Contamination Assessment and Reduction Project
(CARP)

A Model for the Evaluation and Management of Contaminants of Concern in Water, Sediment, and Biota in the NY/NJ Harbor Estuary

Hydrodynamic Sub-model

July, 2007

HydroQual

PREFACE

The modeling work reported here is one of several efforts undertaken in connection with the Contamination Assessment and Reduction Project (CARP). CARP is a landmark project bringing together federal, state and non-government partners in a determined effort to better understand and reduce contamination within the New York/New Jersey Harbor Estuary. This contamination has led to environmental harm and economic hardships. In particular, dredging and disposal activities connected to port activities were severely curtailed in the early 1990ôs as dredging managers and regulators struggled with finding management options for handling contaminated dredged material. While dredging has since proceeded, the costs have escalated to 10 to 30 times previous levels, largely because of sediment contamination. Other negative impacts continue to plague the system, including fish advisories and substandard water quality, which are impeding the recovery and utilization of many of the estuaryôs natural resources.

Through workgroup deliberations in connection with the Dredged Material Forum and the NY/NJ Harbor Estuary Program (HEP), a general plan was developed to address the problem of continued contamination of sediments requiring dredging. The operative management questions included: Which sources of contaminants need to be reduced or eliminated to render future dredged material clean? Which actions can yield the greatest benefits? And, which actions are necessary to achieve the 2040 targets recommended in the Dredged Material Management Plan for the Harbor? CARP was initiated to address these questions. The primary funding mechanism for CARP was the 1996 *Joint Dredging Plan for the Port of New York and New Jersey*, an agreement between the States of New York and New Jersey that was funded by the Port Authority of New York and New Jersey (Port Authority). Additional funds were obtained from the New Jersey Department of Transportation (NJDOT), the Empire State Development Corporation, The U.S. Army Corps of Engineers, the Hudson River Estuary Management Program, HEP, and the Hudson River Foundation.

The specific objectives of the CARP are to:

1. Identify and quantify sources of contaminants of concern to the NY/NJ Harbor Estuary from a dredged material standpoint;
2. Establish baseline levels of contaminants of concern in water, sediments, and biota;
3. Determine the relative significance of contaminant inputs in controlling the concentrations of those contaminants in water, sediment and biota:
4. Forecast future conditions in light of various contaminant reduction scenarios;
5. Take action to reduce levels of contaminants of concern in water, sediments, and fish tissue.

CARP is a unique partnership of governmental and non-governmental entities whose activities have been guided by a management committee composed of representatives from the U.S. Environmental Protection Agency, U.S. Army Corps of Engineers, New Jersey Department of Environmental Protection (NJDEP), New York State Department of Environmental Conservation (NYSDEC), NJDOT, Empire State Development

Corporation, Port Authority, Environmental Defense and the Hudson River Foundation. NYSDEC and NJDEP completed objectives 1 and 2 above through a comprehensive data collection (sampling and testing) program, which represents about 90% of the $32 million total funding for CARP. It was the consensus of the CARP Management Committee that mathematical modeling tools were needed to help understand the results of the data collection program and the fate and transport of contaminants through the Harbor. These models provide a means for integrating data in a mass balance framework such that relationships between loadings and contaminant concentrations in water, sediment and biota can be evaluated and quantified. Moreover, these models can provide the predictive capacity that managers and scientists need to assess the consequences of existing contaminant loads and potential remedial actions. The modeling work performed by HydroQual, Inc., therefore addresses Objectives 3 and 4 above, and represents about 10% of the total funding for CARP.

The major focus of CARP has been on an objective evaluation of the fate and transport of contaminants throughout the entire NY/NJ Harbor Estuary system. The CARP Management Committee hopes that its work will lead to action to reduce both ongoing and historic contamination. The CARP Management Committee includes representatives of federal and state government agencies and is therefore mindful of the various regulatory programs that are in place to address contaminant issues. Consequently, since the inception of CARP, agencies on the Committee have made comments and recommendations to make CARP as relevant as possible to these programs. However, the CARP data collection and modeling efforts were not designed specifically to comply with the requirements of any particular regulatory program. CARP products, particularly the modeling results, will no doubt provide important new information for these programs to consider, but further data collection and model refinement may be necessary to suit the scale and requirements of any particular program. And it is only those charged with regulatory responsibilities that can judge whether CARP products comply with their requirements.

Given the vast complexities of the entire estuary and the processes that affect contaminant fate and transport, modeling of this system has been a great technical challenge. From the initiation of CARP, it was understood that the modeling would be limited in some aspects because of scientific uncertainties in fully understanding all of the relevant processes. To ensure that the model components would be *state-of-the-science* upon completion, a Model Evaluation Group (MEG) was established at the outset of the project. Experts in organic and inorganic geochemistry, hydrodynamics, sediment transport and contaminant modeling were solicited to be members of the MEG. The MEGôs first responsibility was to be part of the team to select a modeling contractor. It then has met repeatedly over the past five years, reviewing and commenting on the acceptability of modeling concepts and formulations to reproduce estuarine processes, including the review of model validation and hindcast results. The comments and suggestions of the MEG have been addressed by HydroQual, Inc., and a summary of the responses are included in this report. In addition, the MEG has provided comments and guidance on the future use and application of the modeling products.

While some model components have been verified, refined and successfully used in other venues, other components were newly designed for this project. The CARP modeling has elements that could be considered *applied science and engineering*, while others would be better characterized as *research and development*. The MEG has generally found that the CARP modeling effort has advanced the understanding of contaminant behavior in the estuary and does a very credible job of characterizing the relationships between contaminant loadings and concentrations in the environment.

One of the more challenging issues that the CARP Management Committee addressed was the development of realistic contaminant reduction scenarios to use as an illustration of the modelôs capability. As the modeling activities progressed, it became increasingly clear that legacy contamination of sediments was a dominant feature in controlling levels of contaminants in the system. Since two large-scale sediment remediation projects (namely the Hudson River Superfund and Lower Passaic River Superfund projects) were being developed, it made sense to include these projects in our initial CARP scenario analyses. While neither project is fully defined as yet, the model scenario gives a glimpse of the potential for these sites (remediated or not) to influence sediment and water quality in the Harbor over the long term.

The completed modeling components should not only be viewed as management tools, but as research tools from which fuller understandings of the fate and transport of contaminants can be gleaned. In addition, it is the hope of the CARP Management Committee that this modeling work serve as a foundation from which more advanced models can be developed and applied to new and emerging management issues.

Dennis J. Suszkowski, Ph.D.
Hudson River Foundation
Co-chair, CARP Management Committee

W. Scott Douglas
NJ Dept. of Transportation
Co-chair, CARP Management Committee

LEGAL NOTICE

CONTENTS

FIGURES

FIGURES (Continued)

TABLES

EXECUTIVE SUMMARY

An existing calibrated, validated, and peer-reviewed three dimensional hydrodynamic circulation model of the NY/NJ Harbor, Sound, and Bight System, the System-Wide Eutrophication Model (SWEM), has been adopted as the Contamination Assessment and Reduction Project (CARP) hydrodynamic model. The model has been applied continuously for four consecutive water years: 1998-99, 1999-2000, 2000-01, and 2001-02. The development of requisite model forcings and inputs for these water years is described in detail. A skill assessment of the model calculations for the four water years as compared to observed physical oceanographic data (water elevations, velocity currents, temperature, and salinity) produced favorable results. The CARP hydrodynamic circulation sub-model is suitable for driving calculations of other CARP sub-models (i.e., suspended sediment transport, nutrient and organic carbon fate and transport, contaminant fate and transport, and bioaccumulation).

CONCLUSIONS

- The previously calibrated, validated, and peer-reviewed CARP hydrodynamic sub-model is appropriate for application under 1998-99, 1999-2000, 2000-01, and 2001-02 conditions. Comparisons between available measured data and model calculations are quite reasonable overall.

- In some instances, there are disagreements between model calculations and observed data which are likely related to model imperfections including improper accounting for salt marsh areas along the Hackensack River, limited grid resolution in Newark Bay, and model bathymetry in the Arthur Kill and Kill van Kull which does not track changes in channel depths due to dredging ongoing during the CARP data collection period.

- Much of the available CARP physical oceanographic data are concentrated in the water years 2000-01 and 2001-02. The model skill assessment would benefit from additional model and data comparisons for the 1998-99 and 1999-00 water years to the extent that, unknown to HydroQual, such data exist. Data collected between 1998 and 2000 now available to HydroQual from several agencies have been utilized in the skill assessment.

- The CARP hydrodynamic sub-model provides sufficient detail on transport and dispersion to support calculations by other CARP sub-models (e.g., contaminant fate and transport model, sediment transport/organic carbon model).

- The CARP hydrodynamic sub-model is amenable to application on an even more finely resolved computational grid than the CARP computational grid as may be warranted to support future modeling efforts within the region.

SECTION 1.0

INTRODUCTION

This report presents the technical details of the development of the Contamination Assessment and Reduction Project (CARP) hydrodynamic sub-model. The report focuses on the application of the CARP hydrodynamic sub-model and its skill assessment for the four water years beginning in October 1998 and ending in September 2002. For consistency, the application of the CARP hydrodynamic sub-model to the 1988-89 and 1994-95 water years used for previous projects is also described. These additional years are useful to CARP for assessing an expanded range of hydrodynamic conditions.

The hydrodynamic model applied for the CARP model is the calibrated, validated, and peer-reviewed hydrodynamic model implemented by HydroQual as part of the System-Wide Eutrophication Model (SWEM). SWEM has been used extensively by the New York City Department of Environmental Protection (NYCDEP) and the NY/NJ Harbor Estuary Program (HEP). Since the SWEM hydrodynamic model is the predecessor model to the CARP hydrodynamic model, some of the features of SWEM which will not be detailed in other sections of this report are described below.

The SWEM hydrodynamic model was calibrated and validated against observed physical oceanographic data collected during two full annual cycles, the 12 month periods from October 1, 1994 to September 30, 1995 and from October 1, 1988 to September 30, 1989. The development, calibration, and validation of the SWEM hydrodynamic model are described in detail in a series of technical reports prepared by HydroQual for NYCDEP. Full citations for these reports are listed in the references section of this report. SWEM reports prepared by HydroQual are available to CARP upon request.

The peer-review process for the SWEM hydrodynamic model development and application includes both oversight by several modeling evaluation groups (MEGs) and publication in the peer-reviewed literature. A MEG with six members was convened in 1994 by HEP. This MEG met on three occasions and provided comprehensive review of the development of the SWEM hydrodynamic model and the supporting physical oceanography field program as well as the initial calibration of the hydrodynamic model in the Harbor portion of the model domain. In 1997, a second MEG was convened by HEP which consisted of four members. This MEG met on four occasions and provided comprehensive review of the calibration/validation of the hydrodynamic model in SWEM over the entire spatial domain. A third MEG was convened by the joint HEP and Long Island Sound Study Nutrient Work Groups in 1999. This MEG met on four occasions and provided detailed review of the

final hydrodynamics. In all three cases, the MEGs also evaluated the SWEM water quality model and the combined suitability of the hydrodynamic and water quality models for application to address nutrient management actions.

Several MEG members were involved with all three phases of the MEG review of SWEM. A complete list of SWEM MEG members includes: Robert Thomann, Donald Pritchard, John Paul, John O'Reilly, Sam Wainwright, Dale Haidvogel, Jay Taft, Peter Hamilton, Chris Uchrin, and Charles Sawyer. More than $250,000.00 was spent on convening MEG, preparing technical presentations for MEG evaluation, responding to written comments from MEG, and modifying SWEM to the satisfaction of MEG.

The hydrodynamic model used for computing SWEM transport has also been described in a peer-reviewed paper (Blumberg et al., 1999) in the Journal of Hydraulic Engineering of the American Society of Civil Engineers. The paper received the Society's Hilgard Prize. A copy of the paper appears in the appendix to this report. The acceptance of the paper by the Journal of Hydraulic Engineering involved the scrutiny of three independent reviewers selected by the Journal editor.

Prior to CARP, additional enhancement of the SWEM calibration in the New Jersey tributaries was performed by HydroQual under oversight by New Jersey Department of Environmental Protection (NJDEP) staff. Enhancement to SWEM in the New Jersey tributaries completed in July 2002 included refinements to model grid geometry in New Jersey waters; adjustments to model bottom friction as a compensating mechanism for limited lateral resolution in some New Jersey waters; and comparisons of adjusted model calculations to measured water elevations, salinity and temperature. A detailed description of this work appears in a technical report prepared by HydroQual for NJDEP which is available to CARP upon request. A full citation for this report is listed in the references section of this report.

The hydrodynamic model source code underlying both the CARP and SWEM applications is the Estuarine and Coastal Ocean Circulation Model (ECOM) derived from the Princeton Ocean Model (POM) developed by Alan F. Blumberg and George L. Mellor. This code has been used to develop numerous models outside of the NY/NJ Harbor region. The model code is well-known and respected within the international hydrodynamic modeling community. The code has been constantly refined and upgraded to include both more realistic physics and more robust numerical solution techniques. Since the early 1990's, HydroQual has maintained a users manual for the ECOM code. The most up to date version of the users manual is available to the CARP MEG upon request and includes a detailed description of the basic equations of the model, characteristics of the model, characteristics of the computer code, and descriptions of input and output files associated with the code.

The principal attributes of the ECOM source code include:

- ECOM is fully three-dimensional.
- ECOM contains imbedded turbulence closure sub-models to provide vertical and horizontal mixing coefficients.
- ECOM is a sigma coordinate model in that the vertical coordinate is scaled on the water column depth.
- The horizontal grid uses curvilinear orthogonal coordinates and a finite difference solution scheme.
- The horizontal time difference calculations are explicit whereas the vertical difference calculations are implicit. The latter eliminates the time constraints for the vertical coordinate and permits the use of fine vertical resolution in the surface and bottom boundary layers.
- ECOM has a free surface and split time step. The external mode portion of the model is two-dimensional and uses a short time step based on the Courant-Friedrich-Level (CFL) numerical stability criteria condition and the external wave speed. The internal mode is three-dimensional and uses a long time step based on the CFL stability criteria condition and the internal wave speed.
- ECOM includes complete thermodynamics, allowing the computation of temperature and salinity.
- Results produced by ECOM source code may be used directly to satisfy input requirements of various water quality models.

The purpose of this report is to provide the CARP MEG with a comprehensive description of the CARP hydrodynamic model and its suitability for use in the calculation of contaminant fate and transport. The report is broken down into three technical sections including CARP hydrodynamic sub-model setup, CARP hydrodynamic sub-model skill assessment, and CARP hydrodynamic sub-model linkages with other CARP sub-models.

SECTION 2.0

CARP HYDRODYNAMIC MODEL SETUP

This report section describes the setup of the CARP hydrodynamic sub-model. The data requirements for the requisite model forcings are described. Also provided is a description of the observed dominant hydrodynamic features of the NY/NJ Harbor Estuary.

2.1 HYDRODYNAMIC FEATURES OF THE NY/NJ HARBOR ESTUARY

New York Harbor, Long Island Sound and the New York Bight are among the most extensively investigated waters in the world. Numerous papers and reports have been published on the tides, currents, and hydrology in this area. Jay and Bowman (1975) gave a comprehensive literature review on the hydrodynamics and water quality in this region from 1848 to the early 1970s. Additional investigations have been conducted since the 1970's. A comprehensive discussion of the circulation in the New York Bight and surrounding coastal waters may be found in Beardsley and Boicourt (1981). Field experiments (Beardsley et al., (1985); Brown et al. (1985); Joyce (1985)) have added a wealth of information on the circulation. Based upon the analysis of Beardsley and Boicourt (1981), Beardsley and Butman (1974), Beardsley and Winant (1979), Chapman et al. (1986), Han et al. (1980) and Mayer et al. (1982) as well as the drifter-bottle studies of Bumpus (1969), it is apparent that the characteristic feature of the circulation in the New York Bight is a southwestward net flow along the shelf of roughly 2 to 10 cm/s with a mean transport on the order of 250,000 cubic meters per second. The average currents generally increase in magnitude in the offshore direction and decrease with depth. This flow is driven by an alongshore sea level slope of approximately 2 cm/100 km at the shelf break, presumably due to large scale circulation offshore.

Simulations of the long-term mean circulation in the Middle Atlantic Bight have been conducted by Blumberg and Mellor (1980), and discussed subsequently by Blumberg and Oey (1985). The main conclusion from their three-dimensional simulations was that the presence of the Gulf Stream is an important factor for the circulation along the continental shelf in the New York Bight. Moreover, a series of observations reported by Garvine, et al., (1988), have shown that eddy-like features are almost always present along the shelf break. The eddies typically appear either as plumes of less saline shelf

water that protrude into slope water curling "backwards," opposite the direction of the mean shelf flow or as eddies with warmer, saltier slope water in their cores, partially or wholly encircled by the plumes. While these plumes can potentially produce vigorous cross-shelf transfer of heat and salt, their influence is, for the most part, restricted to the outer shelf regions.

Diagnostic studies of the mean barotropic and baroclinic circulation in New York Bight have been conducted by Han et al. (1980) and Hopkins and Dieterle (1983, 1987) using a steady, vertically integrated vorticity equation approach. Despite the simplicity of the approach, essentially solving for the free surface elevation only, the investigators were able to capture the major features of the circulation and its response to wind forcing. Among the three-dimensional numerical investigations, the work of Oey et al. (1985 a-c) is noteworthy. Blumberg and Galperin (1990) simulated the summer circulation in New York Bight and contiguous estuarine waters by focusing on the importance of the coupling between New York Bight and Long Island Sound. Three-dimensional hydrodynamic model studies of the Long Island Sound and the New York Bight have also been reported by Schmalz et al. (1994) and Scheffer et al. (1994), respectively.

2.2 FEATURES OF THE CARP COMPUTATIONAL GRID

The CARP hydrodynamic sub-model computational grid covers New York Harbor, Long Island Sound, and the New York Bight from Cape May, New Jersey to Nantucket Shoals, Rhode Island as shown in Figure 2-1a. Selected portions of the model computational grid for the New York-New Jersey Harbor area and the Hudson River are shown in Figures 2-1b and 2-1c, respectively. The complex bathymetry of the model domain is shown in Figures 2-2. The model grid (Figure 2-1a) is curvilinear and orthogonal with resolution from one hundred meters in rivers to fifty kilometers in New York Bight. The model grid includes ten vertical layers.

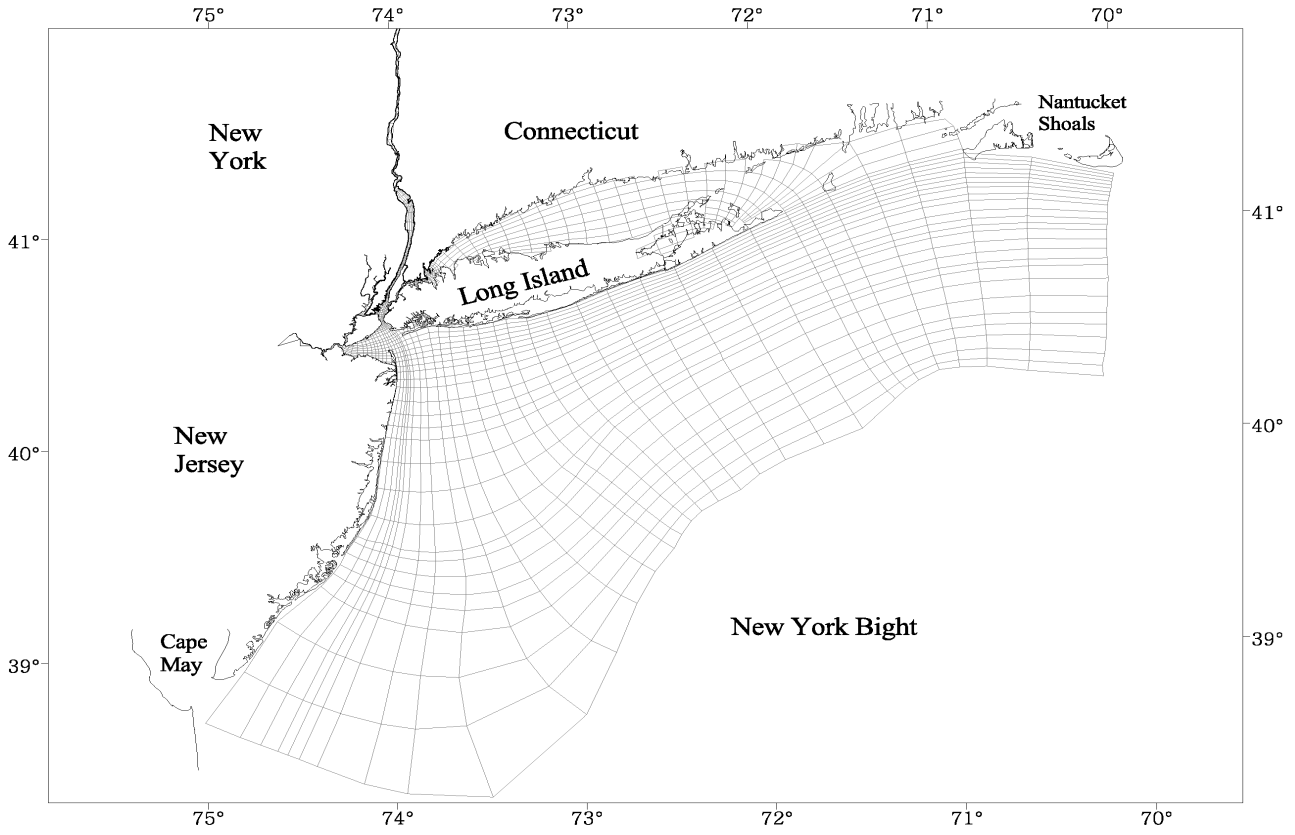

Figure 2-1a. Computational grid for the CARP model.

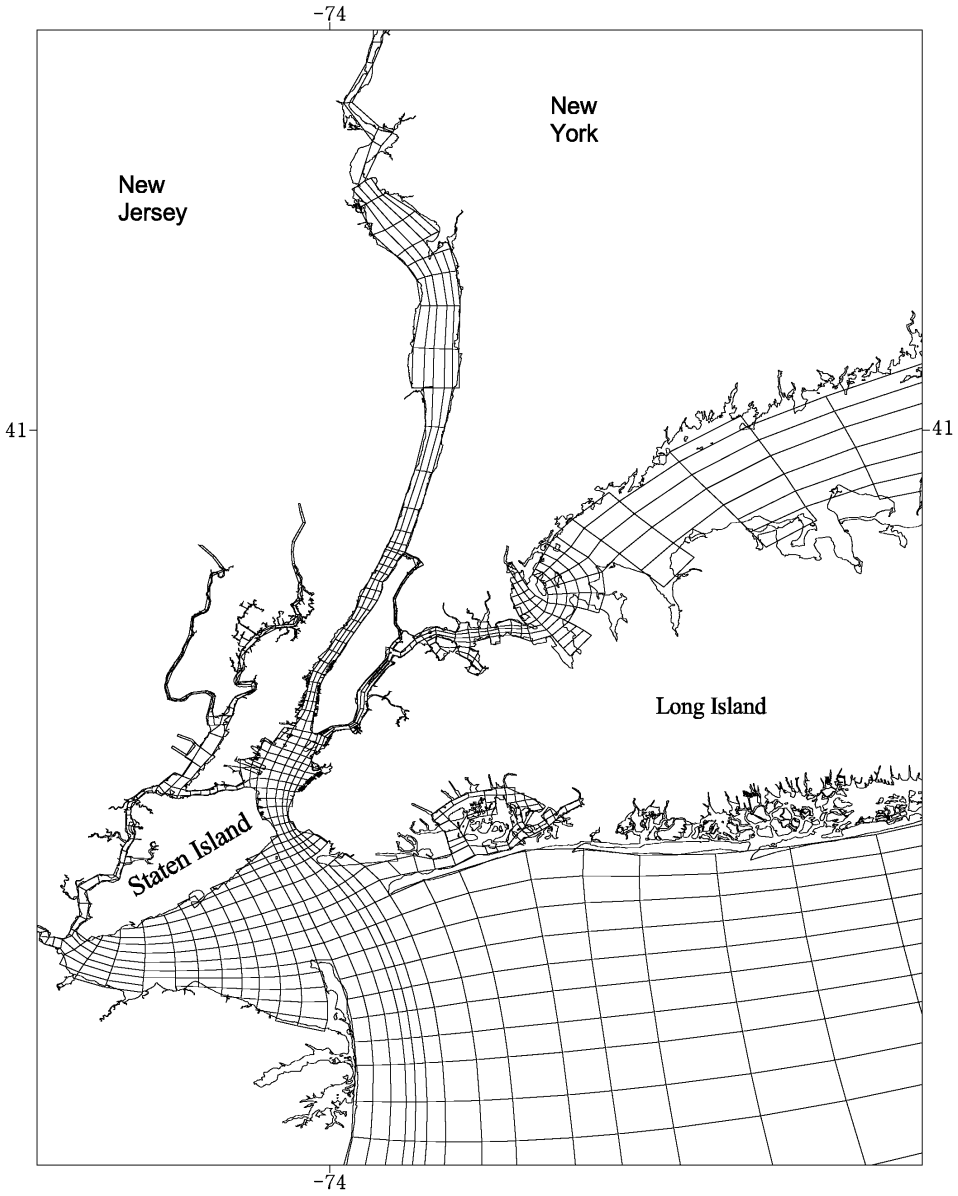

Figure 2-1b. Harbor view of the CARP model computational grid.

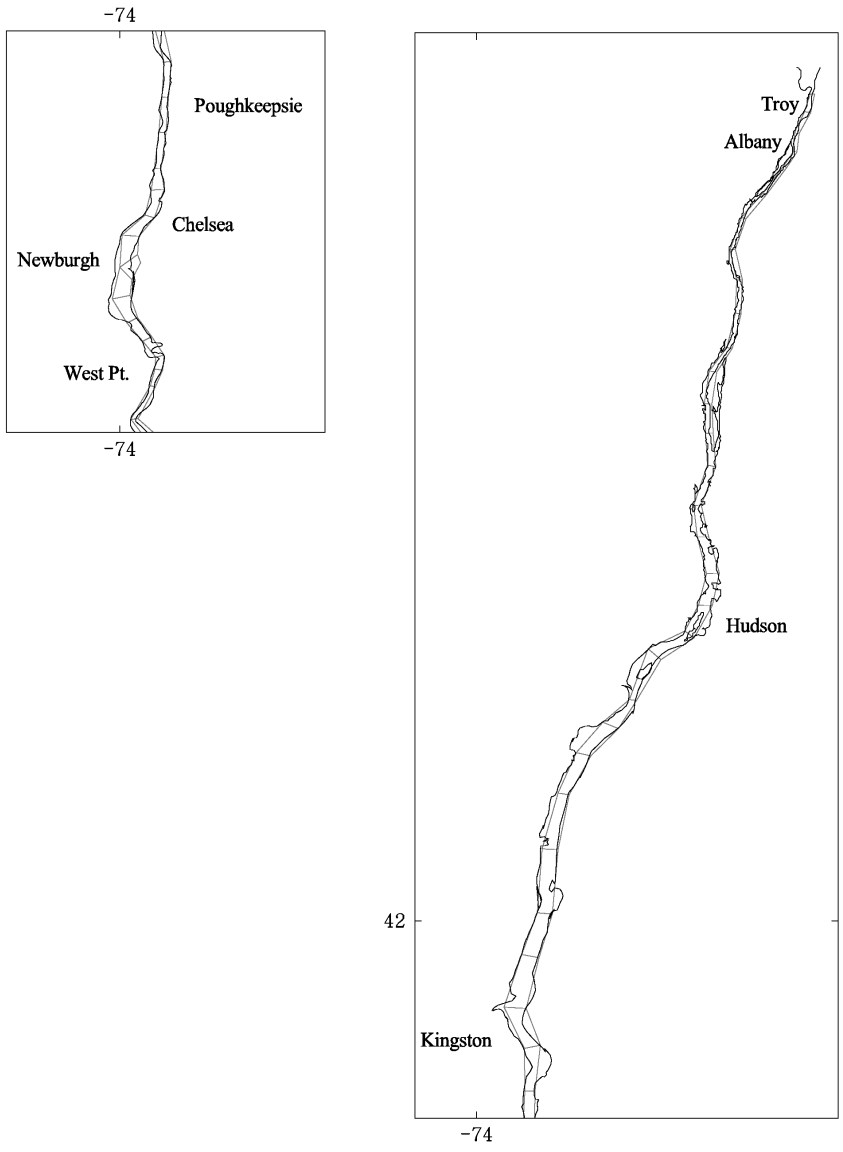

Figure 2-1c. Hudson River view of the CARP model computational grid.

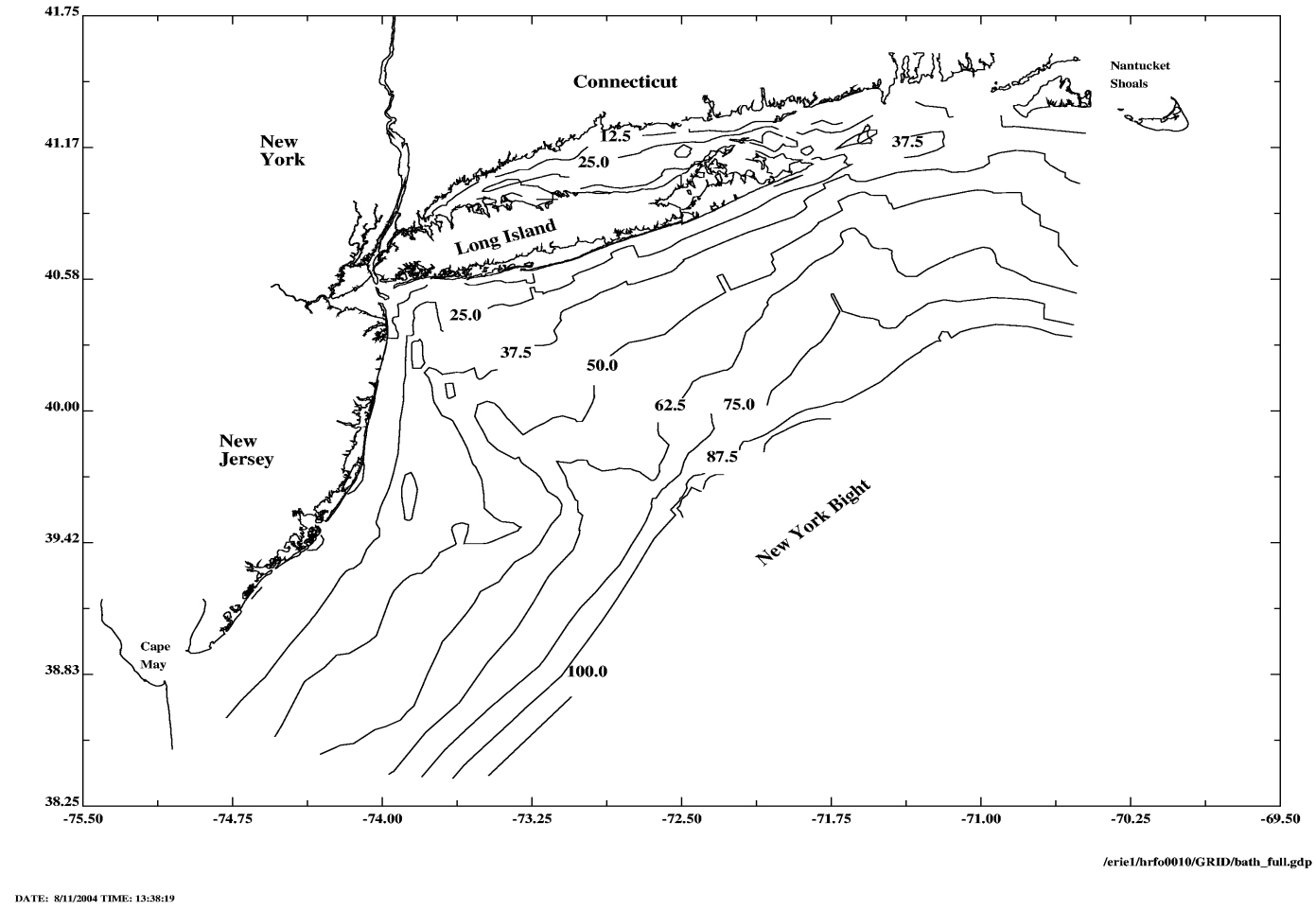

Figure 2-2. Bathymetric features incorporated into the CARP model computational grid.

2.3 CARP HYDRODYNAMIC SUB-MODEL FORCINGS

The CARP hydrodynamic sub-model responds to surface wind stress, heat and salinity fluxes, freshwater discharges and tidal forcing. The boundary conditions, or forcing functions, required by the hydrodynamic model include:

- water surface elevation along open ocean boundaries incorporating astronomical tide, cross-shelf elevation gradient and shelf-break elevation;
- three-dimensional fields of temperature and salinity along the open boundaries;
- meteorological information consisting of wind speed and velocity, shortwave solar radiation, cloud cover, air temperature, atmospheric vapor pressure and relative humidity to compute surface wind stress and heat flux; and
- freshwater inflows from rivers, wastewater treatment plants, combined sewer overflow and surface runoff.

The required meteorological forcings are developed from data collected at J.F.K. Airport, N.Y., Albany Airport, N.Y., Bridgeport Airport, C.T. and several buoys in New York Bight. The water level data along the open boundaries are generated from a combination of output from the Oregon State University (OSU) TPXO.2 global model of ocean tides (Egbert et al. (1994)) and cross-shelf elevation gradients.

Detailed specification of model forcings enables the CARP hydrodynamic sub-model to reproduce hydrodynamic events of various time scales with sufficient accuracy. Times scales of events captured by the hydrodynamic model include semi-diurnal/tidal cycle, diurnal, meteorological (i.e., a few days), spring and neap tidal cycle (i.e., 15 days), monthly, seasonal and annual. The model forcings are described more fully below.

2.3.1 Tidal Elevation

To produce a simulation of the tidal scale circulation, including the effects of baroclinicity, it is necessary to prepare a data base containing the astronomical dynamics and climatological thermodynamic properties prevailing in New York Bight. The low frequency dynamics in the shelf break are important to the circulation in New York Bight. This phenomena has already been addressed by others. (Hopkins and Dieterle, 1983 and 1987; Blumberg and Galperin, 1990) Low frequency dynamics of the continental shelf are associated with a geostrophic balance. Hence, the cross-shelf

slope of the sea surface elevation at the boundaries is highly significant. Because low frequency cross-shelf sea surface elevation records at the CARP model boundaries are not available, a practical approach was developed to define forcing conditions at the CARP model boundaries. The approach was applied previously for SWEM for the 1994-95 and 1988-89 water years and has been repeated for all 4 CARP simulation years between October 1998 and September 2002.

For the model simulation period, the sea surface elevation $\eta(x,t)$ at the boundary is assumed to be composed of three parts. The first part drives the long-term circulation (geostrophic currents) due to the cross-shelf slope ($\eta_g(x,t)$); the second part deals with the tidal fluctuations ($\eta_T(x,t)$); and the third part represents sub-tidal (meteorological) forcing ($\eta_M(t)$). The resulting water surface elevation is given by:

$$\eta(x,t) = \eta_g(x) + \eta_T(x,t) + \eta_M(t) \qquad (2\text{-}1)$$

The effect of the along-shelf elevation gradient imposed at the shelf break on the barotropic circulation in New York Bight has been studied by Hopkins and Dieterle 1983. They found that the parabathic elevation gradient at the shelf-break affects the total transport through the cross-shelf boundary. For August 1978, a typical summertime period, a diabathic gradient of 13 cm across at the Narragansett Bay shelf-break section and an 11 cm gradient across at the Cape May shelf-break section could produce the observed summer along-shelf flux of water. Following their findings, Blumberg and Galperin,1990, adopted the same boundary elevation in a summer average circulation study in the New York Bight.

For the CARP hydrodynamic model, a 13 cm gradient along the northeastern Nantucket Shoals boundary, an 11 cm gradient across the Cape May shelf-break southern boundary and a zero gradient along the shelf boundary are imposed.

Astronomical tide, $\eta_T(x,t)$, which is due to eight primary harmonic constituents (M_2, S_2, N_2, K_2, O_1, P_1 and Q_1), is obtained from a global model of ocean tide, TPXO.2, developed by Oregon State University (Egbert et al., 1994). The input to the tidal synthesis program is gridded data of the harmonic constants. The output is η_T as a function of time and space (longitude and latitude). The tidal synthesis program uses interpolation of the tidal admittances in the diurnal and semi-diurnal bands to include 9 additional minor constituents ($2N_2$, MU_2, NU_2, L_2, T_2, J_1, NO_1, OO_1, RHO_1). The synthesis program also adds the long period constituents MF, MM, SSA using the standard equilibrium forms.

Close examination of low frequency fluctuations of water level at various locations in the region indicates that the response of water elevation to meteorological forcing are essentially in phase.

The differences in amplitude at different locations, due to local bathymetry and coastline, are also small. Therefore, for the CARP hydrodynamic model, $\eta_M(t)$ is expressed as:

$$\eta_M(t) = \alpha\bar{\eta}(t) \qquad (2\text{-}2)$$

where α is a calibration parameter and $\eta(t)$ is the 34 hours low passed water surface elevation at Sandy Hook. As a tidal wave propagates over the continental shelf, its amplitude is increased by shoaling and shallow water effects. As a result, α is expected to have a value less than one. Its value ($\alpha = 0.5$) has been determined by making a series of model runs and comparing model results with data.

Also a modified form of the Sommerfield radiation boundary conditions (Blumberg and Kantha, 1985) is applied across the Cape May shelf-break section with a function which tends to force the elevation to a specified (elevation) boundary condition within a given time scale. Thus, long waves are allowed to propagate and they are free to advect through the boundary.

2.3.2 Salinity and Temperature

Temperature and salinity boundary conditions are obtained from climatological data from the World Ocean Atlas 1998 (WOA98), published by NOAA. The published data set contains gridded monthly temperature and salinity at one-degree latitude-longitude. The monthly data are tabulated at 19 levels from 0 to 1000 m. At the model boundary, temperature and salinity are linearly interpolated from the surrounding gridded data.

As climatological data do not represent true monthly variations of temperature and salinity for 1998 through 2002, it was necessary to adjust the boundary conditions defined from WOA98 so that computed temperature and salinity matched the monthly mean temperature and salinity in Long Island Sound, New York Bay and the Hudson River. The temporal variations of the adjusted salinity and temperature at the boundary are defined as follows:

$$S(x,t) = S_L(x,t) - 2.0 \qquad (2\text{-}3)$$

$$T(x,t) = T_L(x,t) - 2.0 \qquad (2\text{-}4)$$

where S_L and T_L are the climatological salinity and temperature in ppt and ˚C from WOA98.

2.3.3 Meteorological Data

Two major boundary forcings applied on the water surface are wind stress and heat flux. Wind stress is computed from wind speed and wind direction. Heat flux computation requires the specification of air temperature, relative humidity, barometric pressure, shortwave solar radiation and cloud cover. Hourly meteorological data were obtained from NOAA for J.F.K. Airport, N.Y., Albany Airport, N.Y., Bridgeport Airport, C.T. and several buoys in New York Bight. Figure 2-3 shows the locations of the meteorological data stations. Data from J.F.K. are used for heat flux computation (Figure 2-4a through 2-4d). Spatially varying wind stress were computed from these data and were applied in the model.

2.3.4 River Discharge

Fresh water inflows from 34 tributary rivers are considered in the CARP model. Discharge data were compiled from USGS surface water records for New York, New Jersey and Connecticut for the four CARP water years. Table 2-1 lists the 34 tributary rivers. The gauging station locations are shown in Figure 2-5. The flow records from the 34 gaged tributary rivers enter the CARP model at 25 locations as described below and in Table 2-2. The temporal variation of the river discharges entering the CARP model are shown on the figures contained in Appendix 2. The annual mean, maximum, and minimum flows from the rivers are listed in Table 2-2.

The ungauged Catskill Creek includes drainage basins in Green and Columbia Counties. The inflow was calculated based on specific discharge (flow/area) from the adjacent Wallkill and Esopus Creeks. A similar procedure was used to determine discharge from the ungauged Westecunk Creek based on specific discharge from neighboring river basins.

Temporal variation of river water temperature is shown in Figure 2-6. The figure is based on daily surface water temperature measured at the Battery. The maximum, minimum and yearly mean temperatures assigned to river water are 24.5, 1.0 and 12.1˚C respectively.

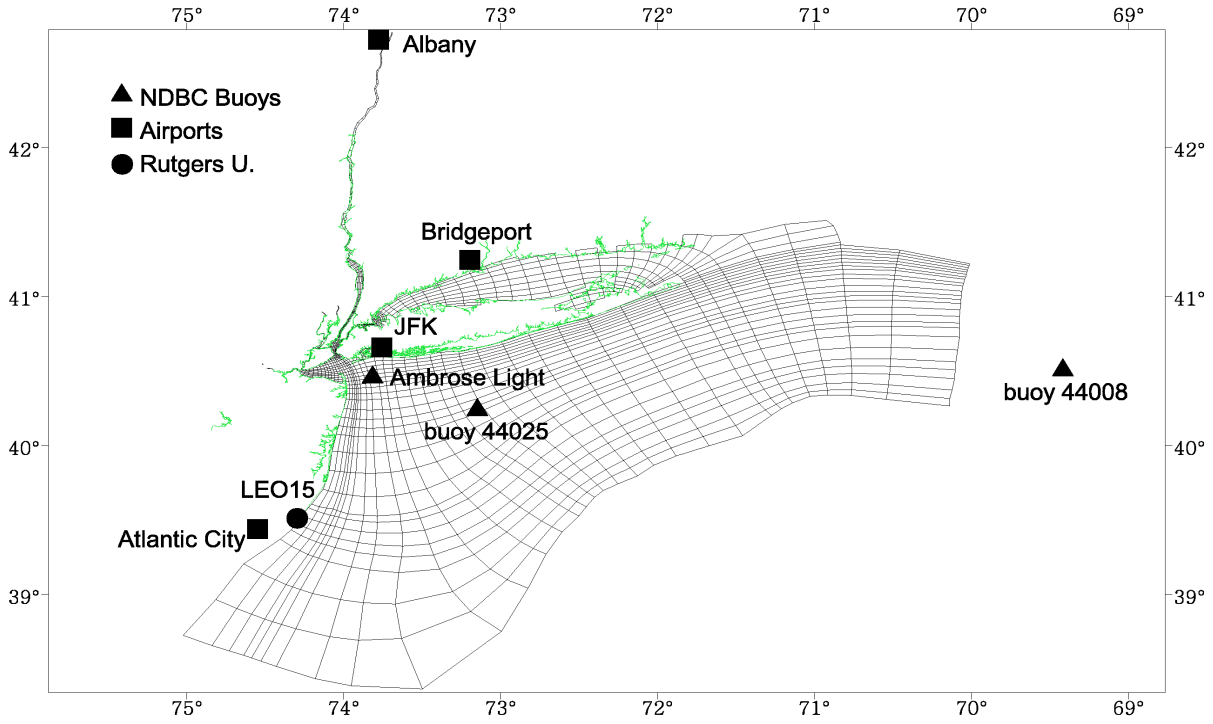

Figure 2-3. Location map for meteorological data stations.

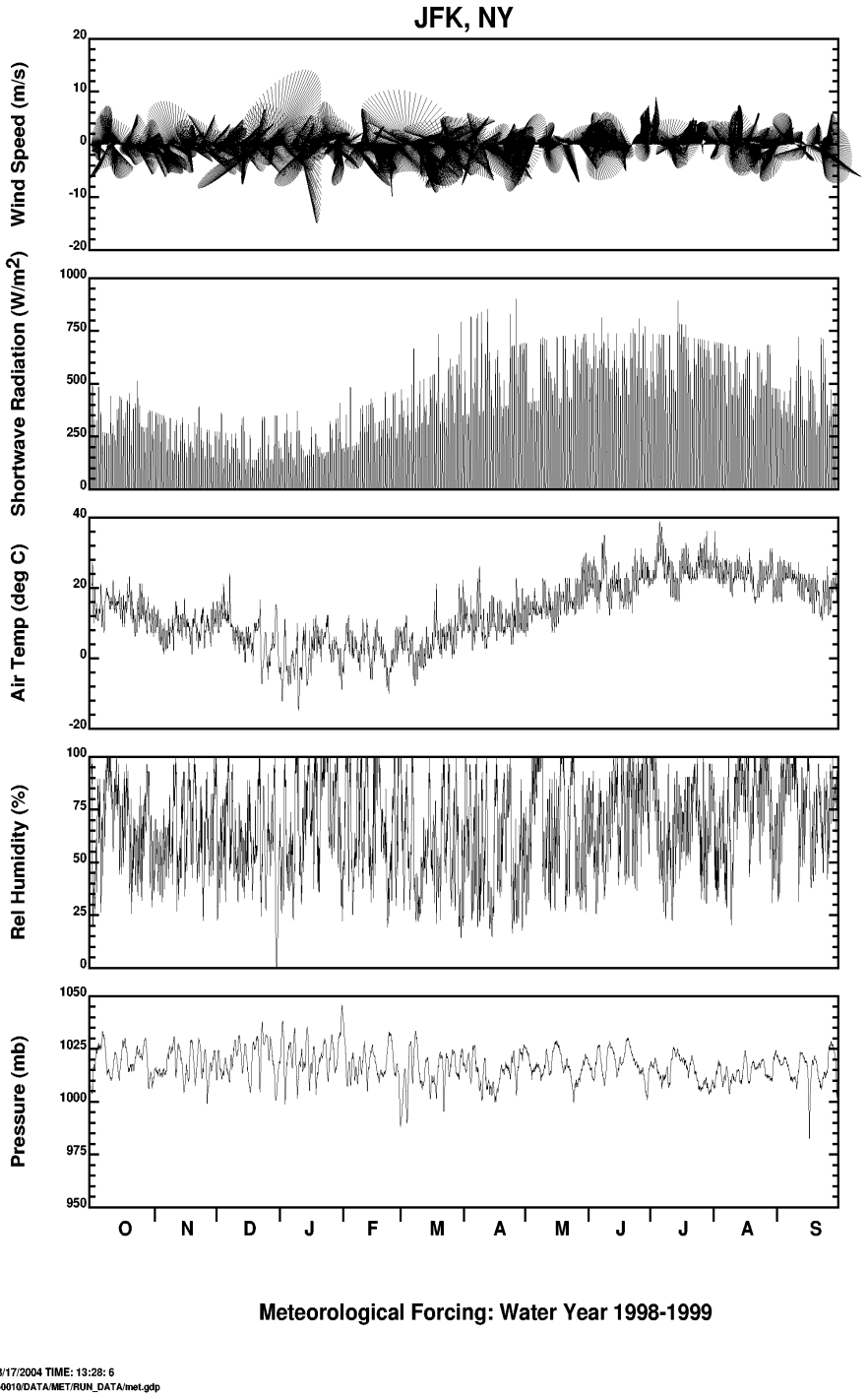

Figure 2-4a. 1998-1999 meteorological data applied for model forcings.

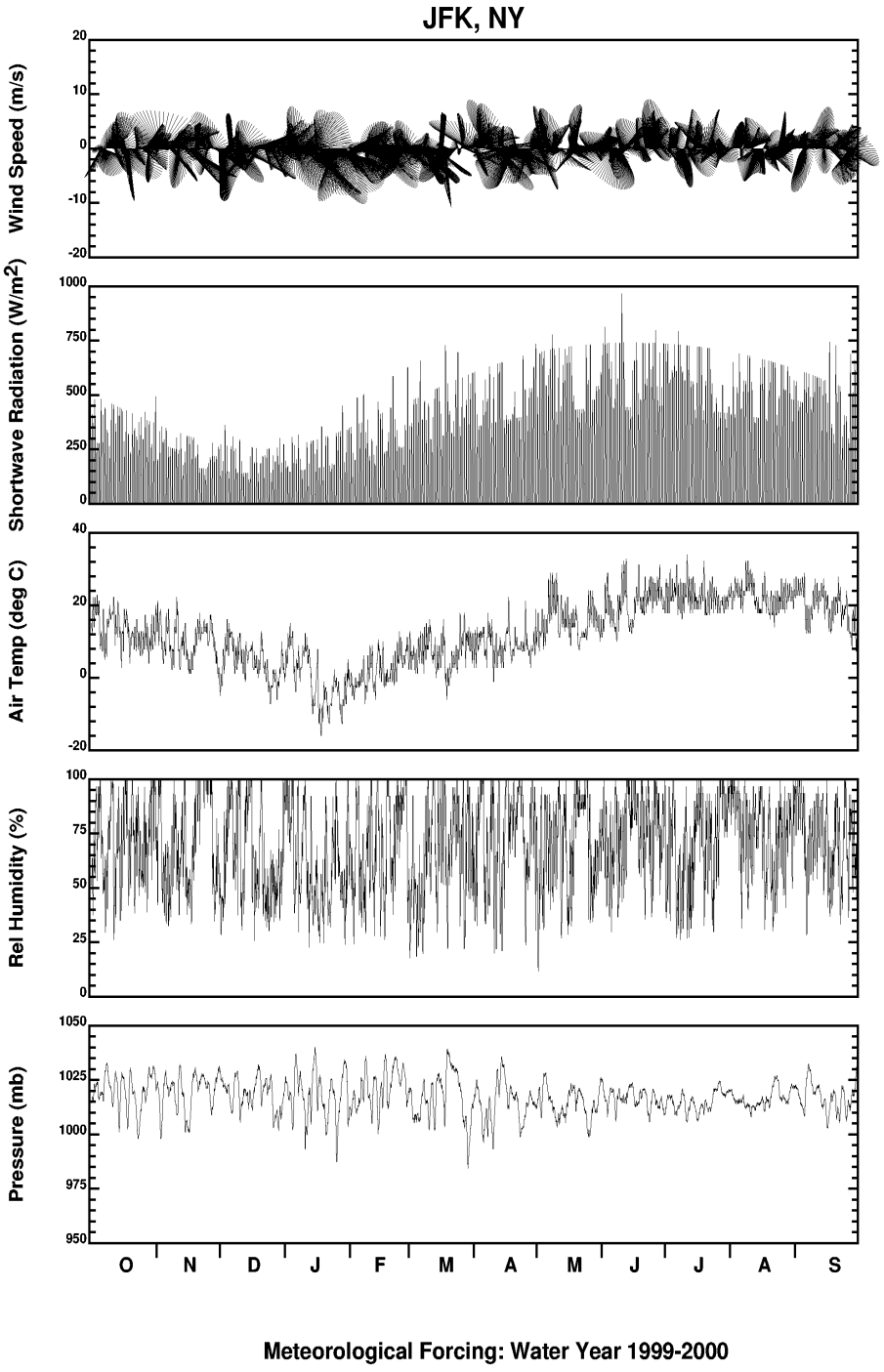

Figure 2-4b. 1999-2000 meteorological data applied for model forcings.

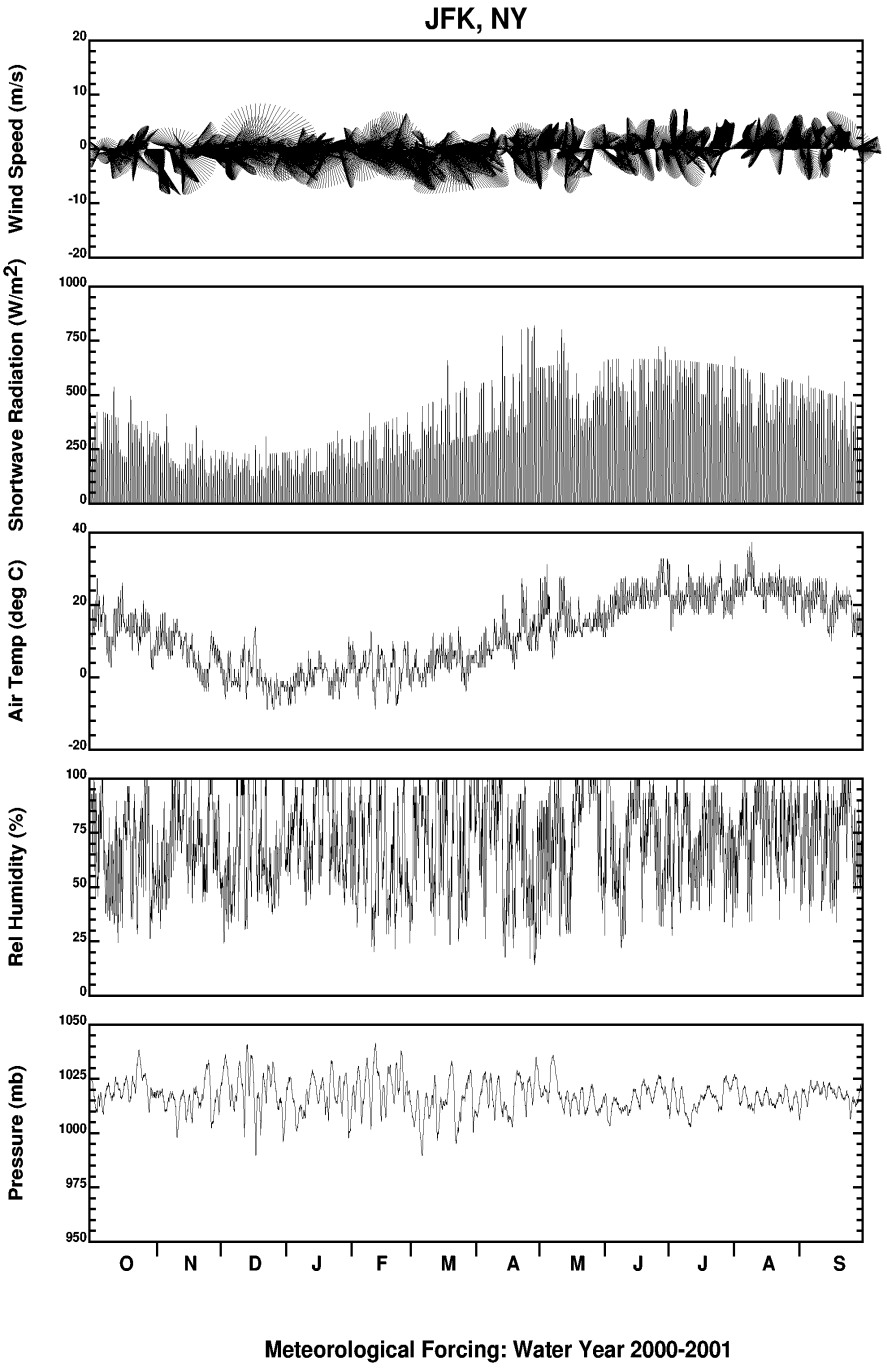

Figure 2-4c. 2000-2001 meteorological data applied for model forcings.

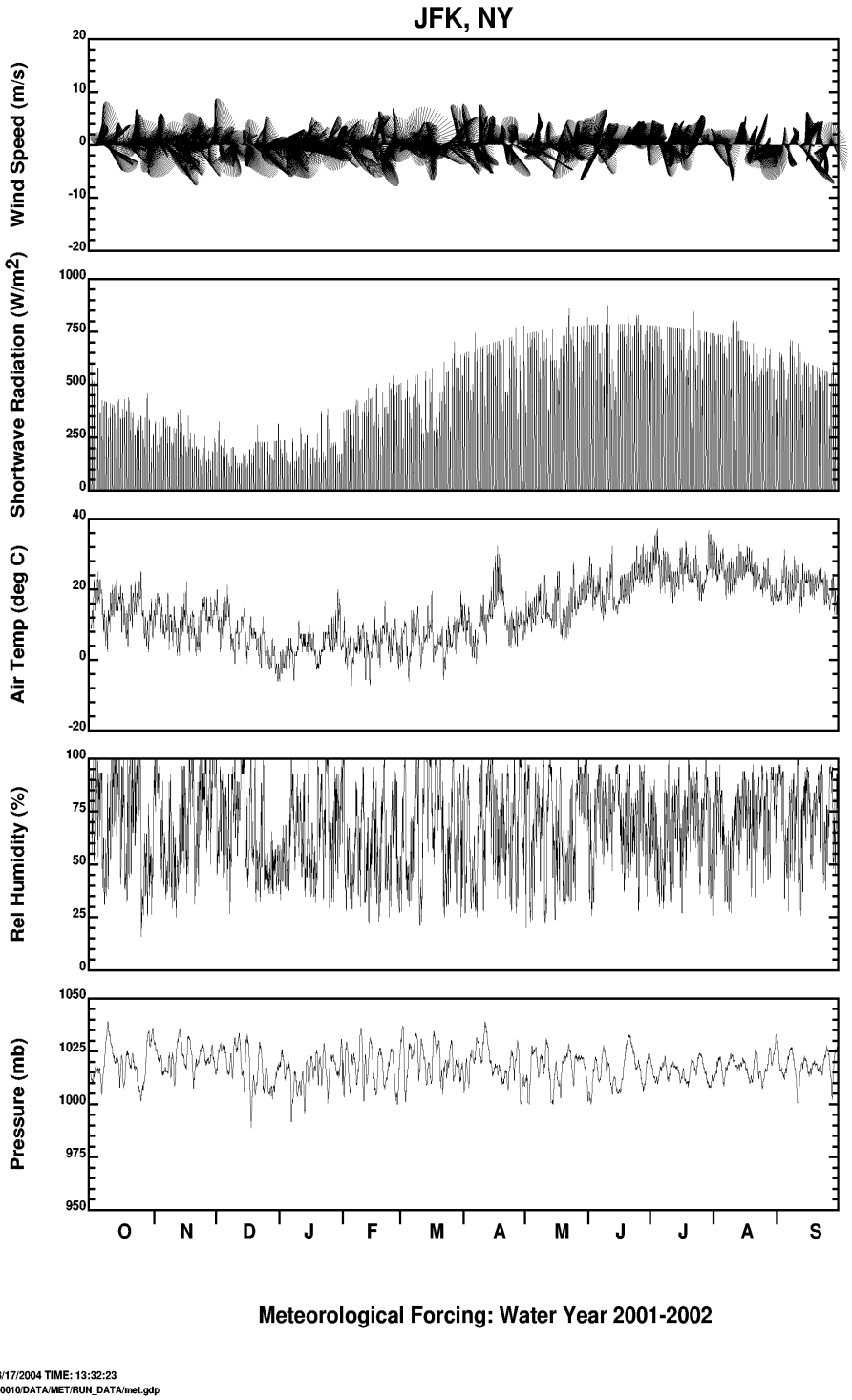

Figure 2-4d. 2001-2002 meteorological data applied for model forcings.

Table 2-1. Listing of Tributary Rivers included in the Model

No.	Gauge Number and Name	Latitude	Longitude
1	USGS 01358000 Hudson River at Green Island, NY	42.75222	-73.68944
2	USGS 01359750 Moordener Kill at Castleton-on-Hudson, NY	42.53389	-73.73750
3	USGS 01357500 Mohawk River at Cohoes, NY	42.78528	-73.70806
4	USGS 01335754 Hudson R Above Lock 1 near Waterford, NY	42.82917	-73.66667
5	USGS 01378500 Hackensack River at New Milford, NJ	40.94833	-74.02667
6	USGS 01389500 Passaic River at Little Falls, NJ	40.88472	-74.22611
7	USGS 01391500 Saddle River at Lodi, NJ	40.89028	-74.08056
8	USGS 01403060 Raritan River Below Calco Dam at Bound Brook, NJ	40.55111	-74.54833
9	USGS 01405400 Manalapan Brook at Spotswood, NJ	40.38944	-74.39056
10	USGS 01405030 Lawrence Brook at Weston Mills, NJ	40.48306	-74.41222
11	USGS 01364500 Esopus Creek at Mount Marion, NJ	42.03778	-73.97250
12	USGS 01367500 Rondout Creek at Rosendale, NY	41.84306	-74.08639
13	USGS 01371500 Wallkill River at Gardiner, NY	41.68611	-74.16556
14	USGS 01372500 Wappinger Creek Near Wappingers Falls, NY	41.65306	-73.87306
15	USGS 01375000 Croton River at New Croton Dam near Croton-on-Hudson, NY	41.22500	-73.85972
16	USGS 01376500 Saw Mill River at Yonkers, NY	40.93722	-73.88944
17	USGS 01407500 Swimming River near Red Bank, NJ	40.31917	-74.11611
18	USGS 01209700 Norwalk R at South Wilton, CT	41.16361	-73.41972
19	USGS 01205500 Housatonic River at Stevenson, CT	41.38389	-73.16806
20	USGS 01208500 Naugatuck River at Beacon Falls, CT	41.44222	-73.06306
21	USGS 01196500 Quinnipiac River at Wallingford, CT	41.44944	-72.84139
22	USGS 01184000 Connecticut River at Thompsonville, CT	41.98722	-72.60583
23	USGS 01122500 Shetucket River near Willimantic, CT	41.70028	-72.18250
24	USGS 01127000 Quinebaug River at Jewett City, CT	41.59778	-71.98472
25	USGS 01408000 Manasquan River at Allenwood, NJ	40.16139	-74.15472
26	USGS 01407705 Shark River Near Neptune City, NJ	40.19861	-74.07028
27	USGS 01408120 North Branch Metedeconk River Near Lakewood, NJ	40.09167	-74.15250
28	USGS 01408500 Toms River Near Toms River, NJ	39.98639	-74.22333
29	USGS 01409400 Mullica River Near Batsto, NJ	39.67444	-74.66500
30	USGS 01410000 Oswego River at Harrisville, NJ	39.66333	-74.52417
31	USGS 01409500 Batsto River at Batsto, NJ	39.64167	-74.65028
32	USGS 01410150 East Branch Bass River near New Gretna, NJ	39.62306	-74.44139
33	USGS 01411300 Tuckahoe River at Head of River, NJ	39.30694	-74.82056
34	USGS 01411000 Great Egg Harbor River at Folsom, NJ	39.59500	-74.85139

Table 2-2. River Flow Statistics for the Model Input for each of the 4 years (cms)

			1998-1999			1999-2000			2000-2001			2001-2002		
River #			Mean	Maximum	Minimum	Mean	Maximum	Minimum	Mean	Maximum	Minimum	Mean	Maximum	Minimum
1	Hudson River[1]	1358000	291.16	1774.79	72.00	512.94	2599.88	148.81	395.86	2719.29	72.10	323.42	1652.45	74.92
		1357500/1335754												
2	Hackensack River	1378500	0.94	158.01	0.00	0.88	14.41	0.01	1.01	32.85	0.01	0.03	0.28	0.00
3	Passaic River	1389500	19.24	319.98	0.91	26.86	88.92	3.85	23.21	126.01	1.84	5.63	57.20	0.18
4	Saddle River	1391500	2.05	51.54	0.15	2.92	19.85	0.79	2.55	26.48	0.57	1.52	15.72	0.37
5	Raritan River	1403060	26.73	1727.33	2.92	24.14	202.75	3.77	28.49	256.27	3.09	12.21	207.28	2.78
6	South River+Lawrence Brook	1404054/14040503	3.77	67.27	0.01	3.86	22.15	1.04	5.15	41.96	1.38	2.62	27.41	0.72
7	Normans Kill[2]	1359750	2.45	12.99	1.27	3.37	12.18	1.69	2.74	16.14	1.29	1.89	9.50	1.29
8	Moordener Kill	1359750	0.48	2.52	0.25	0.65	2.36	0.33	0.53	3.14	0.25	0.37	1.84	0.25
9	Esopus Creek	1364500	6.37	141.02	0.16	11.98	245.51	1.53	8.59	148.38	0.34	3.75	42.48	0.23
10	Rondout Creek+Wallkill River	1367500/1371500	31.64	532.92	1.42	50.50	541.98	9.18	37.39	557.84	2.35	19.16	237.30	2.04
11	Wappinger Creek	1372500	10.72	104.71	0.20	18.91	97.53	3.95	13.29	132.83	0.35	5.72	73.60	0.41
12	Croton River	1375000	9.45	300.16	0.20	16.29	63.15	2.55	12.73	94.01	1.95	1.36	34.83	0.57
13	Sawmill River	1376500	0.75	18.77	0.18	1.17	4.08	0.32	0.95	5.99	0.29	0.25	2.33	0.20
14	Bronx River	1375000	1.17	37.00	0.03	2.01	7.78	0.31	1.57	11.59	0.24	0.17	4.29	0.07
15	Navesink River + Shrewsbury River[3]	1407500	1.64	32.08	0.00	1.77	20.42	0.00	2.24	66.14	0.00	0.19	12.47	0.00
16	Catskill River[4]	1364500/1371500	27.93	442.56	0.60	48.22	598.89	7.79	35.47	524.26	1.49	16.86	189.58	1.11
17	Norwalk River	1209700	1.44	25.26	0.05	1.34	11.02	0.14	1.18	12.60	0.09	0.78	9.49	0.08
18	Housatonic River + Naugatuck River	1205500/1208500	80.14	647.32	4.79	104.65	455.33	6.82	82.69	448.26	5.04	46.23	321.96	4.62
19	Quinnipiac River	1196500	5.73	73.91	0.96	6.52	65.41	2.24	5.97	59.18	1.59	2.99	24.44	1.13
20	Connecticut River	1184000	397.70	2160.57	73.62	566.34	2265.34	126.29	430.08	2712.75	59.75	382.85	2041.64	44.17
21	Thames River[5]	1122500/1127000	48.69	311.49	1.78	56.58	328.76	6.74	49.63	417.39	5.35	28.41	211.81	3.43
22	Manasquan River + Shark River	1408029/1407705	3.86	61.66	0.82	3.66	28.39	0.90	4.03	65.62	1.10	2.07	19.13	0.64
23	Metedeconk River + Toms River	1408120/1408500	16.54	101.57	4.95	18.49	42.34	7.77	19.23	98.00	5.00	11.20	32.47	4.07
24	Westeconk River[6] + Mullica River[7]	1409400/1408500/												
		1410000/1409500/												
		1410150	30.23	184.26	10.13	34.11	100.57	14.90	34.49	128.60	11.67	19.18	65.69	9.05
25	Great Egg Harbour River + Tuckahoe River	1411300/1411000	21.70	95.81	5.41	25.10	134.18	11.80	24.94	87.25	7.55	13.69	43.08	3.97

Notes

[1] If the Hudson River flow at Green Island is unavailable, the flow is calculated using the flow records for the Mohawk River and the Hudson River at Lock #1 near Waterford.

[2] The Normans Kill flow is calculated using the Moordener Kill flow.

[3] Calculated using drainage areas ratios with the Swimming River flow record.

[4] Calculated by summing the Wallkill River and Esopus Creek Flows.

[5] Calculated by summing the Shetucket River and Quinebaug River flows.

[6] The Westeconk River is ungauged. Flows were calculated based on Toms River flows corrected for drainage area.

[7] Calculated using Mullica River, Oswego River, Batso River and Bass River flows.

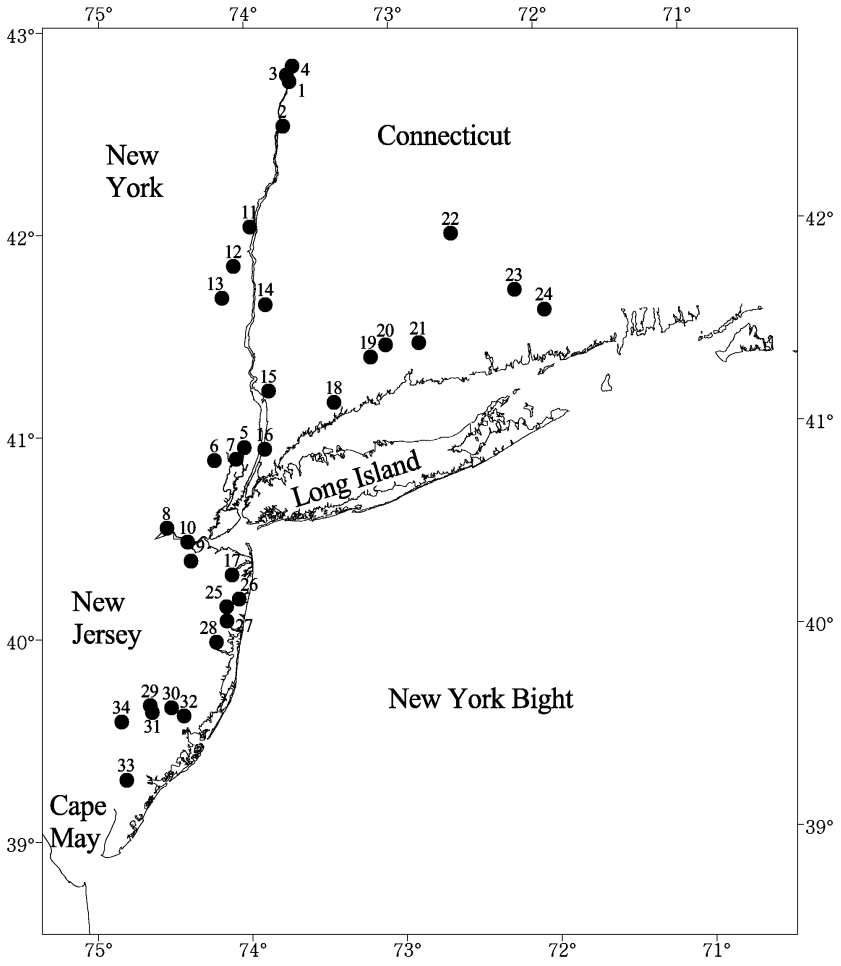

Figure 2-5. Gaging station locations from which USGS flow records were obtained for model input.

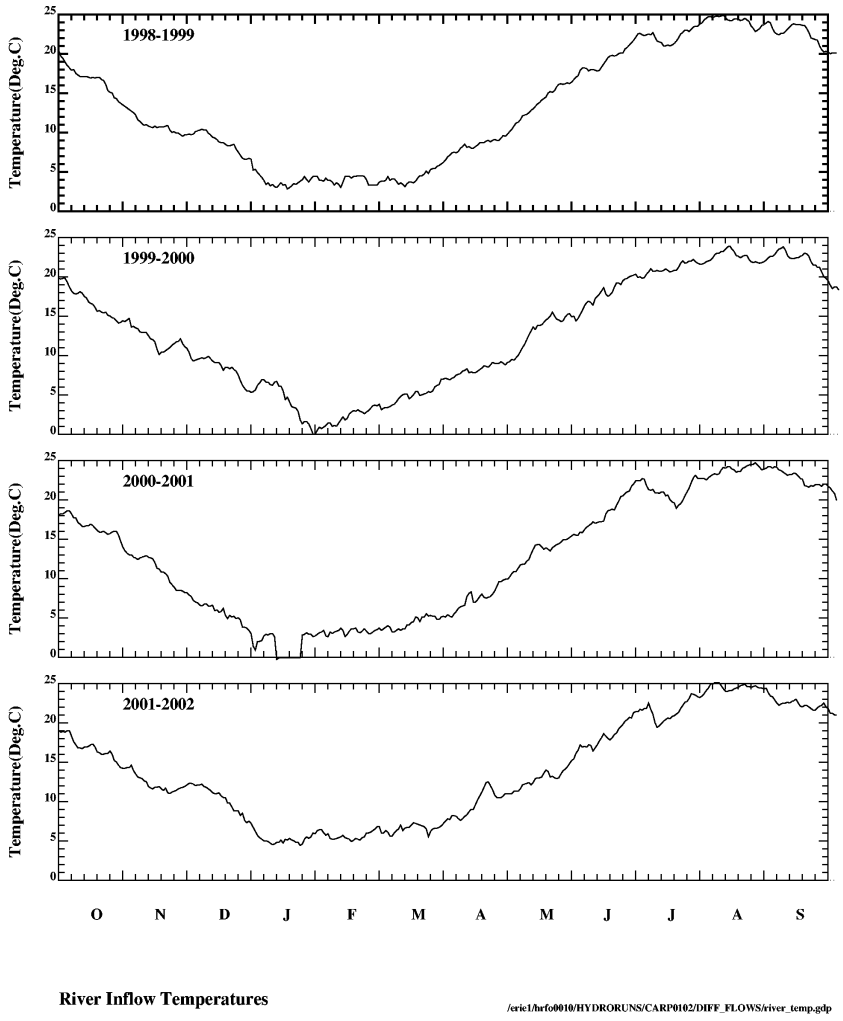

Figure 2-6. Temporal variation of river water temperature.

Figure 2-7 shows the monthly averaged flows of the Hudson River measured at Green Island for the four CARP water years. Table 2-3 lists the statistics of the Hudson River inflow for these years. Figure 2-7 and Table 2-3 indicate that water year 2000 is a relatively wet year and that 2002 is a relatively dry year.

Table 2-3. Monthly Average Flows (cms)
Hudson River, NY
(USGS 01358000 Hudson River at Green Island, NY)

	1998-1999	1999-2000	2000-2001	2001-2002
October	172.0	263.0	263.4	114.9
November	192.0	673.9	308.5	164.3
December	188.0	459.9	494.1	219.1
January	1104.8	471.6	291.4	169.1
February	473.0	2494.7	345.8	423.6
March	584.0	1397.3	412.3	545.8
April	594.0	1636.0	1400.9	690.0
May	218.0	1250.8	341.6	650.9
June	119.0	1094.2	457.4	482.9
July	146.0	310.0	195.8	151.8
August	88.0	389.0	104.8	112.7
September	1421.5	225.0	116.7	138.5
Maximum	1421.5	2494.7	1400.9	690.0
Minimum	88.0	225.0	104.8	112.7
Average	441.7	888.8	394.4	322.0

2.3.5 Wastewater Treatment Plants

The wastewater treatment plants included in the CARP model are shown in Figure 2-8. Their respective discharges, listed in Table 2-4, have been compiled from Discharge Monitoring Reports (DMRs) obtained by HydroQual through EPA's Permit Compliance System (PCS). Additional more detailed records available from NYCDEP were also used. In some cases, monthly flow records

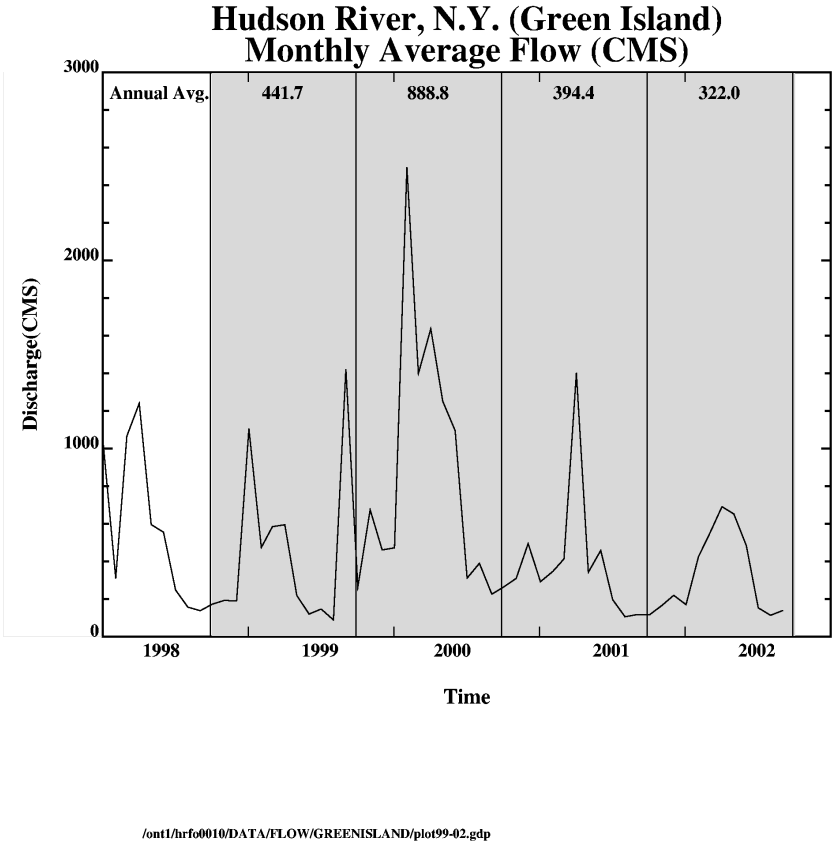

Figure 2-7. Comparison of Hudson River flow for the various CARP model years.

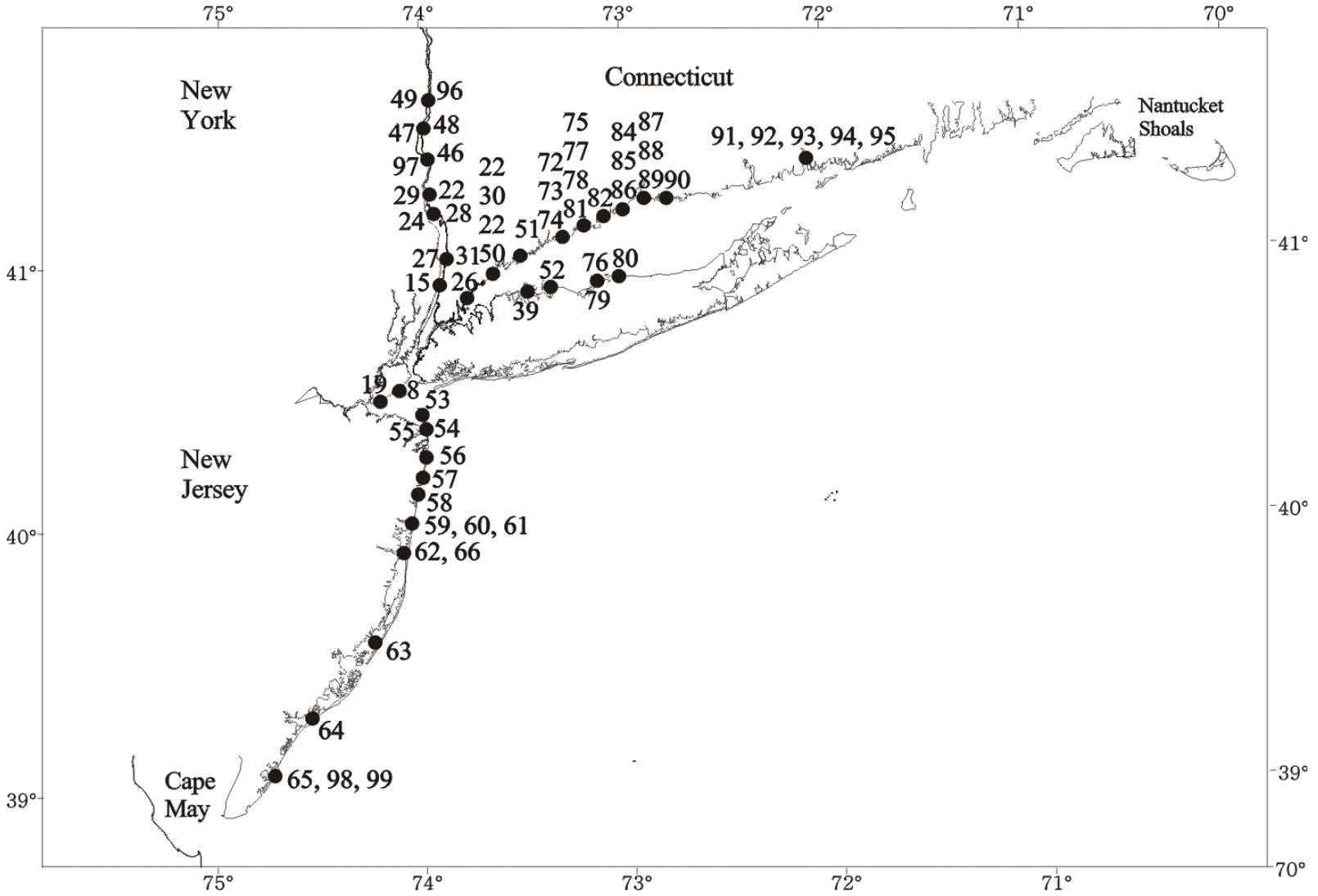

Figure 2-8a. Location map of wastewater treatment plants included in the CARP model Sound/Bight view. Facility identifications are included in Table 2-4.

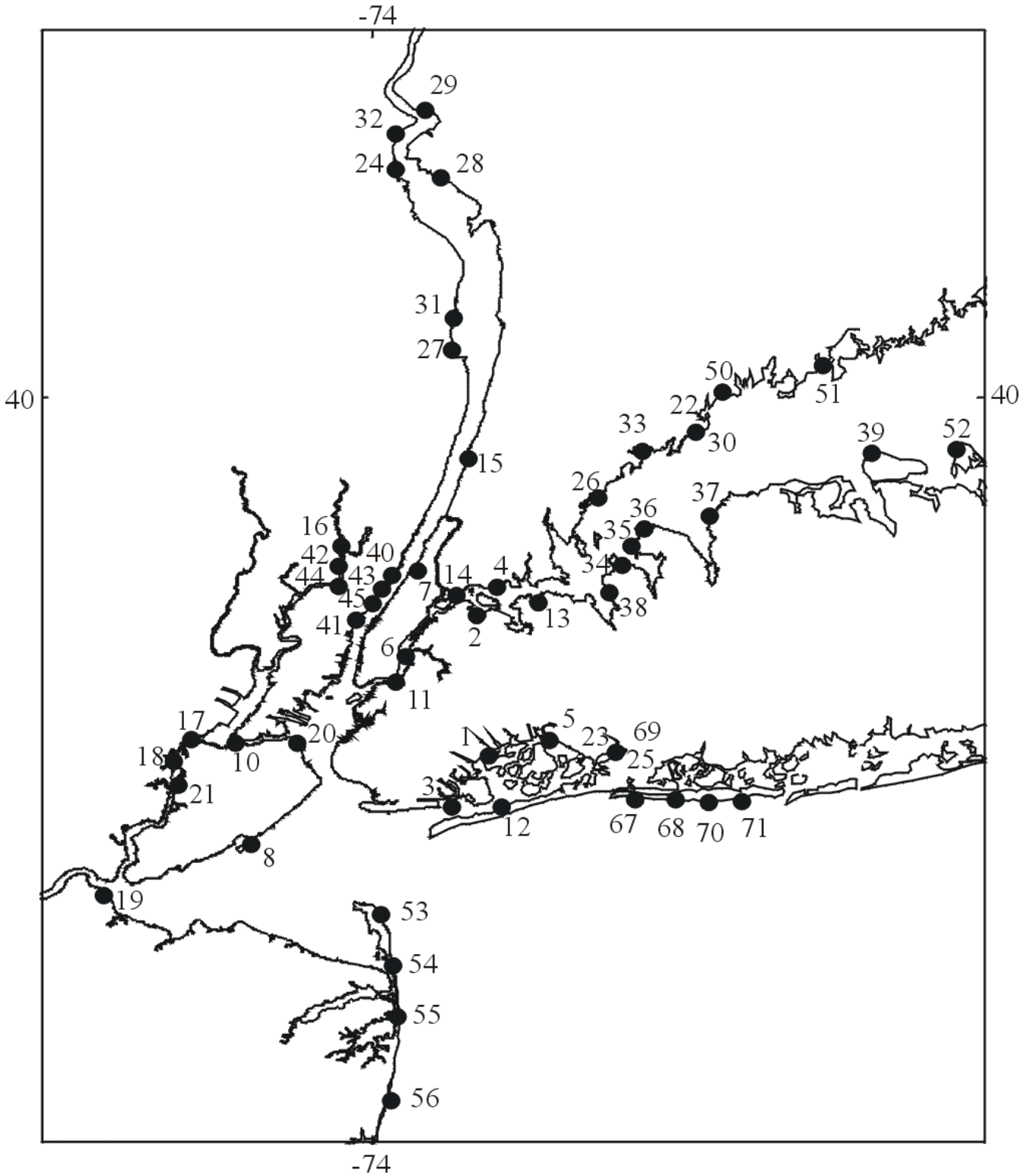

Figure 2-8b. Location map of wastewater treatment plants included in the CARP model - Harbor view. Facility identifications are included in Table 2-4.

Table 2-4. Sewage Treatment Plant Flow Statistics (cms)

		1998-1999			1999-2000			2000-2001			2001-2002		
Number	Facility	Max	Min	Mean	Max	Min	Mean	Max	Min	Mean	Max	Min	Mean
1	26th Ward	6.133	2.004	2.571	6.046	1.936	2.502	5.520	0.000	2.402	6.222	1.834	2.364
2	Bowery Bay	14.984	2.733	4.906	15.334	2.760	5.018	12.268	2.864	5.086	11.611	2.576	4.606
3	Coney Island	8.236	2.906	4.315	8.325	2.814	4.197	7.974	0.000	4.191	9.113	2.692	4.014
4	Hunts Point	12.705	3.071	5.187	12.268	2.988	5.105	9.201	2.933	4.882	15.334	2.600	4.508
5	Jamaica	8.762	2.161	3.525	8.762	2.190	3.580	7.448	0.000	3.708	8.149	1.962	3.213
6	Newtown Creek	28.014	7.231	10.161	27.163	6.871	9.831	24.097	7.463	10.498	27.163	7.100	10.008
7	North River	14.897	3.776	6.359	14.239	3.531	6.045	14.020	3.205	5.473	15.334	3.287	5.582
8	Oakwood Beach	3.768	0.975	1.308	3.505	0.975	1.317	3.505	0.000	1.308	3.505	0.975	1.303
9	Owls Head	10.734	2.797	4.897	10.778	2.666	4.749	10.384	2.666	4.702	10.515	2.507	4.430
10	Port Richmond	5.258	1.030	1.515	5.258	0.936	1.405	5.170	0.000	1.346	5.258	0.905	1.336
11	Red Hook	4.971	0.996	1.511	4.819	0.934	1.455	4.469	0.902	1.394	4.843	0.872	1.346
12	Rockaway	4.160	0.542	0.848	3.290	0.542	0.850	3.492	0.000	0.805	3.947	0.513	0.804
13	Tallman Island	5.476	1.449	2.392	5.696	1.420	2.366	5.476	1.557	2.555	5.520	1.336	2.229
14	Wards Island	23.220	5.067	8.779	23.659	4.753	8.349	21.030	4.596	8.033	20.811	4.436	7.750
15	Yonkers	3.505	3.154	3.312	3.505	3.154	3.312	3.505	3.154	3.312	3.505	3.154	3.312
16	Bergen County	3.254	2.542	2.905	3.254	2.542	2.906	3.254	2.542	2.905	3.254	2.542	2.905
17	Jnt Meeting Essex Union	2.900	2.163	2.523	2.900	2.163	2.523	2.900	2.163	2.523	2.900	2.163	2.523
18	Linden Roselle	0.633	0.464	0.535	0.633	0.464	0.536	0.633	0.464	0.535	0.633	0.464	0.535
19	Middlesex County	5.405	4.259	4.711	5.405	4.259	4.712	5.405	4.259	4.711	5.405	4.259	4.711
20	Passaic Valley	12.136	10.734	11.444	12.136	10.734	11.446	12.136	10.734	11.444	12.136	10.734	11.444
21	Rahway	1.264	0.998	1.100	1.264	0.998	1.101	1.264	0.998	1.100	1.264	0.998	1.100
22	Blind Brook	0.153	0.096	0.120	0.153	0.096	0.120	0.153	0.096	0.120	0.153	0.096	0.120
23	Cedarhurst	0.036	0.030	0.033	0.036	0.030	0.033	0.036	0.030	0.033	0.036	0.030	0.033
24	Haverstraw	0.240	0.143	0.184	0.240	0.143	0.184	0.240	0.143	0.184	0.240	0.143	0.184
25	Inwood	0.048	0.000	0.043	0.000	0.000	0.000	0.000	0.000	0.000	0.048	0.044	0.046
26	New Rochelle	0.670	0.499	0.588	0.670	0.499	0.589	0.670	0.499	0.588	0.670	0.499	0.588
27	Orangetown SD#2	0.535	0.302	0.439	0.535	0.302	0.439	0.535	0.302	0.439	0.535	0.302	0.439
28	Ossining	0.311	0.223	0.263	0.311	0.223	0.264	0.311	0.223	0.263	0.311	0.223	0.263
29	Peekskill	0.337	0.232	0.269	0.337	0.232	0.269	0.337	0.232	0.269	0.337	0.232	0.269
30	Port Chester	0.171	0.145	0.156	0.171	0.145	0.156	0.171	0.145	0.156	0.171	0.145	0.156
31	Rockland County SD#1	0.942	0.716	0.817	0.942	0.716	0.817	0.942	0.716	0.817	0.942	0.716	0.817
32	Stony Point	0.044	0.036	0.039	0.044	0.036	0.039	0.044	0.036	0.039	0.044	0.036	0.039
33	Mamaroneck	0.767	0.434	0.591	0.767	0.434	0.591	0.767	0.434	0.591	0.767	0.434	0.591
34	Great Neck Village	0.048	0.036	0.042	0.048	0.036	0.042	0.048	0.036	0.042	0.048	0.036	0.042
35	Great Neck SD	0.114	0.101	0.108	0.114	0.101	0.108	0.114	0.101	0.108	0.114	0.101	0.108
36	Port Washington	0.118	0.110	0.114	0.118	0.110	0.114	0.118	0.110	0.114	0.118	0.110	0.114
37	Glen Cove STP	0.201	0.185	0.193	0.201	0.185	0.193	0.201	0.185	0.193	0.201	0.185	0.193
38	Bel Grave	0.060	0.055	0.057	0.060	0.055	0.057	0.060	0.055	0.057	0.060	0.055	0.057
39	Oyster Bay	0.052	0.037	0.044	0.052	0.037	0.044	0.052	0.037	0.044	0.052	0.037	0.044
40	Edgewater	0.166	0.107	0.130	0.166	0.107	0.130	0.166	0.107	0.130	0.166	0.107	0.130

Table 2-4. Sewage Treatment Plant Flow Statistics (cms) (Cont.)

		1998-1999			1999-2000			2000-2001			2001-2002		
Number	Facility	Max	Min	Mean	Max	Min	Mean	Max	Min	Mean	Max	Min	Mean
41	Hoboken	0.521	0.428	0.473	0.521	0.428	0.473	0.521	0.428	0.473	0.521	0.428	0.473
42	North Bergen Central	0.309	0.236	0.264	0.309	0.236	0.264	0.309	0.236	0.264	0.309	0.236	0.264
43	North Bergen Woodcliff	0.118	0.101	0.110	0.118	0.101	0.110	0.118	0.101	0.110	0.118	0.101	0.110
44	Secaucus	0.144	0.125	0.134	0.144	0.125	0.134	0.144	0.125	0.134	0.144	0.125	0.134
45	West New York	0.456	0.291	0.394	0.456	0.291	0.394	0.456	0.291	0.394	0.456	0.291	0.394
46	USMA-West Point	0.088	0.068	0.077	0.088	0.068	0.077	0.088	0.068	0.077	0.088	0.068	0.077
47	Town of Cornwall	0.057	0.026	0.037	0.057	0.026	0.037	0.057	0.026	0.037	0.057	0.026	0.037
48	City of Newburgh	0.346	0.241	0.278	0.346	0.241	0.278	0.346	0.241	0.278	0.346	0.241	0.278
49	City of Poughkeepsie	0.403	0.241	0.300	0.403	0.241	0.300	0.403	0.241	0.300	0.403	0.241	0.300
50	Greenwich CT STP	0.421	0.260	0.332	0.421	0.260	0.332	0.421	0.260	0.332	0.421	0.260	0.332
51	Stamford CT	0.675	0.482	0.588	0.675	0.482	0.588	0.675	0.482	0.588	0.675	0.482	0.588
52	Huntington NY	0.079	0.060	0.070	0.079	0.060	0.070	0.079	0.060	0.070	0.079	0.060	0.070
53	Bayshore Region SA	0.390	0.323	0.354	0.390	0.323	0.354	0.390	0.323	0.354	0.390	0.323	0.354
54	Monmouth County Baysh	0.728	0.613	0.673	0.728	0.613	0.673	0.728	0.613	0.673	0.728	0.613	0.673
55	NE Monmouth SA	0.464	0.416	0.444	0.464	0.416	0.444	0.464	0.416	0.444	0.464	0.416	0.444
56	Long Branch SA	0.212	0.121	0.174	0.212	0.121	0.174	0.212	0.121	0.174	0.212	0.121	0.174
57	Ocean Township SA	0.236	0.176	0.206	0.236	0.176	0.206	0.236	0.176	0.206	0.236	0.176	0.206
58	Asbury Park	0.134	0.113	0.124	0.134	0.113	0.124	0.134	0.113	0.124	0.134	0.113	0.124
59	Neptune Township SA	0.276	0.184	0.214	0.276	0.184	0.213	0.276	0.184	0.214	0.276	0.184	0.214
60	S. Monmouth Regional SA	0.236	0.158	0.195	0.236	0.158	0.195	0.236	0.158	0.195	0.236	0.158	0.195
61	Ocean County UA Northe	0.899	0.831	0.867	0.899	0.831	0.867	0.899	0.831	0.867	0.899	0.831	0.867
62	Ocean County UA - Cent	1.008	0.832	0.895	1.008	0.832	0.895	1.008	0.832	0.895	1.008	0.832	0.895
63	Ocean County UA - Sout	0.407	0.210	0.272	0.407	0.210	0.272	0.407	0.210	0.272	0.407	0.210	0.272
64	Atlantic County UA	0.418	0.318	0.365	0.418	0.318	0.365	0.418	0.318	0.365	0.418	0.318	0.365
65	Cape May - Wildwood	0.524	0.232	0.314	0.524	0.232	0.314	0.524	0.232	0.314	0.524	0.232	0.314
66	Ciba-Geigy	0.000	0.000	0.000	0.000	0.000	0.000	0.000	0.000	0.000	0.000	0.000	0.000
67	Long Beach	0.321	0.230	0.265	0.321	0.230	0.265	0.321	0.230	0.265	0.321	0.230	0.265
68	Bay Park	2.607	2.169	2.376	2.607	2.169	2.390	2.607	2.169	2.391	2.559	2.125	2.345
69	Lawrence	0.055	0.049	0.052	0.055	0.049	0.052	0.055	0.049	0.052	0.055	0.049	0.052
70	Suffolk County Swer Dis	0.911	0.846	0.881	0.911	0.846	0.881	0.911	0.846	0.881	0.911	0.846	0.881
71	Cedar Creek	2.572	2.239	2.382	2.572	2.239	2.382	2.572	2.239	2.382	2.572	2.239	2.382
72	New Canaan STP	0.074	0.034	0.052	0.074	0.034	0.052	0.074	0.034	0.052	0.074	0.034	0.052
73	Norwalk WPCF	0.736	0.491	0.588	0.736	0.491	0.588	0.736	0.491	0.588	0.736	0.491	0.588
74	Westport WPCF	0.080	0.057	0.066	0.080	0.057	0.066	0.080	0.057	0.066	0.080	0.057	0.066
75	Fairfield Taown Hall	0.399	0.272	0.329	0.399	0.272	0.329	0.399	0.272	0.329	0.399	0.272	0.329
76	Kings Park SCSD#6	0.031	0.023	0.027	0.031	0.023	0.027	0.031	0.023	0.027	0.031	0.023	0.027
77	Bridgeport Westside	1.205	0.857	0.972	1.205	0.857	0.972	1.205	0.857	0.972	1.205	0.857	0.972
78	Bridgeport Eastside	0.321	0.249	0.294	0.321	0.249	0.295	0.321	0.249	0.294	0.321	0.249	0.294
79	Stonybrook SCSD#21	0.109	0.077	0.094	0.109	0.077	0.094	0.109	0.077	0.094	0.109	0.077	0.094
80	Port Jefferson SCSD#1	0.035	0.023	0.031	0.035	0.023	0.031	0.035	0.023	0.031	0.035	0.023	0.031
81	Stratford WPCF	0.514	0.317	0.402	0.514	0.317	0.402	0.514	0.317	0.402	0.514	0.317	0.402
82	Milford-Beaver Brook	0.092	0.066	0.080	0.092	0.066	0.080	0.092	0.066	0.080	0.092	0.066	0.080

Table 2-4. Sewage Treatment Plant Flow Statistics (cms) (Cont.)

		1998-1999			1999-2000			2000-2001			2001-2002		
Number	Facility	Max	Min	Mean	Max	Min	Mean	Max	Min	Mean	Max	Min	Mean
83	Derby WPCF	0.098	0.066	0.078	0.098	0.066	0.078	0.098	0.066	0.078	0.098	0.066	0.078
84	Shelton WPCF	0.114	0.081	0.094	0.114	0.081	0.094	0.114	0.081	0.094	0.114	0.081	0.094
85	Ansonia WPCF	0.129	0.068	0.091	0.129	0.068	0.091	0.129	0.068	0.091	0.129	0.068	0.091
86	Seymour WPCF	0.063	0.039	0.049	0.063	0.039	0.049	0.063	0.039	0.049	0.063	0.039	0.049
87	West Haven	0.372	0.258	0.313	0.372	0.258	0.313	0.372	0.258	0.313	0.372	0.258	0.313
88	East Shore	1.525	1.296	1.402	1.525	1.296	1.403	1.525	1.296	1.402	1.525	1.296	1.402
89	North Haven	0.184	0.110	0.137	0.184	0.110	0.137	0.184	0.110	0.137	0.184	0.110	0.137
90	Branford	0.188	0.155	0.170	0.188	0.155	0.170	0.188	0.155	0.170	0.188	0.155	0.170
91	New London	0.447	0.267	0.344	0.447	0.267	0.344	0.447	0.267	0.344	0.447	0.267	0.344
92	Groton City	0.161	0.128	0.146	0.161	0.128	0.146	0.161	0.128	0.146	0.161	0.128	0.146
93	Groton Town	0.022	0.003	0.012	0.022	0.003	0.012	0.022	0.003	0.012	0.022	0.003	0.012
94	Montville	0.079	0.042	0.057	0.079	0.042	0.057	0.079	0.042	0.057	0.079	0.042	0.057
95	Norwich	0.342	0.127	0.223	0.342	0.127	0.224	0.342	0.127	0.223	0.342	0.127	0.223
96	Arlington	0.166	0.118	0.135	0.166	0.118	0.135	0.166	0.118	0.135	0.166	0.118	0.135
97	Highland Falls	0.038	0.021	0.027	0.038	0.021	0.027	0.038	0.021	0.027	0.038	0.021	0.027
98	Cape May - Cape May	0.083	0.040	0.055	0.083	0.040	0.055	0.083	0.040	0.055	0.083	0.040	0.055
99	Cape May - Ocean City	0.252	0.102	0.149	0.252	0.102	0.149	0.252	0.102	0.149	0.252	0.102	0.149

retrieved previously for the 1994-95 water year were used for all CARP years. In other cases, hourly records for the CARP years were readily available. Table 2-4 shows maximum, minimum, and mean flows in cms at each facility on an hourly to monthly basis for each of the four CARP water years. Flows for any of the facilities may be updated at a later date if the CARP model is to be used for regulatory purposes.

Representative monthly mean temperatures of the wastewater treatment plant effluents were obtained from NYCDEP. Figure 2-9 shows the temporal variation of temperature of wastewater from wastewater treatment plants. The maximum, minimum and mean temperatures are 23.0, 14.0 and 18.61˚C, respectively.

2.3.6 Combined Sewer Overflows and Stormwater Runoff

Fresh water flow inputs due to combined sewer overflows and stormwater runoff were calculated by HydroQual using previously calibrated models of the CARP model drainage area and sewer system. The landside models include a hybrid of two modeling packages, the Storm Water Management Model (SWMM) and the Rainfall Runoff Modeling Program (RRMP). These models are driven by rainfall records to generate CSO and stormwater volumes. Hourly rainfall data from regional airports or from local rain gauges installed in the drainage area were used as input. The resulting outflows were distributed throughout the CARP model domain at 318 locations. Figure 2-10 shows the highly variable (i.e. rainfall dependent) total flow from combined sewer overflows and stormwater runoff as an increment to the relatively constant wastewater treatment flows. As indicated for some locations, CSOs and stormwater runoff can result in relatively high total flows over the simulation period. The temperature assigned to CSOs is somewhat cooler than that of wastewater treatment plant effluents as shown on Figure 2-9. The temperature of runoff is taken to equal the temperature of the river water as shown previously in Figure 2-6.

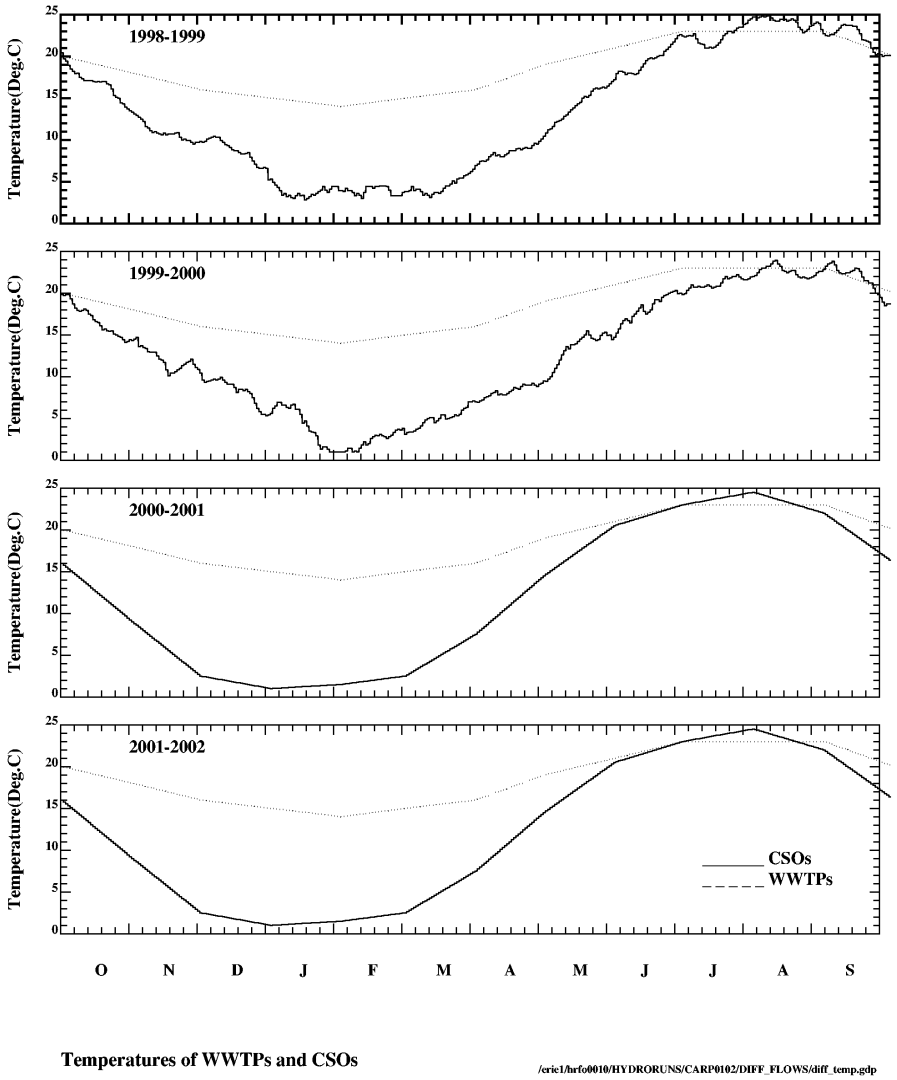

Figure 2-9. Temporal profile of modeled effluent temperature.

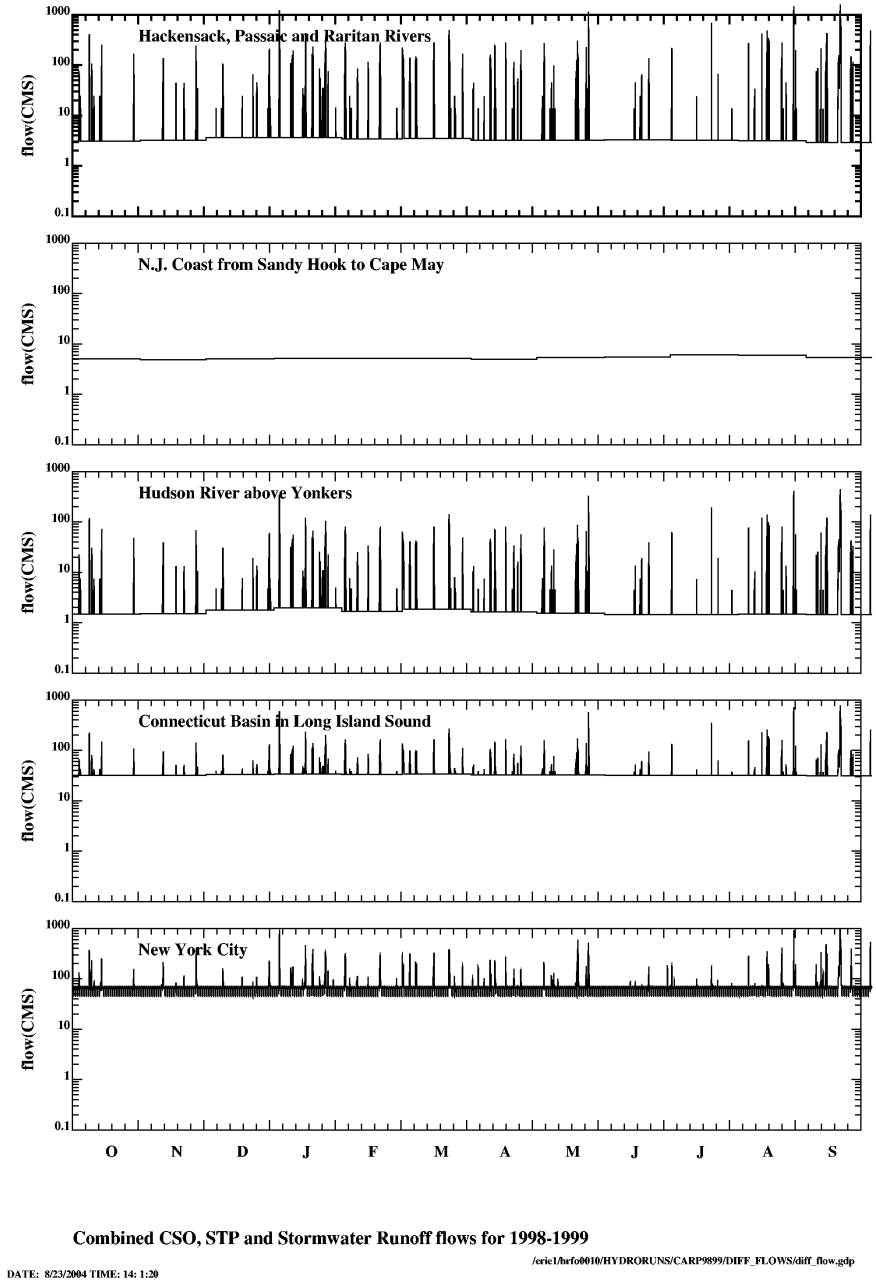

Figure 2-10a. Temporal profiles of various freshwater inputs (i.e., wastewater, CSO, and stormwater) for 1998-99 on a regional basis.

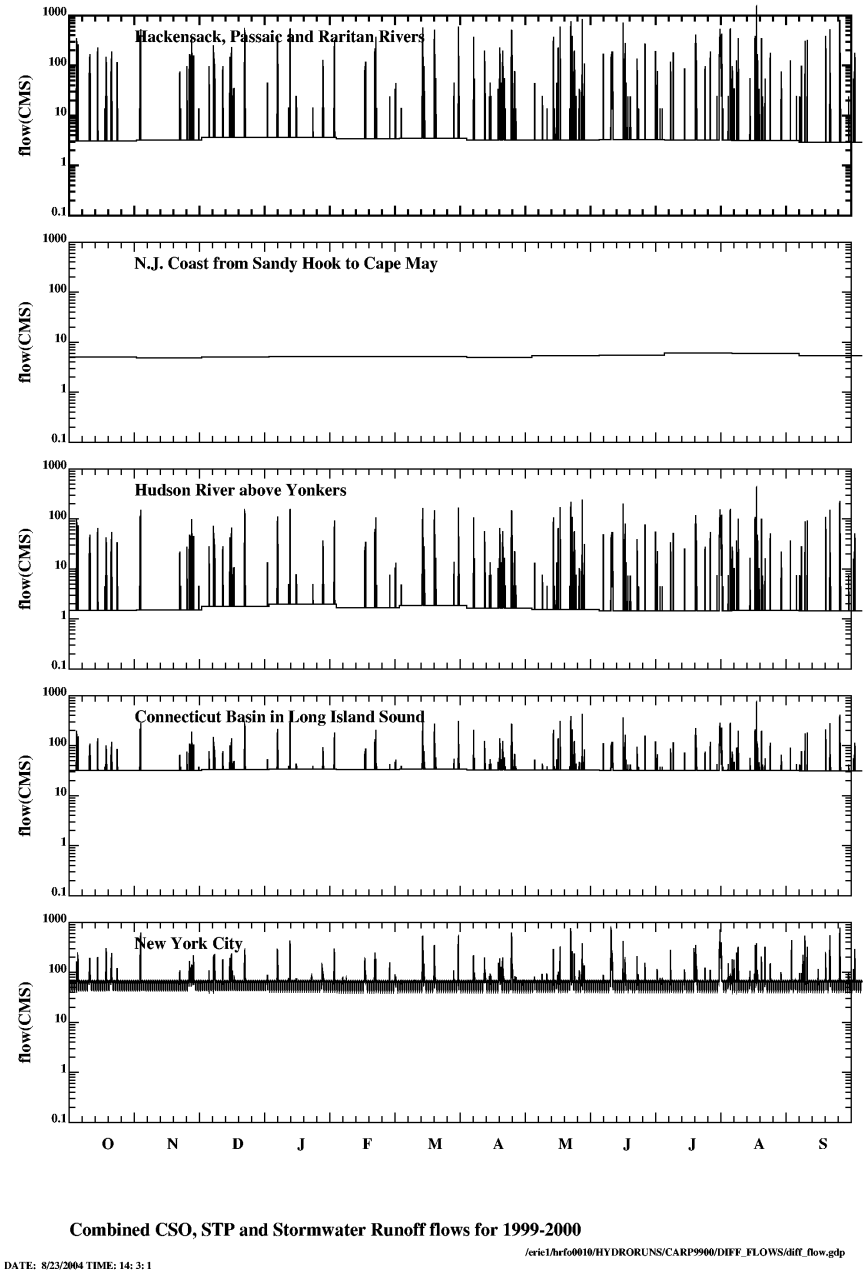

Figure 2-10b. Temporal profiles of various freshwater inputs (i.e., wastewater, CSO, and stormwater) for 1999-2000 on a regional basis.

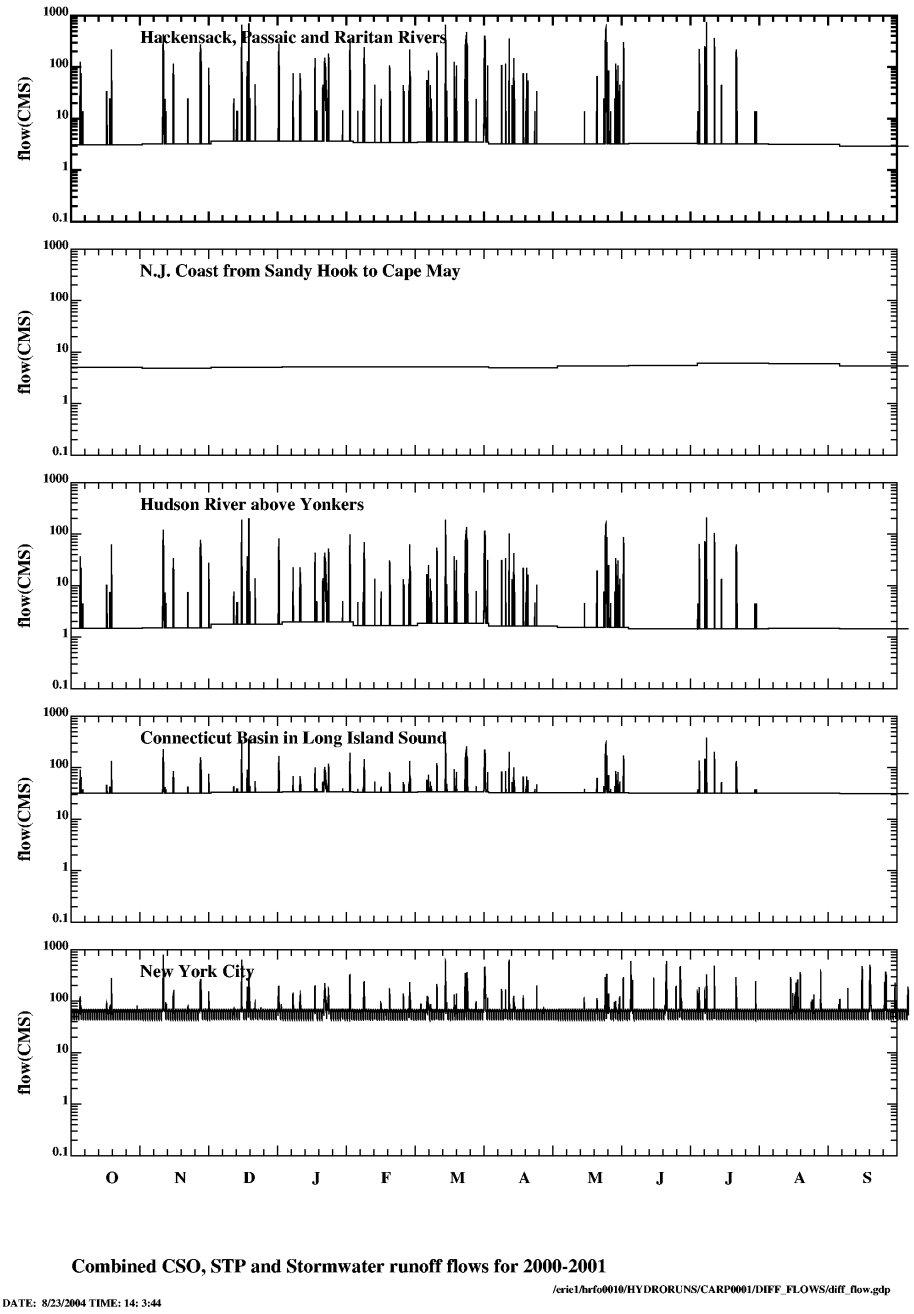

Figure 2-10c. Temporal profiles of various freshwater inputs (i.e., wastewater, CSO, and stormwater) for 2000-2001 on a regional basis.

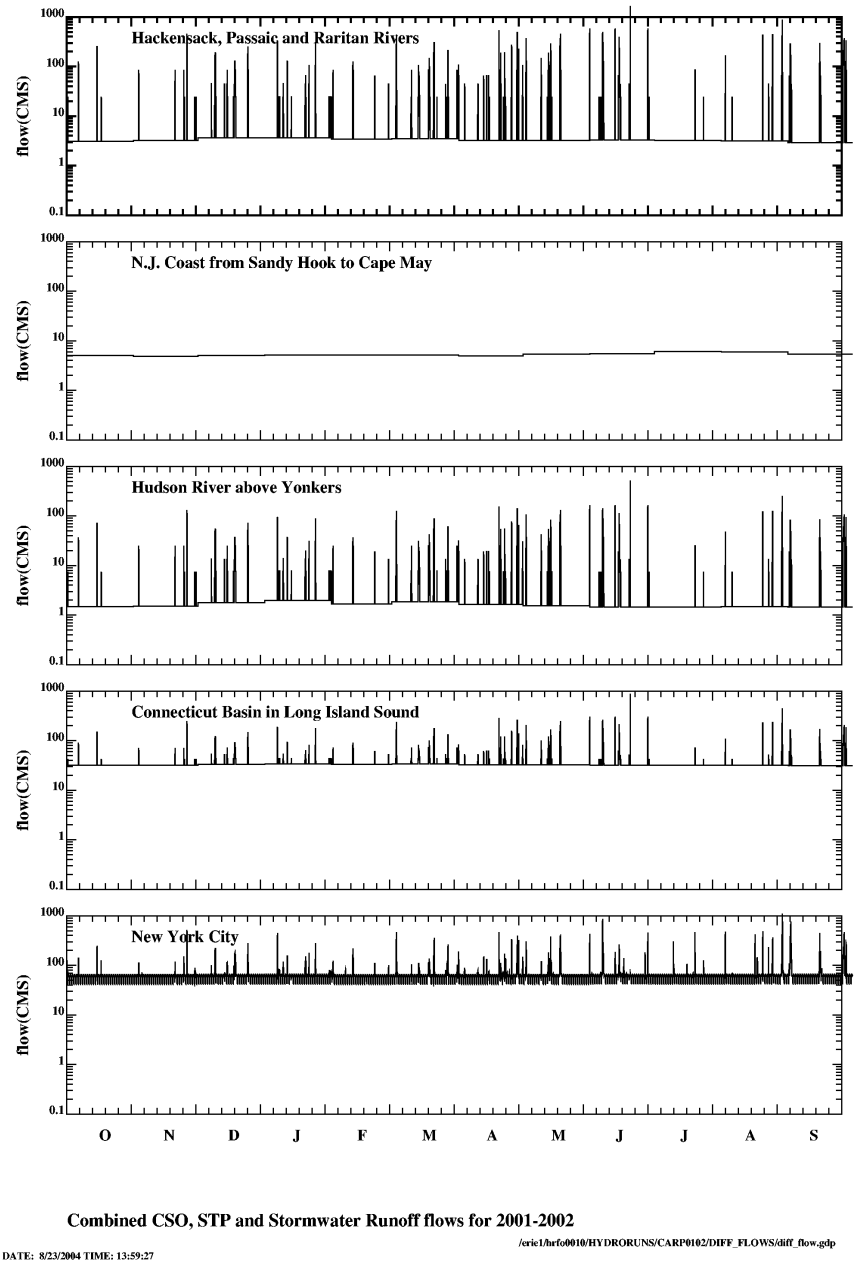

Figure 2-10d. Temporal profiles of various freshwater inputs (i.e., wastewater, CSO, and stormwater) for 2001-2002 on a regional basis.

SECTION 3.0

CARP HYDRODYNAMIC MODEL SKILL ASSESSMENT

The calibration and validation of the CARP hydrodynamic sub-model was completed previously as part of a separate project and is described extensively elsewhere (HydroQual, 1999c, 1999d, and 2002). This report section will focus strictly on the performance of the CARP hydrodynamic sub-model during its application to the CARP modeling period. The skill assessment of the CARP hydrodynamic sub-model involved model and data comparisons for several physical oceanographic parameters (i.e., water level; velocity currents and bottom temperature and salinity; and velocity currents, temperature and salinity over depth) measured by CARP over a two year period from November 2000 through November 2002. The skill assessment also includes model and data comparisons for oceanographic parameters measured routinely between October 1998 and September 2002 by other agencies such as NOAA, NYCDEP, Meadowlands Ecology Research Institute (MERI), Passaic Valley Sewerage Commissioners (PVSC), and CTDEP. The parameters used for the skill assessment are described below and the ability of the model to capture the features of the measured data sets are also discussed.

3.1 SKILL ASSESSMENT USING CARP HYDRODYNAMIC DATA

CARP hydrodynamic sampling locations are shown on Figure 3-1. Also shown on Figure 3-1 are the periods of record for each of the five stations for bottom pressure, temperature, salinity, and ADCP measurements. As described below, a series of summary format (i.e., condensed x-axis time series scale) plots have been developed which show CARP model calculations and CARP data comparisons. Also developed are a more detailed, expanded x-axis scale version of these comparison plots which are presented in Appendix 3.

Figures 3-2a and 3-2b show the model calculated (blue lines) and measured data (red lines) comparisons for water elevations. Figures 3-3a and 3-3b show the model calculated temperature in near surface and near bottom waters (blue lines) and measured near bottom temperature (red lines). Figures 3-4a and 3-4b show analogous comparisons for calculated and observed salinity. Figures 3-5 through 3-9 show model calculated (blue lines) and measured (red lines) velocity at three depths for each of the five stations. A more detailed, expanded x-axis scale presentation of these model and data comparisons is found in Appendix 3.

Overall the comparisons between model calculations and observed data presented in Figures 3-2 through 3-9 and Appendix 3 are very good. Some instances of disagreement, particularly the model

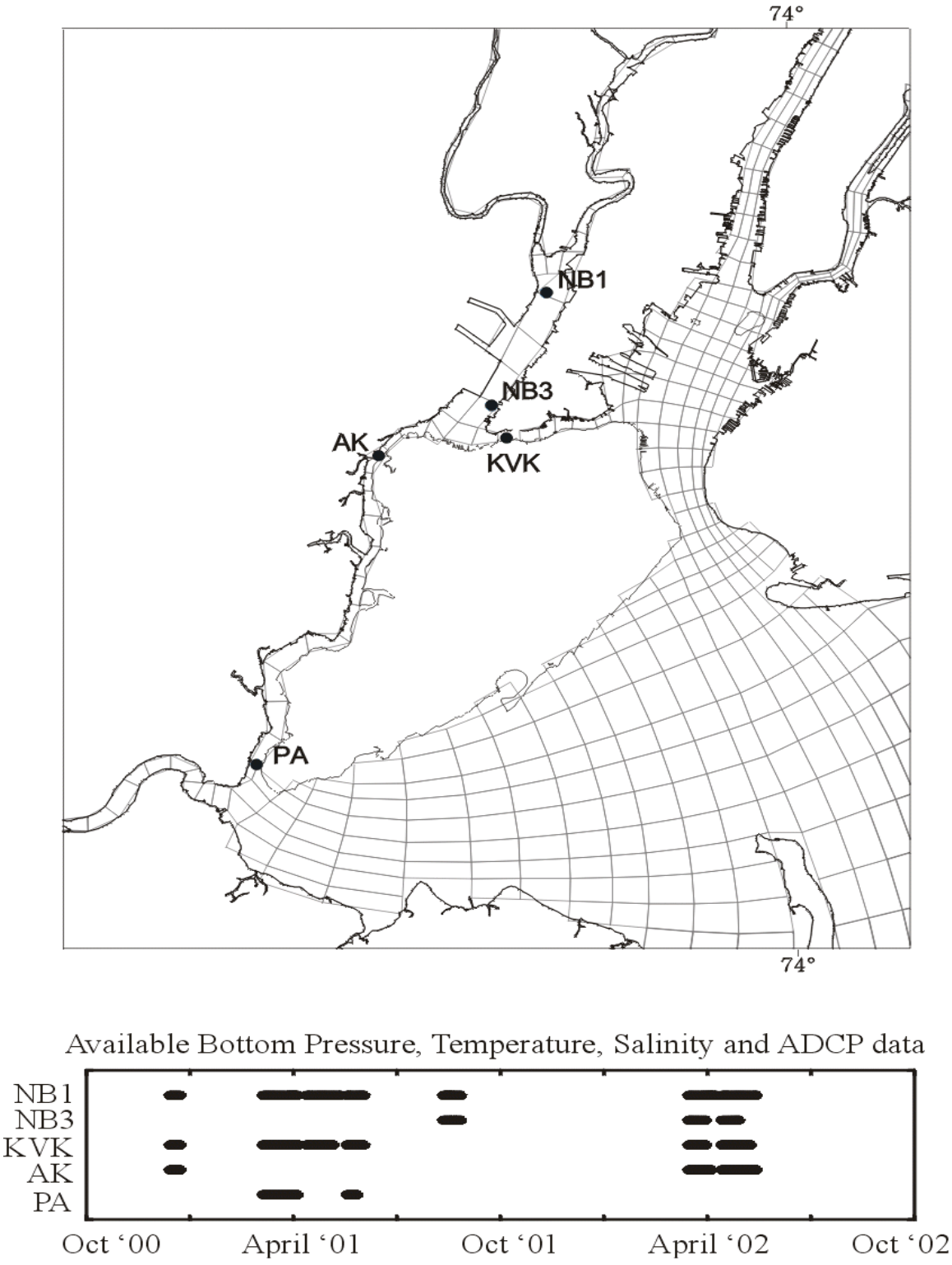

Figure 3-1. CARP hydrodynamic sampling locations and sampling periods.

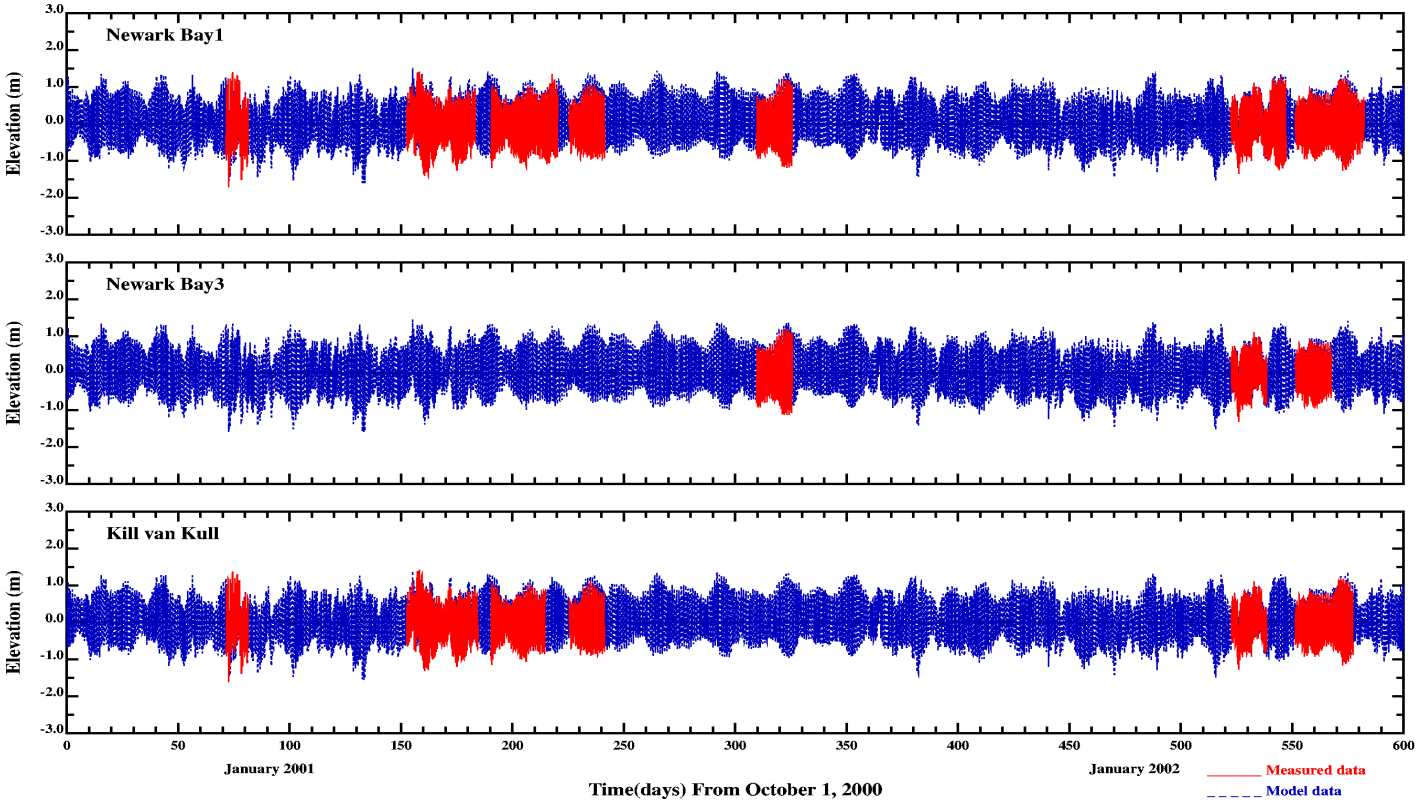

Figure 3-2a. Model and data comparisons for water elevations.

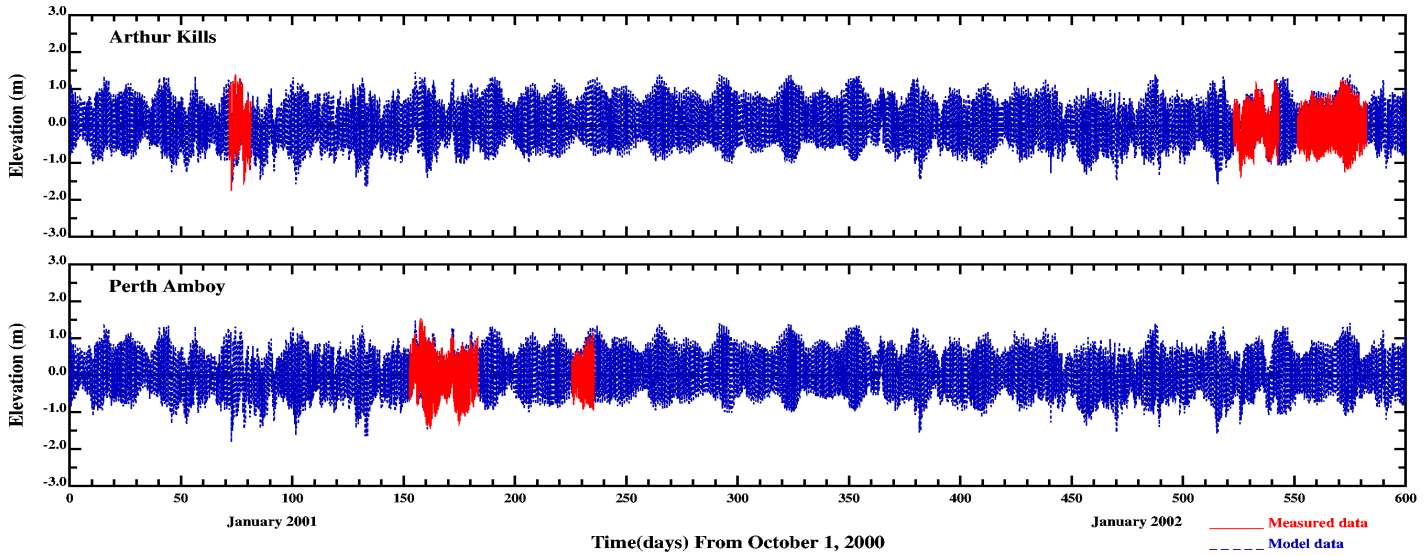

Figure 3-2b. Model and data comparisons for water elevations.

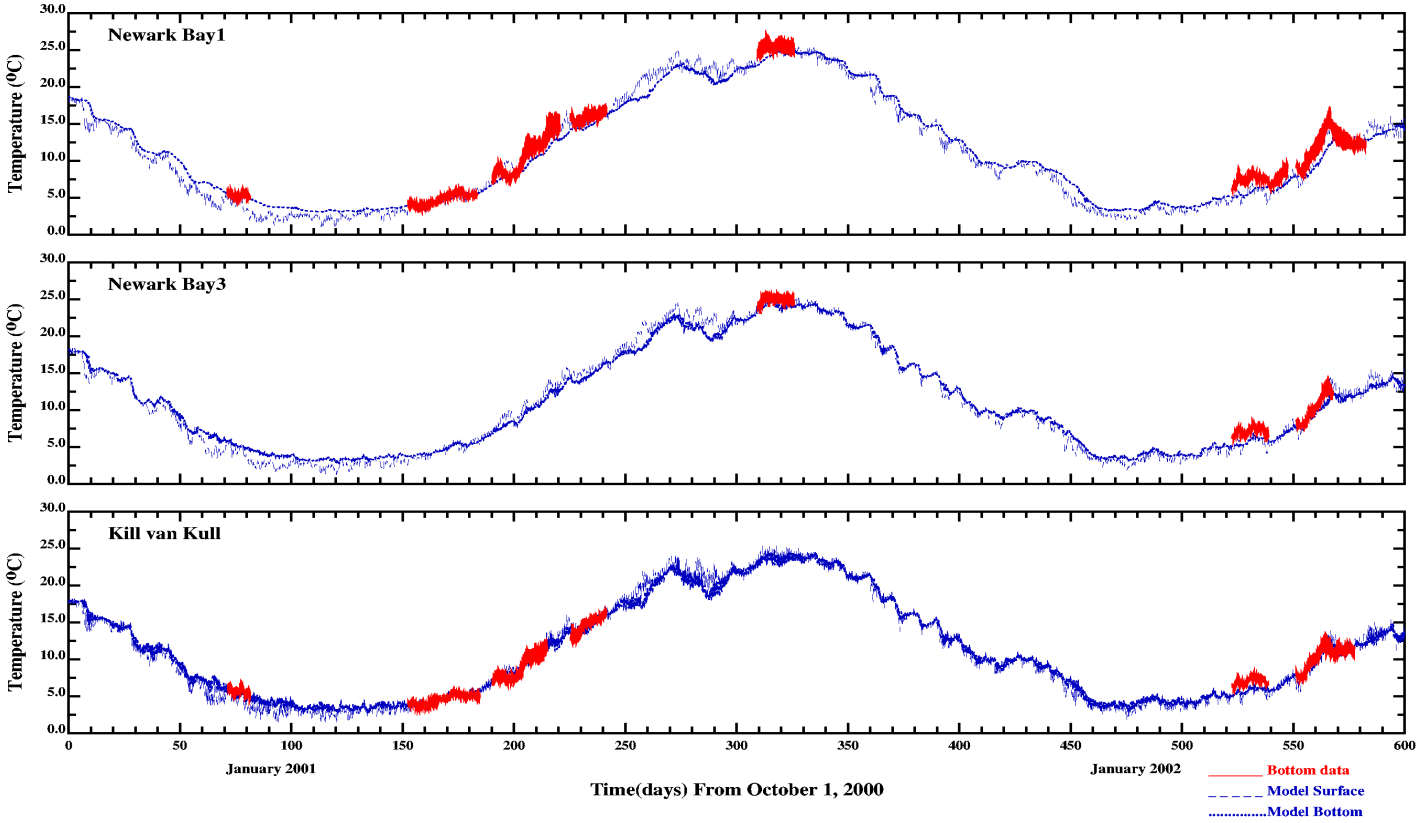

Figure 3-3a. Model and data comparisons for temperature.

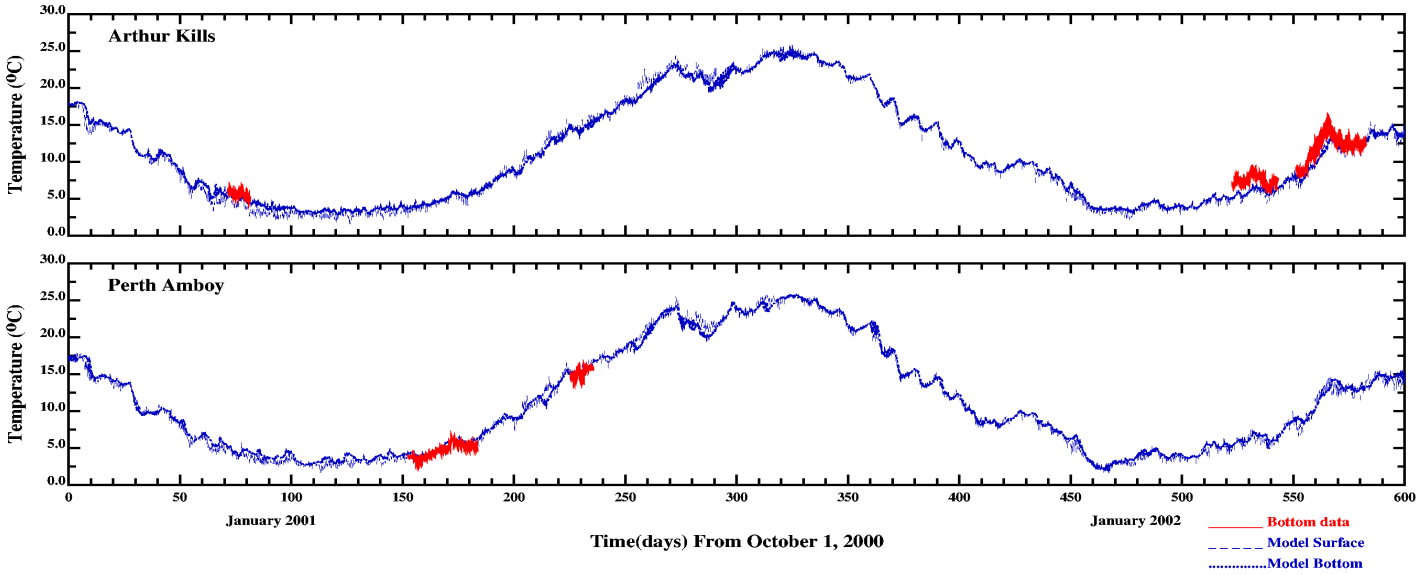

Figure 3-3b. Model and data comparisons for temperature.

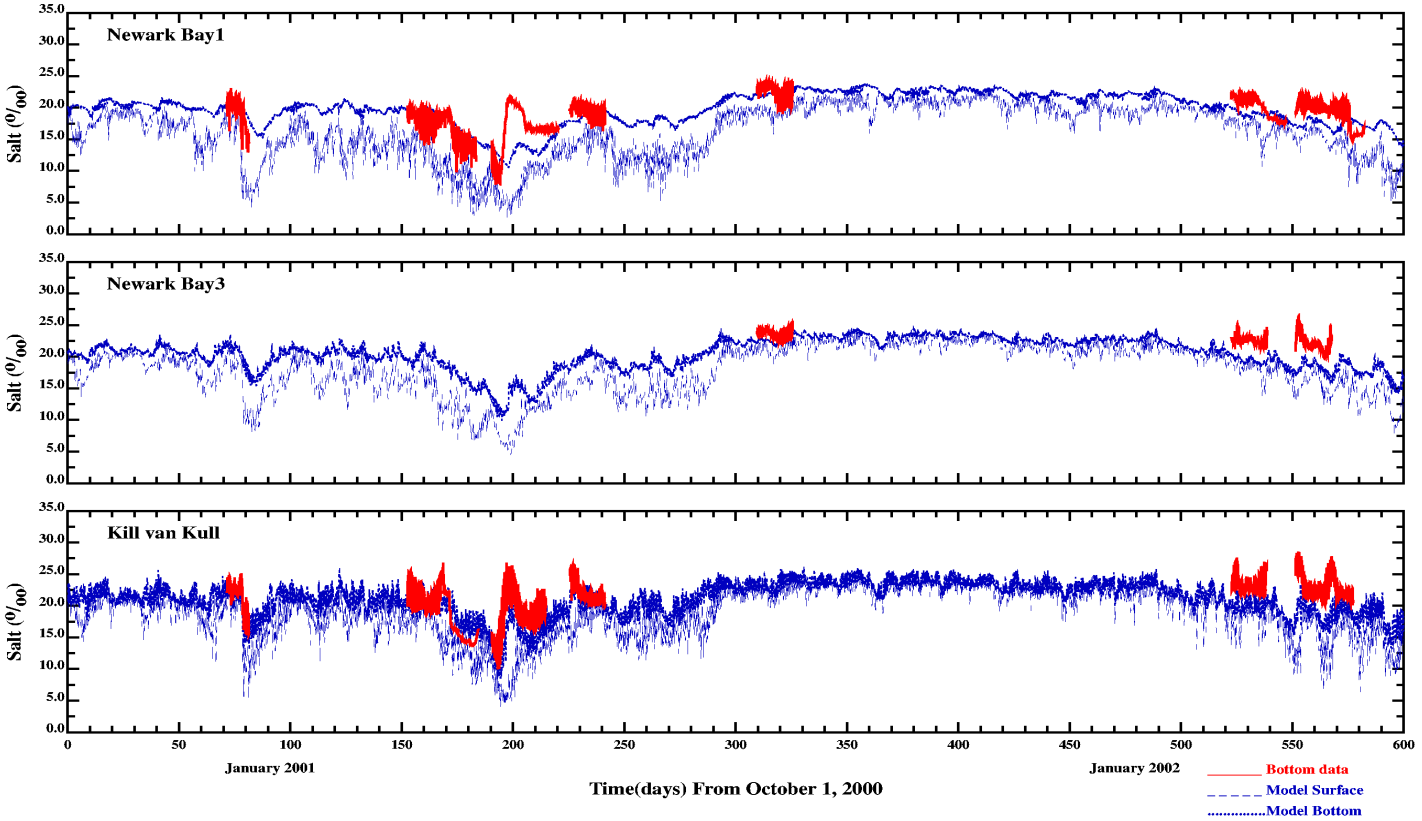

Figure 3-4a. Model and data comparisons for salinity.

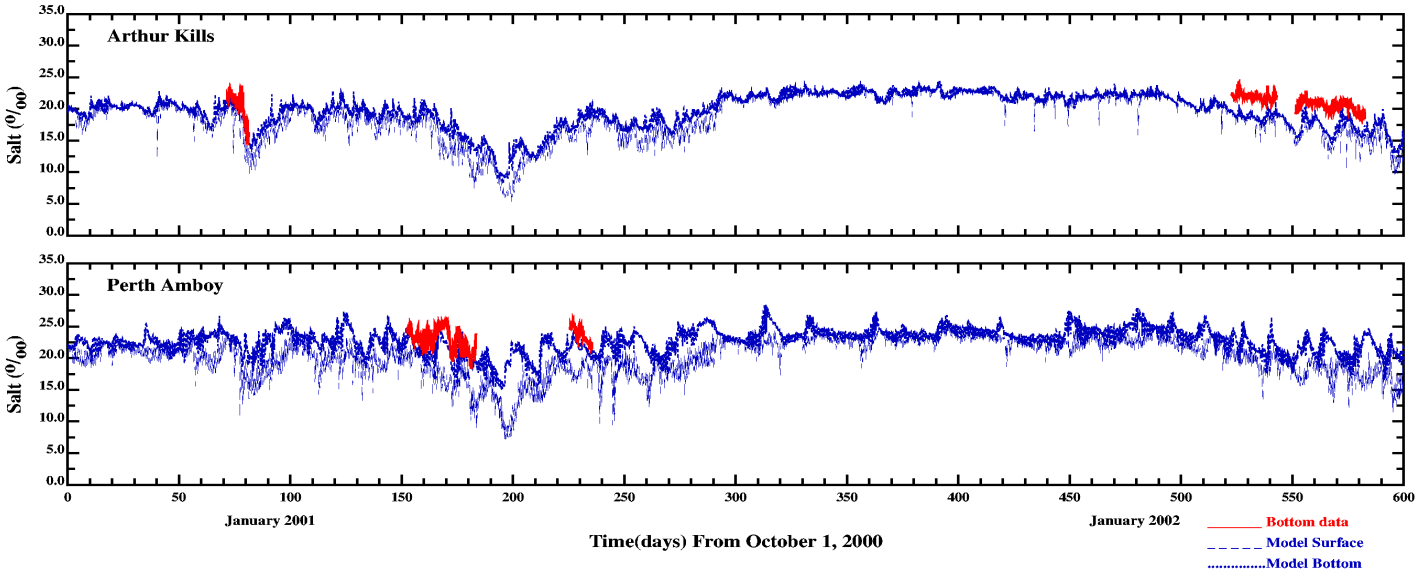

Figure 3-4b. Model and data comparisons for salinty.

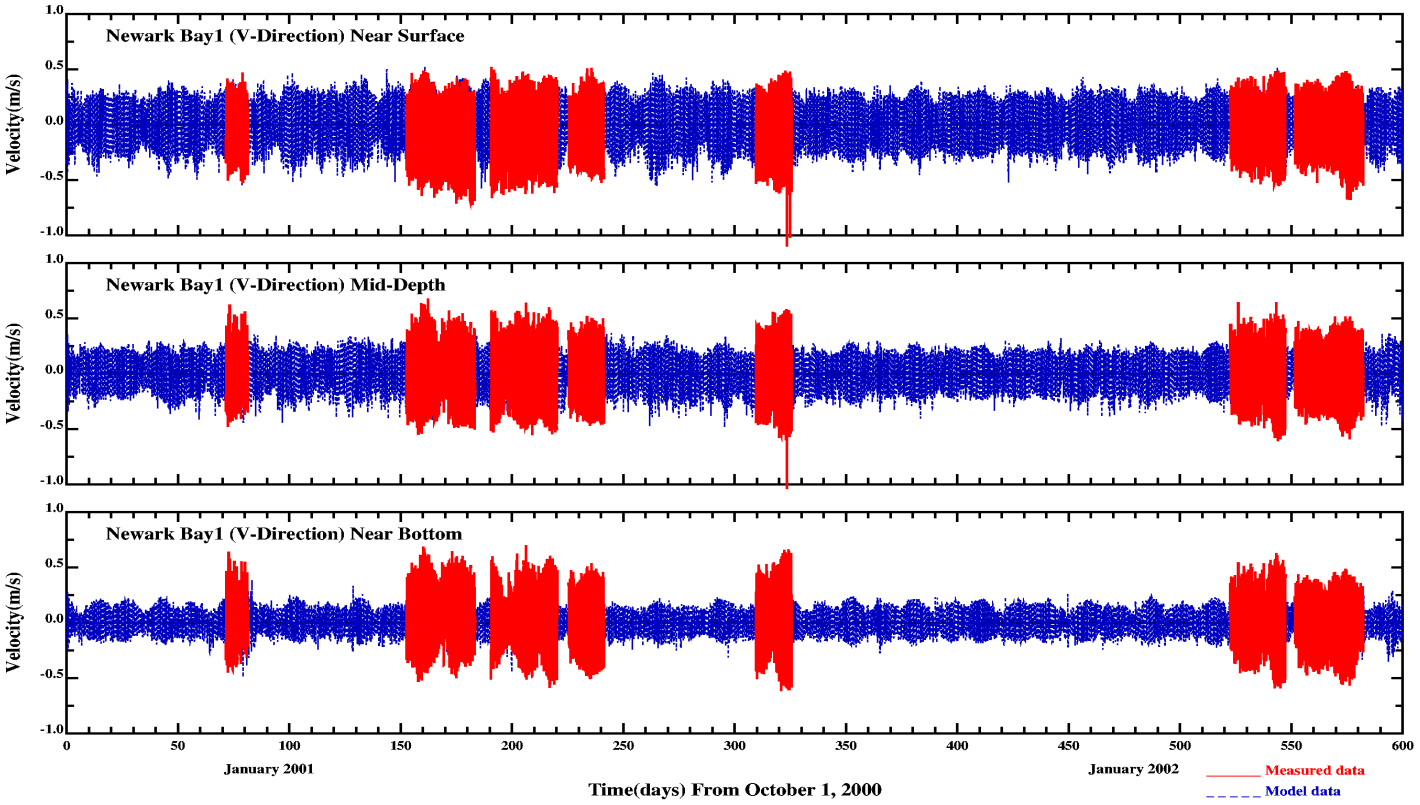

Figure 3-5. Model and data comparisons for velocity, Newark Bay Station 1.

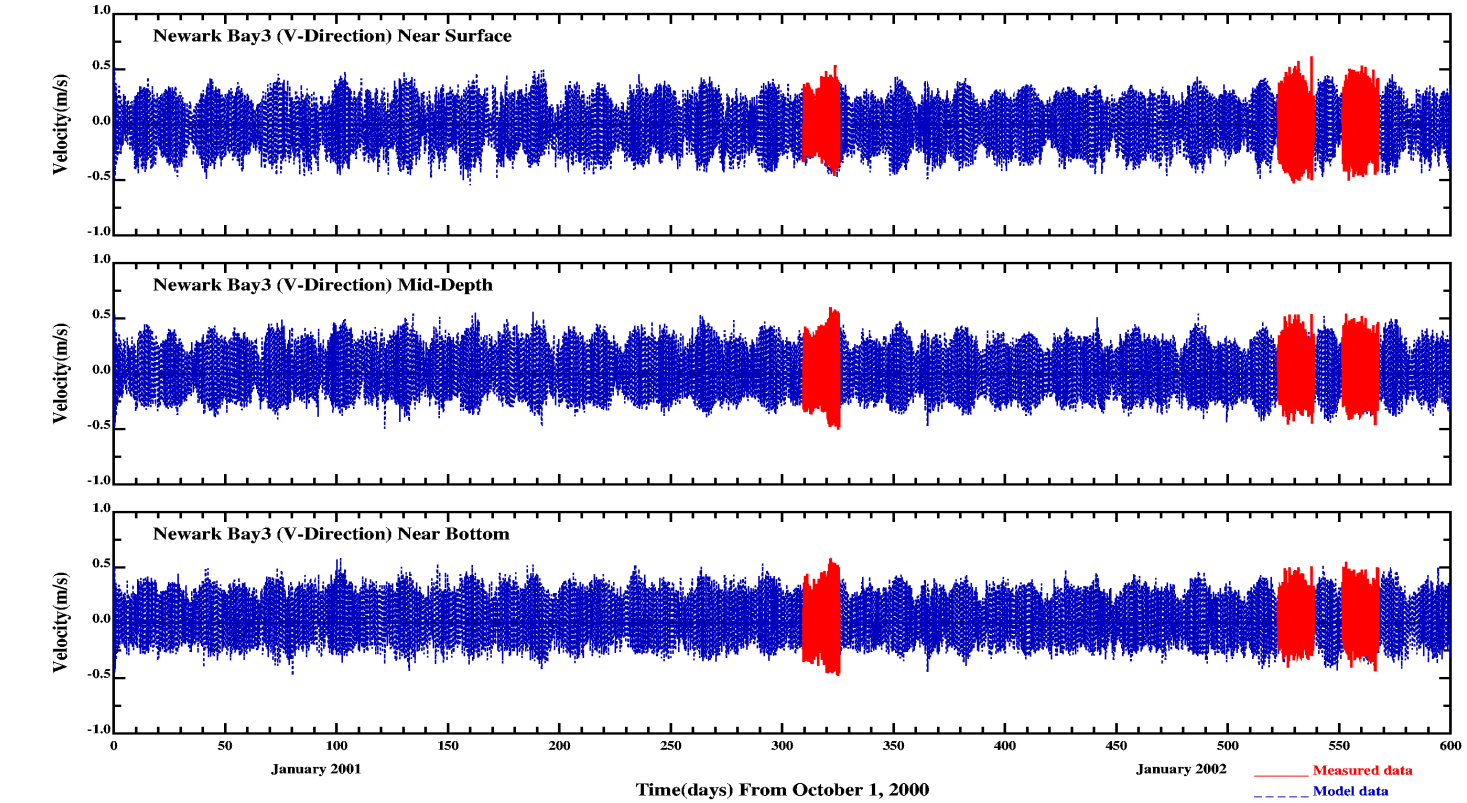

Figure 3-6. Model and data comparisons for velocity, Newark Bay Station 3.

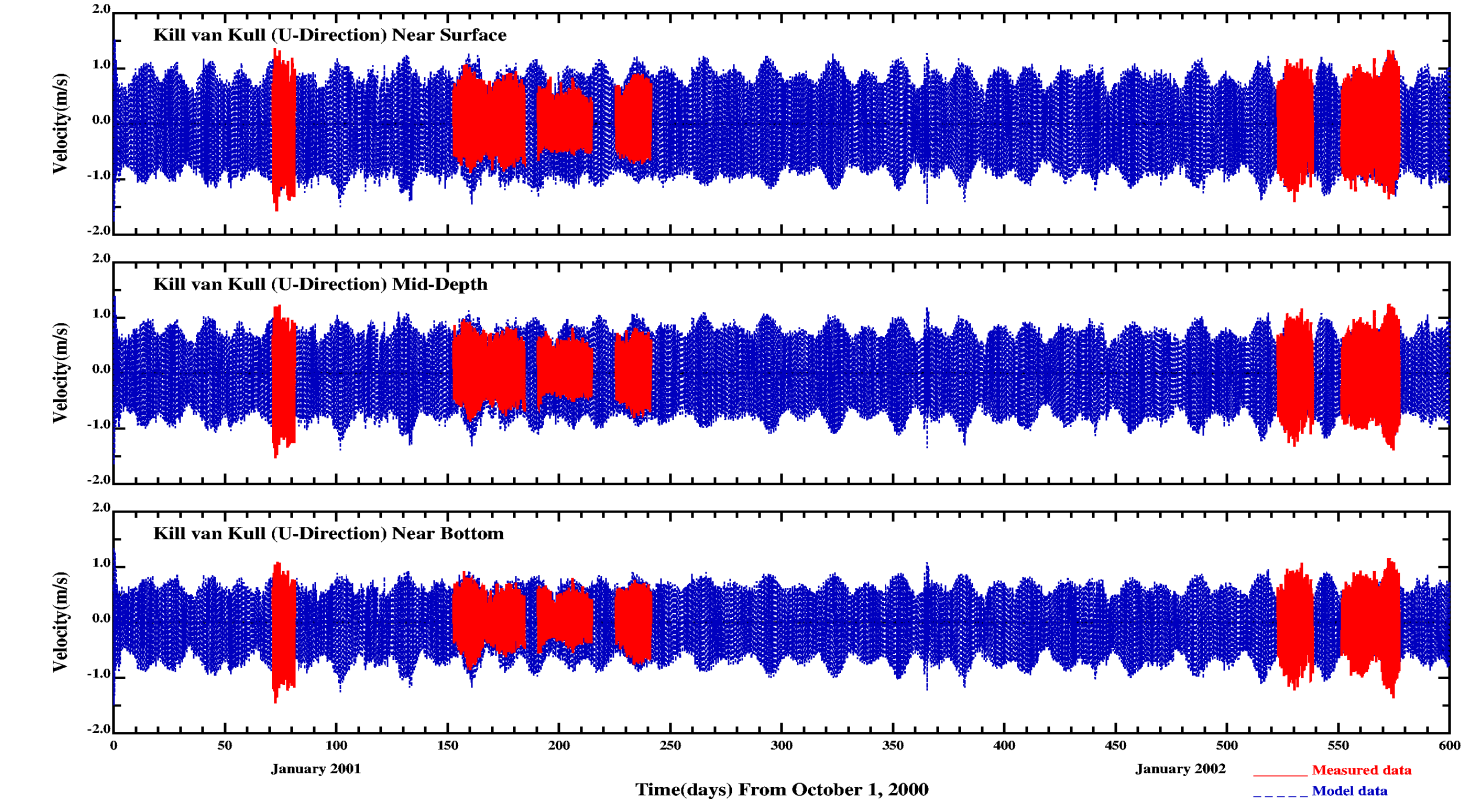

Figure 3-7. Model and data comparisons for velocity, Kill Van Kull Station.

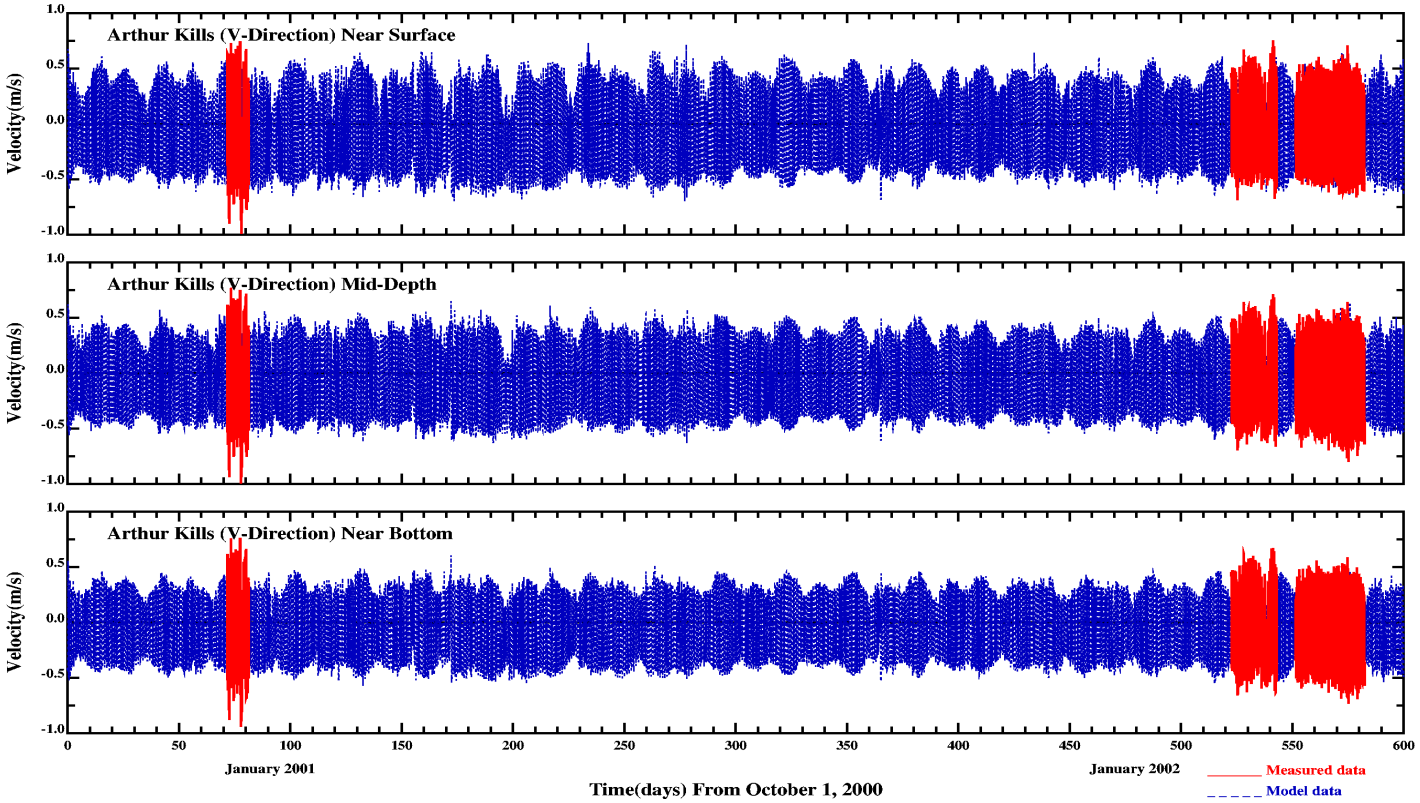

Figure 3-8. Model and data comparisons for velocity, Arthur Kill Station.

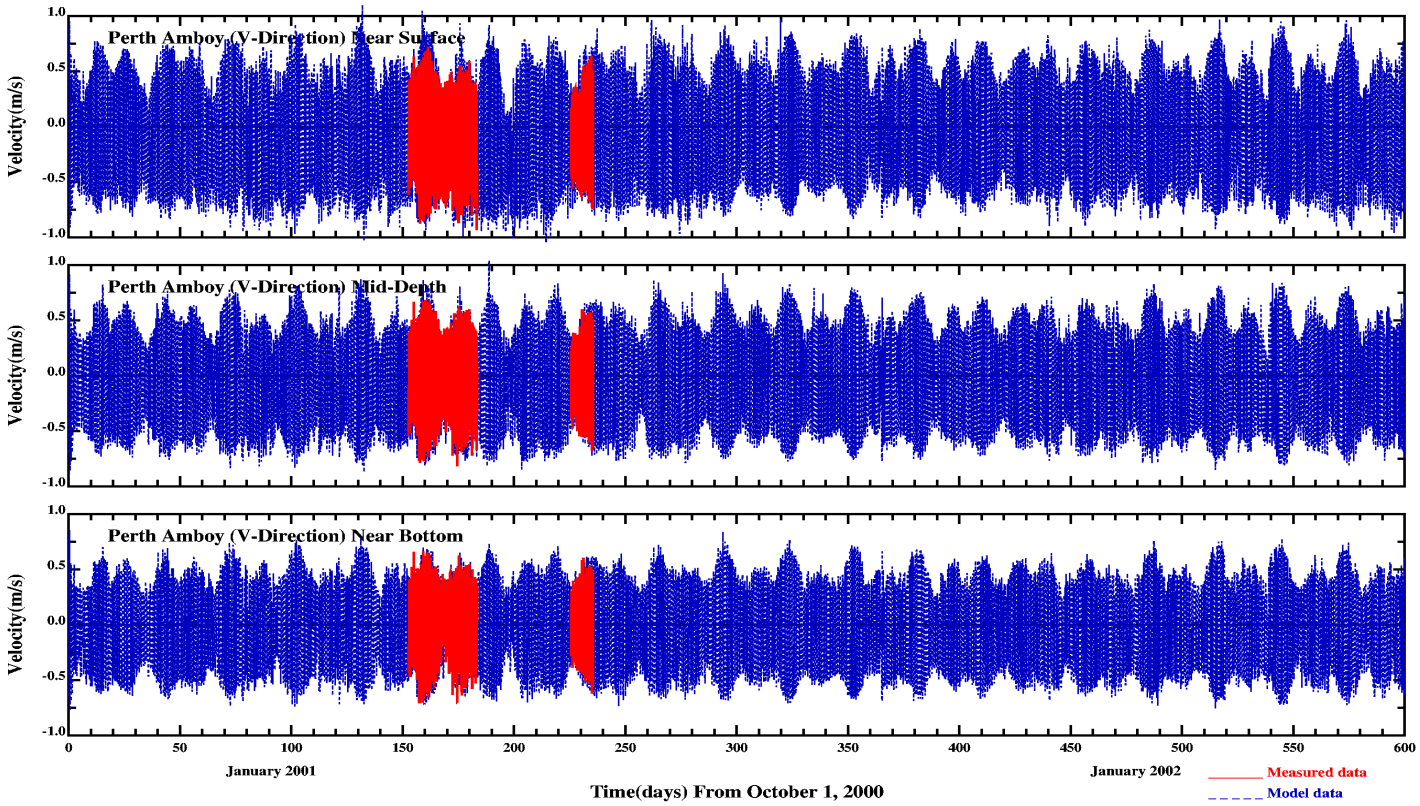

Figure 3-9. Model and data comparisons for velocity, Perth Amboy Station.

over-prediction of the range in near bottom velocities at the Newark Bay 1 station (see Figures 3-1 and 3-5) and salinity under-predictions at all five stations (Figures 3-4a and 3-4b), are described more fully below.

3.1.1 Tidal Elevations

The CARP hydrodynamic model reproduces the measured (i.e., via bottom pressure sensors) tidal and sub-tidal sea surface elevations well at the five locations indicated on Figure 3-1. CARP model computed tidal amplitude at each location follows very well the observed water elevations. The comparison of computed and observed tidal phases can be found in Appendix 3.

3.1.2 Temperature and Salinity

Overall there is good agreement between CARP model results and near bottom observations of salinity and temperature. Observed seasonal temperature variations and freshwater flow events are captured very well by the CARP model. Starting in February/March of 2002, the CARP model tends to under-predict bottom salinity. The under-prediction may be attributed to USACOE dredging activity in the general vicinity of the Kills (i.e., the USACOE started dredging of shipping channels to 41'). The CARP model uses a 24-30' water depth, representative of most of the 1998-2002 CARP modeling period, in the Arthur Kill and Kill van Kull.

3.1.3 Current Veloctity

CARP model calculations of current velocity are plotted at 3 depths (i.e., surface, mid-depth, and bottom (75% of depth)) for model and data comparisons. The calculated amplitude and phase of the currents at these depths agree very well with the measured data at 3 stations in the Kills. However, the CARP model under-predicts current velocities at two stations in Newark Bay. The most probable reason for the CARP model under predictions is that a single lateral grid cell representation of Newark Bay is not adequate for wide and shallow portions of the Bay. The ADCP data were collected at the bottom of a deep shipping channel in Newark Bay. Further lateral refinement of the CARP model grid in Newark Bay, for future projects such as the Passaic River Superfund Study, might improve model results.

3.2 SKILL ASSESSMENT USING NOAA TIDE GAUGE DATA

Several NOAA tidal guages in the CARP model domain are used for skill assessment of model results. Figure 3-10a shows the location of NOAA tidal guages in the NY-NJ harbor area. Hourly time

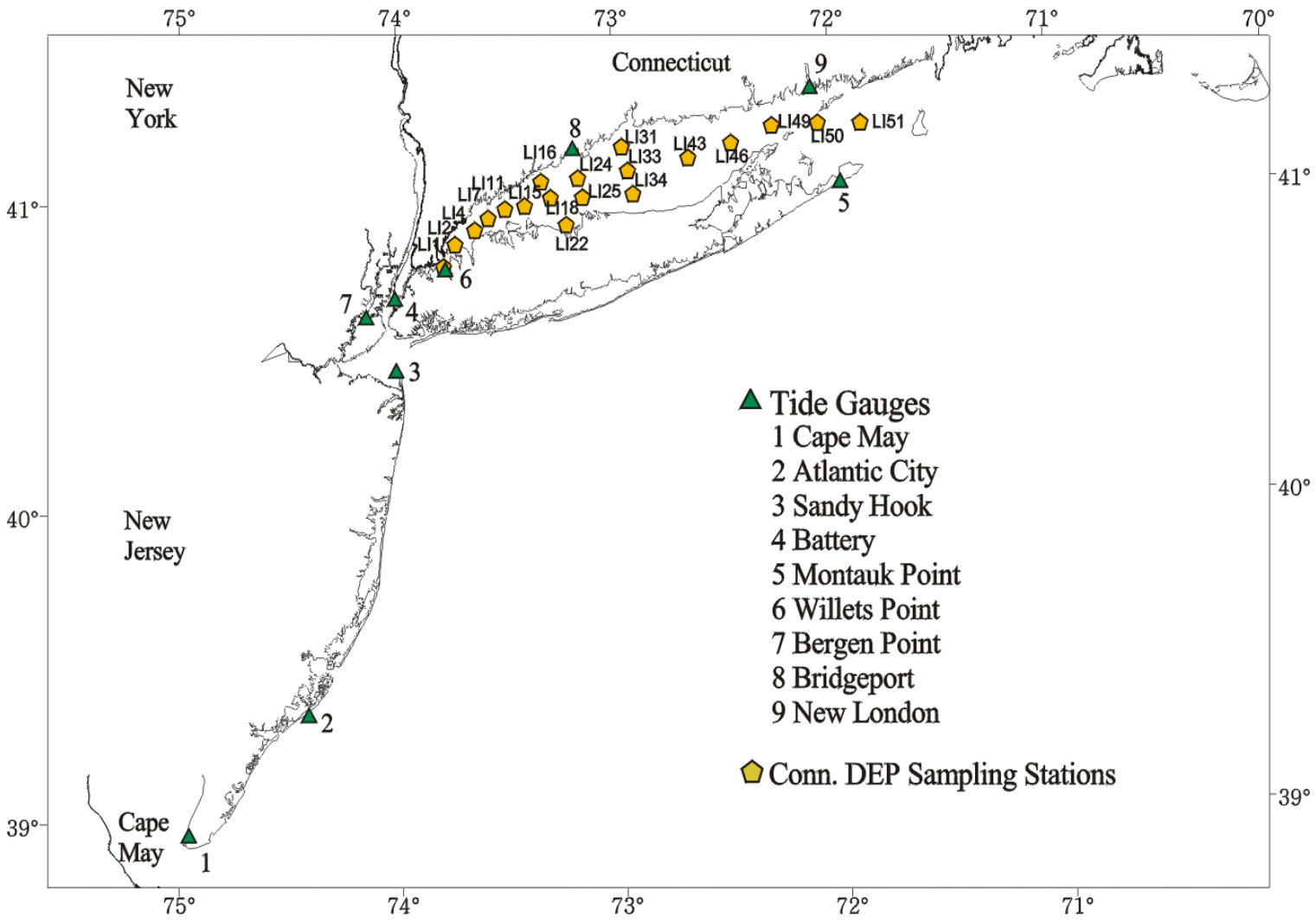

Figure 3-10a. Station map of data available from other programs for CARP model skill assessment.

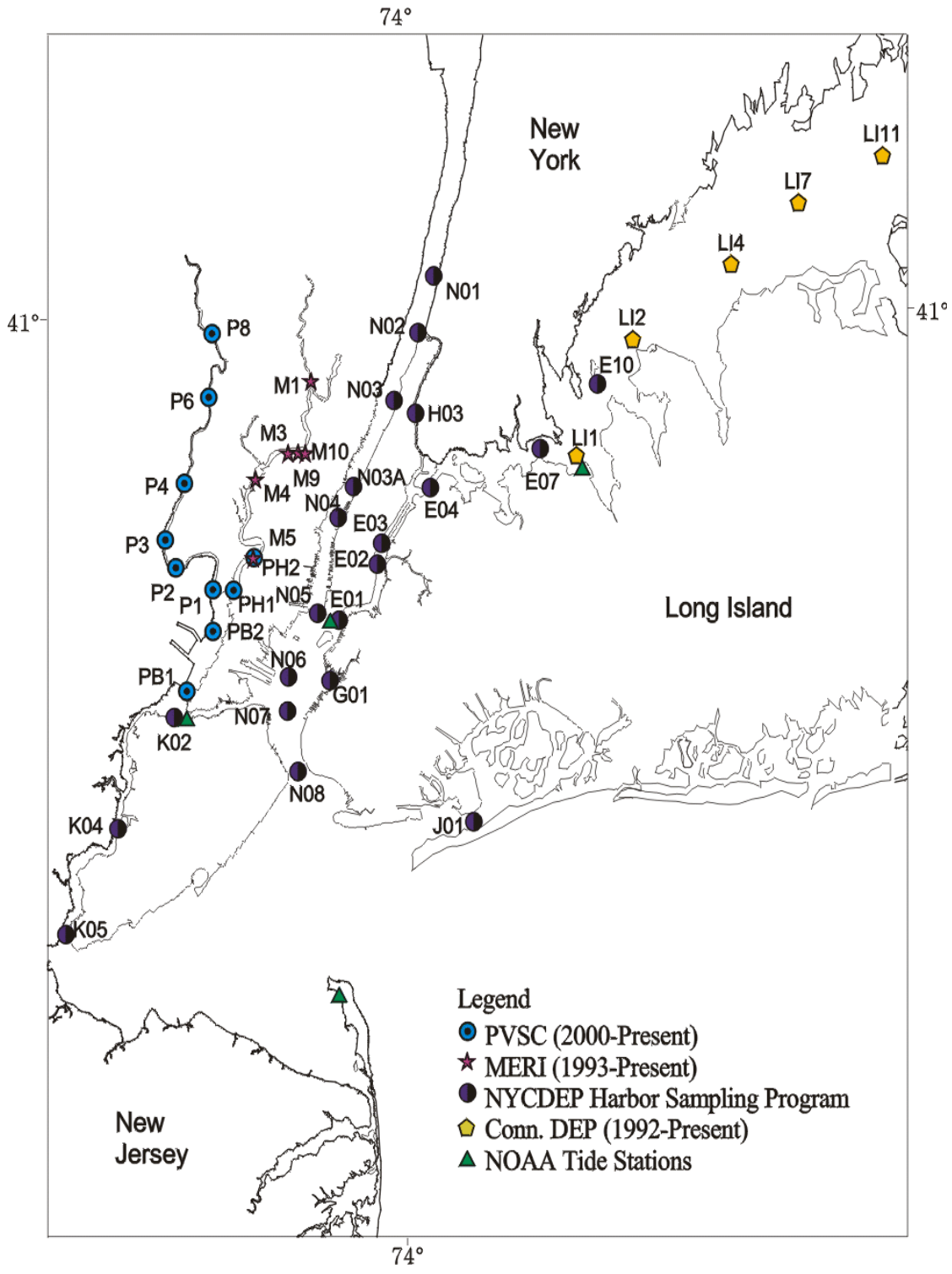

Figure 3-10b. Harbor view station map of data available from other programs for CARP model skill assessment.

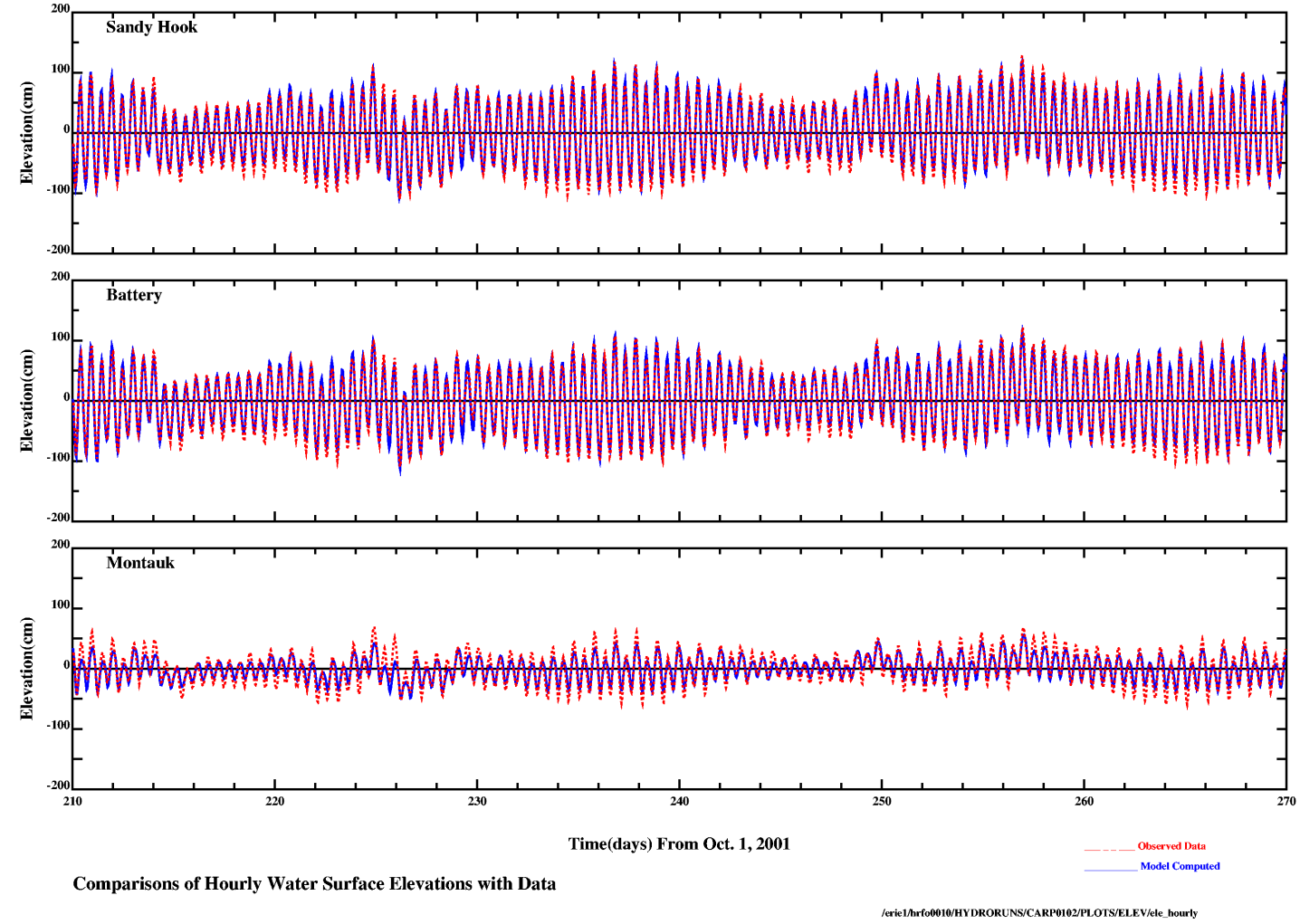

Figure 3-11. Selected Model and data comparisons for water elevations.

series and 35 hour low-passed sea surface elevations for four years are presented in Appendix 4. Selected representative results are shown in Figure 3-11. As demonstrated in earlier efforts (i.e., 88-89 and 94-95 SWEM years), the model reproduced very well the tidal sea level fluctuations in the model domain for all four CARP simulation years.

3.3 SKILL ASSESSMENT USING PVSC SALINITY AND TEMPERATURE DATA

The Passaic Valley Sewerage Commissioners maintained 8 water quality sampling stations in the Passaic River and the Newark Bay area starting in October 2000. These stations are shown in Figure 3-10b with blue circles. Monthly water quality data are available from May through November. Figures 3-12a and 3-12b show hourly temperature and salinity, respectively, during June-July of four years at station P1, which is located at the mouth of Passaic River. While the model computed hourly water temperature is slightly (2-5 °C) lower than observed data in 2001, the model computes the surface and bottom salinity quite well. The model captures strong tidal salinity fluctuations at the mouth of the Passaic River. Figures 3-13a and 3-13b show the yearly variations of 34 hour low-passed temperature and salinity, respectively. The model reproduced seasonal variations of temperature and salinity very well. Additional model skill assessment using PVSC data are shown in Appendix 5

3.4 SKILL ASSESSMENT USING MERI TEMPERATURE AND SALINITY DATA

The Meadowlands Environmental Research Institute, MERI, provided us their field sampling data from 1993 on. The sampling locations are shown in Figure 3-10. Hourly temperature and salinity data for the June-July period for the four CARP water years at Station M4 near Berrys Creek are shown in Figure 3-14a and 3-14b, respectively. Yearly variations of temperature and salinity at the same station are shown in Figure 3-15a and 3-15b. While the model reproduced well both the hourly and 34 hourly low-passed salinity in the Hackensack River, it appears that model consistently under-predicted water temperature in the River. This under-prediction of water temperature may be attributed to the fact that the CARP model does not cover the expansive Meadowlands tidal marsh on both sides of the Hackensack River. This shallow and vast area can retain greater solar energy (i.e., heating of the water) than the narrow River itself. Additional model skill assessment at MERI data stations are shown in Appendix 6.

3.5 SKILL ASSESSMENT USING NYCDEP SALINITY AND TEMPERATURE DATA

NYCDEP maintains a vast array of sampling stations in waters within its jurisdiction. Model and data comparisons at two selected NYCDEP sampling locations (i.e., station N4 near the Lincoln Tunnel and station K2 in the Kill van Kull) are shown in Figures 3-16 to 3-19 and are for the most part

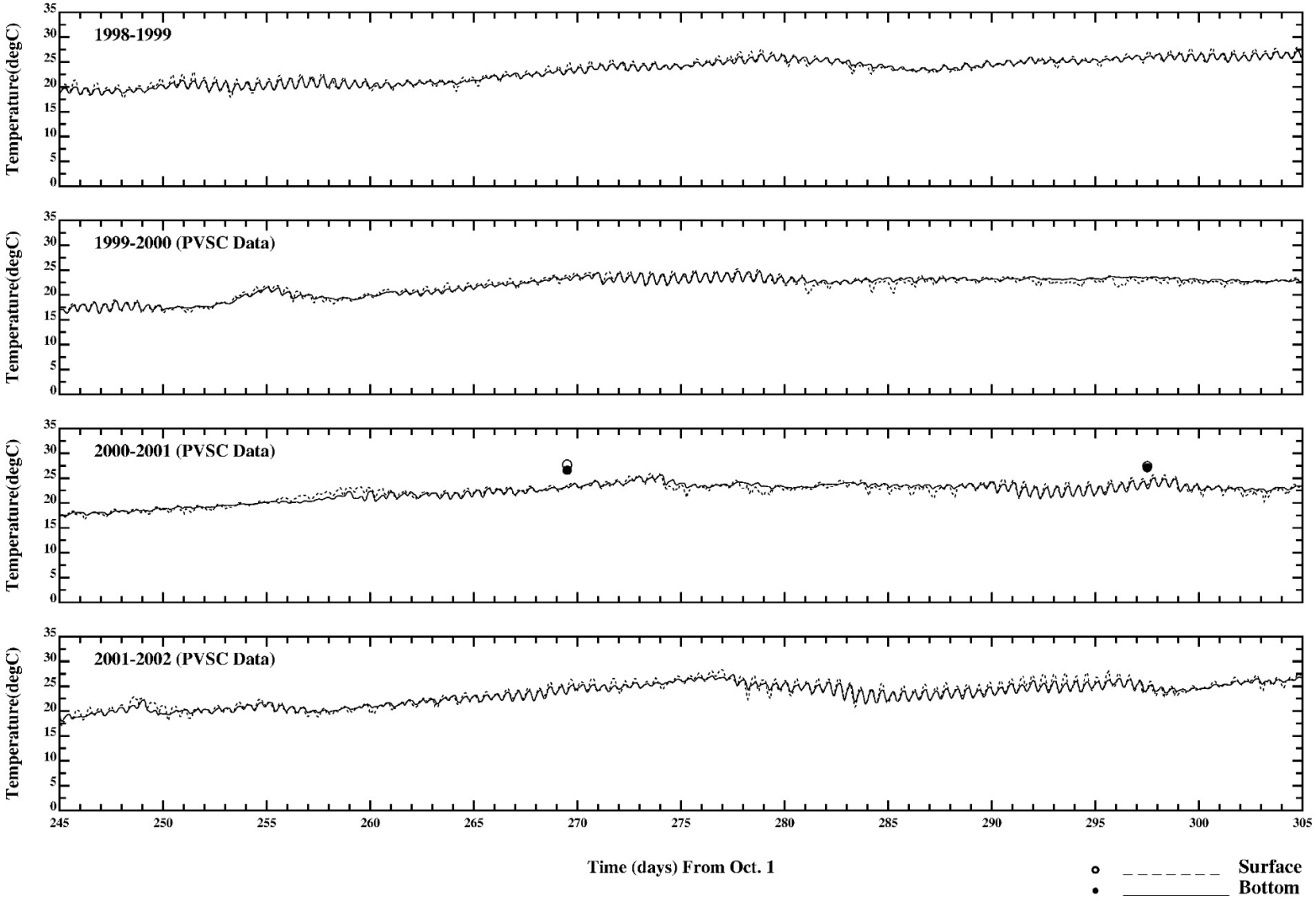

Figure 3-12a. Comparison of data with model results (hourly) for surface and bottom temperature in Passaic River - Upstream (P1)

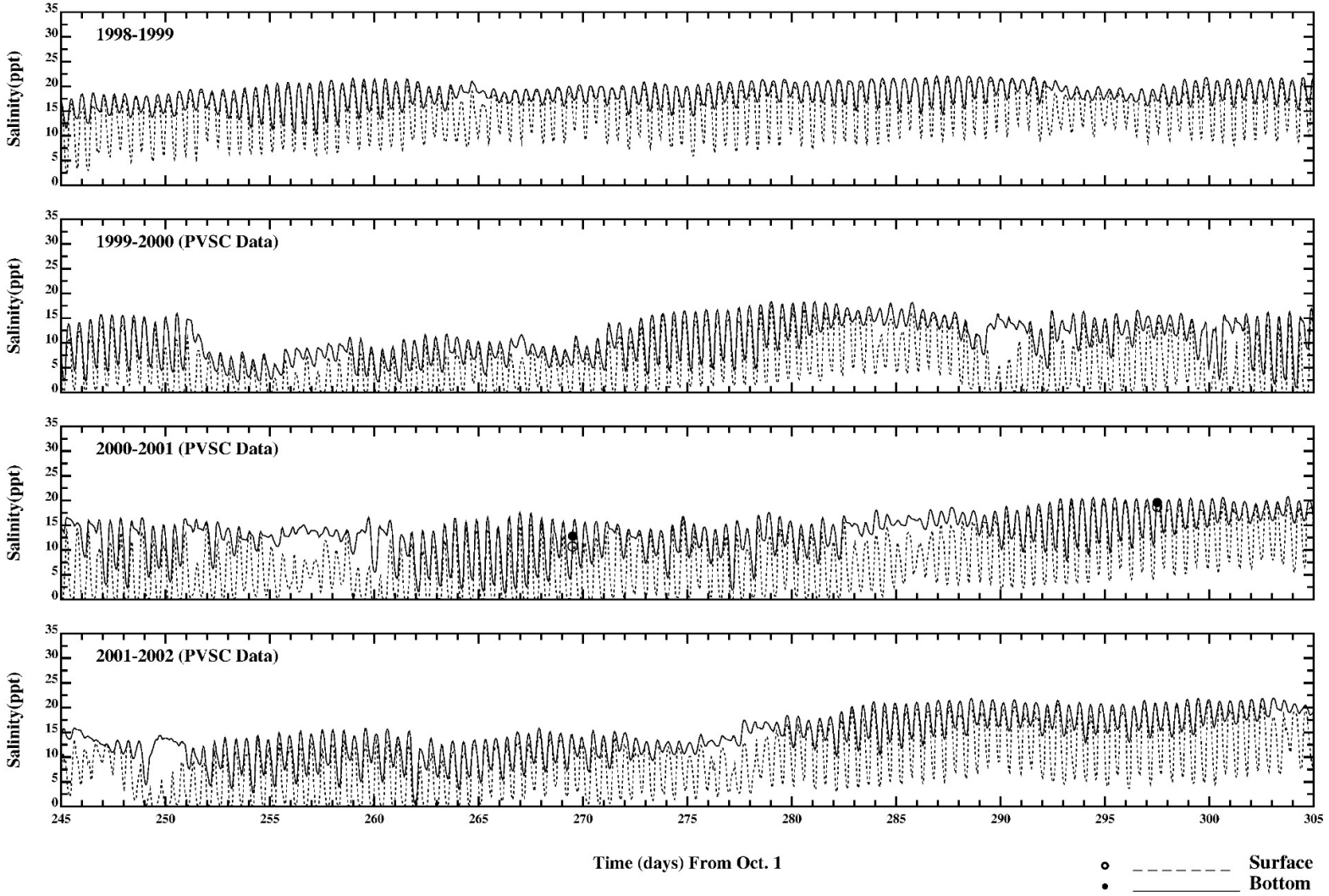

Figure 3-12b. Comparison of data with model results (hourly) for surface and bottom salinity in Passaic River - Upstream (P1)

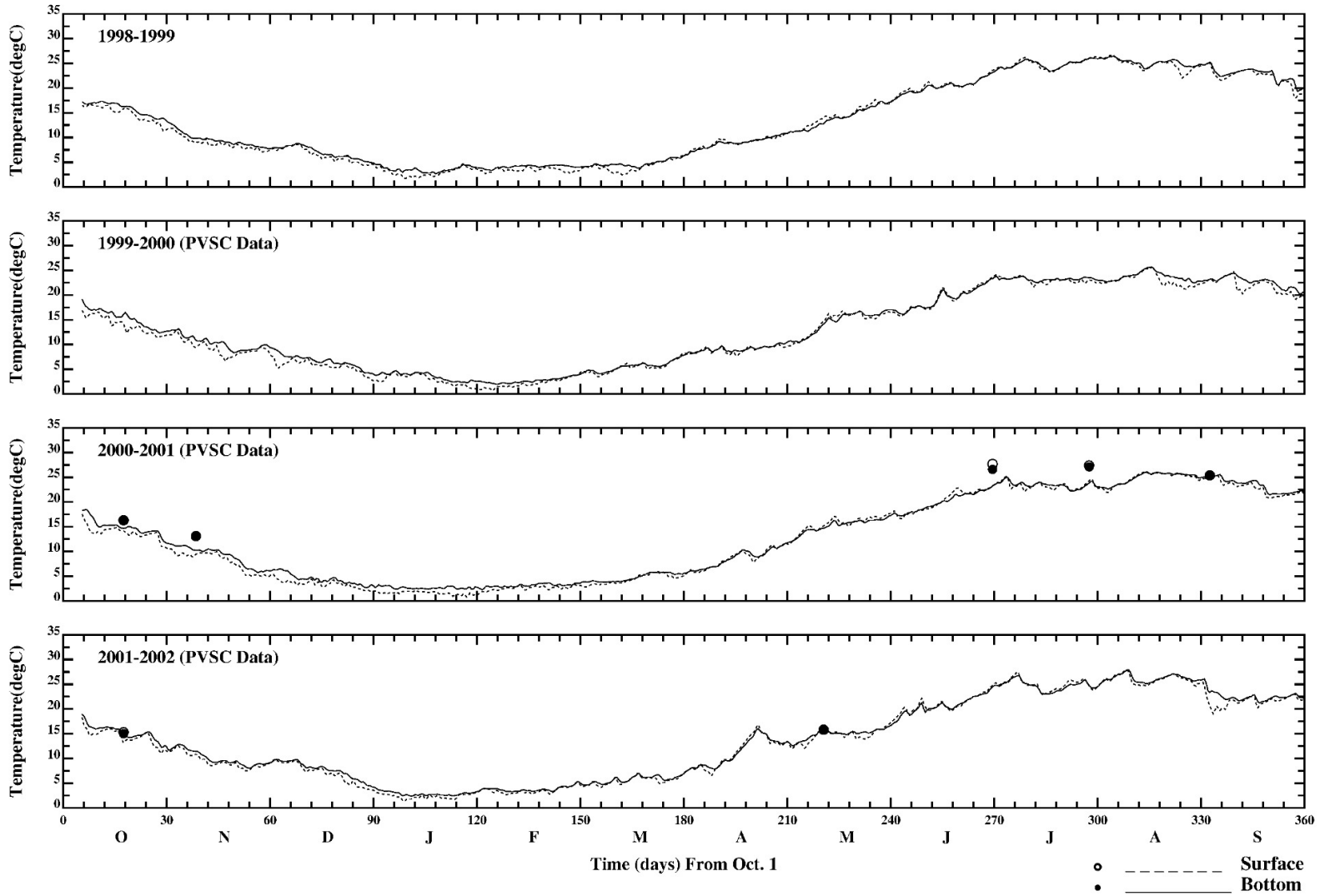

Figure 3-13a. Comparison of data with model results (34 HLP) for surface and bottom temperature at Passaic River - Downstream (P1)

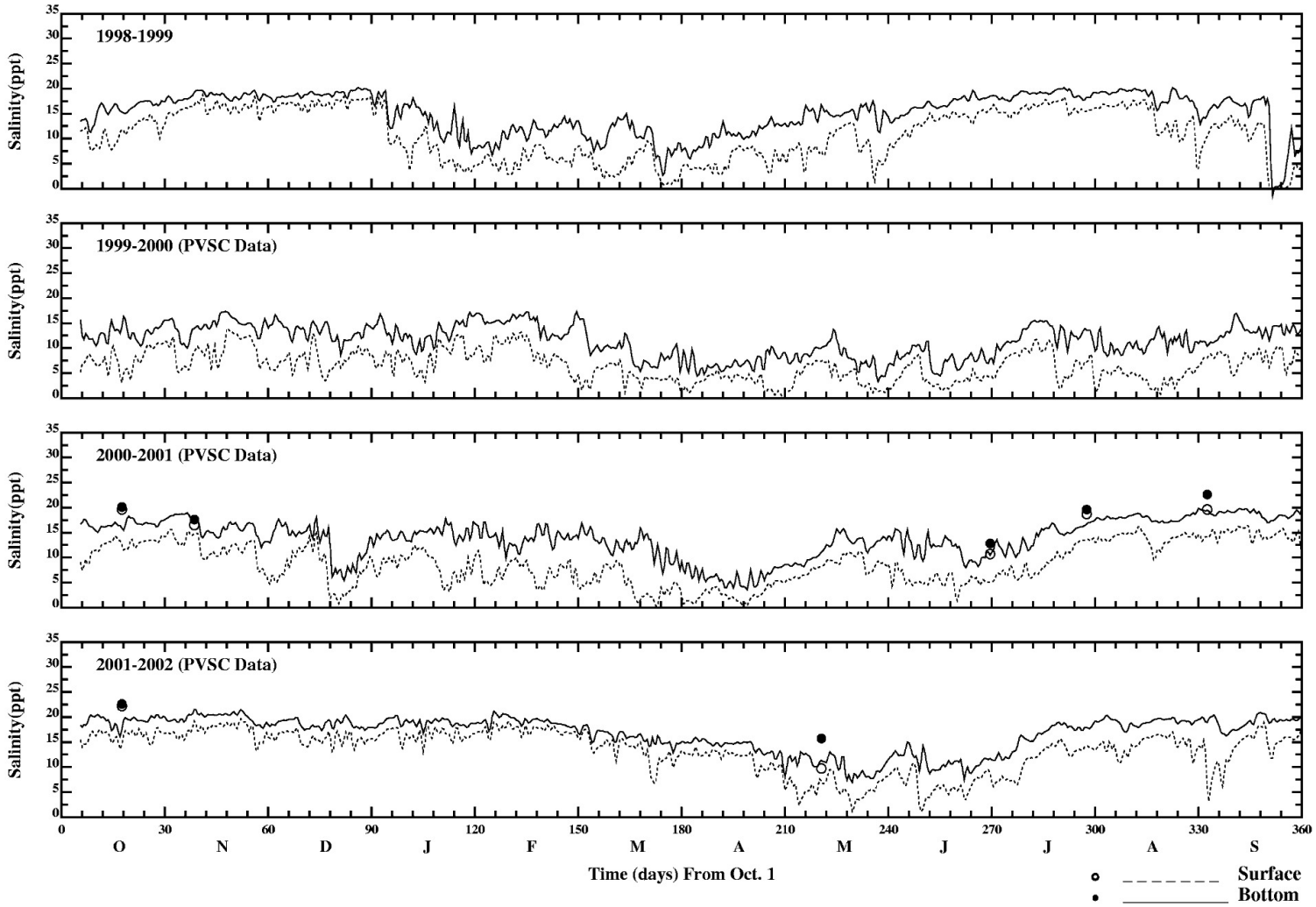

Figure 3-13b. Comparison of data with model results (34 HLP) for surface and bottom salinity at Passaic River - Downstream (P1)

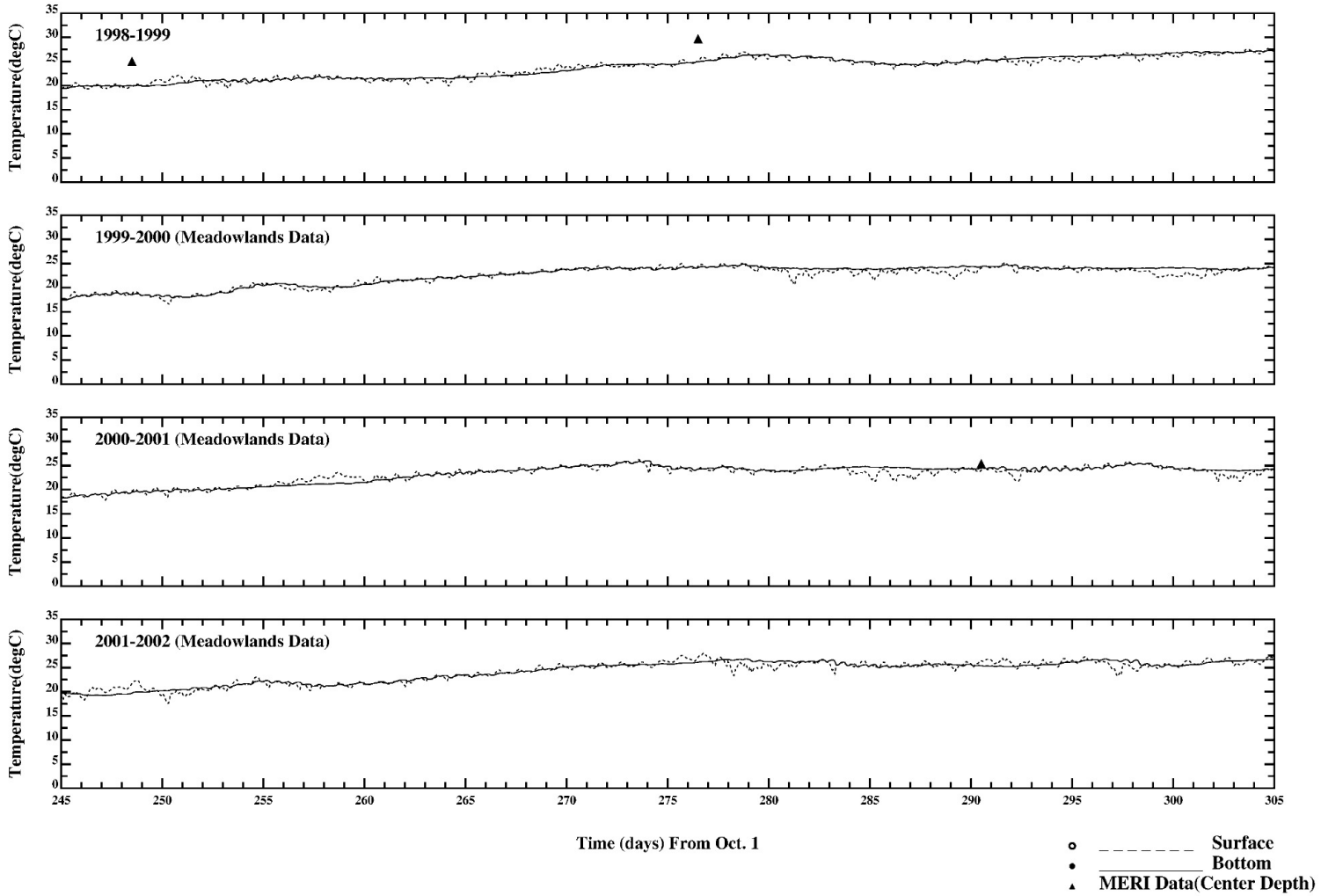

Figure 3-14a. Comparison of data with model results (hourly) for surface and bottom temperature in Hackensack River (M4)

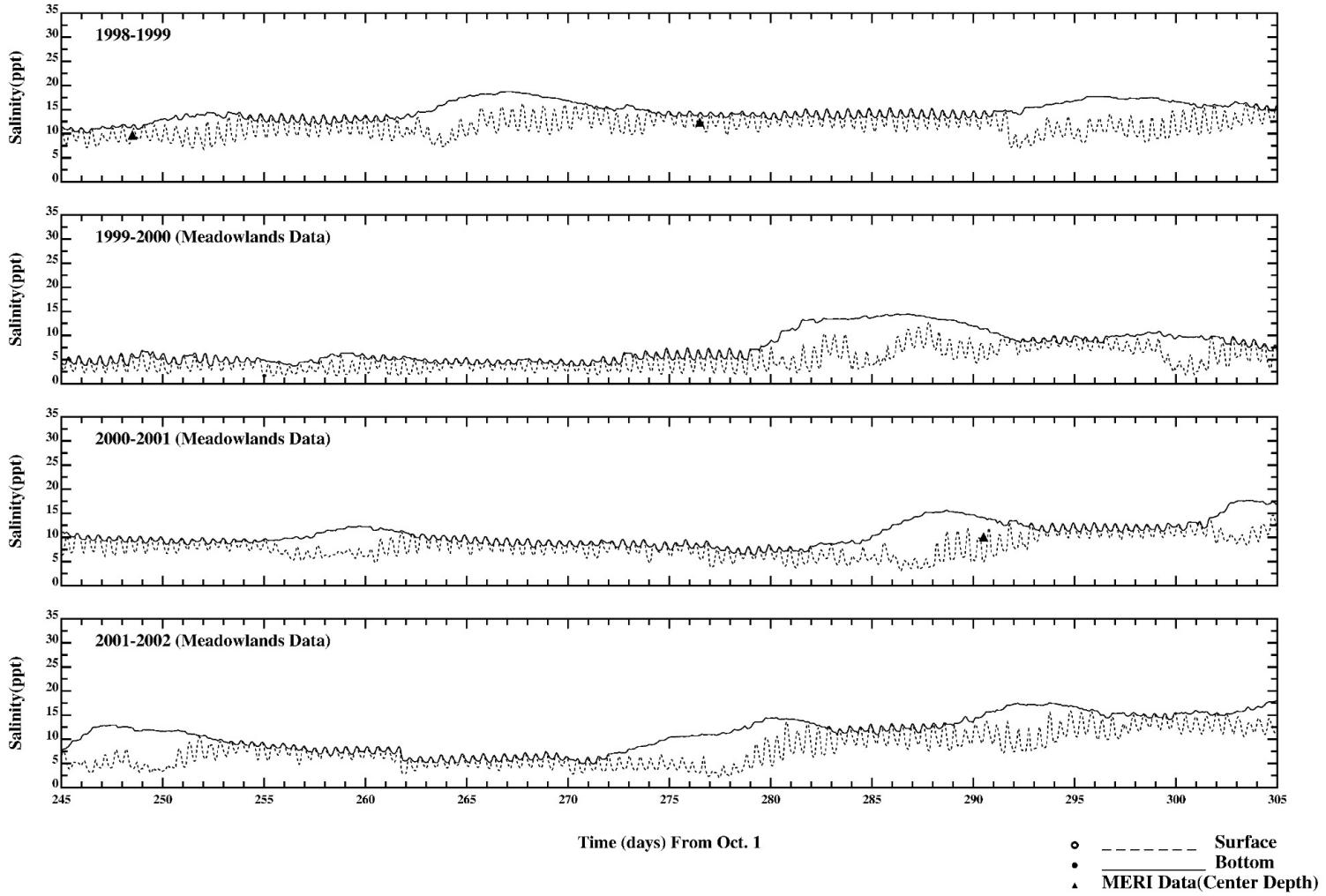

Figure 3-14b. Comparison of data with model results (hourly) for surface and bottom salinity in Hackensack River (M4)

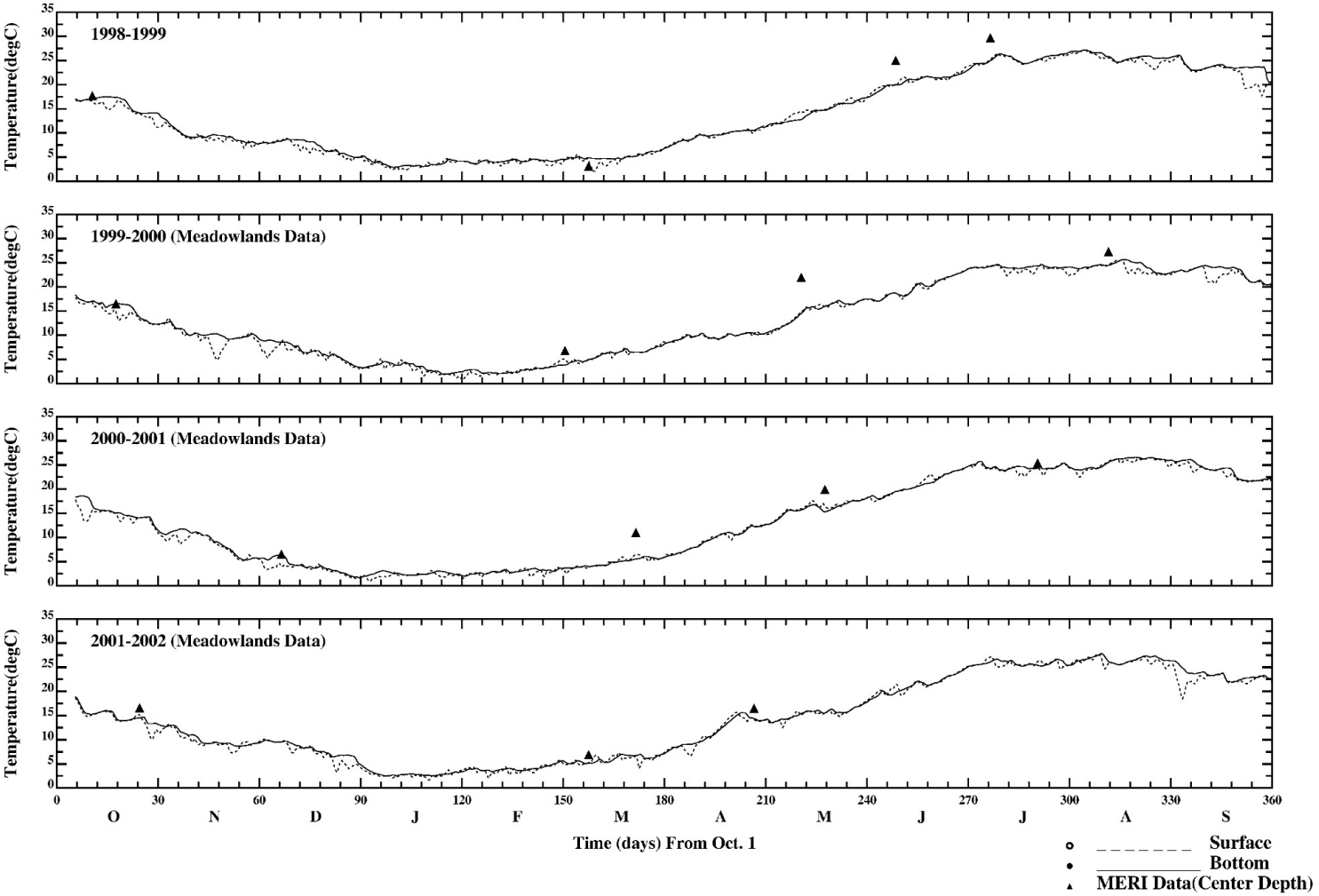

Figure 3-15a. Comparison of data with model results (34 HLP) for surface and bottom temperature at Hackensack River (M4)

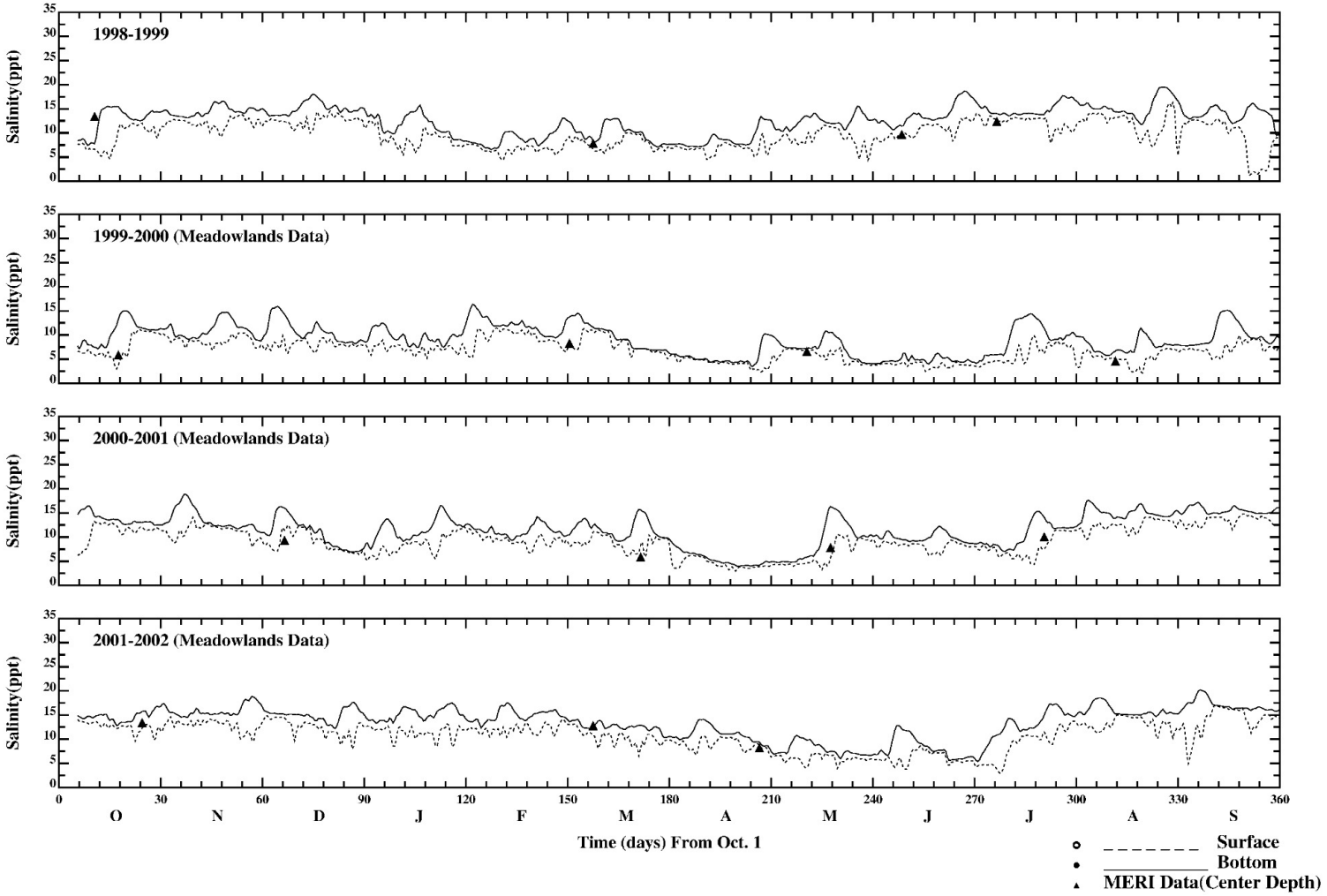

Figure 3-15b. Comparison of data with model results (34 HLP) for surface and bottom salinity at Hackensack River (M4)

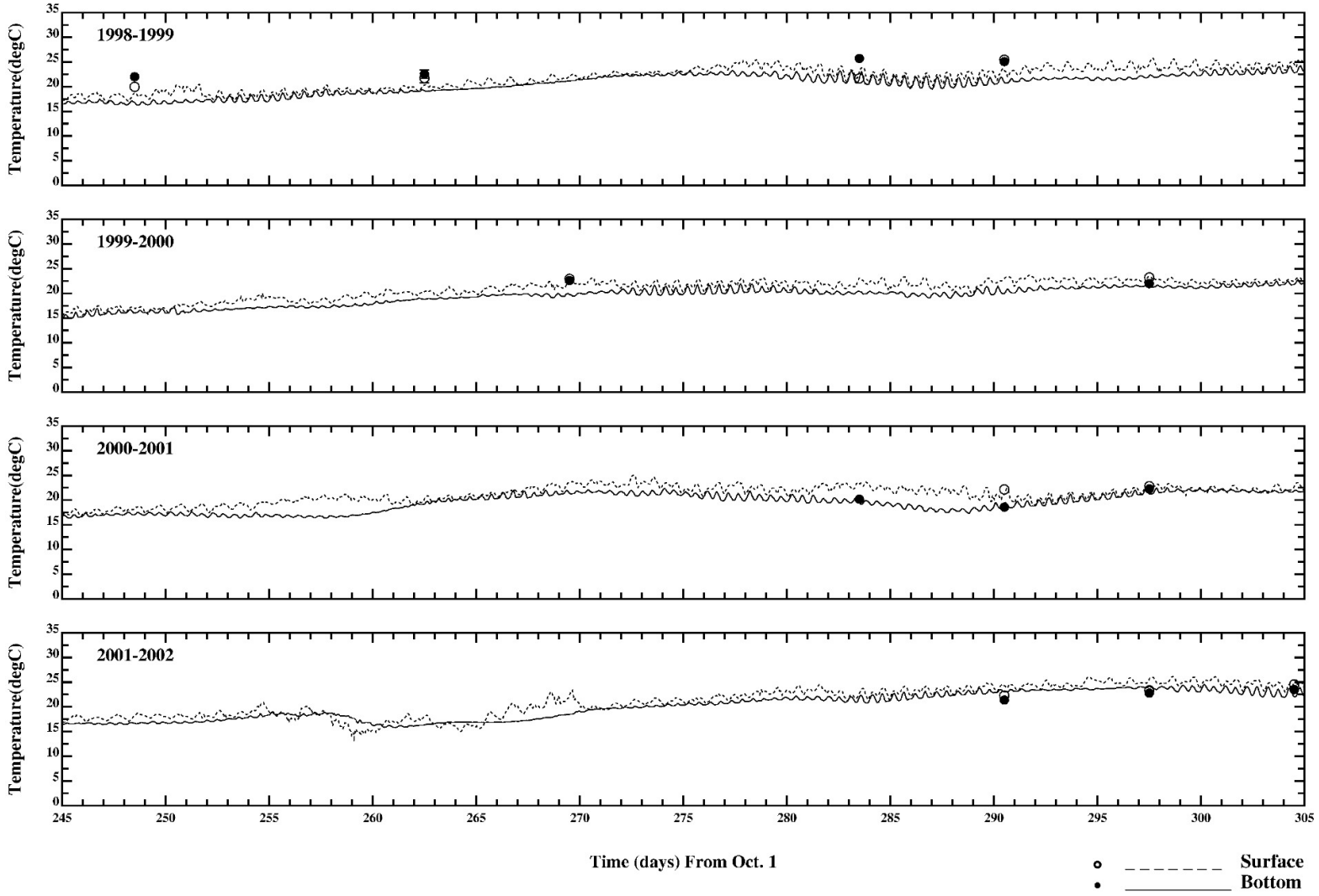

Figure 3-16a. Comparison of data with model results (hourly) for surface and bottom temperature at Lincoln Tunnel (N4)

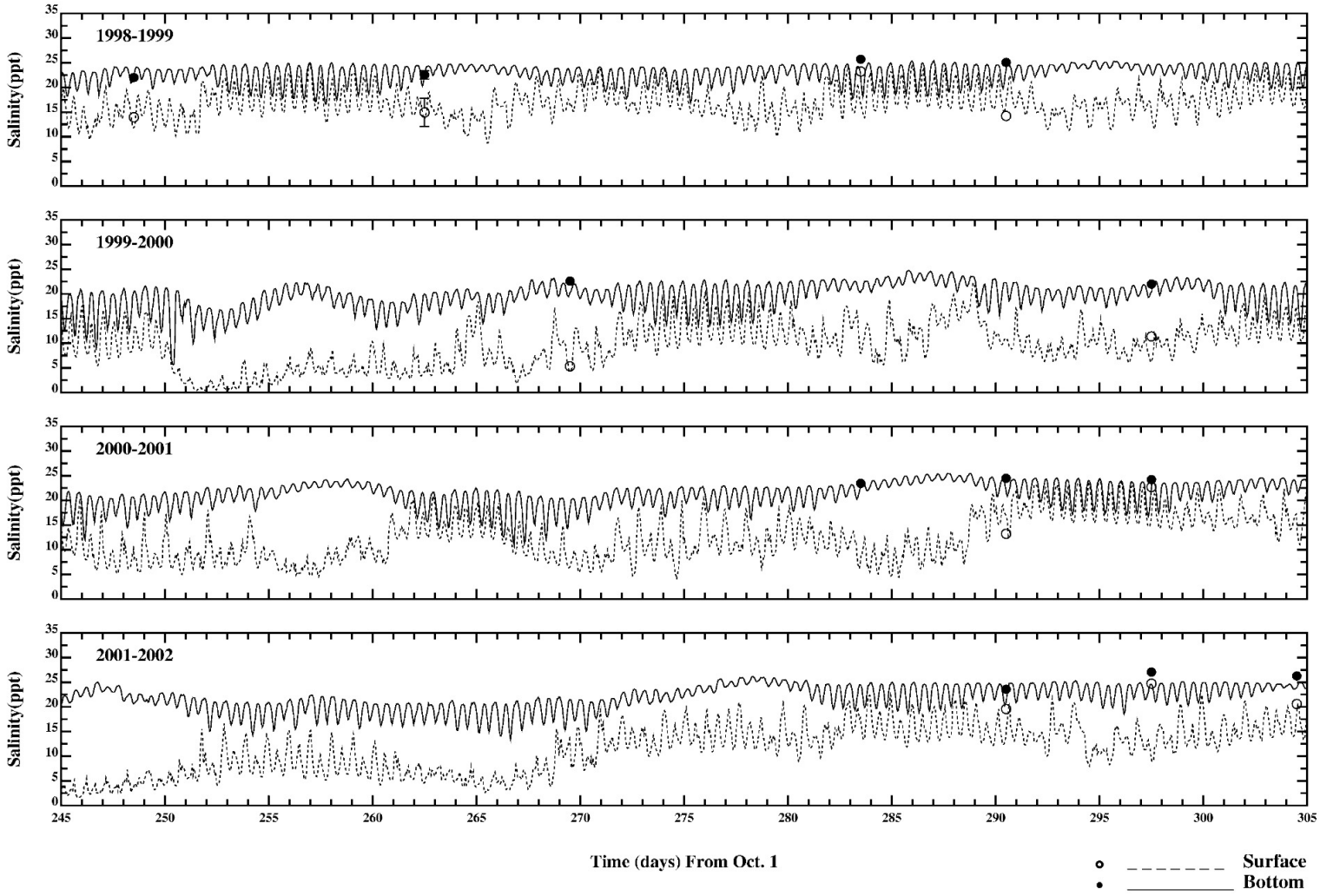

Figure 3-16b. Comparison of data with model results (hourly) for surface and bottom salinity at Lincoln Tunnel (N4)

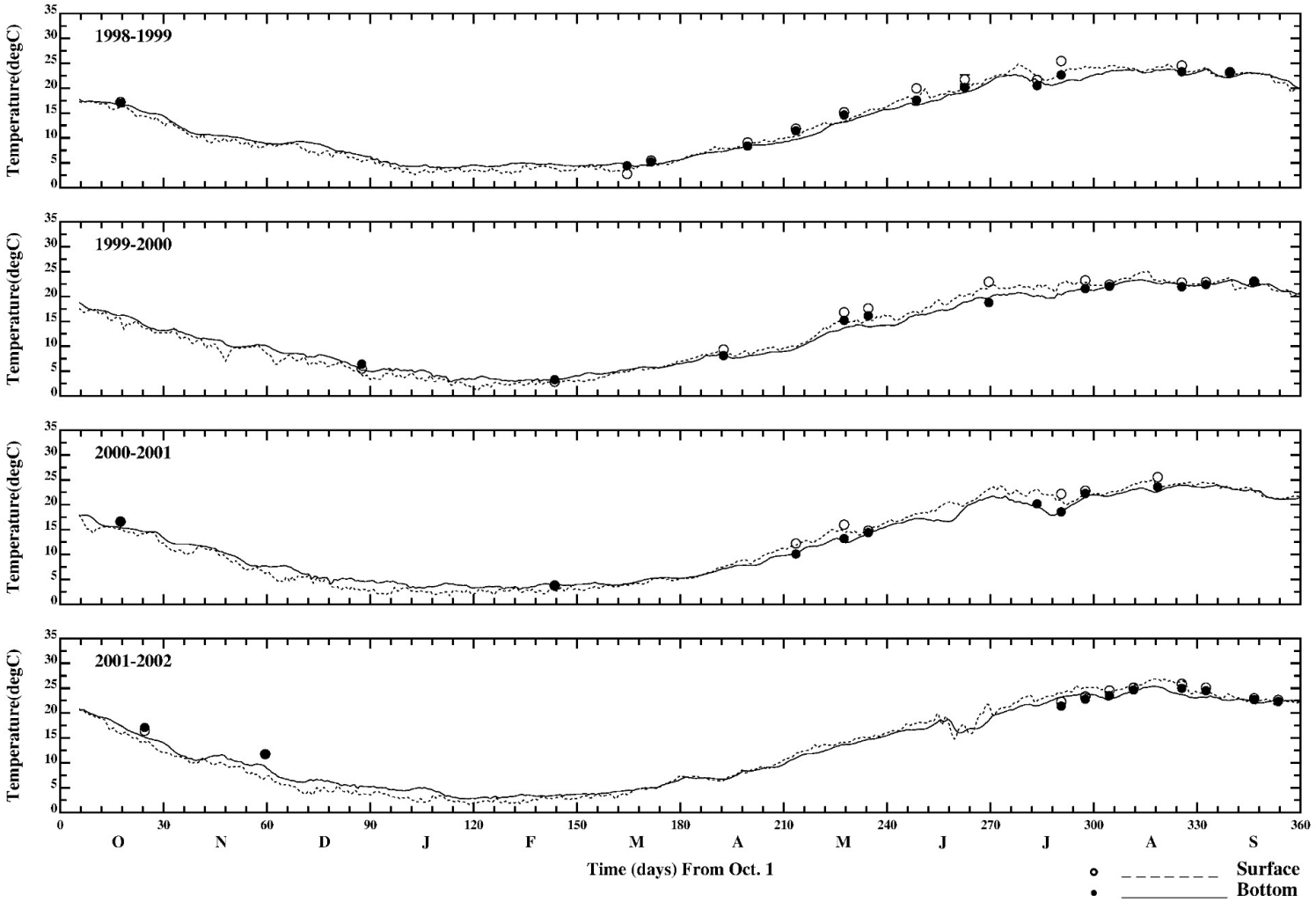

Figure 3-17a. Comparison of data with model results (34 HLP) for surface and bottom temperature at Lincoln Tunnel (N4)

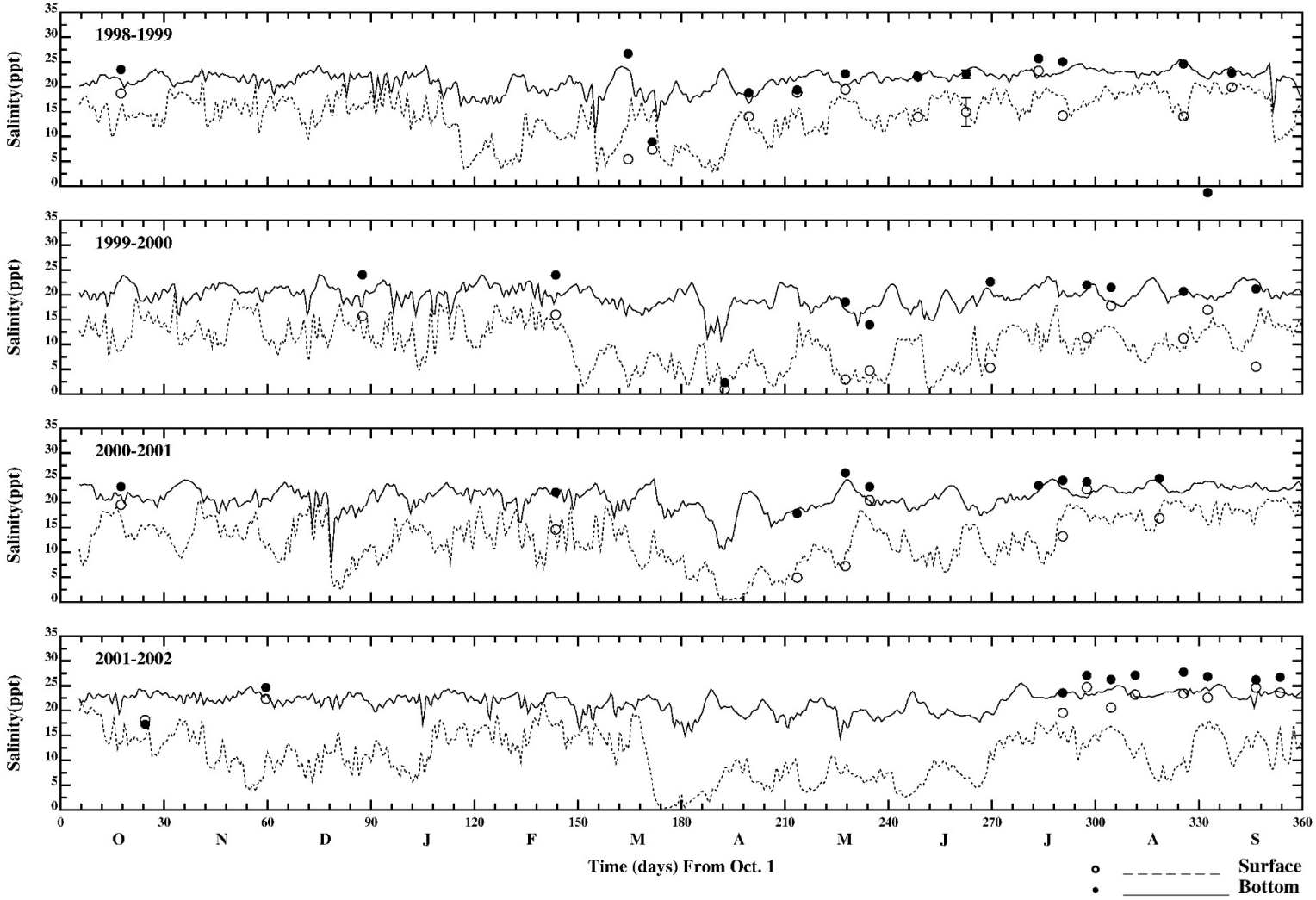

Figure 3-17b. Comparison of data with model results (34 HLP) for surface and bottom salinity at Lincoln Tunnel (N4)

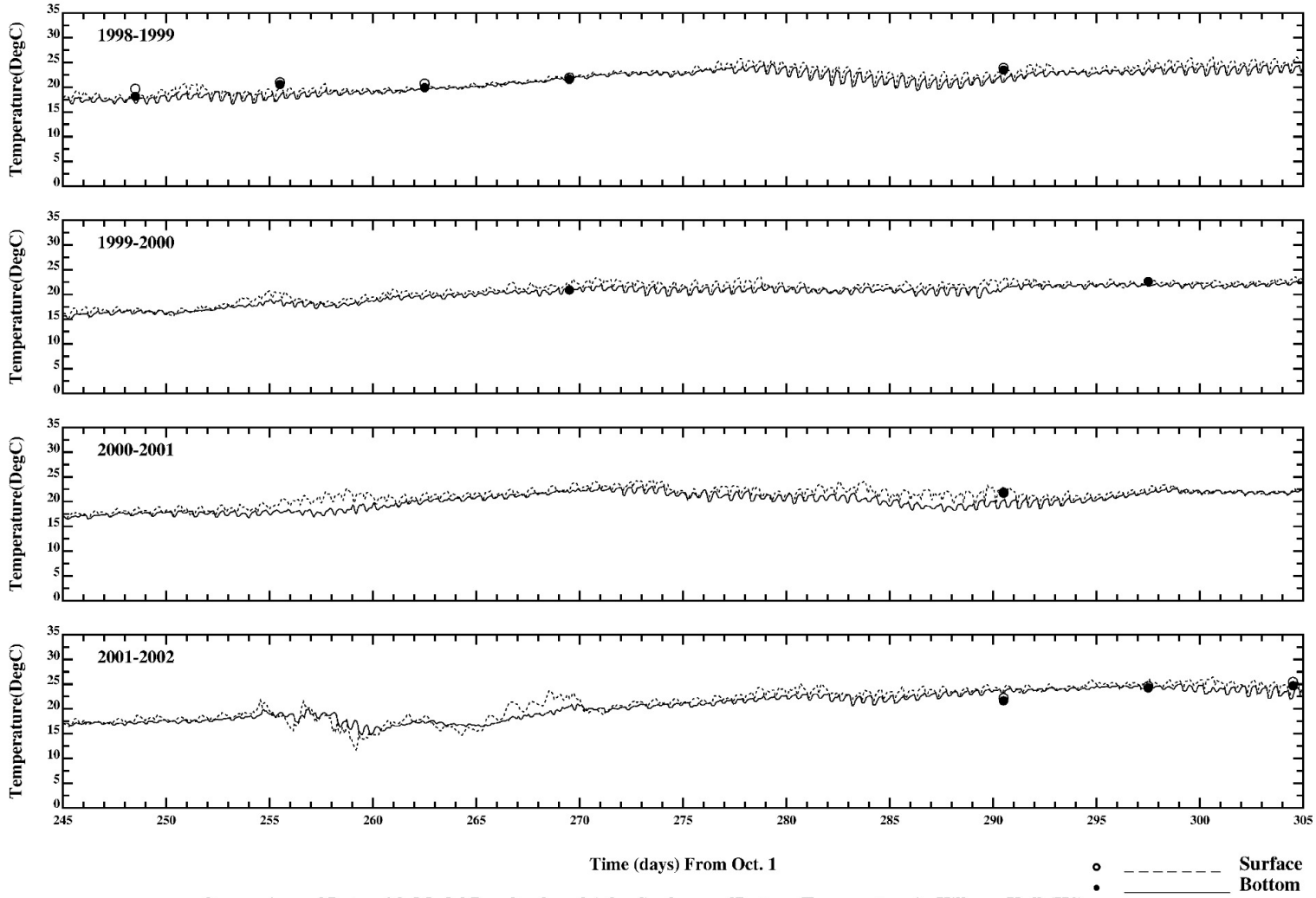

Figure 3-18a. Comparison of data with model results (hourly) for surface and bottom temperature in Kill van Kull (K2)

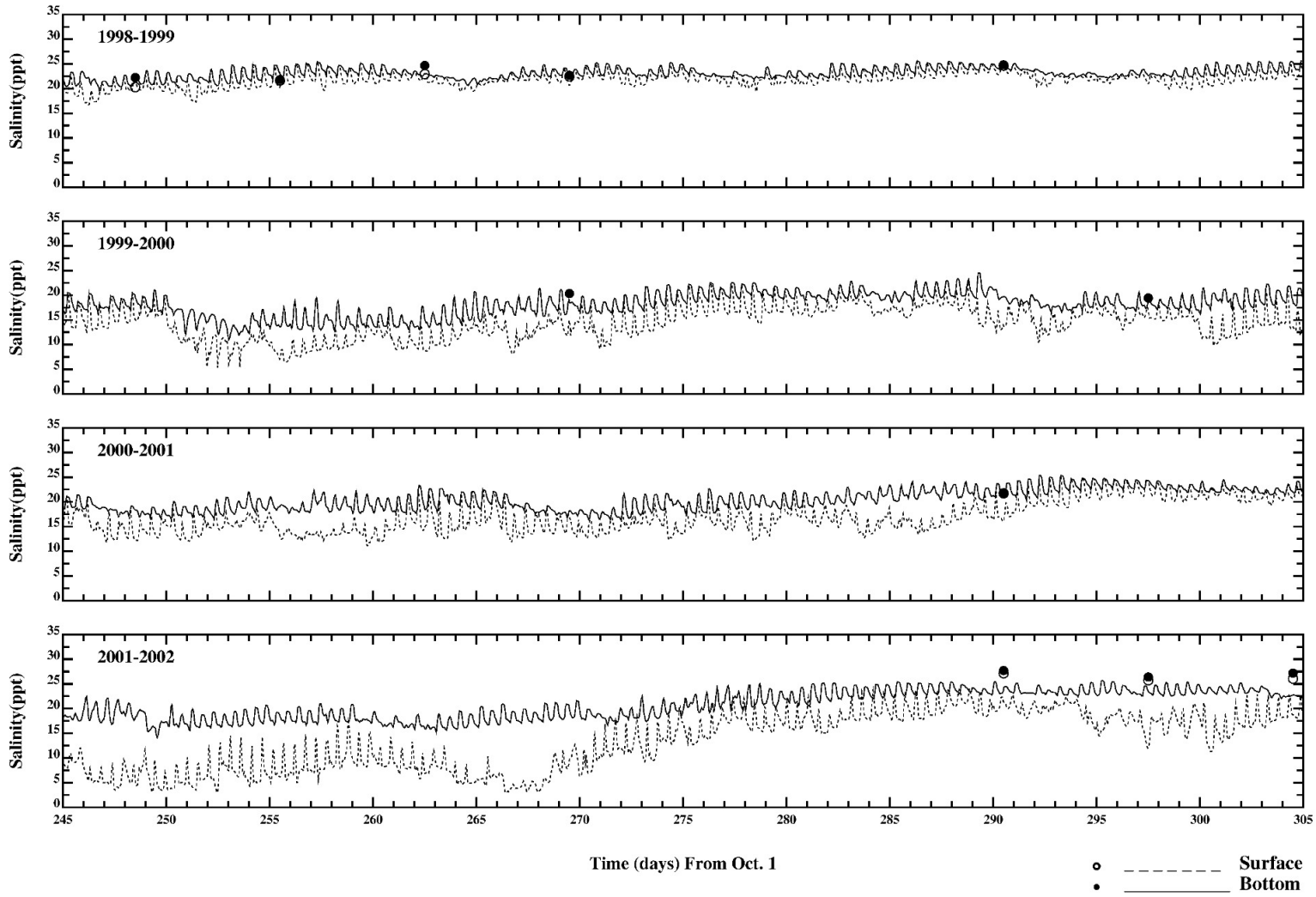

Figure 3-18b. Comparison of data with model results (hourly) for surface and bottom salinity in Kill van Kull (K2)

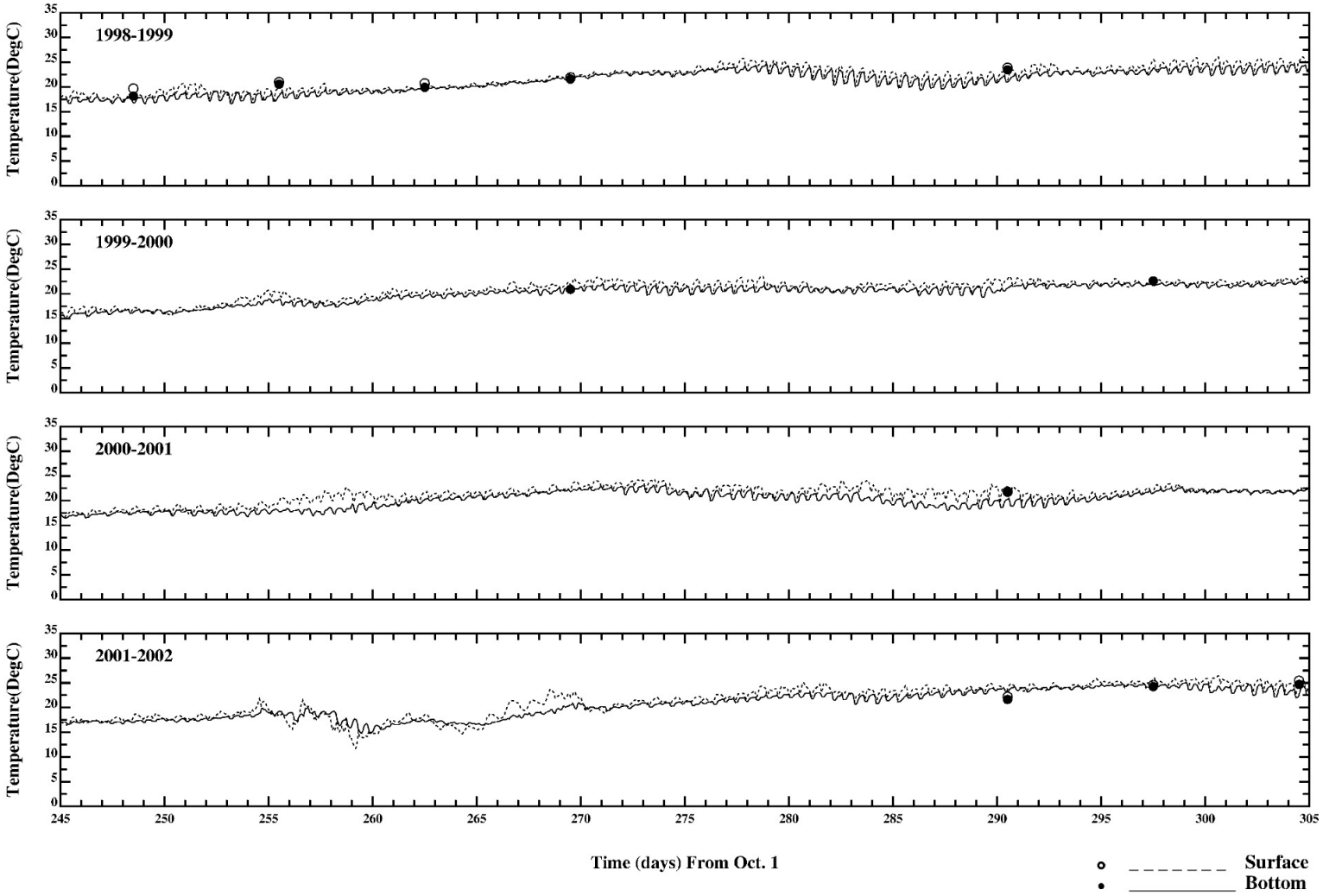

Figure 3-19a. Comparison of data with model results (hourly) for surface and bottom temperature in Kill van Kull (K2)

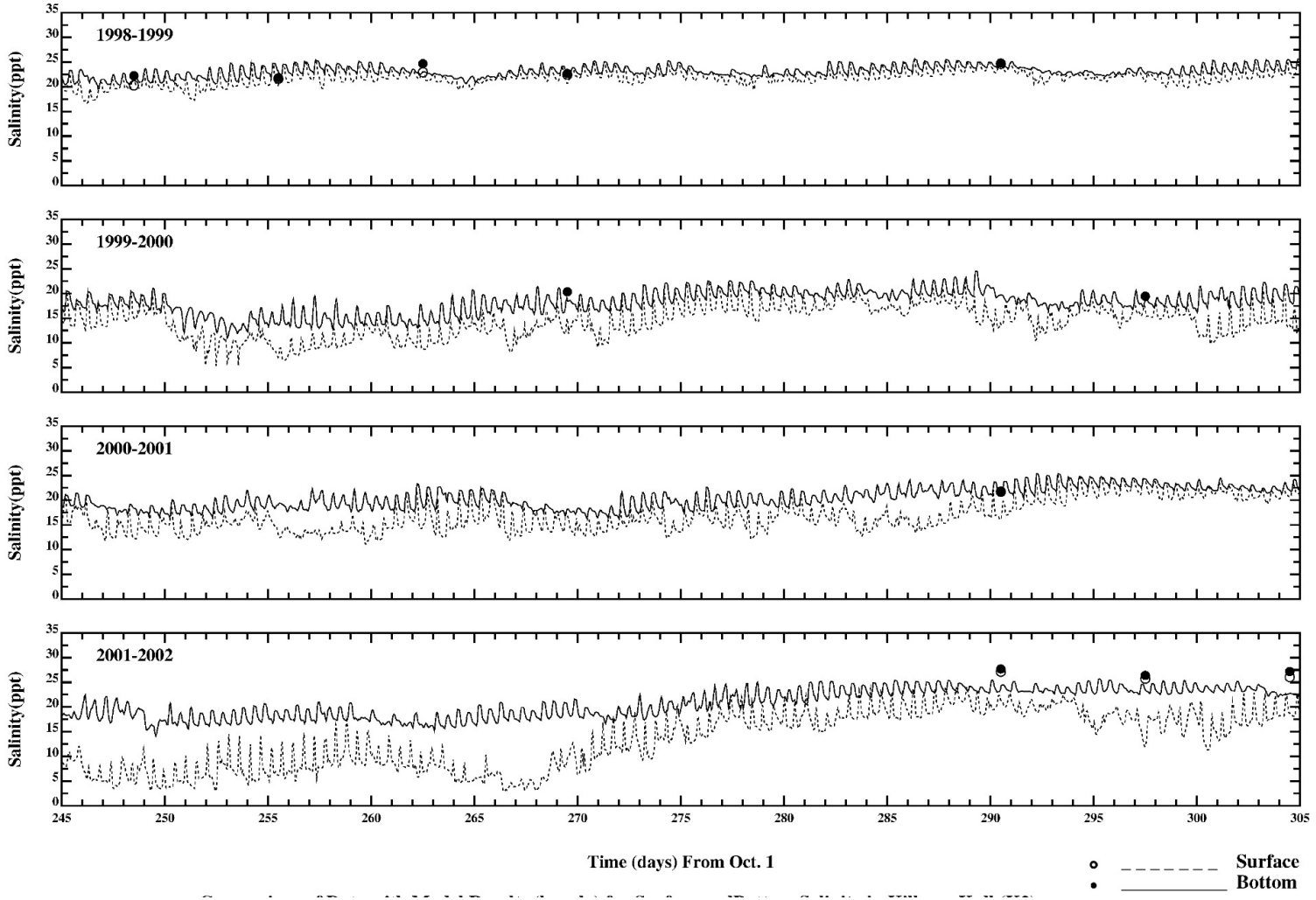

Figure 3-19b. Comparison of data with model results (hourly) for surface and bottom salinity in Kill van Kull (K2)

favorable. However, at station K2 in the Kill van Kull, the model computes surface and bottom salinity very well until the early part of 2002 and then under-predicts the salinity afterwards (see Figure 3-19b). This pattern was also observed when comparing model calculations to CARP observations of salinity in Kill van Kull (see Figure 3-4). In both cases, the model under-prediction may be attributed to dredging activity in the Arthur Kill and Kill van Kull area. Additional model and data comparisons are shown in Appendix 7.

3.6 SKILL ASSESSMENT USING CTDEP SALINITY AND TEMPERATURE DATA

CTDEP maintains both monthly and bi-weekly water quality monitoring stations throughout Long Island Sound. Appendix 8 contains hourly and yearly plots of temperature and salinity at 19 stations in the Sound.

3.7 MODEL-DATA CORRELATION ANALYSES

A correlation analysis between CARP hydrodynamic sub-model results and observed data has been performed. For purposes of the correlation analysis, the CARP model domain has been sub-divided into 6 regions: Newark Bay and Kills; Hackensack and Passaic Rivers (i.e., NJ Tributaries); Raritan Bay; Upper and Lower New York Bays (i.e., Inner Harbor); East and Harlem Rivers; and Long Island Sound. For each water year, model-data correlation plots were prepared for temperature and salinity (both surface and bottom).

For temperature, model calculations and observed data are strongly correlated in most regions for both near surface and near bottom. An exception is the NJ tributaries. The reason for the poor correlation in the Hackensack and Passaic Rivers were already discussed above in Section 3.2. The correlation coefficient, R^2, is better than 0.85 at most locations. The model and data correlations for temperature are shown in Figures 3-20a and 3-20b. R^2 values along with those calculated for salinity are shown in Figure 3-21 and are tabulated in Table 3-1.

For salinity, model and data correlations are shown in Figure 3-22a and 3-22b. The CARP hydrodynamic sub-model is performing well at locations in the Inner Harbor, Long Island Sound, and the East River for both surface and bottom salinity for all four CARP water years. Correlation coefficients, R^2s, for regions in the NJ tributaries, Newark Bay and the Kills are poor for salinity in some cases especially in the 2000-2002 period. Reasons for the poor correlations may be related to sparseness and quality of the observed data, in-progress dredging activities during data collection and limited model grid segmentation.

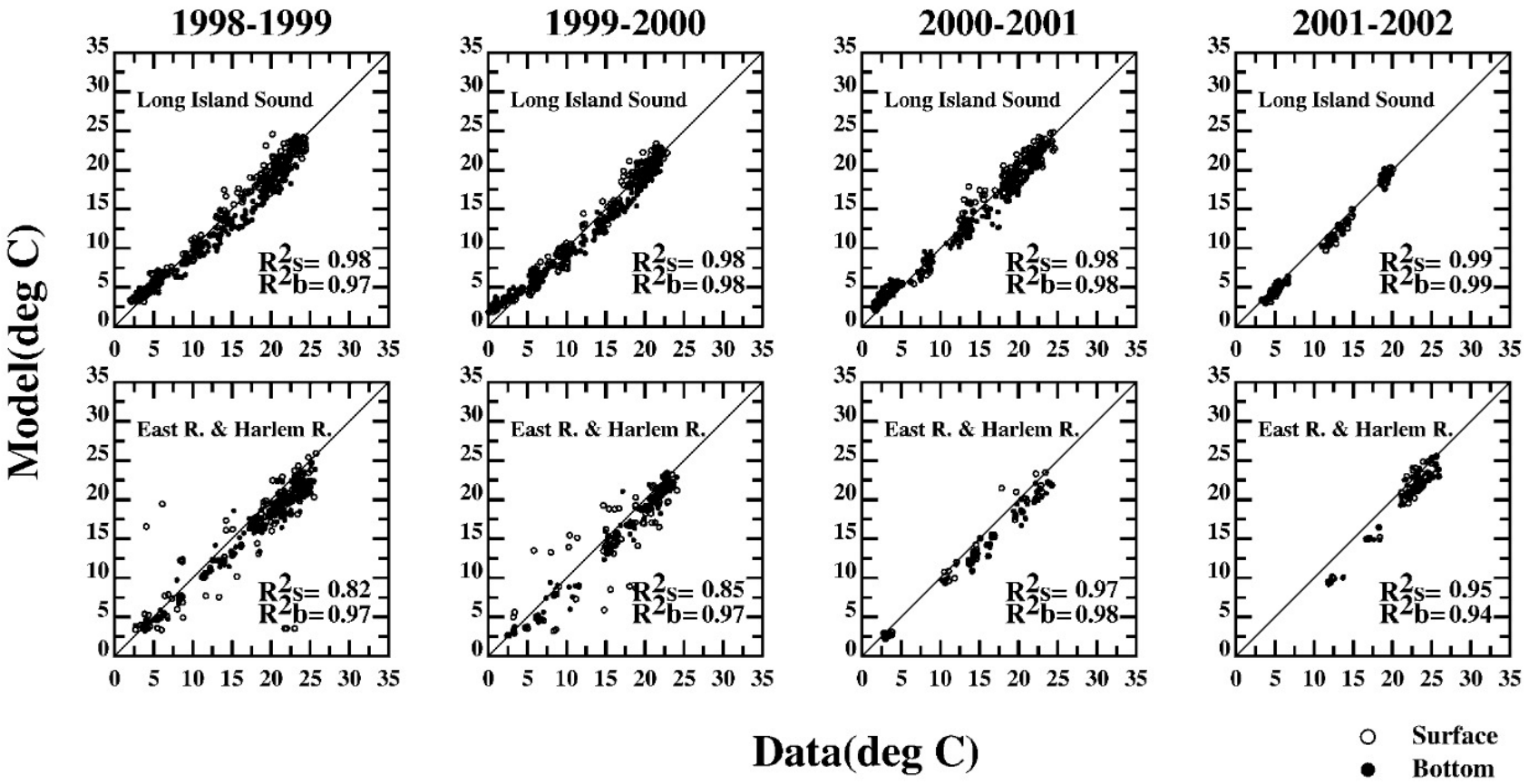

Figure 3-20a. Correlation analysis for temperature.

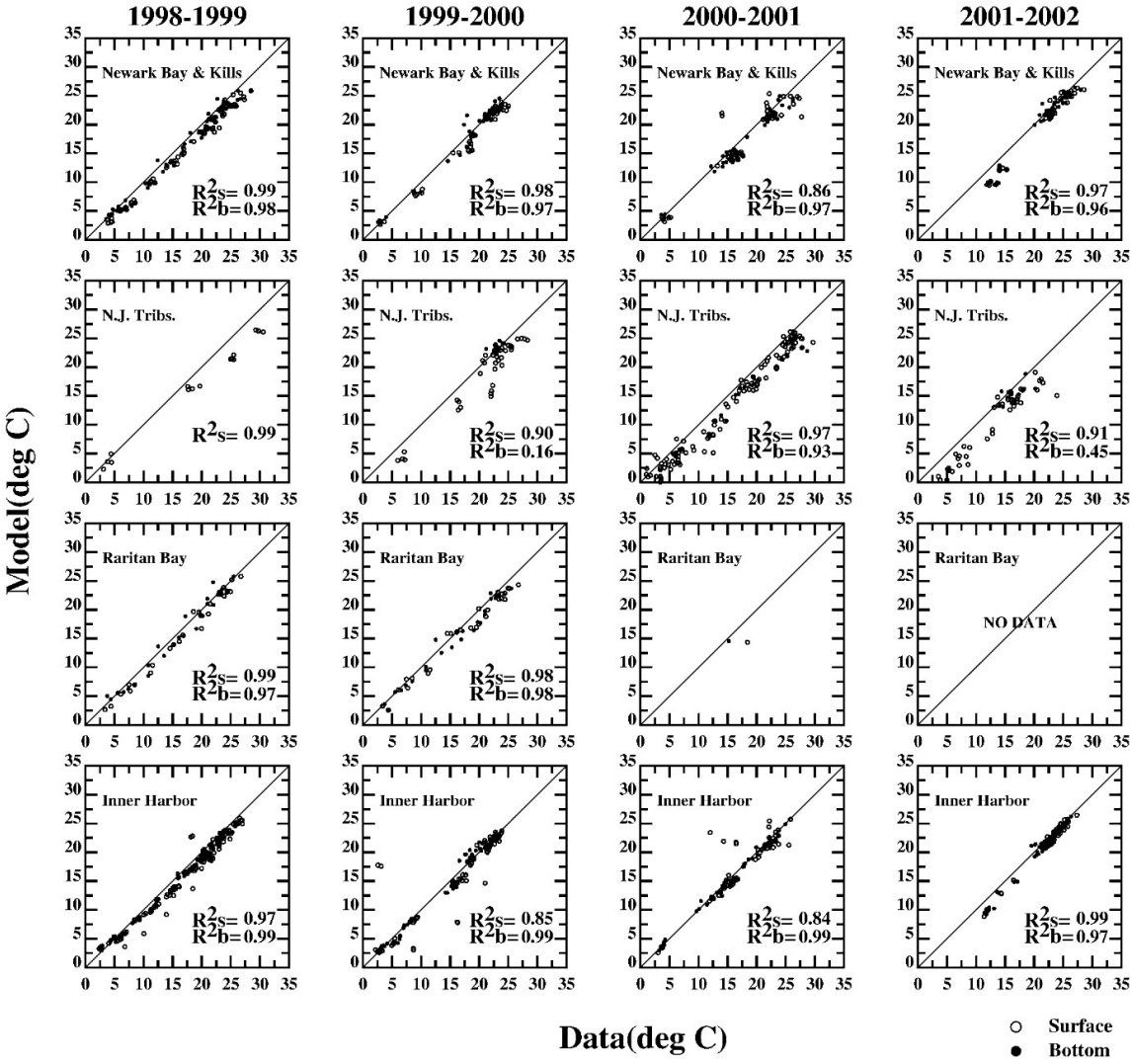

Figure 3-20b. Correlation analysis for temperature.

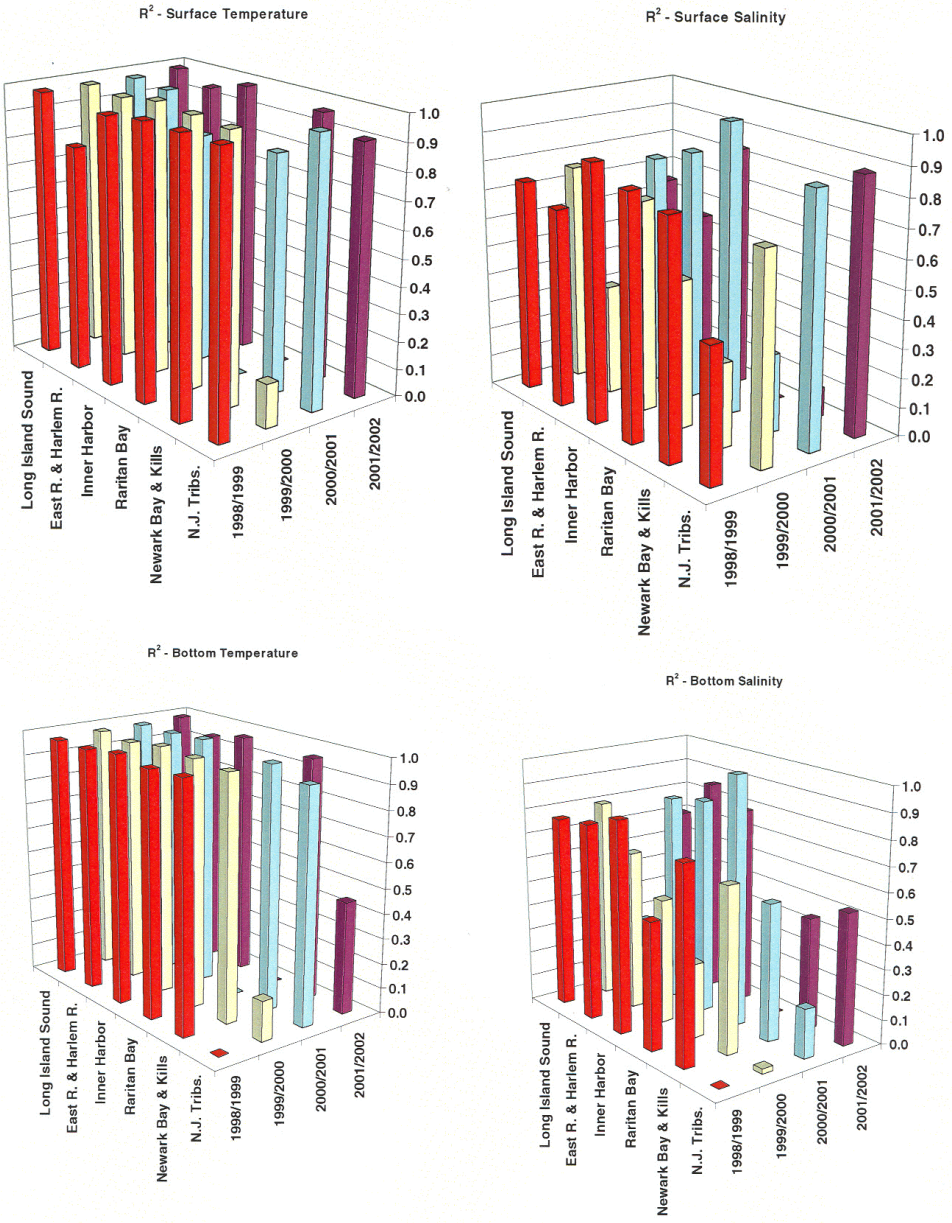

Figure 3-21. Correlation coefficients for temperature and salinity.

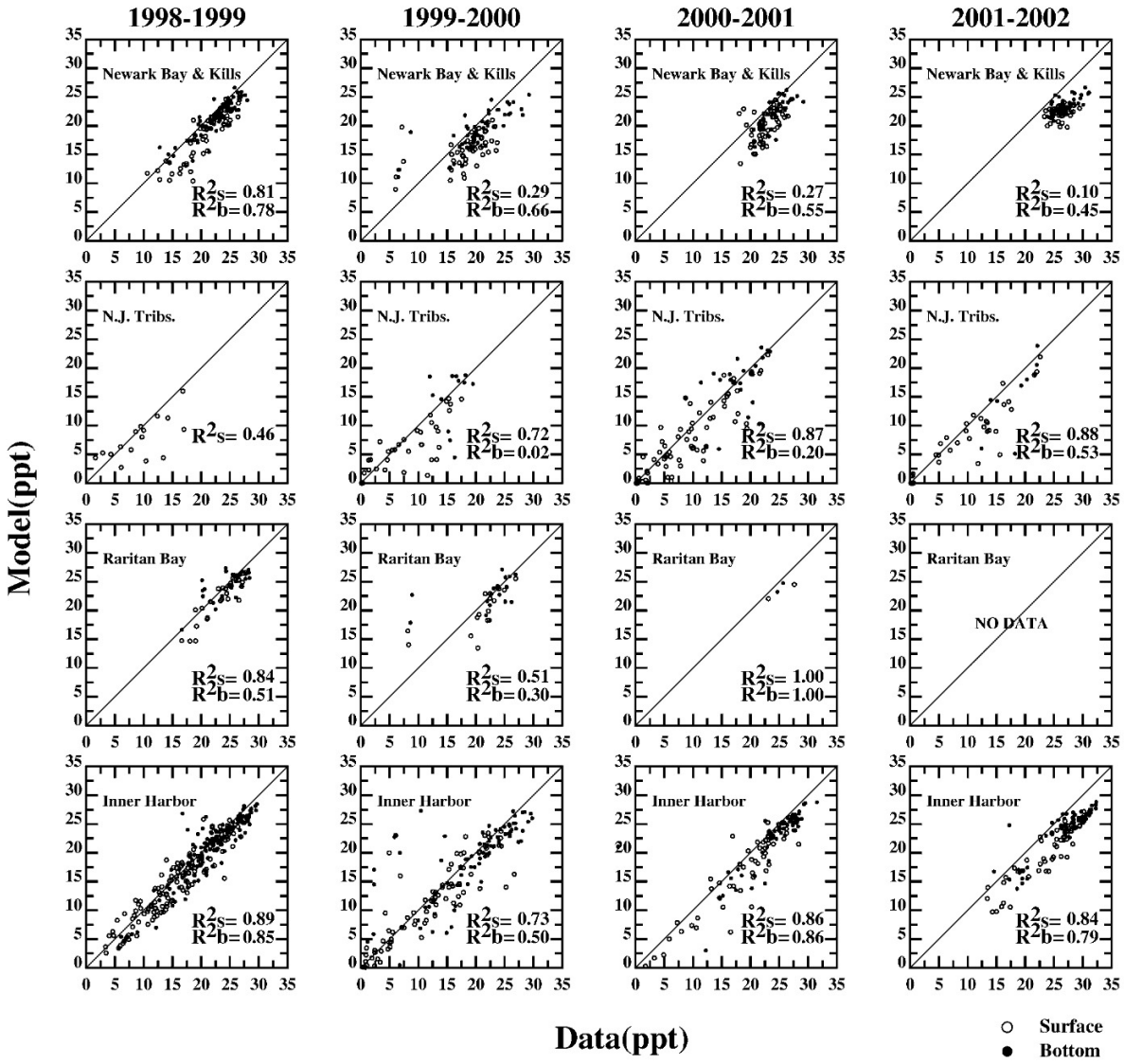

Figure 3-22a. Correlation analysis for salinity.

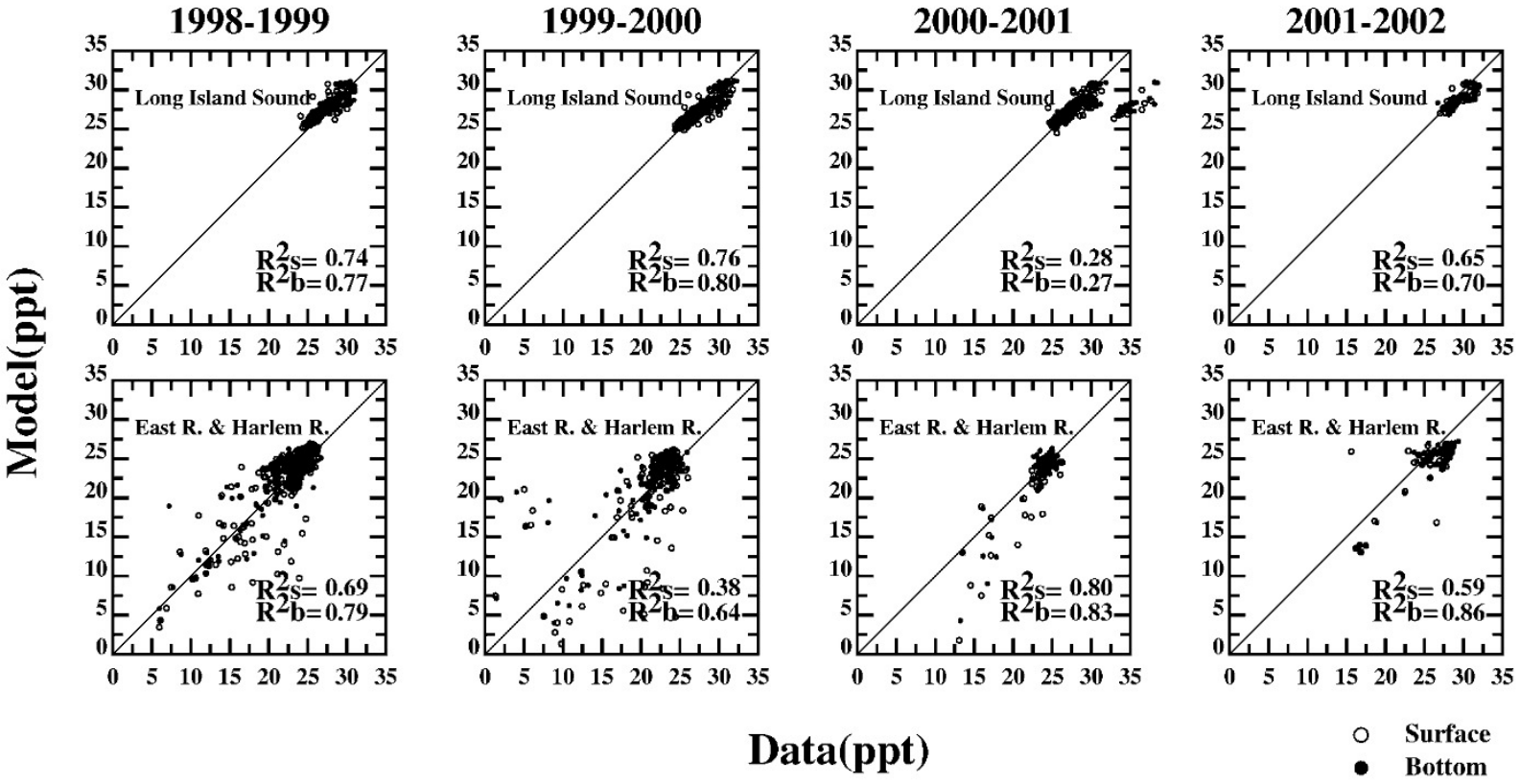

Figure 3-22b. Correlation analysis for salinity.

Table 3-1. Tabulation of Correlation Coefficients

Surface

R^2:Temperature	S	S	S	S
	1998/1999	1999/2000	2000/2001	2001/2002
Long Island Sound	0.98	0.98	0.98	0.99
East R. & Harlem R.	0.82	0.85	0.97	0.95
Inner Harbor	0.97	0.85	0.84	0.99
Raritan Bay	0.99	0.98	NO DATA	NO DATA
Newark Bay & Kills	0.99	0.98	0.86	0.97
N.J. Tribs.	0.99	0.9	0.97	0.91

Bottom

R^2:Temperature	B	B	B	B
	1998/1999	1999/2000	2000/2001	2001/2002
Long Island Sound	0.97	0.98	0.98	0.99
East R. & Harlem R.	0.97	0.97	0.98	0.94
Inner Harbor	0.99	0.99	0.99	0.97
Raritan Bay	0.97	0.98	NO DATA	NO DATA
Newark Bay & Kills	0.98	0.97	0.97	0.96
N.J. Tribs.	NO DATA	0.16	0.93	0.45

Surface

R^2:Salinity	S	S	S	S
	1998/1999	1999/2000	2000/2001	2001/2002
Long Island Sound	0.74	0.76	0.28	0.65
East R. & Harlem R.	0.69	0.38	0.8	0.56
Inner Harbor	0.89	0.73	0.86	0.84
Raritan Bay	0.84	0.51	1	NO DATA
Newark Bay & Kills	0.81	0.29	0.27	0.1
N.J. Tribs.	0.46	0.72	0.87	0.88

Bottom

R^2:Salinity	B	B	B	B
	1998/1999	1999/2000	2000/2001	2001/2002
Long Island Sound	0.77	0.8	0.27	0.7
East R. & Harlem R.	0.79	0.64	0.83	0.86
Inner Harbor	0.85	0.5	0.86	0.79
Raritan Bay	0.51	0.3	1	NO DATA
Newark Bay & Kills	0.78	0.66	0.55	0.45
N.J. Tribs.	NO DATA	0.02	0.2	0.53

In particular, Passaic River temperature data were collected during summer months only, creating a very narrow range in temperature measurements (i.e., 21-25°C). When statistics on the model and data comparisons were performed for the narrow range in data, small errors were exacerbated. The below shows the model and data comparisons for Passaic River temperature:

Surface		**Bottom**	
Model	**Data**	**Model**	**Data**
23.758	25.000	24.194	24.000
23.865	22.800	23.847	22.700
21.642	23.800	24.591	23.500
23.472	25.600	23.307	25.400
23.498	22.900	23.046	22.800
20.322	23.900	24.069	24.300
22.903	23.100	22.266	23.000
22.786	22.600	22.521	22.500
20.758	20.900	23.153	21.200
22.936	23.600	22.643	23.000
22.602	22.700	22.565	22.600
19.667	22.700	23.494	23.100

SECTION 4.0

LINKAGES TO OTHER CARP SUB-MODELS

In general, the CARP hydrodynamic sub-model calculates the water circulation and transport patterns that are passed to the other CARP sub-models on an hourly averaged basis. Transport information across each interface in the CARP model computational grid is passed to each sub-model through the use of an information file, a gcm_tran file, that is output by the hydrodynamic sub-model. Report sections 4.1 and 4.2 describe the content of a gcm_tran file and discuss the importance for modeling contaminant fate and transport of specific pieces of information contained in the gcm_tran file.

4.1 GENERAL INFORMATION PASSED TO CARP SUB-MODELS

The CARP hydrodynamic sub-model produces an output file which includes as time histories in three dimensions the calculated (i.e., one hour average) water depths, volume transport rates, dispersions, salt concentrations, and temperatures. The volume transport rates are reported in the longitudinal, lateral, and vertical directions. The dispersions are reported in the longitudinal and lateral directions as eddy viscosities and in the vertical direction as eddy diffusivities. Calculated water depths are tracked as changes in elevation over time.

4.2 SPECIFIC INFORMATION SHARED WITH CARP SUB-MODELS

The organic carbon production and contaminant fate and transport CARP sub-models rely upon temperature and salinity calculated by the hydrodynamic sub-model for calculating temporally and spatially varying values of various rate constants and kinetic coefficients which have temperature and/or salinity dependencies. These sub-models also reply upon the volume transport rates calculated by ECOM. Specifically for the calculation of suspended sediment, organic carbon, and other particulate matter transport, bottom shear stress provided by the hydrodynamic sub-model is of critical importance (i.e., bottom shear stress determines whether or not resuspension of particulate matter can occur). Bottom shear stresses in ECOM are typically calculated without considering the effects on bottom roughness of wind wave interactions with velocity currents. As part of the CARP specific application of ECOM, the effect of wave-current interaction on the bottom roughness coefficient is considered. Subsequent reports will described the CARP suspended sediment/organic carbon production sub-model in detail.

SECTION 5.0

REFERENCES

Beardsley, R.C. and W.C. Boicourt. 1981. On Estuarine and Continental-Shelf Circulation in the Middle Atlantic Bight. Evolution of Physical Oceanography, Scientific Surveys in Honor of Henry Stommel; B.A. Warren and C. Wunsch, Eds., The MIT Press, 198-233.

Beardsley, R.C. and B. Butman. 1974. Circulation on the New England Continental Shelf: Response to Strong Winter Storms. Geophysical Res. Let. 1(4).

Beardsley, R.C., D.C. Chapman, K.H. Brink, S.R. Ramp and R. Schlitz. 1985. The Nantucket Shoals Flux Experiment (NSFE79). Part I: A Basic Description of the Current and Temperature Variability. J. Phys. Oceanogr, (15) 713-748.

Beardsley, R.C. and C.D. Winant. 1979. On the Mean Circulation in the Middle Atlantic Bight. J. Phys. Oceanogr. 9.

Blumberg, A.F. and B. Galperin. 1990. On the Summer Circulation in New York Bight and Contiguous Estuarine Waters. In: Coastal and Estuarine Studies, Vol. 38, Residual Currents and Long-Term Transport, D.T. Cheng (Ed.), Springer-Verlag, New York.

Blumberg, A.F. and G.L. Mellor. 1980. A Coastal Ocean Numerical Model. In: Mathematical Modelling of Estuarine Physics. Proceedings of an International Symposium, Hamburg, August 24-26, 1978. J. Sundermann and K.P. Holz, Eds., Springer-Verlag, Berlin.

Blumberg, A.F. and L.Y. Oey. 1985. Modeling Circulation and Mixing in Estuaries and Coastal Oceans. Adv. In Geophysics, 28A.

Blumberg, A.F., L.A. Khan, and J.P. St. John. 1999. Three-Dimensional Hydrodynamic Model of New York Harbor Region. J. Hydraulic Engr., ASCE, 125(8): 799-816.

Brown, W.S., N.R. Pettigrew and J.D Irish. 1985. The Nantucket Shoals Flux Experiment (NSFE79). Part II: The Structure and Variability of Across-Shelf Pressure Gradients. J. Phys. Oceanogr., (15) 749-771.

Bumpus, D.F. 1969. Reversal in the Surface Drift in the Middle Atlantic Bight Areas,. Deep-Sea Res. 16 (suppl.).

Chapman, J., A. Barth, R.C. Beardsley and R.G. Fairbanks. 1986. On the Continuity of Mean Flow Between the Scotian Shelf and the Middle Atlantic Bight. J. Phys. Oceangr., 16.

Egbert, G.D., A.F. Bennett and M.G.G Forman. 1994. TOPE/POSEISON Tides Estimated Using a Global Inverse Model. J. Geophy. Res., 99 (C12), 24, 821-852.

Garvine, R.W., K.-C. Wong, G.G. Gawarkiewicz, R.K. McCarthy, R.W. Houghton and F. Aikman III. 1988. The Morphology of Shelf-Break Eddies. J. Geo. Res., 93, 15, December 1988, pp. 593, 607.

Han, G., D.V. Hansen and J.A. Galt. 1980. Steady-State Diagnostic Model of the New York Bight. J. Phys. Oceanogr., 10.

Hopkins, T.S. and D.A. Dieterle. 1983. An Externally Forced Barotropic Circulation Model for the New York Bight. Cont. Shelf Res., 2.

Hopkins, T.S. and D.A. Dieterle. 1987. Analysis of the Baroclinic Circulation of the New York Bight with a 3-D Diagnostic Model. Cont. Shelf Res., (7): 237-265.

HydroQual, Inc. 1999a. Newton Creek Water Pollution Control Project East River Water Quality Plan, Report to NYCDEP. Task 10.0 System-Wide Eutrophication Model (SWEM) Sub-task 10.1 Construct SWEM. Prepared under subcontract to Greeley and Hansen, New York, NY.

HydroQual, Inc. 1999b. Newton Creek Water Pollution Control Project East River Water Quality Plan, Report to NYCDEP. Task 10.0 System-Wide Eutrophication Model (SWEM) Sub-task 10.2 Obtain and Reduce Loading/Water Quality Data. Prepared under subcontract to Greeley and Hansen, New York, NY.

HydroQual, Inc. 1999c. Newton Creek Water Pollution Control Project East River Water Quality Plan, Report to NYCDEP. Task 10.0 System-Wide Eutrophication Model (SWEM) Sub-task 10.3 Calibrate SWEM Hydrodynamics. Prepared under subcontract to Greeley and Hansen, New York, NY.

HydroQual, Inc. 1999d. Newton Creek Water Pollution Control Project East River Water Quality Plan, Report to NYCDEP. Task 10.0 System-Wide Eutrophication Model (SWEM) Sub-task 10.6 Validate SWEM Hydrodynamics. Prepared under subcontract to Greeley and Hansen, New York, NY.

HydroQual, Inc. 2002. Calibration Enhancement of the System-Wide Eutrophication Model (SWEM) in the New Jersey Tributaries, Report to NJDEP. Final Technical Report April 23, 2001 through July 31, 2002. Prepared under subcontract to Passaic Valley Sewerage Commissioners, Newark, NJ.

Jay, D.A., M.J. Bowman. 1975. The Physical Oceanography and Water Quality of New York Harbor and Western Long Island Sound. Tech. Rpt. 23, Marine Sciences Research Center, State University of New York at Stony brook.

Joyce, T.M. (Editor). 1985. Warm-Core Rings Collection. J. Geophys. Res. (Special Section), (90) 8801-8951.

Mayer, D.A., G.C. Han and D.V. Hansen. 1982. The Structure of Circulation: MESA Physical Oceanographic Studies in New York Bight, 2, J. Geophys. Res., (87) 9579-9588.

NOAA, 1998. World Ocean Atlas.

Oey, L.Y., G.L. Mellor and R.I. Hires. 1985a. Tidal Modeling of the Hudson Raritan Estuary. Estuarine Coastal Shelf Science (20) 511-527.

Oey, L.Y., G.L. Mellor and R.I. Hires. 1985b. A Three Dimensional Simulation of the Hudson-Raritan Estuary. Part I: Description of the Model and Model Simulations, Journal of Physical Oceanography, (15) 1676-1692.

Oey, L.Y., G.L. Mellor and R.I. Hires. 1985c. A Three Dimensional Simulation of the Hudson-Raritan Estuary. Part II: Comparison with Observations, Journal of Physical Oceanography, (15) 1693-1709.

Scheffner, N.W., S.R. Vermulakonda, D.J. Mark, H.L. Butler and K.W. Kim. 1994. New York Bight Study, Report 1: Hydrodynamic Modeling, Tech-Rept. CERC-94-4, U.S. Army Corps of Engineers, Vicksburg, MS.

Schmalz, Jr.., R.A., M.F. Devine and P.H. Richardson. 1994. Long Island Sound Oceanography Project, Summary Report, volume 2: Residual Circulation and Thermohaline Structure, NOAA Tech. Rpt. NOSOES 003, Silver Spring, Maryland.

APPENDIX 1

SWEM HYDRODYNAMICS PAPER

THREE-DIMENSIONAL HYDRODYNAMIC MODEL OF NEW YORK HARBOR REGION

By Alan F. Blumberg,[1] Liaqat Ali Khan,[2] P.E., and John P. St. John,[3] P.E.

ABSTRACT: Three-dimensional simulations of estuarine circulation in the New York Harbor complex, Long Island Sound, and the New York Bight have been conducted using the Estuarine, Coastal and Ocean Model (ECOM) within the framework of a single grid system. The model grid is curvilinear and orthogonal, with resolution from 100 m in rivers to about 50 km in the bight. The model forcing functions consist of (1) meteorological data; (2) water level elevation and temperature and salinity fields along the open boundary; and (3) freshwater inflows from 30 rivers, 110 wastewater treatment plants, and 268 point sources from combined sewer overflows and surface runoffs. Because the goal of this study is to maximize, to the extent possible, the predictive skill of the modeling system, the motivation for and a detailed description of the construction of these boundary forcing functions are presented. Two 12-month periods are considered: (1) October 1988 to September 1989 for model calibration; and (2) October 1994 to September 1995 for model validation. For model calibration, the results are compared with water levels at 14 stations, currents at six stations, and temperature and salinity at 35 stations. Model validation is accomplished using data from an extensive hydrodynamic monitoring program. Mean errors in predicted elevations and currents are less than 10% and 15%, respectively. Correlation coefficients for salinity and temperature are as high as 0.86 and 1.0, respectively. The level of skill shown by these statistical measures suggests that the model is capable of describing the entire spectrum of time scales for the computed quantities, from the semidiurnal to the annual scales.

INTRODUCTION

Hydrodynamic and water quality investigations of New York Harbor, Long Island Sound, and New York Bight have attracted the attention of citizens concerned with environmental quality and federal, state, and local authorities. It is in part prompted by concern over water quality management, and in part due to the desire to better understand the estuarine circulation and mixing produced by wind, tidal forcing, and freshwater inflows in the presence of varying topography. Numerous papers and reports have been published on the tides, currents, hydrography, and hydrology of this area. Jay and Bowman (1975) have reviewed the hydrodynamics and water quality of this region from 1848 to the early 1970s. A comprehensive discussion on the circulation in the New York Bight and surrounding coastal waters can be found in Beardsley and Boicourt (1981). Field experiments (Beardsley et al. 1985; Brown et al. 1985; Joyce 1985; Chapman et al. 1986) have added a wealth of information on the circulation patterns. Based upon these field experiments, the characteristic feature of the circulation in the New York Bight is a southwestward mean flow along the shelf of roughly 2–10 $cm \cdot s^{-1}$ with a mean transport of the order of 250,000 $m^3 \cdot s^{-1}$.

A large number of numerical model studies of the New York Bight have been reported. Diagnostic studies of the mean barotropic and baroclinic circulation in the New York Bight have been conducted by Han et al. (1980) and Hopkins and Dieterle (1983, 1987). Simulation of the long-term mean circulation in the Middle Atlantic Bight has been reported by Blumberg and Mellor (1980). Their main conclusion was that the presence of the Gulf Stream is an important factor for the circulation along the continental shelf in the New York Bight. Blumberg and Galperin (1990) simulated the summer circulation in the New York Bight and contiguous estuarine waters by focusing on the importance of the coupling between New York Bight and Long Island Sound. Buoyancy and wind induced circulations in the New York Bight have also been analyzed by Oey et al. (1995). In these studies, climatological forcing functions were used to understand the main features of the mean circulation pattern.

Recently, Scheffner et al. (1994) have reported the development of a coupled three-dimensional model of New York Bight, Long Island Sound, and New York Bay. Model calibration and validation were performed for short periods (a few months) using limited data sets. Discrepancies between the model and data (for currents, salinity, and temperature) are quite high. Oey et al. (1985) have reported a numerical model of New York Harbor, comparing model results with short-term data for model calibration. Blumberg and Prichard (1997) have concentrated on the East River, which connects New York Harbor to Long Island Sound, in an attempt to estimate mass transports through the system. Numerical models of Long Island Sound, a comparison of model results with data, and analyses of the residual circulation can be found in Schmalz et al. (1994). In these studies, only parts of New York Harbor, Long Island Sound, and New York Bight are considered. Consequently, interactions between the interconnected water bodies became difficult to analyze.

In the present study, a three-dimensional hydrodynamic model of the New York Harbor, Long Island Sound, and the New York Bight is presented within the framework of a single model. Figs. 1(a) and 1(b) show the model domain and the horizontal, orthogonal curvilinear grid system employed in the current study. The model is driven by water level, meteorological forcing, spatially and temporally varying surface heat flux, and freshwater fluxes from 30 rivers, 110 wastewater treatment plants, and 268 point sources of combined sewer overflows and storm runoffs. Salinity and temperature boundary conditions are, however, partially derived from climatological data. Two 12-month modeling periods, October 1988 to September 1989 and October 1994 to September 1995, are considered. Model skill assessment for the two significantly different hydrologic years consists of comparing water levels at 19 stations, currents at 12 locations, and salinity and temperature at 37 locations distributed throughout the model domain. Performance of the model is also quantified in terms of root-mean square (RMS) errors and correlation coefficients following suggestions of the ASCE Task Committee (1988). Considerable effort has been devoted to developing model

[1]PhD, Exec. Vice Pres. and Prin. Sci., HydroQual, 1 Lethbridge Plaza, Mahwah, NJ 07430.

[2]PhD, Proj. Engr., HydroQual, 1 Lethbridge Plaza, Mahwah, NJ.

[3]Prin. Engr., HydroQual, 1 Lethbridge Plaza, Mahwah, NJ.

Note. Discussion open until January 1, 2000. To extend the closing date one month, a written request must be filed with the ASCE Manager of Journals. The manuscript for this paper was submitted for review and possible publication on April 6, 1998. This paper is part of the ***Journal of Hydraulic Engineering***, Vol. 125, No. 8, August, 1999. ©ASCE, ISSN 0733-9429/99/0008-0799–0816/$8.00 + $.50 per page. Paper No. 18077.

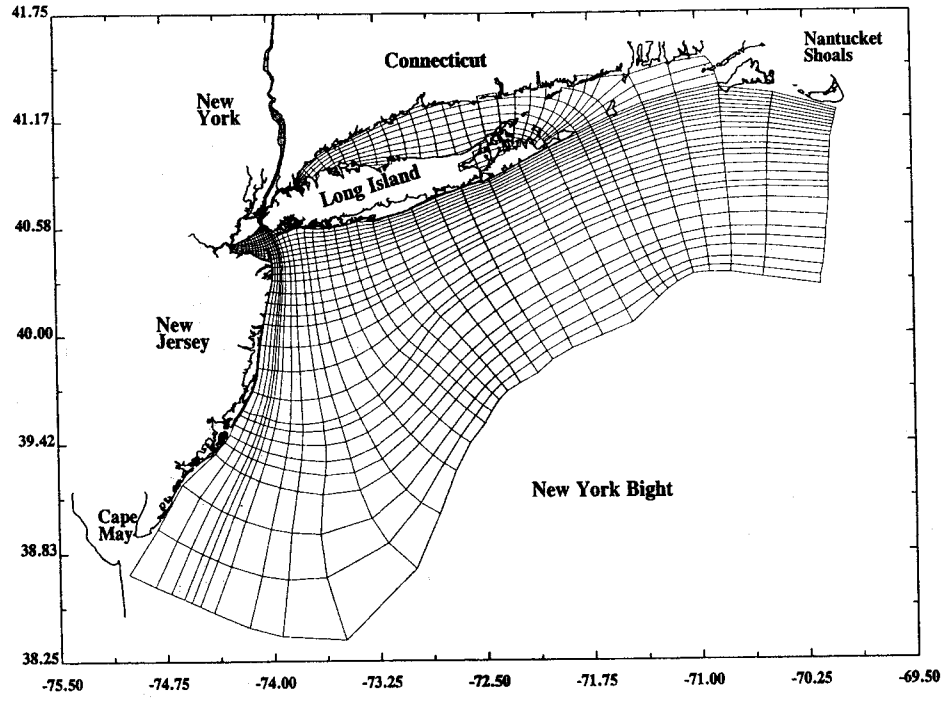

FIG. 1(a). Model Domain and Orthogonal Curvilinear Coordinate System

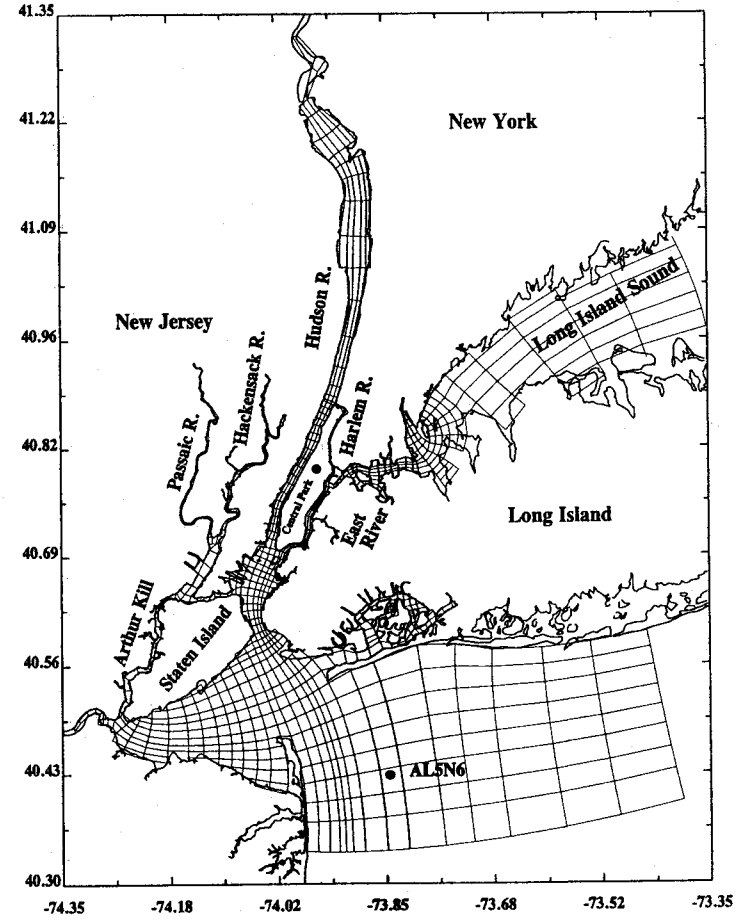

FIG. 1(b). Model Grid of Hudson River, East River, New York Bay, Raritan Bay, and Apex of New York Bight

forcing functions and assessing model skill, because a goal of the present study is to as accurately as possible predict the hydrodynamic behavior of the system. The study indicates that accurate estimation of relevant sources of freshwater significantly enhances the ability of the model to predict salinity.

The present study is one of the first attempts to model such a complex estuarine system and the contiguous continental shelf as a coupled hydrodynamic and thermodynamic system over annual cycles. Calibration and validation of large-scale hydrodynamic models over annual cycles are rare. An example of a similar attempt for a much smaller system, the Chesapeake Bay, is given in Johnson et al. (1993). In the context of hydraulic engineering, most of the three-dimensional models incorporating second-order turbulent closure schemes have been applied to small-scale problems (Cokljat and Younis 1995; Ouillon and Dartus 1997; Sinha et al. 1998) for investigating local phenomena.

MODEL DESCRIPTION

The hydrodynamic model used in the present study is a three-dimensional, time-dependent model developed by Blumberg and Mellor (1980, 1987). This model, called Estuarine, Coastal and Ocean Model (ECOM), has a long history of successful applications to oceanic, coastal, and estuarine waters. Some recent applications of the model include the Chesapeake Bay (Blumberg and Goodrich 1990), New York Bight (Blumberg and Galperin 1990), Delaware Bay and Delaware River (Galperin and Mellor 1990), Gulf Stream region (Ezer and Mellor 1992), Massachusetts Bay (Blumberg et al. 1993), Georges Bank (Chen and Beardsley 1995), and the Oregon continental shelf (Allen et al. 1995).

The numerical model solves a coupled system of differential, prognostic equations describing conservation of mass, momentum, heat, and salt. The governing equations in terms of velocity $U_i = (U, V, W)$, temperature T, and salinity S are (Blumberg and Mellor 1980, 1987) as follows:

$$\frac{\partial U_i}{\partial x_i} = 0 \tag{1}$$

$$\frac{\partial}{\partial t}(U, V) + \frac{\partial}{\partial x_i}[U_i(U, V)] + f(-V, U) = -\frac{1}{\rho_o}\left(\frac{\partial P}{\partial x}, \frac{\partial P}{\partial y}\right) + \frac{\partial}{\partial z}\left[K_M \frac{\partial}{\partial z}(U, V)\right] + (F_U, F_V) \tag{2}$$

$$\frac{\partial T}{\partial t} + \frac{\partial}{\partial x_i}(U_i T) = \frac{\partial}{\partial z}\left(K_H \frac{\partial T}{\partial z}\right) + F_T \tag{3}$$

$$\frac{\partial S}{\partial t} + \frac{\partial}{\partial x_i}(U_i S) = \frac{\partial}{\partial z}\left(K_H \frac{\partial S}{\partial z}\right) + F_S \tag{4}$$

The hydrostatic approximation yields

$$\frac{P}{\rho_o} = g(\eta - z) + \int_z^\eta g \frac{\rho' - \rho_o}{\rho_o} dz' \tag{5}$$

where $\eta(x, y, t)$ = water level; P = pressure; f = Coriolis parameter; ρ_o = reference density; and ρ = density, which is a function of S and T, as defined in Fofonoff (1962).

The vertical mixing coefficients K_M and K_H in (2)–(4) are calculated using the Mellor and Yamada (1982) turbulence closure scheme, as modified by Galperin et al. (1988) and Blumberg et al. (1992). The terms (F_U, F_V), F_T, and F_S are related to small-scale mixing processes not directly resolved by the model. They are parameterized as horizontal diffusion in terms of the Smagorinsky (1963) horizontal diffusion formulation. This parameterization contains two coefficients, A_M for F_U and F_V, and A_H for F_T and F_S, which are functions of an adjustable parameter C_S. An additional adjustable parameter is the bottom frictional drag coefficient, C_D, relating bottom stress to bottom velocity. Recently, Davis et al. (1997) have reviewed the developments of turbulence closure schemes in the context of hydrodynamic models.

Eqs. (1)–(4) are transformed to an orthogonal curvilinear coordinate system in the horizontal plane. They are further transformed to a bottom and free surface following the σ coordinate system in the vertical plane. The model recognizes fast, barotropic external waves and slow, baroclinic internal waves, and solves corresponding barotropic and baroclinic equations with different time steps. Further details of the numerical model can be found in Blumberg and Mellor (1980, 1987).

The model domain and the orthogonal curvilinear grid system used in the present study are shown in Figs. 1(a) and 1(b). The grid consists of 49 × 84 segments in the horizontal plane, and 11 σ levels in the vertical plane. The model domain encompasses New York Bight from Cape May, N.J. to Nantucket Shoals off the coast of Massachusetts, Long Island Sound, New York Harbor, and the adjoining rivers in New York and New Jersey, as shown in Fig. 1(a). The model grid of the Hudson River extends to the dam at Troy, N.Y. The open boundary follows the 100 m isobath along the continental shelf break. The resolution of the computational grid varies from 100 m in the rivers to about 50 km in the New York Bight. The depth of the water column varies from approximately 150 m to less than 2 m. A computational time step of 50 s was used for the external mode, while the internal mode used 500 s.

MODEL FORCING FUNCTIONS

In the last two decades, significant progress has been made in three-dimensional, time-dependent, numerical modeling of geophysical systems. Models such as ECOM have combined sophisticated physics with highly accurate numerical procedures. Therefore, in many cases, specification of proper boundary conditions determines the success of the model application. This is especially true when data for boundary conditions are not directly available. At present, there is no uniform practice in specifying necessary and sufficient boundary conditions for hydrodynamic models. Therefore, the ASCE Task Committee (Wang et al. 1990) suggested that all "boundary conditions be accurately stated with their associated assumptions."

In this section, boundary conditions and model forcing functions for the simulation periods of October 1988 to September 1989 and October 1994 to September 1995 are presented. The first modeling period was selected for model calibration using data available from a previous study ("Newtown" 1995). In the latter simulation period, a field program was conducted so that the hydrodynamic model could be throughly validated.

Elevation Boundary Condition

Measured elevation data are not available for specifying boundary conditions in this model domain. Therefore, as an approximation, the sea surface elevation $\eta(x_b, t)$, where x_b and t are open ocean boundary and time, respectively, is assumed to be composed of three parts. The first part drives the long-term circulation (geostrophic currents) due to the cross-shelf climatological slope $[\eta_G(x_b, t)]$, the second part deals with the tidal fluctuations $[\eta_T(x_b, t)]$, and the third part represents subtidal (meteorological) forcing $[\eta_M(t)]$. The resulting water level is expressed as

$$\eta(x_b, t) = \eta_G(x_b) + \eta_T(x_b, t) + \eta_M(t) \tag{6}$$

The effect of the cross-shelf elevation gradient imposed at the shelf break by the large-scale offshore circulation has been studied by Hopkins and Dieterle (1983). They found that the

elevation gradient across the shelf affects the total transport through the cross-shelf boundaries. For a typical summertime period, a gradient of 13 cm across a Narragansett Bay shelf-break section and an 11 cm gradient across a Cape May shelf-break section could produce the observed summer along-shelf flux of water. Following their findings, Blumberg and Galperin (1990) used the same boundary elevation for analyzing summer circulations in the New York Bight. These gradients have been adopted in the present study.

The astronomical tide, $\eta_T(x, t)$, due to the eight primary harmonic constituents (M_2, S_2, N_2, K_2, O_1, P_1, and Q_1) was obtained from a global model of ocean tides, TPX0.2, developed by Oregon State University (Egbert et al. 1994). This model covers the globe on a 512 × 256 grid.

Most of the previous models of New York Bight have been driven by either cross-shelf slopes (Blumberg and Galperin 1990) or astronomical tides (Scheffner et al. 1994; Oey et al. 1995) only. In the present study, the influence of the offshore meteorological conditions is also incorporated into the boundary condition. Wong (1990) has analyzed variations of subtidal water levels in the Long Island Sound, including Montauk and Sandy Hook (Fig. 2 shows locations of these stations). An analysis similar to that of Wong (1990) for data at Montauk, Sandy Hook, Atlantic City, and Cape May indicates that the response of the water surface to meteorological forcing is essentially in phase throughout the New York Bight and the adjacent estuarine waters. The differences in amplitude and phase at different locations, due to the local bathymetry and coastline, are small. Therefore, in the current study the meteorological component of the water level, $\eta_M(t)$, is expressed as

$$\eta_M(t) = \alpha \eta_{SH}(t) \tag{7}$$

where α = additional calibration parameter; and $\eta_{SH}(t)$ is taken as the 34-h low-passed water level at Sandy Hook. The parameter α is expected to have a value less than one because the amplitude of the wave is amplified by shoaling and shallow water effects as it propagates over the continental shelf toward the coastline.

Salinity and Temperature Boundary Conditions

For 1988–89, temperature and salinity boundary conditions were extracted from the climatological data set constructed by Levitus (1984). This data set contains gridded monthly data at 1° latitude-longitude intervals. At each point, data are tabulated at 19 levels from 0 to 1,000 m. Climatological data, of course, do not represent true monthly variations of temperature and salinity for a particular simulation period. Therefore, boundary conditions based on the work of Levitus (1984) were adjusted so that computed temperature and salinity approximately matched the observed 1988–89 monthly mean temperature and salinity data in Long Island Sound and New York Harbor. The boundary condition adjustments are

$$S(x, t) = S_L(x, t) - 2.0; \quad T(x, t) = T_L(x, t) - 2.0 \tag{8}$$

where S_L and T_L = climatological salinity and temperature in ppt and °C from Levitus (1984).

During 1994–95, salinity and temperature data were collected at three moorings along the open boundary of the model. However, these data contain gaps that were filled with the climatological data (Levitus 1984). The reconstructed data were smoothed to remove any discontinuity between the measured and climatological data.

Meteorological Forcing Function

Two major boundary forcing functions applied at the water surface are the heat flux and the wind stress. The heat flux computation requires the specification of the air temperature, relative humidity, barometric pressure, wind speed, shortwave solar radiation, and cloud cover (Rosati and Miyakoda 1988). Hourly meteorological data for these quantities were obtained from the National Oceanic and Atmospheric Administration (NOAA) at Central Park, N.Y. and a buoy (AL5N6) at the apex of New York Bight. Data from Central Park were used for the heat flux computation. The wind stress computed from buoy wind speed and direction was applied only to New York Bight and Long Island Sound. In the rest of the domain the wind stress resulting from data recorded at Central Park was used. The wind speed at the offshore buoy is, in general, higher. The ratio of yearly mean wind speed at the buoy to Central Park is 1.75. For 1988–89 and 1994–95, the yearly mean shortwave solar radiation is 158 and 148 $W \cdot m^{-2}$, respectively. Therefore, the 1988–89 simulation period was a relatively warmer year.

Freshwater Inflow

Freshwater inflows from 30 rivers and tributaries are considered in the modeling framework. Daily discharge data were compiled from U.S. Geological Survey (USGS) surface water records for New York, New Jersey, and Connecticut. The annual mean flows from all of the rivers are 1,420 and 870 $m^3 \cdot s^{-1}$ for the simulation periods 1988–89 and 1994–95, respectively. Thus, in 1994–95, the freshwater inflow into the model domain is approximately 40% smaller. The Connecticut River has the highest discharge, followed by the Hudson River. The mean flow of the Hudson is about 65% that of the Connecticut River. Temperature specified for the river inflows is based on historical data analyzed by Ashizawa and Cole (1994). Riverine water temperature for both of the simulation periods varied from 1°C to 25°C.

Two other sources of freshwater are from wastewater treatment plants and storm-water runoffs. Effluents from 110 wastewater treatment plants are included in the model. Temperature and discharge data were obtained from the Interstate Sanitation Commission. The total effluent from the treatment plants is 114 $m^3 \cdot s^{-1}$, and temperature varied from 11°C to 12°C. Surface runoffs, including combined sewer overflows, from catchments adjacent to the model domain were computed through the use of the Storm-Water Management Model (SWMM). These point sources of freshwater were distributed over 268 computational cells. These runoffs are highly transient, and are a function of rainfall intensity. Temperature for these runoffs is taken as that of the river inflows.

INITIAL CONDITIONS

To start the computations, it is necessary to specify initial conditions for elevation, velocity, salinity, and temperature. Three-dimensional initial conditions for salinity and temperature were constructed from climatological data of Levitus (1984), which are tabulated on a 1° square grid. They were supplemented by field measurements in 1994–95. For both of the simulation periods, initial water surface was assumed horizontal, and velocity components were set to zero through the model domain. To remove the effects of approximate initial conditions, the model was run for one year, and model results were compared with measurements in the second year of computations.

MODEL SKILL ASSESSMENT

An extensive set of data for the 1988–89 simulation period were available ("Newtown" 1995) for model calibration. These data were collected from agencies, including the NOAA and the Department of Environmental Protection of New York, New Jersey, and Connecticut. As part of the present study, a year-long field program from October 1994 to September 1995

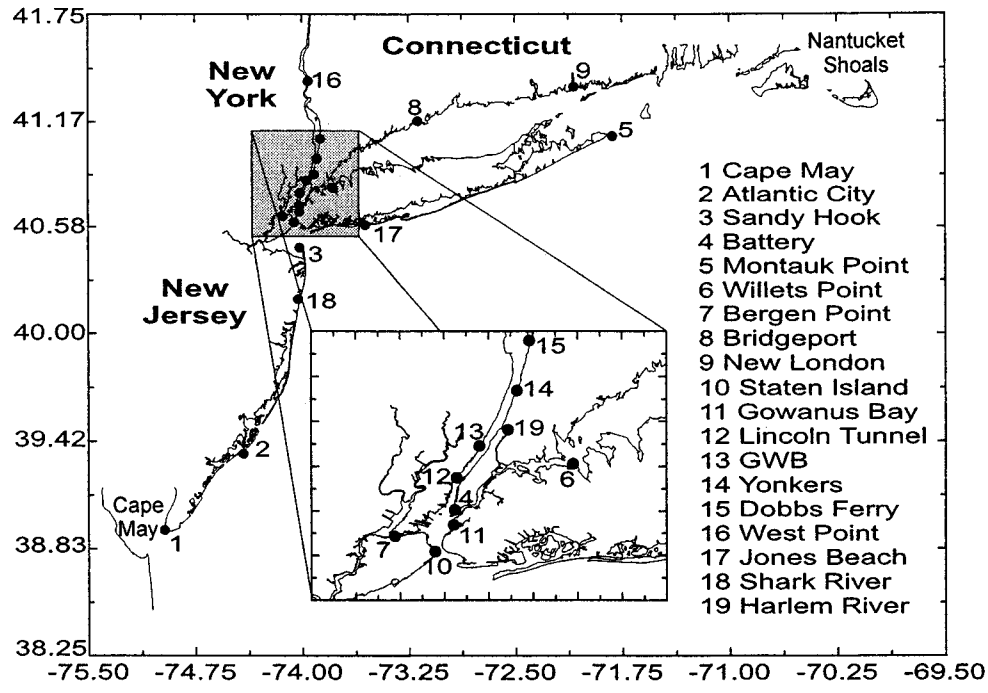

FIG. 2. Locations of Tide Gauges

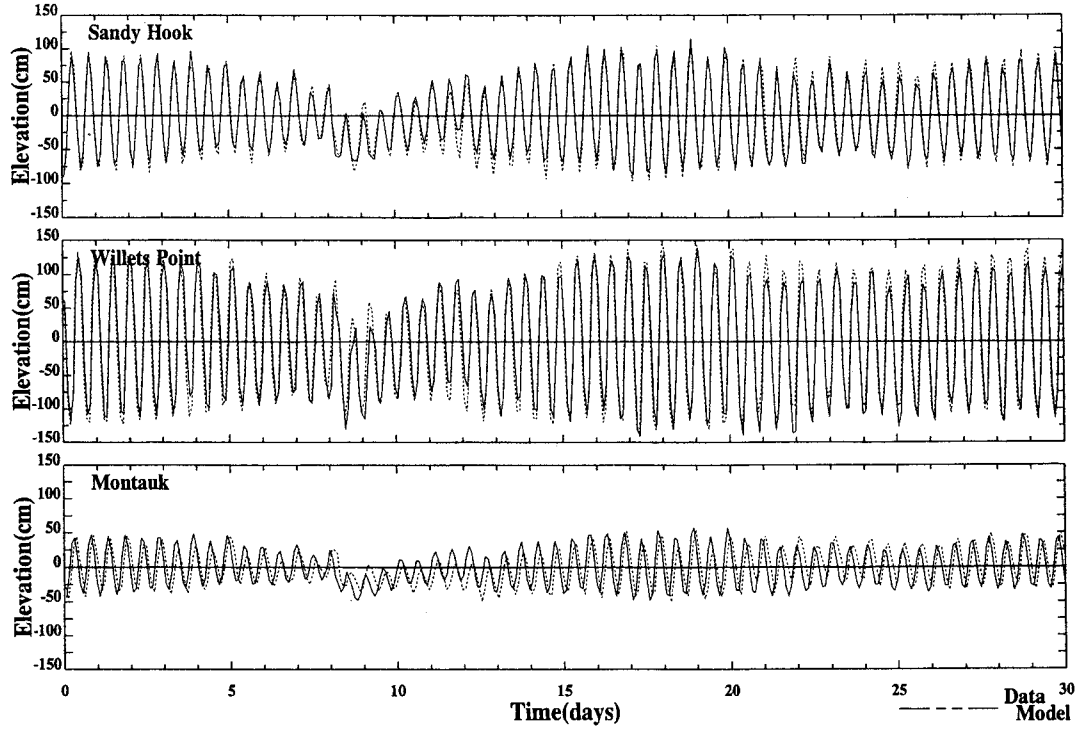

FIG. 3. Comparison of Instantaneous Water Levels in April 1995

was conducted. A total of 16 stations in the New York Harbor, Long Island Sound, and New York Bight were instrumented. A description of the Acoustic Doppler Current Profiler (ADCP) deployments and data collection procedure can be found in Coomes (1996).

The model was calibrated by adjusting (1) the inverse shoaling coefficient, α, defined by (7); (2) the subgrid scale horizontal mixing coefficient, C_S, defined by Smagorinsky's horizontal diffusion parameterization in (2)–(4); and (3) the bottom frictional drag coefficient, C_D. These coefficients are adjusted to reproduce measured tidal elevations, currents, salinity, and temperature in 1988–89. Initial runs were made using α = 1.0, 0.75, 0.50, and 0.25. Comparisons of 34-h low-passed water levels suggest that α = 0.50 provides the best match between the model and data at all of the tide gauges. With this value of α, additional model runs were made for different values of C_S and C_D.

During the calibration process, it was observed that the model consistently overestimated monthly mean salinity and temperature in the Long Island Sound and New York Harbor. Various reasons for the discrepancy were investigated. Finally, it was concluded that the climatological data (Levitus 1984) were too different from the actual salinity and temperature conditions in the New York Bight during 1988–89. Therefore,

TABLE 1. Statistical Evaluation of Model Performance for Instantaneous Elevation

Number (1)	Station (2)	Number of data (3)	Data range (cm) (4)	RMS error (%) (5)	Correlation coefficient (6)
1	Cape May	8,640	165.8	9.2	0.97
2	Atlantic City	8,640	147.8	9.5	0.96
3	Sandy Hook	8,640	173.1	7.6	0.97
4	The Battery	8,640	166.4	7.3	0.97
5	Montauk	5,682	80.5	29.8	0.60
6	Willets Point	8,640	254.5	10.5	0.95
7	Bergen Point	8,640	183.2	8.1	0.97
8	Bridgeport	8,640	236.5	8.2	0.97
9	New London	8,640	96.3	11.1	0.94
10	Staten Island	8,739	157.3	8.5	0.97
11	Gowanus Bay	6,794	140.0	9.6	0.97
12	Lincoln Tunnel	6,733	154.0	11.9	0.92
13	GWB	2,878	110.0	9.5	0.98
14	Yonkers	6,802	93.0	10.4	0.98
15	Dobbs Ferry	6,786	129.0	10.0	0.97
16	West Point	7,833	97.6	17.2	0.93
17	Jones Inlet	7,823	147.3	11.3	0.94
18	Shark River	7,814	164.4	13.4	0.90
19	Harlem River	7,854	138.3	9.9	0.95
[Maximum]	—	—	254.5	29.8	0.98
[Minimum]	—	—	80.0	7.6	0.60
[Mean]	—	—	149.2	11.2	0.94

TABLE 2. Statistical Evaluation of Model Performance for Subtidal Elevation Variations

		34-h Low-Passed Water Level		Five-Day Low-Passed Water Level	
Number (1)	Station (2)	RMS error (cm) (3)	Correlation coefficient (4)	RMS error (cm) (5)	Correlation coefficient (6)
1	Cape May	6.5	0.92	4.4	0.95
2	Atlantic City	8.8	0.87	7.2	0.88
3	Sandy Hook	6.9	0.92	5.4	0.92
4	The Battery	6.7	0.92	5.2	0.93
5	Montauk	7.0	0.81	5.0	0.85
6	Willets Point	12.9	0.79	8.7	0.84
7	Bergen Point	6.5	0.93	5.1	0.93
8	Bridgeport	9.2	0.86	7.1	0.86
9	New London	7.7	0.83	6.1	0.83
[Maximum]	—	12.9	0.93	8.7	0.95
[Minimum]	—	6.5	0.79	4.4	0.83
[Mean]	—	8.0	0.87	6.2	0.89

salinity and temperature boundary conditions were adjusted, as indicated by (8). It should be noted that the computed temperature in New York Harbor is not significantly affected by the data used for the temperature boundary condition. Far from the open boundary, surface heat flux is a more important factor in determining water temperature.

The calibrated value of C_S is 0.01 throughout the model domain. The friction coefficient C_D is 0.003, except in the East River and Harlem River, where C_D is much higher, equal to 0.06. This higher value of C_D is the result of relatively coarse grid representation of the rivers in this region. They involve one computational cell width [Figs. 1(a) and 1(b)] from the Harlem River to the connection between the Upper and Lower East Rivers at Hell Gate.

Because of the large number of locations where data were available for model calibration and validation, only some representative visual comparisons of the model results with data are presented in this section. However, overall agreement between the model and data is based on all data, and it is presented in tabular form in terms of RMS errors and correlation coefficients.

Water Levels

The locations of 19 tide gauges in the model domain are shown in Fig. 2. Fig. 3 compares instantaneous water levels at Sandy Hook, Willets Point, and Montauk for the month of April in 1995. Comparisons at other locations for both of the simulation periods are similar. The results indicate that the model slightly underestimates amplitudes at Cape May, Atlantic City, and Willets Point, and there is a phase shift of about 1 h at Montauk. This phase shift is present in both of the simulation periods. It is probably the result of the tide gauge at Montauk being located in an embayment, which is not included in the model. Otherwise, the agreement between the model and data is very good. The tidal ranges between the spring and neap tidal cycle, and times of high and low waters are very well reproduced. The amplification of the tidal range in Long Island Sound, from approximately 0.80 m at Montauk to 2.5 at Willets Point, is very well reproduced. Except at Montauk, phase differences between the model and data are negligible.

Statistical evaluation of the model performance for the instantaneous water level is presented in Table 1. Data from both of the simulation periods, 1988–89 and 1994–95, are included in the analysis contained in the table. A maximum RMS error of about 30% of the local tidal range and the lowest correlation of 0.60 occur at Montauk. At the rest of the stations, correlation coefficients exceed 0.90. Except for Montauk and West Point, RMS errors at all of the stations are less than 15% of the local tidal range. For all of the tide stations, the mean RMS error and mean correlation coefficient are 10% and 0.94, respectively.

A comparison of 34-h low-passed water levels at Sandy Hook, Willets Point, and Montauk for the model calibration period, when the appropriate value of α was determined, is presented in Fig. 4. At the NOAA tide gauges that contain long-term continuous data, RMS errors and correlation coefficients are presented for subtidal (34-h and five-day low-passed) water level variations in Table 2. For these subtidal frequencies, the correlation coefficients vary from 0.79 to 0.95. At these frequencies, the phase shift between the model and data at Montauk becomes less significant, resulting in a higher correlation coefficient. The mean correlation coefficients are 0.87 and 0.89 for the 34-h and five-day low-passed water levels, respectively. The corresponding RMS errors are 8.0 cm and 6.2 cm. A part of the error in the computed instantaneous and subtidal elevations is obviously the result of approximations made in the formulation of the elevation boundary condition [(7)].

Errors in the computed amplitudes and phases of the M_2 tidal constituent at 25 locations are compared in Table 3. The table includes six additional stations, station numbers 20–25, in the New York Bight. At these stations, computed results are compared with those reported in the *U.S. Geological Survey Bulletin 1611* (Moody et al. 1984). In the study area, the M_2 is the dominant tidal constituent, and its amplitude is computed to within 10 cm. Excluding Montauk, maximum phase errors for the M_2 are less than 20°. The errors in the computed amplitude and phase for the other constituents are higher. However, their magnitudes, when compared with M_2, are relatively small, resulting in very good agreement between the model and data, as shown in Figs. 3 and 4 and Tables 1 and 2.

Current Velocities

The locations of ADCPs and current meter moorings are shown in Fig. 5. Note that there are two ADCP stations de-

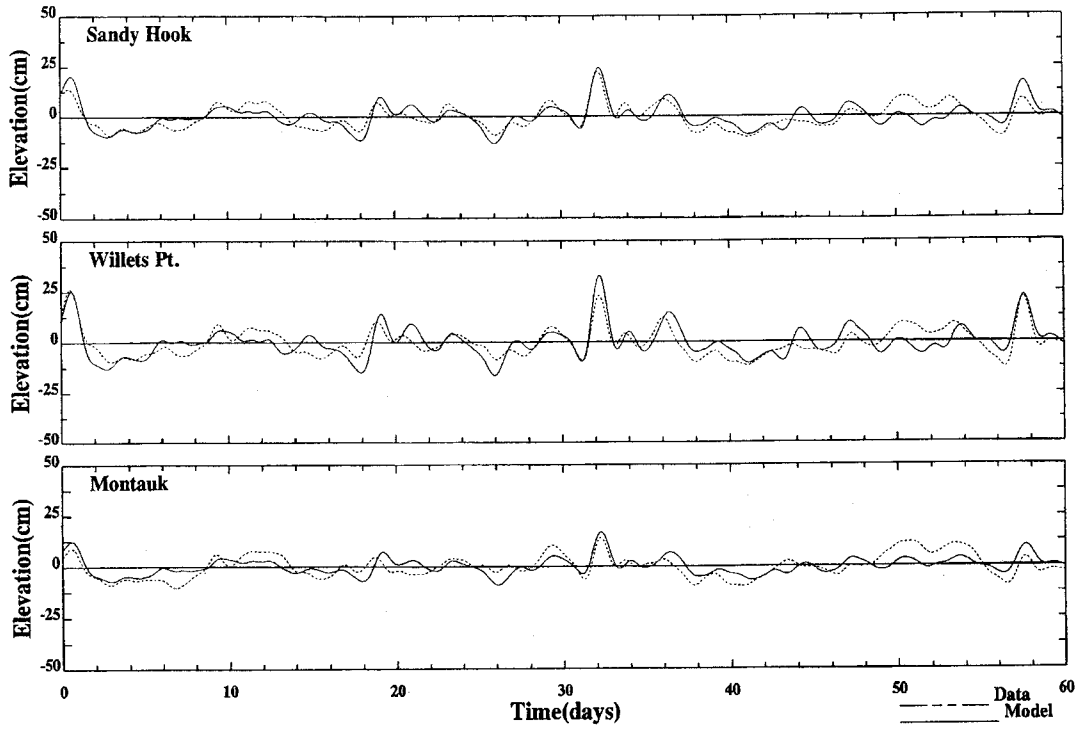

FIG. 4. Comparisons of 34 h Low-Passed Water Levels from June 1 to July 30, 1989

TABLE 3. Comparison of M_2 Elevation Tidal Constituents

Number (1)	Station (2)	Latitude (north) (3)	Longitude (west) (4)	Observed		Calculated	
				Amplitude (cm) (5)	Phase (°) (6)	Amplitude (cm) (7)	Phase (°) (8)
1	Cape May	74°87′	38°88′	69	245	59	234
2	Atlantic City	74°55′	39°51′	58	211	60	221
3	Sandy Hook	74°30′	40°70′	68	223	63	216
4	The Battery	74°31′	40°72′	66	235	62	231
5	Montauk	71°87′	41°32′	29	263	32	204
6	Willets Point	73°76′	40°77′	112	332	102	342
7	Bergen Point	74°38′	40°68′	73	237	65	230
8	Bridgeport	73°40′	41°40′	96	325	88	334
9	New London	72°35′	41°51′	36	274	33	275
10	Staten Island	74°33′	40°66′	65	229	64	245
11	Gowanus Bay	74°31′	40°69′	69	234	65	252
12	Lincoln Tunnel	74°30′	40°76′	56	254	59	263
13	GWB	73°87′	40°80′	58	265	54	277
14	Yonkers	73°83′	40°87′	53	277	56	302
15	Dobbs Ferry	73°82′	41°34′	54	292	58	312
16	West Point	73°87′	41°53′	43	327	52	312
17	Jones Inlet	73°63′	40°65′	53	220	59	202
18	Shark River	74°31′	40°41′	47	281	56	235
19	Harlem River	74°84′	40°82′	49	276	53	264
20	Picket	40°43′	71°19′	44	349	35	327
21	LT5	40°12′	72°00′	46	349	39	321
22	MESA10	40°00′	73°14′	55	351	52	320
23	AMBROSE	40°28′	73°50′	65	353	61	321
24	LT2	39°24′	73°44′	54	353	51	326
25	MD	38°59′	74°02′	52	354	54	339

noted by NC. Short-term data at two ADCPs (SC and one of the NCs) were available for 1989. The rest of the ADCPs (NC, RH, and HR) were installed during the 1994–95 period. At the ADCP stations, currents were reported at a large number of vertical bins (Coomes 1996). To limit the presentation, results are presented for near-surface, middepth, and near-bottom bins. Current meter velocities are compared at their depths of deployment.

The computed velocity is compared with ADCP data at College Point, N.Y. for the month of July 1995 in Fig. 6. Comparisons of data versus the model at other ADCP stations are very similar. At CP and HR, the model underestimates the near-bottom velocity significantly, which is the result of using a higher C_D in the East River. Table 4 presents a statistical evaluation of model performance at all of the ADCPs and current meter moorings in New York Harbor for 1989. Note that at these moorings, currents were measured at only one depth. In addition, only the analysis of the main component of velocities is presented in the table, as transverse velocities across the channel are small. RMS errors are generally less than 15%,

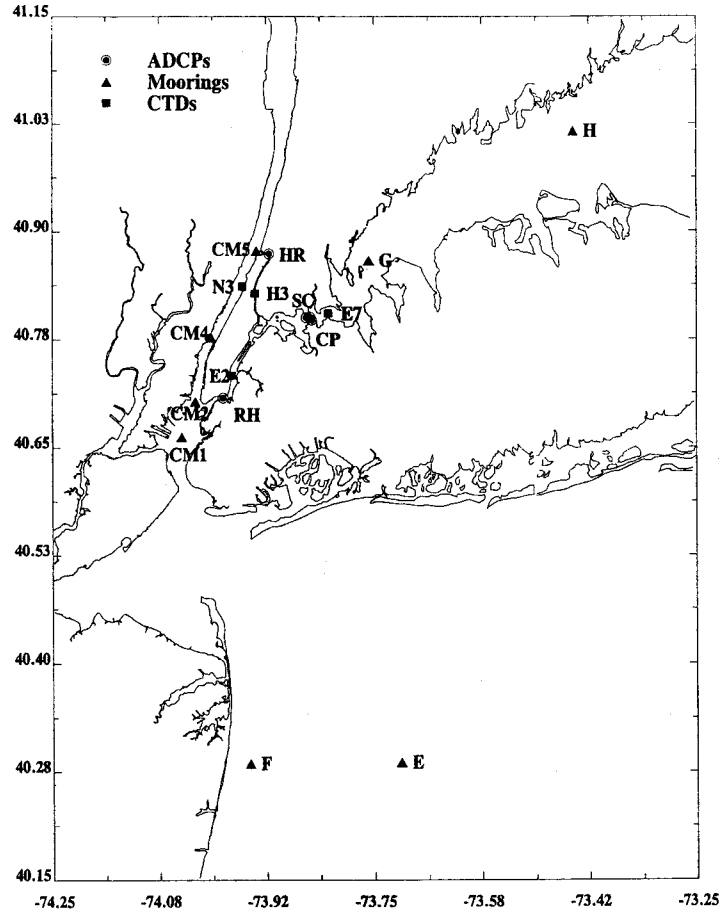

FIG. 5. Locations of ADCPs, Moorings, and Four CTDs

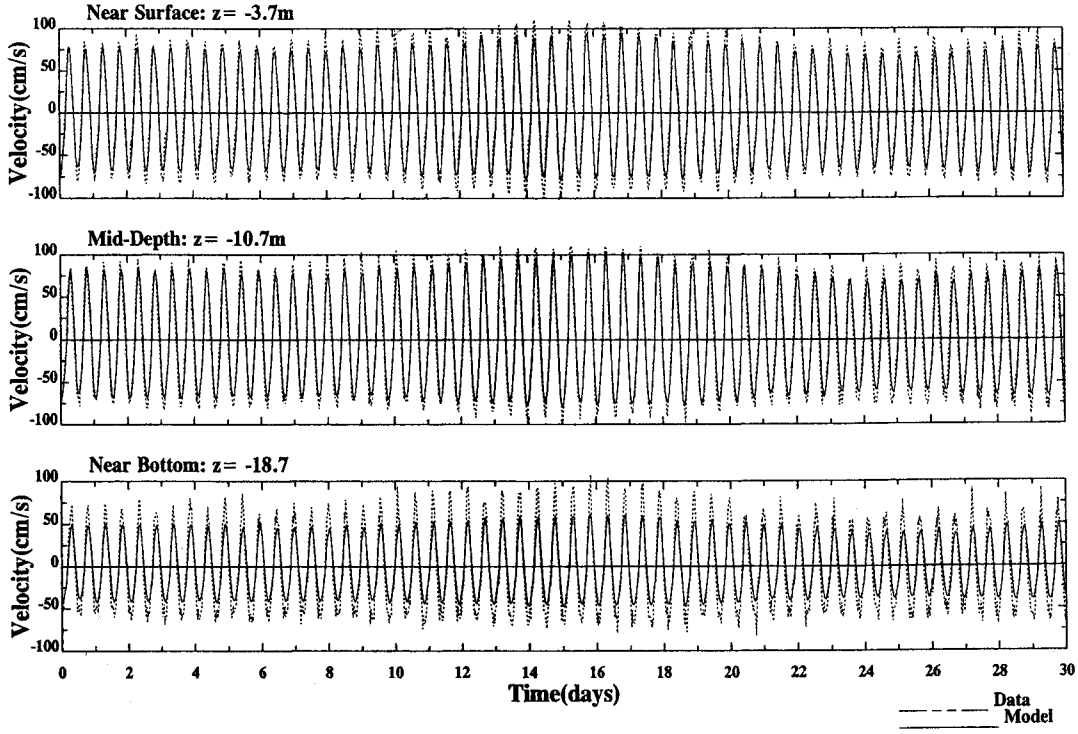

FIG. 6. Comparisons of Instantaneous Velocity at College Point in June 1995

TABLE 4. Statistical Evaluation of Model Performance for Currents in Harbor

Number (1)	Station (2)	Depth (3)	Number of data (4)	Data range (cm/s) (5)	RMS error (%) (6)	Correlation coefficient (7)
1	College Point (CP)[a]	Near surface	10,807	187.0	7.1	0.97
1	College Point[a]	Middepth	10,807	193.1	7.8	0.97
1	College Point[a]	Near bottom	10,807	148.5	12.2	0.95
2	College Point[b]	Near surface	936	179.2	7.8	0.97
2	College Point[b]	Middepth	936	157.7	10.9	0.97
2	College Point[b]	Near bottom	936	131.7	10.0	0.96
3	South Clason (SC)	Near surface	2,736	143.7	12.4	0.96
3	South Clason	Middepth	2,736	172.3	9.1	0.97
3	South Clason	Near bottom	2,736	152.4	8.9	0.97
4	Red Hook (RH)	Near surface	15,103	373.9	9.9	0.98
4	Red Hook	Middepth	15,103	336.3	12.9	0.99
4	Red Hook	Near bottom	15,103	303.5	16.6	0.99
5	Harlem River (HR)	Near surface	14,240	203.0	10.8	0.96
5	Harlem River	Middepth	14,240	197.0	11.8	0.95
5	Harlem River	Near bottom	14,240	176.1	15.2	0.95
6	Upper Bay (CM1)	Near bottom	423	116.9	12.1	0.95
7	The Battery (CM2)	Near bottom	1,773	95.3	12.9	0.96
8	Weehawken (CM4)	Near bottom	1,778	113.9	14.2	0.95
9	Spuyten Duyvil (CM5)	Near bottom	1,767	136.3	12.1	0.94
[Maximum]	—	—	—	373.9	16.4	0.99
[Minimum]	—	—	—	95.3	7.1	0.94
[Mean]	—	—	—	185.1	11.3	0.96

[a]1994–95.
[b]1988–89.

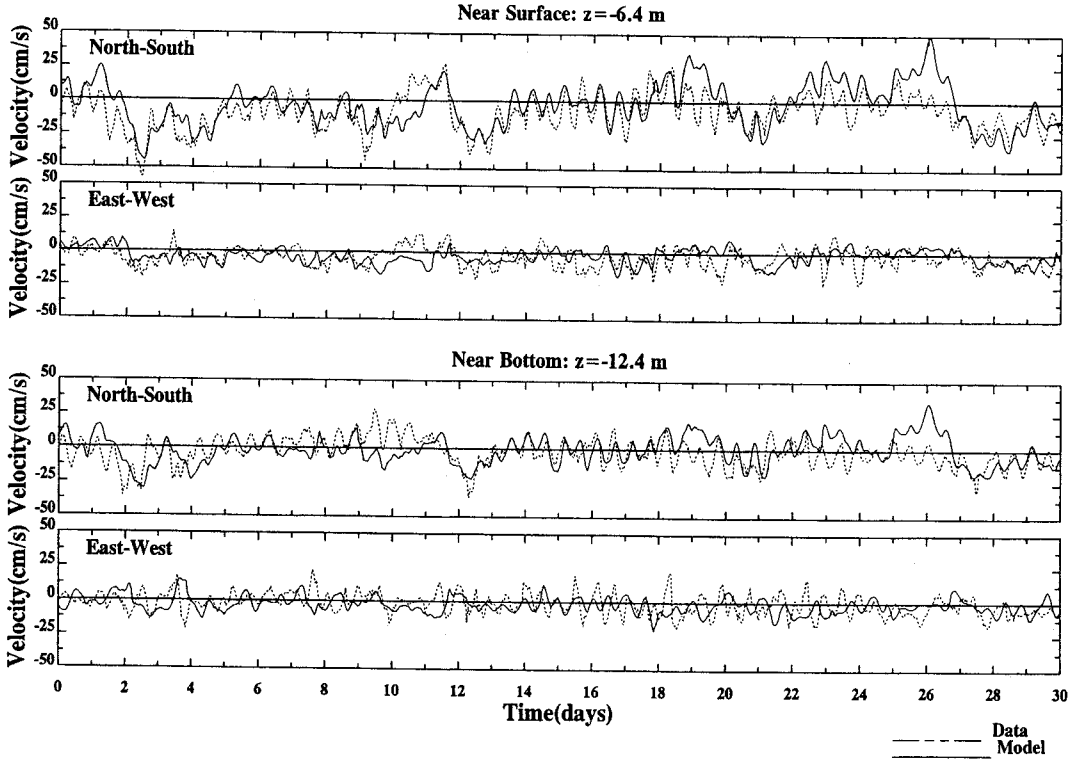

FIG. 7. Comparisons of Currents at Mooring F in June 1995

and the correlation coefficients are higher than 0.94. The overall agreement between the model and data is very good.

During 1994–95, near-surface and near-bottom currents at three moorings, shown in Fig. 5, were available. In Fig. 7, computed velocities for the month of April of 1995 are compared with data at mooring E in the New York Bight. Agreement between the model and data in the New York Bight at all of the moorings is considerably lower than that obtained for ADCP current measurements in the New York Harbor. However, the model reproduces the overall trends in the data. RMS errors and correlation coefficients at the mooring stations are presented in Table 5.

The table indicates that RMS errors are less than 20% of the velocity range. Correlation coefficients vary from 0.03 for the U component of velocity at the deep location at mooring F to 0.72 for the V component at shallow mooring F. The correlation coefficients are, in general, higher for near-surface velocities. The lowest correlation is at mooring F, located just outside the mouth of the Shark River. The model does not include the Shark River in the computational domain. Only its

TABLE 5. Statistical Evaluation of Model Performance for Offshore Currents

Station (1)	Depth (m) (2)	Velocity Range (cm/s) U (3)	Velocity Range (cm/s) V (4)	RMS Error (%) U (5)	RMS Error (%) V (6)	Correlation Coefficient U (7)	Correlation Coefficient V (8)
E	5.3	58	64	15	13	0.65	0.59
E	20.9	63	82	15	13	0.49	0.43
F	6.4	32	95	20	13	0.35	0.72
F	12.4	47	76	18	14	0.03	0.48
H	3.0	108	57	9	13	0.87	0.53
H	25.0	85	55	8	12	0.92	0.70

discharge is included as a point source of freshwater. Therefore, the oscillatory flow field in the east-west direction in the vicinity of Shark River is not simulated well by the model. The model, however, does a much better job in the north-south direction at mooring F. At mooring H, where velocities are significantly higher than those at moorings E and F, correlation coefficients are also considerably higher. The same is true for moorings in the New York Harbor.

A comparison of 34-h low-passed currents at three different levels is shown in Fig. 8. Though the model reproduces most of the subtidal variabilities, their amplitudes are underestimated and there are significant phase differences. Computed currents toward New York Harbor (negative currents) are considerably weaker than those suggested by the data. Compared with data of Blumberg and Prichard (1997), the deterioration of the results is due to approximations made in specifying elevation boundary conditions, and the simplified geometrical representation of the Upper East River using only three computational cells.

Energy spectra (in variance-preserving form) for currents and elevation at the SC station are compared in Fig. 9. The current spectra are presented for near-surface, middepth, and near-bottom bins. Both the data and the model indicate that the prominent peaks in the energy spectra occur at the M_2 and K_1 periods. Energy contained in the M_2 frequency is significantly higher than in other frequencies. The figures indicate that the model reproduces the variations in energy spectra very well for frequencies greater than 0.6 cycles per day (cpd). At lower frequencies, the model underestimates energy, resulting in the smaller subtidal velocity of Fig. 8.

Salinity and Temperature

The model was calibrated by comparing computed near-surface and near-bottom salinity, and temperature at 35 stations in 1988–89. These stations are distributed throughout the model domain. Data density was fairly high at 10 stations in the Hudson River, New York Harbor, and Lower East River in the summer of 1989. Daily near-surface data were available at four locations (The Battery, Willets Point, Bridgeport, and Montauk). At the rest of the locations, data mostly consisted of weekly and biweekly samples during the entire simulation period. Model results were compared with data at 27 locations for model validation. This included approximately hourly near-surface and near-bottom data at four moorings in the New York Bight and Long Island Sound. Fig. 5 shows the mooring locations along with the monitoring stations used for the model and data comparisons presented in this paper.

Comparisons of instantaneous salinity at stations N3 in the Hudson River, E2 in the Lower East River, E7 in the Upper East River, and H3 in the Harlem River from June 1, 1989 to July 30, 1989 are presented in Fig. 10. The variations in subtidal salinity (34-h low-passed) at these locations over the complete simulation period are shown in Fig. 11. These figures indicate that the model simulates the surface and bottom salinity very well. The vertical salinity stratification and its temporal variations in the Hudson River, due to spring and neap tidal cycles, are well reproduced. The well-mixed water columns of the Lower East River and the seasonal stratification found in the Upper East River are also correctly simulated by the model. The range of salinity variations in the Harlem River is significantly higher than in the East River. Unlike the Hudson River, the Harlem River remains well mixed throughout the spring-neap tidal cycles. Comparisons of salinity at all of

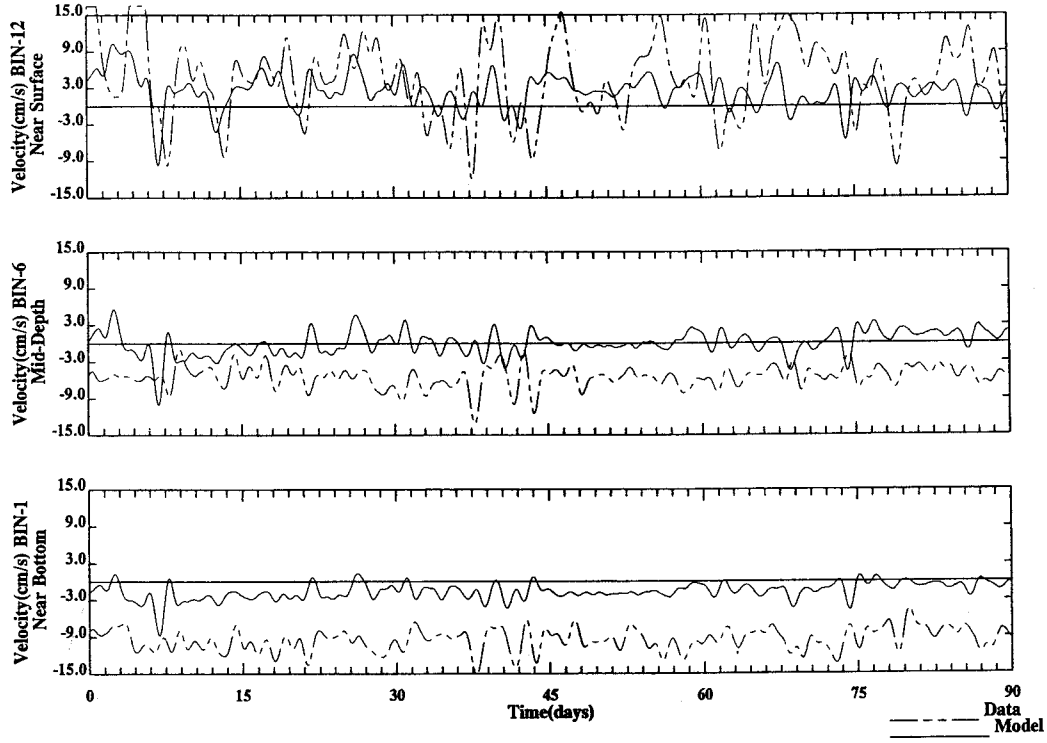

FIG. 8. Comparisons of 34-h Low-Passed Velocity at South of Clason from May 1 to June 1989

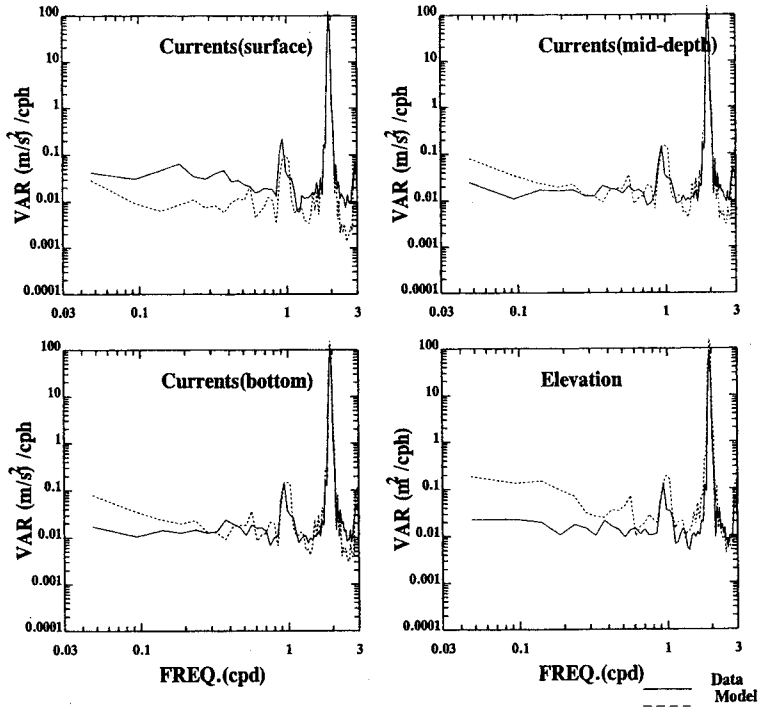

FIG. 9. Comparisons of Power Spectral Density of Currents and Elevations at South of Clason

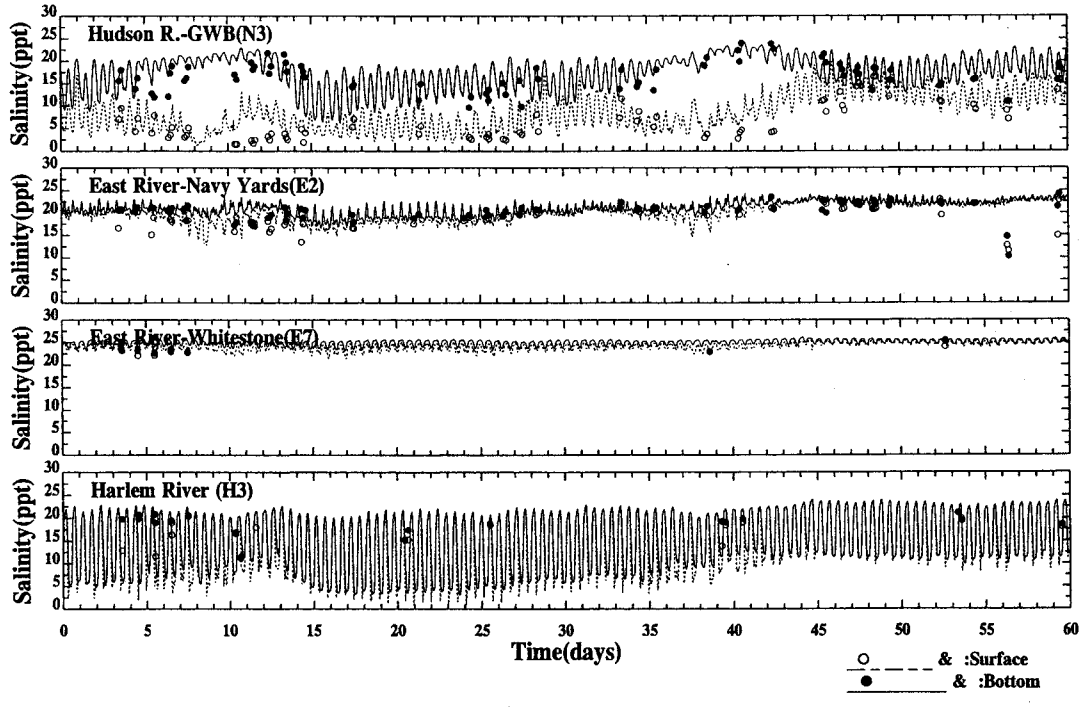

FIG. 10. Comparisons of Instantaneous Surface and Bottom Salinity from June 1 to July 30, 1989

the stations for both 1988–89 and 1994–94 appear similar. At mooring stations E, F, G, and H, tidal variations in salinity and vertical stratification are significantly smaller than those in New York Harbor, and the agreement between the model and data is similar to that shown in Figs. 10 and 11.

Semidiurnal and diurnal variations in temperature as much smaller than those for salinity. Therefore, Fig. 12 compares the subtidal variations of temperature over an annual cycle at mooring stations E, F, G, and H. The corresponding variations in temperature at stations N3, E2, E7, and H3 are shown in Fig. 13. The model overestimates temperature in Long Island Sound and New York Bight from the latter half of January to early March, as indicated at moorings F, G, and H in Fig. 13 and station E7 in Fig. 13. The situation is quite similar for the 1988–89 simulation period. However, in the New York Harbor area, the computed temperatures are within the variability of the data, as indicated by mode versus data comparisons at stations N3, E2, and H3 in Fig. 13. Sensitivity analysis indicates that lowering the offshore boundary temperature does not significantly improve the computed results in Long Island Sound and New York Bight. The possible source of error appears to be associated with the computation of surface heat flux based on air temperatures from Central Park for the whole model domain. The overall agreement between the computed

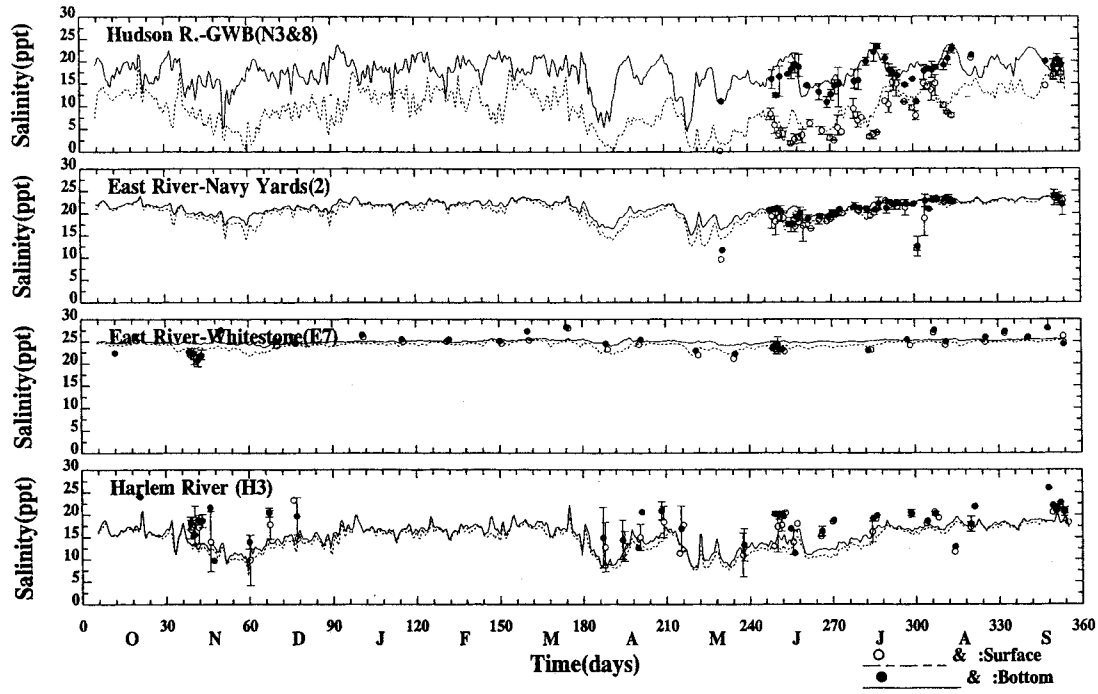

FIG. 11. Comparisons of Subtidal Surface and Bottom Salinity Variations for 1988–89

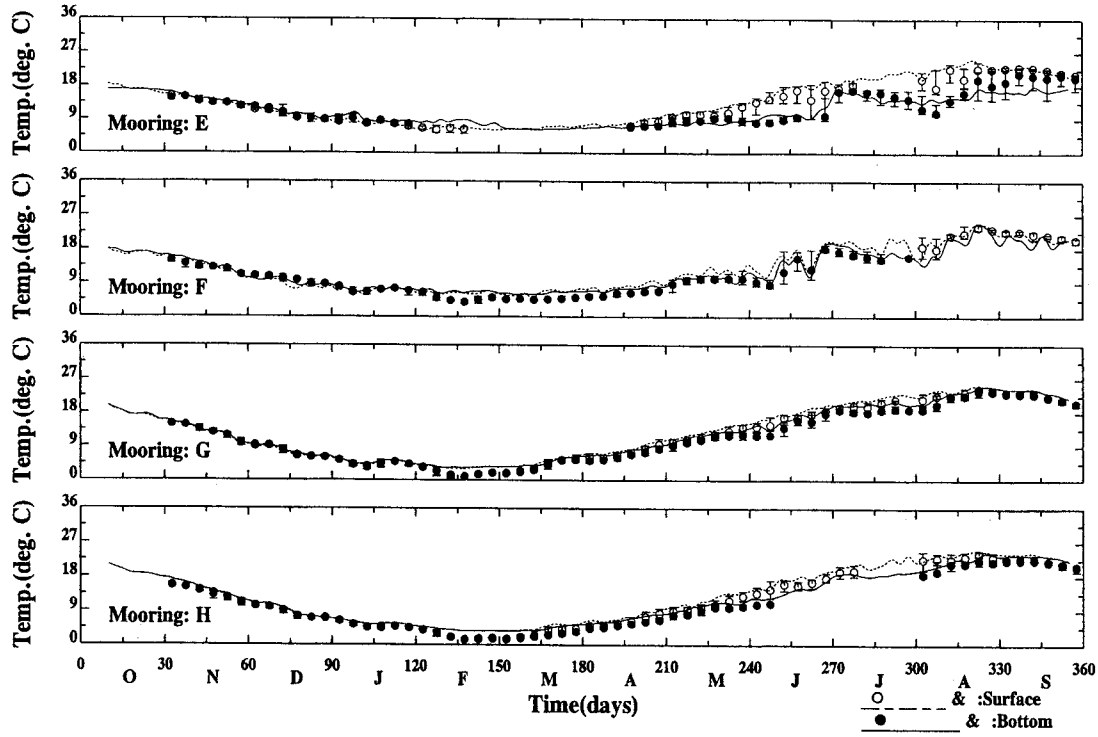

FIG. 12. Comparisons of Subtidal Surface and Bottom Temperature at Moorings for 1994–95

temperature and data was considered reasonable, and further refinement was not warranted.

Because of the large number of salinity and temperature stations involved in the current study, the model's skill for bottom and surface salinity and temperature is presented in Figs. 14 and 15, respectively. The results are aggregated into subregions in the model domain. These subdivisions are (1) the Hudson River north of The Battery; (2) the East River; (3) the New York Bay; (4) the Kill area including Newark Bay; (5) Long Island Sound; and (6) the New York Bight. As the number of data points at moorings is large, only 12 h mean values are plotted and analyzed. Fig. 14 indicates that for surface and bottom salinity, the lowest correlation is 0.58. It occurs in the East River. In the Hudson River, where the tidal variations in salinity are large, the correlation between the data and the model exceeds 0.80. The correlation between the model and data for temperature varies from 0.77 in the East River to almost 1.0 in Long Island Sound. Except for the surface temperature in the East River, the correlation at all of the regions exceeds 0.90.

SENSITIVITY ANALYSIS

The forcing functions developed in the present study are based on a large number of assumptions and approximations.

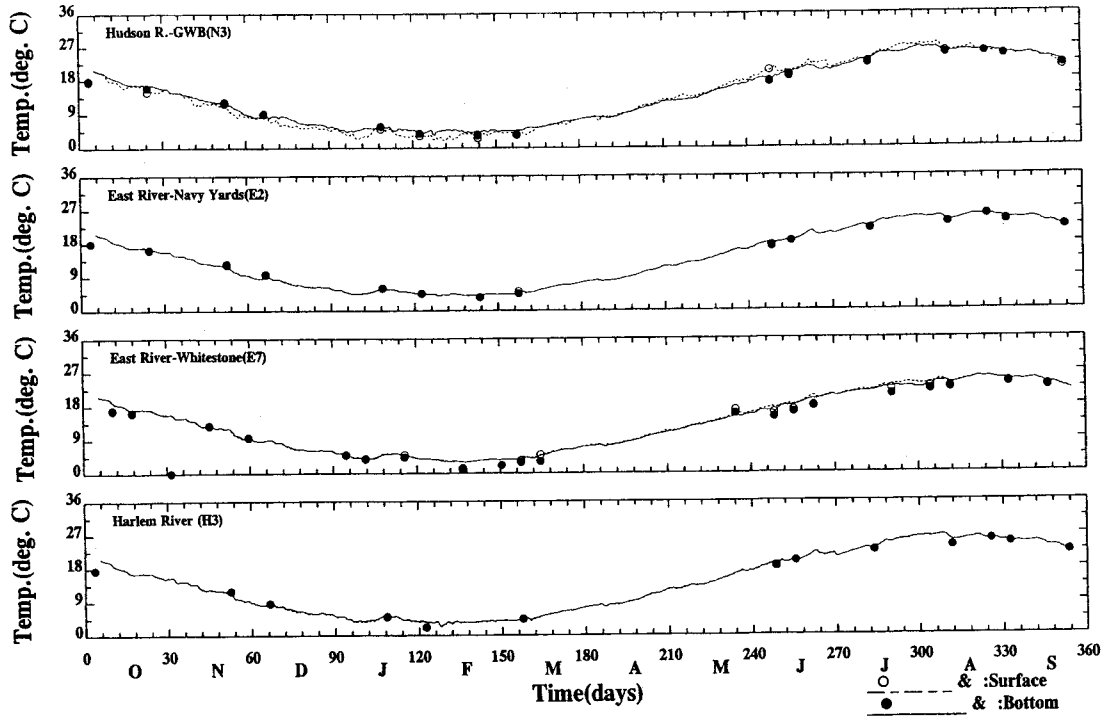

FIG. 13. Comparisons of Subtidal Surface and Bottom Temperature Variations in New York Harbor for 1994–95

The effects of these assumptions and approximations were analyzed while calibrating the model. In this section, effects of using daily mean, monthly mean, and yearly mean freshwater inflows from the Hudson River and Connecticut River on the computed salinity are discussed. Most of the previous studies of the New York Bight and New York Harbor (Oey et al. 1985; Blumberg and Galperin 1990; Oey et al. 1995) have used these approximations to simplify their model applications. The Hudson and Connecticut Rivers contribute about 65% of total freshwater inflows from 30 rivers and tributaries included in the current study.

Computed surface and bottom salinities in May 1989 at station N3 in the Hudson River for three different temporal distributions of freshwater inflows are compared in Fig. 16. These discharge distributions are (1) daily mean flows from 30 rivers and tributaries; (2) historical monthly mean flows from the Hudson and Connecticut Rivers only; and (3) the same as in case 2, but using historical annual mean flows. Moreover, following previous studies on New York Harbor, New York Bight, and Long Island Sound, point sources of surface runoffs are also neglected in cases 2 and 3. The historical monthly and annual mean values were determined from USGS data from 1946 to 1996 for the Hudson River and from 1928 to 1996 for the Connecticut River.

The figure indicates that both surface and bottom salinity distributions are significantly different for the three river inflow conditions. The difference between salinity distributions resulting from monthly and annual mean flows is relatively smaller. Compared with daily discharge, the maximum increase in salinity for using monthly and annual discharges is 12 and 16 ppt, respectively. The corresponding increase for bottom salinity is 12 and 13 ppt, respectively. The latter river inflow conditions result in significantly higher salinity in the New York Harbor, Long Island Sound, and the apex of New York Bight.

The correlations between the model and salinity data for the three discharge conditions for 1988–89 are shown in Table 6. In the table, New York Bight is not included, as sufficient data were not available. Note that correlation coefficients shown in Fig. 14 and Table 6 are not identical, as the figure is based on all available data for 1988–89 and 1994–95, whereas Table 6 is based on data for 1988–89 only. The use of monthly discharge lowers the correlation between the model and data by 0.02–0.40. For annual mean flow, correlation coefficients deteriorate by 0.11–0.44. For monthly mean flow, the largest decrease in correlation coefficients occurs in Long Island Sound. However, for annual mean flow, the largest decrease occurs in the New York Bay. Degradation in correlation for surface salinity is higher than the correlation for bottom salinity. This analysis clearly illustrates the need for accurate and detailed information about forcing functions to achieve the objectives of developing hydrodynamic models.

RESIDUAL CIRCULATION IN NEW YORK HARBOR

Residual circulation in New York Harbor is one of the important factors responsible for the transport and distribution of pollutants from various sources located along the Hudson River, East River, and Long Island Sound (Blumberg and Prichard 1997). Therefore, an objective of the present study was to analyze residual circulations at different time scales, indicating whether pollutants could be transported to Long Island Sound or to New York Harbor, and how these pollutants are flushed into the New York Bight.

Residual circulations in the model domain, including New York Harbor, Long Island Sound, and the New York Bight, were analyzed at time scales ranging from tidal and meteorological (4–10 days) to monthly, seasonal, and annual. The annual mean distribution of fluxes through key locations in New York Harbor from the 1988–89 simulation period is shown in Fig. 17. At each section, the net flow is split into upper layer (Q_u) and lower layer (Q_l) flows based on the change in flow direction in the vertical. The negative sign indicates flow in the direction opposite to the arrow, representing the direction of net flow. The results of the 1988–89 simulation period are presented, as they are representative of a typical hydrological year, with the yearly mean freshwater flows being close to their historical annual means.

The annual mean freshwater into the Hudson River at West Point in 1988–89 was 520 m^3/s, resulting from eight upstream

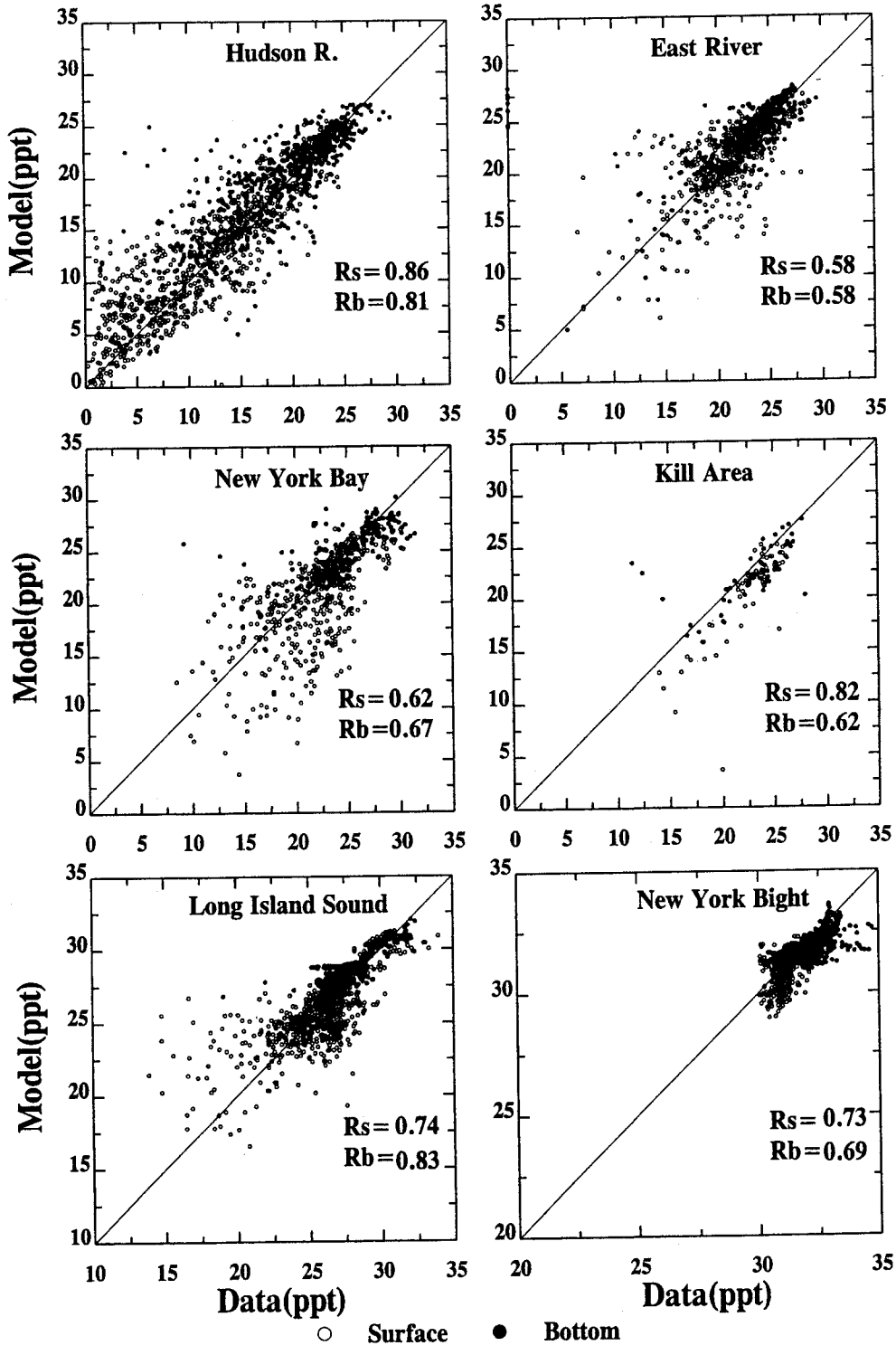

FIG. 14. Correlation between Computed and Observed Surface (*Rs*) and Bottom (*Rb*) Salinity

rivers and tributaries, surface runoffs, and wastewater treatment plants. This flow consisted of 685 m^3/s less dense, lighter water mass flowing downstream over 165 m^3/s denser and saltier water intruding upstream. The exchange of water between New York Harbor and Long Island Sound, through the East River at Throgs Neck, consisted of a near-surface flow of 50 m^3/s to Long Island Sound and a near-bottom flow of 250 m^3/s toward New York Harbor. The resulting net flux was 200 m^3/s toward New York Harbor. That transport of water was joined by additional flow from the Harlem River. Vertical stratification in both Upper and Lower East Rivers was weak, and the Harlem River was well mixed. Local sources of freshwater, wastewater treatment plants, and rainfall added 55 m^3/s to the flow reaching the Hudson River. It should be noted that previous estimates of transport through the East River vary from 22 to 620 m^3/s toward New York Harbor and 102–1,100 m^3/s toward Long Island Sound (Jay and Bowman 1975; Blumberg and Prichard 1997).

In the 1988–89 simulation period, the annual net outflow to the New York Bight through the Sandy Hook–Rockaway transect was 960 m^3/s. The upper layer flow to the New York Bight consisted of 3,335 m^3/s, while 2,375 m^3/s of more saline

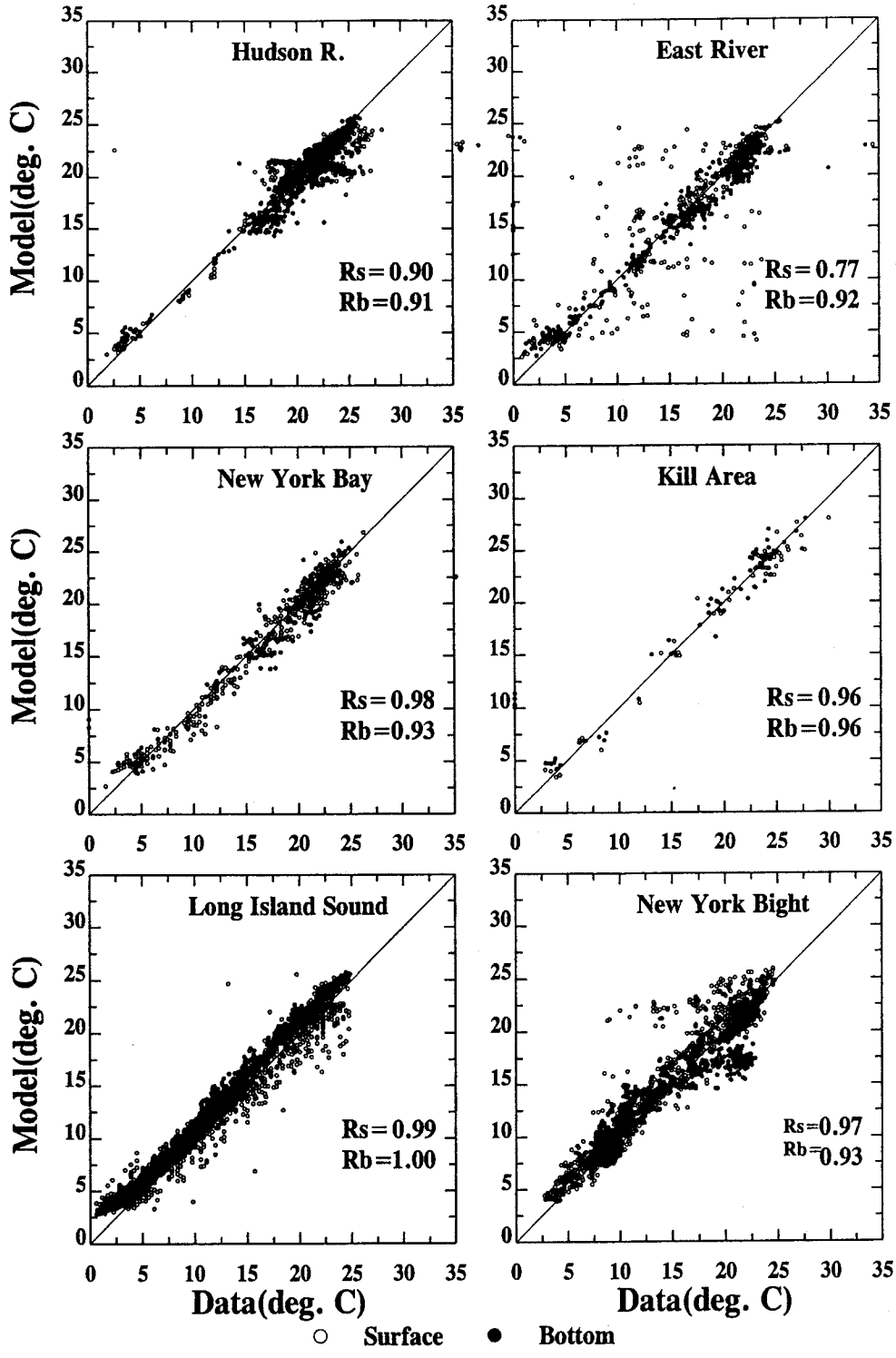

FIG. 15. Correlation between Computed and Observed Surface (*Rs*) and Bottom (*Rb*) Temperature

water intruded into New York Harbor. The Kill van Kull received 95 m^3/s of flow from the Upper New York Bay. This flow, combined with that from the Newark Bay, was transported through the Arthur Kill. Both Newark Bay and the Arthur Kill were well mixed, while the Kill van Kull showed weak vertical stratification. A very small amount of freshwater from the Hackensack and Passaic Rivers was transported directly to the Upper New York Bay. Within the boundaries of New York Harbor shown in Fig. 17, local sources of freshwater, wastewater treatment plants, and rainfall contributed about 140 m^3/s to the net outflow to the New York Bight.

The ratio Q_u/Q_l can be used as an indicator of vertical stratification in an estuary receiving freshwater from upstream. For a constant upstream river flow, a higher value of Q_u/Q_l indicates a higher exchange of water mass between the lower and upper layers and smaller vertical stratification. The Hudson River from West Point to the George Washington Bridge (GWB) showed smaller vertical stratification, with Q_u/Q_l varying from 4.1 to 4.8. The interface between the denser bottom water and lighter surface water gradually becomes sharper in the downstream direction, as indicated by Q_u/Q_l values of 1.7 and 1.4 at the Narrows and Sandy Hook–Rockaway transect,

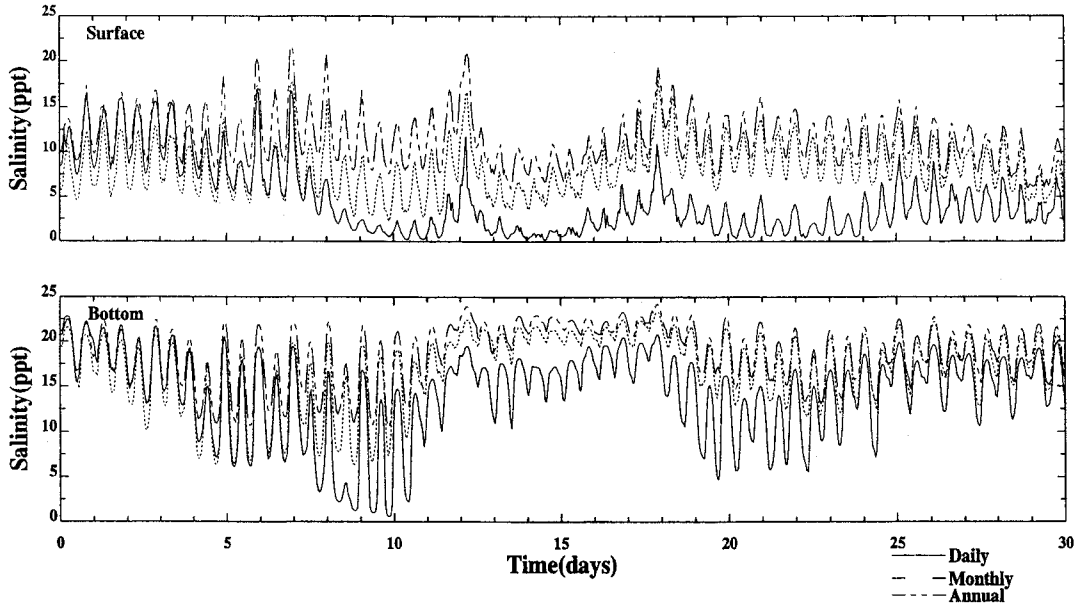

FIG. 16. Comparison of Salinity in Hudson River at GWB(N3) for Different River Inflows in May 1989

TABLE 6. Correlation between Model and Salinity Data As Function of River Discharge Approximations

Location (1)	Depth (2)	Mean Discharge		
		Daily (3)	Monthly (4)	Annual (5)
Hudson River	Surface	0.88	0.76	0.68
Hudson River	Bottom	0.69	0.67	0.66
East River	Surface	0.65	0.58	0.49
East River	Bottom	0.69	0.61	0.53
New York Bay	Surface	0.54	0.30	0.12
New York Bay	Bottom	0.53	0.50	0.42
Kill Area	Surface	0.67	0.65	0.47
Kill Area	Bottom	0.68	0.58	0.46
Long Island Sound	Surface	0.62	0.22	0.18
Long Island Sound	Bottom	0.65	0.46	0.39

respectively. Along the reach of the Hudson River shown in Fig. 17, the ratio Q_u/Q_l changed by a factor of three in 1988–89. In 1994–95, a period of relatively low flow, Q_u/Q_l at the Narrows and Sandy Hook–Rockaway transect was approximately the same (1.6 and 1.4, respectively). However, at West Point the ratio decreased to 2.5, indicating higher vertical stratification and salinity intrusion in the Hudson River.

SUMMARY AND CONCLUSIONS

A three-dimensional hydrodynamic model of the New York Bight, Long Island Sound, and New York Harbor has been presented within the framework of a single grid system. The study utilizes ECOM, a three-dimensional hydrodynamic model developed by Blumberg and Mellor (1980, 1987), for simulating water level, velocity, salinity, and temperature. ECOM has a long history of successful applications to many coastal and estuarine systems. For such models, specification of boundary forcing functions greatly influences the success of the model application. Therefore, a detailed description of derived boundary conditions—elevations, salinity, temperature, surface heat flux, freshwater inflows from rivers, wastewater treatment plants, and surface runoff—has been presented. Sensitivity analyses indicate the need for accurate and detailed information on boundary conditions. Otherwise, computed hydrodynamic parameters will be significantly different from the field condition. For example, if monthly mean freshwater inflows from rivers are used as boundary conditions, correlations between the computed salinity and data can be reduced by 0.40. Numerical experiments indicate that accurate estimations of all sources of freshwater significantly improve the simulation accuracy of the model.

The model was calibrated by comparing water levels at 14 locations, current velocities at six locations, and salinity and temperature at 35 locations over a period of one year from October 1988 to September 1989. A hydrologically different simulation period, October 1994 to September 1995, was used for model validation. Compared with 1988–89, the latter period is relatively colder, with 10 W/m^2 lower yearly mean shortwave solar radiation, and significantly drier, with only 66% of inflows from rivers. The model was validated against elevation data at 13 locations, current data at five locations, and salinity and temperature data at 27 locations.

The model skill assessment has been quantified in terms of RMS errors and correlation coefficients. At most of the locations, errors in computed water levels are less than 10% of the local tidal range, and correlations between the data and model exceed 0.95. The M_2 amplitudes and phases at 24 locations are predicted within 10 cm and 20°, respectively. In the New York Harbor, currents are computed within 15% of observations. Though the model reproduces the overall trends in observed velocities in the New York Bight, the correlation between the model and data is lower. The performance of the model in predicting salinity and temperature is very encouraging. The model reproduces not only stratification and destratification over the spring and neap tidal cycles, but also the simultaneous existence of stratified, well-mixed, and partially well-mixed conditions in different regions in the model domain. Correlation coefficients for different subregions of the model domain vary from 0.58 to 0.86 for salinity and from 0.77 to almost 1.0 for temperature.

Two 12-month simulations indicate that the model is capable of describing the entire spectrum of time scales of the computed quantities, including the semidiurnal tidal scale, diurnal scale, meteorological scale (a few days), spring and neap tidal scale (15 days), and monthly, seasonal, and annual scales. An analysis of the annual mean residual circulation pattern in the New York Harbor has been presented. Therefore, the model is expected to be a useful tool for water quality modeling and water resources management of the modeled region. The paper attempts to rectify the lack of information on constructing open boundary conditions for hydrodynamic models

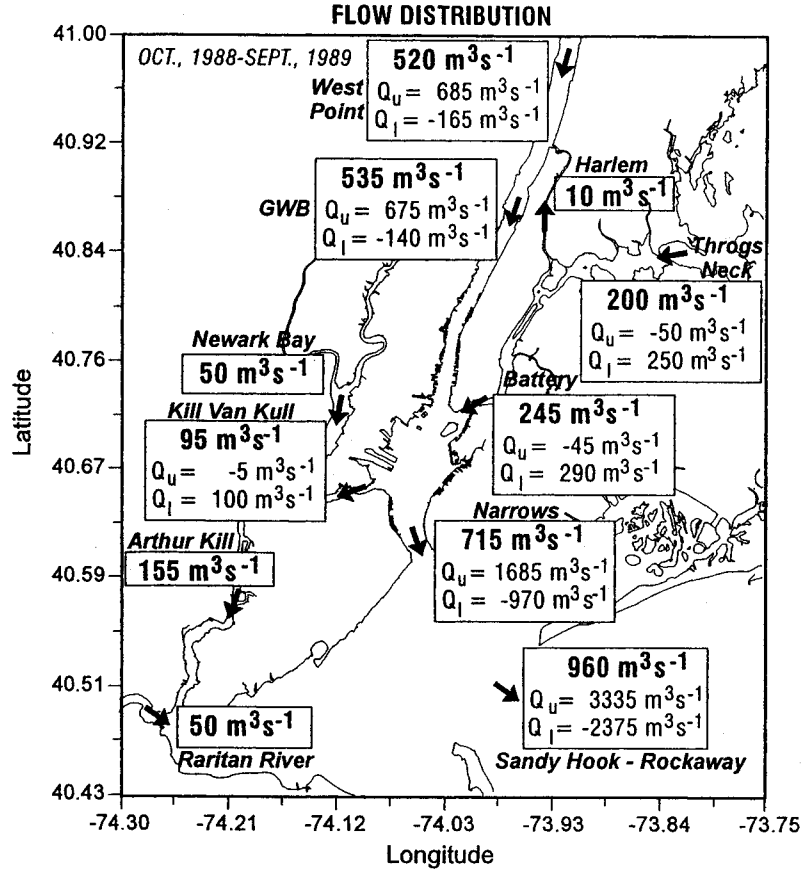

FIG. 17. Annual Circulation Pattern in New York Harbor in 1988–89

(Wang et al. 1990) and statistical evaluation of model performance (ASCE Task Committee 1988) in most of the published papers and reports.

ACKNOWLEDGMENTS

The work summarized in the present paper was supported by the New York City Department of Environmental Protection, and was performed under subcontract to Greeley and Hansen in association with Hazen and Sawyer, P. C., and Malcolm Pirnie, Inc. The work was performed as part of engineering services for facilities planning for the Newtown Creek Water Pollution Control Plant.

APPENDIX. REFERENCES

Allen, J. S., Newberger, P. A., and Federiuk, J. (1995). "Upwelling circulation on the Oregon continental shelf." *J. Phys. Oceanography*, 35, 1843–89.

ASCE Task Committee on Turbulence Models in Hydraulic Computations. (1988). "Turbulence modeling of surface water flow and transport." *J. Hydr. Engrg.*, ASCE, 114(3), 970–1073.

Ashizawa, D., and Cole, J. J. (1994). "Long-term temperature trends of the Hudson River: A study of the historical data." *Estuaries*, 17(1B), 166–71.

Beardsley, R. C., and Boicourt, W. C. (1981). "On estuarine and continental-shelf circulation in the Middle Atlantic Bight." *Evolution of physical oceanography*, B. A. Warren C. Wunsch, eds., MIT Press, Cambridge, Mass., 198–233.

Beardsley, R. C., Chapman, D. C., Brink, K. H., Ramp, S. R., and Schlitz, R. (1985). "The Nantucket shoals flux experiment (NSFE79). Part I: A basic description of the current and temperature variability." *J. Phys. Oceanography*, 15, 713–748.

Blumberg, A. F., and Galperin, B. (1990). "On the summer circulation in New York Bight and contiguous estuarine waters." *Coastal and estuarine studies. Volume 38: Residual currents and long-term transport*, D. T. Cheng, ed., Springer, New York, 451–68.

Blumberg, A. F., Galperin, B., and O'Conner, D. J. (1992). "Modeling vertical structure of open-channel flows." *J. Hydr. Engrg.*, ASCE, 118(8), 1119–1134.

Blumberg, A. F., and Goodrich, D. M. (1990). "Modeling of wind-induced destratification in Chesapeake Bay." *Estuaries*, 13(3), 236–249.

Blumberg, A. F., and Mellor, G. L. (1980). "A coastal ocean numerical model." *Proc., Int. Symp. on Math. Modelling of Estuarine Phys.*, J. Sundermann and K. P. Holz, eds., Springer, Berlin, 202–19.

Blumberg, A. F., and Mellor, G. L. (1987). "A description of a three-dimensional coastal ocean circulation model." *Three-dimensional coastal ocean models. Coastal and estuarine sciences: Volume 4*, N. Heaps, ed., American Geophysical Union, Washington, D.C., 1–16.

Blumberg, A. F., and Prichard, D. W. (1997). "Estimates of the transport through the East River, New York." *J. Geophys. Res.*, 102(3), 5685–5703.

Blumberg, A. F., Signell, R. P., and Jenter, H. L. (1993). "Modeling transport processes in the coastal ocean." *J. Marine Envir. Engrg.*, 1, 3–52.

Brown, W. S., Pettigrew, N. R., and Irish, J. D. (1985). "The Nantucket shoals flux experiment (NSFE79). Part II: The structure and variability of across-shelf pressure gradients." *J. Phys. Oceanography*, 15, 749–771.

Chapman, J. A., Beardsley, R. C., and Fairbanks, R. G. (1986). "On the continuity of mean flow between the Scotian shelf and the Middle Atlantic Bight." *J. Phys. Oceanography*, 16, 722–58.

Chen, C., and Beardsley, R. C. (1995). "A numerical study of stratified tidal rectification over finite amplitude banks." *J. Phys. Oceanography*, 25, 2090–128.

Cokljat, D., and Younis, B. A. (1995). "Second-order closure study of open-channel flows." *J. Hydr. Engrg.*, ASCE, 121(2), 94–107.

Coomes, C. (1996). "Bottom-mounted real-time ADCPs." *Sea Technol.*, (Feb.), 29–33.

Davis, A. M., Jones, J. E., and Xing, J. (1997). "Review of recent developments in tidal hydrodynamic modeling. II: Turbulence energy models." *J. Hydr. Engrg.*, ASCE, 123(4), 293–302.

Egbert, G. D., Bennett, A. F., and Forman, M. G. G. (1994). "TOPEX/POSEIDON tides estimated using a global inverse model." *J. Geophys. Res.*, 99(C12), 24,821–24,852.

Ezer, T., and Mellor, G. L. (1992). "A numerical study of the variability and the separation of the Gulf Stream, induced by surface atmosphere forcing and lateral boundary." *J. Phys. Oceanography*, 22, 660–82.

Fofonoff, N. P. (1962). "Physical properties of sea water." *The sea: Volume 1*, N. M. Hill, ed., Interscience, New York, 3–30.

Galperin, B., Kantha, L. H., Hassid, S., and Rosati, A. (1988). "A quasi-equilibrium turbulent energy model for geophysical flows." *J. Atmospheric Sci.*, 45, 55–62.

Galperin, B., and Mellor, G. L. (1990). "Time-dependent, three-dimensional model of the Delaware Bay and River system. Part 1: Description of the model and tidal analysis." *Estuarine, Coast. and Shelf Sci.*, 31, 231–53.

Han, G., Hansen, D. V., and Galt, J. A. (1980). "Steady-state diagnostic model of the New York Bight." *J. Phys. Oceanography*, 10, 1998–2020.

Hopkins, T. S., and Dieterle, D. A. (1983). "An externally forced barotropic circulation model for the New York Bight." *Continental Shelf Res.*, 2, 49–73.

Hopkins, T. S., and Dieterle, D. A. (1987). "Analysis of the baroclinic circulation of the New York Bight with a 3-D diagnostic model." *Continental Shelf Res.*, 7, 237–265.

Jay, D. A., and Bowman, M. J. (1975). "The physical oceanography and water quality of New York Harbor and western Long Island Sound." *Tech. Rep. 23*, Marine Sciences Research Center, State University of New York at Stony Brook.

Johnson, B. H., Kim, K. W., Heath, R. E., Hsieh, B. B., and Butler, H. L. (1993). "Validation of three-dimensional hydrodynamic model of Chesapeake Bay." *J. Hydr. Engrg.*, ASCE, 119(1), 2–20.

Joyce, T. M., ed. (1985). "Warm-core rings collection." *J. Geophys. Res.*, 90, 8801–8951.

Levitus, S. (1984). "Climatological atlas of the world oceans." *NOAA Profl. Paper 13*, National Oceanic and Atmospheric Administration, Rockville, Md.

Mellor, G. L., and Yamada, T. (1982). "Development of a turbulence closure model for geophysical fluid problems." *Rev. Geophys. Space Phys.*, 20, 851–875.

Moody, J. A., et al. (1984). *Atlas of tidal elevation and current observations on the northeast American continental shelf and slope. U.S. Geological Survey Bull. 1611*, U.S. Department of the Interior, Denver.

"Newtown Creek Water Pollution Control project, East River water quality plan, Task 9.0—Harbor eutrophication model (HEM). Subtask 9.3: Calibrate HEM for hydrodynamics." (1995). *Rep. Prepared for City of New York Dept. of Envir. Protection*, HydroQual, Inc., Mahwah, N.J.

Oey, L.-Y., Manning, J., Jo, H. T., and You, K. W. (1995). "A plume and wind driven circulation of the New York Bight." *Quantitative skill assessment for coastal ocean model. Coastal and estuarine studies: Volume 42*. American Geophysical Union, Washington, D.C., 329–347.

Oey, L.-Y., Mellor, G. L., and Hires, R. I. (1985). "A three dimensional simulation of the Hudson-Raritan Estuary. Part I: Description of the model and model simulations." *J. Phys. Oceanography*, 15, 1676–1692.

Ouillon, S., and Dartus, D. (1997). "Three-dimensional computation of flow around Groyne." *J. Hydr. Engrg.*, ASCE, 123(11), 962–70.

Rosati, A., and Miyakoda, K. (1988). "A general circulation model for the upper ocean simulation." *J. Phys. Oceanography*, 18, 1601–26.

Scheffner, N. W., Vermulakonda, S. R., Mark, D. J., Butler, H. L., and Kim, K. W. (1994). "New York Bight study. Report 1: Hydrodynamic modeling." *Tech. Rep. CERC-94-4*, U.S. Army Corps of Engineers, Vicksburg, Miss.

Schmalz, R. A. Jr., Devine, M. F., and Richardson, P. H. (1994). "Long Island Sound oceanography project." *Summary Rep. Vol. 2: Residual Circulation and Thermohaline Struct., NOAA Tech. Rep. NOSOES 003*, Silver Spring, Md.

Sinha, S. K., Sotiropoulos, F., and Odgaard, J. (1998). "Three-dimensional numerical model for flow through natural rivers." *J. Hydr. Engrg.*, ASCE, 124(1), 13–23.

Smagorinsky, J. (1963). "General circulation experiments with the primitive equations. I: The basic experiment." *Monthly Weather Rev.*, 91, 99–164.

Wang, J. D., Blumberg, A. F., Butler, H. L., and Hamilton, P. (1990). "Transport predication in partially stratified tidal water." *J. Hydr. Engrg.*, ASCE, 116(3), 380–96.

Wong, K.-C. (1990). "Sea level variability in Long Island Sound." *Estuaries*, 13(4), 362–72.

APPENDIX 2

TEMPORAL VARIATION OF RIVER DISCHARGES ENTERING THE CARP MODEL

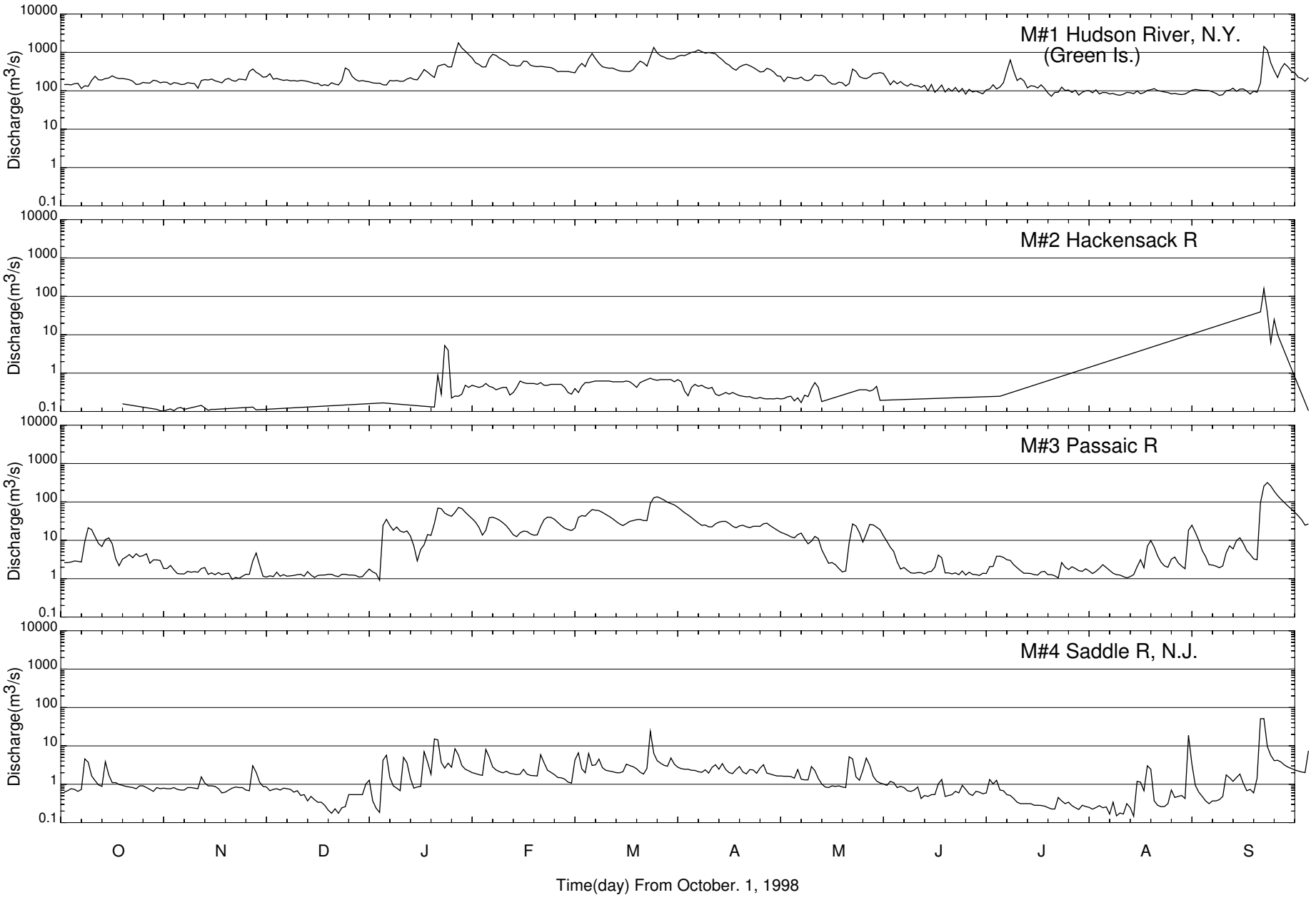

River Inflow Boundary Conditions

DATE: 8/23/2004 TIME: 11:39:28

/ont1/hrfo0010/DATA/FLOW/flow_9899.gdp

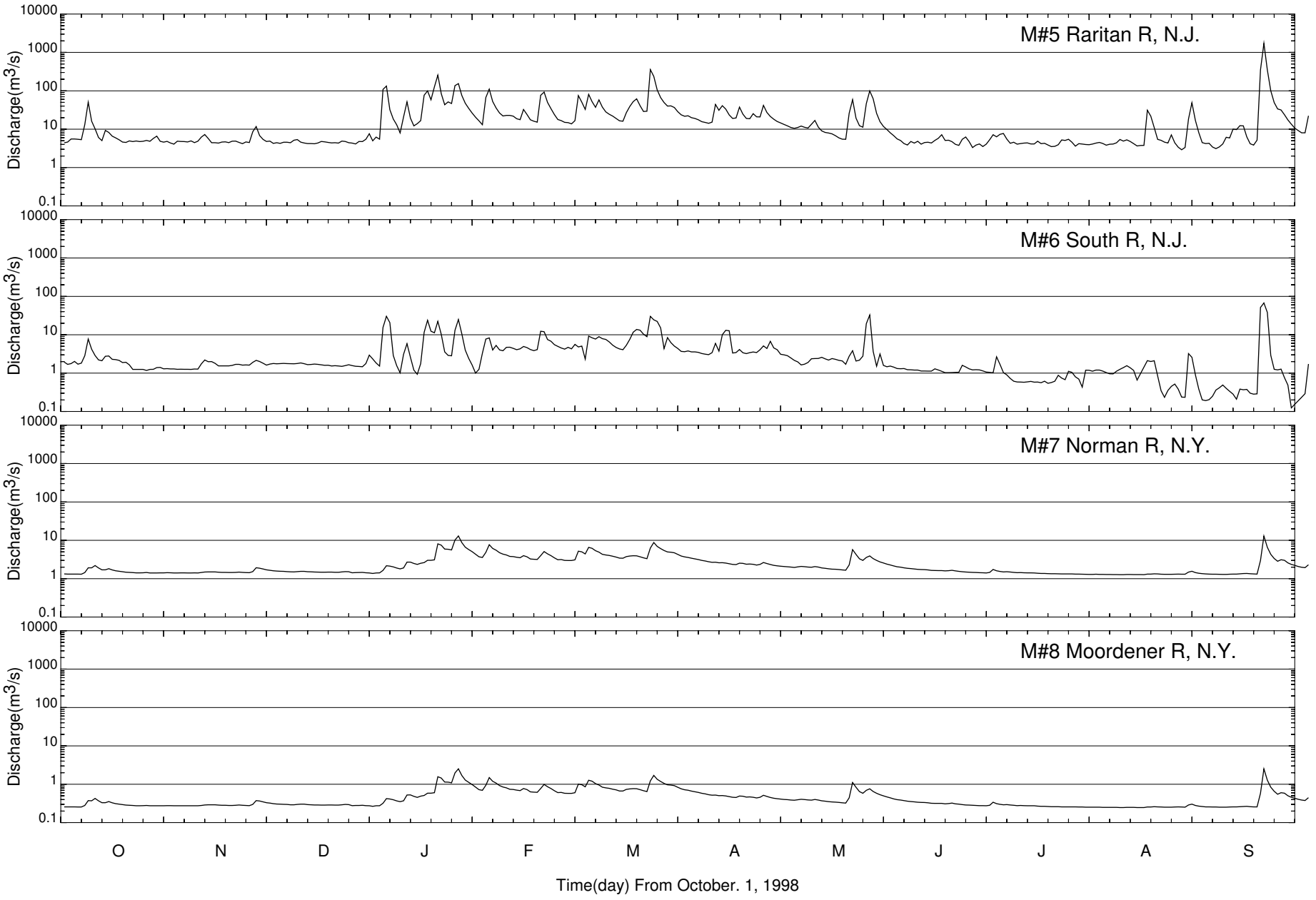

River Inflow Boundary Conditions

DATE: 8/23/2004 TIME: 11:39:28

/ont1/hrfo0010/DATA/FLOW/flow_9899.gdp

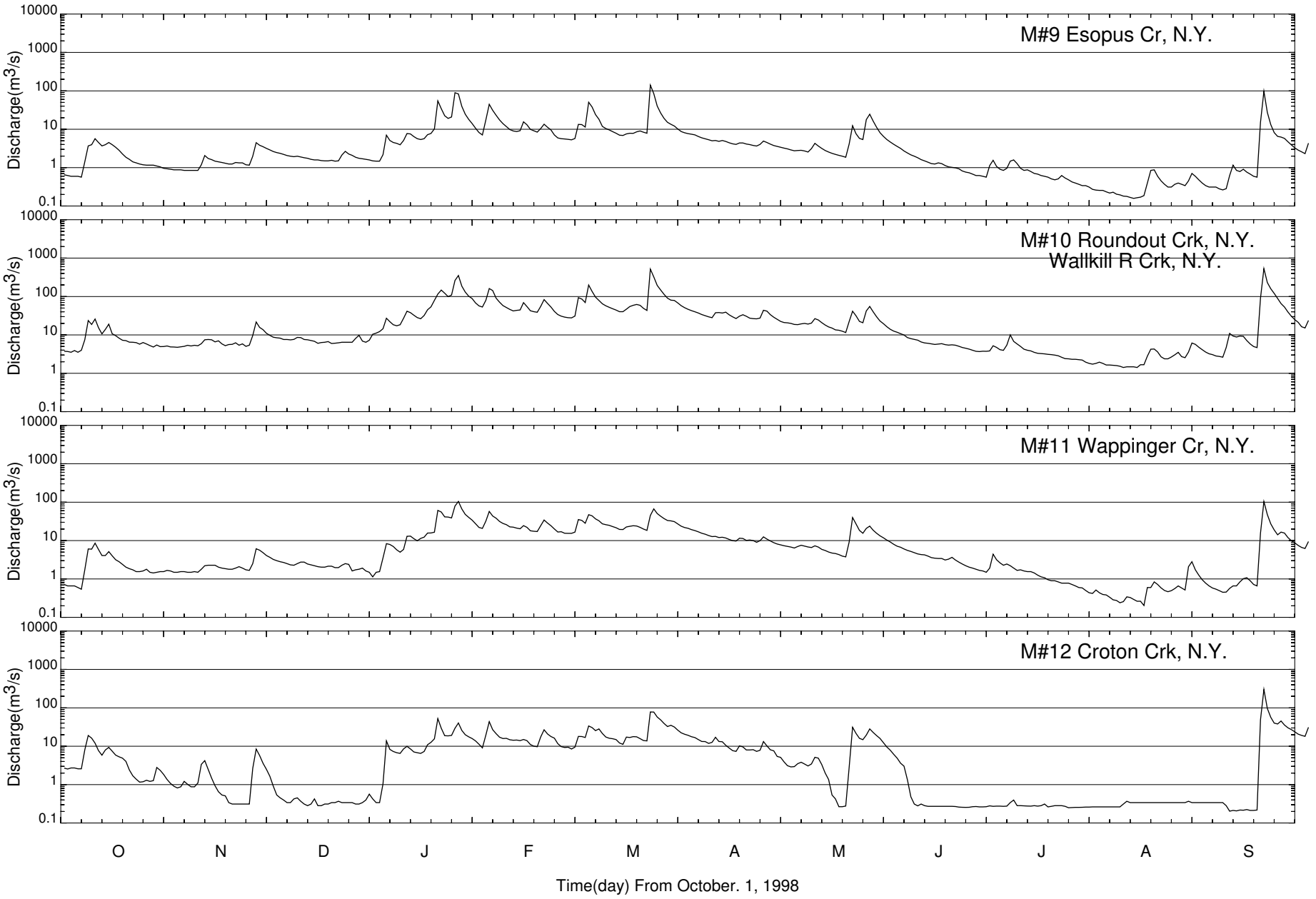

River Inflow Boundary Conditions

DATE: 8/23/2004 TIME: 11:39:28

/ont1/hrfo0010/DATA/FLOW/flow_9899.gdp

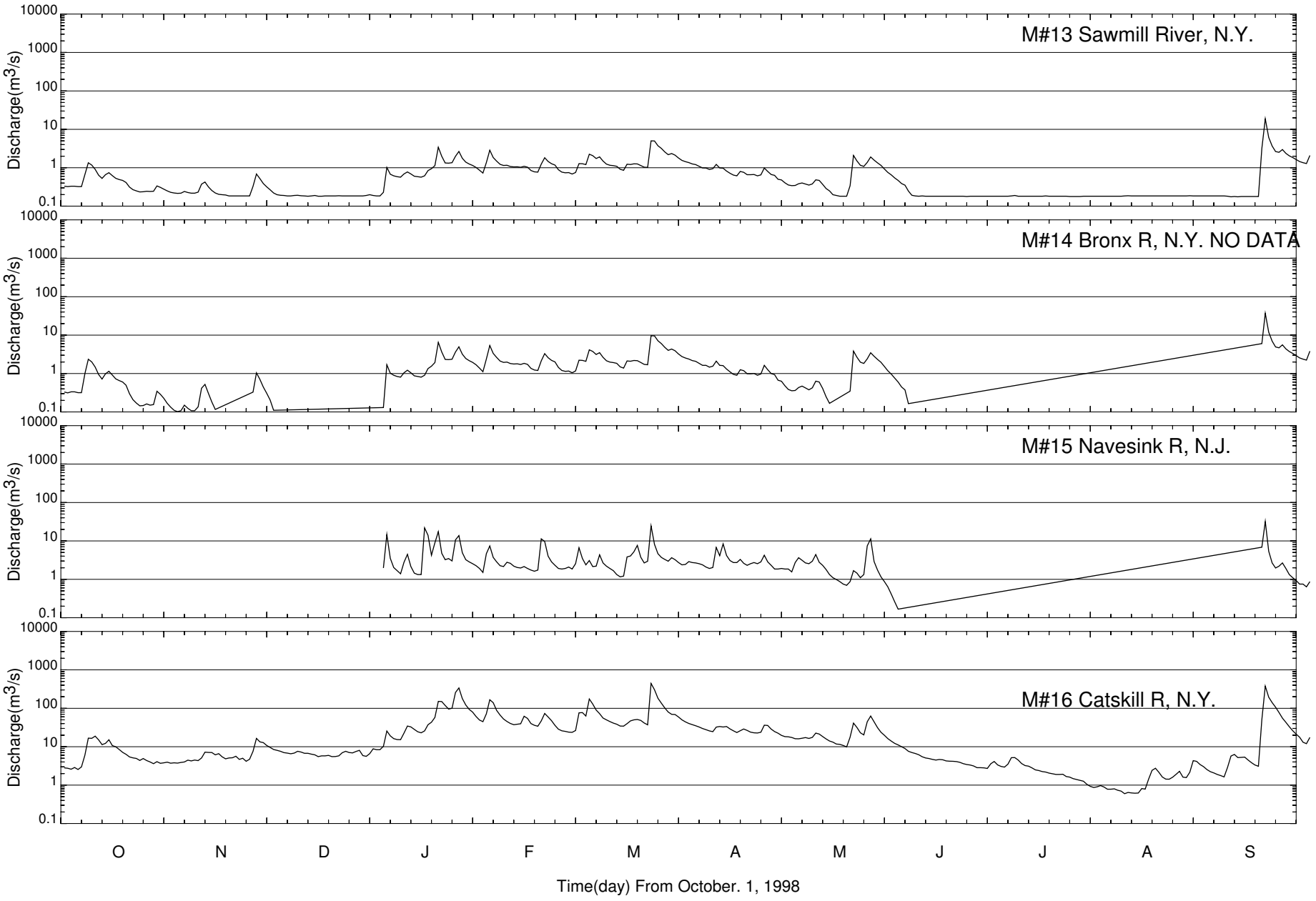

River Inflow Boundary Conditions

DATE: 8/23/2004 TIME: 11:39:28

/ont1/hrfo0010/DATA/FLOW/flow_9899.gdp

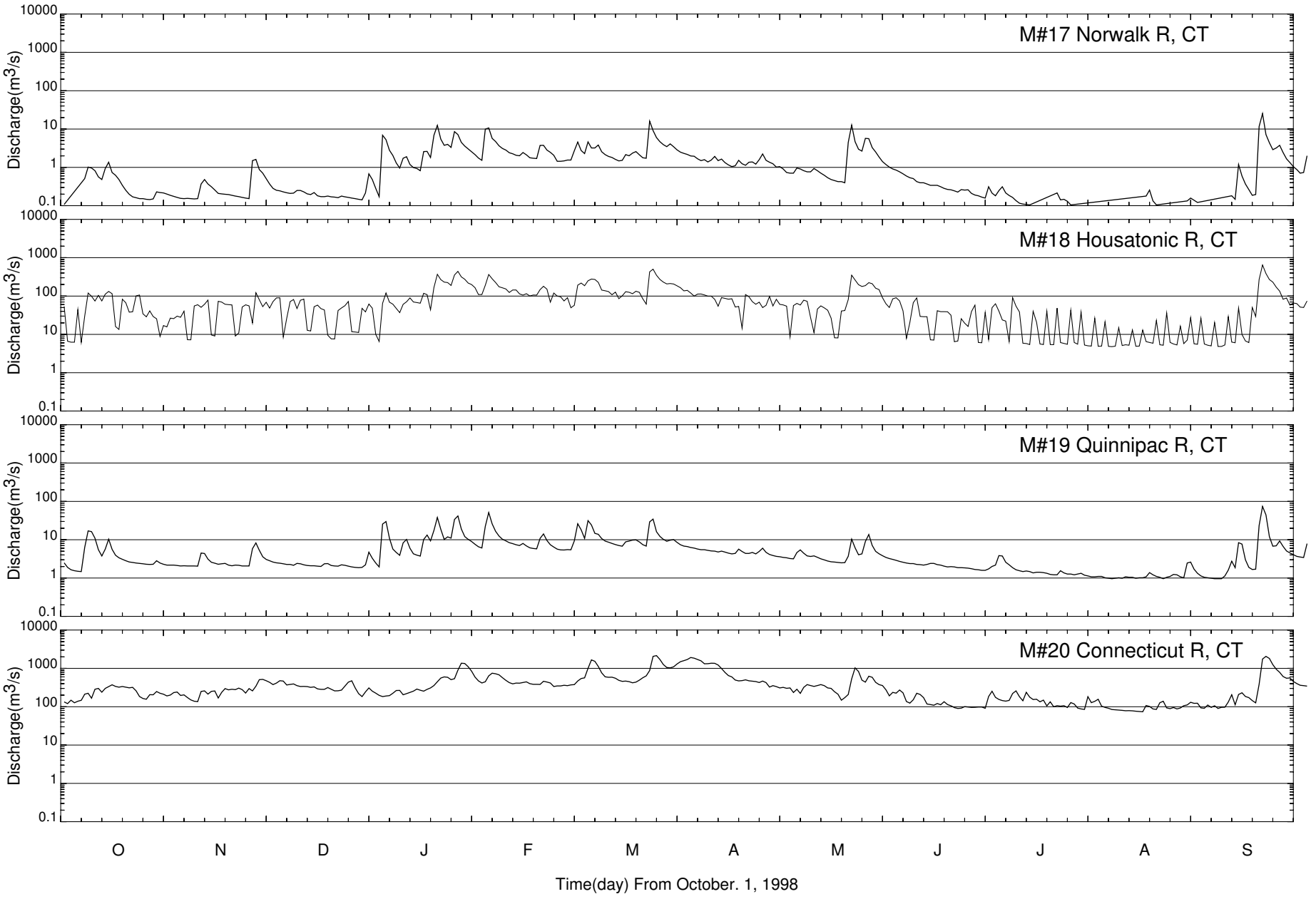

River Inflow Boundary Conditions

DATE: 8/23/2004 TIME: 11:39:28

/ont1/hrfo0010/DATA/FLOW/flow_log_9899.gdp

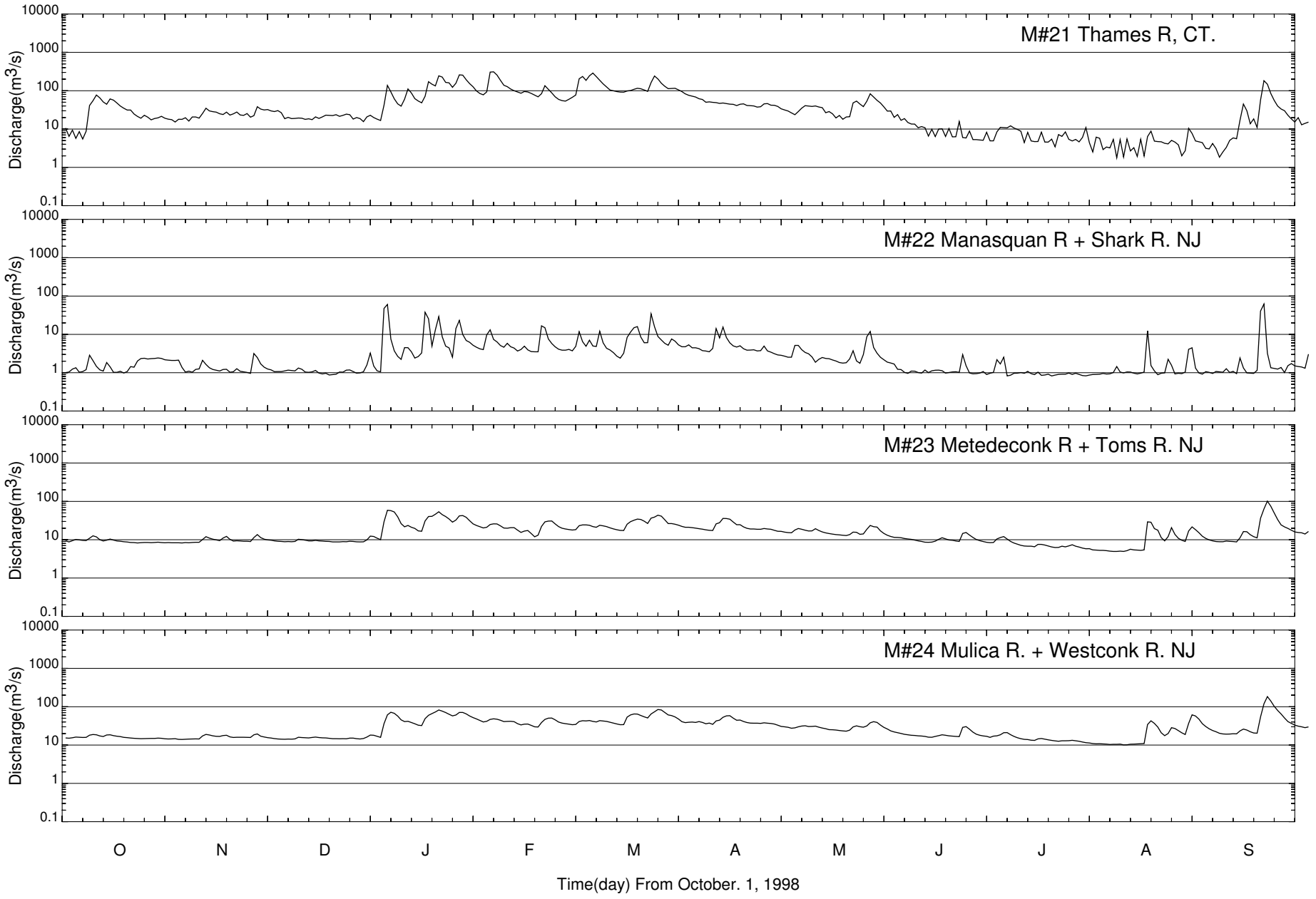

River Inflow Boundary Conditions

DATE: 8/23/2004 TIME: 11:39:28

/ont1/hrfo0010/DATA/FLOW/flow_9899.gdp

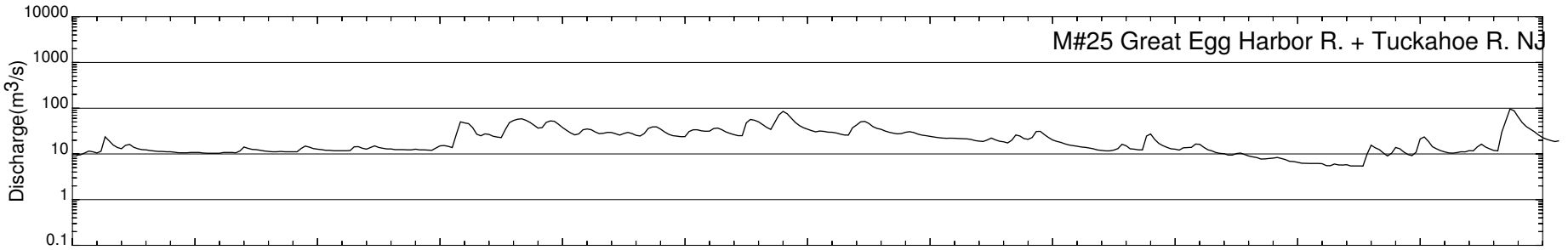
M#25 Great Egg Harbor R. + Tuckahoe R. NJ
Discharge(m3/s)
10000
1000
100
10
1
0.1

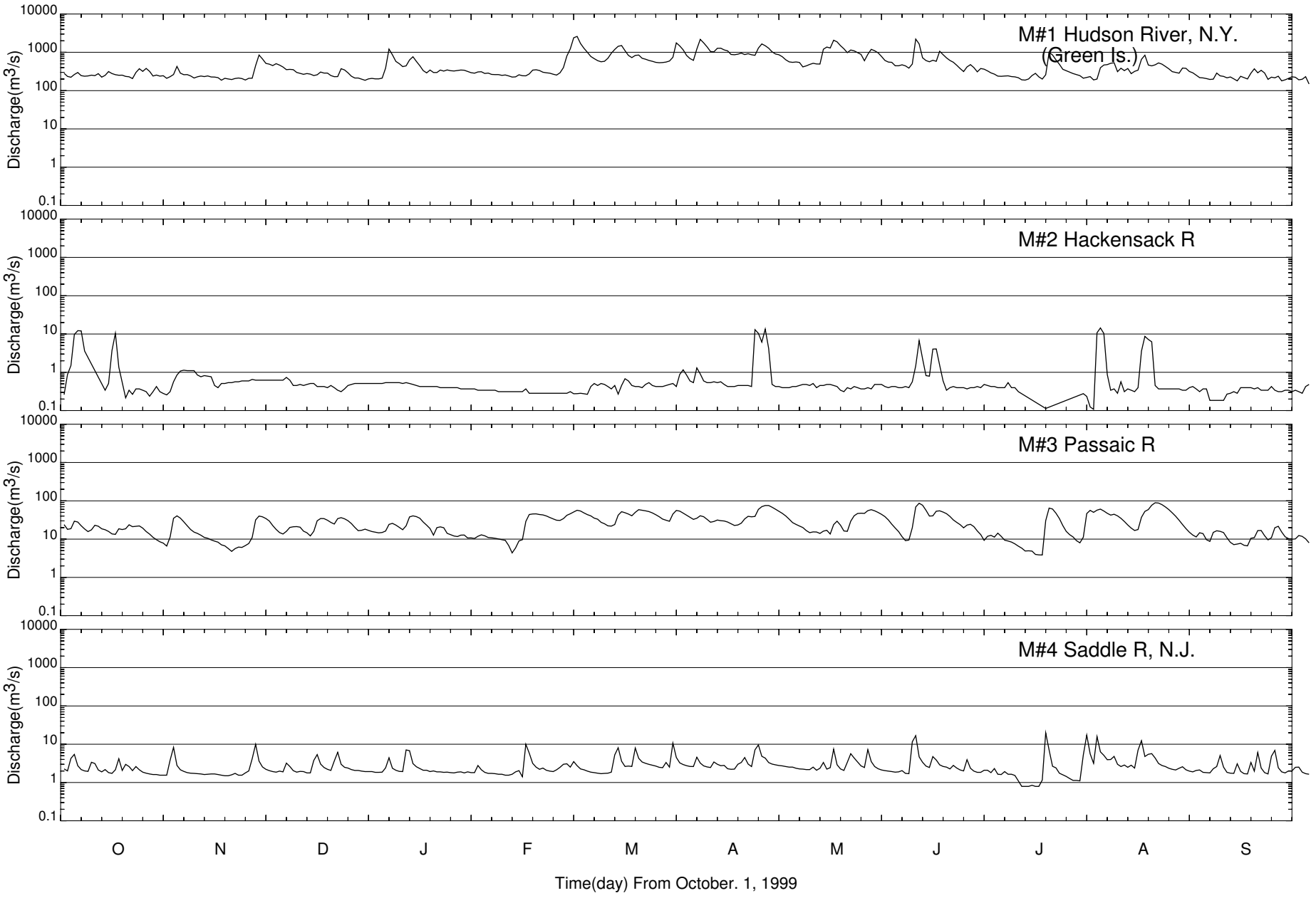

River Inflow Boundary Conditions

DATE: 8/23/2004 TIME: 11:39:33

/ont1/hrfo0010/DATA/FLOW/flow_9900.gdp

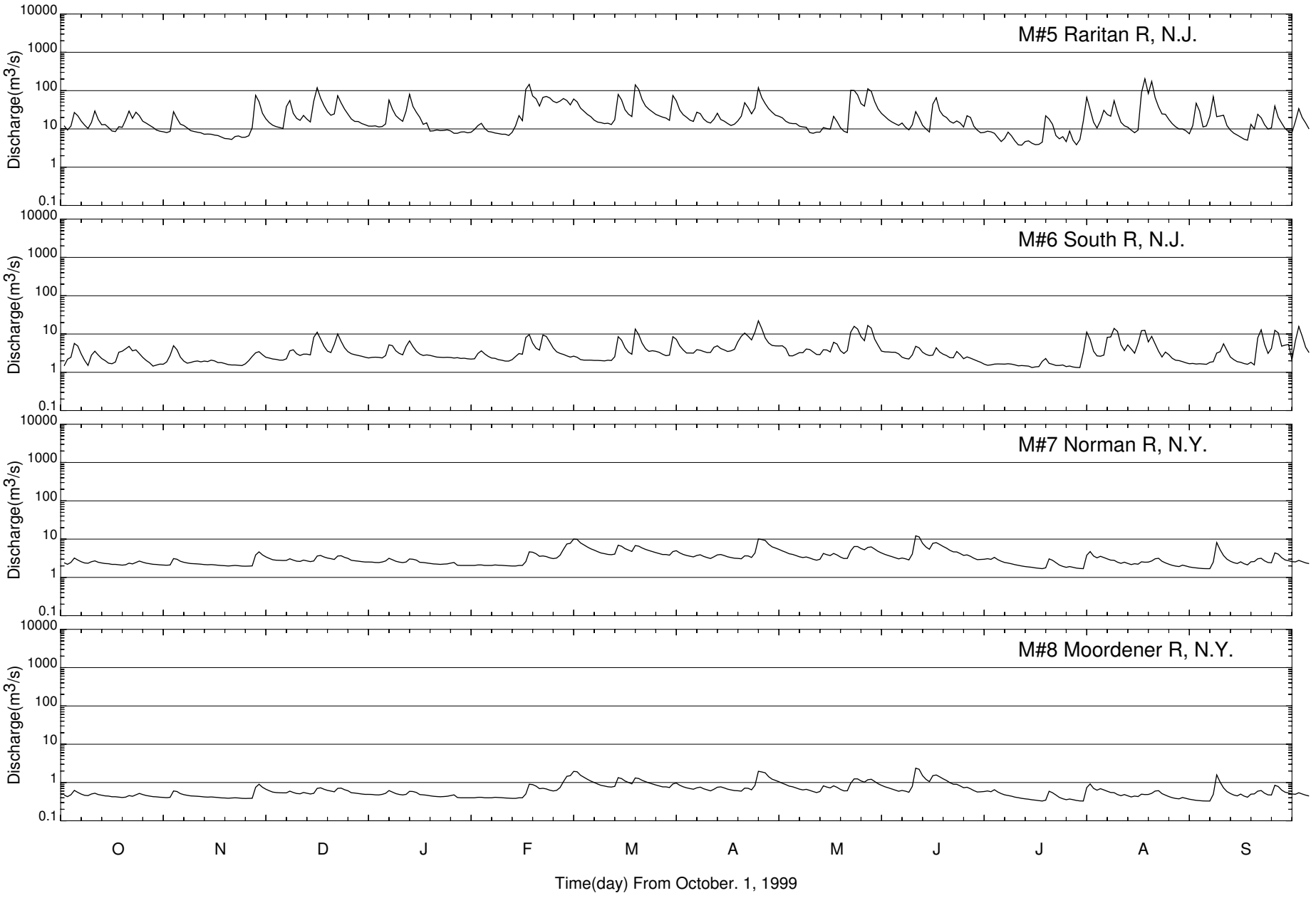

River Inflow Boundary Conditions

DATE: 8/23/2004 TIME: 11:39:33

/ont1/hrfo0010/DATA/FLOW/flow_9900.gdp

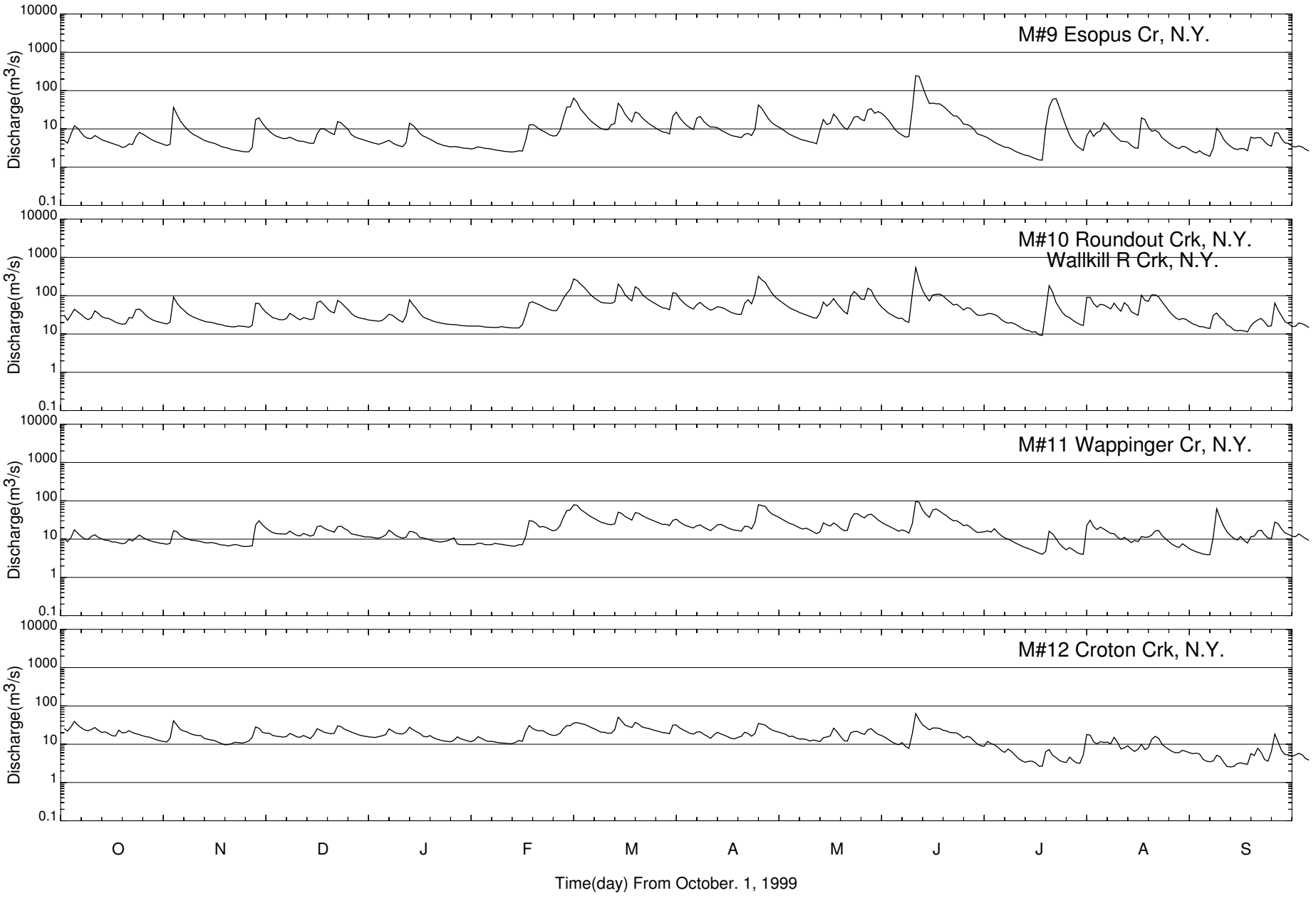

River Inflow Boundary Conditions

DATE: 8/23/2004 TIME: 11:39:33

/ont1/hrfo0010/DATA/FLOW/flow_9900.gdp

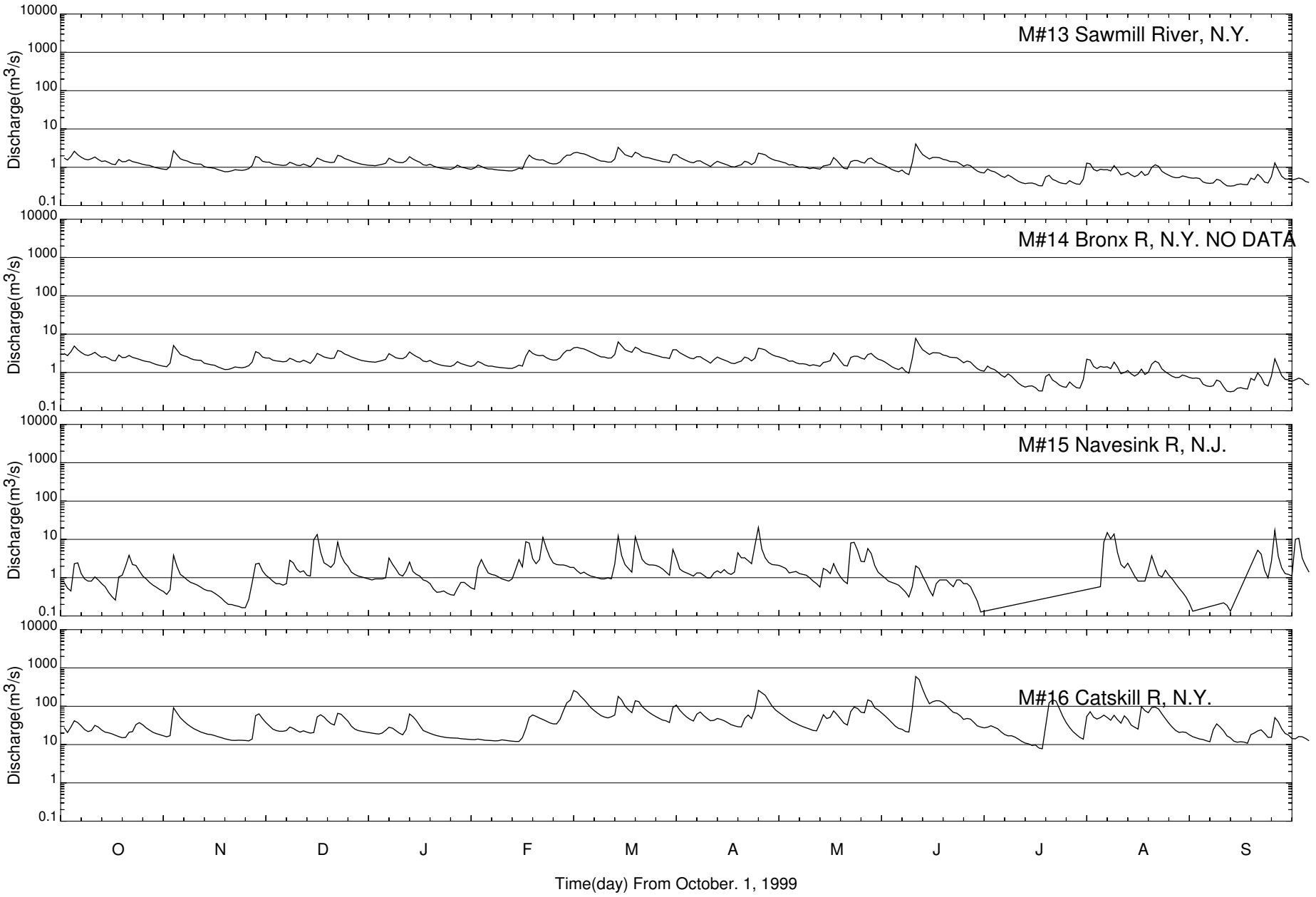

River Inflow Boundary Conditions

DATE: 8/23/2004 TIME: 11:39:33

/ont1/hrfo0010/DATA/FLOW/flow_9900.gdp

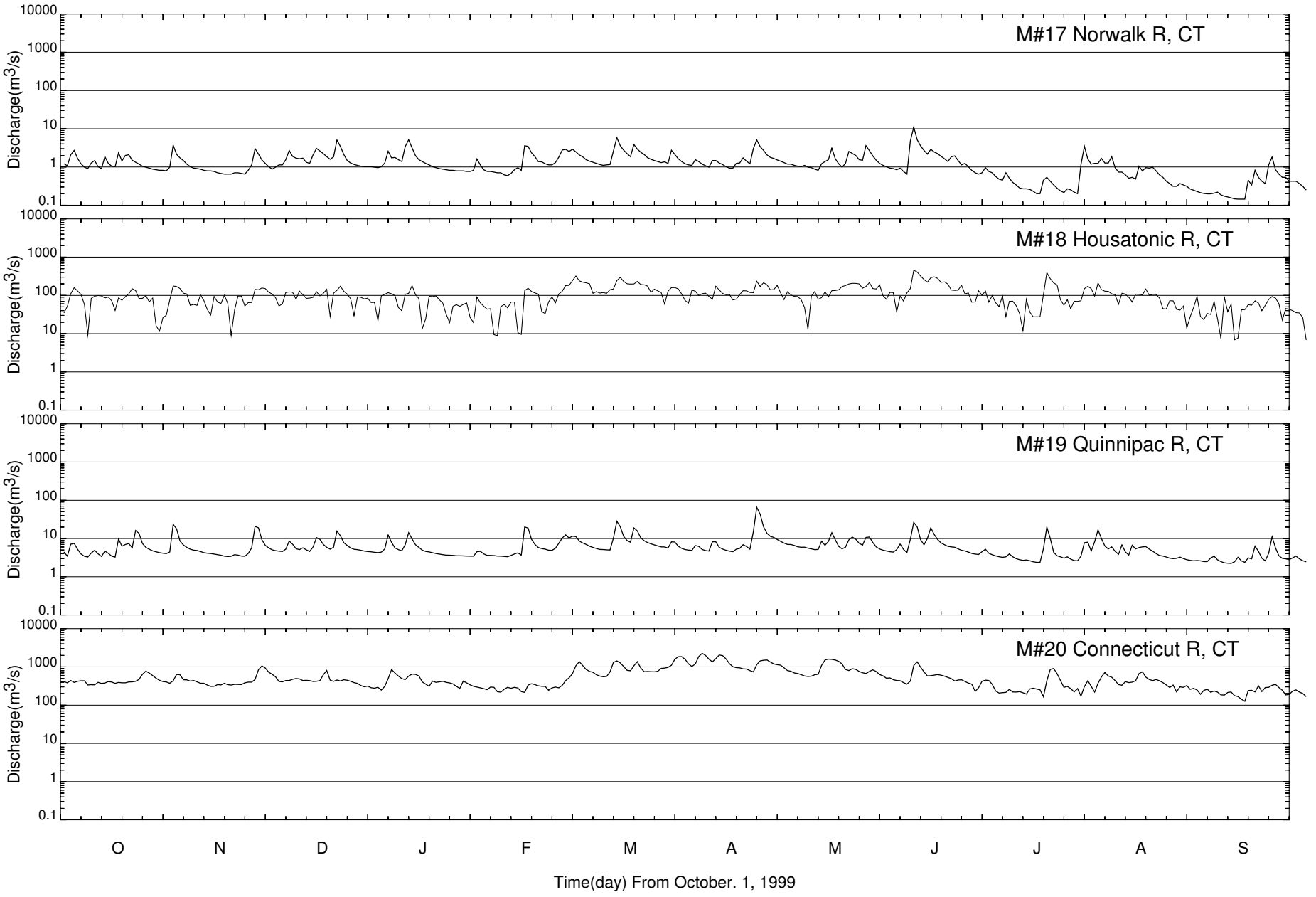

River Inflow Boundary Conditions

DATE: 8/23/2004 TIME: 11:39:33

/ont1/hrfo0010/DATA/FLOW/flow_log_9900.gdp

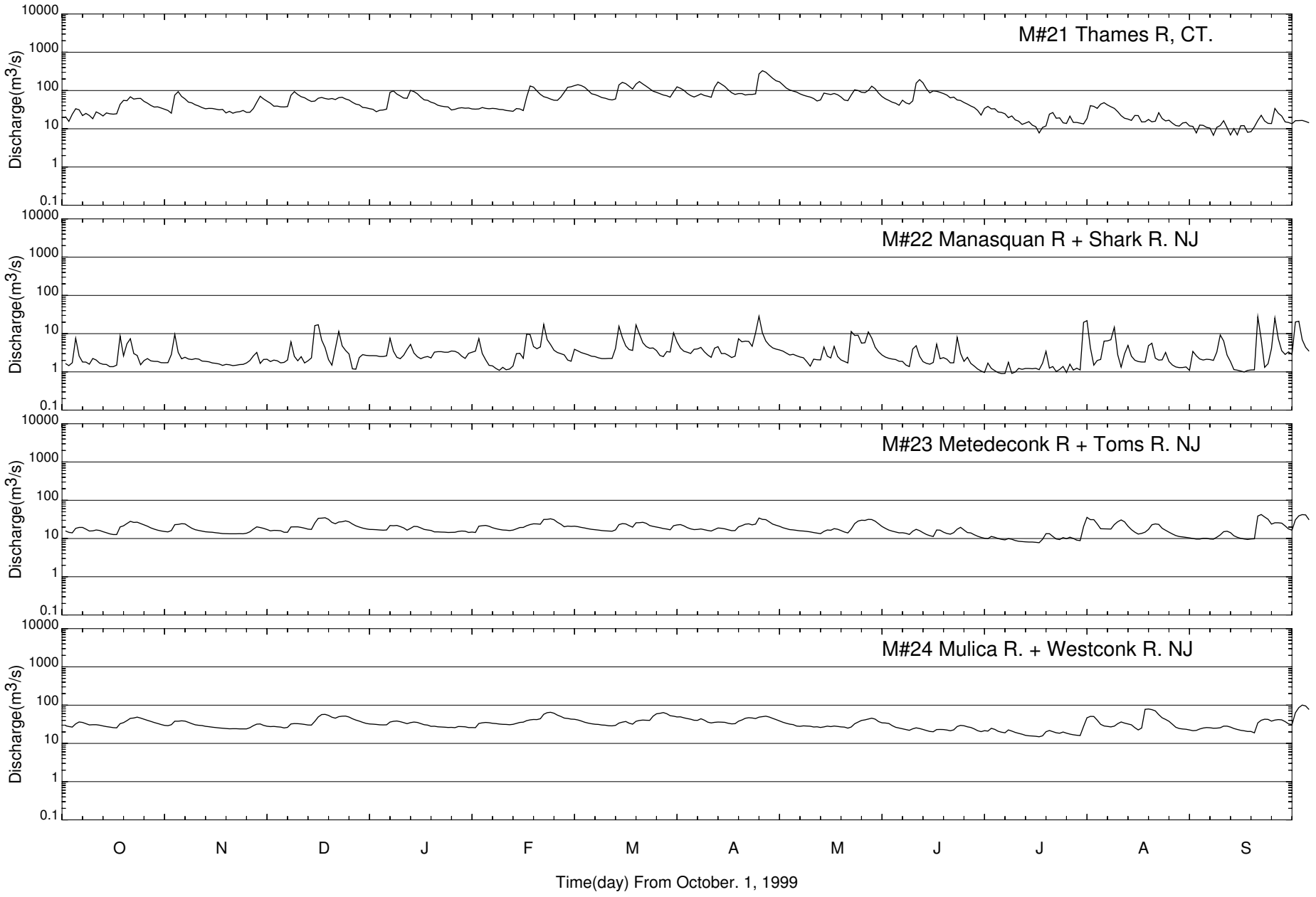

River Inflow Boundary Conditions

DATE: 8/23/2004 TIME: 11:39:33

/ont1/hrfo0010/DATA/FLOW/flow_9900.gdp

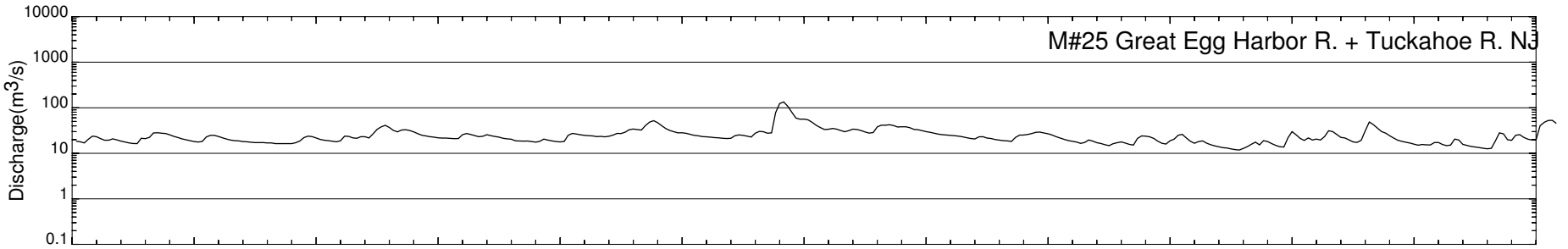
M#25 Great Egg Harbor R. + Tuckahoe R. NJ
Discharge(m3/s)
10000
1000
100
10
1
0.1

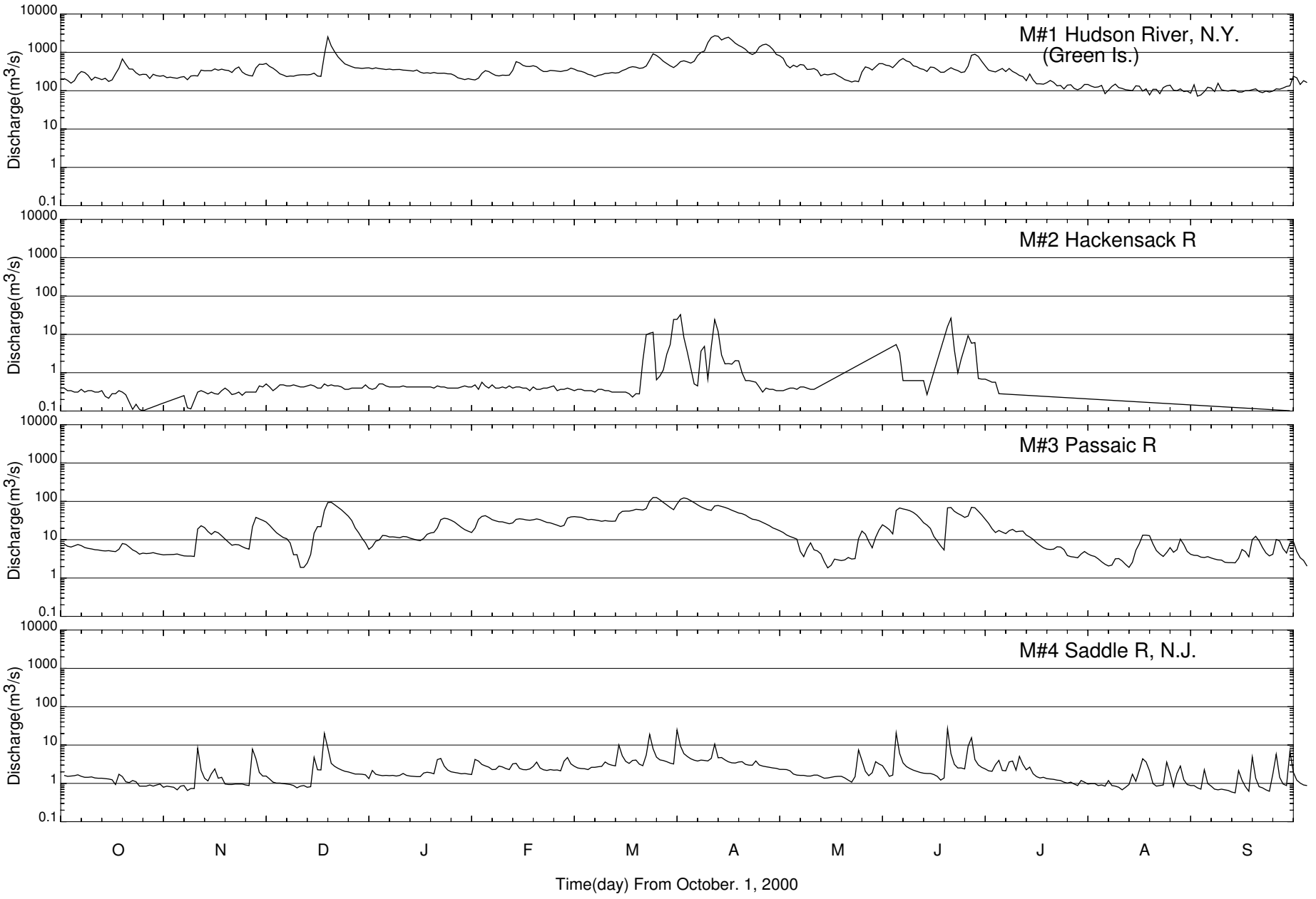

River Inflow Boundary Conditions

DATE: 8/23/2004 TIME: 11:42:19

/ont1/hrfo0010/DATA/FLOW/flow_9900.gdp

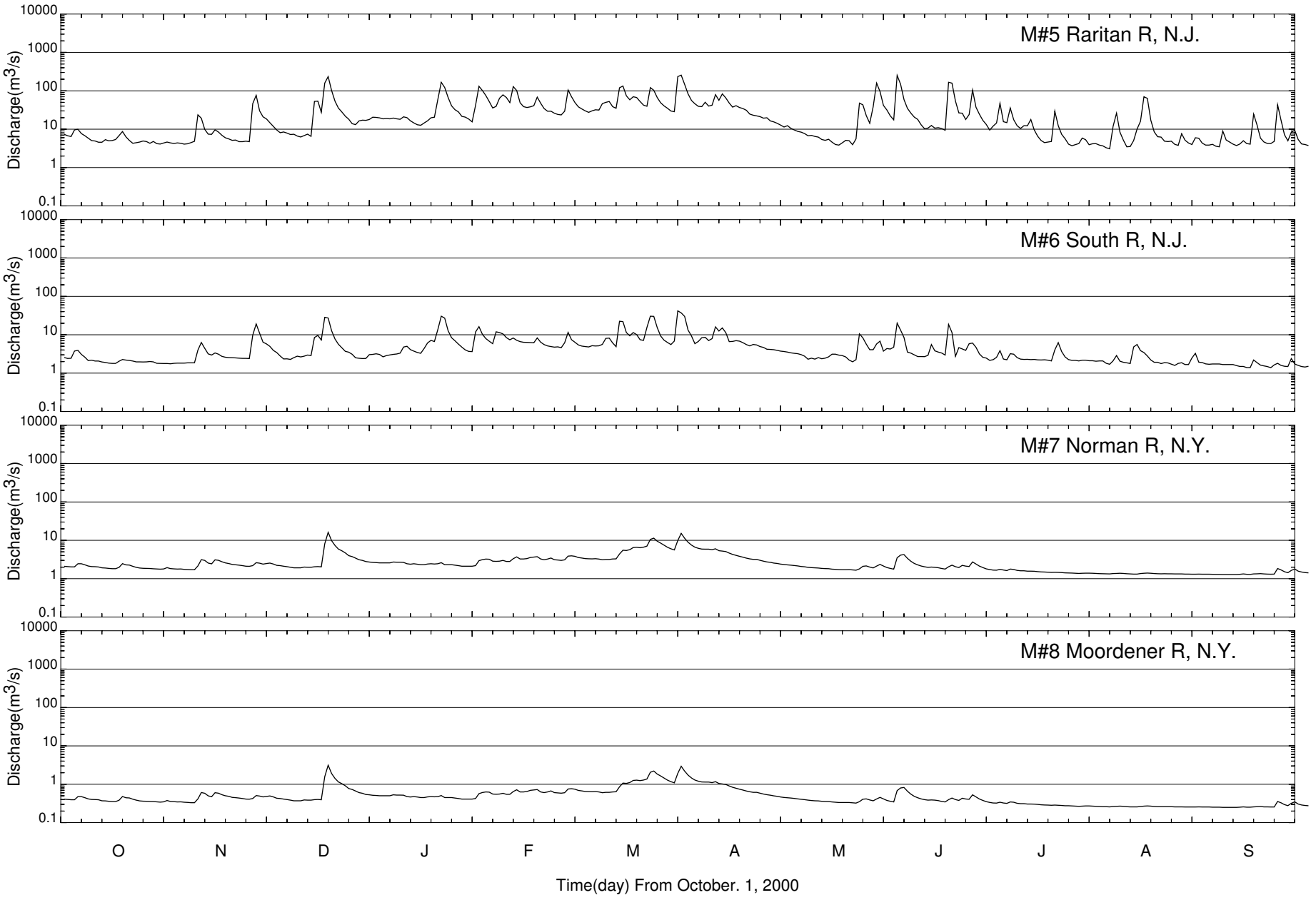

River Inflow Boundary Conditions

DATE: 8/23/2004 TIME: 11:42:19

/ont1/hrfo0010/DATA/FLOW/flow_9900.gdp

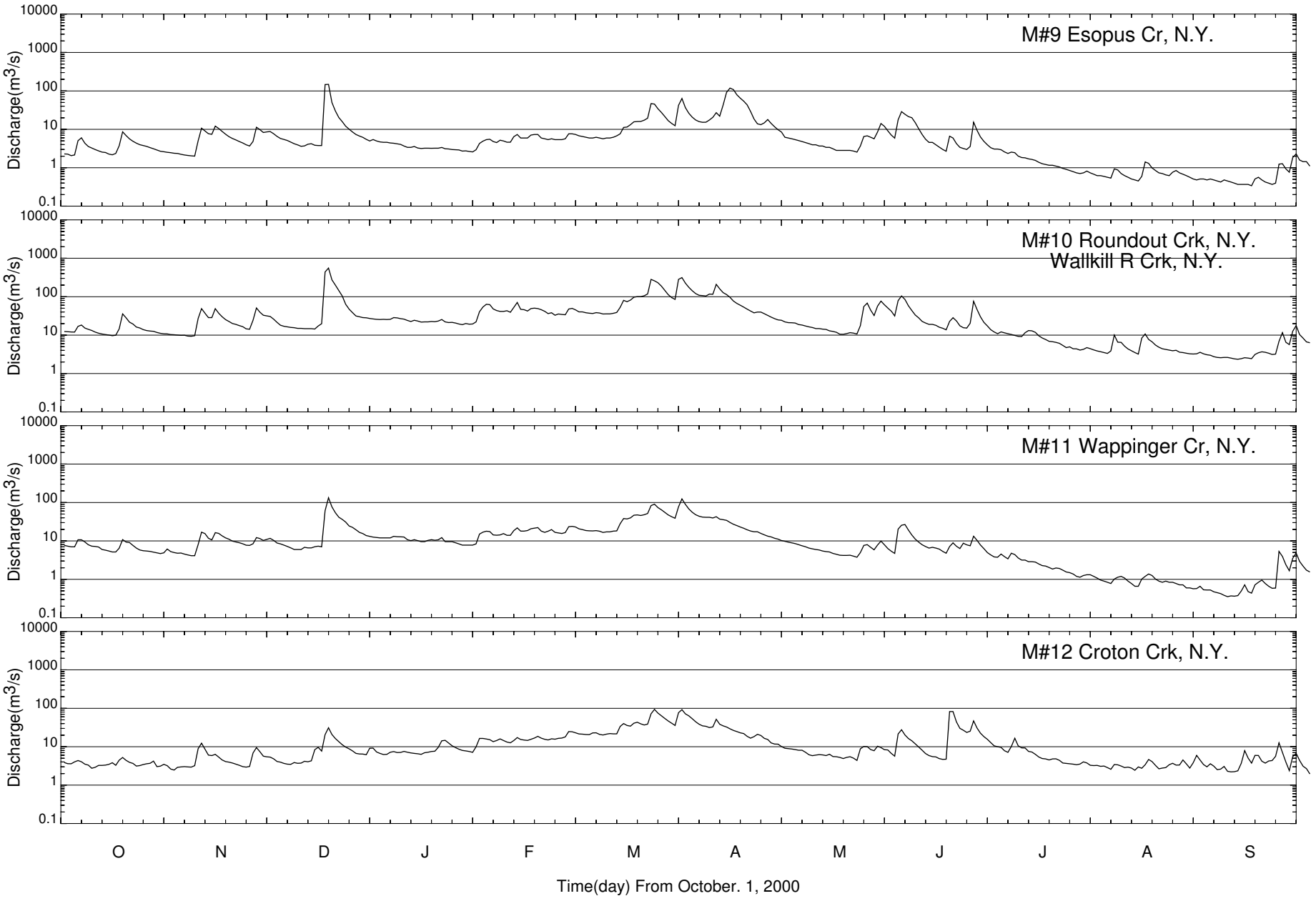

River Inflow Boundary Conditions

DATE: 8/23/2004 TIME: 11:42:19

/ont1/hrfo0010/DATA/FLOW/flow_9900.gdp

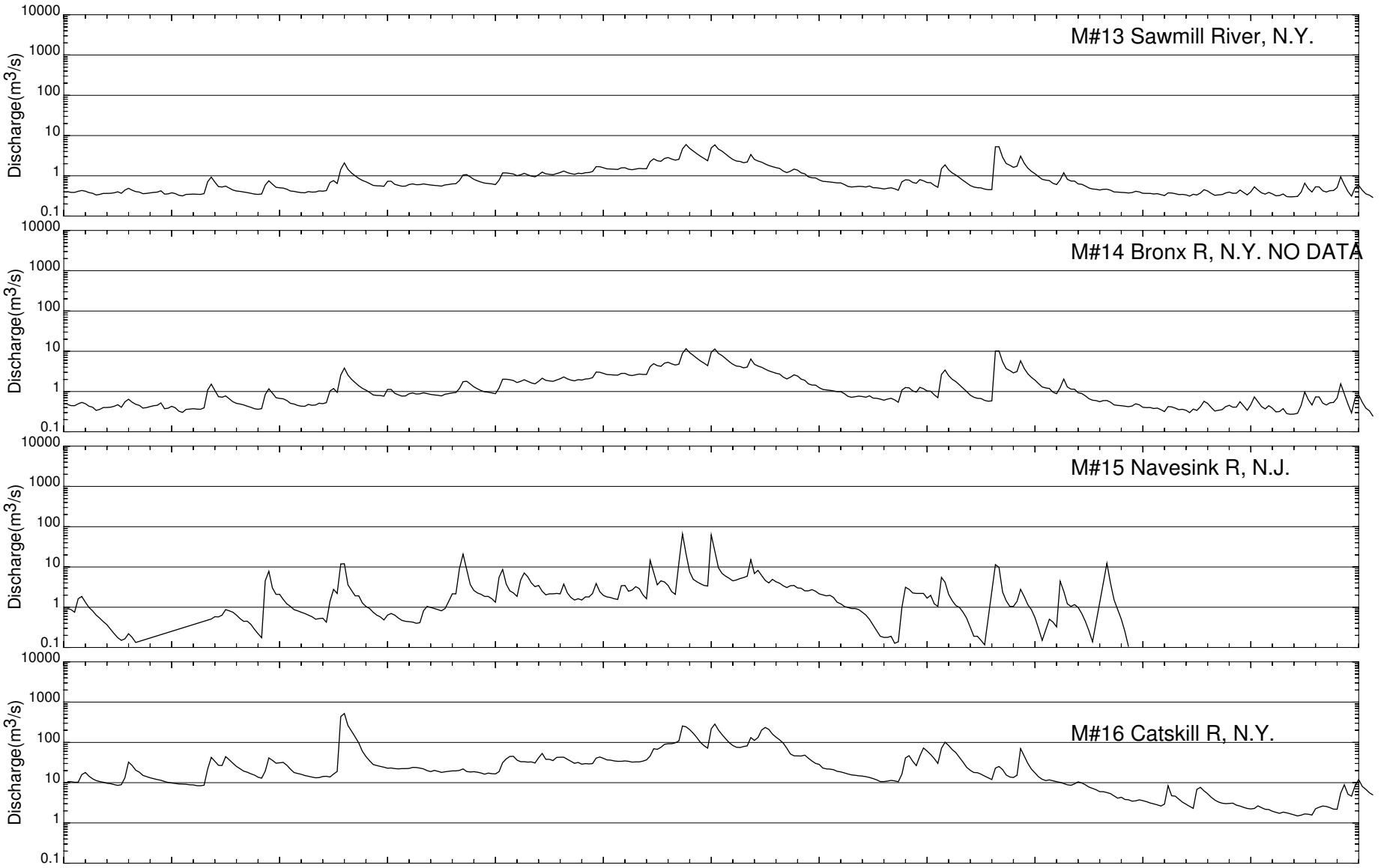

River Inflow Boundary Conditions

DATE: 8/23/2004 TIME: 11:42:19

/ont1/hrfo0010/DATA/FLOW/flow_9900.gdp

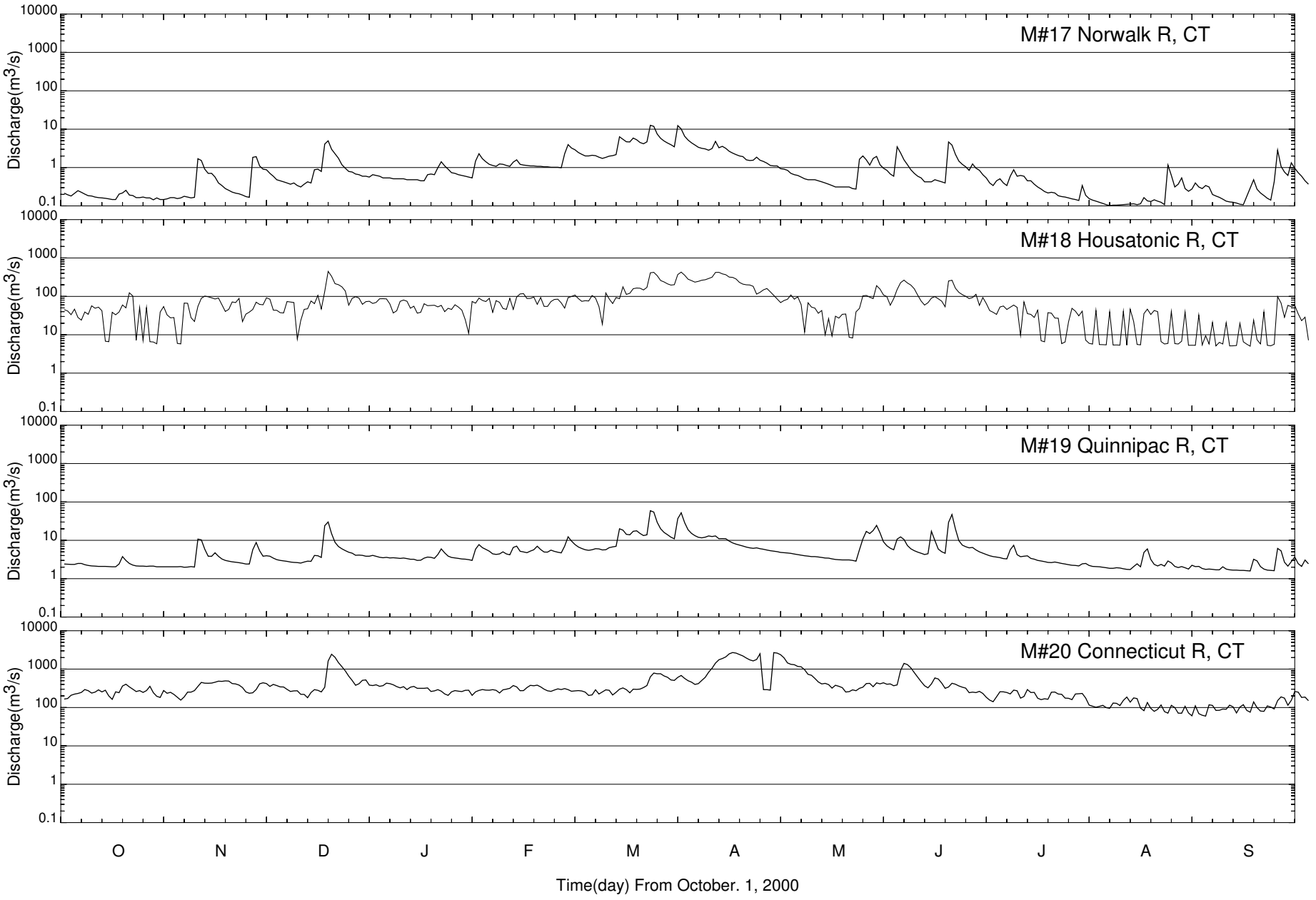

River Inflow Boundary Conditions

DATE: 8/23/2004 TIME: 11:42:19

/ont1/hrfo0010/DATA/FLOW0002/flow_log_0001.gdp

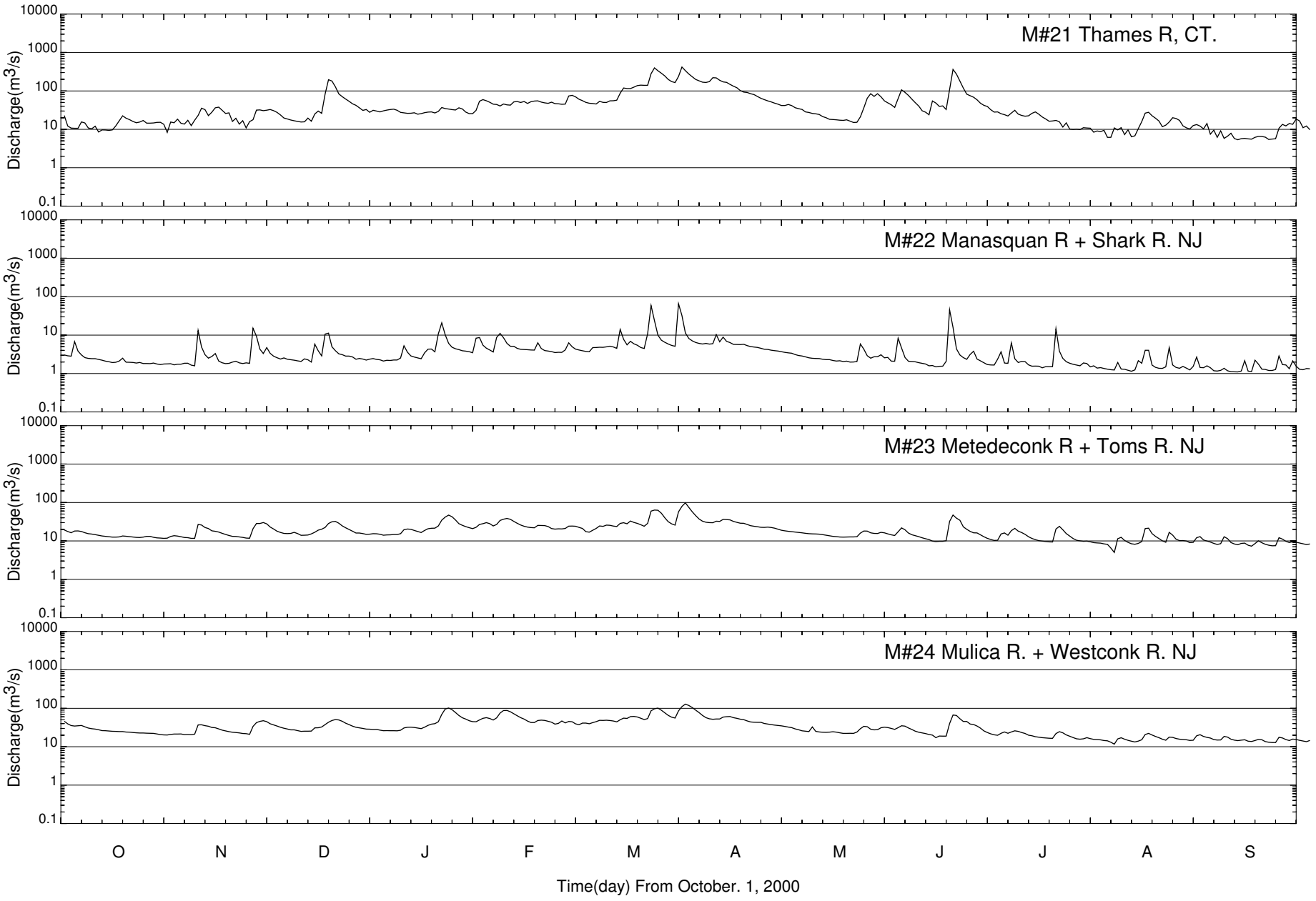

River Inflow Boundary Conditions

DATE: 8/23/2004 TIME: 11:42:19

/ont1/hrfo0010/DATA/FLOW/flow_9900.gdp

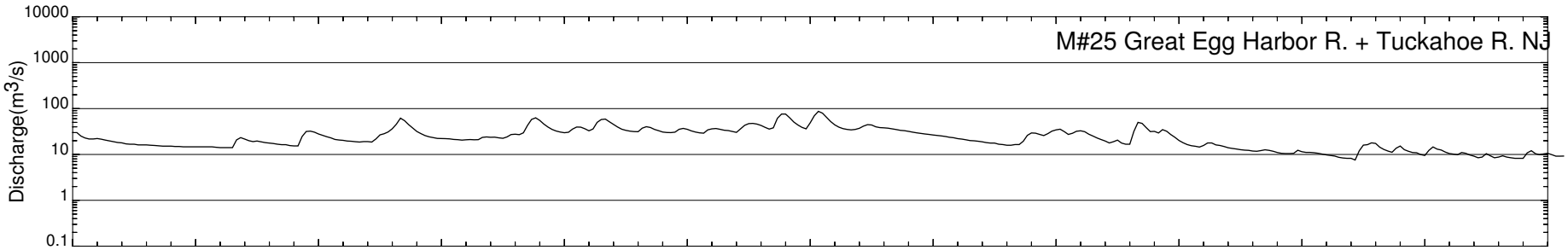
M#25 Great Egg Harbor R. + Tuckahoe R. NJ
Discharge(m3/s)
10000
1000
100
10
1
0.1

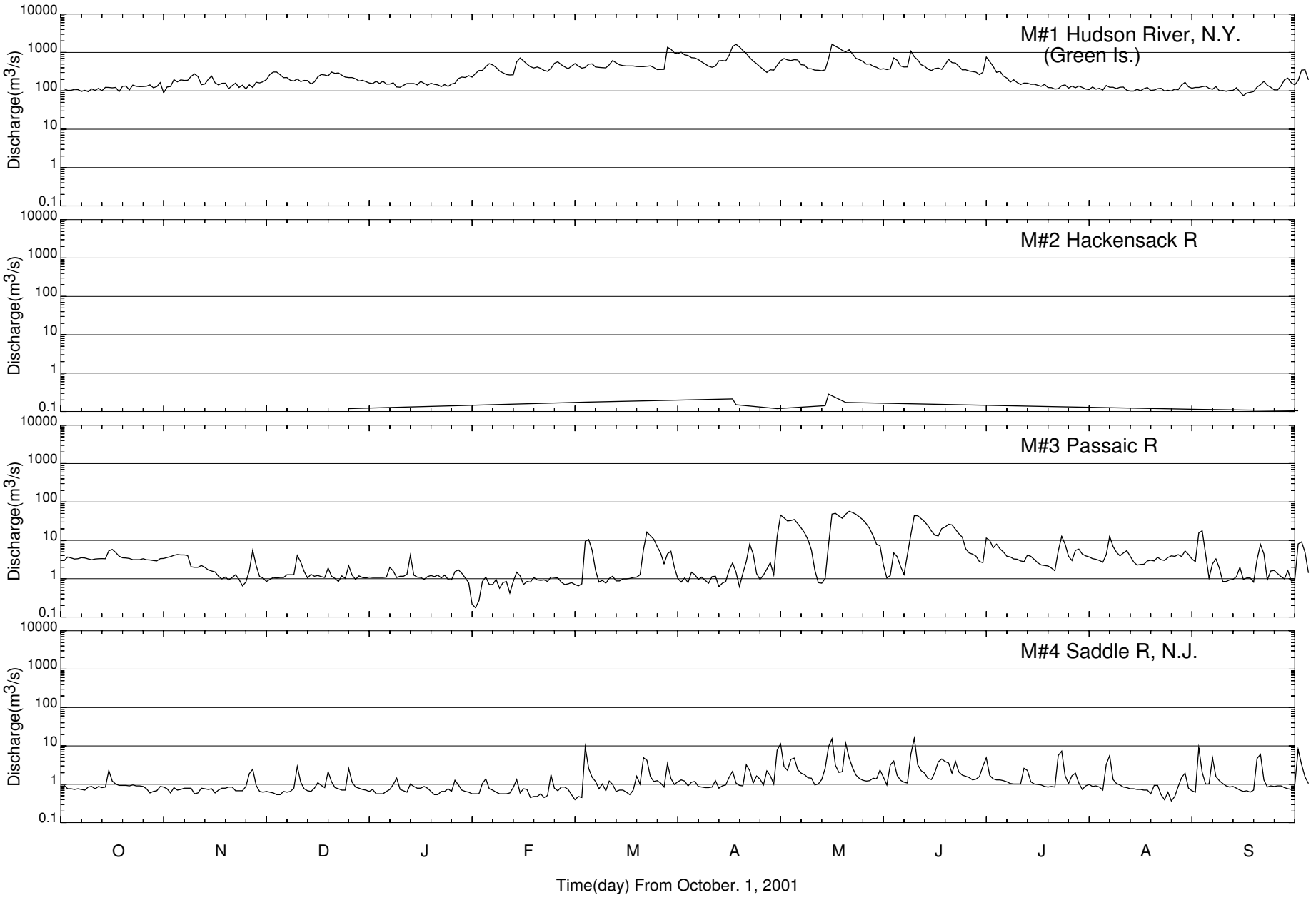

River Inflow Boundary Conditions

DATE: 8/23/2004 TIME: 11:42:24

/ont1/hrfo0010/DATA/FLOW/flow_9900.gdp

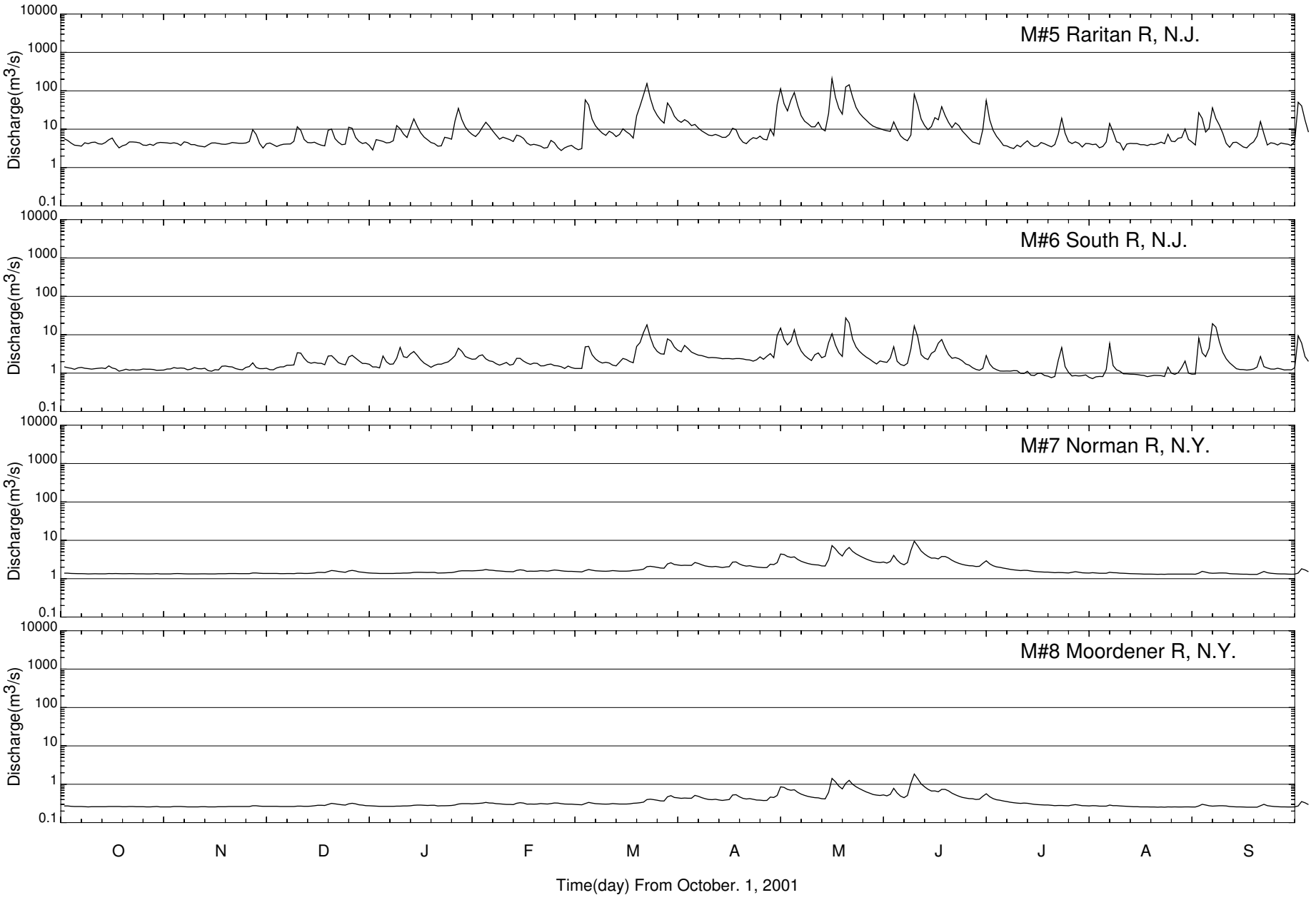

River Inflow Boundary Conditions

DATE: 8/23/2004 TIME: 11:42:24

/ont1/hrfo0010/DATA/FLOW/flow_9900.gdp

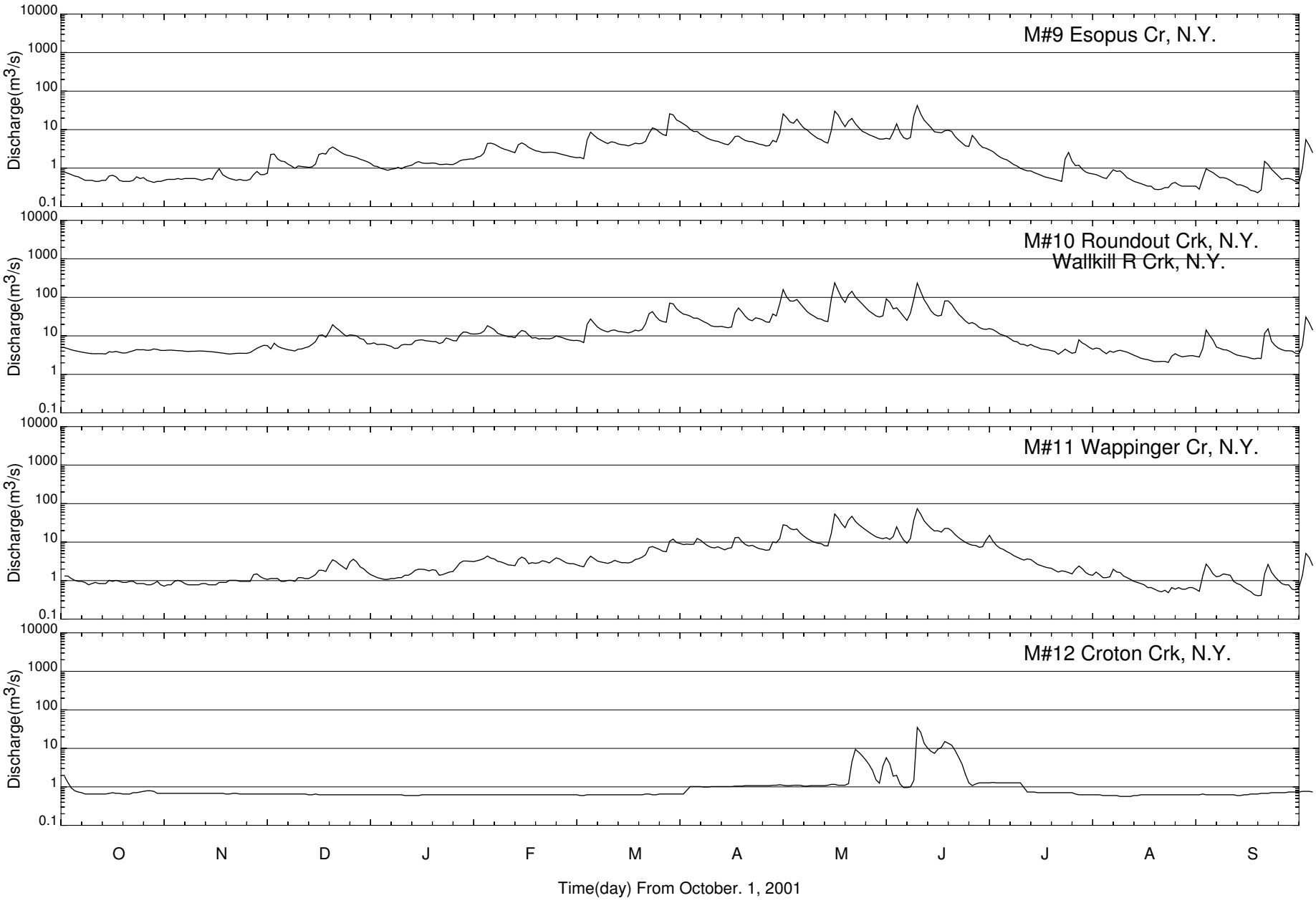

River Inflow Boundary Conditions

DATE: 8/23/2004 TIME: 11:42:24 /ont1/hrfo0010/DATA/FLOW/flow_9900.gdp

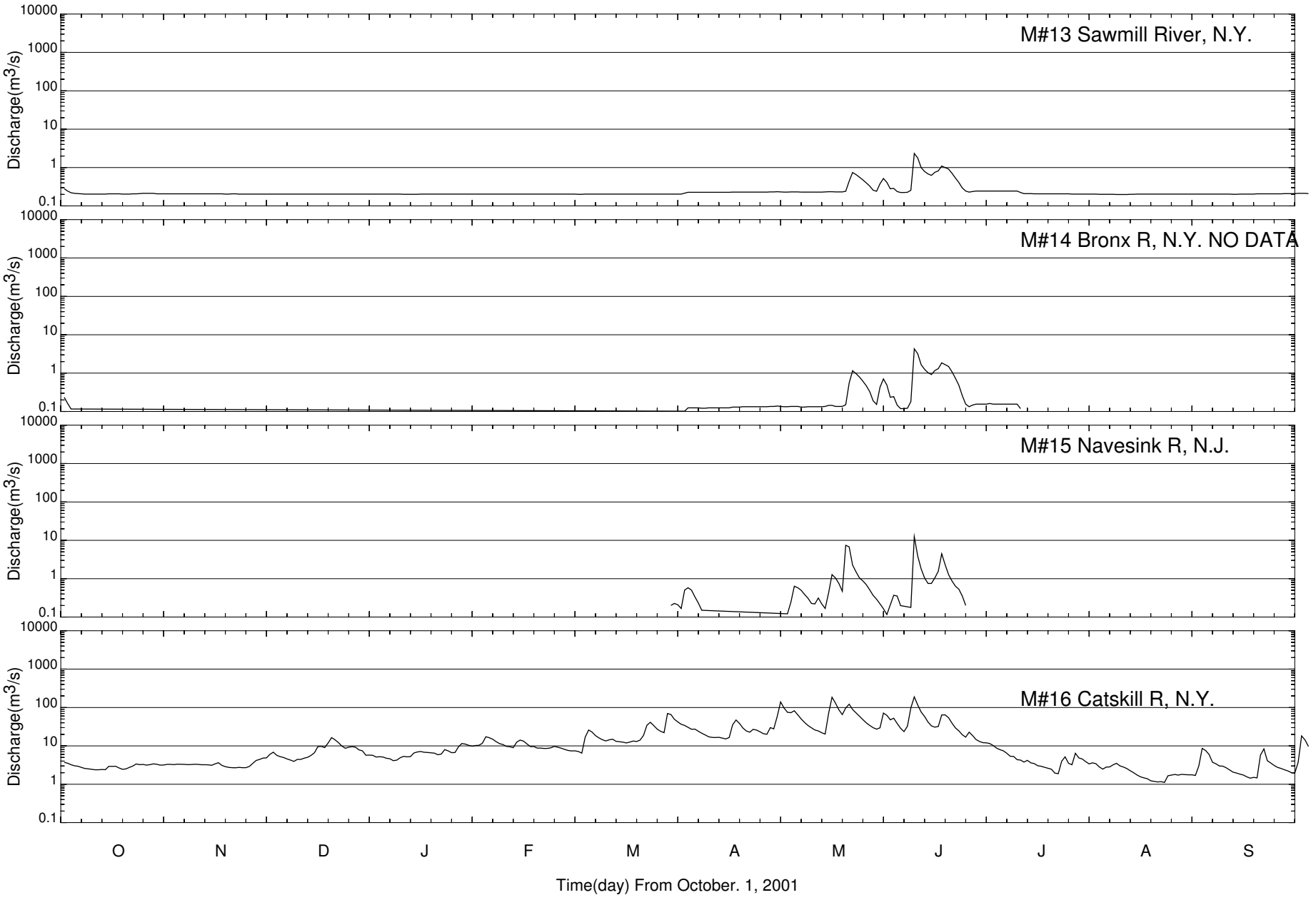

River Inflow Boundary Conditions

DATE: 8/23/2004 TIME: 11:42:24

/ont1/hrfo0010/DATA/FLOW/flow_9900.gdp

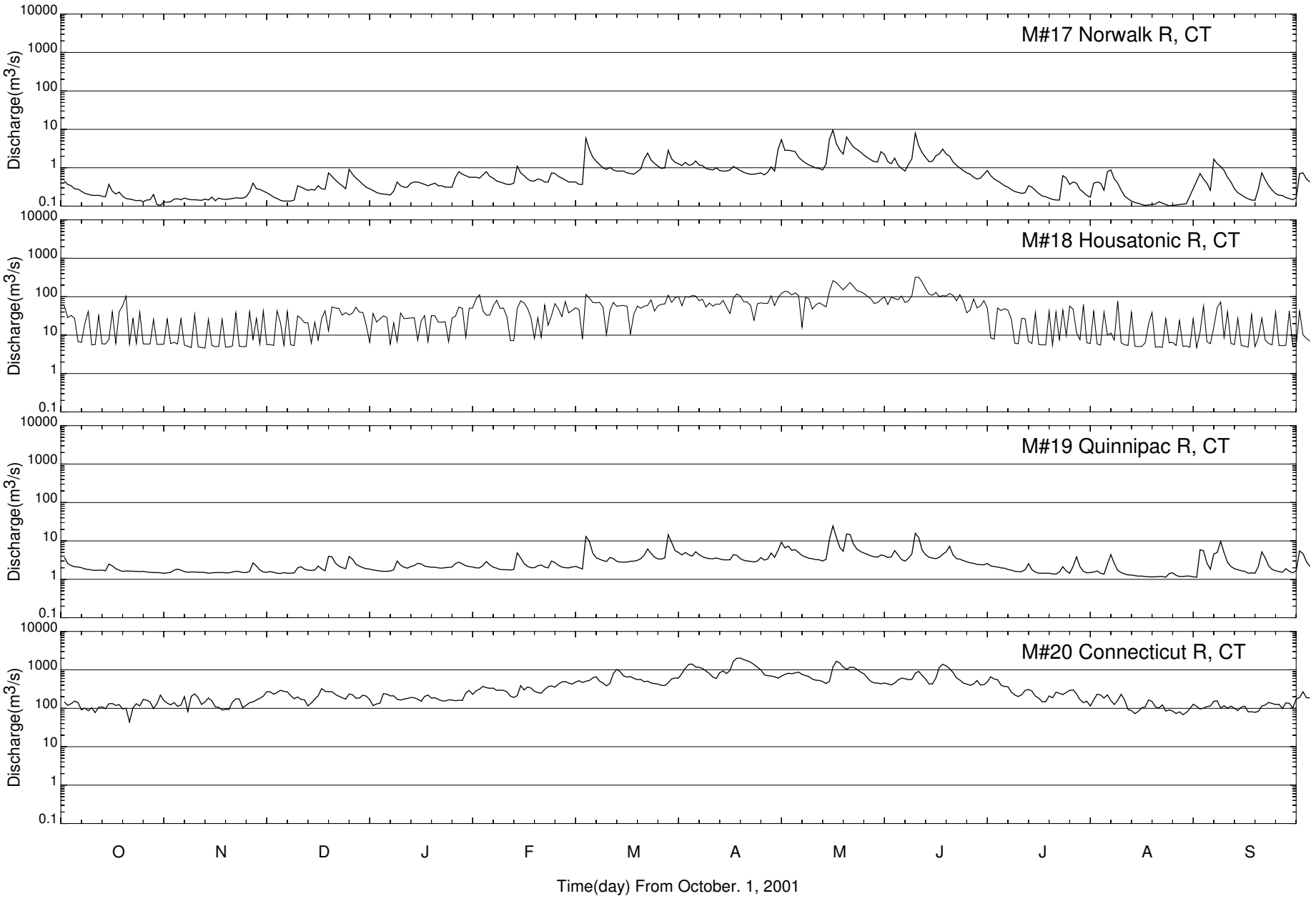

River Inflow Boundary Conditions

DATE: 8/23/2004 TIME: 11:42:24

/ont1/hrfo0010/DATA/FLOW0002/flow_log_0102.gdp

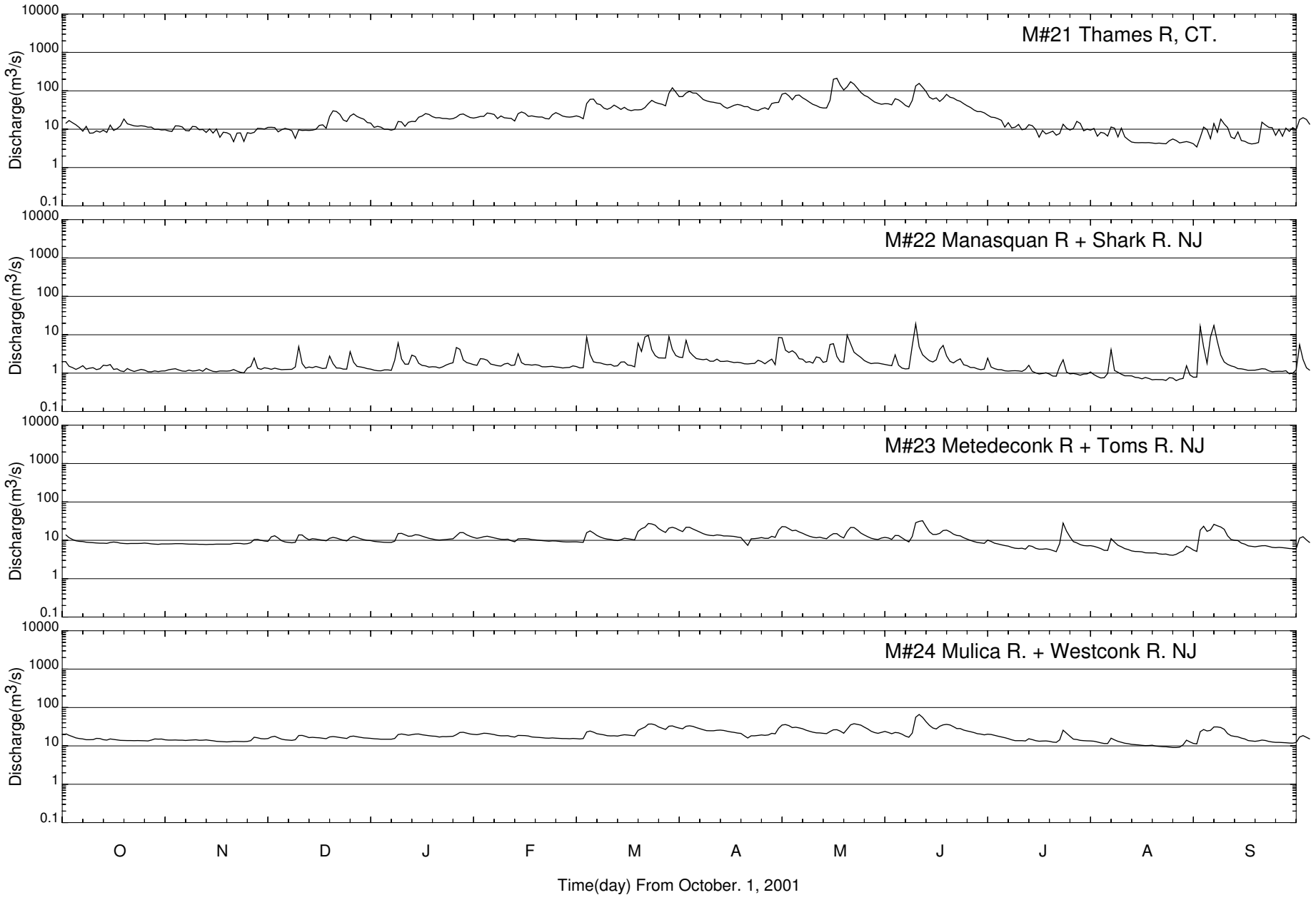

River Inflow Boundary Conditions

DATE: 8/23/2004 TIME: 11:42:24

/ont1/hrfo0010/DATA/FLOW/flow_9900.gdp

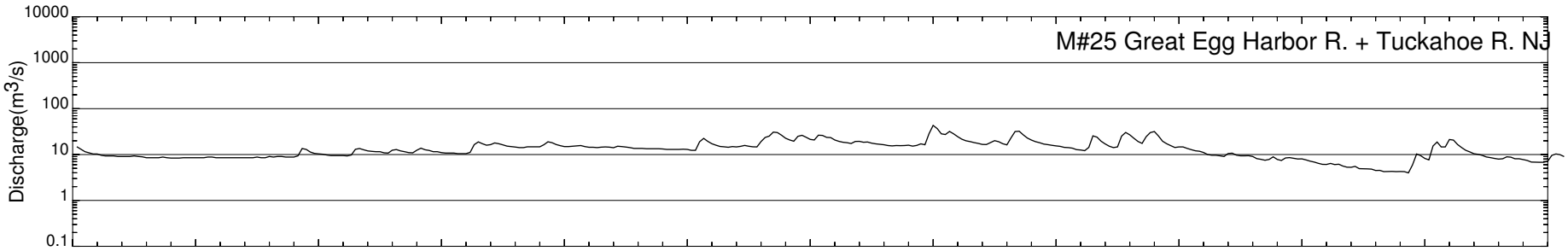
M#25 Great Egg Harbor R. + Tuckahoe R. NJ
Discharge(m3/s)
10000
1000
100
10
1
0.1

APPENDIX 3

ADDITIONAL SKILL ASSESSMENT USING CARP HYDRODYNAMIC DATA

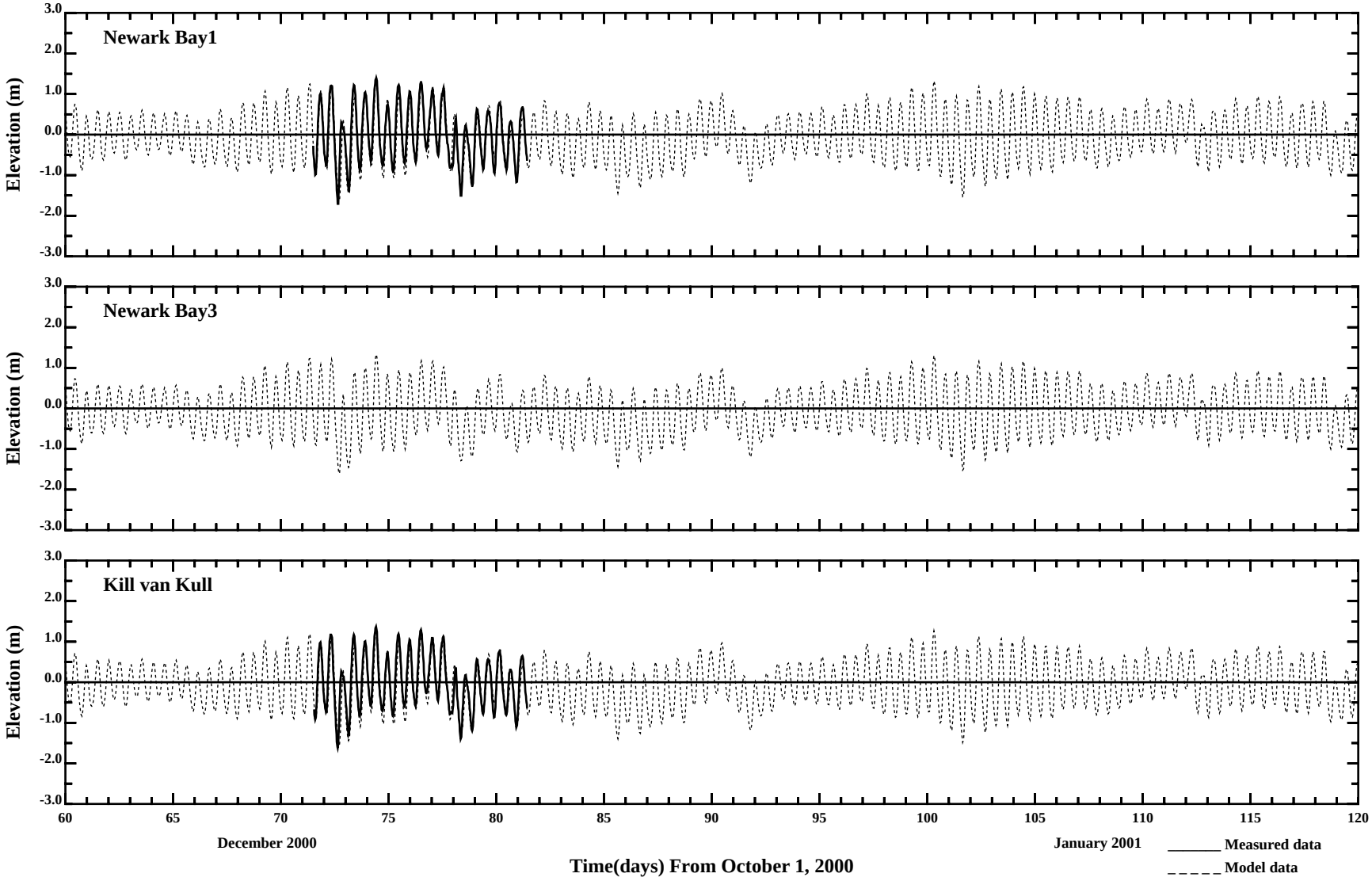

/erie1/hrfo0010/HYDRORUNS/RUTGERS/elev.gdp
DATE: 8/16/2004 TIME: 14: 5: 5

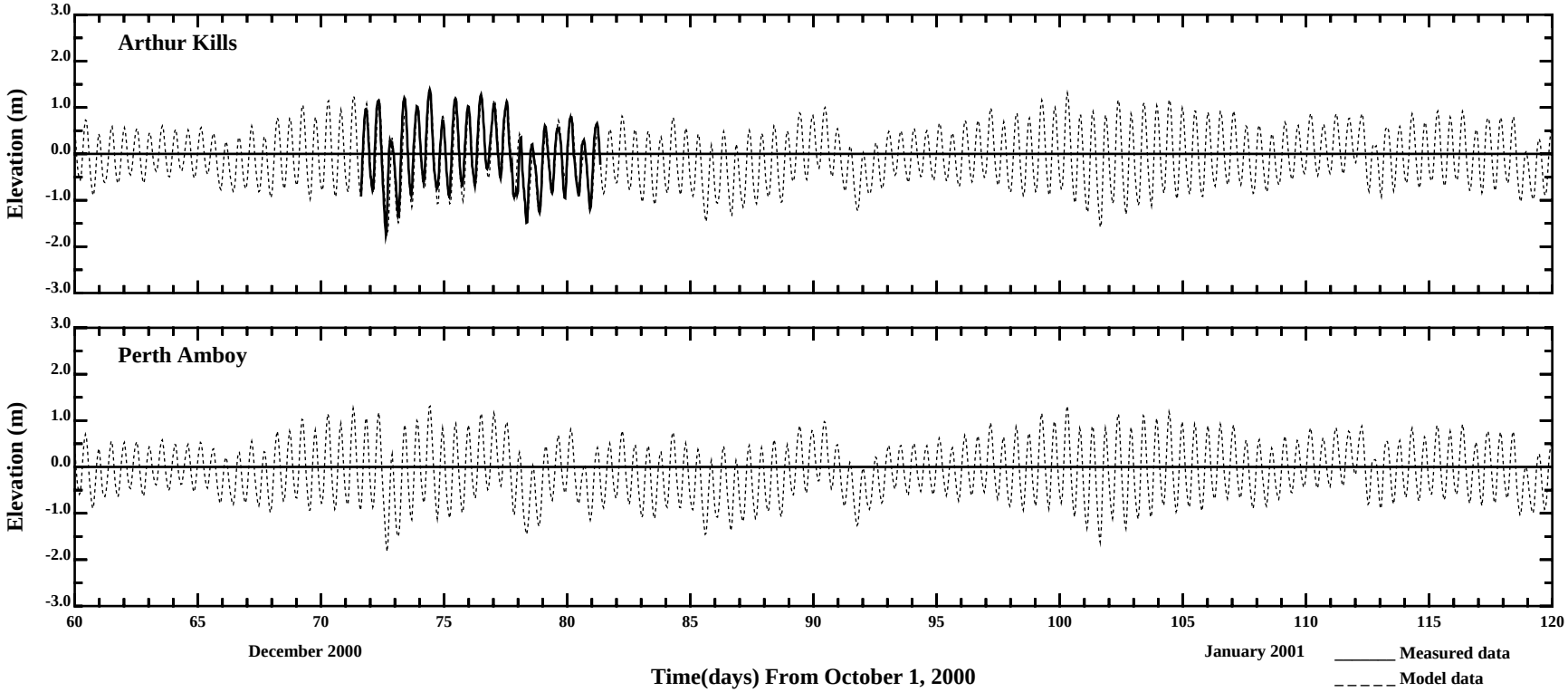

/erie1/hrfo0010/HYDRORUNS/RUTGERS/elev.gdp

DATE: 8/16/2004 TIME: 14: 5: 5

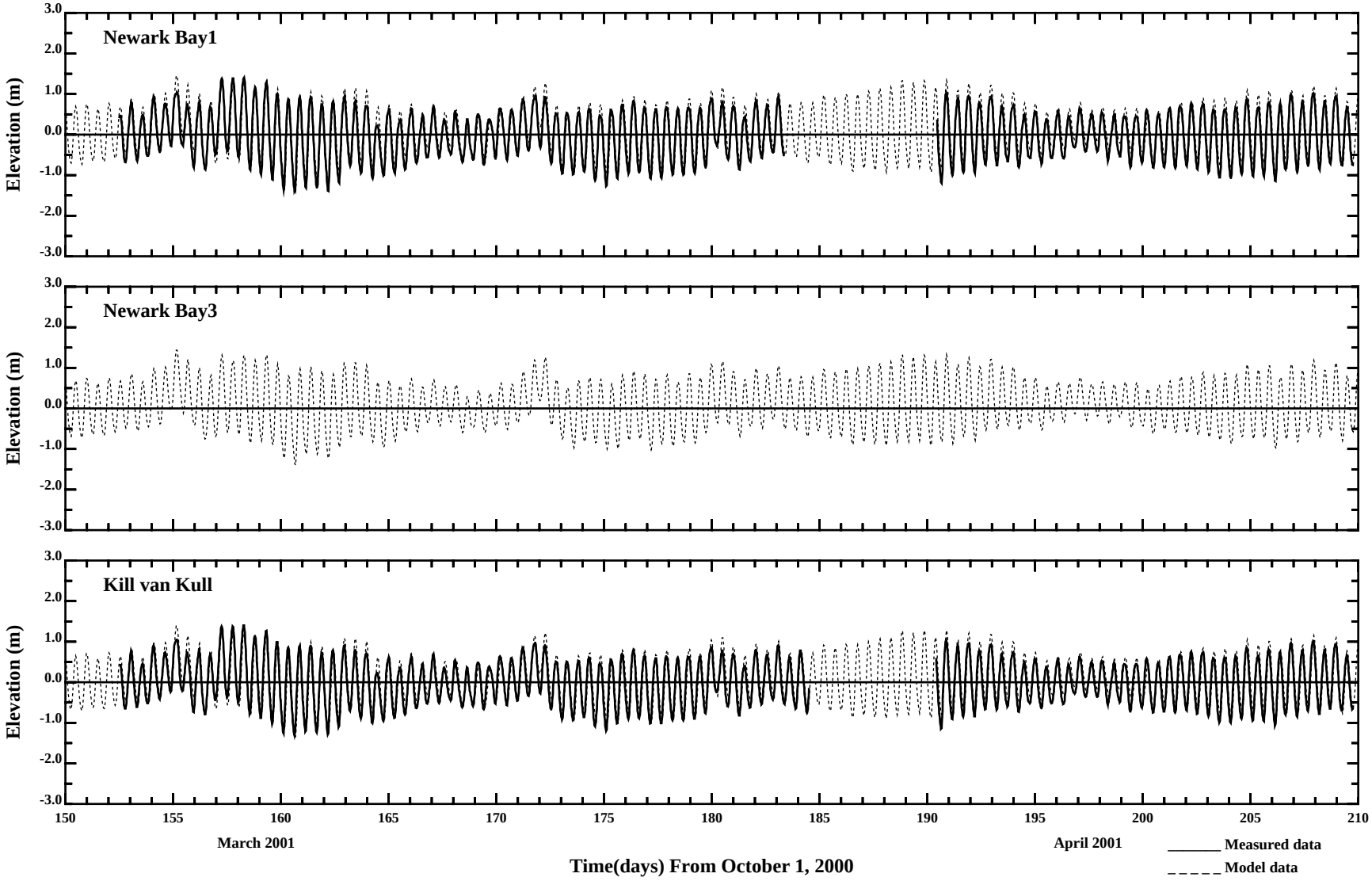

/erie1/hrfo0010/HYDRORUNS/RUTGERS/elev.gdp
DATE: 8/16/2004 TIME: 14: 5:15

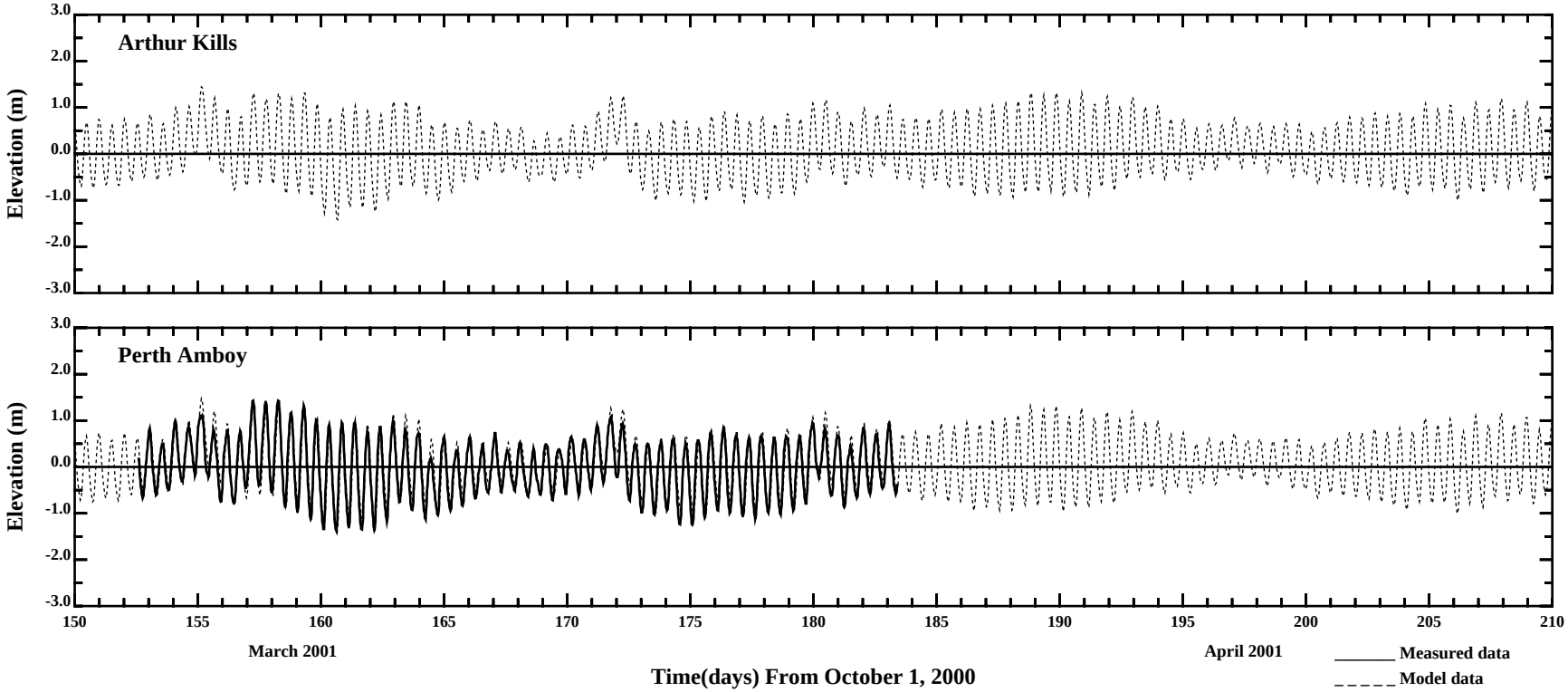

/erie1/hrfo0010/HYDRORUNS/RUTGERS/elev.gdp

DATE: 8/16/2004 TIME: 14: 5:15

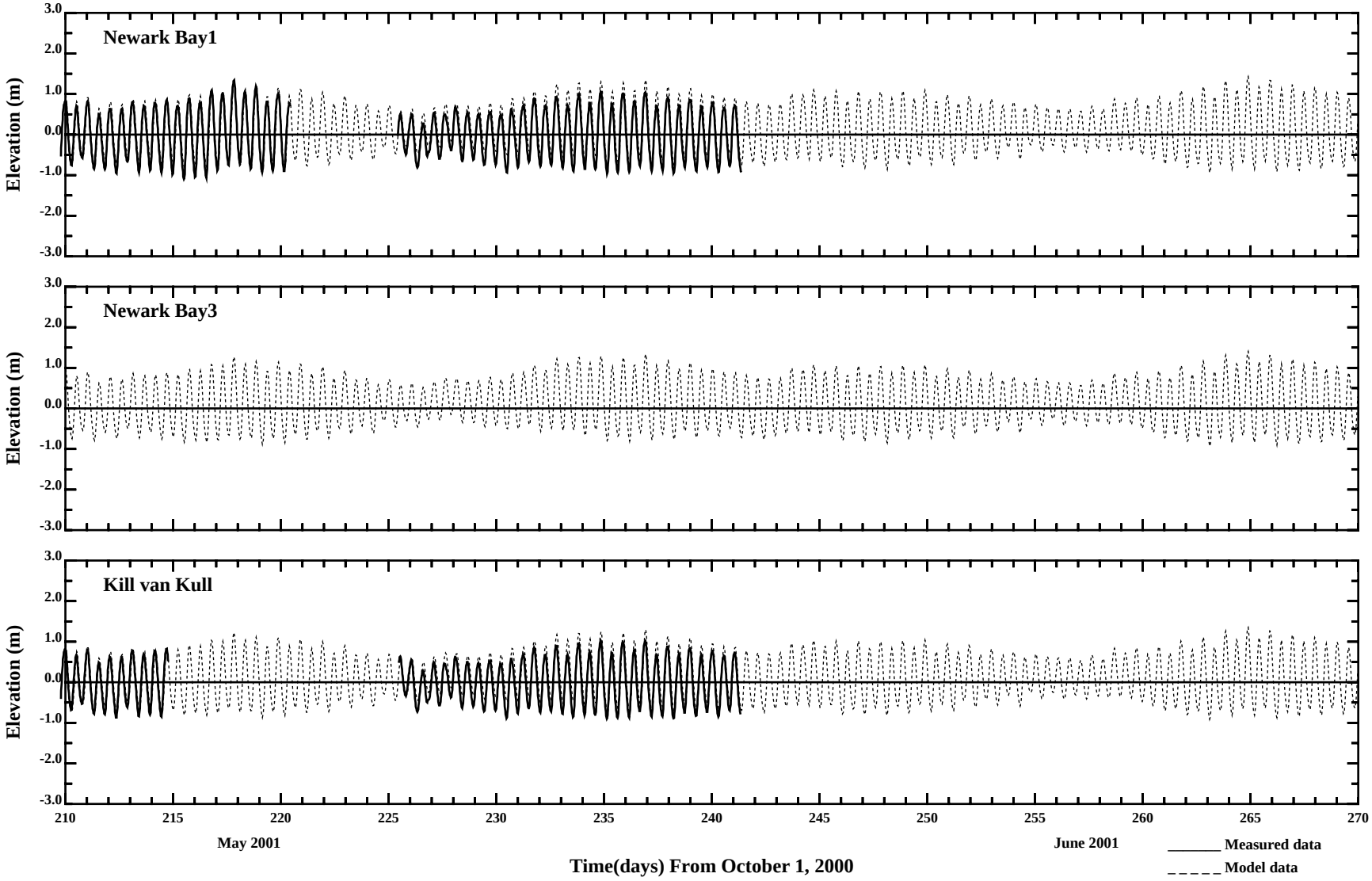

/erie1/hrfo0010/HYDRORUNS/RUTGERS/elev.gdp
DATE: 8/16/2004 TIME: 14: 5:24

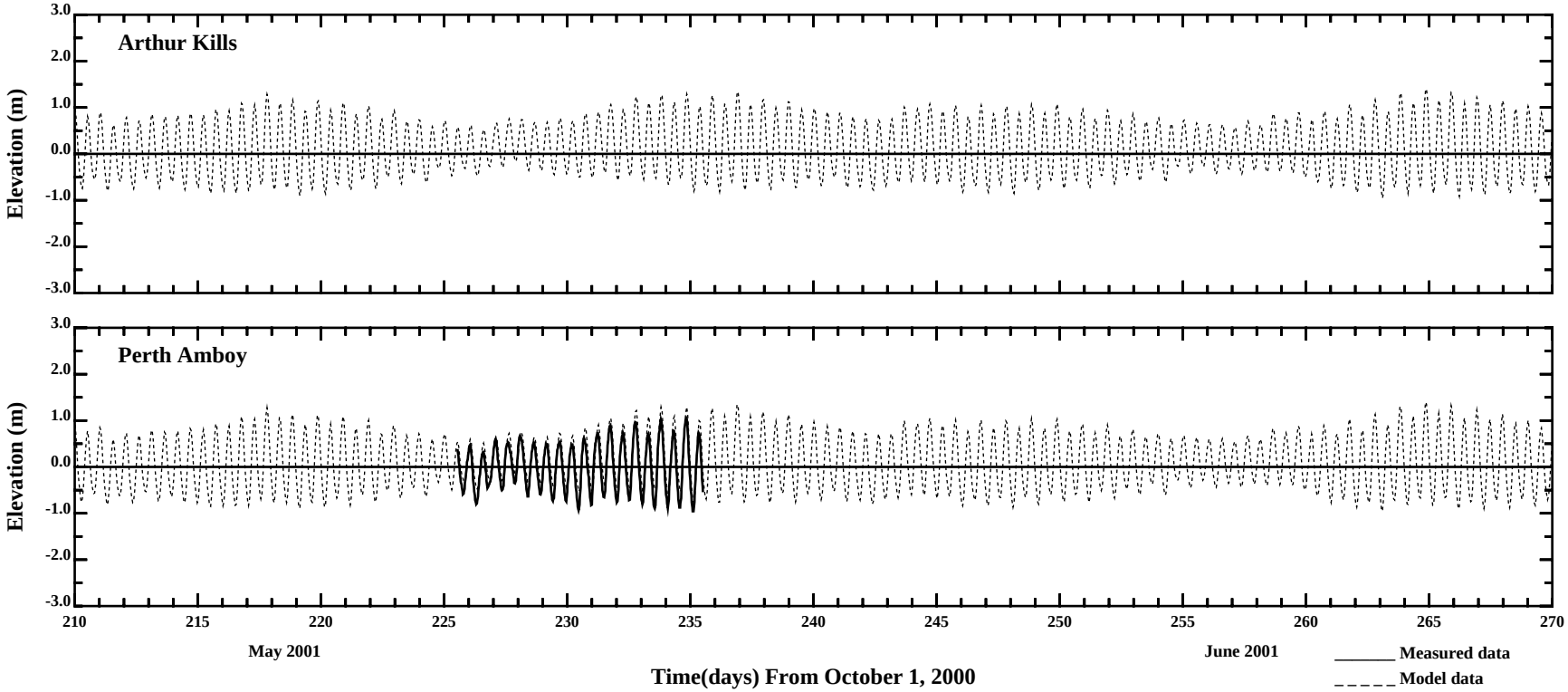

/erie1/hrfo0010/HYDRORUNS/RUTGERS/elev.gdp

DATE: 8/16/2004 TIME: 14: 5:24

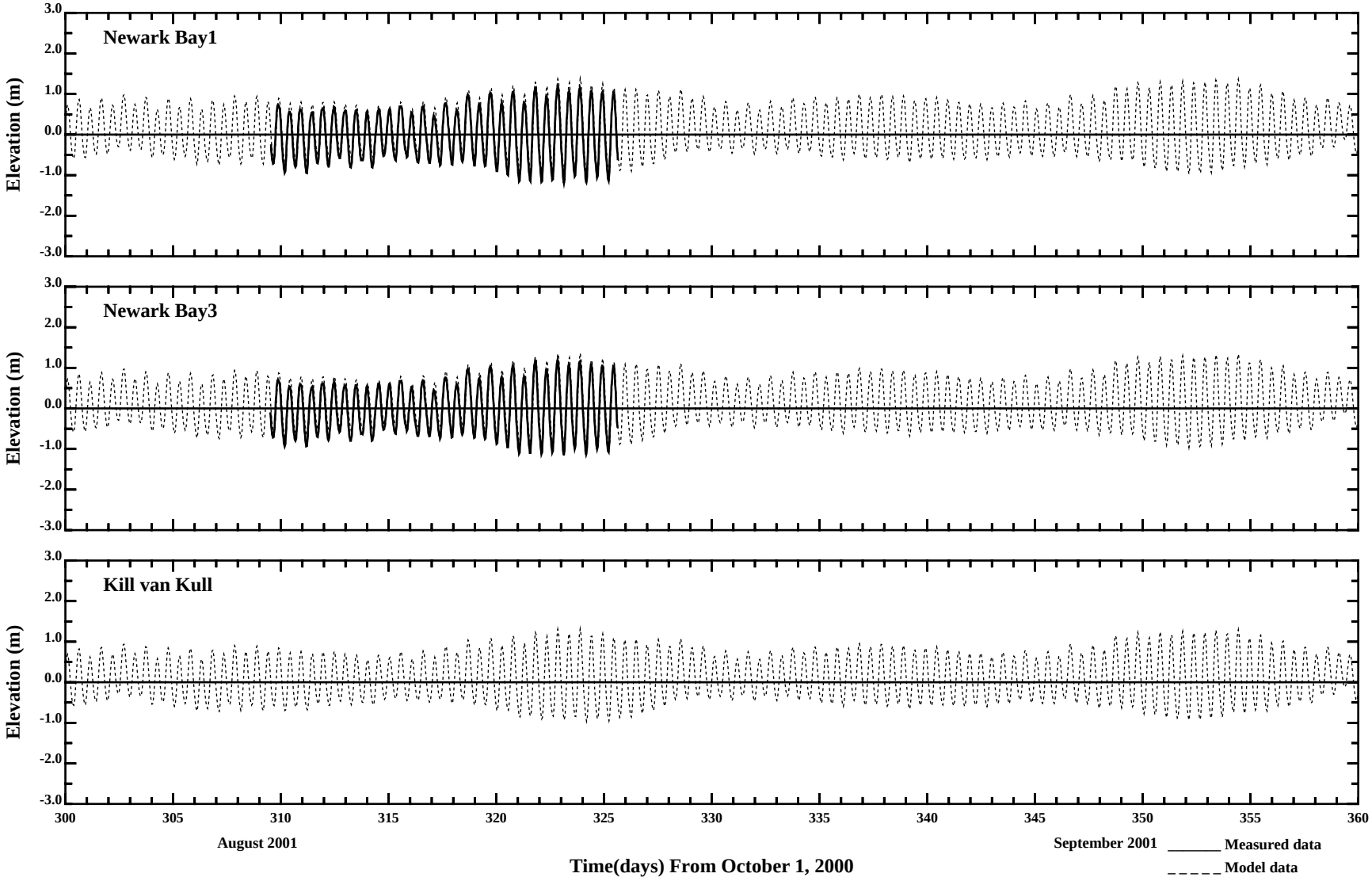

/erie1/hrfo0010/HYDRORUNS/RUTGERS/elev.gdp
DATE: 8/16/2004 TIME: 14: 5:33

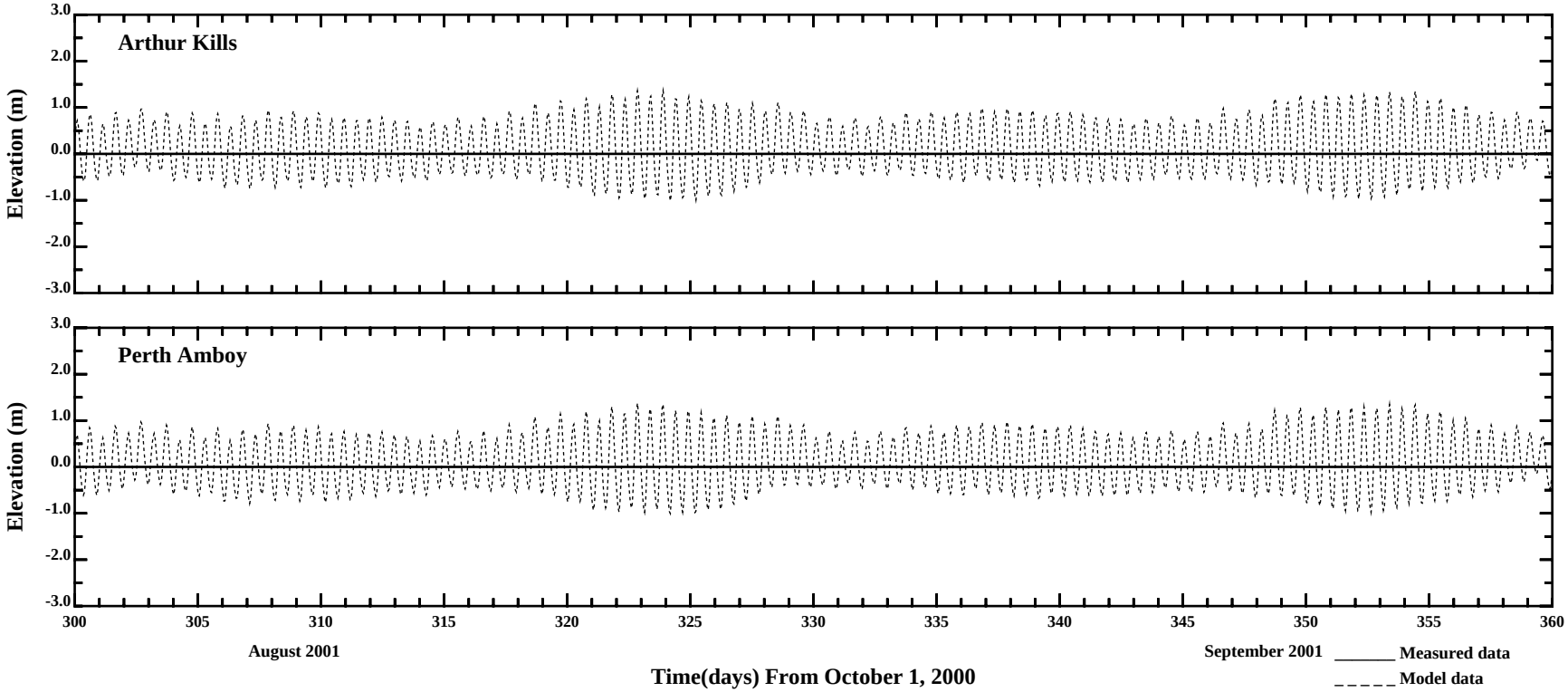

/erie1/hrfo0010/HYDRORUNS/RUTGERS/elev.gdp

DATE: 8/16/2004 TIME: 14: 5:33

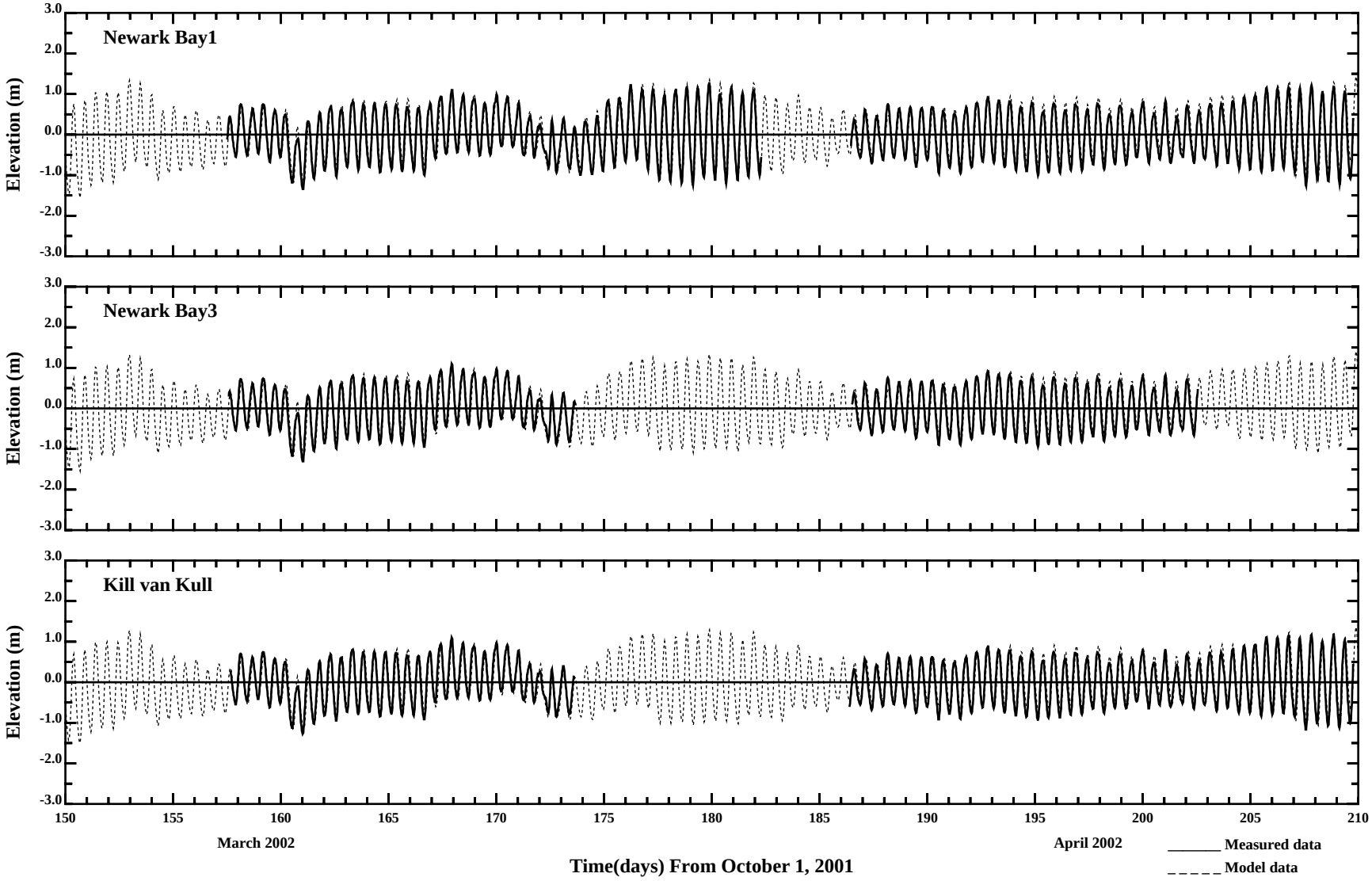

/erie1/hrfo0010/HYDRORUNS/RUTGERS/elev.gdp
DATE: 8/16/2004 TIME: 14: 5:42

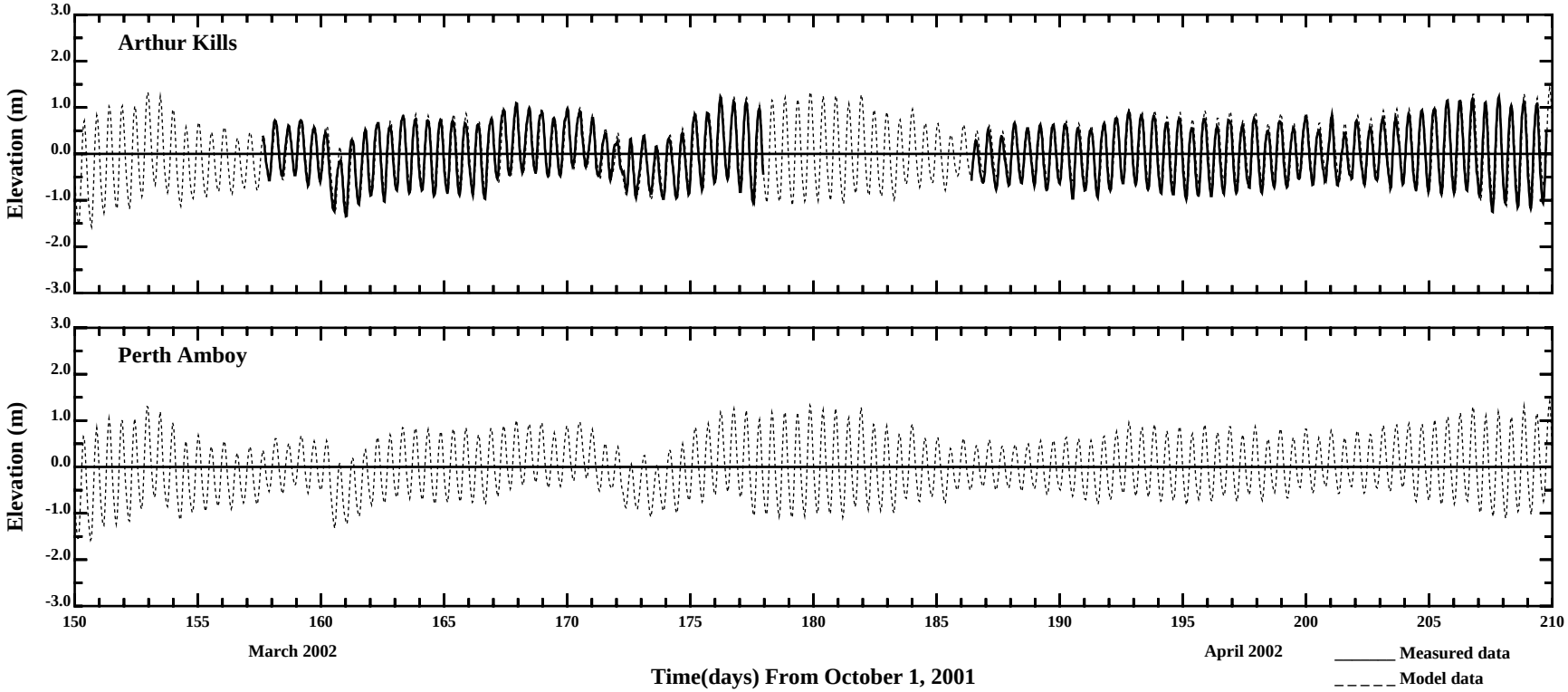

/erie1/hrfo0010/HYDRORUNS/RUTGERS/elev.gdp

DATE: 8/16/2004 TIME: 14: 5:42

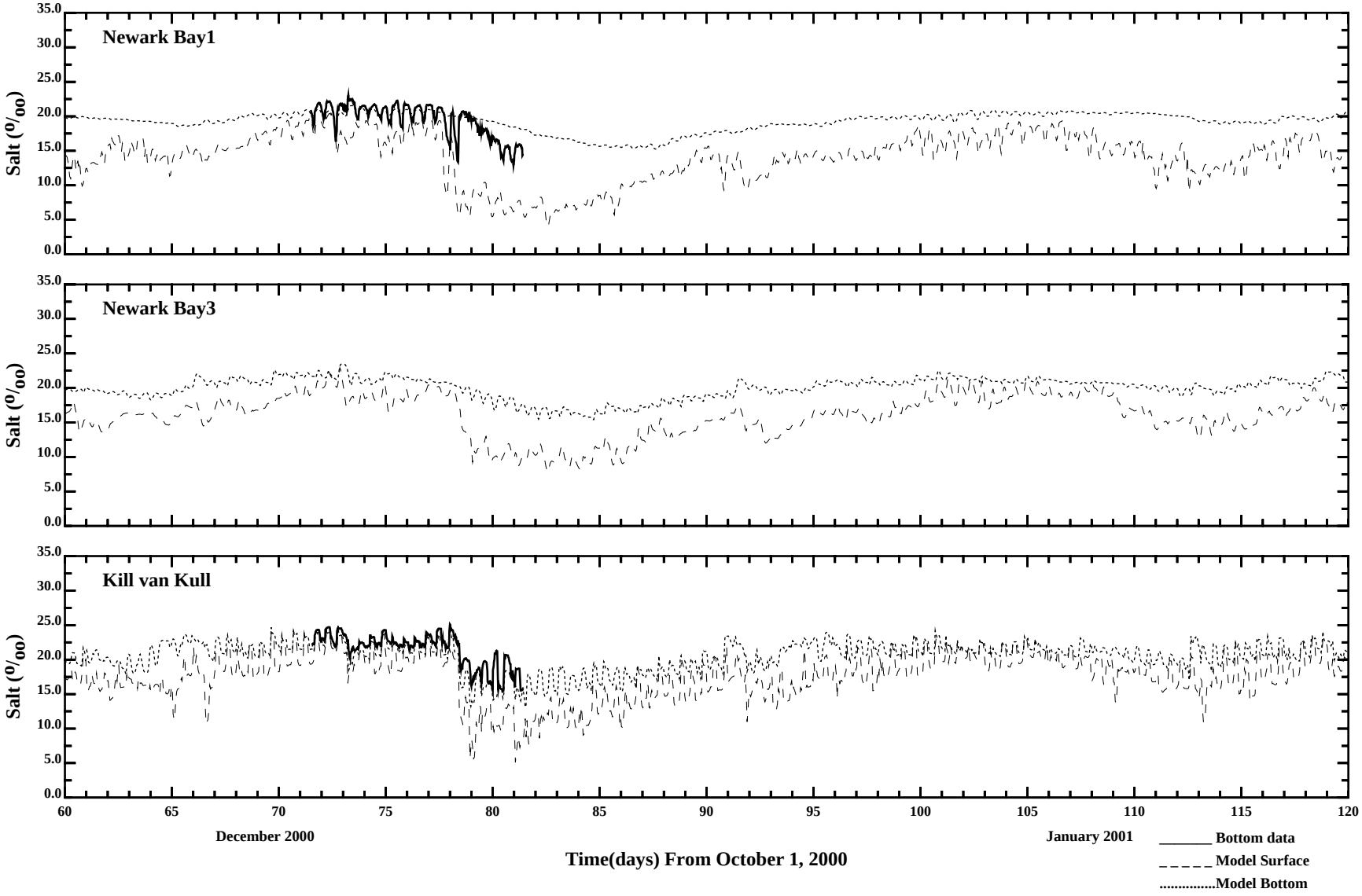

/erie1/hrfo0010/HYDRORUNS/RUTGERS/salt.gdp

DATE: 8/16/2004 TIME: 14: 4:20

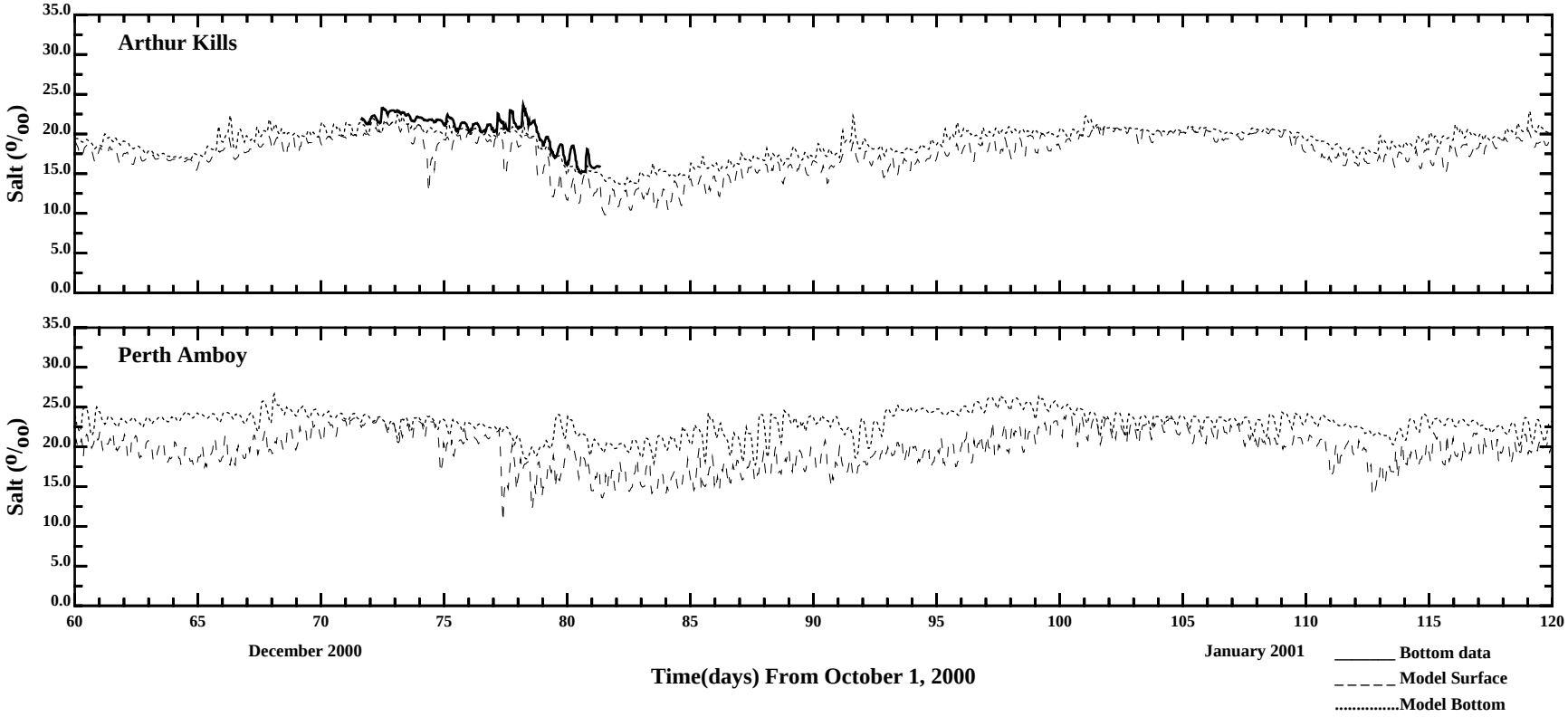

/erie1/hrfo0010/HYDRORUNS/RUTGERS/salt.gdp

DATE: 8/16/2004 TIME: 14: 4:20

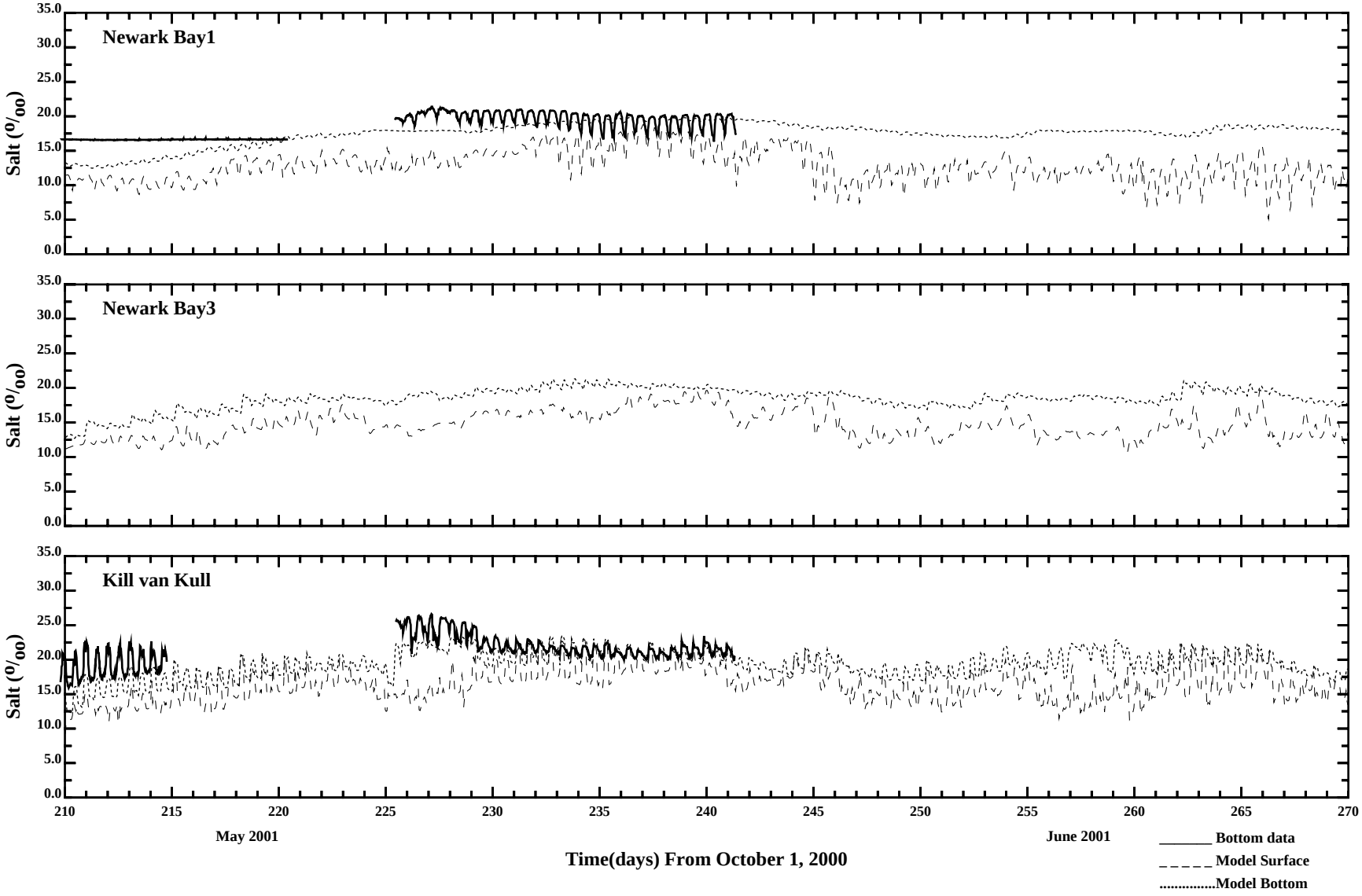

/erie1/hrfo0010/HYDRORUNS/RUTGERS/salt.gdp
DATE: 8/16/2004 TIME: 14: 4:38

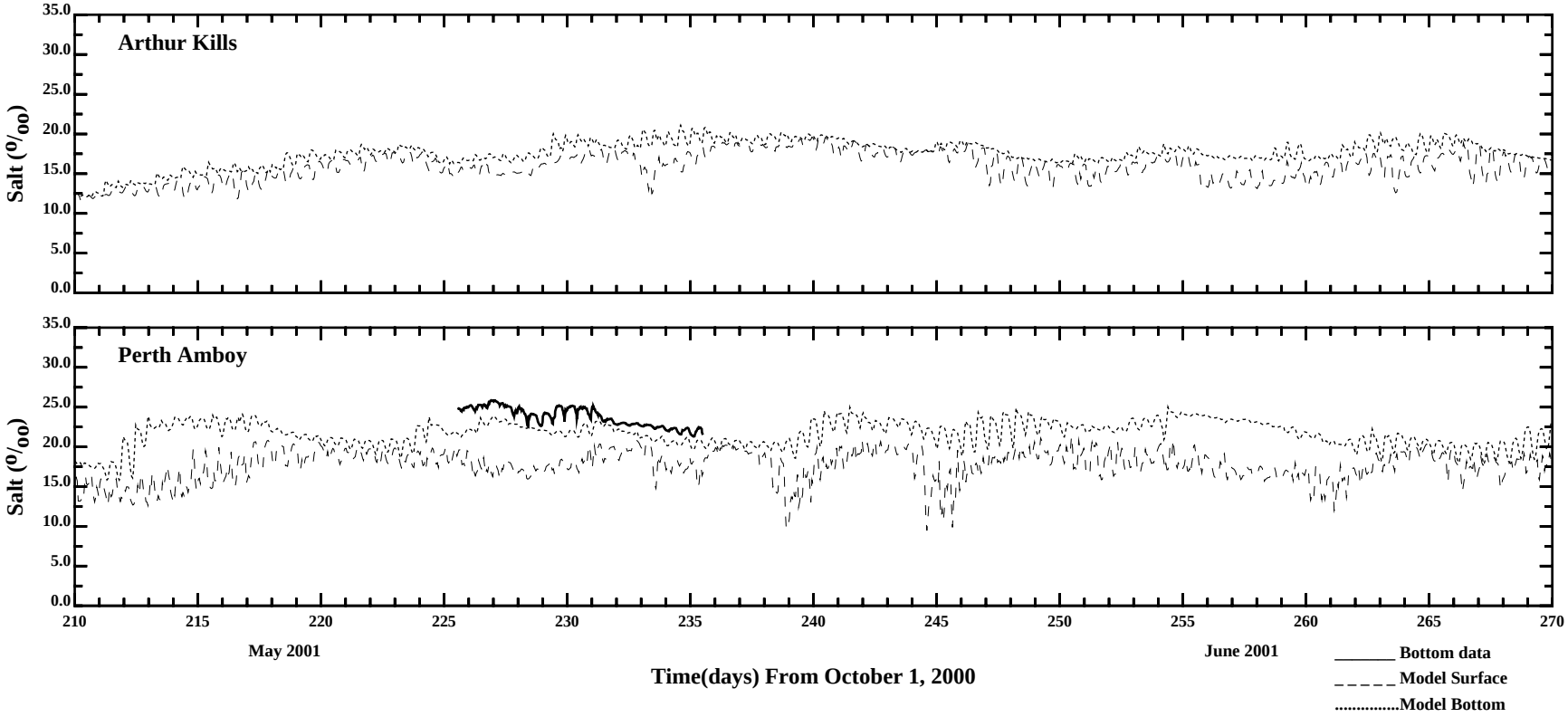

/erie1/hrfo0010/HYDRORUNS/RUTGERS/salt.gdp

DATE: 8/16/2004 TIME: 14: 4:38

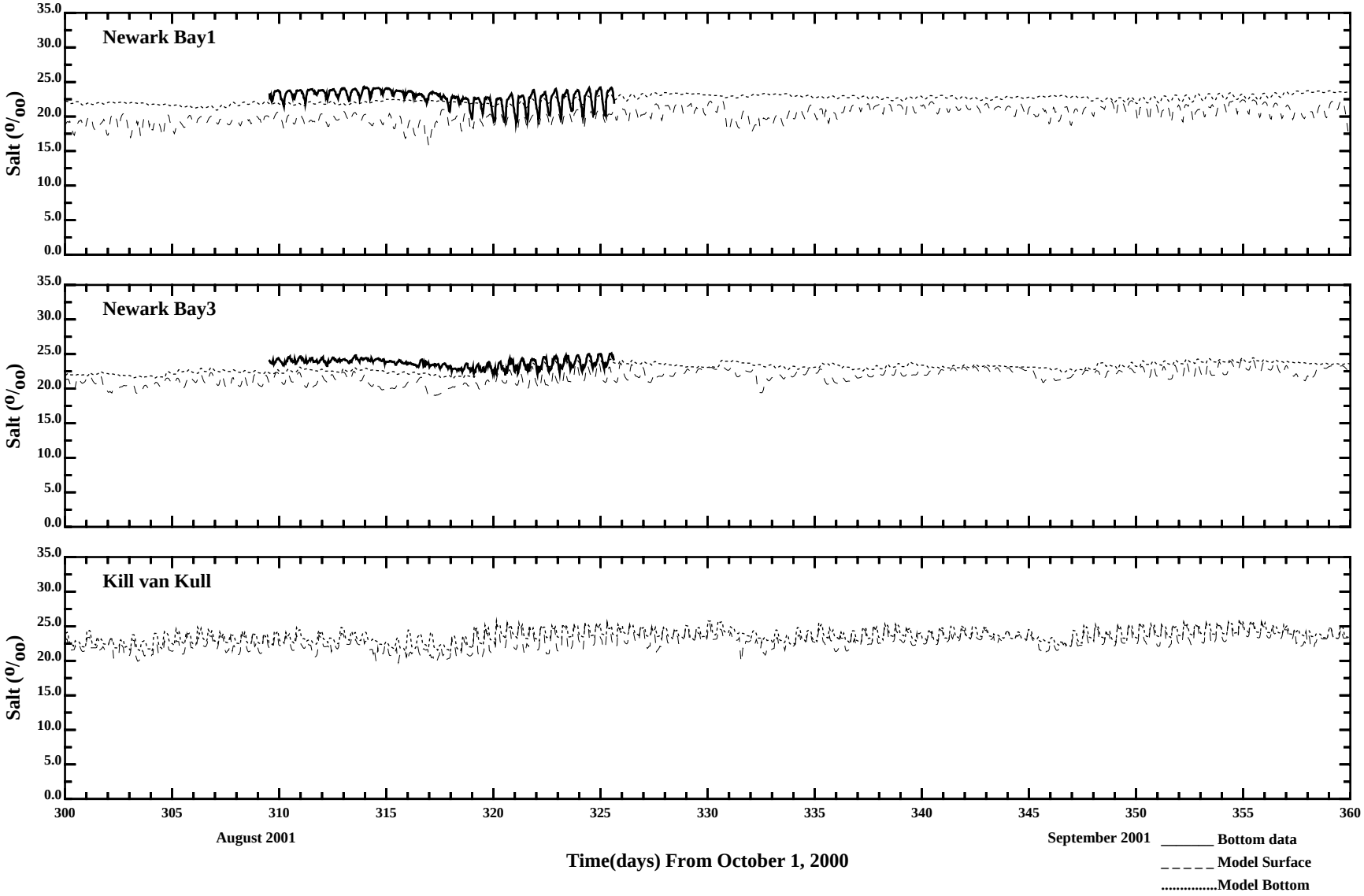

/erie1/hrfo0010/HYDRORUNS/RUTGERS/salt.gdp
DATE: 8/16/2004 TIME: 14: 4:47

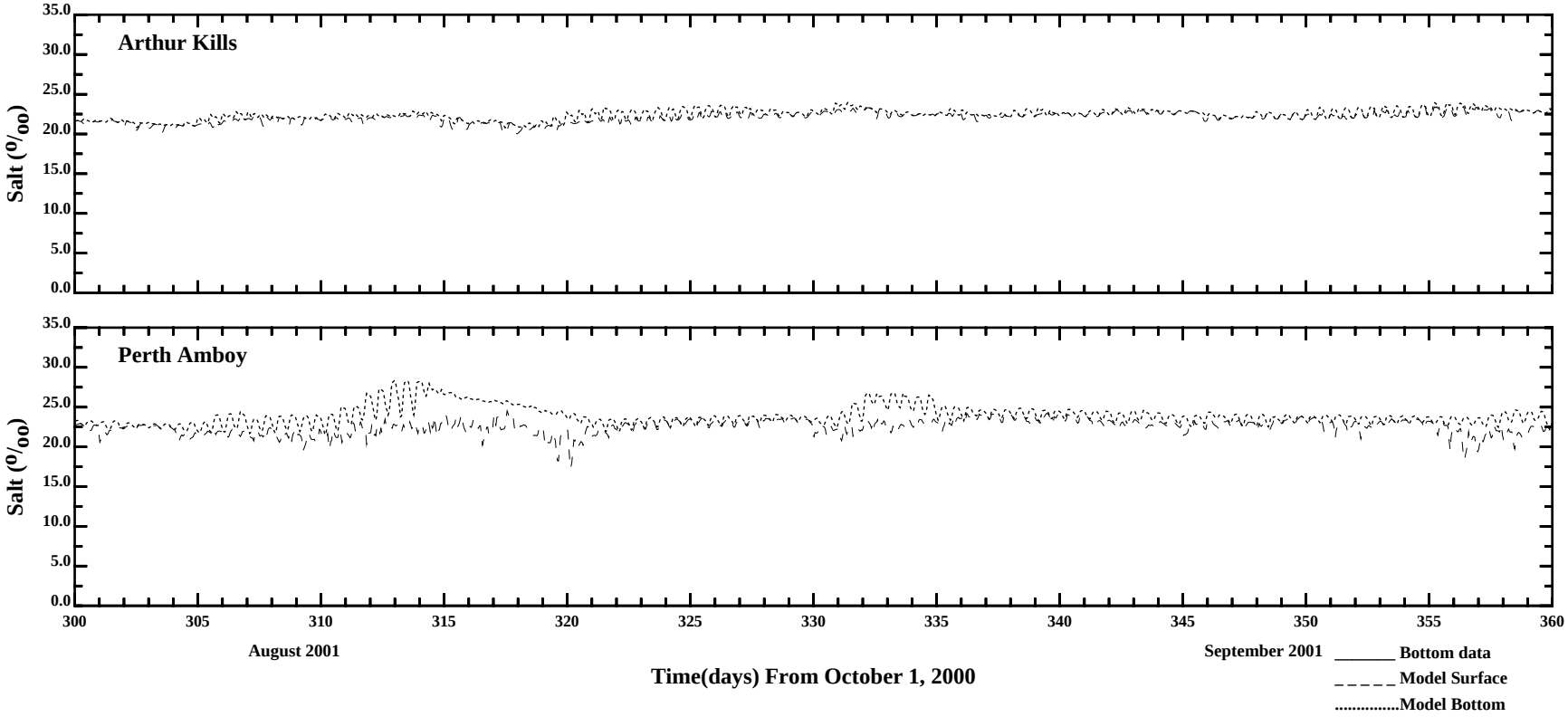

/erie1/hrfo0010/HYDRORUNS/RUTGERS/salt.gdp

DATE: 8/16/2004 TIME: 14: 4:47

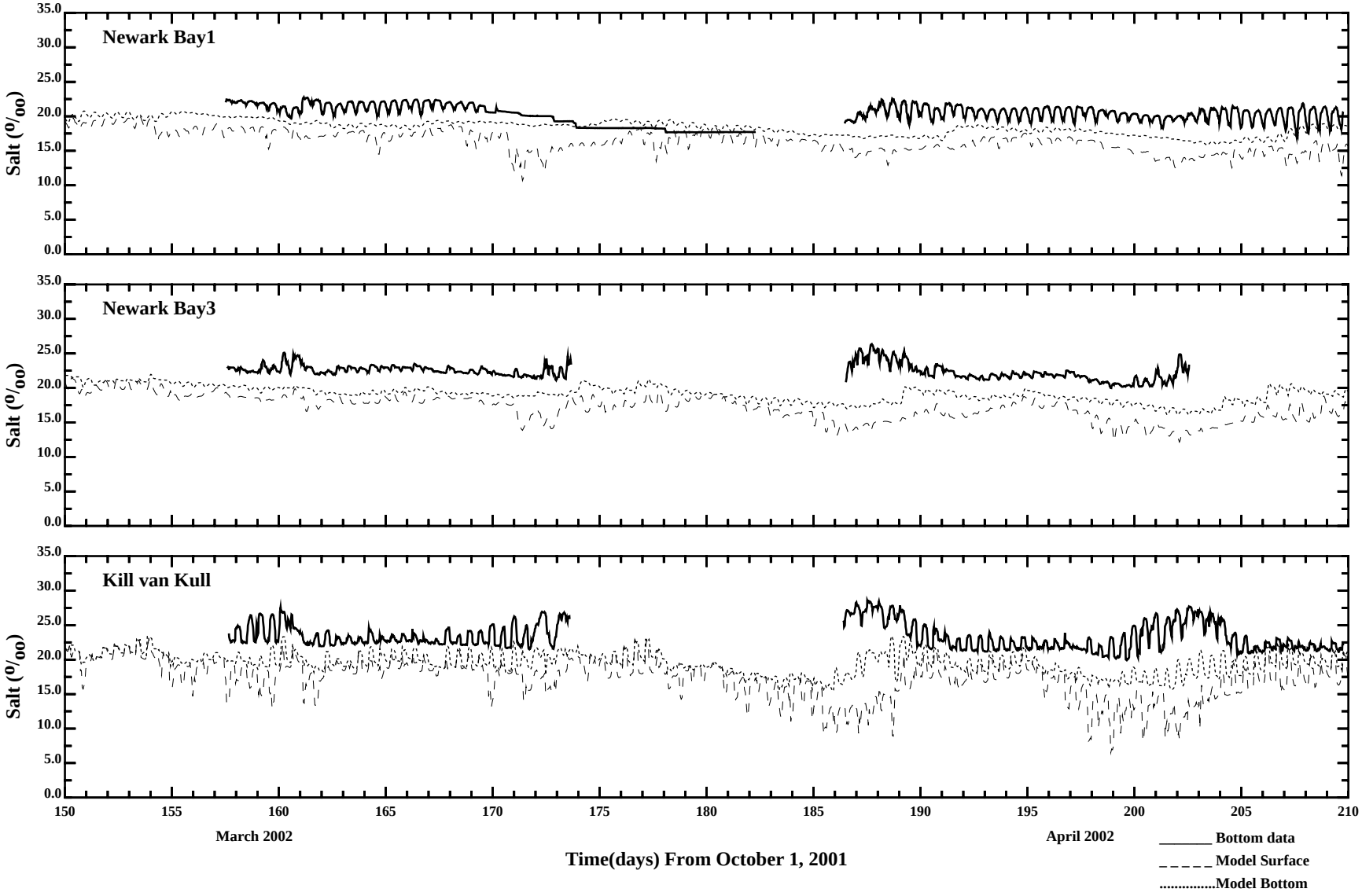

/erie1/hrfo0010/HYDRORUNS/RUTGERS/salt.gdp

DATE: 8/16/2004 TIME: 14: 4:56

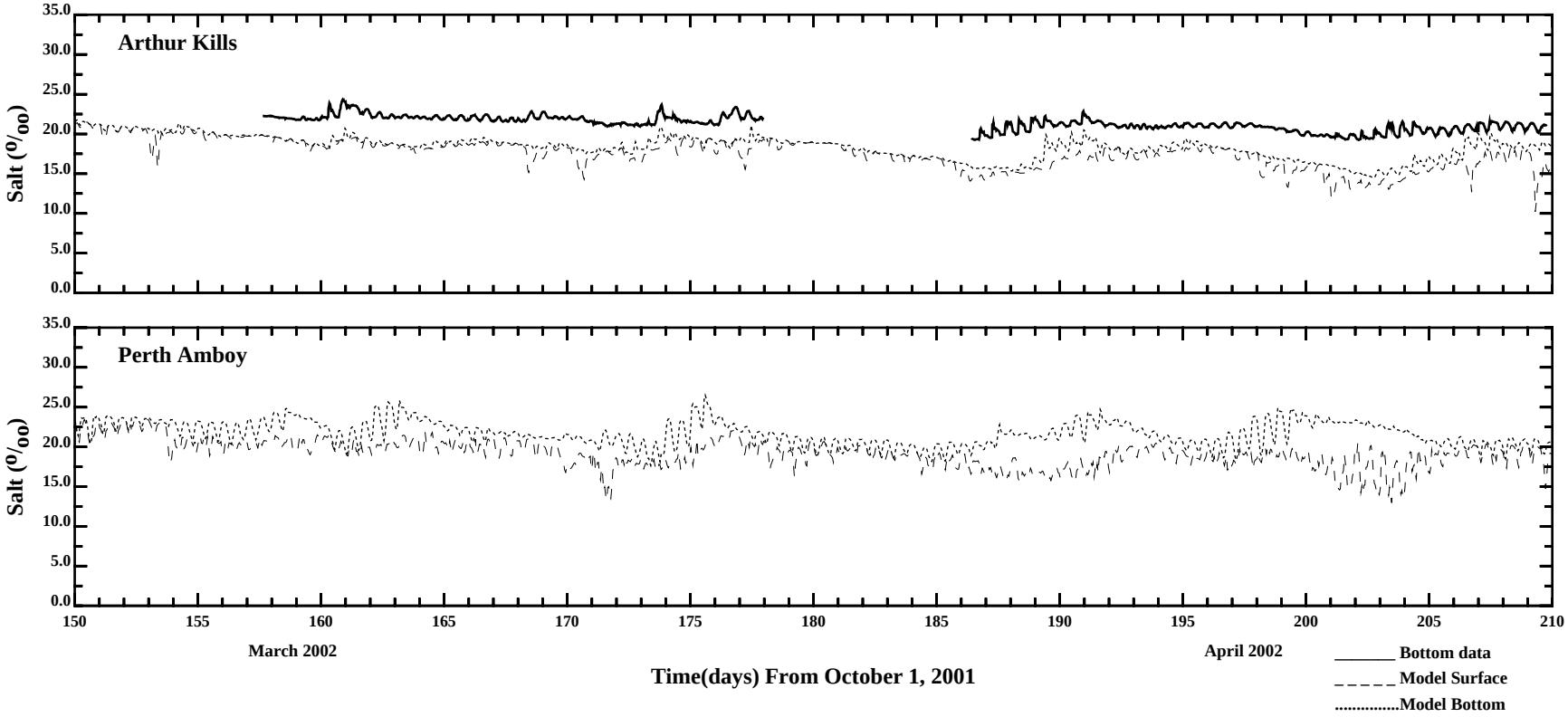

/erie1/hrfo0010/HYDRORUNS/RUTGERS/salt.gdp

DATE: 8/16/2004 TIME: 14: 4:56

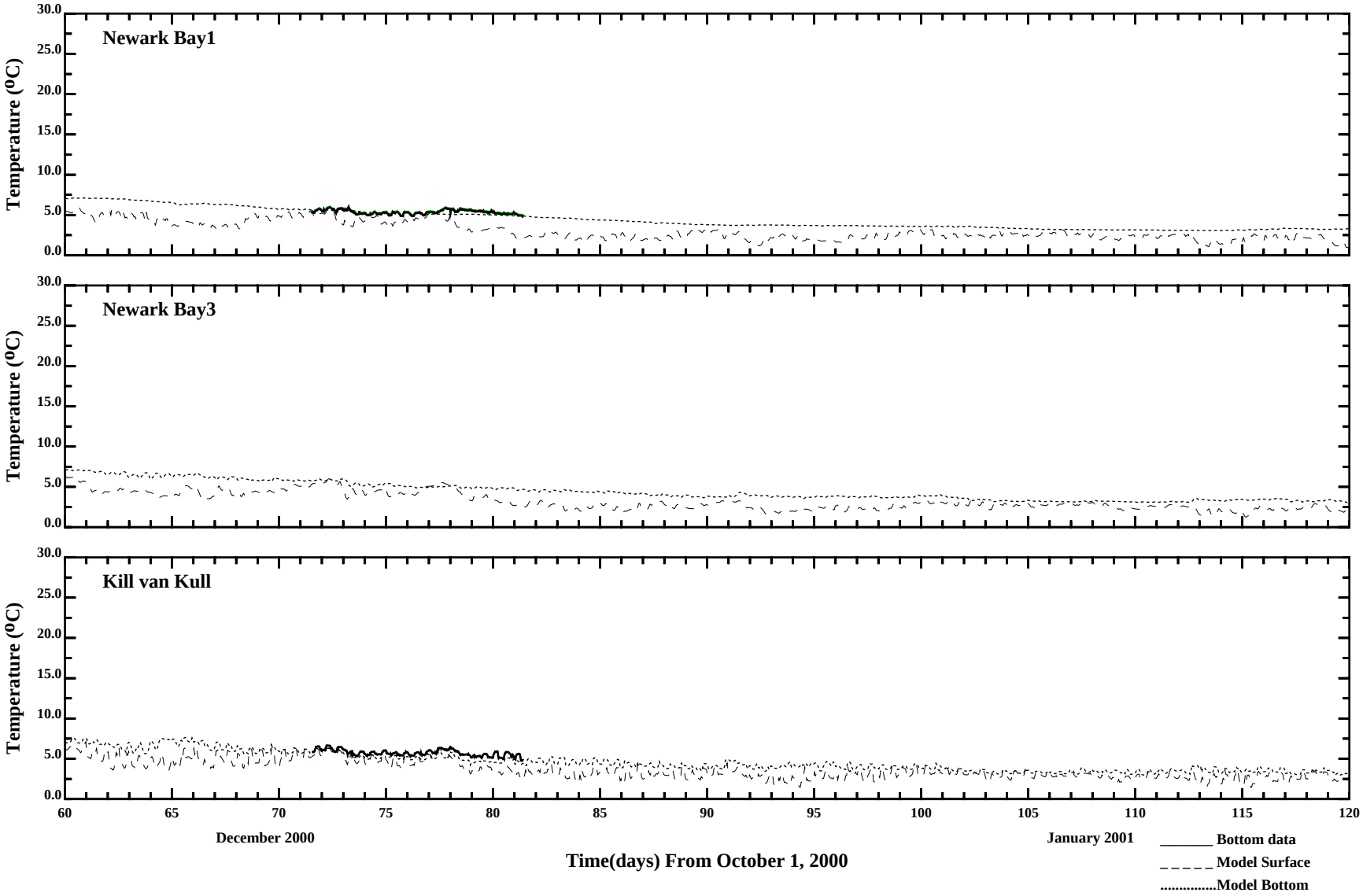

/erie1/hrfo0010/HYDRORUNS/RUTGERS/temp.gdp
DATE: 8/16/2004 TIME: 14: 3:37

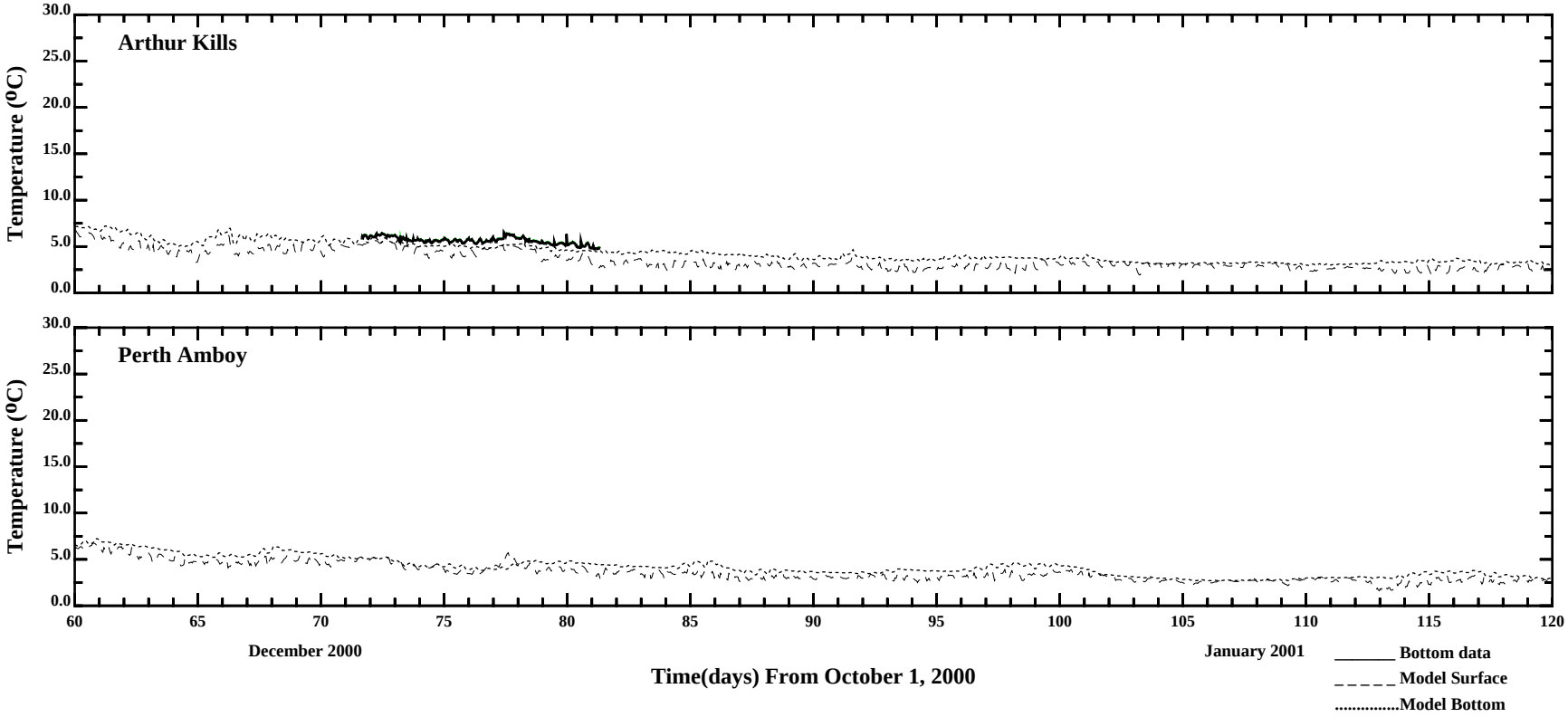

/erie1/hrfo0010/HYDRORUNS/RUTGERS/temp.gdp

DATE: 8/16/2004 TIME: 14: 3:37

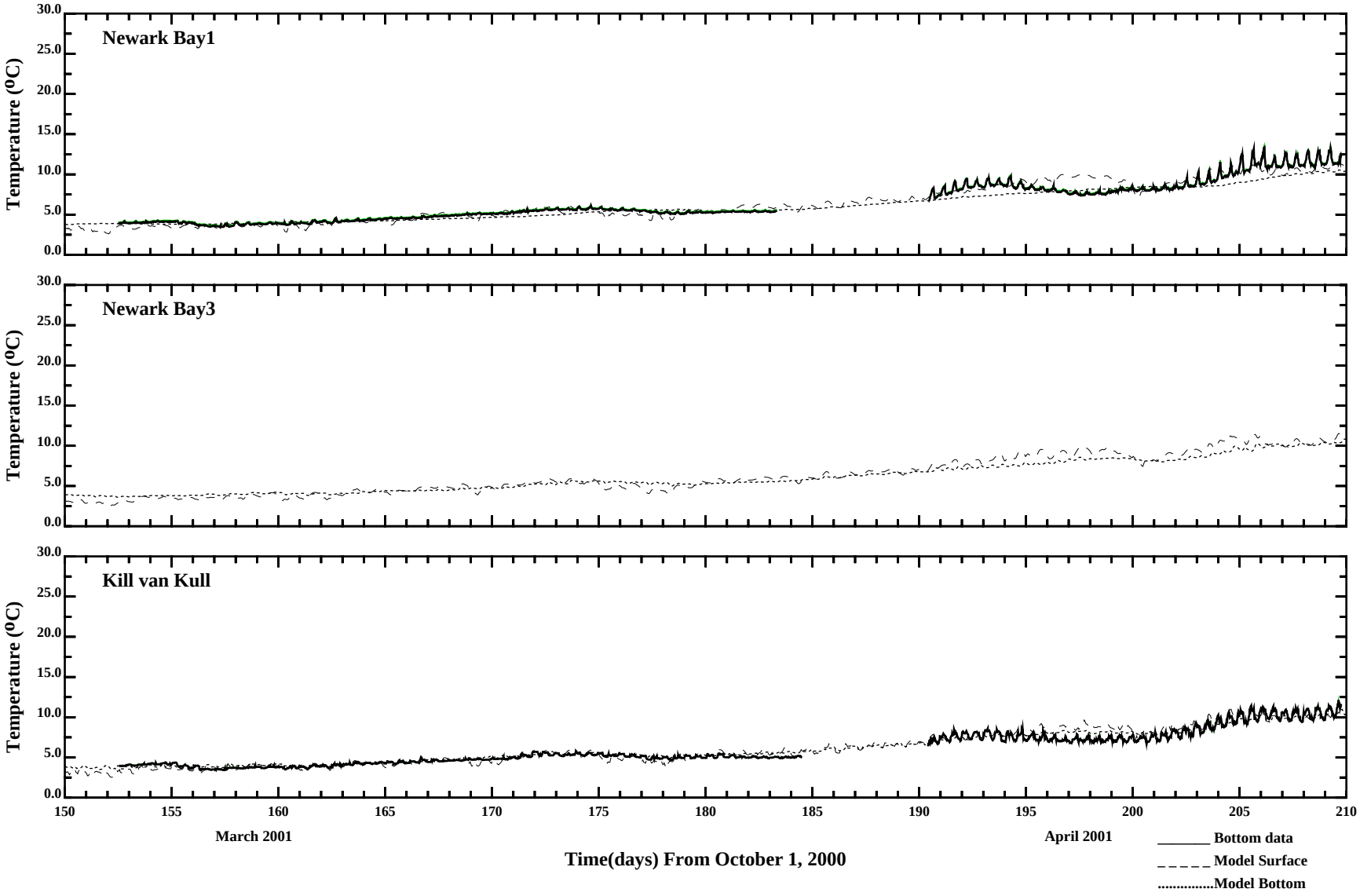

/erie1/hrfo0010/HYDRORUNS/RUTGERS/temp.gdp
DATE: 8/16/2004 TIME: 14: 3:45

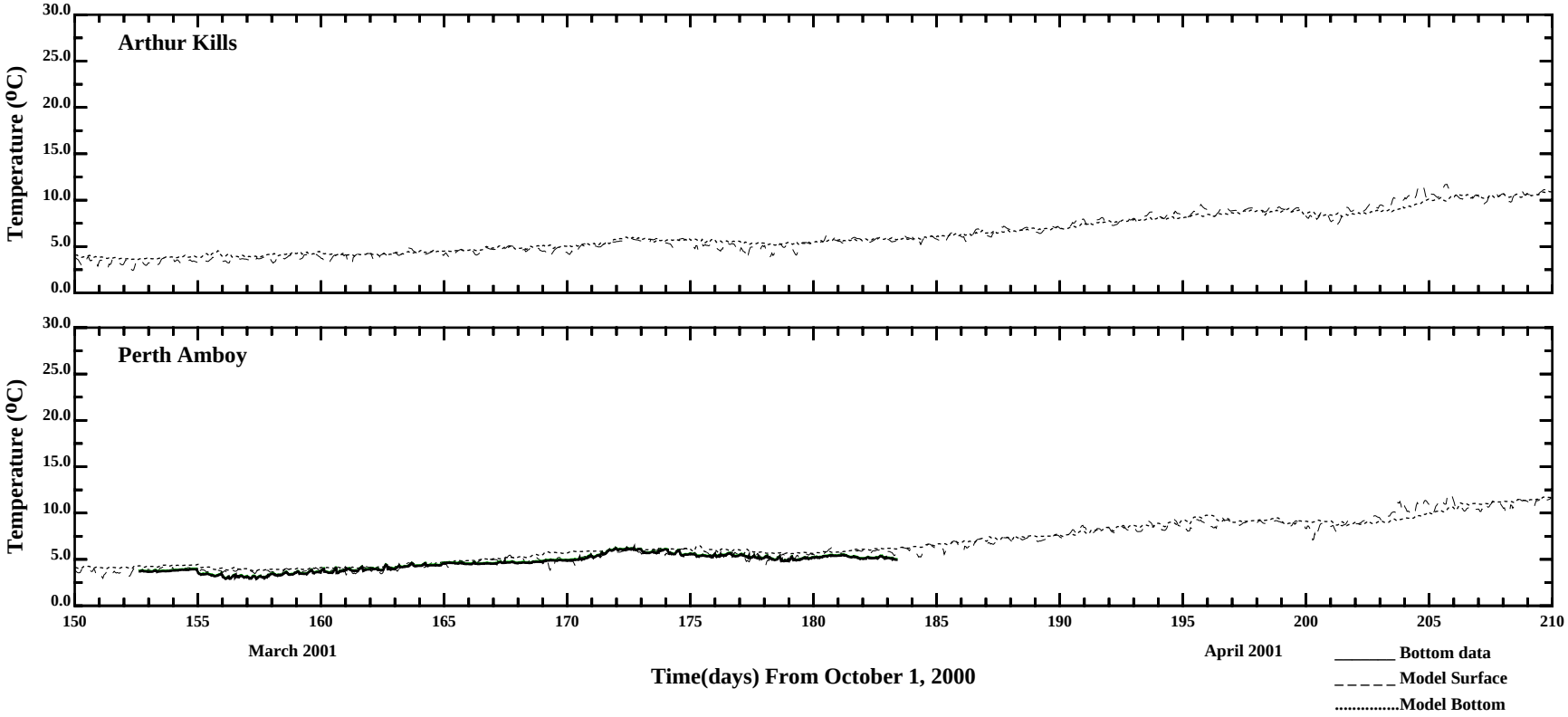

/erie1/hrfo0010/HYDRORUNS/RUTGERS/temp.gdp

DATE: 8/16/2004 TIME: 14: 3:45

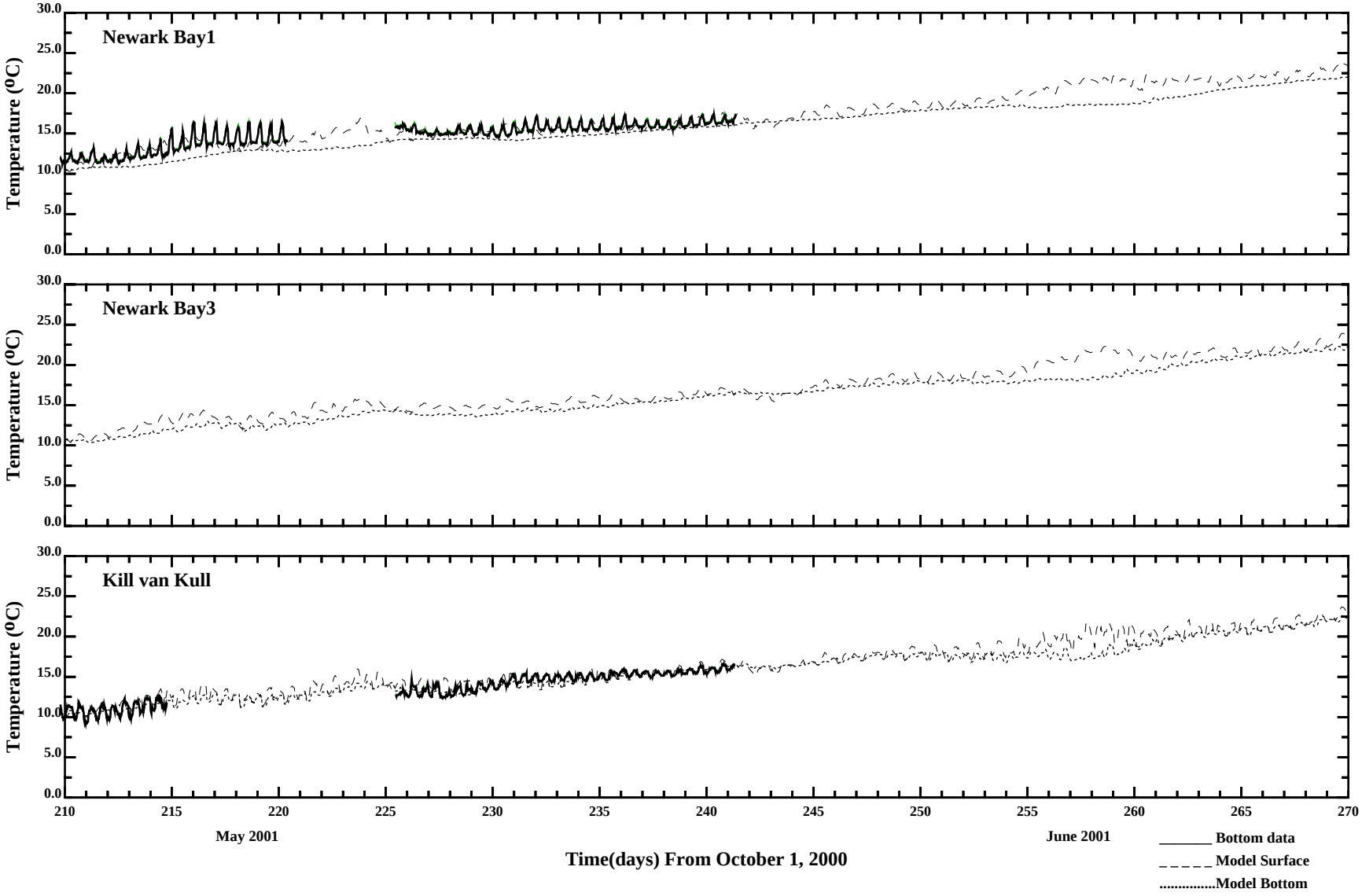

/erie1/hrfo0010/HYDRORUNS/RUTGERS/temp.gdp

DATE: 8/16/2004 TIME: 14: 3:54

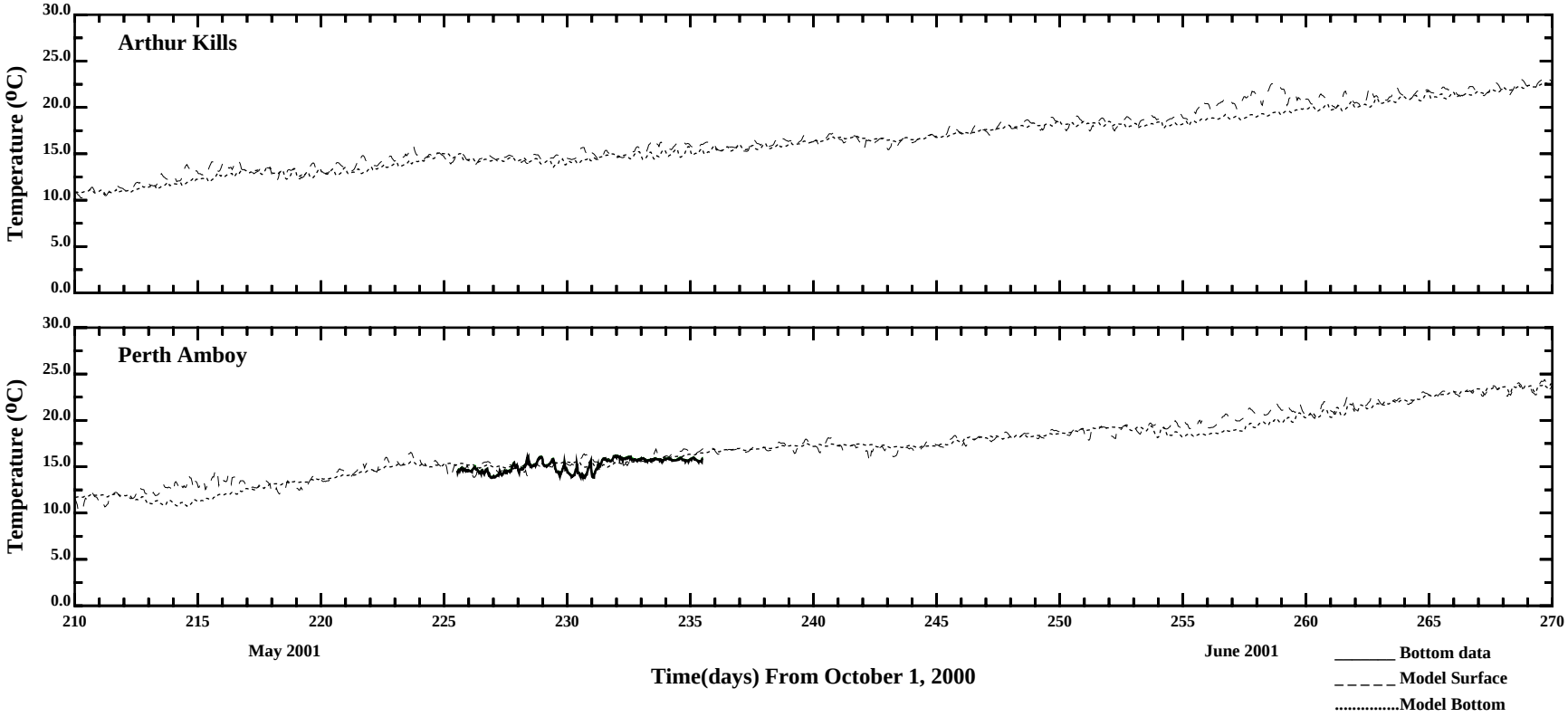

/erie1/hrfo0010/HYDRORUNS/RUTGERS/temp.gdp

DATE: 8/16/2004 TIME: 14: 3:54

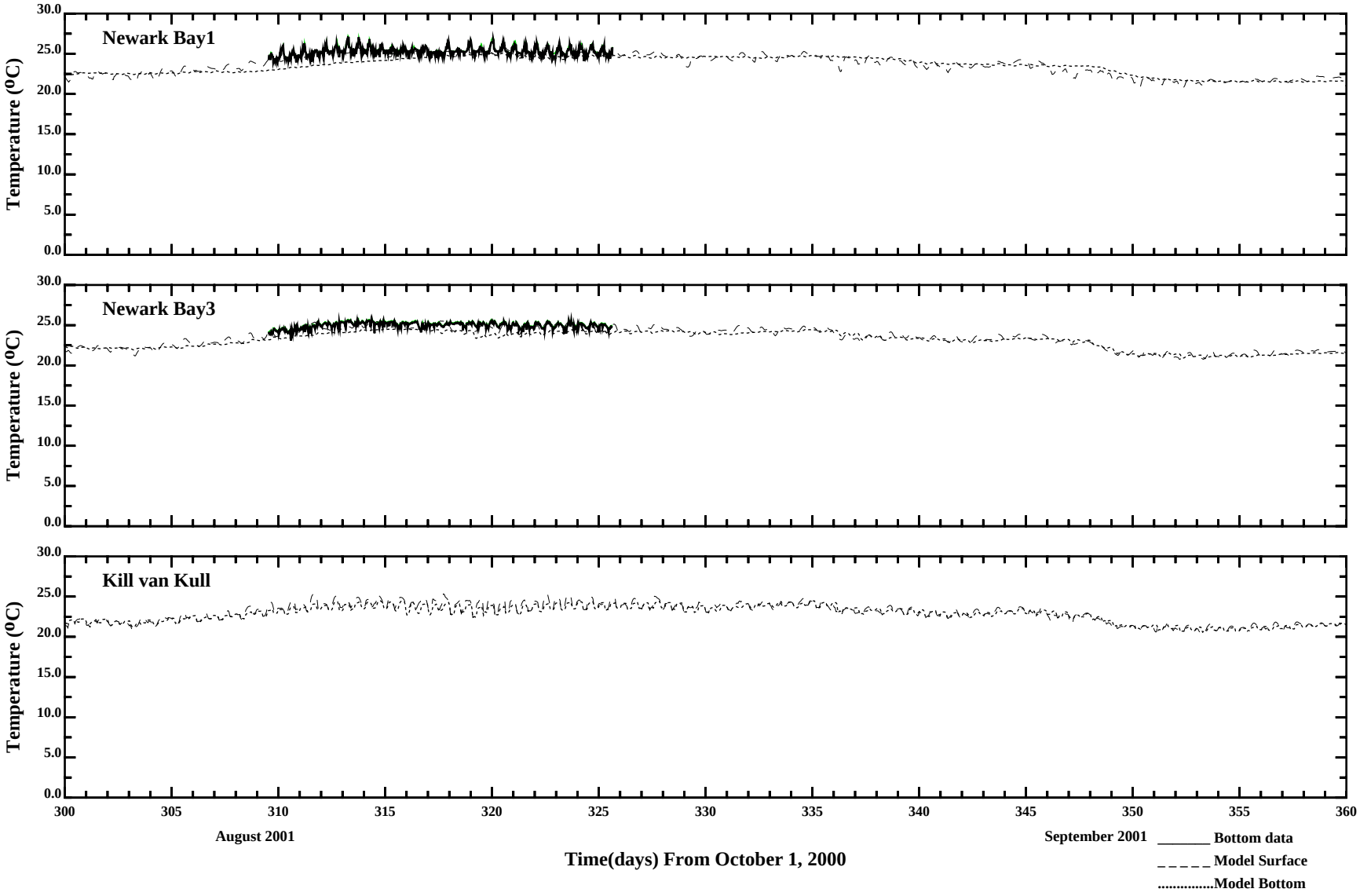

/erie1/hrfo0010/HYDRORUNS/RUTGERS/temp.gdp
DATE: 8/16/2004 TIME: 14: 4: 2

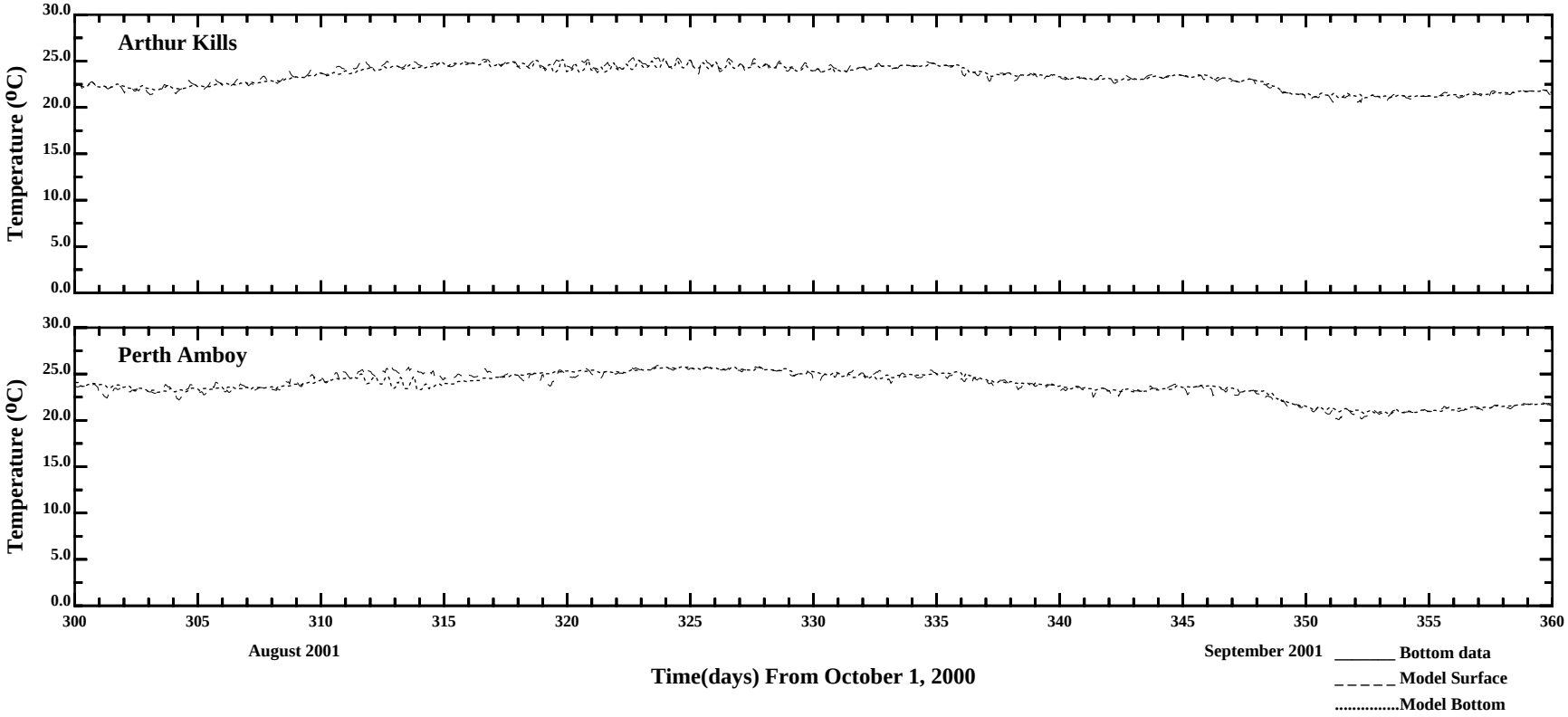

/erie1/hrfo0010/HYDRORUNS/RUTGERS/temp.gdp

DATE: 8/16/2004 TIME: 14: 4: 2

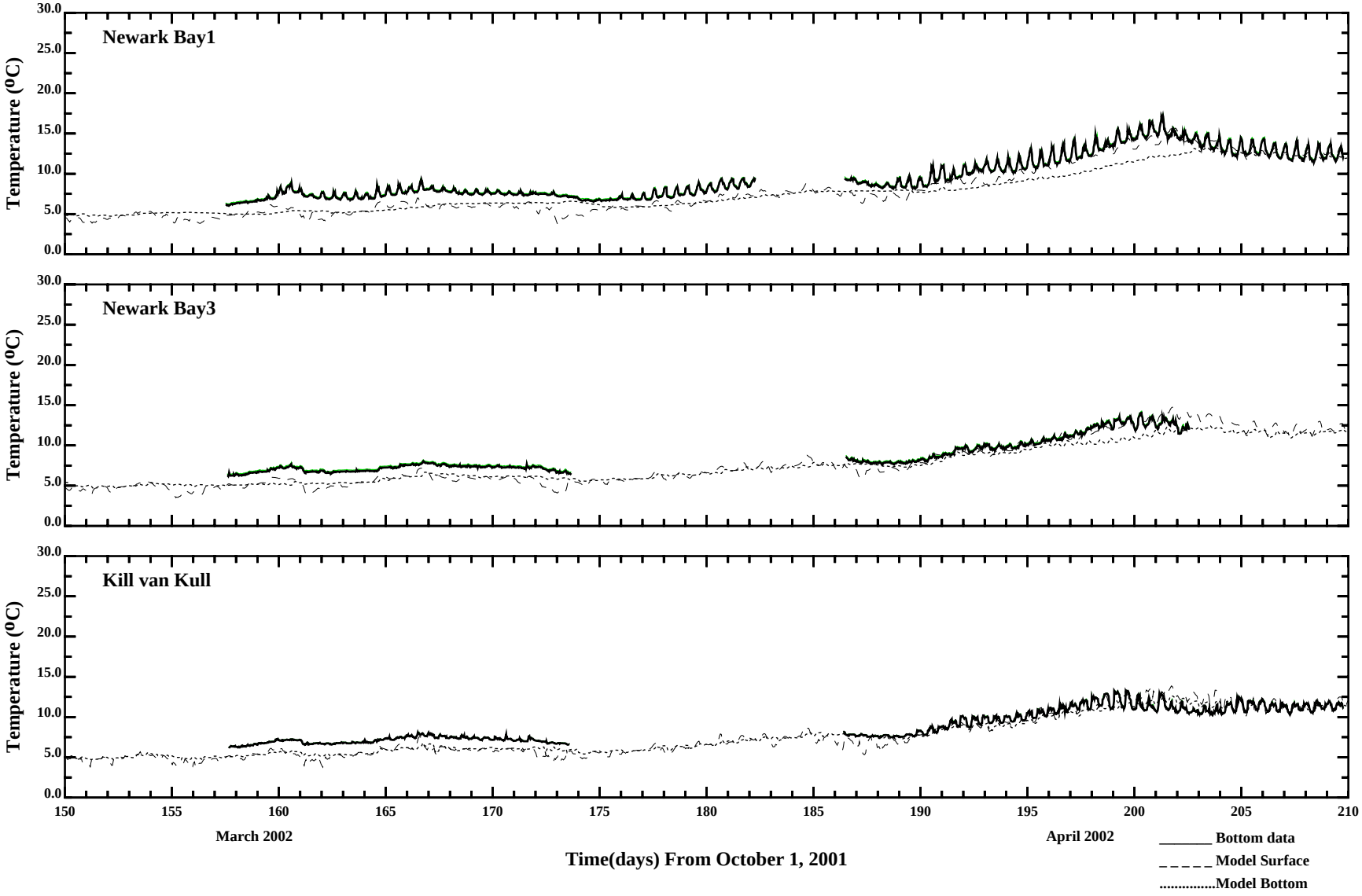

/erie1/hrfo0010/HYDRORUNS/RUTGERS/temp.gdp
DATE: 8/16/2004 TIME: 14: 4:11

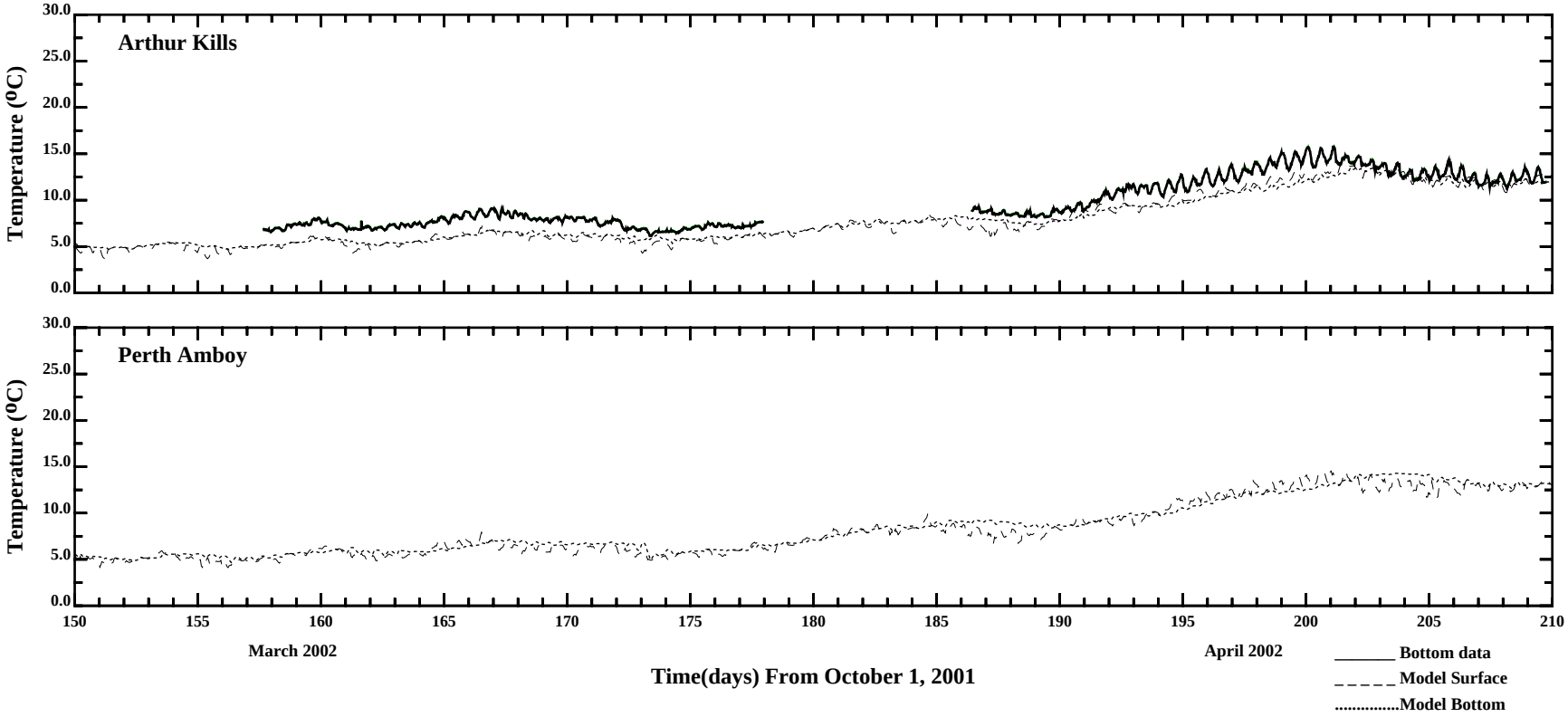

/erie1/hrfo0010/HYDRORUNS/RUTGERS/temp.gdp

DATE: 8/16/2004 TIME: 14: 4:11

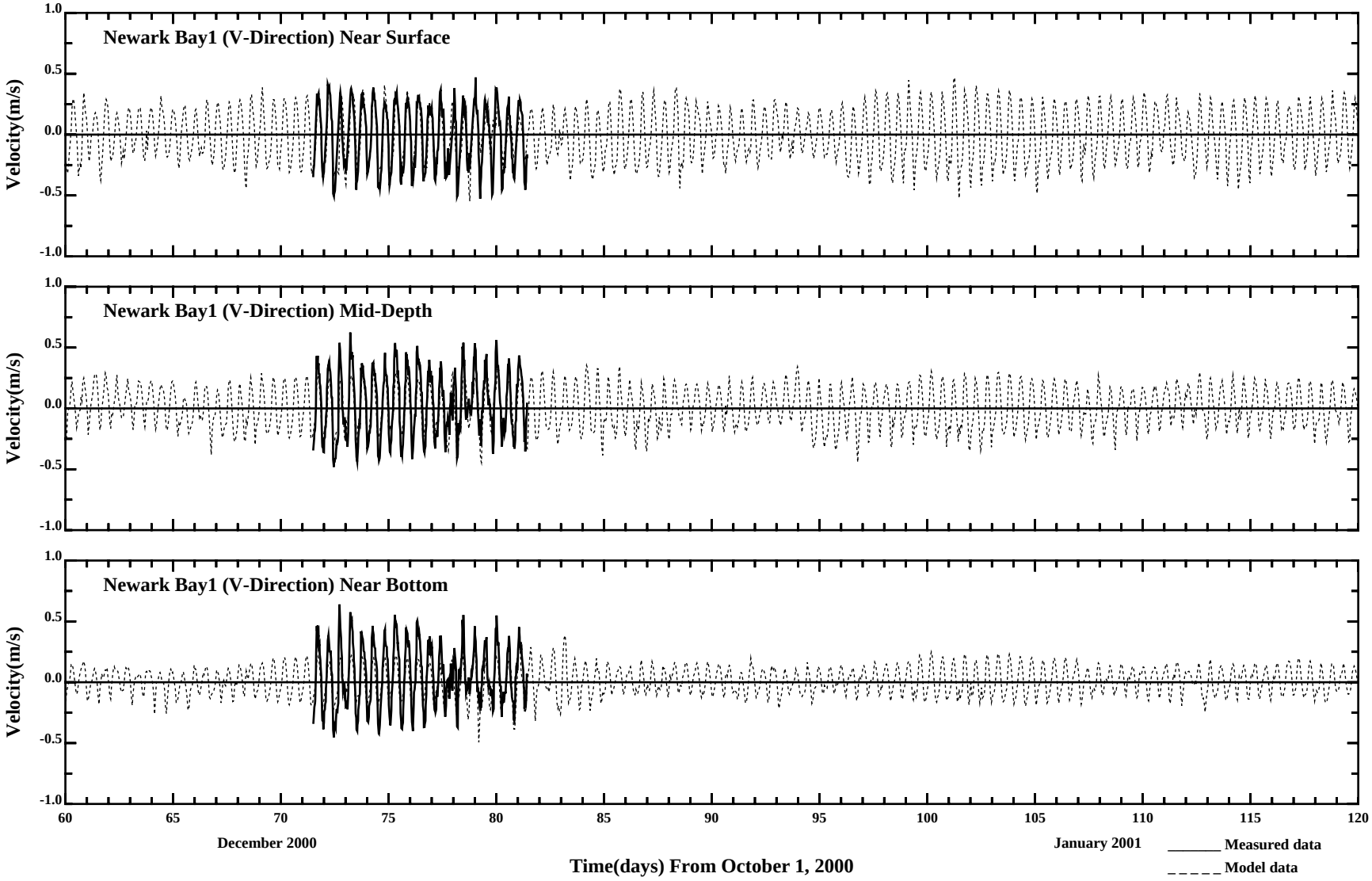

/erie1/hrfo0010/HYDRORUNS/RUTGERS/velocity.gdp
DATE: 8/16/2004 TIME: 14:24:21

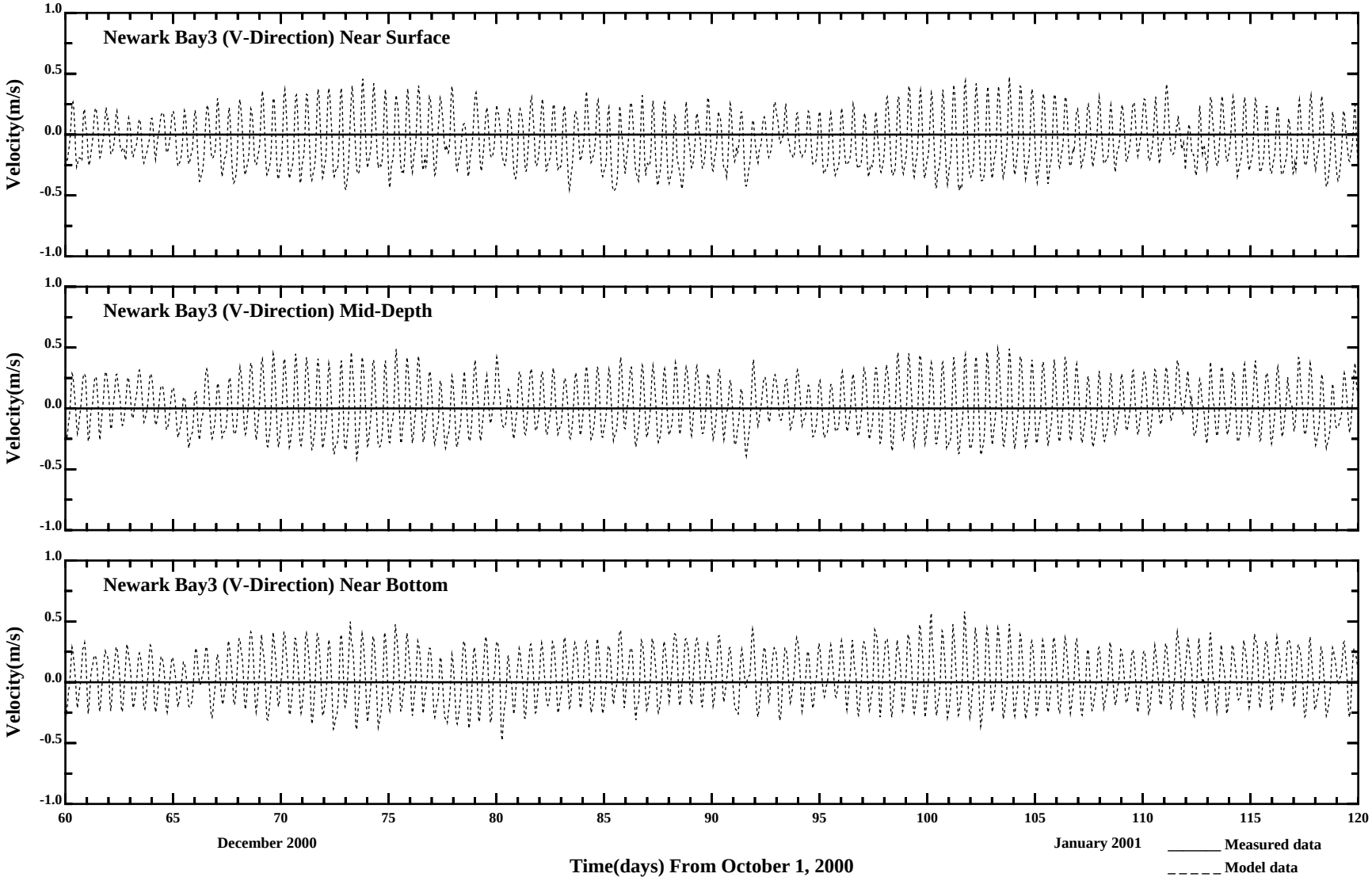

/erie1/hrfo0010/HYDRORUNS/RUTGERS/velocity.gdp
DATE: 8/16/2004 TIME: 14:24:21

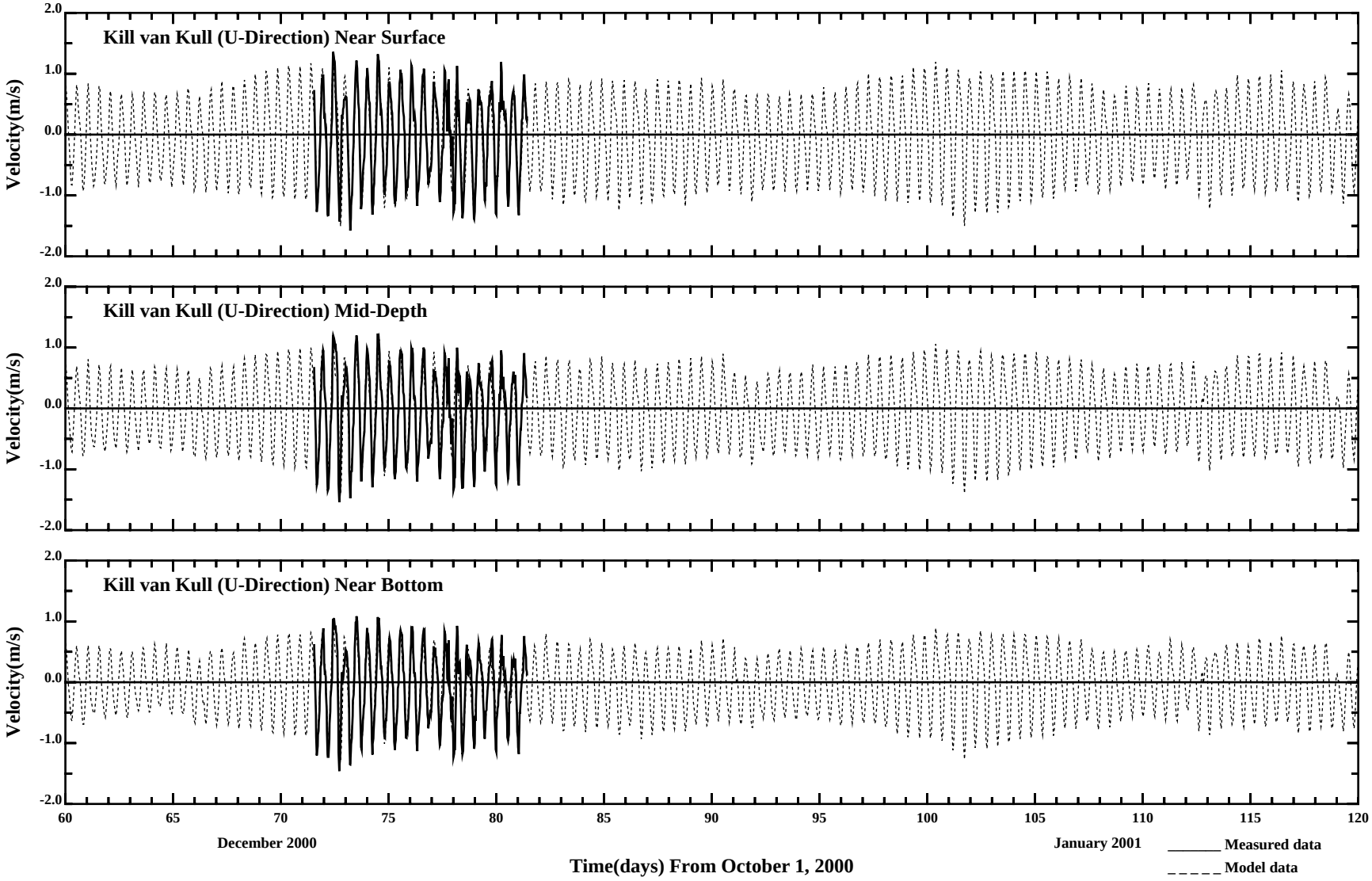

/erie1/hrfo0010/HYDRORUNS/RUTGERS/velocity.gdp
DATE: 8/16/2004 TIME: 14:24:21

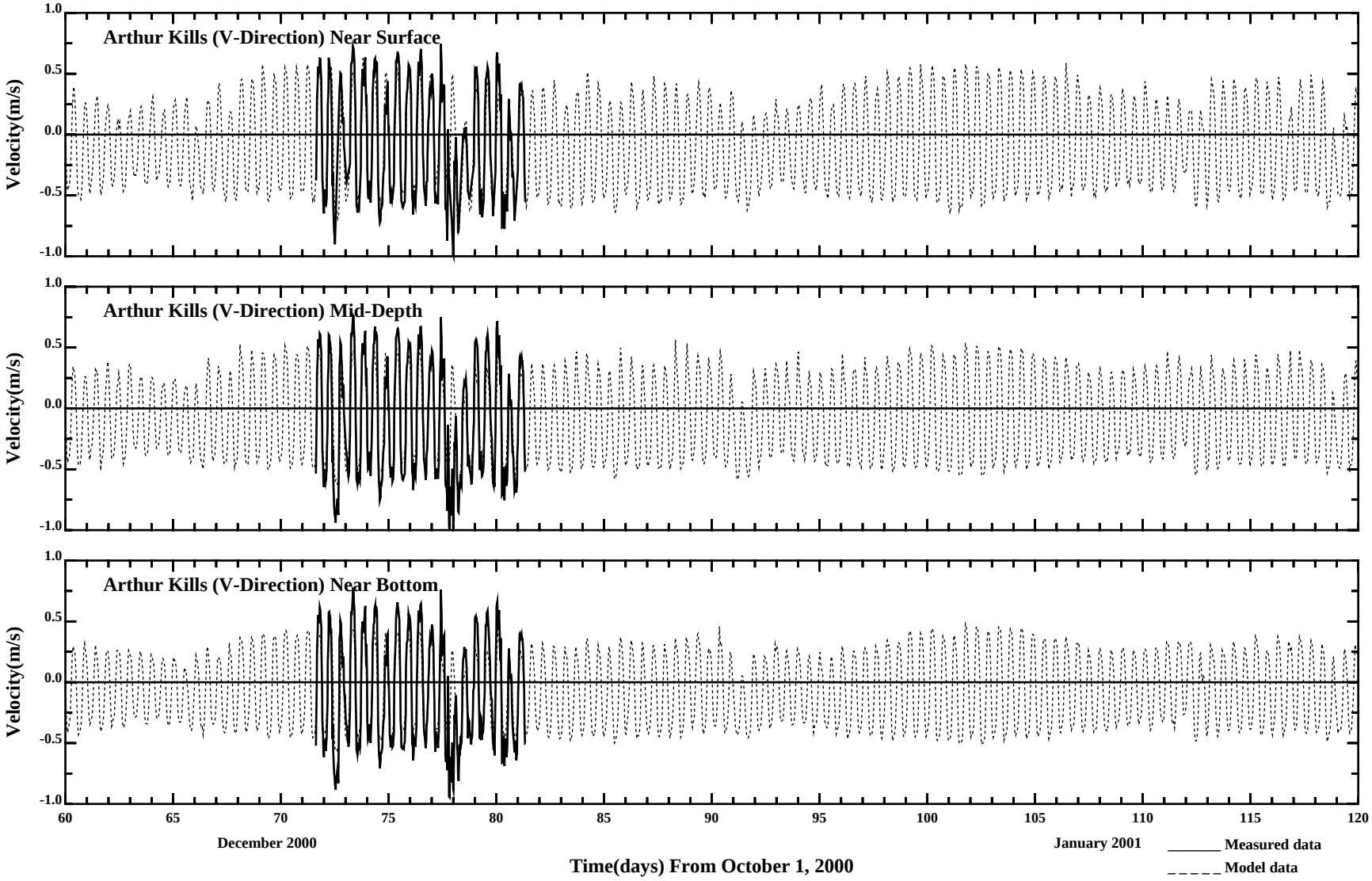

/erie1/hrfo0010/HYDRORUNS/RUTGERS/velocity.gdp
DATE: 8/16/2004 TIME: 14:24:21

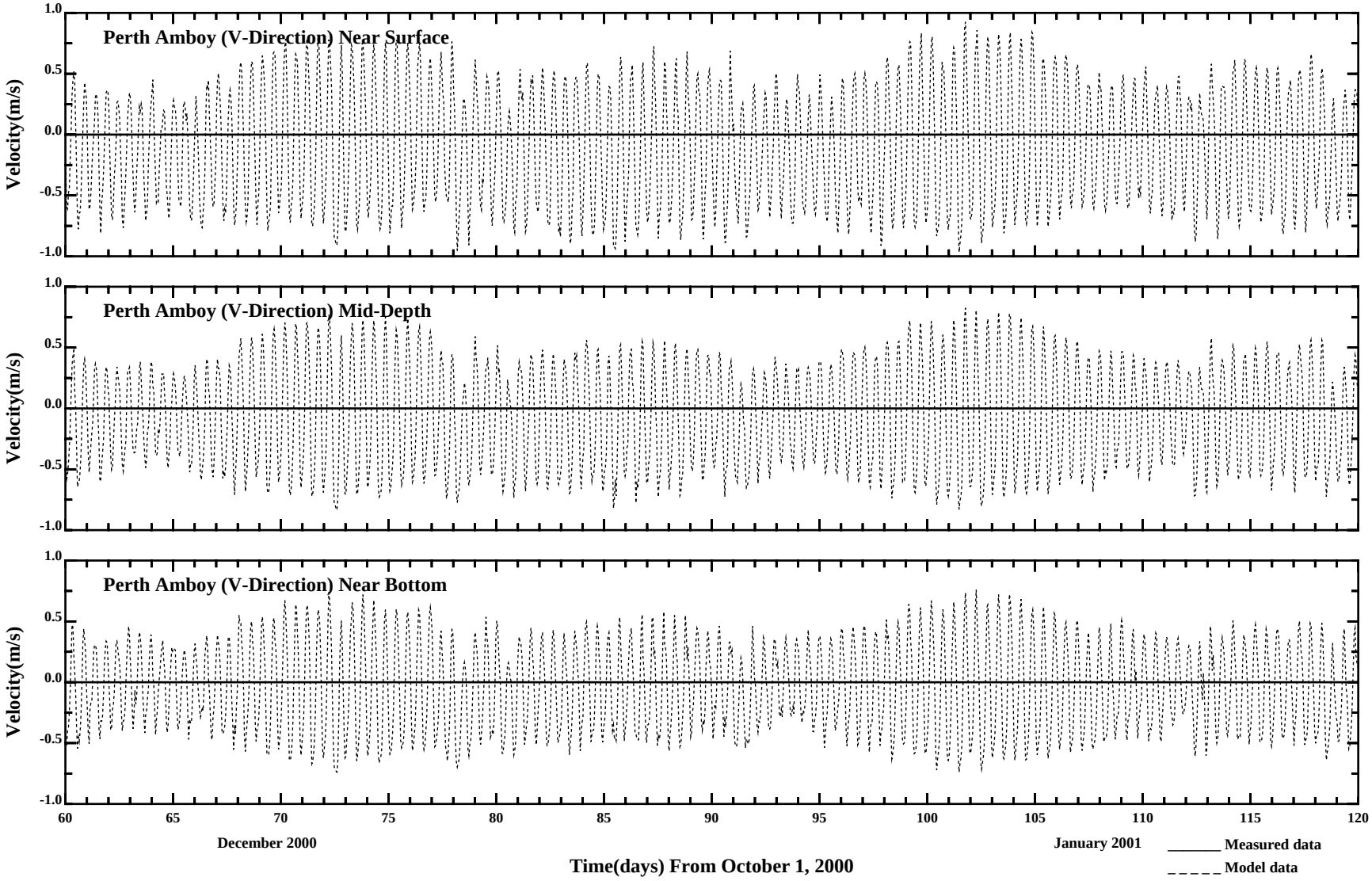

/erie1/hrfo0010/HYDRORUNS/RUTGERS/velocity.gdp
DATE: 8/16/2004 TIME: 14:24:21

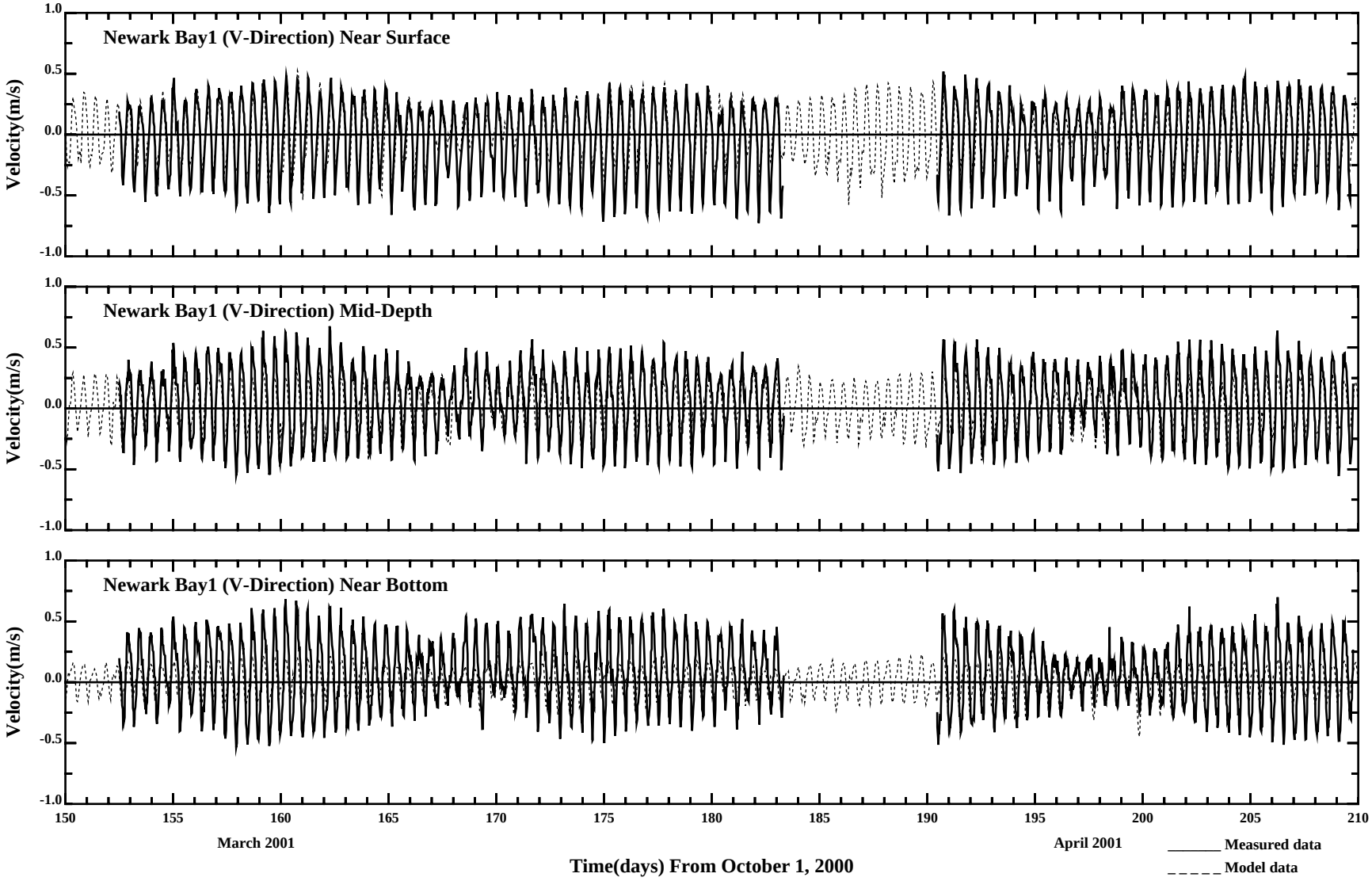

/erie1/hrfo0010/HYDRORUNS/RUTGERS/velocity.gdp
DATE: 8/16/2004 TIME: 14:25: 3

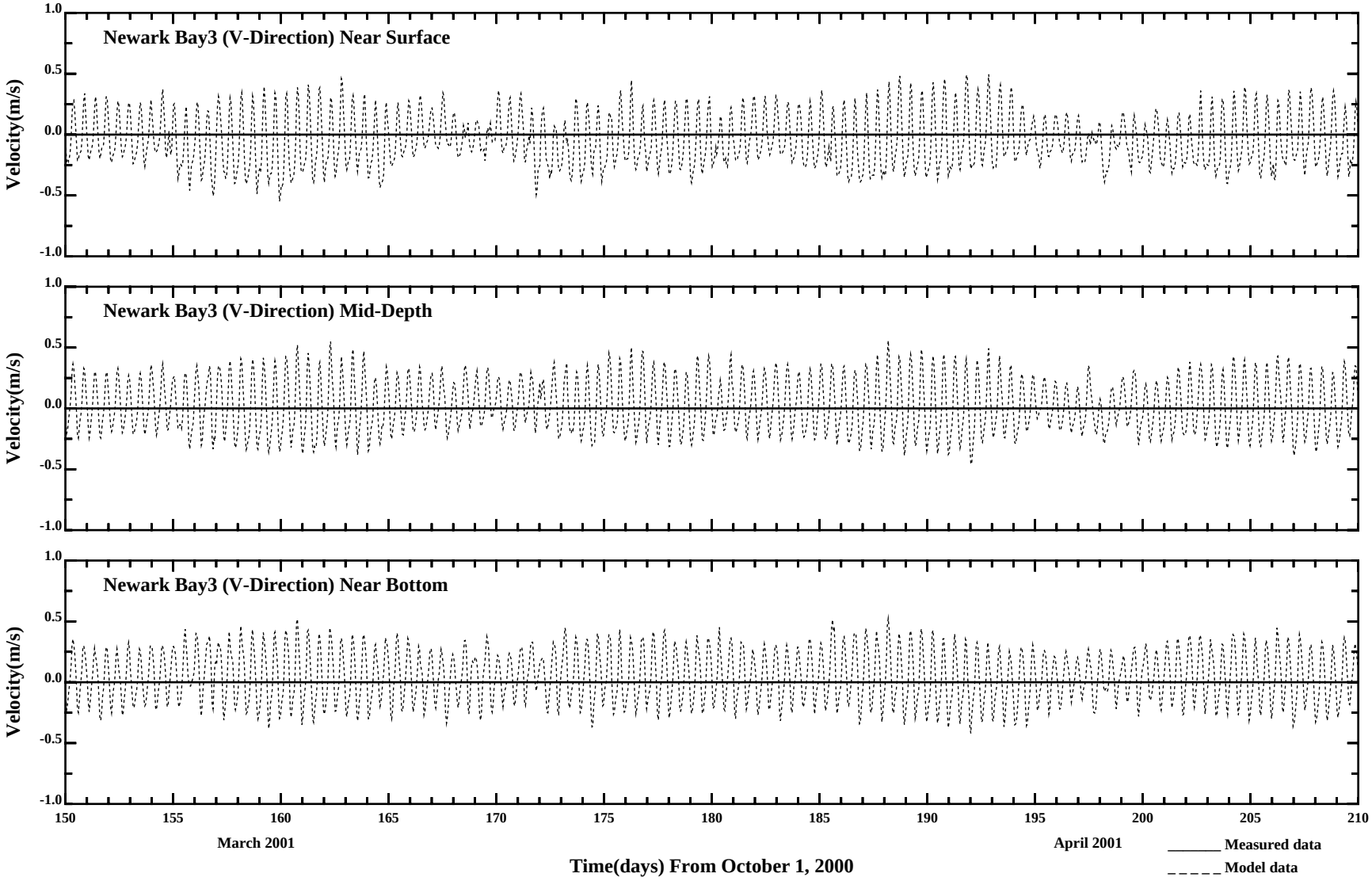

/erie1/hrfo0010/HYDRORUNS/RUTGERS/velocity.gdp
DATE: 8/16/2004 TIME: 14:25: 3

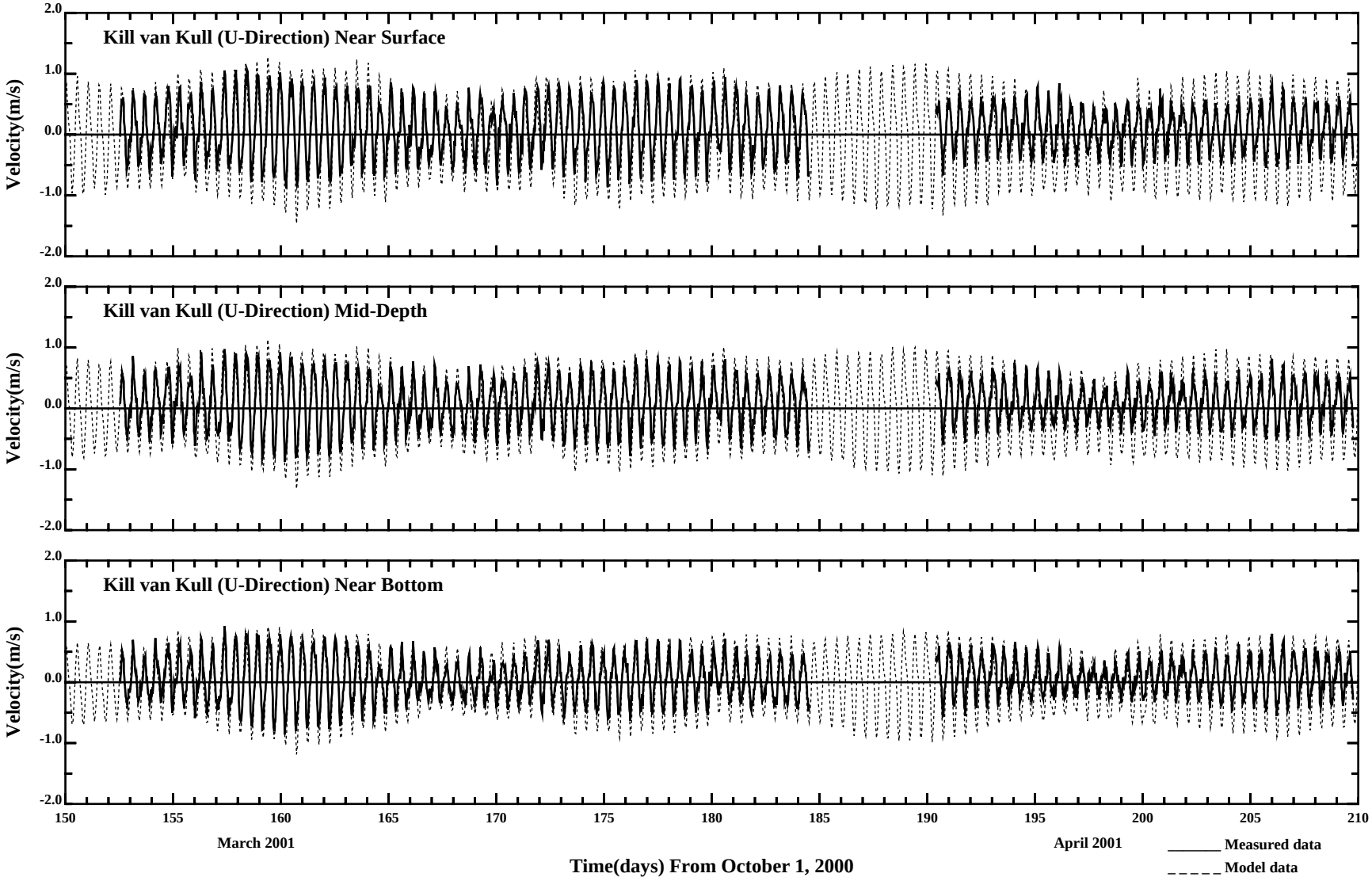

/erie1/hrfo0010/HYDRORUNS/RUTGERS/velocity.gdp
DATE: 8/16/2004 TIME: 14:25: 3

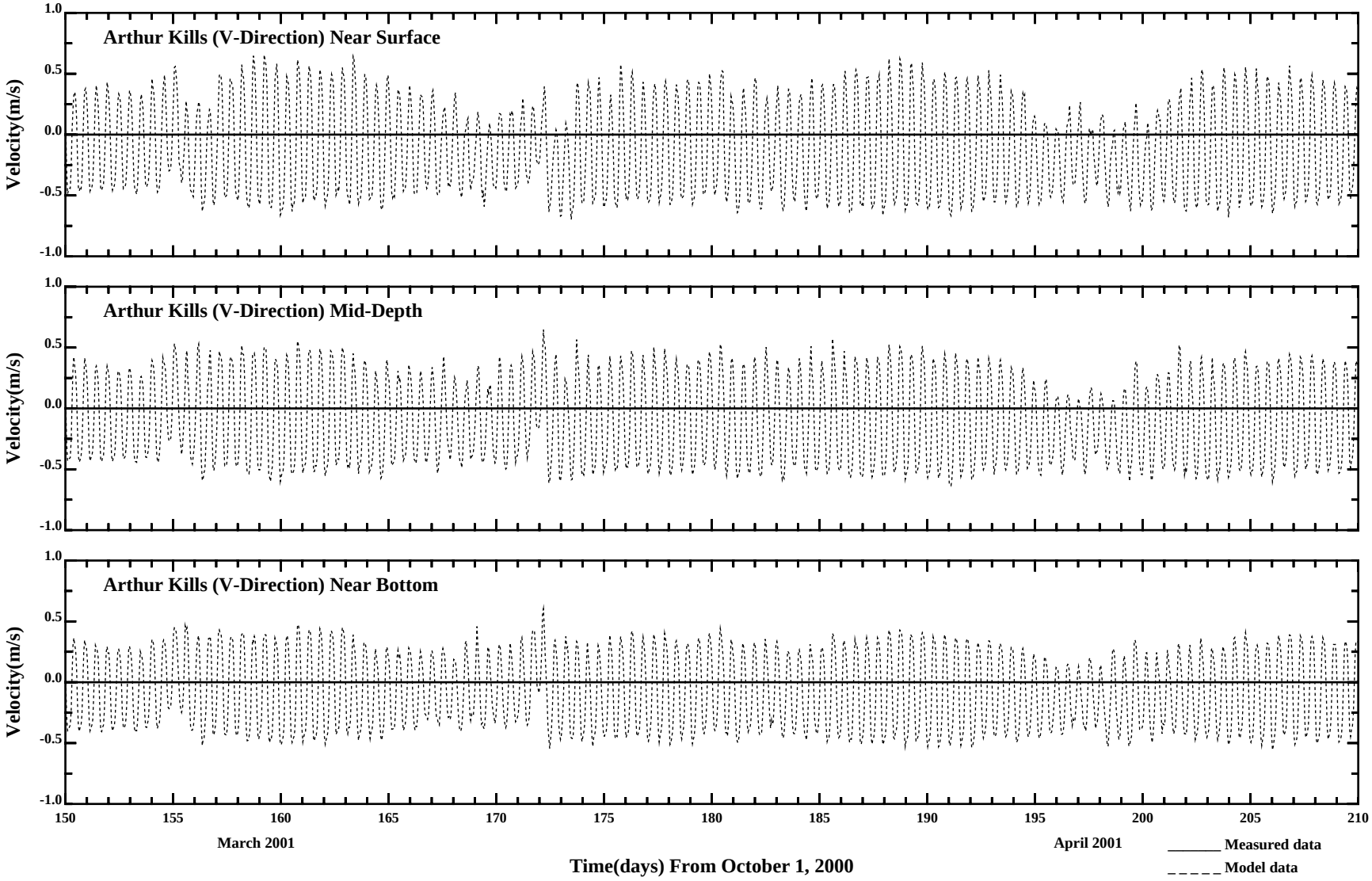

/erie1/hrfo0010/HYDRORUNS/RUTGERS/velocity.gdp
DATE: 8/16/2004 TIME: 14:25: 3

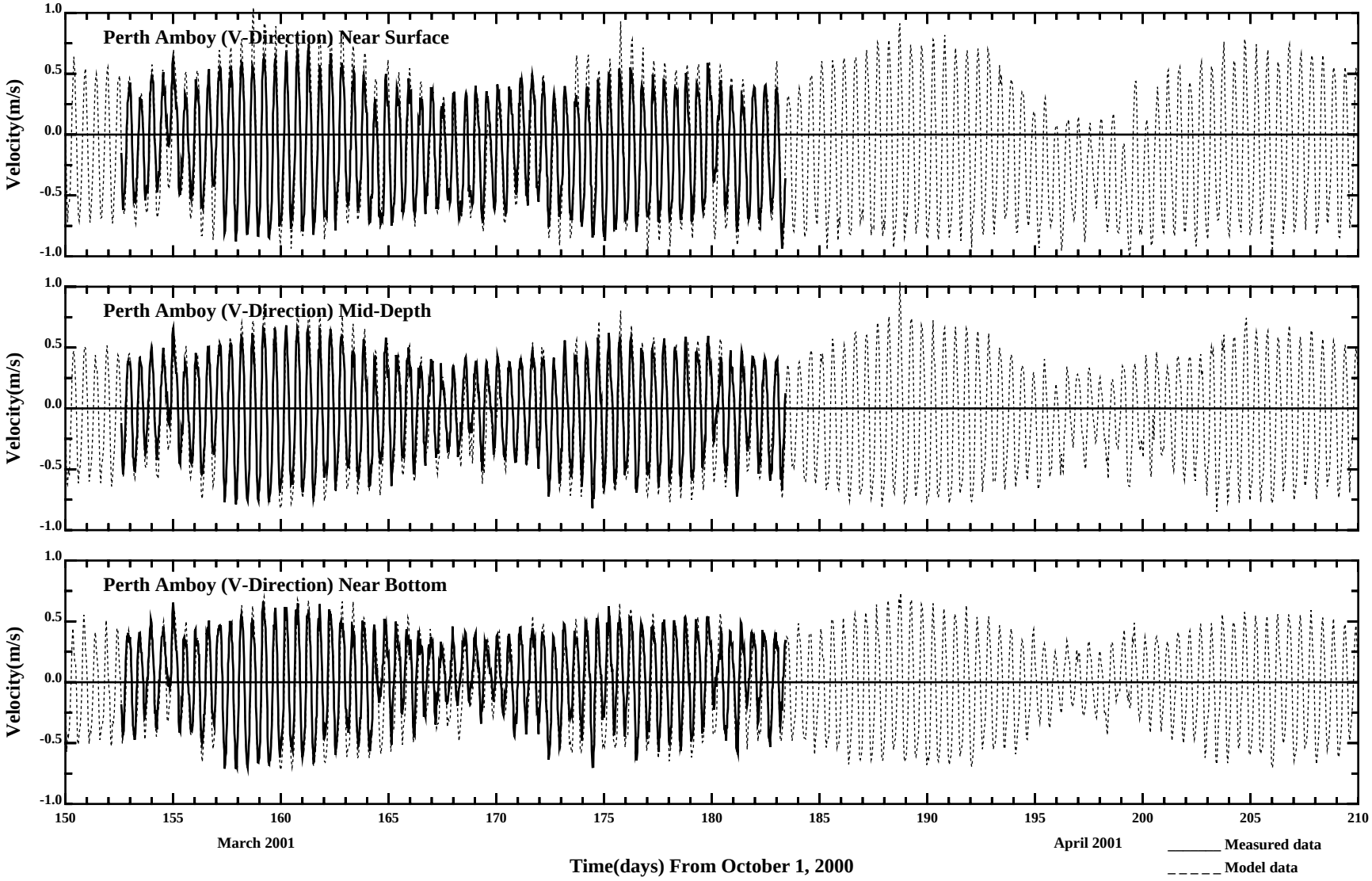

/erie1/hrfo0010/HYDRORUNS/RUTGERS/velocity.gdp
DATE: 8/16/2004 TIME: 14:25: 3

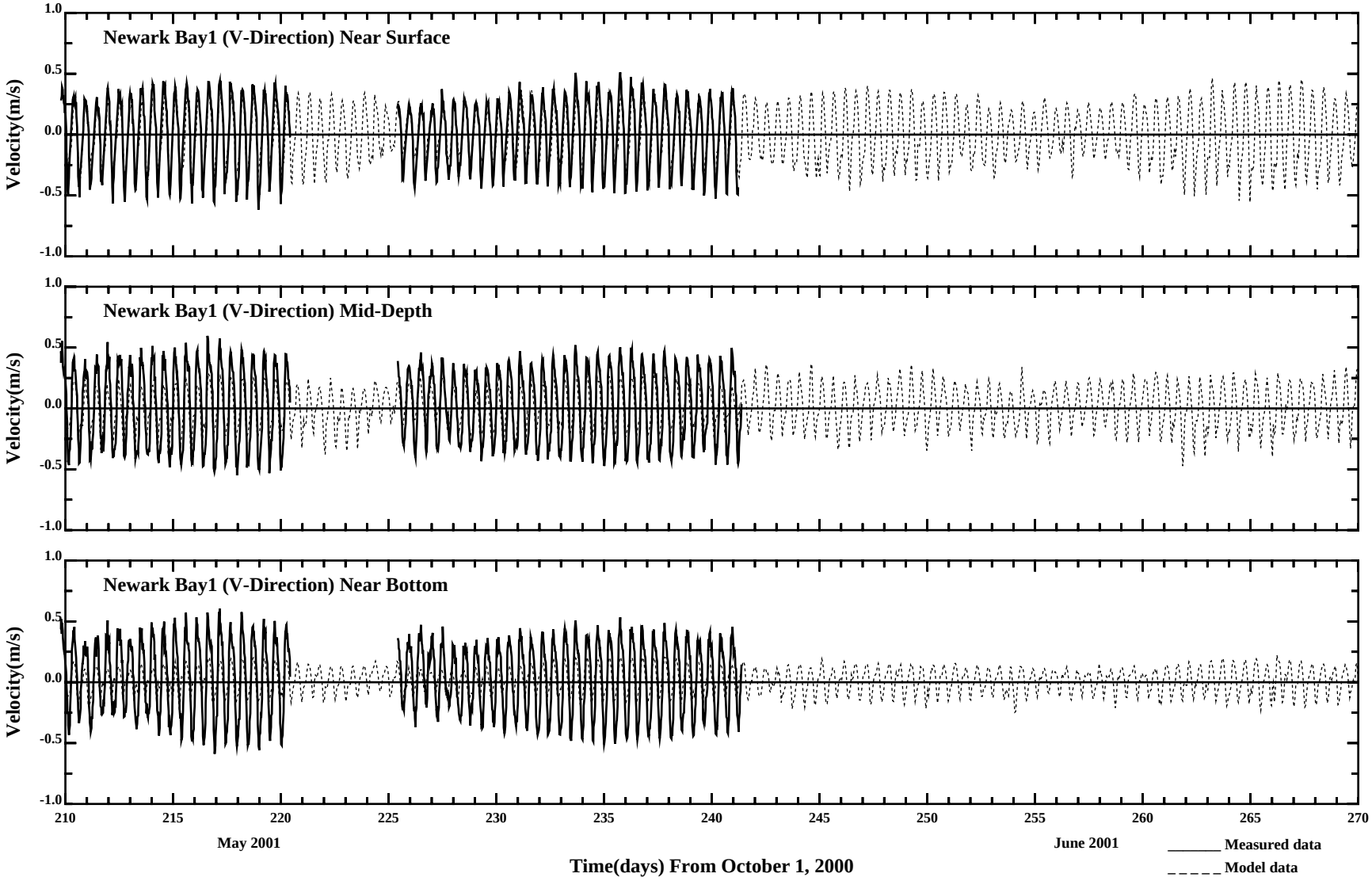

/erie1/hrfo0010/HYDRORUNS/RUTGERS/velocity.gdp
DATE: 8/16/2004 TIME: 14:25:44

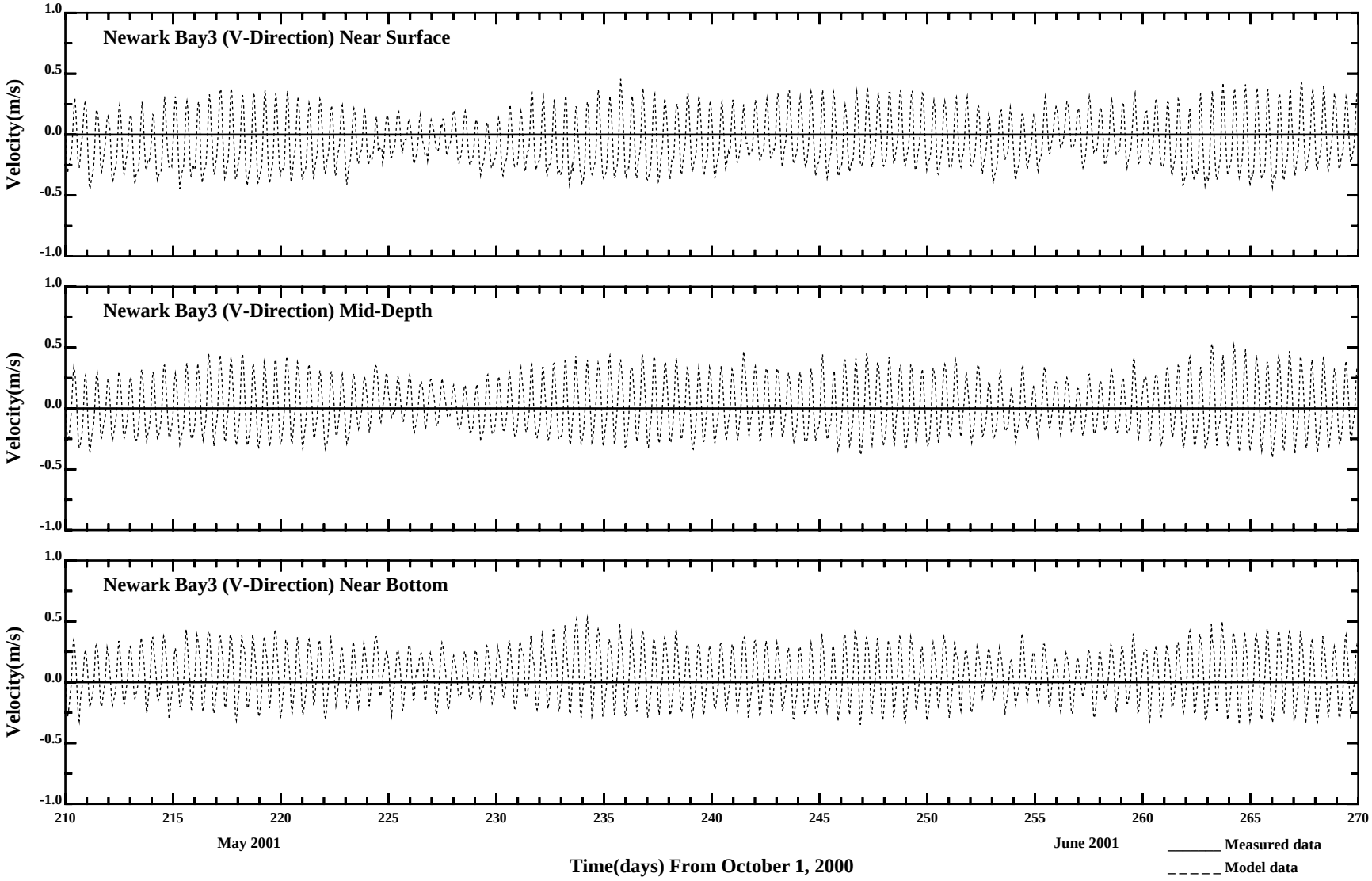

/erie1/hrfo0010/HYDRORUNS/RUTGERS/velocity.gdp
DATE: 8/16/2004 TIME: 14:25:44

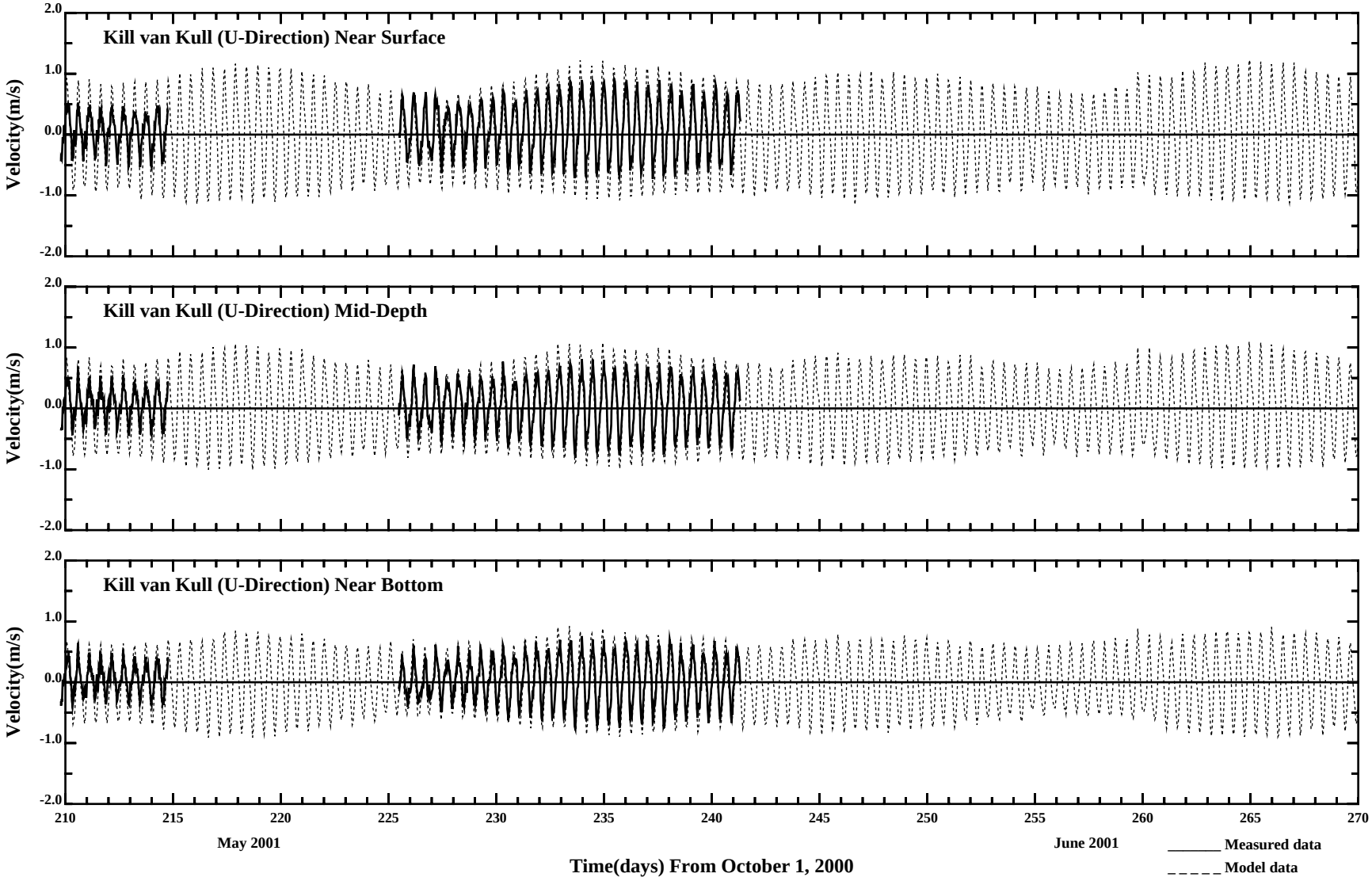

/erie1/hrfo0010/HYDRORUNS/RUTGERS/velocity.gdp
DATE: 8/16/2004 TIME: 14:25:44

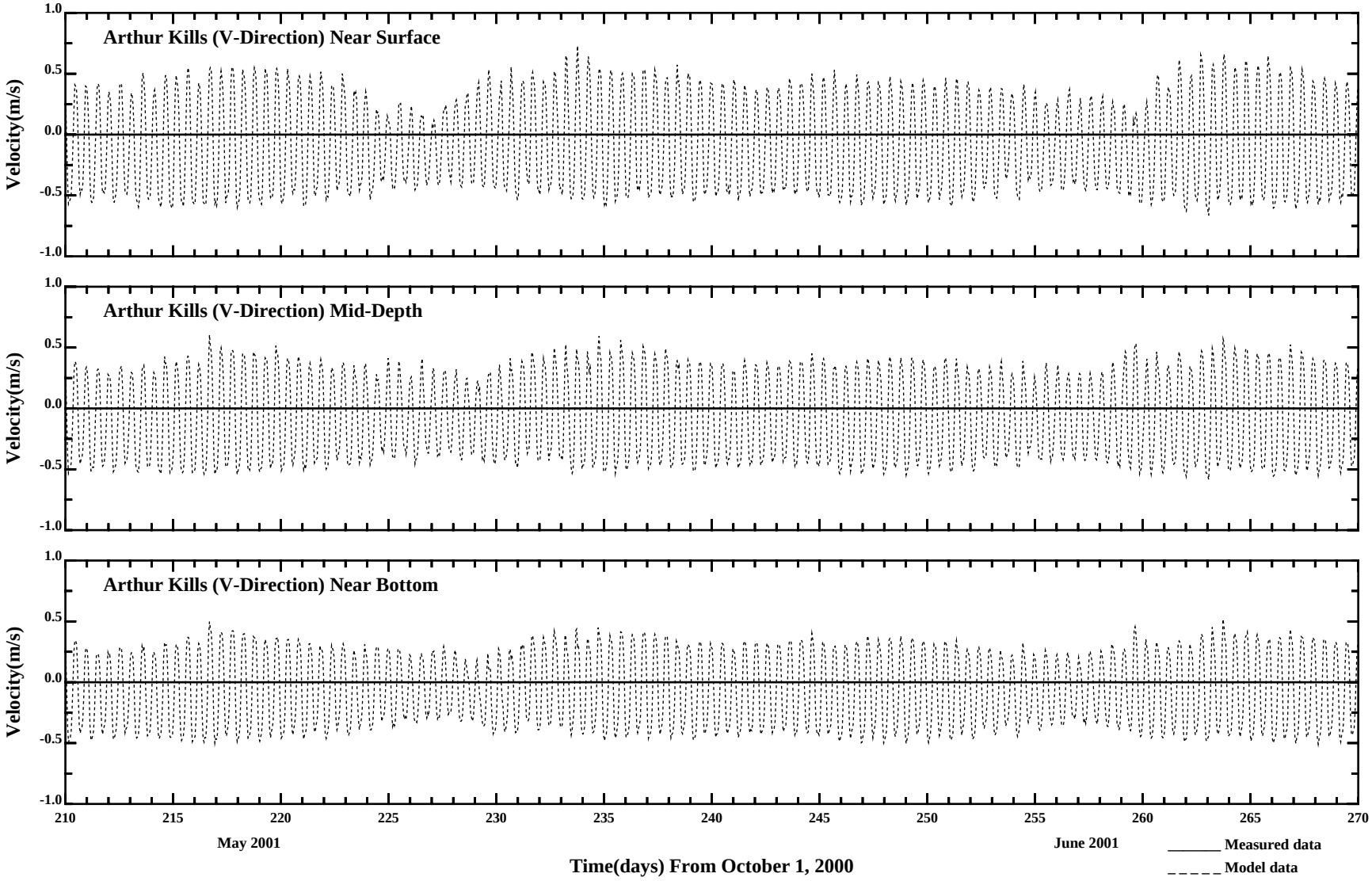

/erie1/hrfo0010/HYDRORUNS/RUTGERS/velocity.gdp
DATE: 8/16/2004 TIME: 14:25:44

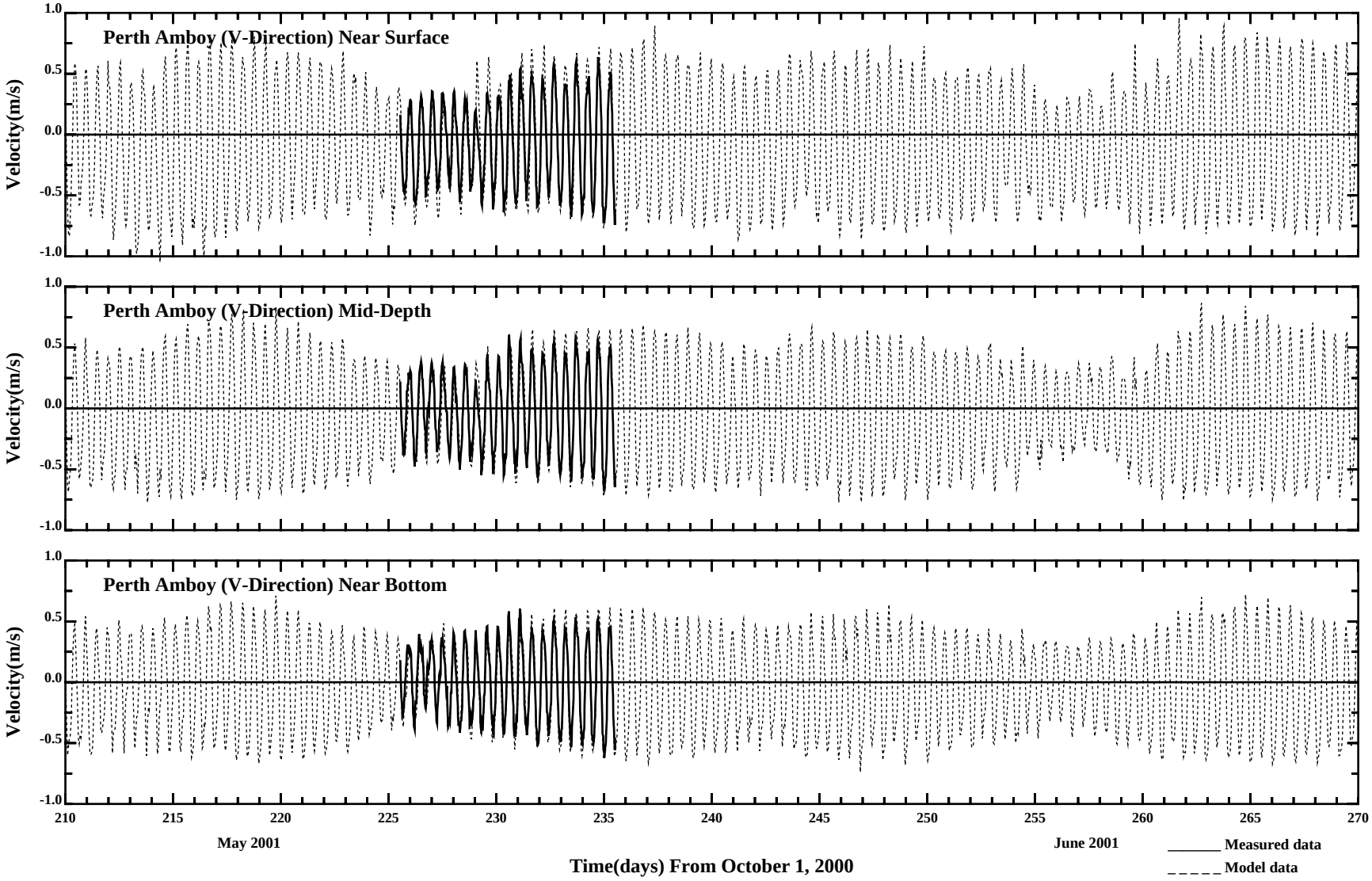

/erie1/hrfo0010/HYDRORUNS/RUTGERS/velocity.gdp
DATE: 8/16/2004 TIME: 14:25:44

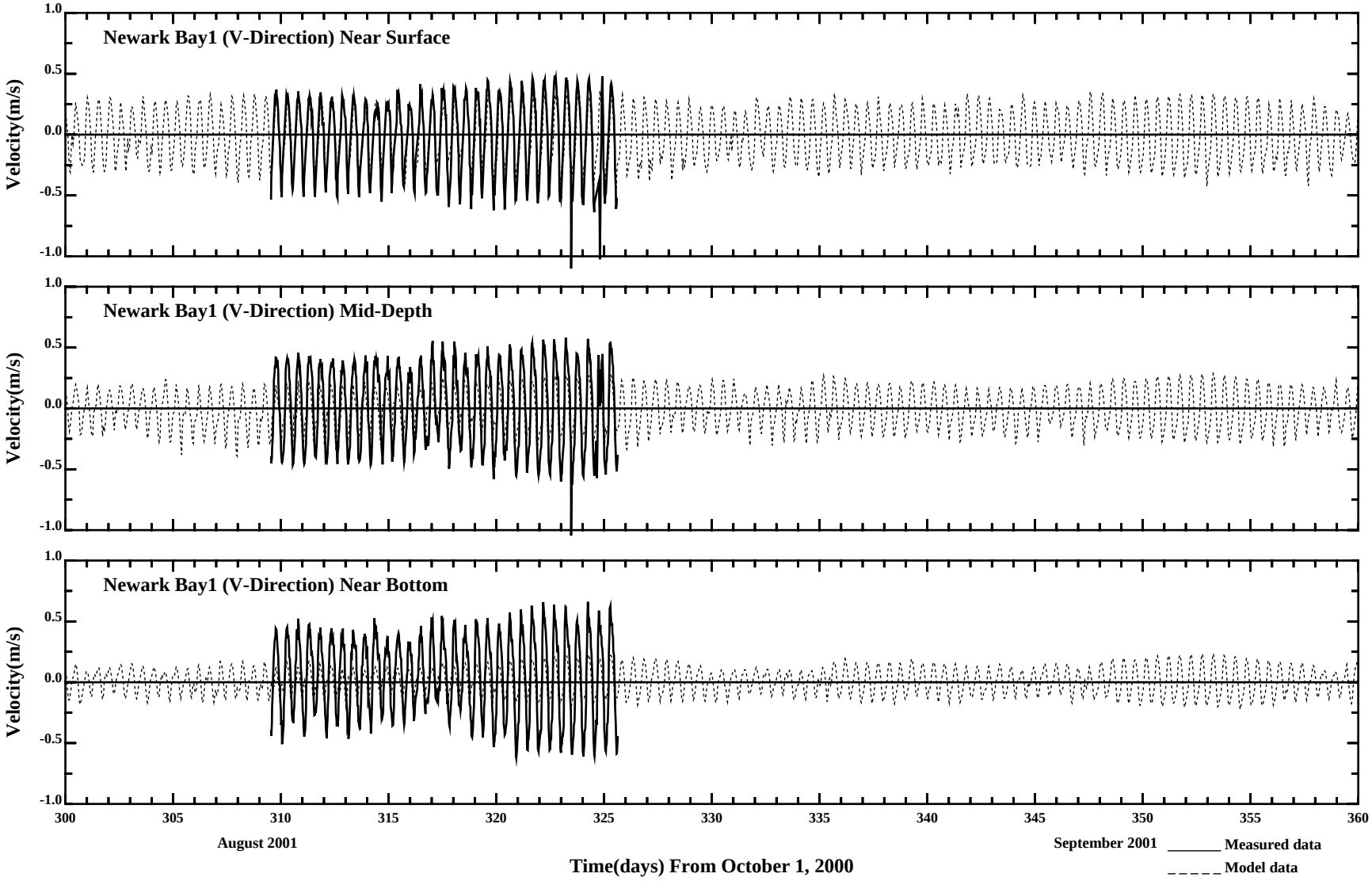

/erie1/hrfo0010/HYDRORUNS/RUTGERS/velocity.gdp
DATE: 8/16/2004 TIME: 14:26:25

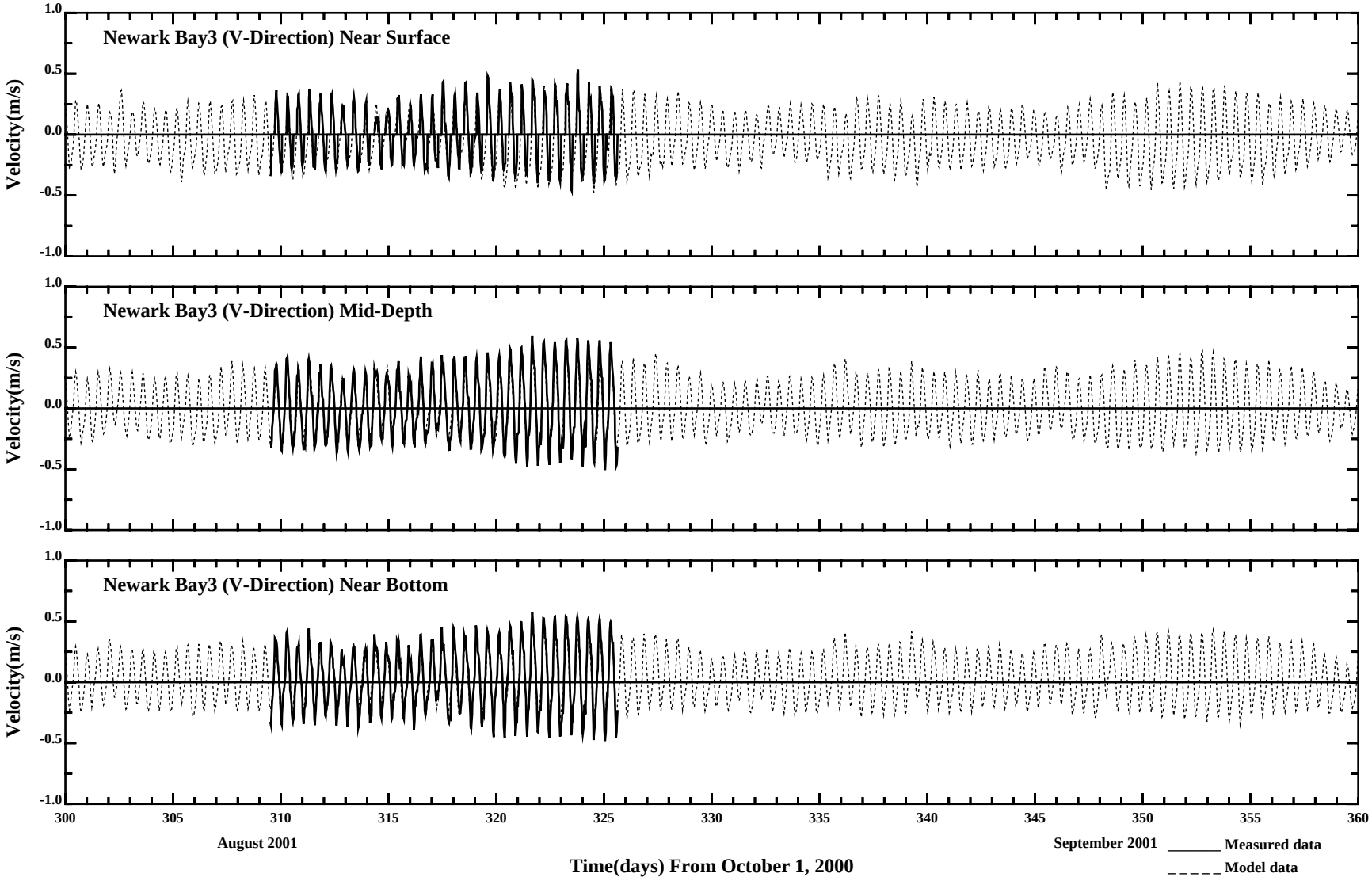

/erie1/hrfo0010/HYDRORUNS/RUTGERS/velocity.gdp
DATE: 8/16/2004 TIME: 14:26:25

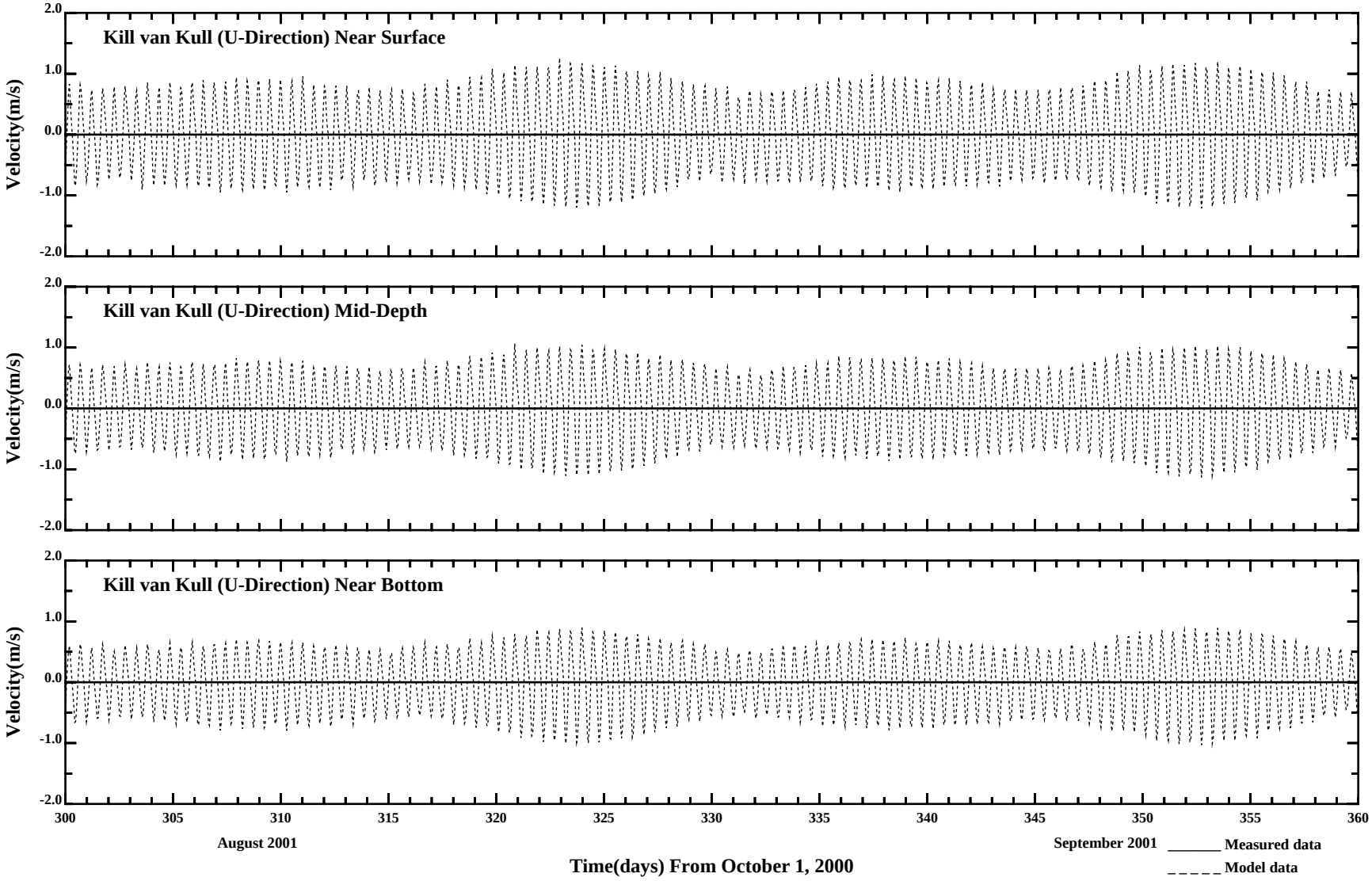

/erie1/hrfo0010/HYDRORUNS/RUTGERS/velocity.gdp
DATE: 8/16/2004 TIME: 14:26:25

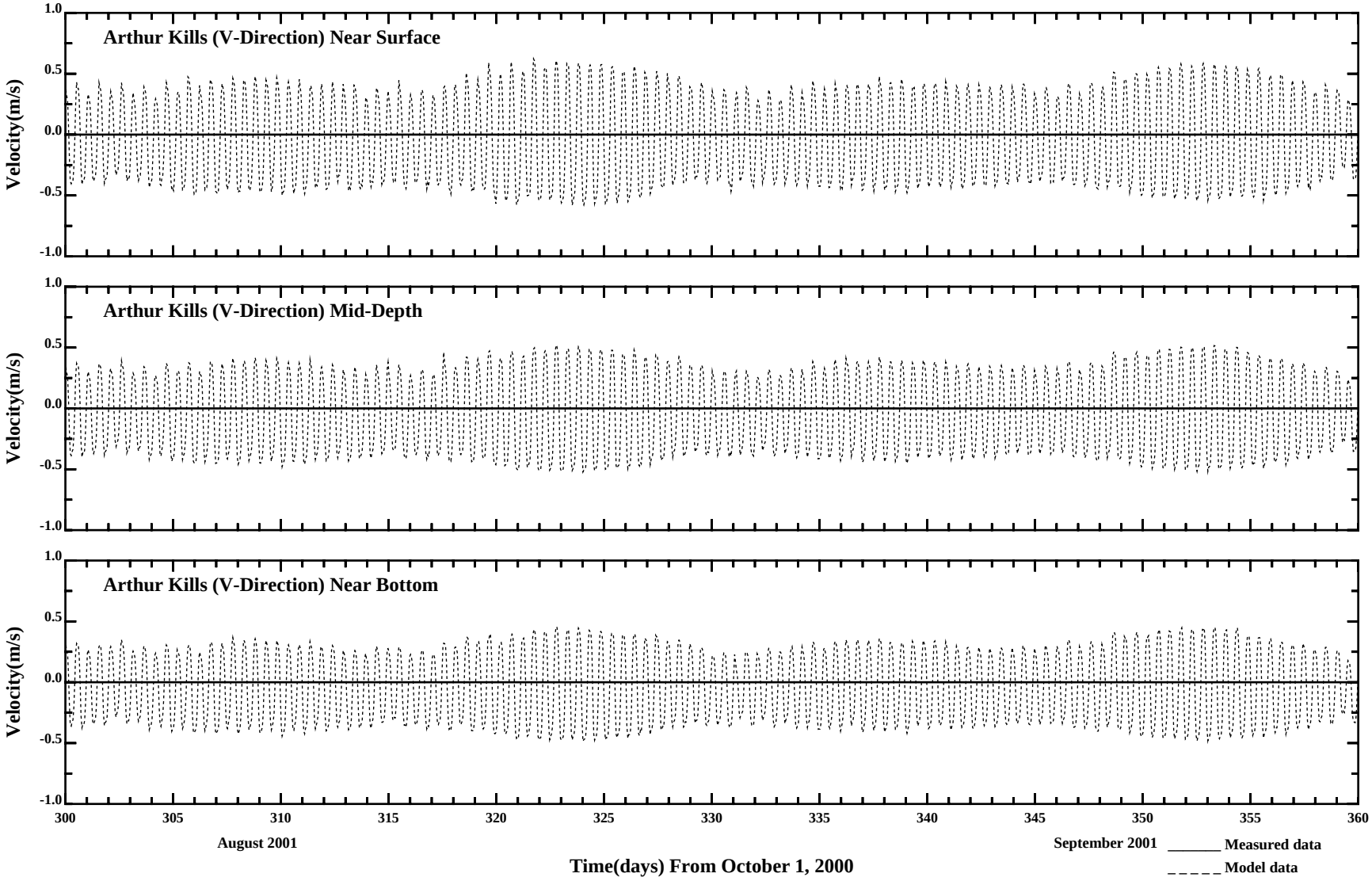

/erie1/hrfo0010/HYDRORUNS/RUTGERS/velocity.gdp
DATE: 8/16/2004 TIME: 14:26:25

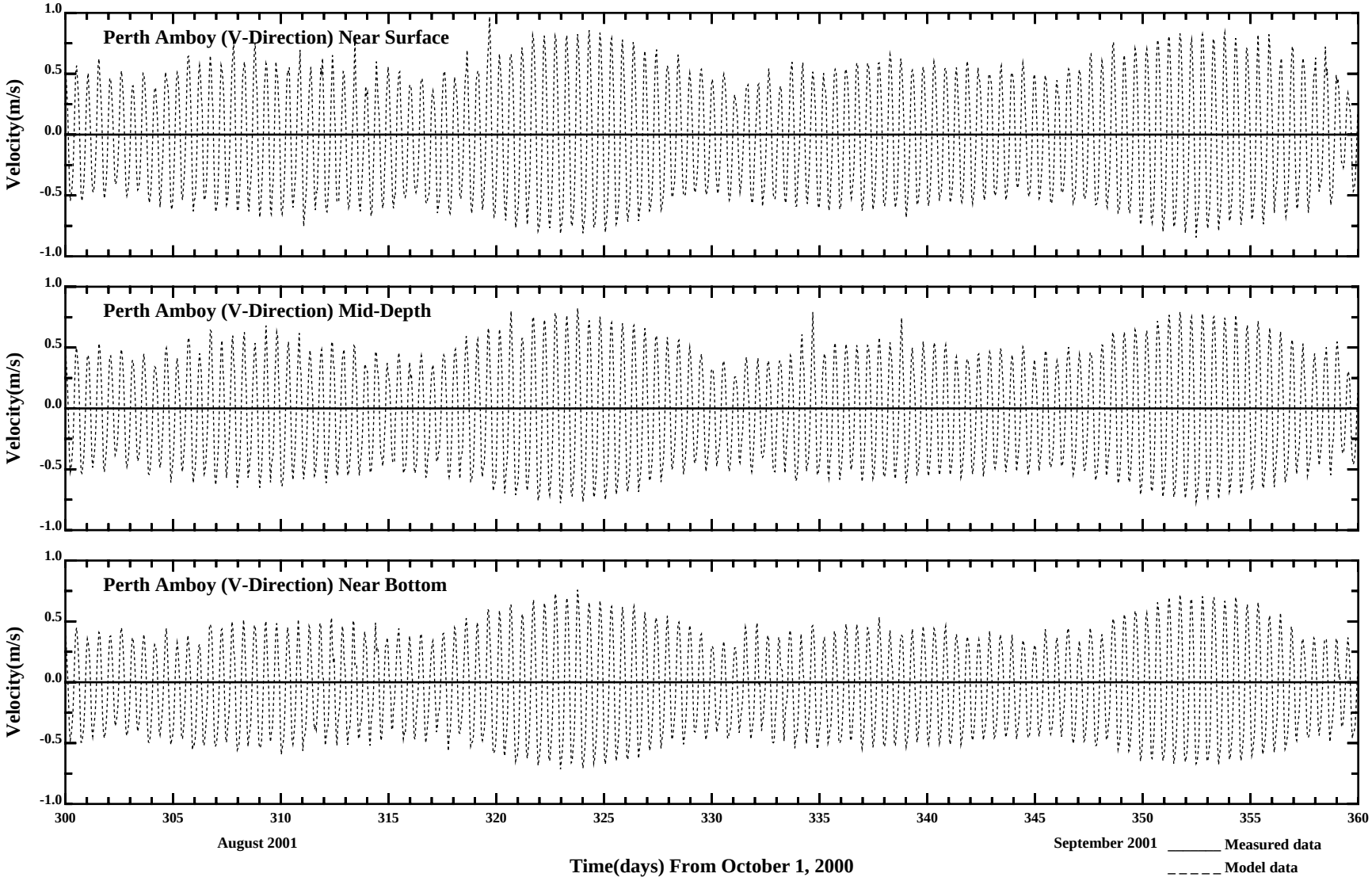

/erie1/hrfo0010/HYDRORUNS/RUTGERS/velocity.gdp
DATE: 8/16/2004 TIME: 14:26:25

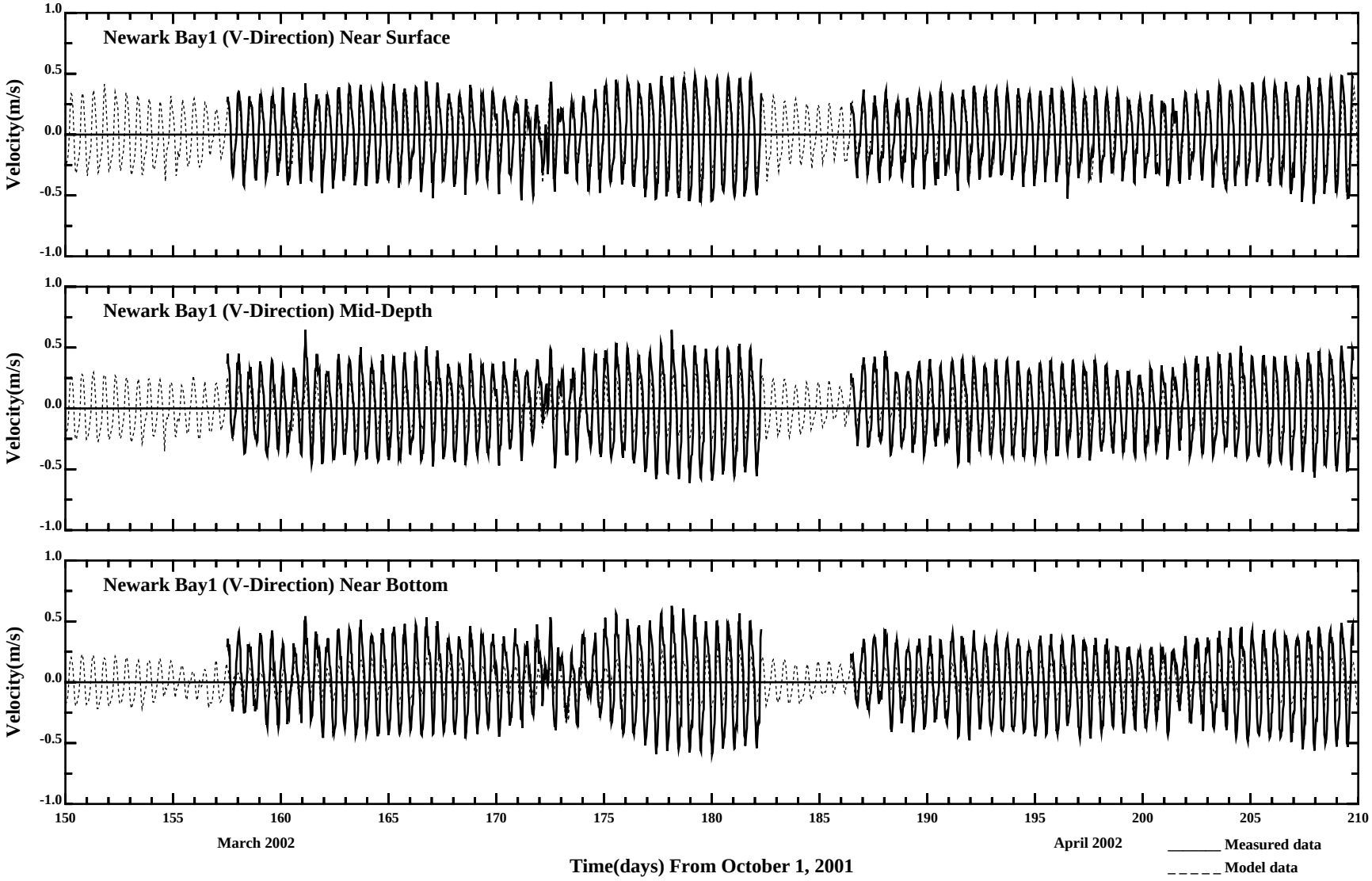

/erie1/hrfo0010/HYDRORUNS/RUTGERS/velocity.gdp
DATE: 8/16/2004 TIME: 14:27: 7

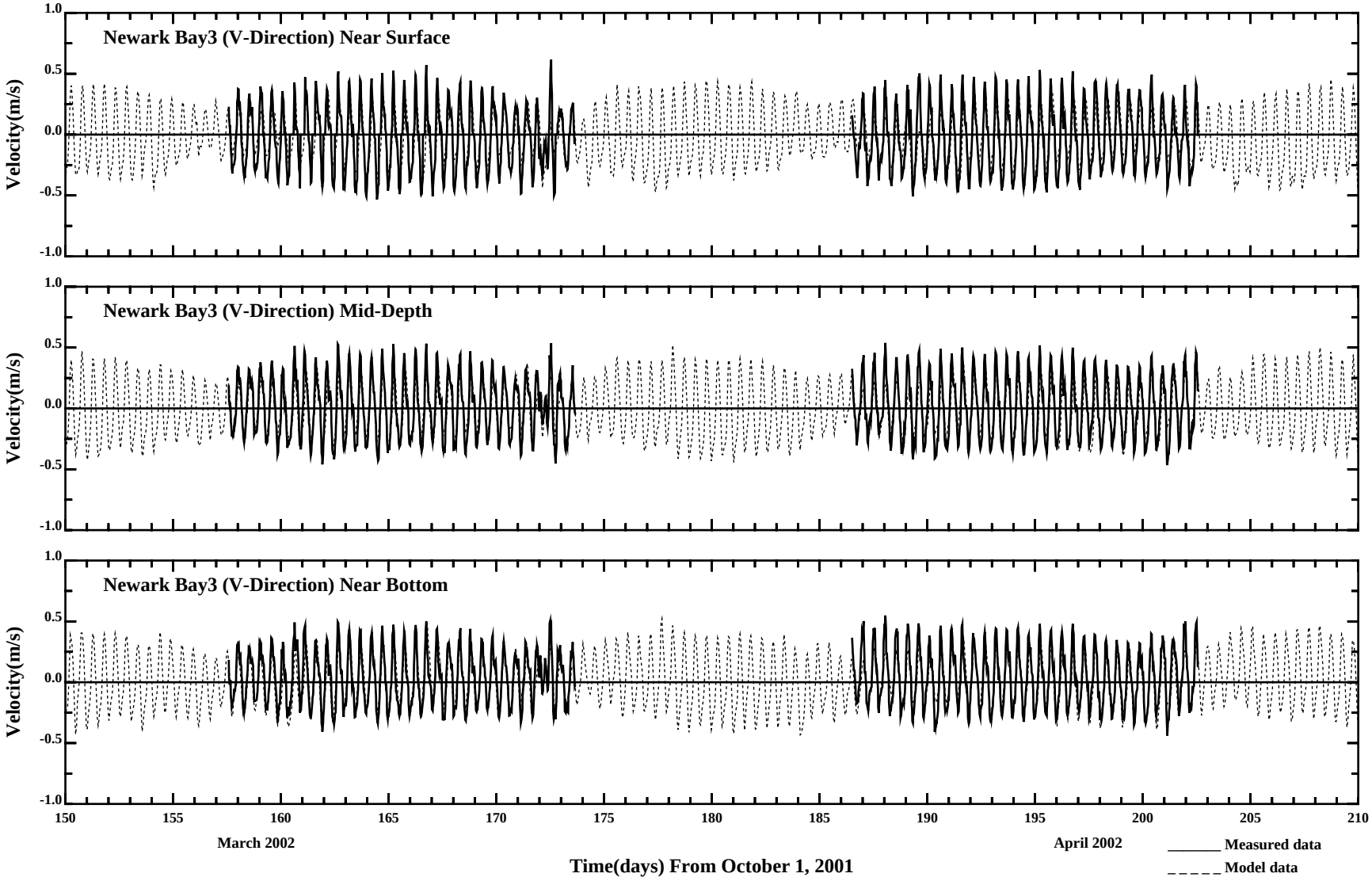

/erie1/hrfo0010/HYDRORUNS/RUTGERS/velocity.gdp
DATE: 8/16/2004 TIME: 14:27: 7

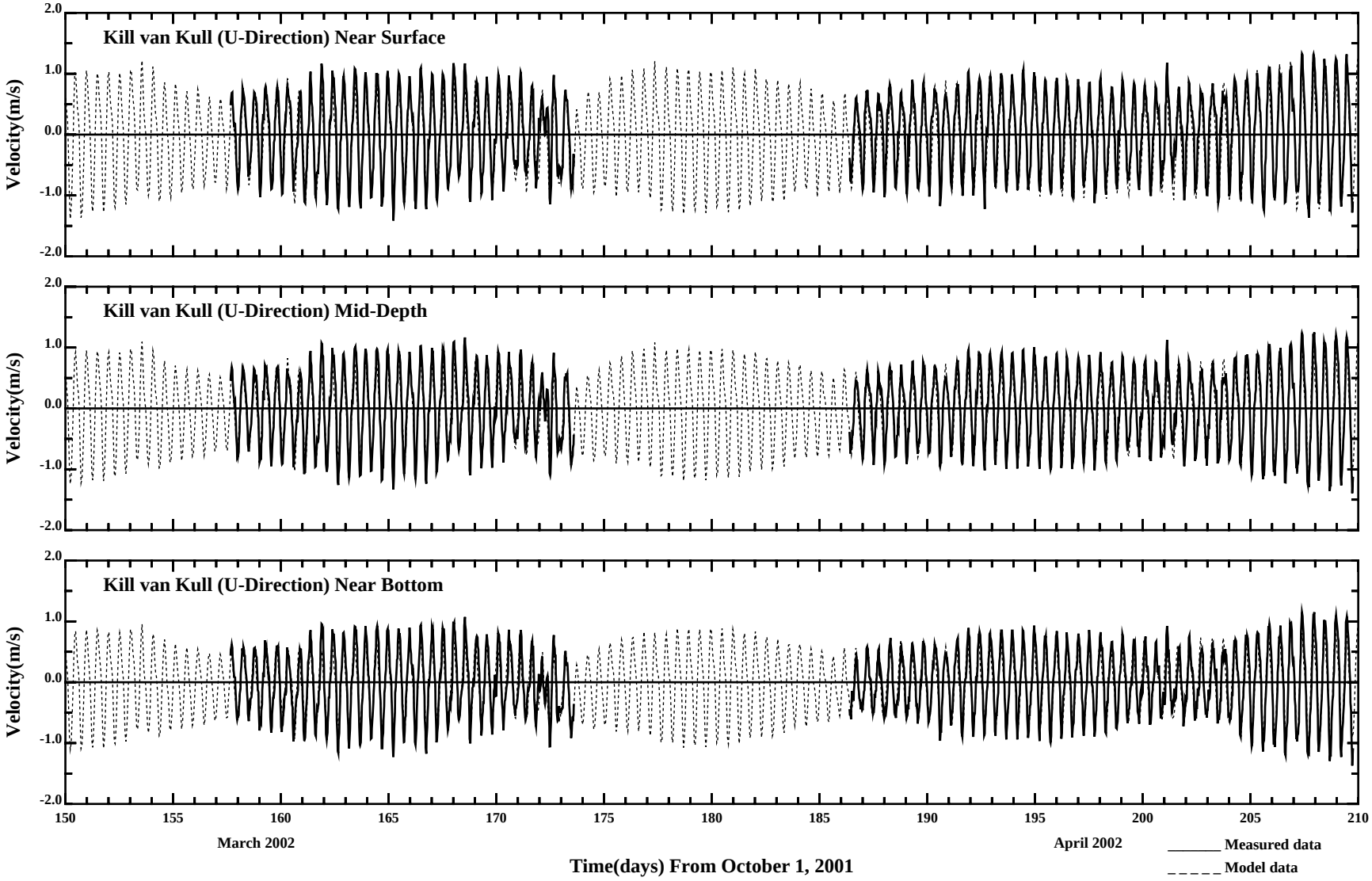

/erie1/hrfo0010/HYDRORUNS/RUTGERS/velocity.gdp
DATE: 8/16/2004 TIME: 14:27: 7

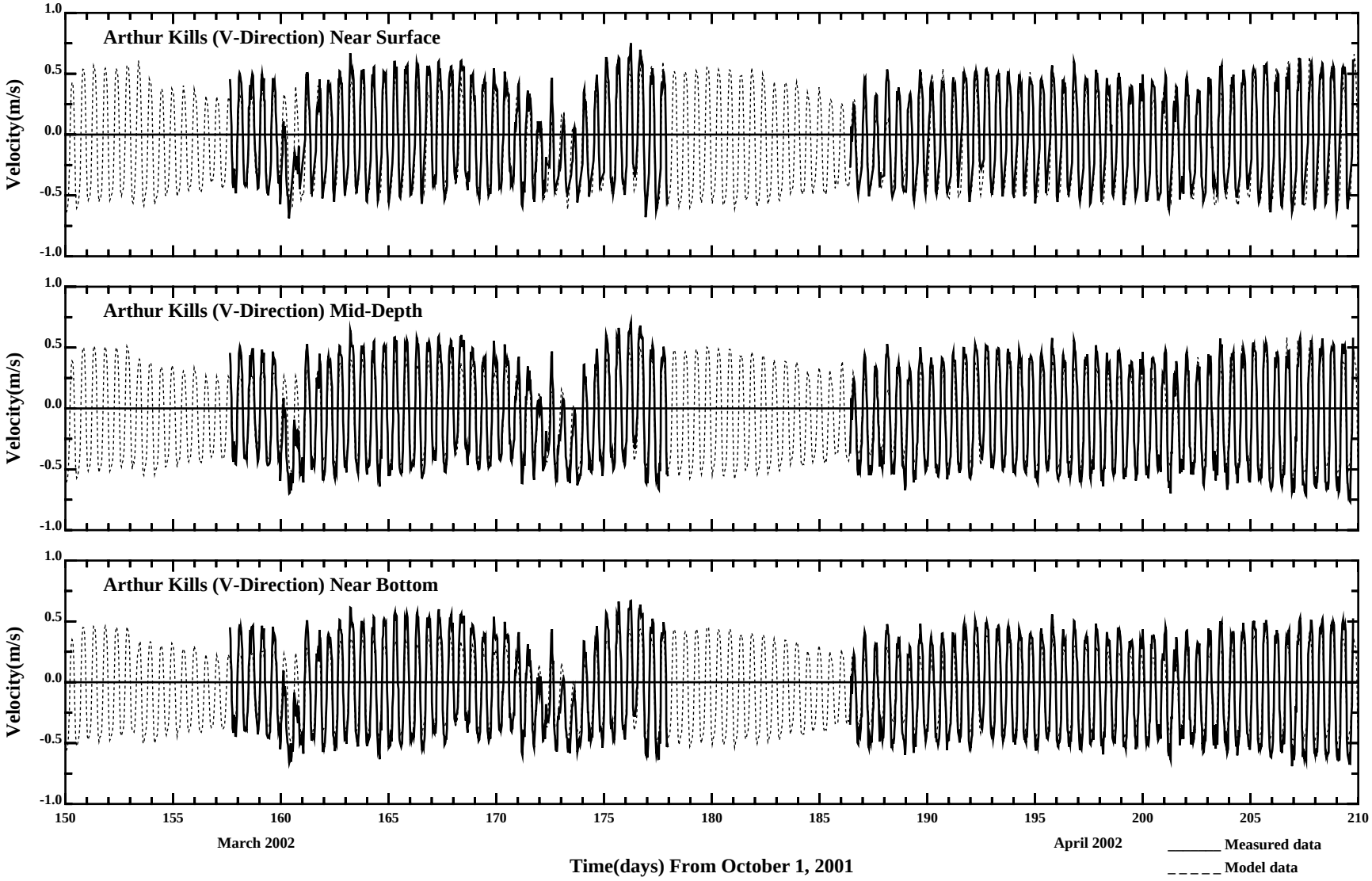

/erie1/hrfo0010/HYDRORUNS/RUTGERS/velocity.gdp
DATE: 8/16/2004 TIME: 14:27: 7

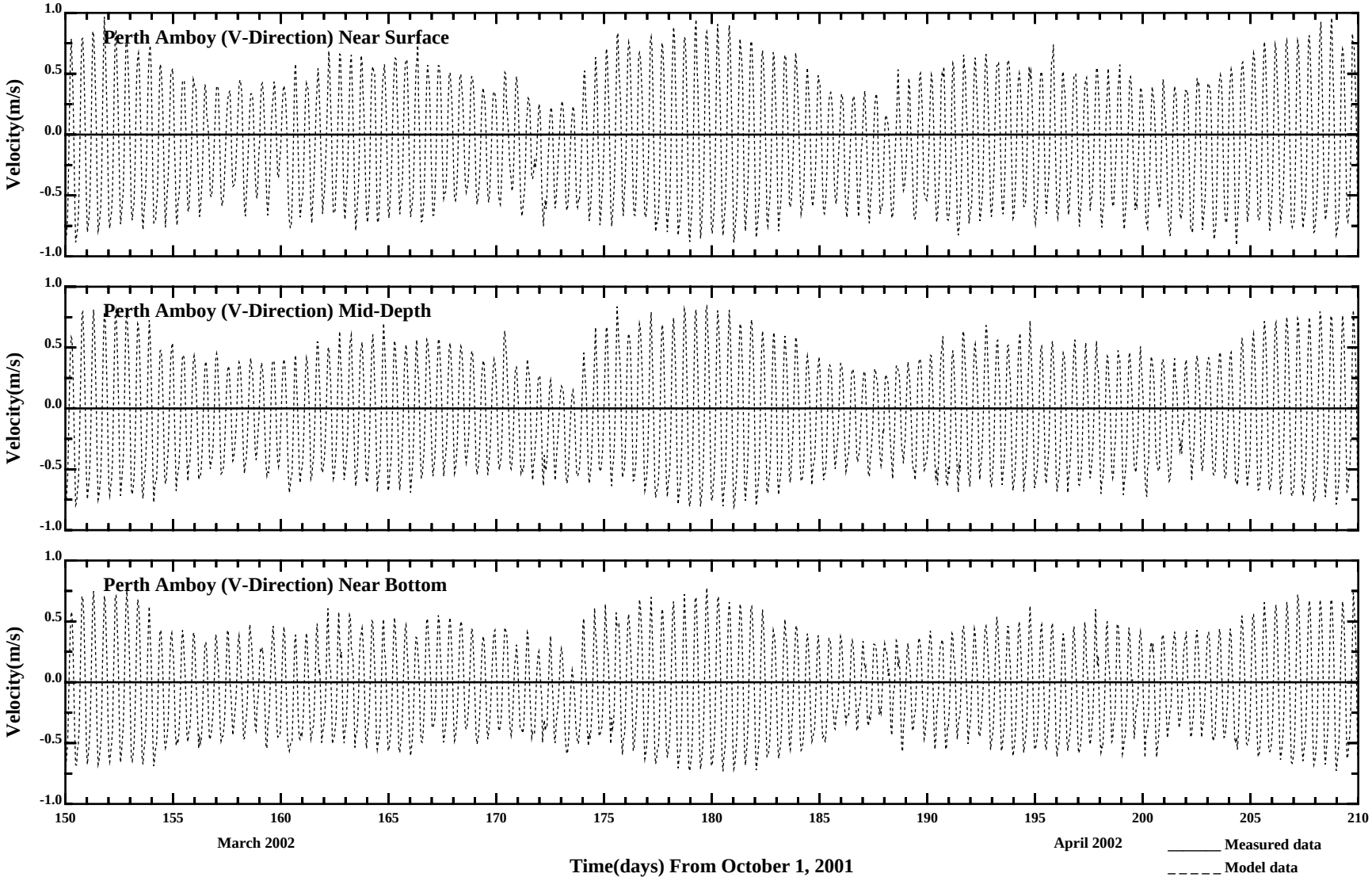

/erie1/hrfo0010/HYDRORUNS/RUTGERS/velocity.gdp
DATE: 8/16/2004 TIME: 14:27: 7

APPENDIX 4

SKILL ASSESSMENT
USING NOAA TIDE GAUGE DATA

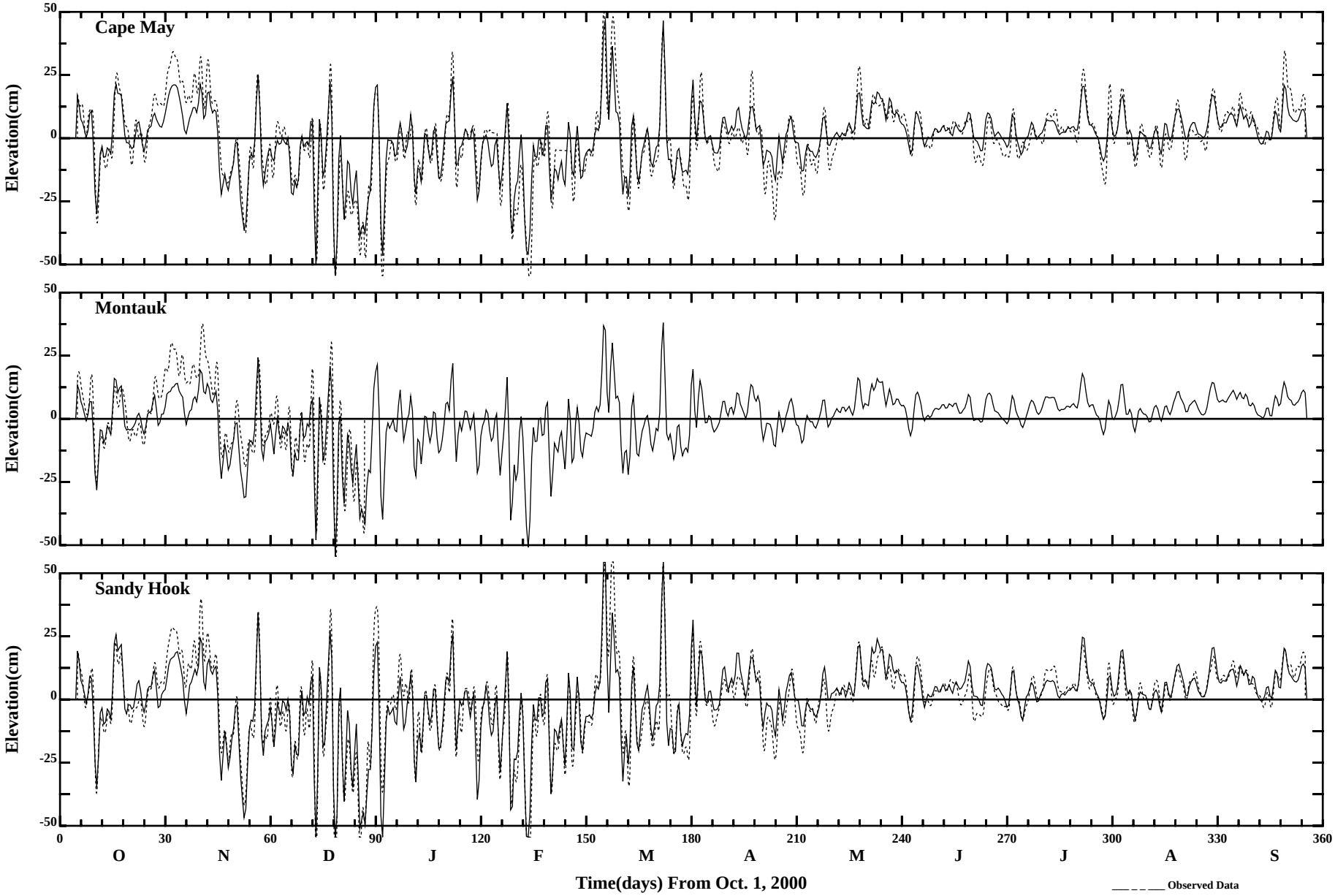

Comparisons of 35 Hour Low Passed Water Surface Elevations With Data

DATE: 11/17/2003 TIME: 10:37:47

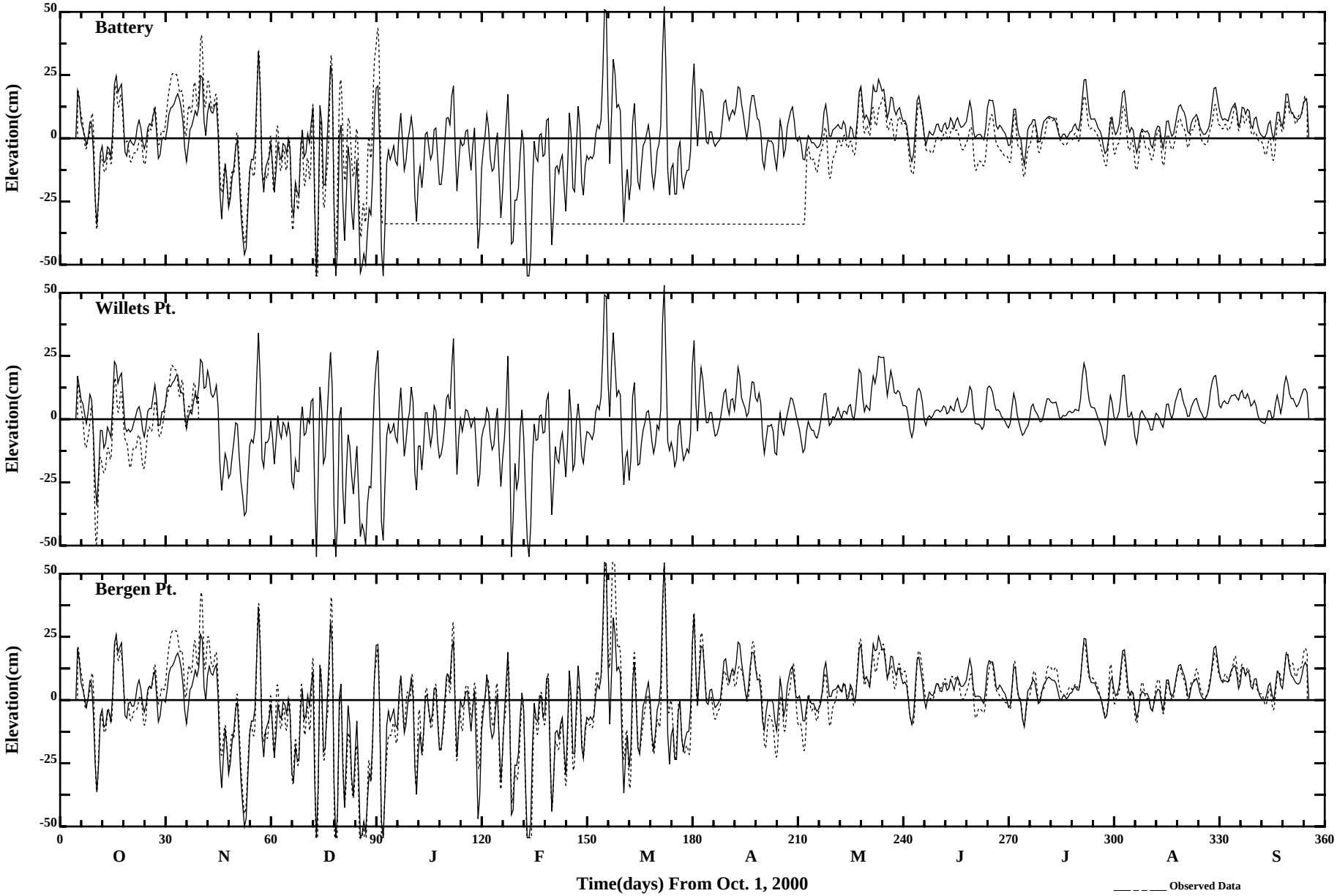

Comparisons of 35 Hour Low Passed Water Surface Elevations With Data

DATE: 11/17/2003 TIME: 10:37:47

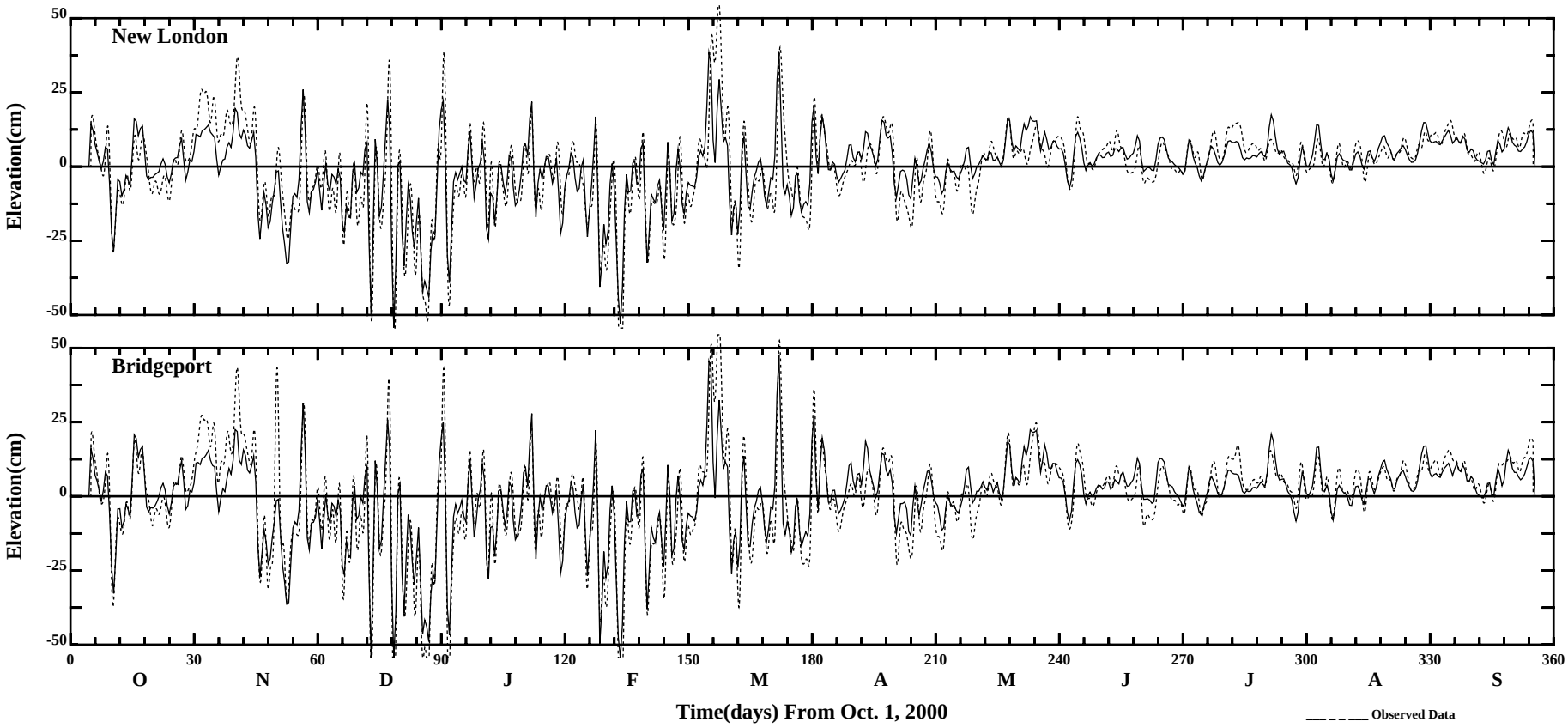

Comparisons of 35 Hour Low Passed Water Surface Elevations With Data

/e1/hrfo0010/HYDRORUNS/CARP0001/PLOTS/ELEV/pele5

DATE: 11/17/2003 TIME: 10:37:47

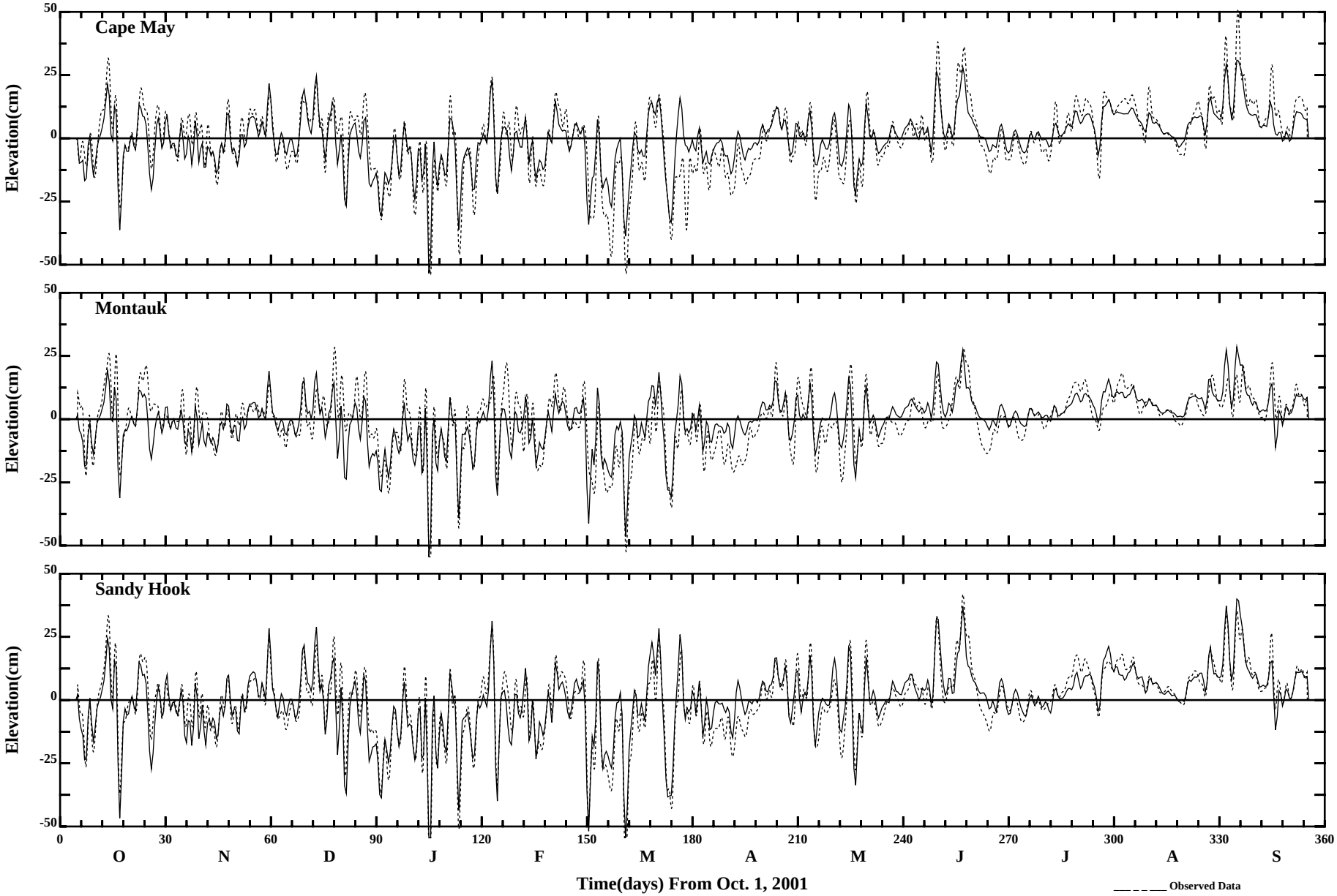

Comparisons of 35 Hour Low Passed Water Surface Elevations With Data

/ont6/hrfo0010/RUNS/ECOMSED-SED/ECOMSED-0102/PLOTS/ELEV/ele_35hlp

DATE: 11/21/2003 TIME: 9: 2:23

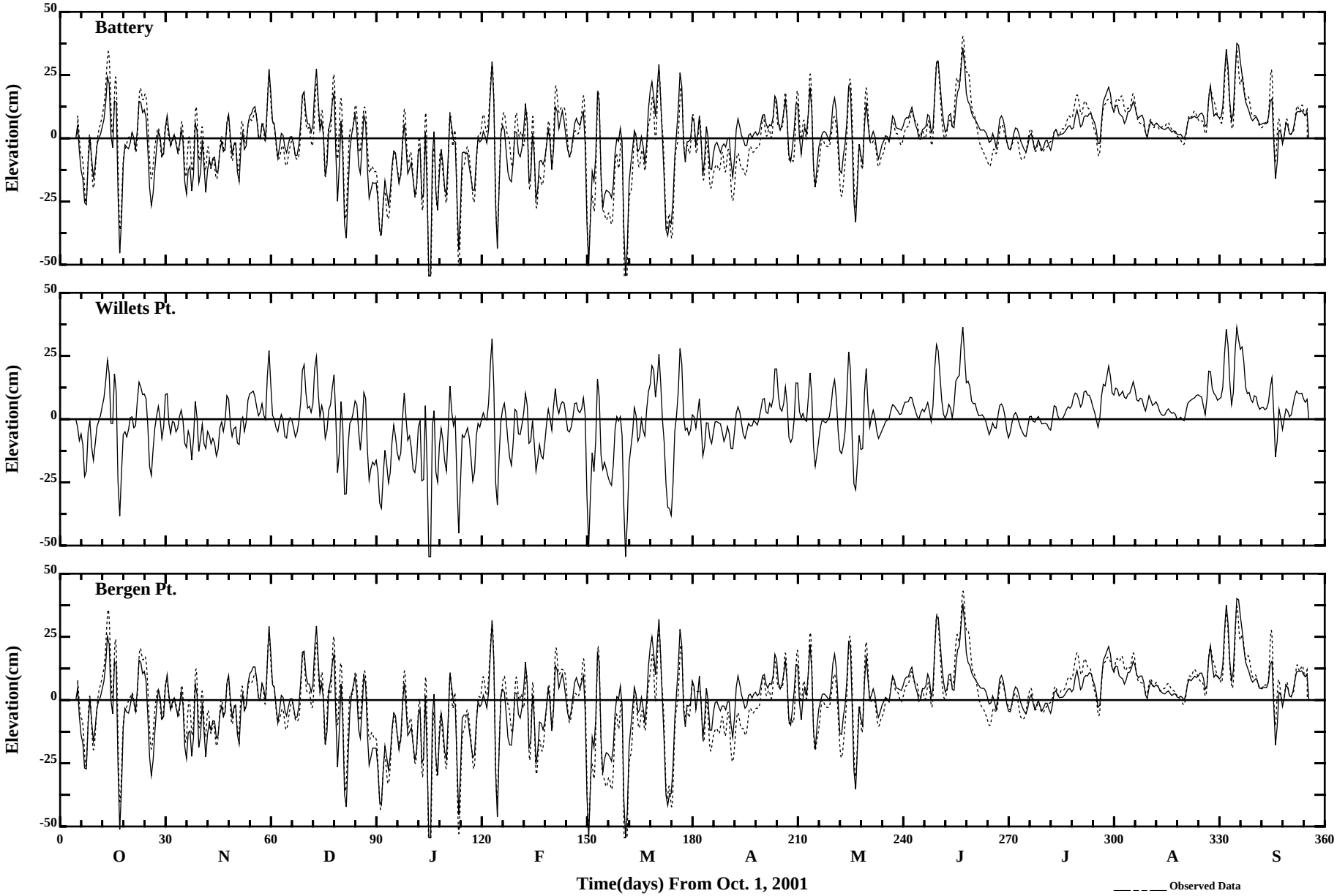

Comparisons of 35 Hour Low Passed Water Surface Elevations With Data

/ont6/hrfo0010/RUNS/ECOMSED-SED/ECOMSED-0102/PLOTS/ELEV/ele_35hlp

DATE: 11/21/2003 TIME: 9: 2:23

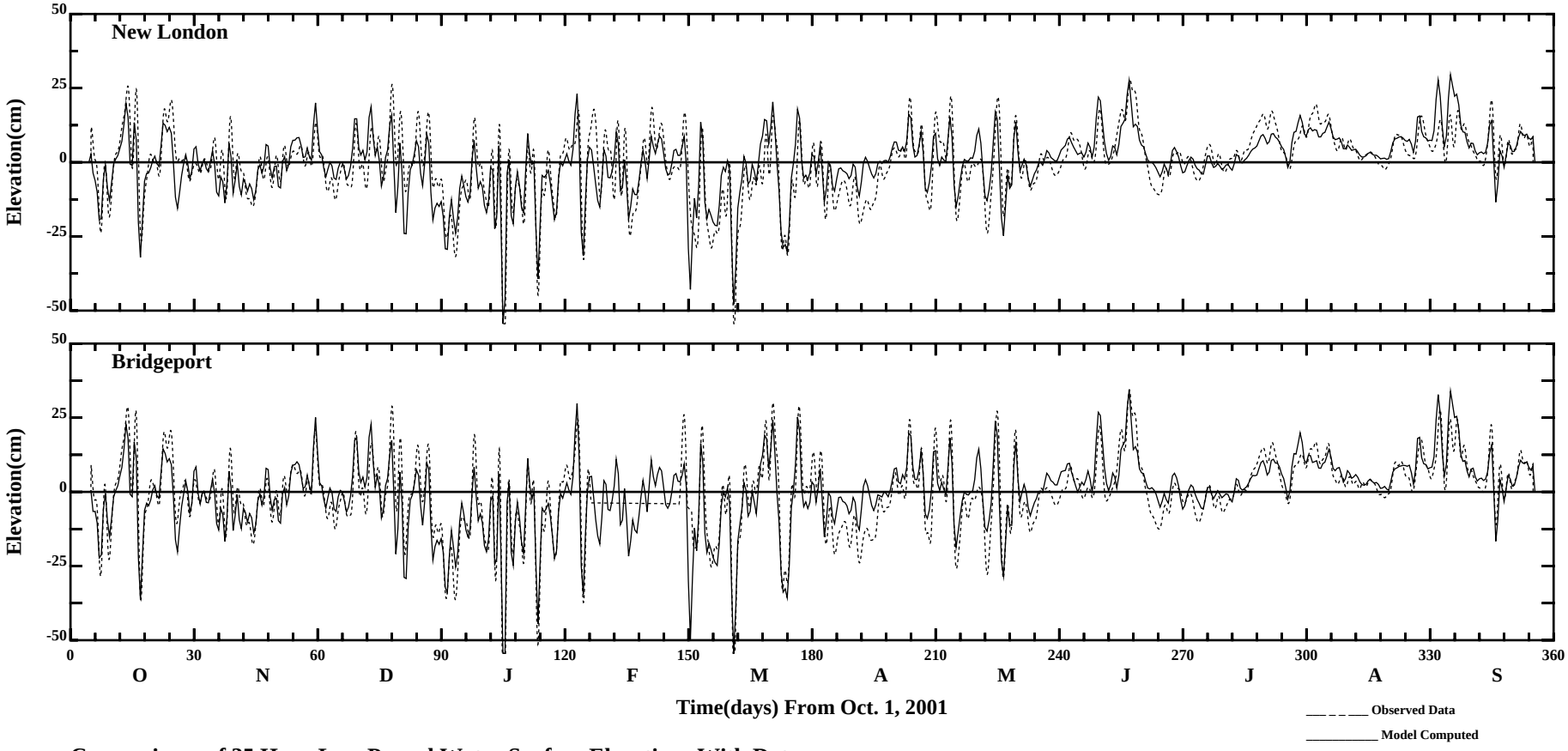

Comparisons of 35 Hour Low Passed Water Surface Elevations With Data

/ont6/hrfo0010/RUNS/ECOMSED-SED/ECOMSED-0102/PLOTS/ELEV/ele_35hlp

DATE: 11/21/2003 TIME: 9: 2:23

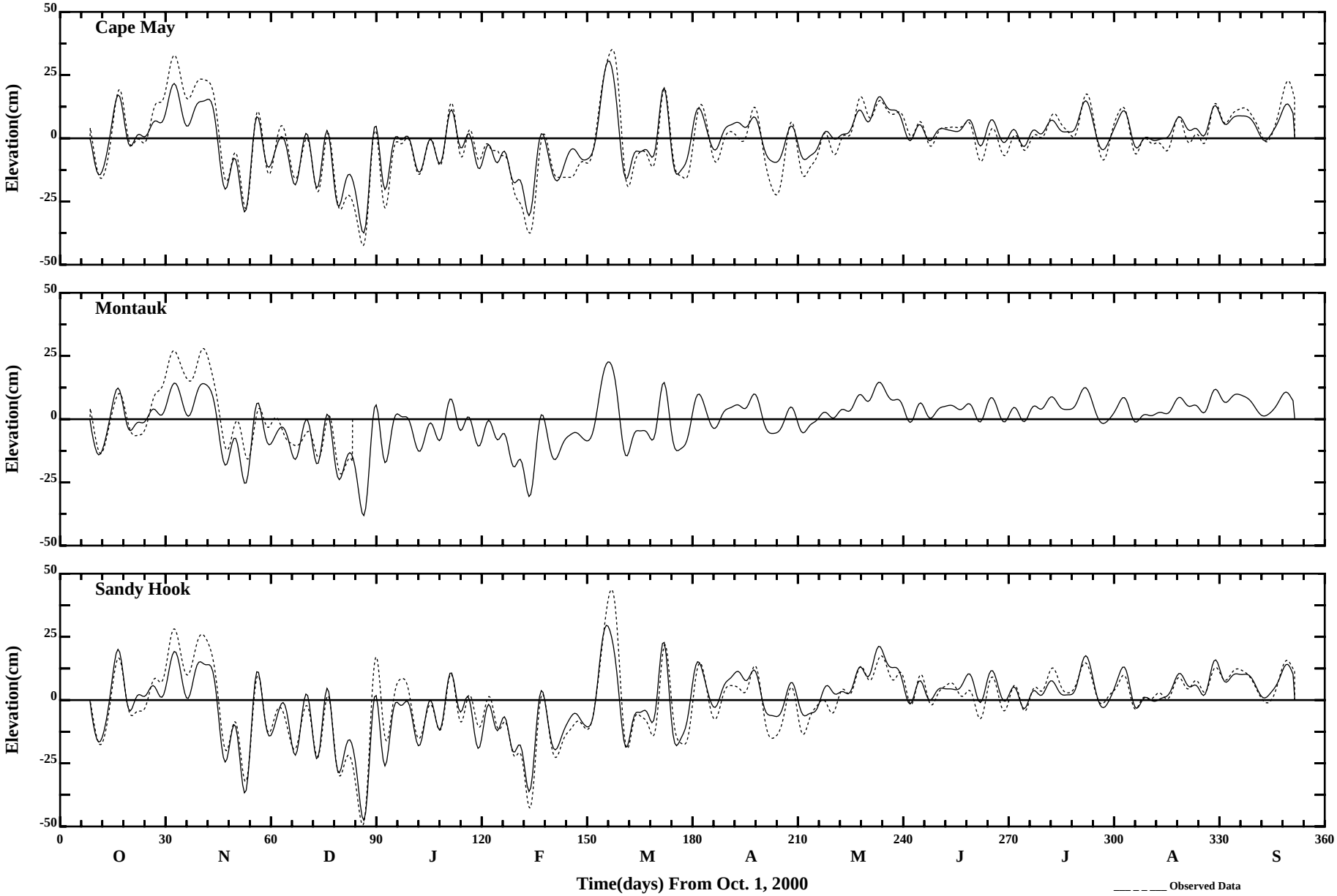

Comparisons of 5 Days Low Passed Water Surface Elevations With Data

/e1/hrfo0010/HYDRORUNS/CARP0001/PLOTS/ELEV/pele4

DATE: 11/17/2003 TIME: 10:38:15

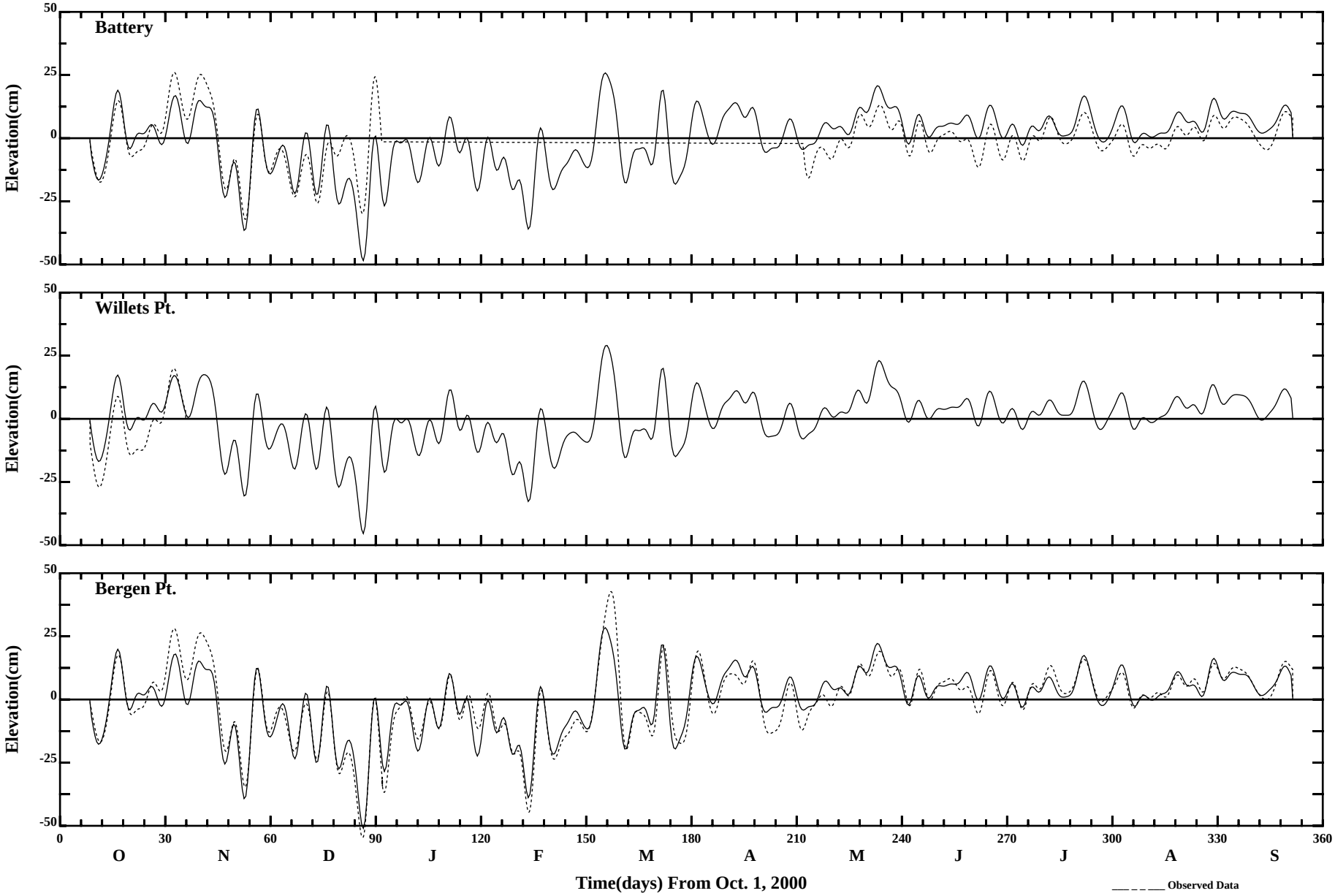

Comparisons of 5 Days Low Passed Water Surface Elevations With Data

/e1/hrfo0010/HYDRORUNS/CARP0001/PLOTS/ELEV/pele4

DATE: 11/17/2003 TIME: 10:38:15

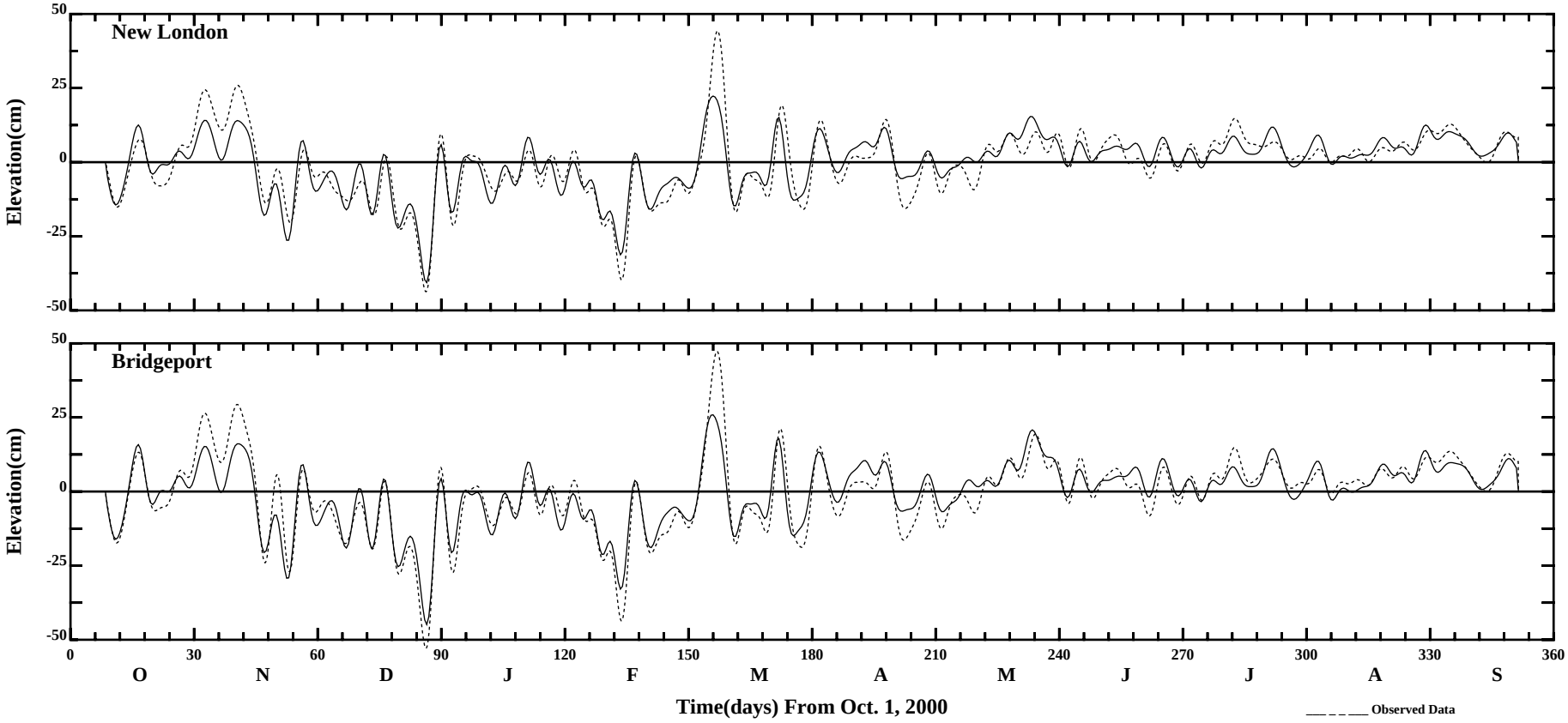

Comparisons of 5 Days Low Passed Water Surface Elevations With Data

/e1/hrfo0010/HYDRORUNS/CARP0001/PLOTS/ELEV/pele4

DATE: 11/17/2003 TIME: 10:38:15

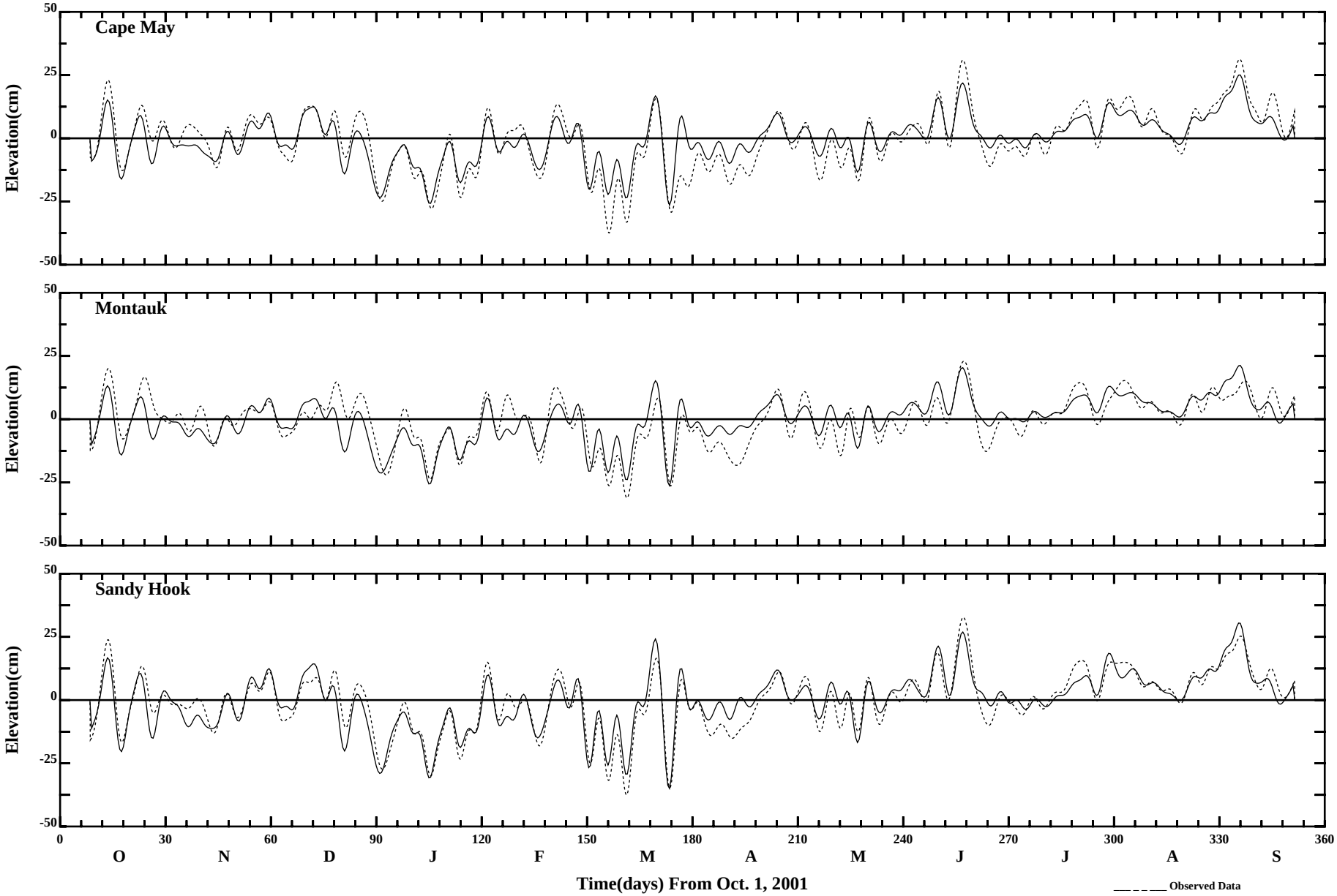

Comparisons of 5 Days Low Passed Water Surface Elevations With Data

DATE: 11/21/2003 TIME: 9: 2:41

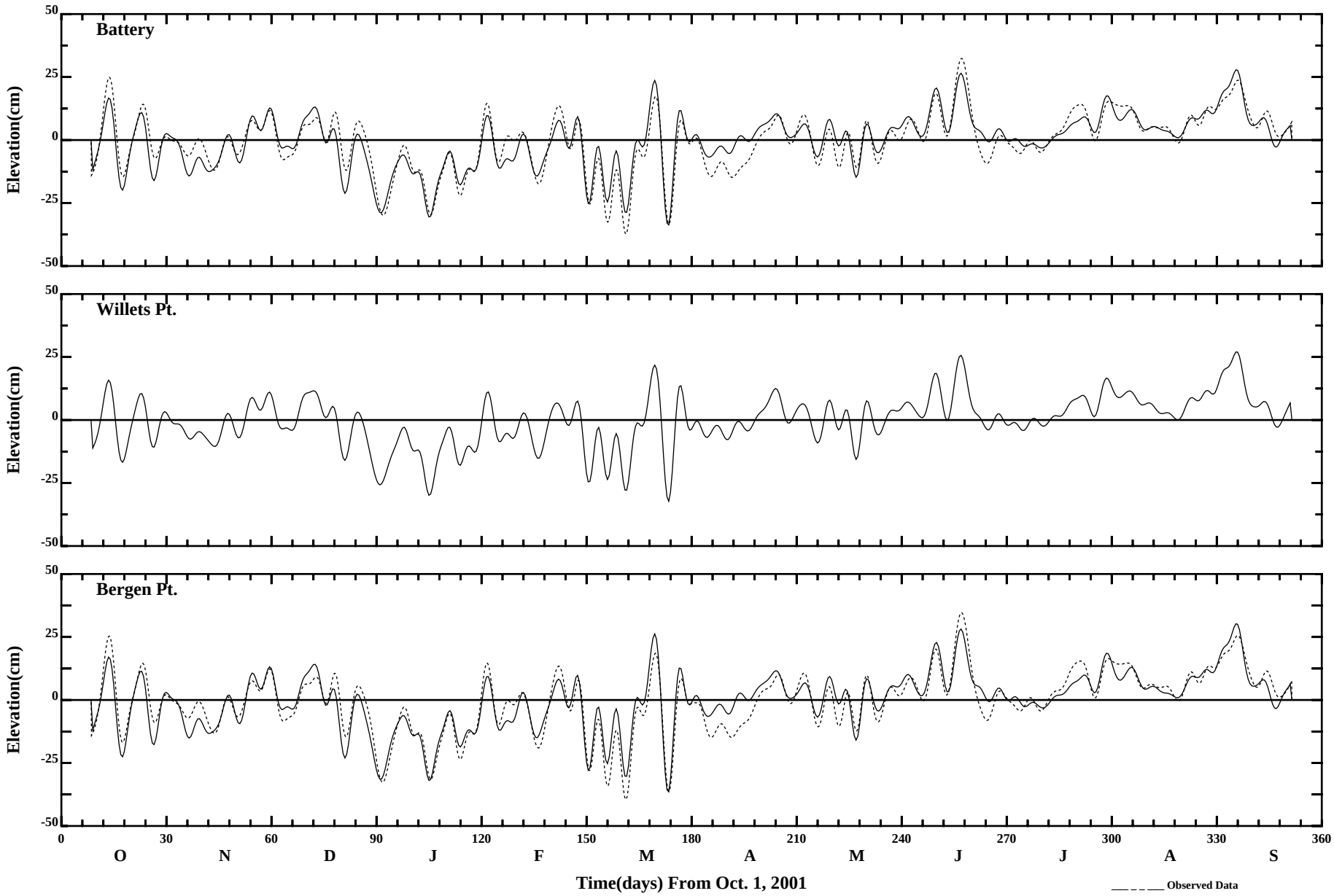

Comparisons of 5 Days Low Passed Water Surface Elevations With Data

/ont6/hrfo0010/RUNS/ECOMSED-SED/ECOMSED-0102/PLOTS/ELEV/ele_5dlp

DATE: 11/21/2003 TIME: 9: 2:41

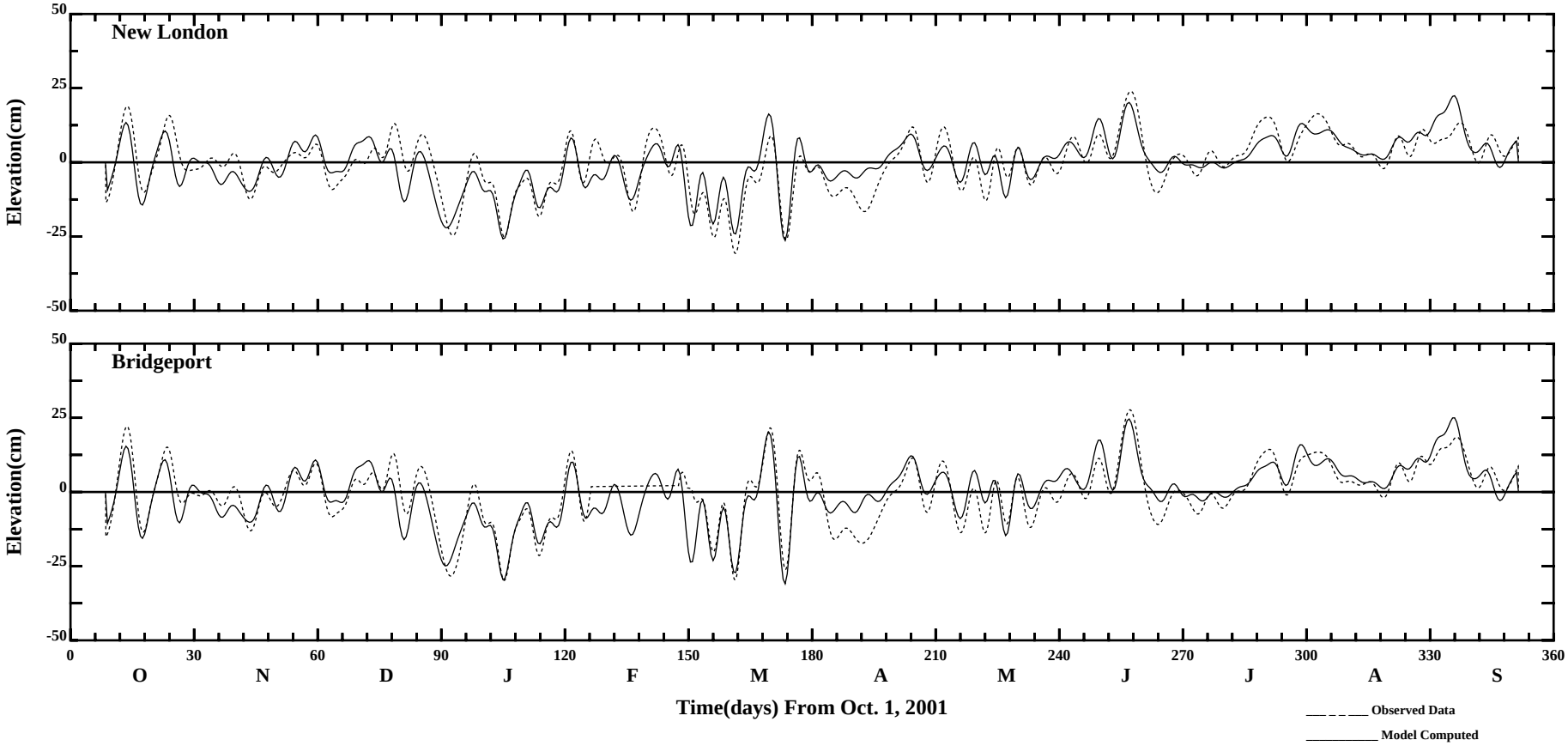

Comparisons of 5 Days Low Passed Water Surface Elevations With Data

/ont6/hrfo0010/RUNS/ECOMSED-SED/ECOMSED-0102/PLOTS/ELEV/ele_5dlp

DATE: 11/21/2003 TIME: 9: 2:41

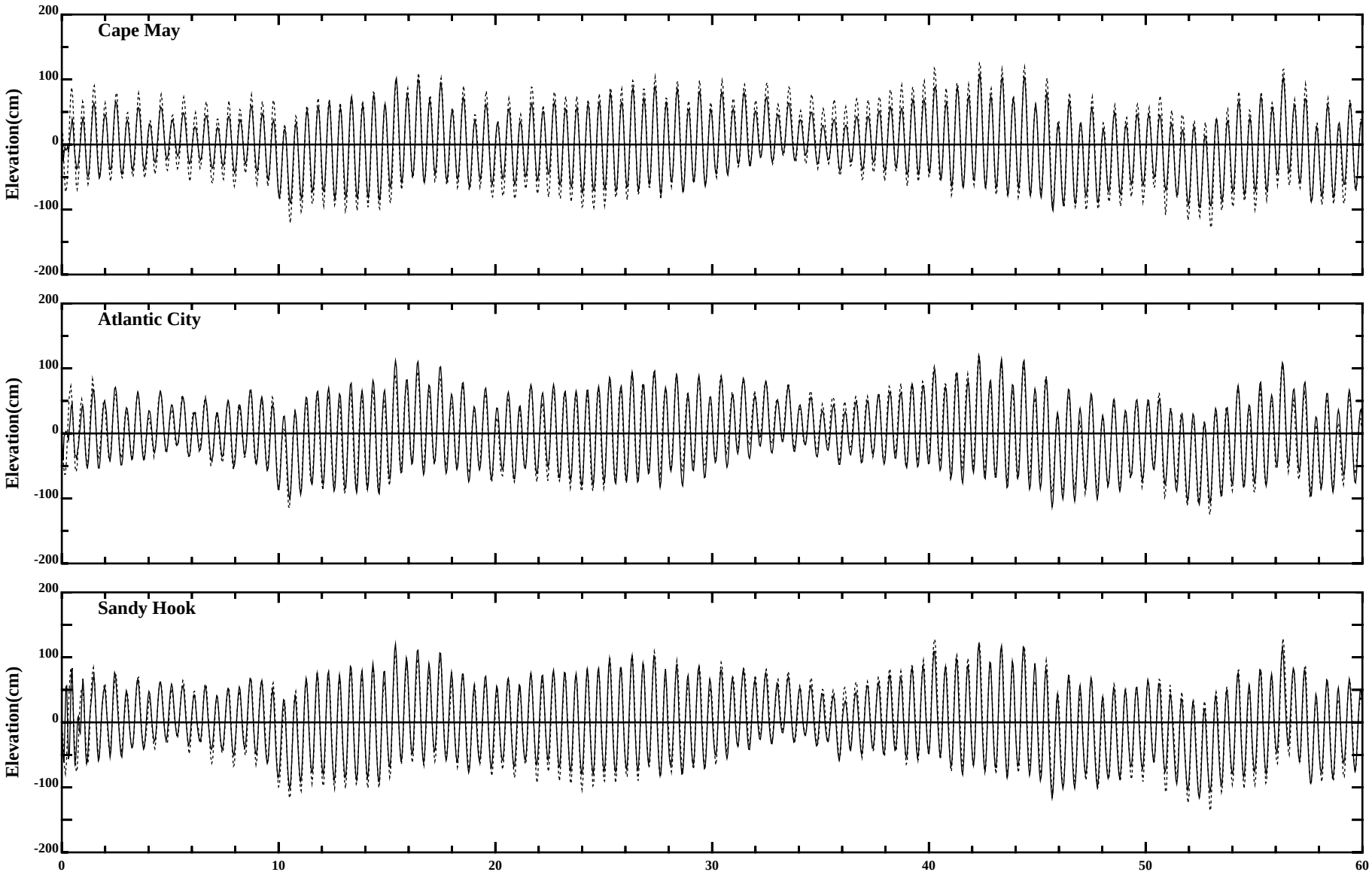

Comparisons of Hourly Water Surface Elevations with Data

/e1/hrfo0010/HYDRORUNS/CARP0001/PLOTS/ELEV/pele3

DATE: 11/17/2003 TIME: 10:36:56

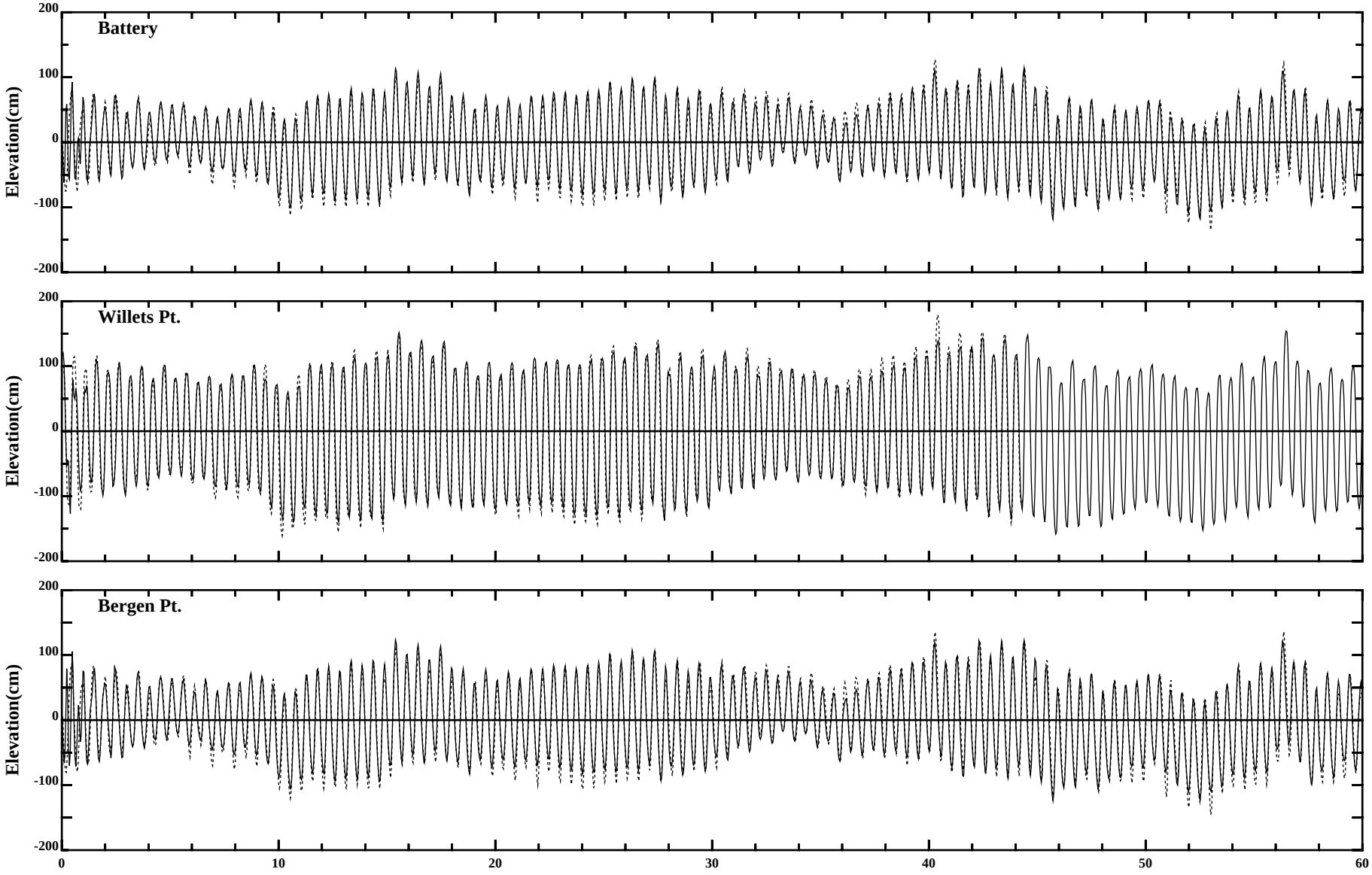

Comparisons of Hourly Water Surface Elevations with Data

/e1/hrfo0010/HYDRORUNS/CARP0001/PLOTS/ELEV/pele3

DATE: 11/17/2003 TIME: 10:36:56

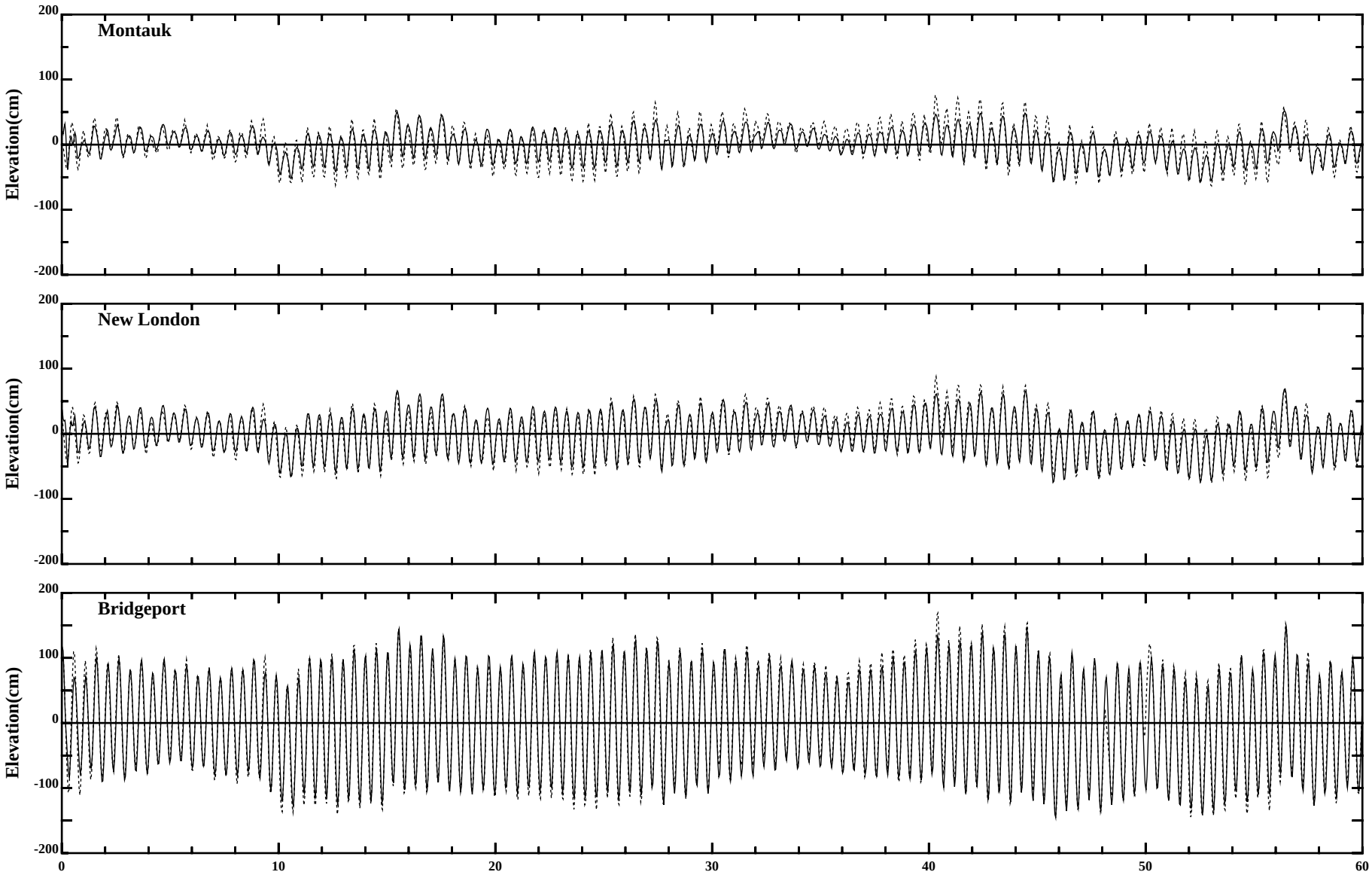

Comparisons of Hourly Water Surface Elevations with Data

/e1/hrfo0010/HYDRORUNS/CARP0001/PLOTS/ELEV/pele3

DATE: 11/17/2003 TIME: 10:36:56

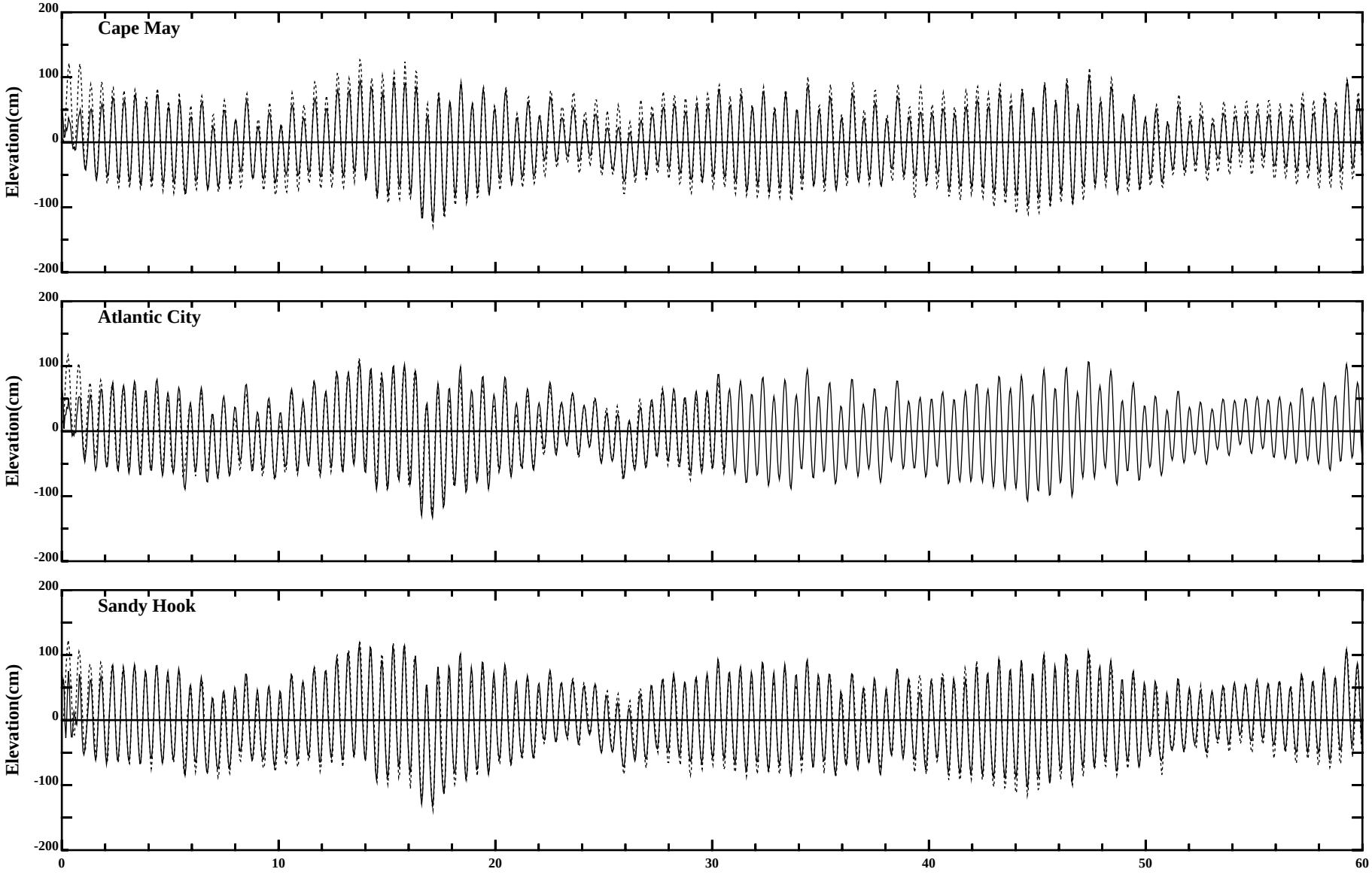

Comparisons of Hourly Water Surface Elevations with Data

DATE: 11/21/2003 TIME: 9: 8:46

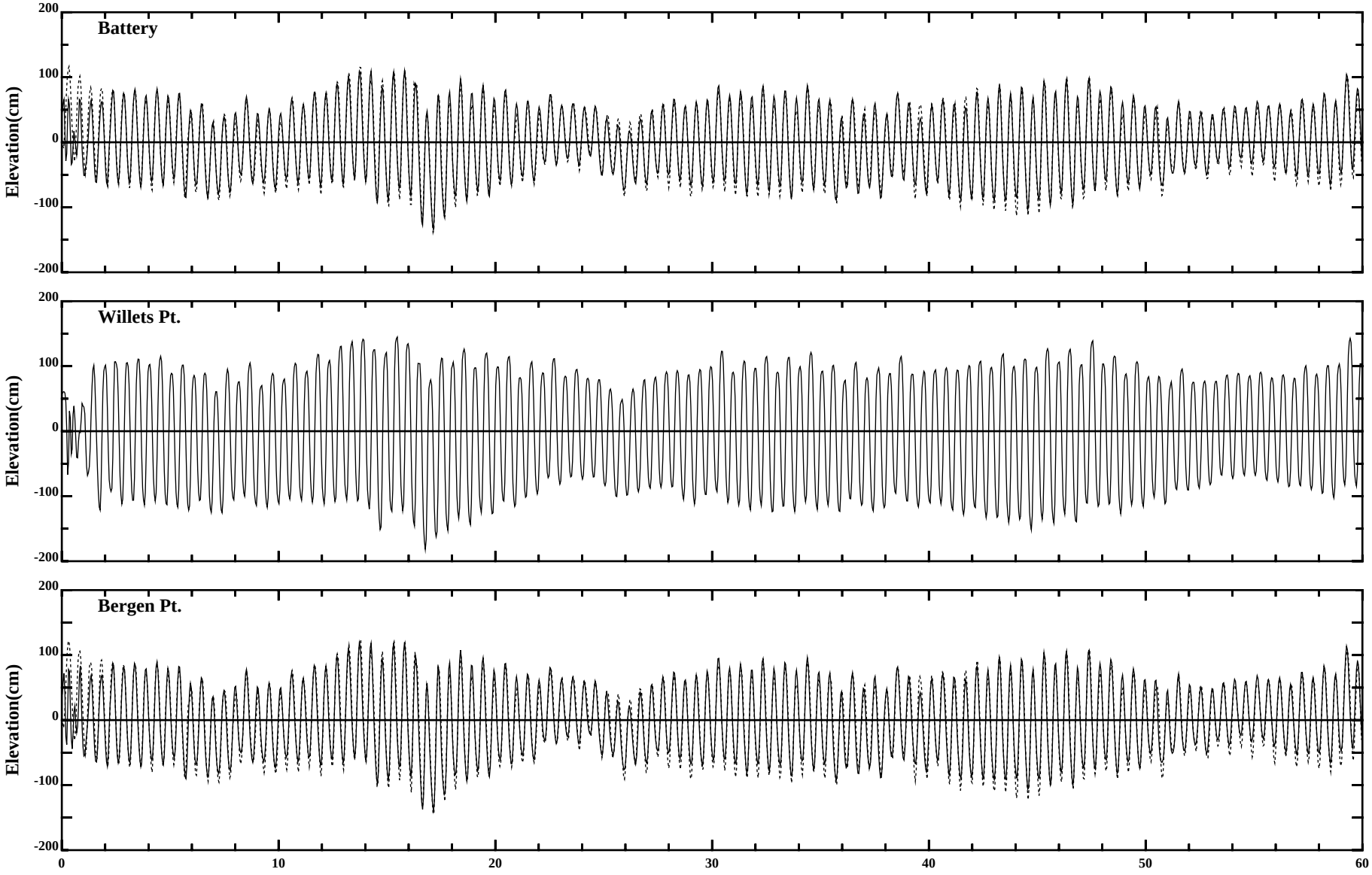

Comparisons of Hourly Water Surface Elevations with Data

/ont6/hrfo0010/RUNS/ECOMSED-SED/ECOMSED-0102/PLOTS/ELEV/ele_hourly

DATE: 11/21/2003 TIME: 9: 8:46

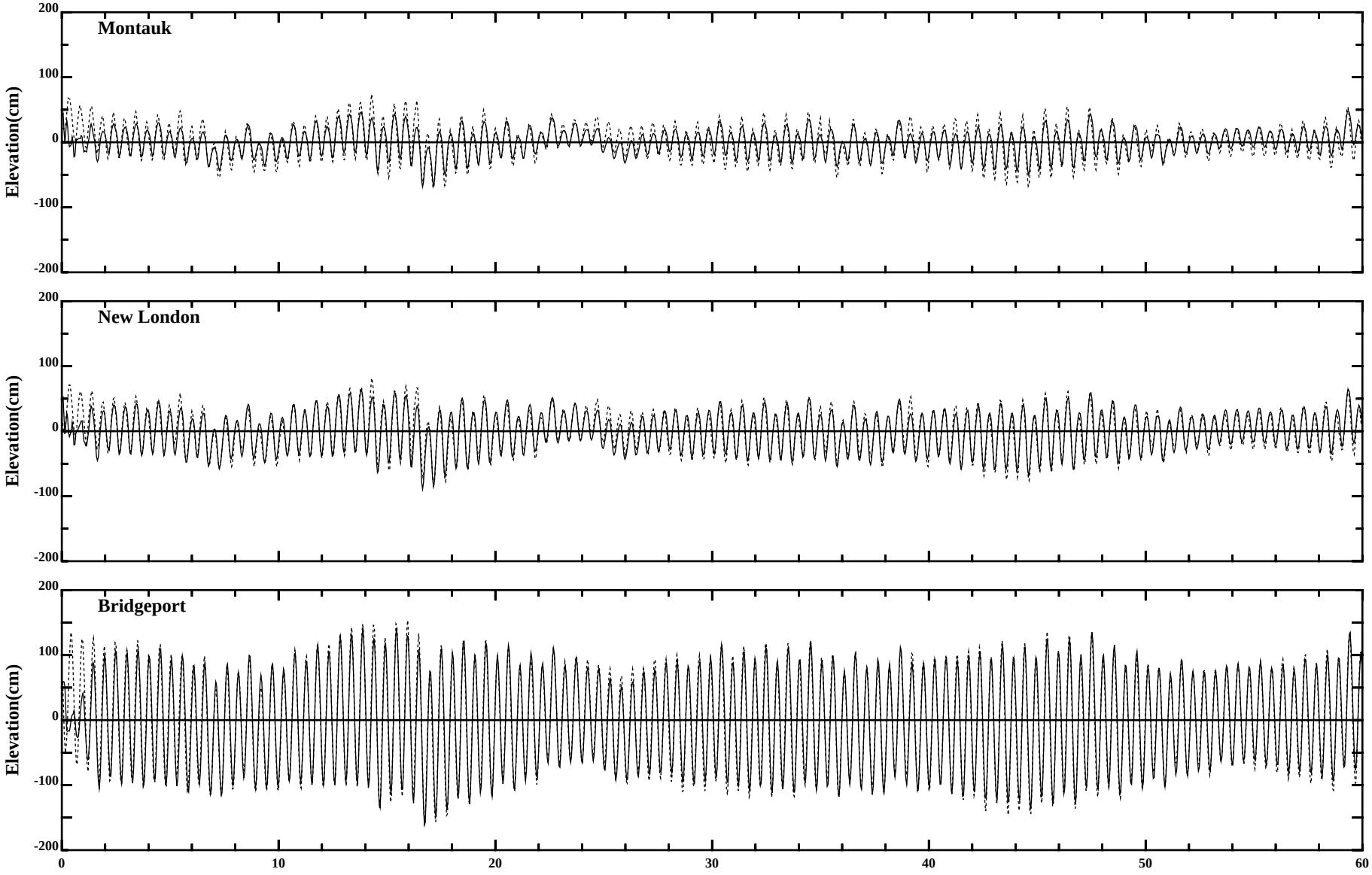

Comparisons of Hourly Water Surface Elevations with Data

/ont6/hrfo0010/RUNS/ECOMSED-SED/ECOMSED-0102/PLOTS/ELEV/ele_hourly

DATE: 11/21/2003 TIME: 9: 8:46

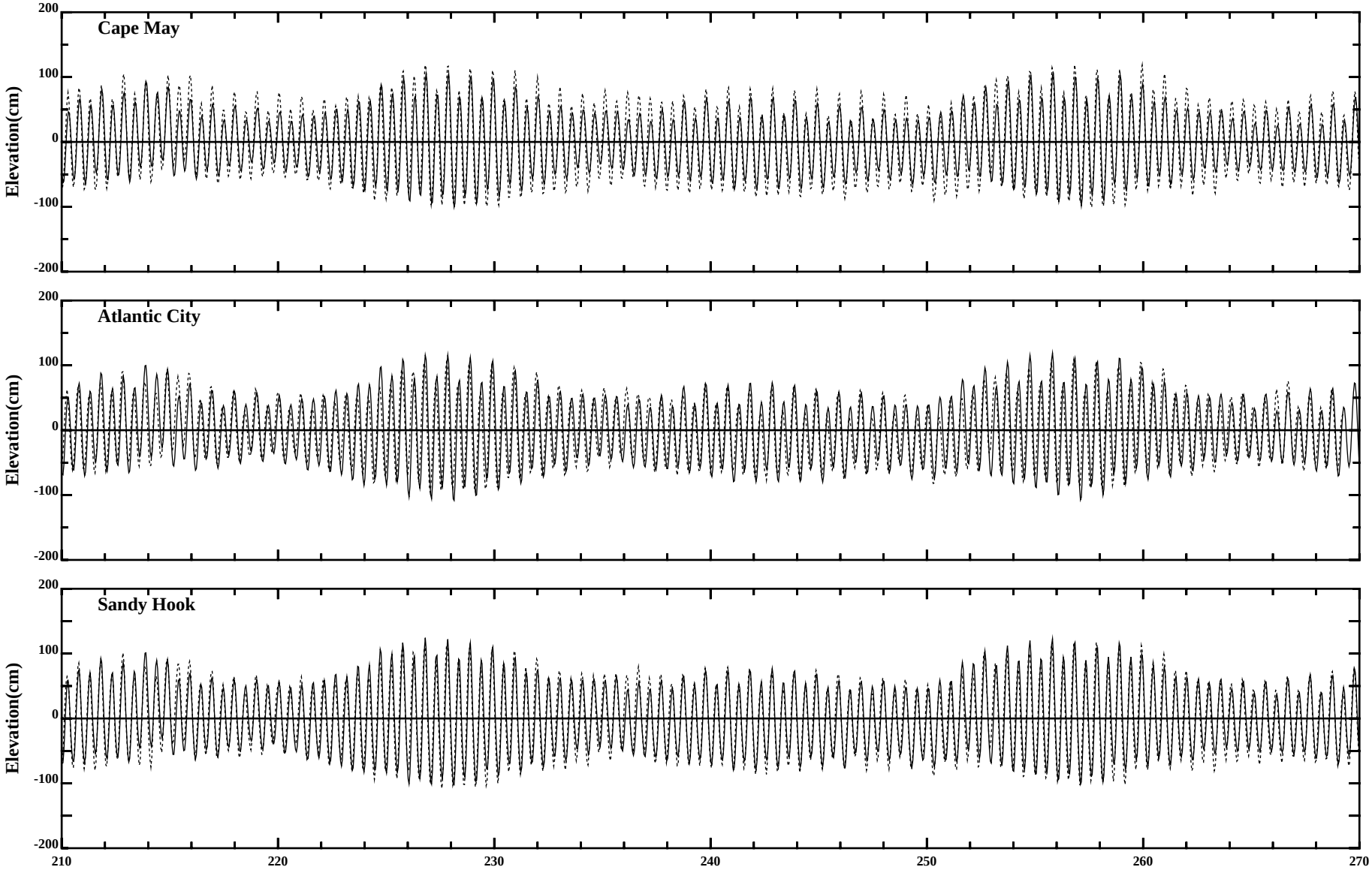

Comparisons of Hourly Water Surface Elevations with Data

/erie1/hrfo0010/HYDRORUNS/CARP9899/PLOTS/ELEV/pele3

DATE: Tue Nov 19 TIME: 12:07:07

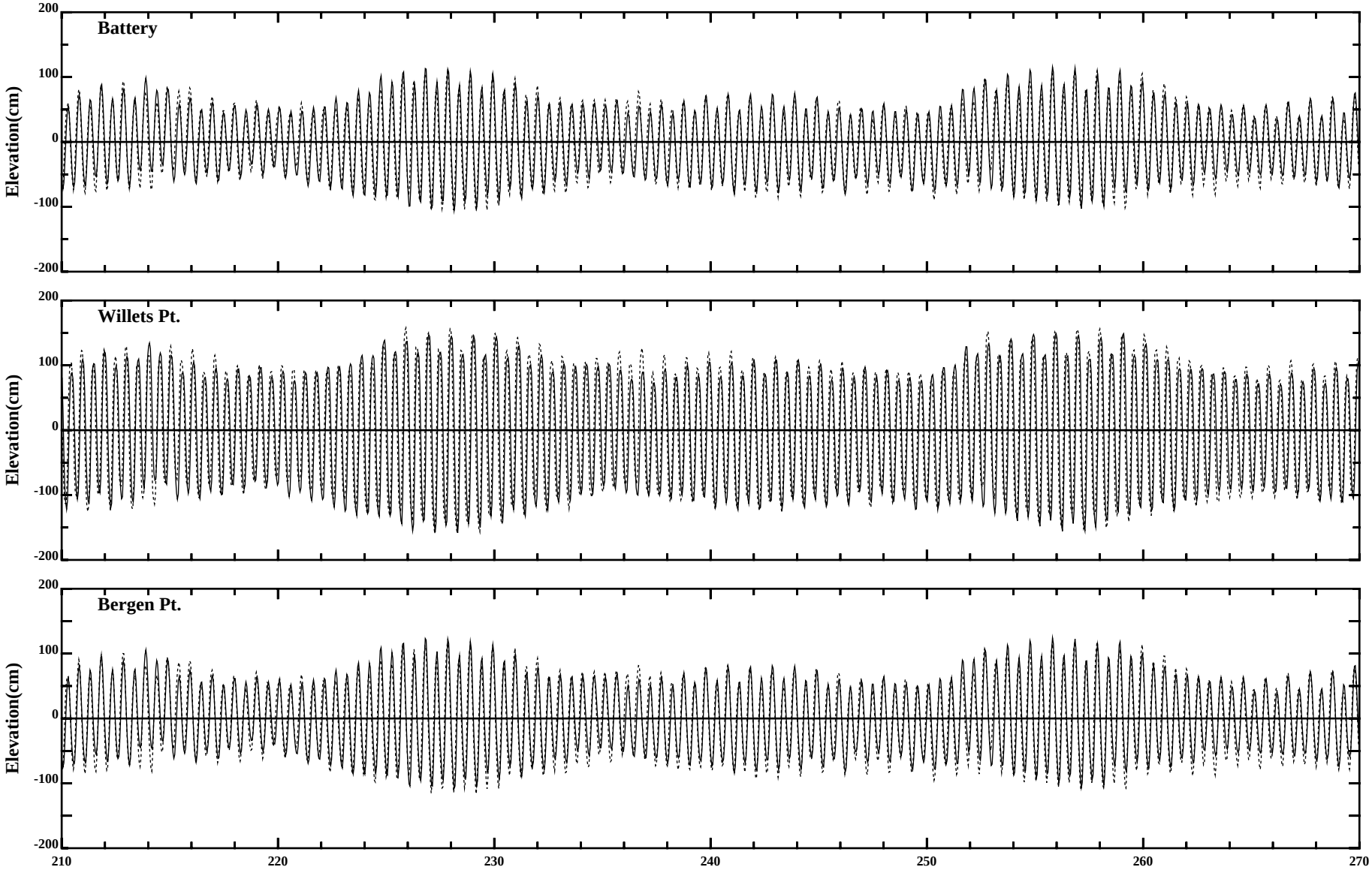

Comparisons of Hourly Water Surface Elevations with Data

/erie1/hrfo0010/HYDRORUNS/CARP9899/PLOTS/ELEV/pele3

DATE: Tue Nov 19 TIME: 12:07:07

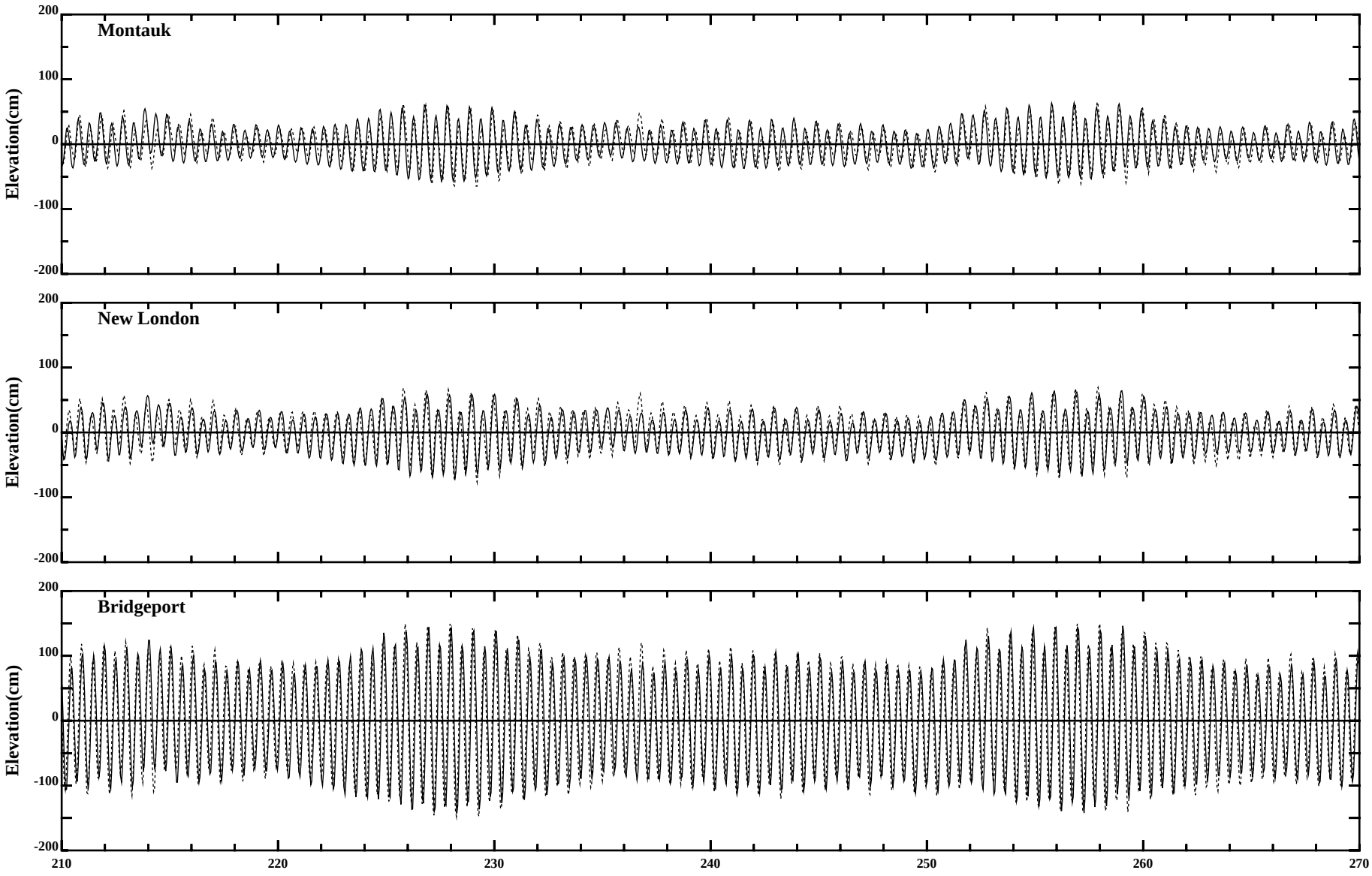

Comparisons of Hourly Water Surface Elevations with Data

DATE: Tue Nov 19 TIME: 12:07:07

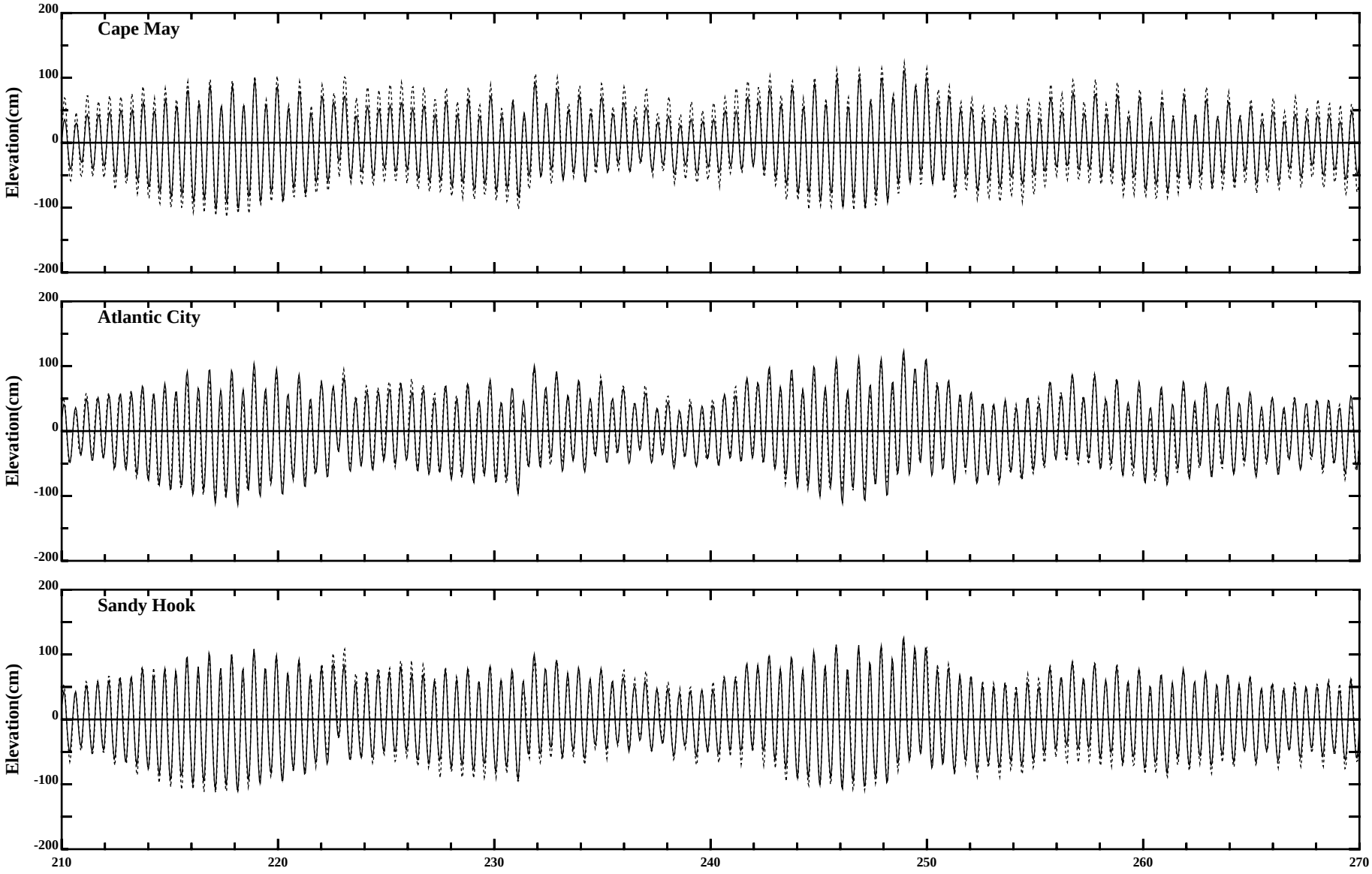

Comparisons of Hourly Water Surface Elevations with Data

/erie1/hrfo0010/HYDRORUNS/CARP9900/PLOTS/ELEV/pele3

DATE: 10/15/2003 TIME: 15: 9: 3

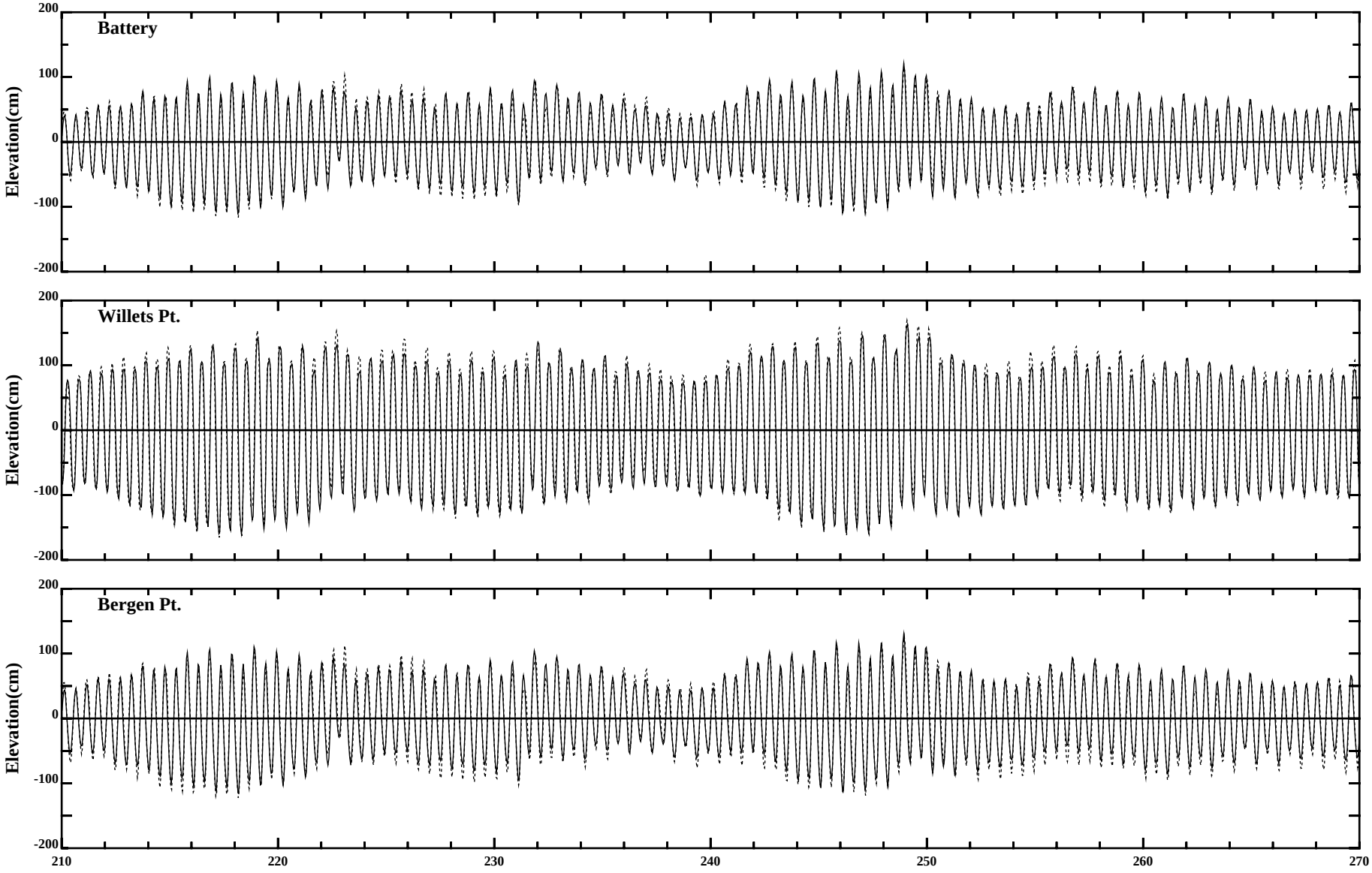

Comparisons of Hourly Water Surface Elevations with Data

/erie1/hrfo0010/HYDRORUNS/CARP9900/PLOTS/ELEV/pele3

DATE: 10/15/2003 TIME: 15: 9: 3

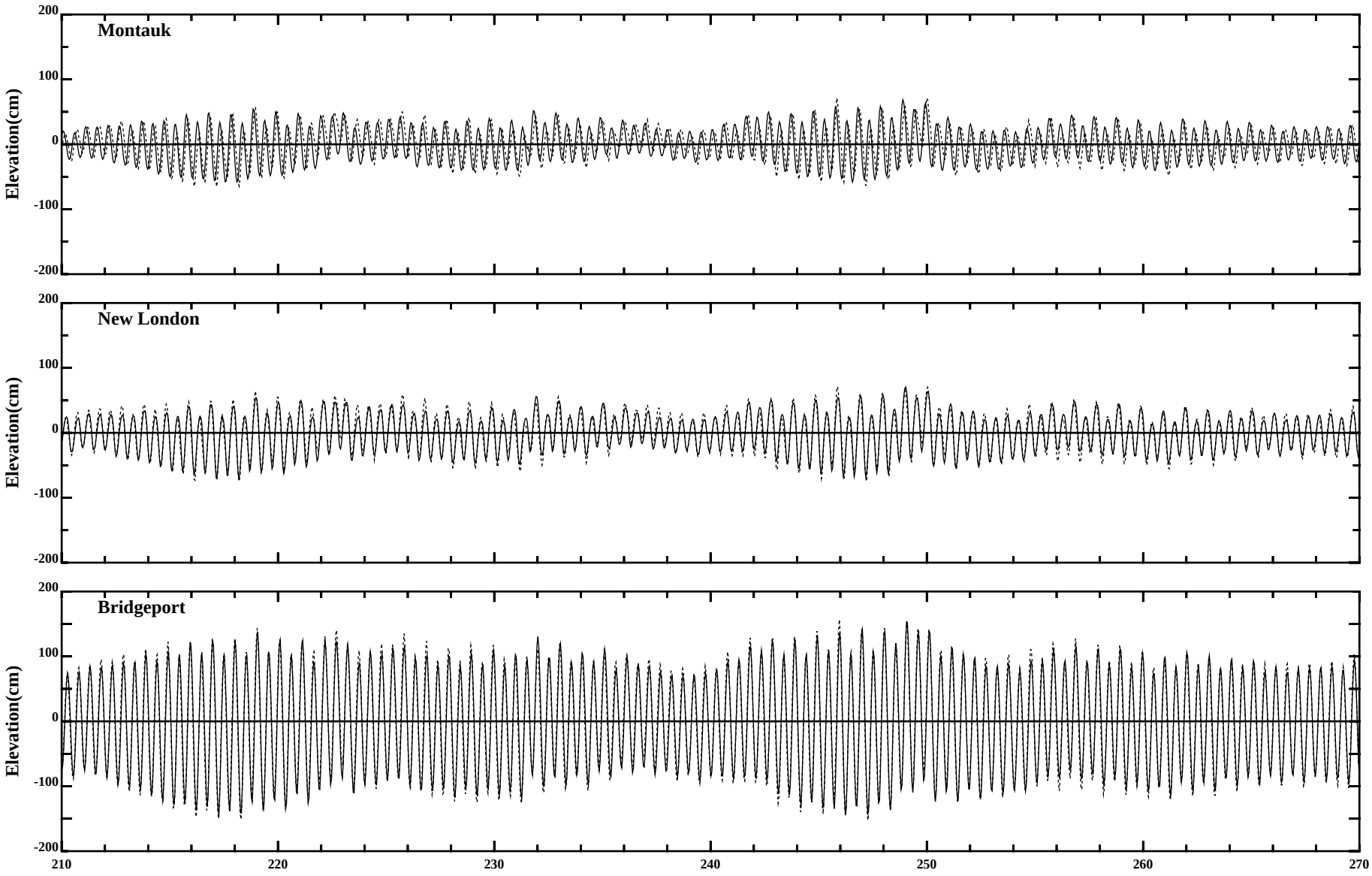

Comparisons of Hourly Water Surface Elevations with Data

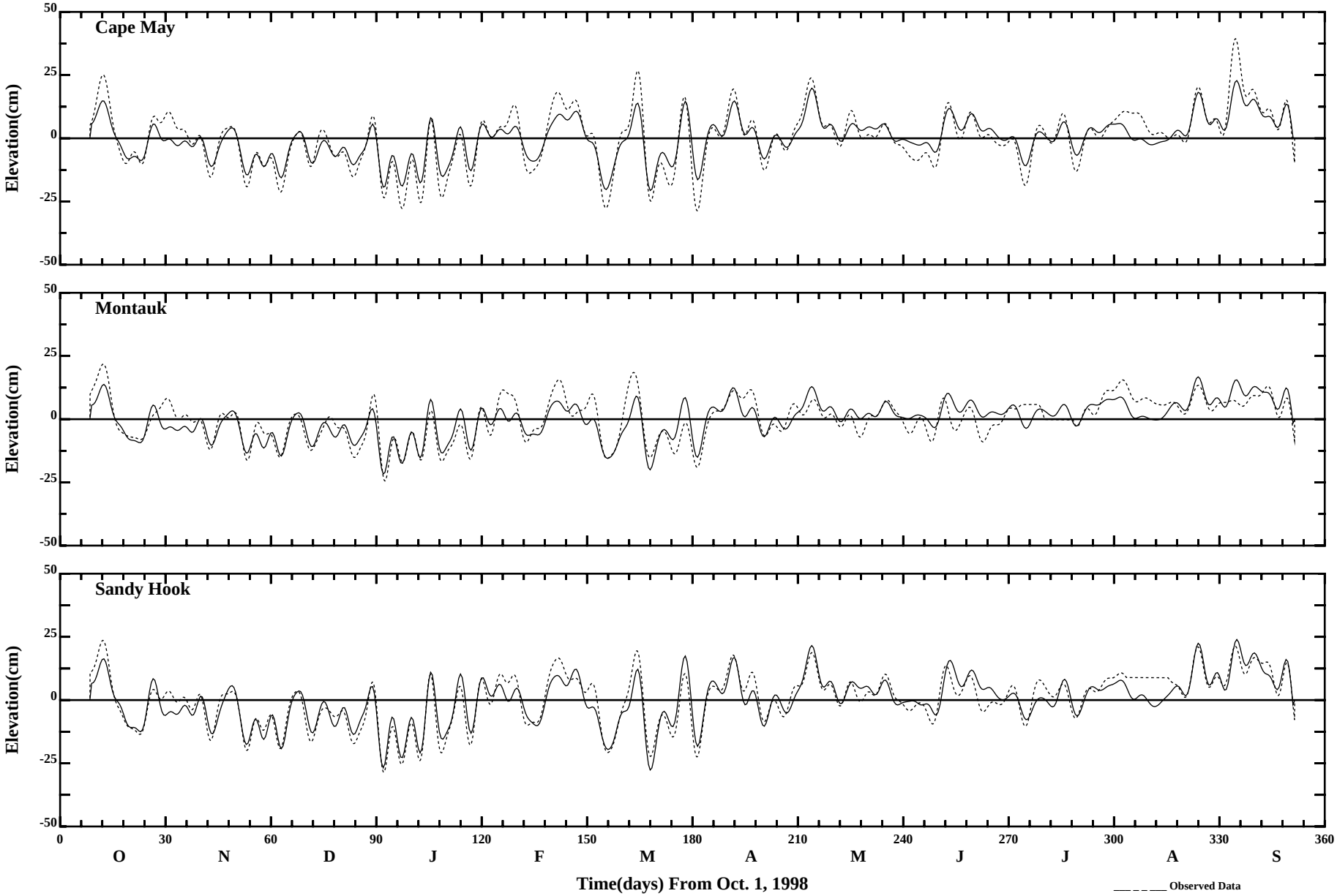

Comparisons of 5 Days Low Passed Water Surface Elevations With Data

/erie1/hrfo0010/HYDRORUNS/CARP9899/PLOTS/ELEV/pele4

DATE: Tue Nov 19 TIME: 12:07:26

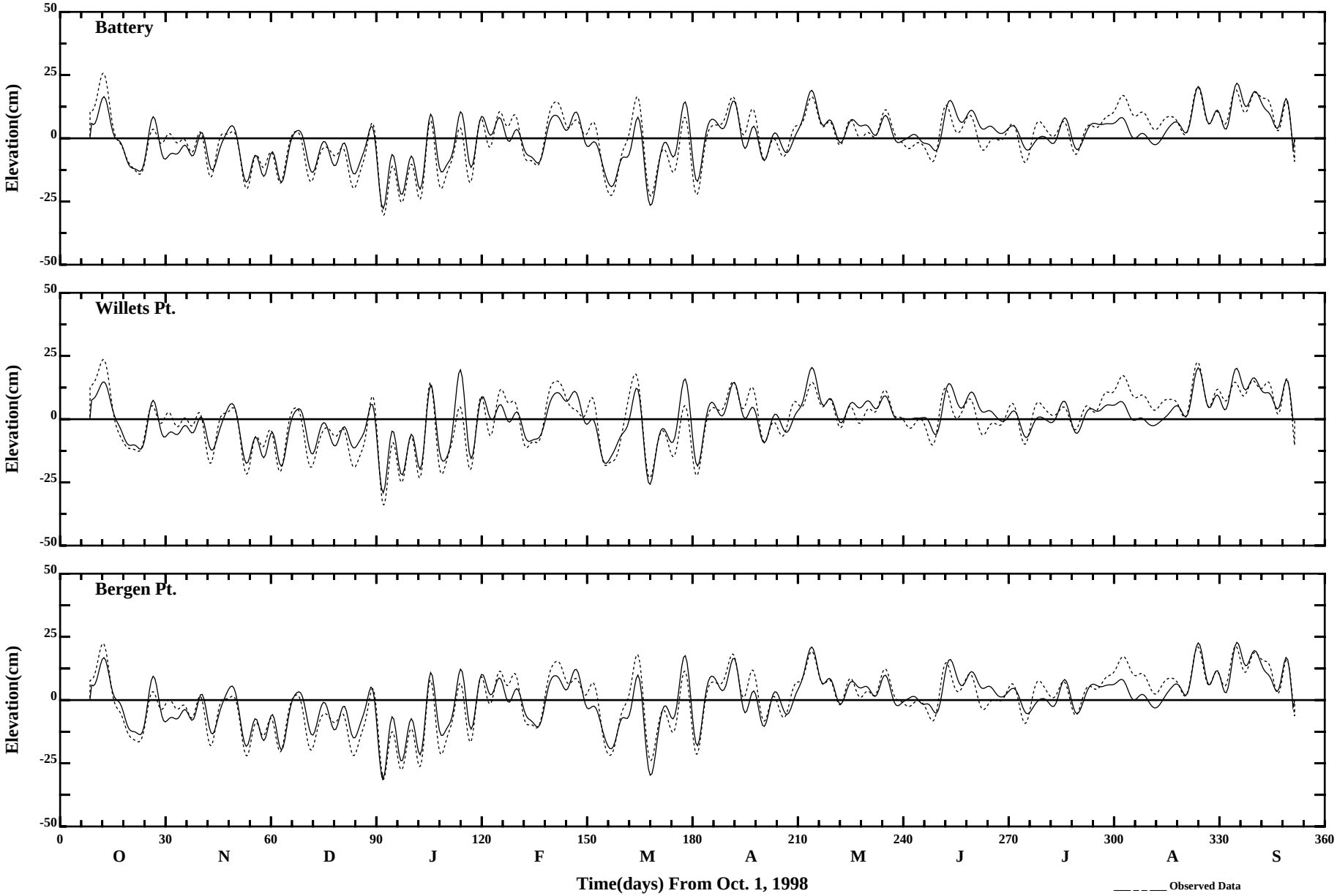

Comparisons of 5 Days Low Passed Water Surface Elevations With Data

DATE: Tue Nov 19 TIME: 12:07:26

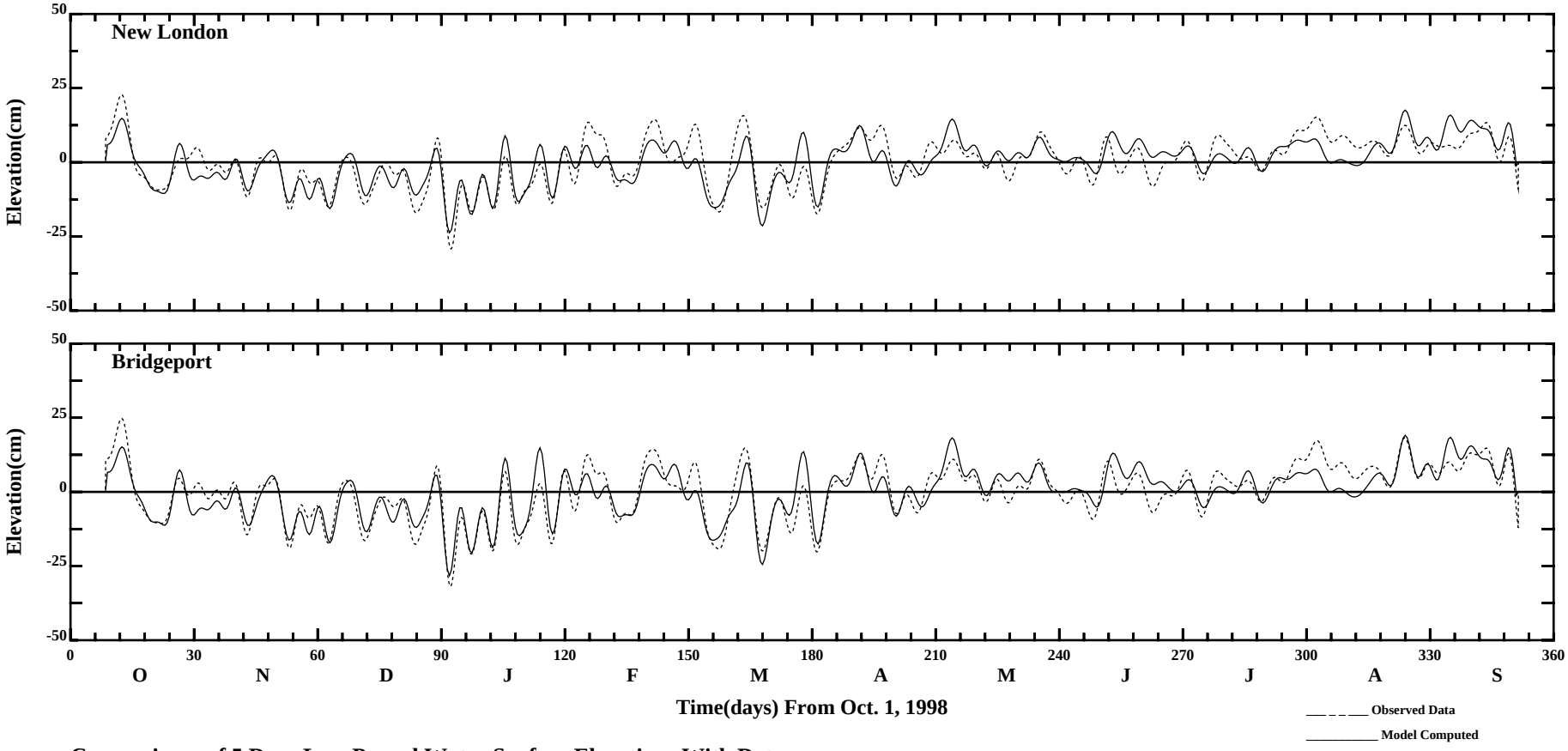

Comparisons of 5 Days Low Passed Water Surface Elevations With Data

/erie1/hrfo0010/HYDRORUNS/CARP9899/PLOTS/ELEV/pele4

DATE: Tue Nov 19 TIME: 12:07:26

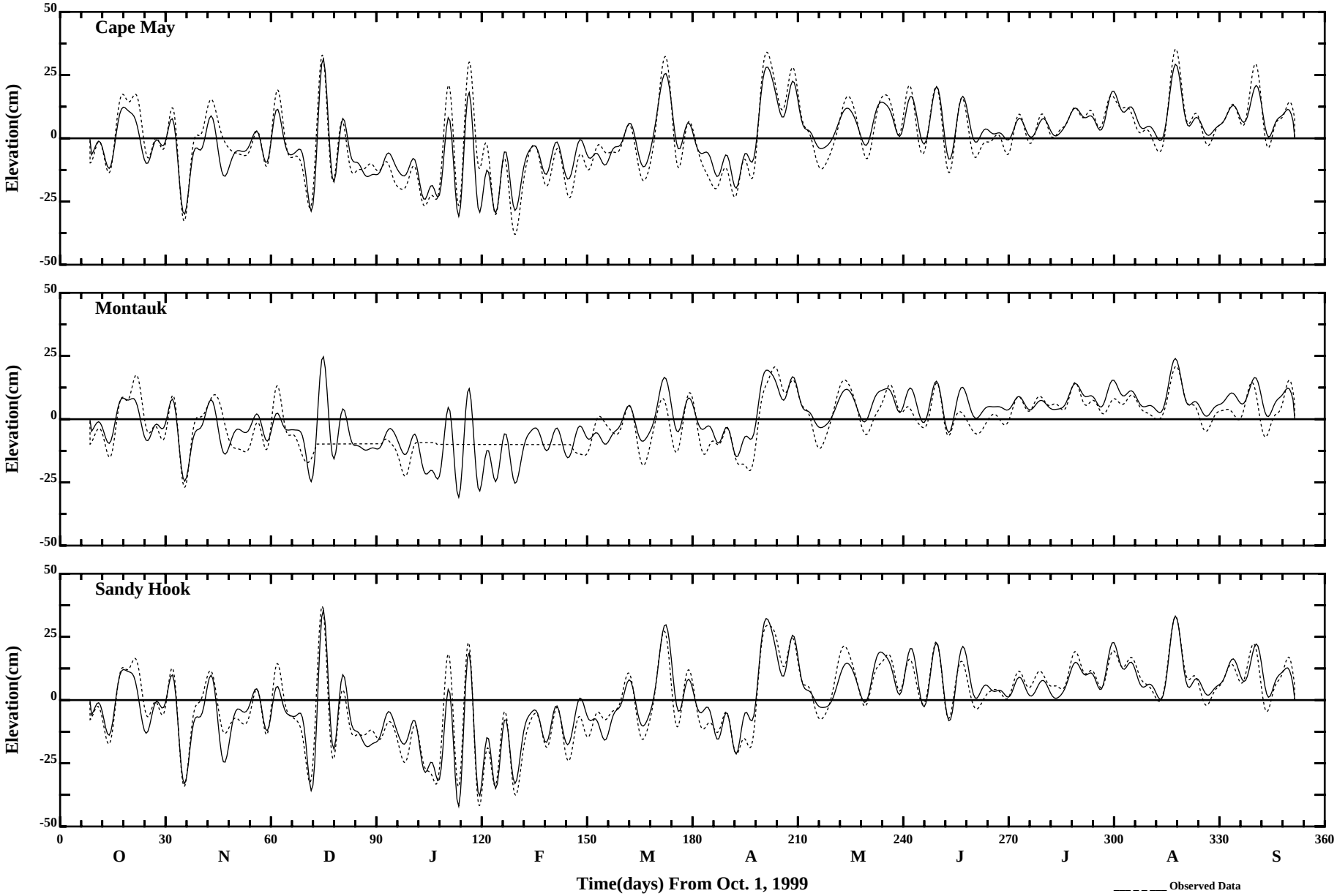

Comparisons of 5 Days Low Passed Water Surface Elevations With Data

DATE: Tue Nov 19 TIME: 12:38:54

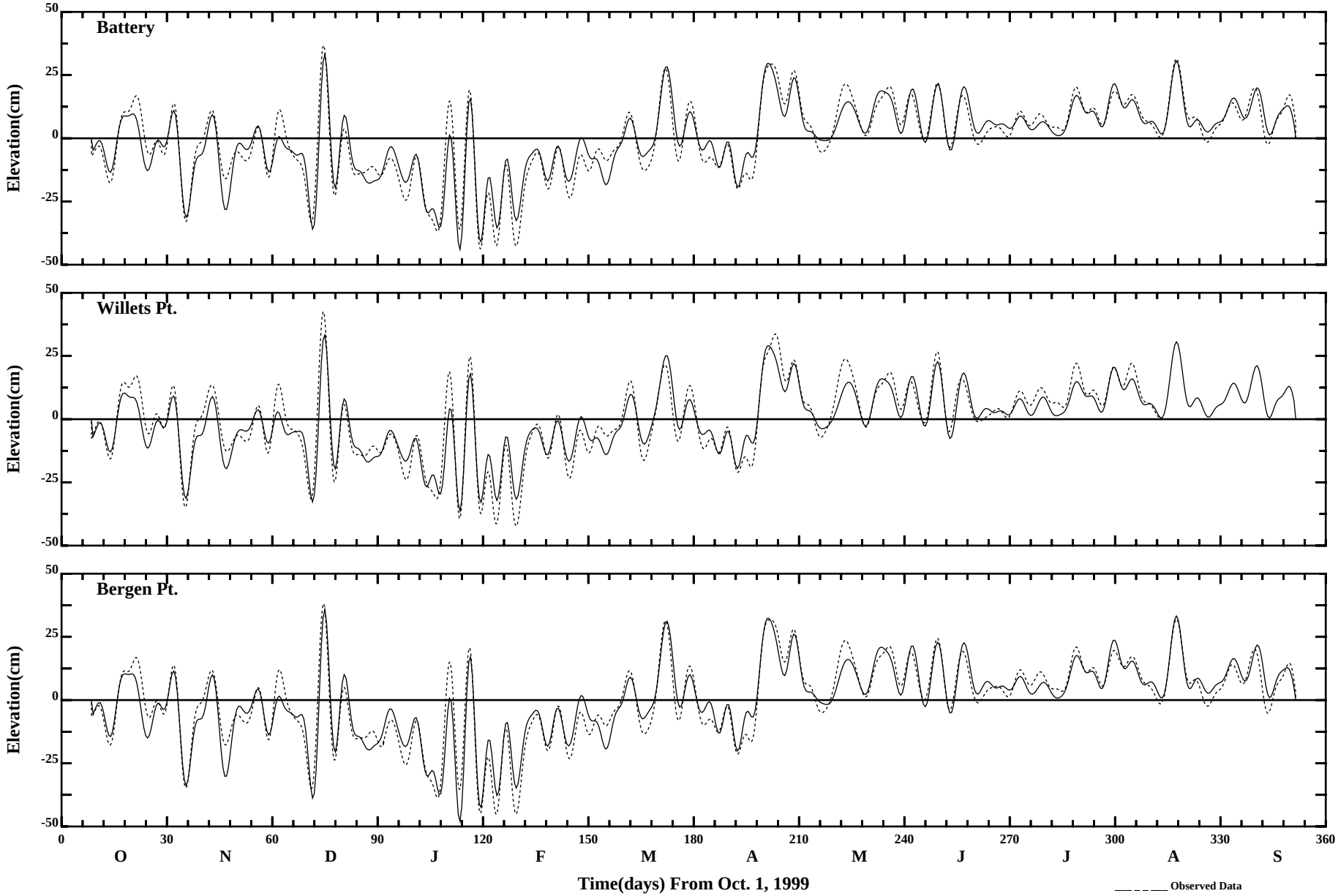

Comparisons of 5 Days Low Passed Water Surface Elevations With Data

DATE: Tue Nov 19 TIME: 12:38:54

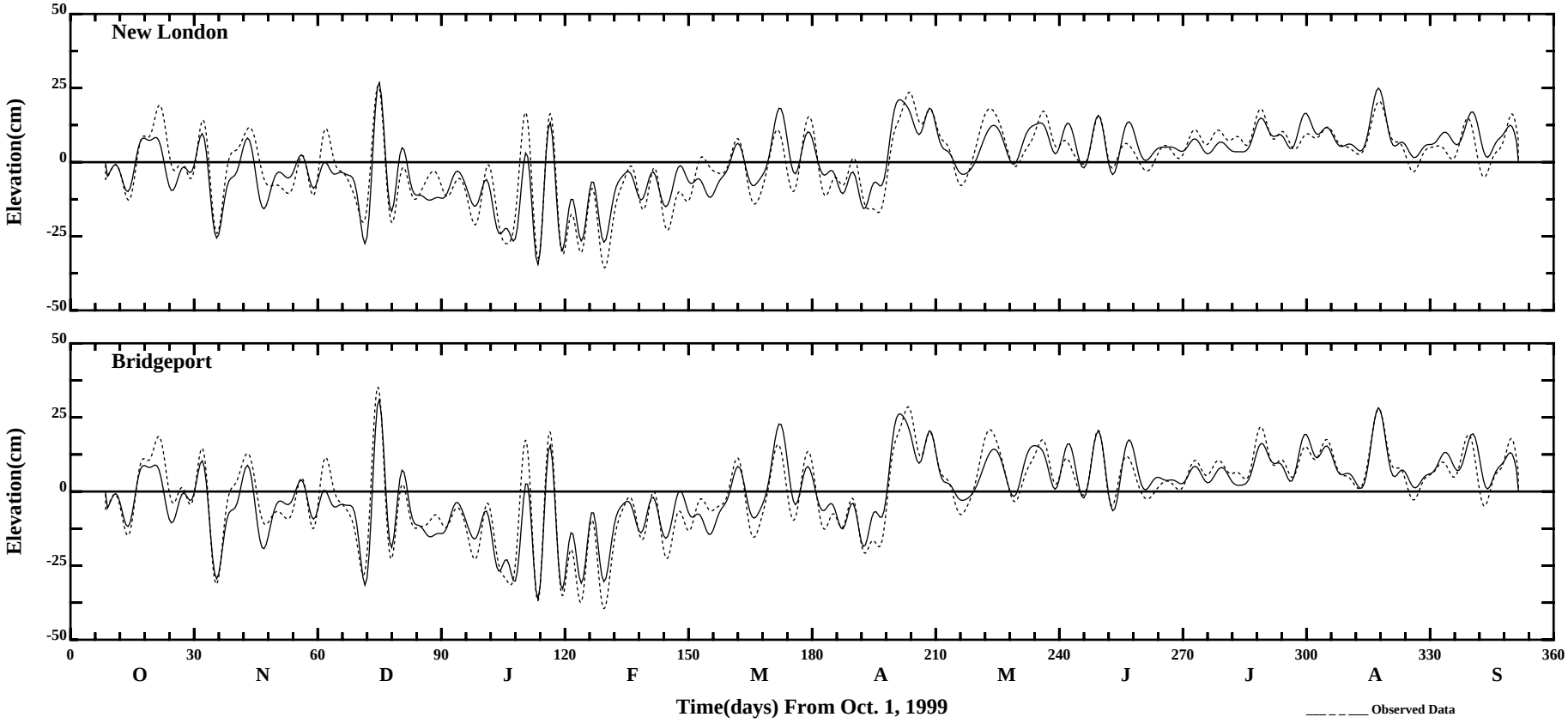

Comparisons of 5 Days Low Passed Water Surface Elevations With Data

/erie1/hrfo0010/HYDRORUNS/CARP9900/PLOTS/ELEV/pele4

DATE: Tue Nov 19 TIME: 12:38:54

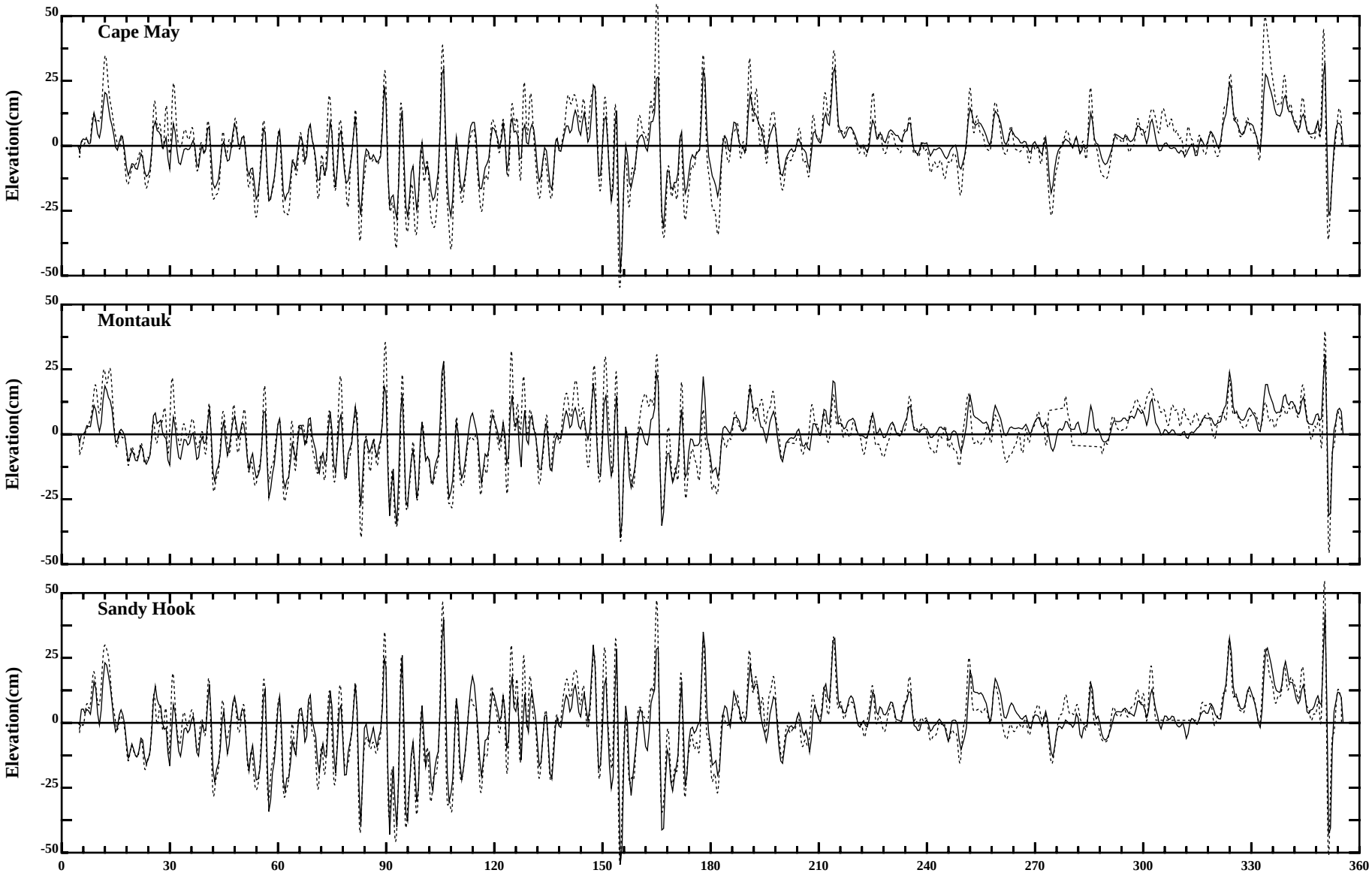

Comparisons of 35 Hour Low Passed Water Surface Elevations With Data

DATE: Tue Nov 19 TIME: 12:07:50

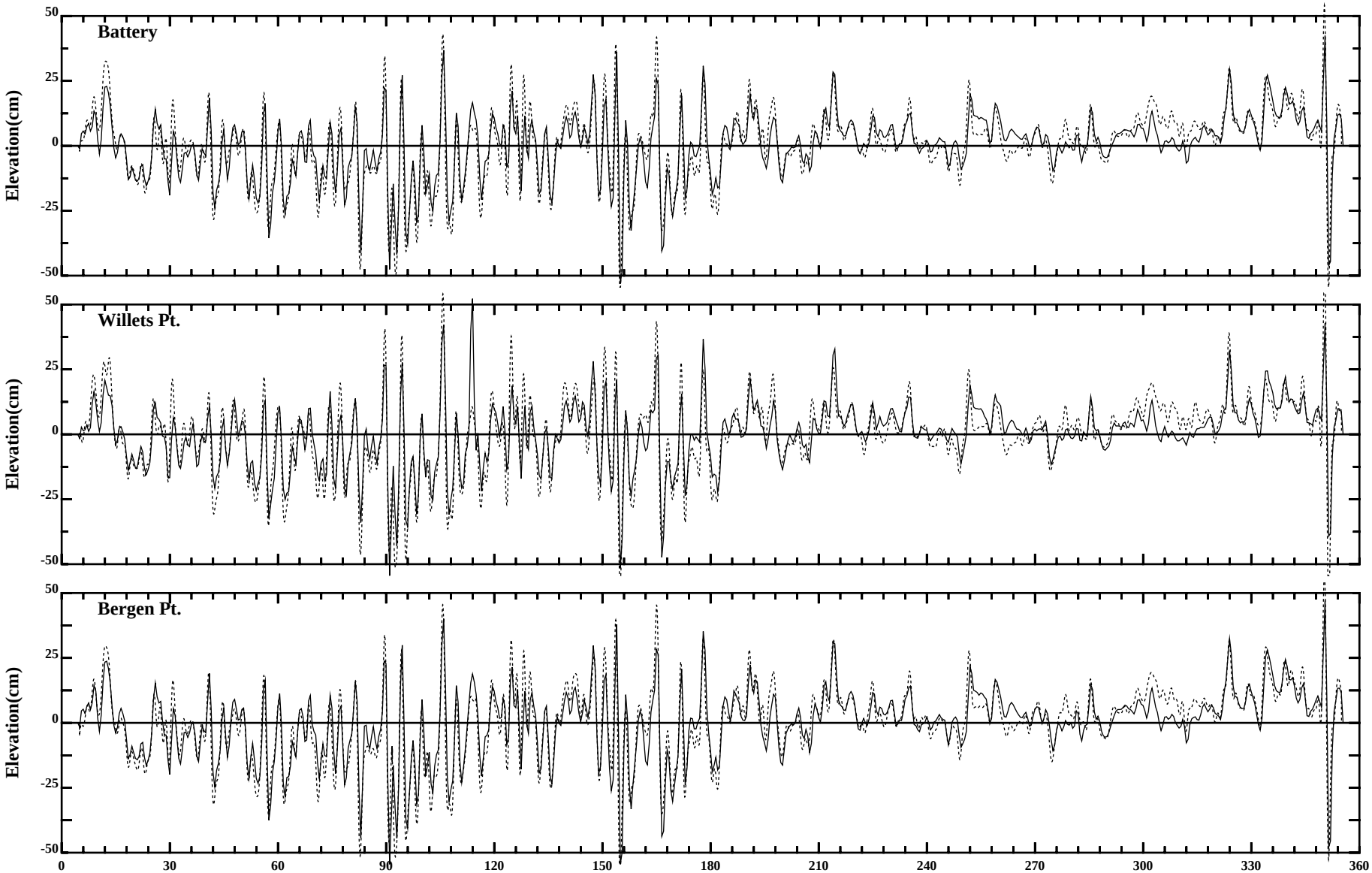

Comparisons of 35 Hour Low Passed Water Surface Elevations With Data

/erie1/hrfo0010/HYDRORUNS/CARP9899/PLOTS/ELEV/pele5

DATE: Tue Nov 19 TIME: 12:07:50

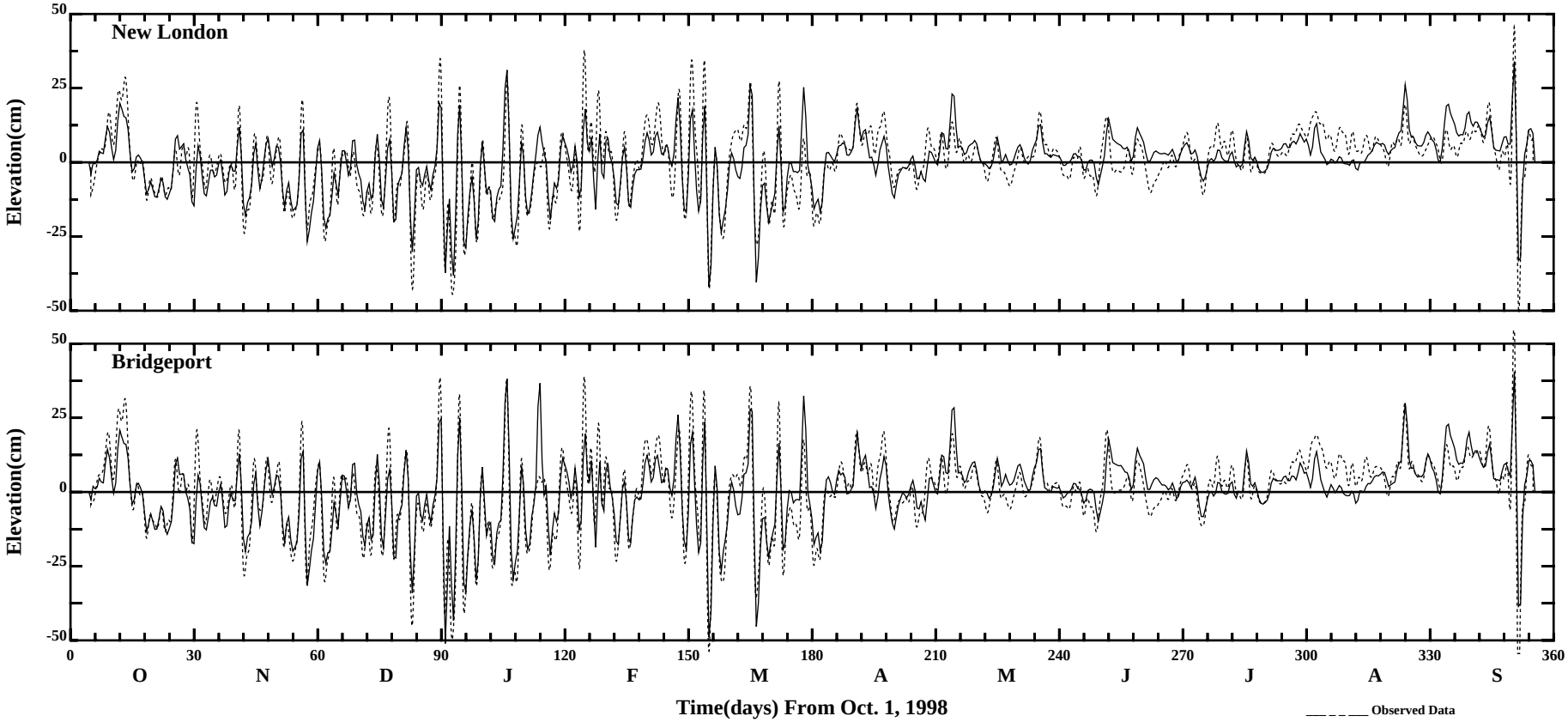

Comparisons of 35 Hour Low Passed Water Surface Elevations With Data

/erie1/hrfo0010/HYDRORUNS/CARP9899/PLOTS/ELEV/pele5

DATE: Tue Nov 19 TIME: 12:07:50

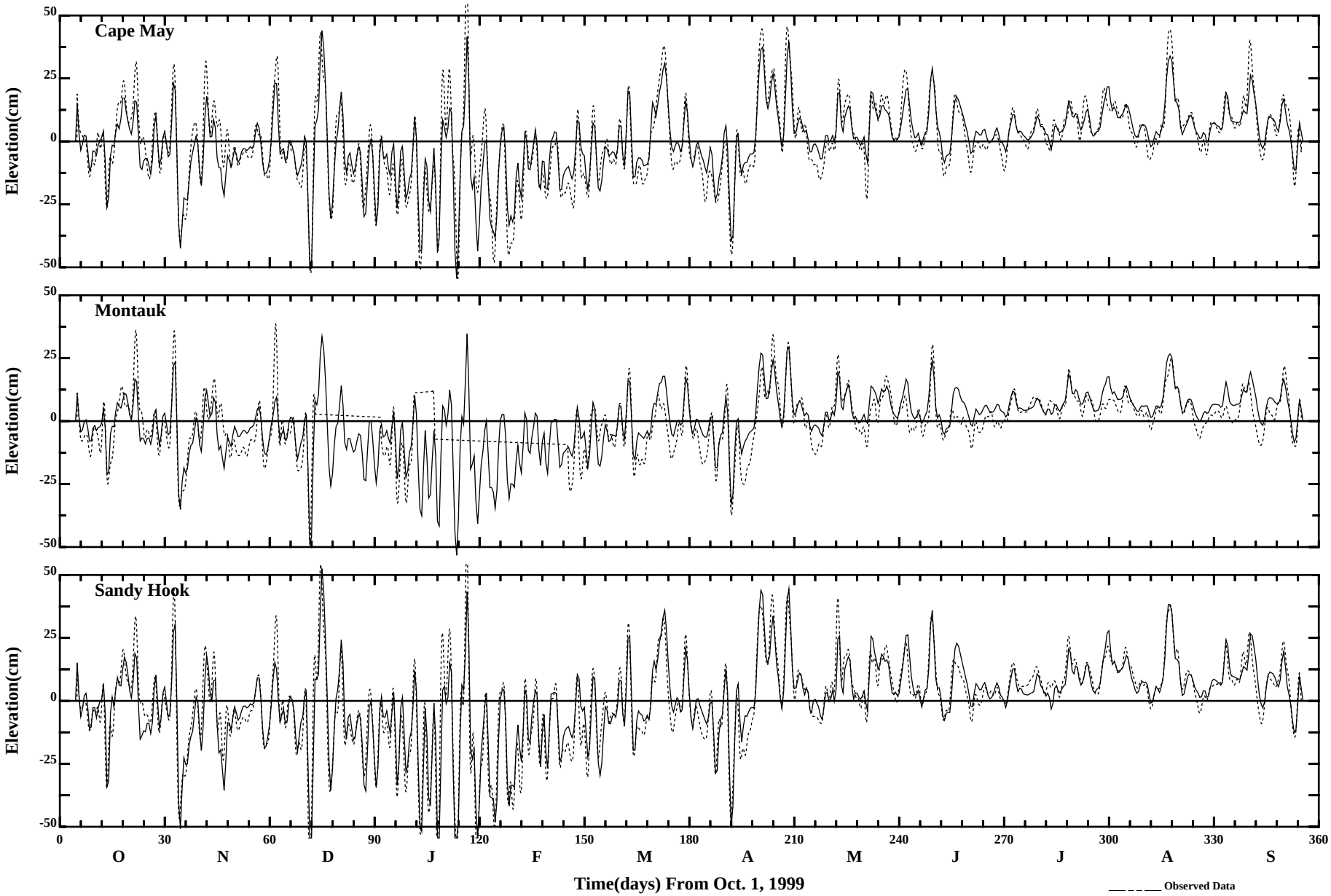

Comparisons of 35 Hour Low Passed Water Surface Elevations With Data

DATE: Tue Nov 19 TIME: 12:39:19

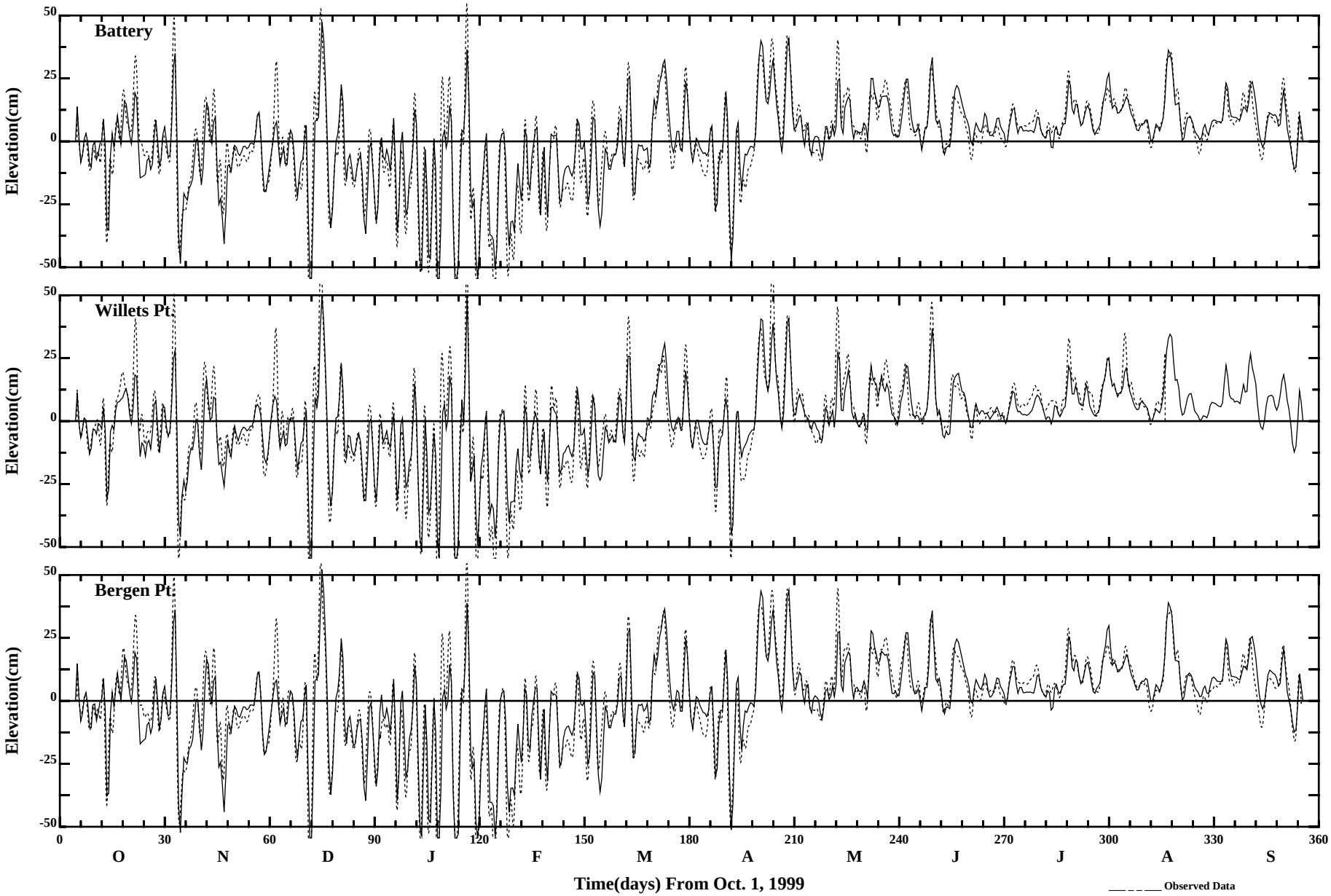

Comparisons of 35 Hour Low Passed Water Surface Elevations With Data

/erie1/hrfo0010/HYDRORUNS/CARP9900/PLOTS/ELEV/pele5

DATE: Tue Nov 19 TIME: 12:39:19

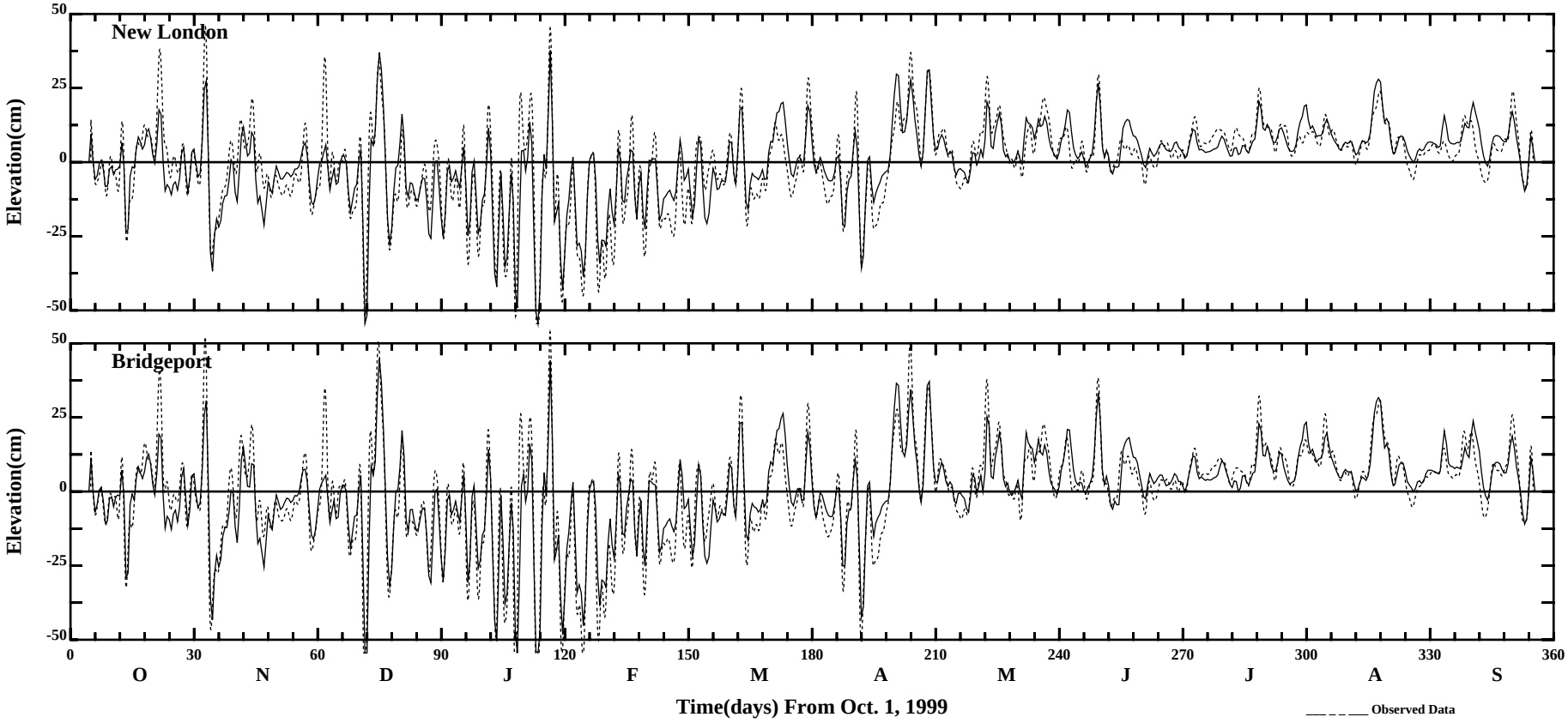

Comparisons of 35 Hour Low Passed Water Surface Elevations With Data

/erie1/hrfo0010/HYDRORUNS/CARP9900/PLOTS/ELEV/pele5

DATE: Tue Nov 19 TIME: 12:39:19

APPENDIX 5

SKILL ASSESSMENT USING PVSC DATA

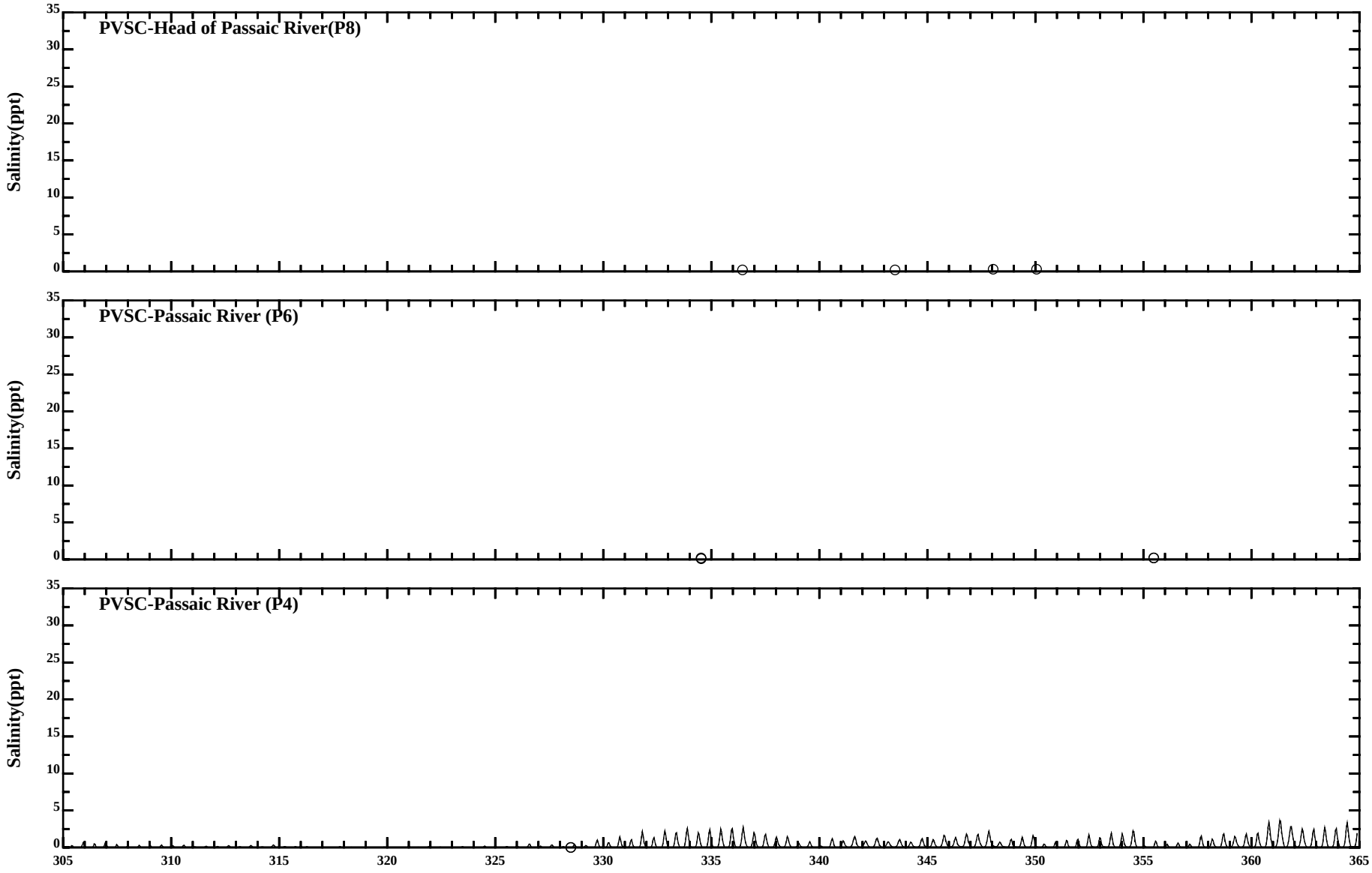

Comparison of Instantaneous Surface and Bottom Salinity

DATE: 8/02/2004 TIME: 12: 7:32

/erie1/hrfo0010/HYDRORUNS/CARP9900/PLOTS/TANDS/salt61

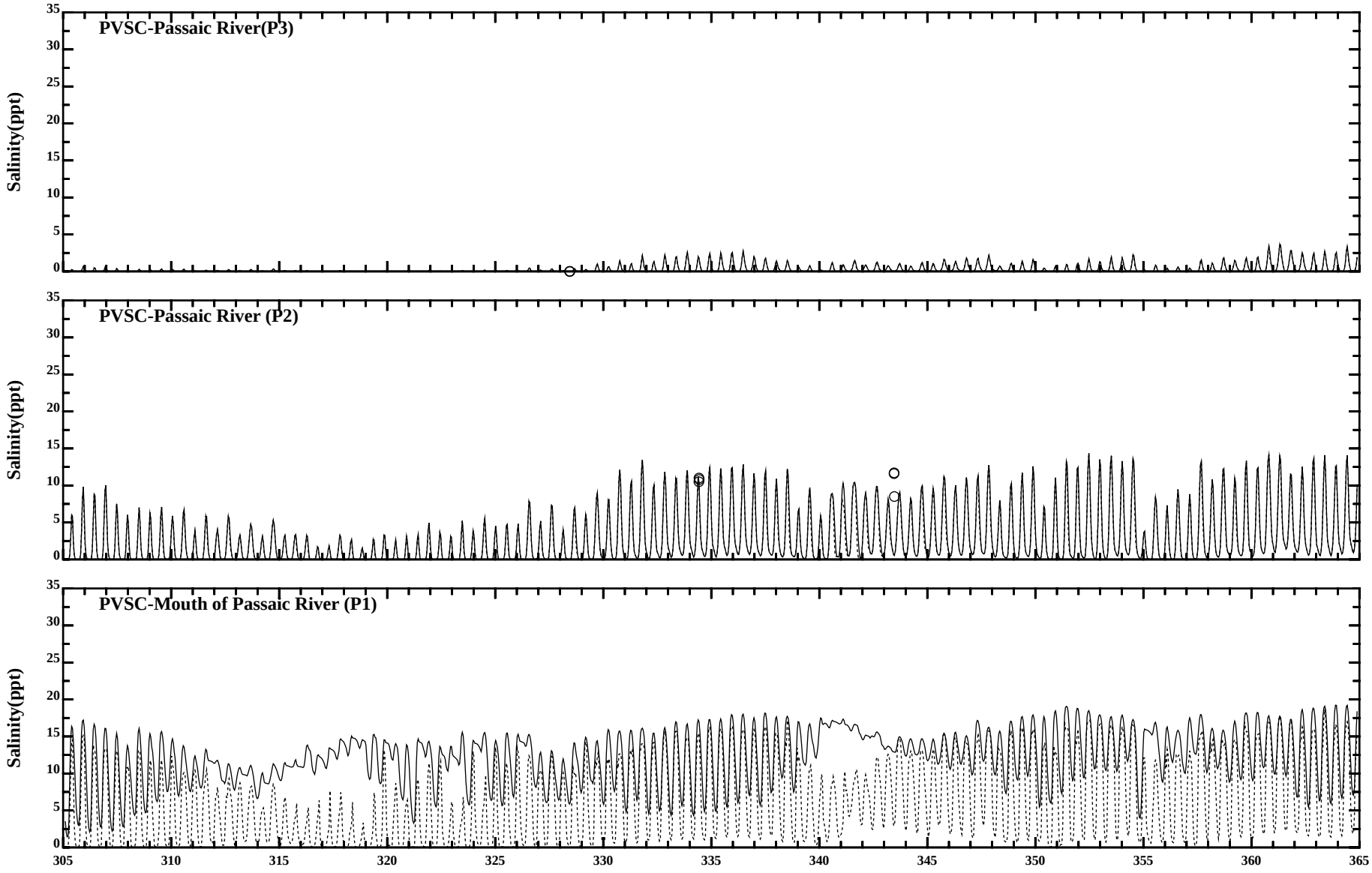

Comparison of Instantaneous Surface and Bottom Salinity

DATE: 8/02/2004 TIME: 12: 7:32

/erie1/hrfo0010/HYDRORUNS/CARP9900/PLOTS/TANDS/salt61

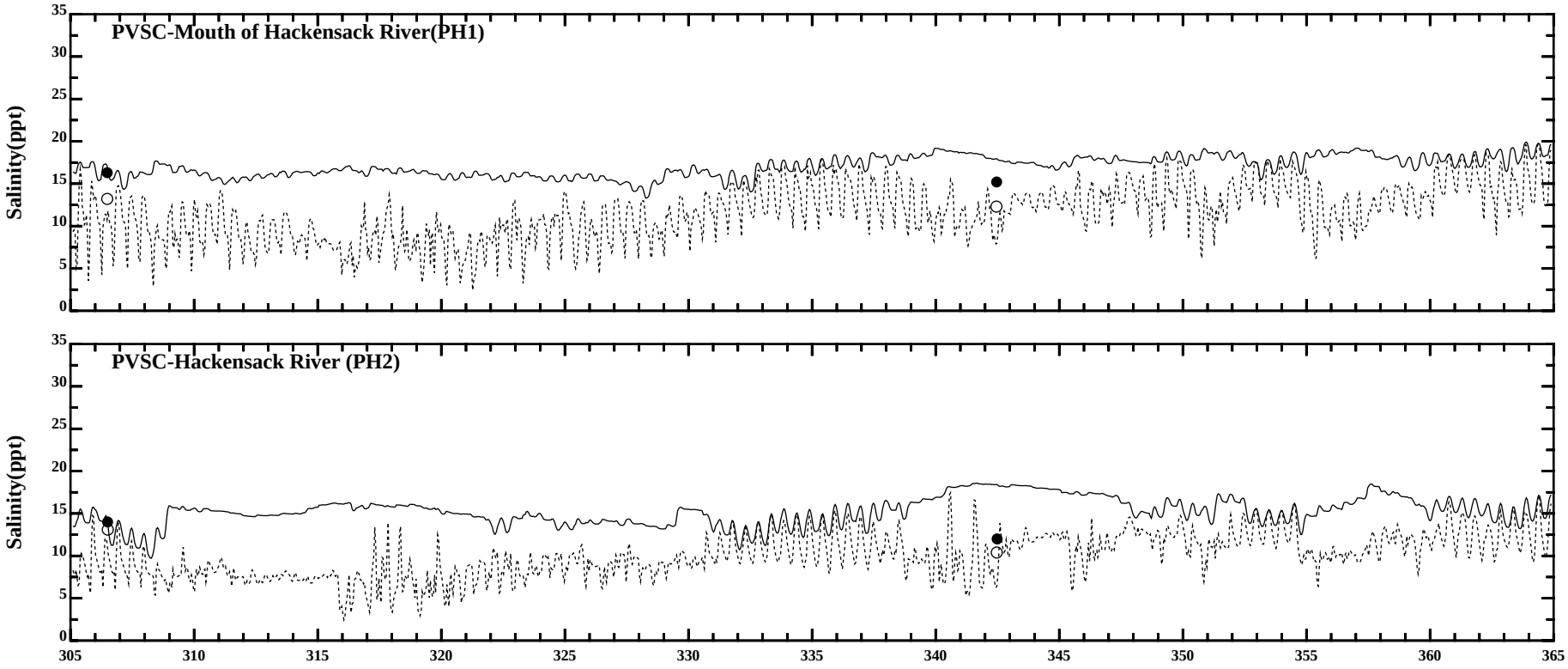

Comparison of Instantaneous Surface and Bottom Salinity

/erie1/hrfo0010/HYDRORUNS/CARP9900/PLOTS/TANDS/salt61

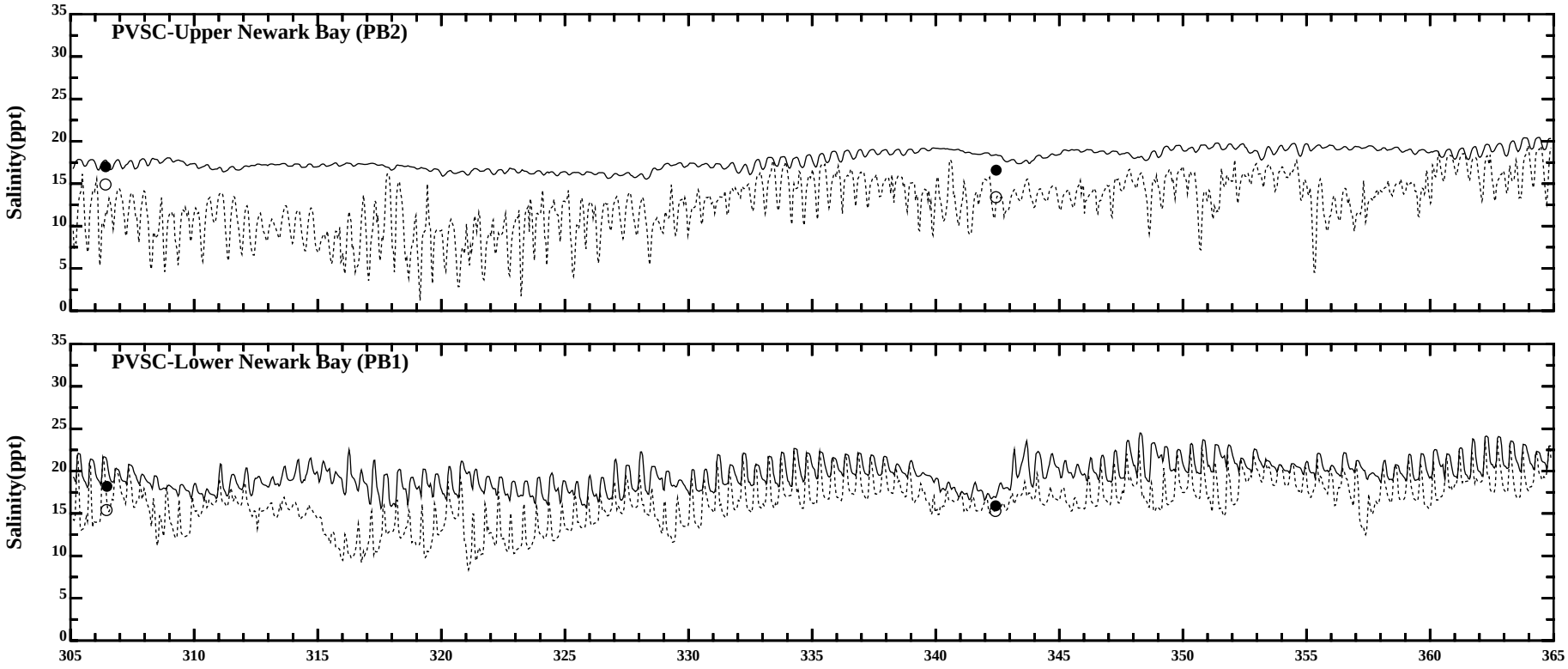

Comparison of Instantaneous Surface and Bottom Salinity

/erie1/hrfo0010/HYDRORUNS/CARP9900/PLOTS/TANDS/salt61

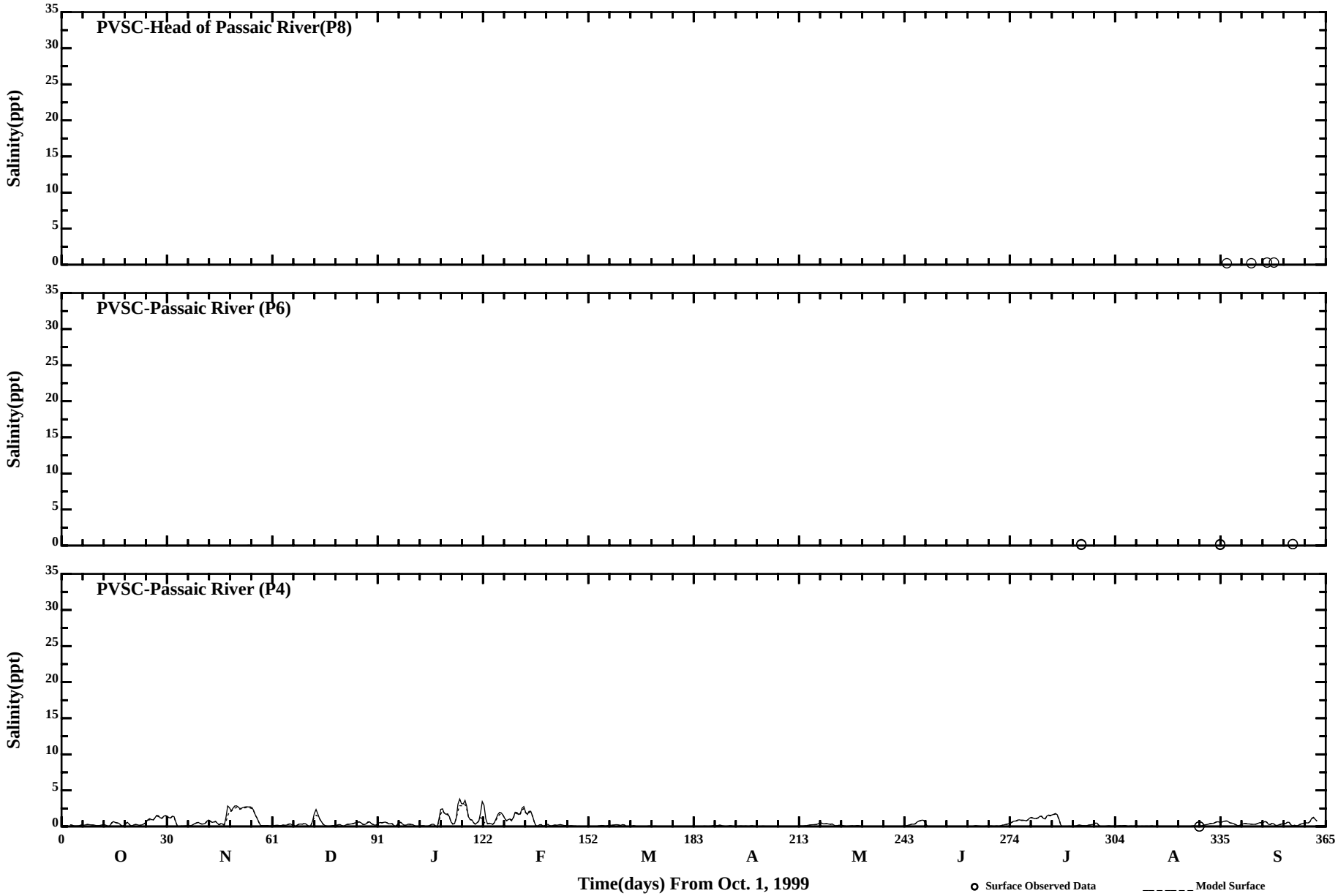

Comparison of 34 Hour Lowpass Surface and Bottom Salinity

DATE: 8/02/2004 TIME: 12: 7:28

/erie1/hrfo0010/HYDRORUNS/CARP9900/PLOTS/TANDS/psalt51_34hlp

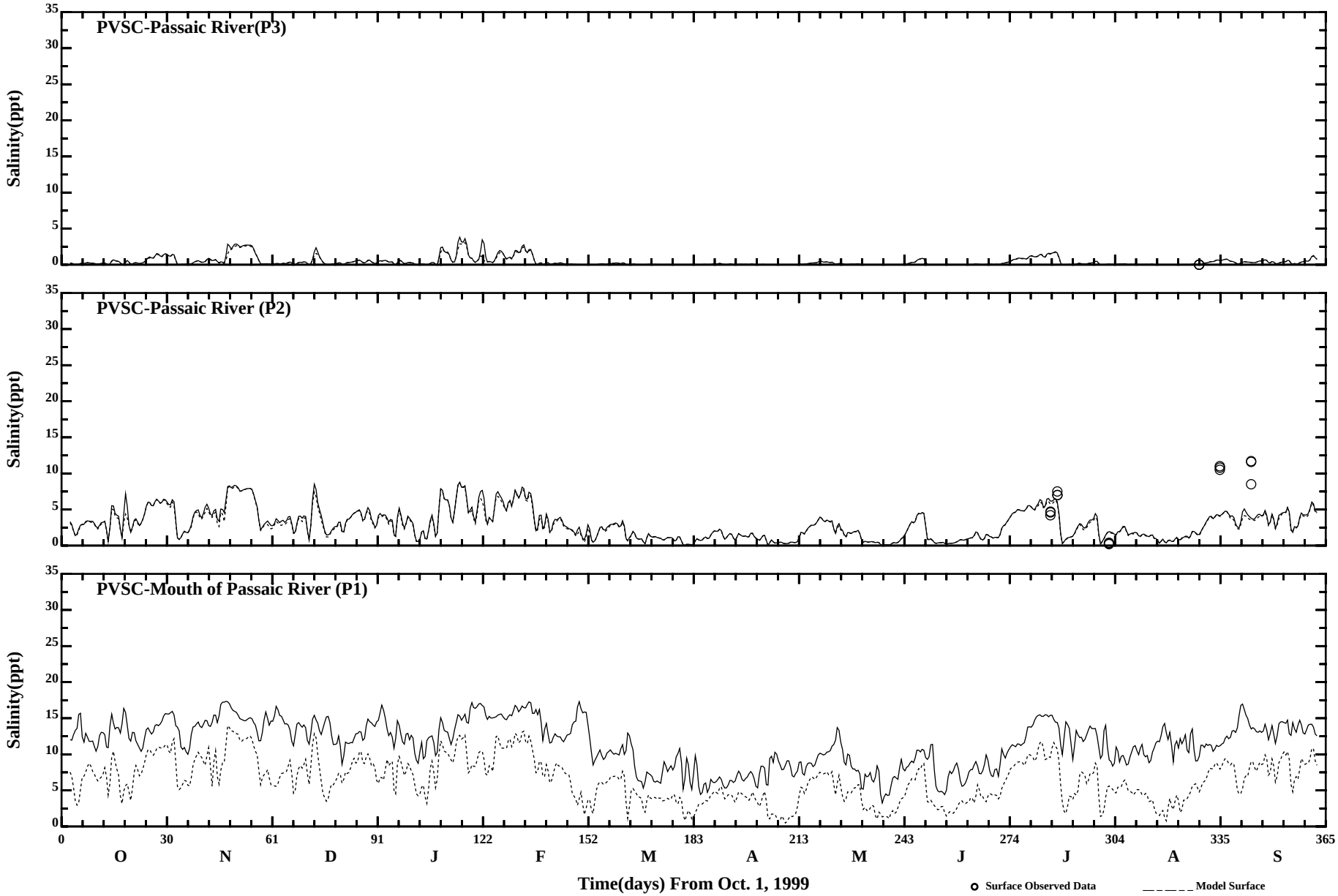

Comparison of 34 Hour Lowpass Surface and Bottom Salinity

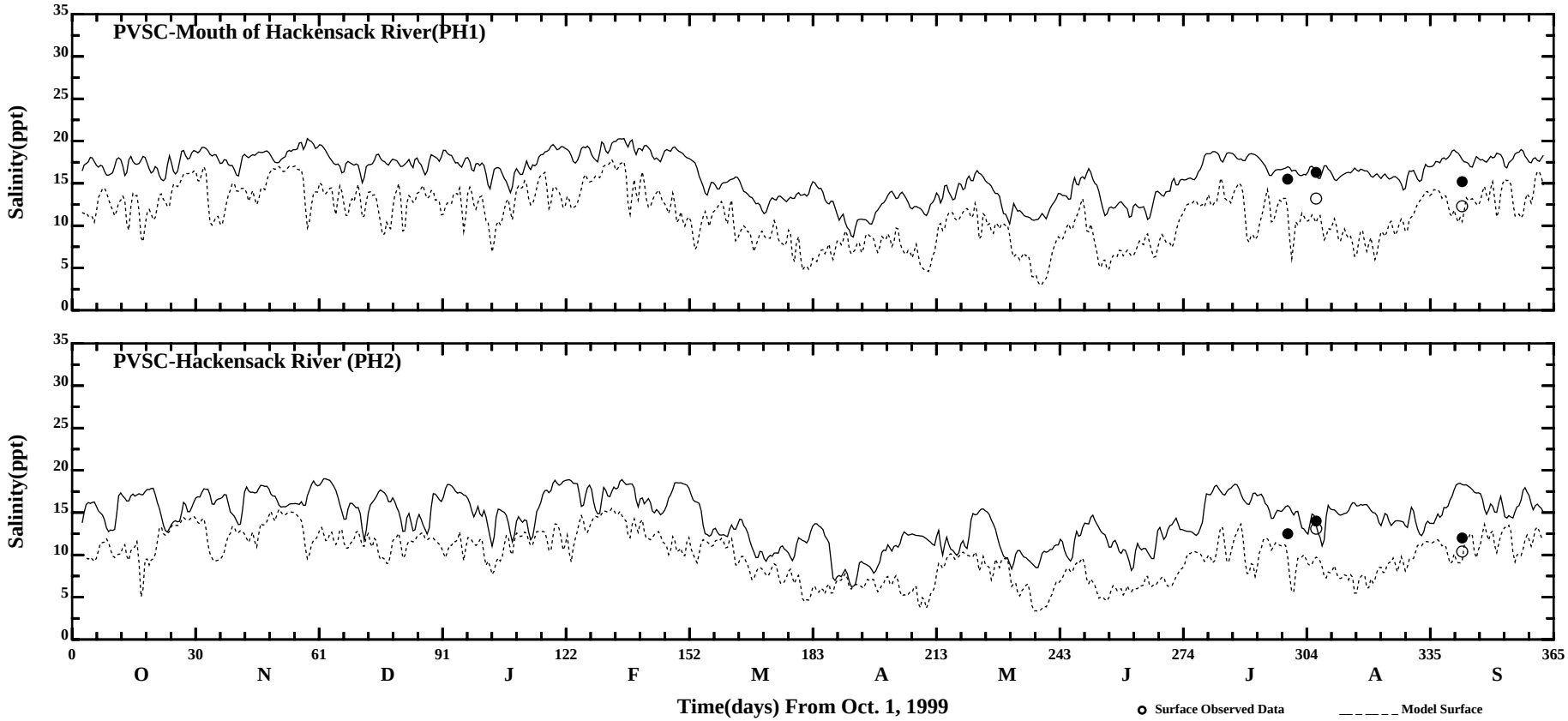

Comparison of 34 Hour Lowpass Surface and Bottom Salinity

/erie1/hrfo0010/HYDRORUNS/CARP9900/PLOTS/TANDS/psalt51_34hlp

DATE: 8/02/2004 TIME: 12: 7:28

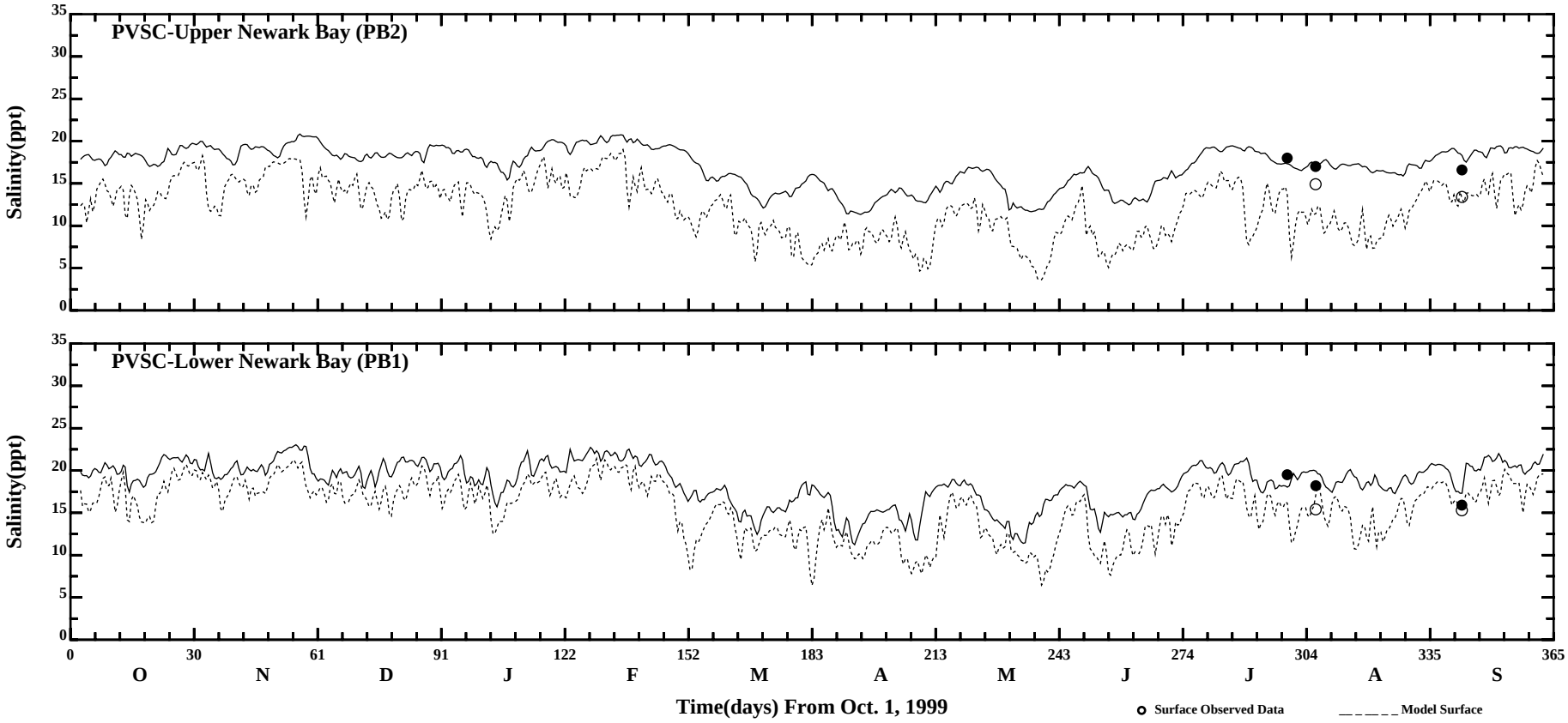

Comparison of 34 Hour Lowpass Surface and Bottom Salinity

Page:4/4

/erie1/hrfo0010/HYDRORUNS/CARP9900/PLOTS/TANDS/psalt51_34hlp

DATE: 8/02/2004 TIME: 12: 7:28

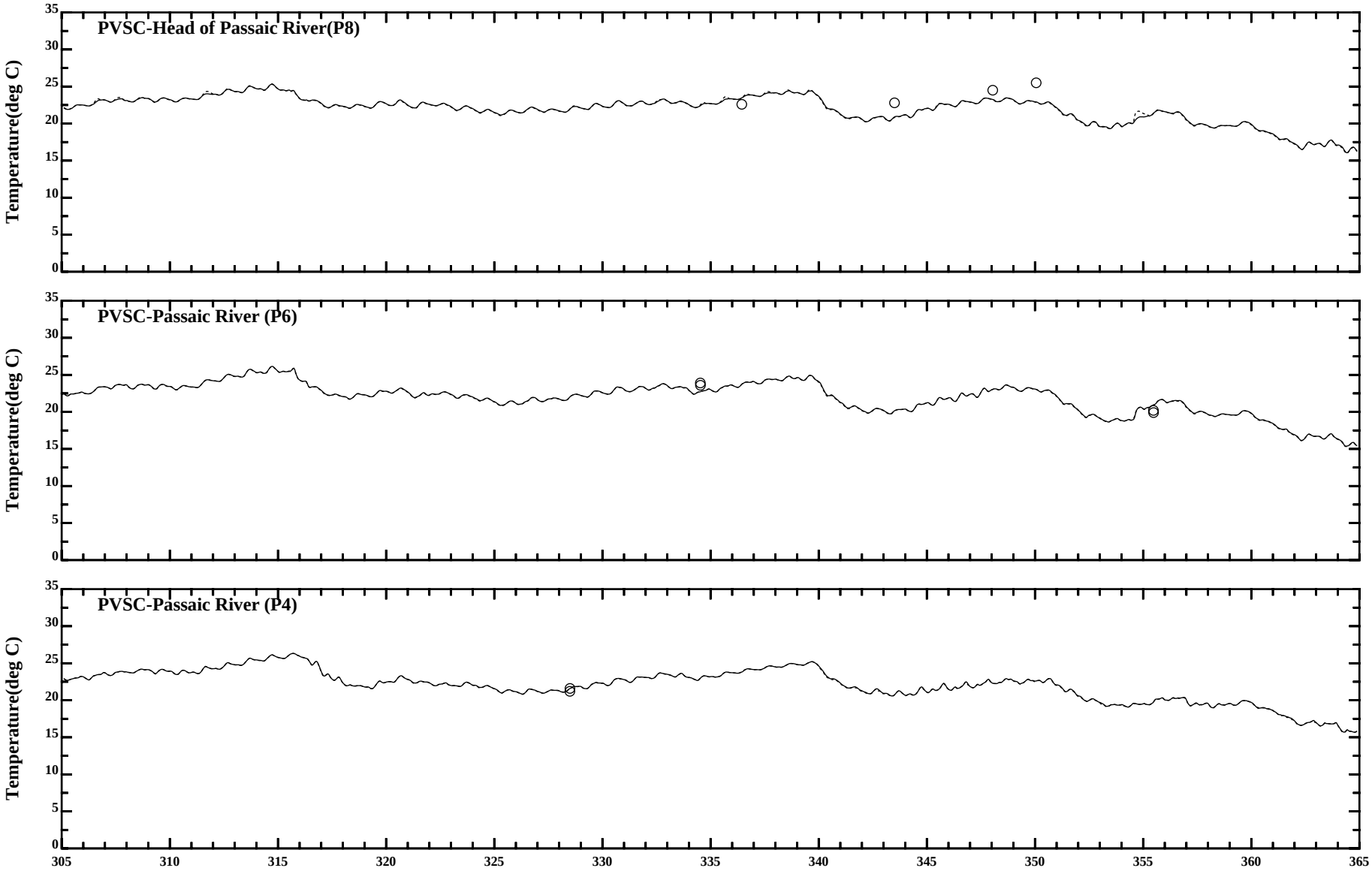

Comparison of Instantaneous Surface and Bottom Temperature

DATE: 8/02/2004 TIME: 12: 7:24

/erie1/hrfo0010/HYDRORUNS/CARP9900/PLOTS/TANDS/temp61

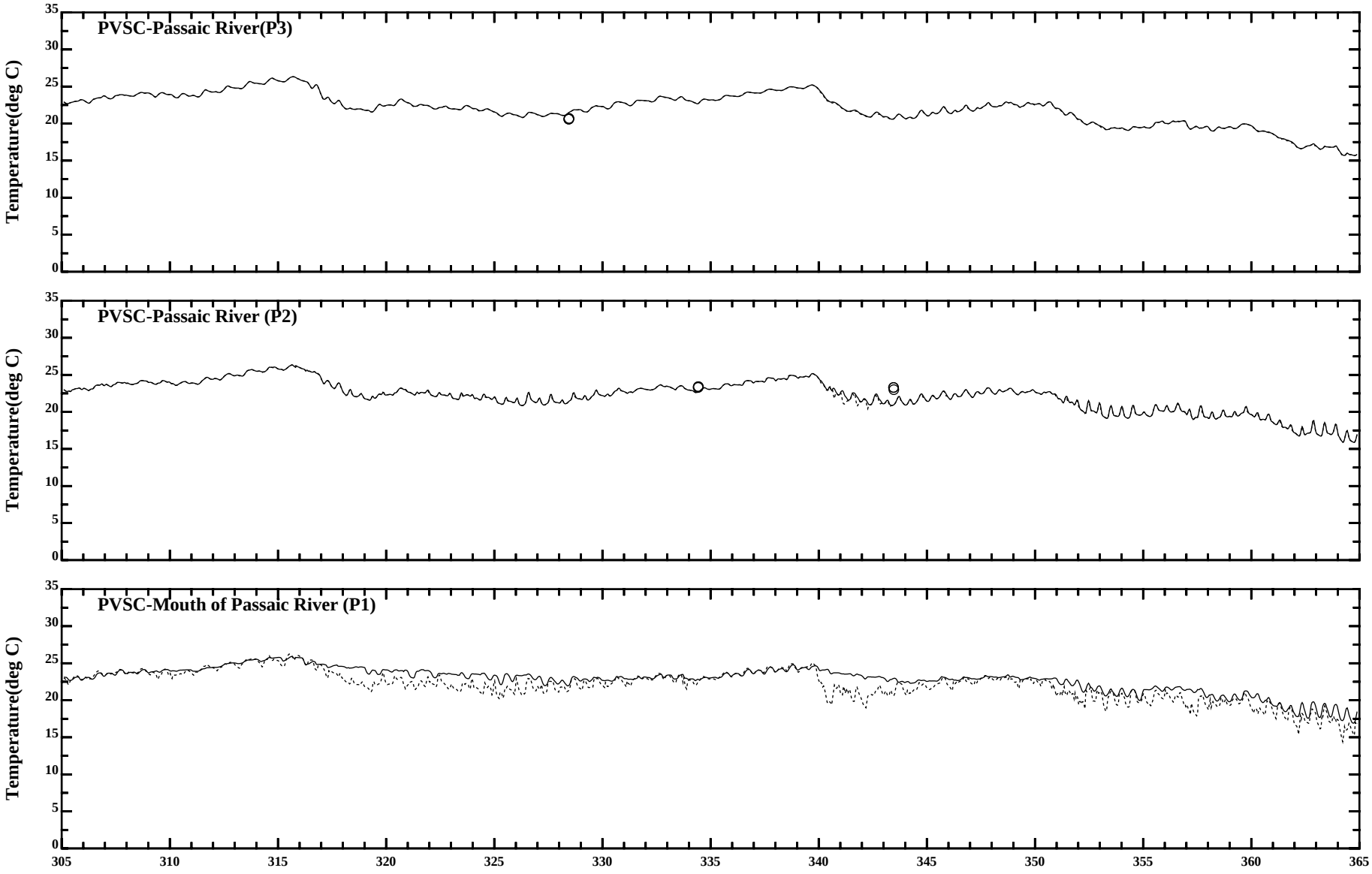

Comparison of Instantaneous Surface and Bottom Temperature

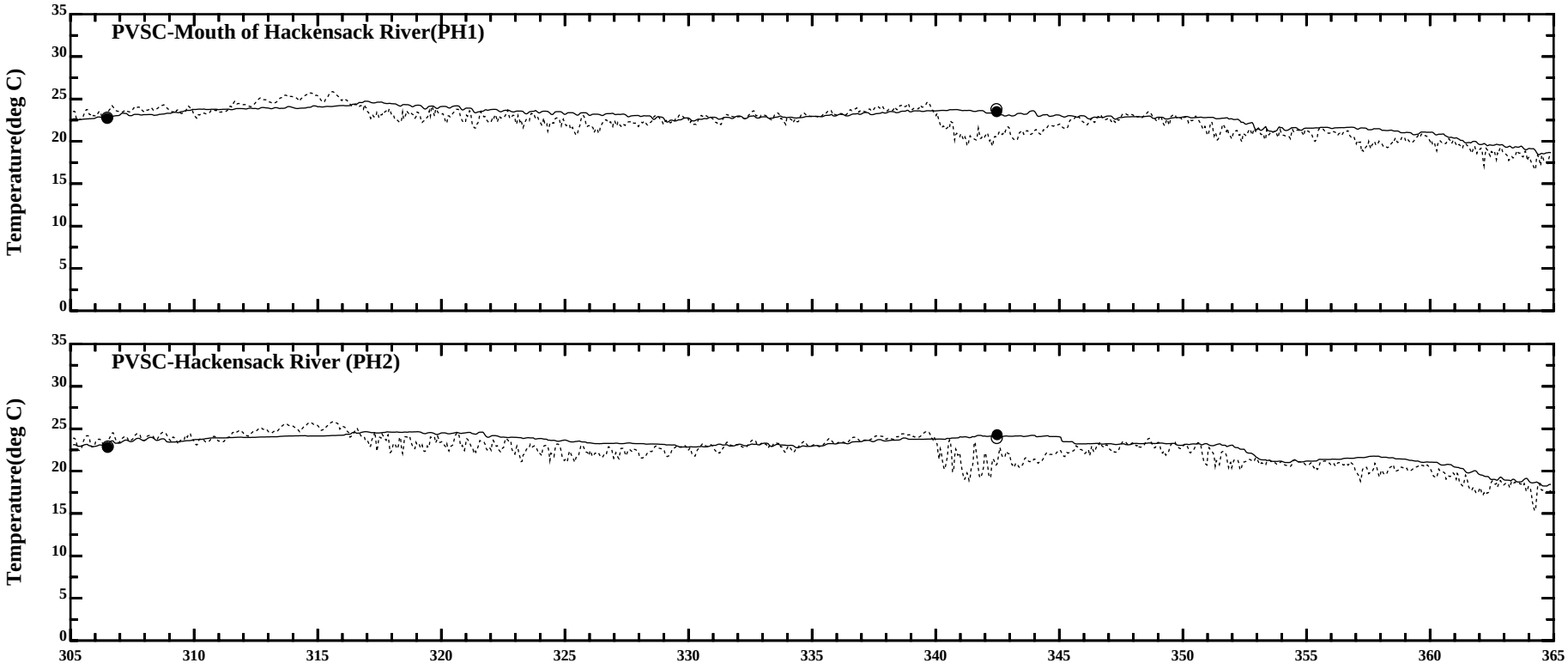

Comparison of Instantaneous Surface and Bottom Temperature

/erie1/hrfo0010/HYDRORUNS/CARP9900/PLOTS/TANDS/temp61

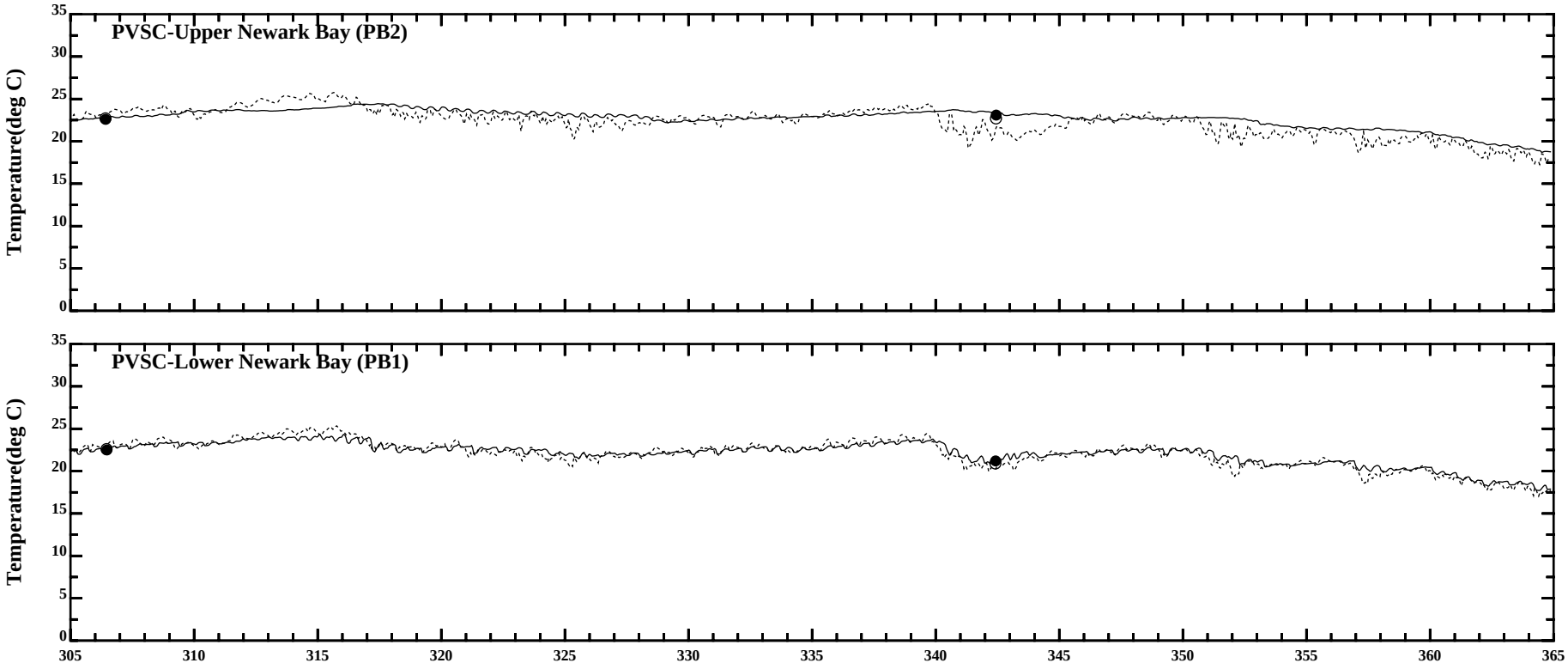

Comparison of Instantaneous Surface and Bottom Temperature

/erie1/hrfo0010/HYDRORUNS/CARP9900/PLOTS/TANDS/temp61

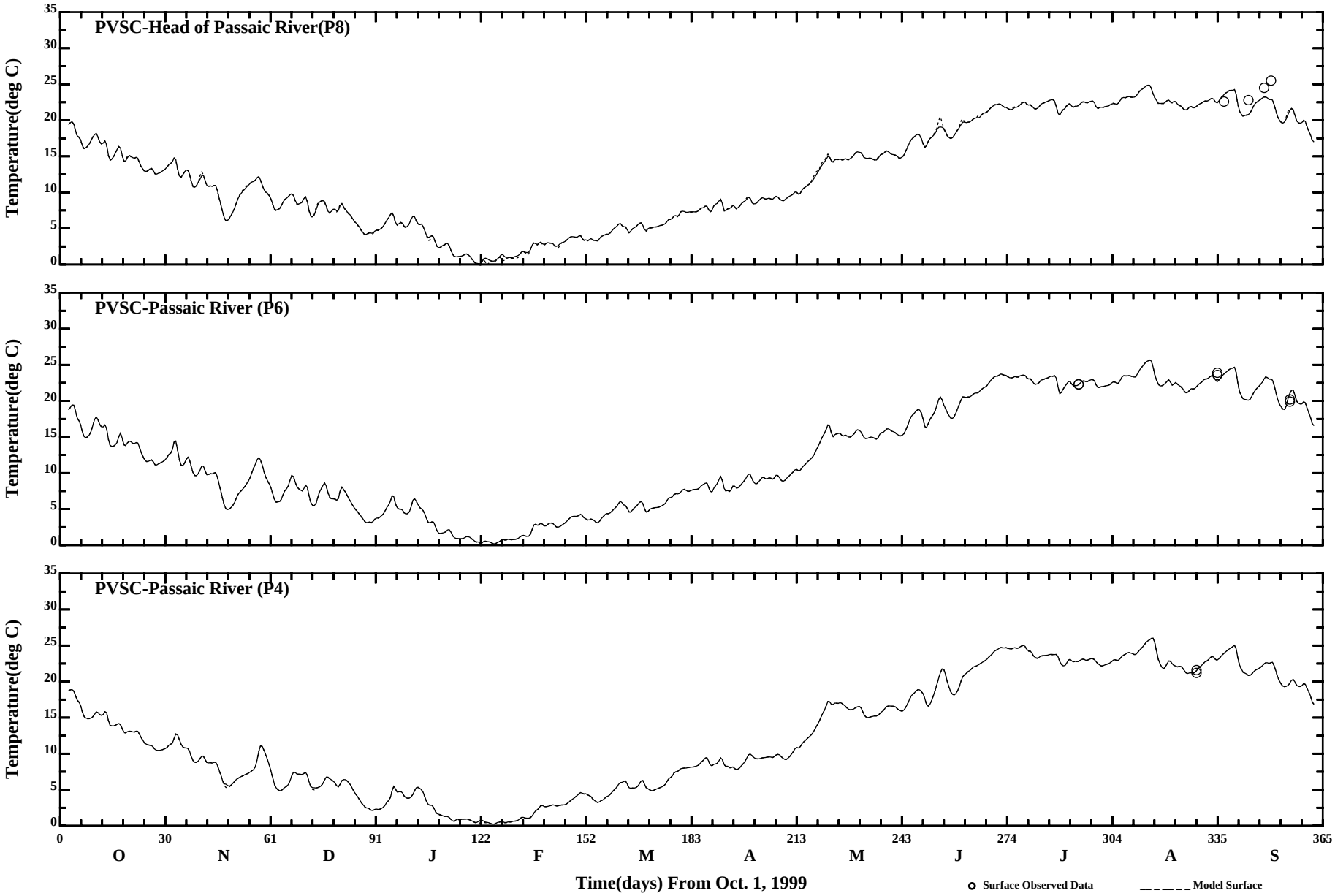

Comparison of 34 Hour Lowpass Surface and Bottom Temperature

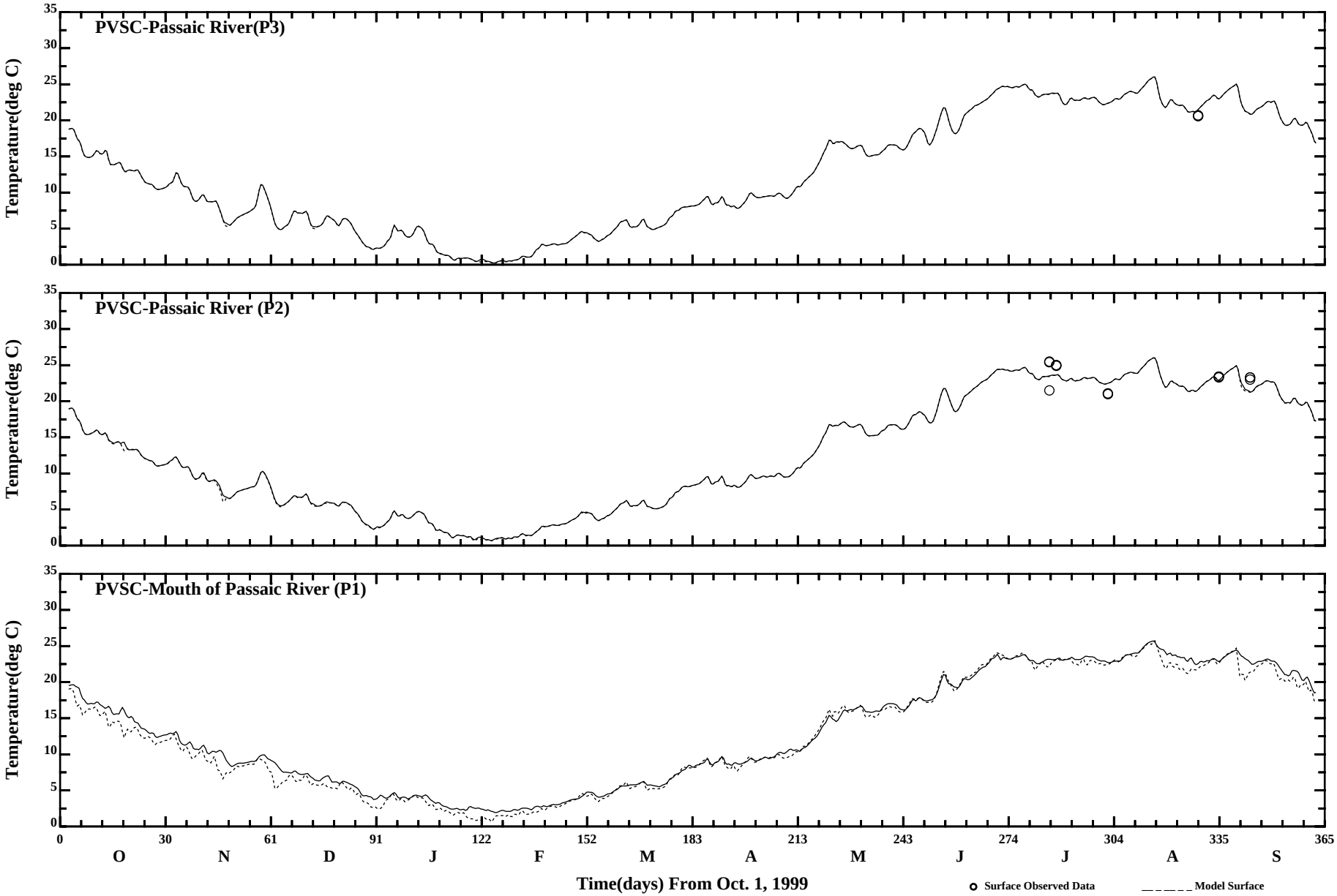

Comparison of 34 Hour Lowpass Surface and Bottom Temperature

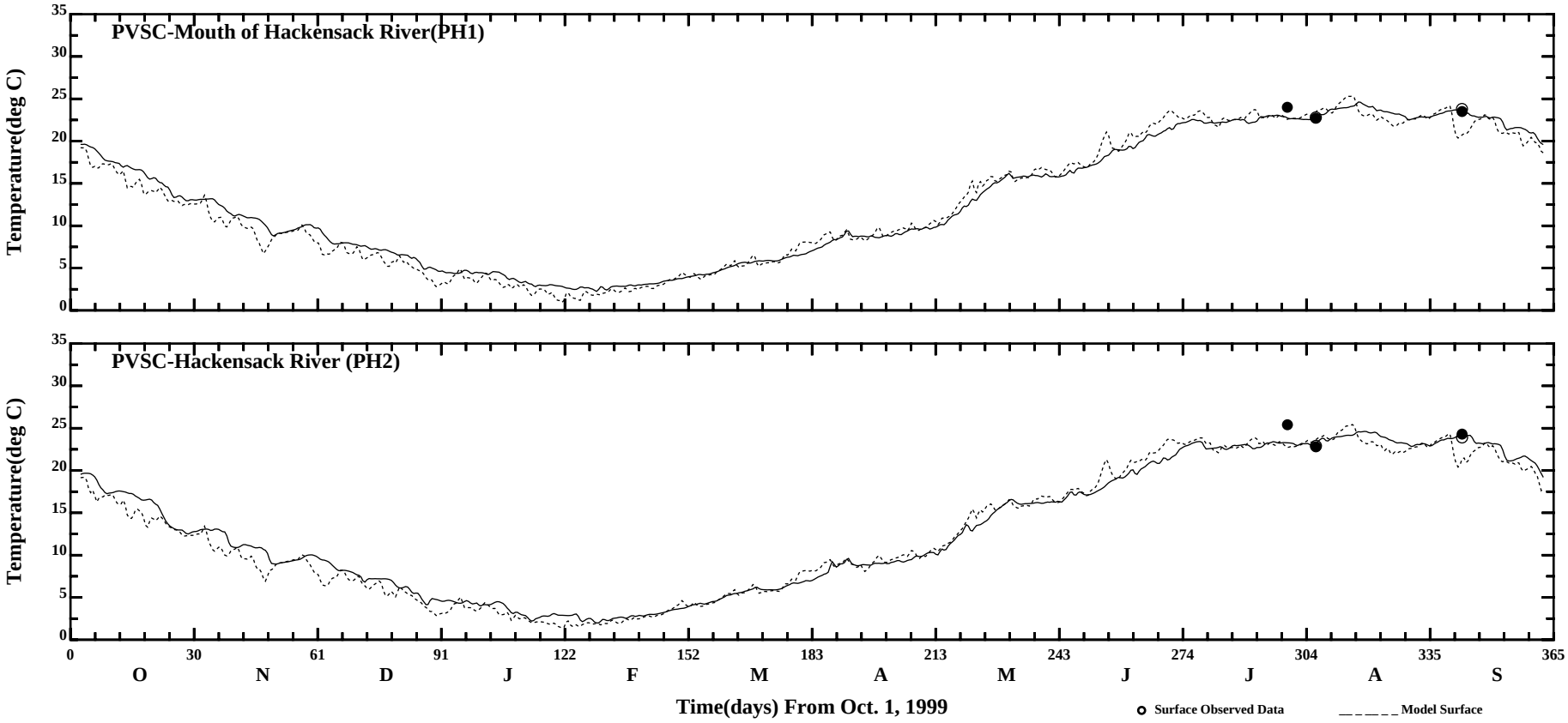

Comparison of 34 Hour Lowpass Surface and Bottom Temperature

/erie1/hrfo0010/HYDRORUNS/CARP9900/PLOTS/TANDS/ptemp51_34hlp

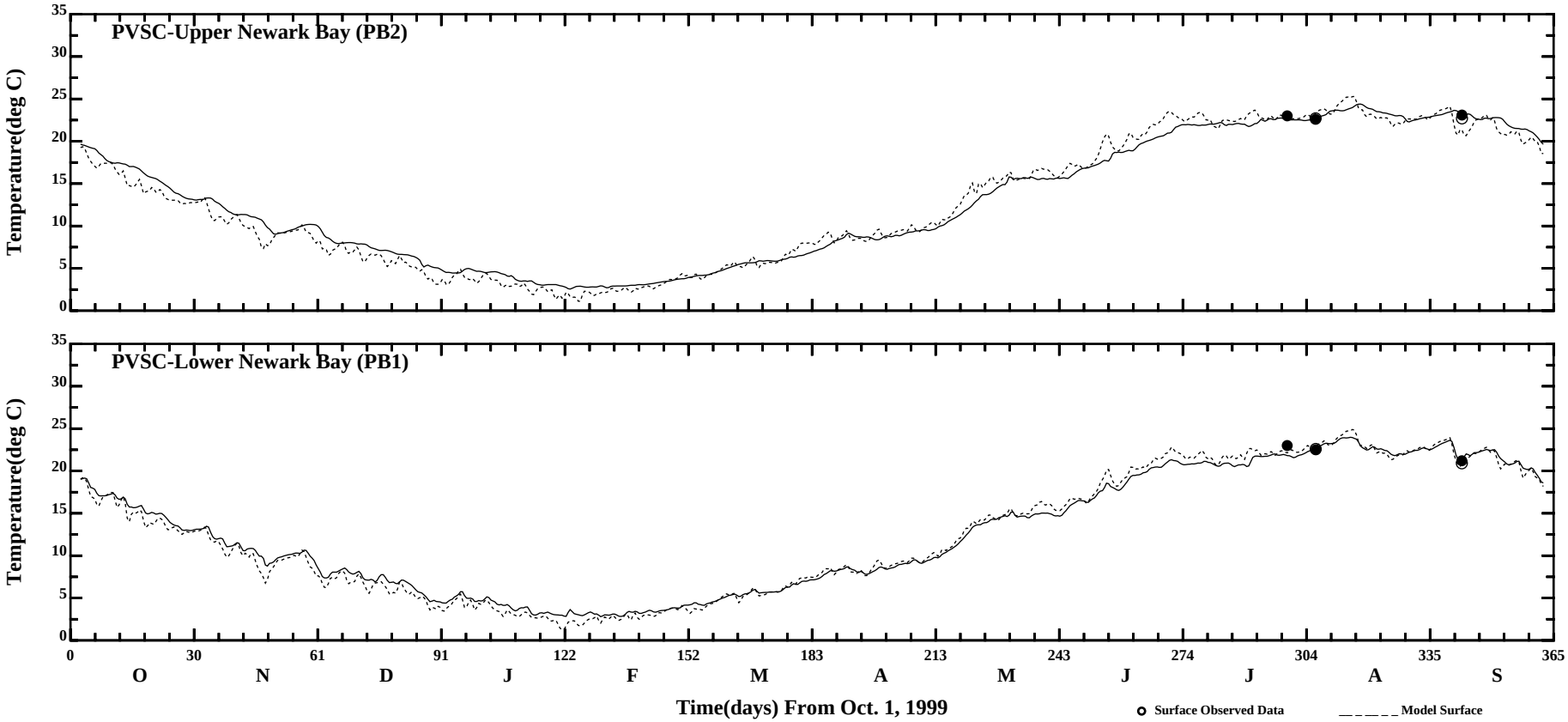

Comparison of 34 Hour Lowpass Surface and Bottom Temperature

/erie1/hrfo0010/HYDRORUNS/CARP9900/PLOTS/TANDS/ptemp51_34hlp

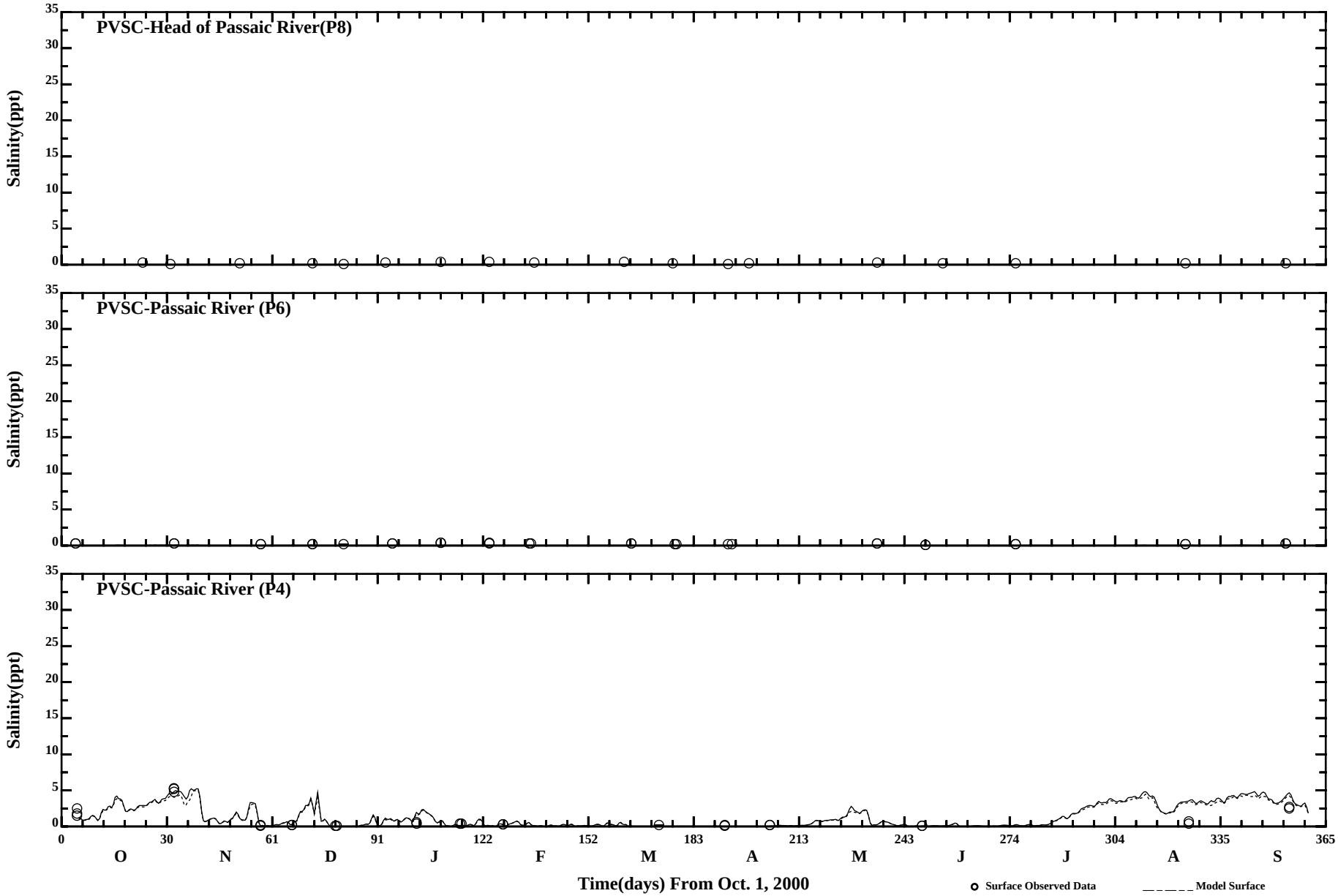

Comparison of 35 Hour Lowpass Surface and Bottom Salinity

DATE: 8/02/2004 TIME: 12:30: 7

/erie1/hrfo0010/HYDRORUNS/CARP0001/PLOTS/TANDS/psalt51_35hlp

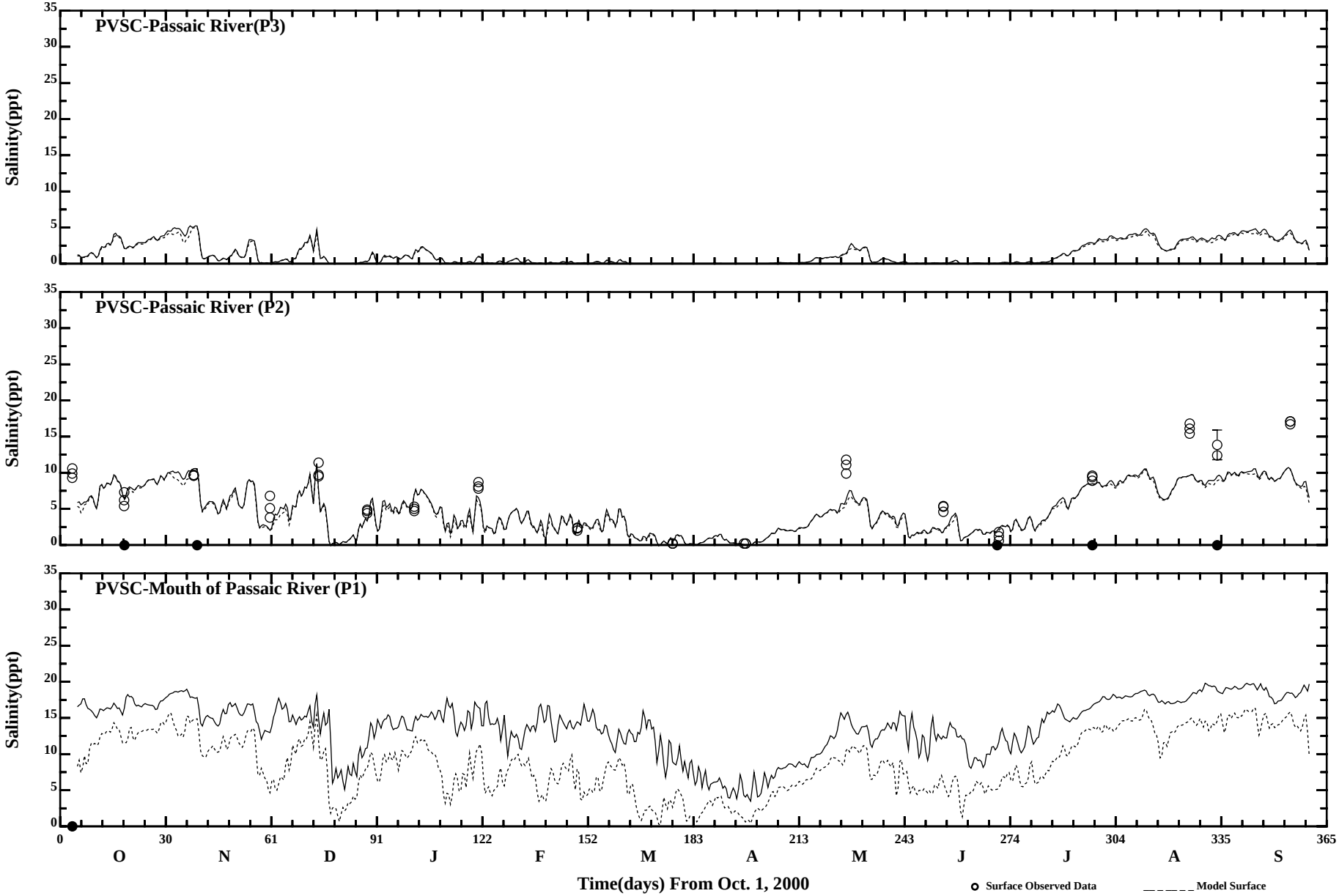

Comparison of 35 Hour Lowpass Surface and Bottom Salinity

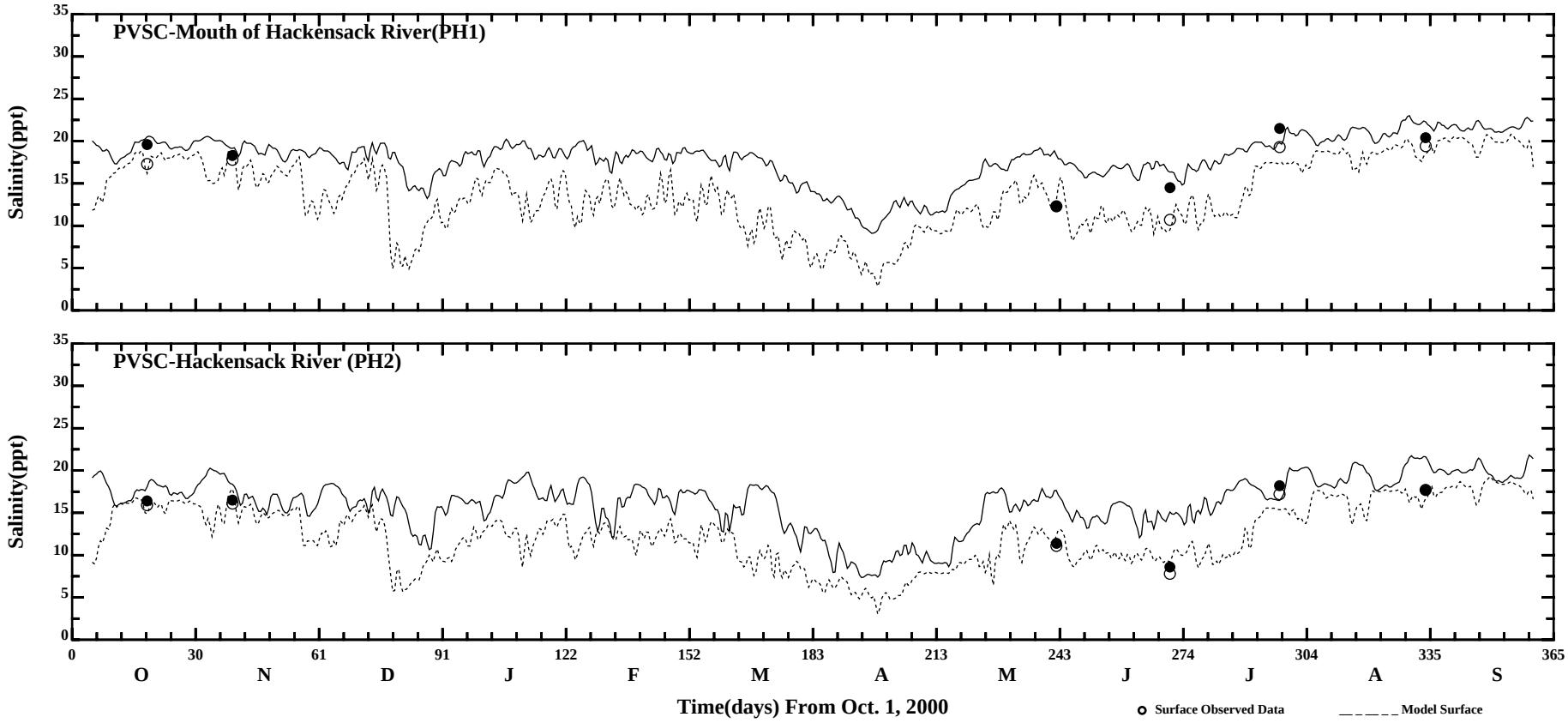

Comparison of 35 Hour Lowpass Surface and Bottom Salinity

/erie1/hrfo0010/HYDRORUNS/CARP0001/PLOTS/TANDS/psalt51_35hlp

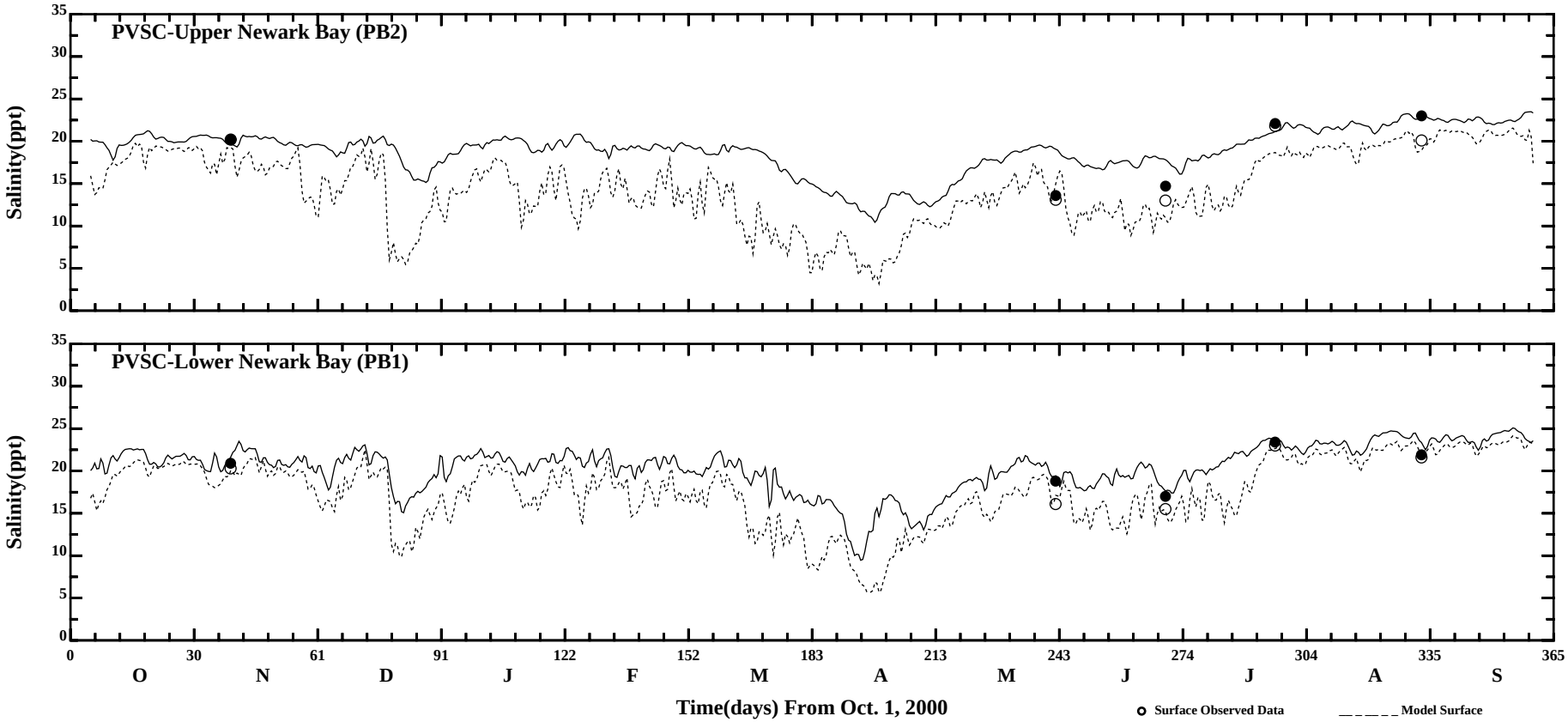

Comparison of 35 Hour Lowpass Surface and Bottom Salinity

/erie1/hrfo0010/HYDRORUNS/CARP0001/PLOTS/TANDS/psalt51_35hlp

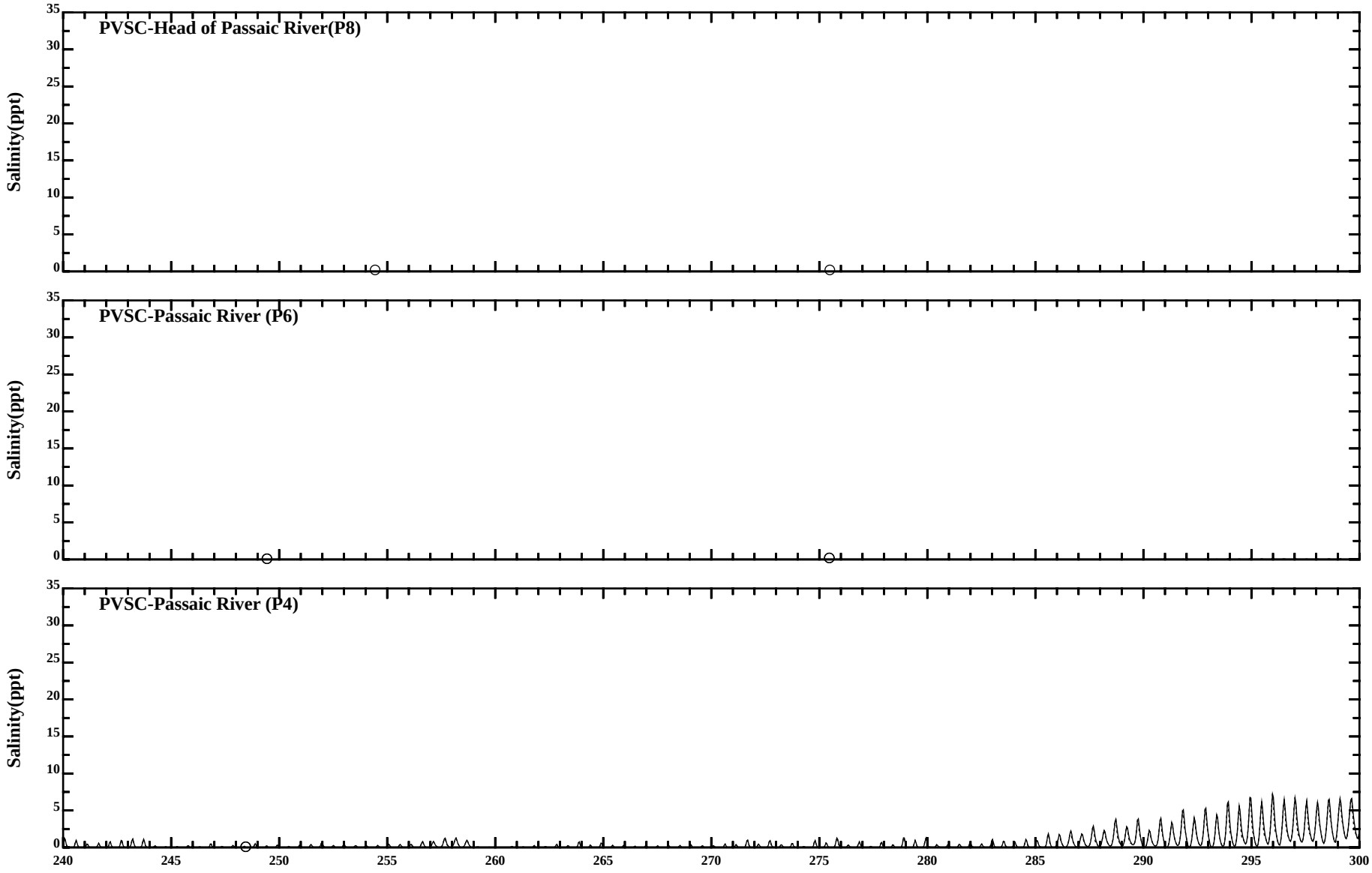

Comparison of Instantaneous Surface and Bottom Salinity

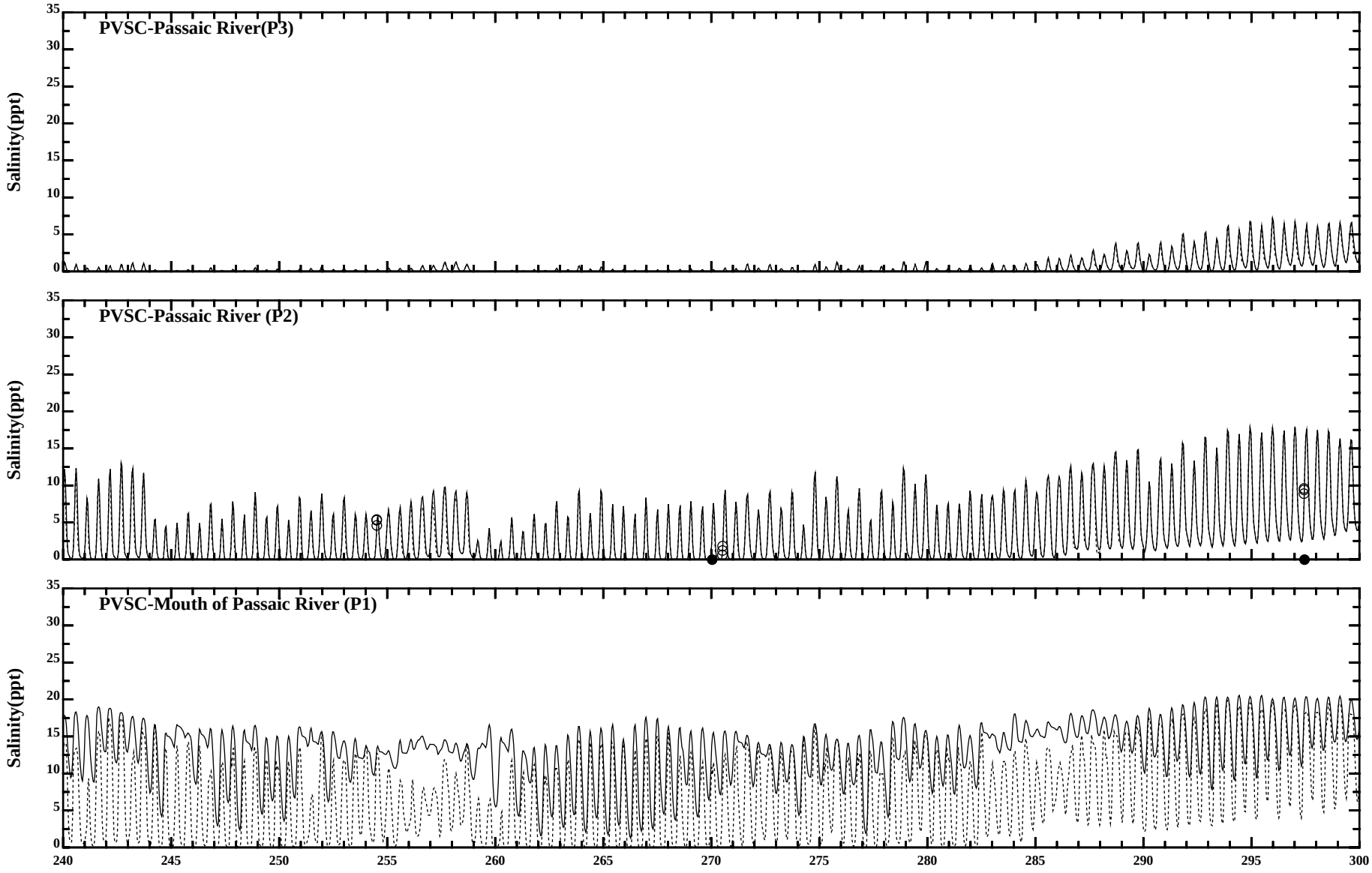

Comparison of Instantaneous Surface and Bottom Salinity

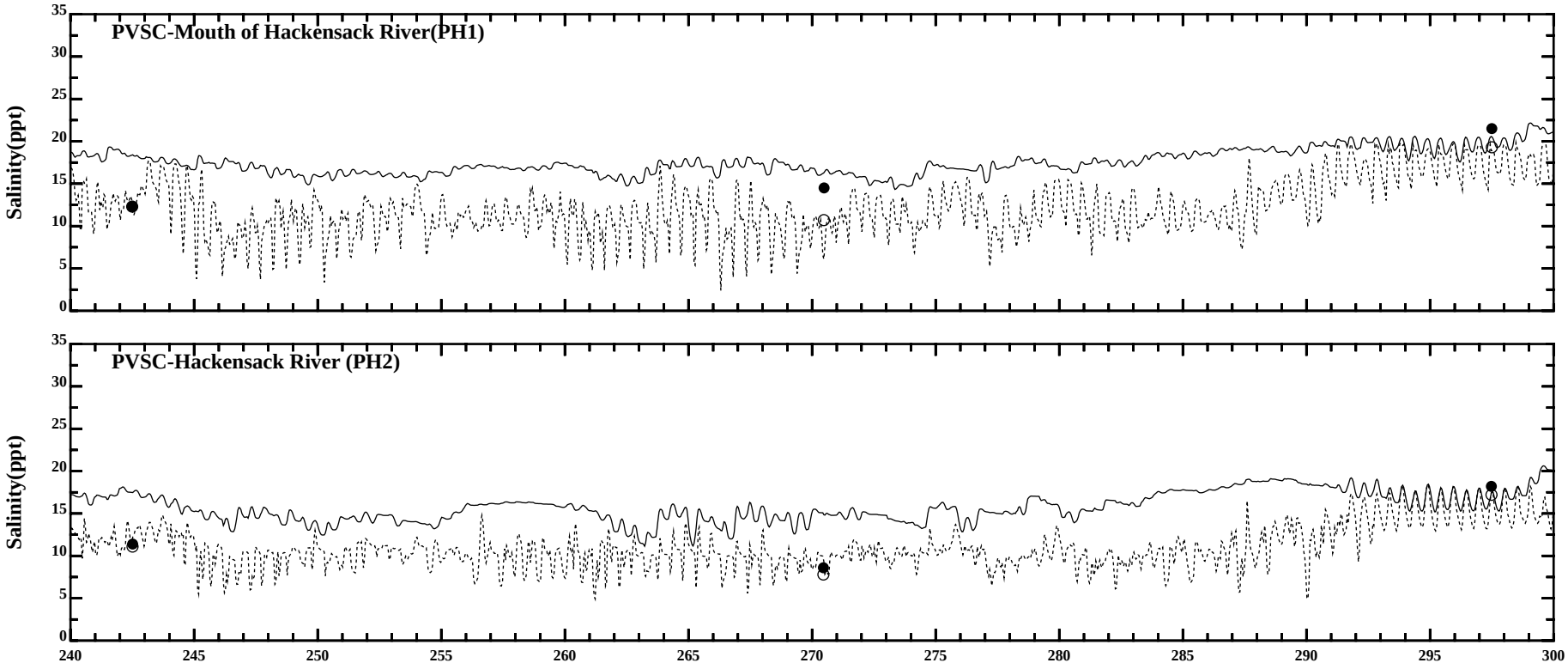

Comparison of Instantaneous Surface and Bottom Salinity

/e1/hrfo0010/HYDRORUNS/CARP0001/PLOTS/TANDS/salt61

DATE: 8/02/2004 TIME: 12:30:11

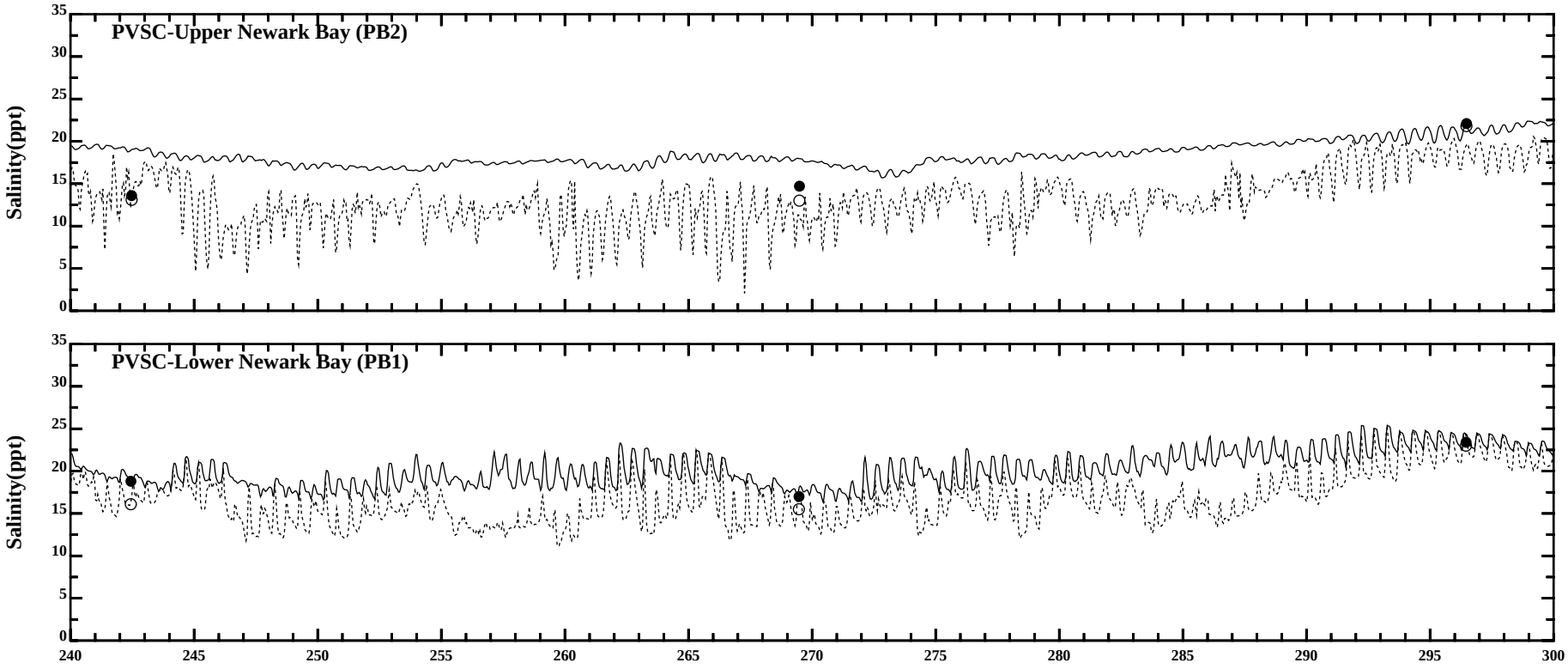

Comparison of Instantaneous Surface and Bottom Salinity

/e1/hrfo0010/HYDRORUNS/CARP0001/PLOTS/TANDS/salt61

DATE: 8/02/2004 TIME: 12:30:11

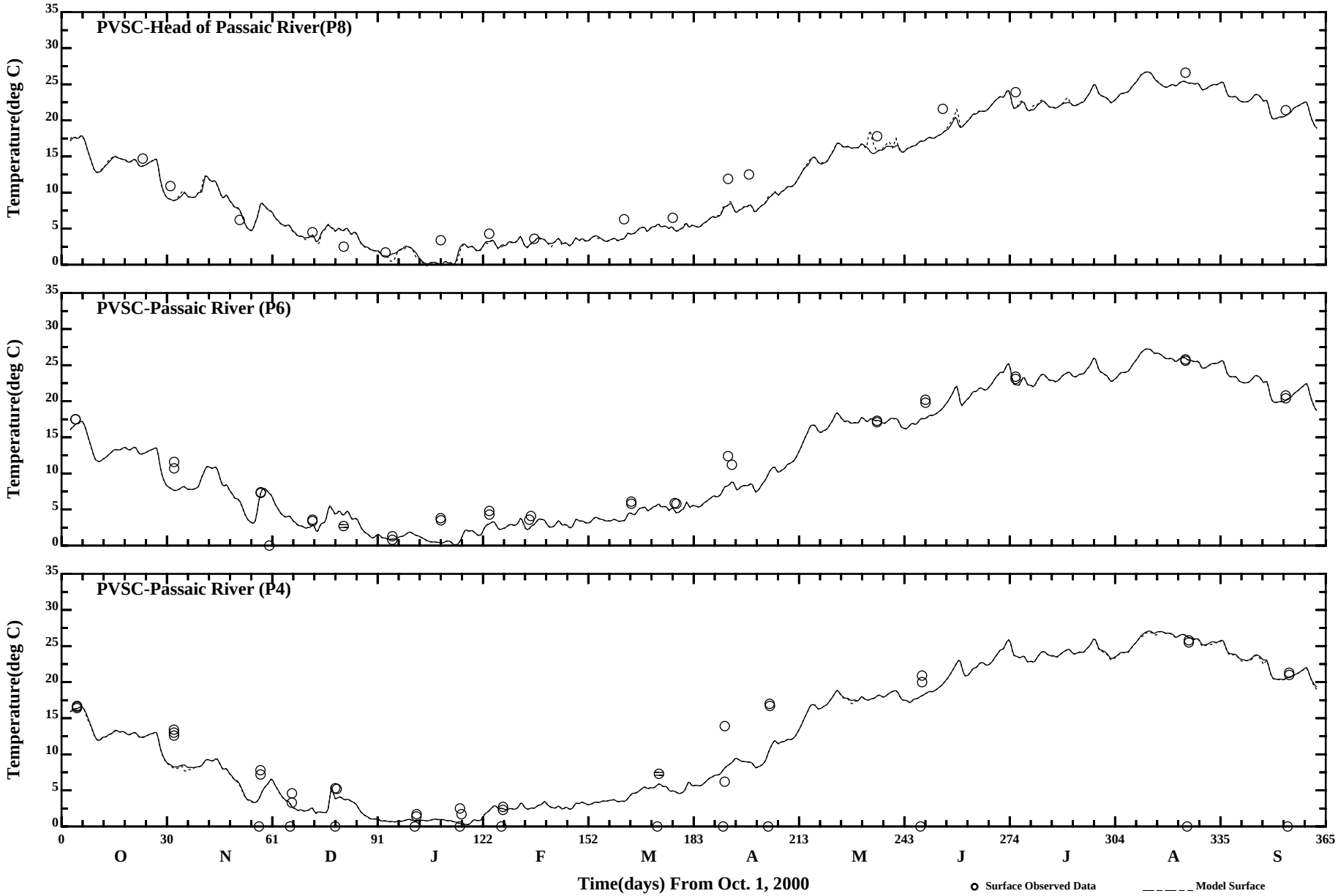

Comparison of 34 Hour Lowpass Surface and Bottom Temperature

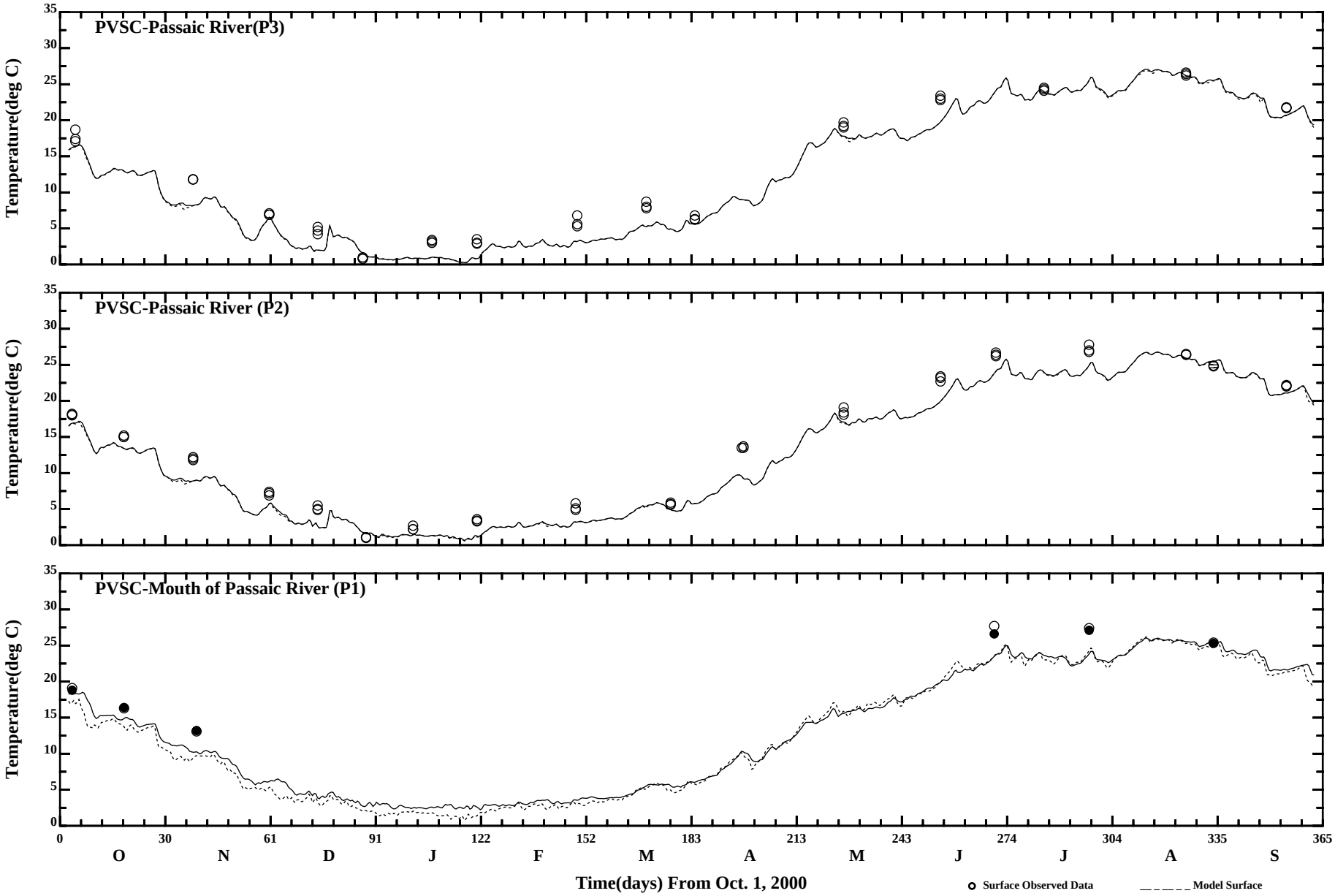

Comparison of 34 Hour Lowpass Surface and Bottom Temperature

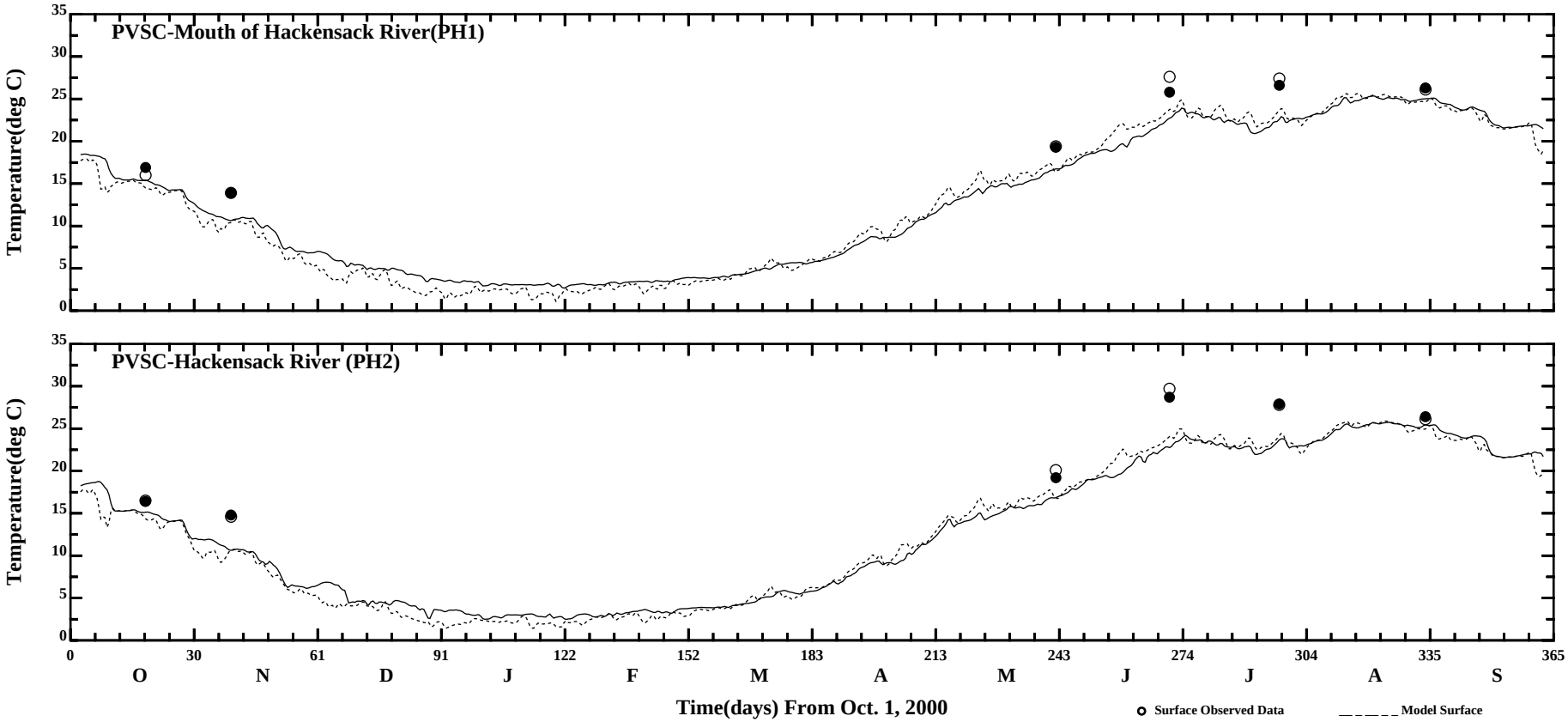

Comparison of 34 Hour Lowpass Surface and Bottom Temperature

/e1/hrfo0010/HYDRORUNS/CARP0001/PLOTS/TANDS/ptemp51_34hlp

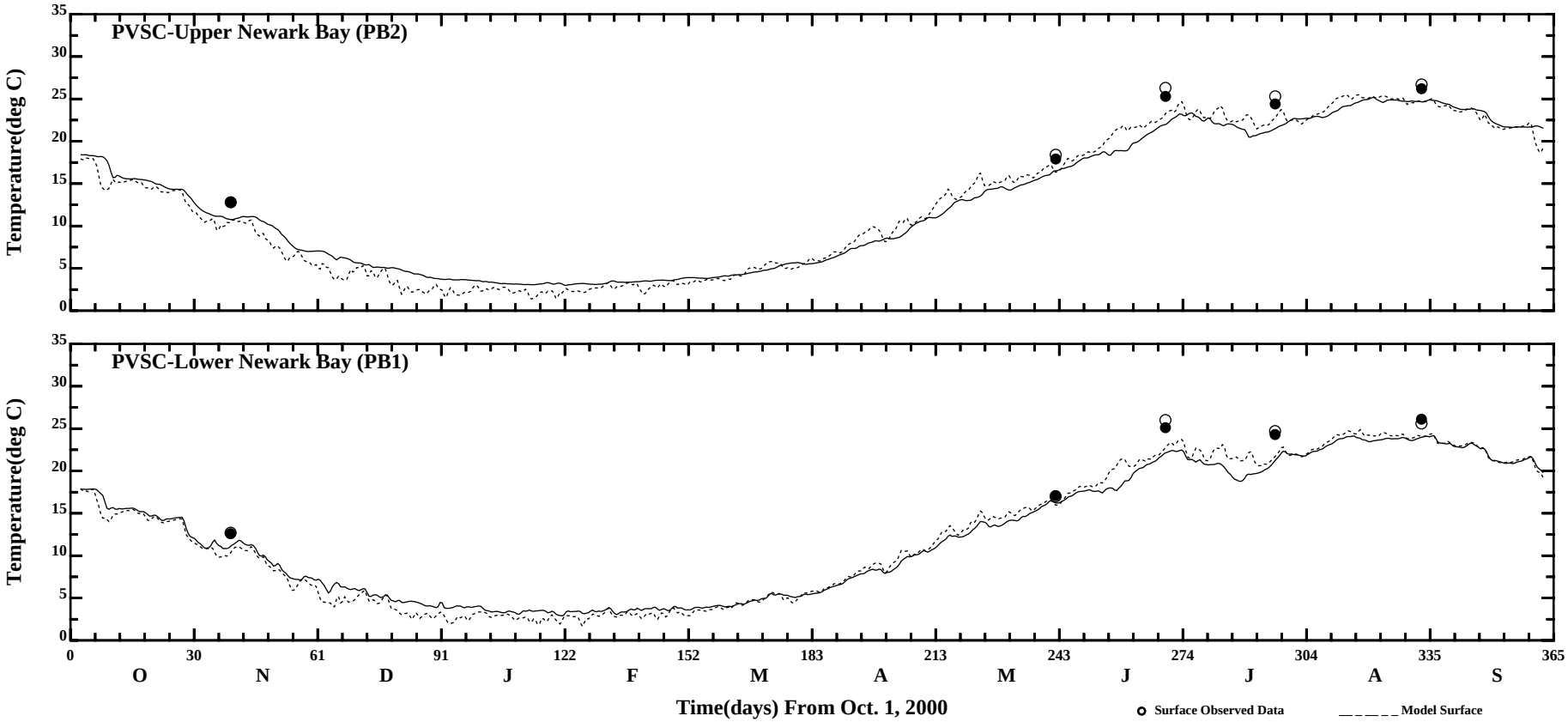

Comparison of 34 Hour Lowpass Surface and Bottom Temperature

/e1/hrfo0010/HYDRORUNS/CARP0001/PLOTS/TANDS/ptemp51_34hlp

DATE: 8/02/2004 TIME: 12:28:58

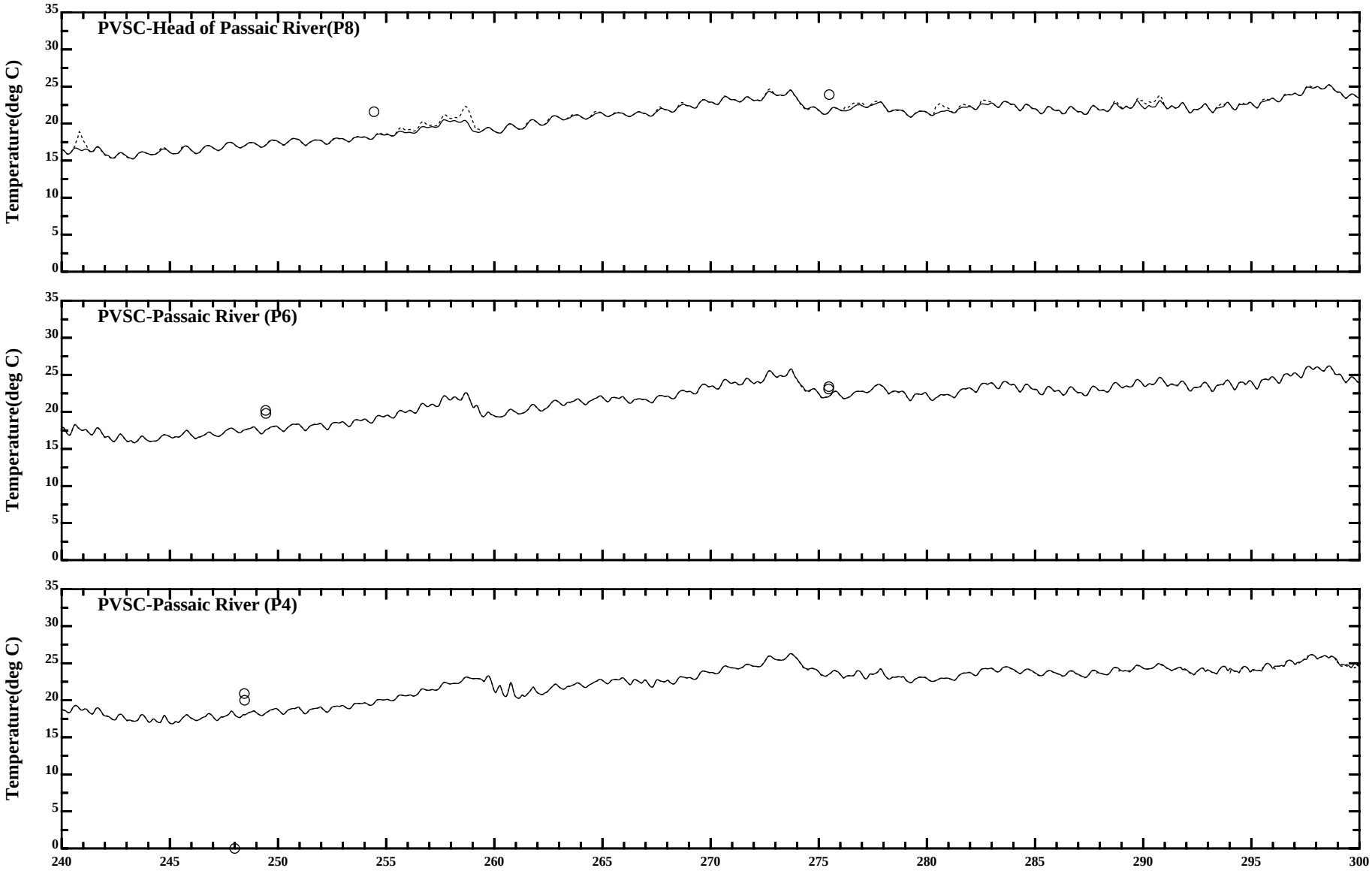

Comparison of Instantaneous Surface and Bottom Temperature

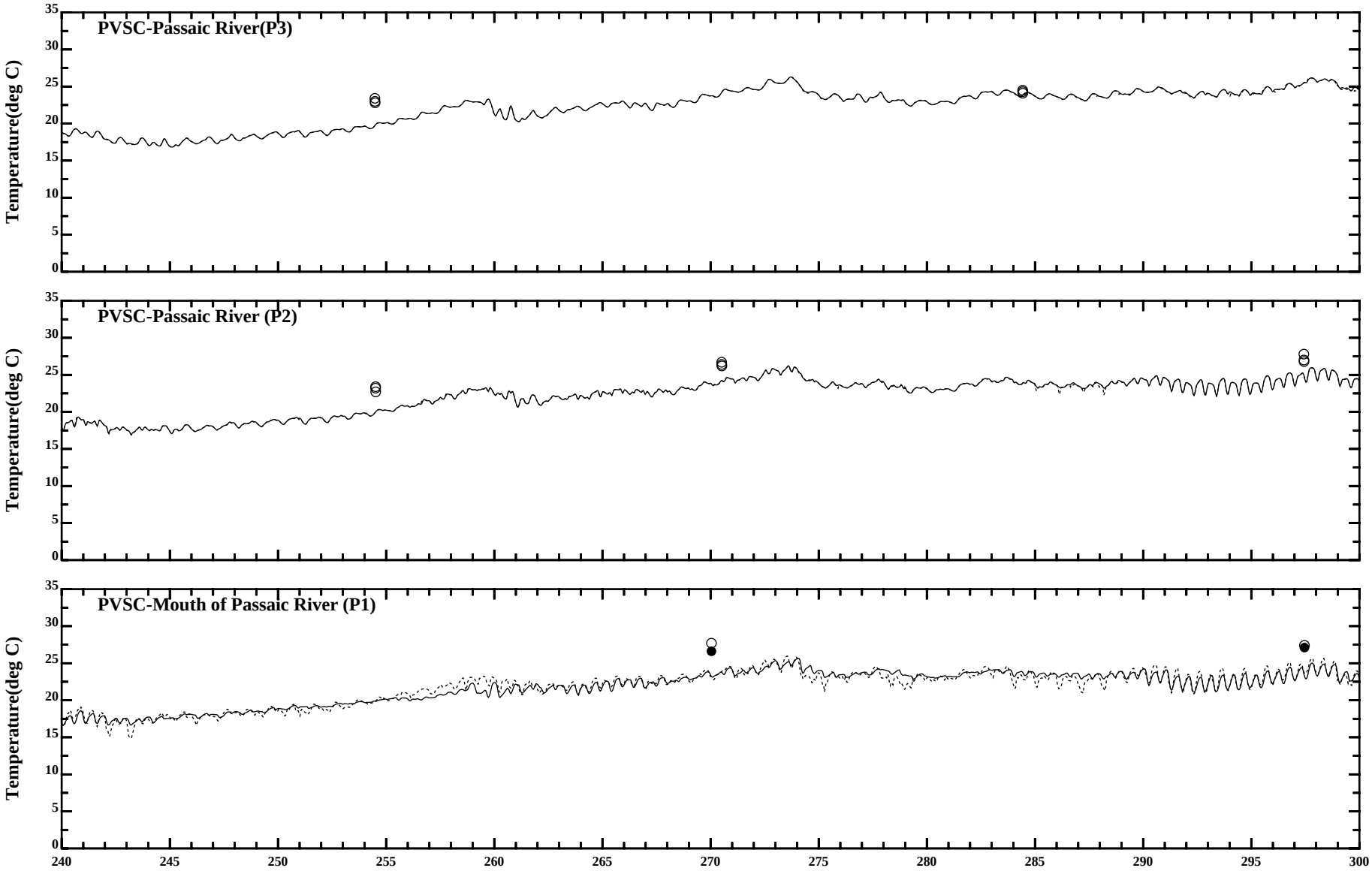

Comparison of Instantaneous Surface and Bottom Temperature

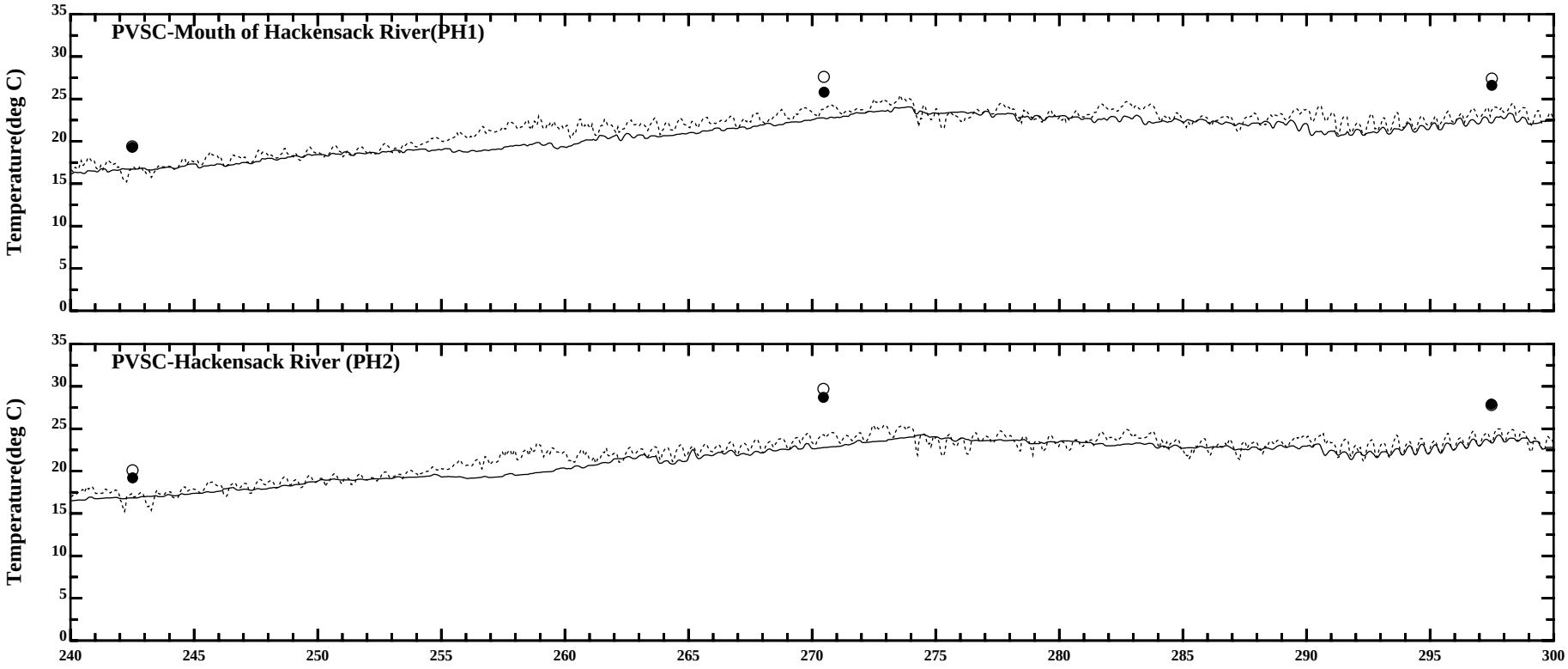

Comparison of Instantaneous Surface and Bottom Temperature

/e1/hrfo0010/HYDRORUNS/CARP0001/PLOTS/TANDS/temp61

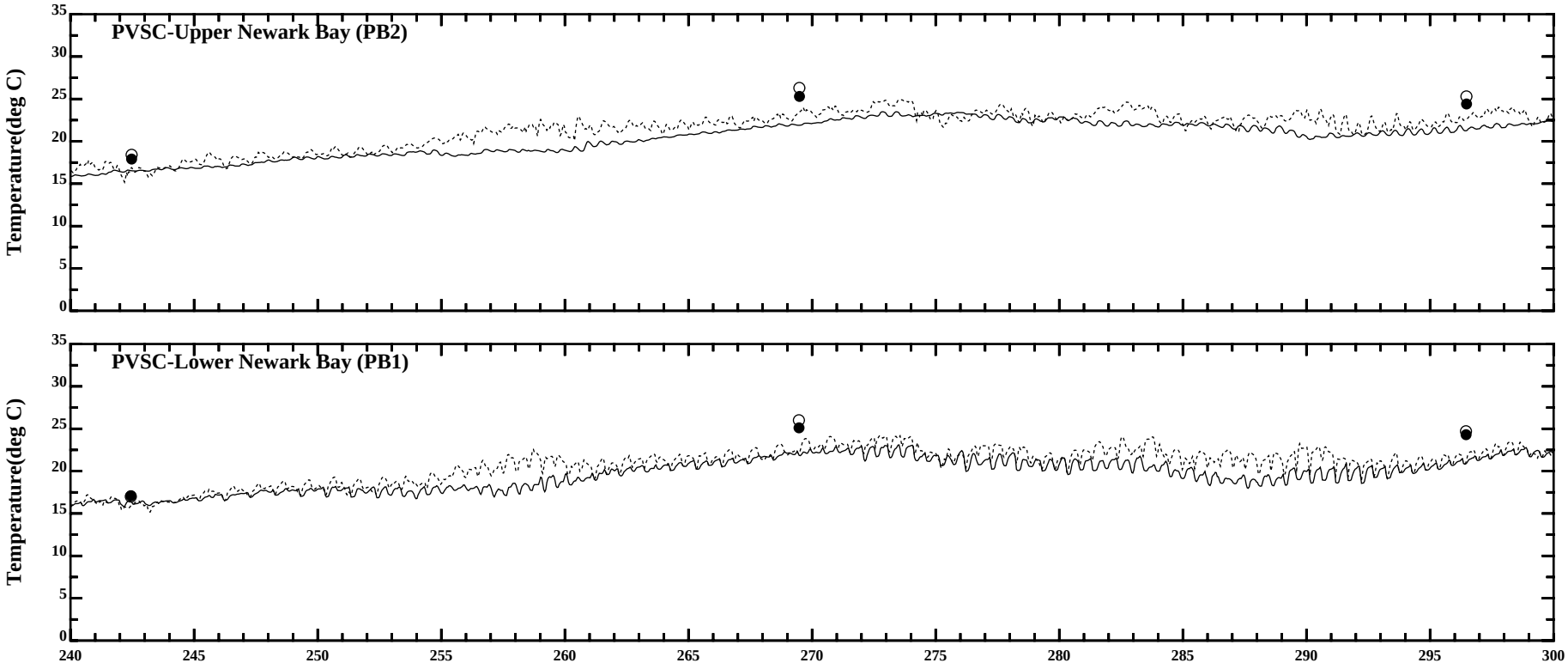

Comparison of Instantaneous Surface and Bottom Temperature

/e1/hrfo0010/HYDRORUNS/CARP0001/PLOTS/TANDS/temp61

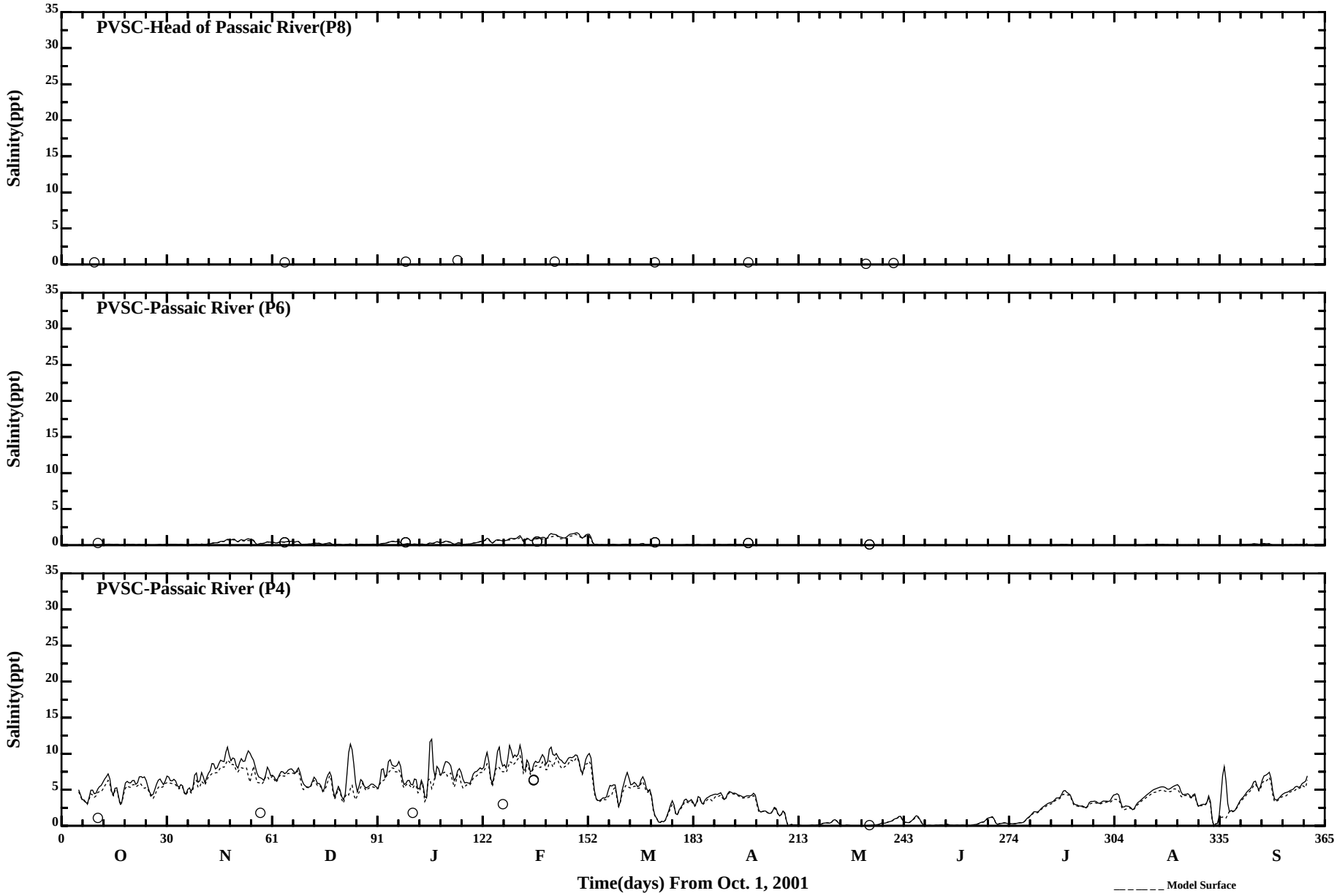

Comparison of 35 Hour Lowpass Surface and Bottom Salinity

/ont6/hrfo0010/RUNS/ECOMSED-SED/ECOMSED-0102/PLOTS/TANDS/salt_pass_35hlp

DATE: 11/21/2003 TIME: 10:41:55

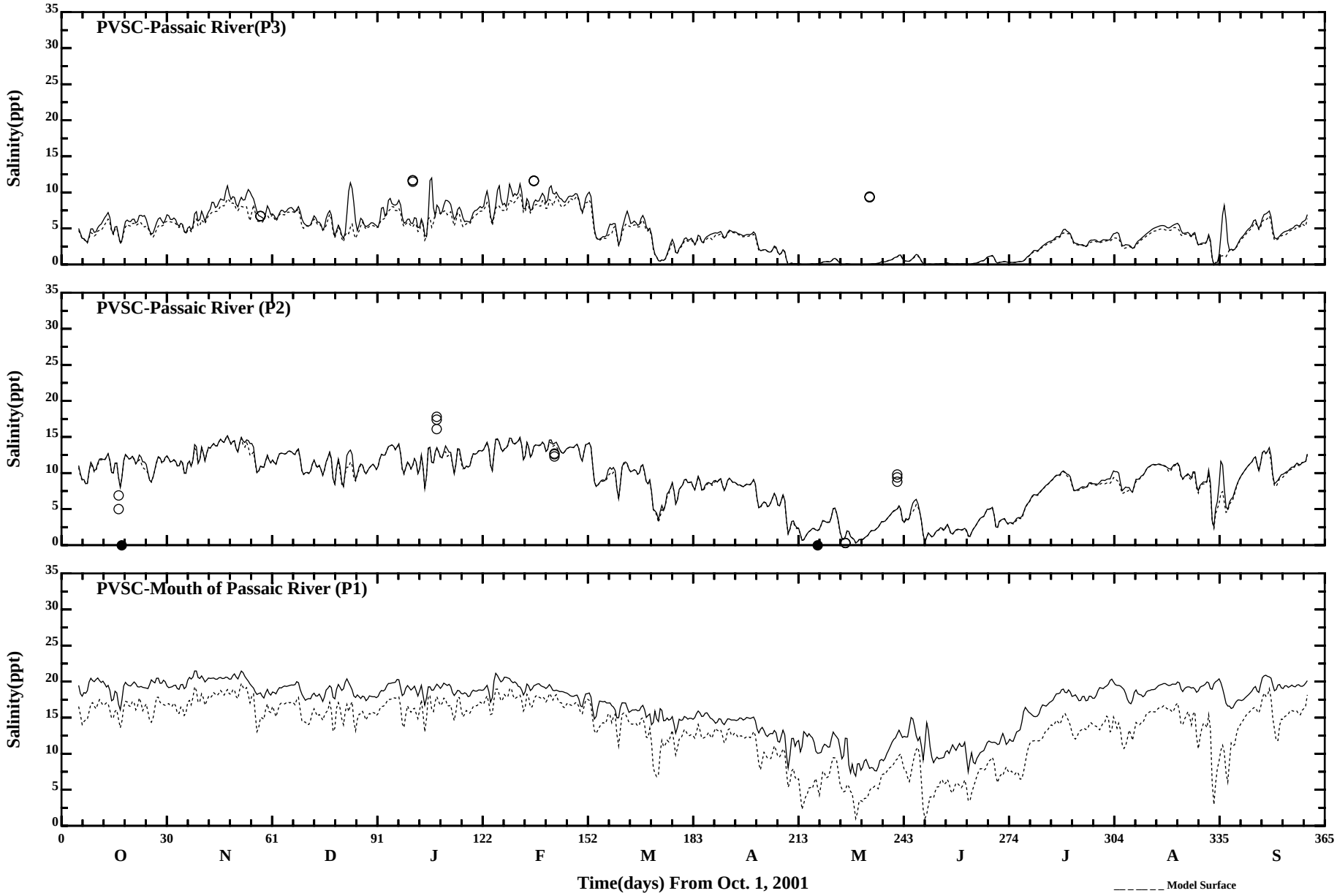

Comparison of 35 Hour Lowpass Surface and Bottom Salinity

/ont6/hrfo0010/RUNS/ECOMSED-SED/ECOMSED-0102/PLOTS/TANDS/salt_pass_35hlp

DATE: 11/21/2003 TIME: 10:41:55

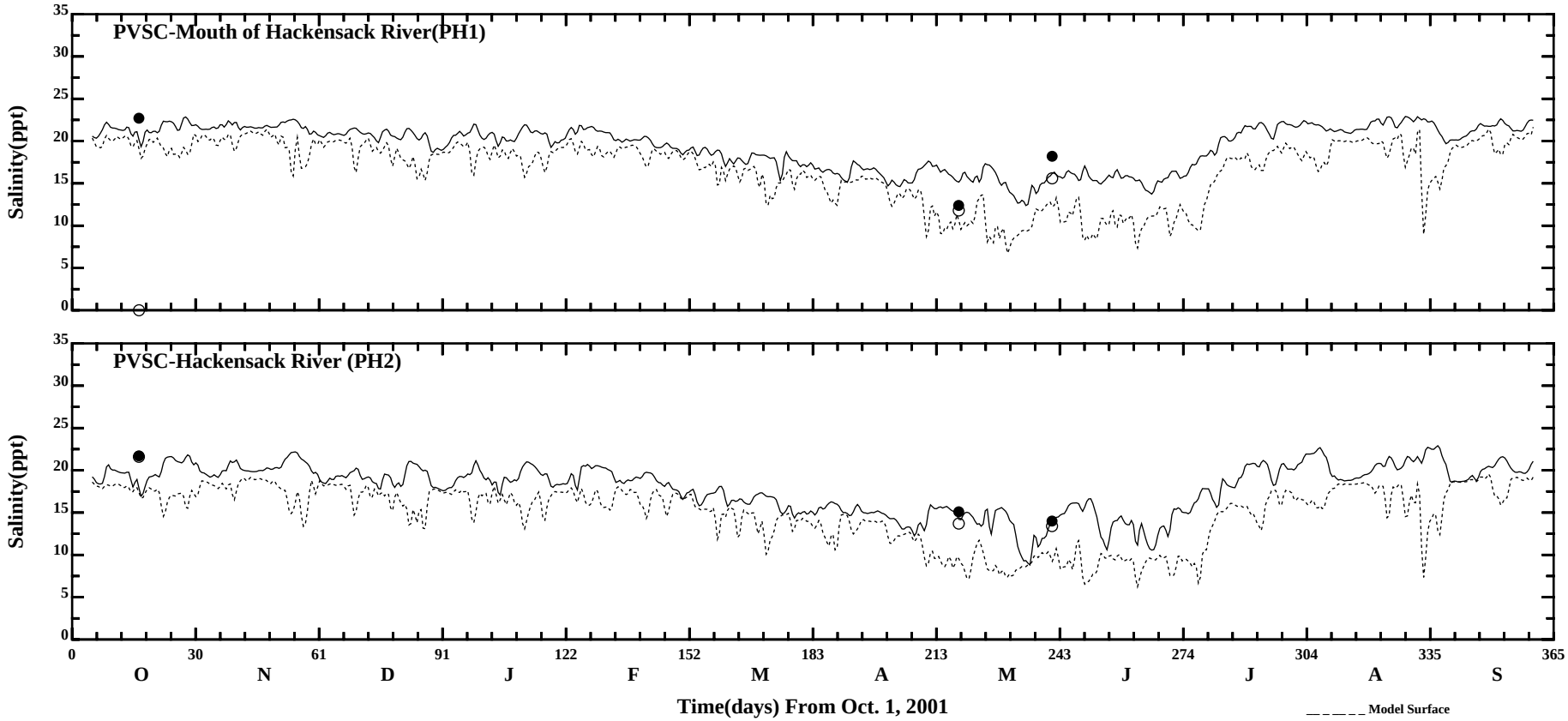

Comparison of 35 Hour Lowpass Surface and Bottom Salinity

/ont6/hrfo0010/RUNS/ECOMSED-SED/ECOMSED-0102/PLOTS/TANDS/salt_pass_35hlp

DATE: 11/21/2003 TIME: 10:41:55

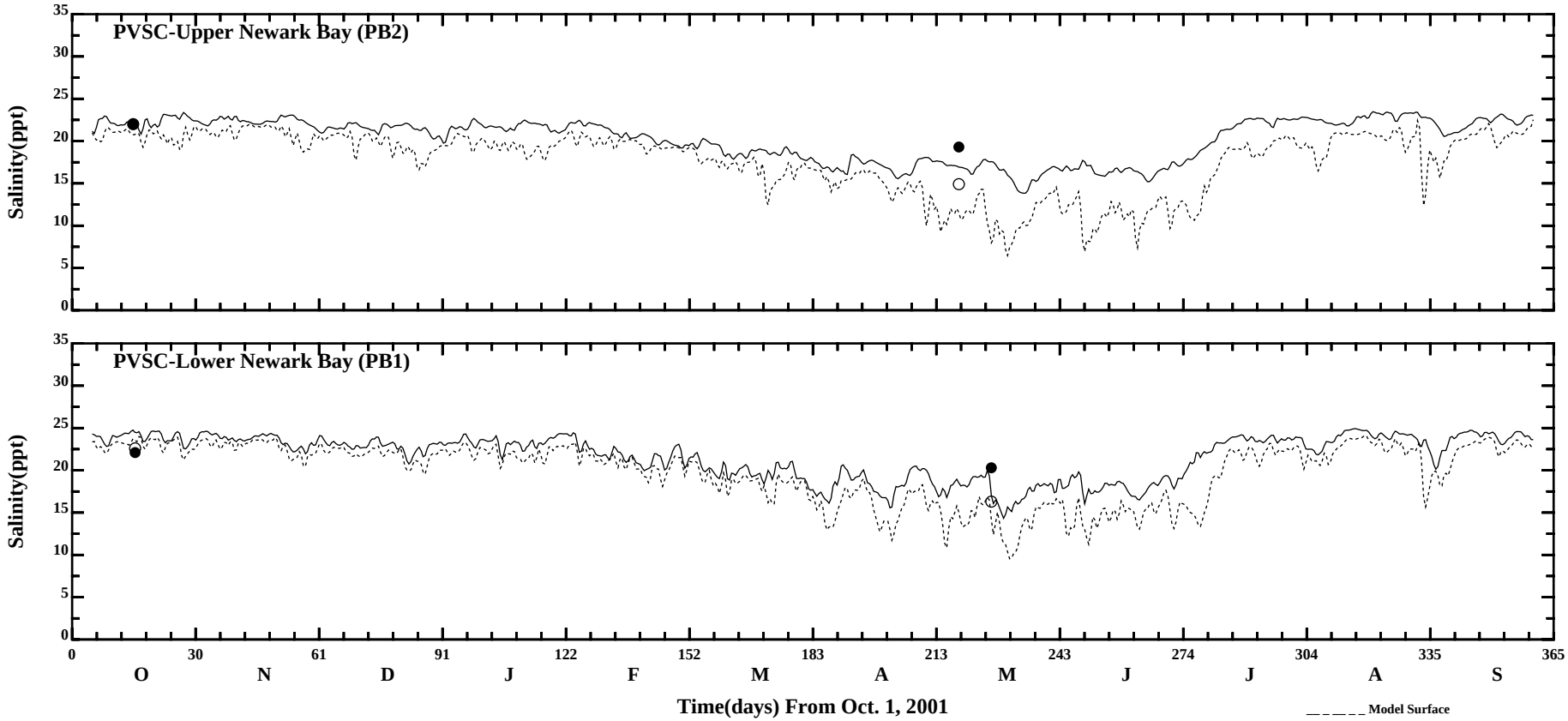

Comparison of 35 Hour Lowpass Surface and Bottom Salinity

/ont6/hrfo0010/RUNS/ECOMSED-SED/ECOMSED-0102/PLOTS/TANDS/salt_pass_35hlp

DATE: 11/21/2003 TIME: 10:41:55

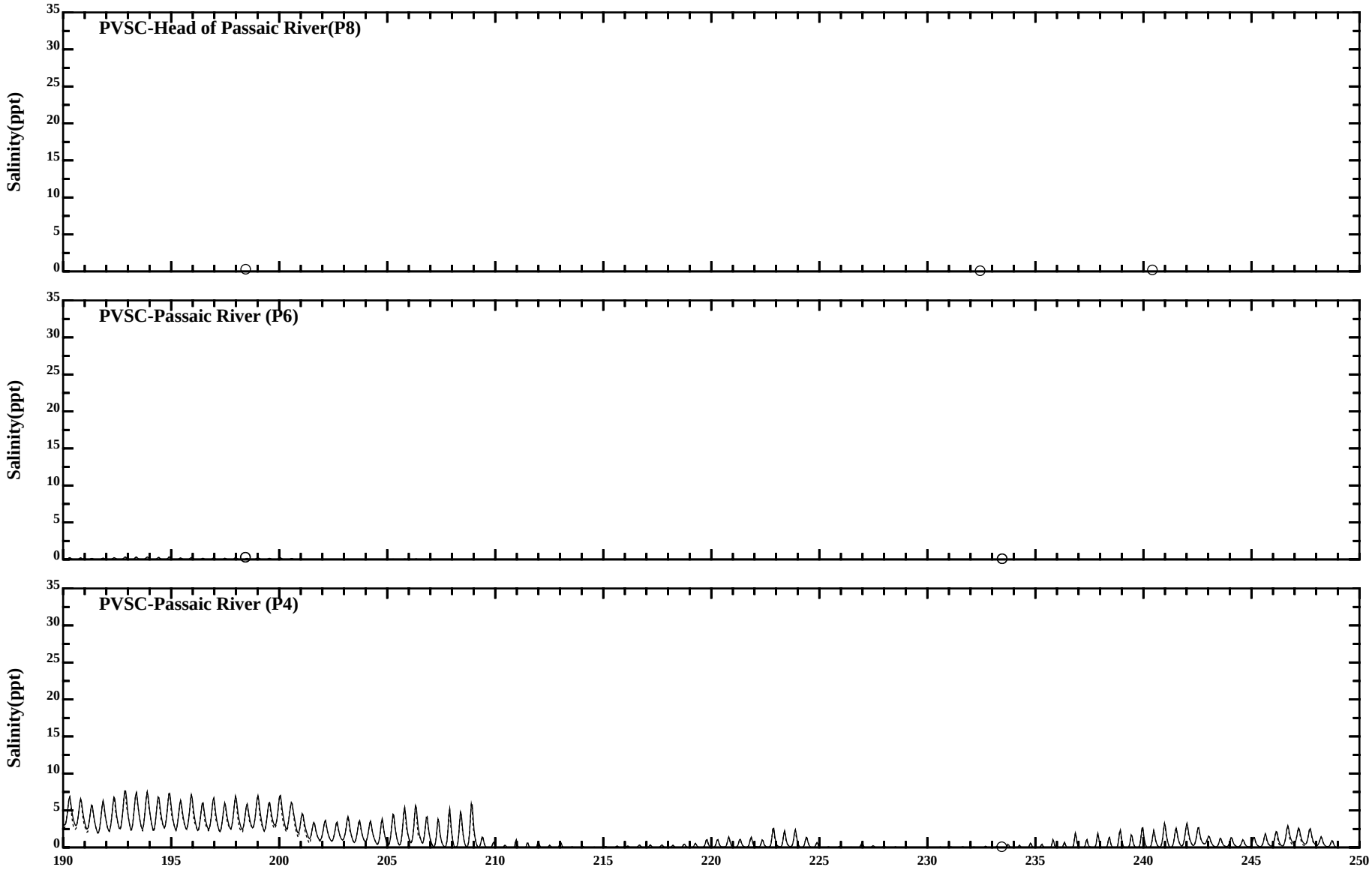

Comparison of Instantaneous Surface and Bottom Salinity

/ont6/hrfo0010/RUNS/ECOMSED-SED/ECOMSED-0102/PLOTS/TANDS/salt_pass_hrly

DATE: 11/21/2003 TIME: 10:42: 1

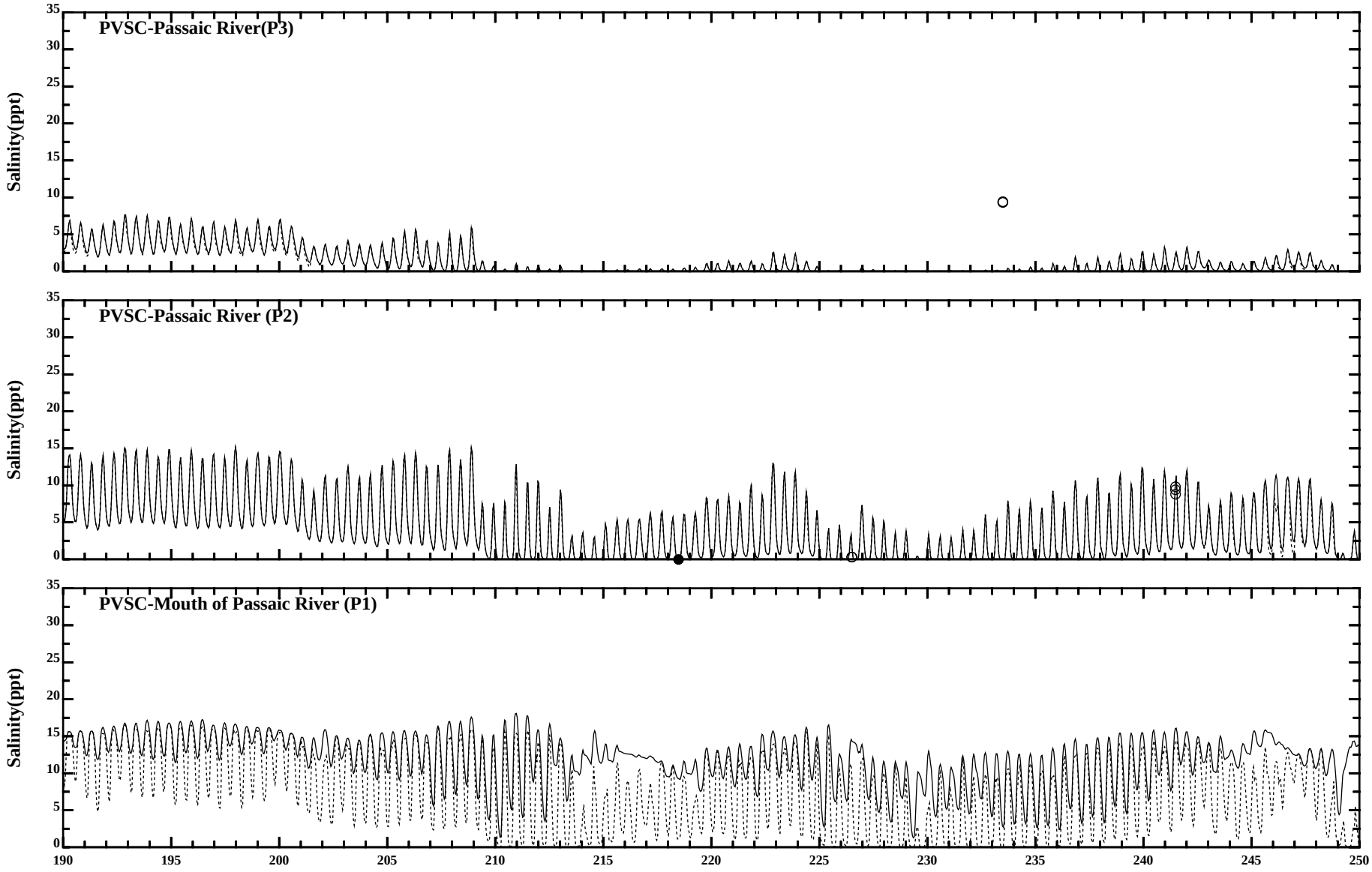

Comparison of Instantaneous Surface and Bottom Salinity

/ont6/hrfo0010/RUNS/ECOMSED-SED/ECOMSED-0102/PLOTS/TANDS/salt_pass_hrly

DATE: 11/21/2003 TIME: 10:42: 1

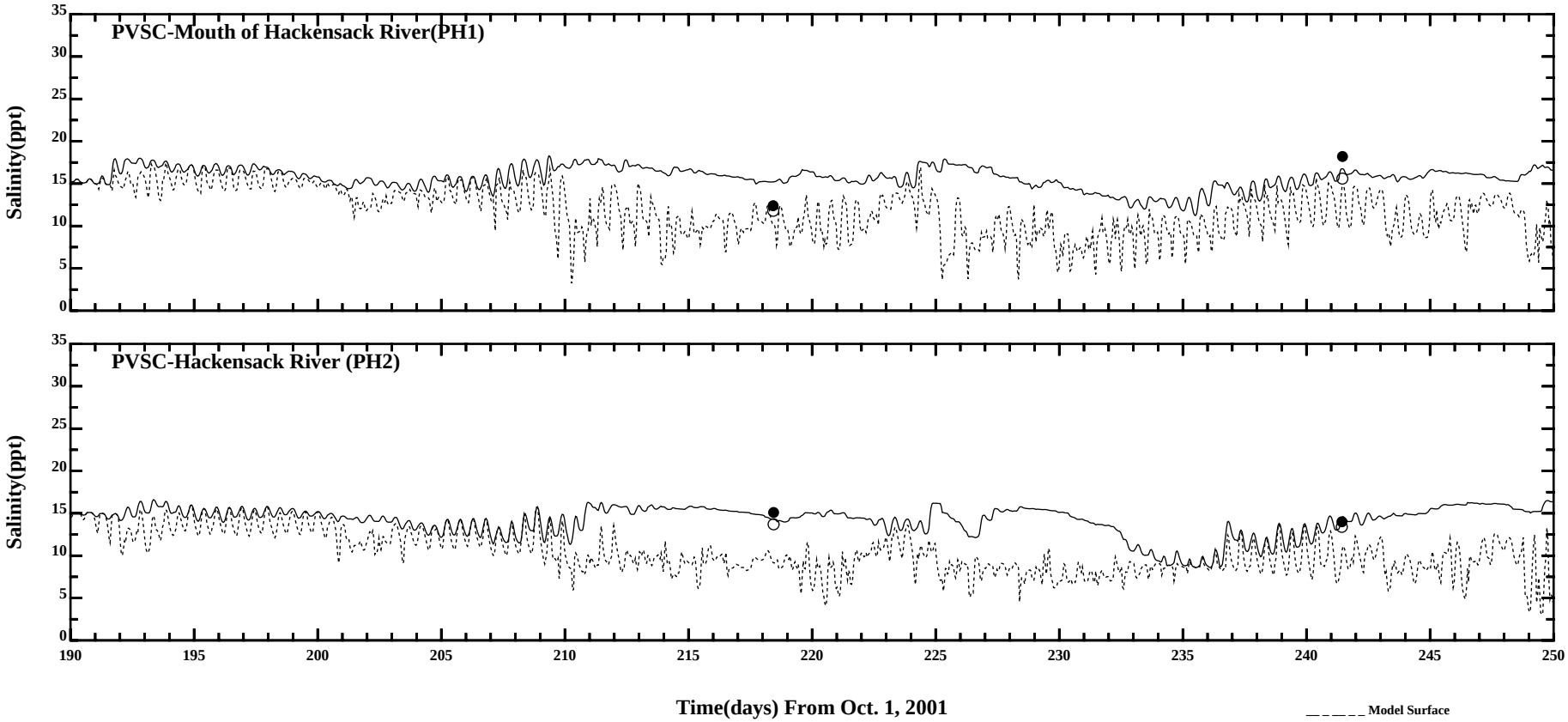

Comparison of Instantaneous Surface and Bottom Salinity

/ont6/hrfo0010/RUNS/ECOMSED-SED/ECOMSED-0102/PLOTS/TANDS/salt_pass_hrly

DATE: 11/21/2003 TIME: 10:42: 1

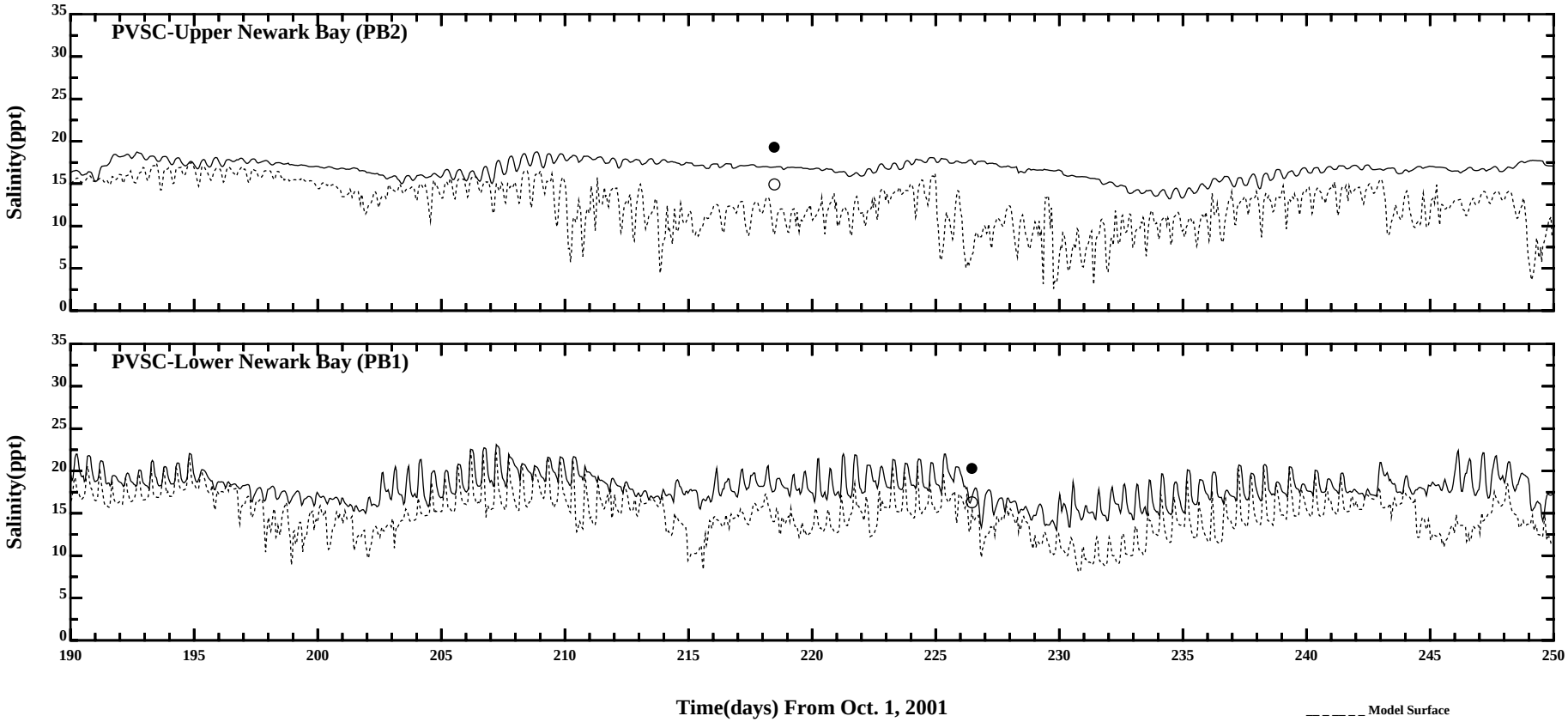

Comparison of Instantaneous Surface and Bottom Salinity

/ont6/hrfo0010/RUNS/ECOMSED-SED/ECOMSED-0102/PLOTS/TANDS/salt_pass_hrly

DATE: 11/21/2003 TIME: 10:42: 1

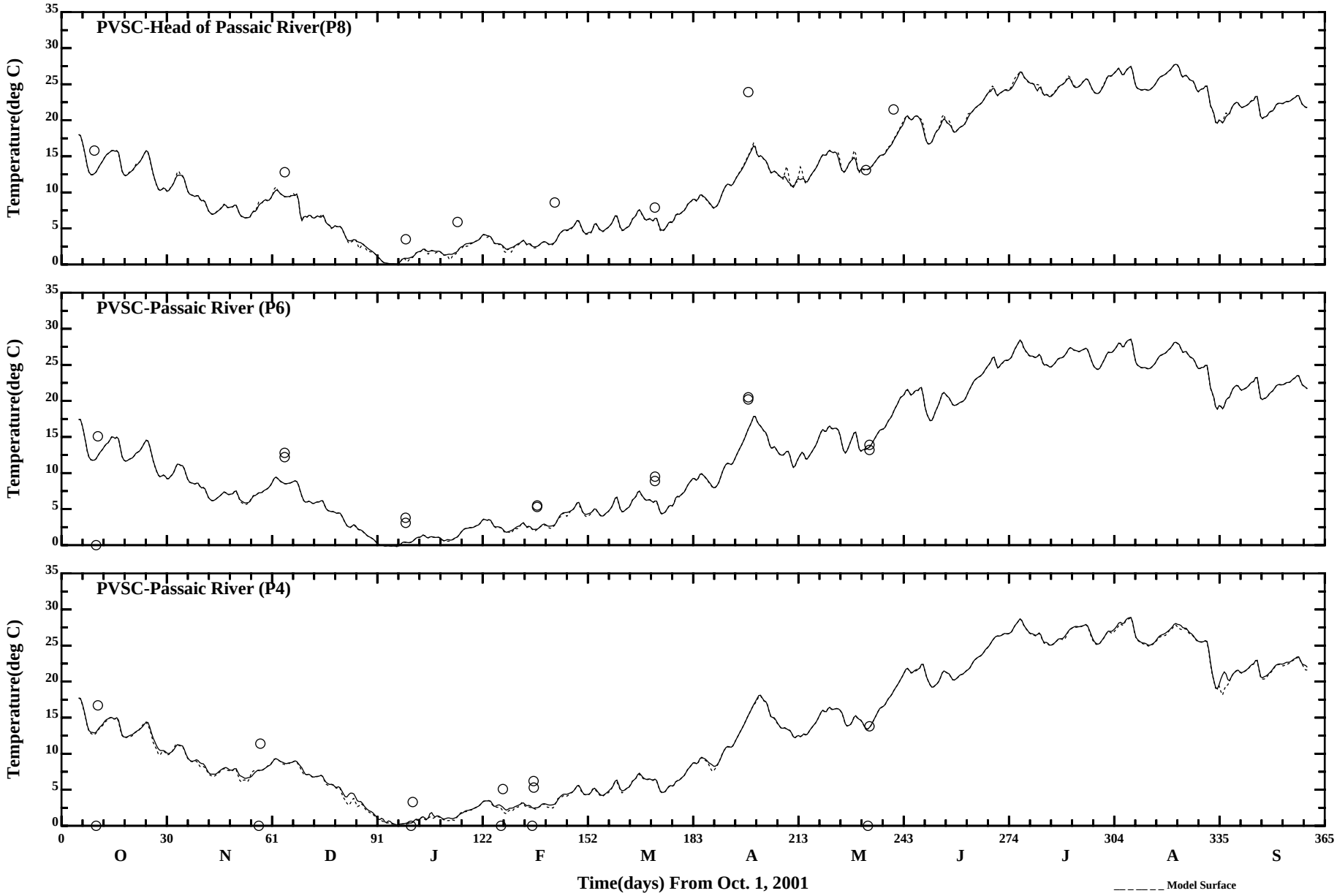

Comparison of 35 Hour Lowpass Surface and Bottom Temperature

/ont6/hrfo0010/RUNS/ECOMSED-SED/ECOMSED-0102/PLOTS/TANDS/temp_pass_35hlp

DATE: 11/21/2003 TIME: 10:40:18

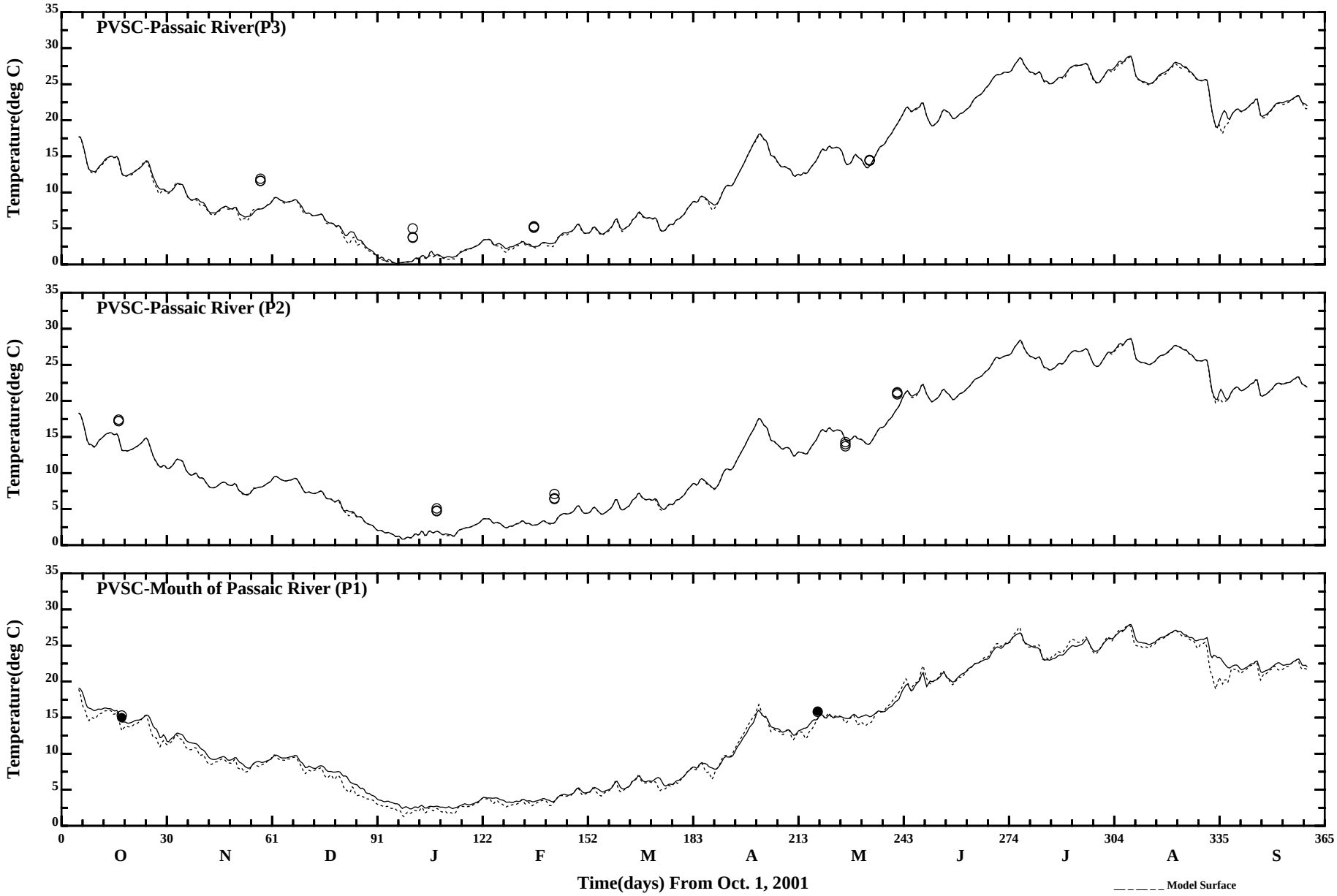

Comparison of 35 Hour Lowpass Surface and Bottom Temperature

/ont6/hrfo0010/RUNS/ECOMSED-SED/ECOMSED-0102/PLOTS/TANDS/temp_pass_35hlp

DATE: 11/21/2003 TIME: 10:40:18

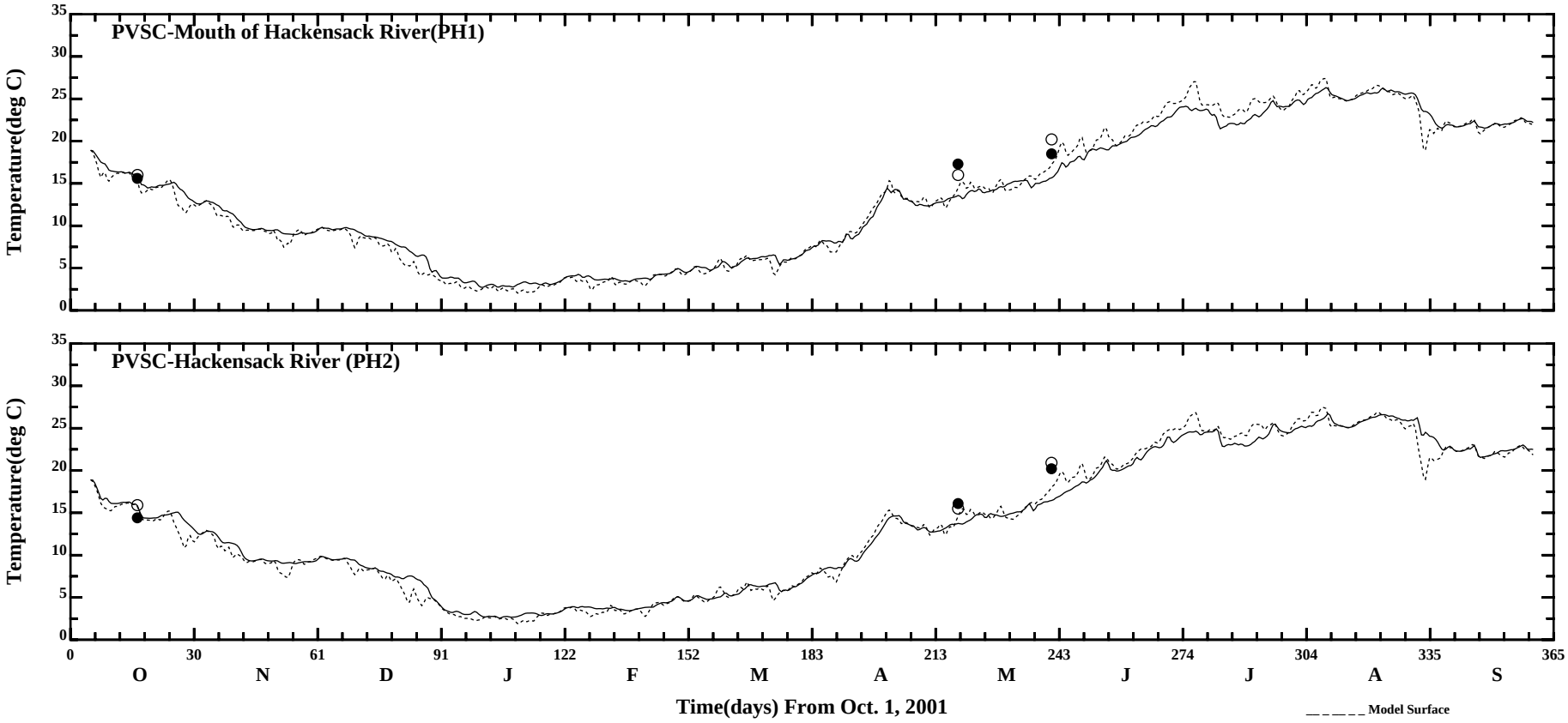

Comparison of 35 Hour Lowpass Surface and Bottom Temperature

/ont6/hrfo0010/RUNS/ECOMSED-SED/ECOMSED-0102/PLOTS/TANDS/temp_pass_35hlp

DATE: 11/21/2003 TIME: 10:40:18

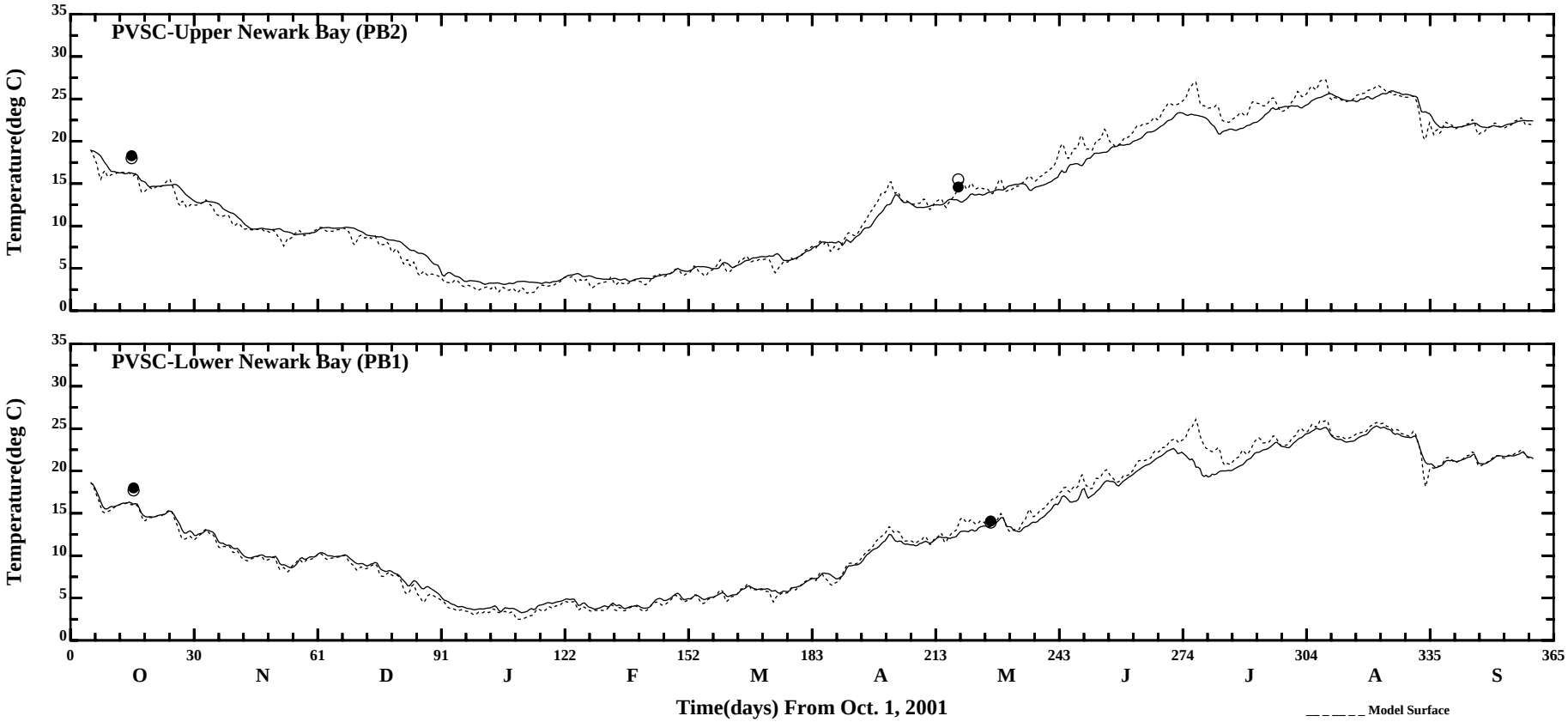

Comparison of 35 Hour Lowpass Surface and Bottom Temperature

/ont6/hrfo0010/RUNS/ECOMSED-SED/ECOMSED-0102/PLOTS/TANDS/temp_pass_35hlp

DATE: 11/21/2003 TIME: 10:40:18

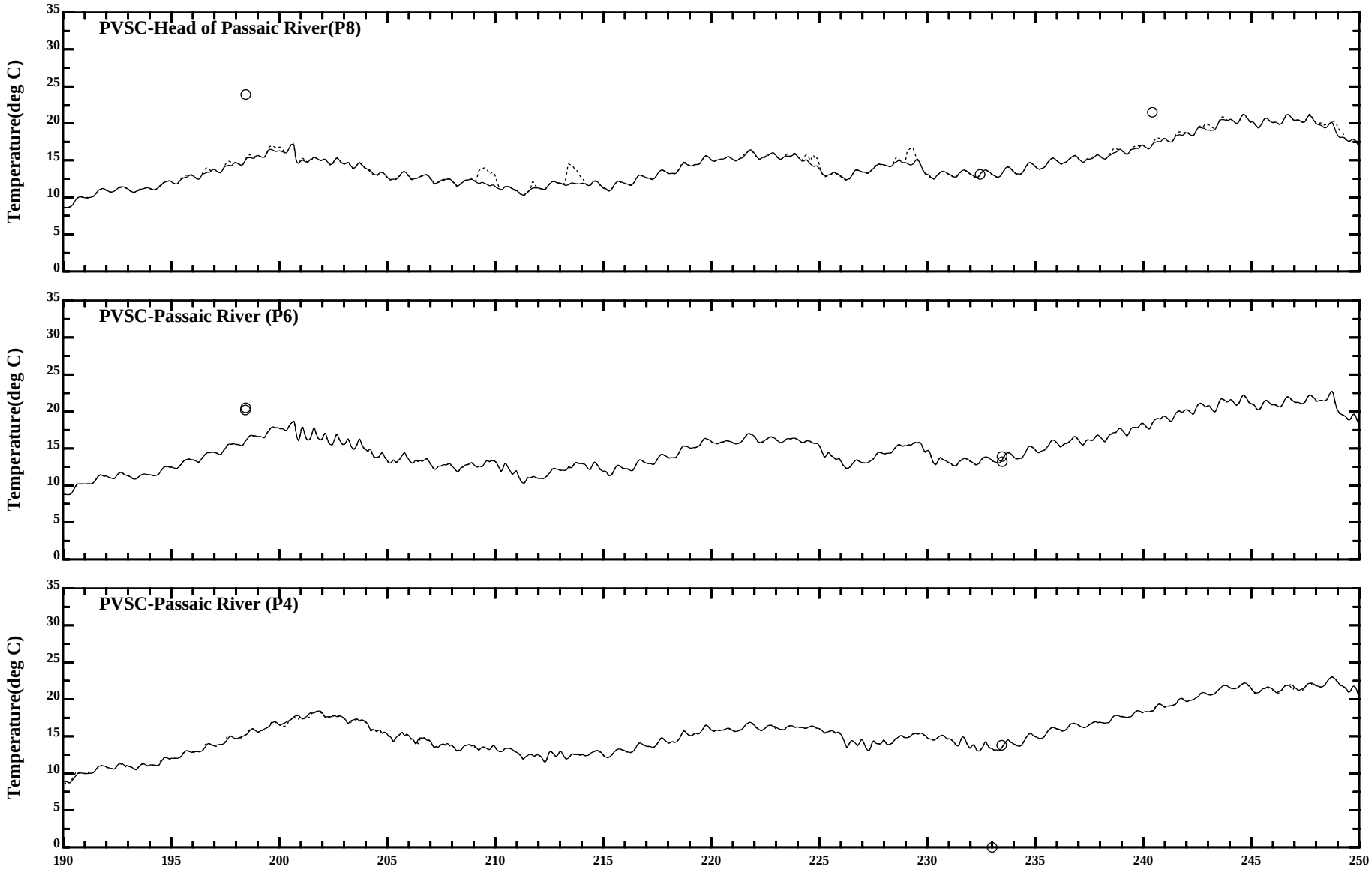

Comparison of Instantaneous Surface and Bottom Temperature

/ont6/hrfo0010/RUNS/ECOMSED-SED/ECOMSED-0102/PLOTS/TANDS/temp_pass_hrly

DATE: 11/21/2003 TIME: 10:40:24

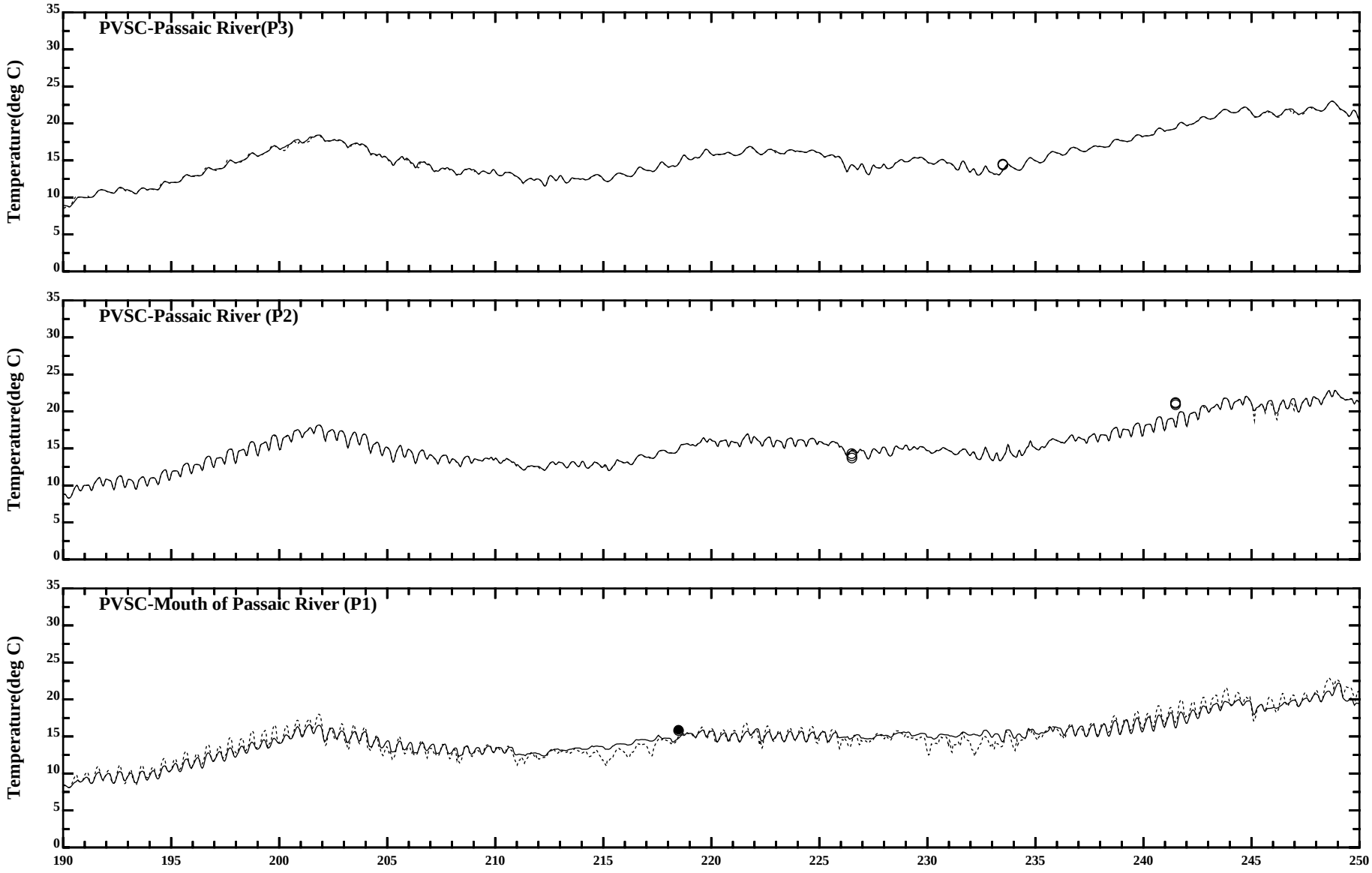

Comparison of Instantaneous Surface and Bottom Temperature

/ont6/hrfo0010/RUNS/ECOMSED-SED/ECOMSED-0102/PLOTS/TANDS/temp_pass_hrly

DATE: 11/21/2003 TIME: 10:40:24

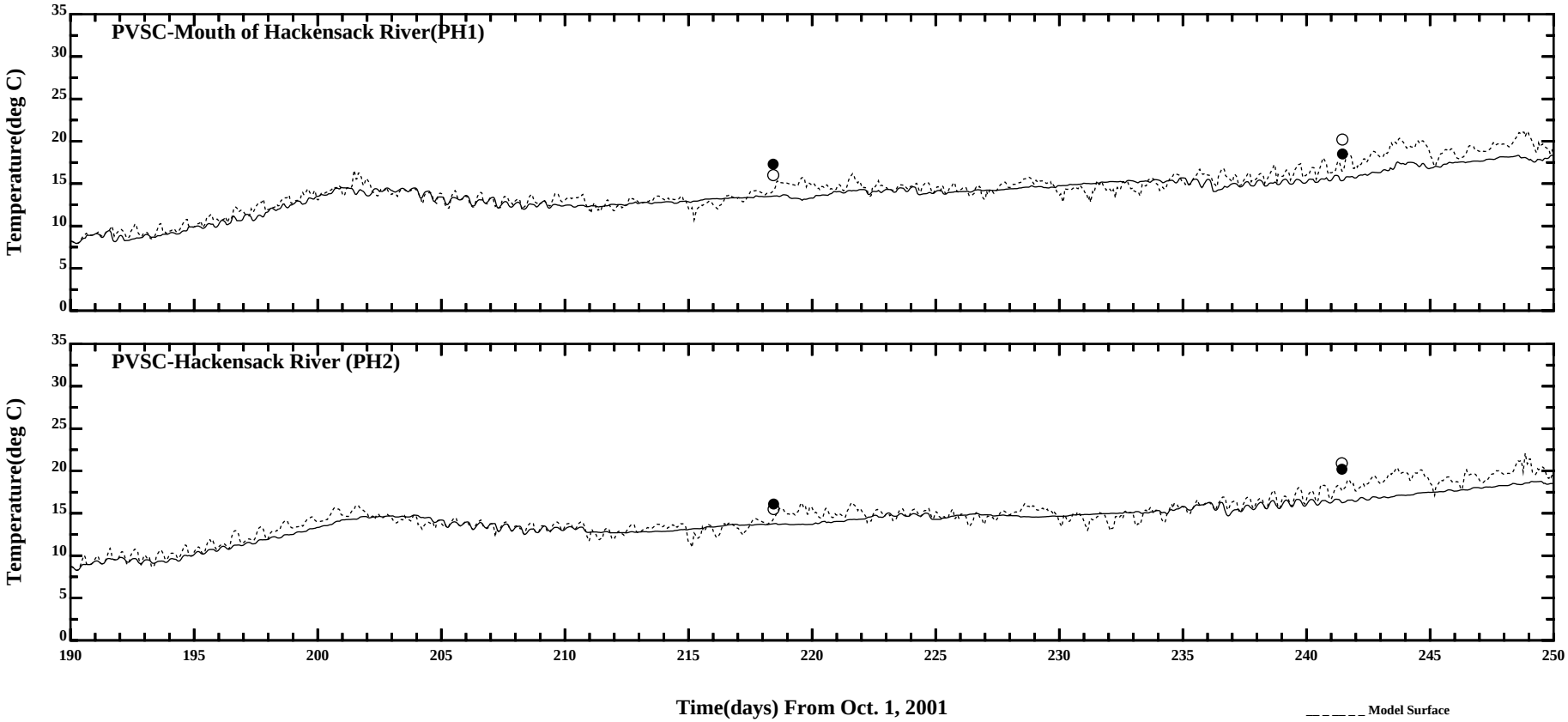

Comparison of Instantaneous Surface and Bottom Temperature

/ont6/hrfo0010/RUNS/ECOMSED-SED/ECOMSED-0102/PLOTS/TANDS/temp_pass_hrly

DATE: 11/21/2003 TIME: 10:40:24

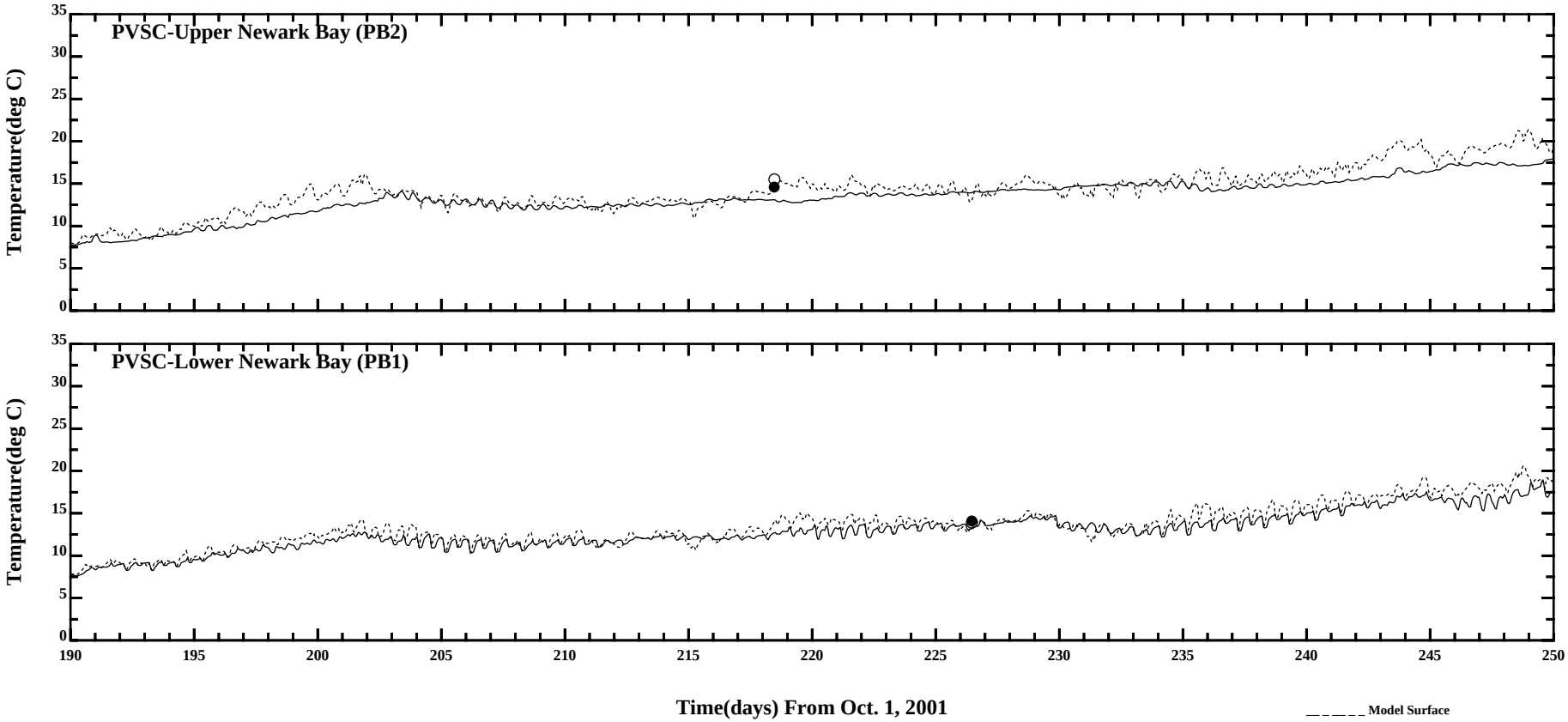

Comparison of Instantaneous Surface and Bottom Temperature

/ont6/hrfo0010/RUNS/ECOMSED-SED/ECOMSED-0102/PLOTS/TANDS/temp_pass_hrly

DATE: 11/21/2003 TIME: 10:40:24

APPENDIX 6

SKILL ASSESSMENT USING MERI DATA

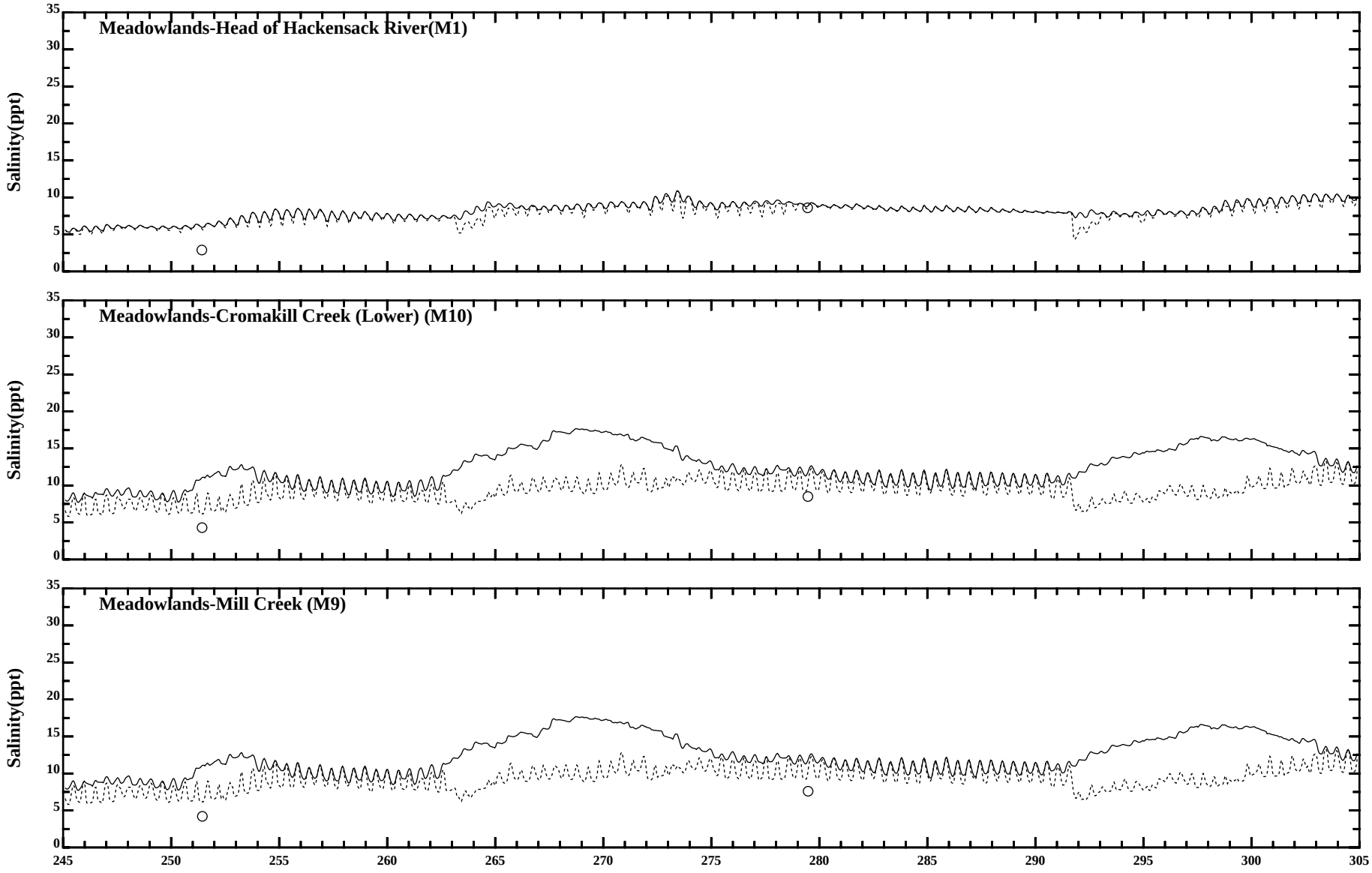

Comparison of Instantaneous Surface and Bottom Salinity

DATE: 8/02/2004 TIME: 11:48:26

/erie1/hrfo0010/HYDRORUNS/CARP9899/PLOTS/TANDS/temp51

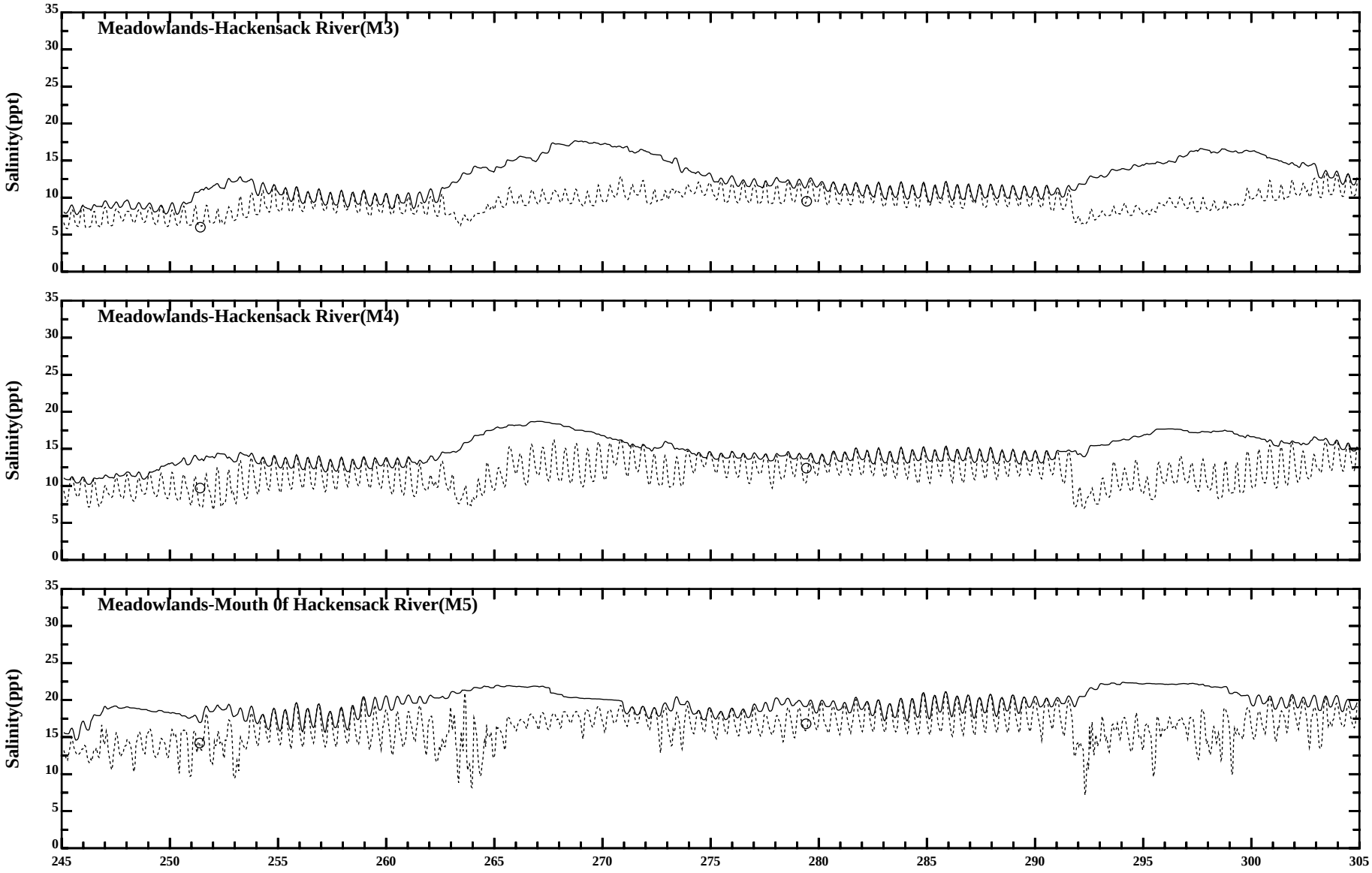

Comparison of Instantaneous Surface and Bottom Salinity

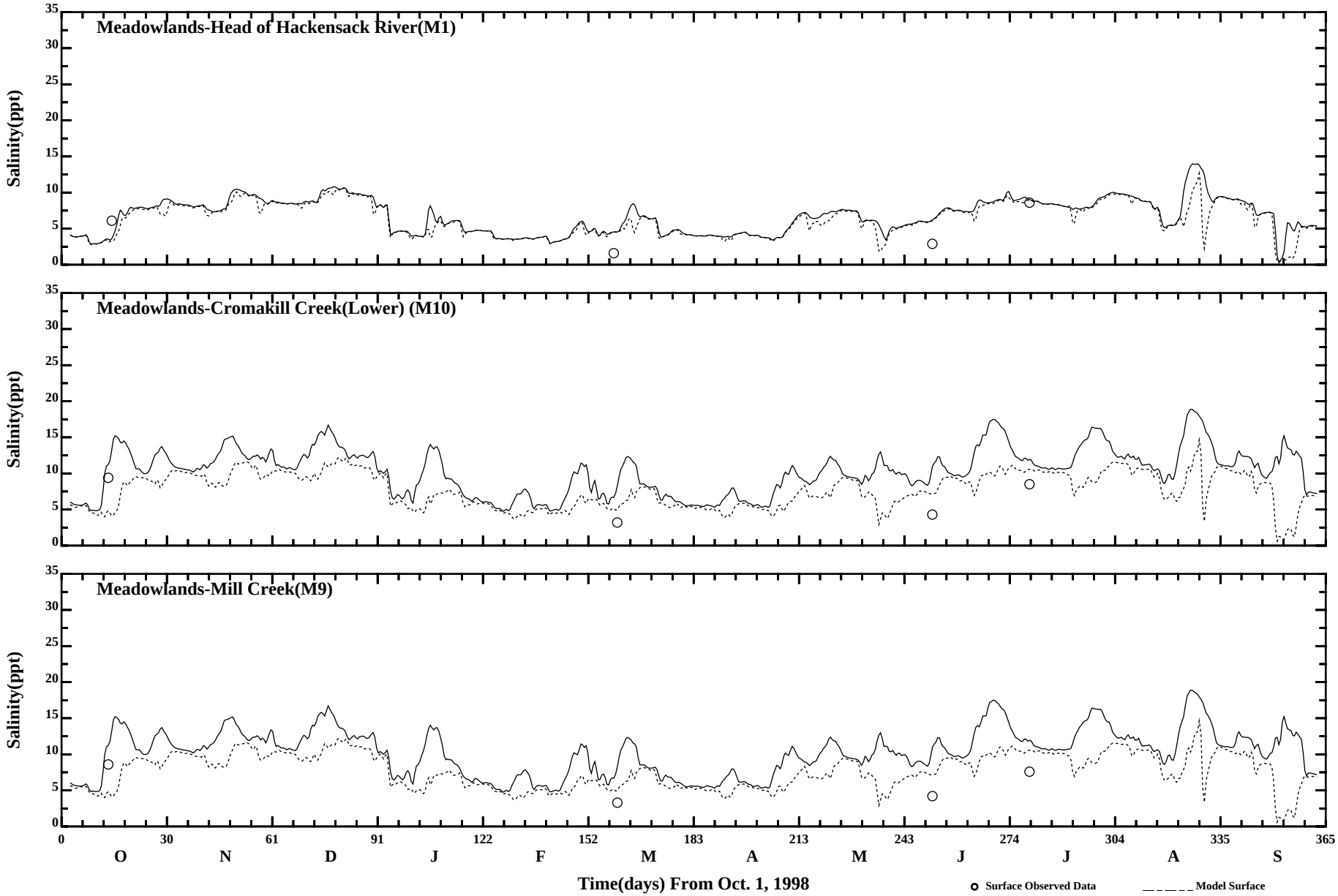

Comparison of 34 Hour Lowpass Surface and Bottom Salinity

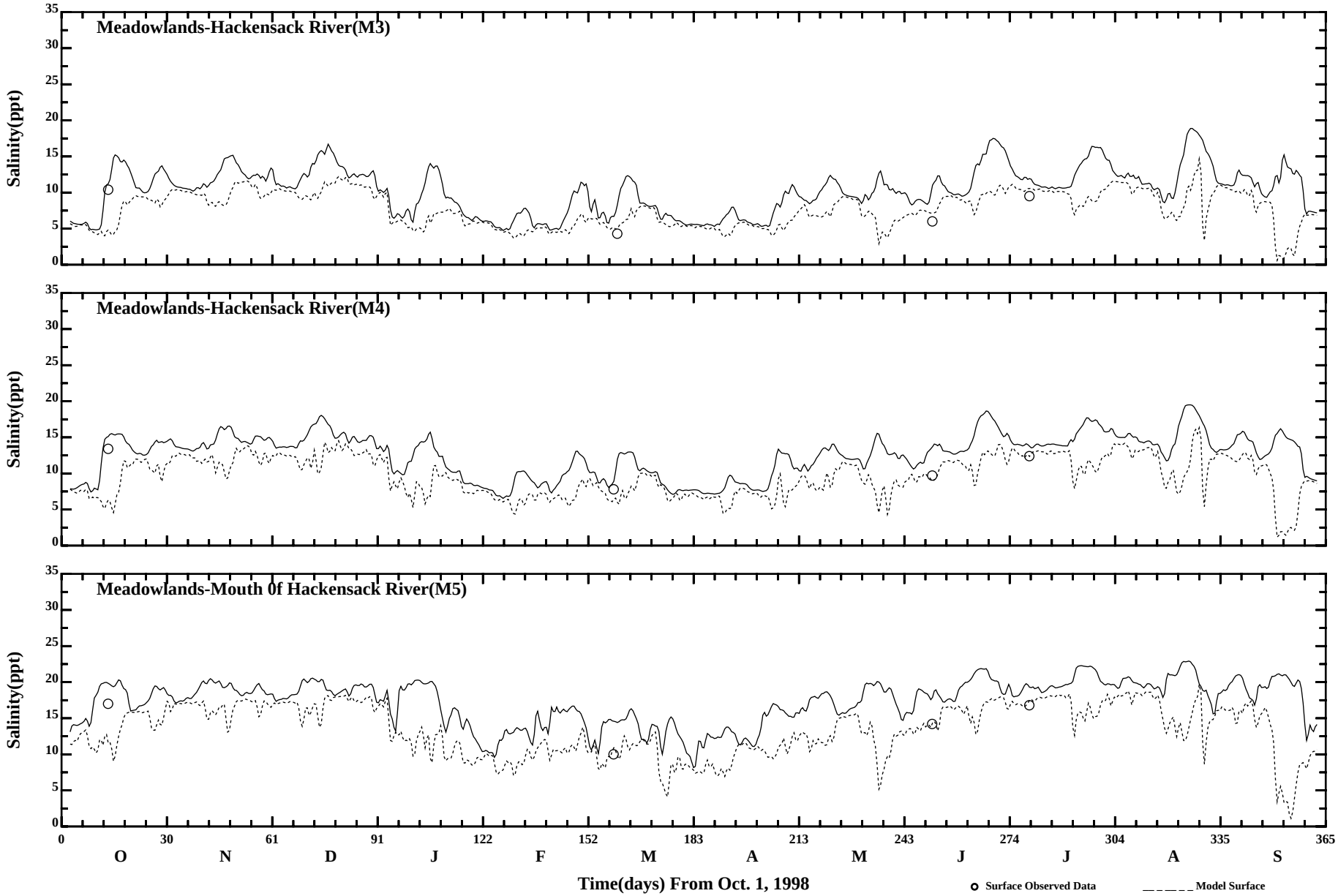

Comparison of 34 Hour Lowpass Surface and Bottom Salinity

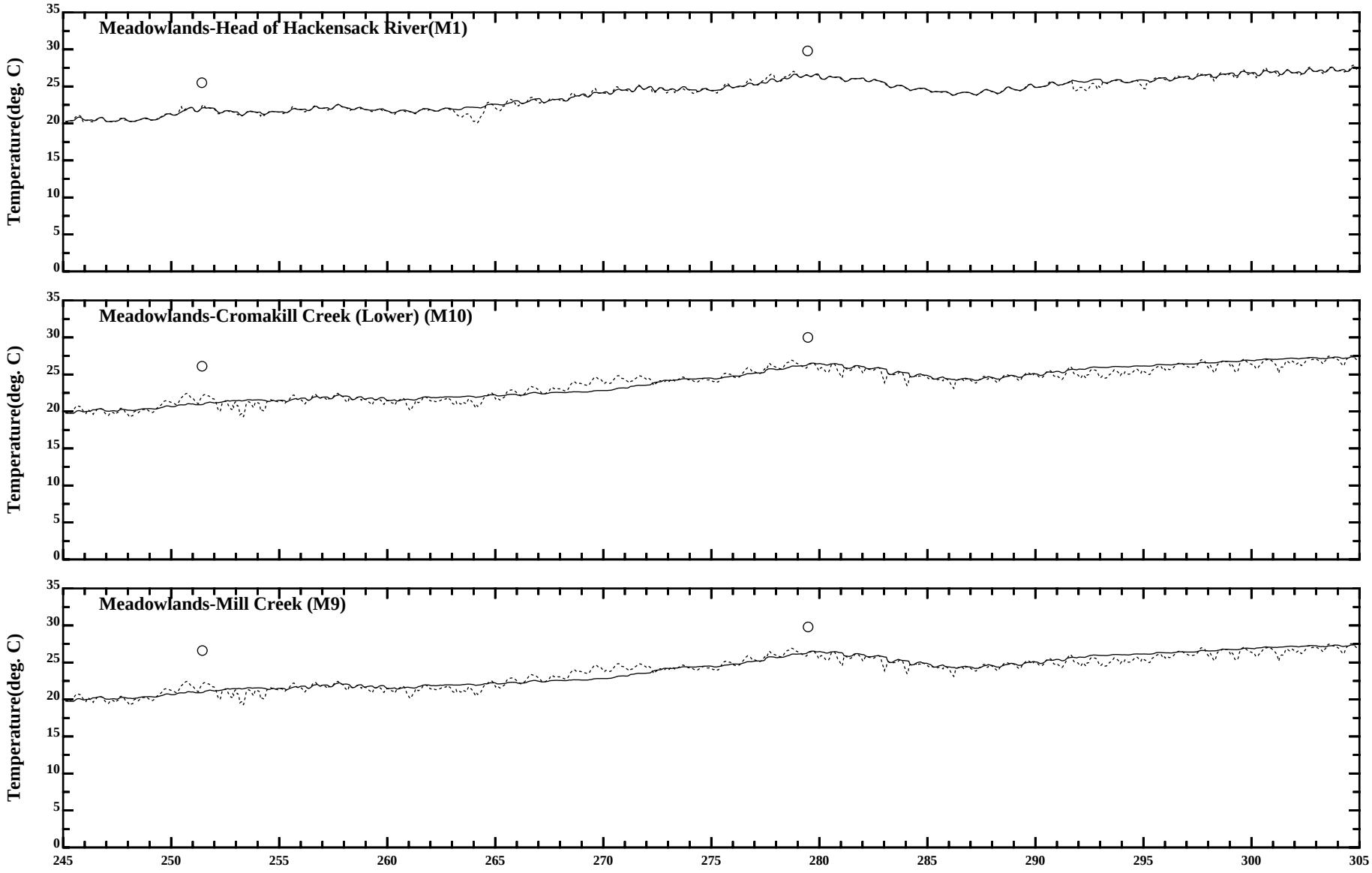

Comparison of Instantaneous Surface and Bottom Temperature

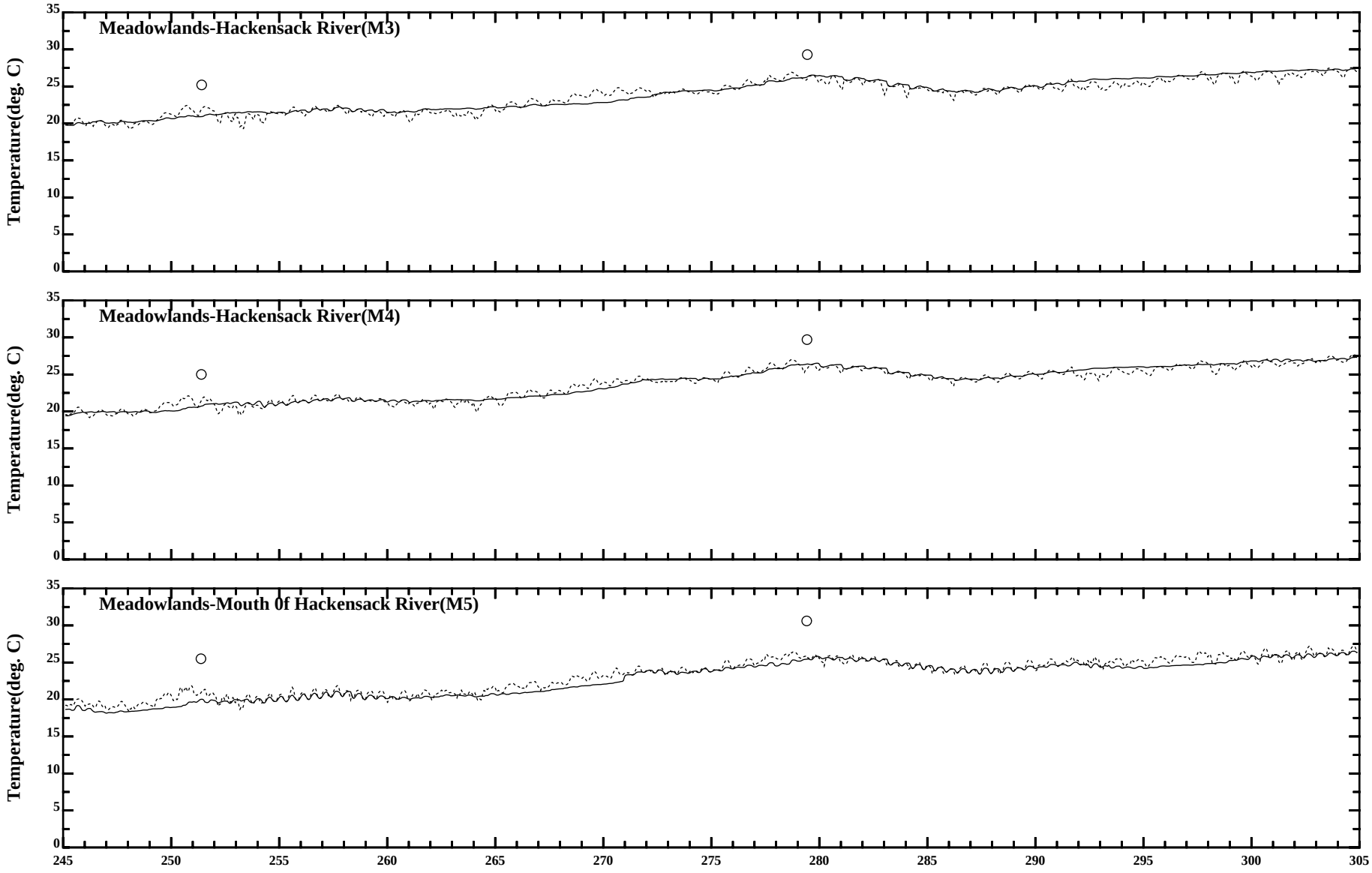

Comparison of Instantaneous Surface and Bottom Temperature

DATE: 8/02/2004 TIME: 11:48:21

/erie1/hrfo0010/HYDRORUNS/CARP9899/PLOTS/TANDS/temp51

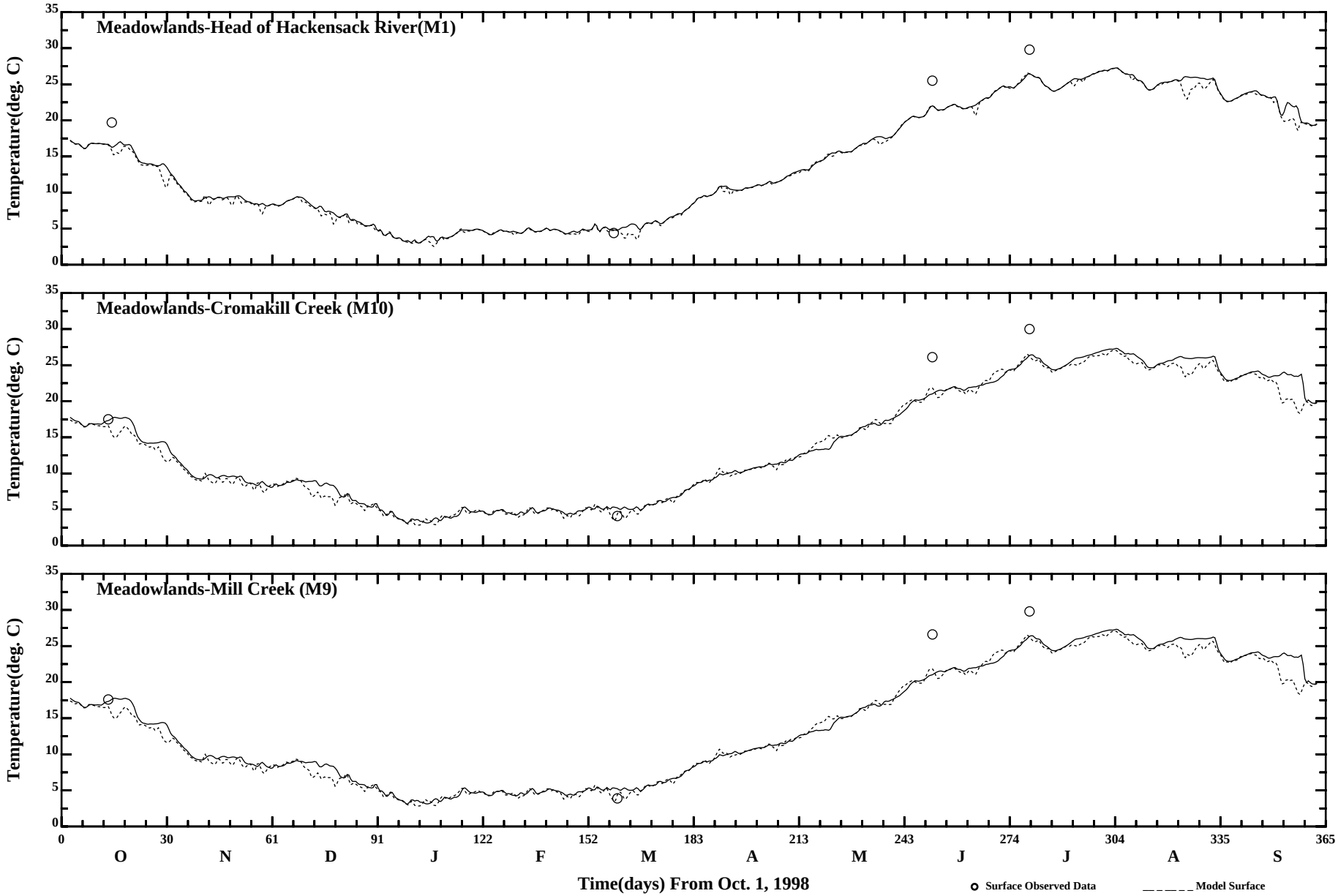

Comparison of 34 Hour Lowpass Surface and Bottom Temperature

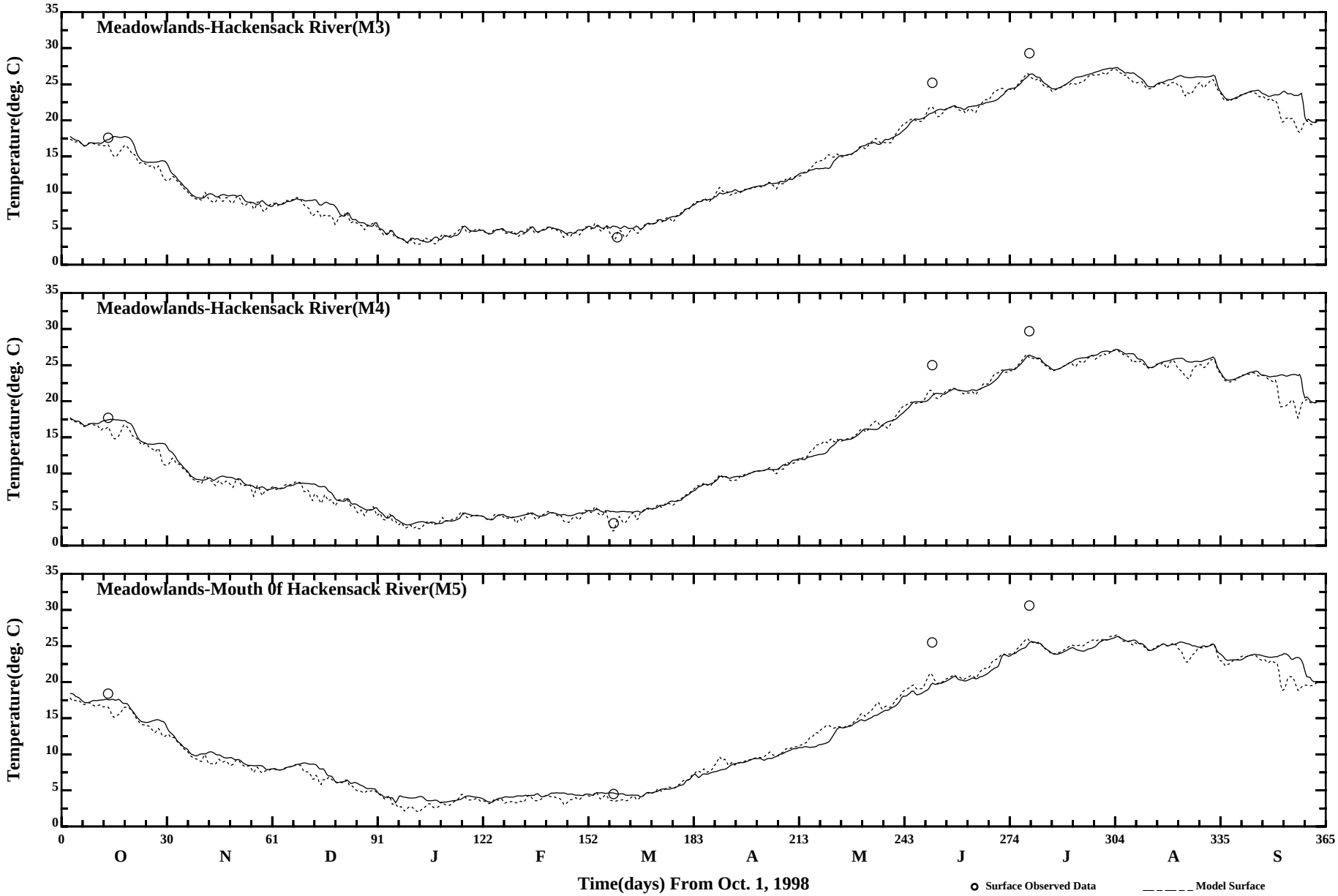

Comparison of 34 Hour Lowpass Surface and Bottom Temperature

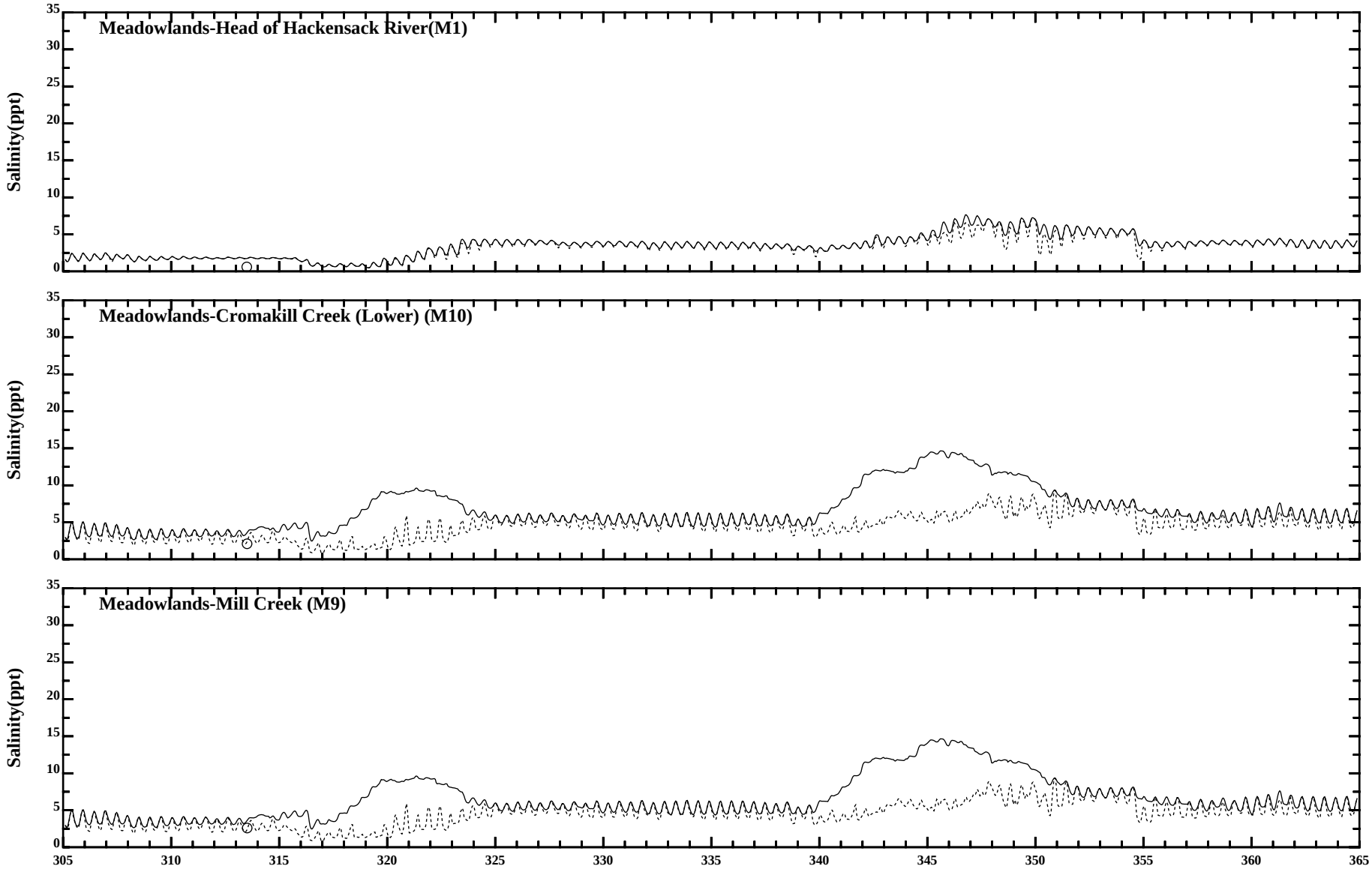

Comparison of Instantaneous Surface and Bottom Salinity

DATE: 8/02/2004 TIME: 12: 7:19

/erie1/hrfo0010/HYDRORUNS/CARP9900/PLOTS/TANDS/salt51

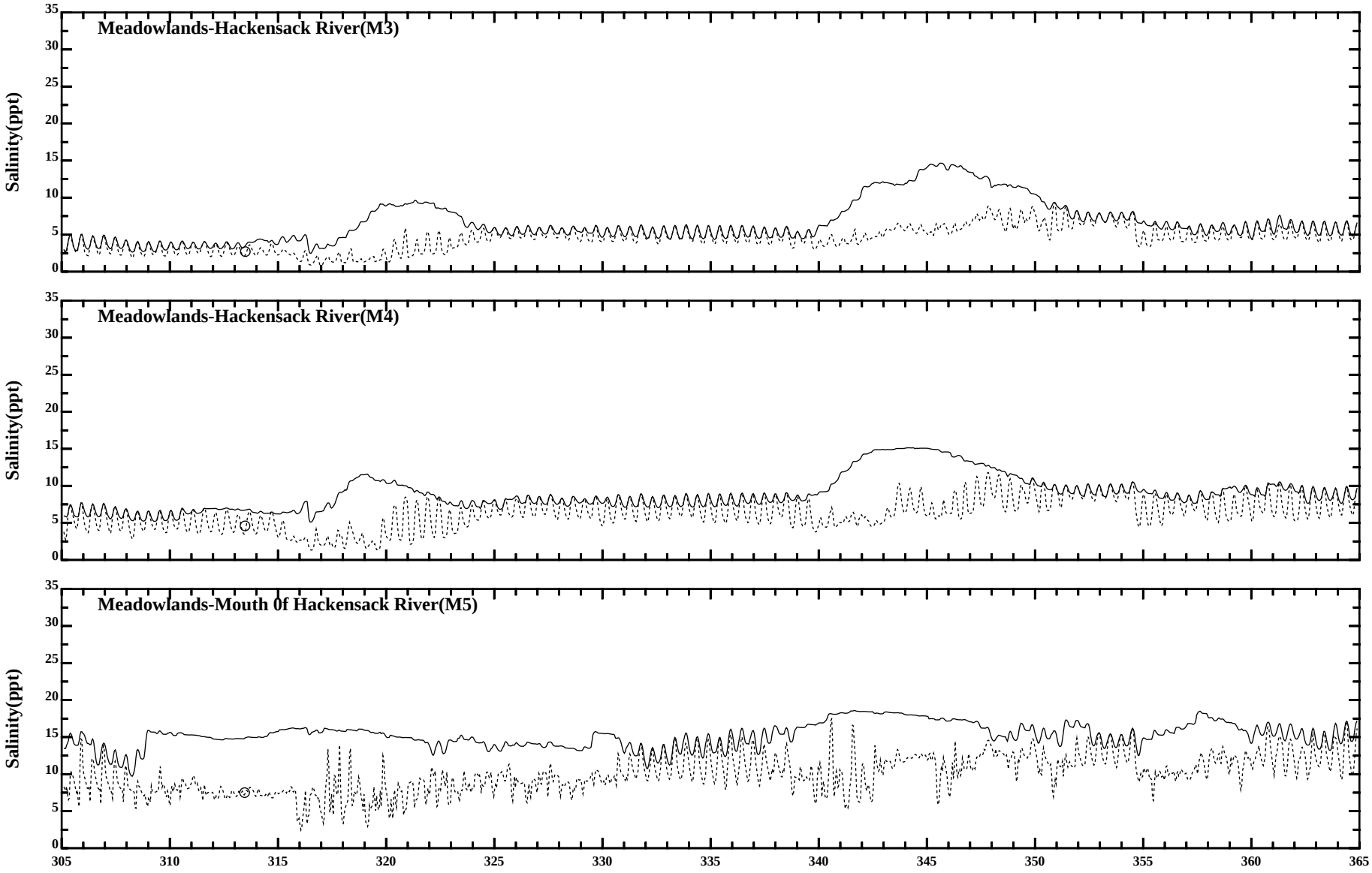

Comparison of Instantaneous Surface and Bottom Salinity

DATE: 8/02/2004 TIME: 12: 7:19

/erie1/hrfo0010/HYDRORUNS/CARP9900/PLOTS/TANDS/salt51

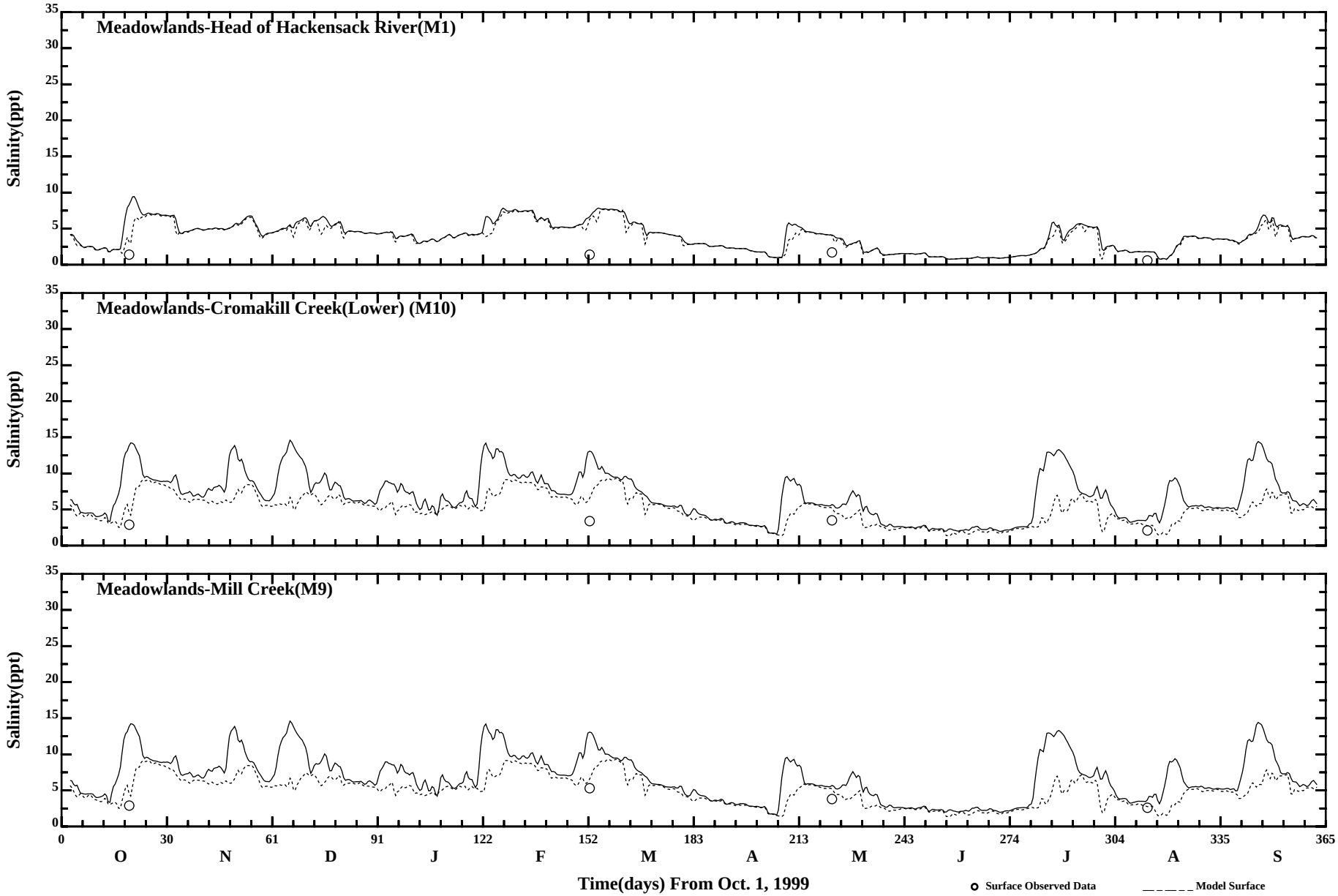

Comparison of 34 Hour Lowpass Surface and Bottom Salinity

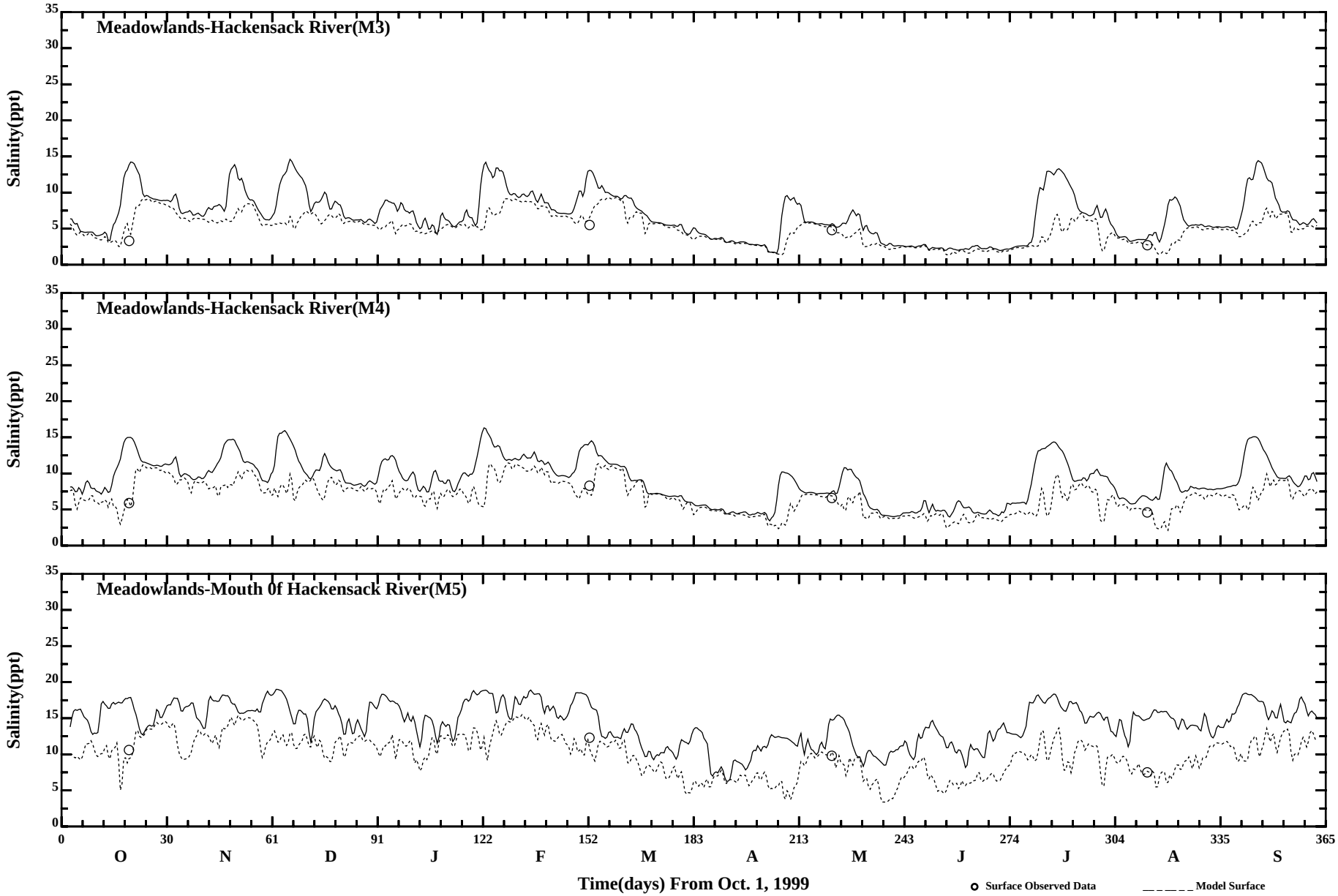

Comparison of 34 Hour Lowpass Surface and Bottom Salinity

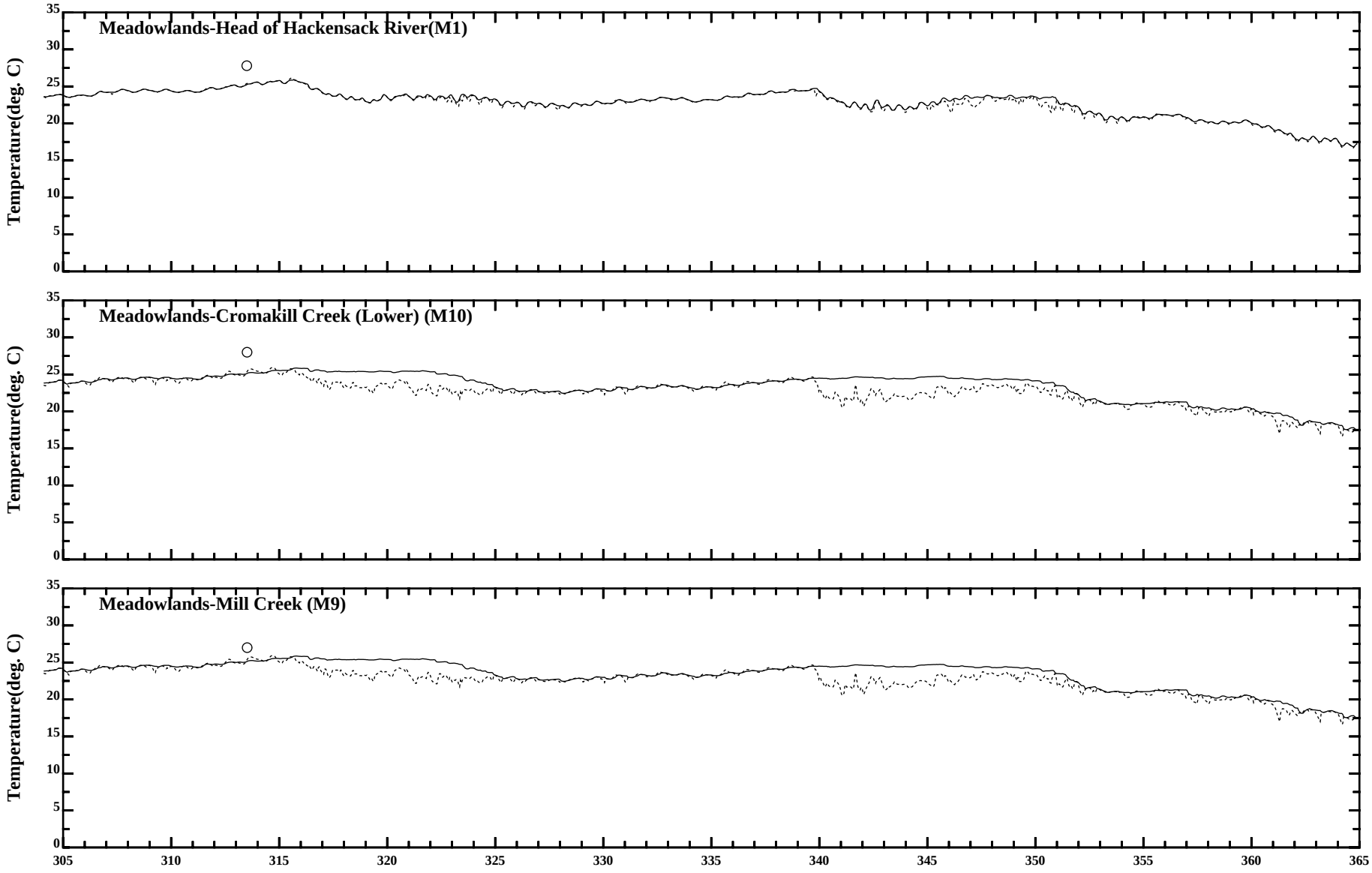

Comparison of Instantaneous Surface and Bottom Temperature

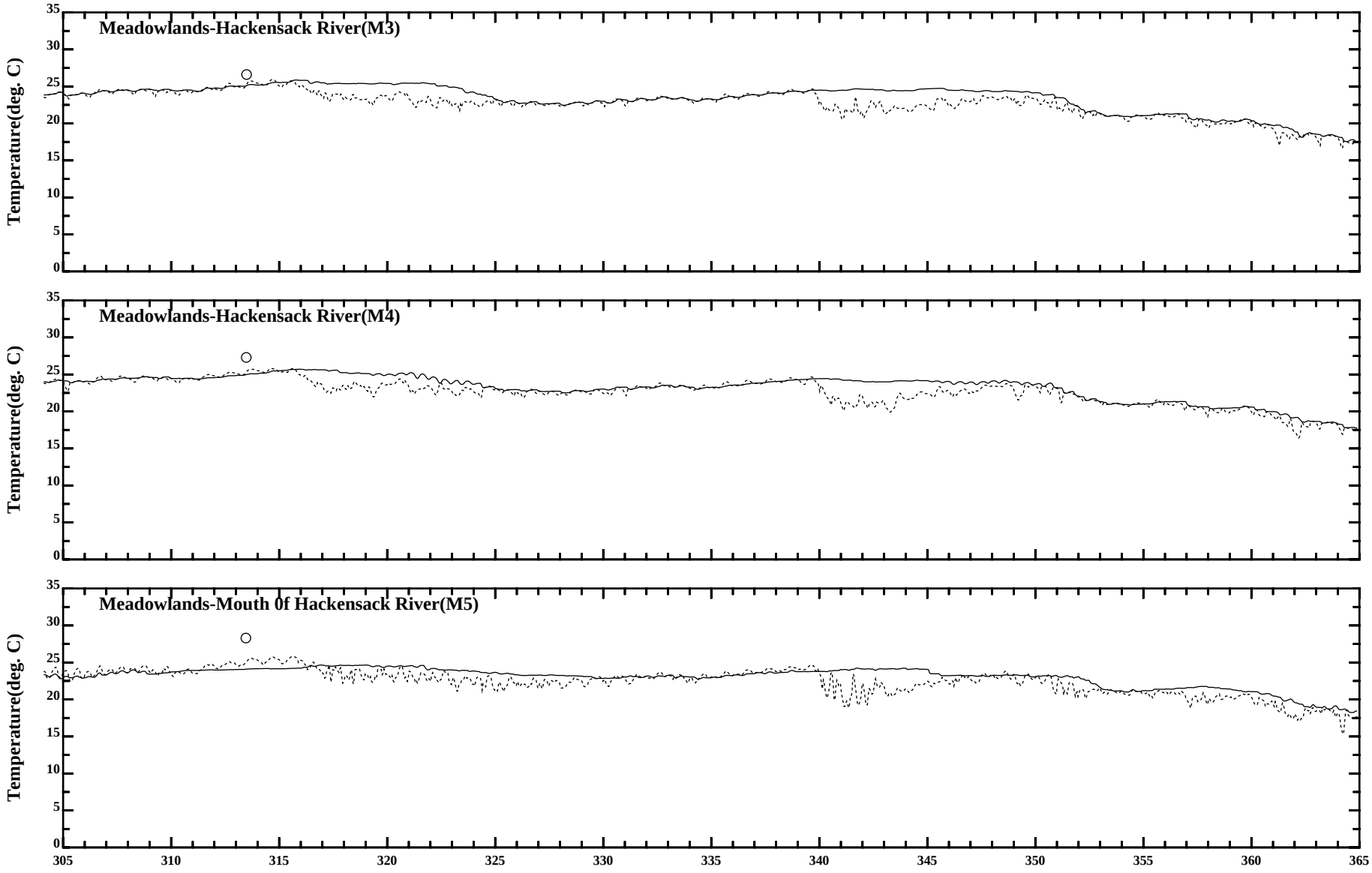

Comparison of Instantaneous Surface and Bottom Temperature

DATE: 8/02/2004 TIME: 12: 7:15

/erie1/hrfo0010/HYDRORUNS/CARP9900/PLOTS/TANDS/temp51

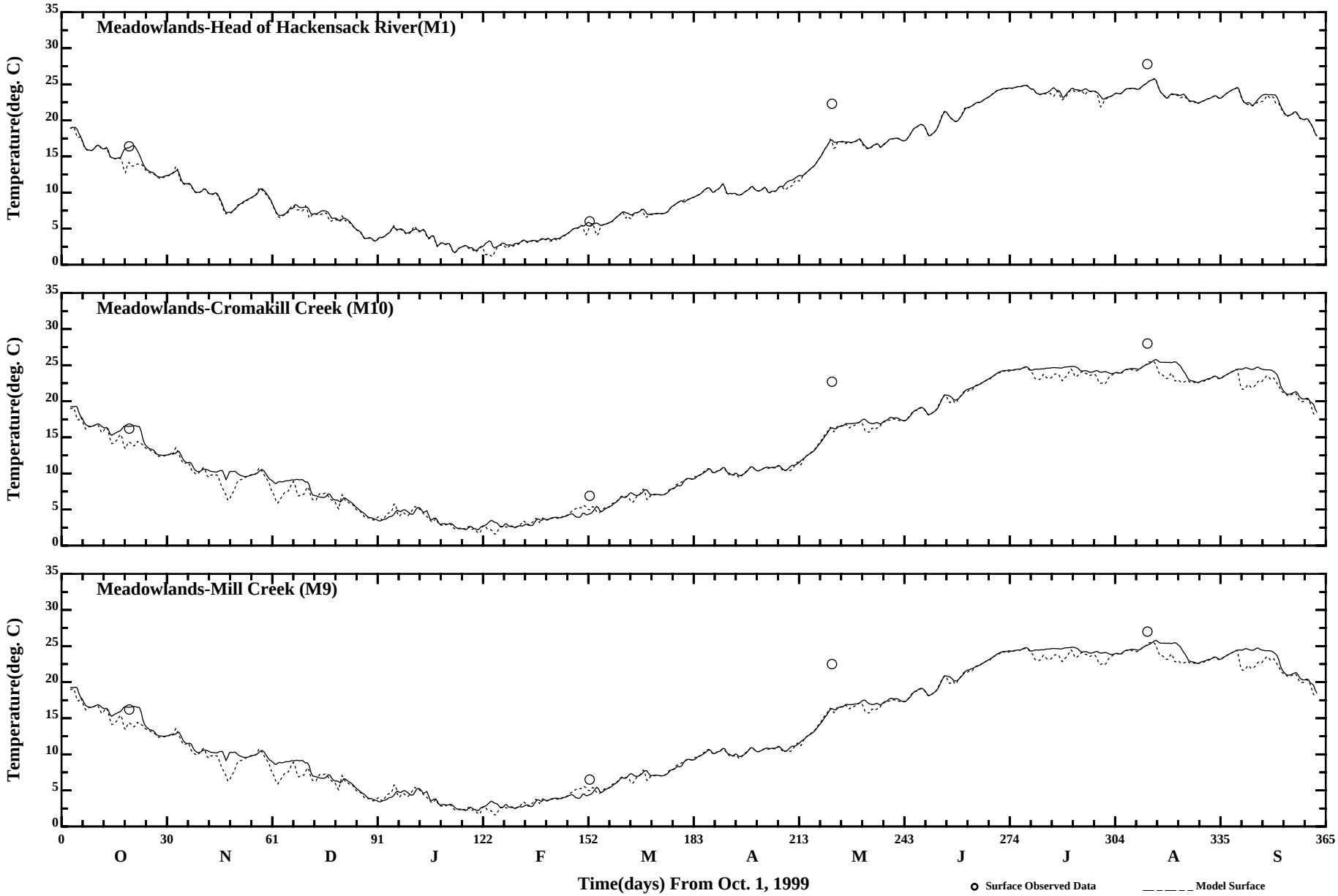

Comparison of 34 Hour Lowpass Surface and Bottom Temperature

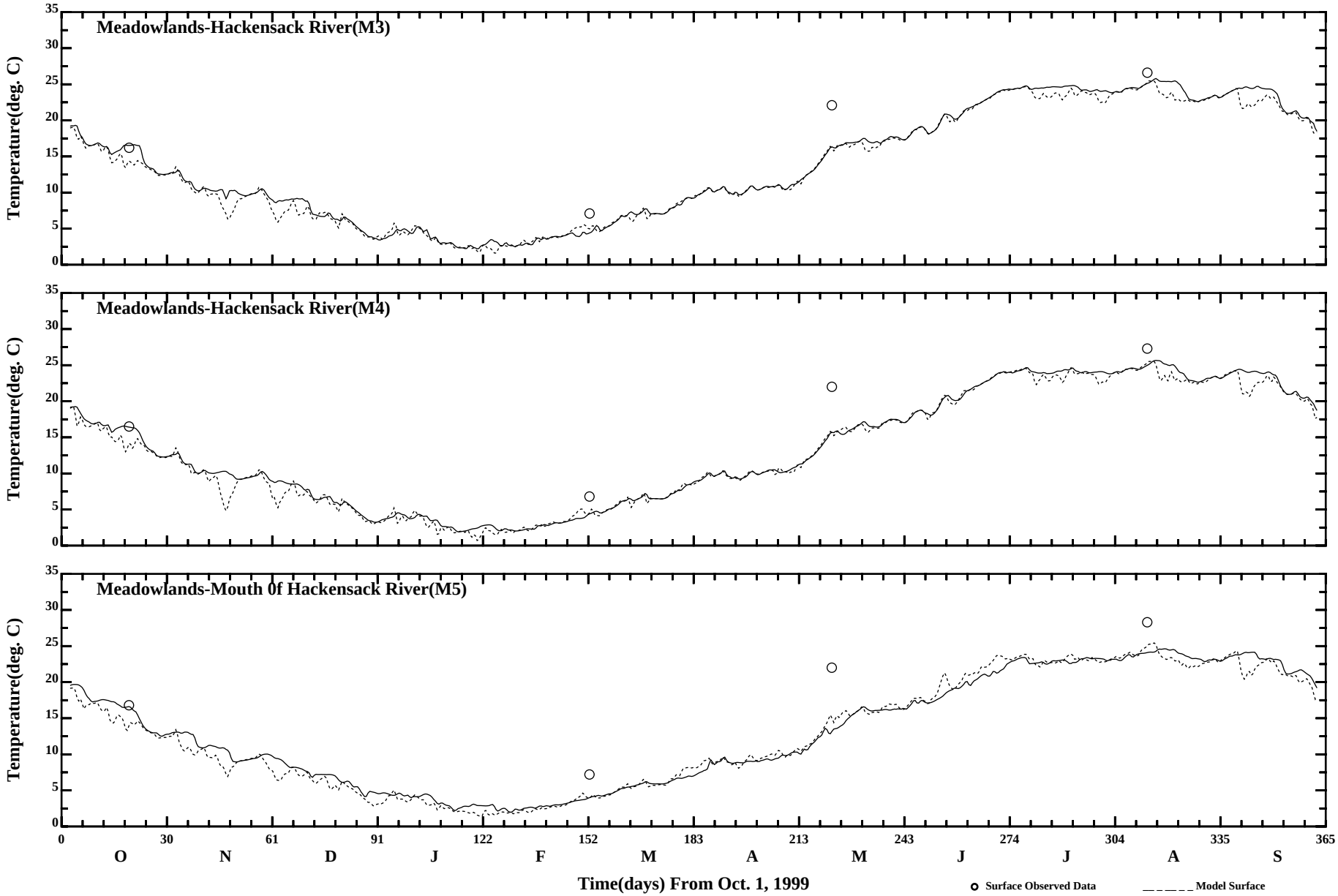

Comparison of 34 Hour Lowpass Surface and Bottom Temperature

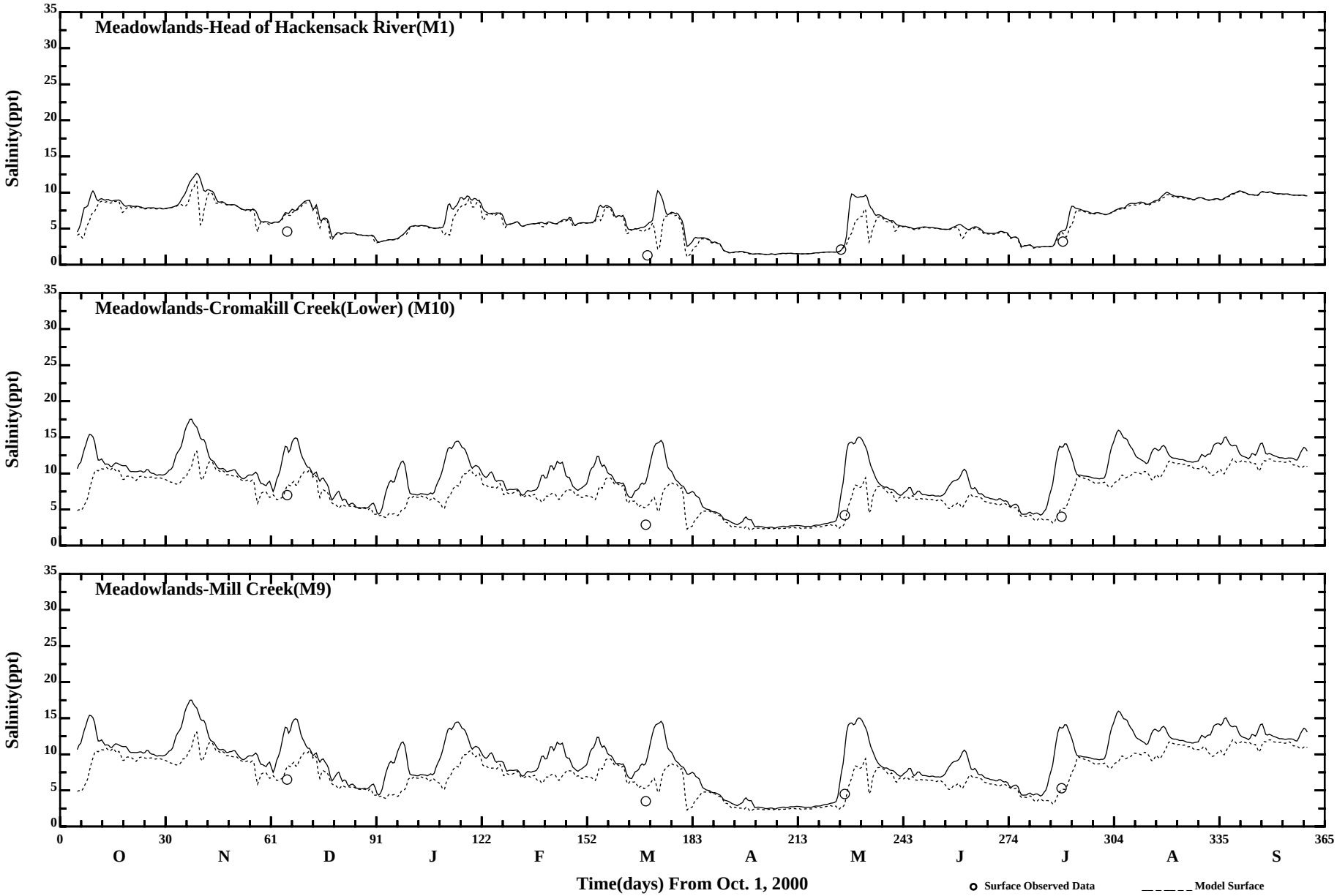

Comparison of 35 Hour Lowpass Surface and Bottom Salinity

DATE: 8/02/2004 TIME: 12:30:15

/erie1/hrfo0010/HYDRORUNS/CARP0001/PLOTS/TANDS/psalt51_35hlp

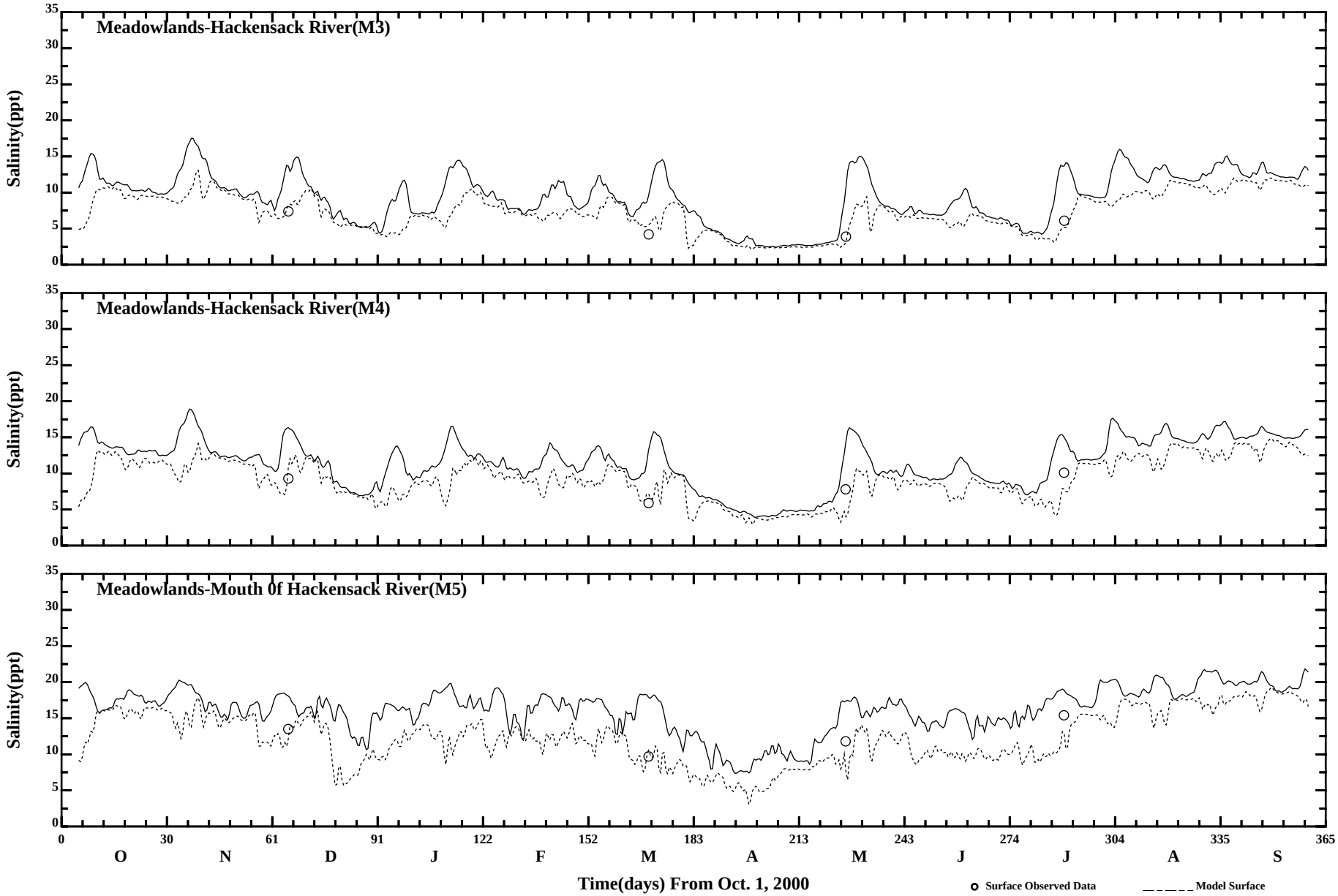

Comparison of 35 Hour Lowpass Surface and Bottom Salinity

DATE: 8/02/2004 TIME: 12:30:15

/erie1/hrfo0010/HYDRORUNS/CARP0001/PLOTS/TANDS/psalt51_35hlp

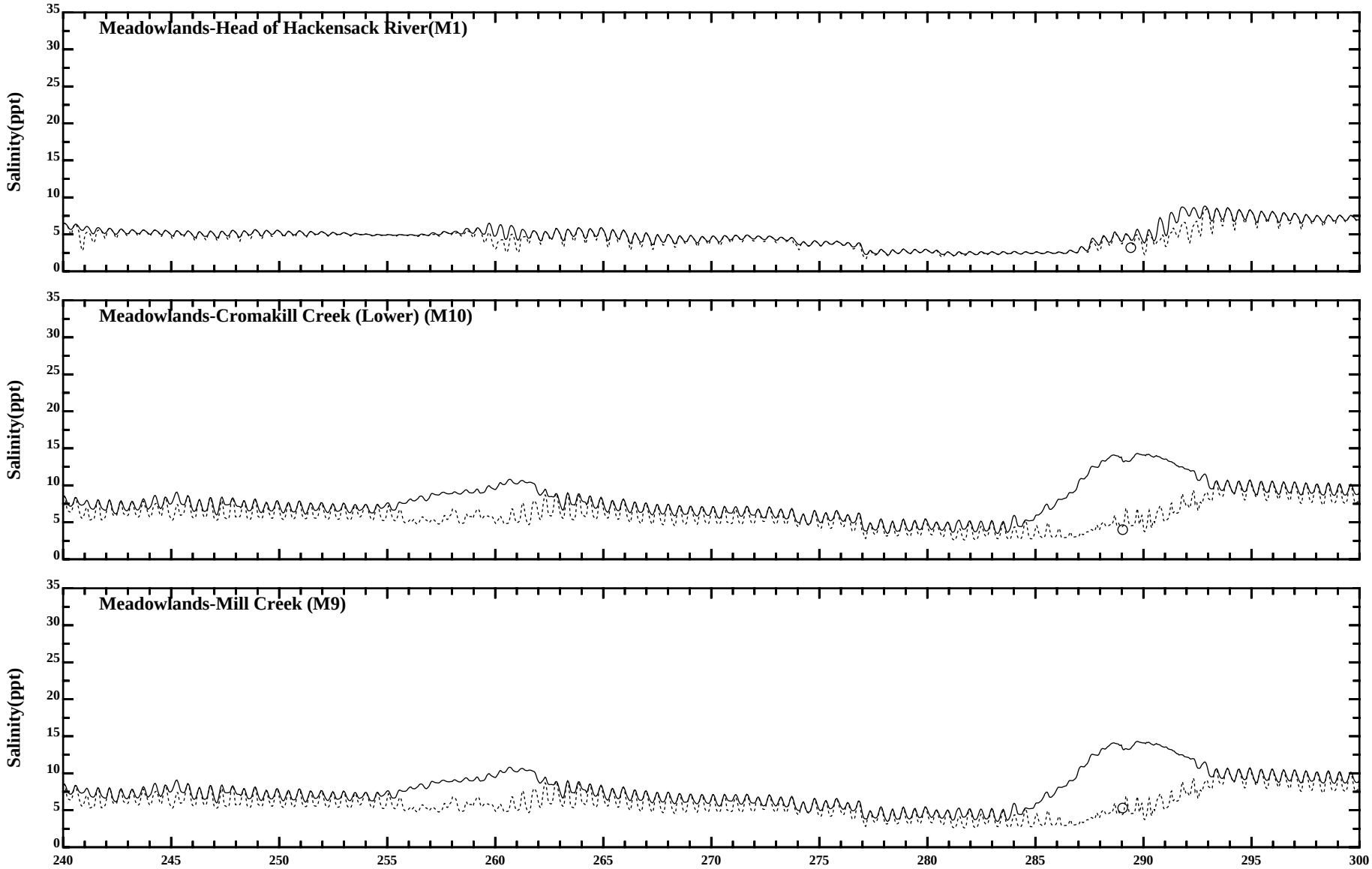

Comparison of Instantaneous Surface and Bottom Salinity

DATE: 8/02/2004 TIME: 12:30:17

/e1/hrfo0010/HYDRORUNS/CARP0001/PLOTS/TANDS/salt51

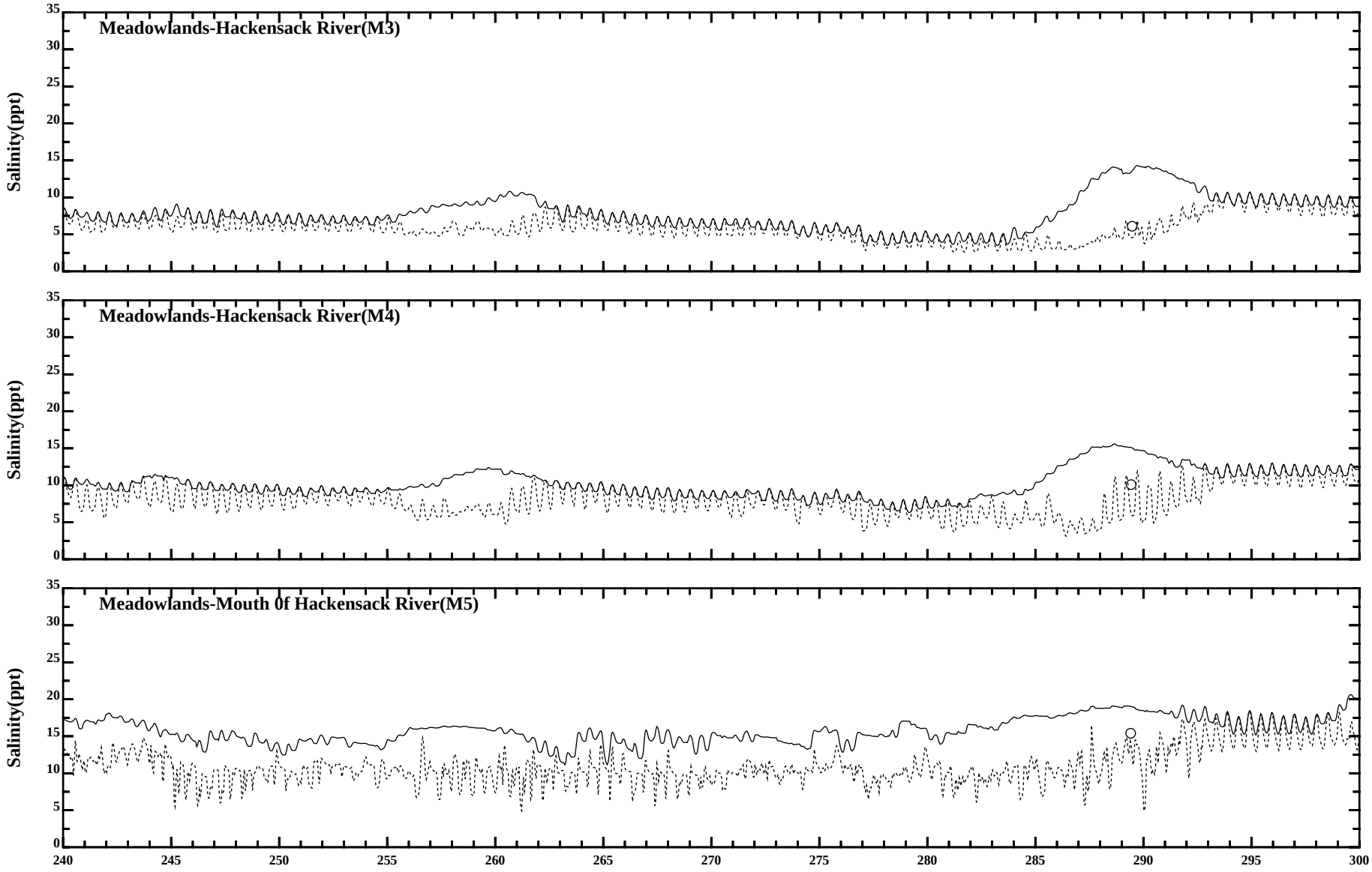

Comparison of Instantaneous Surface and Bottom Salinity

DATE: 8/02/2004 TIME: 12:30:17

/e1/hrfo0010/HYDRORUNS/CARP0001/PLOTS/TANDS/salt51

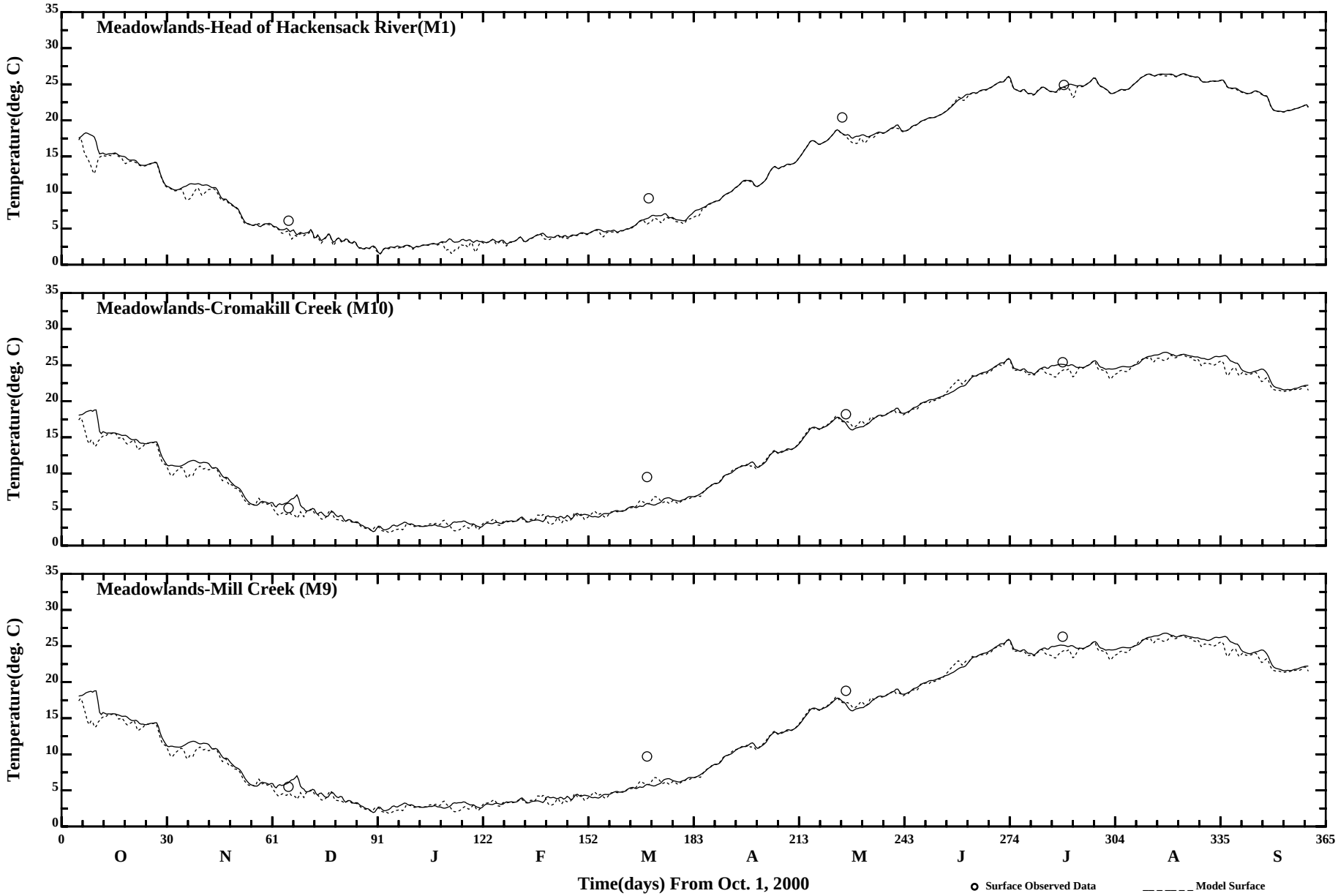

Comparison of 35 Hour Lowpass Surface and Bottom Temperature

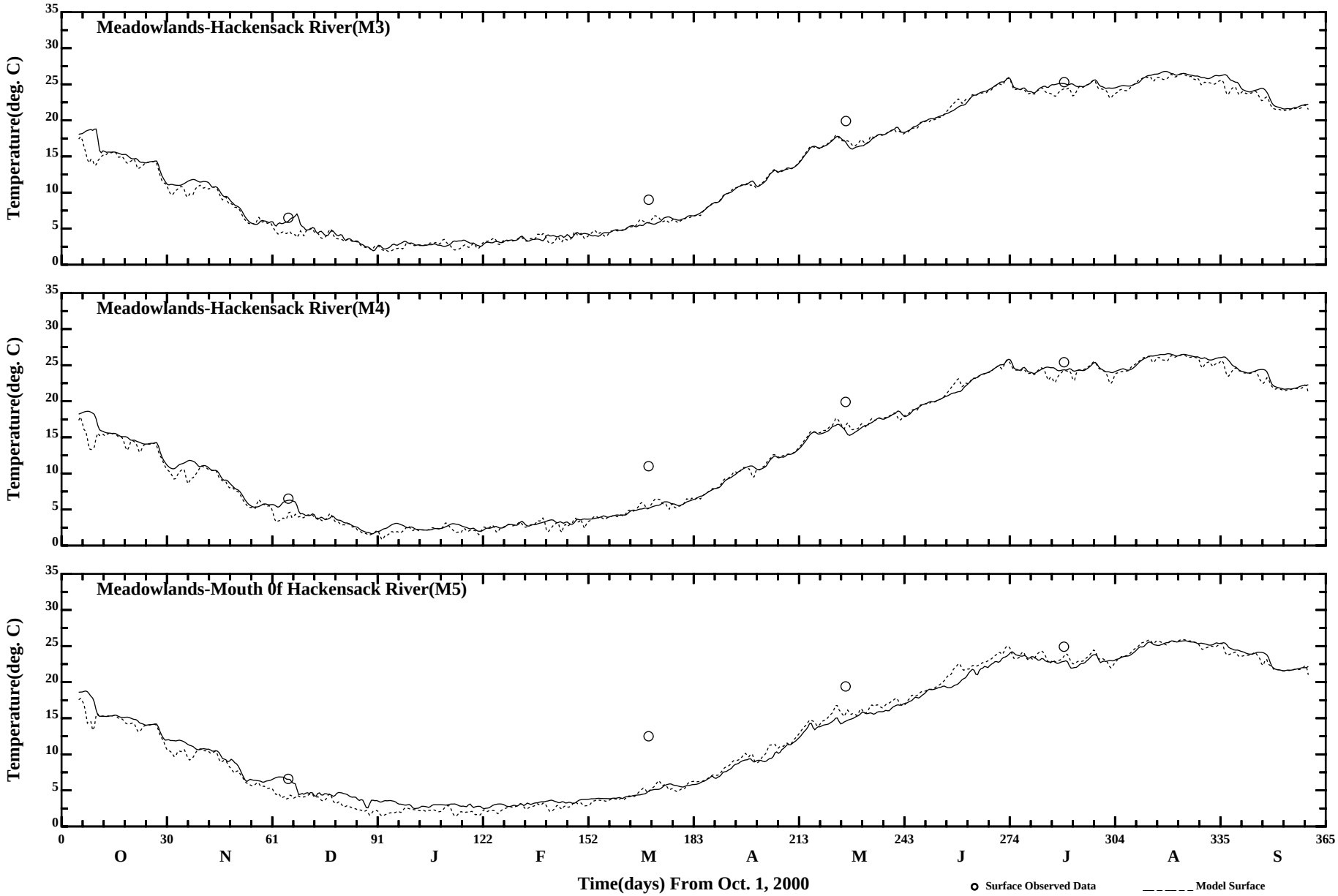

Comparison of 35 Hour Lowpass Surface and Bottom Temperature

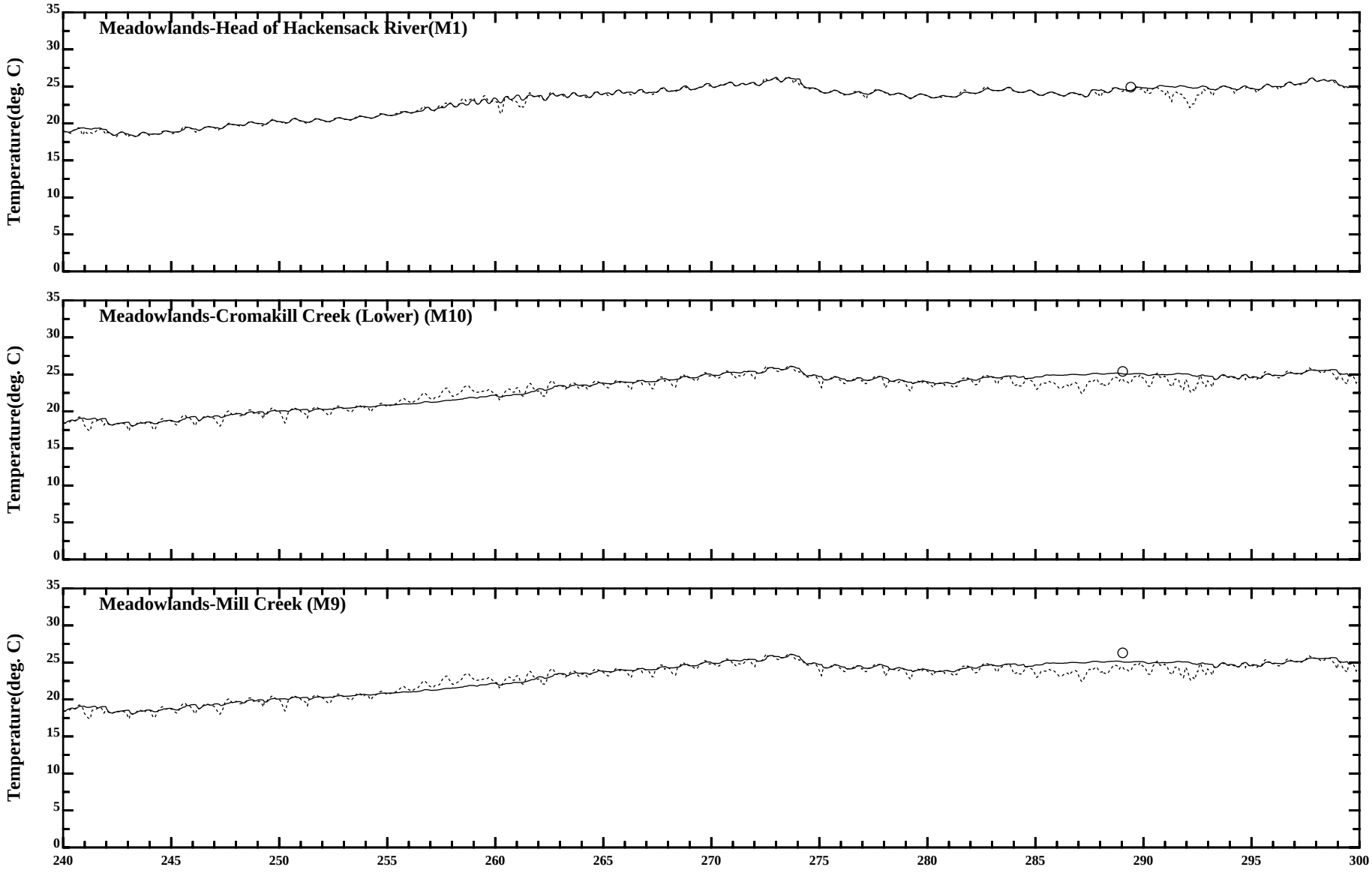

Comparison of Instantaneous Surface and Bottom Temperature

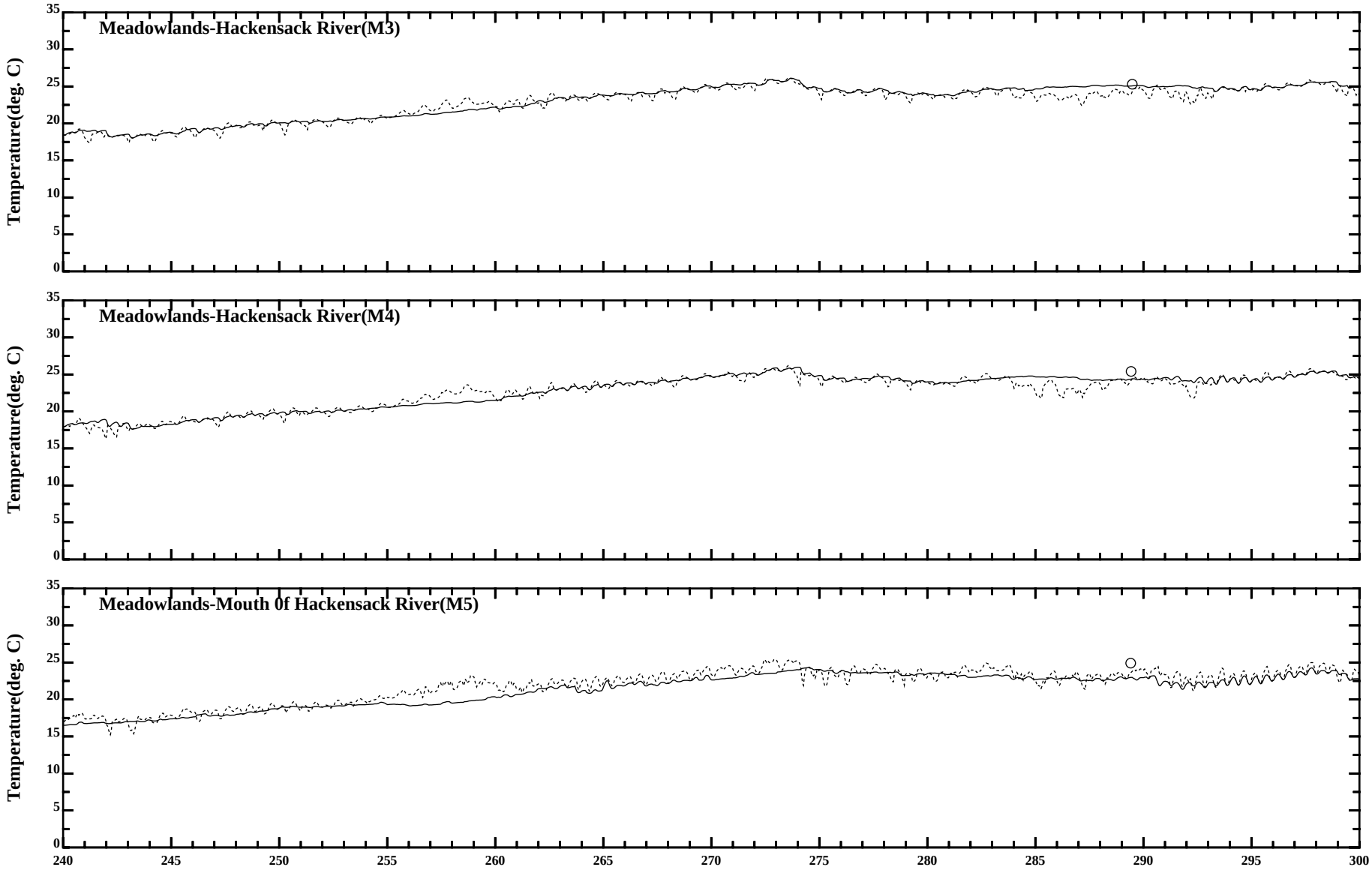

Comparison of Instantaneous Surface and Bottom Temperature

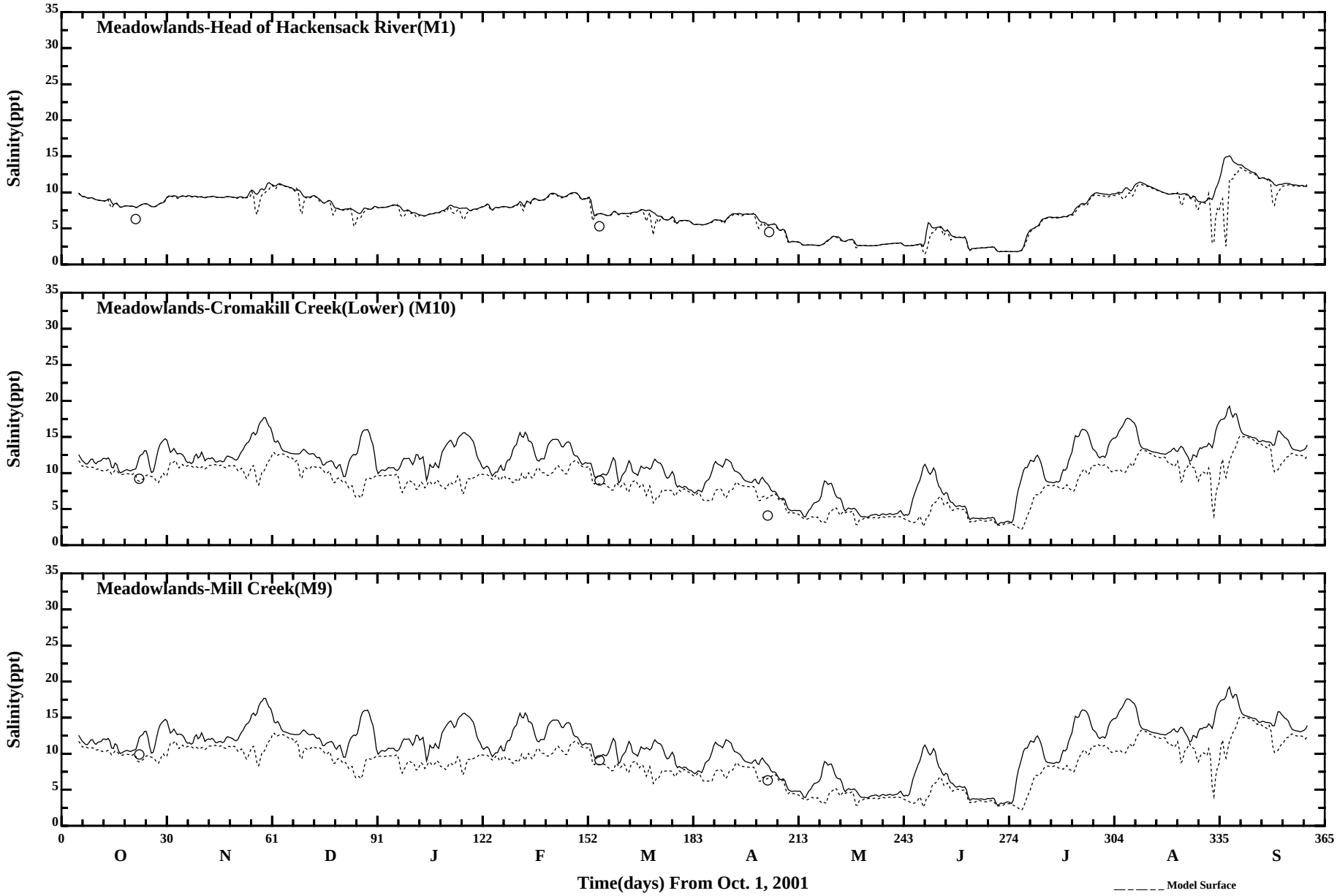

Comparison of 35 Hour Lowpass Surface and Bottom Salinity

/ont6/hrfo0010/RUNS/ECOMSED-SED/ECOMSED-0102/PLOTS/TANDS/salt_hack_35hlp

DATE: 11/21/2003 TIME: 10:42: 7

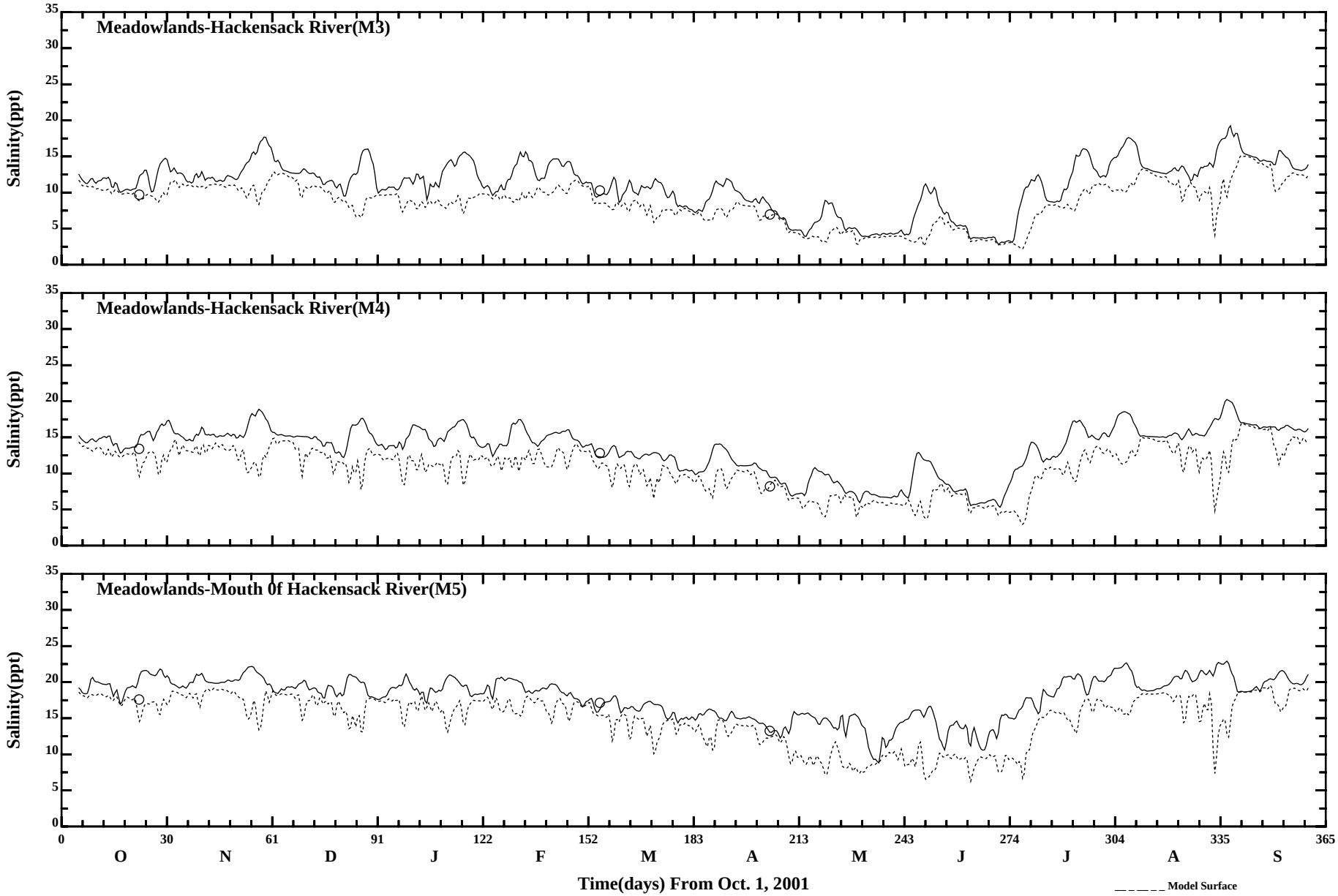

Comparison of 35 Hour Lowpass Surface and Bottom Salinity

/ont6/hrfo0010/RUNS/ECOMSED-SED/ECOMSED-0102/PLOTS/TANDS/salt_hack_35hlp

DATE: 11/21/2003 TIME: 10:42: 7

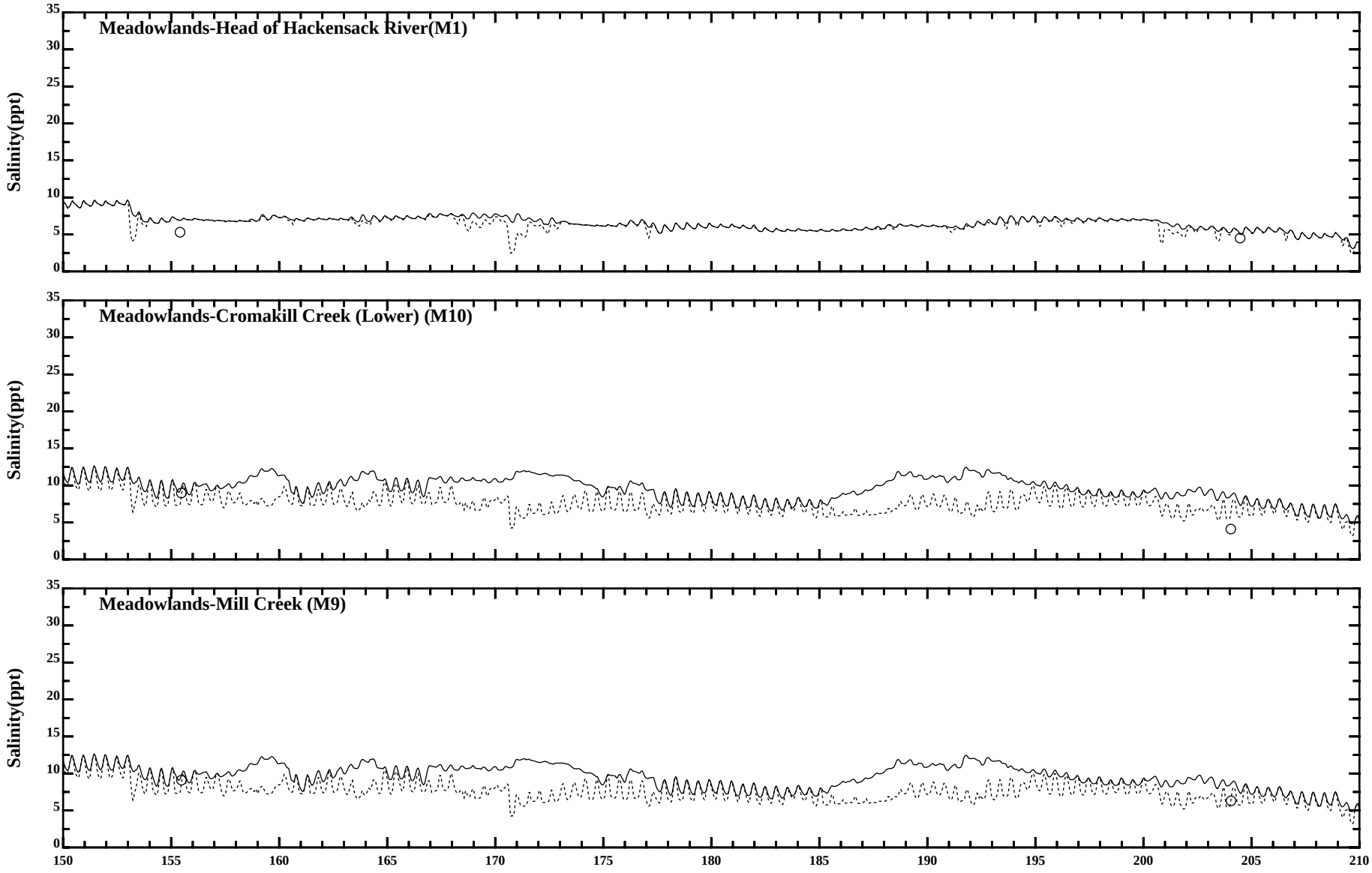

/ont6/hrfo0010/RUNS/ECOMSED-SED/ECOMSED-0102/PLOTS/TANDS/salt_hack_hourly

DATE: 11/21/2003 TIME: 10:42:11

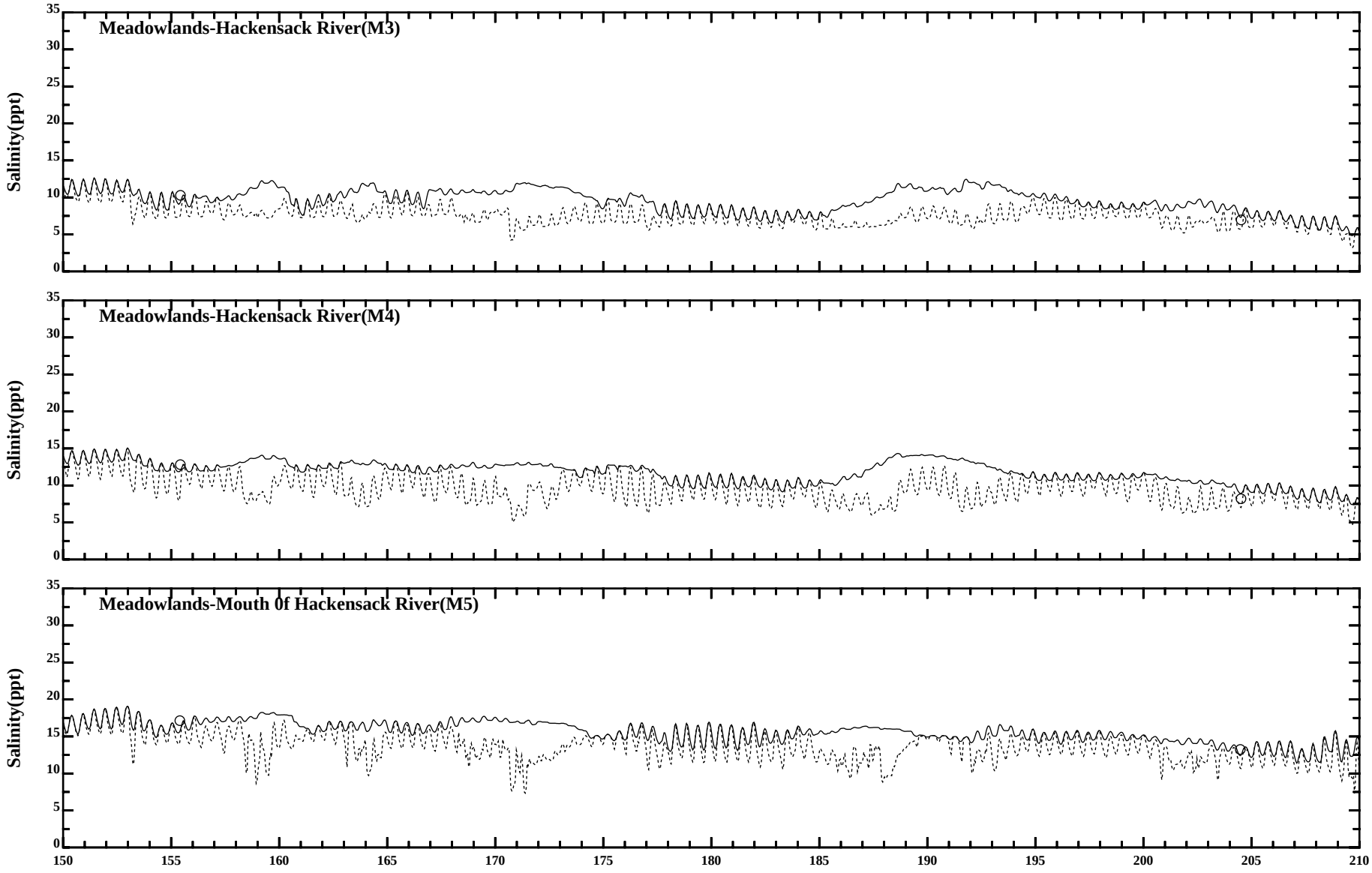

/ont6/hrfo0010/RUNS/ECOMSED-SED/ECOMSED-0102/PLOTS/TANDS/salt_hack_hourly

DATE: 11/21/2003 TIME: 10:42:11

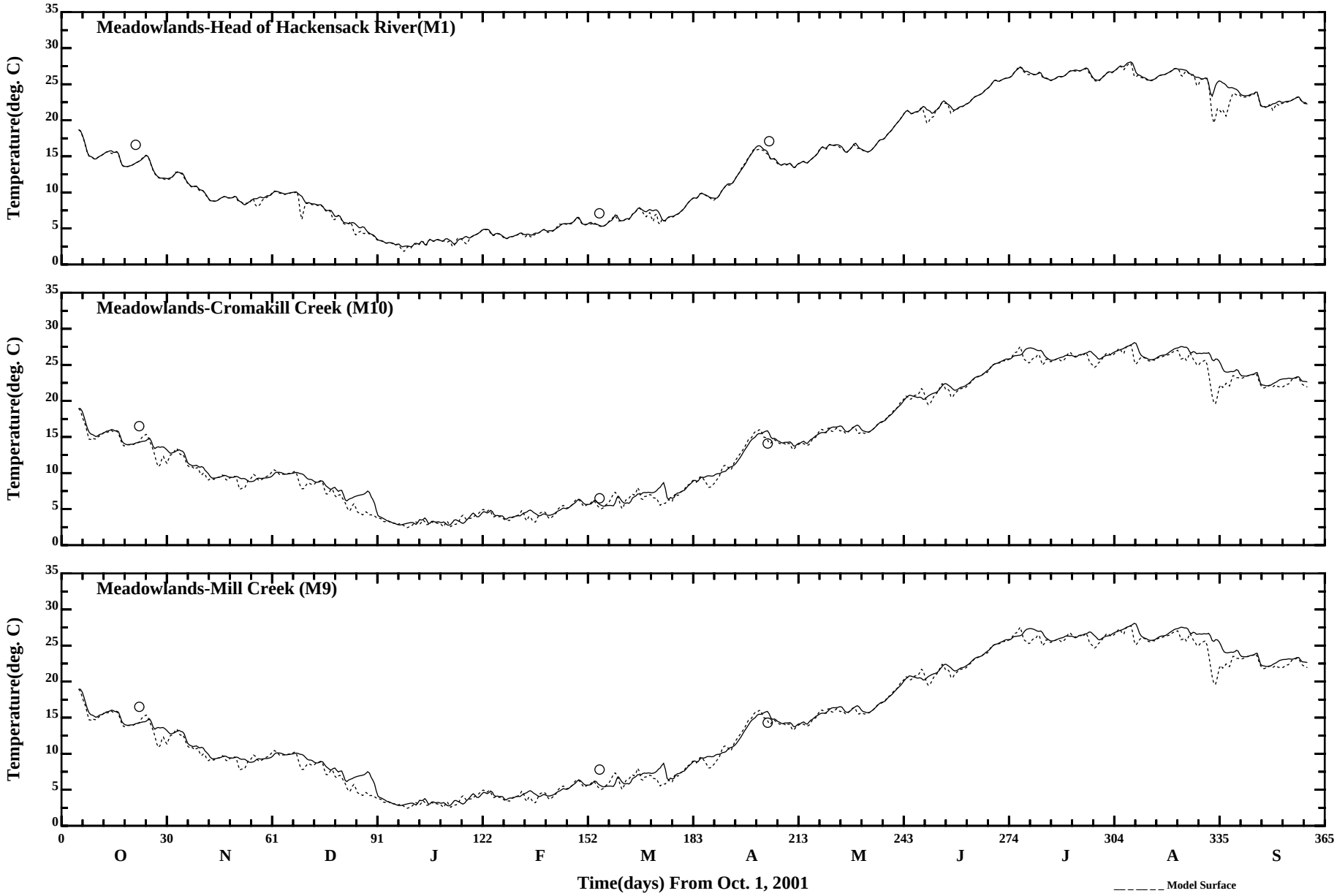

Comparison of 35 Hour Lowpass Surface and Bottom Temperature

/ont6/hrfo0010/RUNS/ECOMSED-SED/ECOMSED-0102/PLOTS/TANDS/temp_hack_35hlp

DATE: 11/21/2003 TIME: 10:40:31

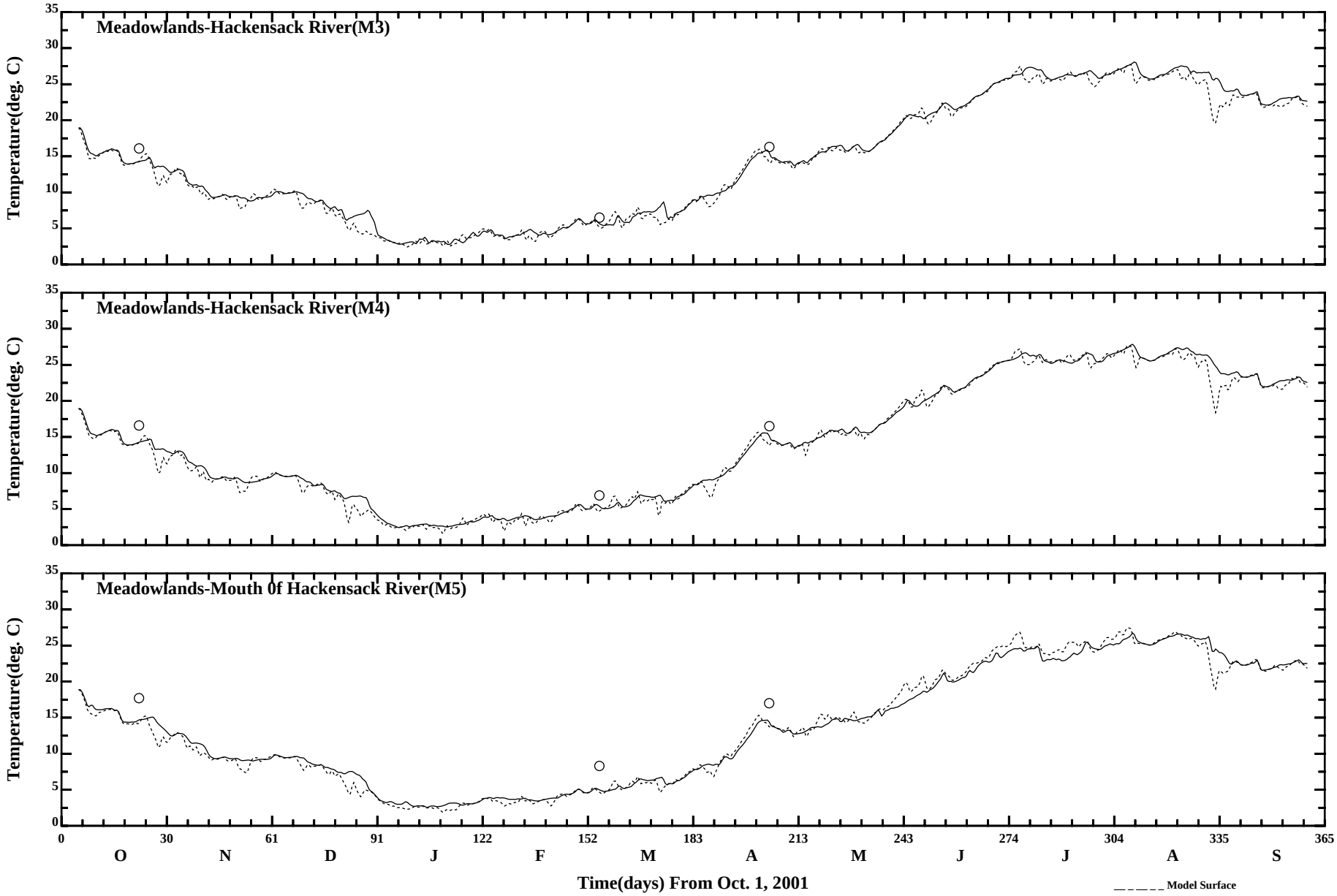

Comparison of 35 Hour Lowpass Surface and Bottom Temperature

/ont6/hrfo0010/RUNS/ECOMSED-SED/ECOMSED-0102/PLOTS/TANDS/temp_hack_35hlp

DATE: 11/21/2003 TIME: 10:40:31

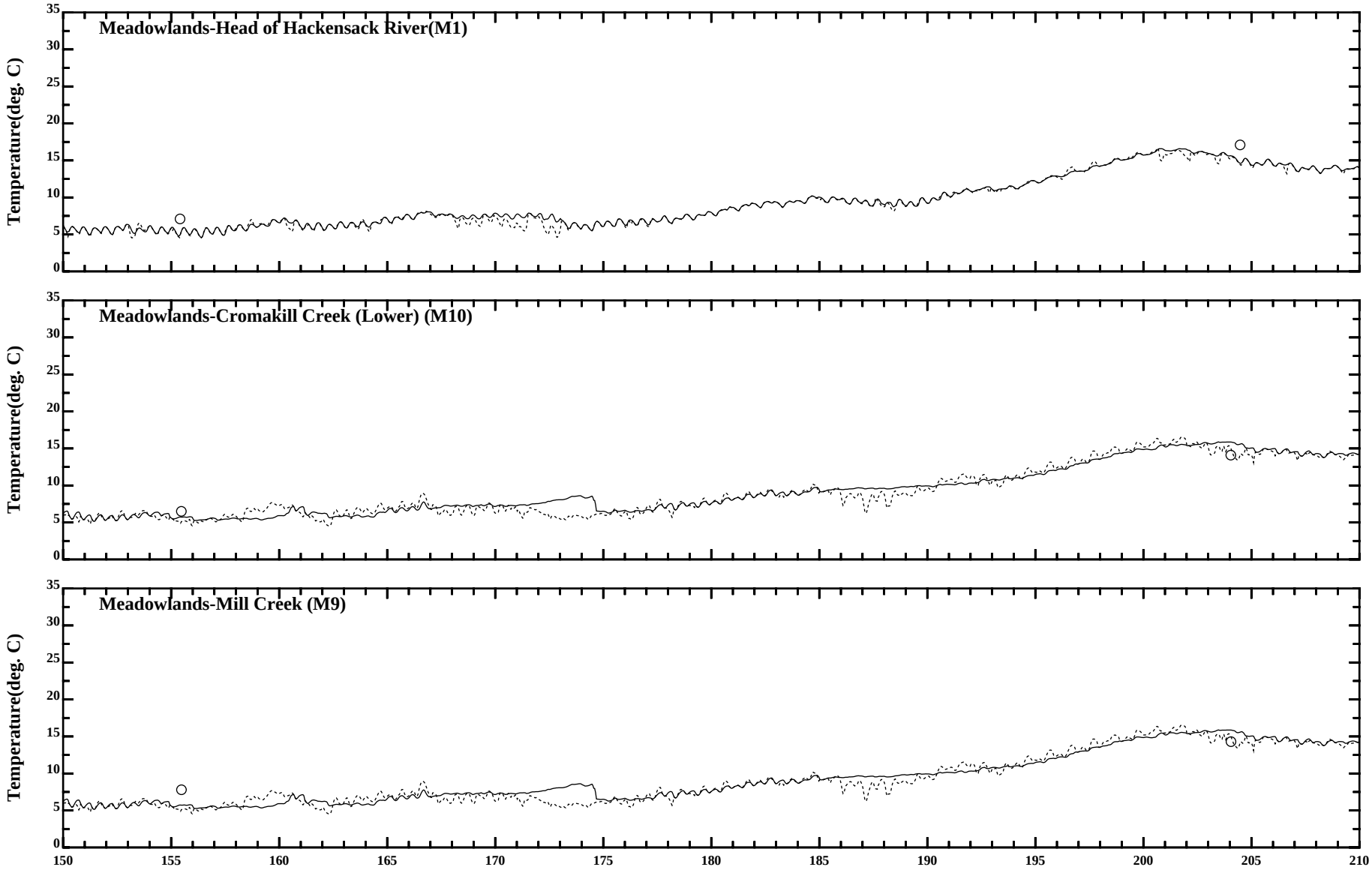
Meadowlands-Head of Hackensack River(M1)
Meadowlands-Cromakill Creek (Lower) (M10)
Meadowlands-Mill Creek (M9)
Temperature(deg. C)
0
5
10
15
20
25
30
35
150
155
160
165
170
175
180
185
190
195
200
205
210
Time(days) From Oct. 1, 2001
Model Surface
Model Bottom
MERI Data Surface
MERI Data Bottom

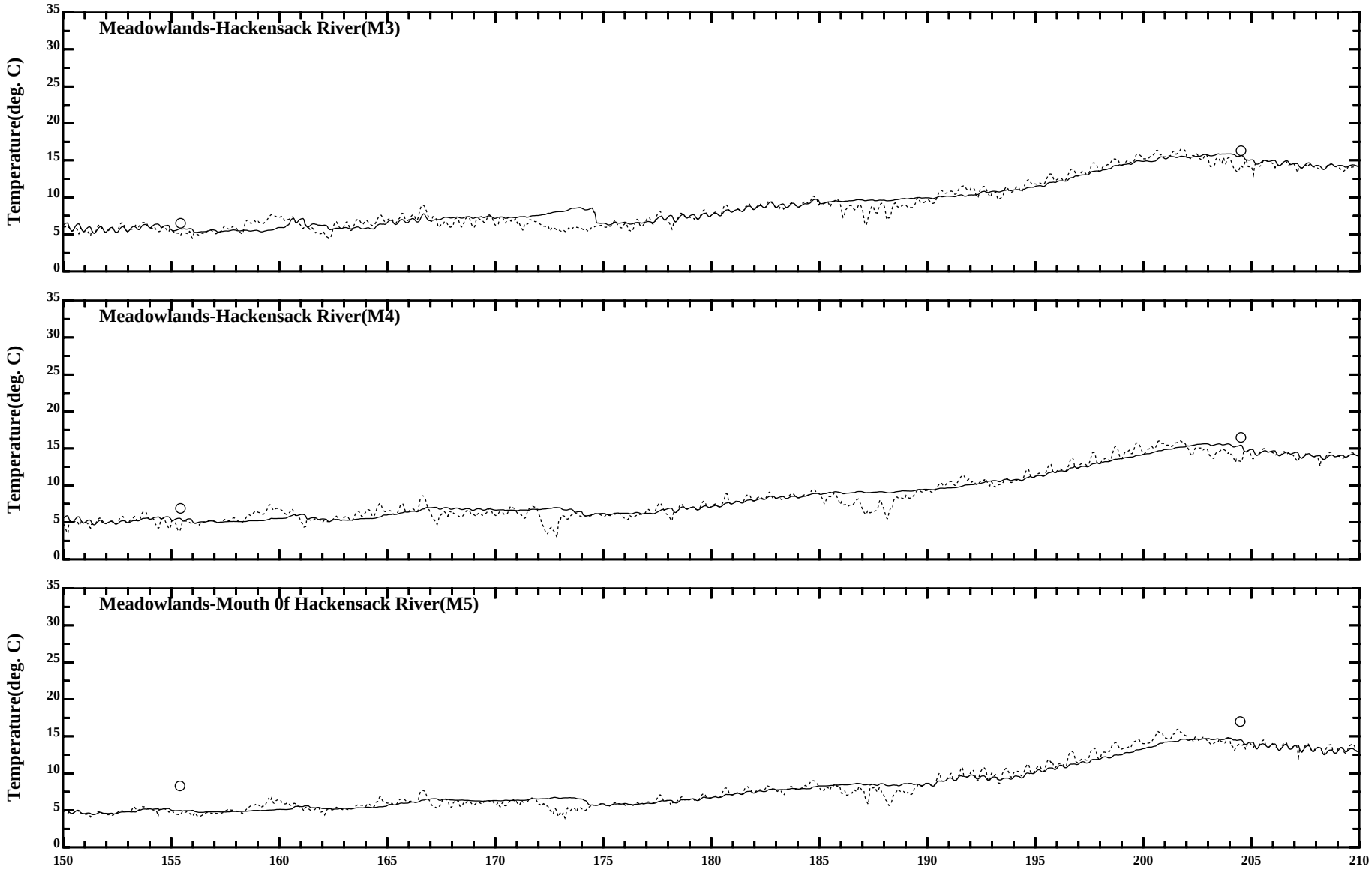
Meadowlands-Hackensack River(M3)
Meadowlands-Hackensack River(M4)
Meadowlands-Mouth 0f Hackensack River(M5)
Temperature(deg. C)
0
5
10
15
20
25
30
35
150
155
160
165
170
175
180
185
190
195
200
205
210
Time(days) From Oct. 1, 2001
Model Surface
Model Bottom
MERI Data Surface
MERI Data Bottom

APPENDIX 7

SKILL ASSESSMENT USING NYCDEP DATA

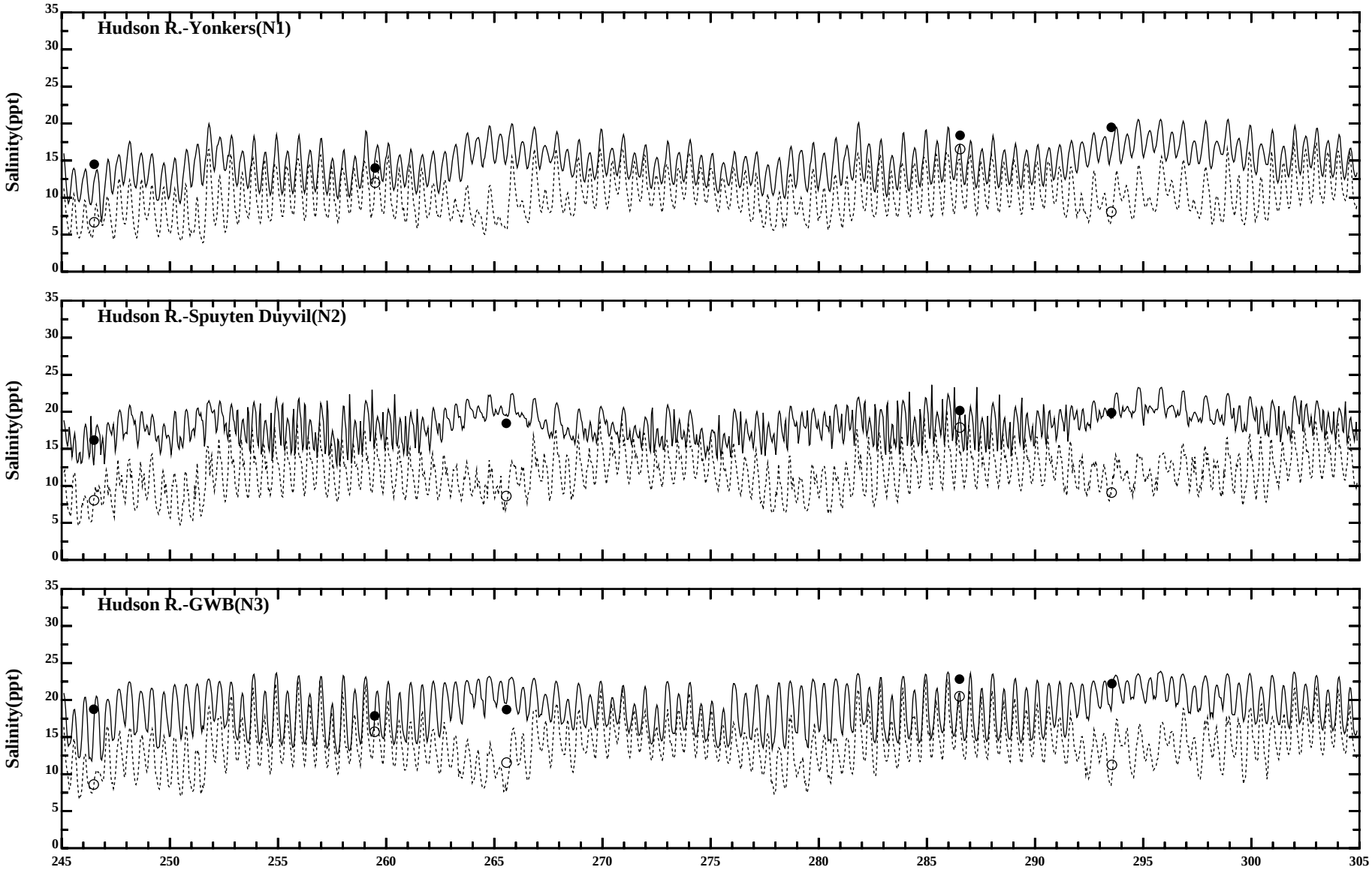

Comparison of Instantaneous Surface and Bottom Salinity

DATE: 8/02/2004 TIME: 11:47:37

/erie1/hrfo0010/HYDRORUNS/CARP9899/PLOTS/TANDS/salt31

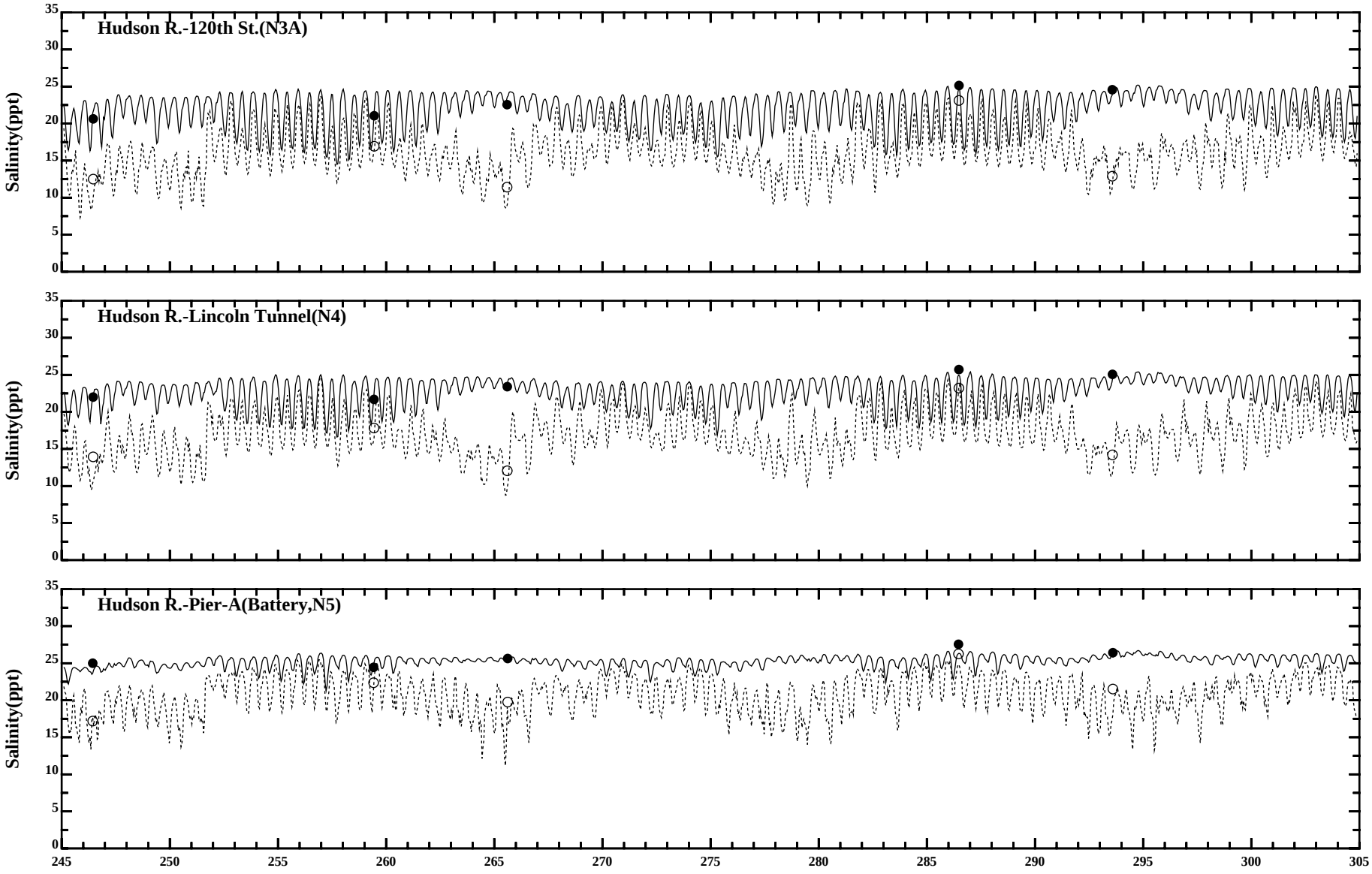

Comparison of Instantaneous Surface and Bottom Salinity

DATE: 8/02/2004 TIME: 11:47:37

/erie1/hrfo0010/HYDRORUNS/CARP9899/PLOTS/TANDS/salt31

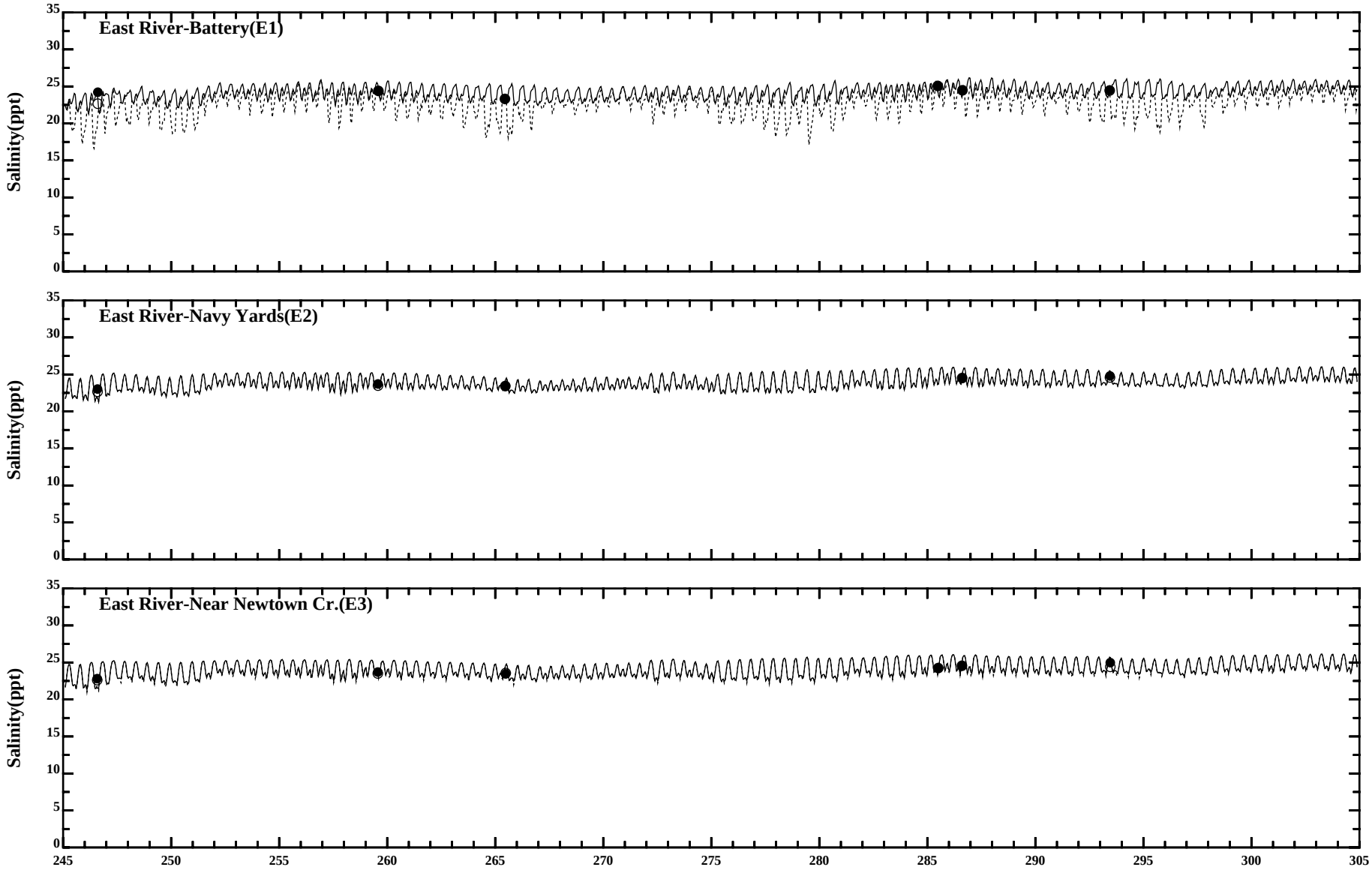

Comparison of Instantaneous Surface and Bottom Salinity

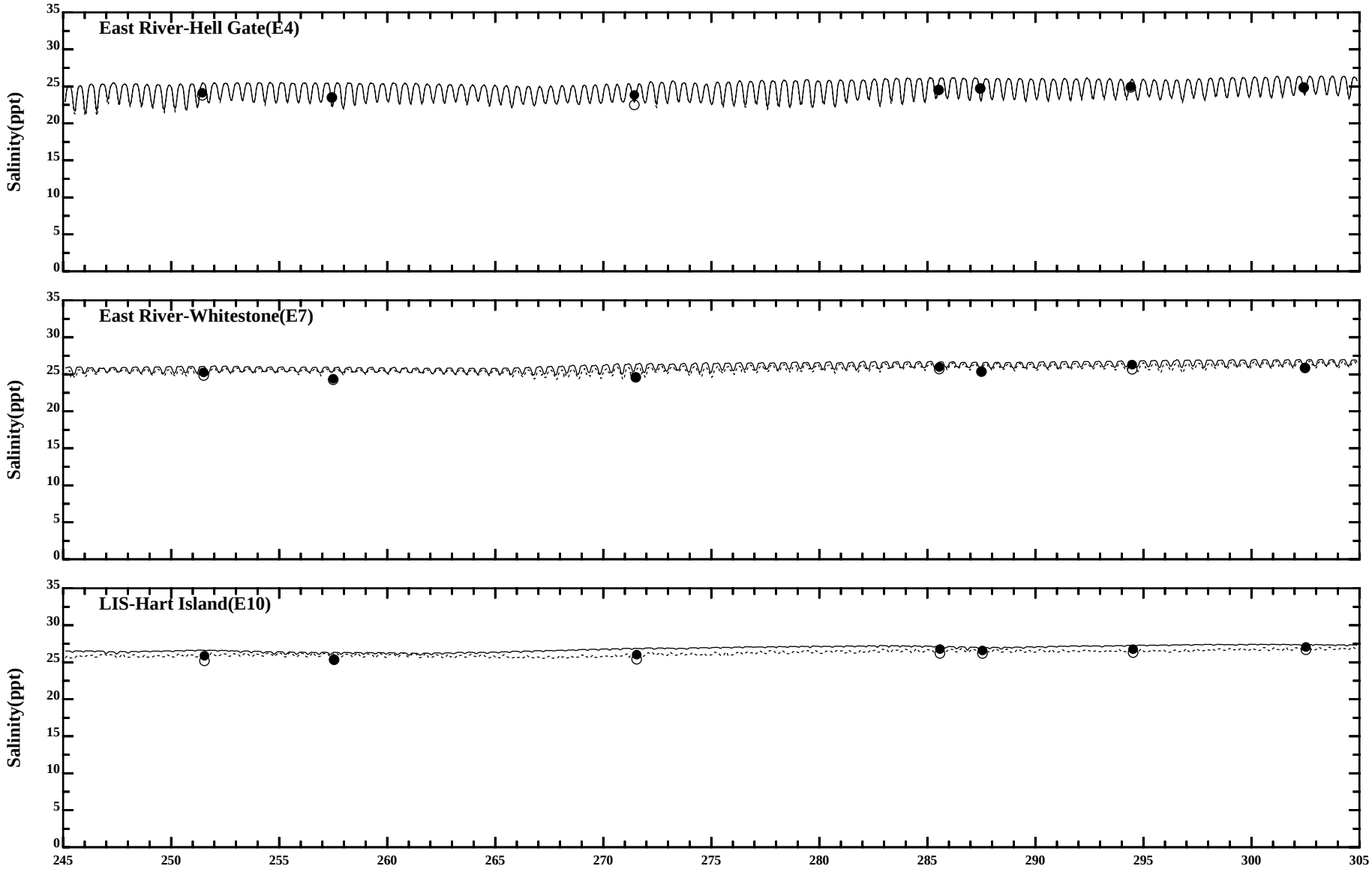

Comparison of Instantaneous Surface and Bottom Salinity

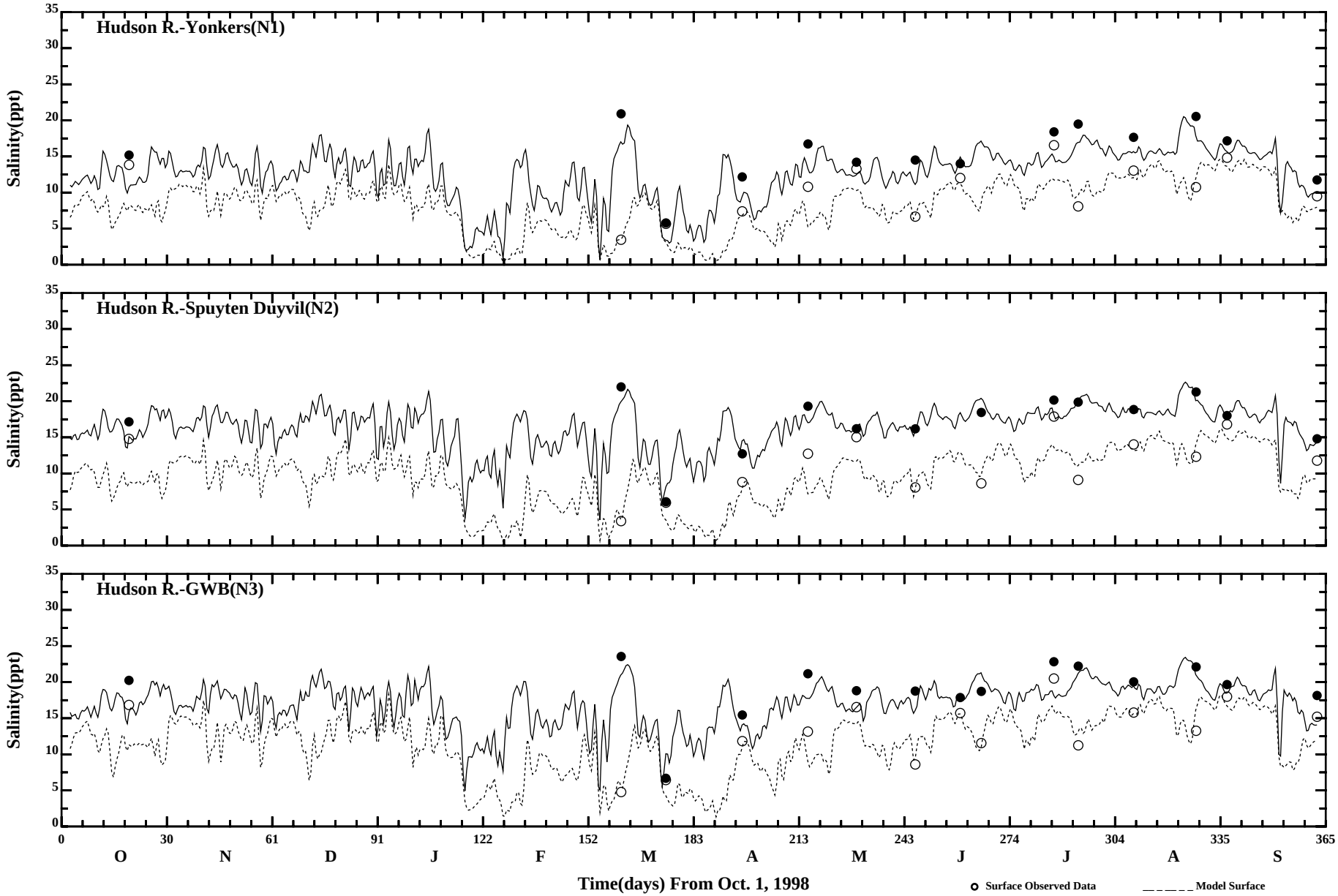

Comparison of 34 Hour Lowpass Surface and Bottom Salinity

DATE: 8/02/2004 TIME: 11:47:16

/erie1/hrfo0010/HYDRORUNS/CARP9899/PLOTS/TANDS/psalt31_34hlp

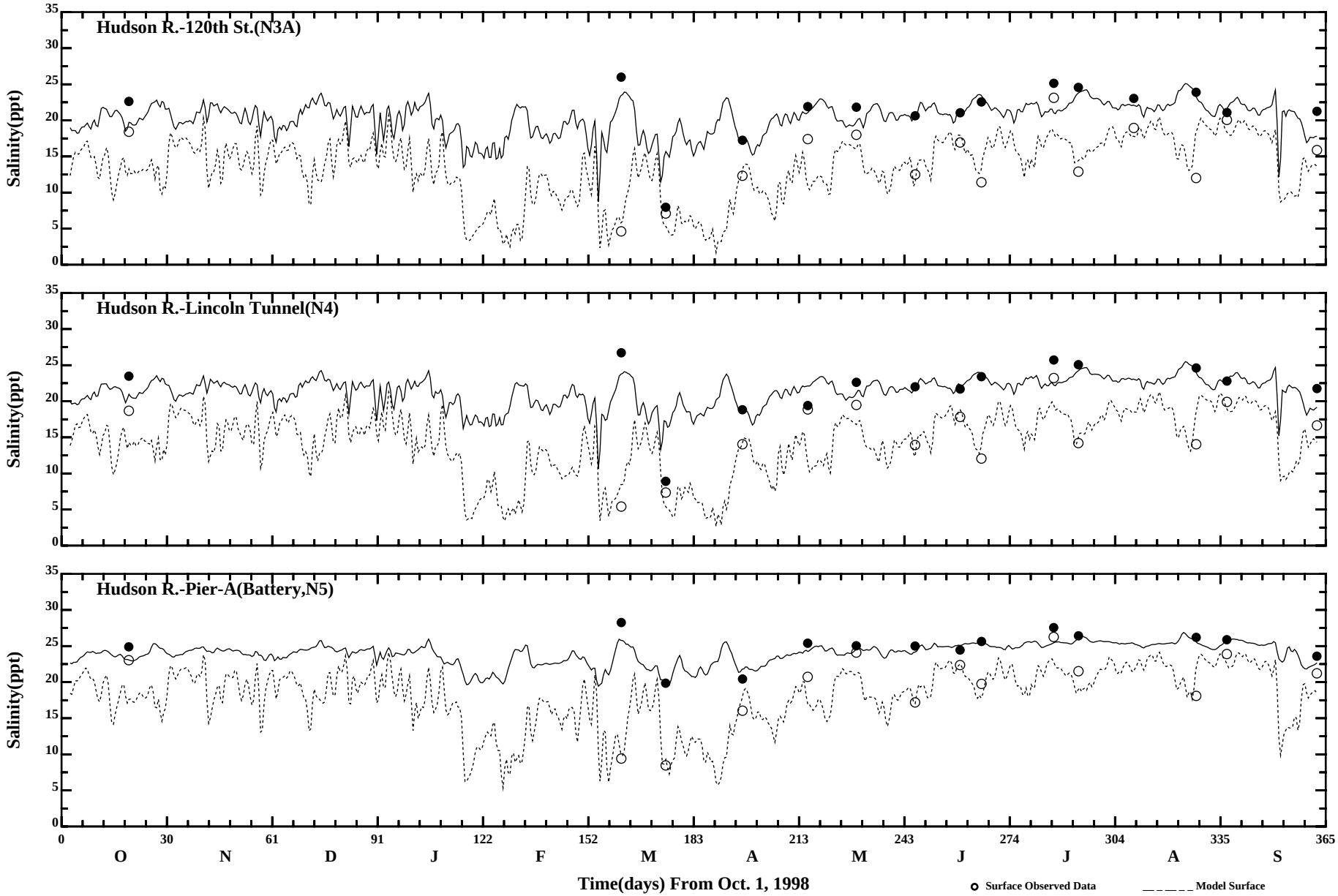

Comparison of 34 Hour Lowpass Surface and Bottom Salinity

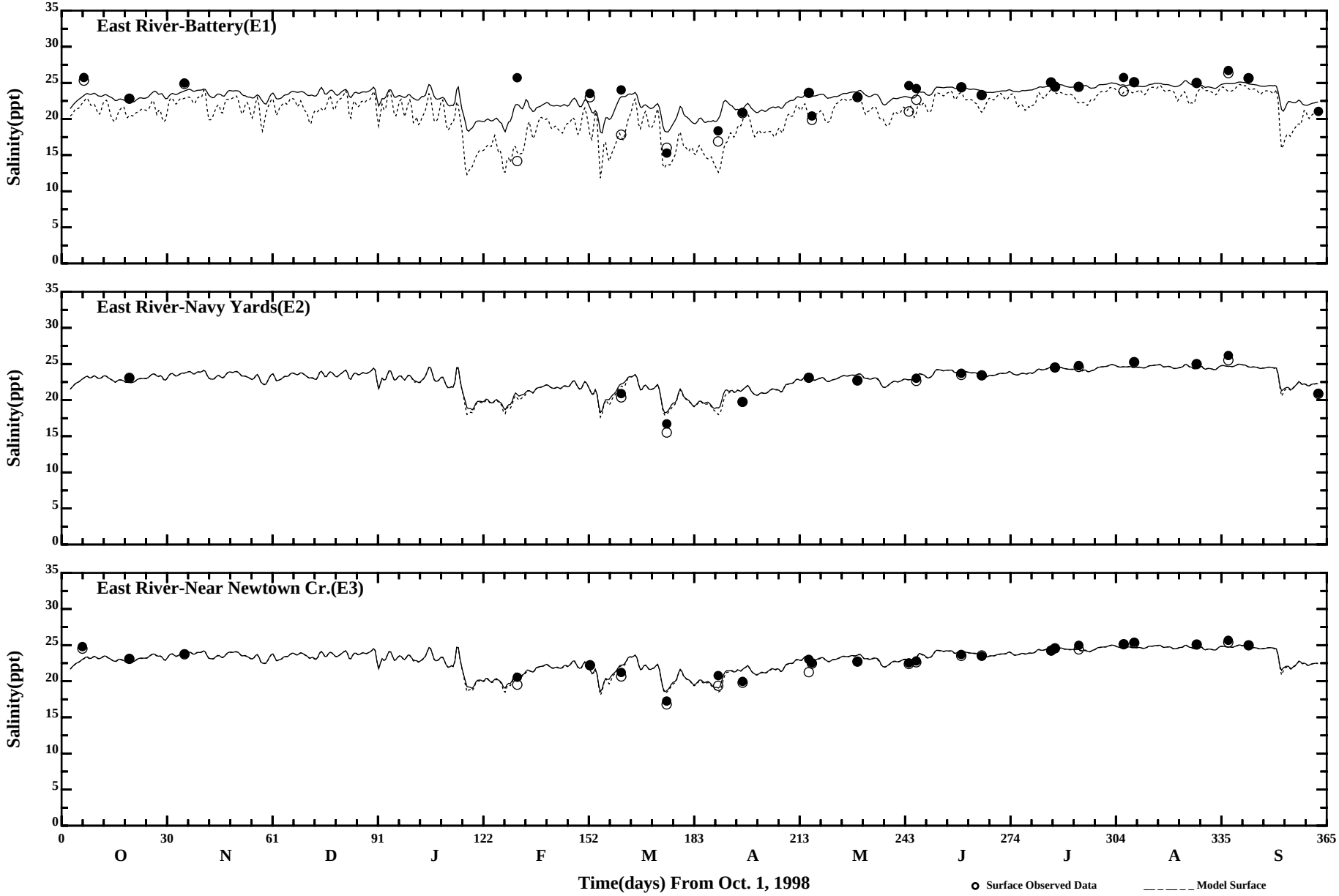

Comparison of 34 Hour Lowpass Surface and Bottom Salinity

DATE: 8/02/2004 TIME: 11:47:16

/erie1/hrfo0010/HYDRORUNS/CARP9899/PLOTS/TANDS/psalt31_34hlp

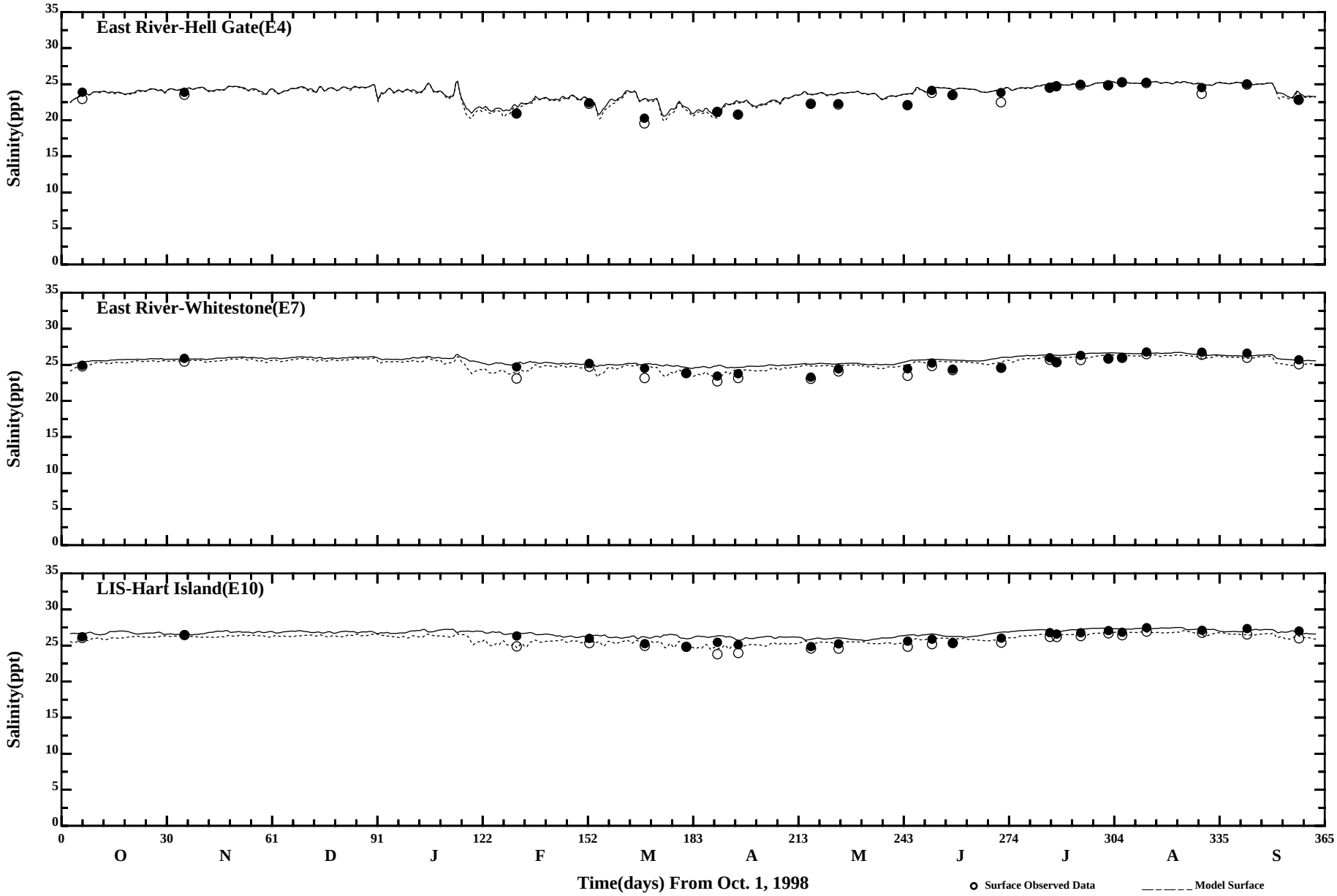

Comparison of 34 Hour Lowpass Surface and Bottom Salinity

DATE: 8/02/2004 TIME: 11:47:16

/erie1/hrfo0010/HYDRORUNS/CARP9899/PLOTS/TANDS/psalt31_34hlp

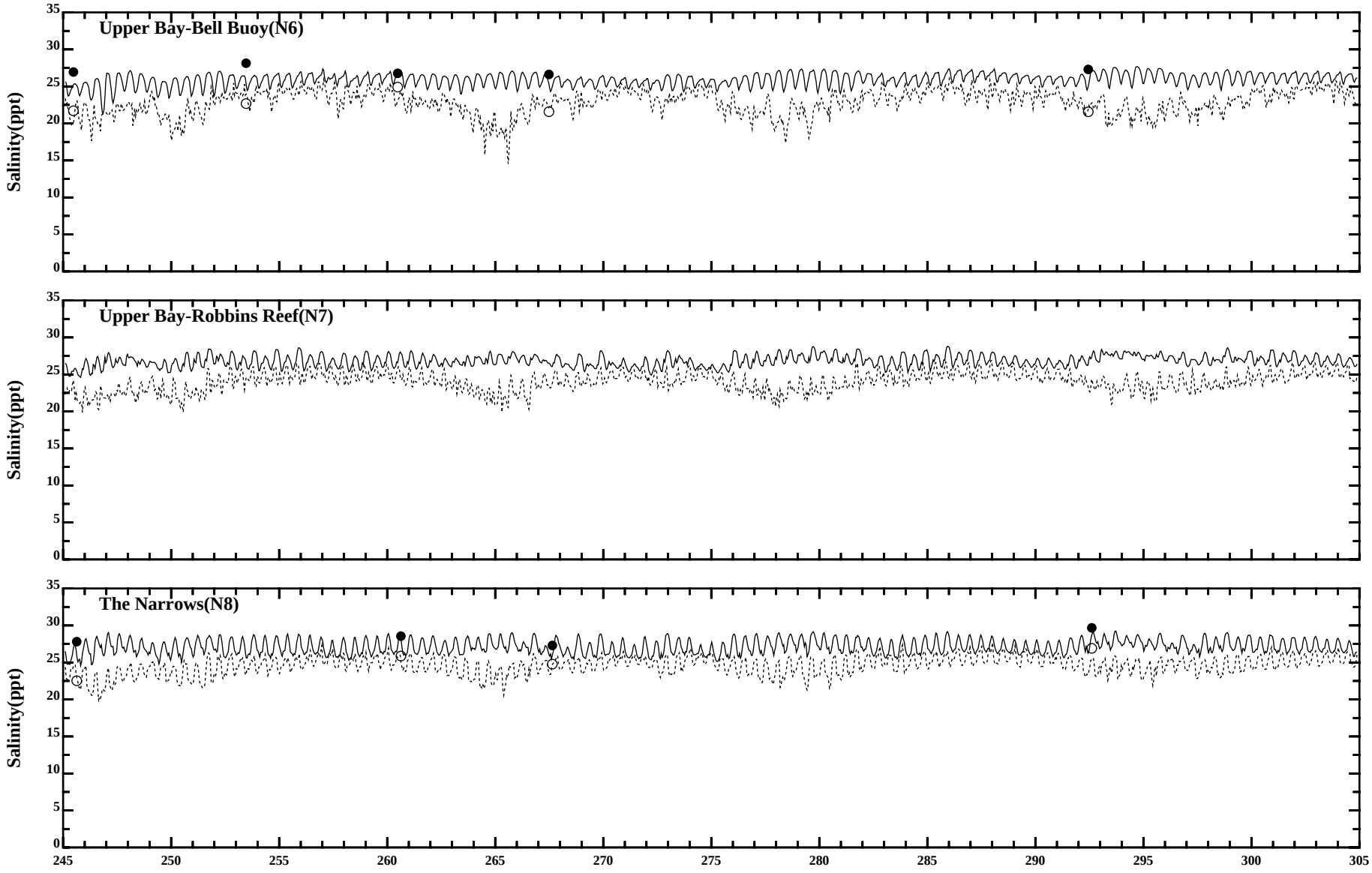

Comparison of Instantaneous Surface and Bottom Salinity

DATE: 8/02/2004 TIME: 11:47:46

/erie1/hrfo0010/HYDRORUNS/CARP9899/PLOTS/TANDS/salt32.gdp

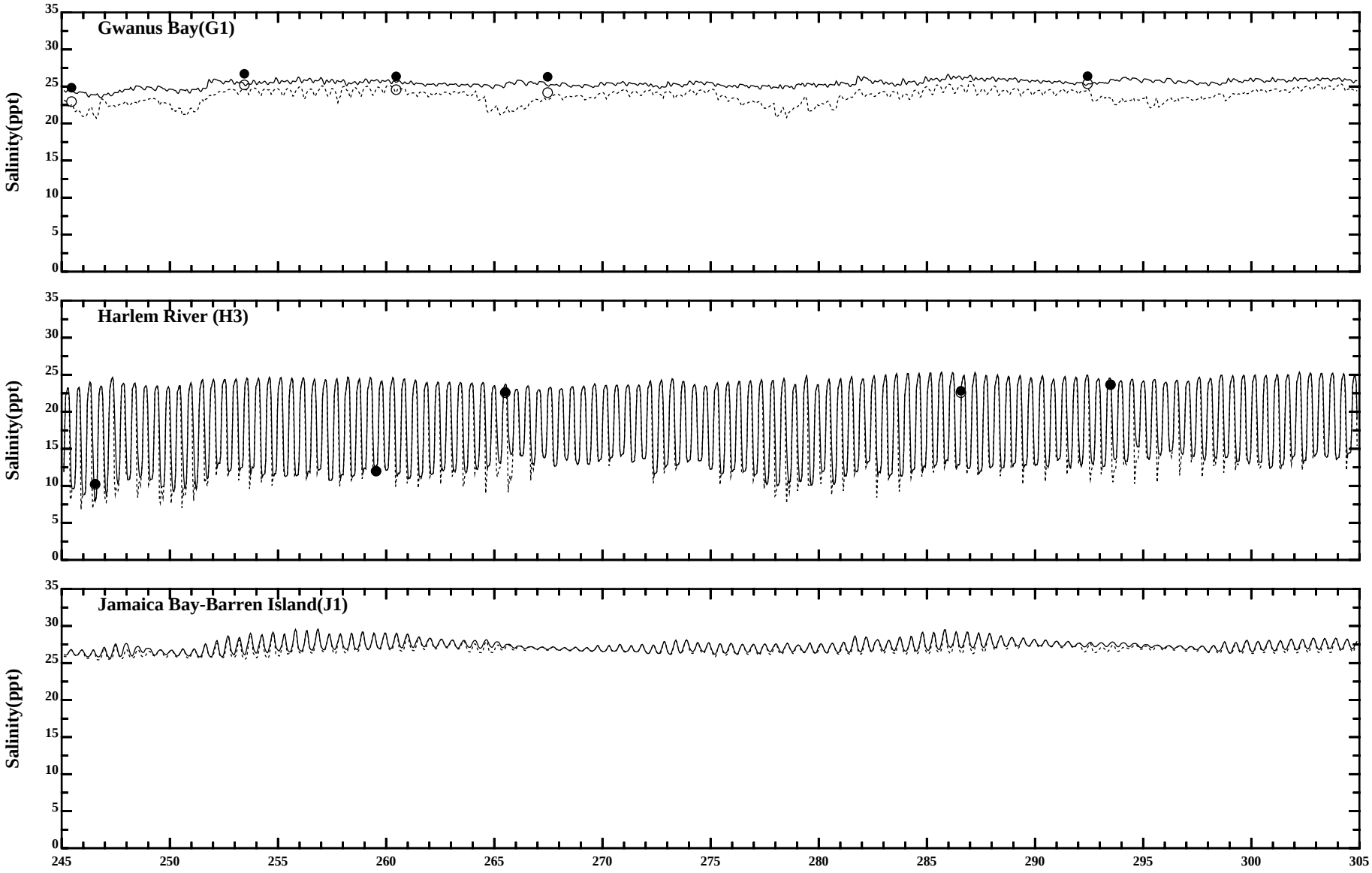

Comparison of Instantaneous Surface and Bottom Salinity

DATE: 8/02/2004 TIME: 11:47:46

/erie1/hrfo0010/HYDRORUNS/CARP9899/PLOTS/TANDS/salt32.gdp

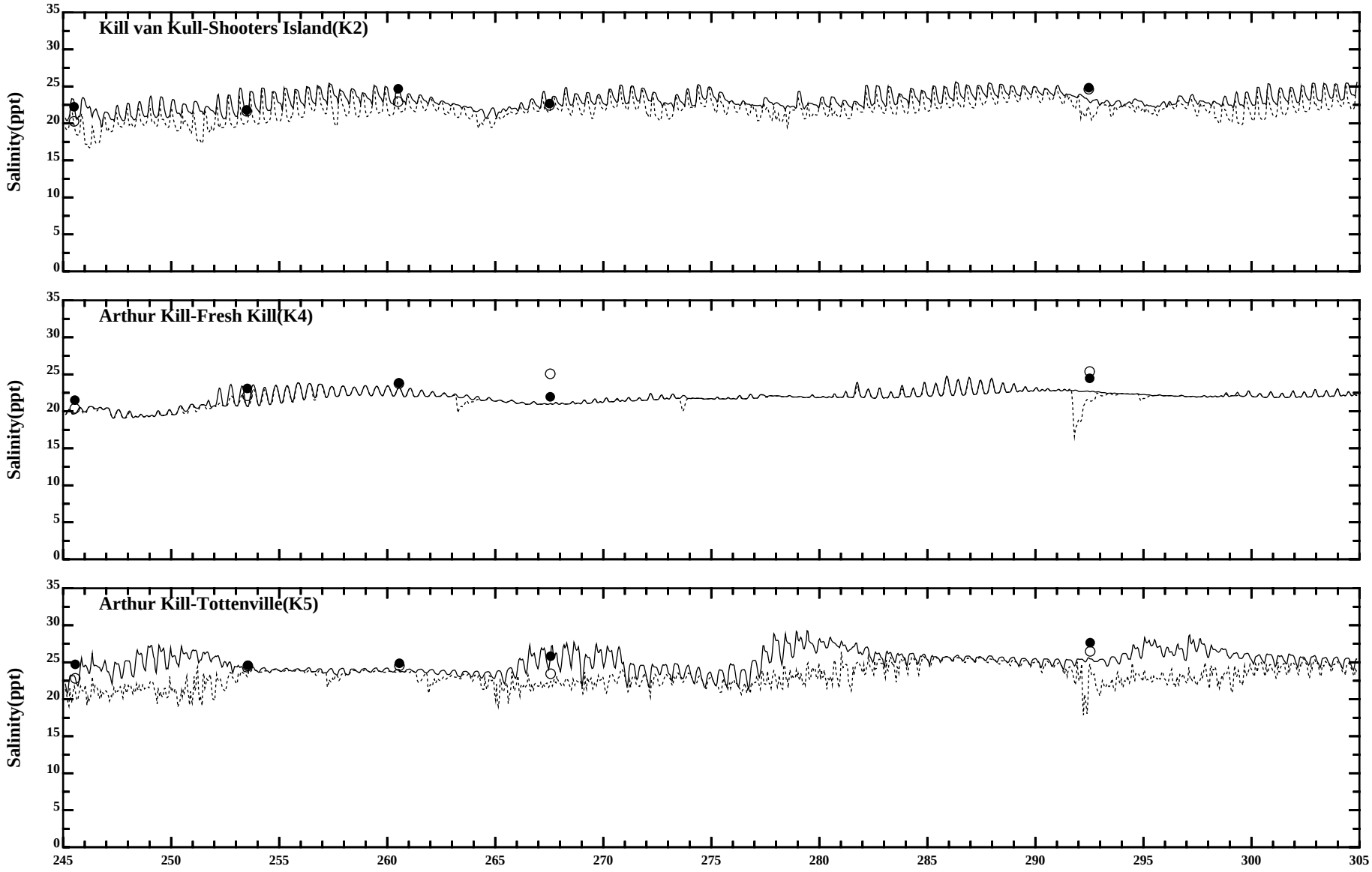

Comparison of Instantaneous Surface and Bottom Salinity

DATE: 8/02/2004 TIME: 11:47:46

/erie1/hrfo0010/HYDRORUNS/CARP9899/PLOTS/TANDS/salt32.gdp

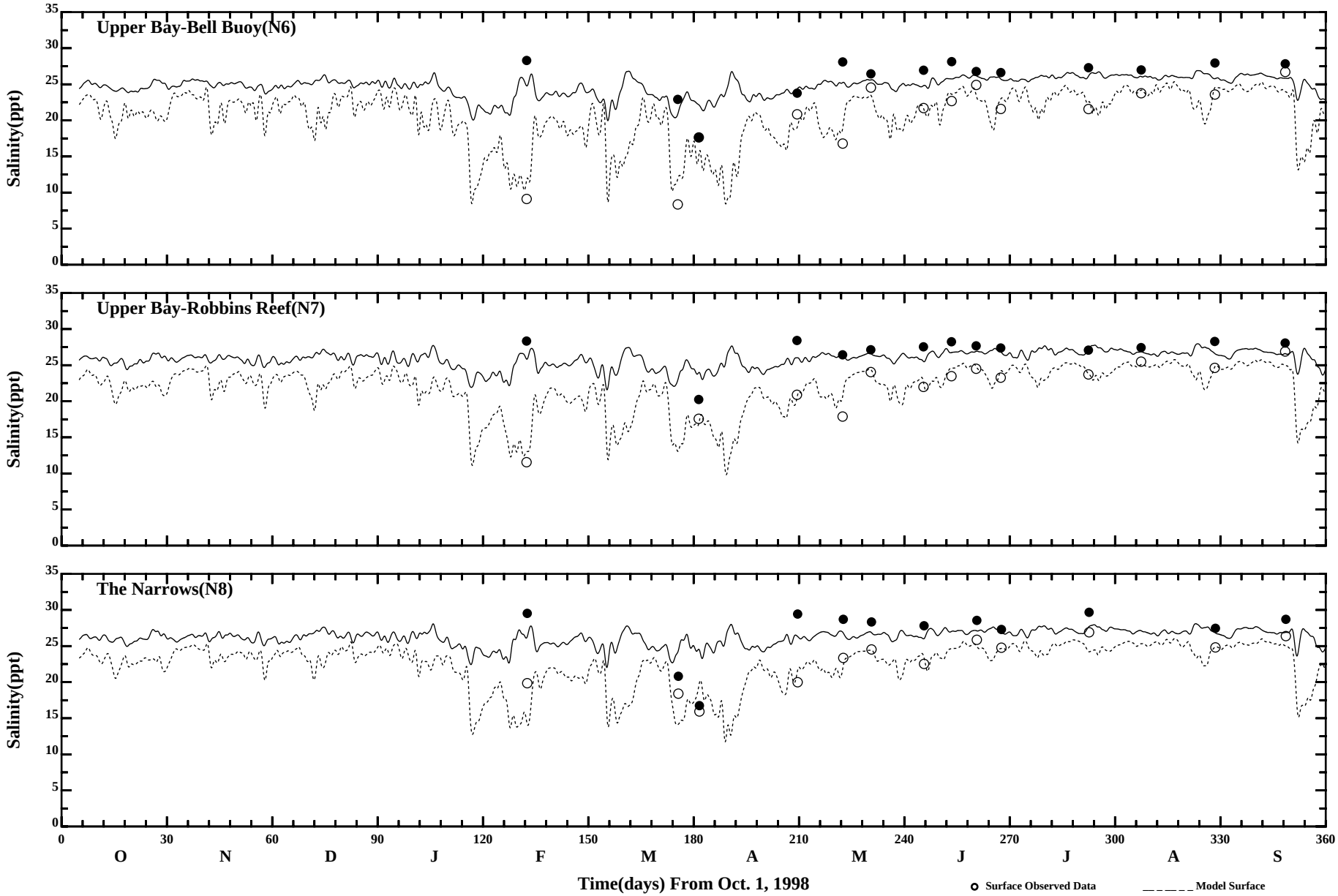

Comparison of 34 Hr LP Surface and Bottom Salinity

DATE: 8/02/2004 TIME: 11:47:27

/erie1/hrfo0010/HYDRORUNS/CARP9899/PLOTS/TANDS/salt32_34hlp.gdp

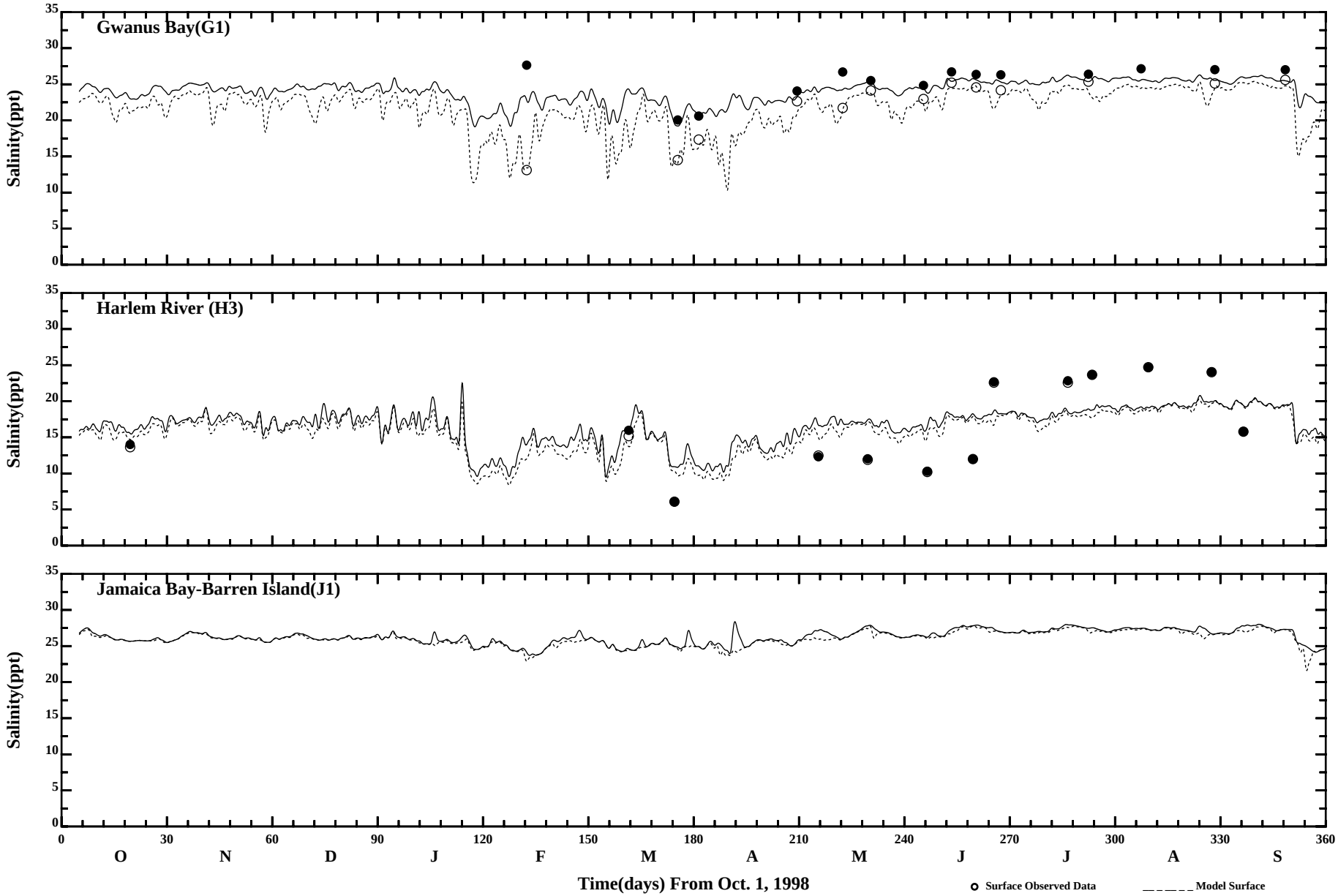

Comparison of 34 Hr LP Surface and Bottom Salinity

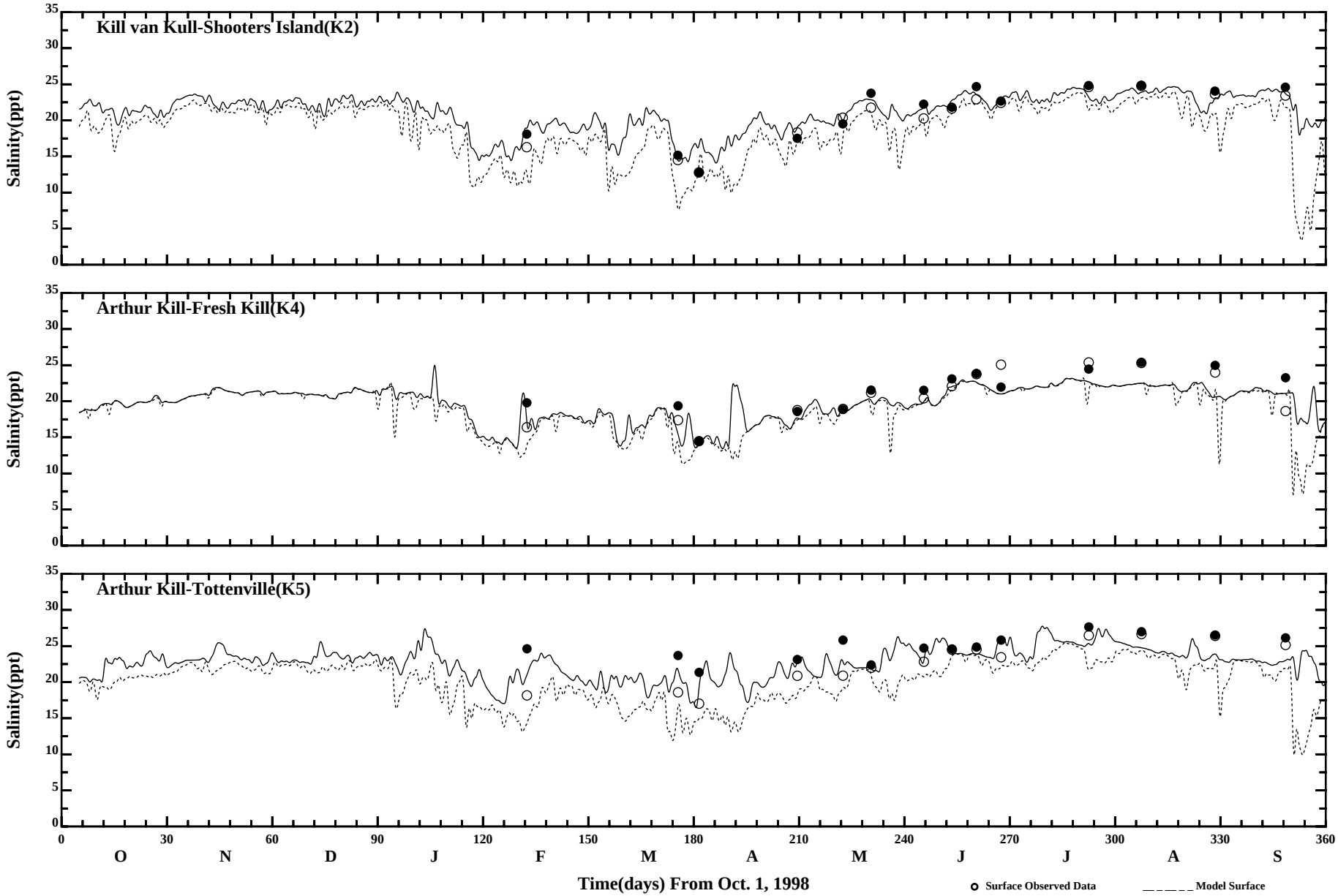

Comparison of 34 Hr LP Surface and Bottom Salinity

DATE: 8/02/2004 TIME: 11:47:27

/erie1/hrfo0010/HYDRORUNS/CARP9899/PLOTS/TANDS/salt32_34hlp.gdp

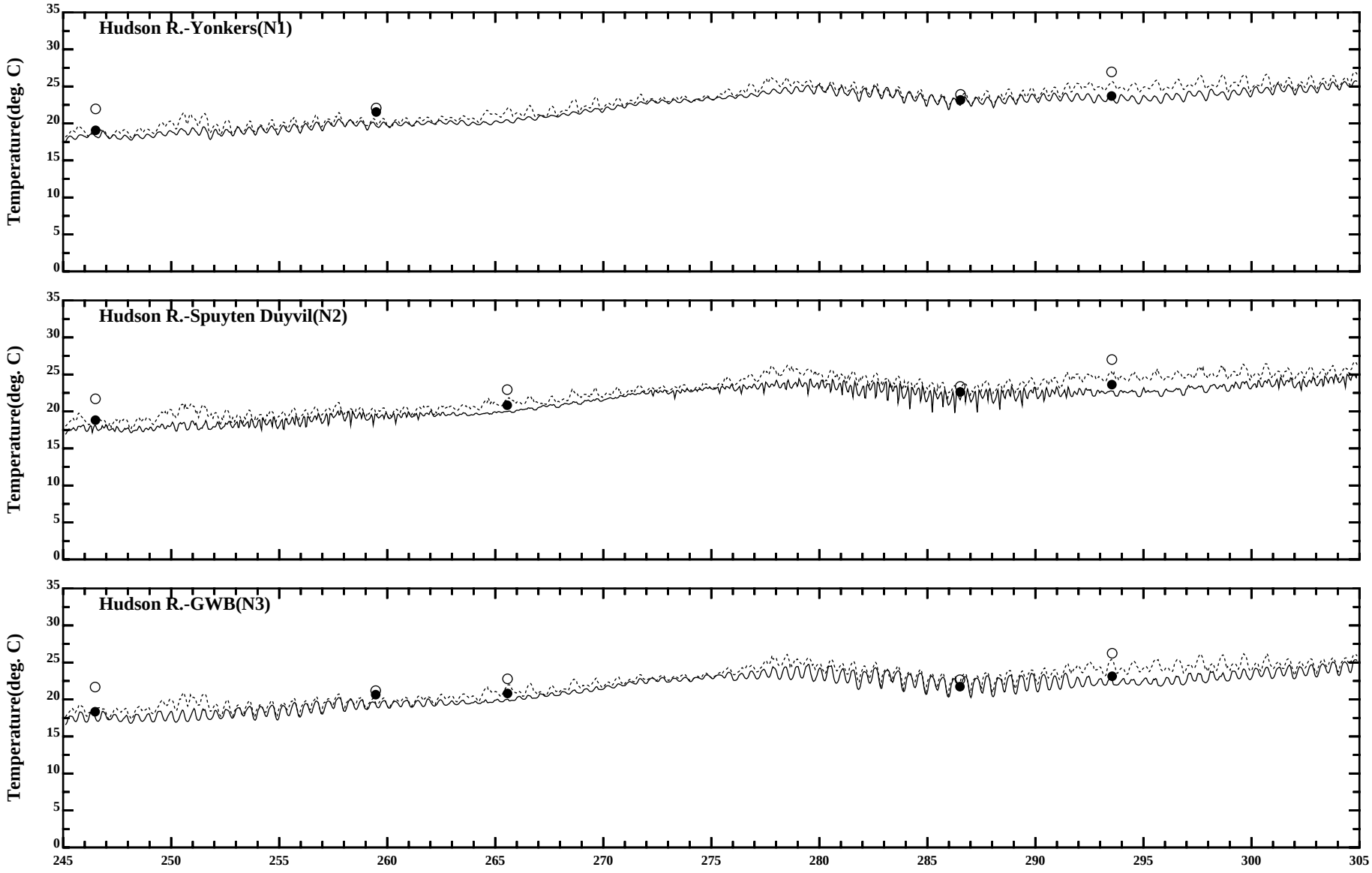

Comparison of Instantaneous Surface and Bottom Temperature

DATE: 8/02/2004 TIME: 11:46:58

/erie1/hrfo0010/HYDRORUNS/CARP9899/PLOTS/TANDS/temp31

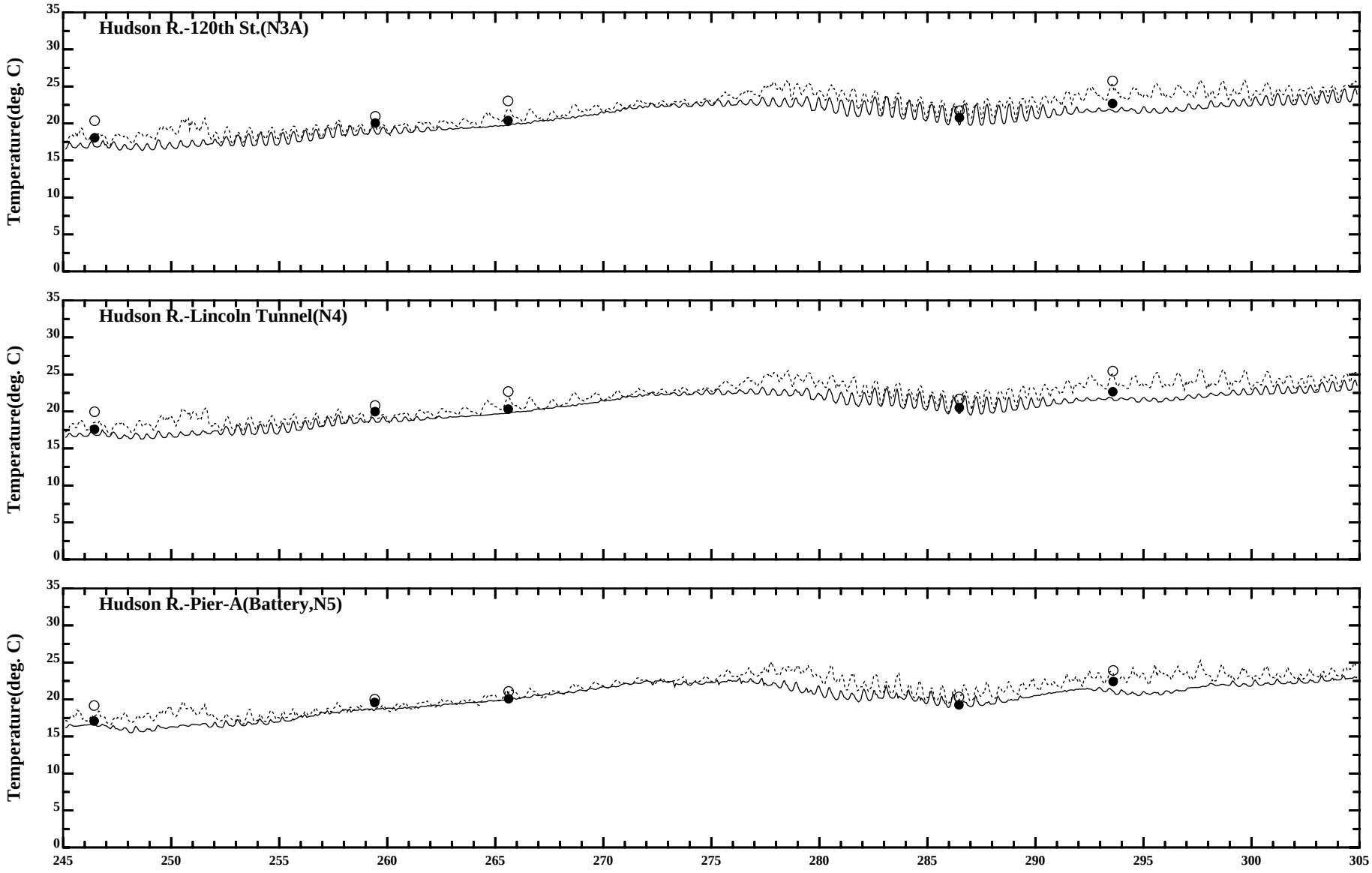

Comparison of Instantaneous Surface and Bottom Temperature

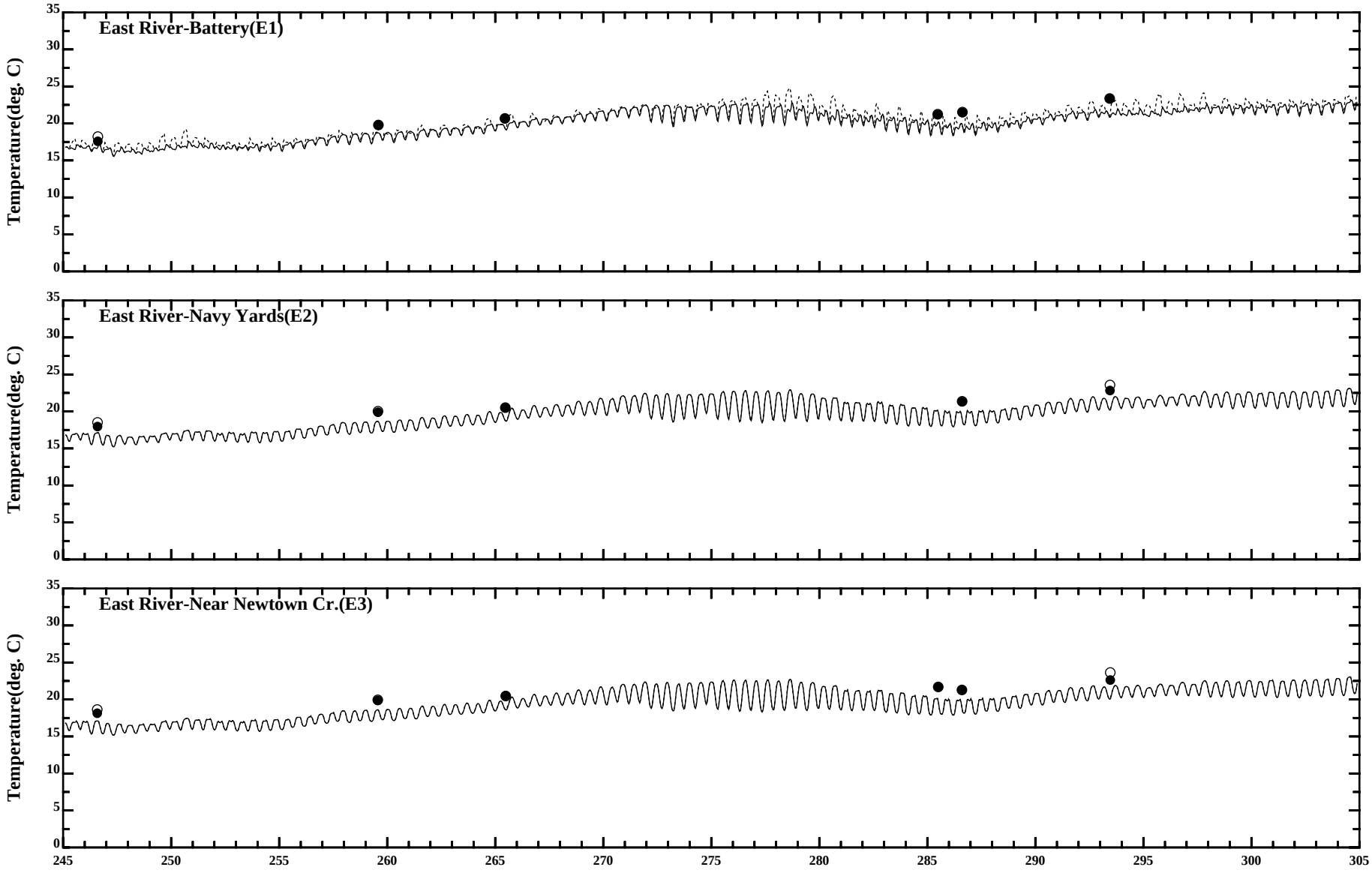

Comparison of Instantaneous Surface and Bottom Temperature

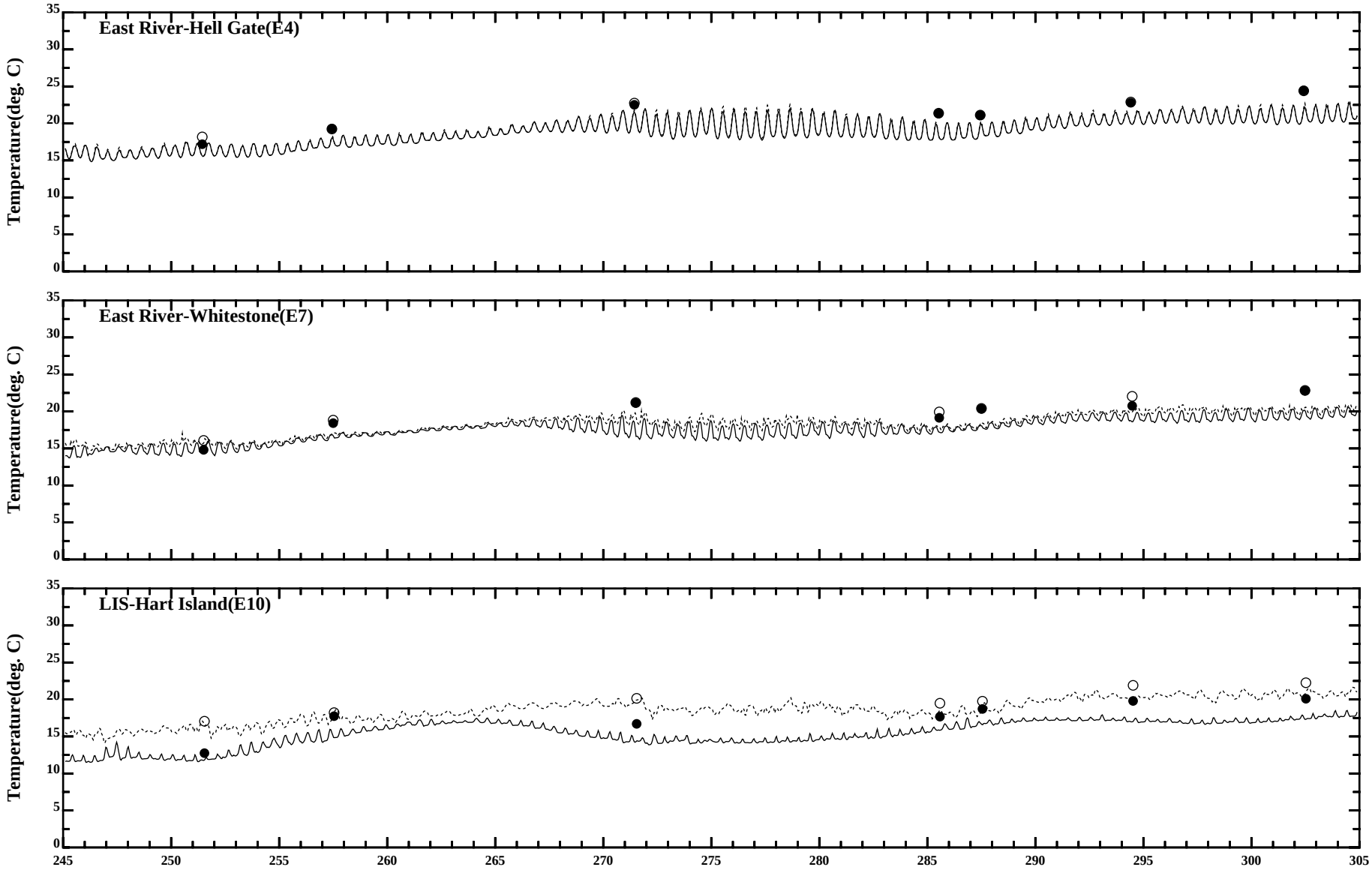

Comparison of Instantaneous Surface and Bottom Temperature

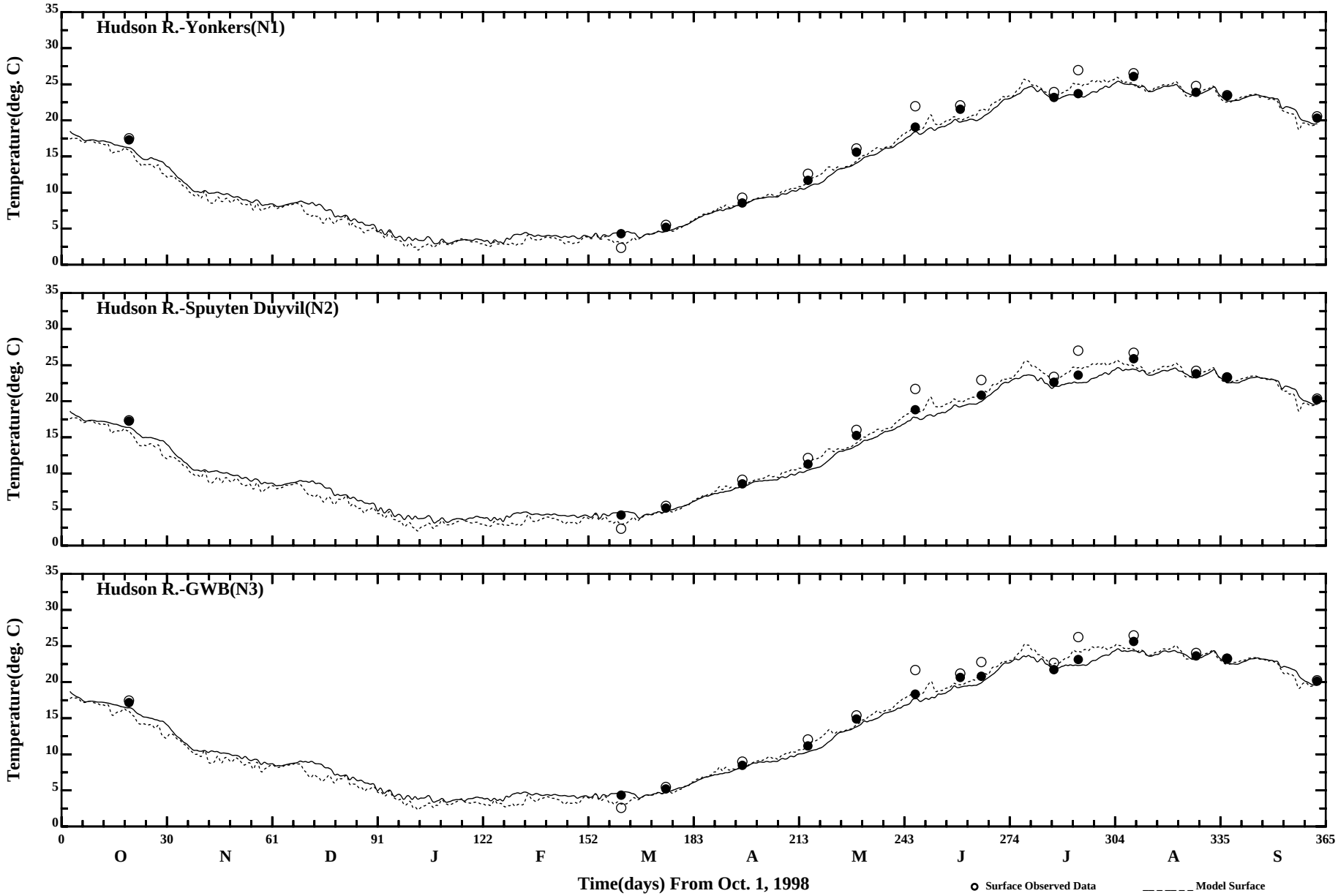

Comparison of 34 Hour Lopass Surface and Bottom Temperature

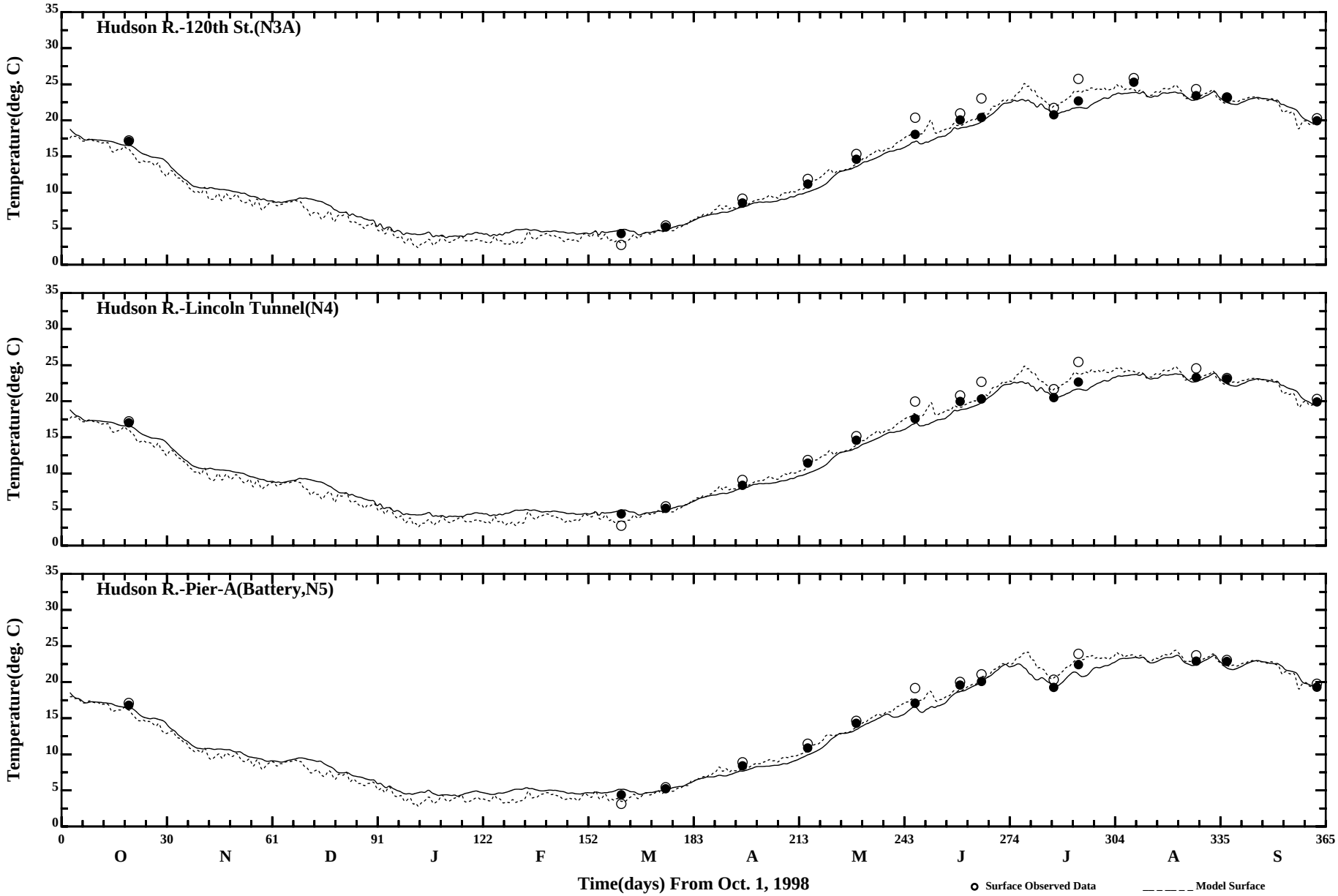

Comparison of 34 Hour Lopass Surface and Bottom Temperature

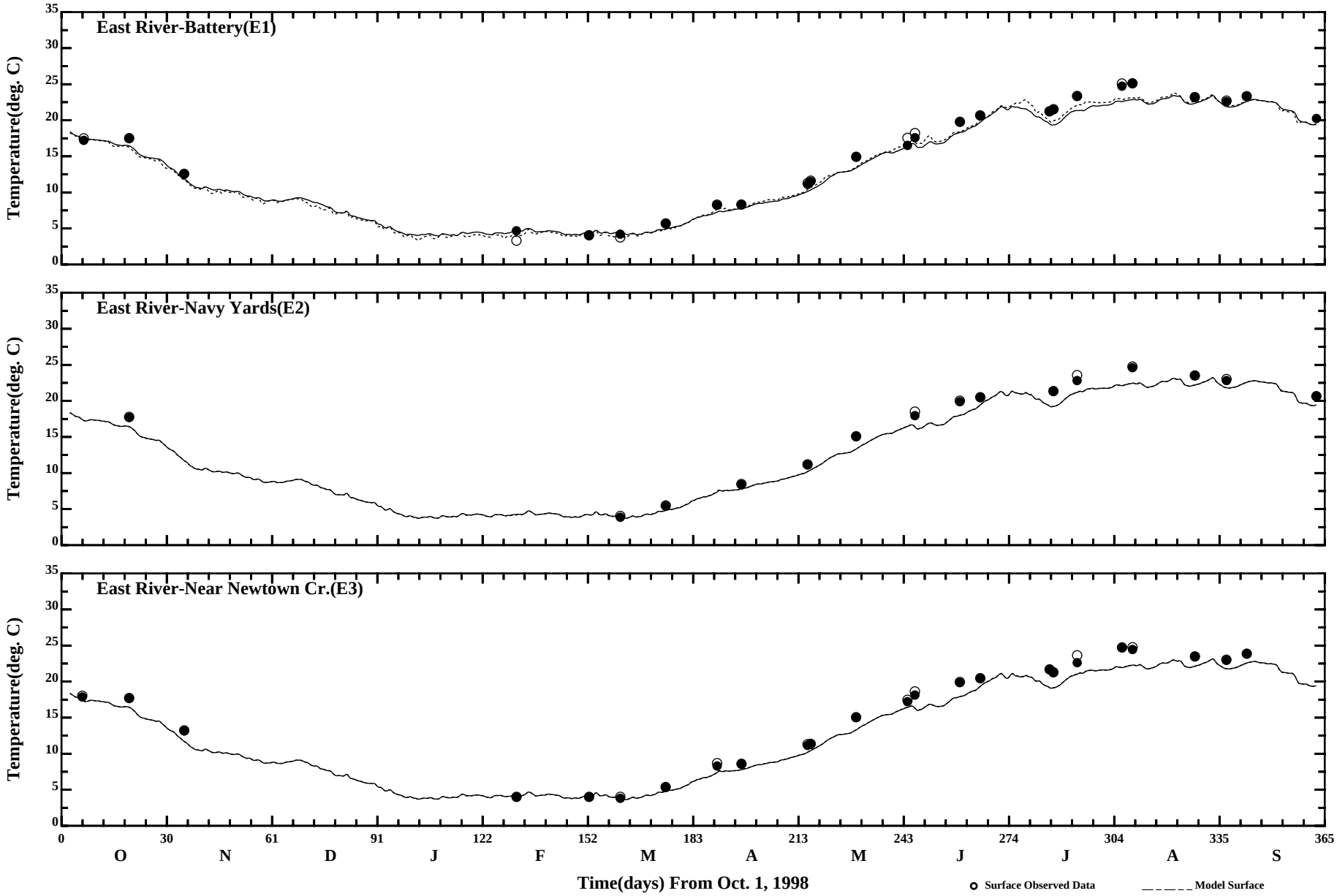

Comparison of 34 Hour Lopass Surface and Bottom Temperature

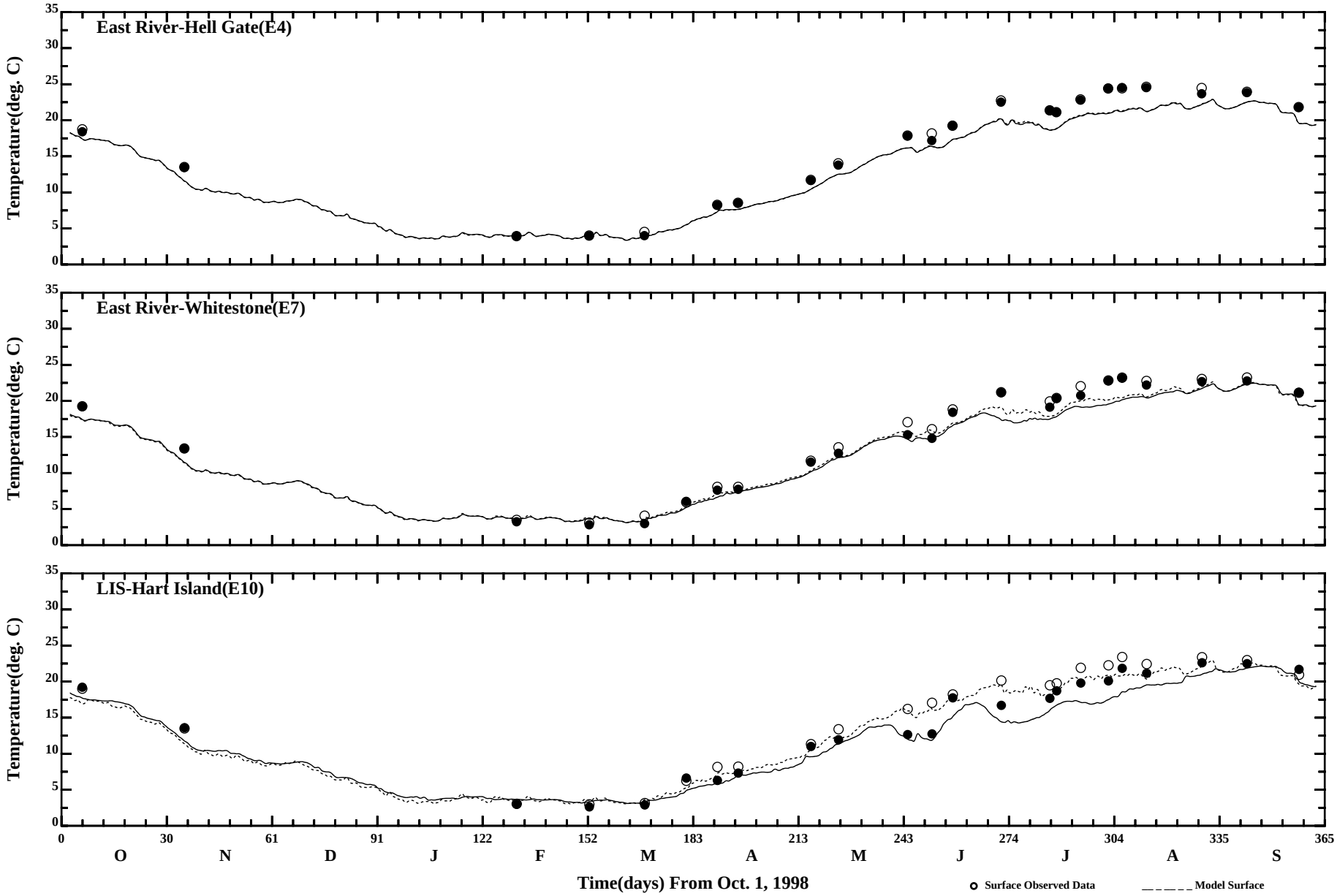

Comparison of 34 Hour Lopass Surface and Bottom Temperature

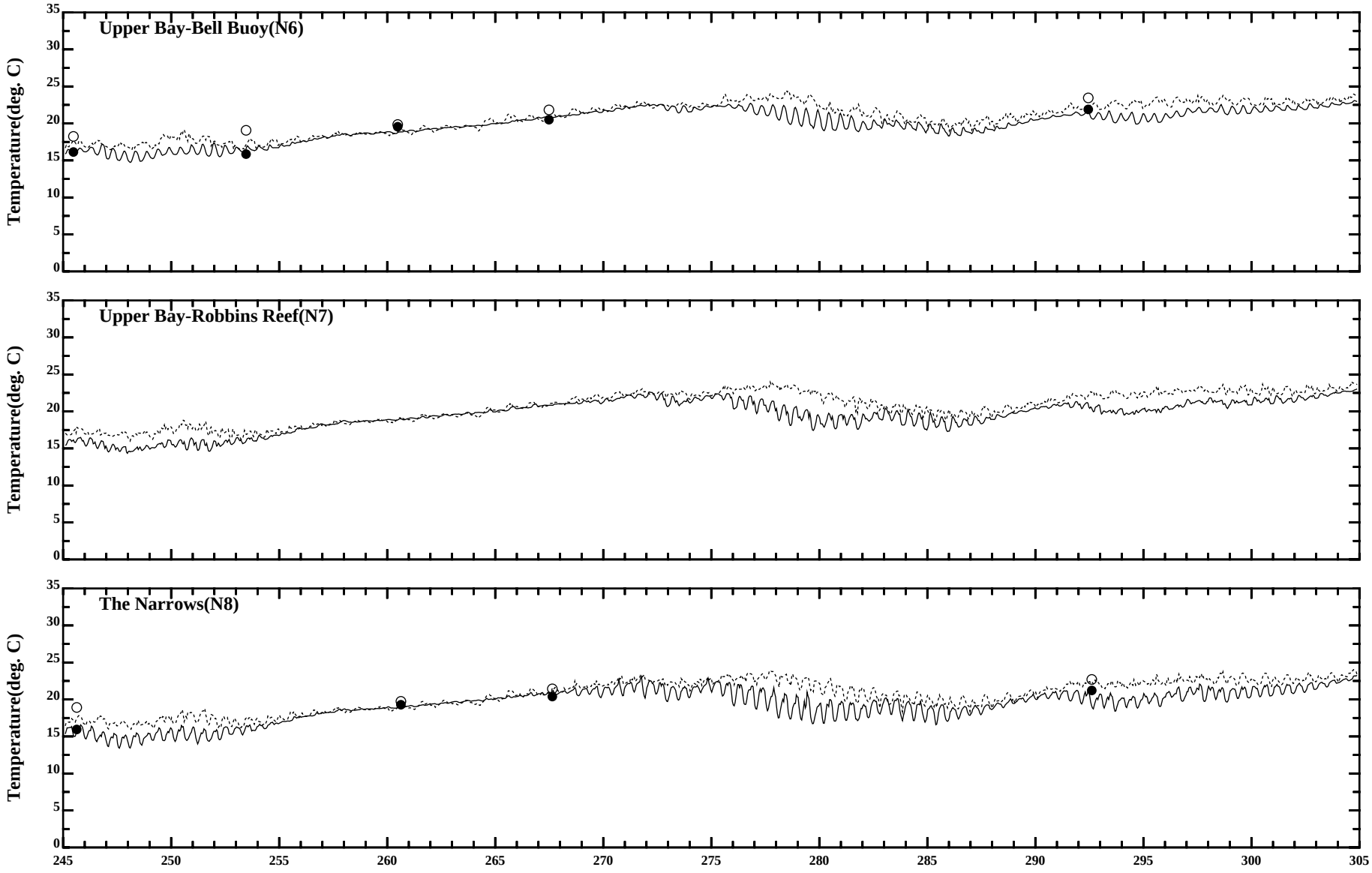

Comparison of Instantaneous Surface and Bottom Temperature

DATE: 8/02/2004 TIME: 11:47: 7

/erie1/hrfo0010/HYDRORUNS/CARP9899/PLOTS/TANDS/temp32.gdp

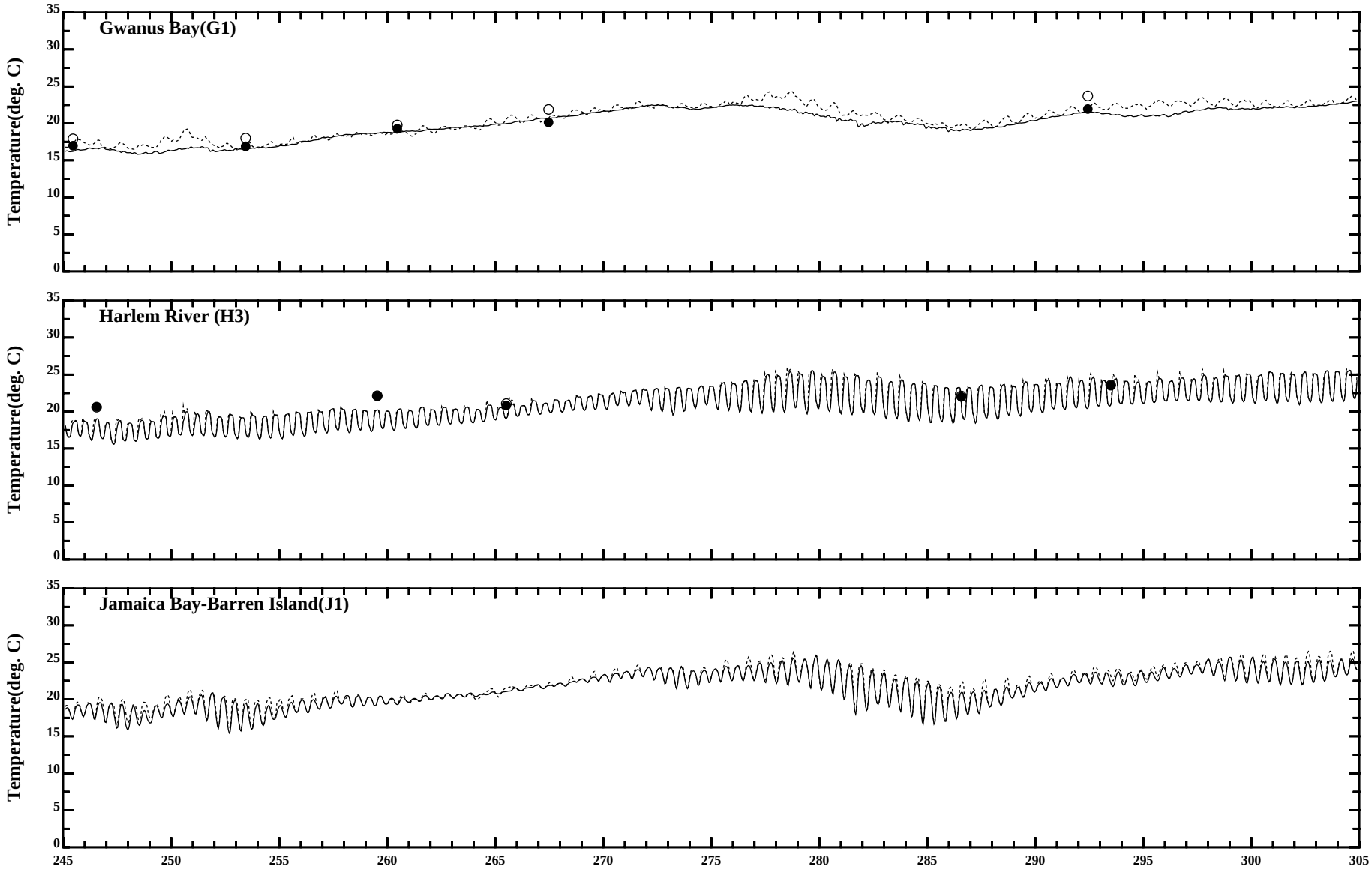

Comparison of Instantaneous Surface and Bottom Temperature

DATE: 8/02/2004 TIME: 11:47: 7

/erie1/hrfo0010/HYDRORUNS/CARP9899/PLOTS/TANDS/temp32.gdp

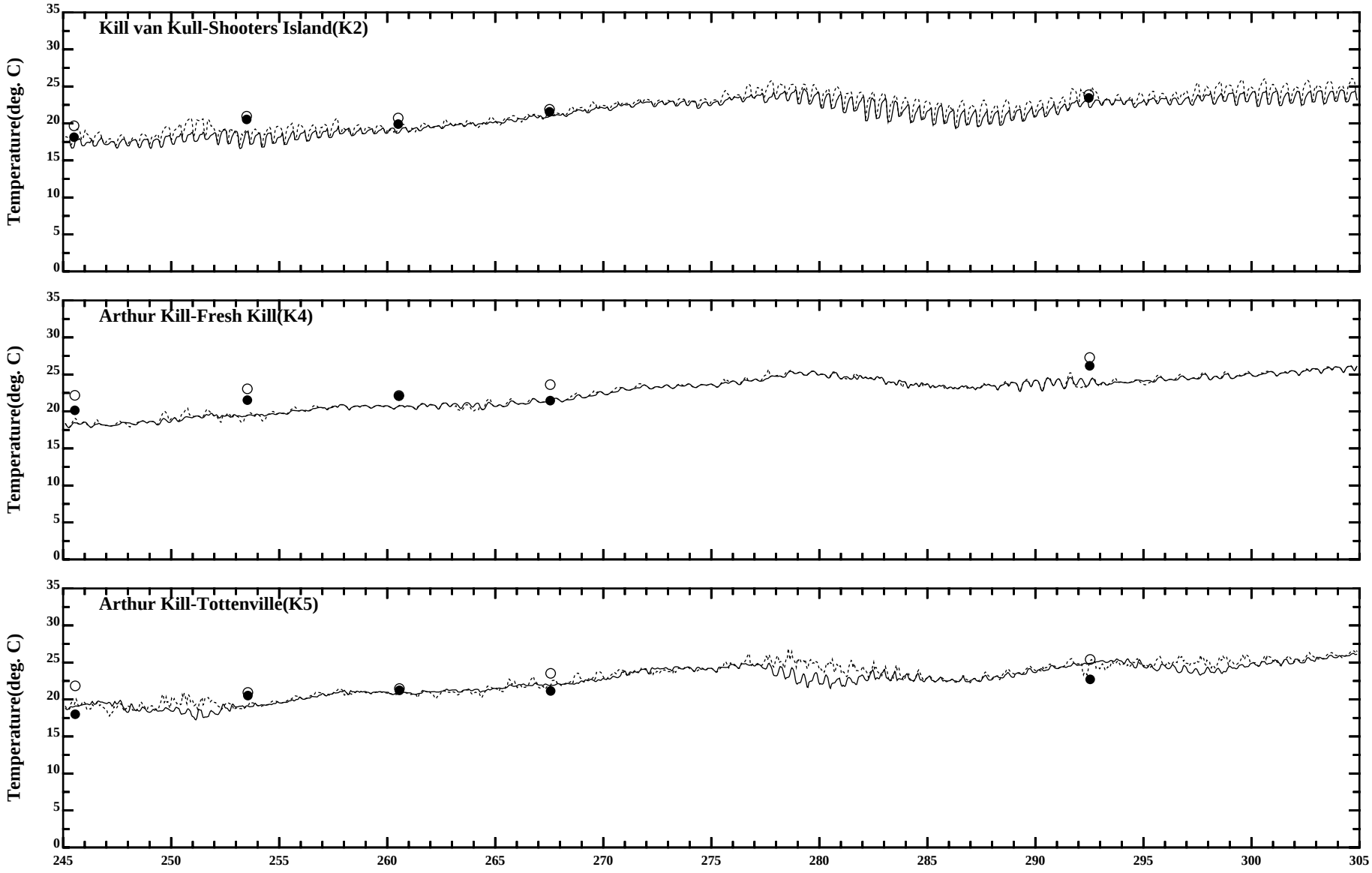

Comparison of Instantaneous Surface and Bottom Temperature

DATE: 8/02/2004 TIME: 11:47: 7

/erie1/hrfo0010/HYDRORUNS/CARP9899/PLOTS/TANDS/temp32.gdp

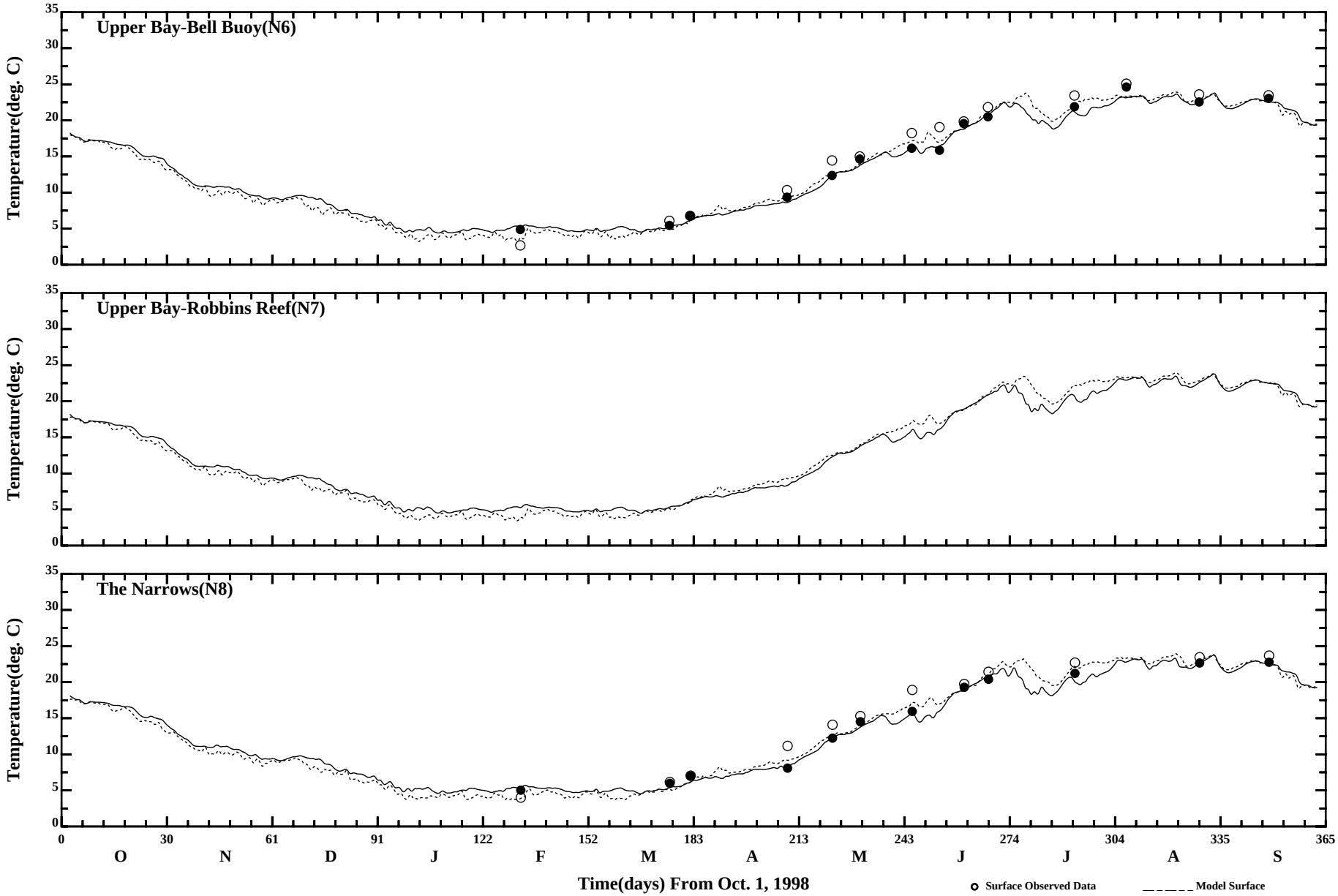

Comparison of 34 Hour Lopass Surface and Bottom Temperature

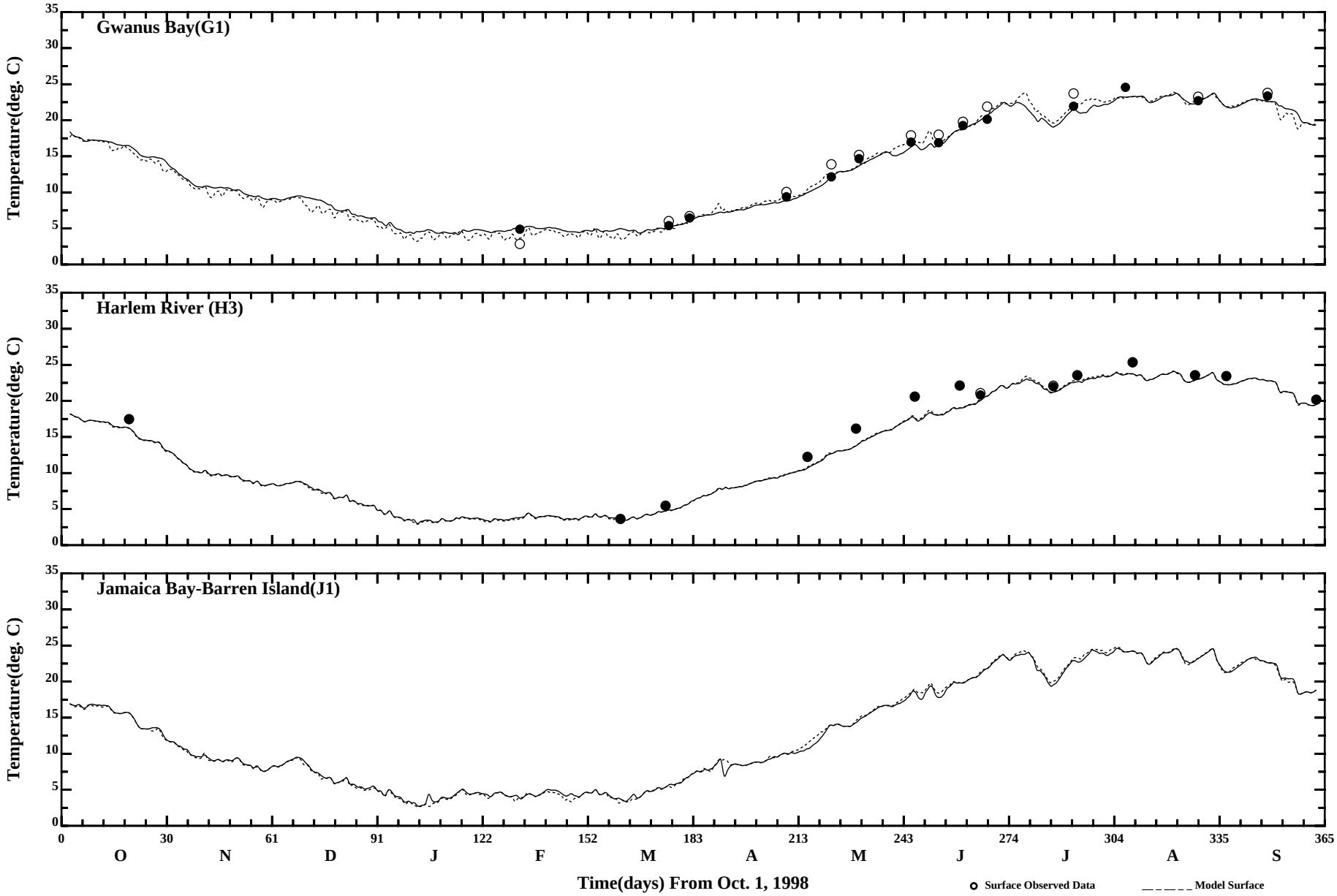

Comparison of 34 Hour Lopass Surface and Bottom Temperature

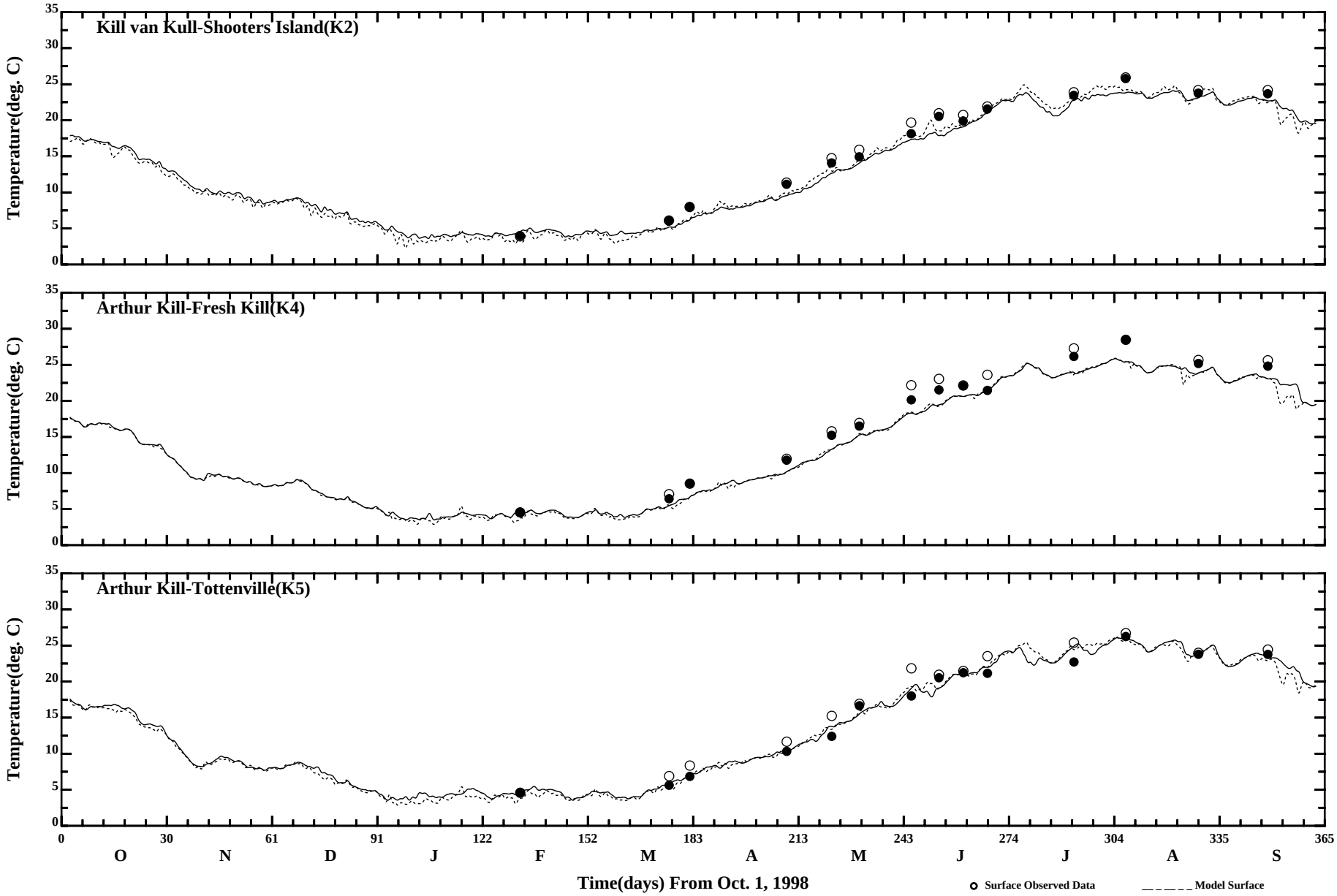

Comparison of 34 Hour Lopass Surface and Bottom Temperature

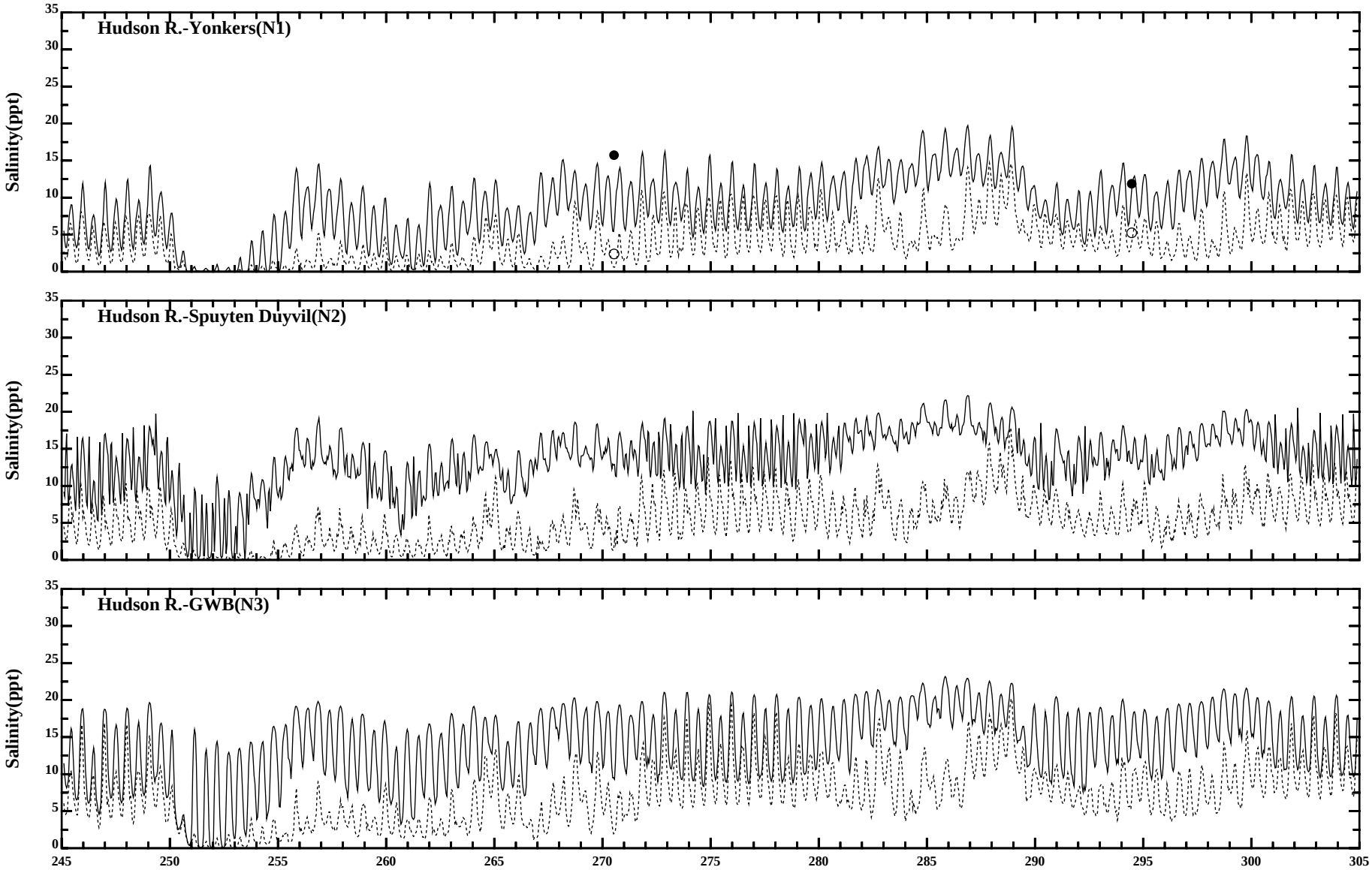

Comparison of Instantaneous Surface and Bottom Salinity

DATE: 8/02/2004 TIME: 12: 6:37

/erie1/hrfo0010/HYDRORUNS/CARP9900/PLOTS/TANDS/salt31

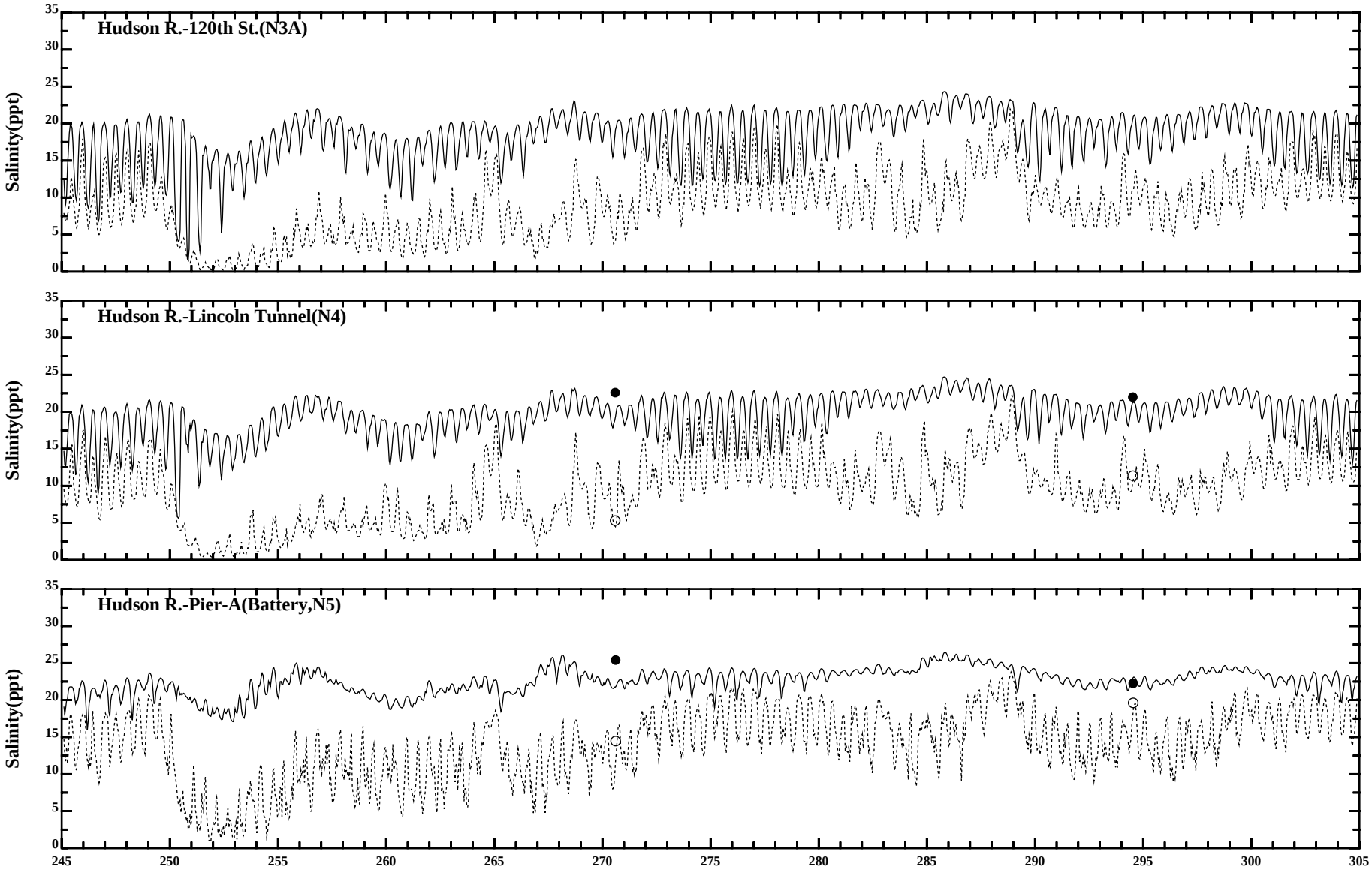

Comparison of Instantaneous Surface and Bottom Salinity

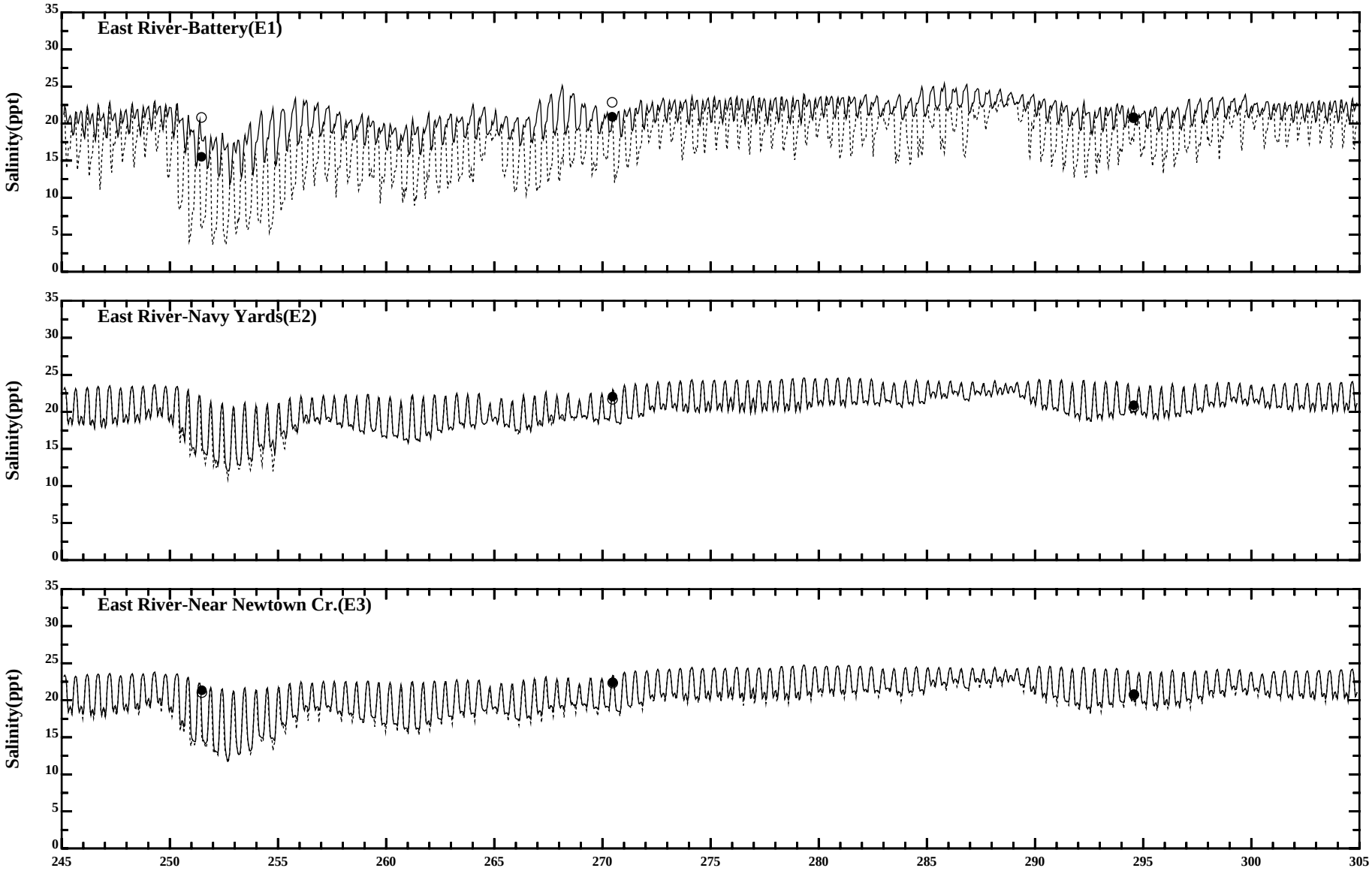

Comparison of Instantaneous Surface and Bottom Salinity

DATE: 8/02/2004 TIME: 12: 6:37

/erie1/hrfo0010/HYDRORUNS/CARP9900/PLOTS/TANDS/salt31

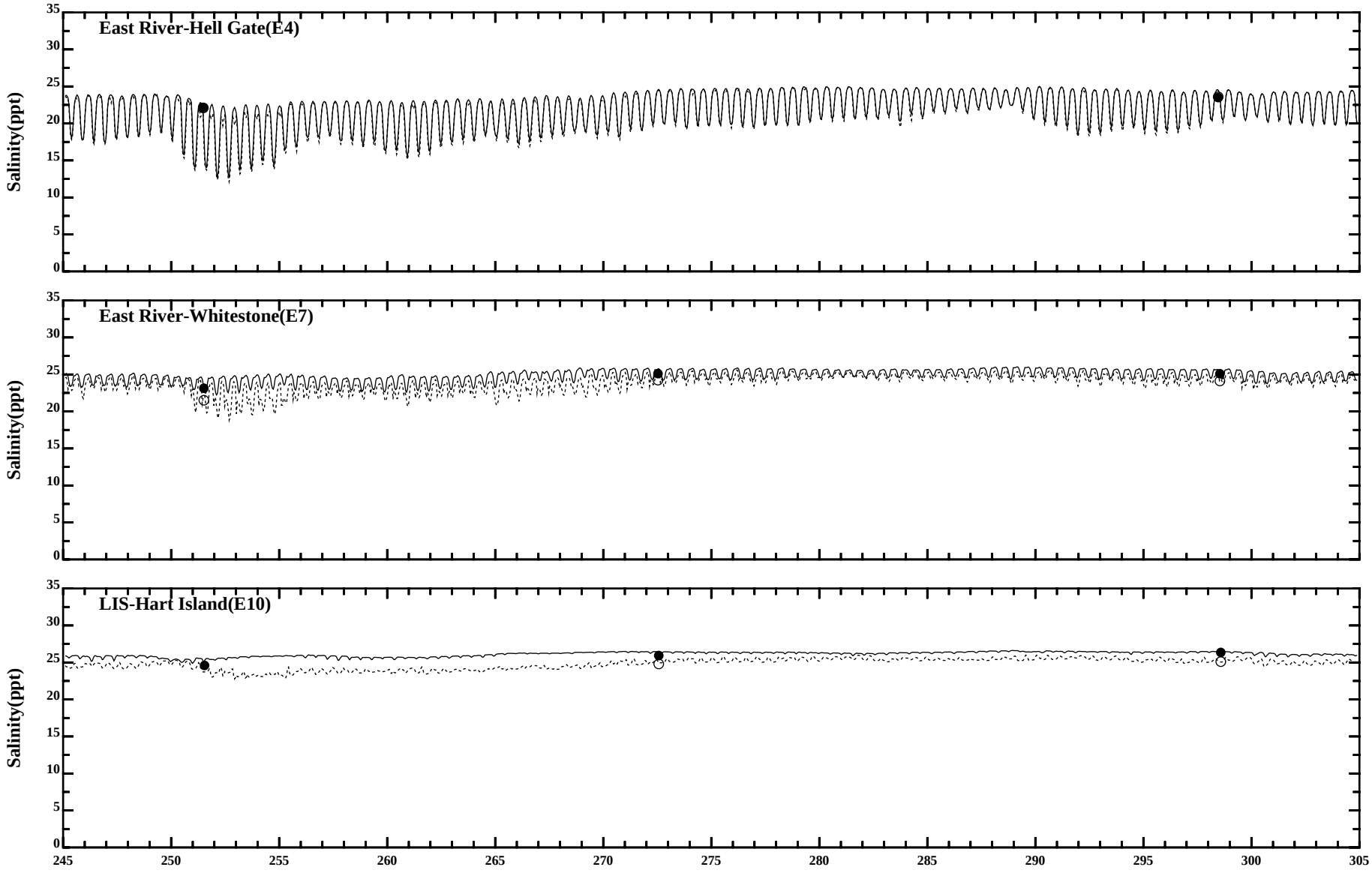

Comparison of Instantaneous Surface and Bottom Salinity

DATE: 8/02/2004 TIME: 12: 6:37

/erie1/hrfo0010/HYDRORUNS/CARP9900/PLOTS/TANDS/salt31

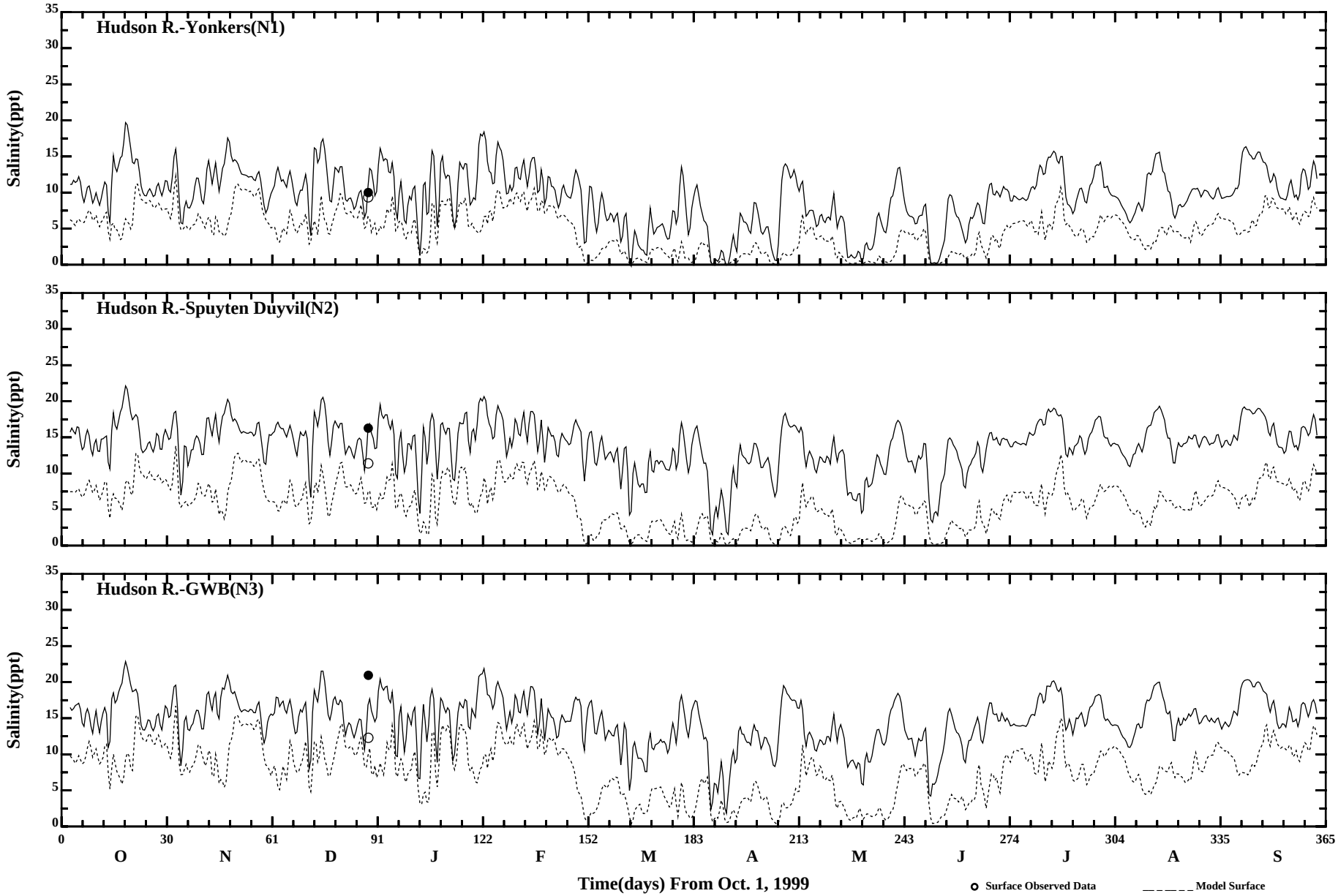

Comparison of 34 Hour Lowpass Surface and Bottom Salinity

DATE: 8/13/2004 TIME: 11:39:35

/erie1/hrfo0010/HYDRORUNS/CARP9900/PLOTS/TANDS/psalt31_34hlp

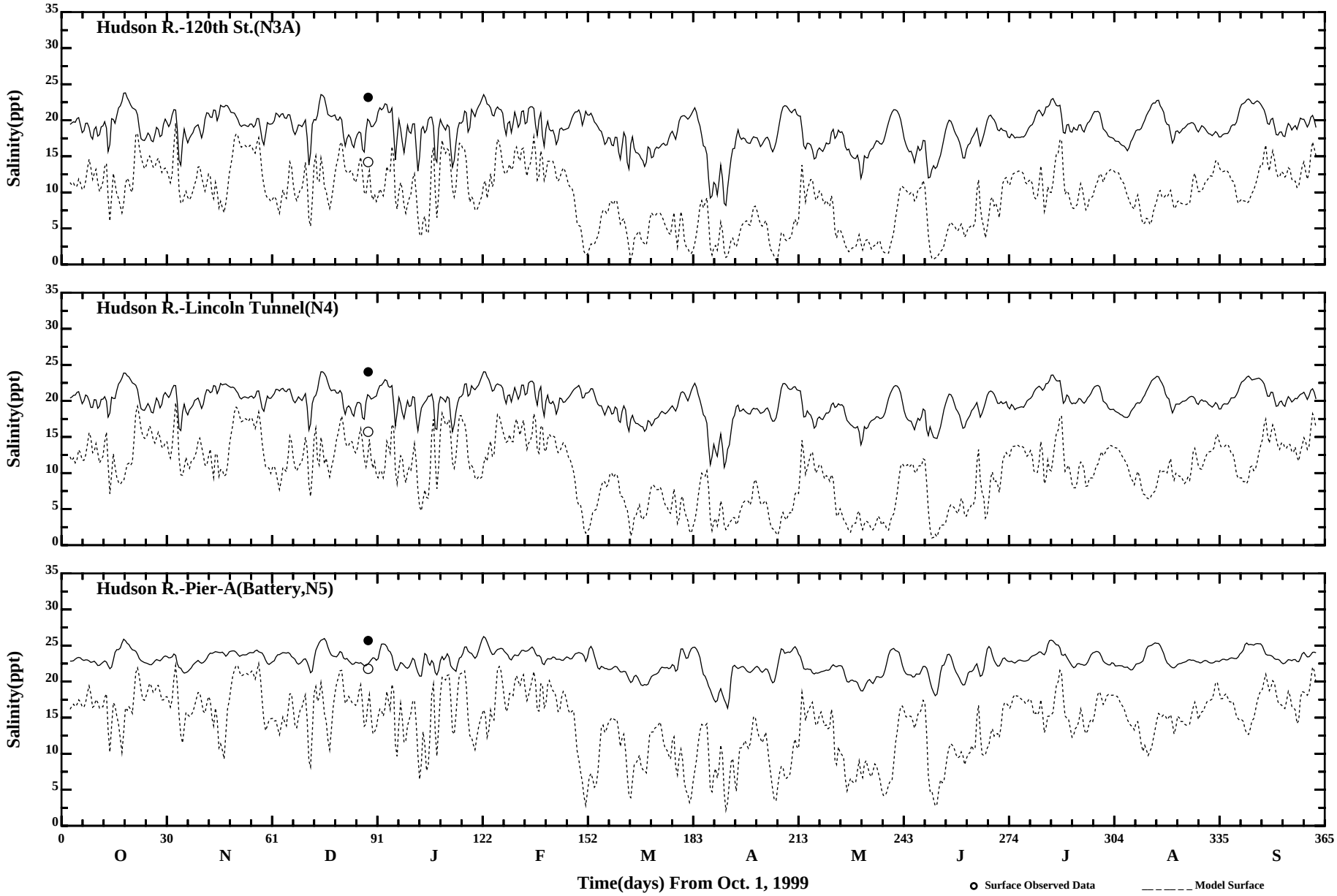

Comparison of 34 Hour Lowpass Surface and Bottom Salinity

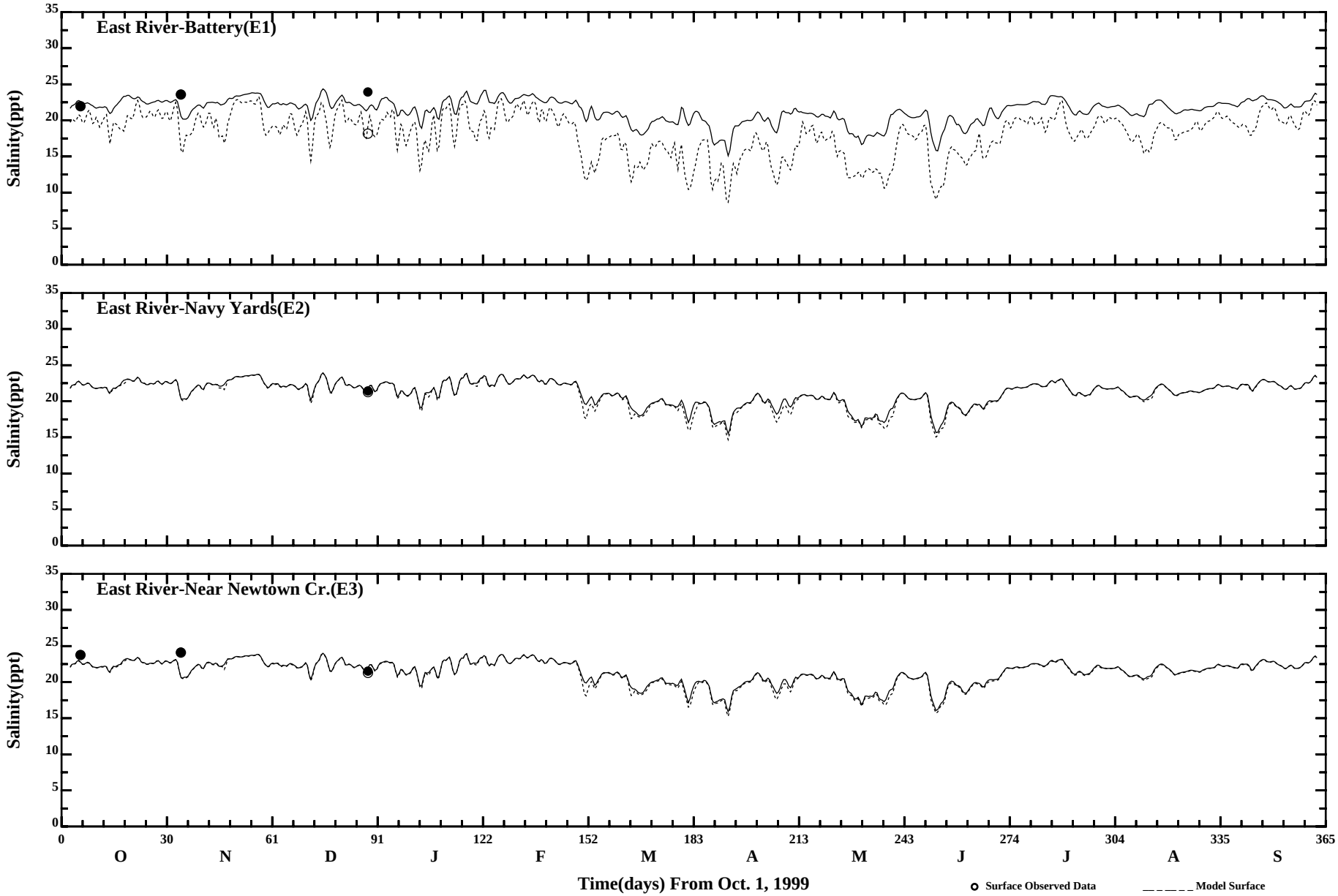

Comparison of 34 Hour Lowpass Surface and Bottom Salinity

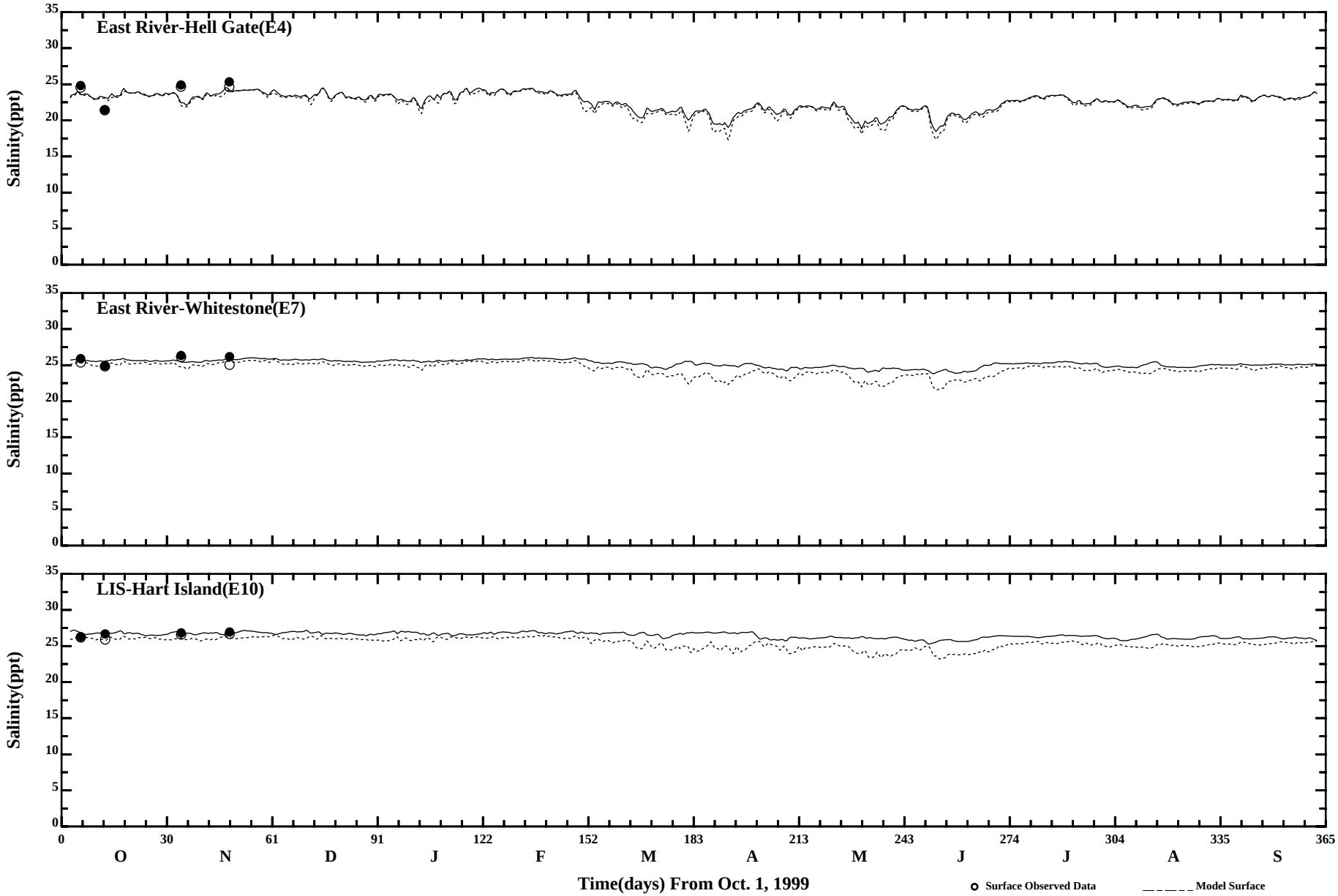

Comparison of 34 Hour Lowpass Surface and Bottom Salinity

DATE: 8/13/2004 TIME: 11:39:35

/erie1/hrfo0010/HYDRORUNS/CARP9900/PLOTS/TANDS/psalt31_34hlp

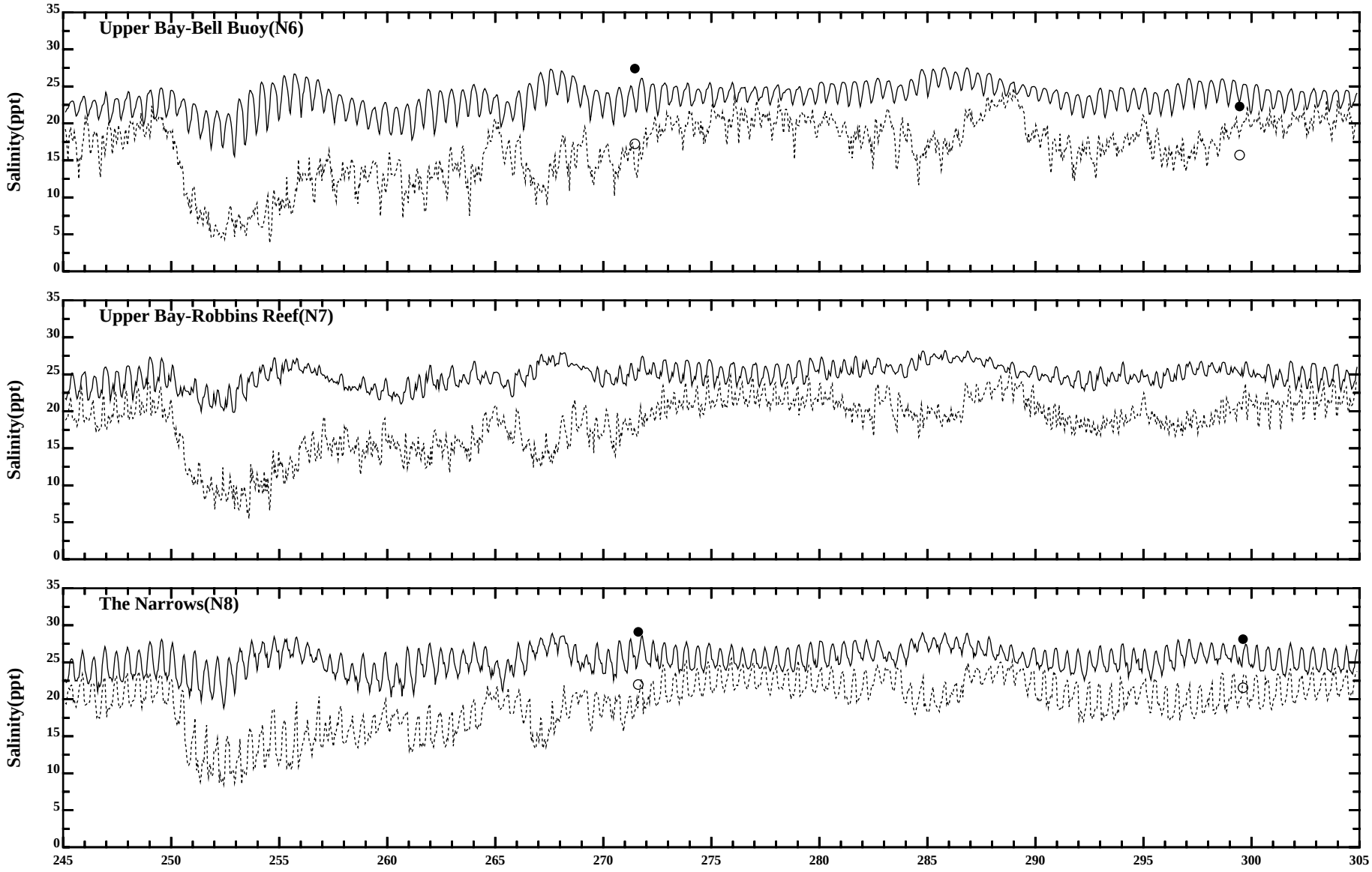

Comparison of Instantaneous Surface and Bottom Salinity

DATE: 8/02/2004 TIME: 12: 6:44

/erie1/hrfo0010/HYDRORUNS/CARP9900/PLOTS/TANDS/salt32.gdp

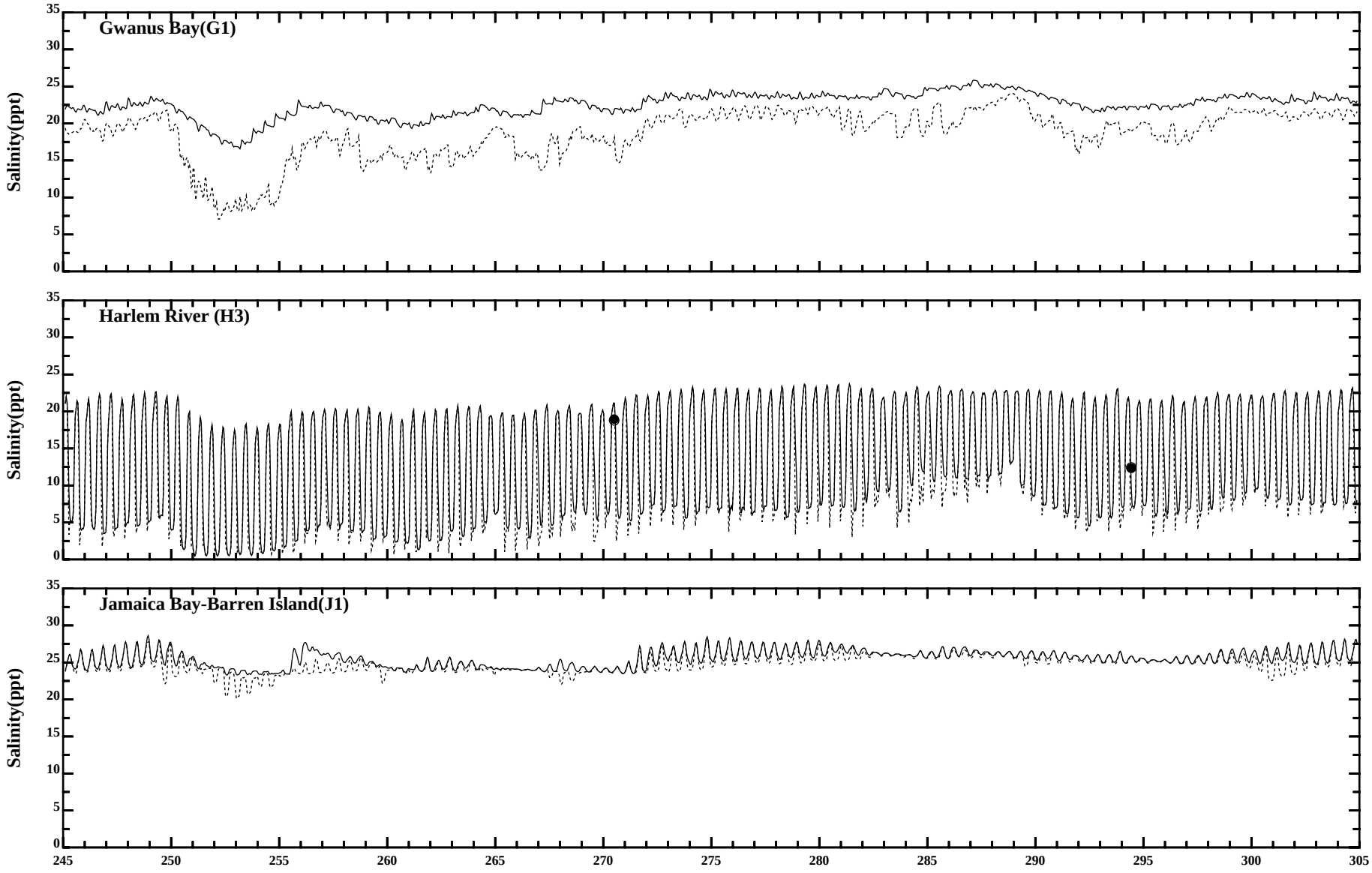

Comparison of Instantaneous Surface and Bottom Salinity

DATE: 8/02/2004 TIME: 12: 6:44

/erie1/hrfo0010/HYDRORUNS/CARP9900/PLOTS/TANDS/salt32.gdp

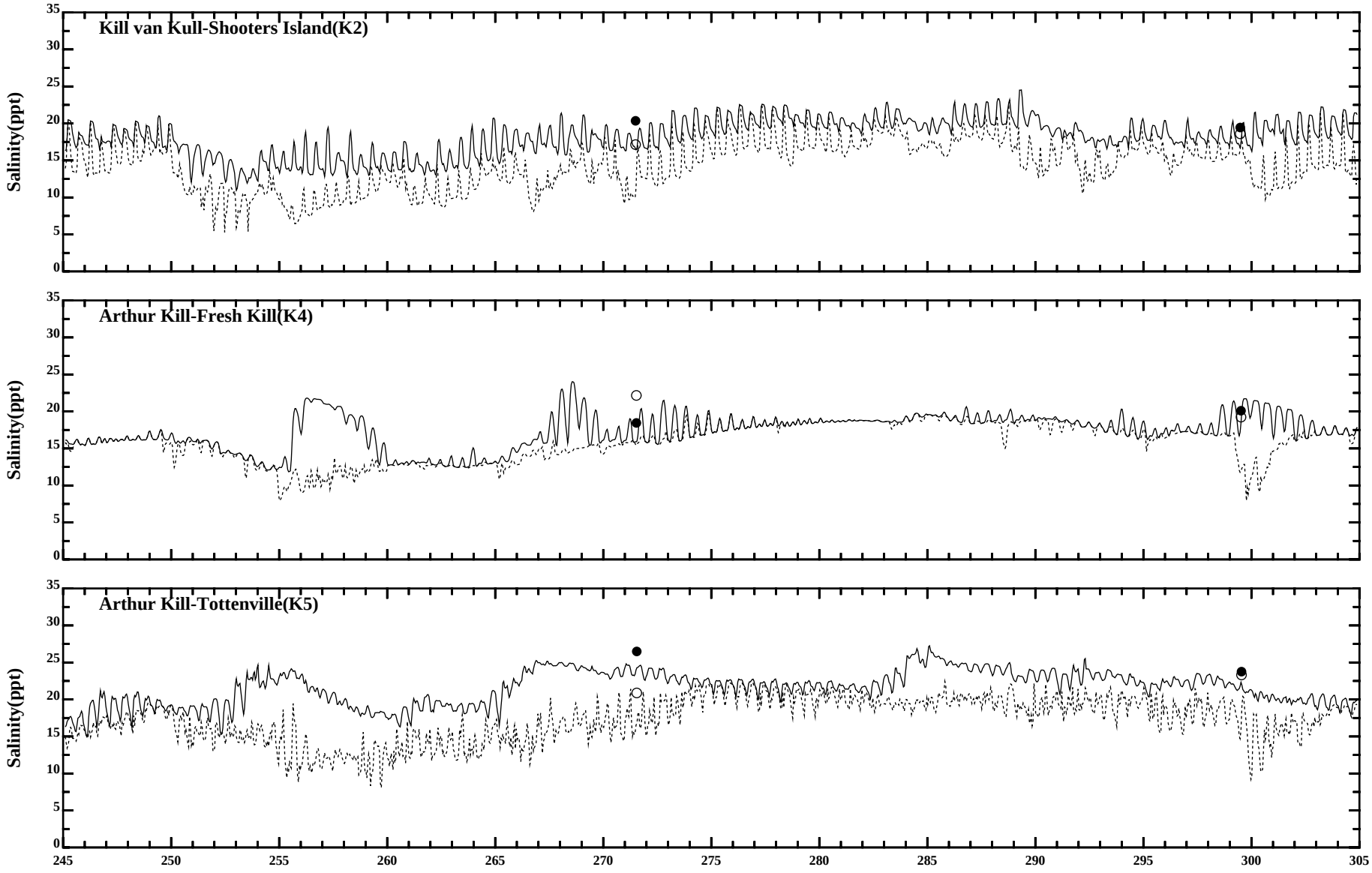

Comparison of Instantaneous Surface and Bottom Salinity

DATE: 8/02/2004 TIME: 12: 6:44

/erie1/hrfo0010/HYDRORUNS/CARP9900/PLOTS/TANDS/salt32.gdp

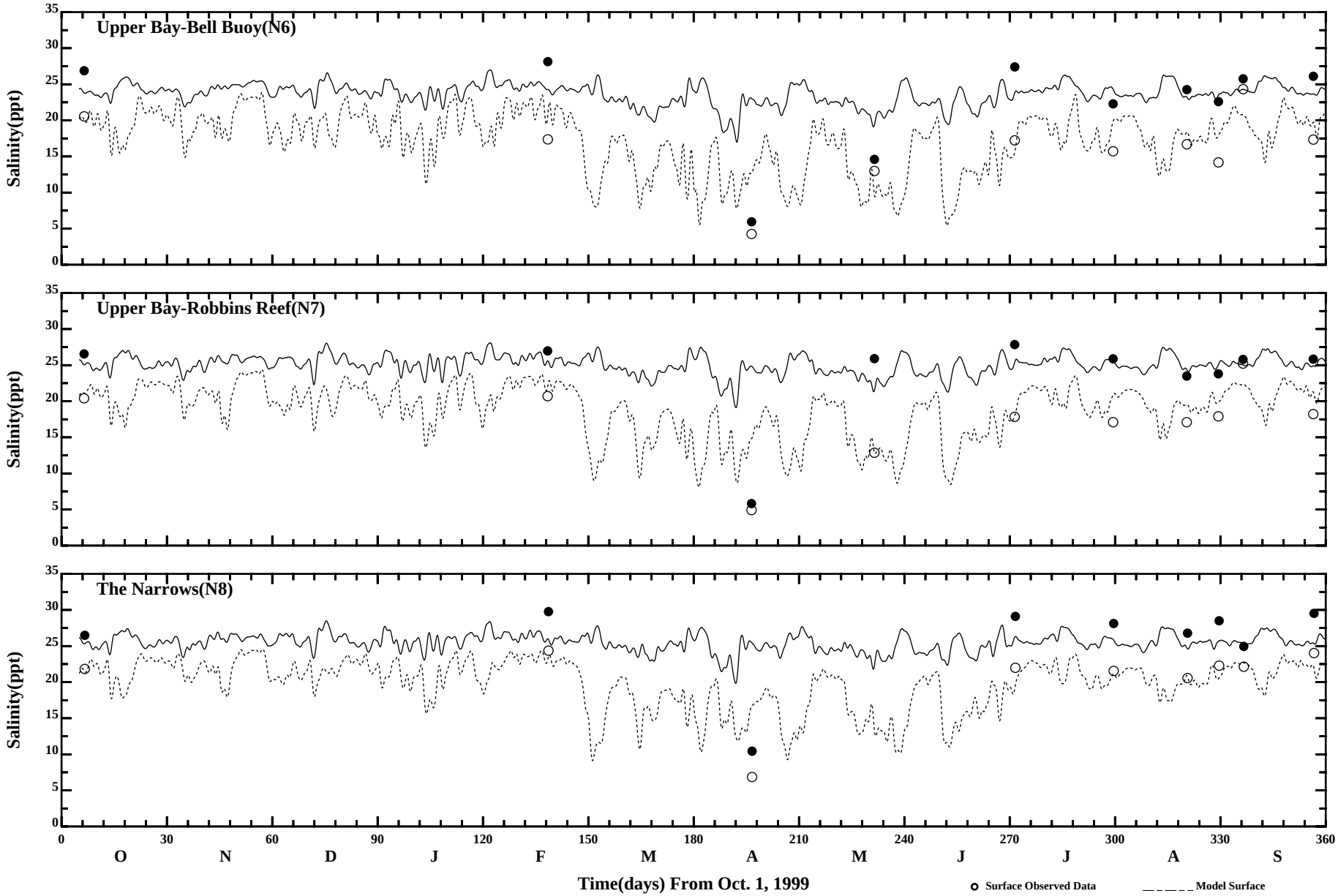

Comparison of 34 Hr LP Surface and Bottom Salinity

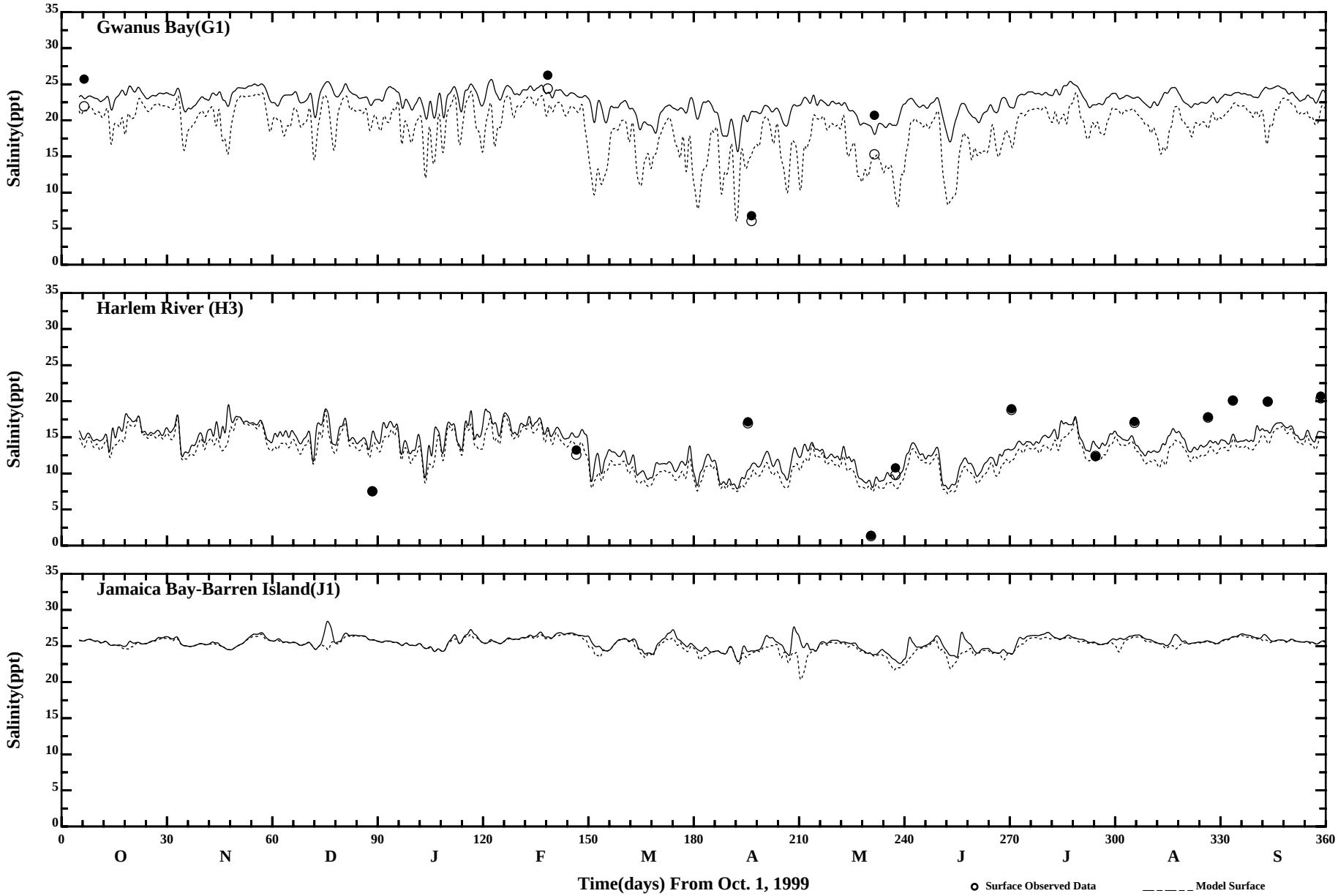

Comparison of 34 Hr LP Surface and Bottom Salinity

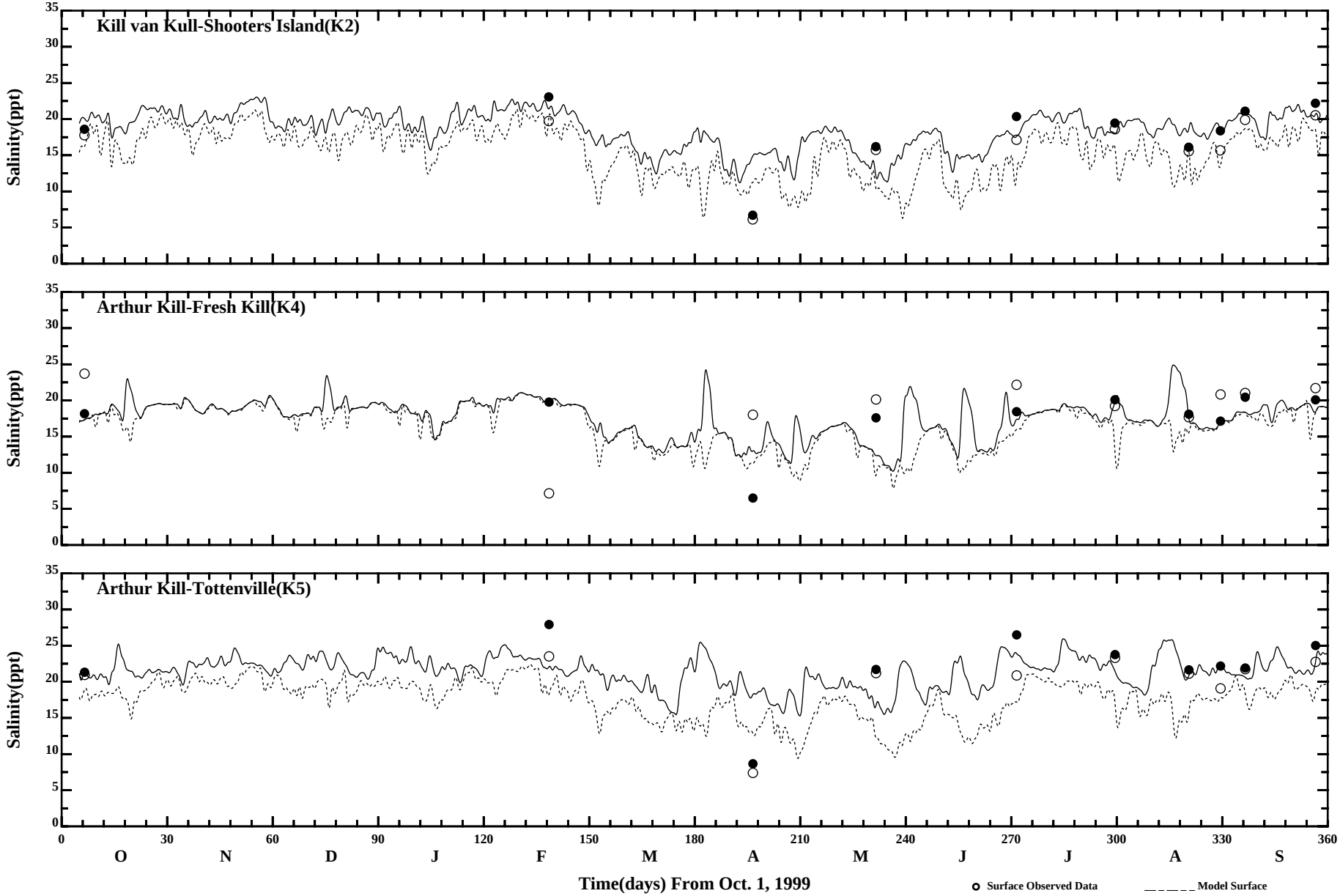

Comparison of 34 Hr LP Surface and Bottom Salinity

DATE: 8/02/2004 TIME: 12: 6:28

/erie1/hrfo0010/HYDRORUNS/CARP9900/PLOTS/TANDS/salt32_34hlp.gdp

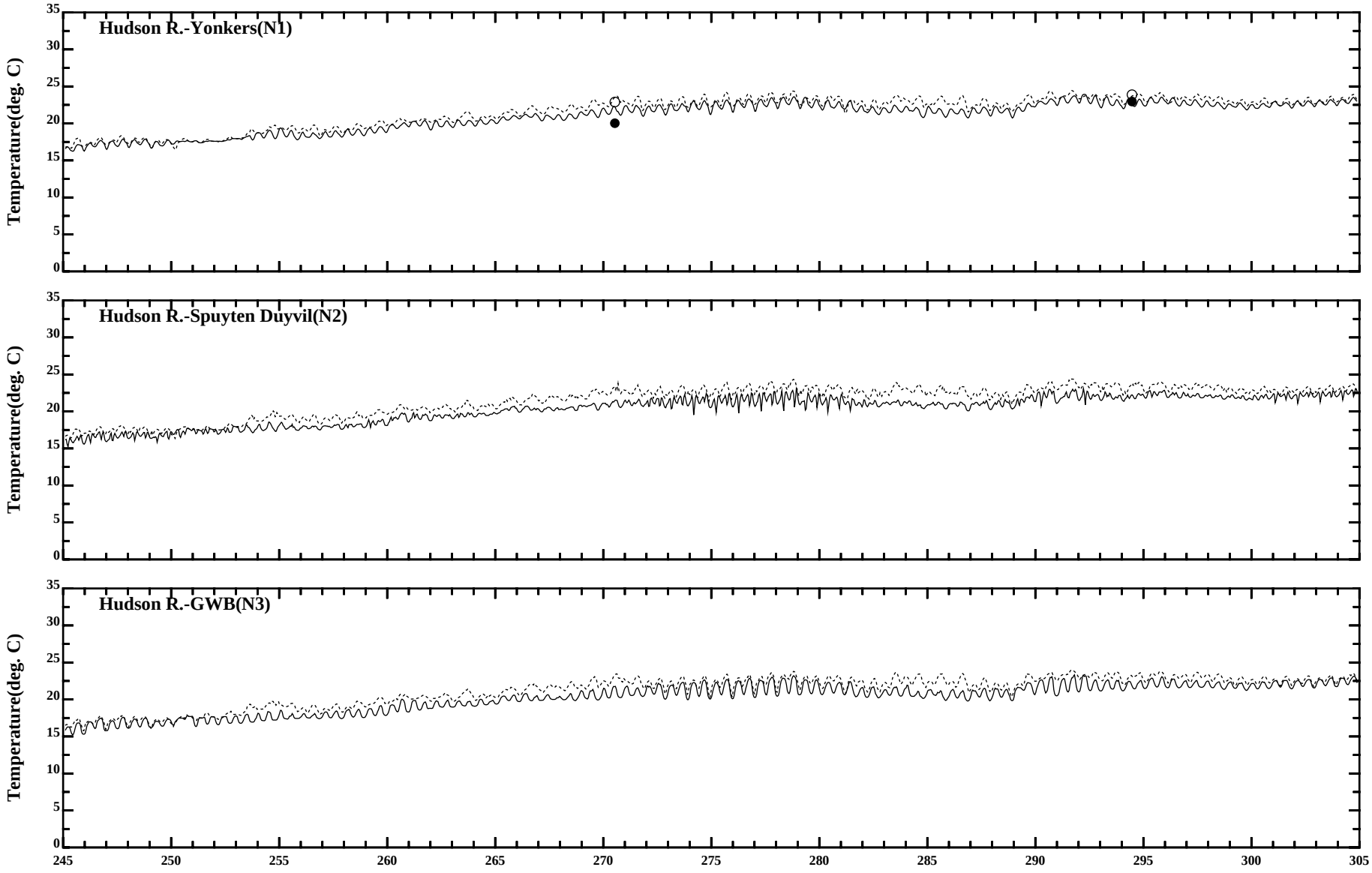

Comparison of Instantaneous Surface and Bottom Temperature

DATE: 8/02/2004 TIME: 12: 6:15

/erie1/hrfo0010/HYDRORUNS/CARP9900/PLOTS/TANDS/temp31

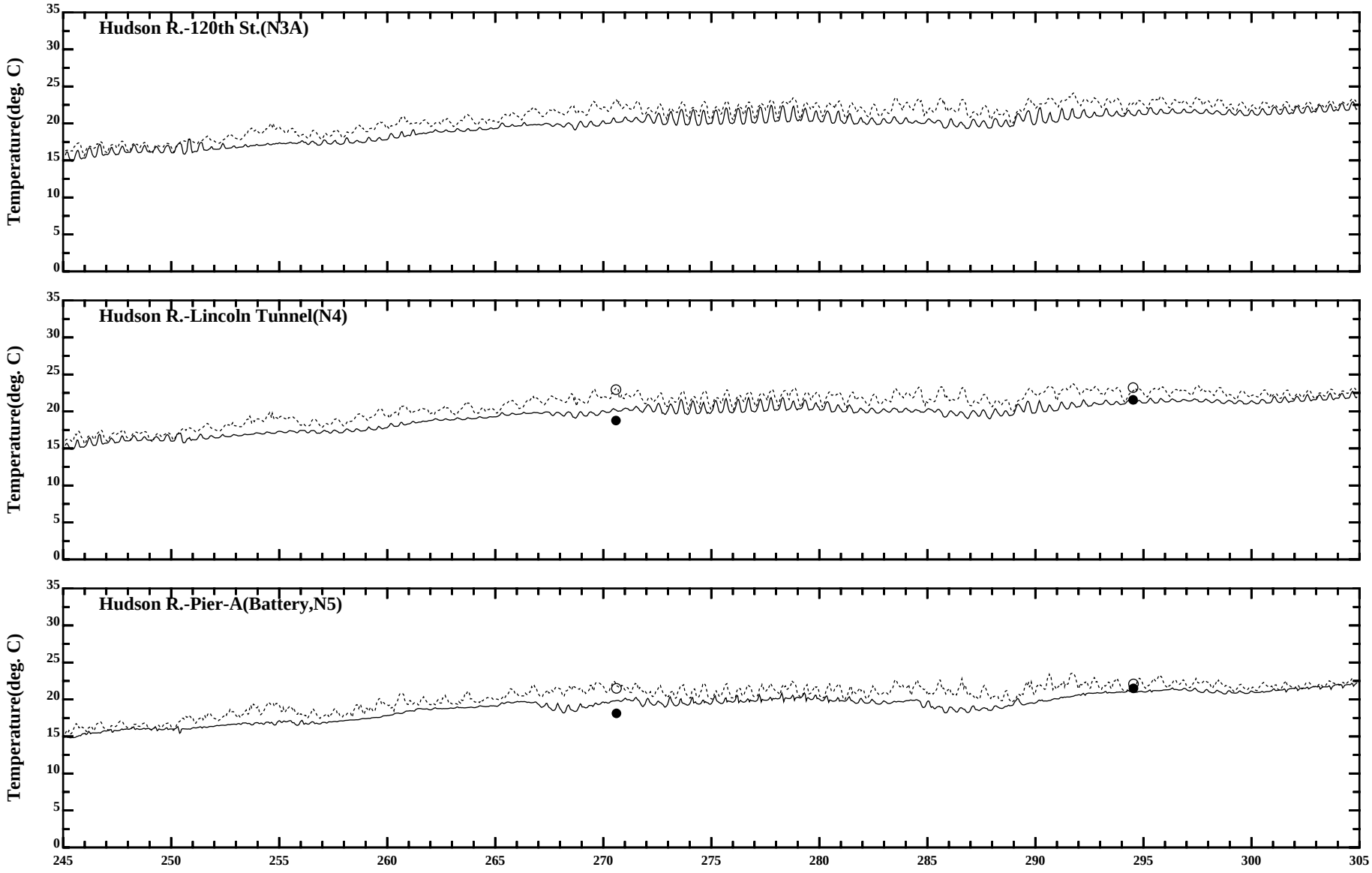

Comparison of Instantaneous Surface and Bottom Temperature

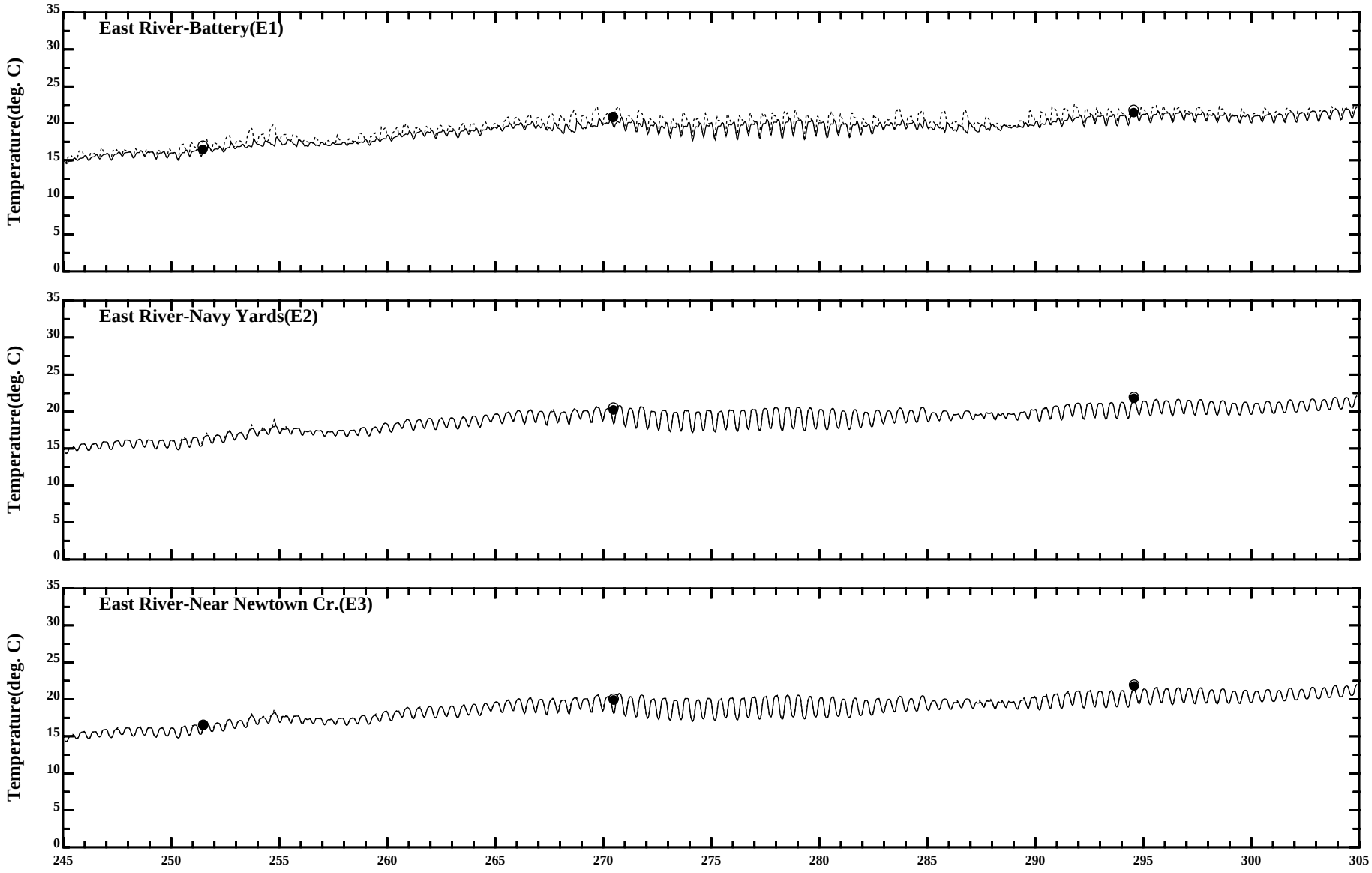

Comparison of Instantaneous Surface and Bottom Temperature

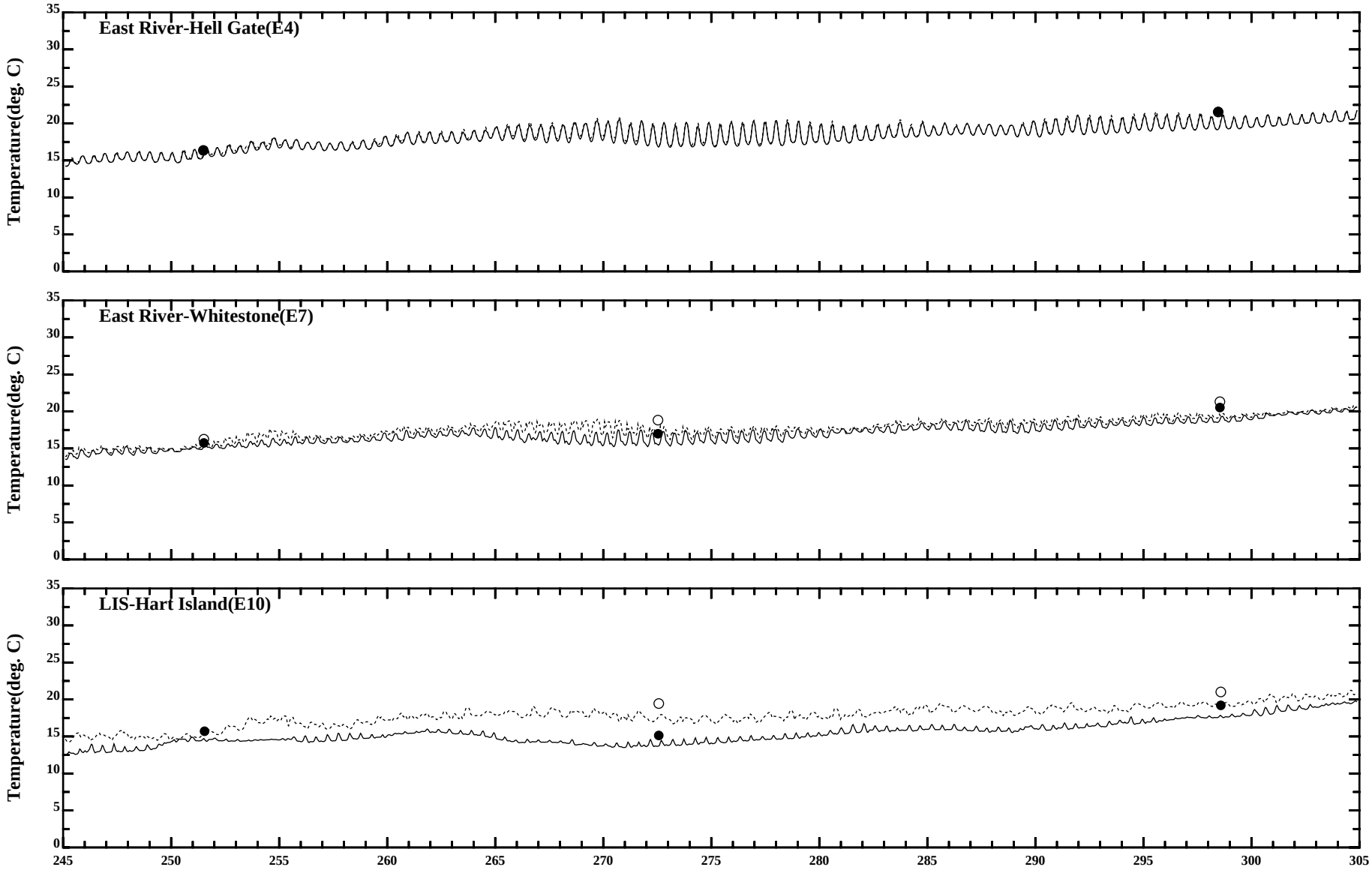

Comparison of Instantaneous Surface and Bottom Temperature

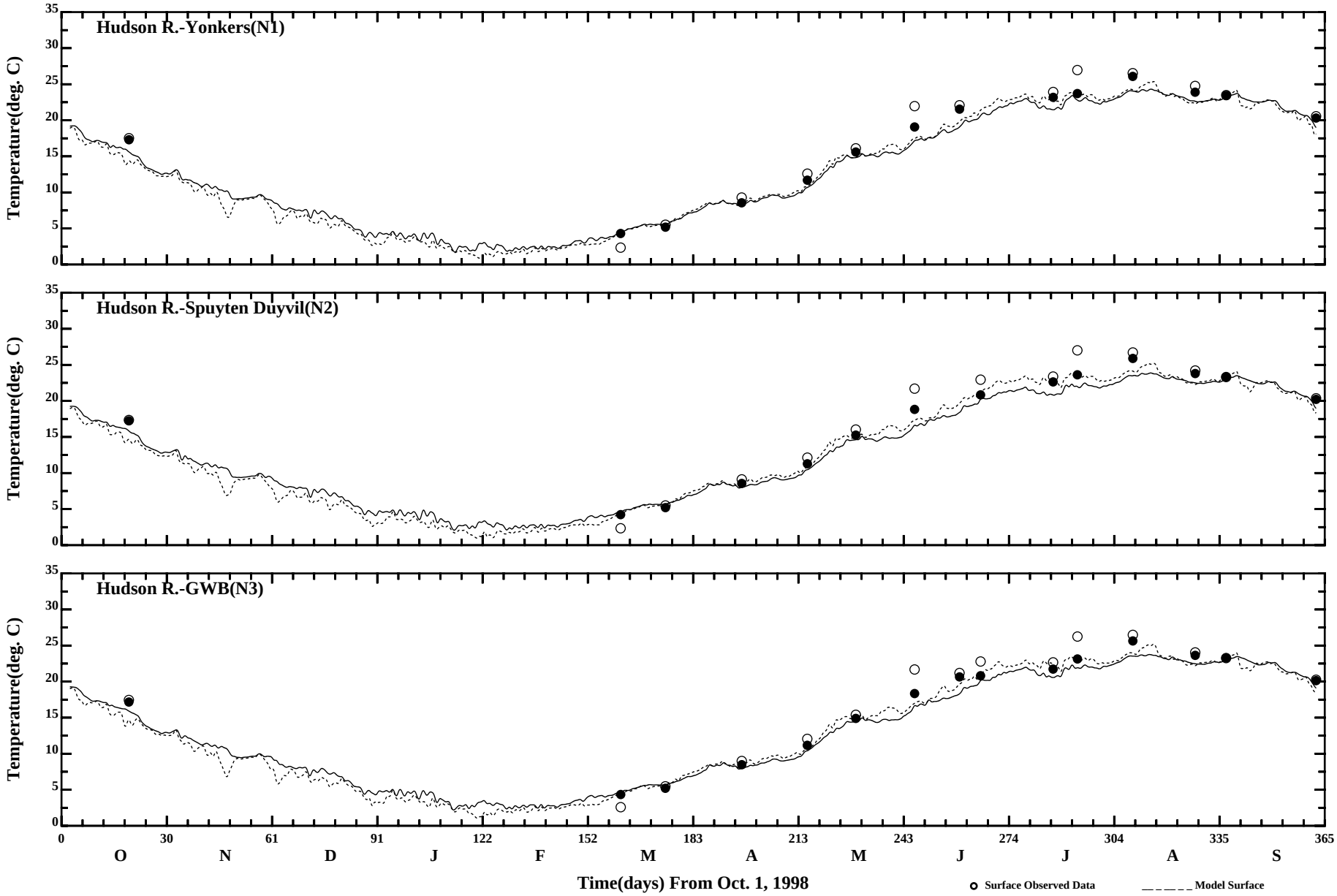

Comparison of 34 Hour Lopass Surface and Bottom Temperature

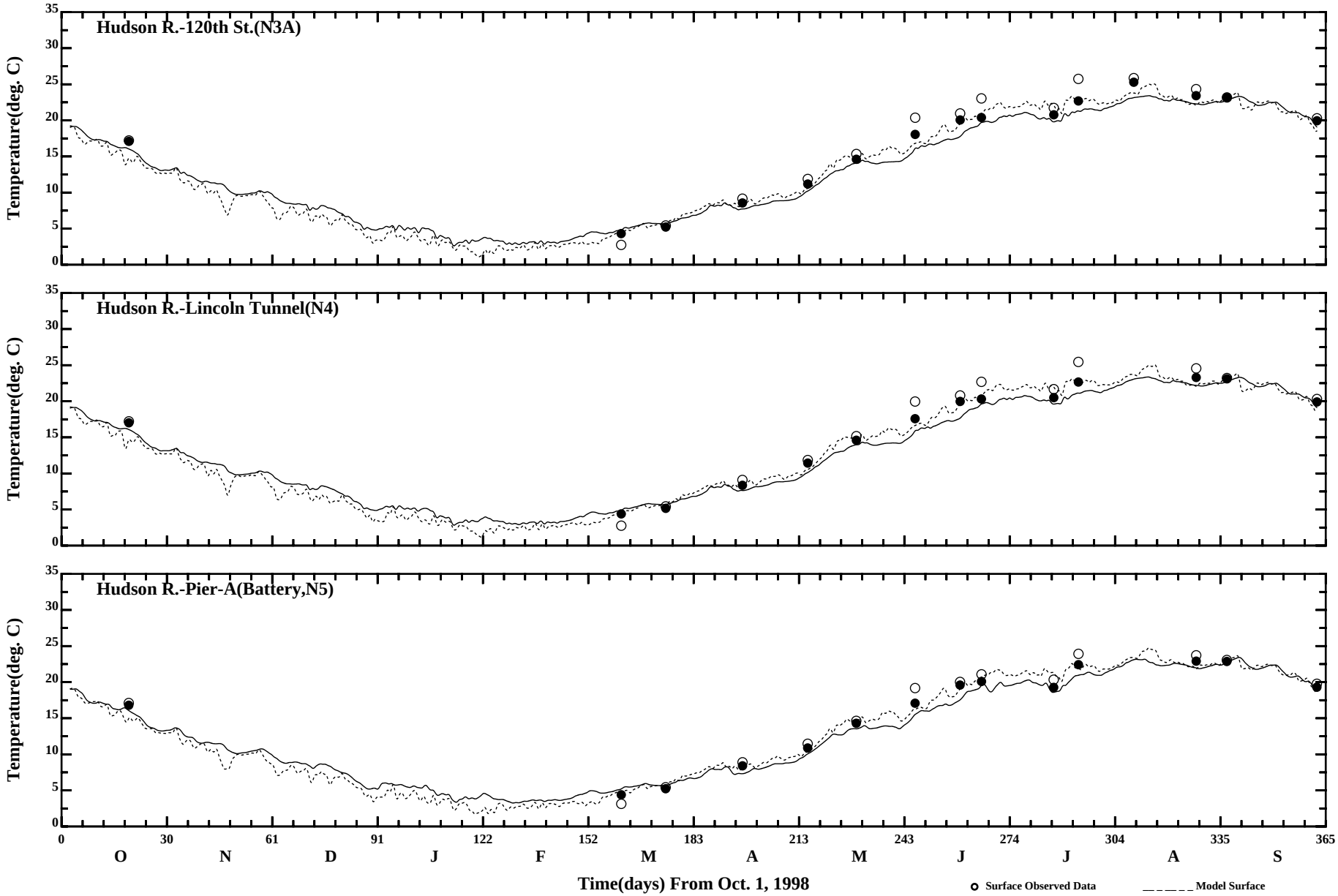

Comparison of 34 Hour Lopass Surface and Bottom Temperature

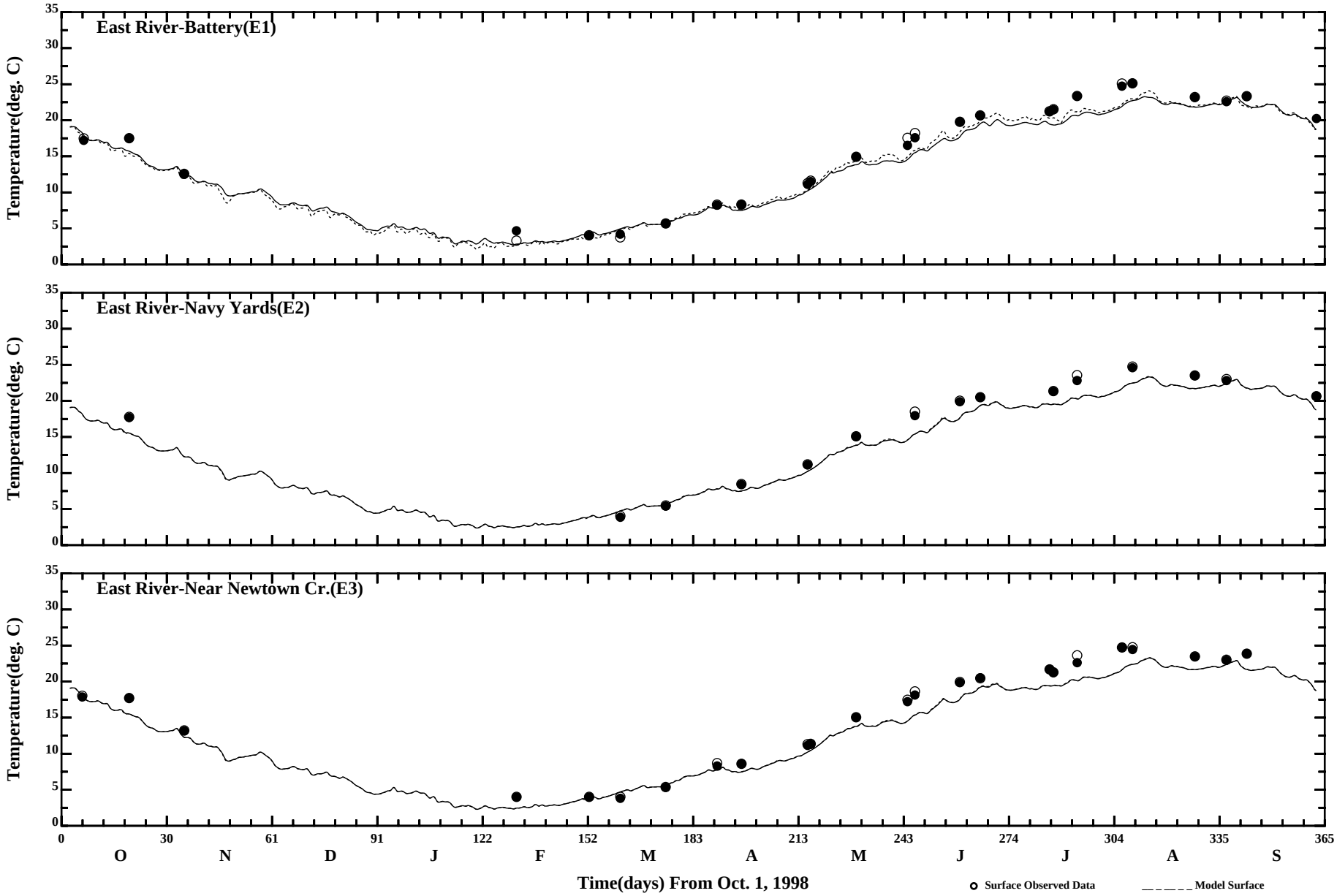

Comparison of 34 Hour Lopass Surface and Bottom Temperature

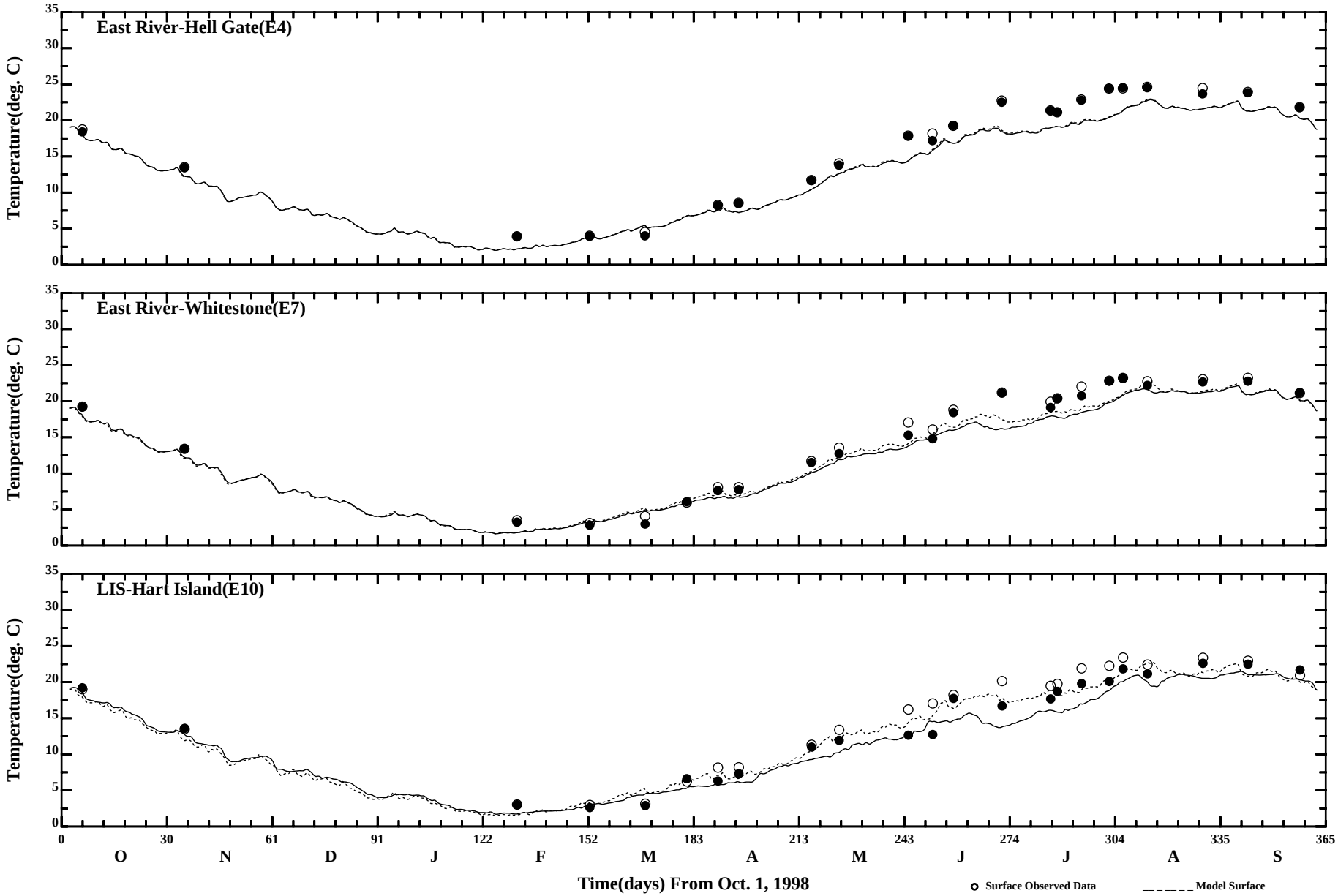

Comparison of 34 Hour Lopass Surface and Bottom Temperature

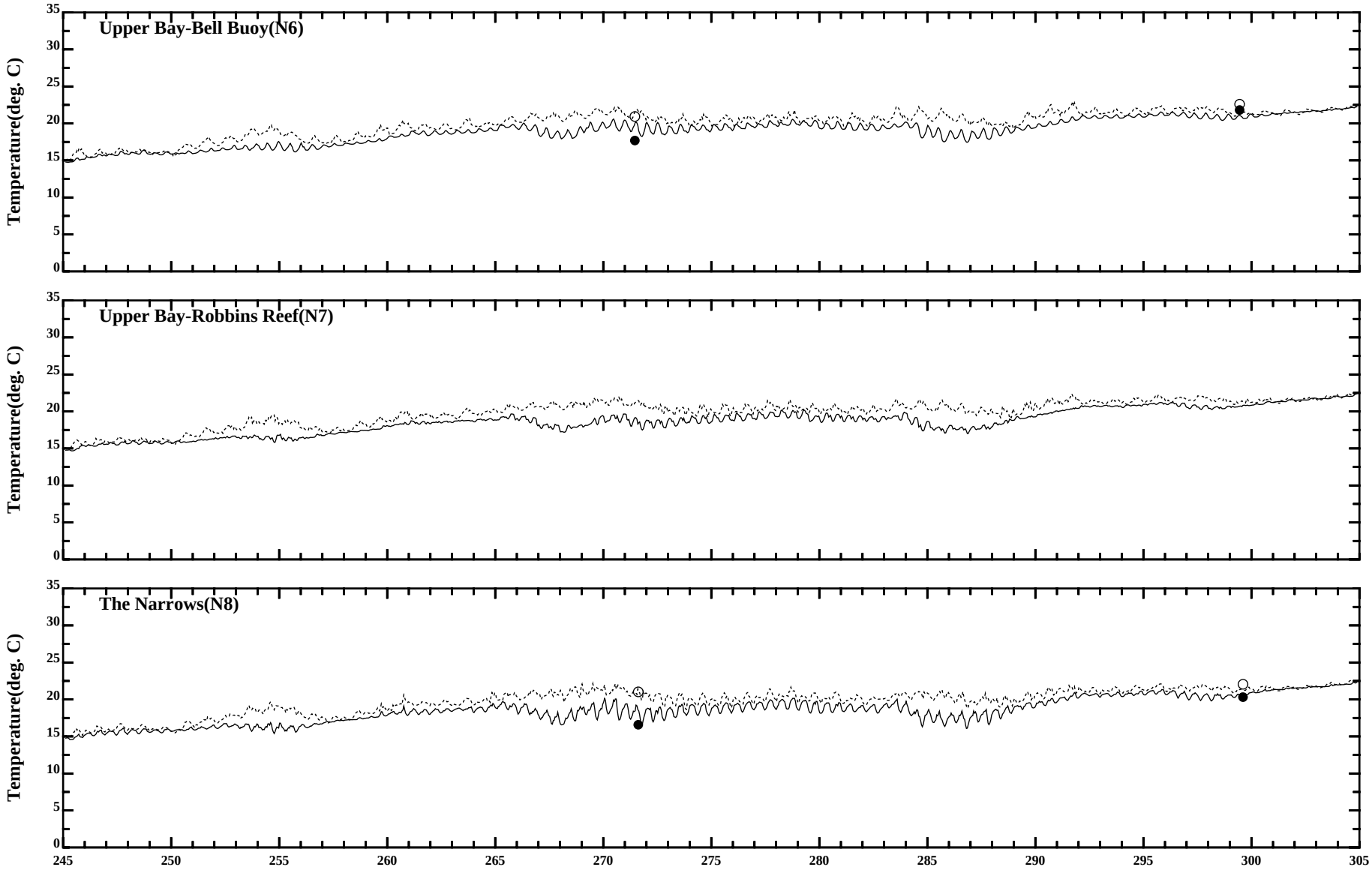

Comparison of Instantaneous Surface and Bottom Temperature

DATE: 8/02/2004 TIME: 12: 6:22

/erie1/hrfo0010/HYDRORUNS/CARP9900/PLOTS/TANDS/temp32.gdp

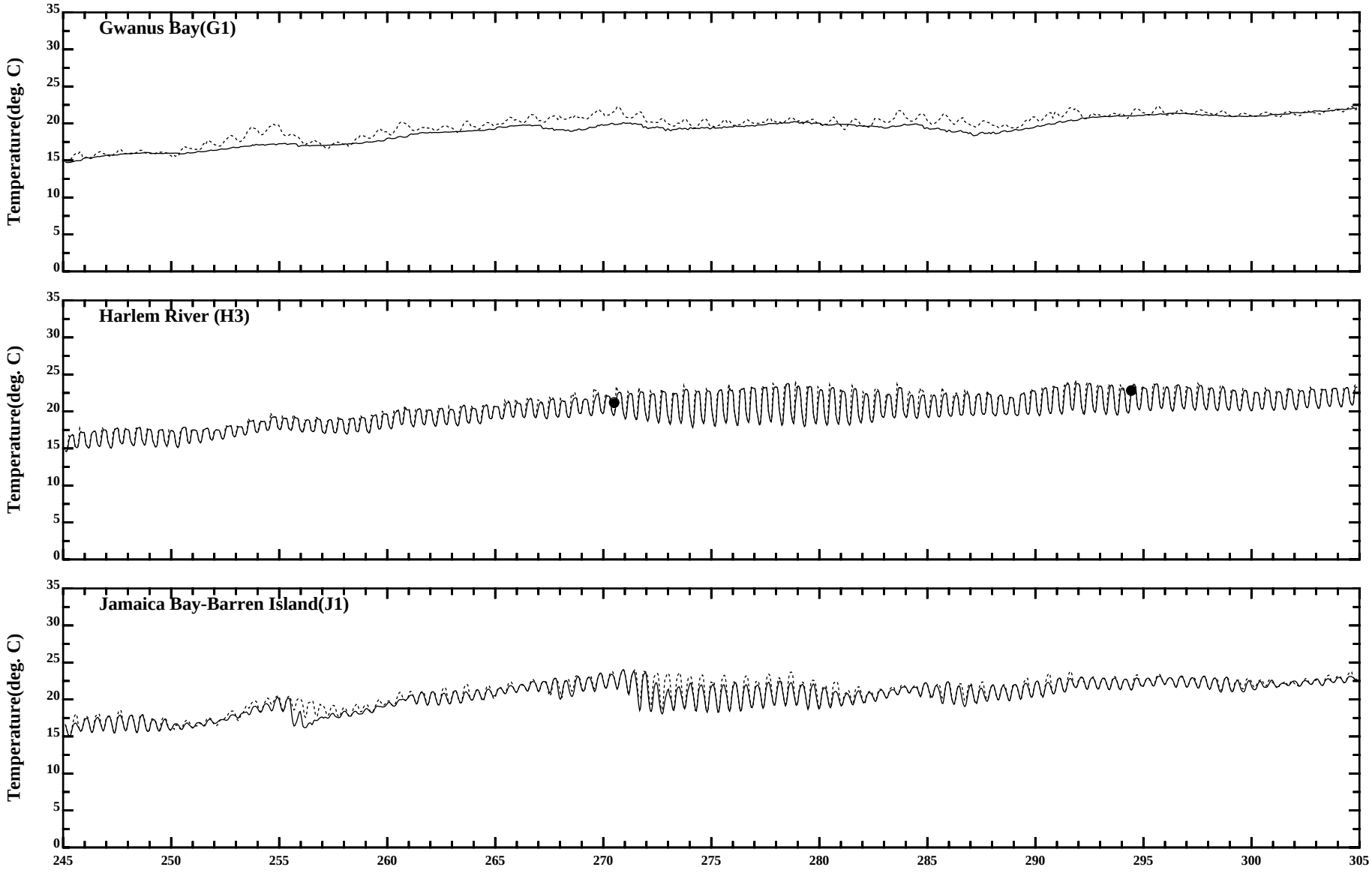

Comparison of Instantaneous Surface and Bottom Temperature

DATE: 8/02/2004 TIME: 12: 6:22

/erie1/hrfo0010/HYDRORUNS/CARP9900/PLOTS/TANDS/temp32.gdp

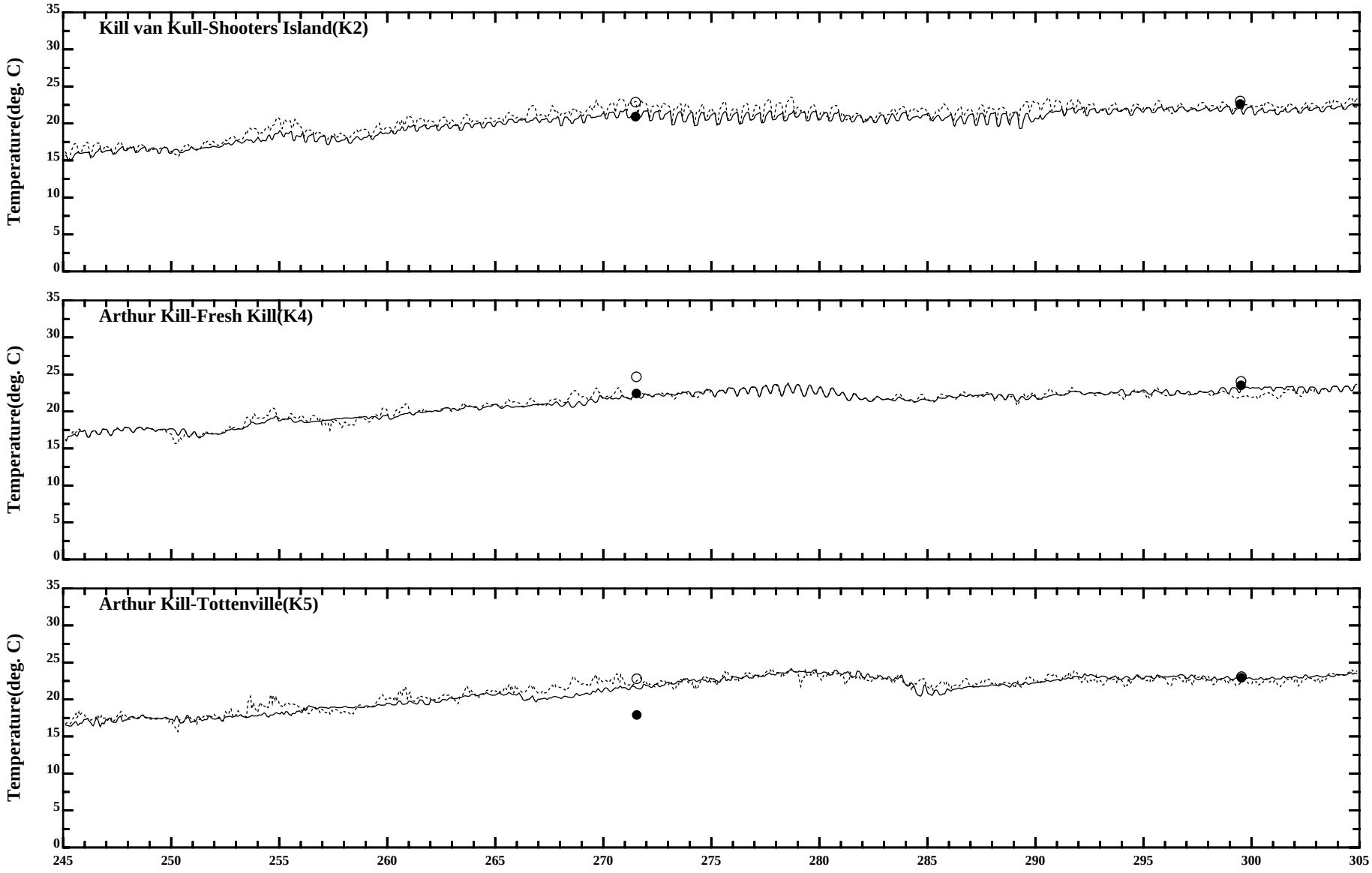

Comparison of Instantaneous Surface and Bottom Temperature

DATE: 8/02/2004 TIME: 12: 6:22

/erie1/hrfo0010/HYDRORUNS/CARP9900/PLOTS/TANDS/temp32.gdp

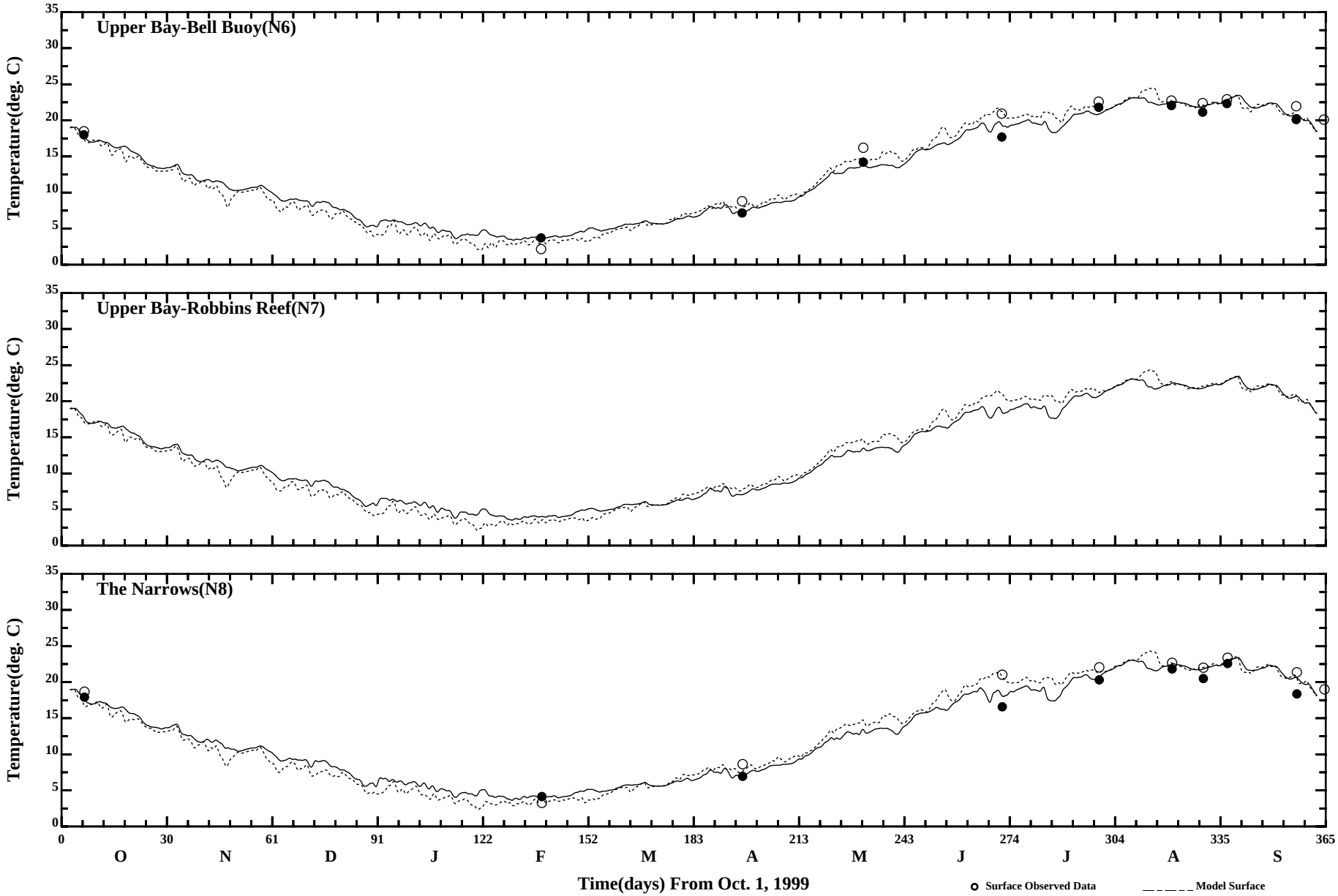

Comparison of 34 Hour Lopass Surface and Bottom Temperature

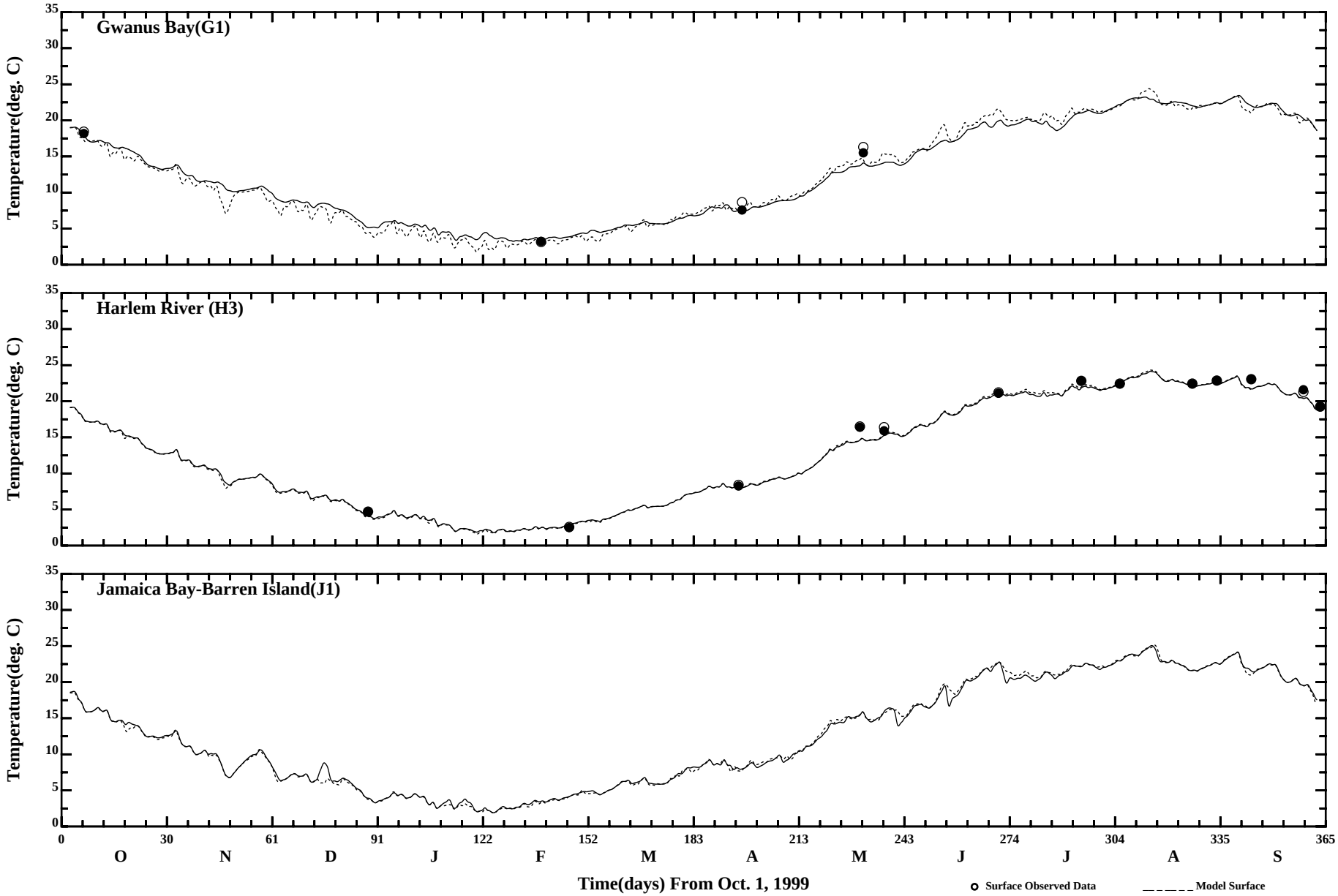

Comparison of 34 Hour Lopass Surface and Bottom Temperature

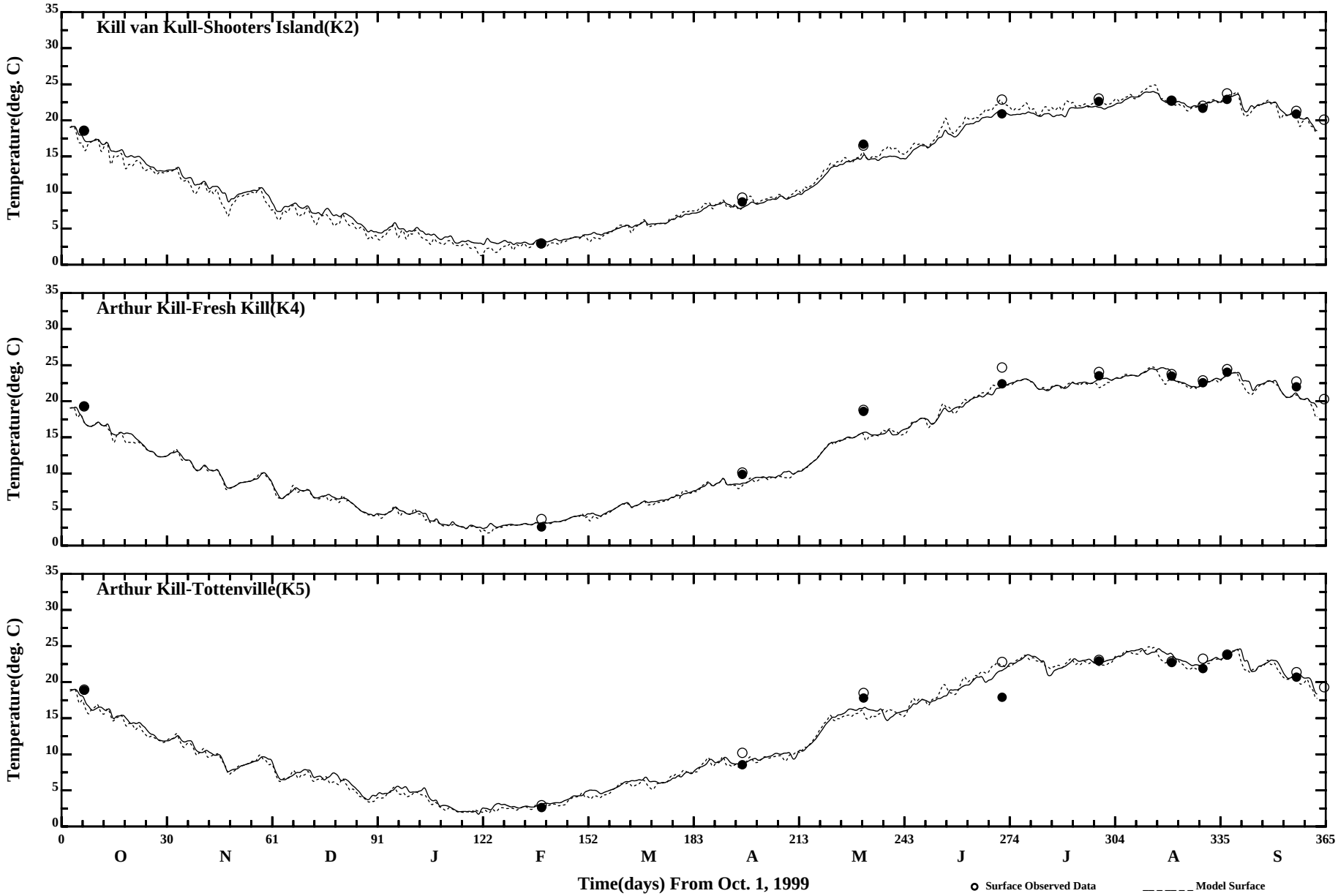

Comparison of 34 Hour Lopass Surface and Bottom Temperature

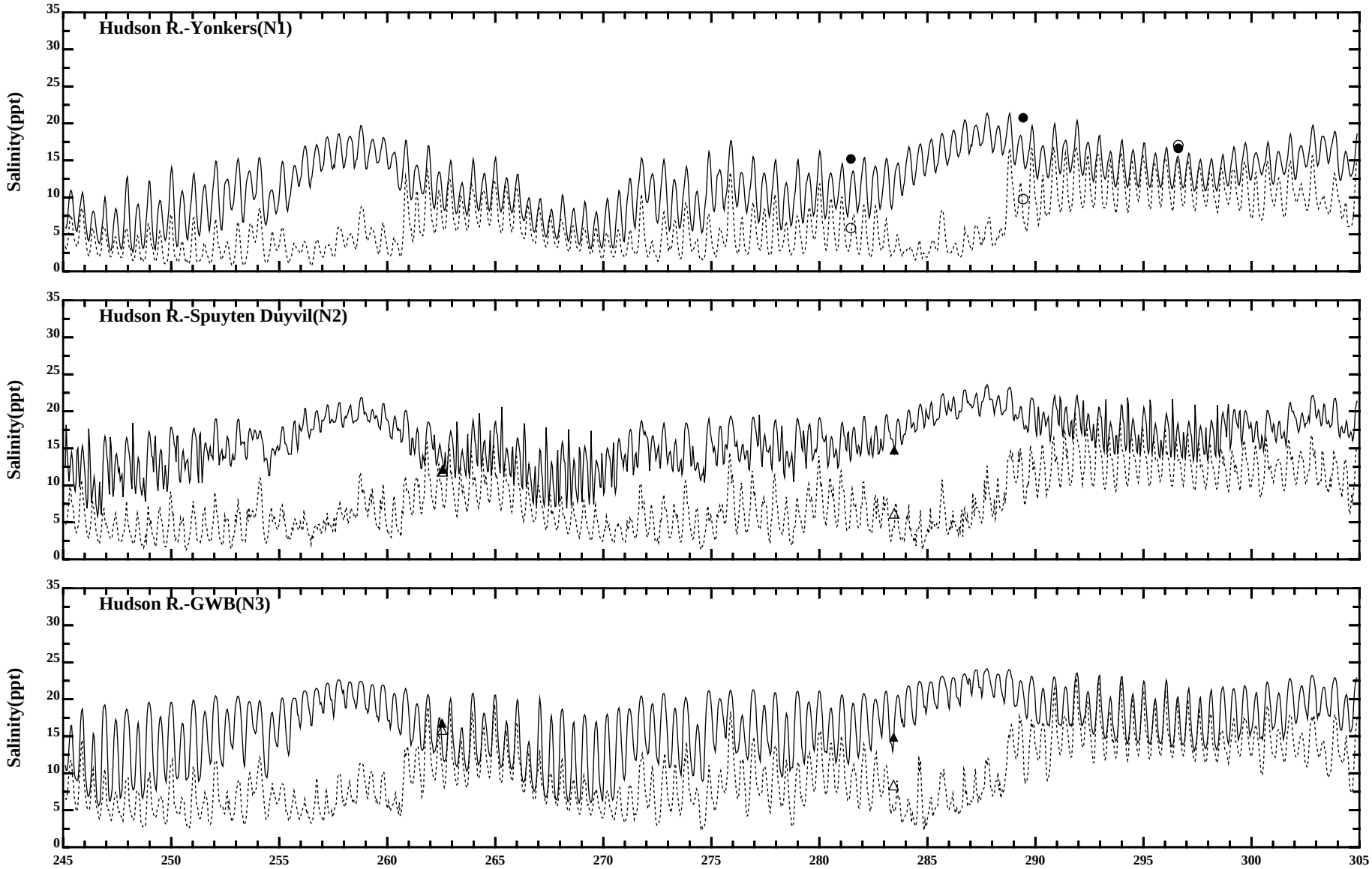

Comparison of Instantaneous Surface and Bottom Salinity

/e1/hrfo0010/HYDRORUNS/CARP0001/PLOTS/TANDS/salt31

DATE: 8/02/2004 TIME: 13:26: 2

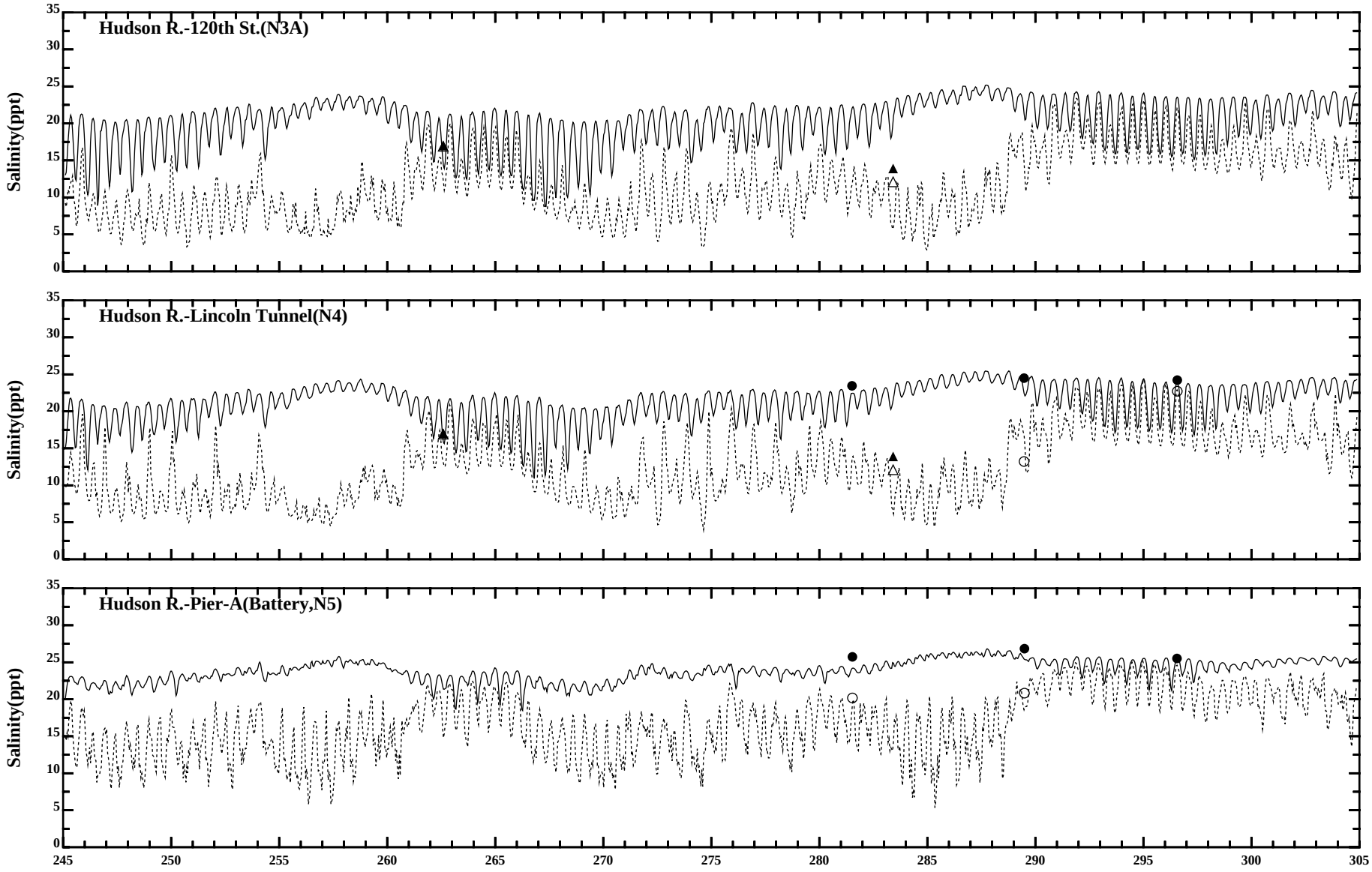

Comparison of Instantaneous Surface and Bottom Salinity

/e1/hrfo0010/HYDRORUNS/CARP0001/PLOTS/TANDS/salt31

DATE: 8/02/2004 TIME: 13:26: 2

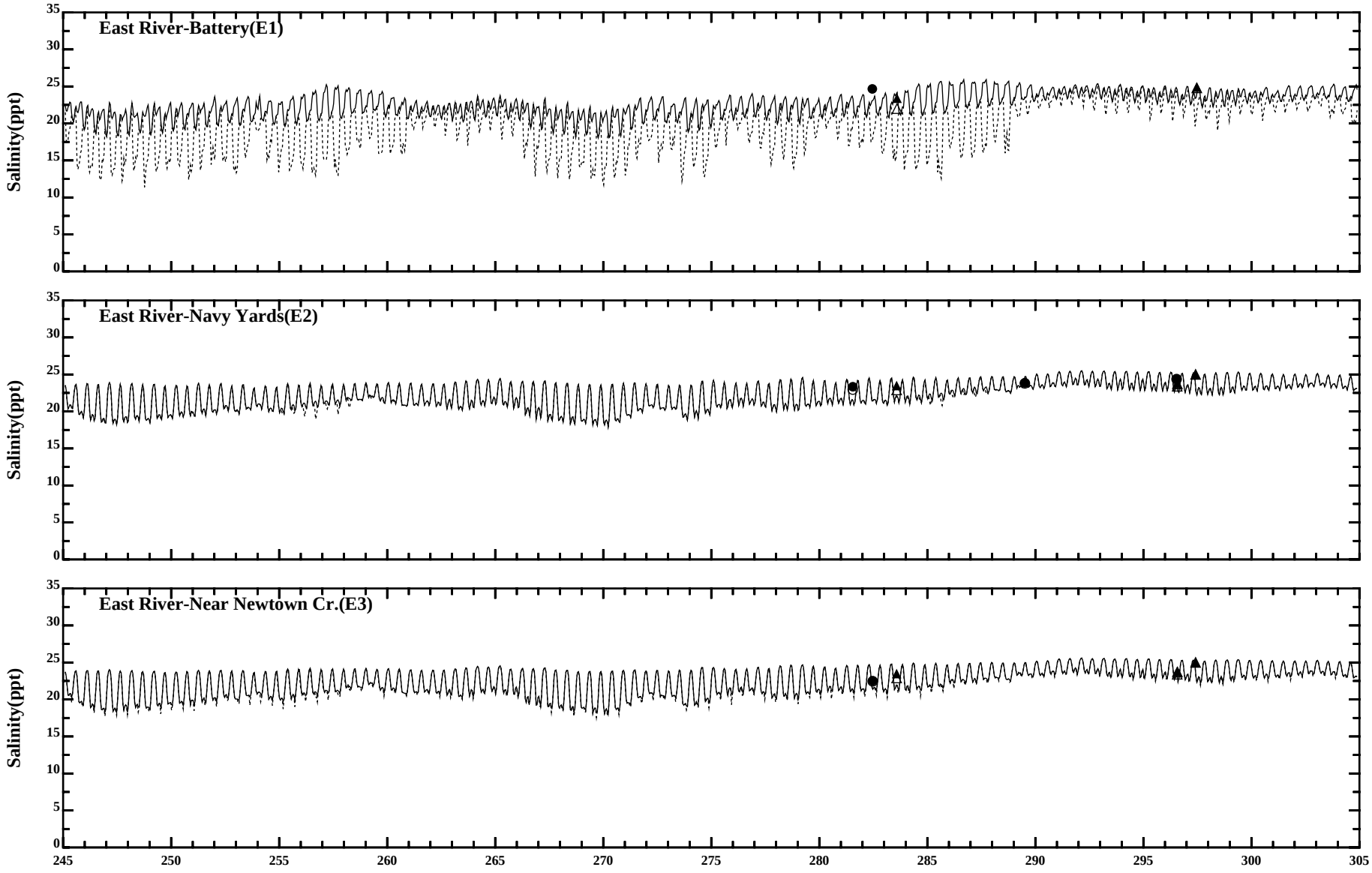

Comparison of Instantaneous Surface and Bottom Salinity

/e1/hrfo0010/HYDRORUNS/CARP0001/PLOTS/TANDS/salt31

DATE: 8/02/2004 TIME: 13:26: 2

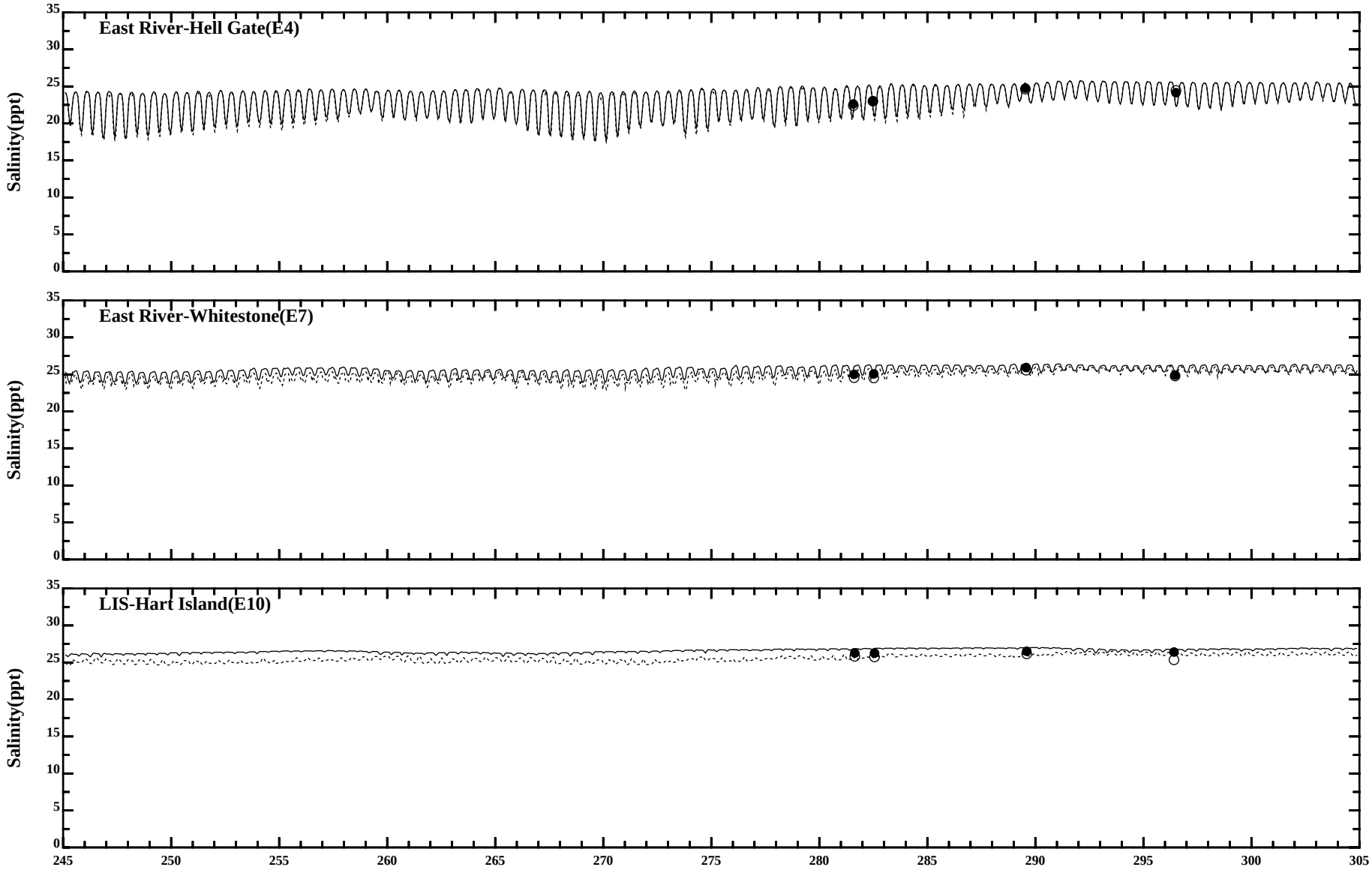

Comparison of Instantaneous Surface and Bottom Salinity

/e1/hrfo0010/HYDRORUNS/CARP0001/PLOTS/TANDS/salt31

DATE: 8/02/2004 TIME: 13:26: 2

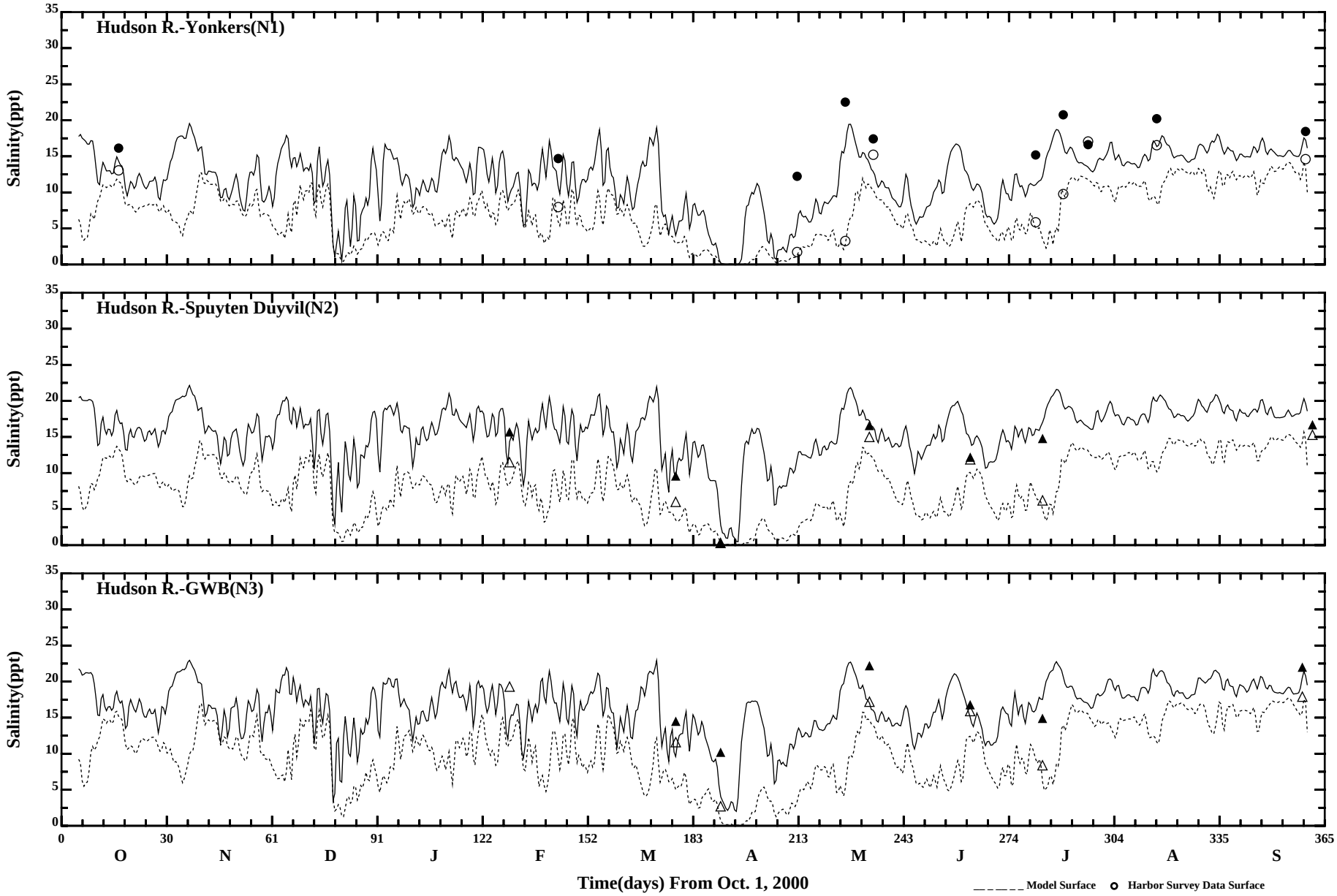

Comparison of 35 Hour Lowpass Surface and Bottom Salinity

/e1/hrfo0010/HYDRORUNS/CARP0001/PLOTS/TANDS/salt31_35hlp

DATE: 8/02/2004 TIME: 13:23:36

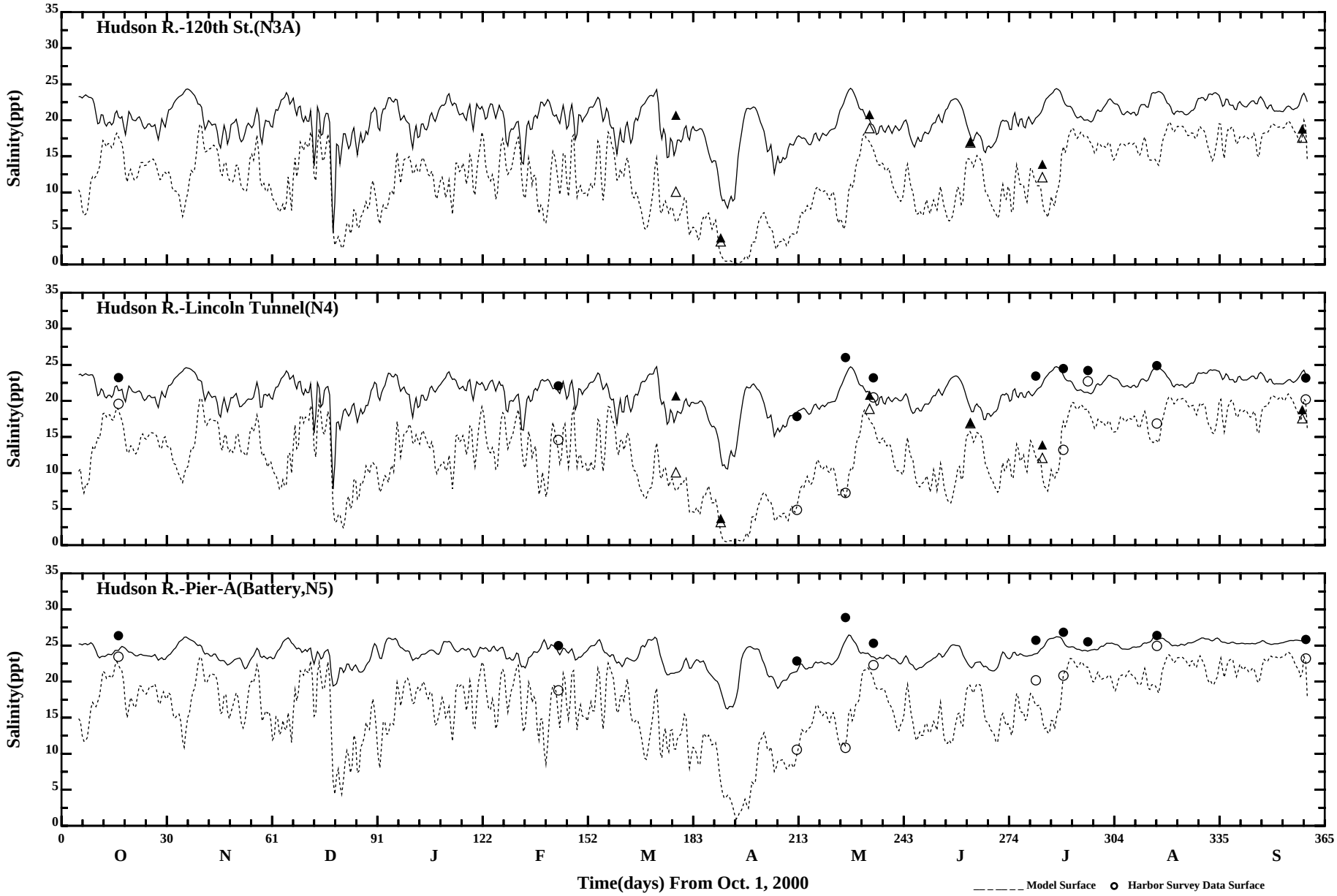

Comparison of 35 Hour Lowpass Surface and Bottom Salinity

/e1/hrfo0010/HYDRORUNS/CARP0001/PLOTS/TANDS/salt31_35hlp

DATE: 8/02/2004 TIME: 13:23:36

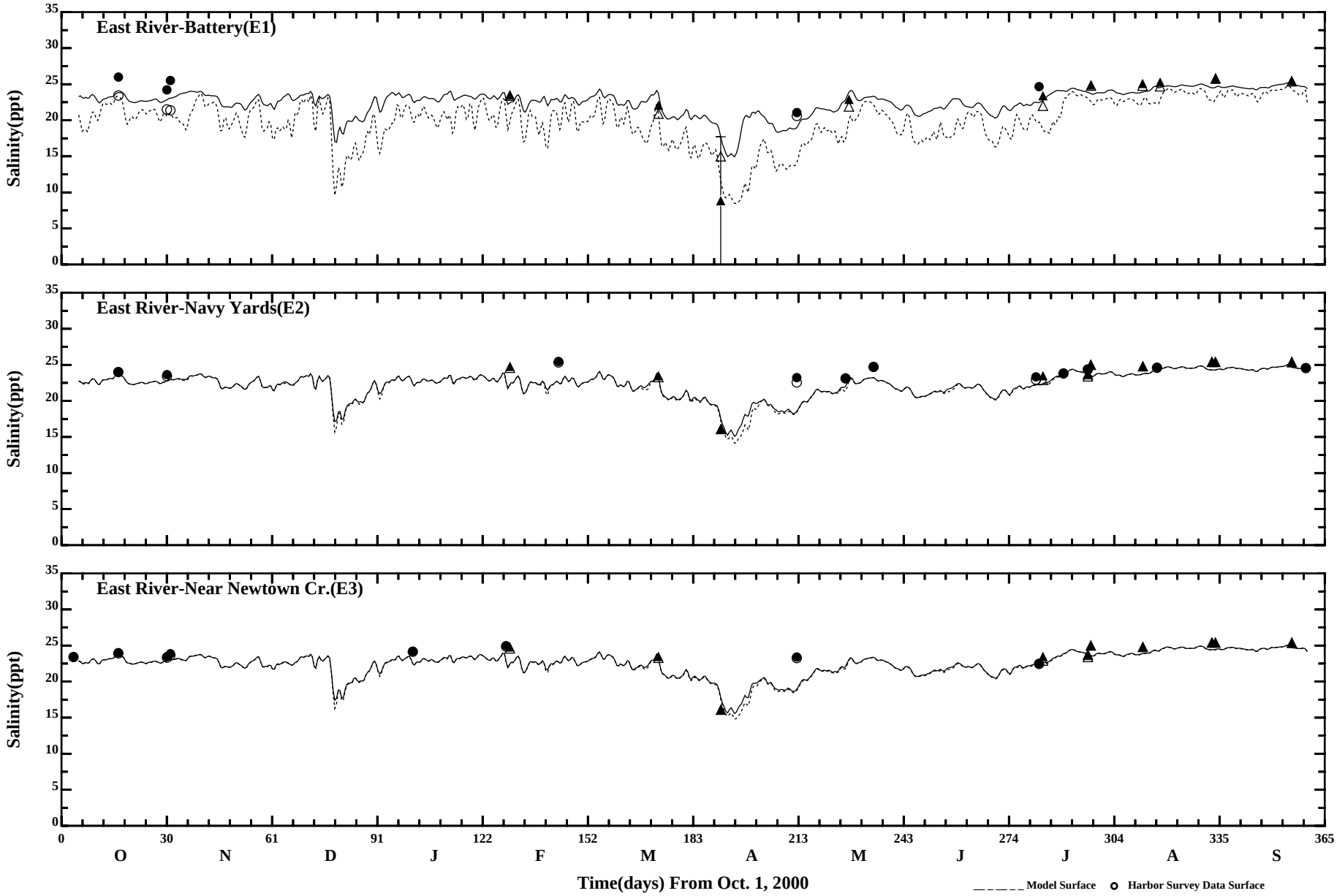

Comparison of 35 Hour Lowpass Surface and Bottom Salinity

/e1/hrfo0010/HYDRORUNS/CARP0001/PLOTS/TANDS/salt31_35hlp

DATE: 8/02/2004 TIME: 13:23:36

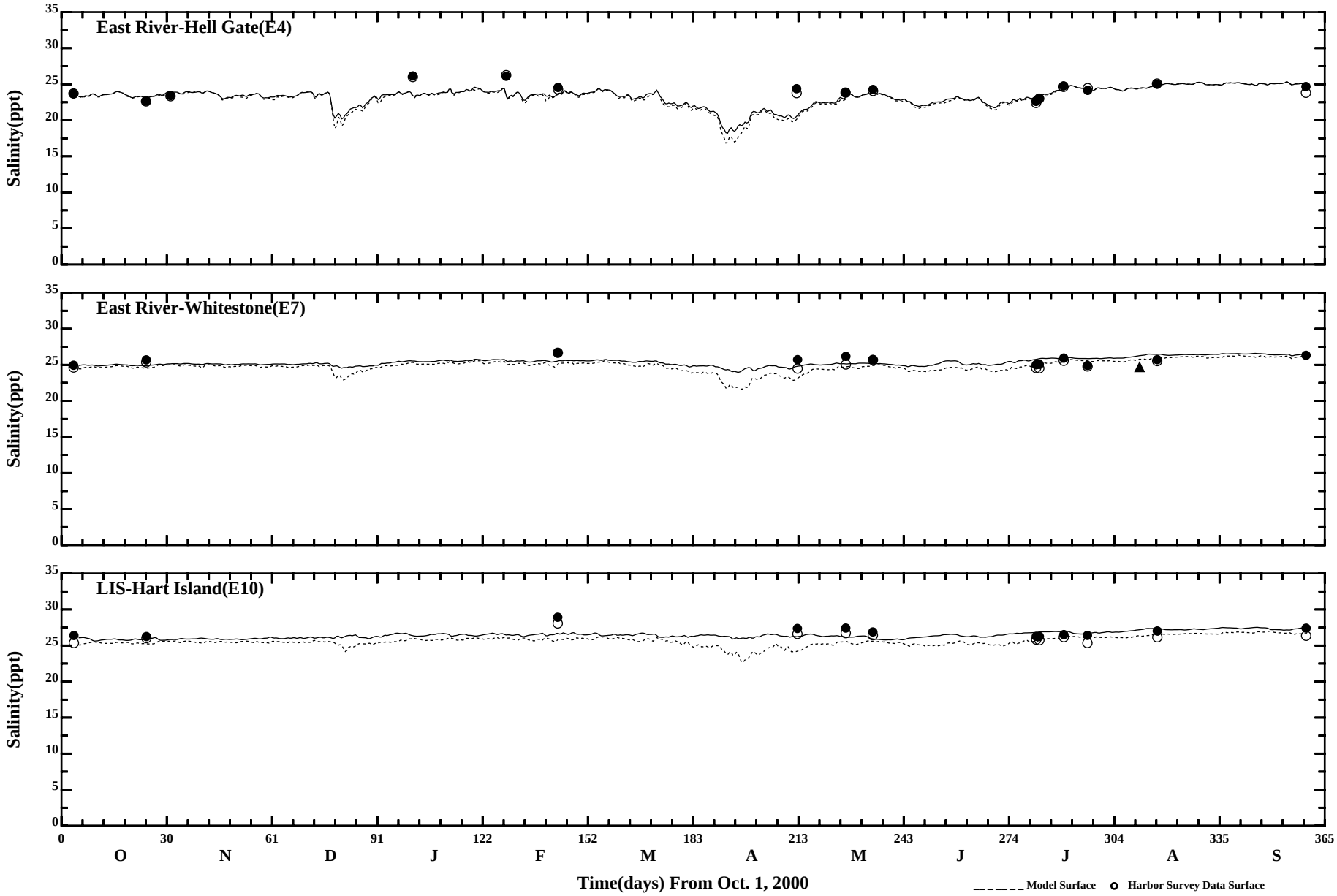

Comparison of 35 Hour Lowpass Surface and Bottom Salinity

/e1/hrfo0010/HYDRORUNS/CARP0001/PLOTS/TANDS/salt31_35hlp

DATE: 8/02/2004 TIME: 13:23:36

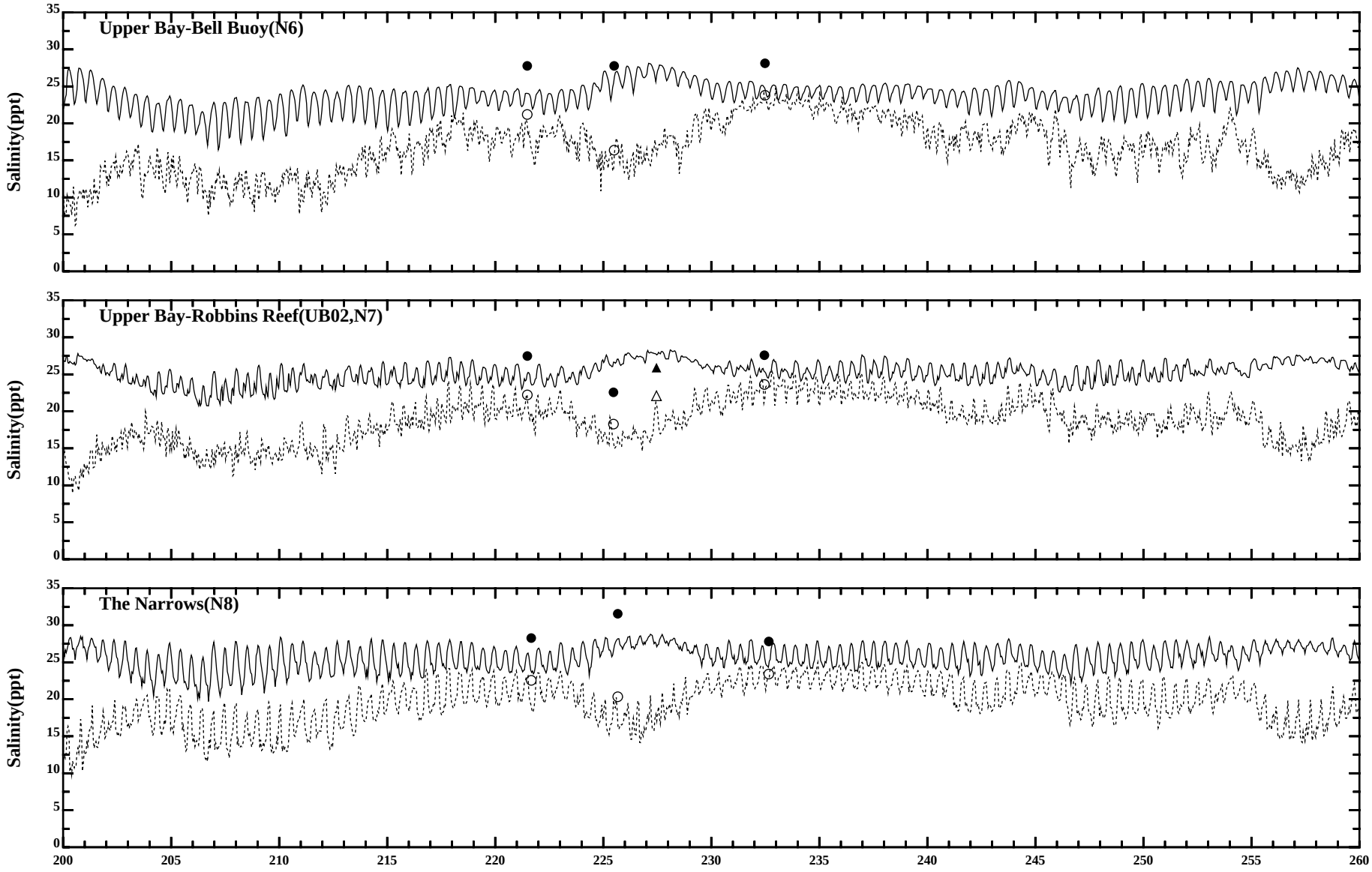

Comparison of Instantaneous Surface and Bottom Salinity

/e1/hrfo0010/HYDRORUNS/CARP0001/PLOTS/TANDS/salt32

DATE: 8/02/2004 TIME: 13:23:54

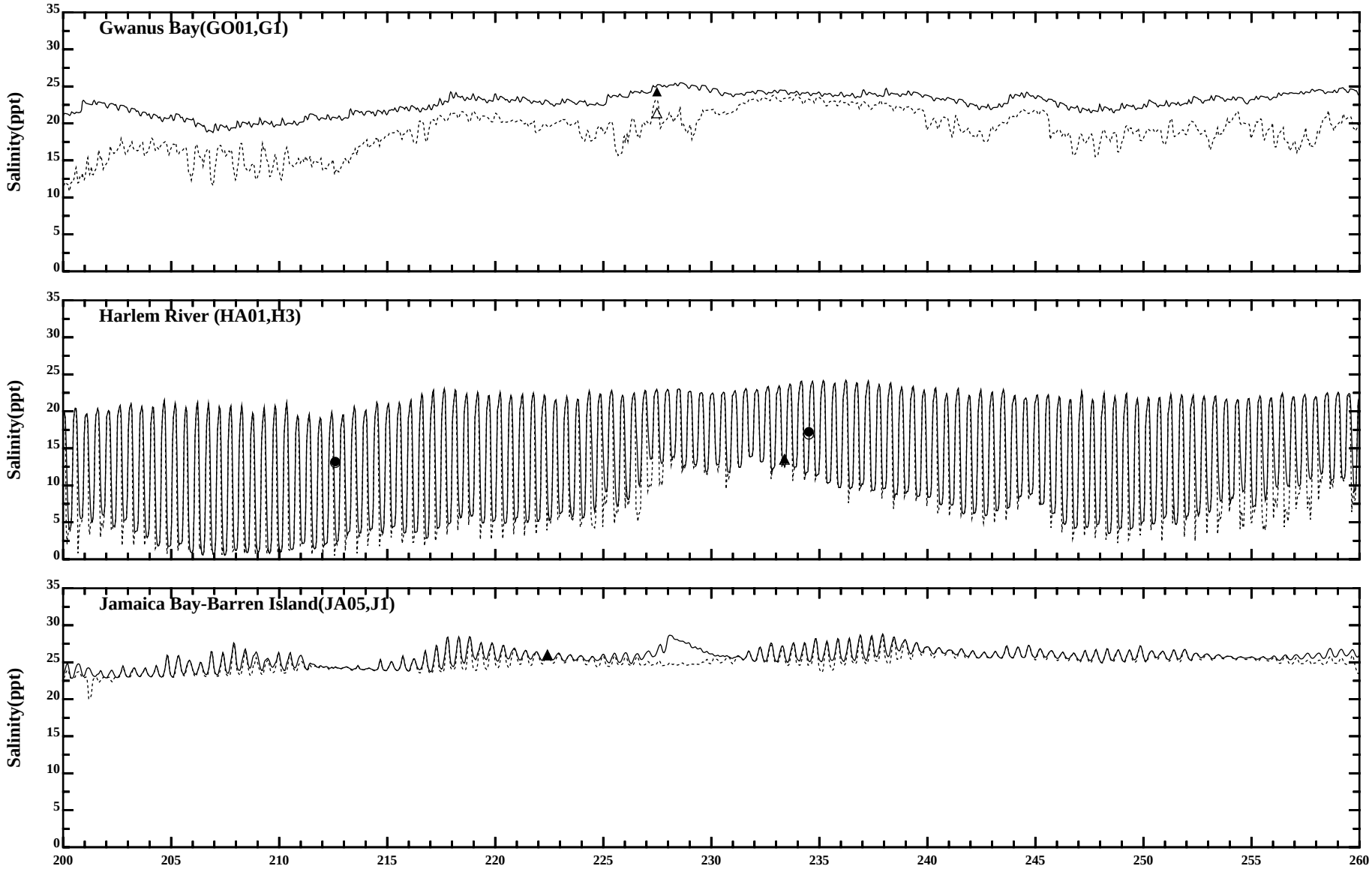

Comparison of Instantaneous Surface and Bottom Salinity

/e1/hrfo0010/HYDRORUNS/CARP0001/PLOTS/TANDS/salt32

_ _ _ _ _ Model Surface
_____ Model Bottom
○ Harbor Survey Data Surface
● Harbor Survey Data Bottom
△ USA Data Surface
▲ USA Data Bottom
□ US ARMY CORPS. OF ENGRS Data Surface
■ US ARMY CORPS. OF ENGRS Data Bottom

DATE: 8/02/2004 TIME: 13:23:54

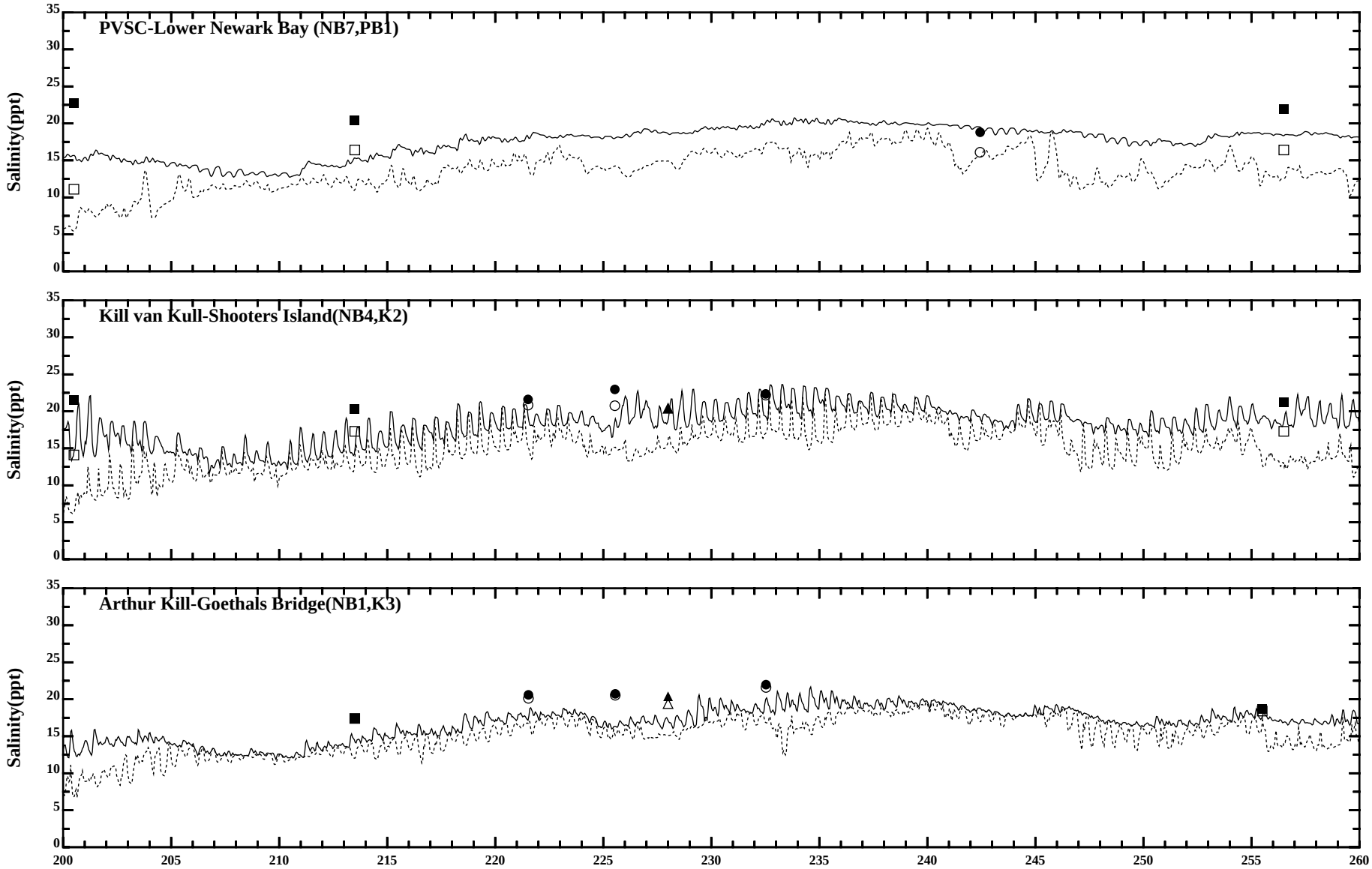

Comparison of Instantaneous Surface and Bottom Salinity

/e1/hrfo0010/HYDRORUNS/CARP0001/PLOTS/TANDS/salt32

DATE: 8/02/2004 TIME: 13:23:54

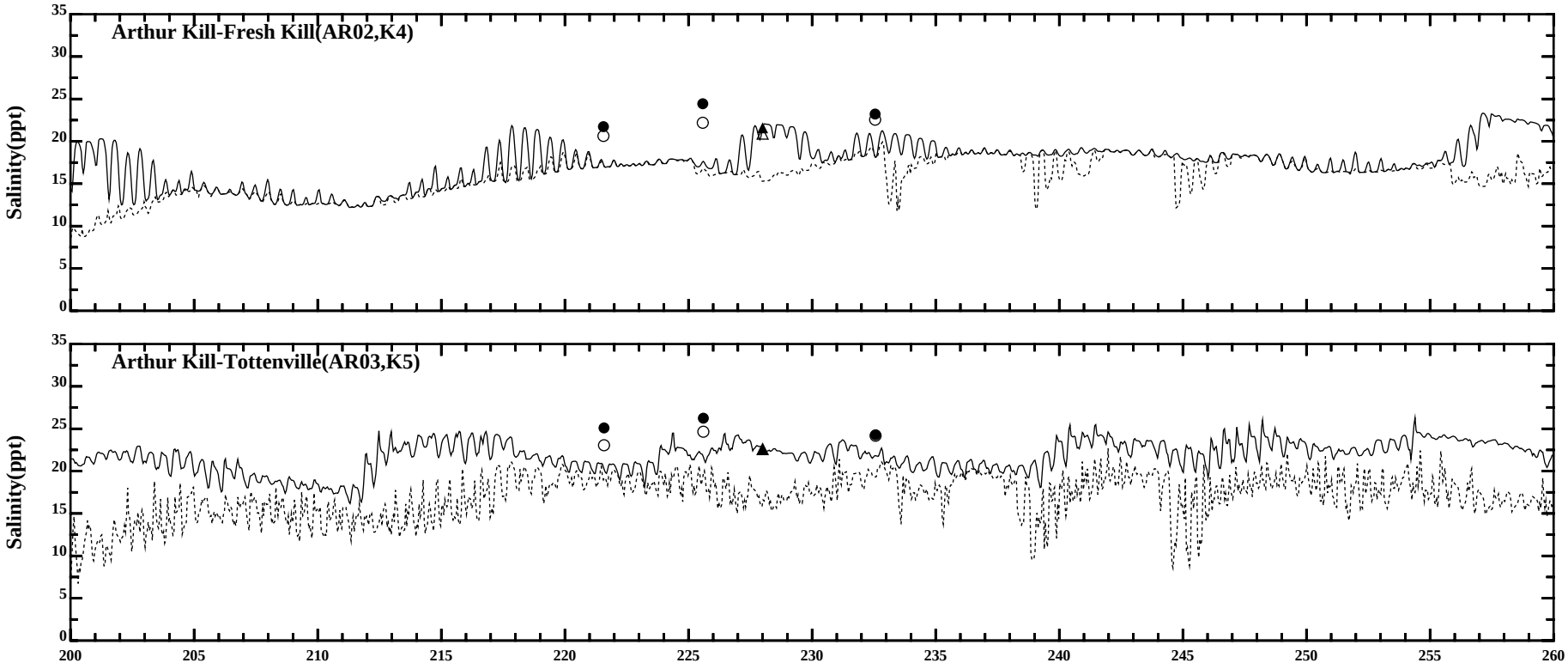

Comparison of Instantaneous Surface and Bottom Salinity

/e1/hrfo0010/HYDRORUNS/CARP0001/PLOTS/TANDS/salt32

DATE: 8/02/2004 TIME: 13:23:54

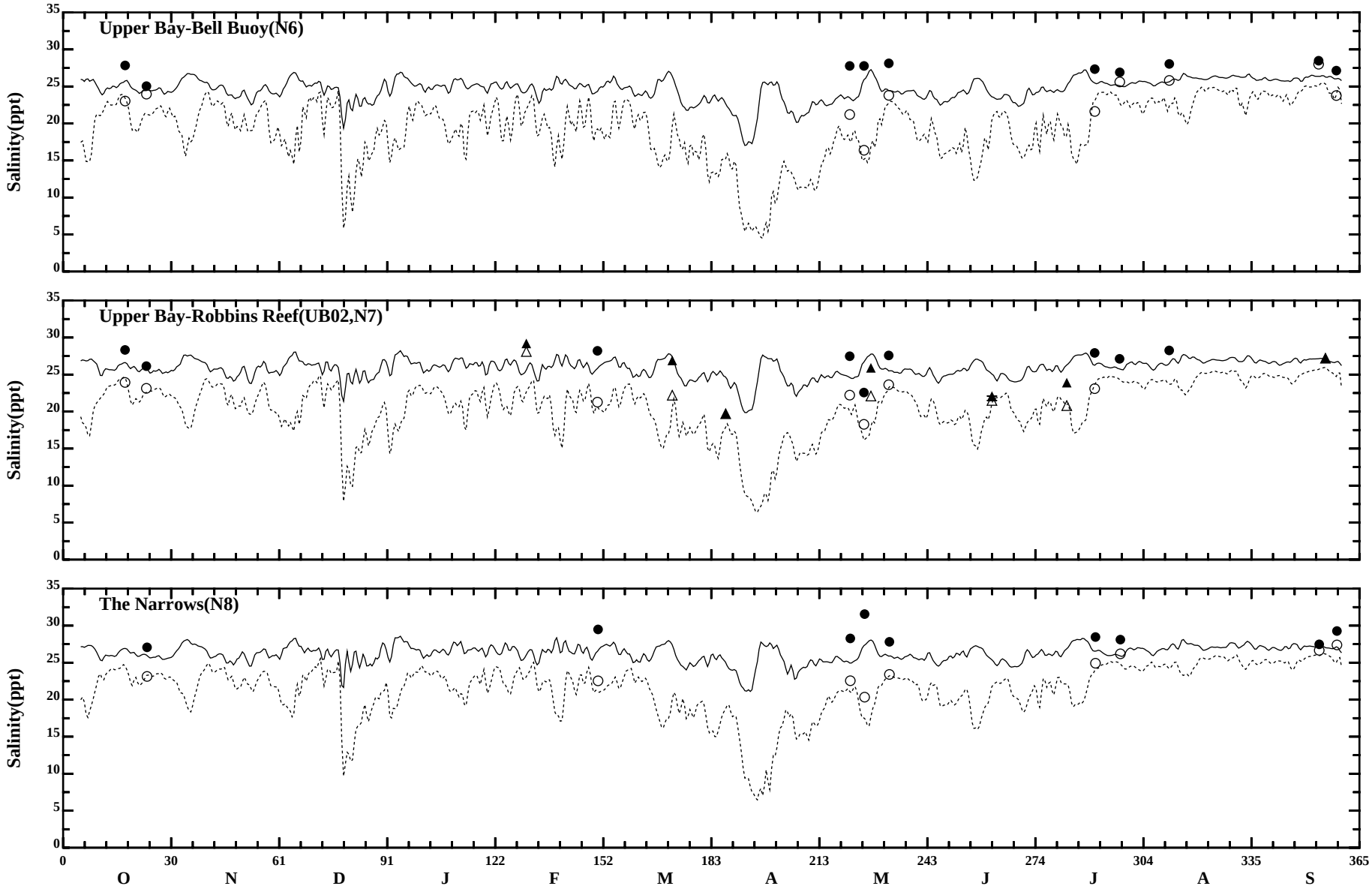

Comparison of 35 Hour Lowpass Surface and Bottom Salinity

/e1/hrfo0010/HYDRORUNS/CARP0001/PLOTS/TANDS/salt32_35hlp

DATE: 8/02/2004 TIME: 12:29:23

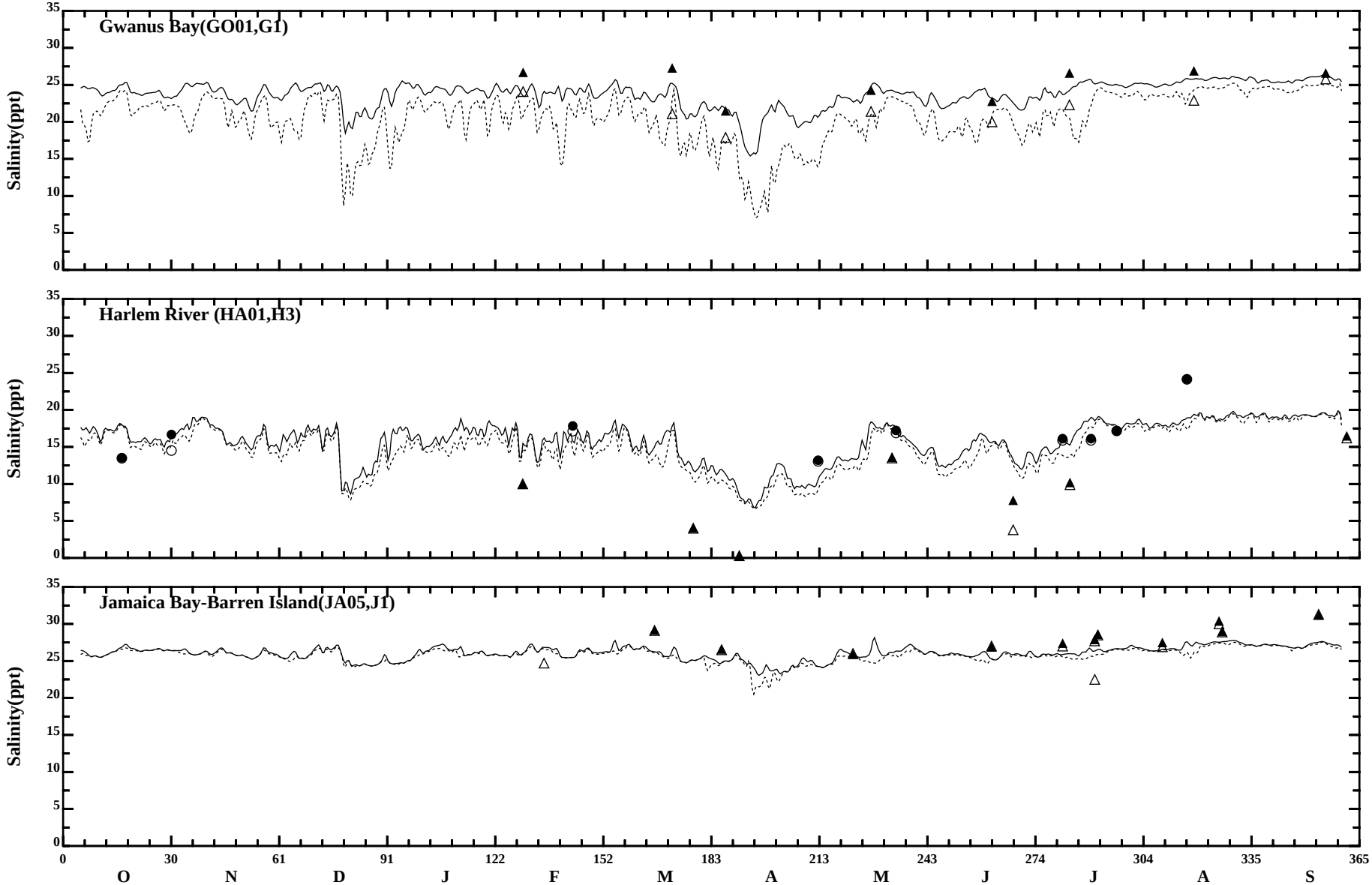

Comparison of 35 Hour Lowpass Surface and Bottom Salinity

/e1/hrfo0010/HYDRORUNS/CARP0001/PLOTS/TANDS/salt32_35hlp

DATE: 8/02/2004 TIME: 12:29:23

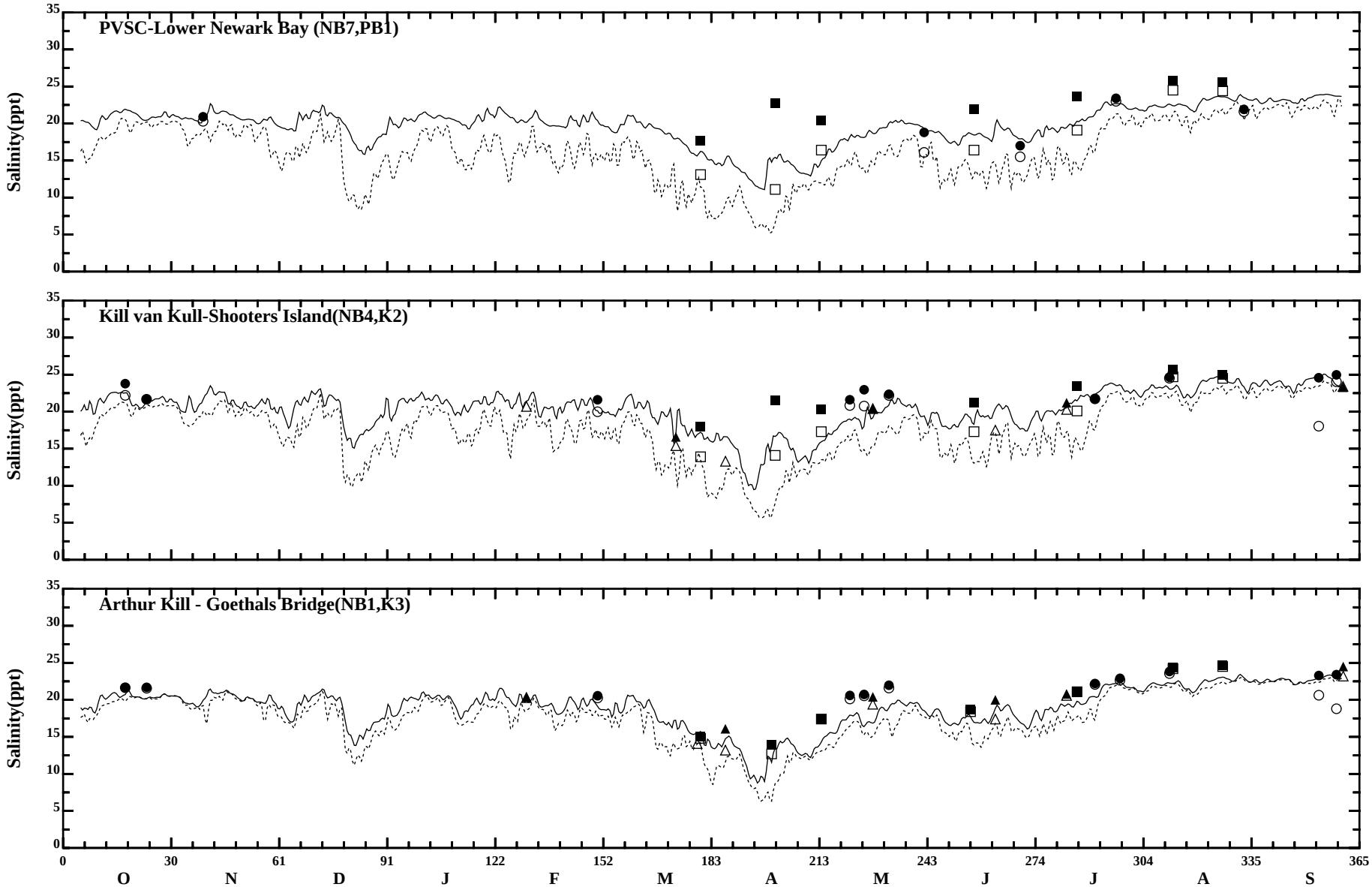

Comparison of 35 Hour Lowpass Surface and Bottom Salinity

/e1/hrfo0010/HYDRORUNS/CARP0001/PLOTS/TANDS/salt32_35hlp

DATE: 8/02/2004 TIME: 12:29:23

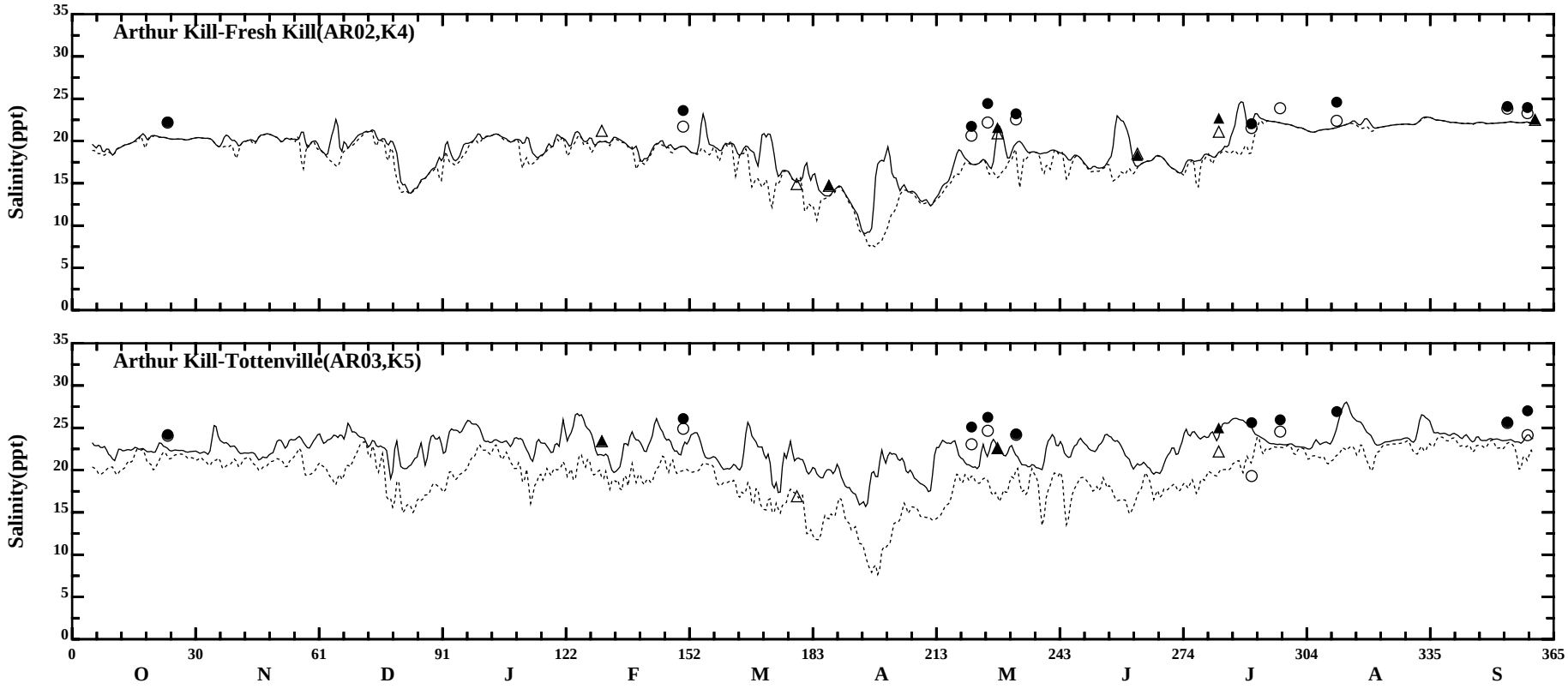

Comparison of 35 Hour Lowpass Surface and Bottom Salinity

/e1/hrfo0010/HYDRORUNS/CARP0001/PLOTS/TANDS/salt32_35hlp

DATE: 8/02/2004 TIME: 12:29:23

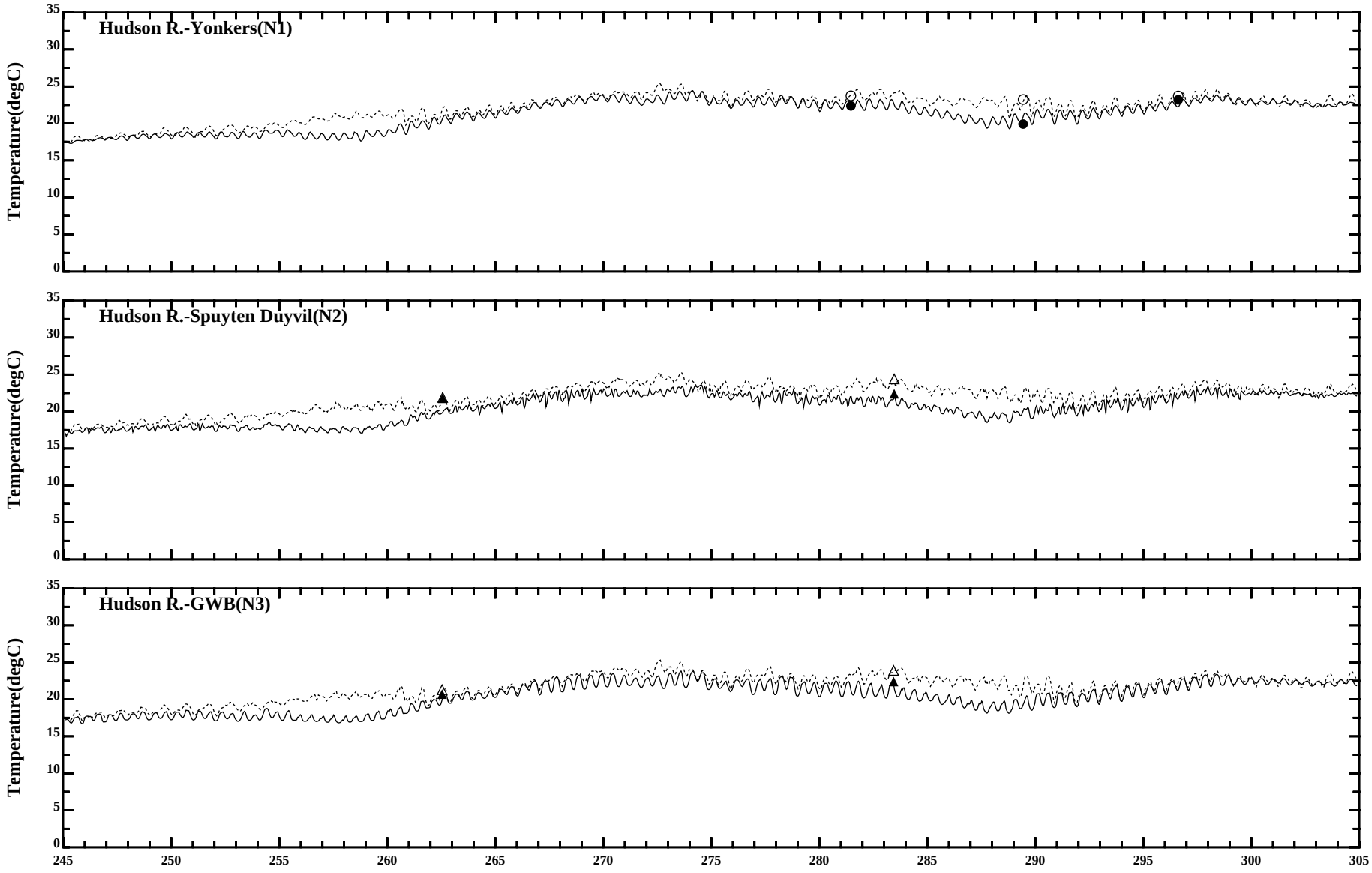

Comparison of Instantaneous Surface and Bottom Temperature

/e1/hrfo0010/HYDRORUNS/CARP0001/PLOTS/TANDS/temp31

DATE: 8/02/2004 TIME: 13:26:28

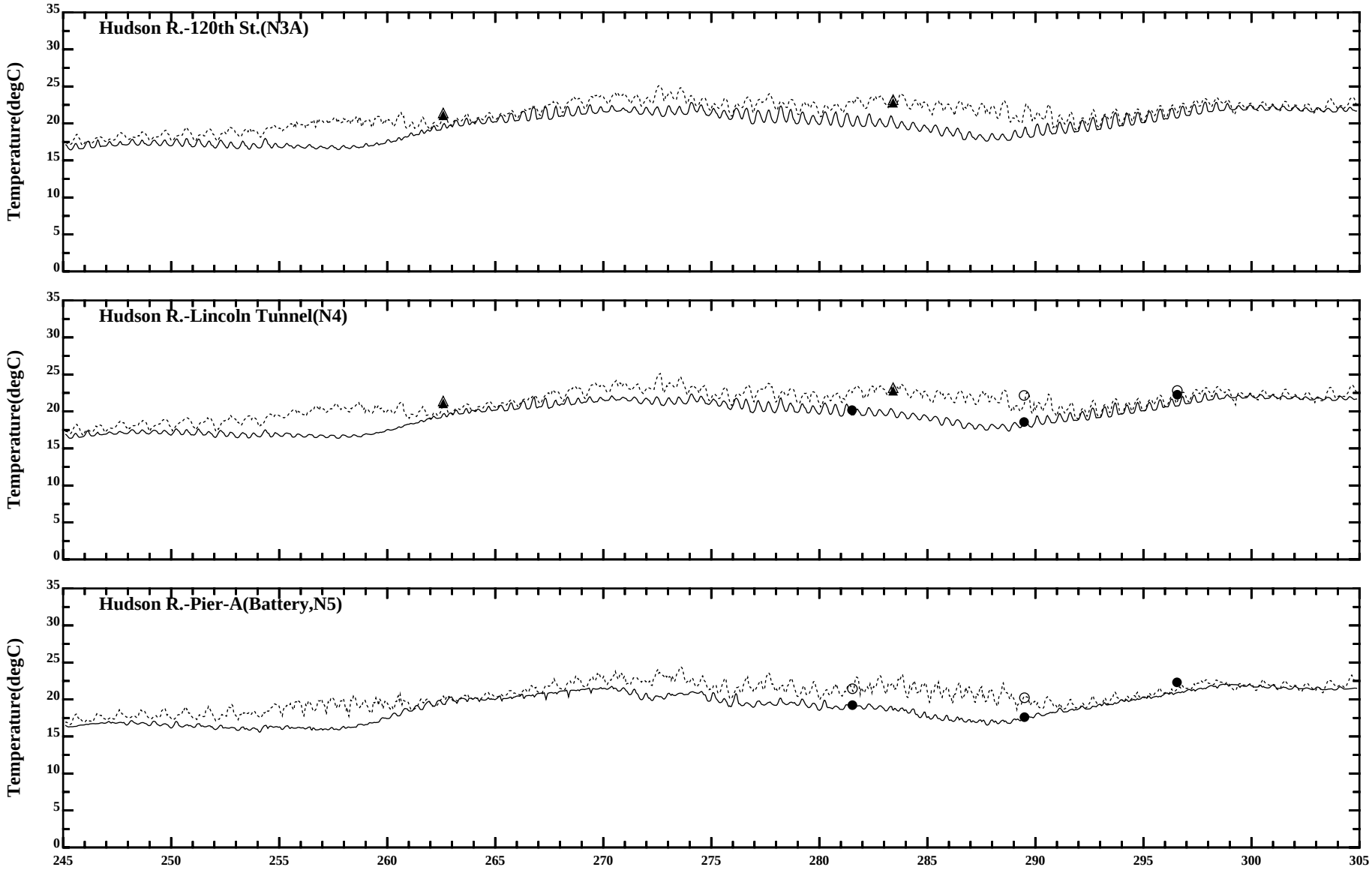

Comparison of Instantaneous Surface and Bottom Temperature

/e1/hrfo0010/HYDRORUNS/CARP0001/PLOTS/TANDS/temp31

DATE: 8/02/2004 TIME: 13:26:28

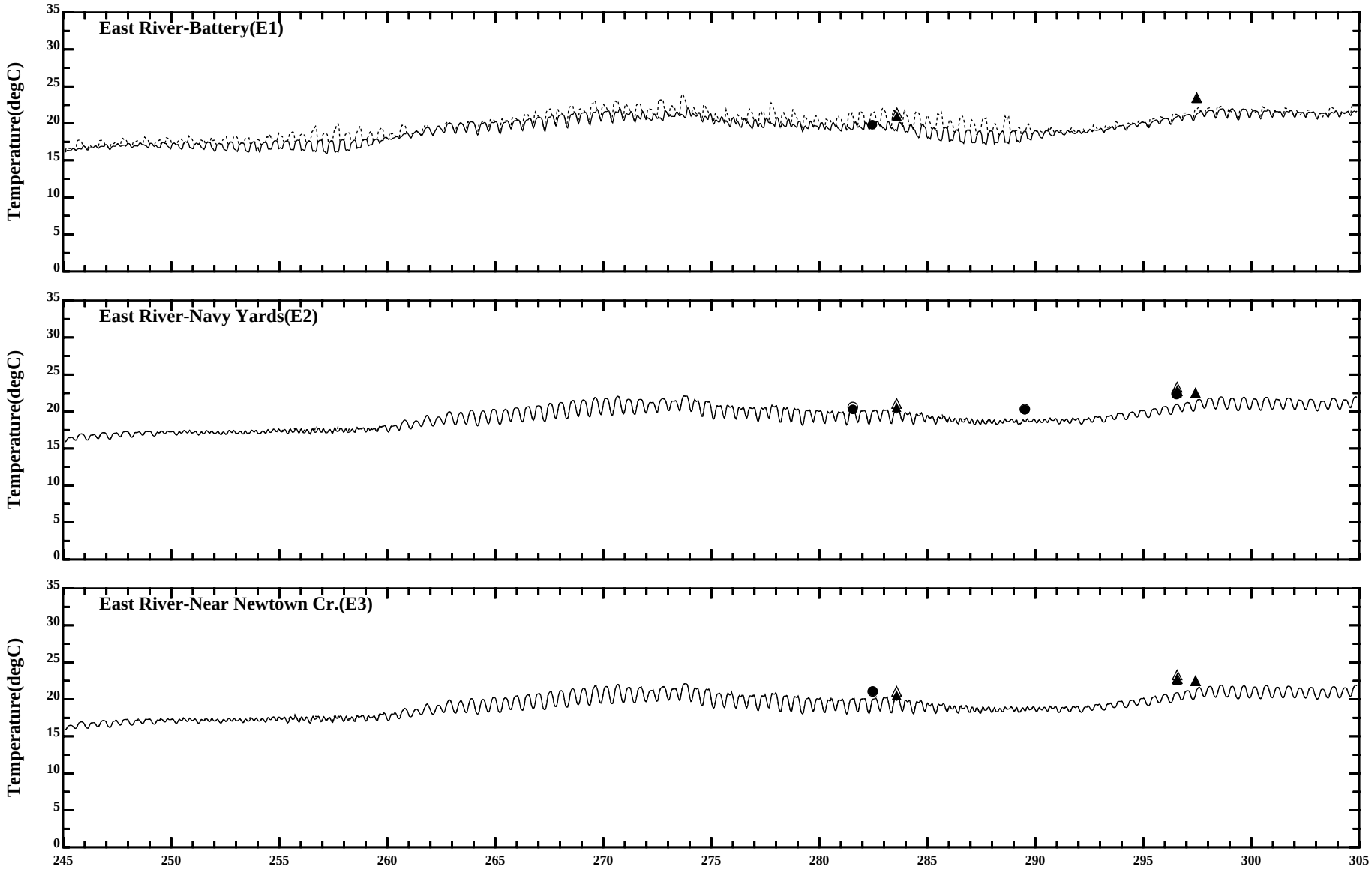

Comparison of Instantaneous Surface and Bottom Temperature

/e1/hrfo0010/HYDRORUNS/CARP0001/PLOTS/TANDS/temp31

DATE: 8/02/2004 TIME: 13:26:28

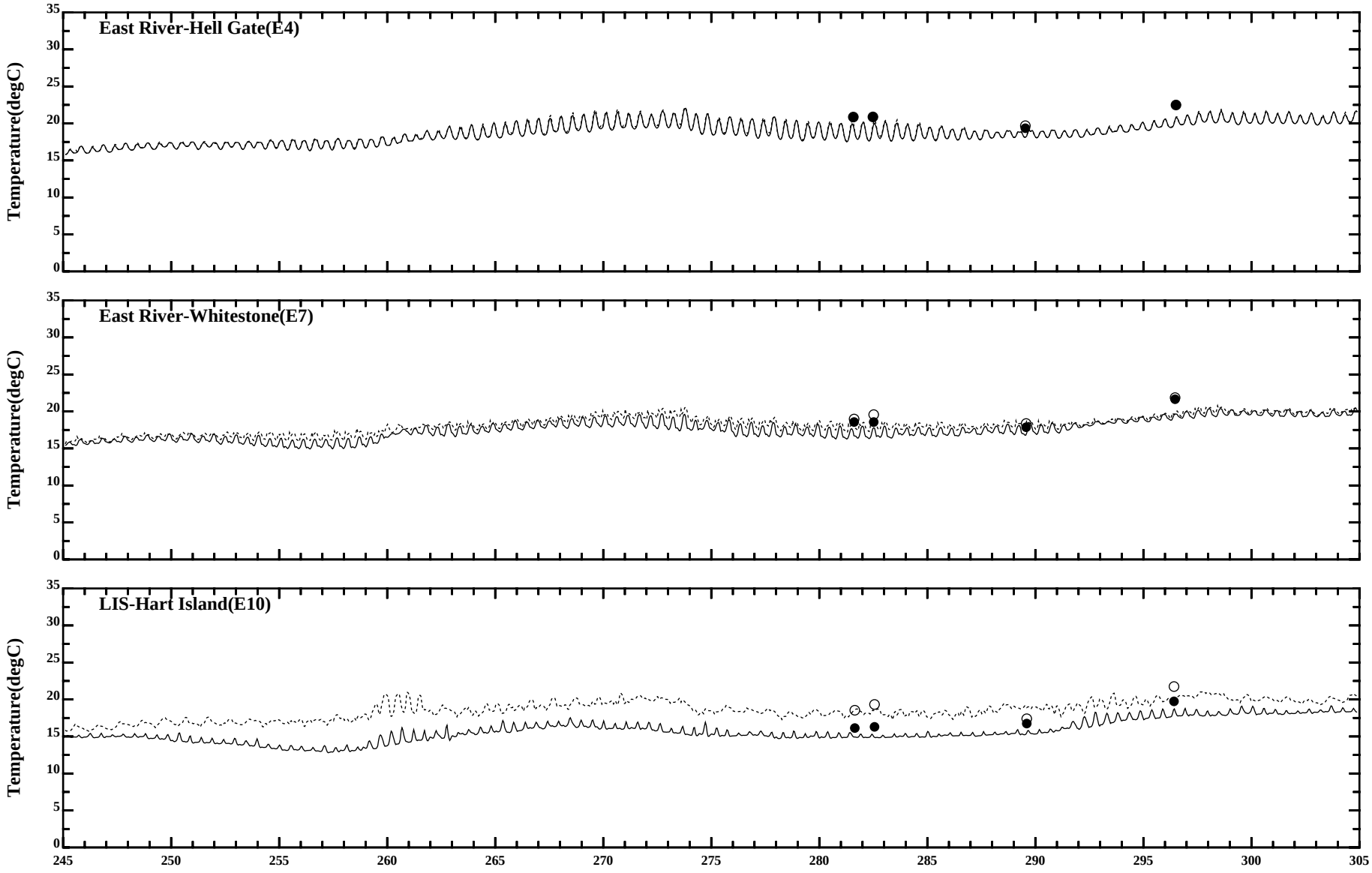

Comparison of Instantaneous Surface and Bottom Temperature

/e1/hrfo0010/HYDRORUNS/CARP0001/PLOTS/TANDS/temp31

DATE: 8/02/2004 TIME: 13:26:28

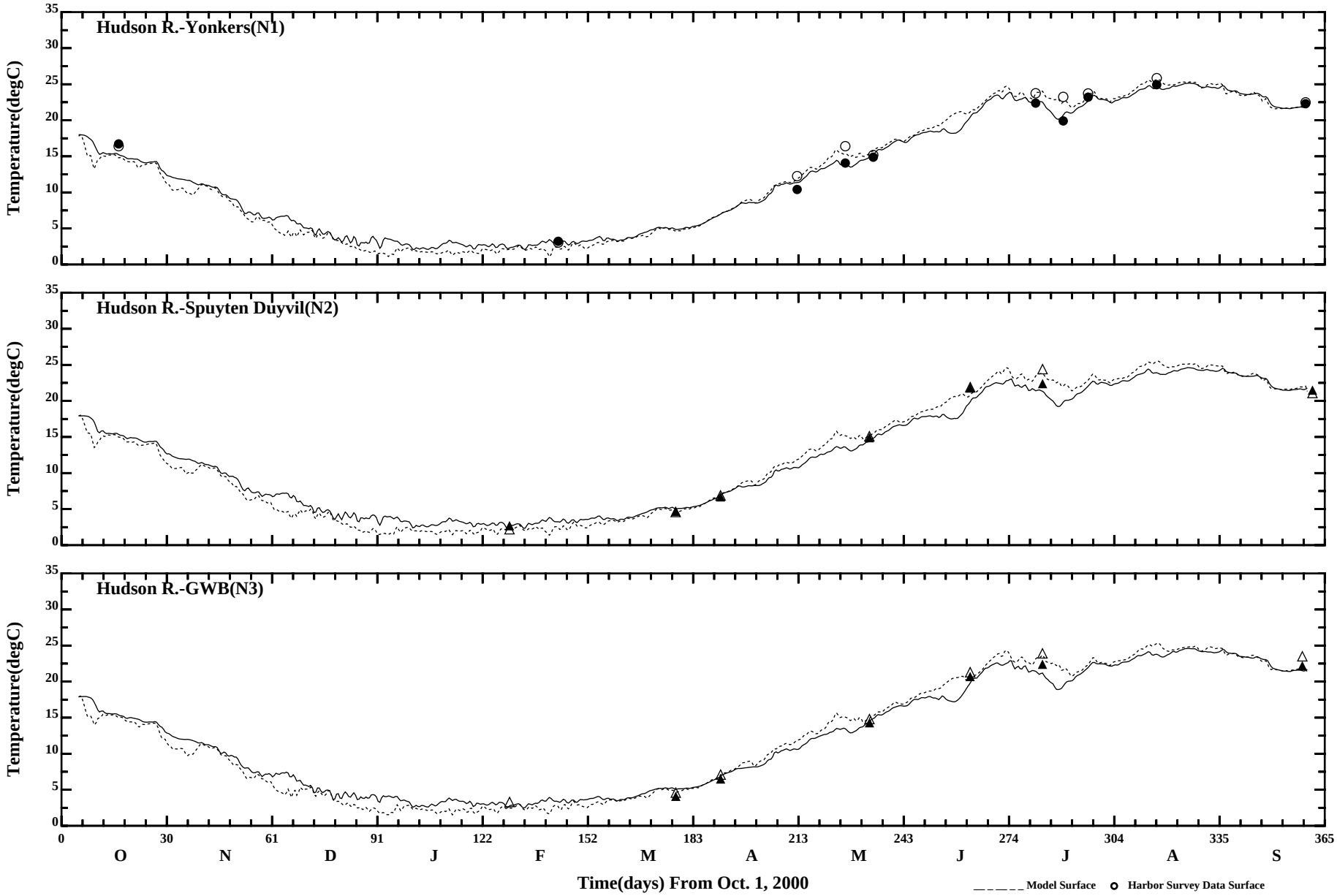

Comparison of 35 Hour Lowpass Surface and Bottom Temperature

/e1/hrfo0010/HYDRORUNS/CARP0001/PLOTS/TANDS/temp31

DATE: 8/02/2004 TIME: 13:27:30

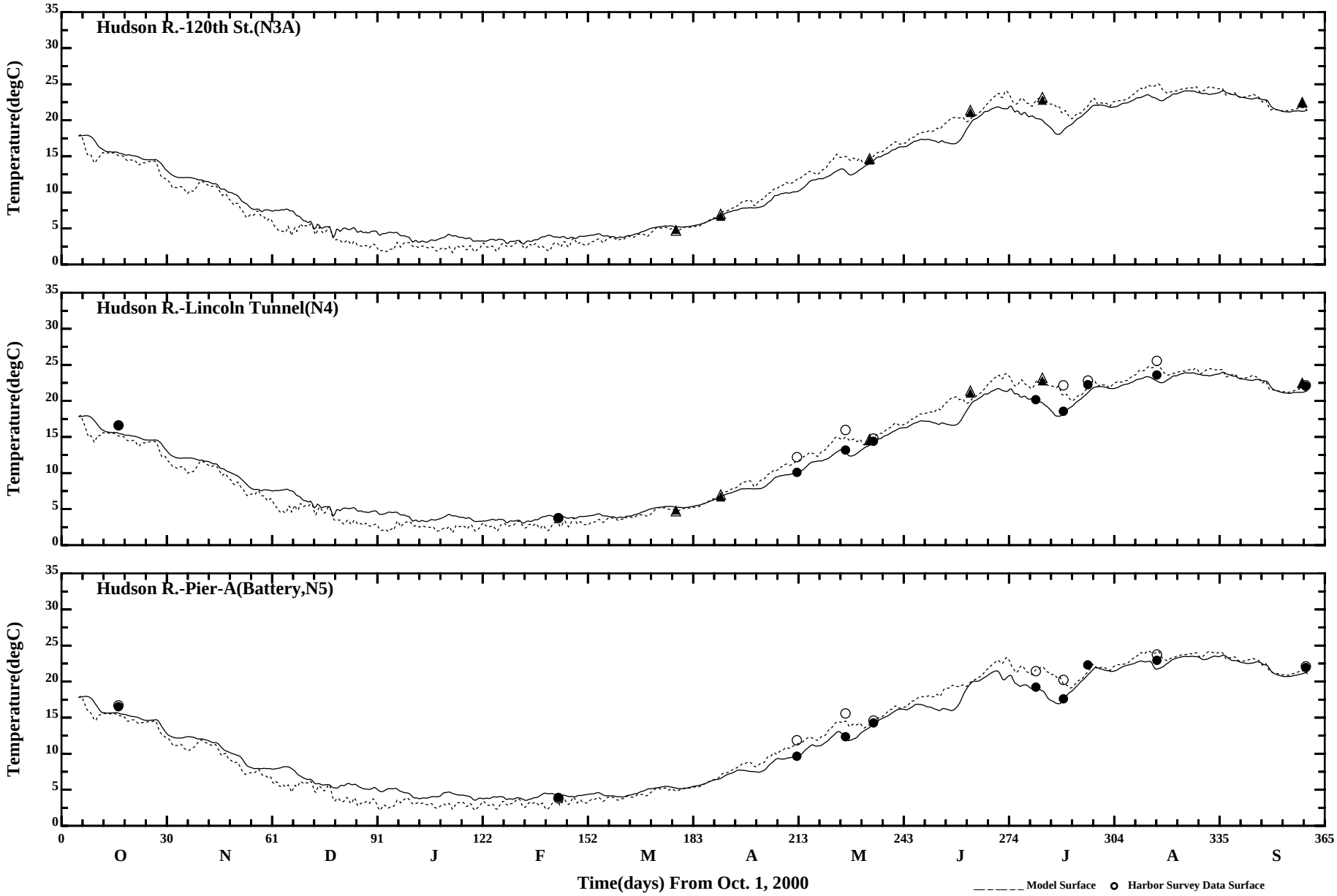

Comparison of 35 Hour Lowpass Surface and Bottom Temperature

/e1/hrfo0010/HYDRORUNS/CARP0001/PLOTS/TANDS/temp31

DATE: 8/02/2004 TIME: 13:27:30

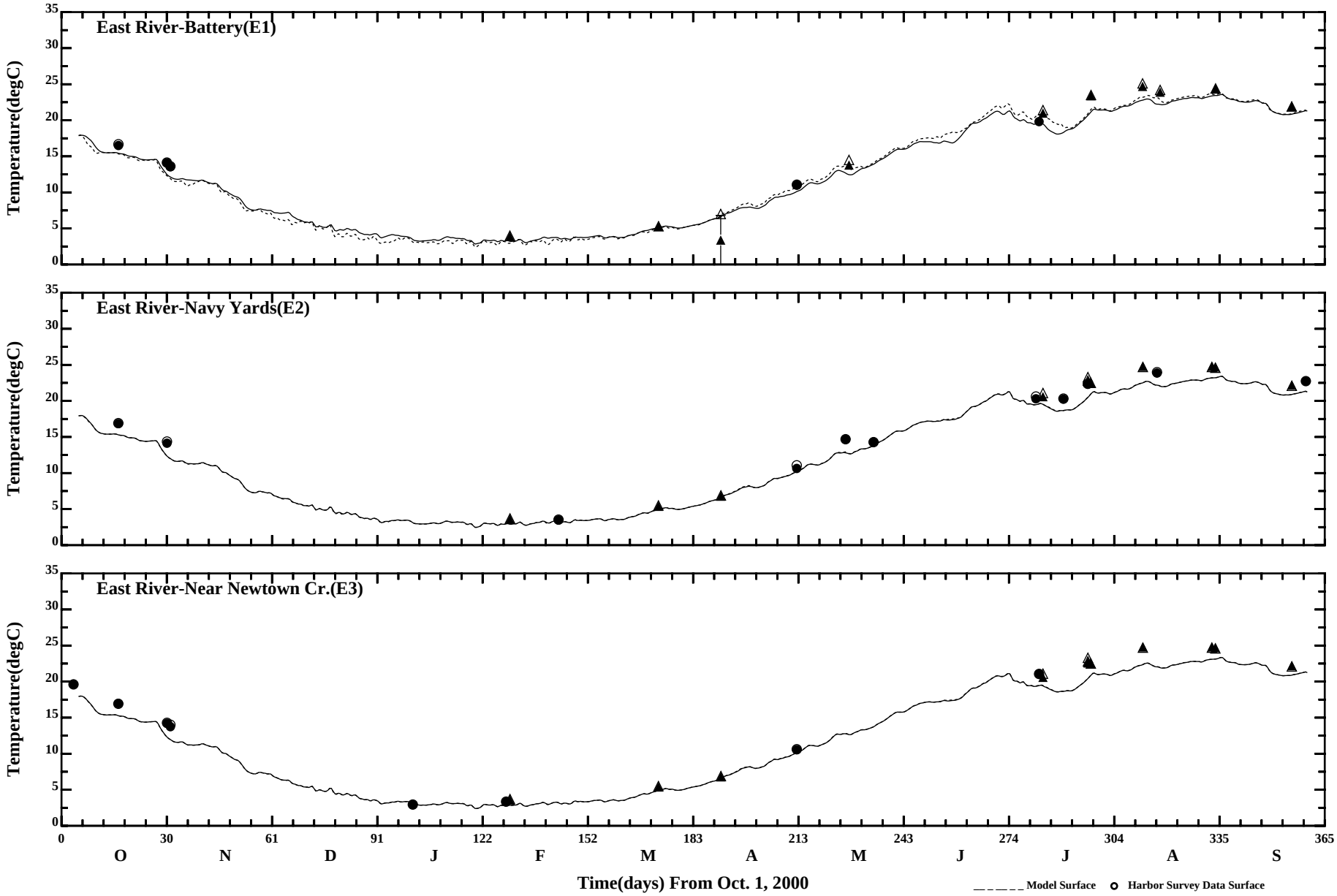

Comparison of 35 Hour Lowpass Surface and Bottom Temperature

/e1/hrfo0010/HYDRORUNS/CARP0001/PLOTS/TANDS/temp31

DATE: 8/02/2004 TIME: 13:27:30

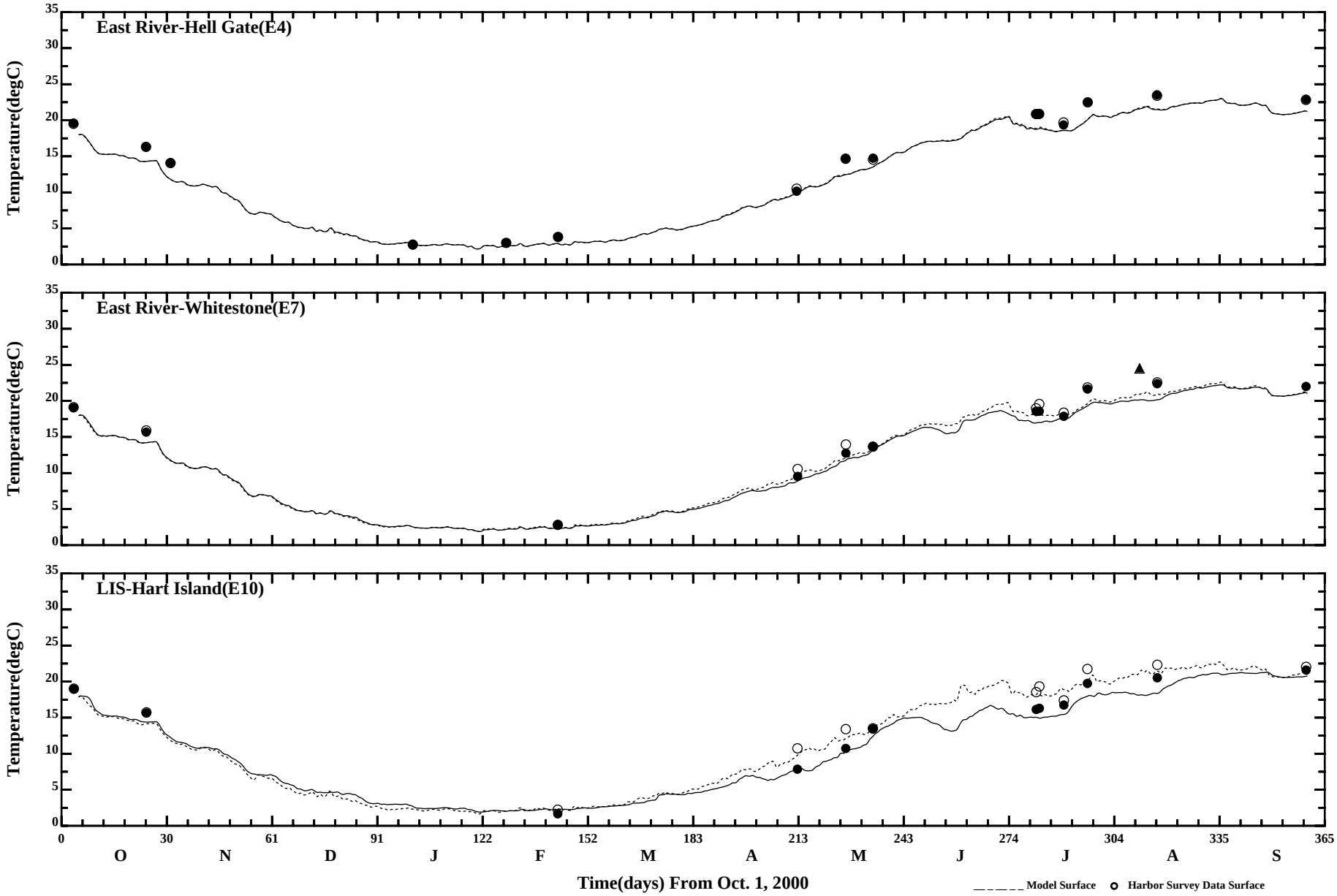

Comparison of 35 Hour Lowpass Surface and Bottom Temperature

/e1/hrfo0010/HYDRORUNS/CARP0001/PLOTS/TANDS/temp31

DATE: 8/02/2004 TIME: 13:27:30

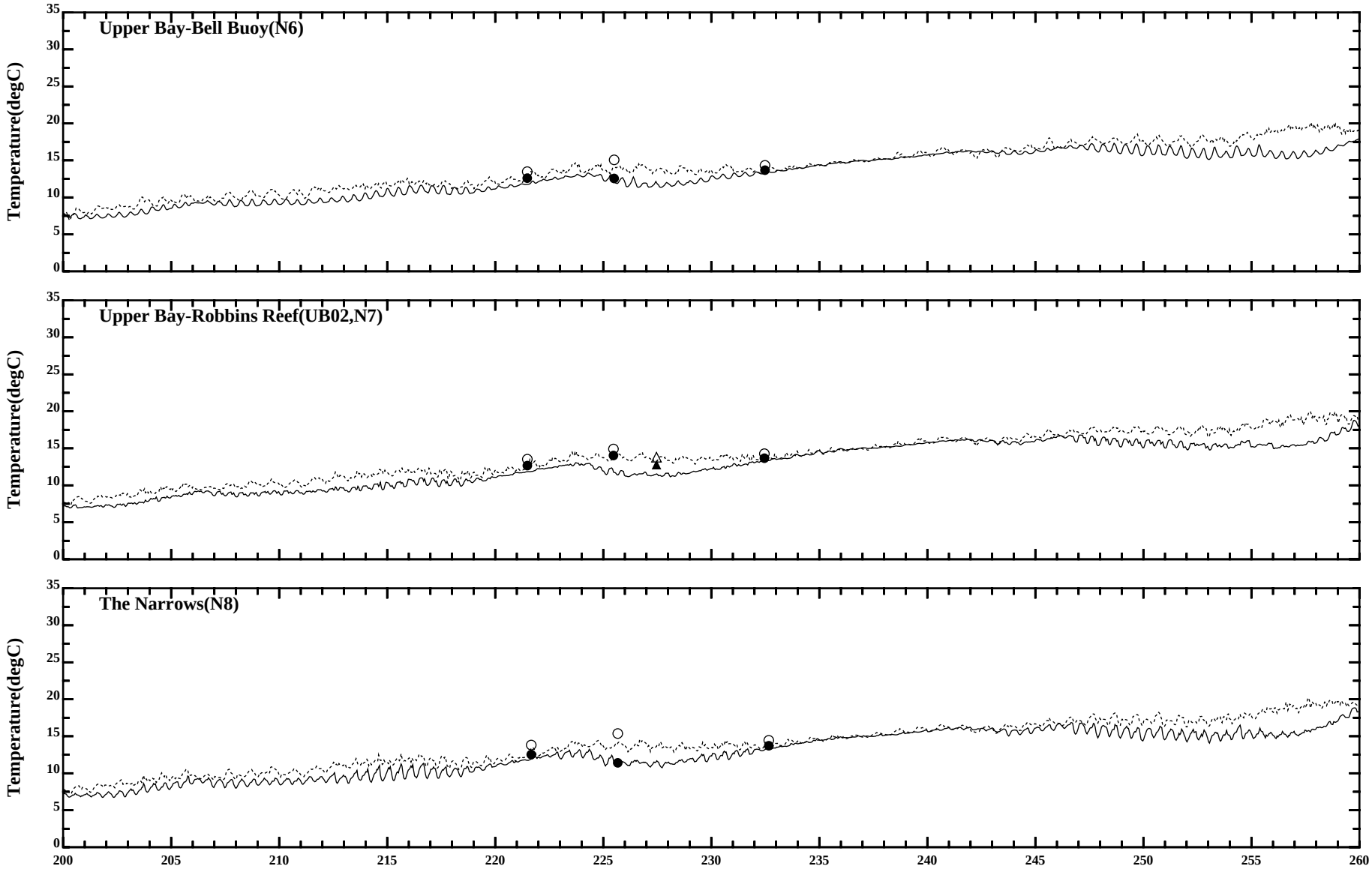

Comparison of Instantaneous Surface and Bottom Temperature

/e1/hrfo0010/HYDRORUNS/CARP0001/PLOTS/TANDS/temp32

DATE: 8/02/2004 TIME: 13:28:19

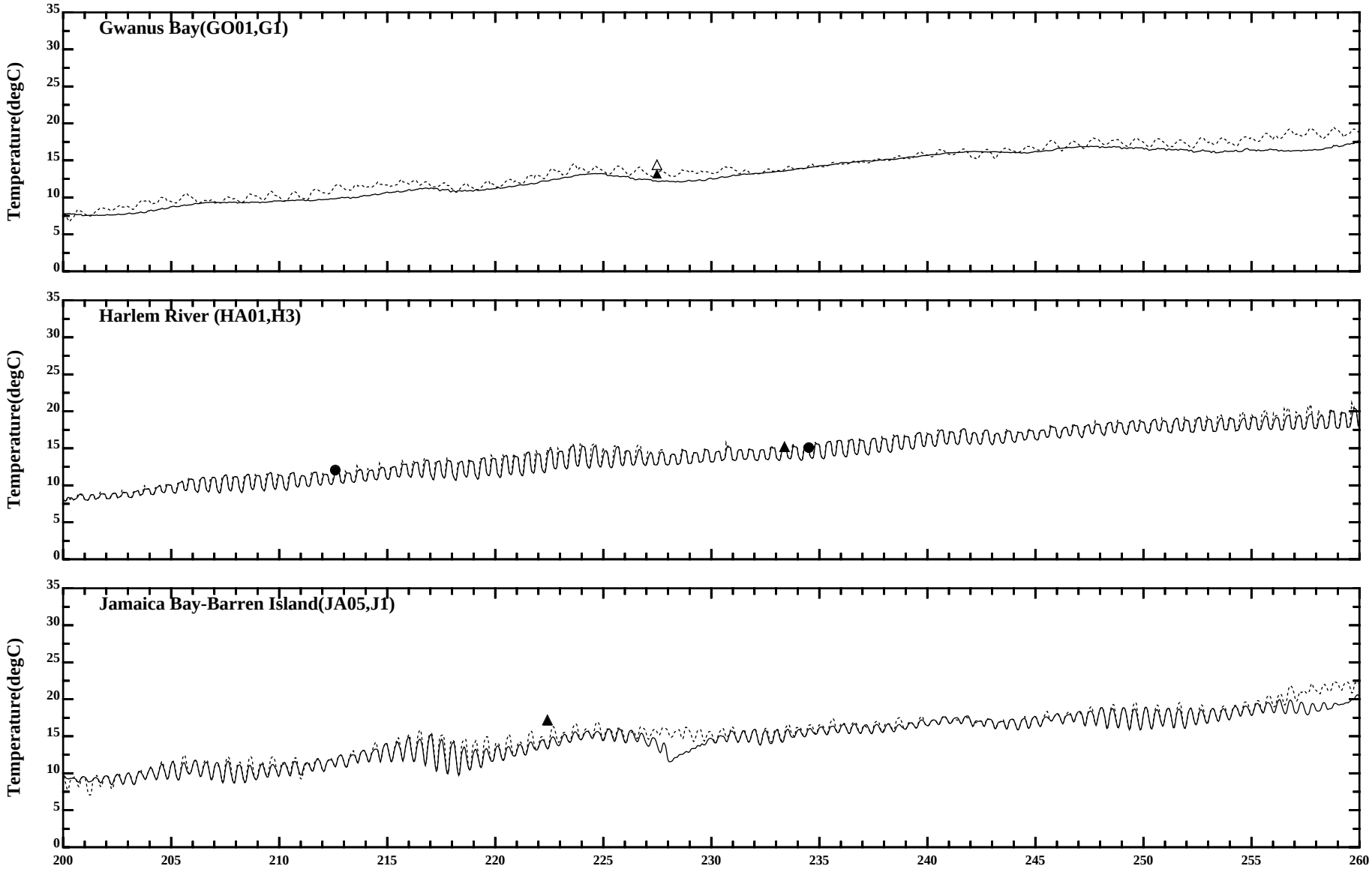

Comparison of Instantaneous Surface and Bottom Temperature

/e1/hrfo0010/HYDRORUNS/CARP0001/PLOTS/TANDS/temp32

DATE: 8/02/2004 TIME: 13:28:19

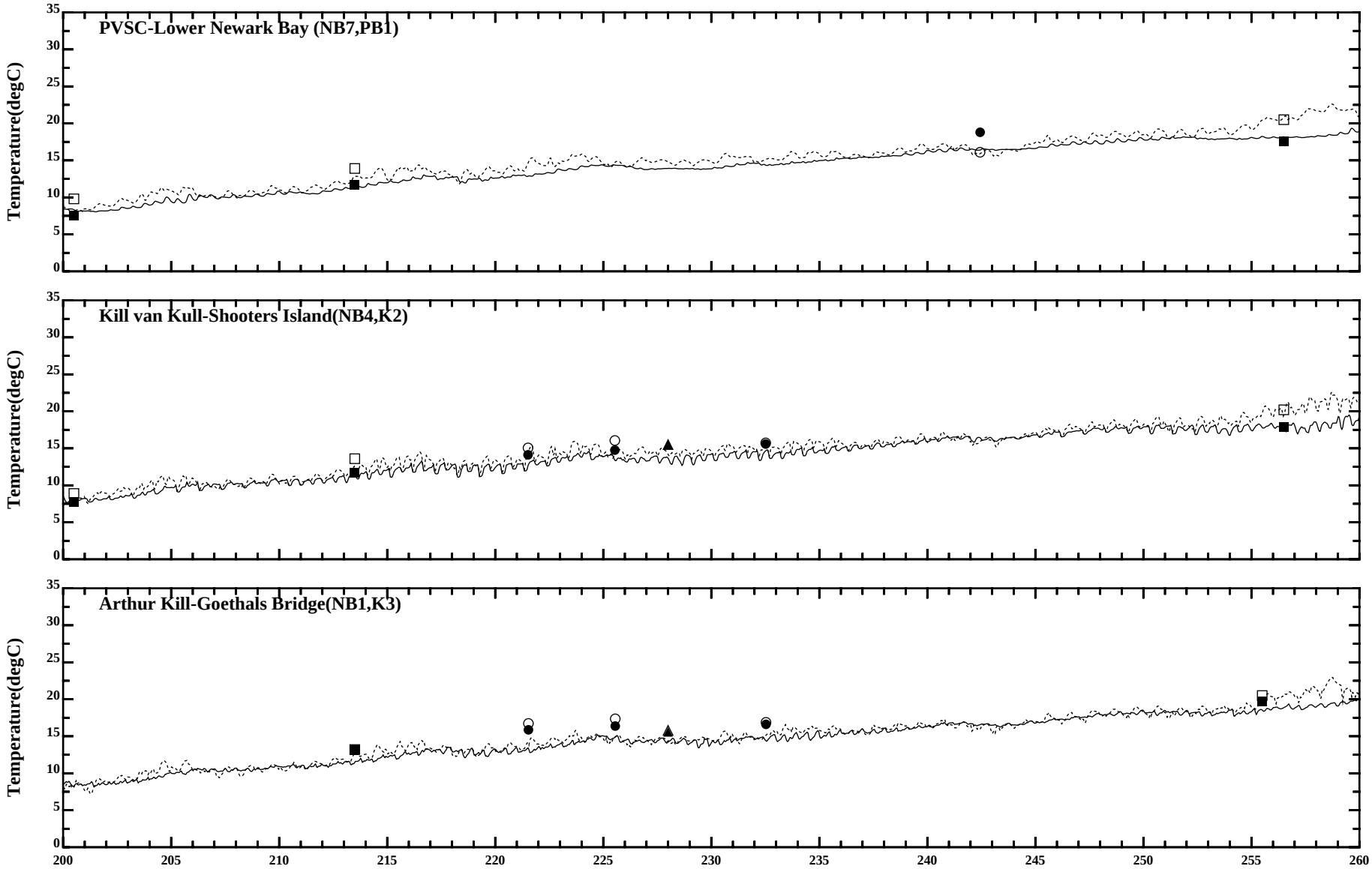

Comparison of Instantaneous Surface and Bottom Temperature

/e1/hrfo0010/HYDRORUNS/CARP0001/PLOTS/TANDS/temp32

DATE: 8/02/2004 TIME: 13:28:19

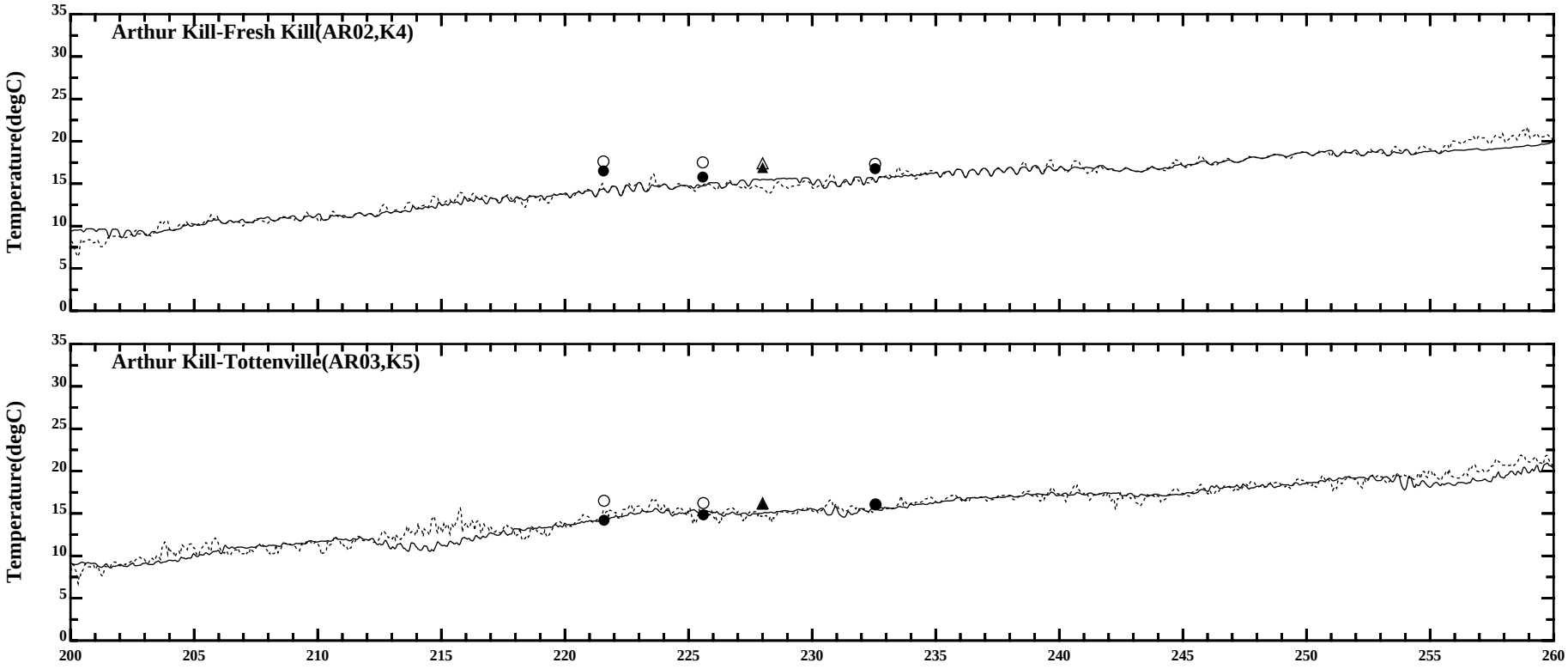

Comparison of Instantaneous Surface and Bottom Temperature

/e1/hrfo0010/HYDRORUNS/CARP0001/PLOTS/TANDS/temp32

DATE: 8/02/2004 TIME: 13:28:19

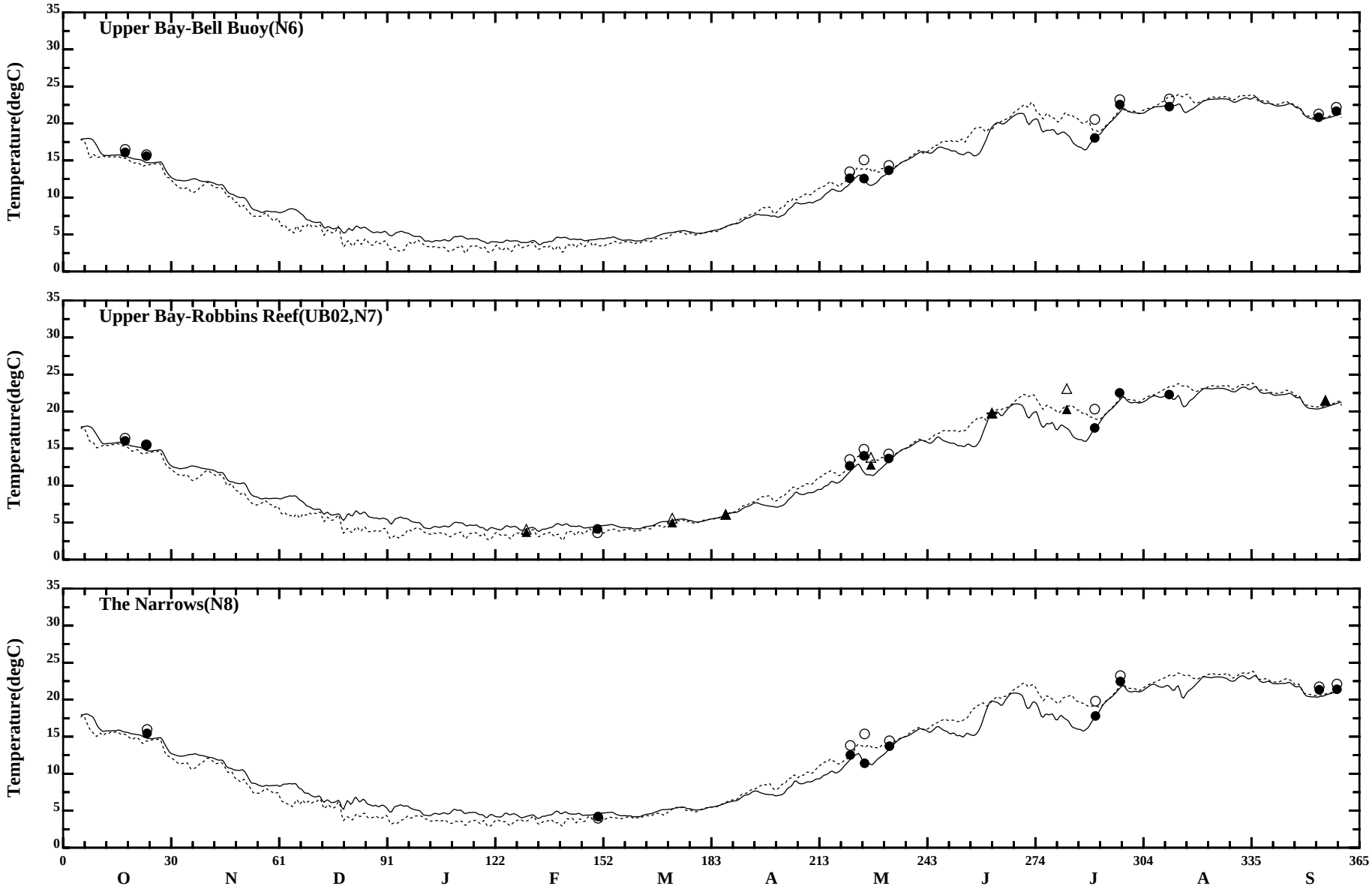

Comparison of 35 Hour Lowpass Surface and Bottom Temperature

/e1/hrfo0010/HYDRORUNS/CARP0001/PLOTS/TANDS/temp32_35hlp

DATE: 8/02/2004 TIME: 12:28:12

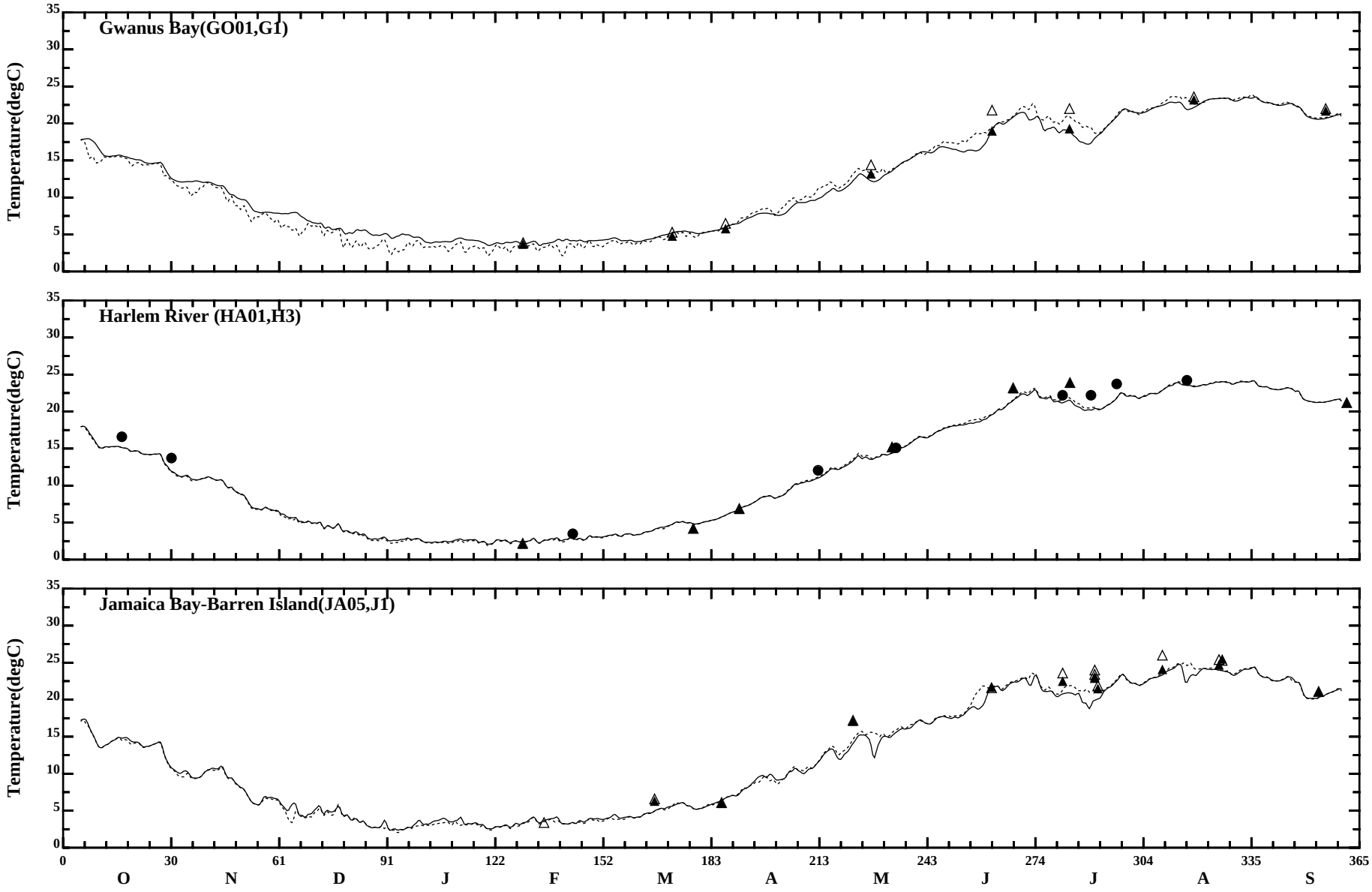

Comparison of 35 Hour Lowpass Surface and Bottom Temperature

/e1/hrfo0010/HYDRORUNS/CARP0001/PLOTS/TANDS/temp32_35hlp

DATE: 8/02/2004 TIME: 12:28:12

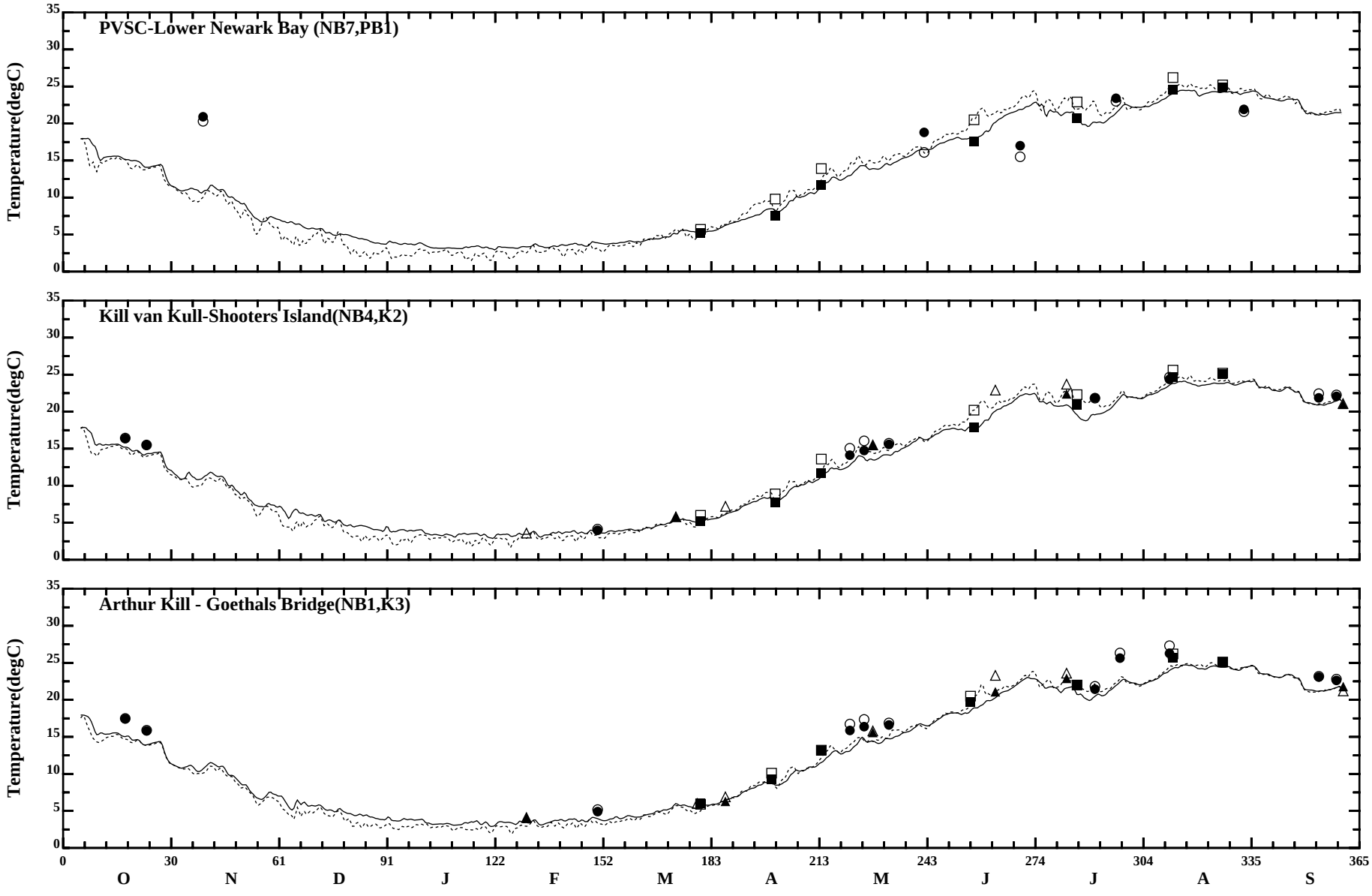

Comparison of 35 Hour Lowpass Surface and Bottom Temperature

/e1/hrfo0010/HYDRORUNS/CARP0001/PLOTS/TANDS/temp32_35hlp

DATE: 8/02/2004 TIME: 12:28:12

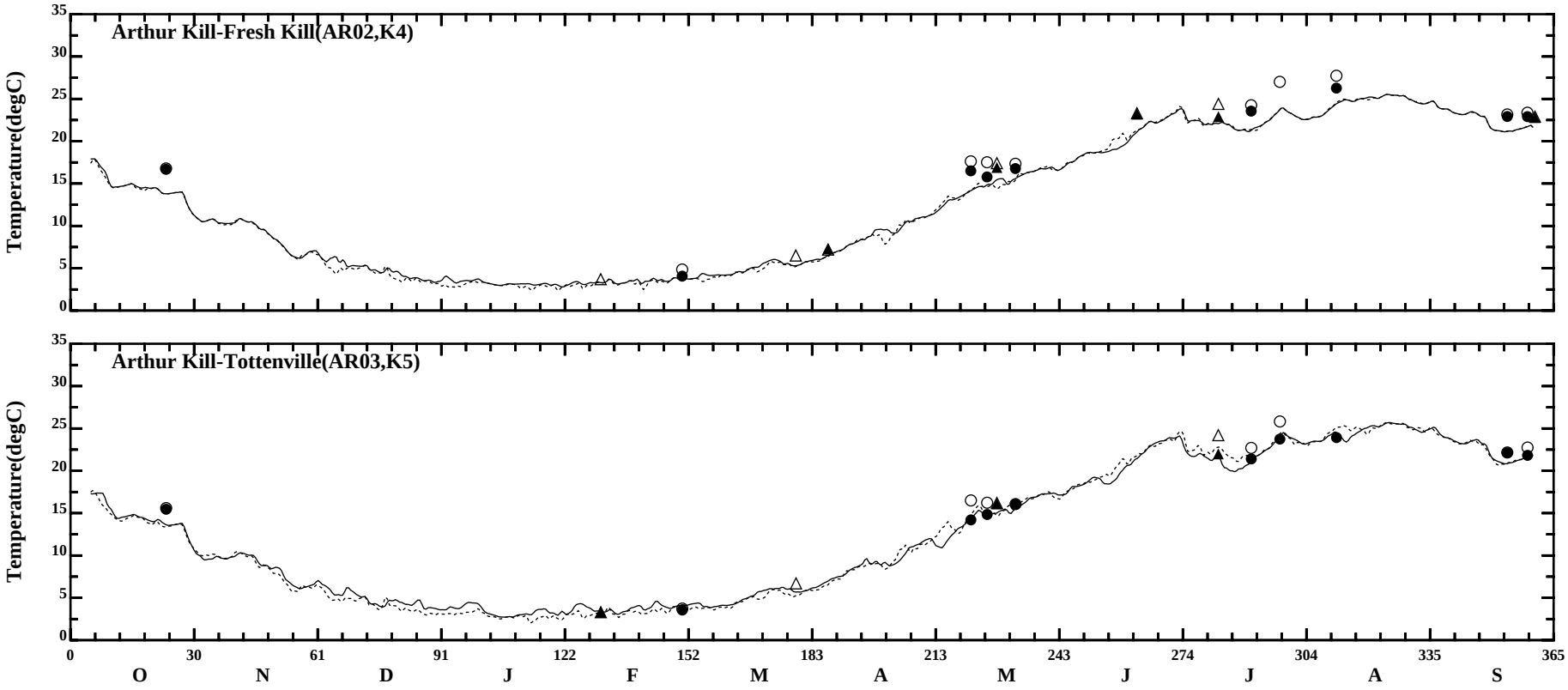

Comparison of 35 Hour Lowpass Surface and Bottom Temperature

/e1/hrfo0010/HYDRORUNS/CARP0001/PLOTS/TANDS/temp32_35hlp

DATE: 8/02/2004 TIME: 12:28:12

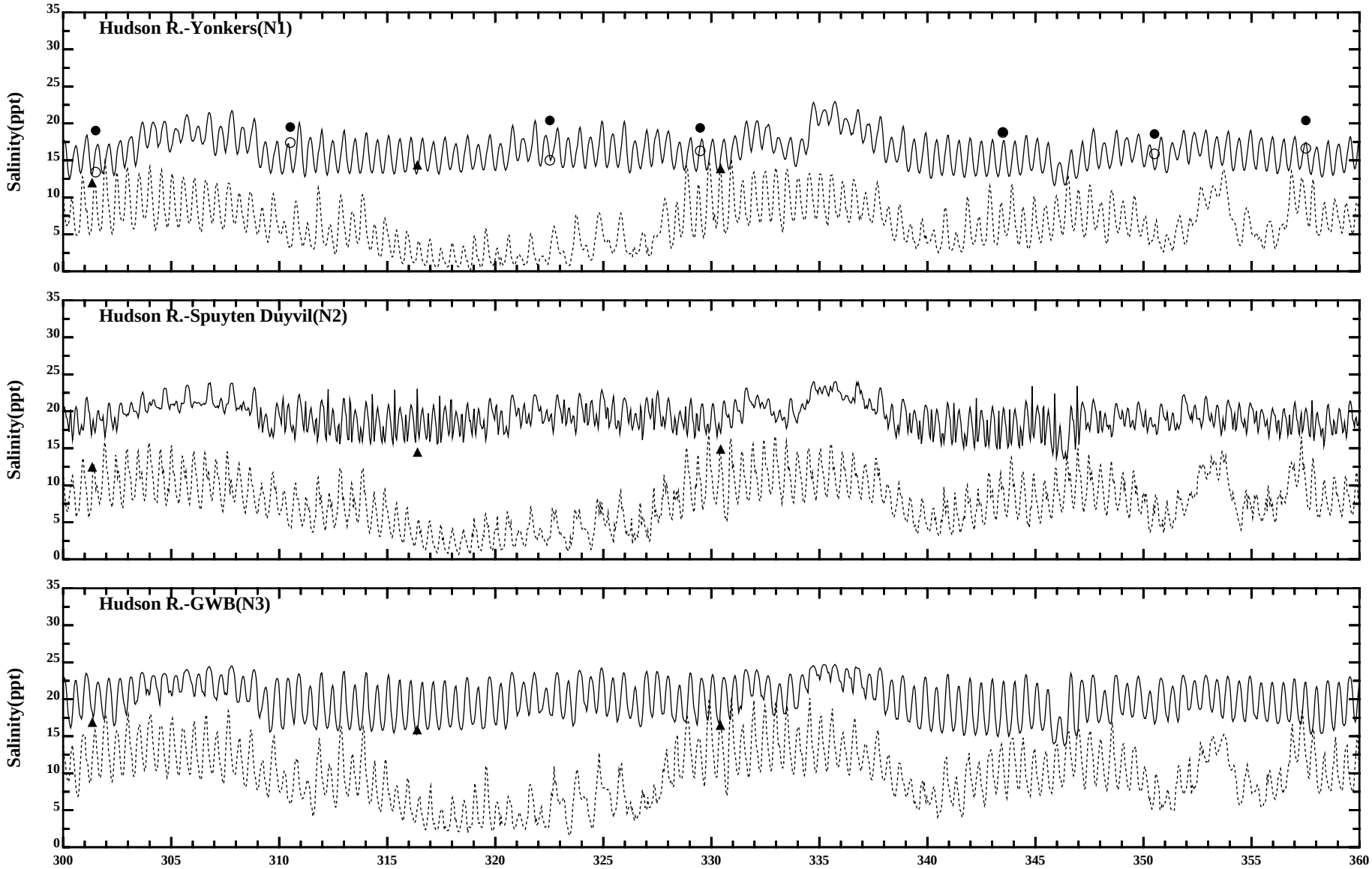

Comparison of Instantaneous Surface and Bottom Salinity

//ont6/hrfo0010/RUNS/ECOMSED-SED/ECOMSED-0102/PLOTS/TANDS/salt31

DATE: 8/02/2004 TIME: 13:43:45

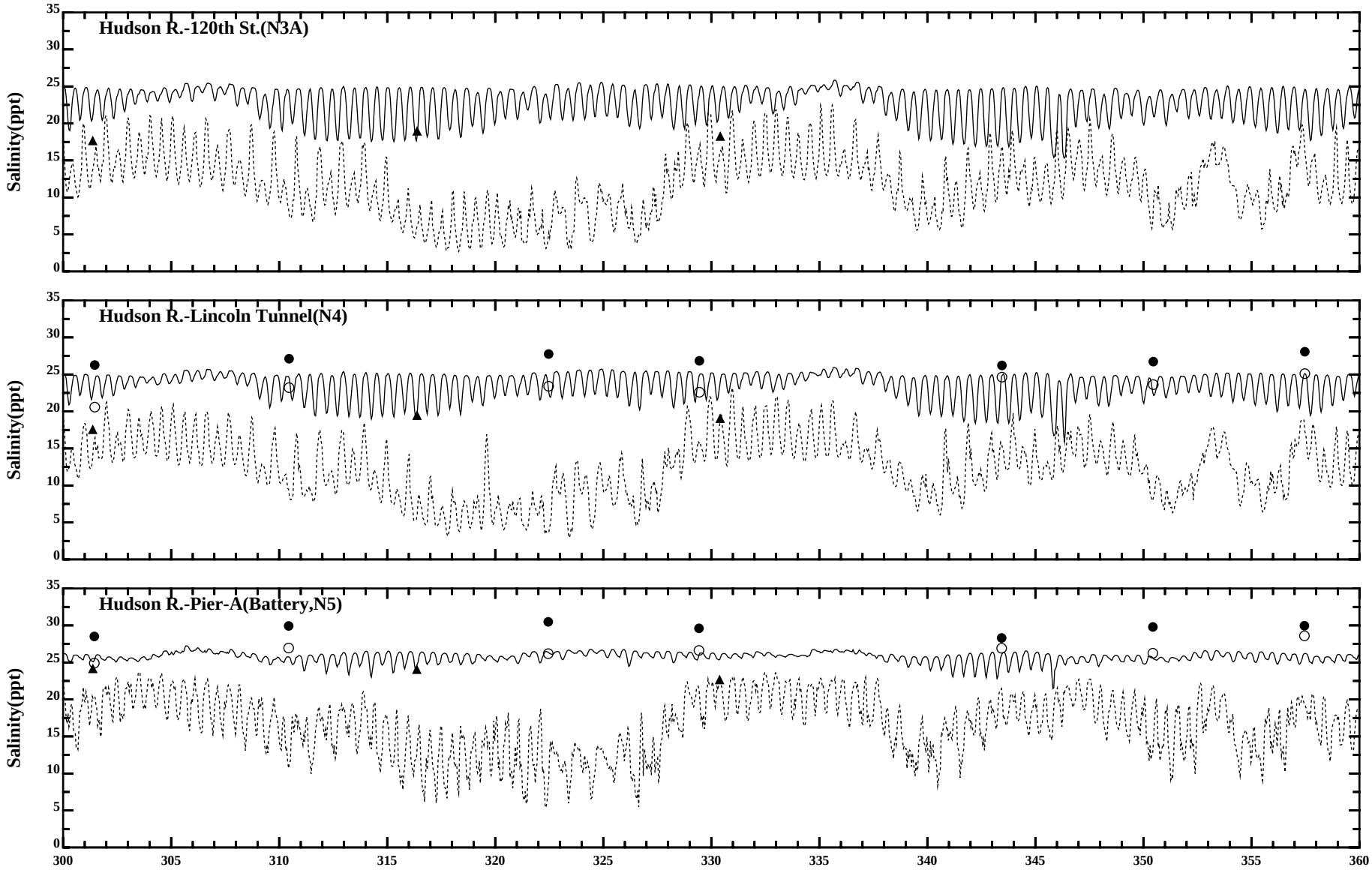

Comparison of Instantaneous Surface and Bottom Salinity

//ont6/hrfo0010/RUNS/ECOMSED-SED/ECOMSED-0102/PLOTS/TANDS/salt31

DATE: 8/02/2004 TIME: 13:43:45

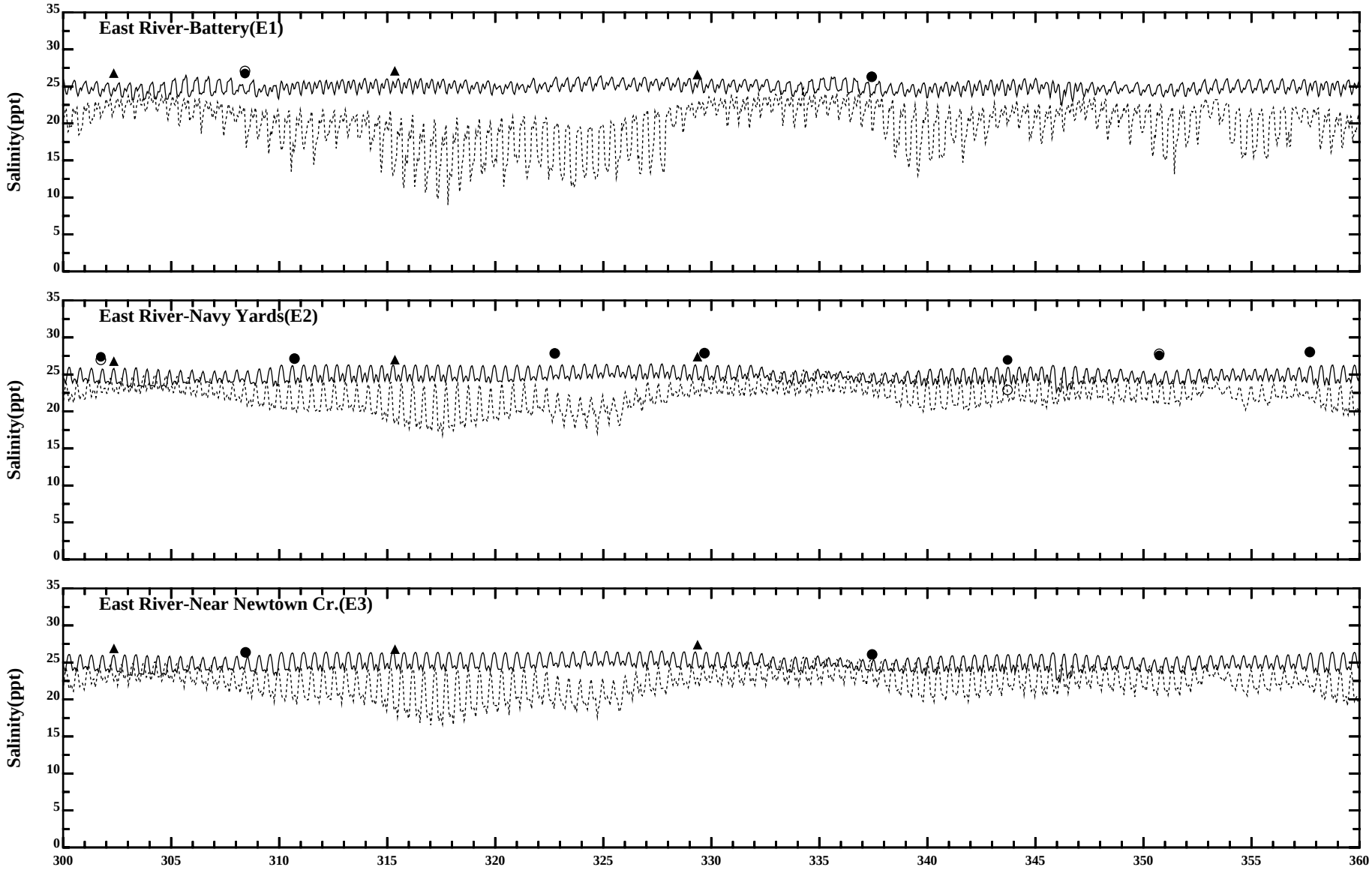

Comparison of Instantaneous Surface and Bottom Salinity

//ont6/hrfo0010/RUNS/ECOMSED-SED/ECOMSED-0102/PLOTS/TANDS/salt31

DATE: 8/02/2004 TIME: 13:43:45

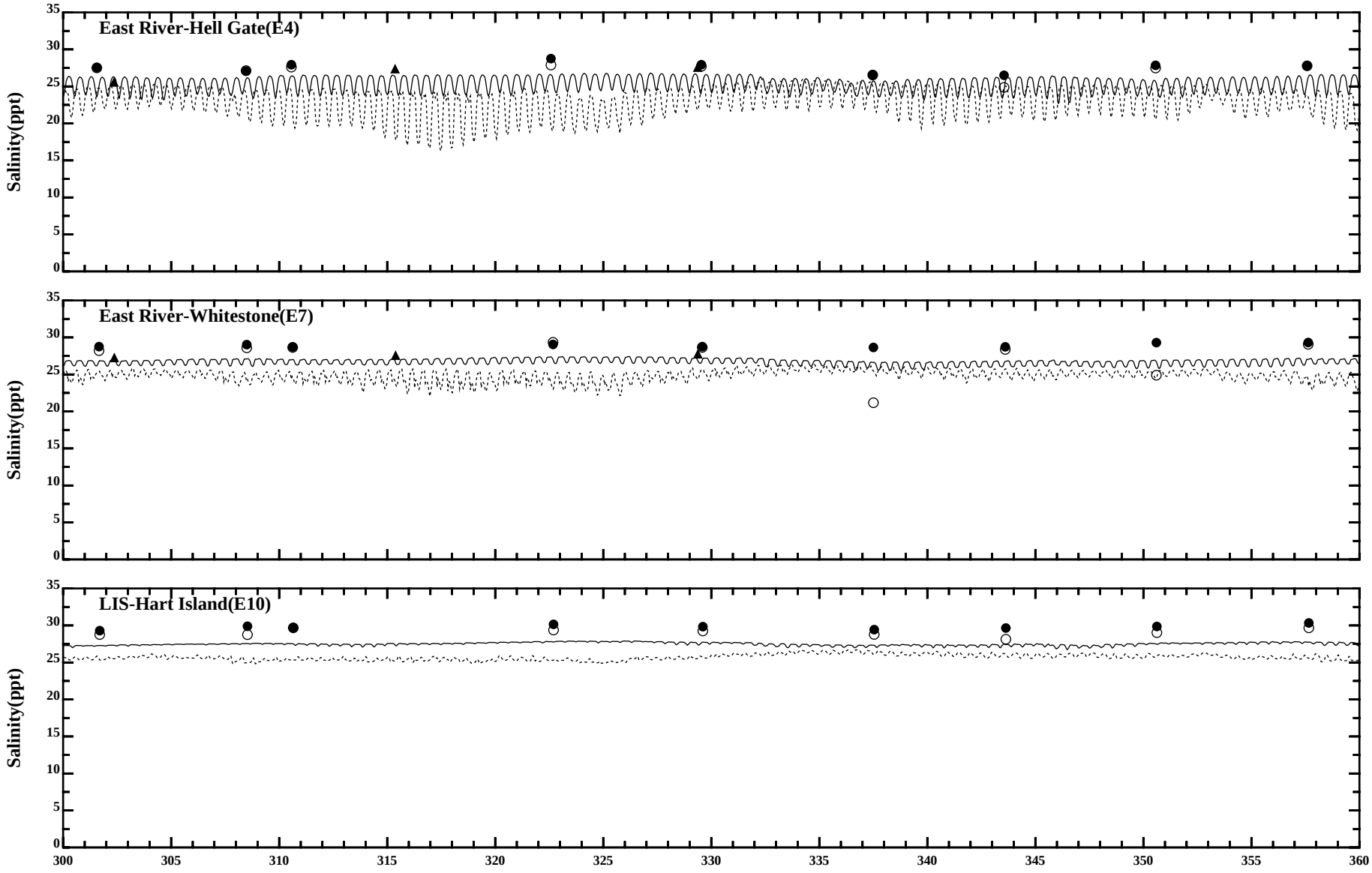

Comparison of Instantaneous Surface and Bottom Salinity

//ont6/hrfo0010/RUNS/ECOMSED-SED/ECOMSED-0102/PLOTS/TANDS/salt31

DATE: 8/02/2004 TIME: 13:43:45

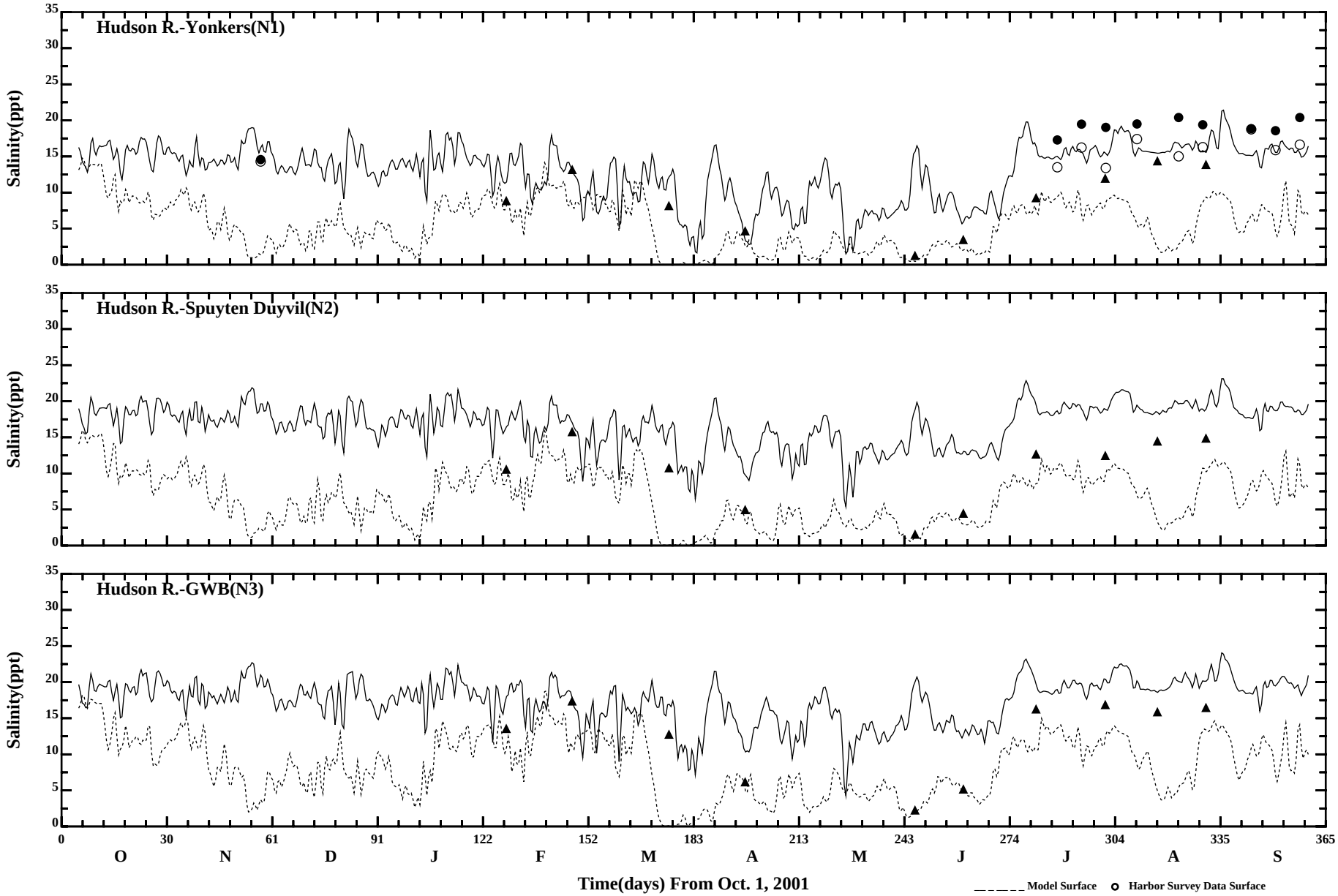

Comparison of 35 Hour Lowpass Surface and Bottom Salinity

//ont6/hrfo0010/RUNS/ECOMSED-SED/ECOMSED-0102/PLOTS/TANDS/salt31_35hlp

DATE: 8/02/2004 TIME: 13:45:38

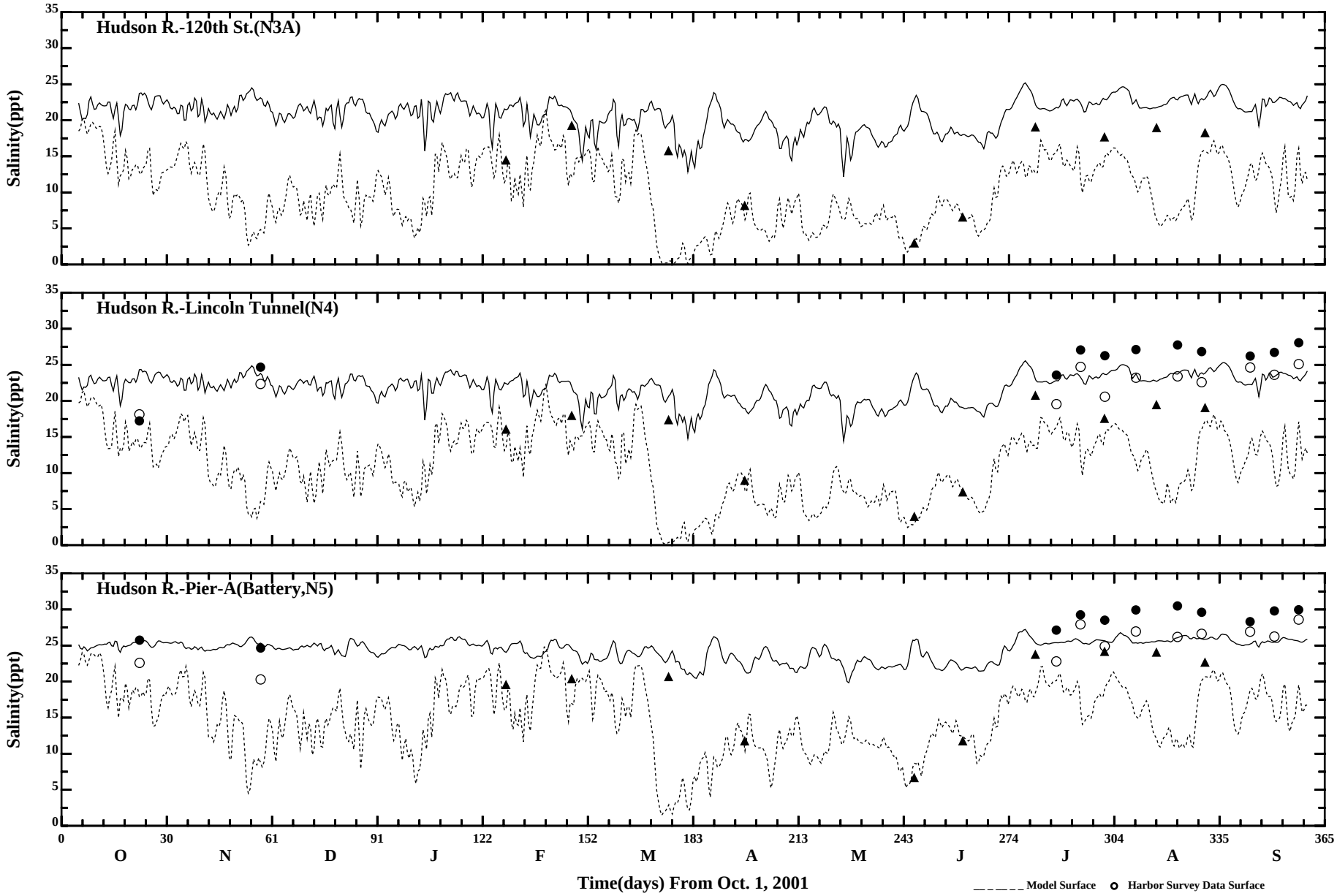

Comparison of 35 Hour Lowpass Surface and Bottom Salinity

//ont6/hrfo0010/RUNS/ECOMSED-SED/ECOMSED-0102/PLOTS/TANDS/salt31_35hlp

DATE: 8/02/2004 TIME: 13:45:38

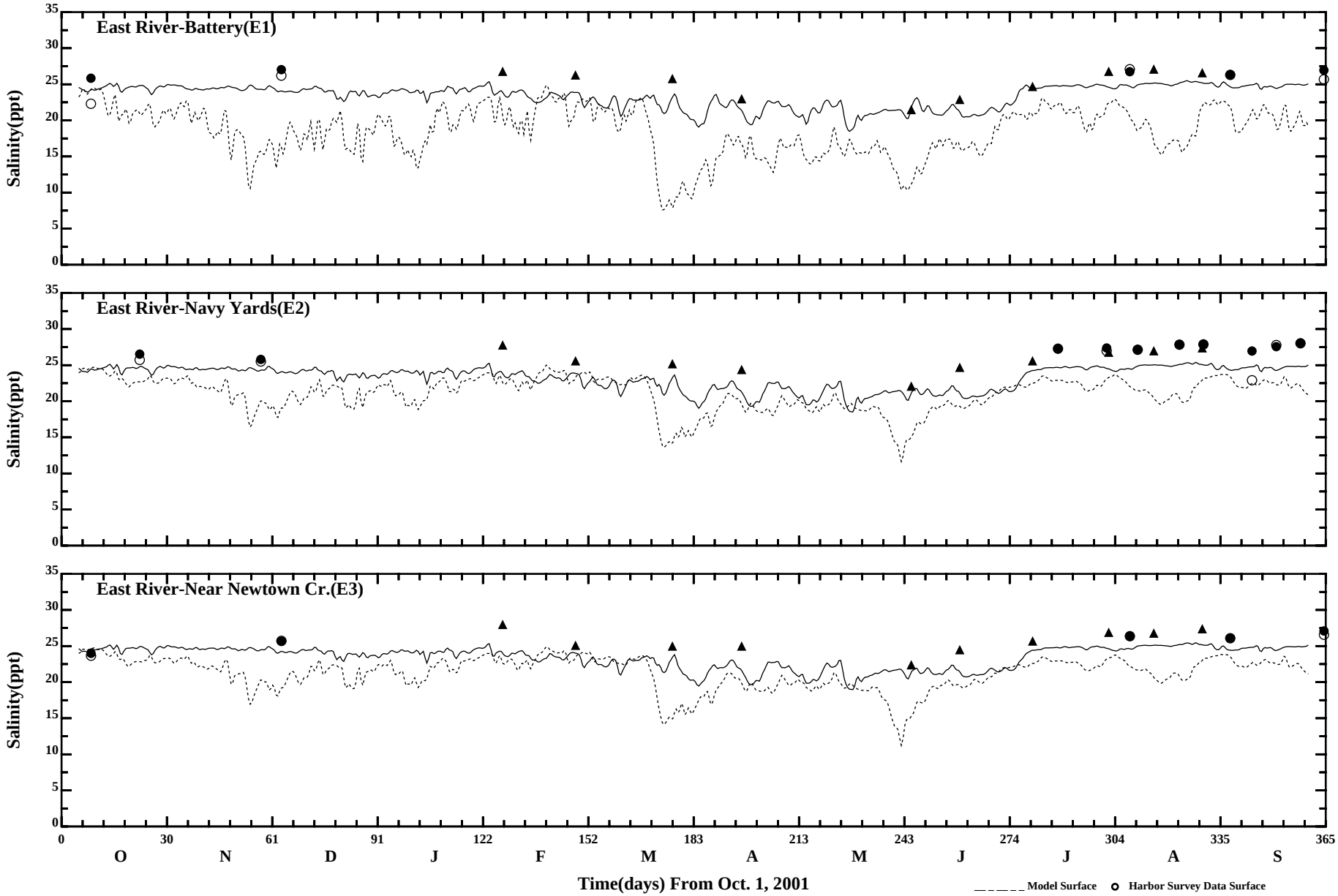

Comparison of 35 Hour Lowpass Surface and Bottom Salinity

//ont6/hrfo0010/RUNS/ECOMSED-SED/ECOMSED-0102/PLOTS/TANDS/salt31_35hlp

DATE: 8/02/2004 TIME: 13:45:38

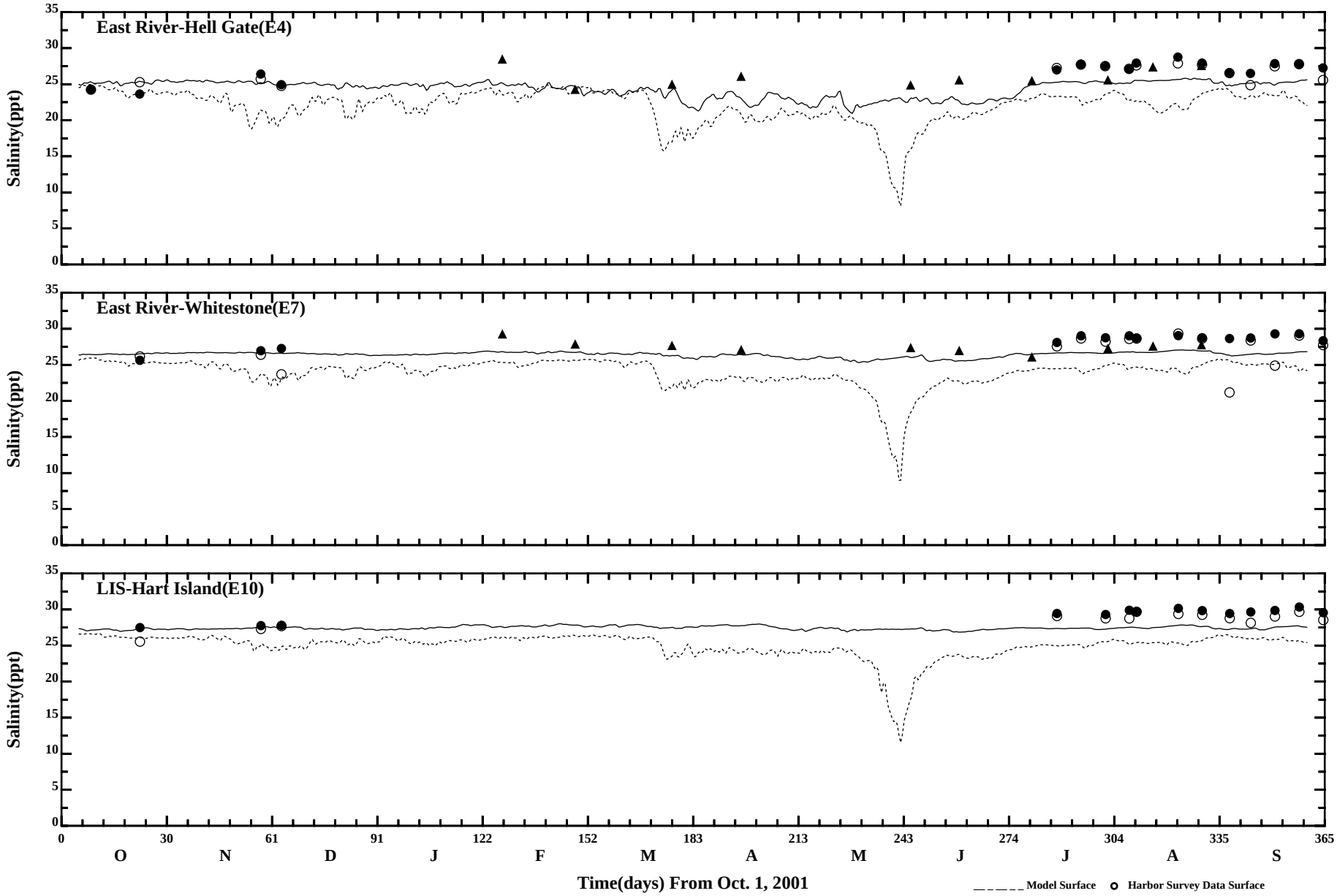

Comparison of 35 Hour Lowpass Surface and Bottom Salinity

//ont6/hrfo0010/RUNS/ECOMSED-SED/ECOMSED-0102/PLOTS/TANDS/salt31_35hlp

DATE: 8/02/2004 TIME: 13:45:38

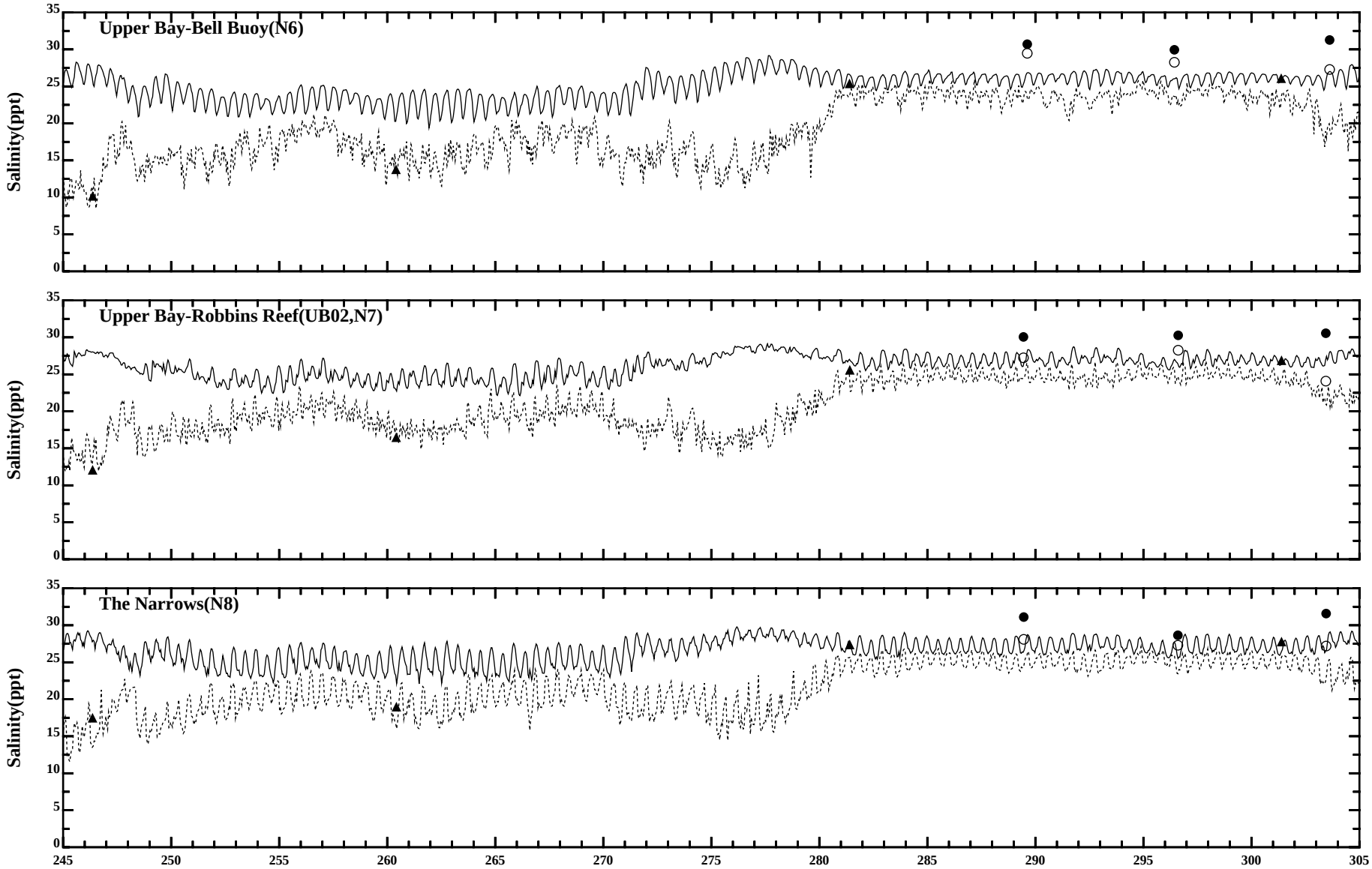

Comparison of Instantaneous Surface and Bottom Salinity

/ont6/hrfo0010/HYDRORUNS/CARP01-02/PLOTS/TANDS/salt32

DATE: 11/24/2003 TIME: 11:14:32

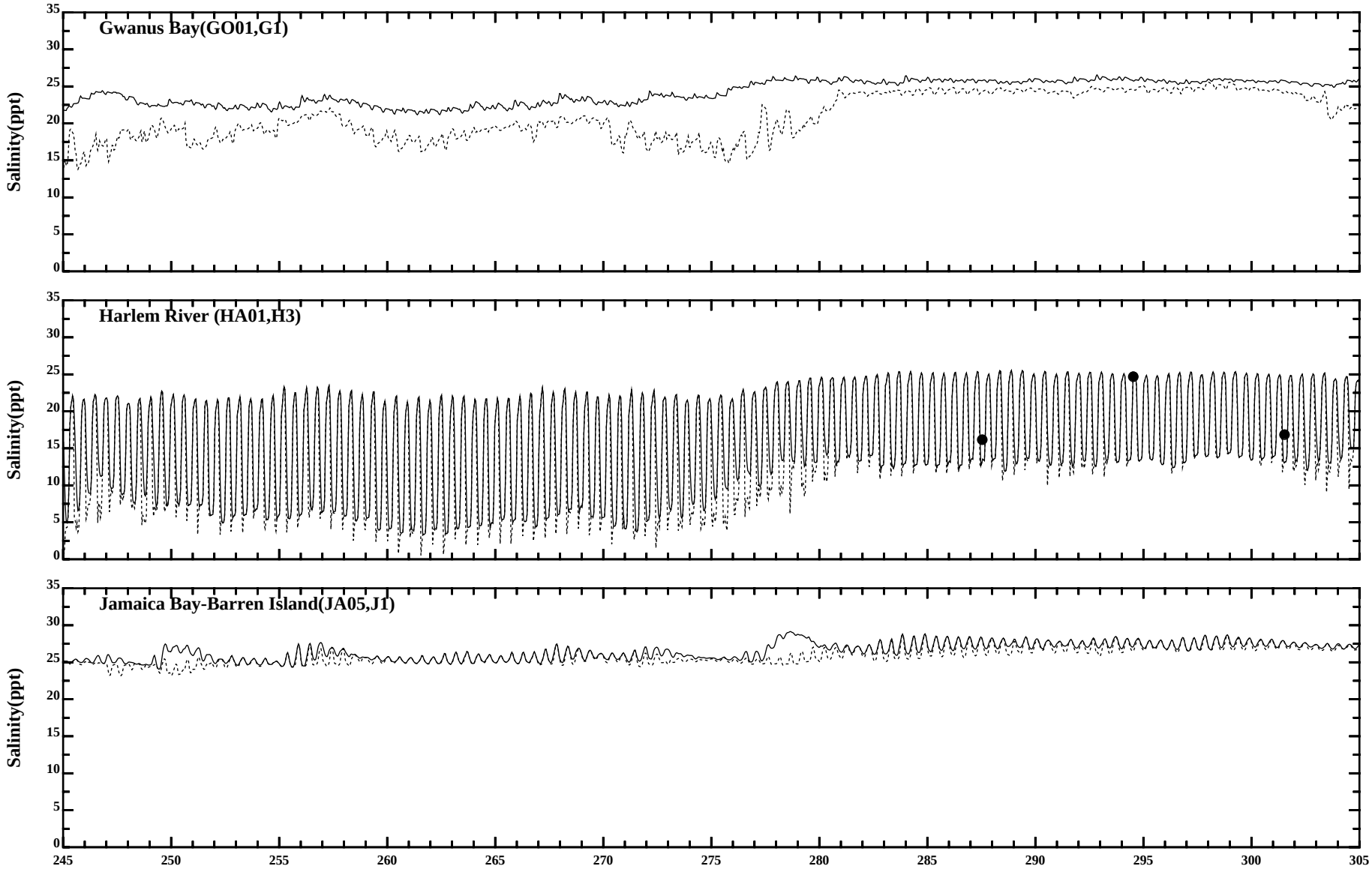

Comparison of Instantaneous Surface and Bottom Salinity

/ont6/hrfo0010/HYDRORUNS/CARP01-02/PLOTS/TANDS/salt32

_ _ _ _ _ Model Surface

_____ Model Bottom

○ Harbor Survey Data Surface

● Harbor Survey Data Bottom

▲ IEC Data at 3 meters Depth

□ US ARMY CORPS. OF ENGRS Data Surface

■ US ARMY CORPS. OF ENGRS Data Bottom

DATE: 11/24/2003 TIME: 11:14:32

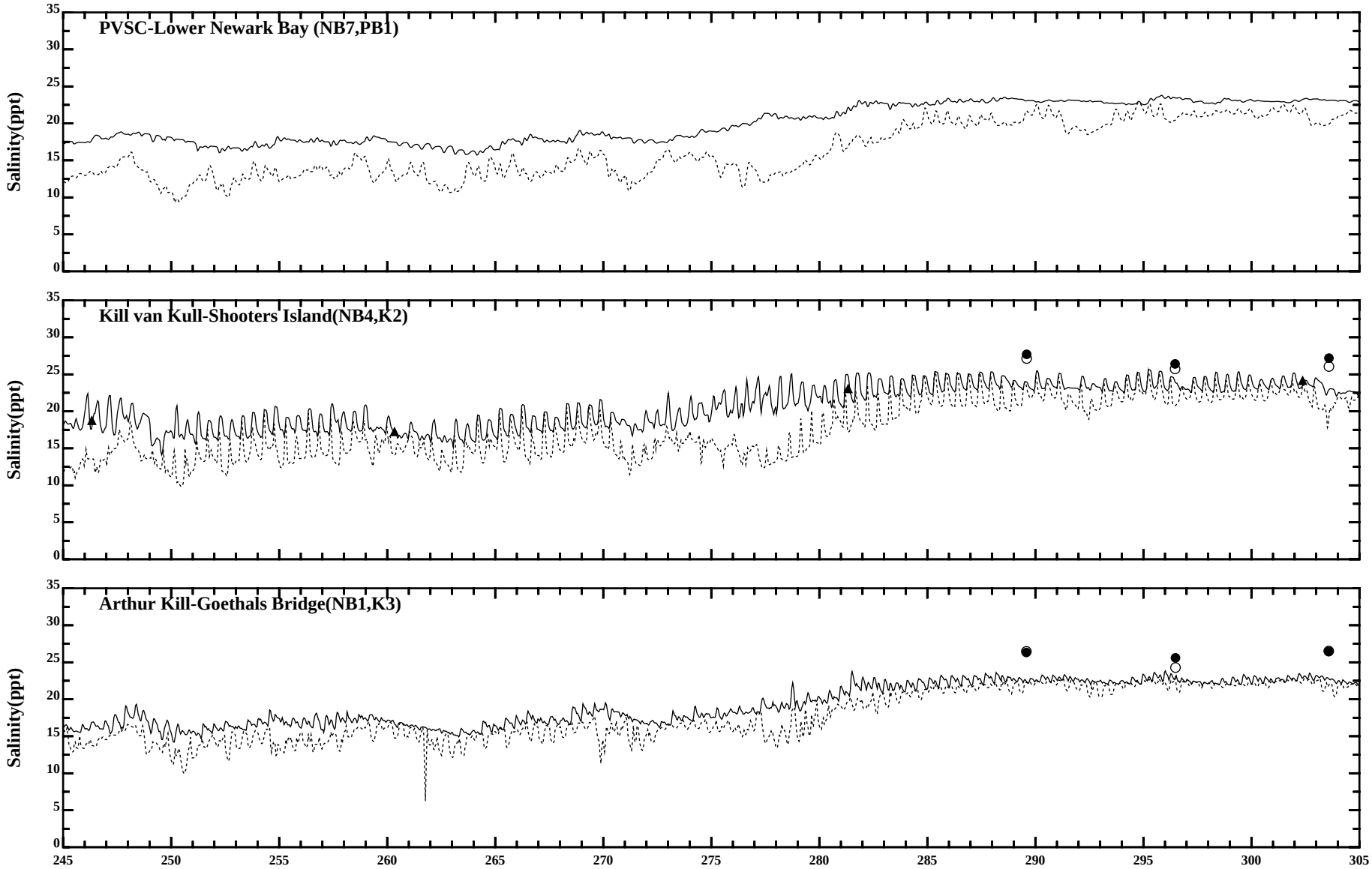

Comparison of Instantaneous Surface and Bottom Salinity

/ont6/hrfo0010/HYDRORUNS/CARP01-02/PLOTS/TANDS/salt32

DATE: 11/24/2003 TIME: 11:14:32

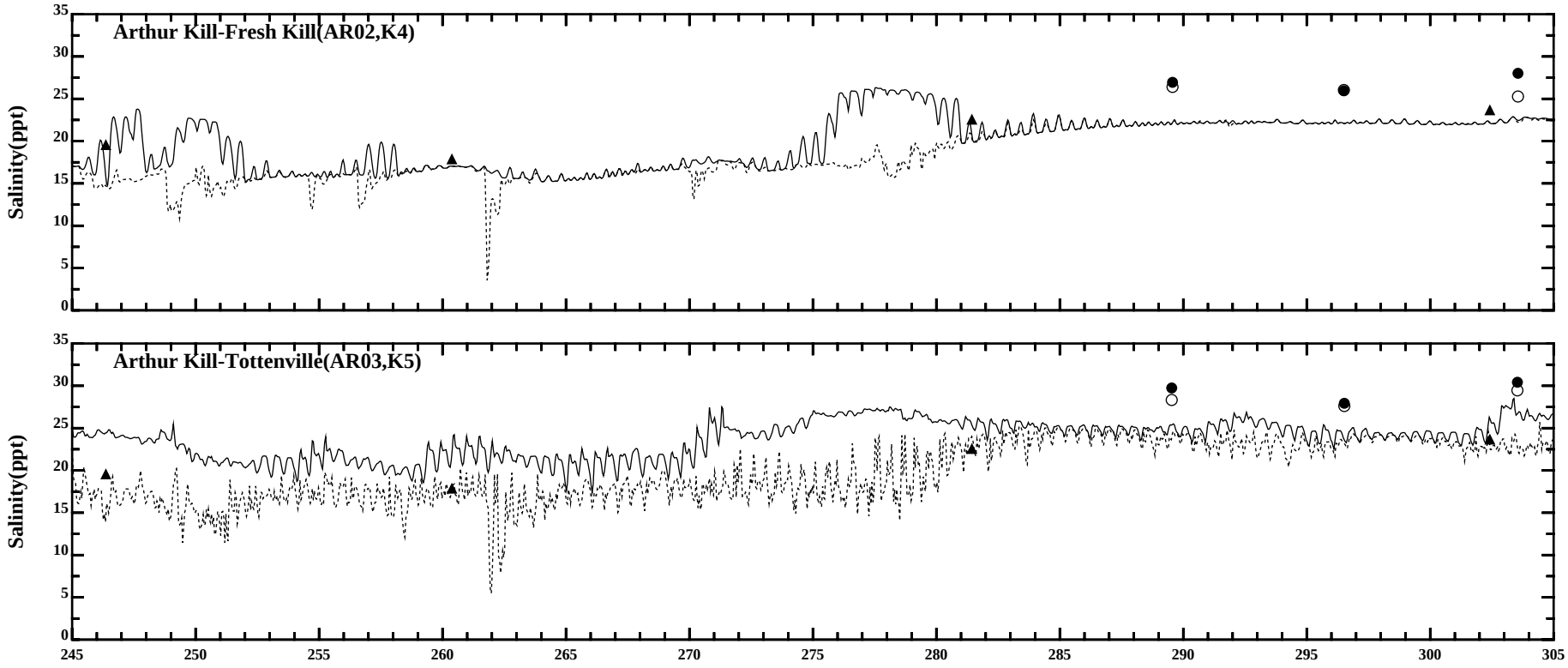

Comparison of Instantaneous Surface and Bottom Salinity

/ont6/hrfo0010/HYDRORUNS/CARP01-02/PLOTS/TANDS/salt32

DATE: 11/24/2003 TIME: 11:14:32

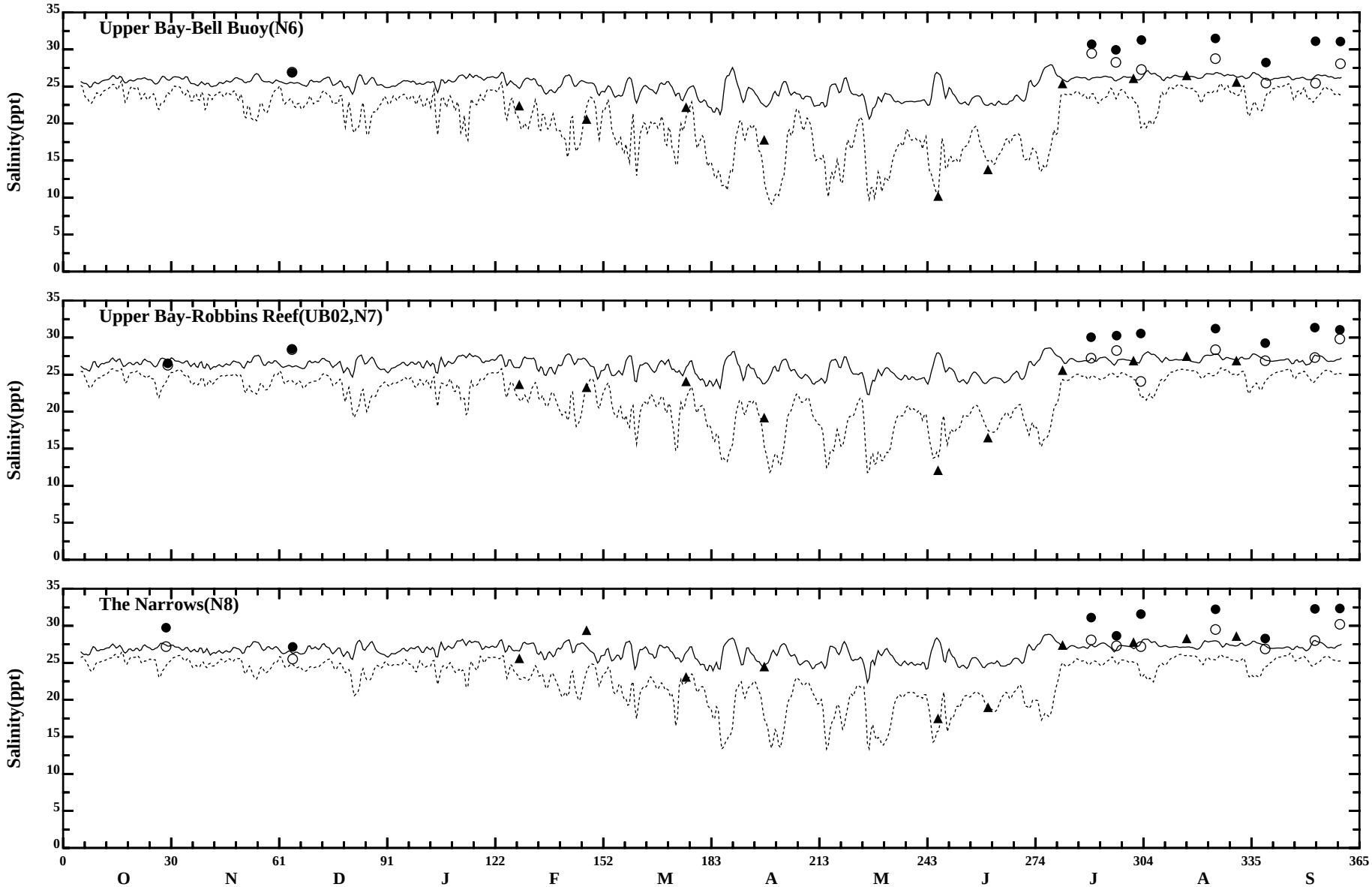

Comparison of 35 Hour Lowpass Surface and Bottom Salinity

/ont6/hrfo0010/HYDRORUNS/CARP01-02/PLOTS/TANDS/salt32_35hlp

DATE: 11/24/2003 TIME: 11:14:24

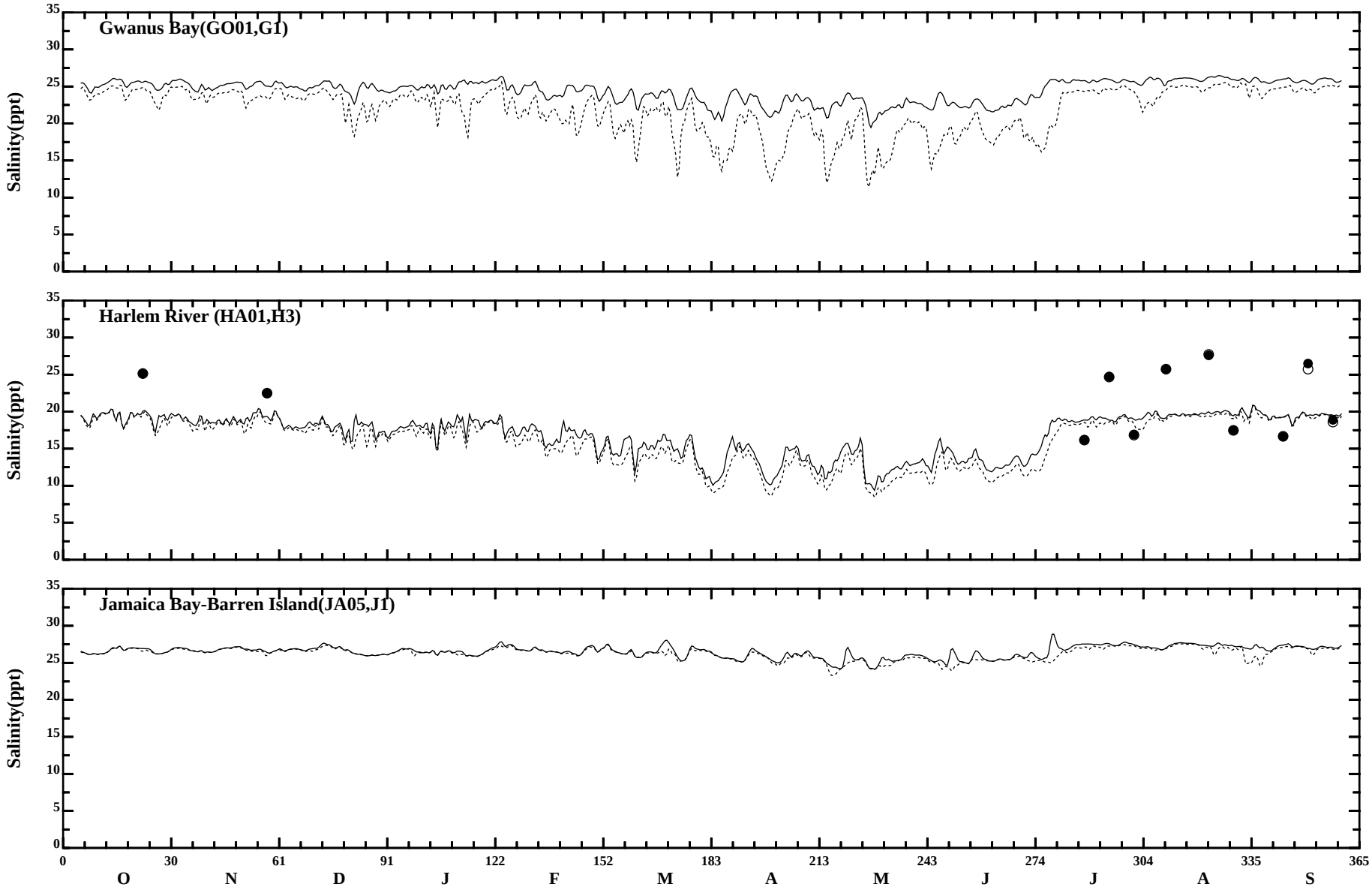

Comparison of 35 Hour Lowpass Surface and Bottom Salinity

/ont6/hrfo0010/HYDRORUNS/CARP01-02/PLOTS/TANDS/salt32_35hlp

DATE: 11/24/2003 TIME: 11:14:24

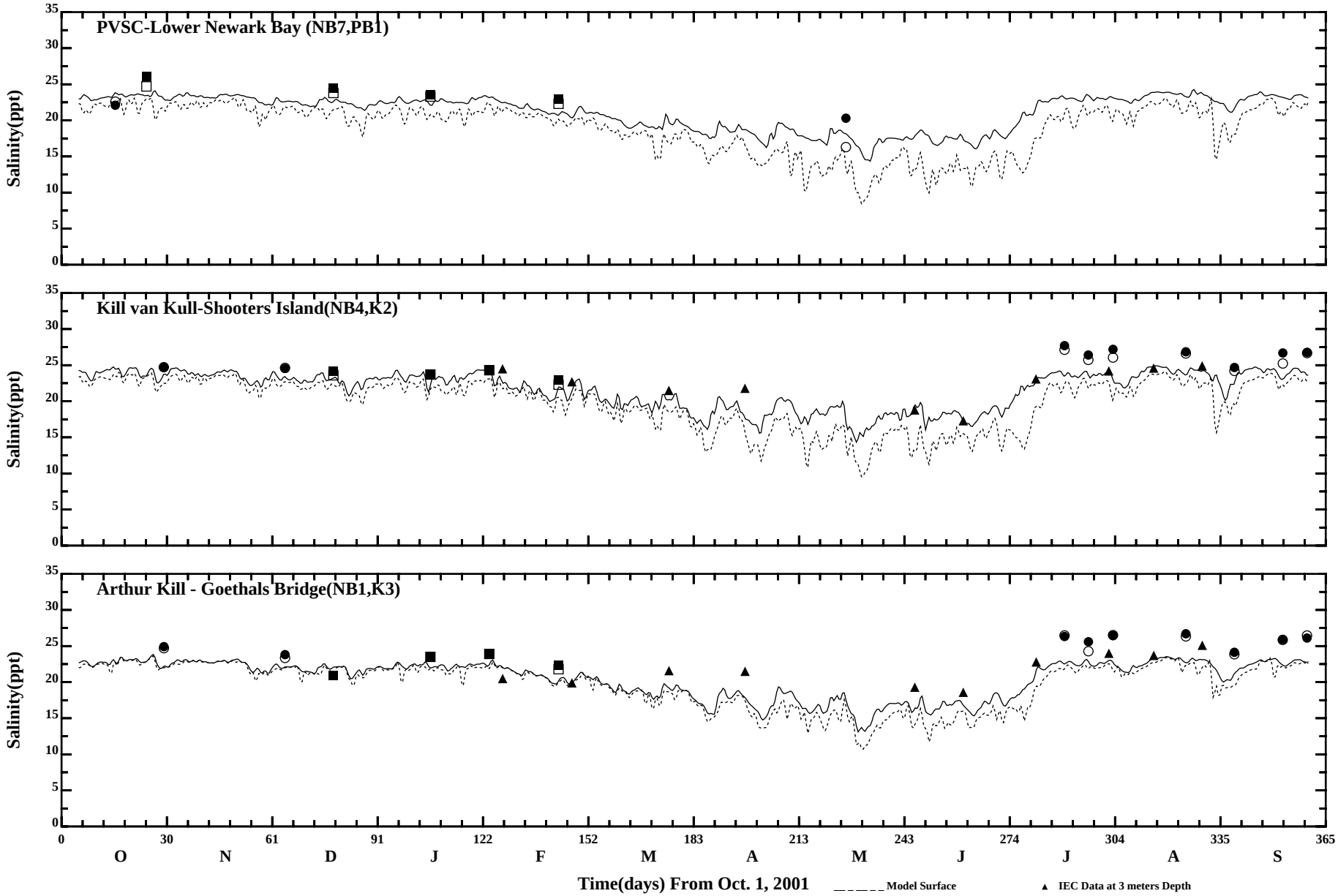

Comparison of 35 Hour Lowpass Surface and Bottom Salinity

/ont6/hrfo0010/HYDRORUNS/CARP01-02/PLOTS/TANDS/salt32_35hlp

DATE: 11/24/2003 TIME: 11:14:24

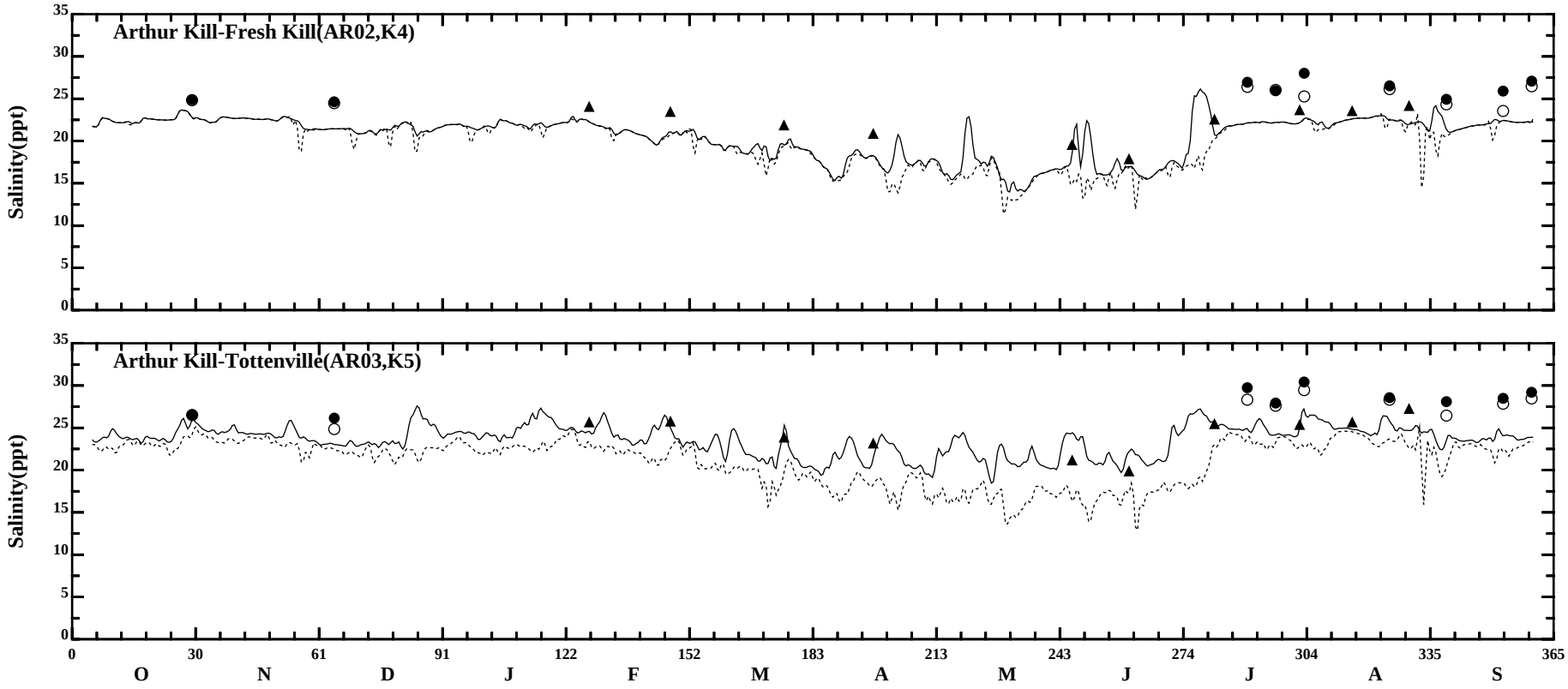

Comparison of 35 Hour Lowpass Surface and Bottom Salinity

/ont6/hrfo0010/HYDRORUNS/CARP01-02/PLOTS/TANDS/salt32_35hlp

DATE: 11/24/2003 TIME: 11:14:24

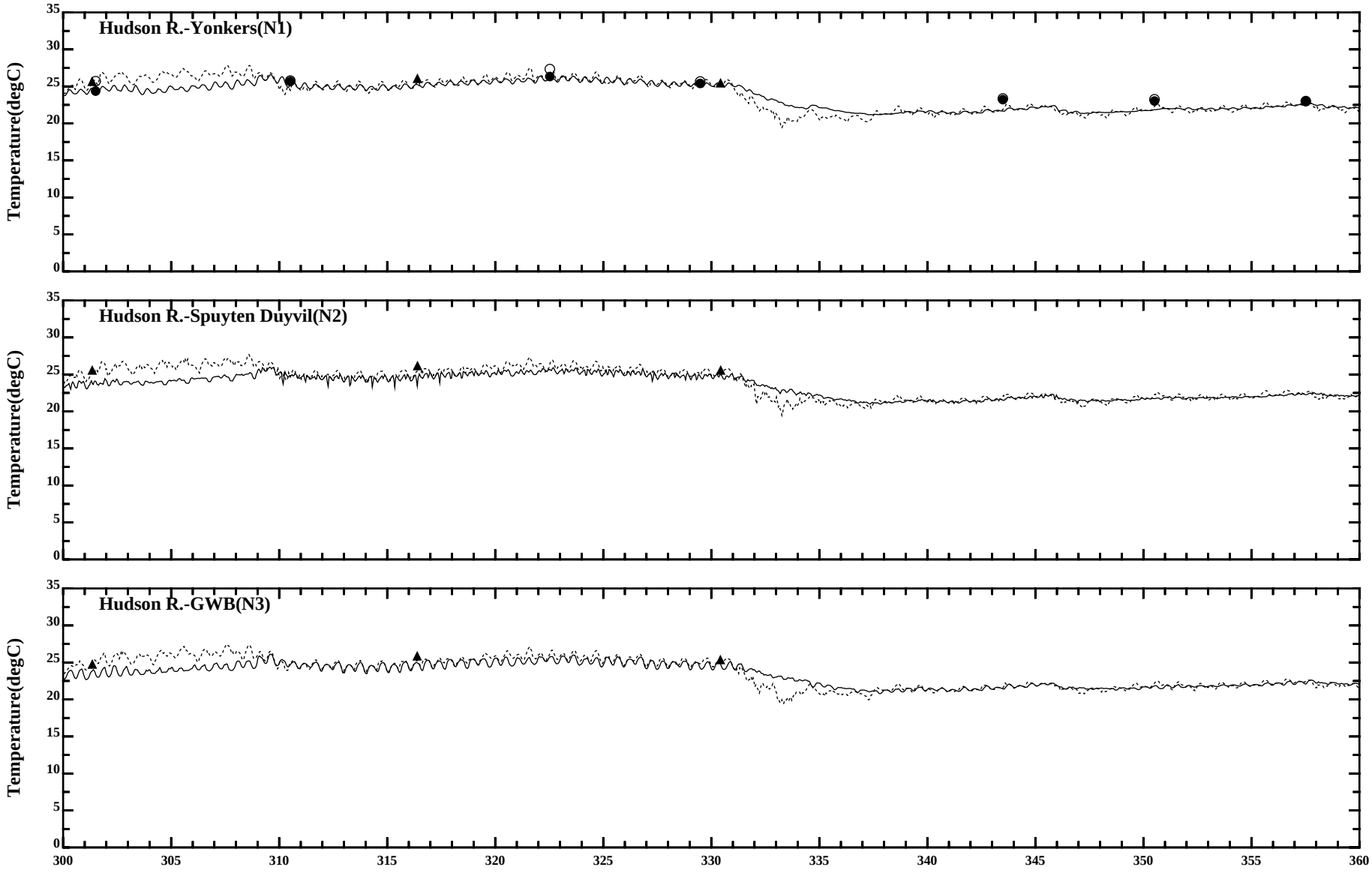

Comparison of Instantaneous Surface and Bottom Temperature

//ont6/hrfo0010/RUNS/ECOMSED-SED/ECOMSED-0102/PLOTS/TANDS/temp31

_ _ _ _ _ Model Surface

_____ Model Bottom

o Harbor Survey Data Surface

● Harbor Survey Data Bottom

▲ IEC Data at 3 meters depth

DATE: 11/24/2003 TIME: 11:28:45

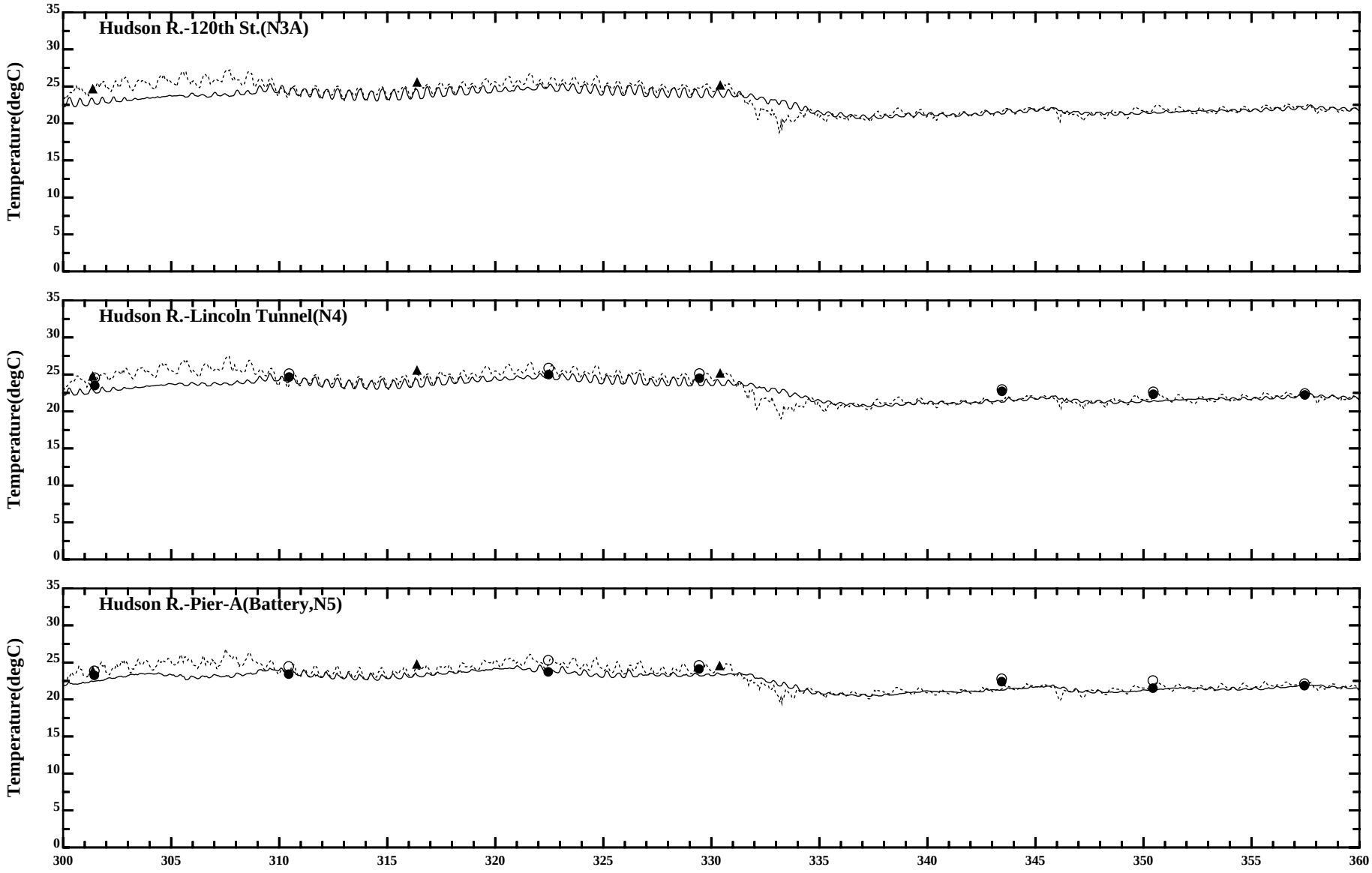

Comparison of Instantaneous Surface and Bottom Temperature

//ont6/hrfo0010/RUNS/ECOMSED-SED/ECOMSED-0102/PLOTS/TANDS/temp31

DATE: 11/24/2003 TIME: 11:28:45

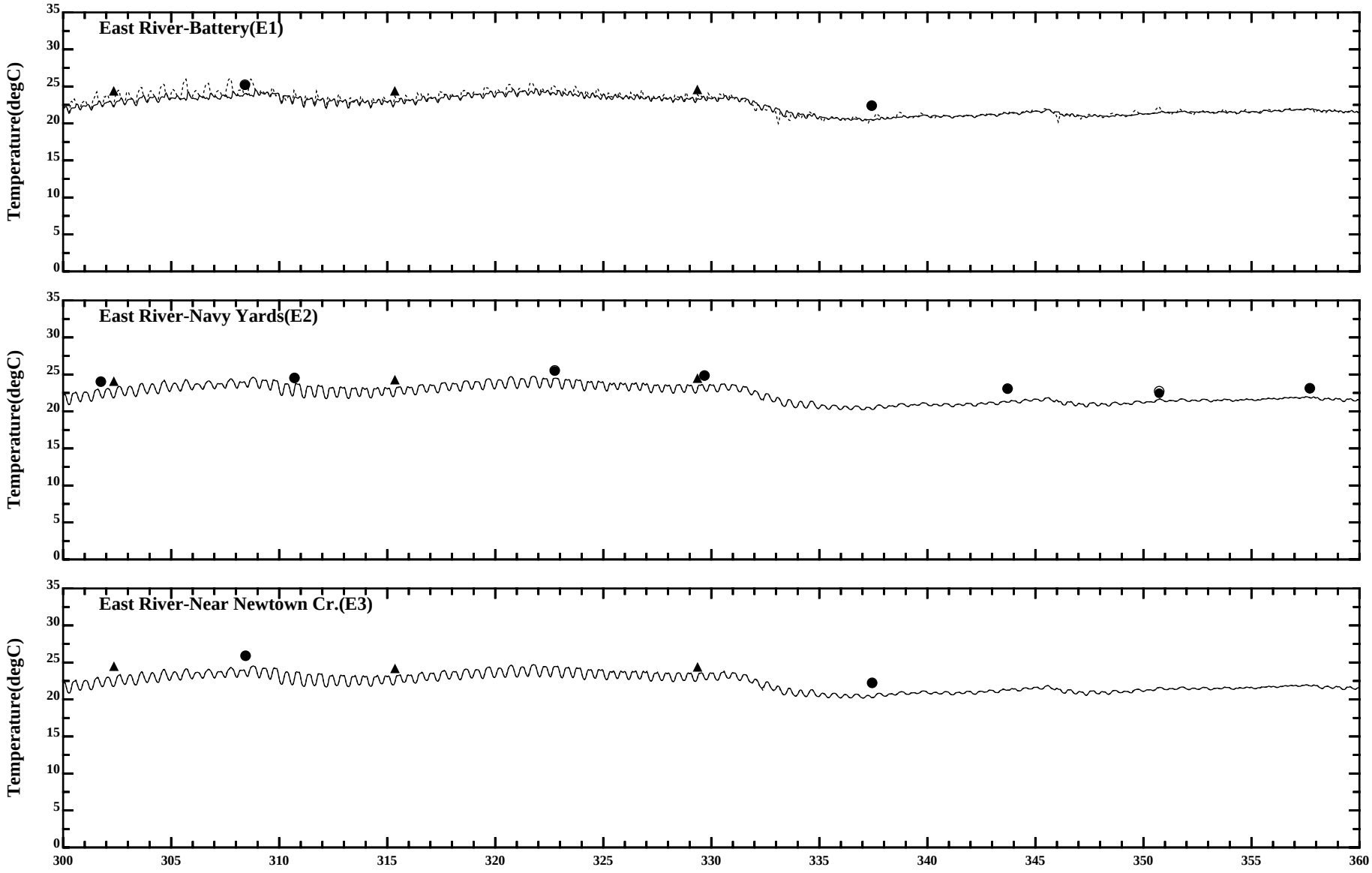

Comparison of Instantaneous Surface and Bottom Temperature

//ont6/hrfo0010/RUNS/ECOMSED-SED/ECOMSED-0102/PLOTS/TANDS/temp31

DATE: 11/24/2003 TIME: 11:28:45

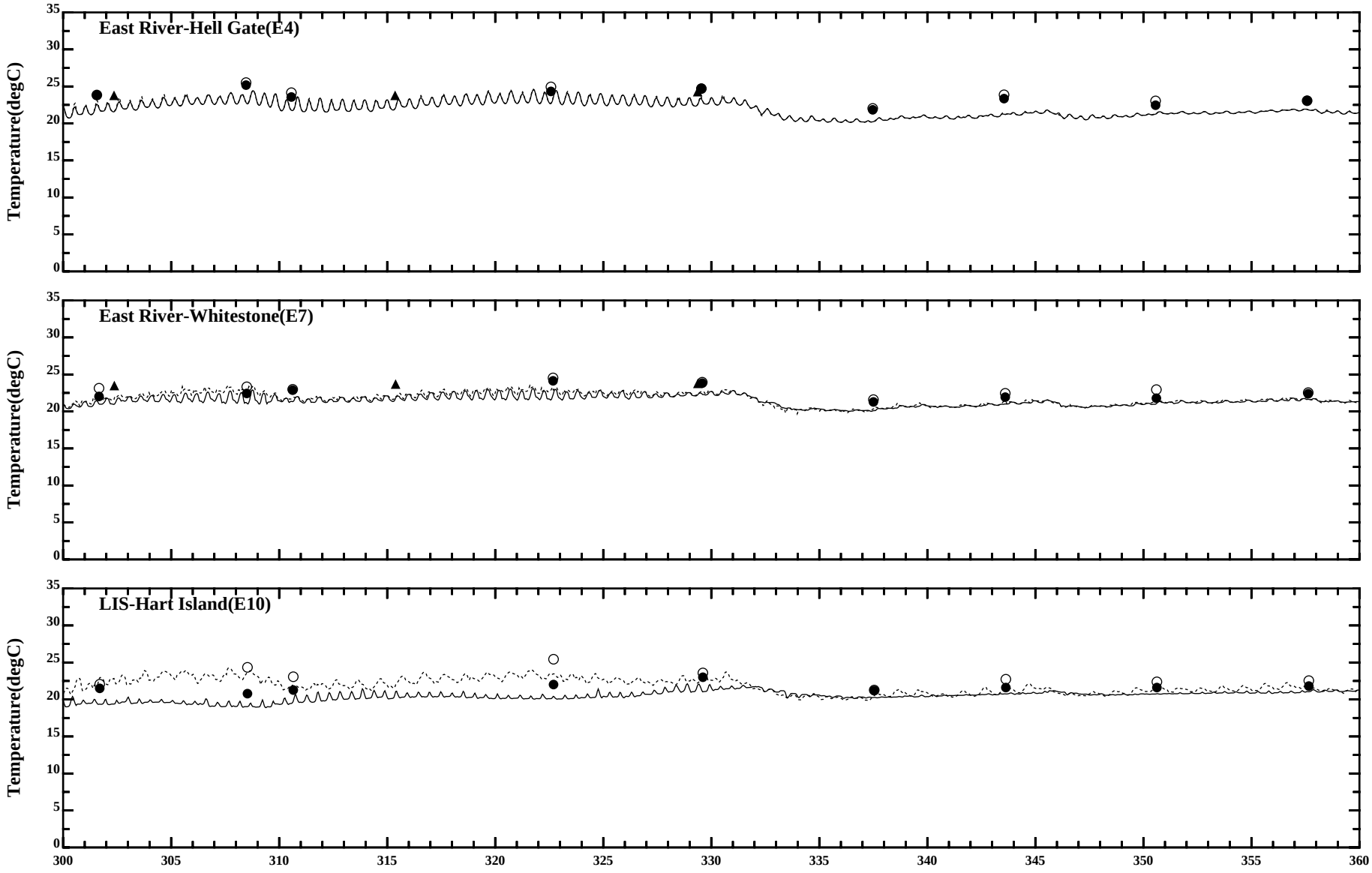

Comparison of Instantaneous Surface and Bottom Temperature

//ont6/hrfo0010/RUNS/ECOMSED-SED/ECOMSED-0102/PLOTS/TANDS/temp31

DATE: 11/24/2003 TIME: 11:28:45

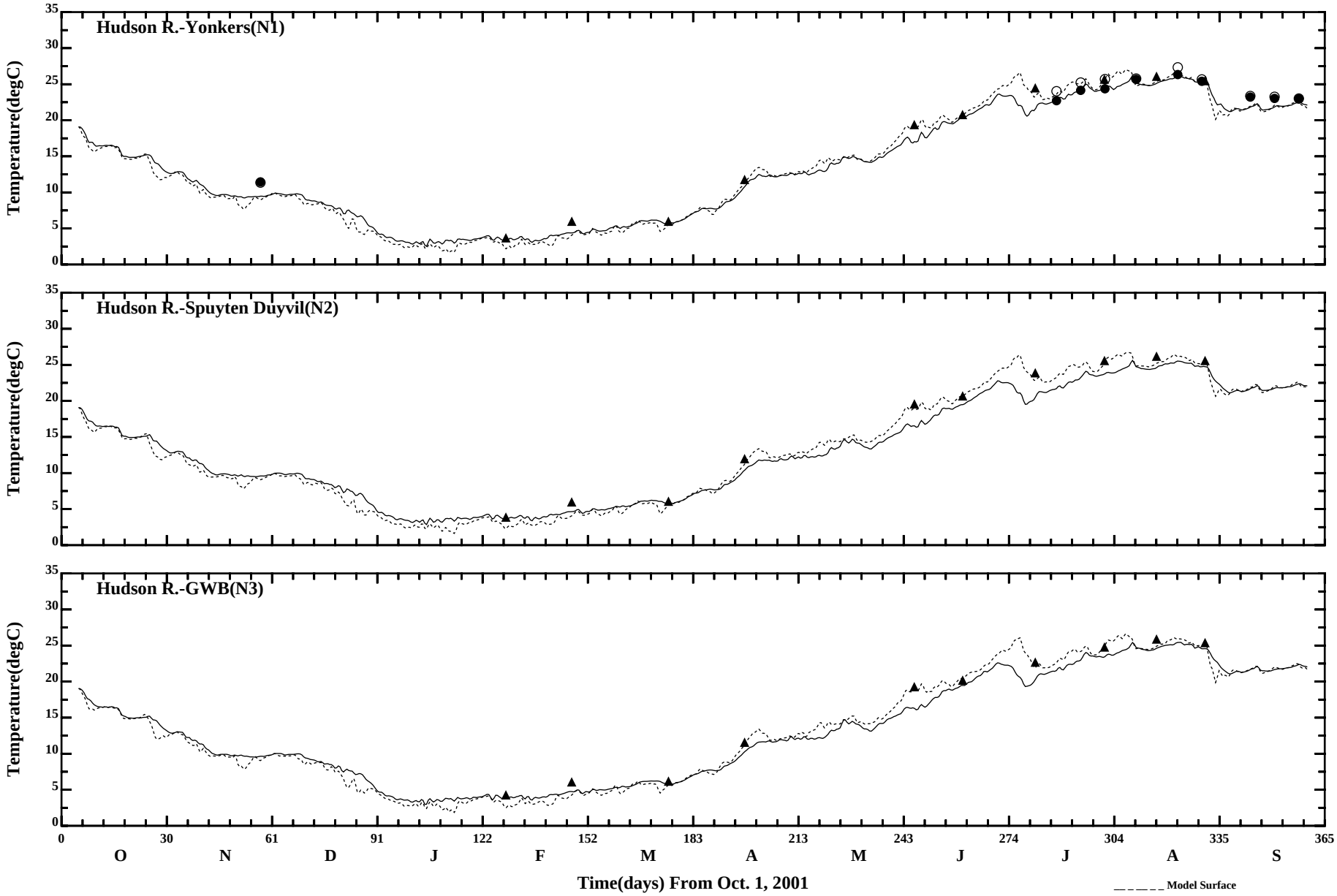

Comparison of 35 Hour Lowpass Surface and Bottom Temperature

//ont6/hrfo0010/RUNS/ECOMSED-SED/ECOMSED-0102/PLOTS/TANDS/temp31_35hlp

DATE: 11/21/2003 TIME: 10:39: 2

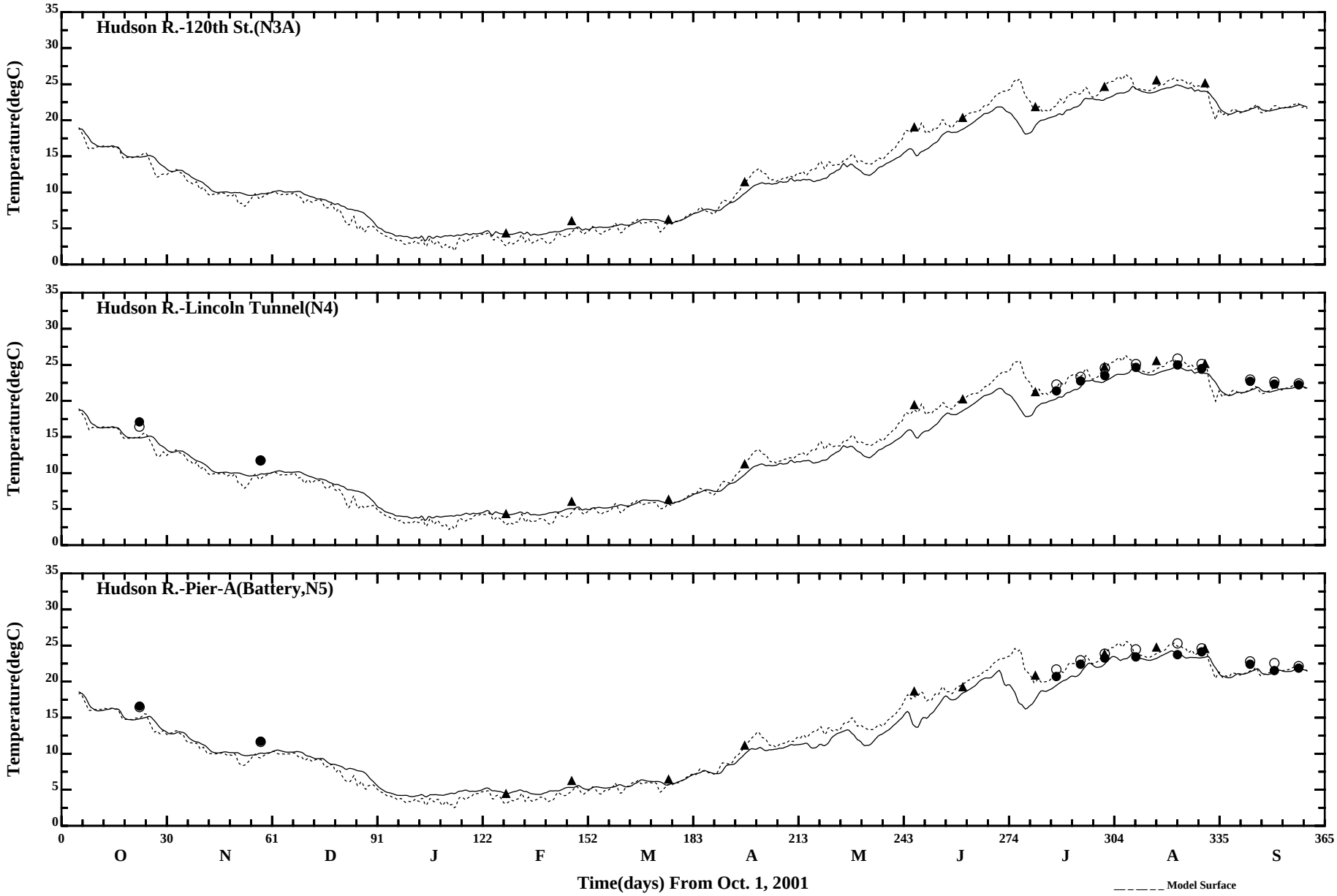

Comparison of 35 Hour Lowpass Surface and Bottom Temperature

//ont6/hrfo0010/RUNS/ECOMSED-SED/ECOMSED-0102/PLOTS/TANDS/temp31_35hlp

DATE: 11/21/2003 TIME: 10:39: 2

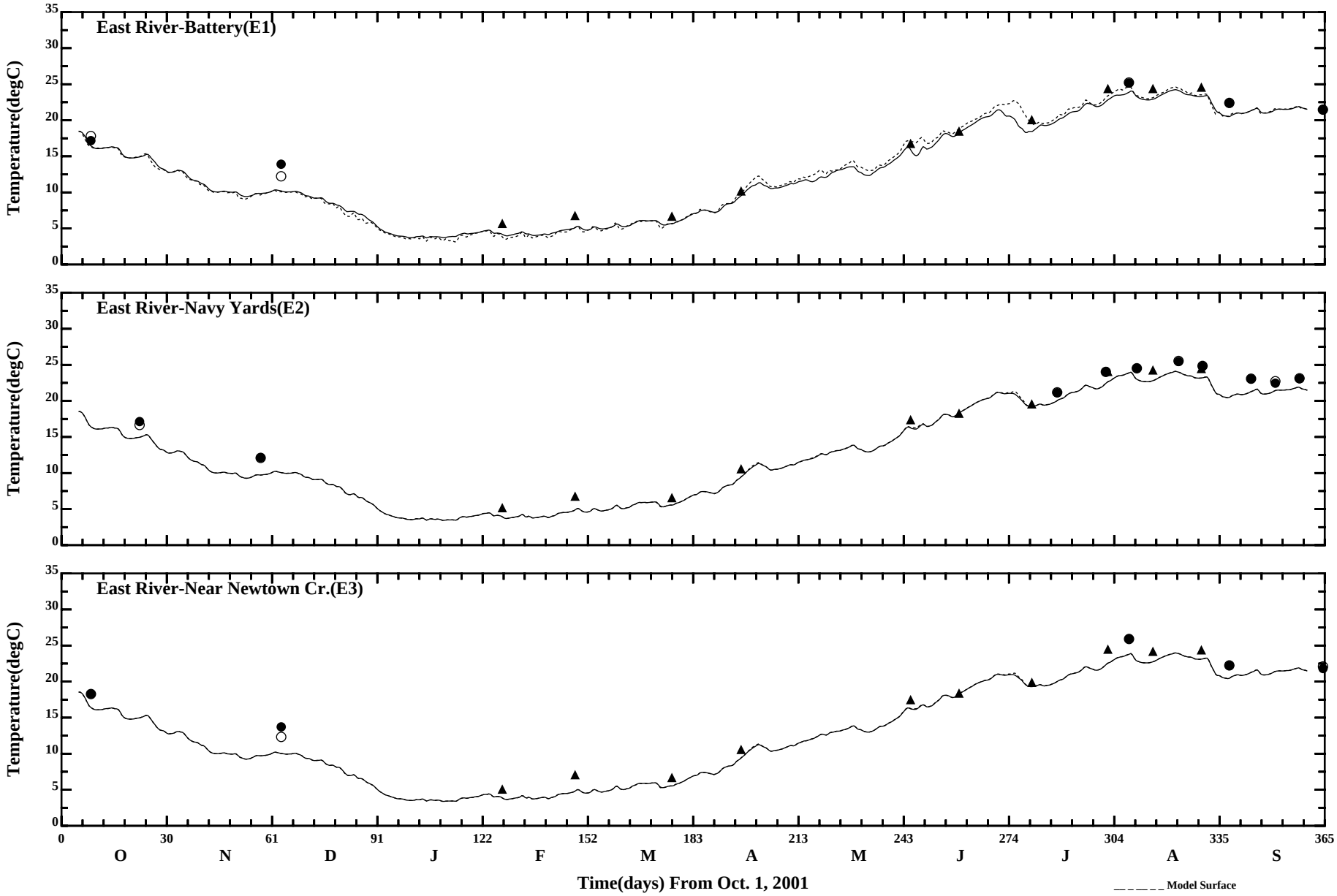

Comparison of 35 Hour Lowpass Surface and Bottom Temperature

//ont6/hrfo0010/RUNS/ECOMSED-SED/ECOMSED-0102/PLOTS/TANDS/temp31_35hlp

DATE: 11/21/2003 TIME: 10:39: 2

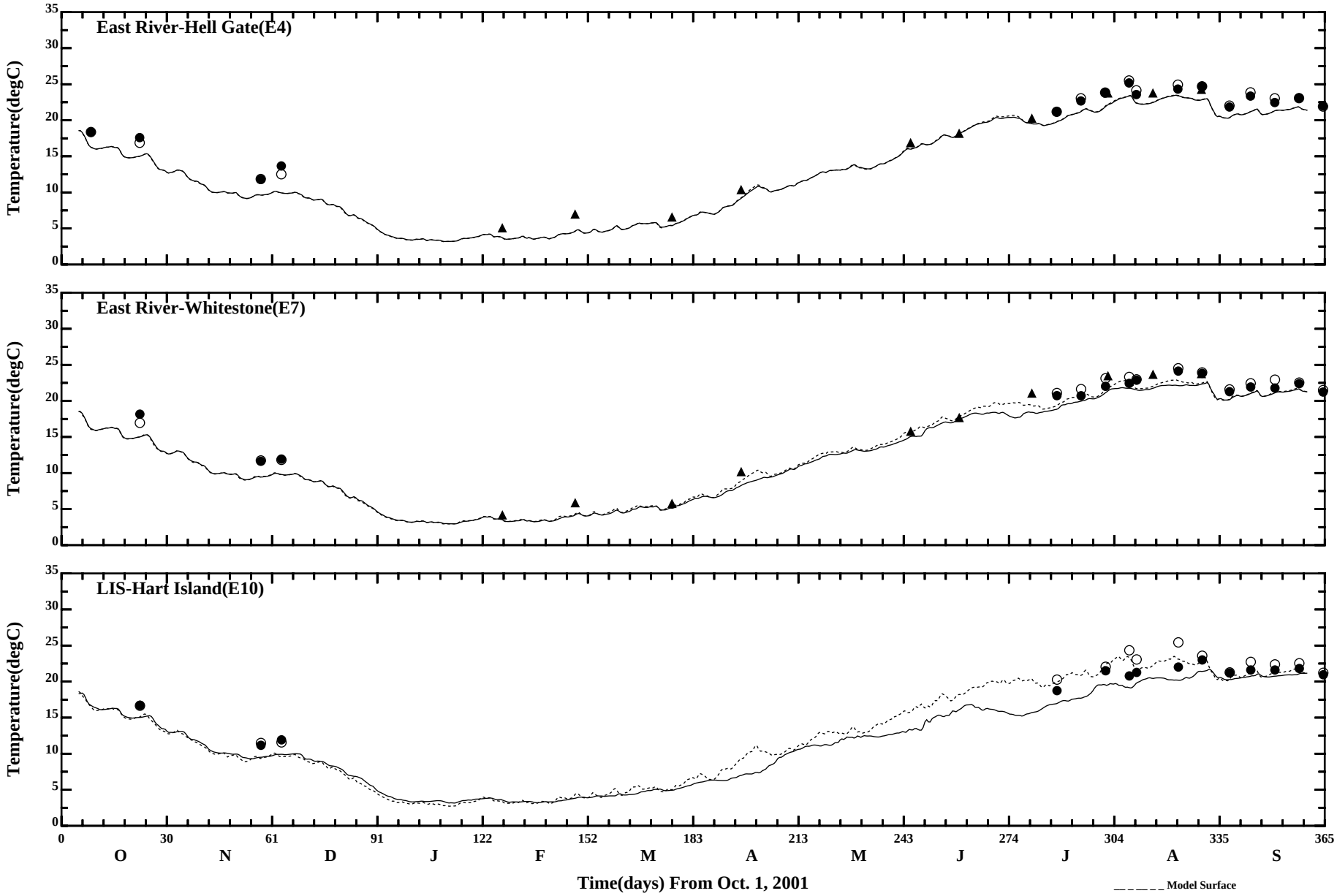

Comparison of 35 Hour Lowpass Surface and Bottom Temperature

//ont6/hrfo0010/RUNS/ECOMSED-SED/ECOMSED-0102/PLOTS/TANDS/temp31_35hlp

DATE: 11/21/2003 TIME: 10:39: 2

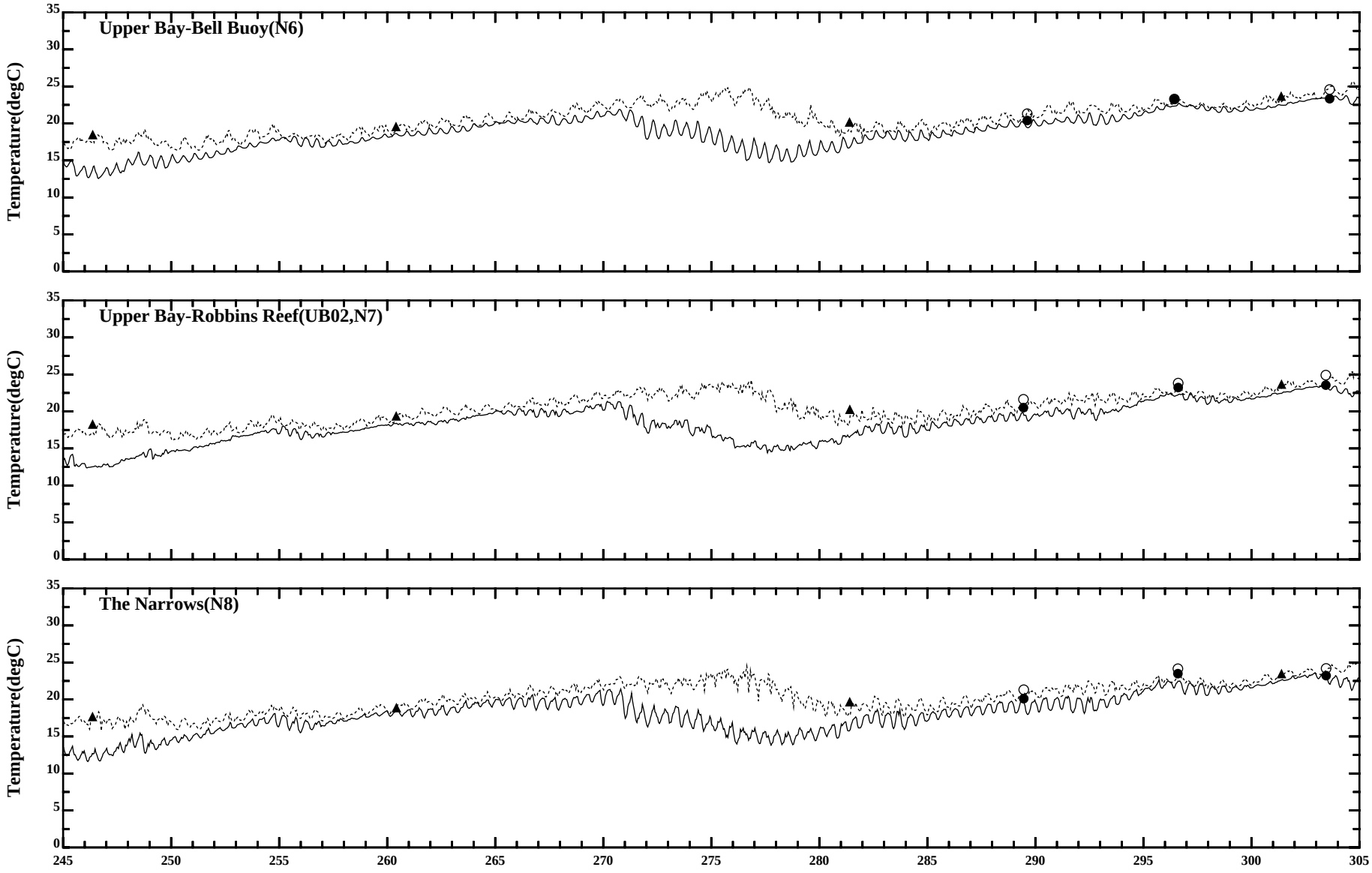

Comparison of Instantaneous Surface and Bottom Temperature

/ont6/hrfo0010/HYDRORUNS/CARP01-02/PLOTS/TANDS/salt32

DATE: 11/24/2003 TIME: 11:14:16

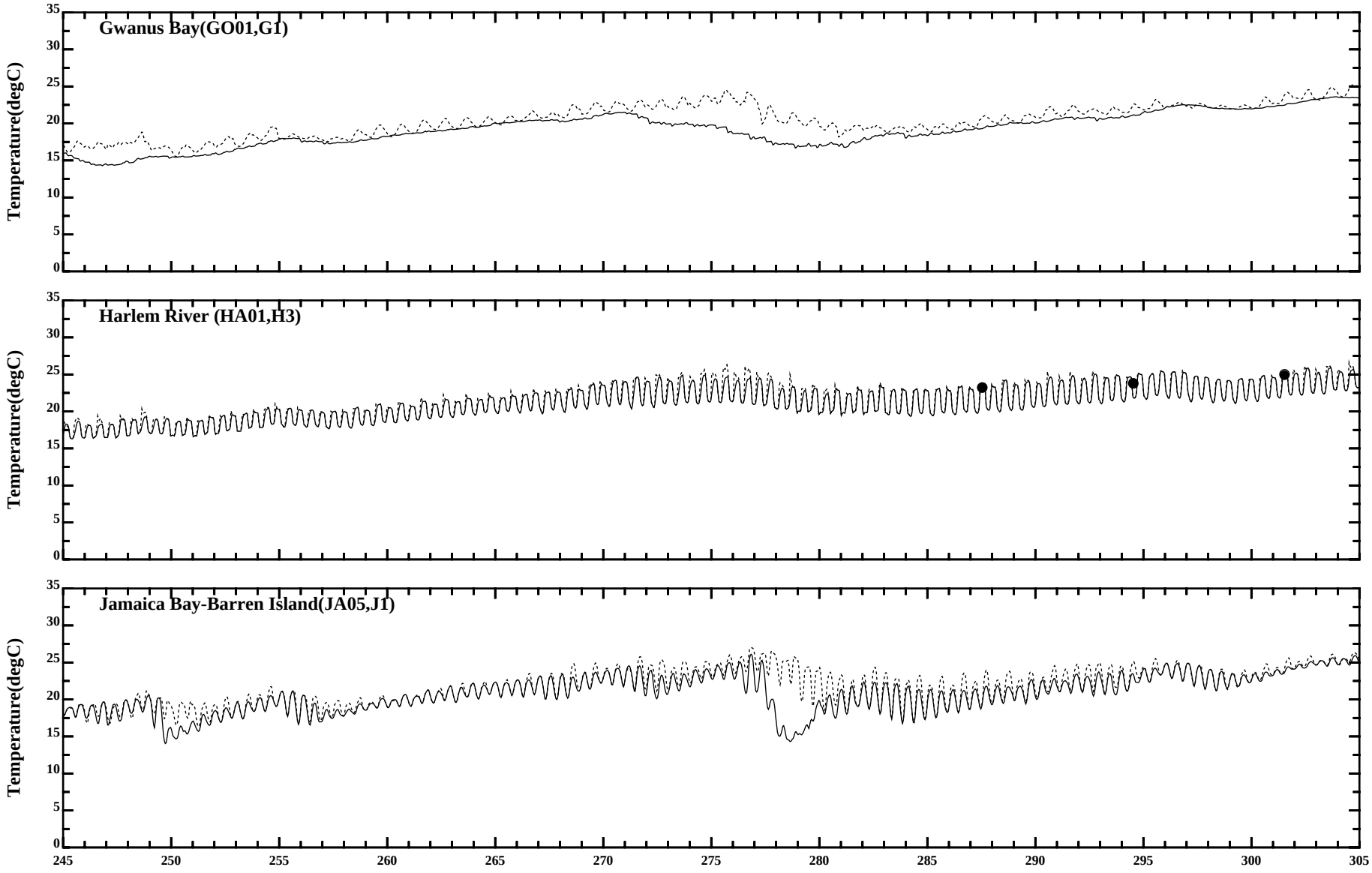

Comparison of Instantaneous Surface and Bottom Temperature

/ont6/hrfo0010/HYDRORUNS/CARP01-02/PLOTS/TANDS/salt32

_ _ _ _ _ Model Surface

_____ Model Bottom

○ Harbor Survey Data Surface

● Harbor Survey Data Bottom

▲ IEC Data at 3 meters Depth

□ US ARMY CORPS. OF ENGRS Data Surface

■ US ARMY CORPS. OF ENGRS Data Bottom

DATE: 11/24/2003 TIME: 11:14:16

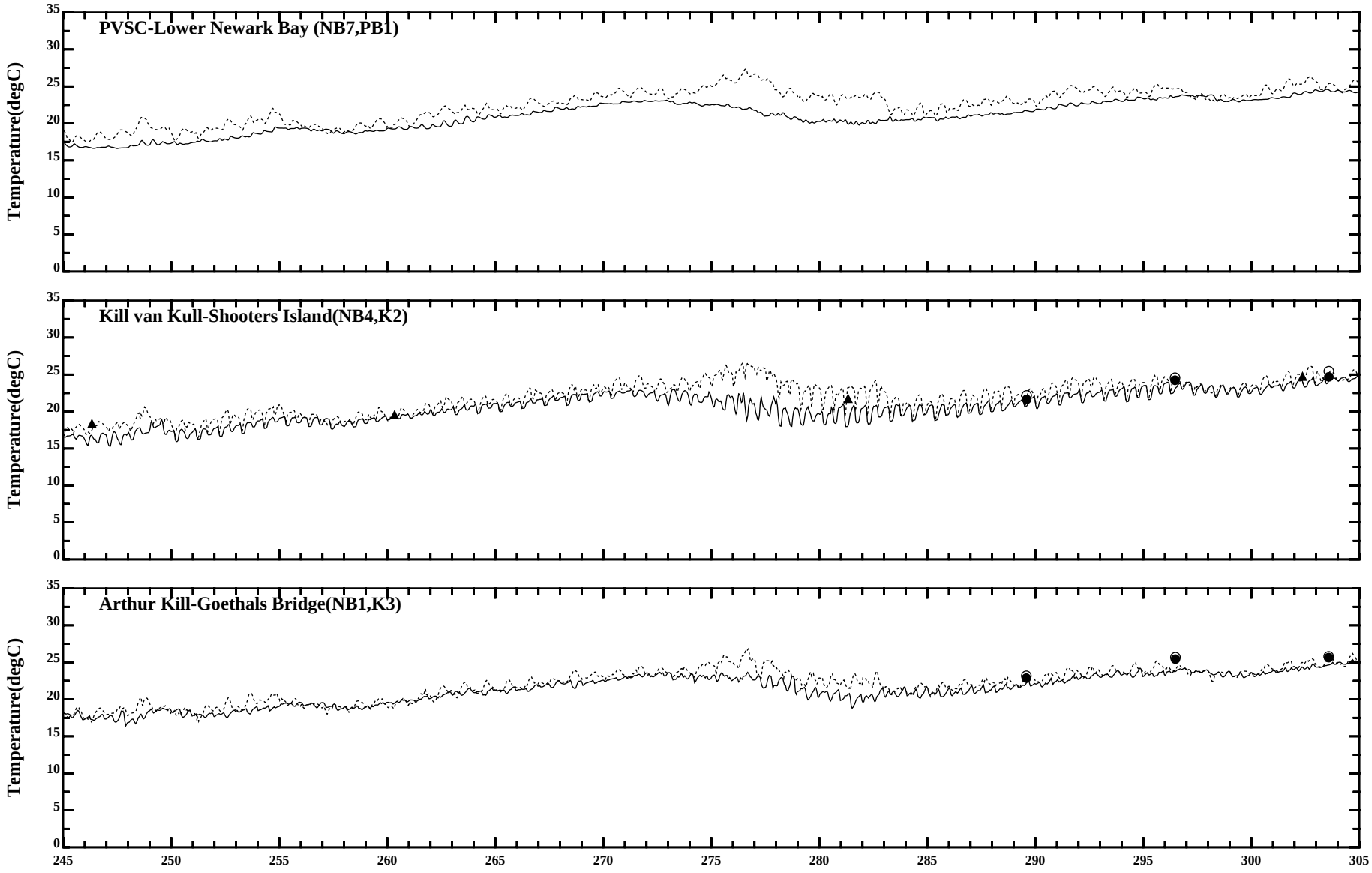

Comparison of Instantaneous Surface and Bottom Temperature

/ont6/hrfo0010/HYDRORUNS/CARP01-02/PLOTS/TANDS/salt32

DATE: 11/24/2003 TIME: 11:14:16

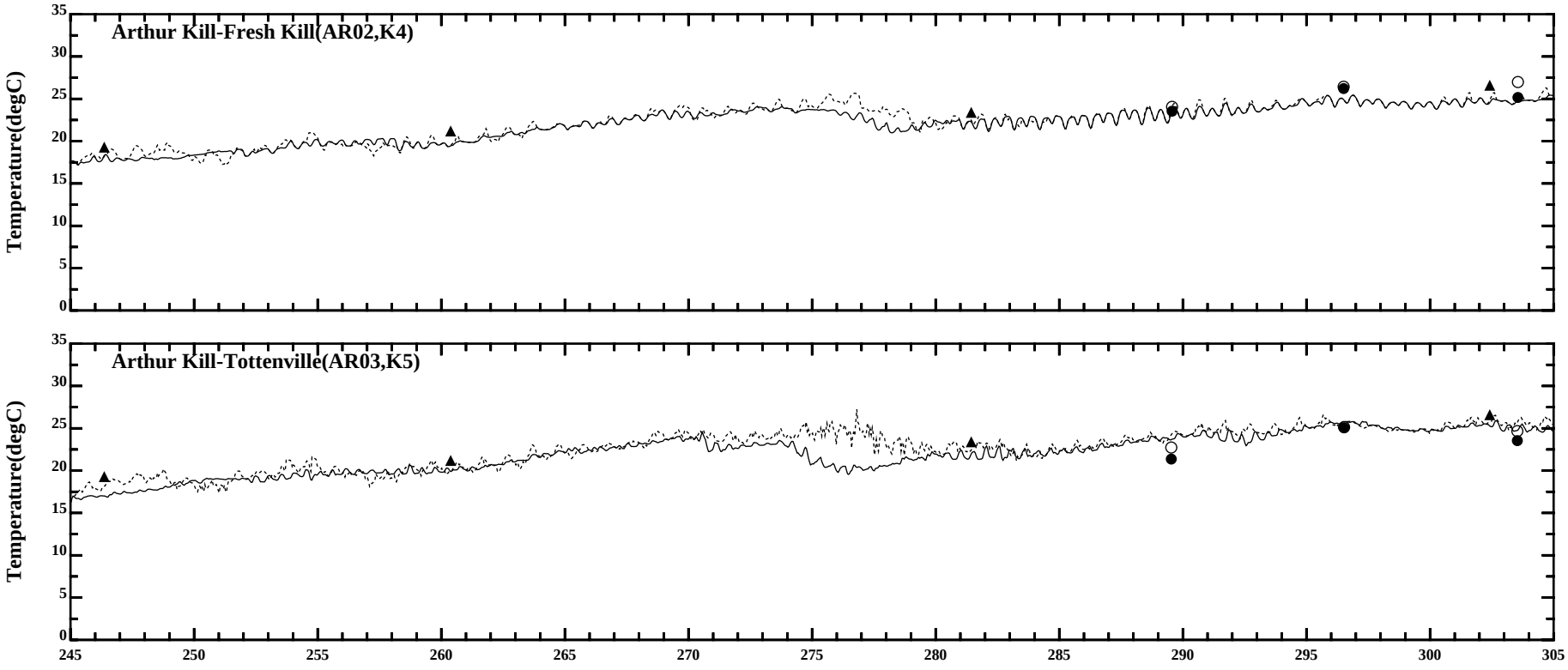

Comparison of Instantaneous Surface and Bottom Temperature

/ont6/hrfo0010/HYDRORUNS/CARP01-02/PLOTS/TANDS/salt32

DATE: 11/24/2003 TIME: 11:14:16

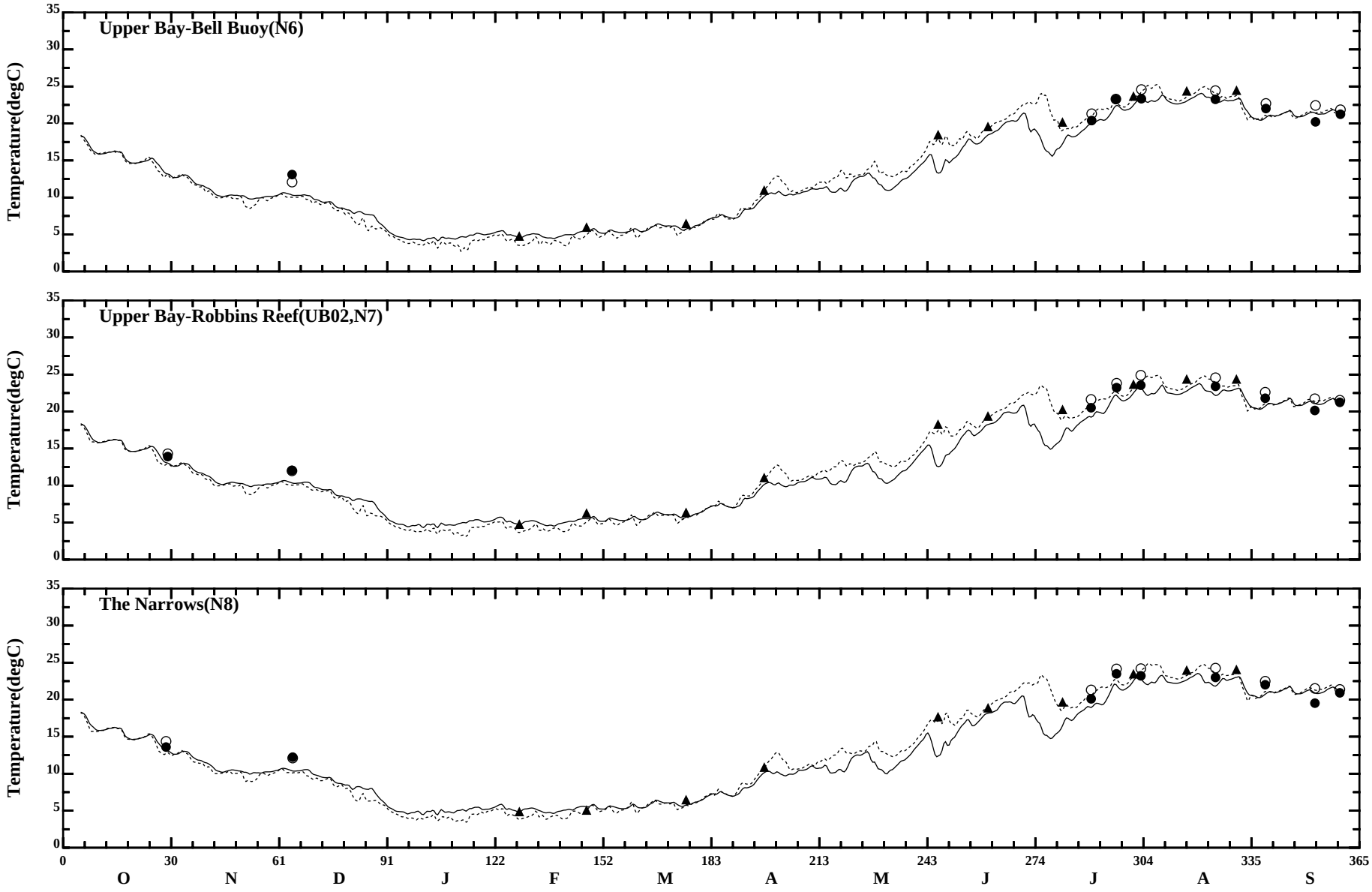

Comparison of 35 Hour Lowpass Surface and Bottom Temperature

/ont6/hrfo0010/HYDRORUNS/CARP01-02/PLOTS/TANDS/salt32_35hlp

DATE: 11/24/2003 TIME: 11:14: 8

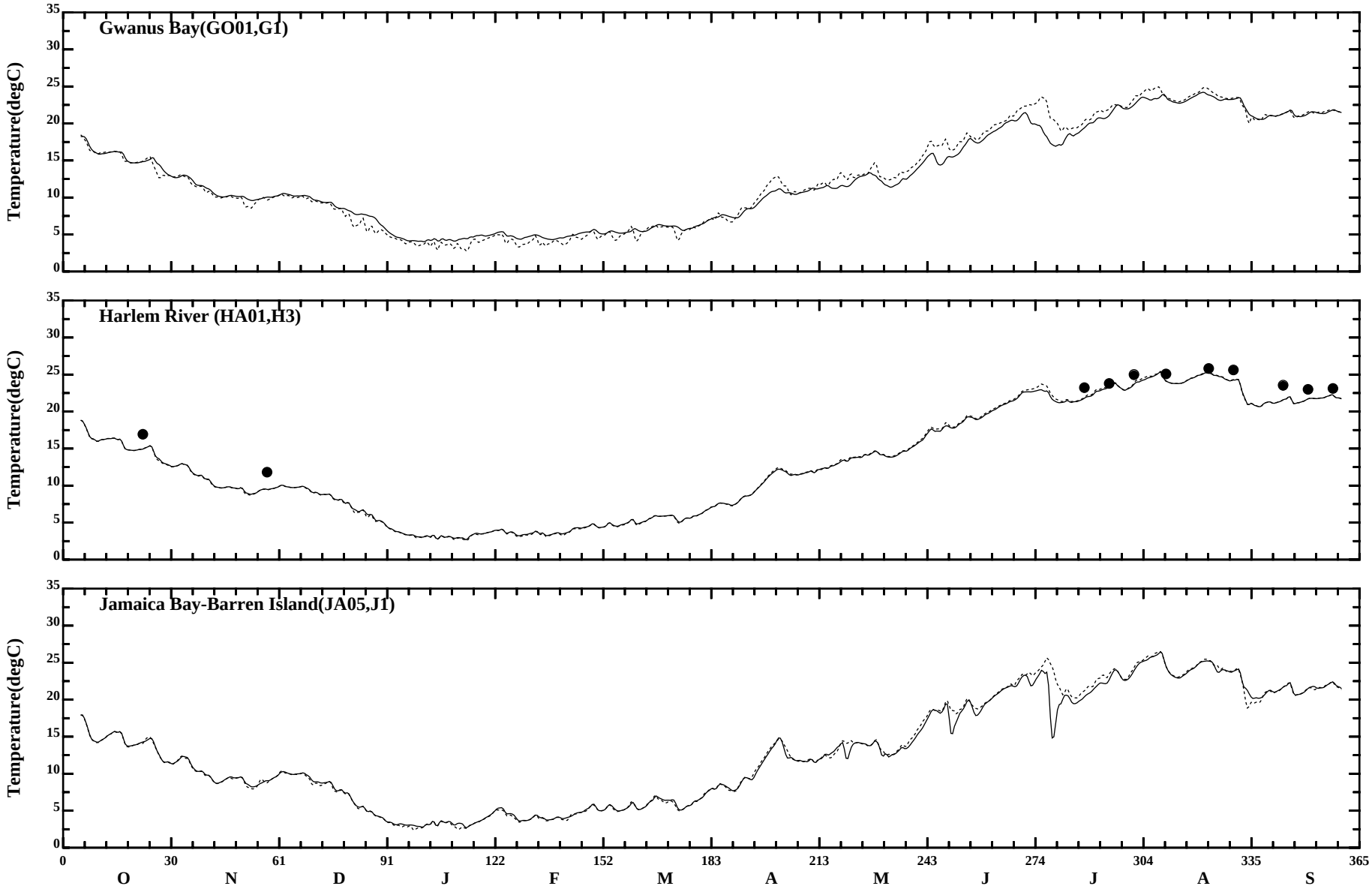

Comparison of 35 Hour Lowpass Surface and Bottom Temperature

/ont6/hrfo0010/HYDRORUNS/CARP01-02/PLOTS/TANDS/salt32_35hlp

DATE: 11/24/2003 TIME: 11:14: 8

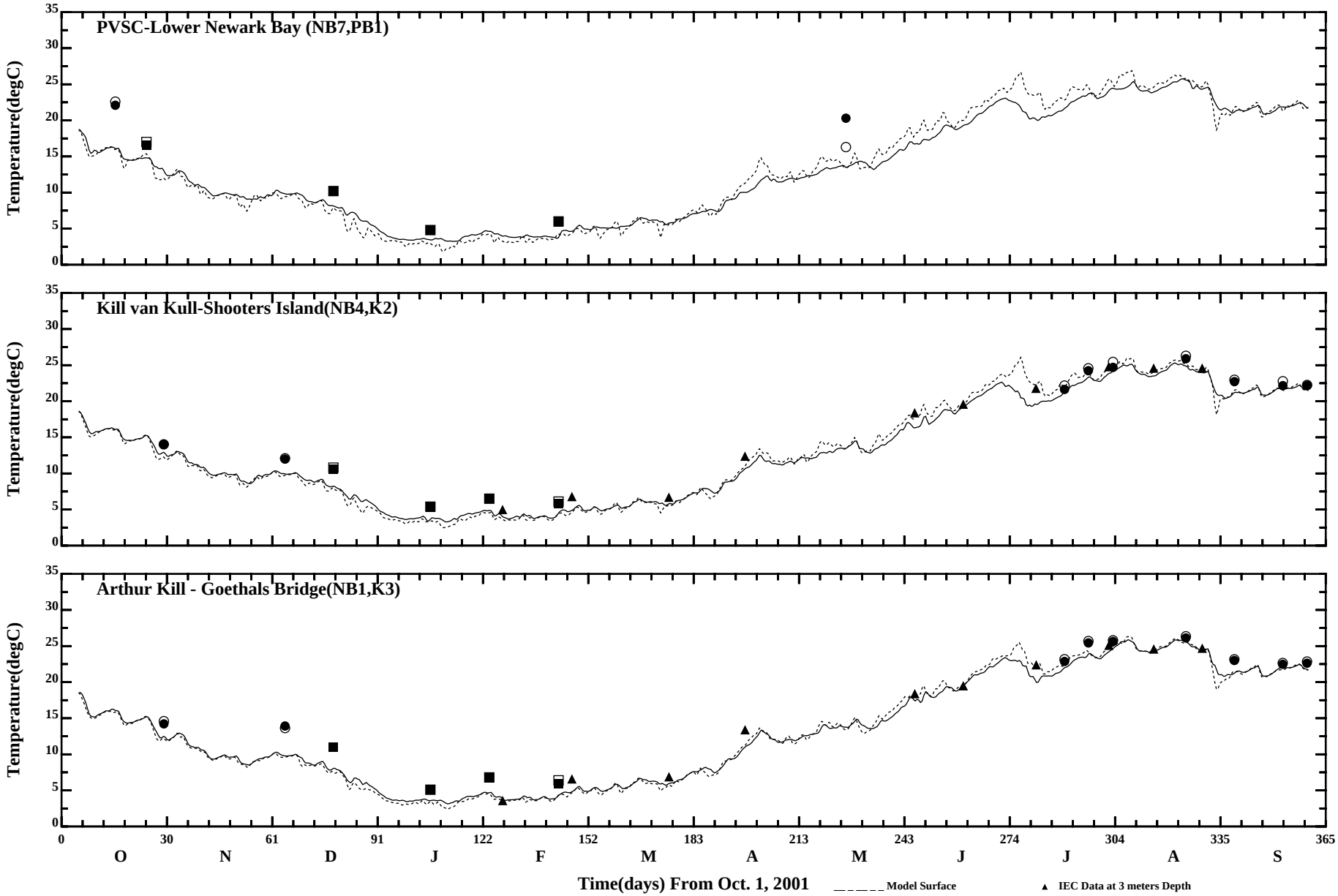

Comparison of 35 Hour Lowpass Surface and Bottom Temperature

/ont6/hrfo0010/HYDRORUNS/CARP01-02/PLOTS/TANDS/salt32_35hlp

DATE: 11/24/2003 TIME: 11:14: 8

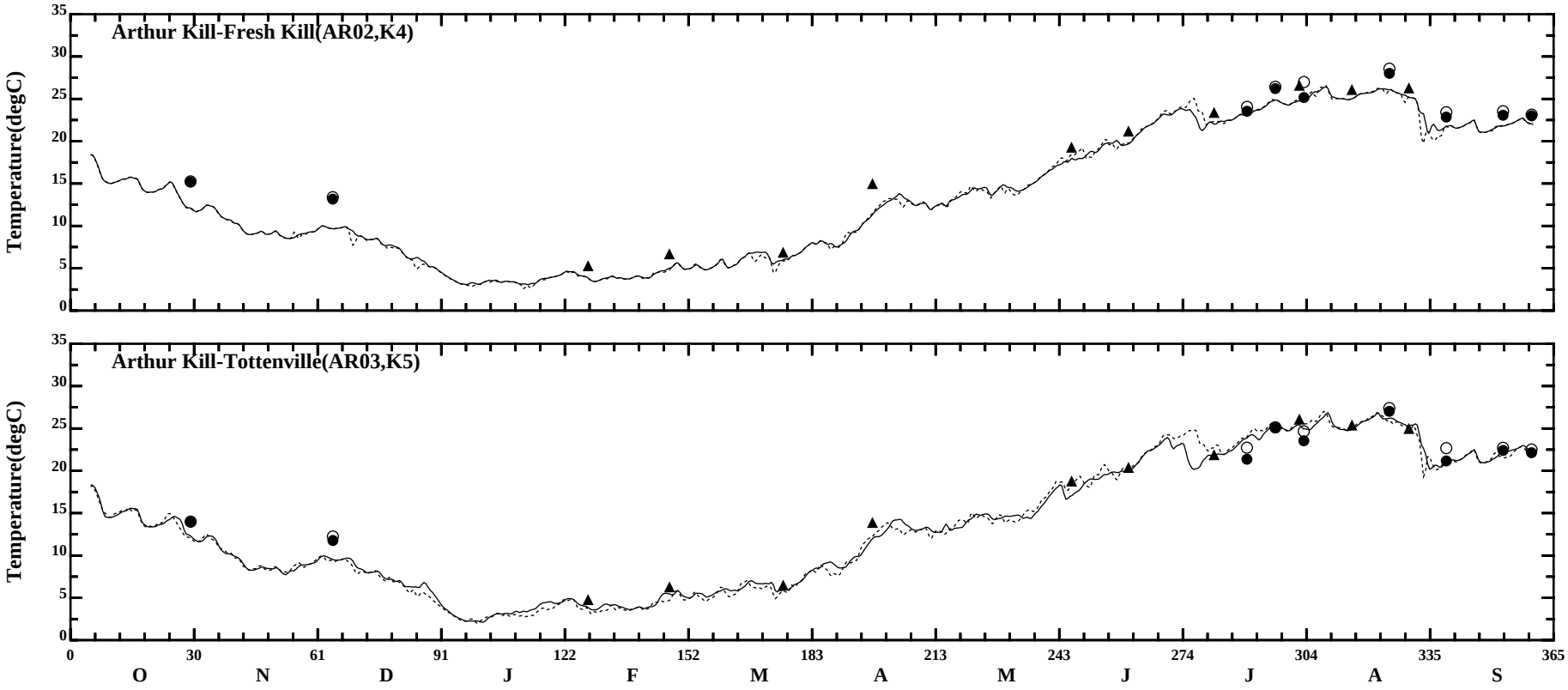

Comparison of 35 Hour Lowpass Surface and Bottom Temperature

/ont6/hrfo0010/HYDRORUNS/CARP01-02/PLOTS/TANDS/salt32_35hlp

APPENDIX 8

SKILL ASSESSMENT USING CTDEP DATA

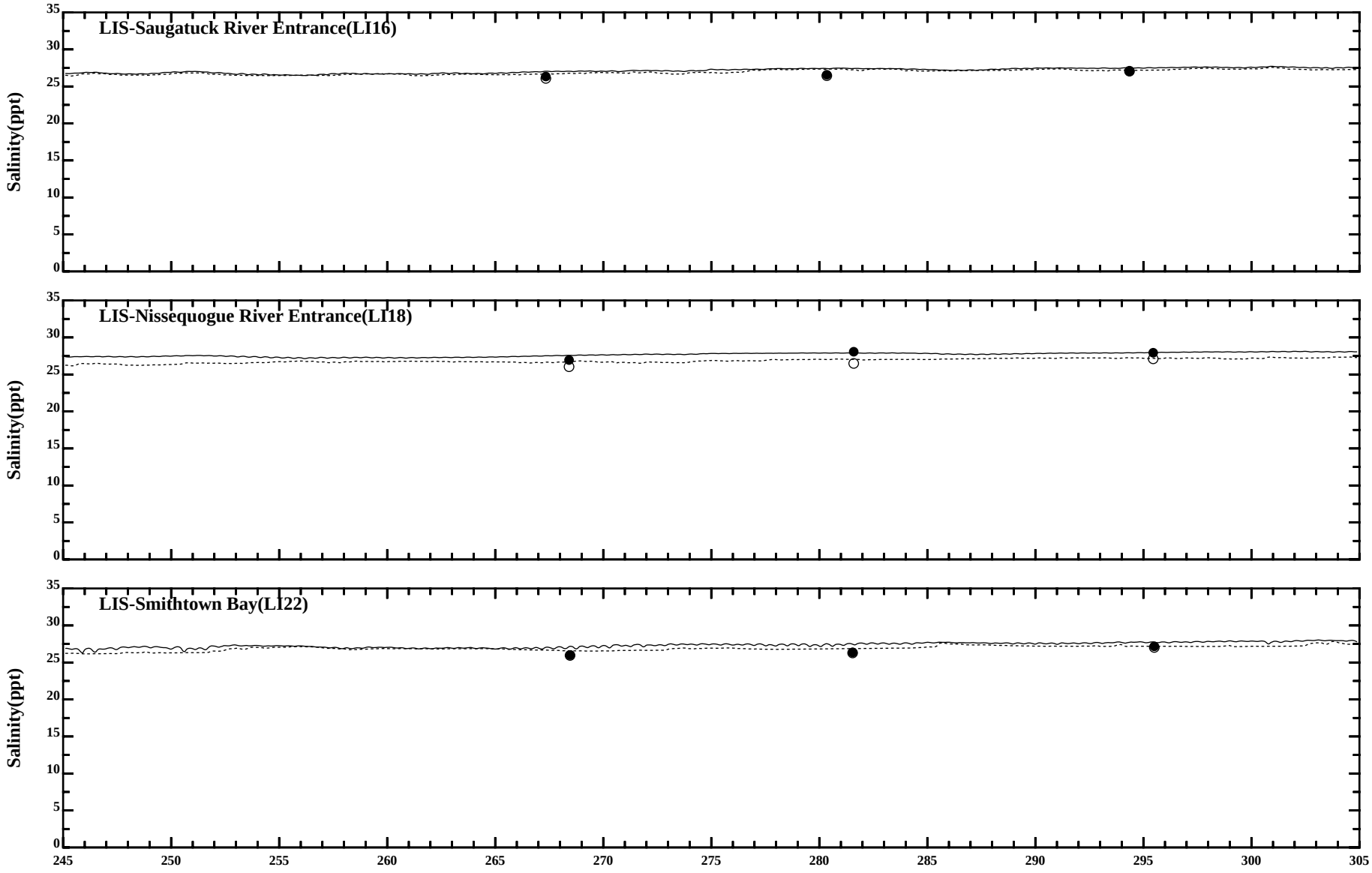

Comparison of Instantaneous Surface and Bottom Salinity

DATE: 8/02/2004 TIME: 11:48:13

/erie1/hrfo0010/HYDRORUNS/CARP9899/PLOTS/TANDS/salt41

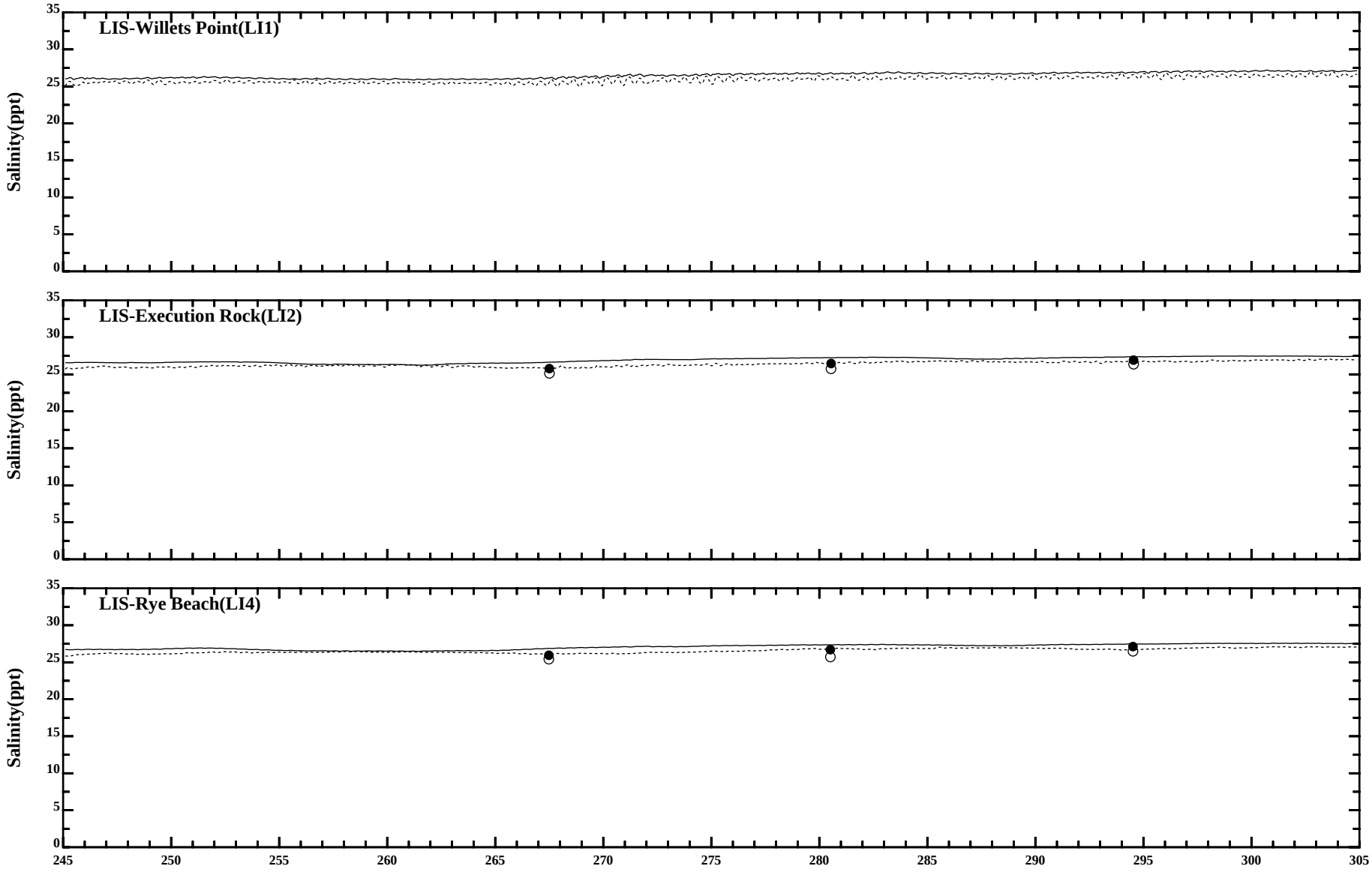

Comparison of Instantaneous Surface and Bottom Salinity

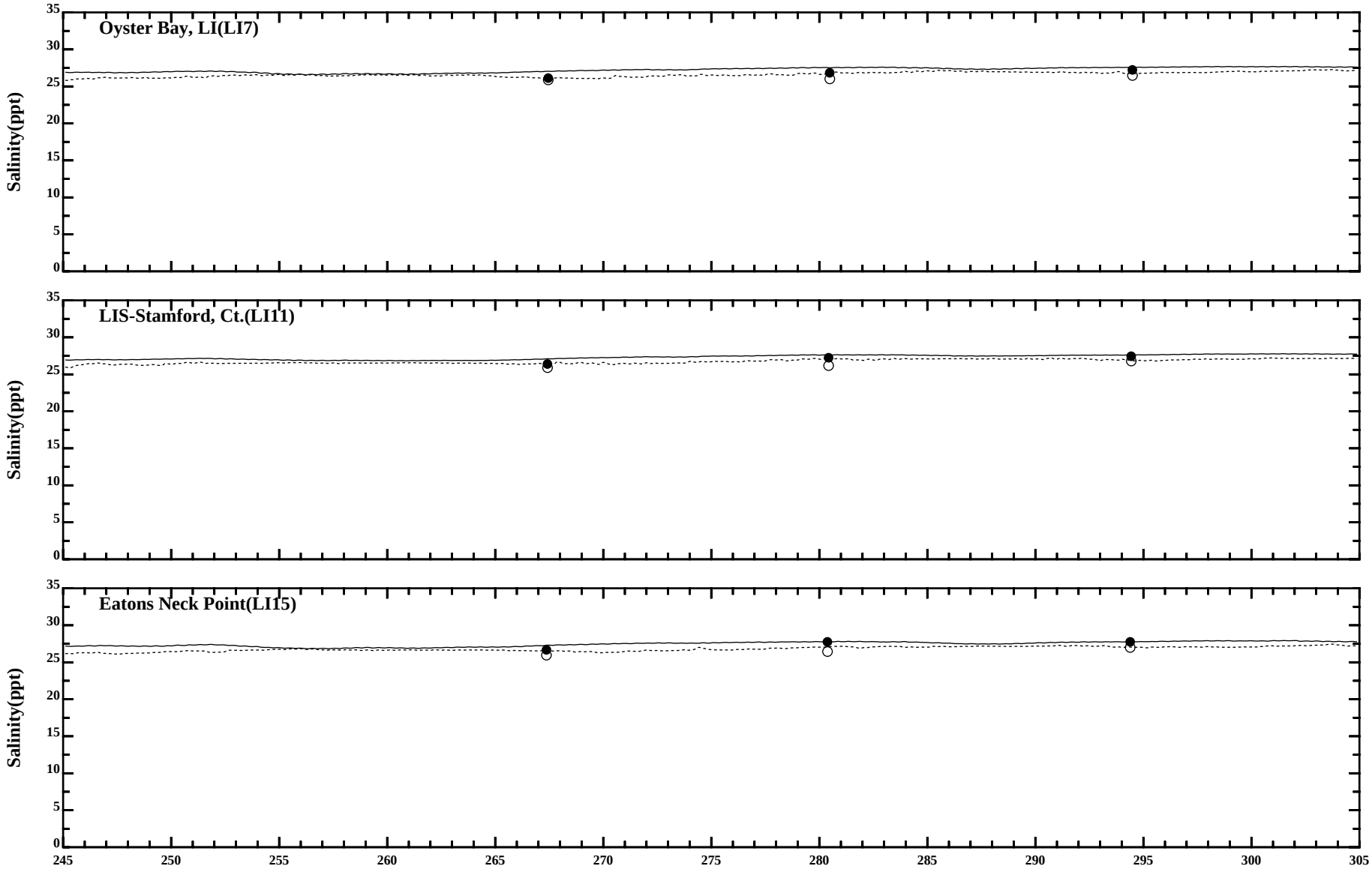

Comparison of Instantaneous Surface and Bottom Salinity

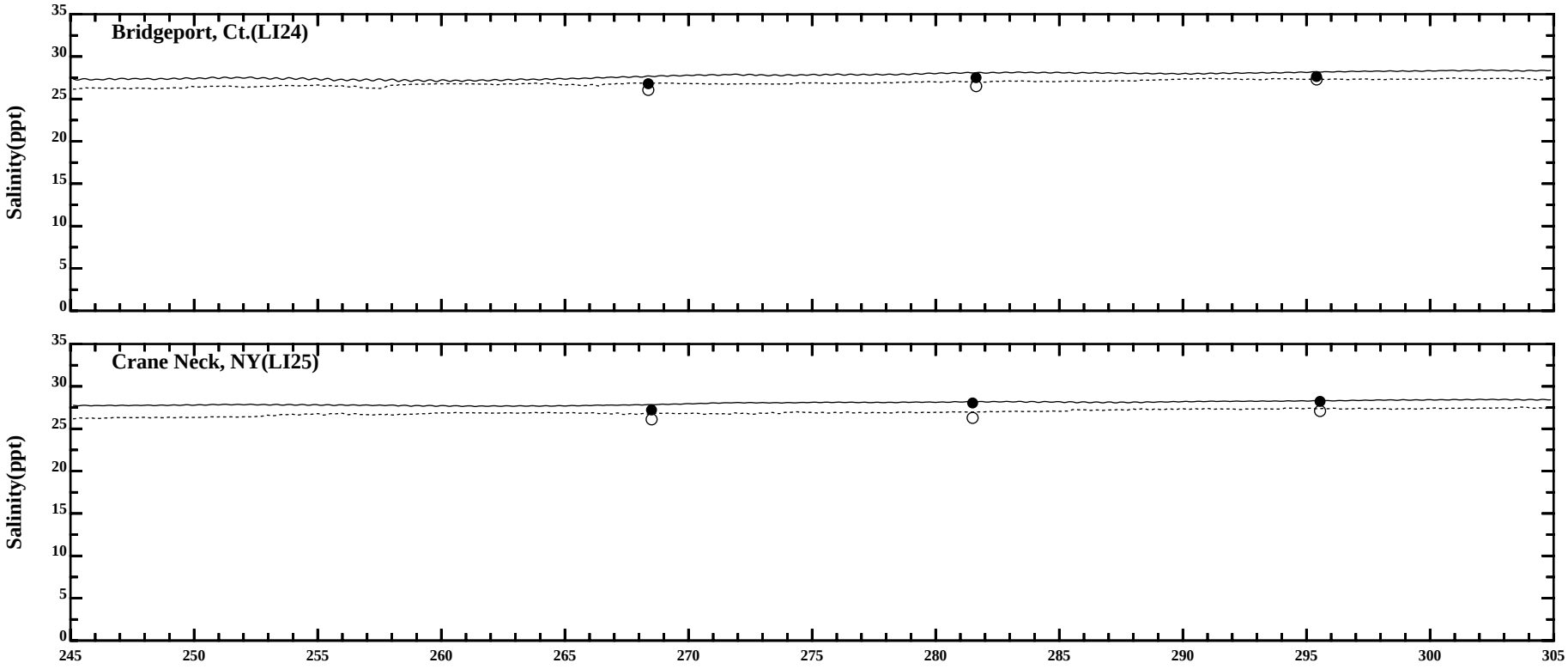

Comparison of Instantaneous Surface and Bottom Salinity

/erie1/hrfo0010/HYDRORUNS/CARP9899/PLOTS/TANDS/salt41

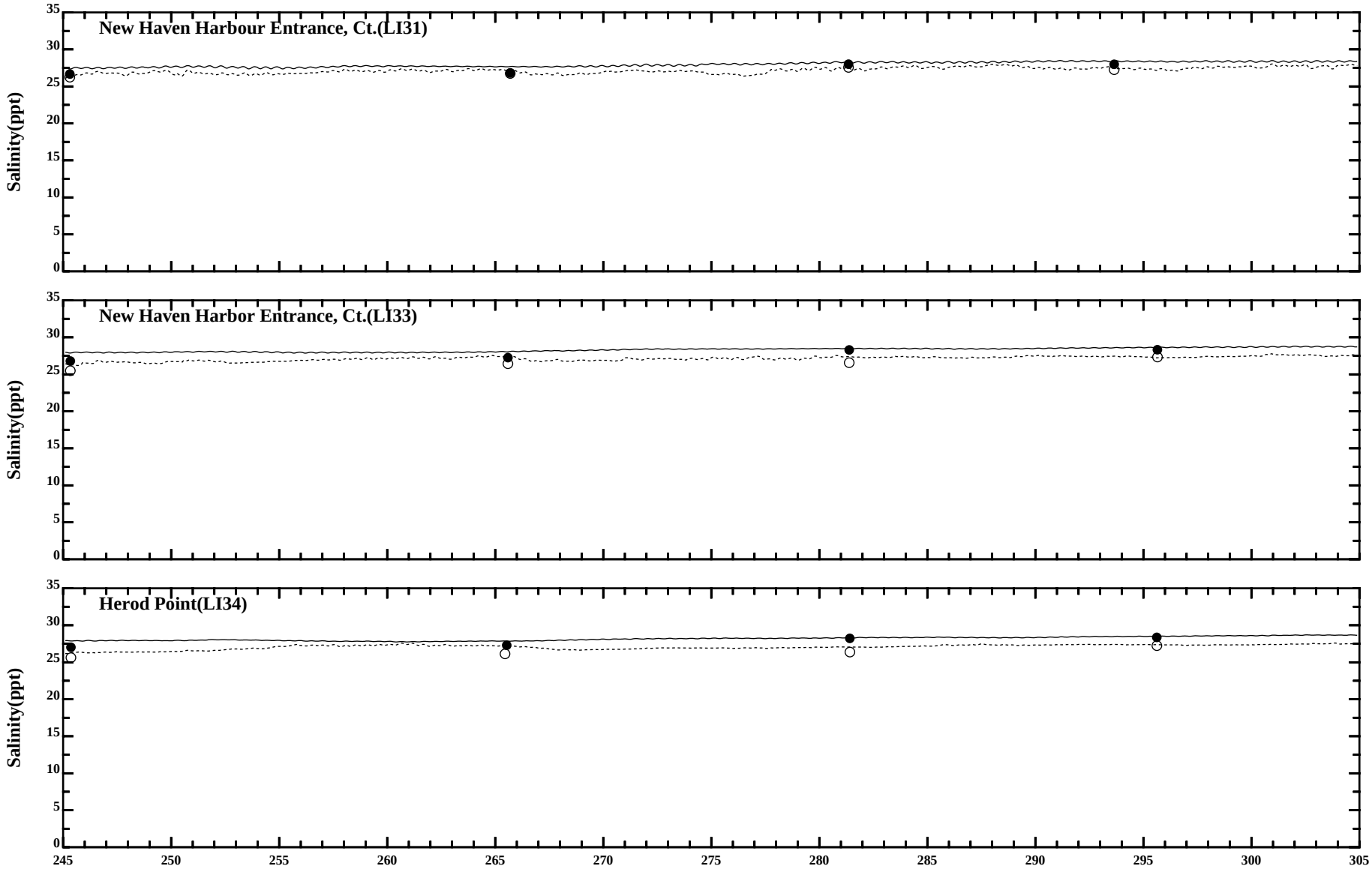

Comparison of Instantaneous Surface and Bottom Salinity

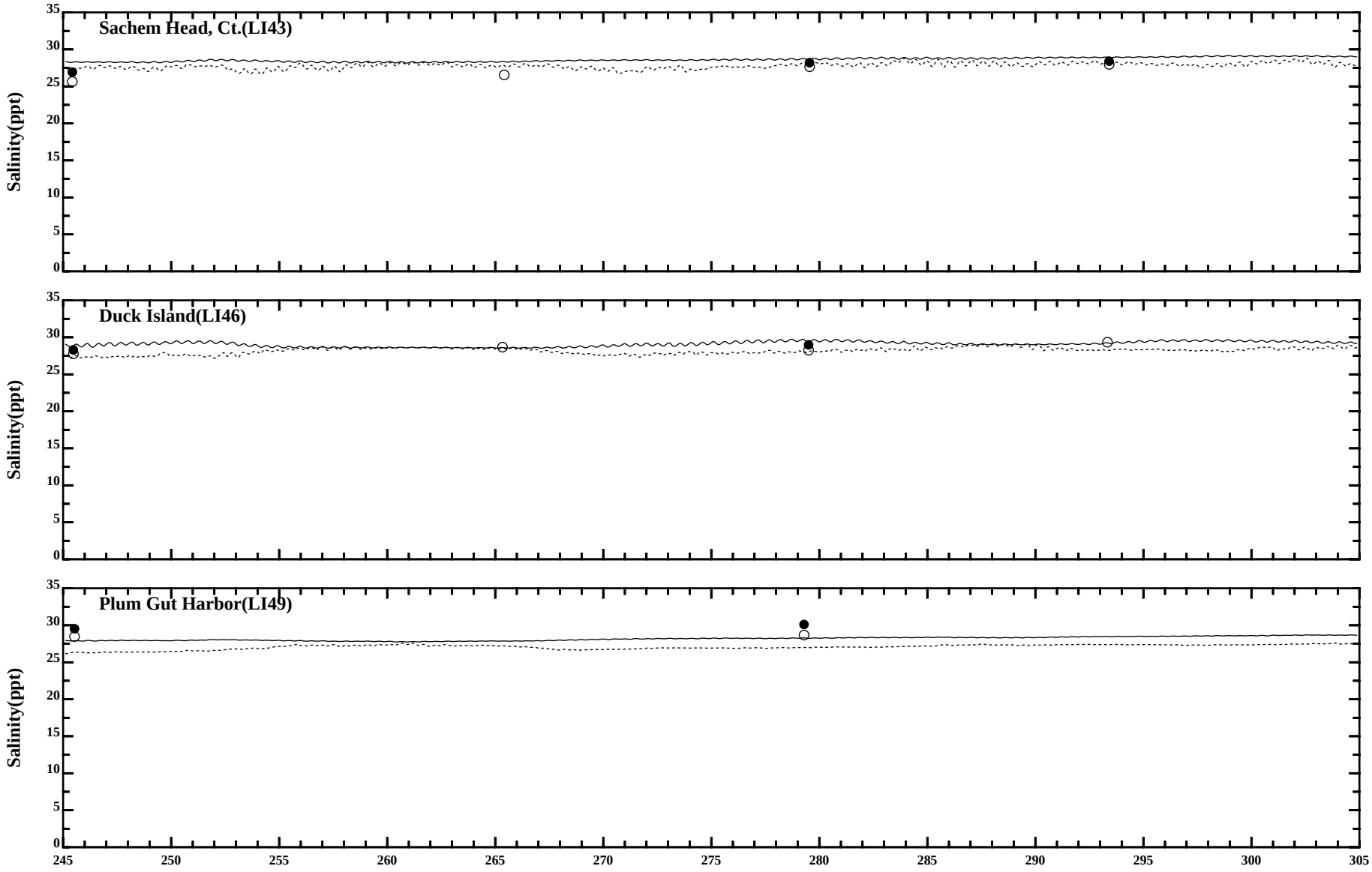

Comparison of Instantaneous Surface and Bottom Salinity

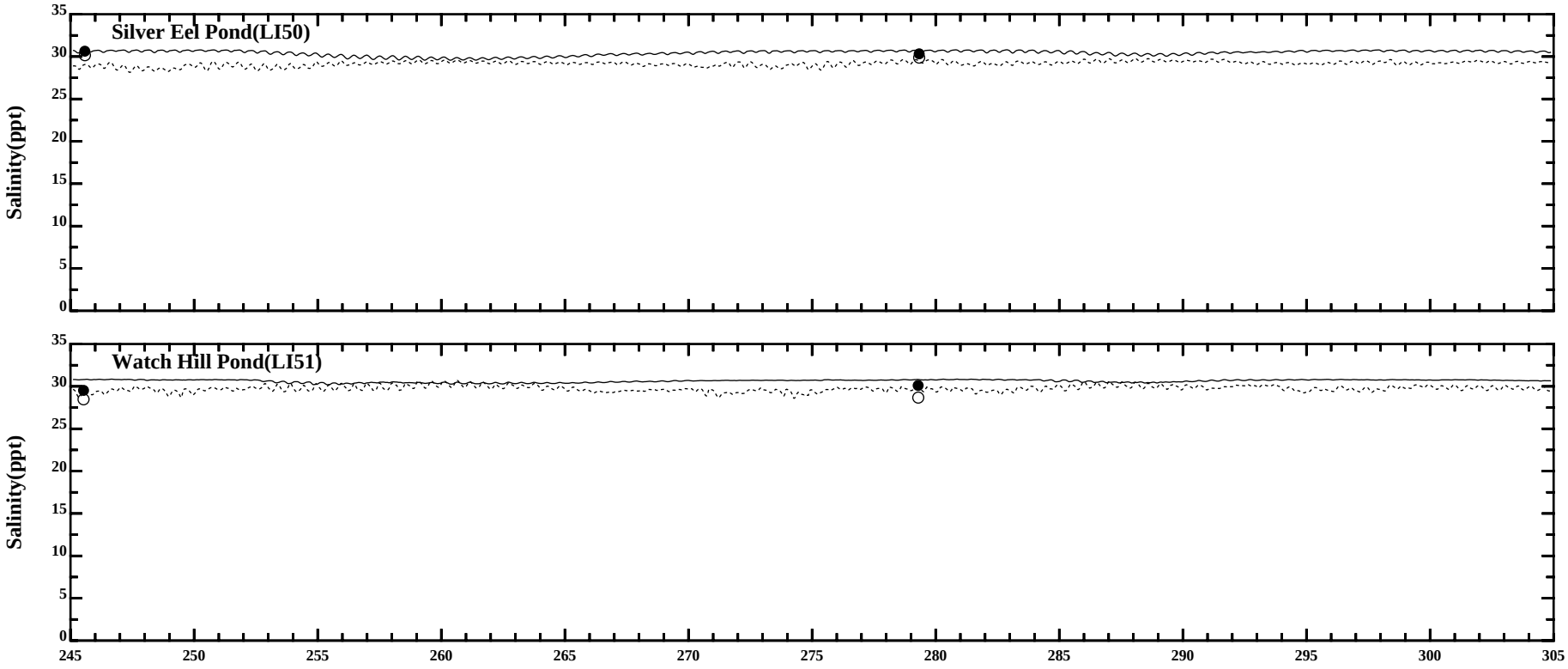

Comparison of Instantaneous Surface and Bottom Salinity

/erie1/hrfo0010/HYDRORUNS/CARP9899/PLOTS/TANDS/salt41

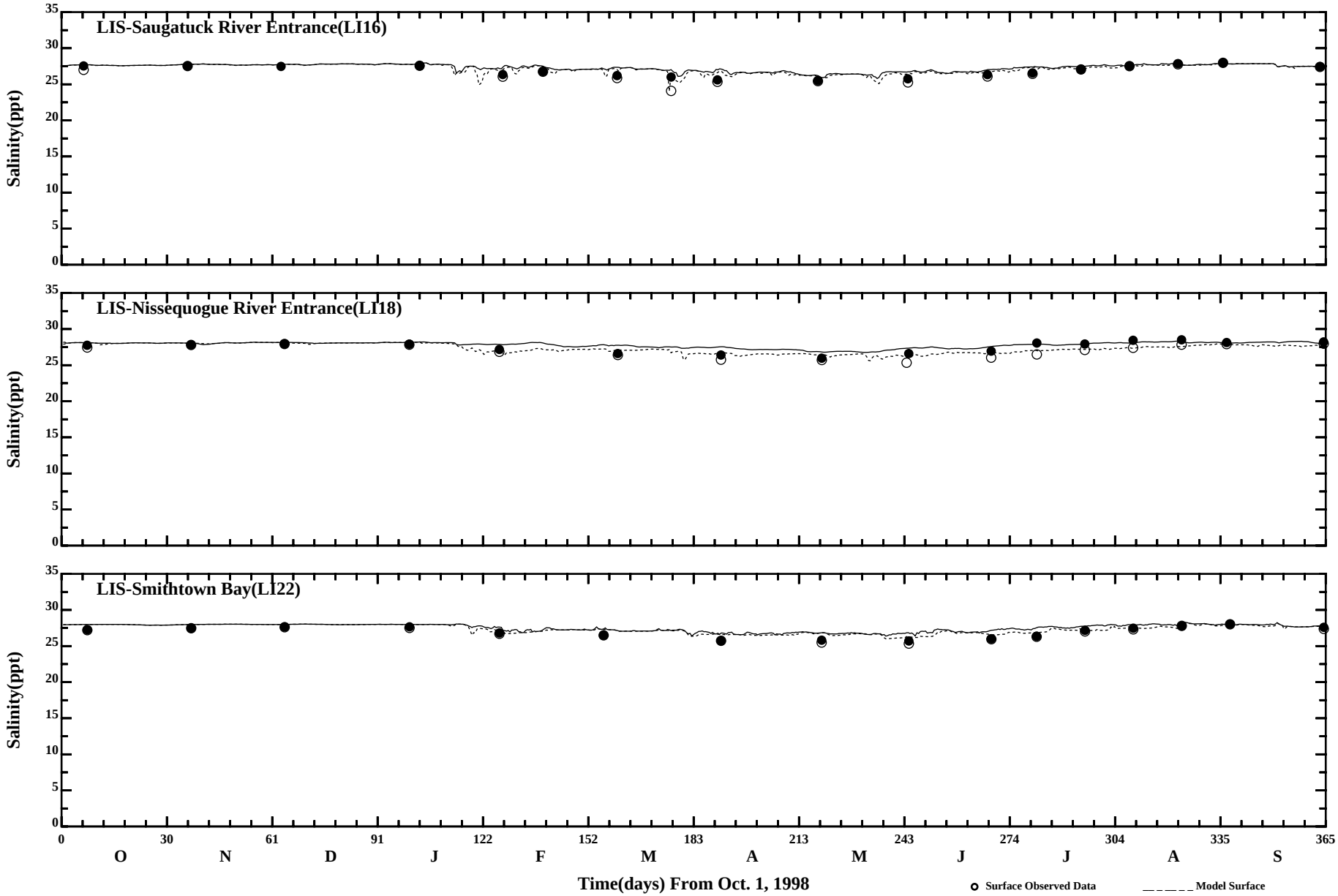

Comparison of 34 Hour Lowpass Surface and Bottom Salinity

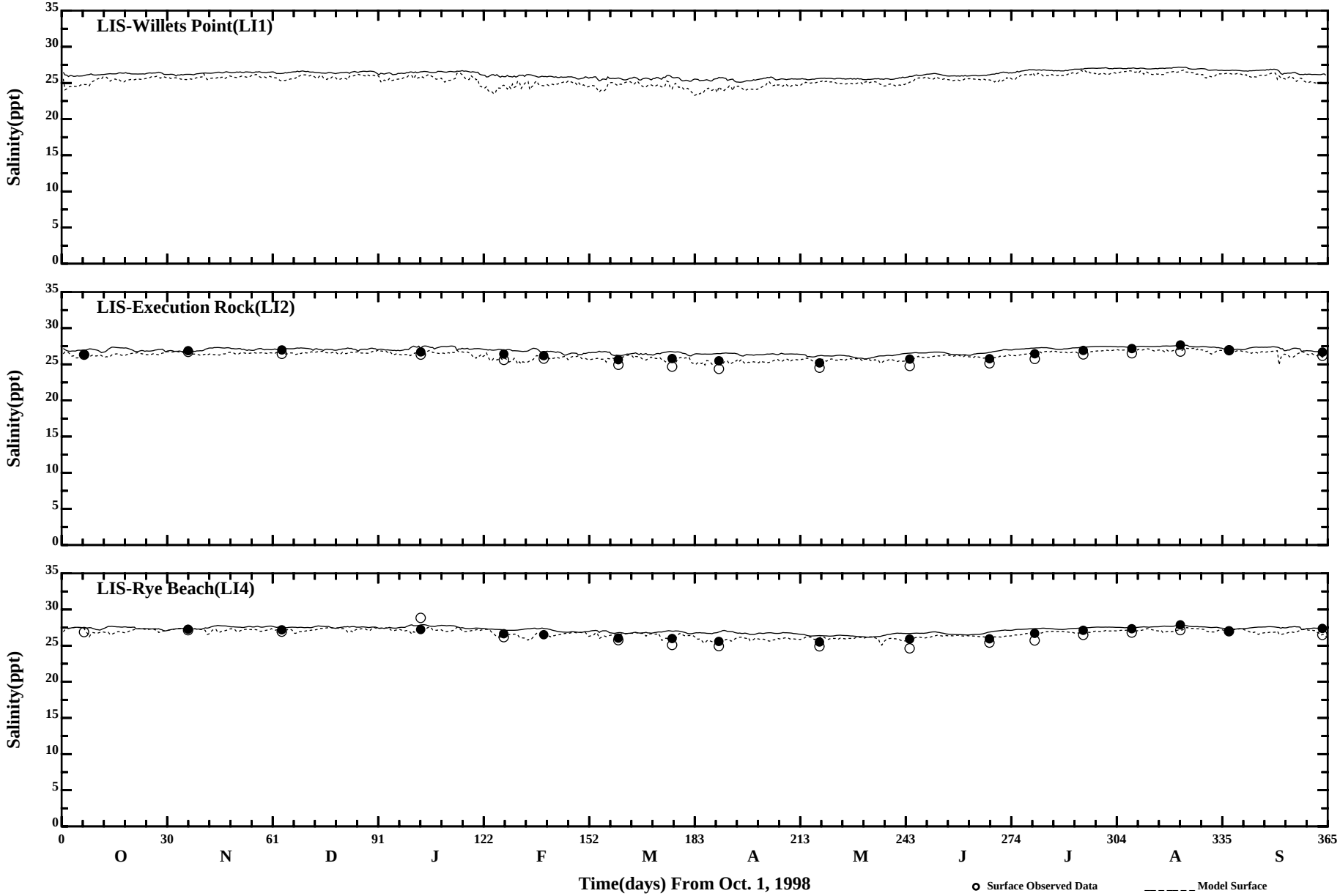

Comparison of 34 Hour Lowpass Surface and Bottom Salinity

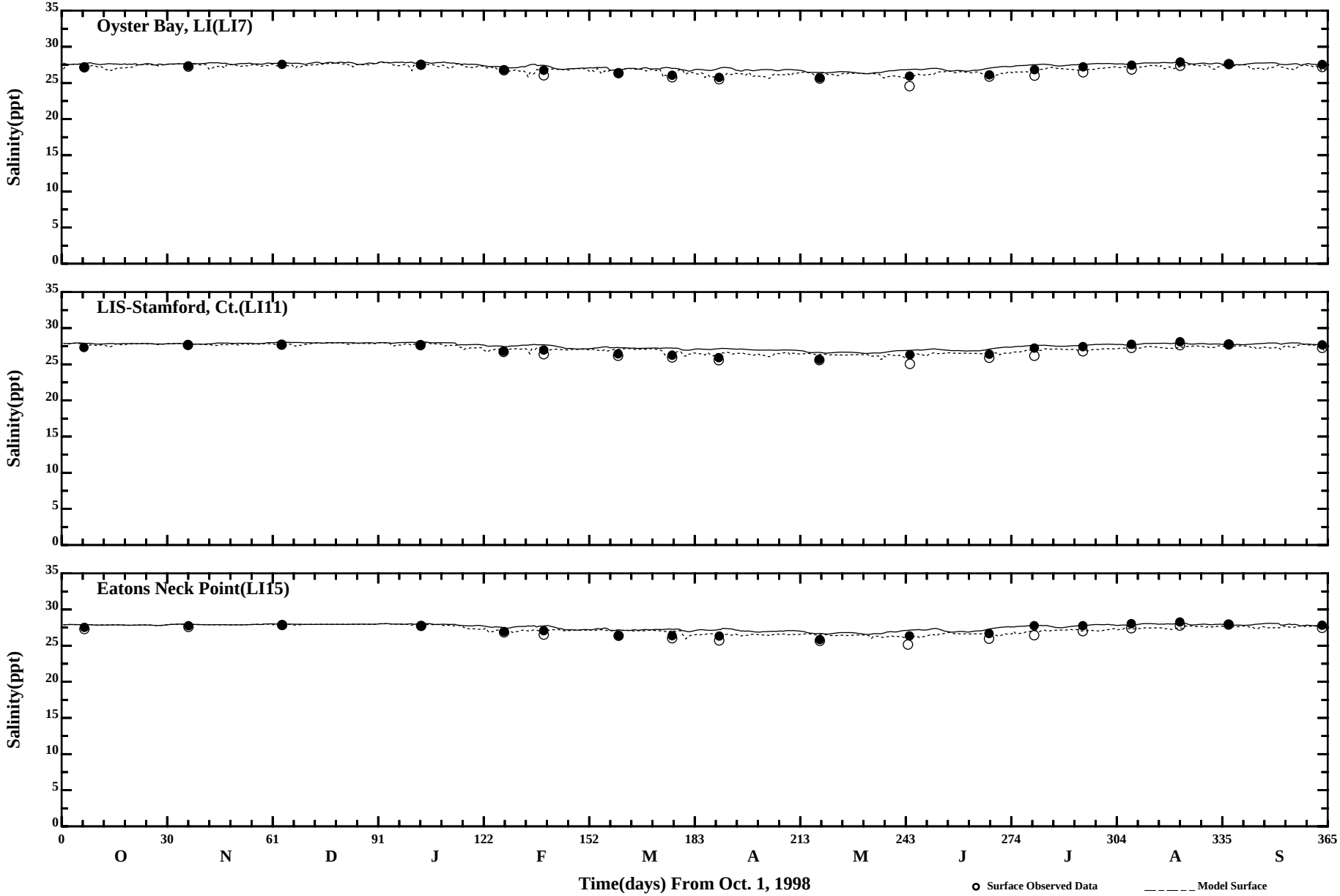

Comparison of 34 Hour Lowpass Surface and Bottom Salinity

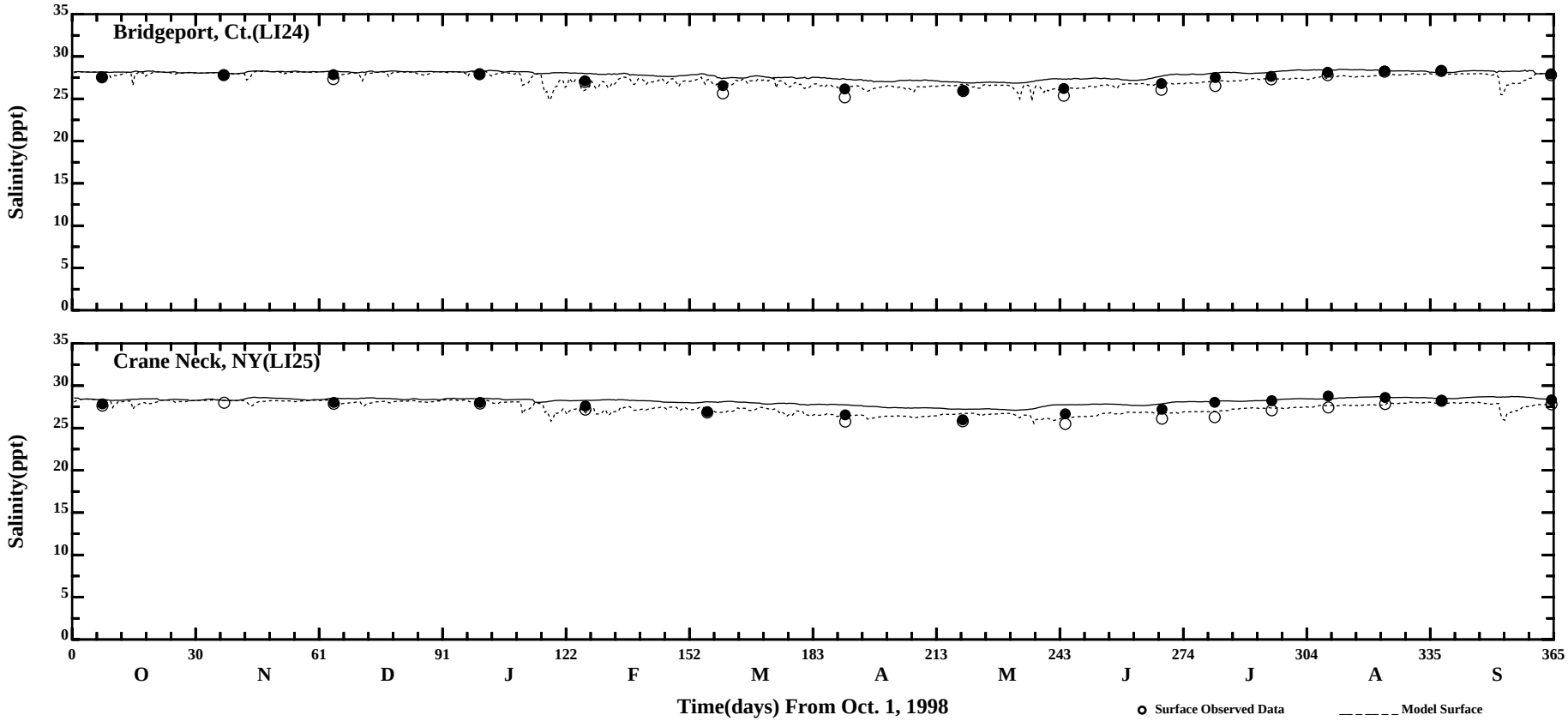

Comparison of 34 Hour Lowpass Surface and Bottom Salinity

/erie1/hrfo0010/HYDRORUNS/CARP9899/PLOTS/TANDS/psalt41_34hlp

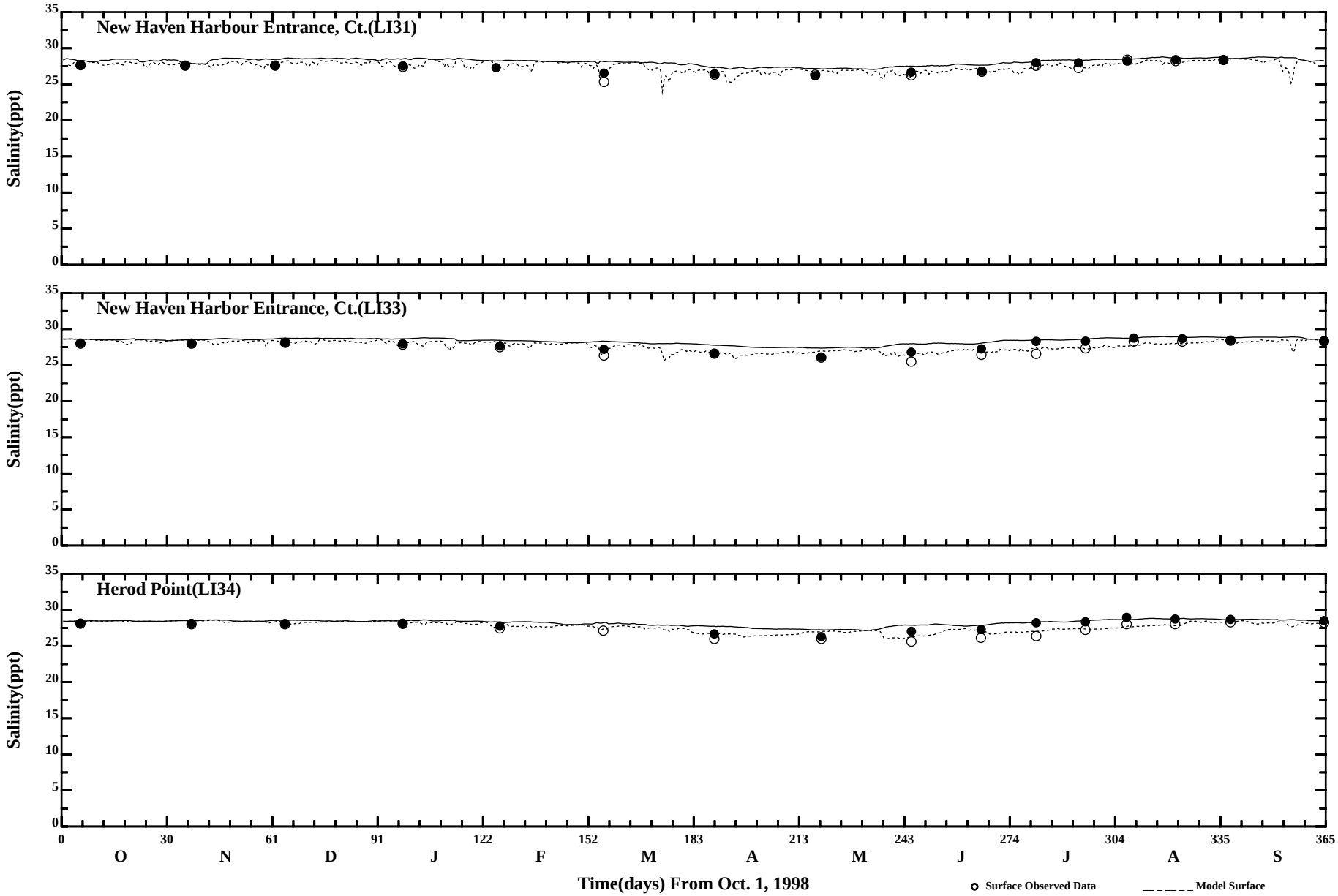

Comparison of 34 Hour Lowpass Surface and Bottom Salinity

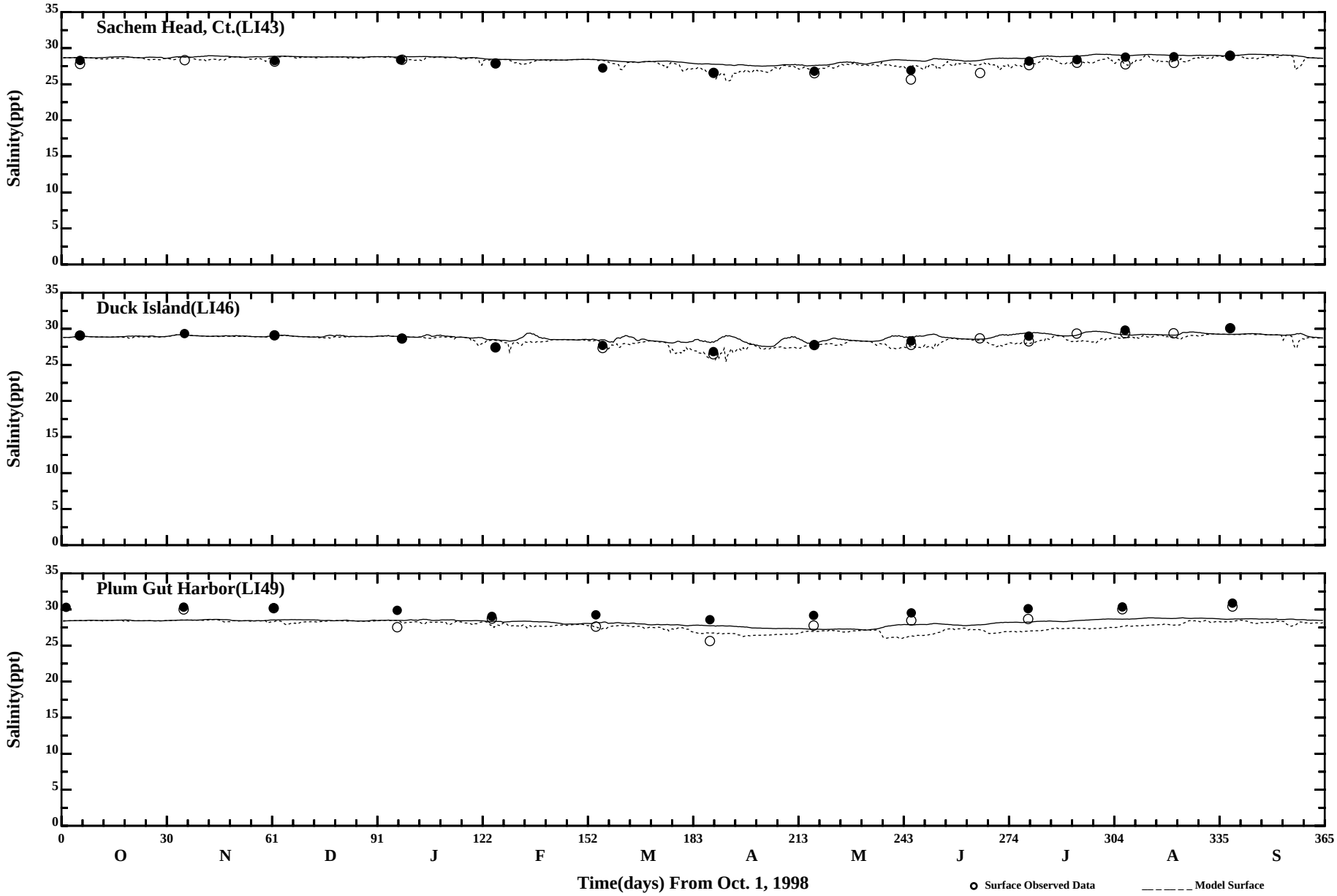

Comparison of 34 Hour Lowpass Surface and Bottom Salinity

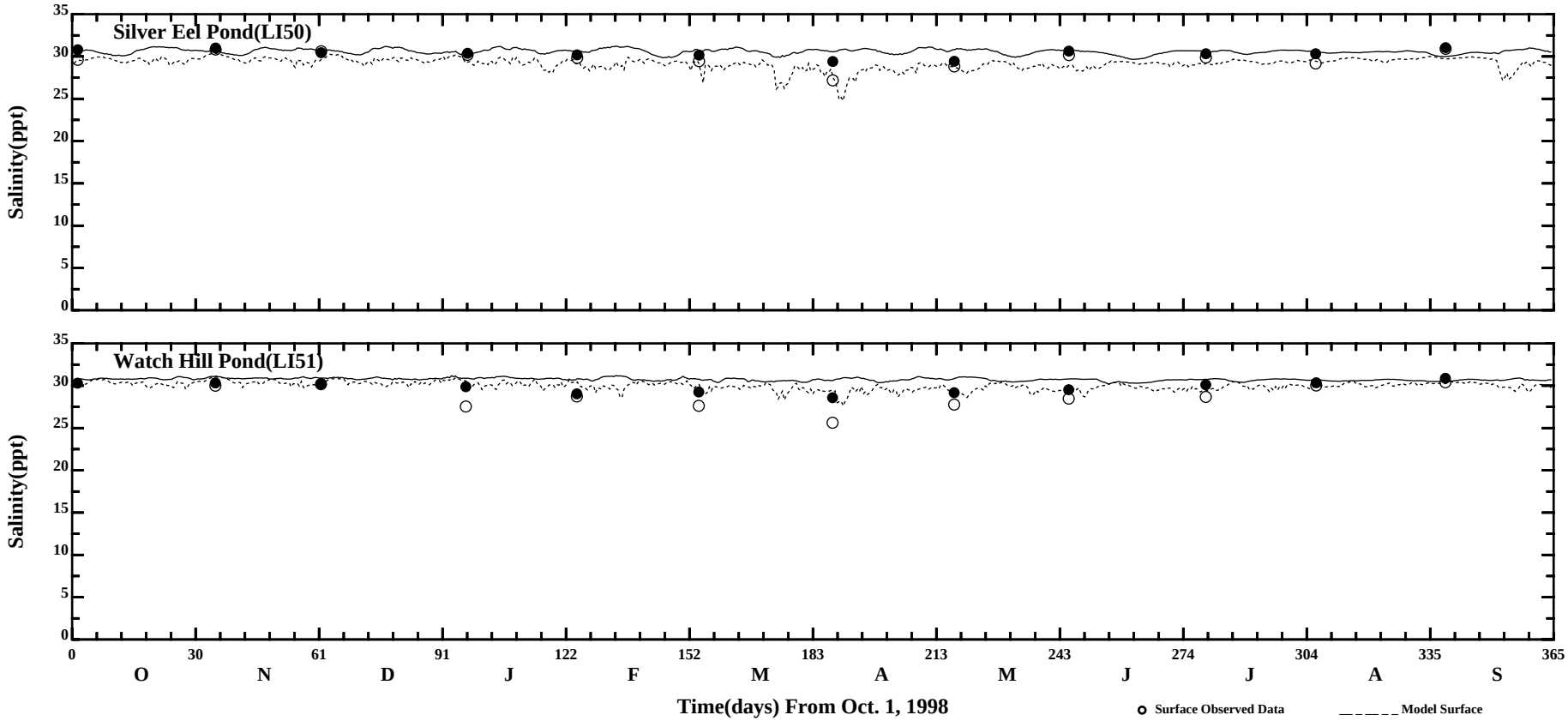

Comparison of 34 Hour Lowpass Surface and Bottom Salinity

/erie1/hrfo0010/HYDRORUNS/CARP9899/PLOTS/TANDS/psalt41_34hlp

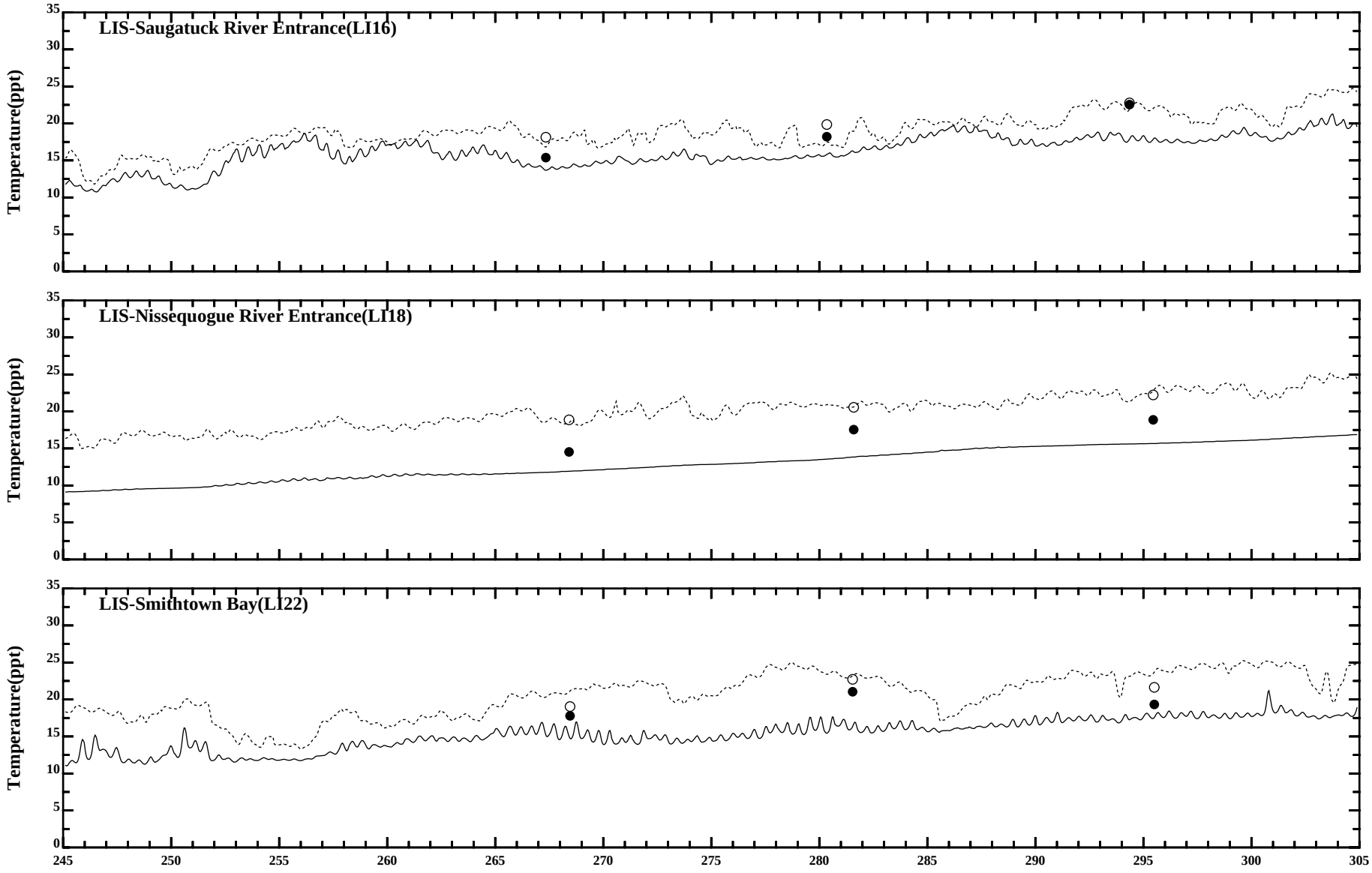

Comparison of Instantaneous Surface and Bottom Temperature

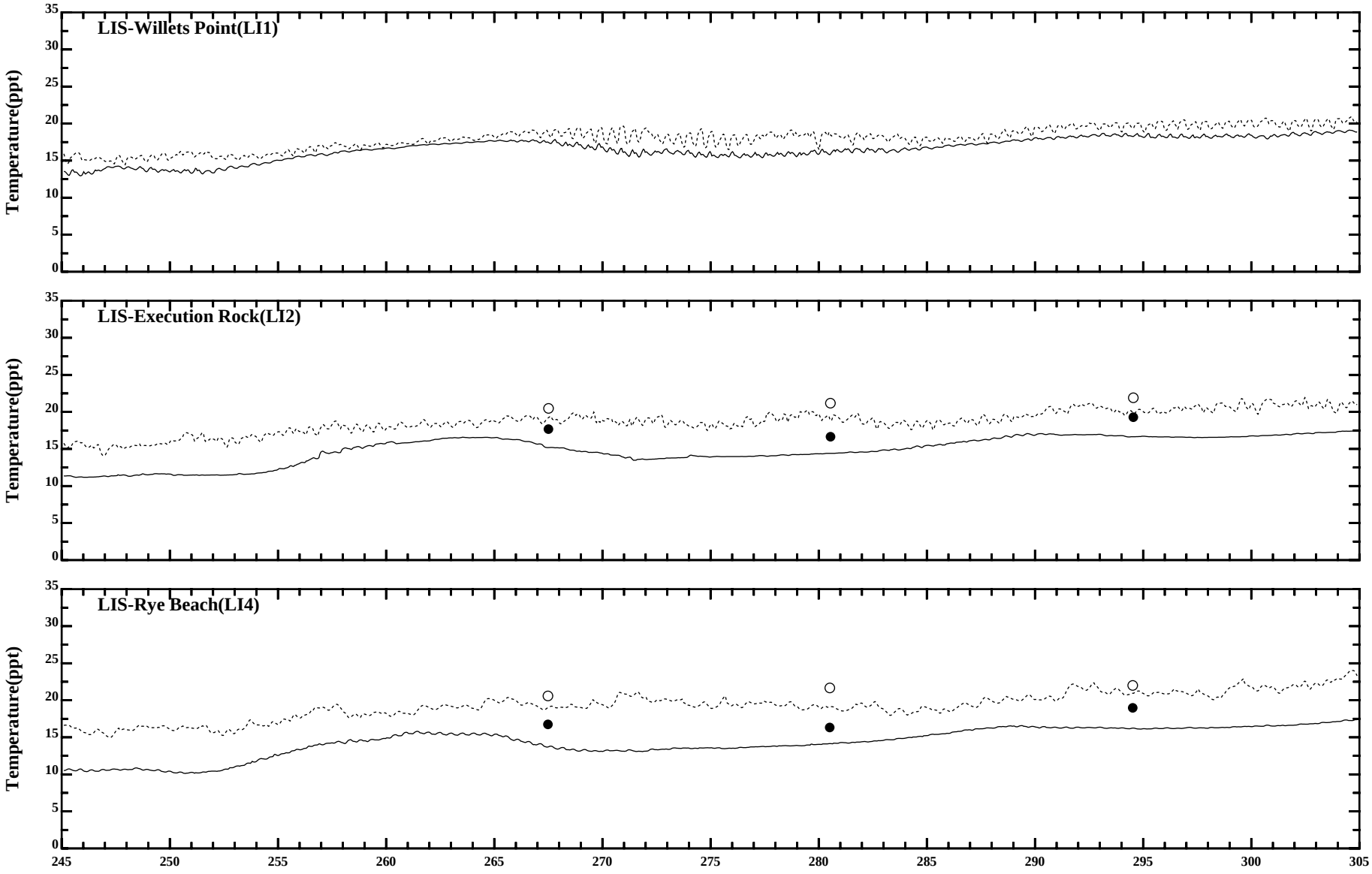

Comparison of Instantaneous Surface and Bottom Temperature

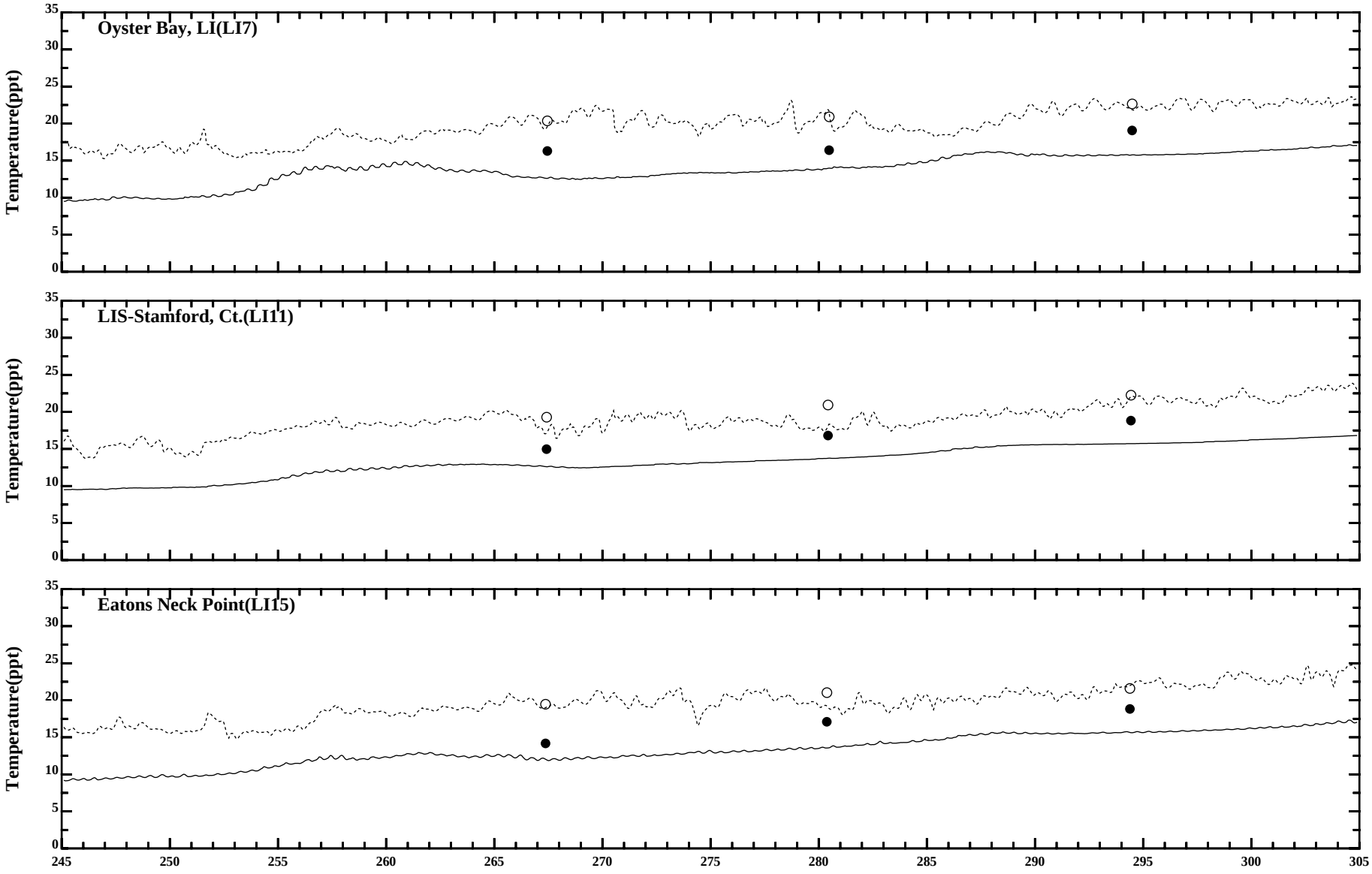

Comparison of Instantaneous Surface and Bottom Temperature

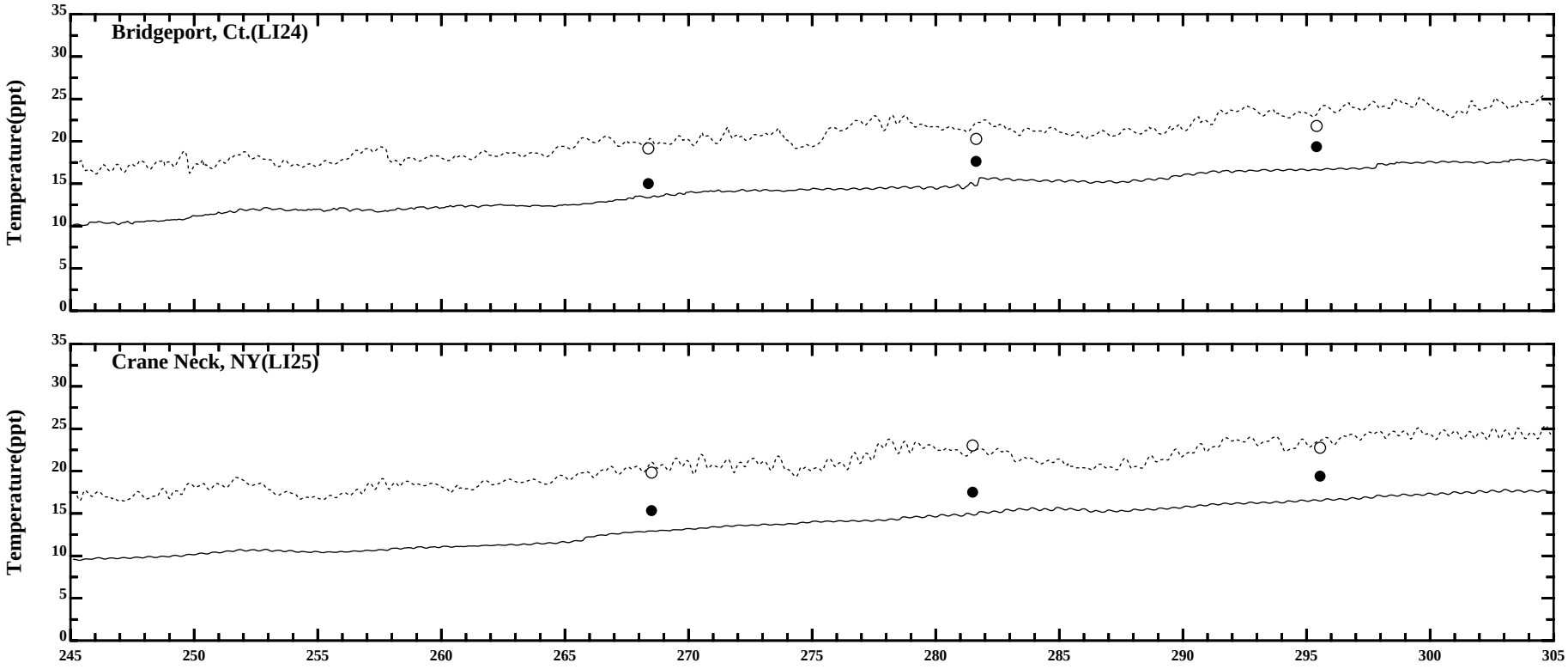

Comparison of Instantaneous Surface and Bottom Temperature

/erie1/hrfo0010/HYDRORUNS/CARP9899/PLOTS/TANDS/temp41

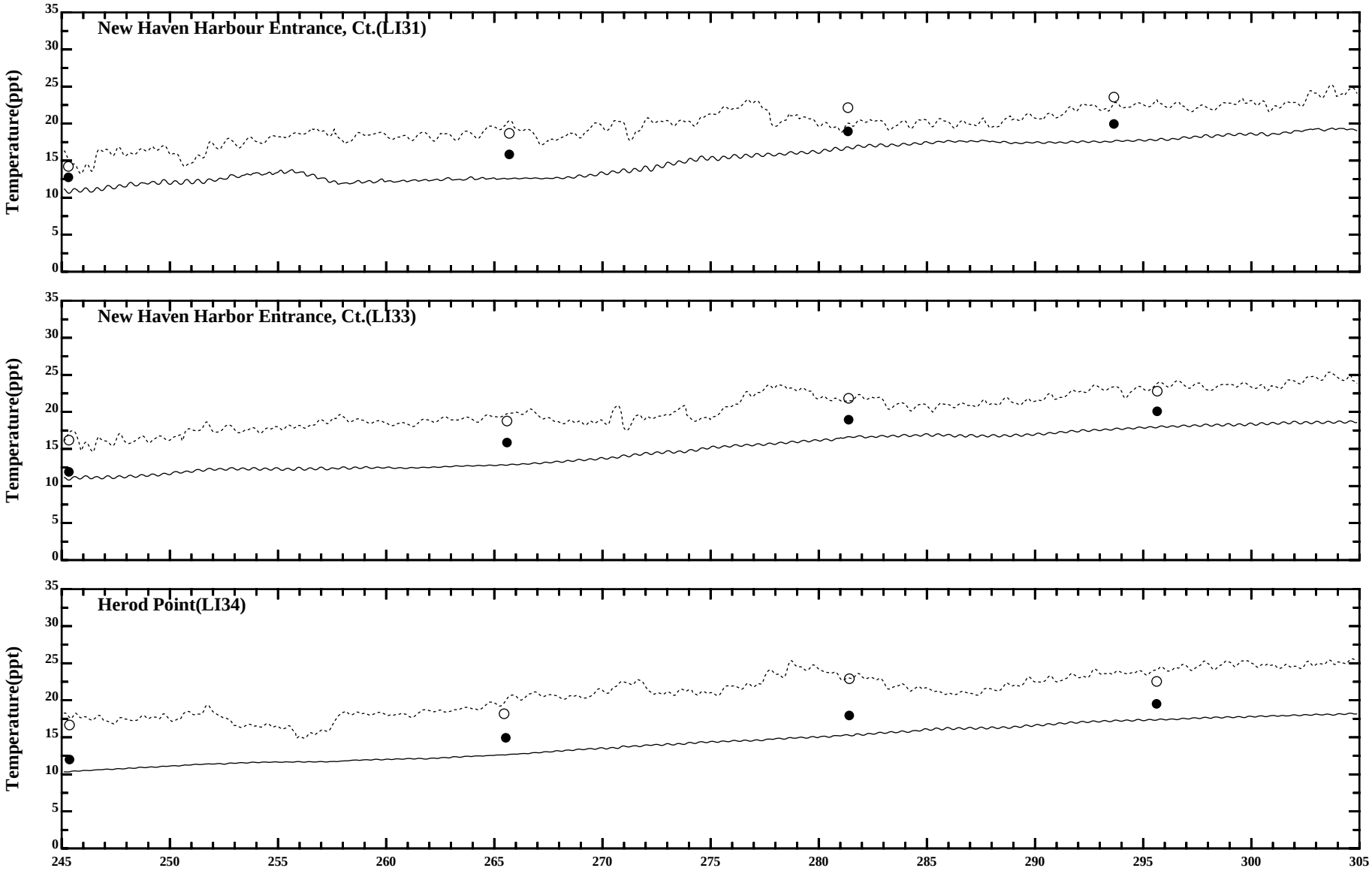

Comparison of Instantaneous Surface and Bottom Temperature

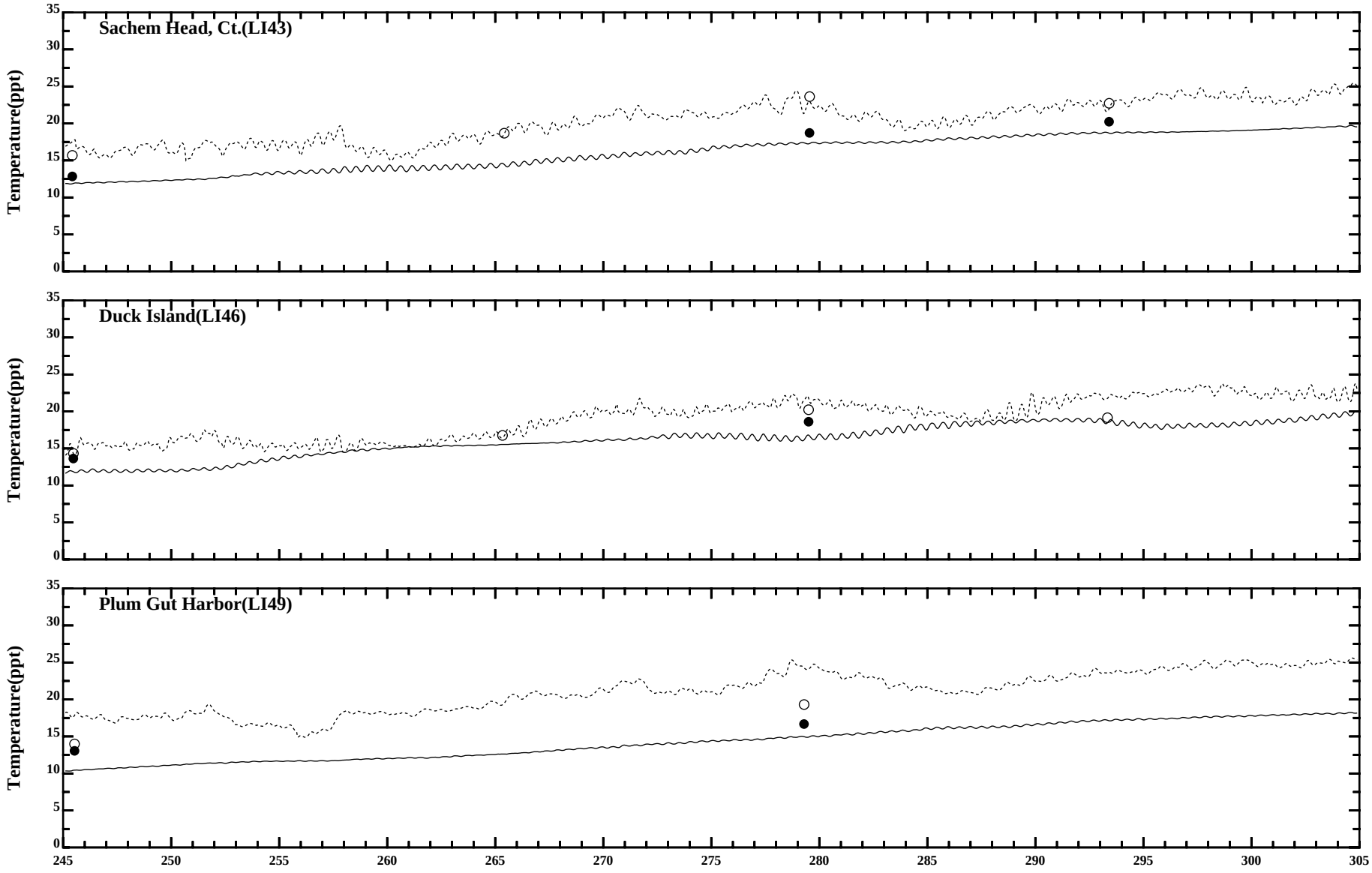

Comparison of Instantaneous Surface and Bottom Temperature

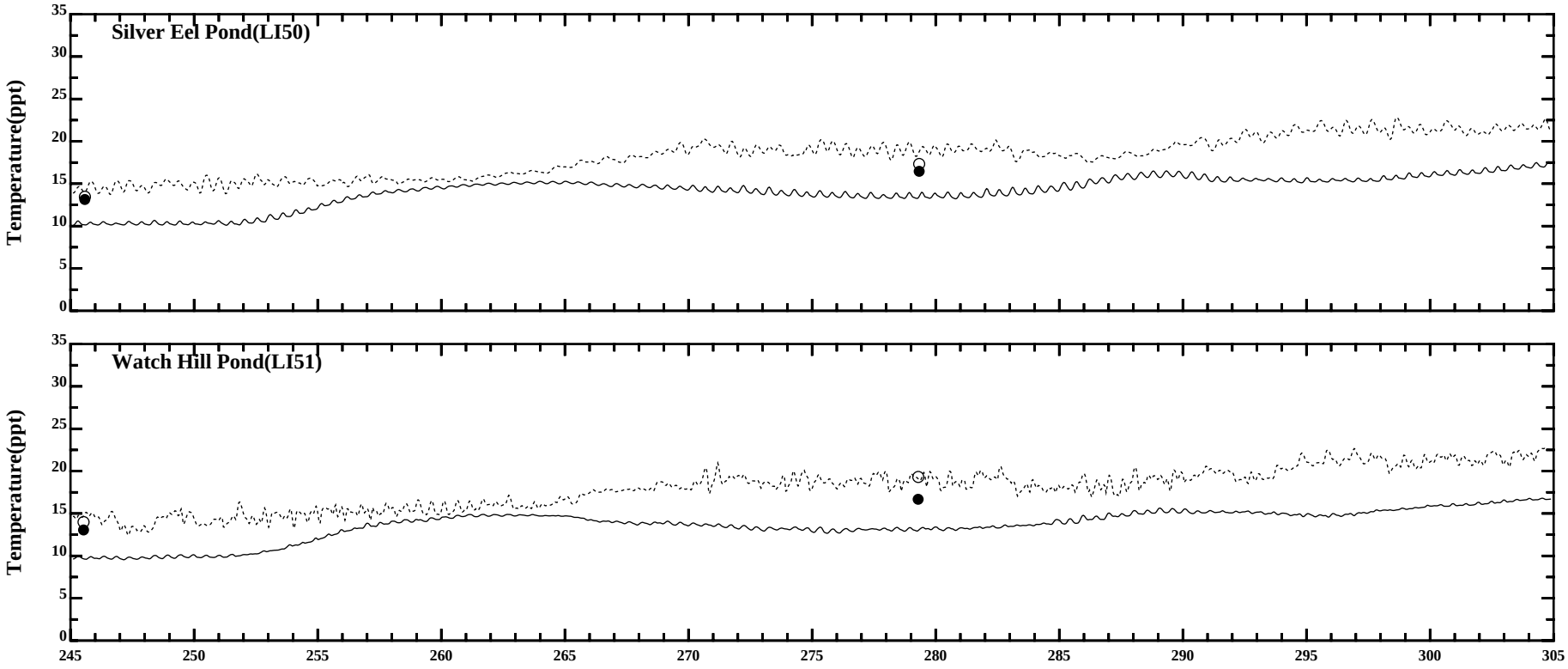

Comparison of Instantaneous Surface and Bottom Temperature

/erie1/hrfo0010/HYDRORUNS/CARP9899/PLOTS/TANDS/temp41

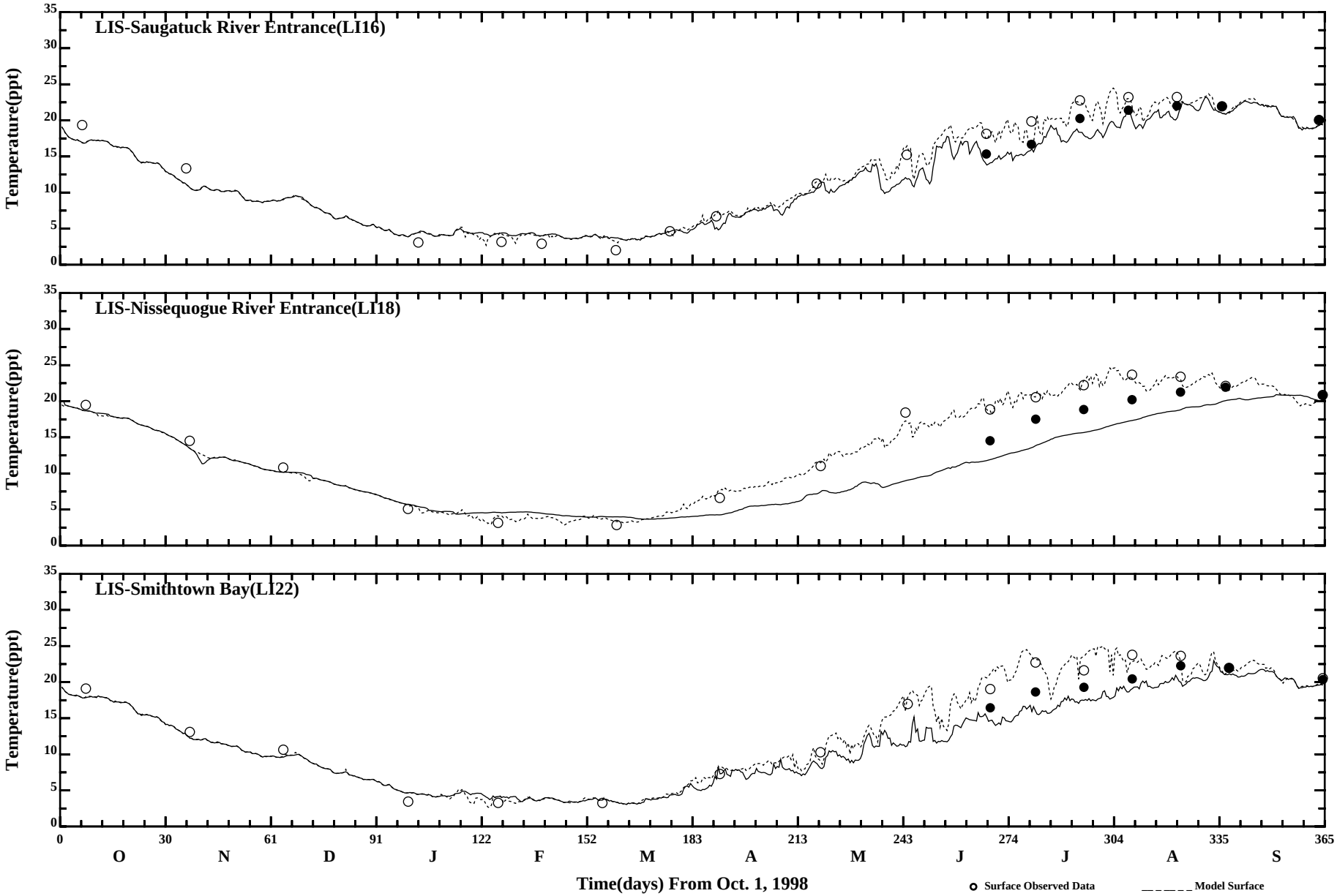

Comparison of 34 Hour Lowpass Surface and Bottom Temperature

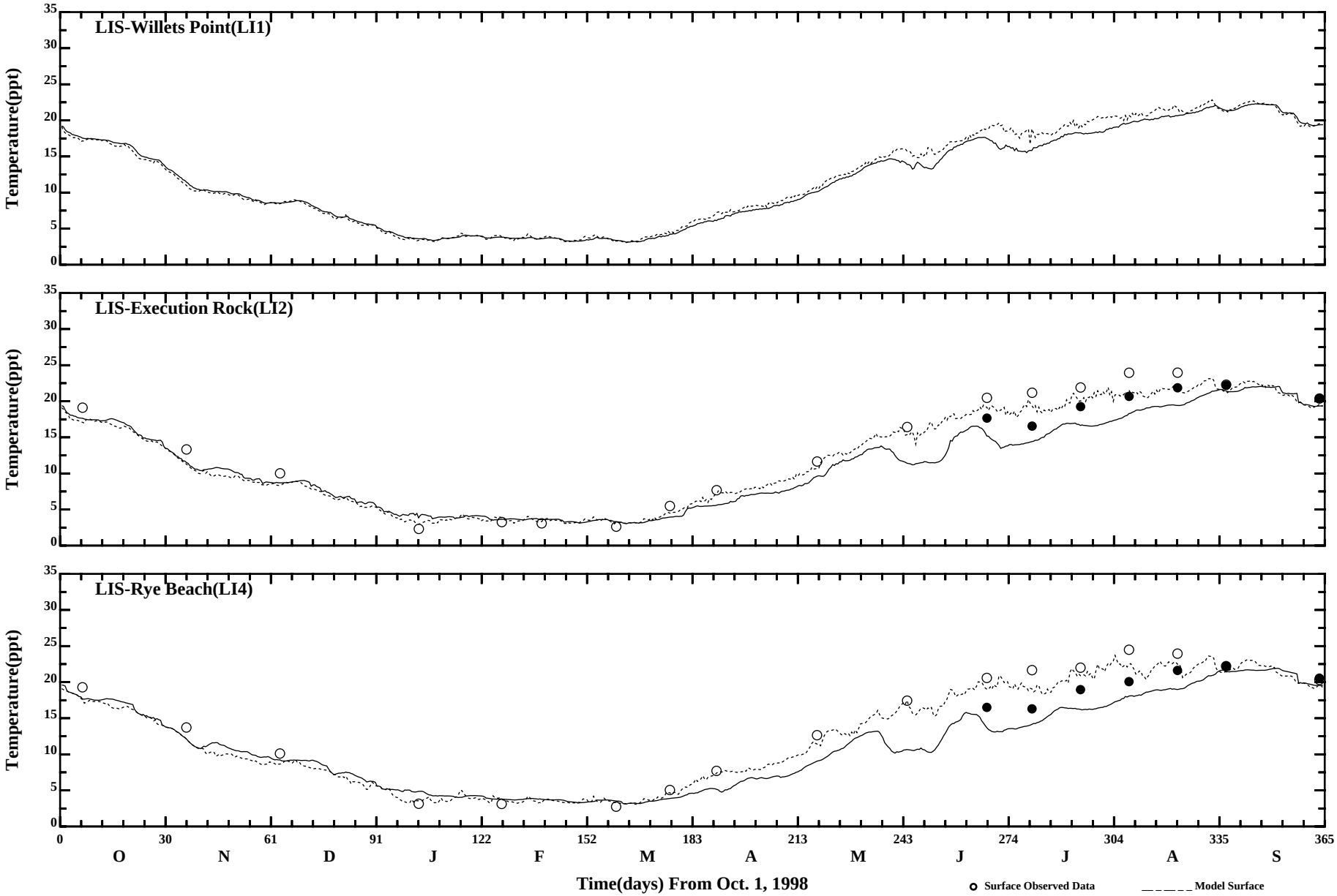

Comparison of 34 Hour Lowpass Surface and Bottom Temperature

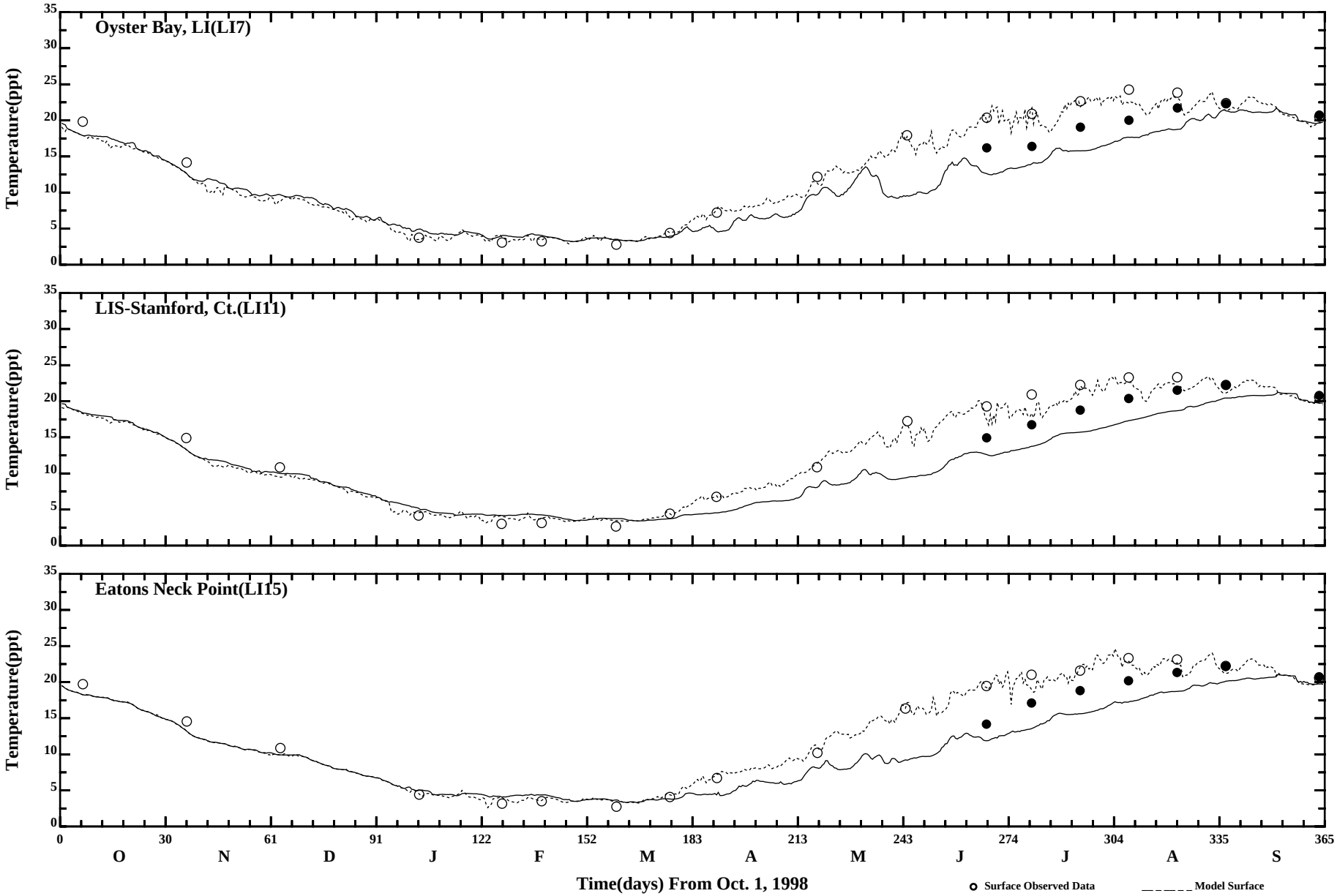

Comparison of 34 Hour Lowpass Surface and Bottom Temperature

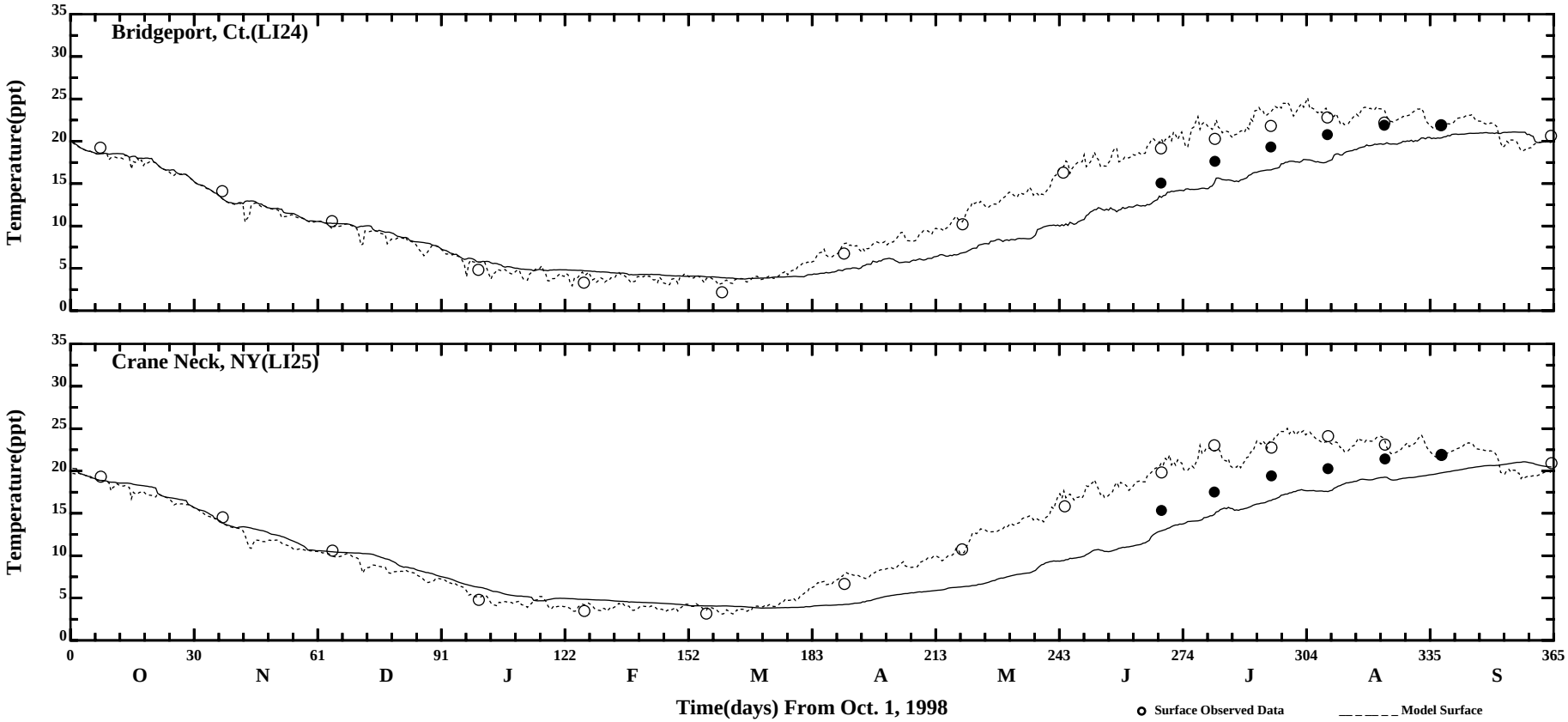

Comparison of 34 Hour Lowpass Surface and Bottom Temperature

/erie1/hrfo0010/HYDRORUNS/CARP9899/PLOTS/TANDS/ptemp41_34hlp

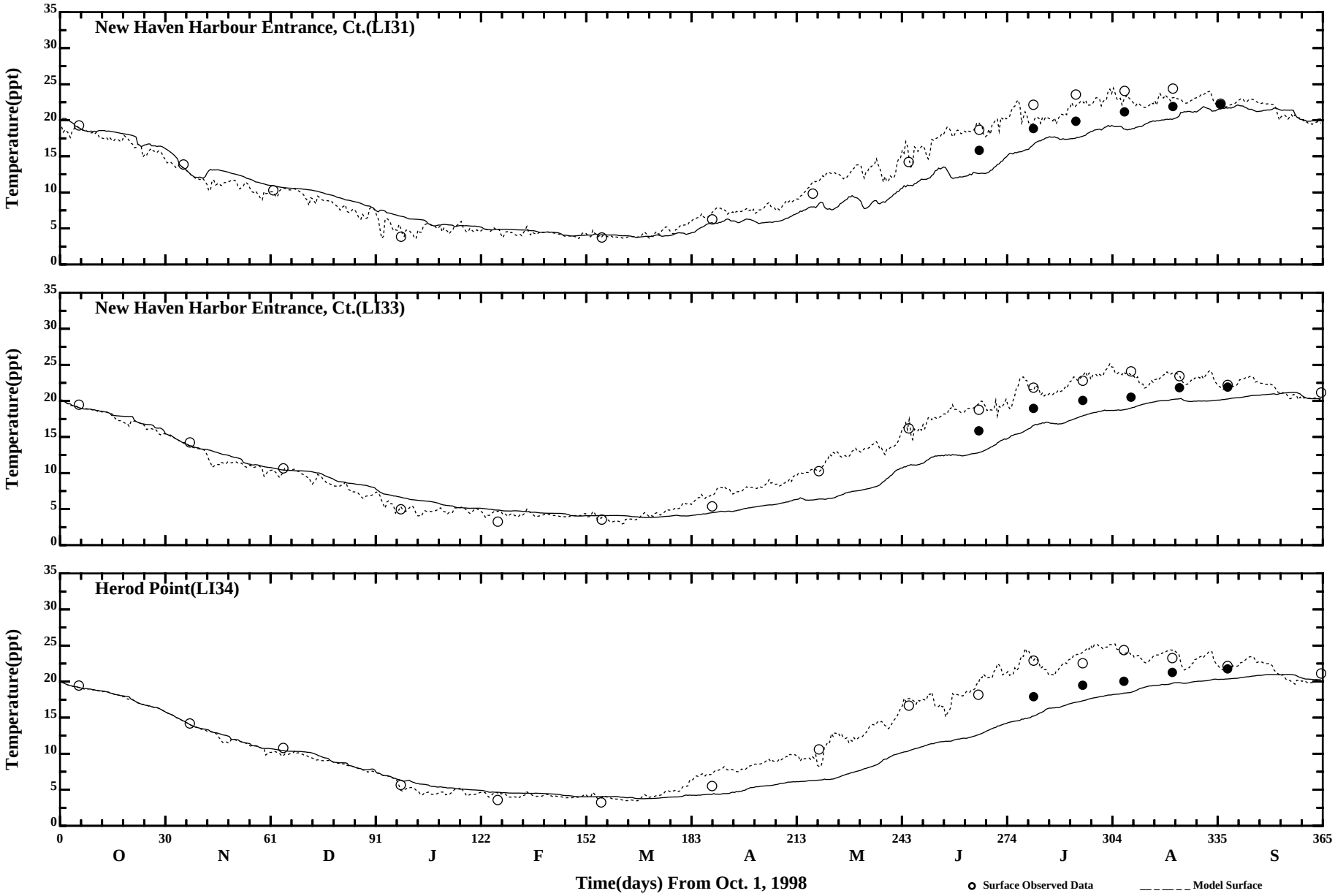

Comparison of 34 Hour Lowpass Surface and Bottom Temperature

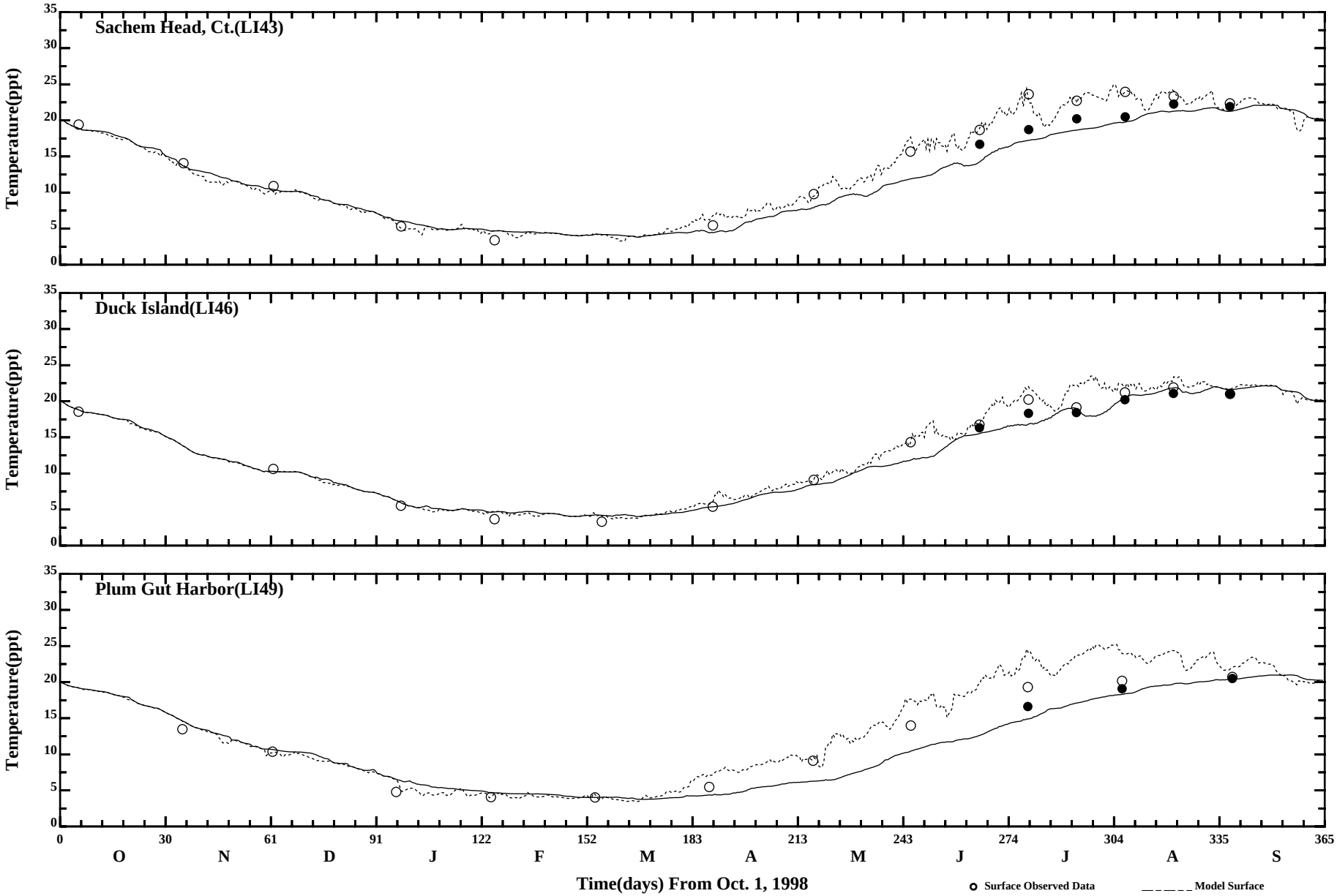

Comparison of 34 Hour Lowpass Surface and Bottom Temperature

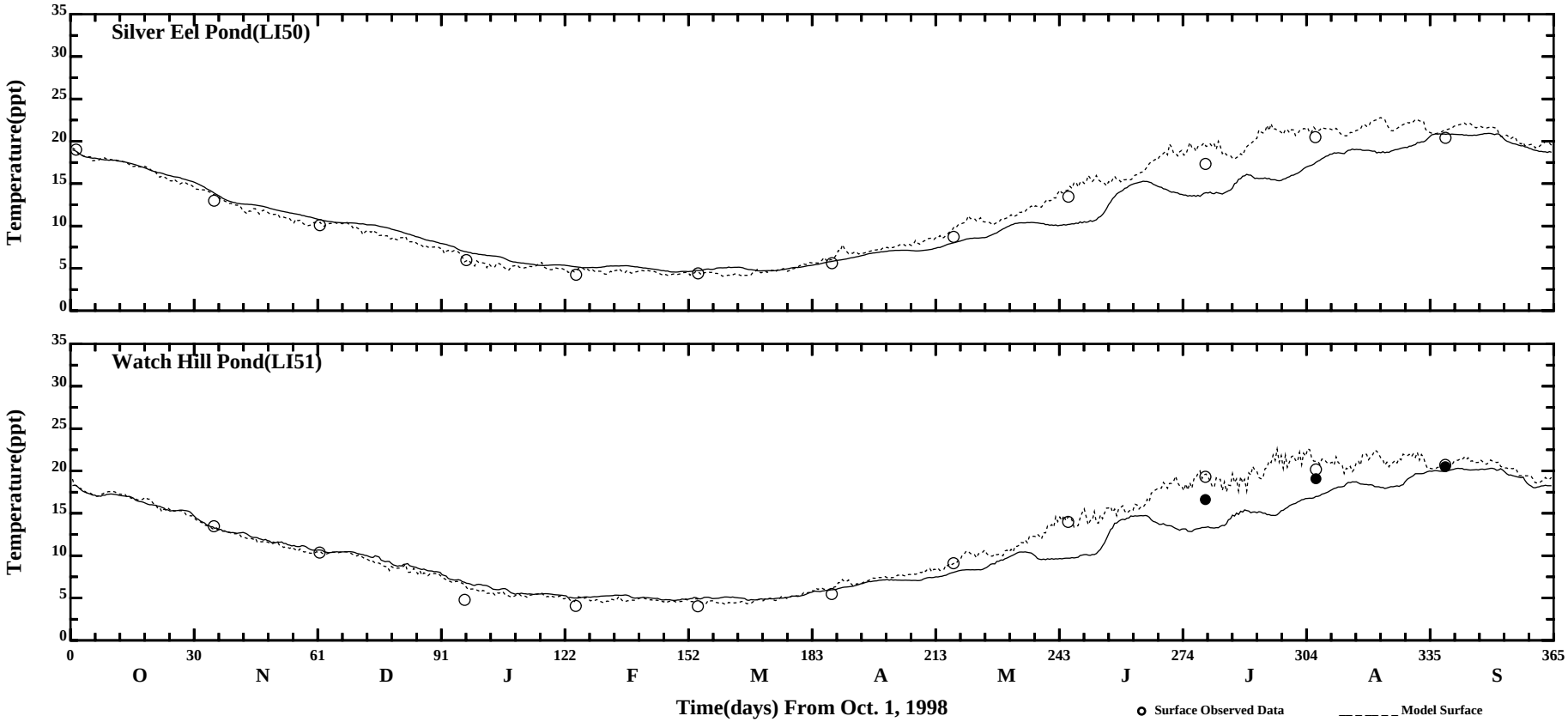

Comparison of 34 Hour Lowpass Surface and Bottom Temperature

/erie1/hrfo0010/HYDRORUNS/CARP9899/PLOTS/TANDS/ptemp41_34hlp

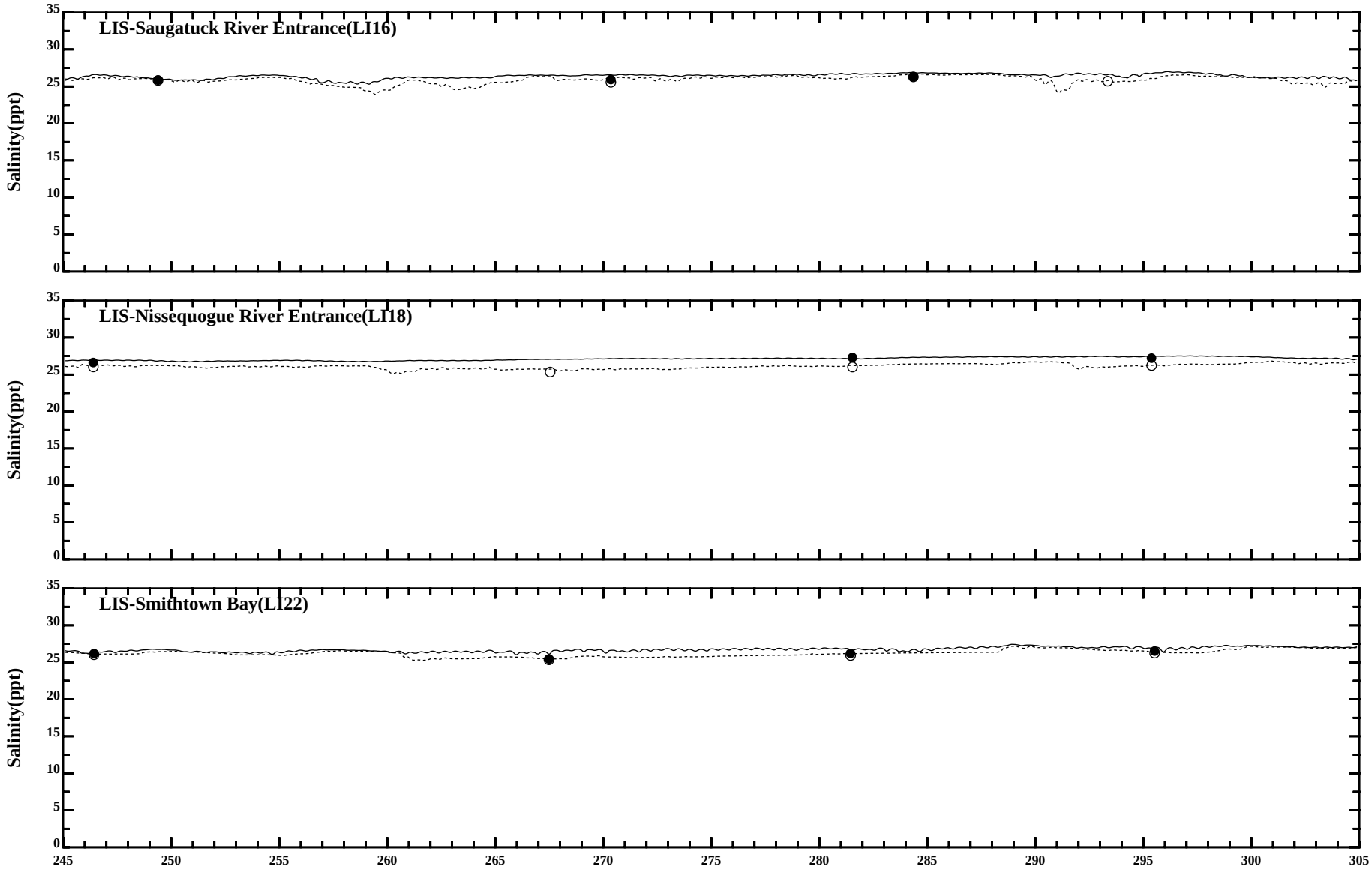

Comparison of Instantaneous Surface and Bottom Salinity

DATE: 8/02/2004 TIME: 12: 7: 8

/erie1/hrfo0010/HYDRORUNS/CARP9900/PLOTS/TANDS/salt41

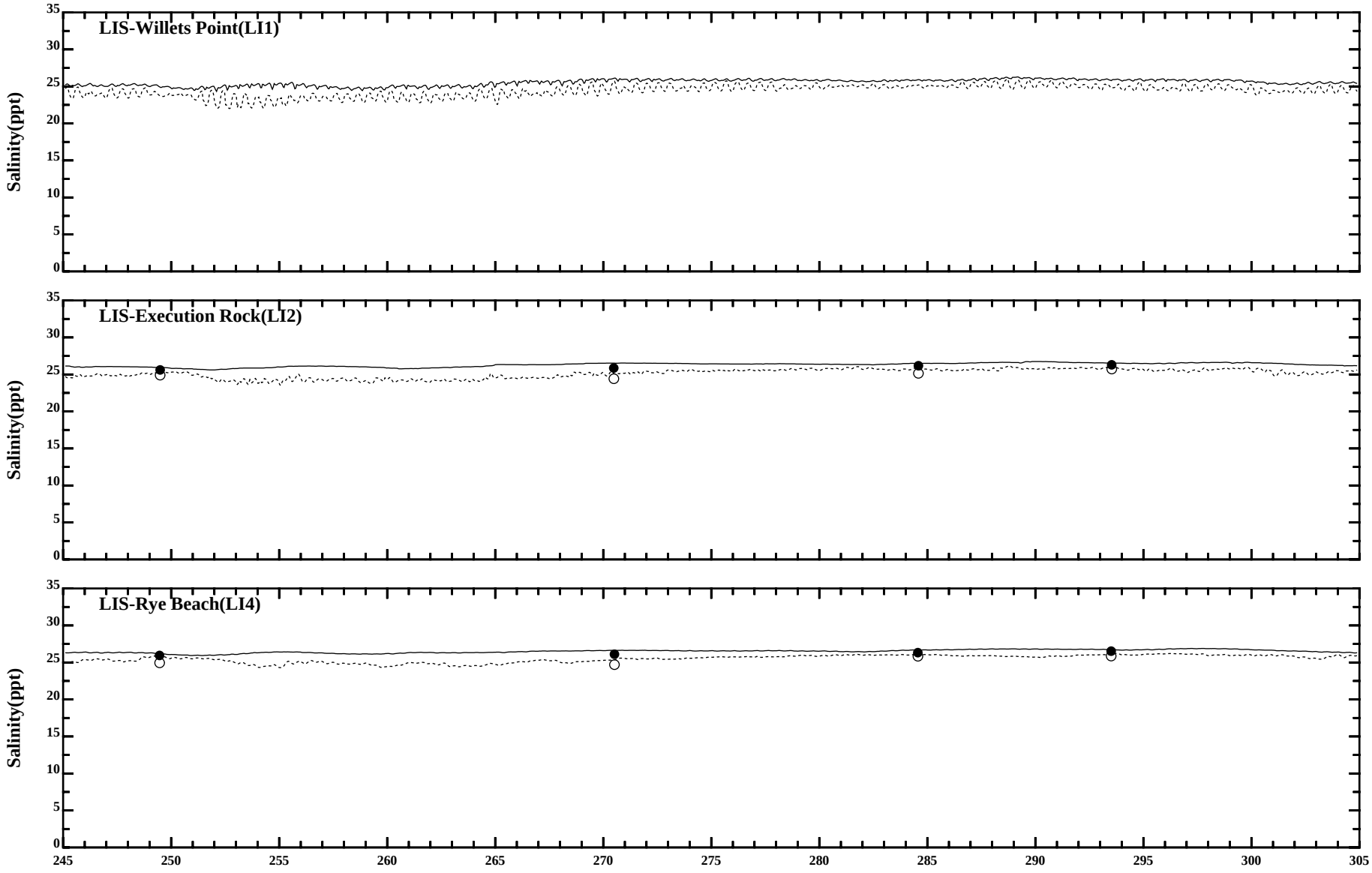

Comparison of Instantaneous Surface and Bottom Salinity

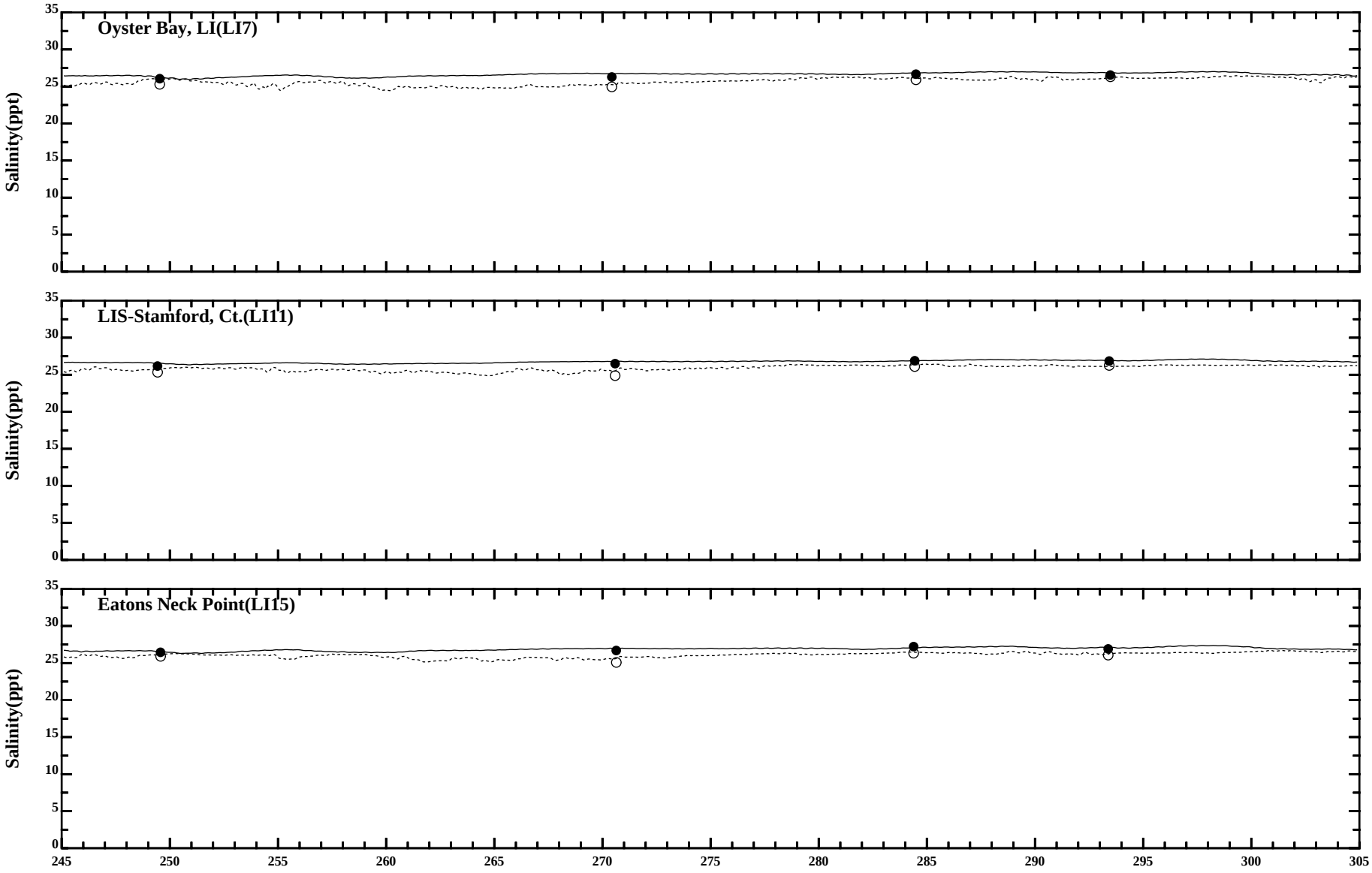

Comparison of Instantaneous Surface and Bottom Salinity

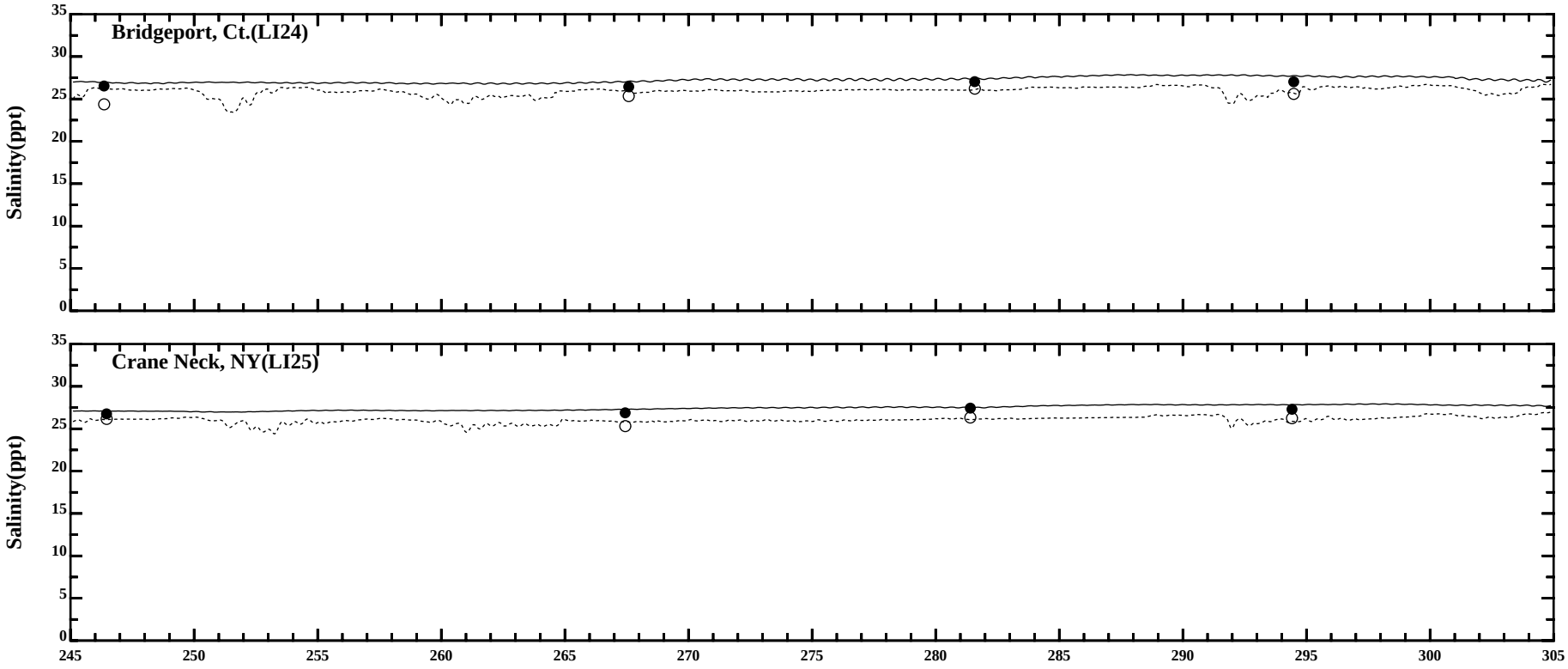

Comparison of Instantaneous Surface and Bottom Salinity

/erie1/hrfo0010/HYDRORUNS/CARP9900/PLOTS/TANDS/salt41

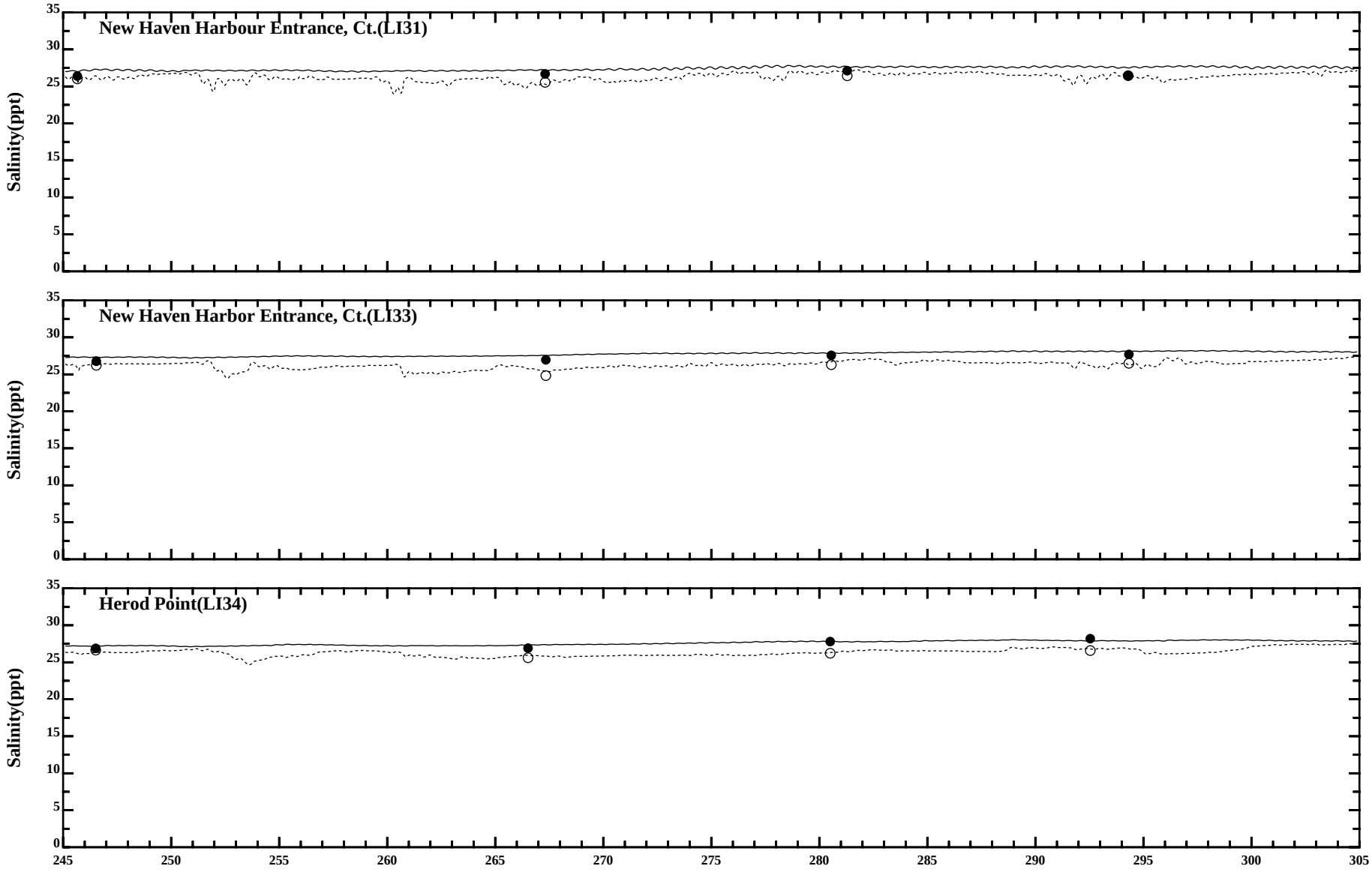

Comparison of Instantaneous Surface and Bottom Salinity

DATE: 8/02/2004 TIME: 12: 7: 8

/erie1/hrfo0010/HYDRORUNS/CARP9900/PLOTS/TANDS/salt41

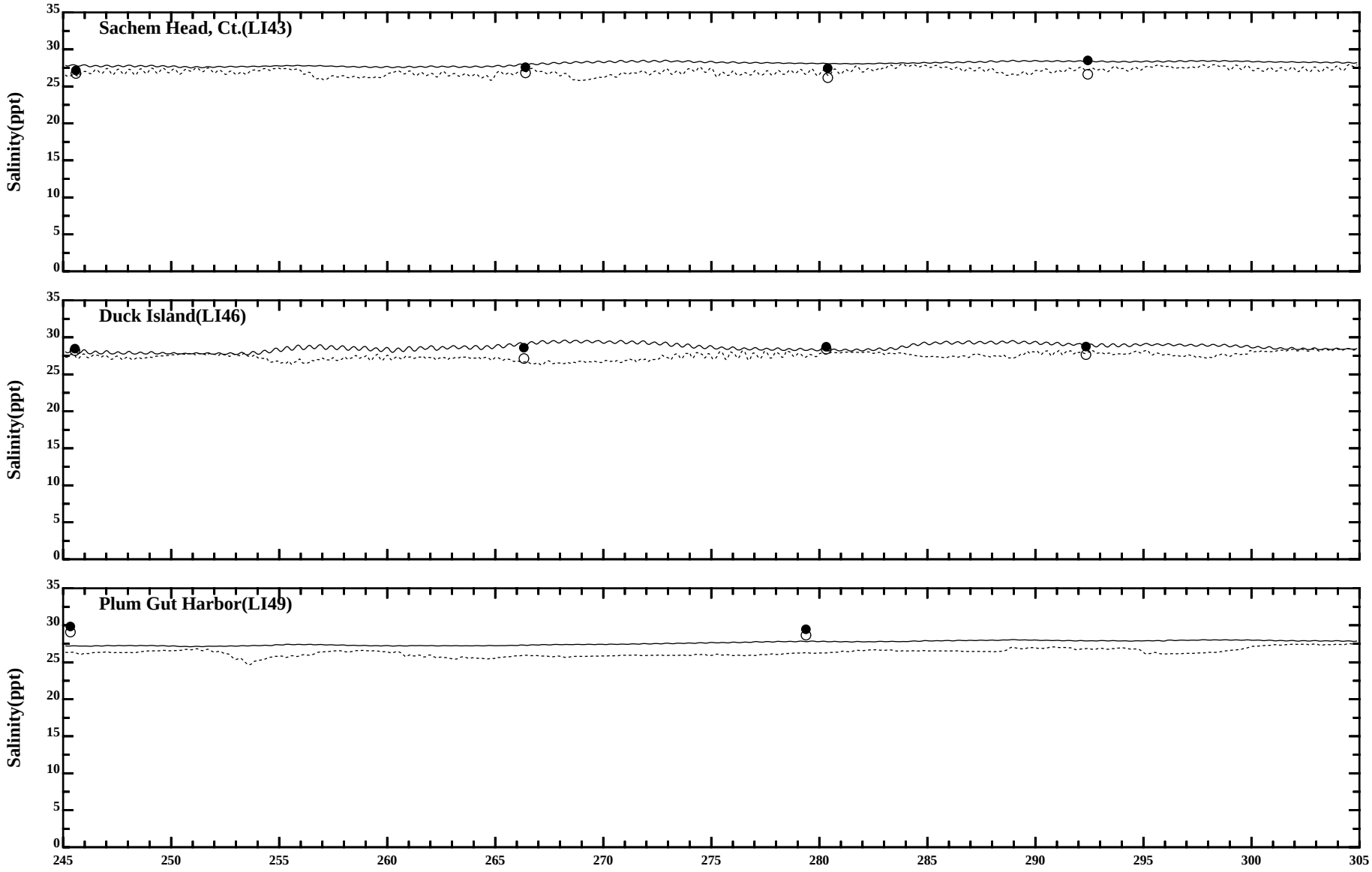

Comparison of Instantaneous Surface and Bottom Salinity

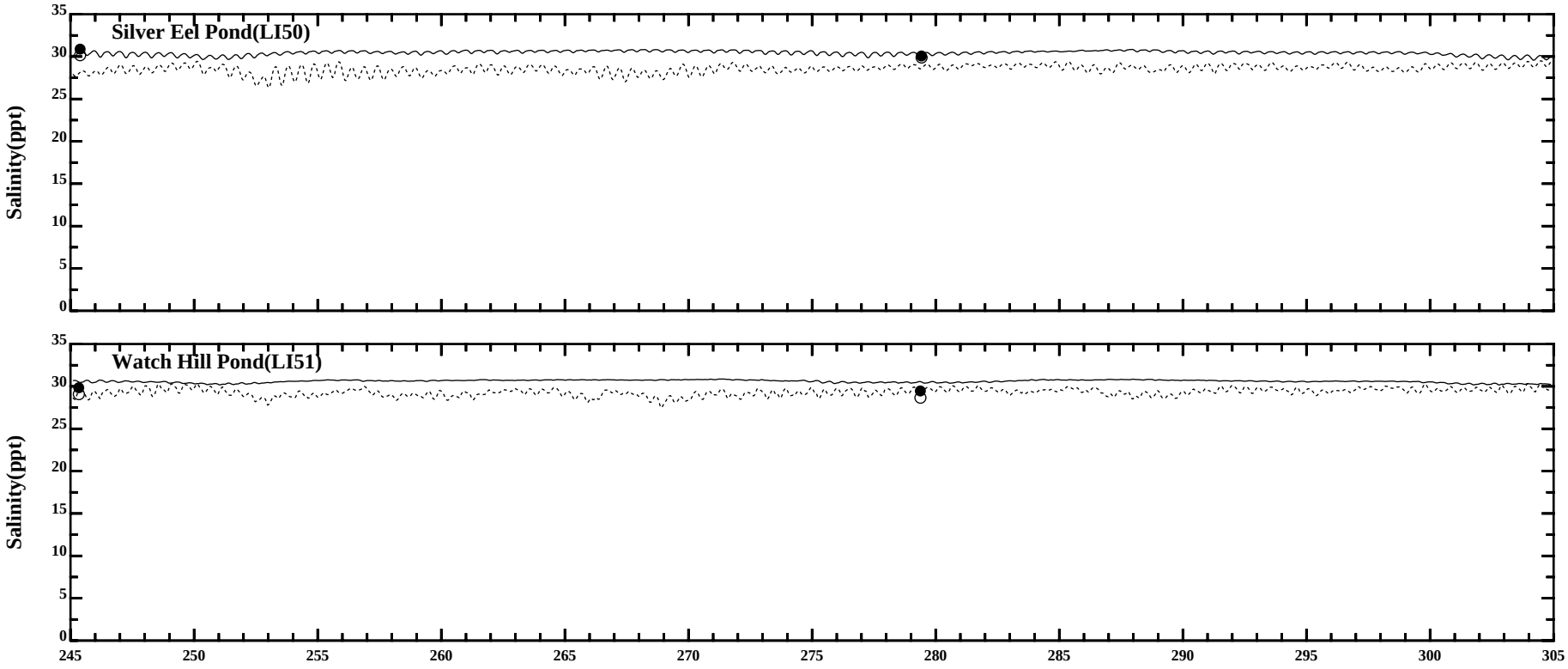

Comparison of Instantaneous Surface and Bottom Salinity

Page:7/7

/erie1/hrfo0010/HYDRORUNS/CARP9900/PLOTS/TANDS/salt41

DATE: 8/02/2004 TIME: 12: 7: 8

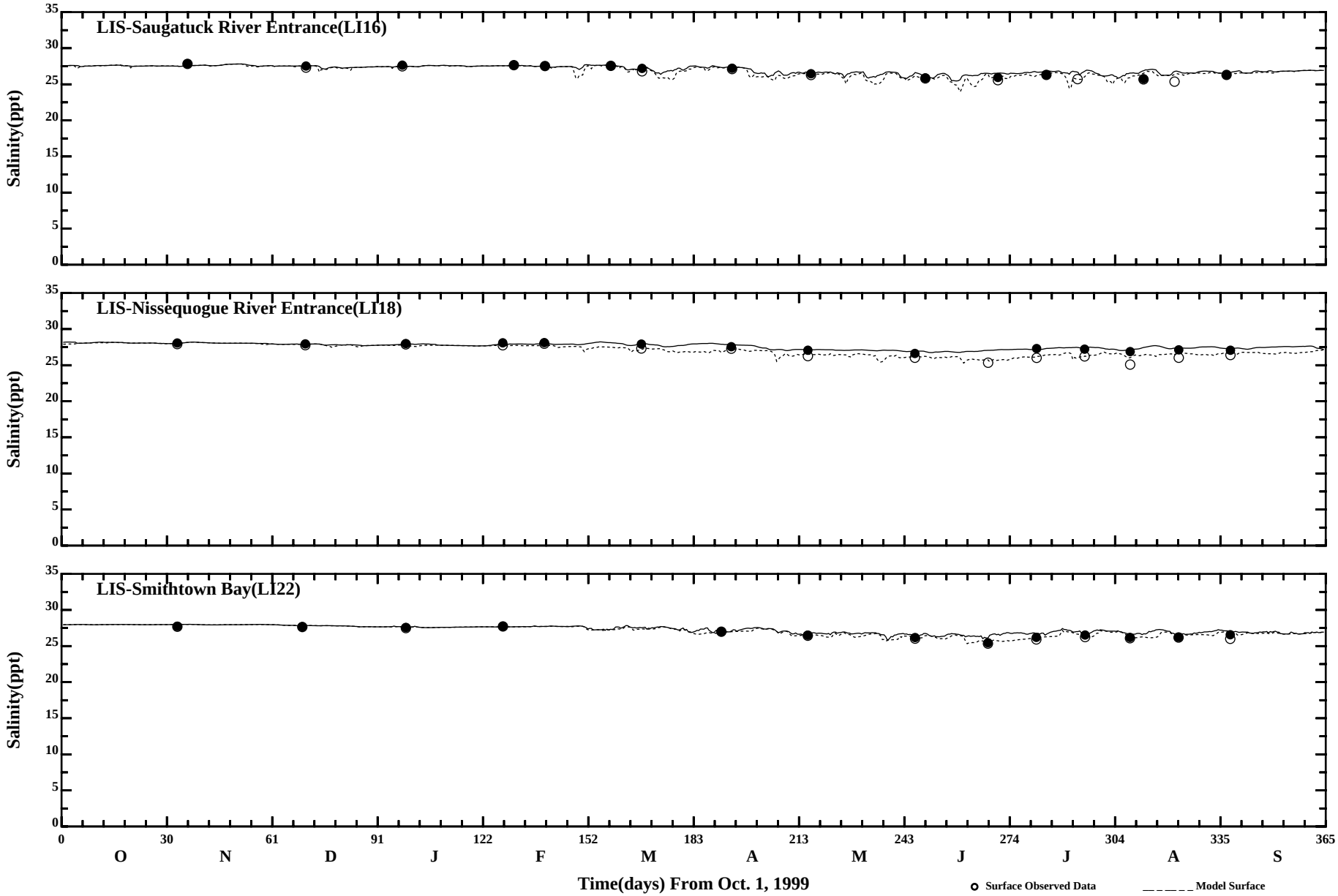

Comparison of 34 Hour Lowpass Surface and Bottom Salinity

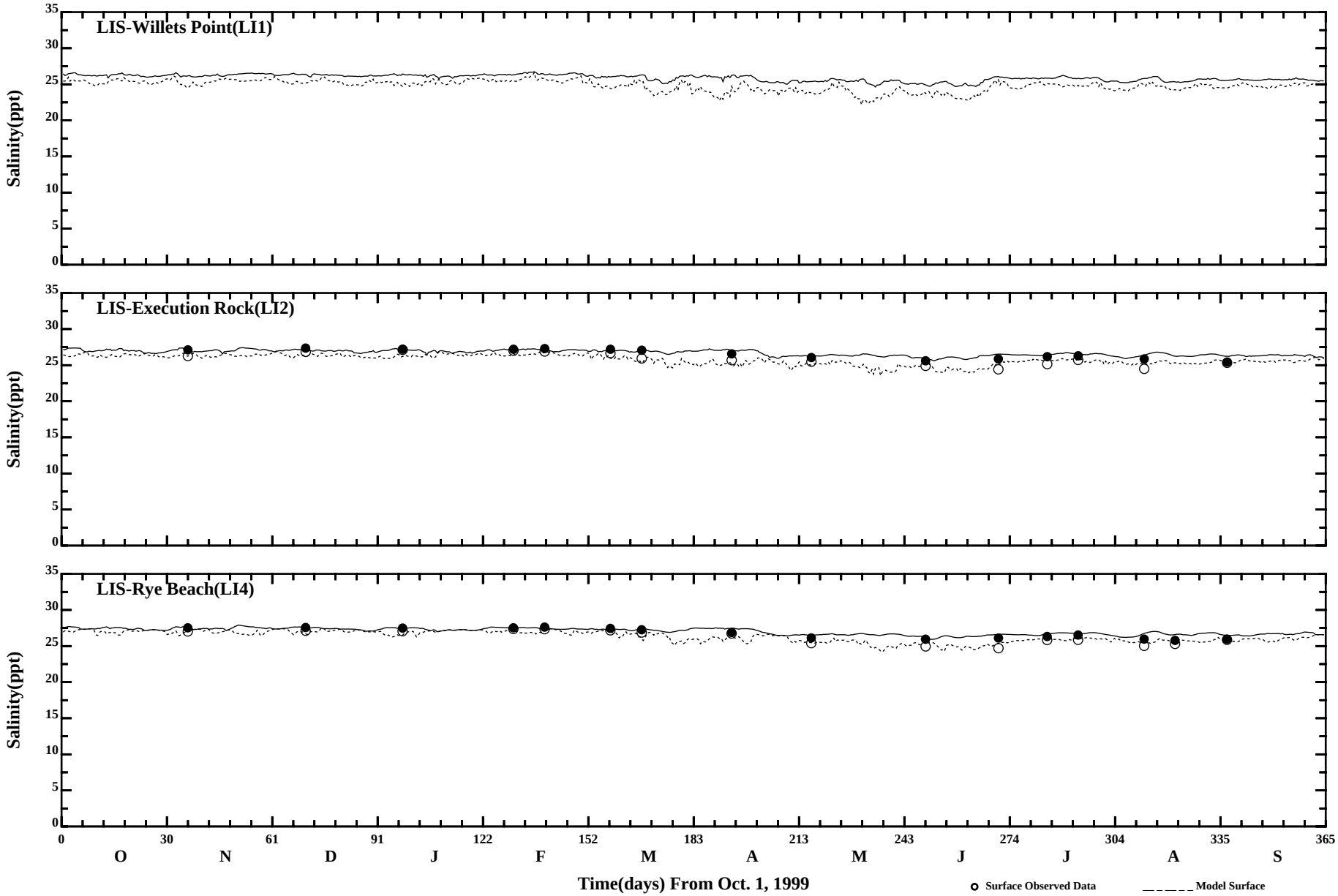

Comparison of 34 Hour Lowpass Surface and Bottom Salinity

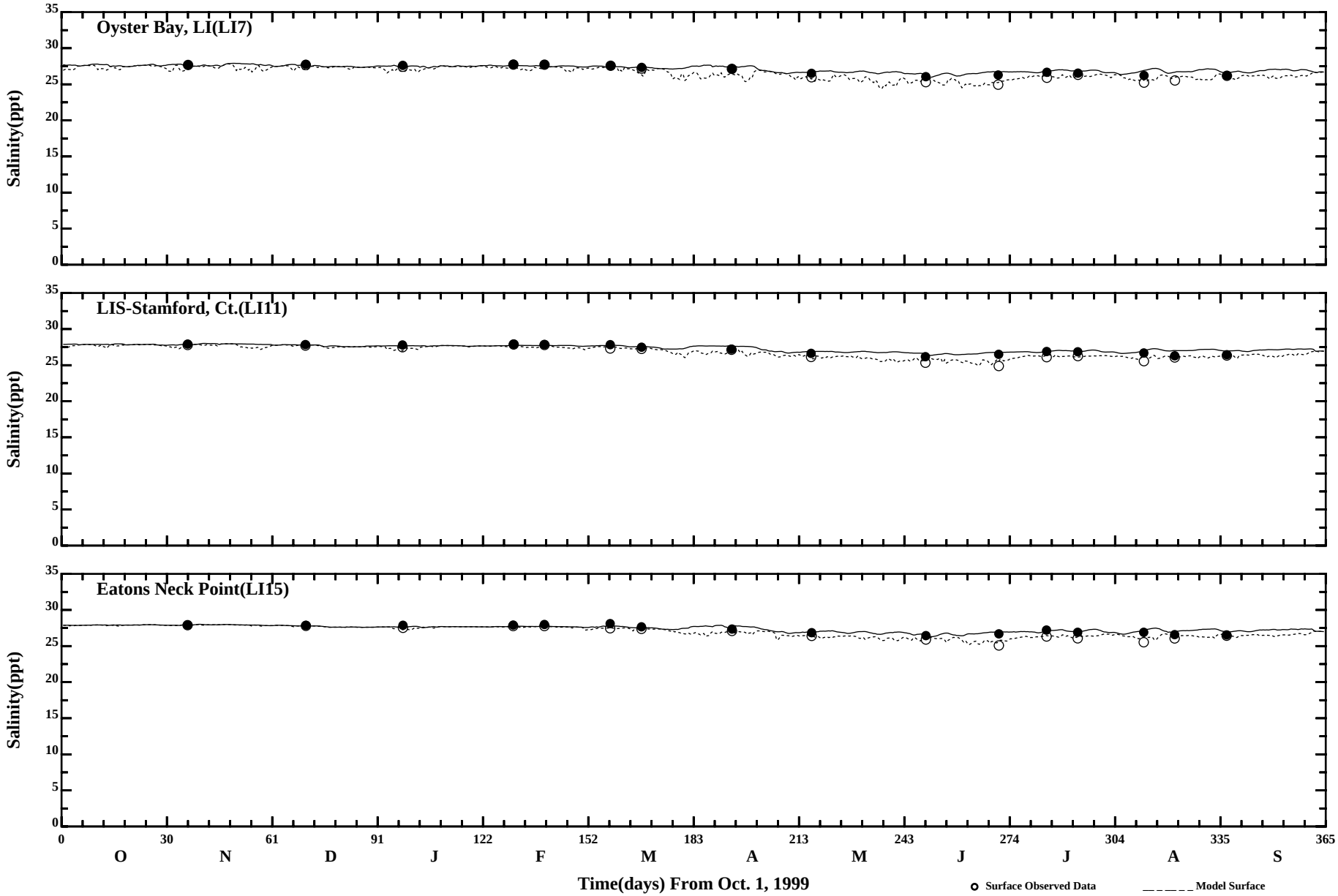

Comparison of 34 Hour Lowpass Surface and Bottom Salinity

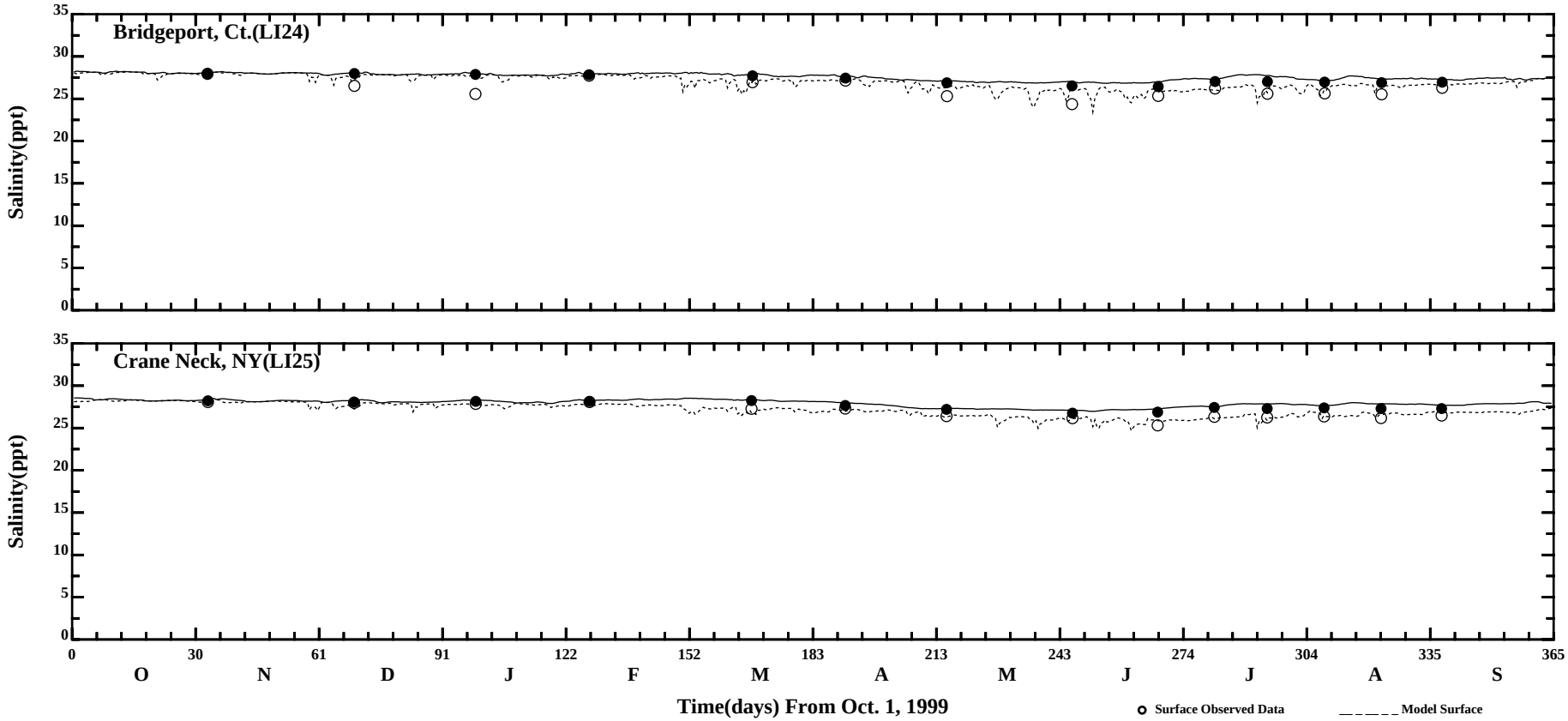

Comparison of 34 Hour Lowpass Surface and Bottom Salinity

/erie1/hrfo0010/HYDRORUNS/CARP9900/PLOTS/TANDS/psalt41_34hlp

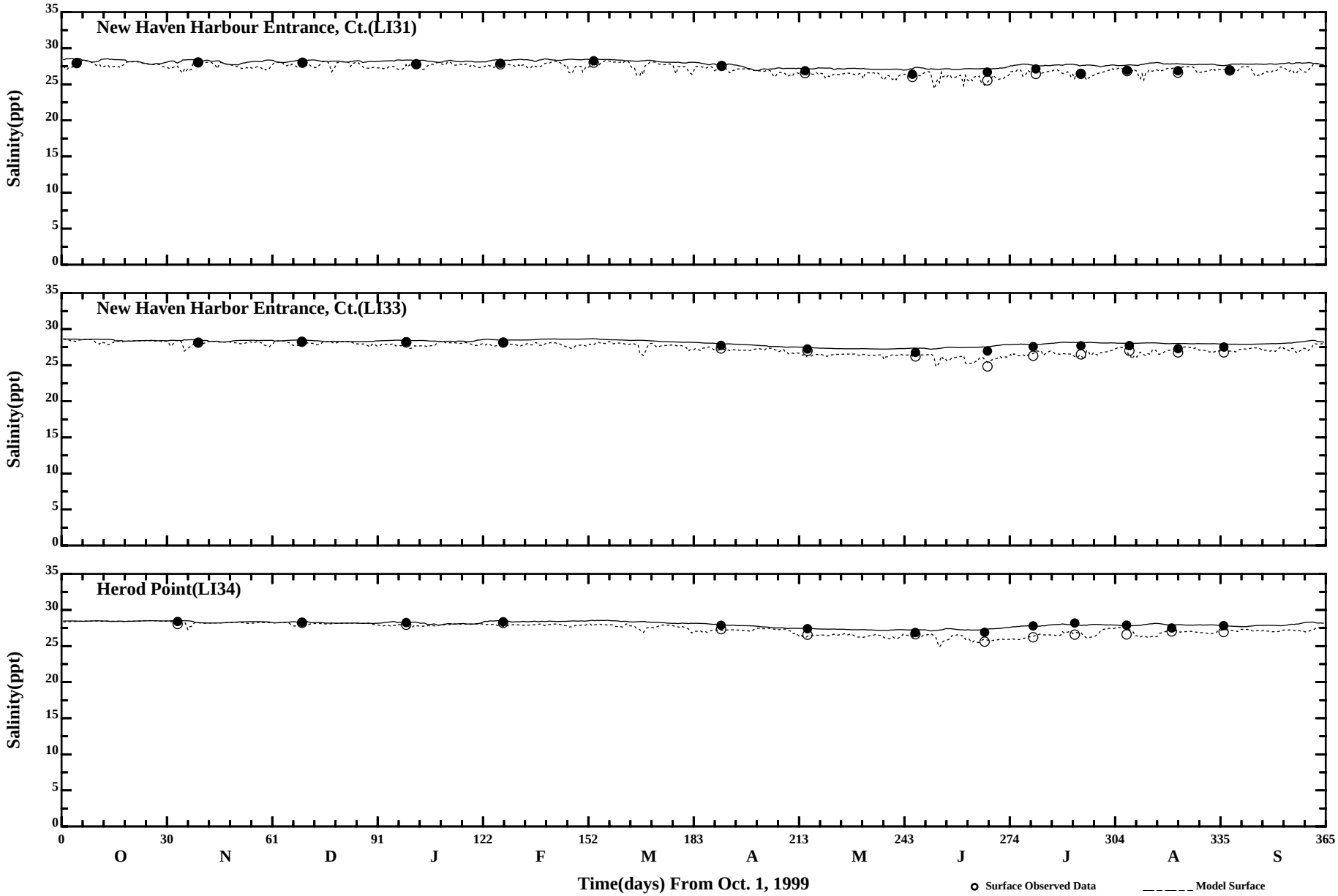

Comparison of 34 Hour Lowpass Surface and Bottom Salinity

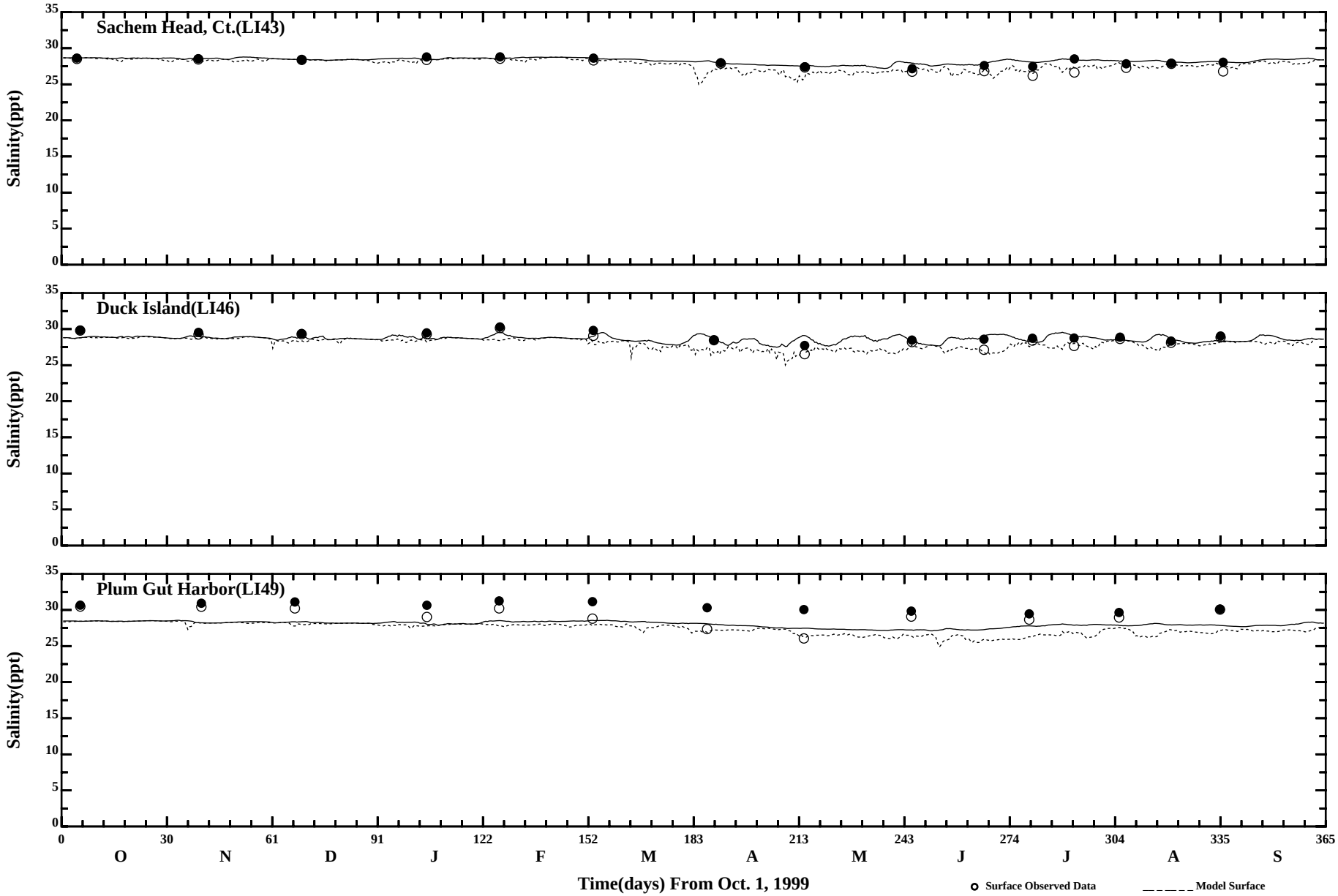

Comparison of 34 Hour Lowpass Surface and Bottom Salinity

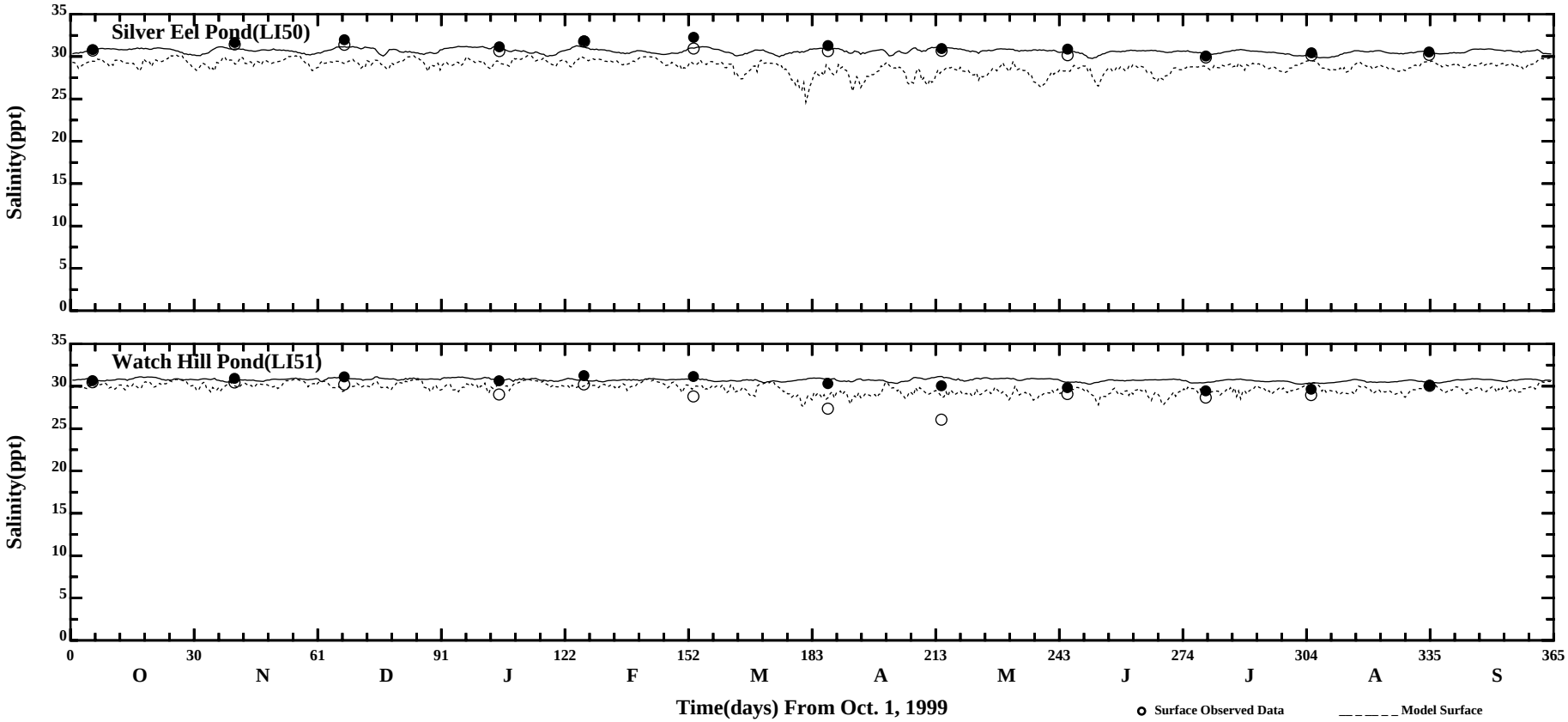

Comparison of 34 Hour Lowpass Surface and Bottom Salinity

/erie1/hrfo0010/HYDRORUNS/CARP9900/PLOTS/TANDS/psalt41_34hlp

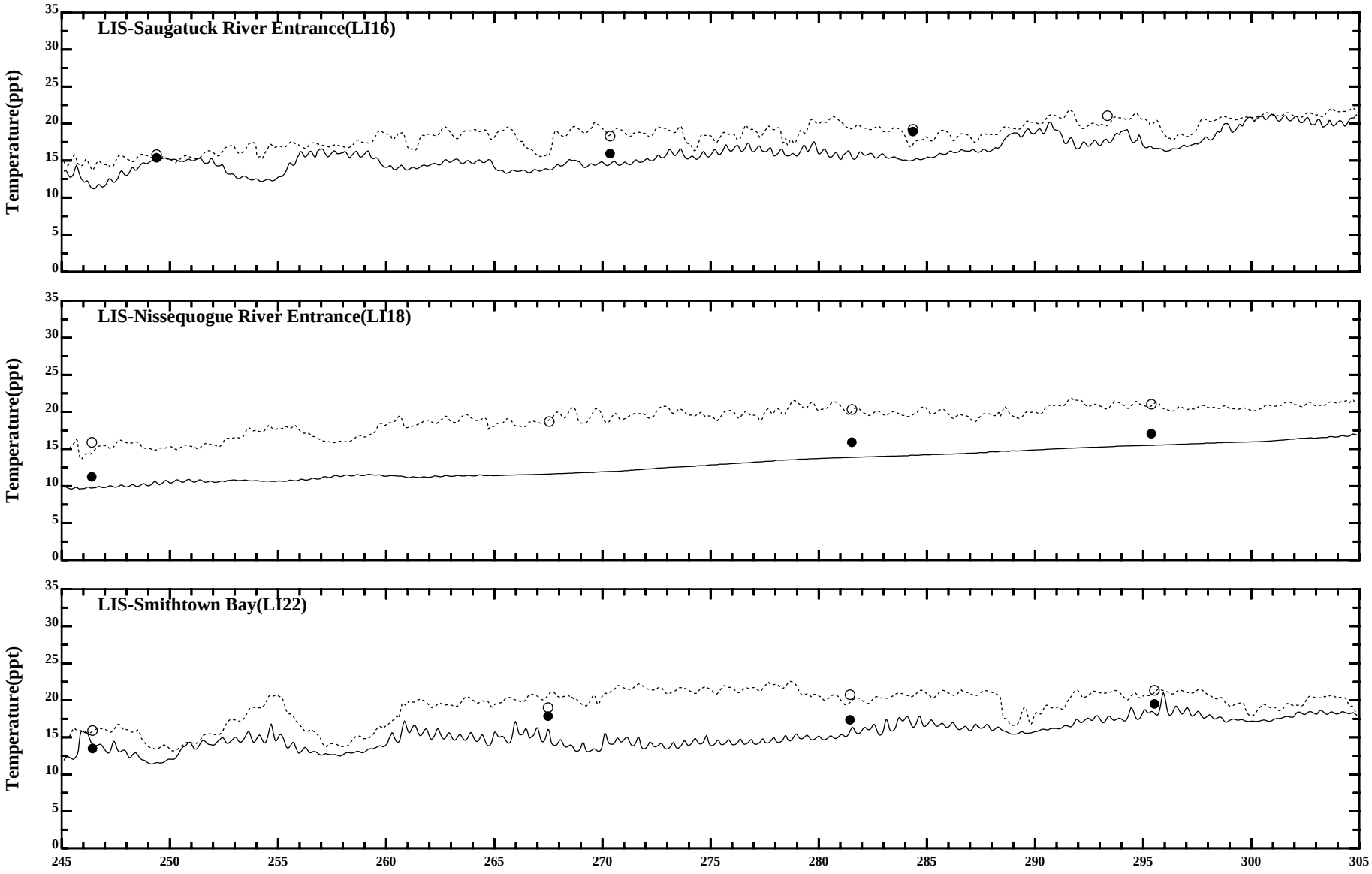

Comparison of Instantaneous Surface and Bottom Temperature

DATE: 8/02/2004 TIME: 12: 6:56

/erie1/hrfo0010/HYDRORUNS/CARP9900/PLOTS/TANDS/temp41

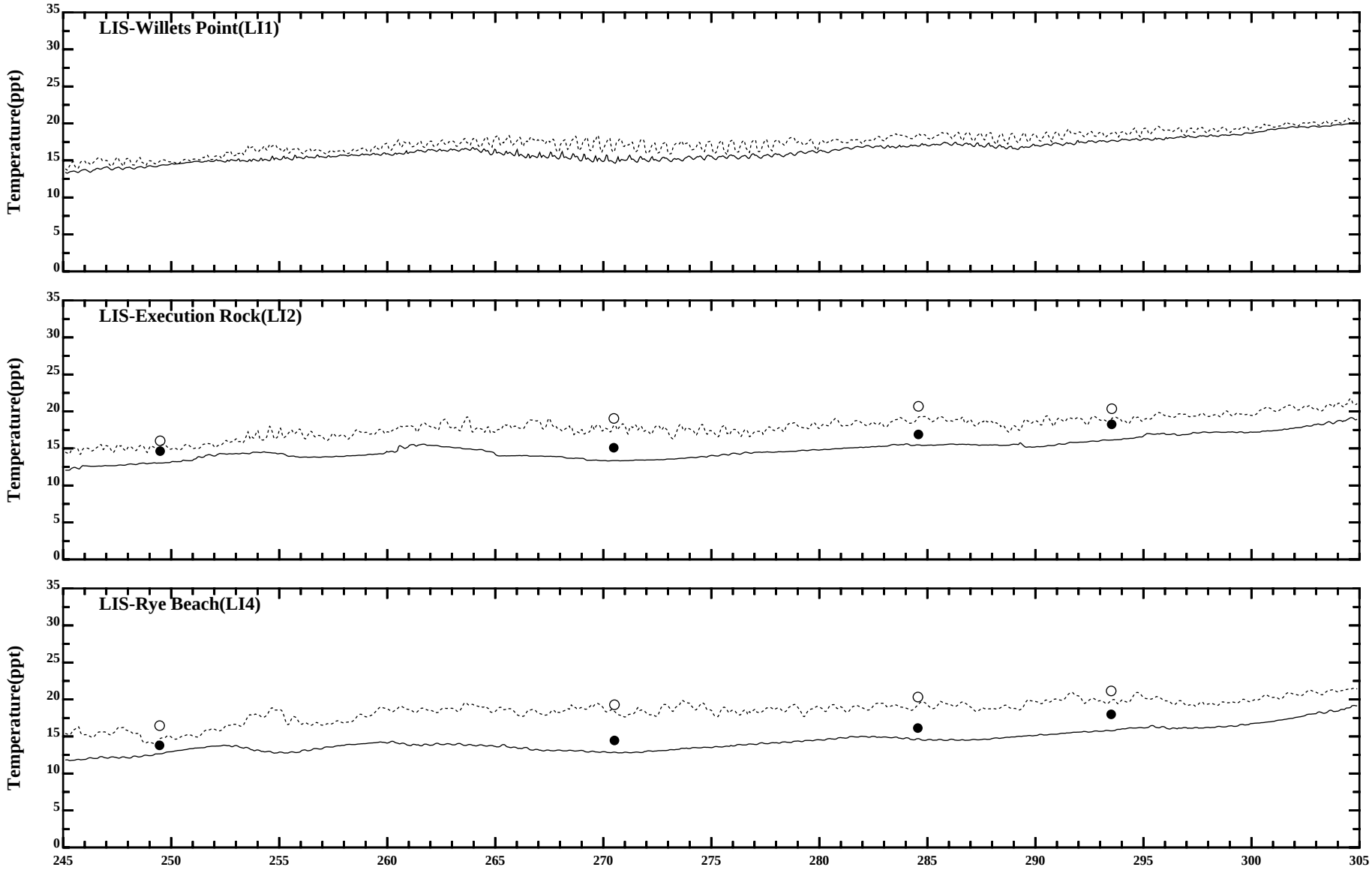

Comparison of Instantaneous Surface and Bottom Temperature

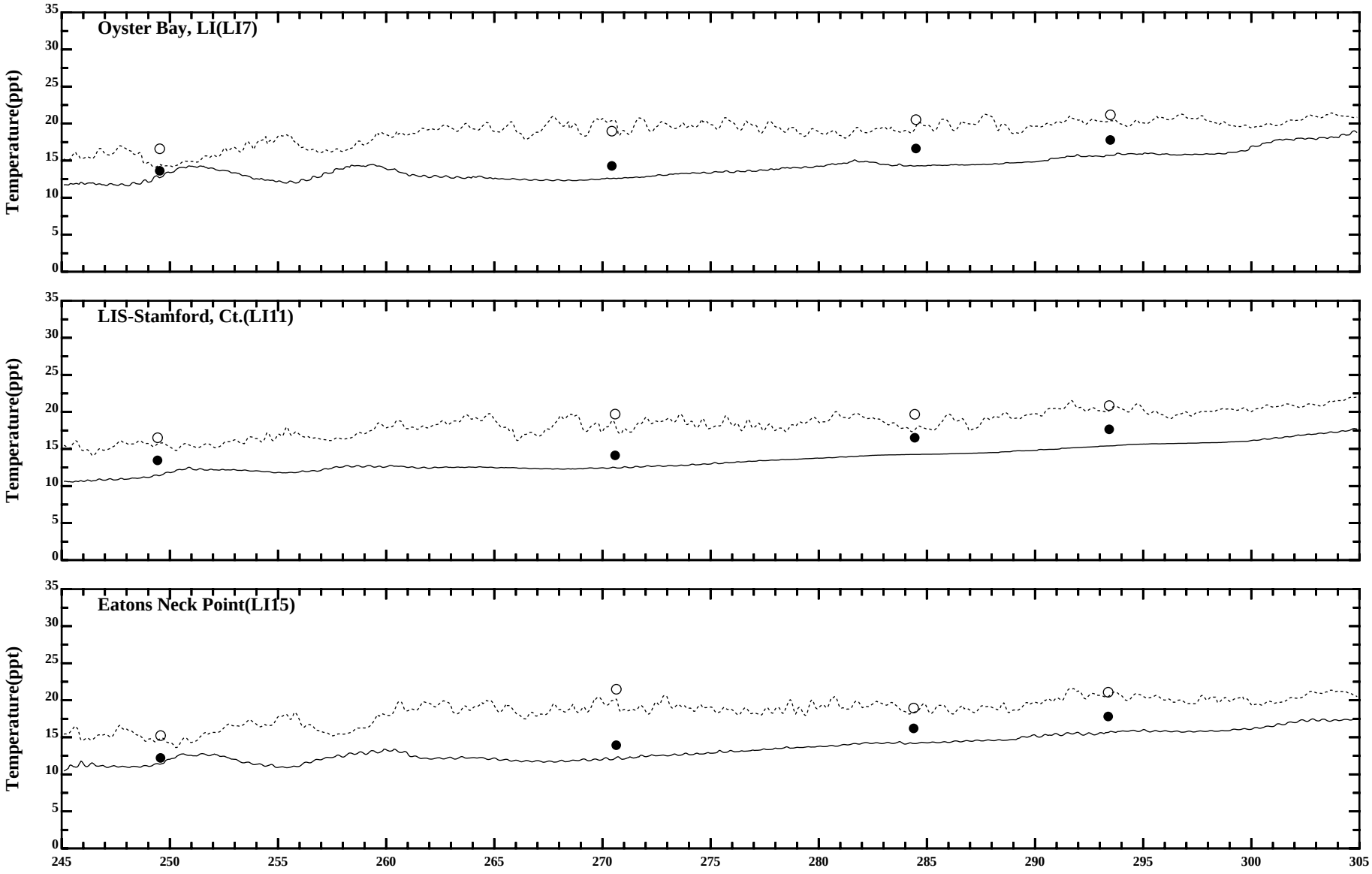

Comparison of Instantaneous Surface and Bottom Temperature

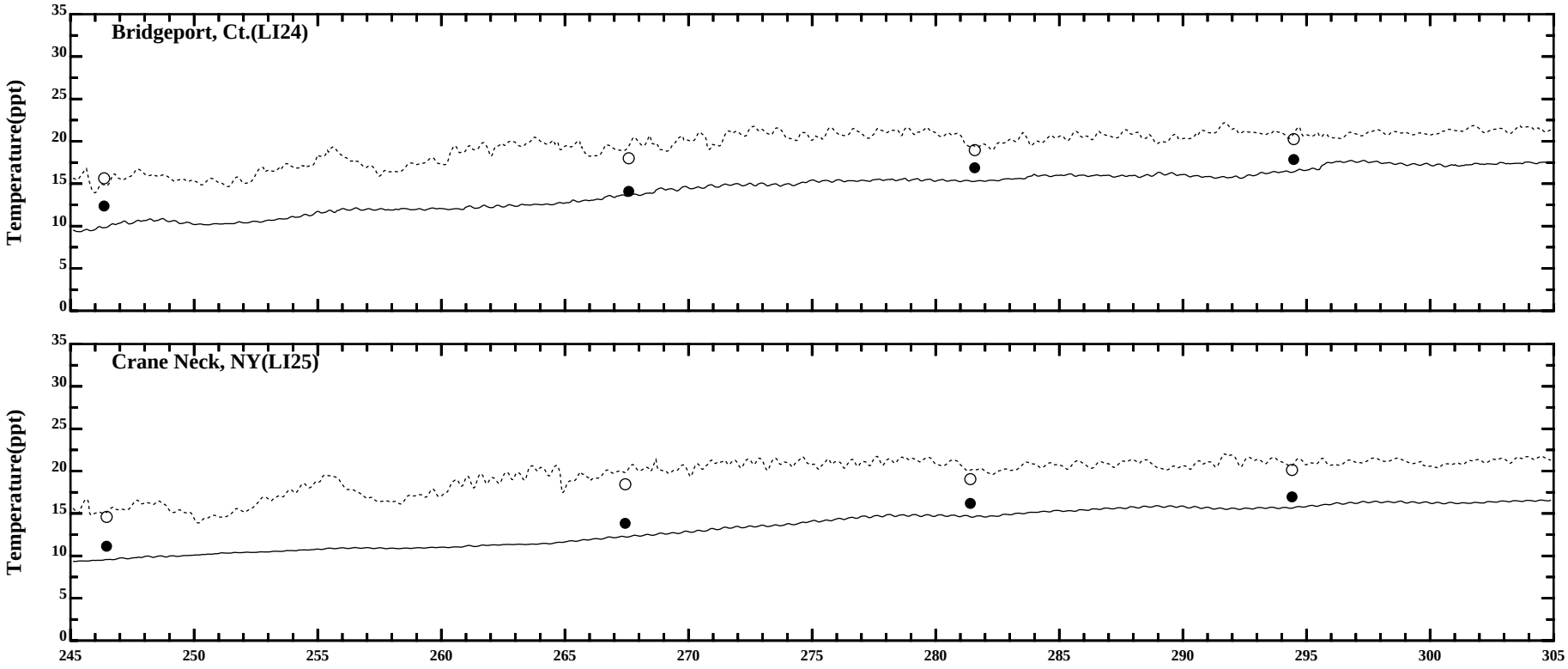

Comparison of Instantaneous Surface and Bottom Temperature

/erie1/hrfo0010/HYDRORUNS/CARP9900/PLOTS/TANDS/temp41

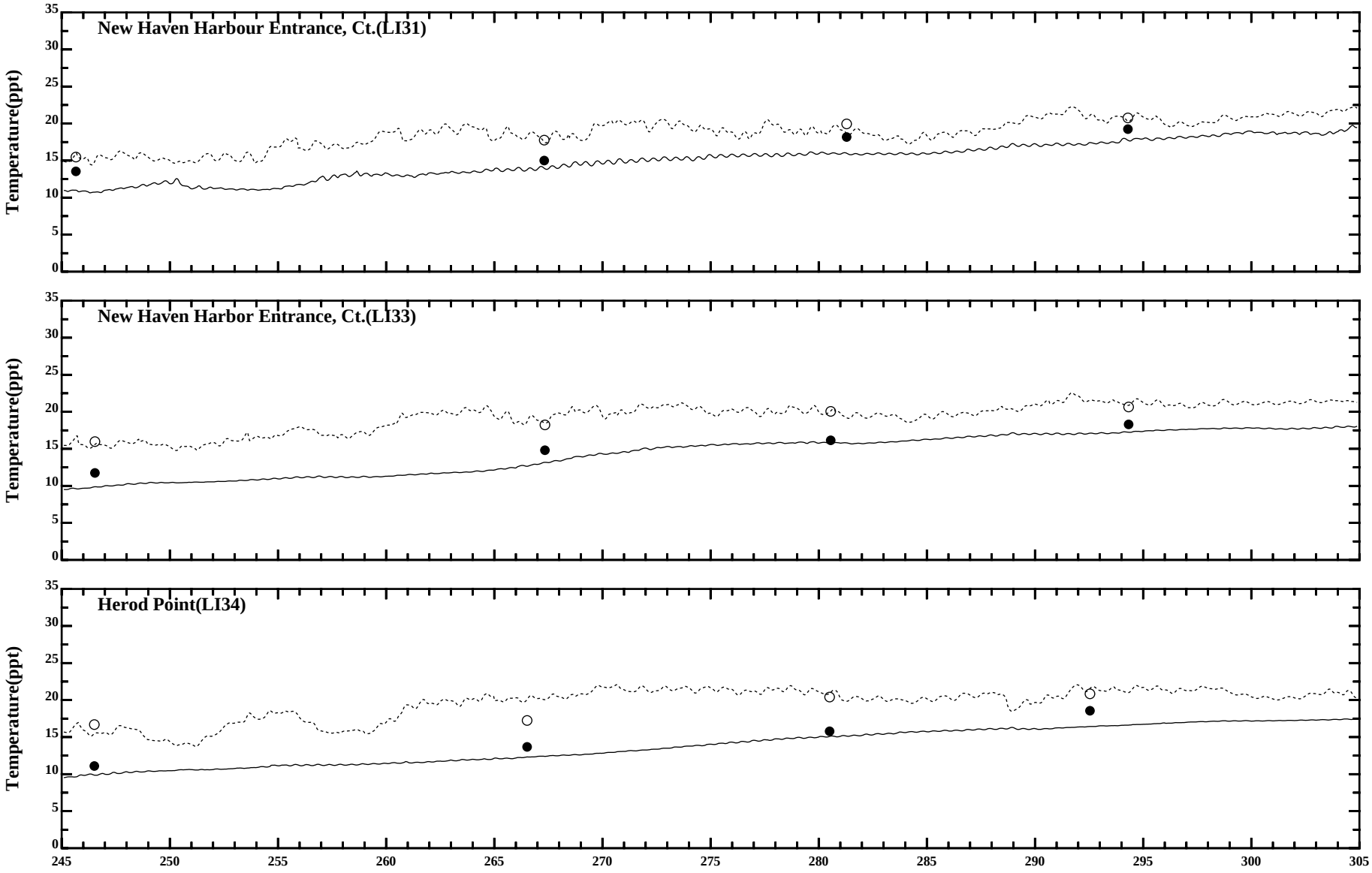

Comparison of Instantaneous Surface and Bottom Temperature

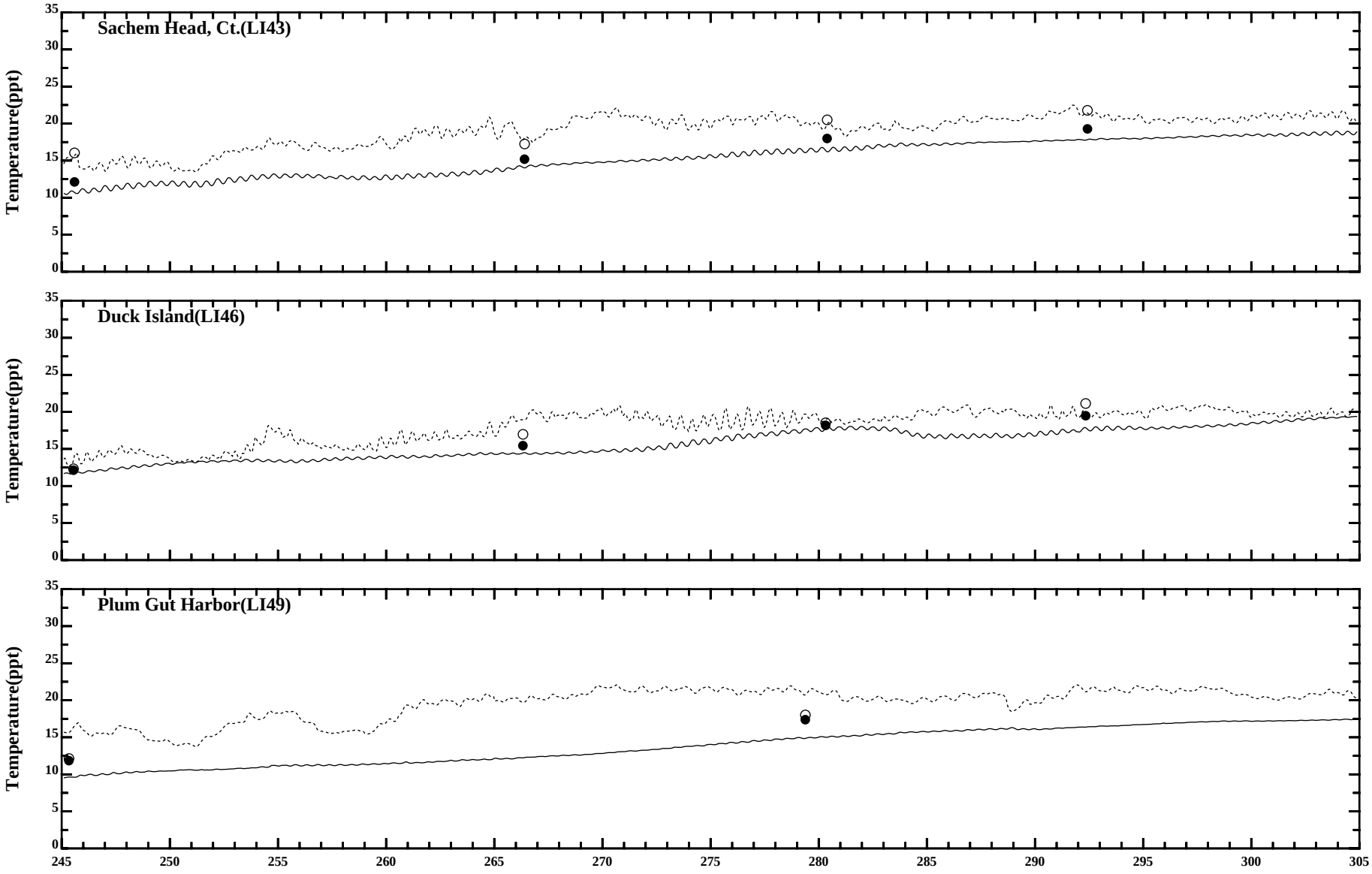

Comparison of Instantaneous Surface and Bottom Temperature

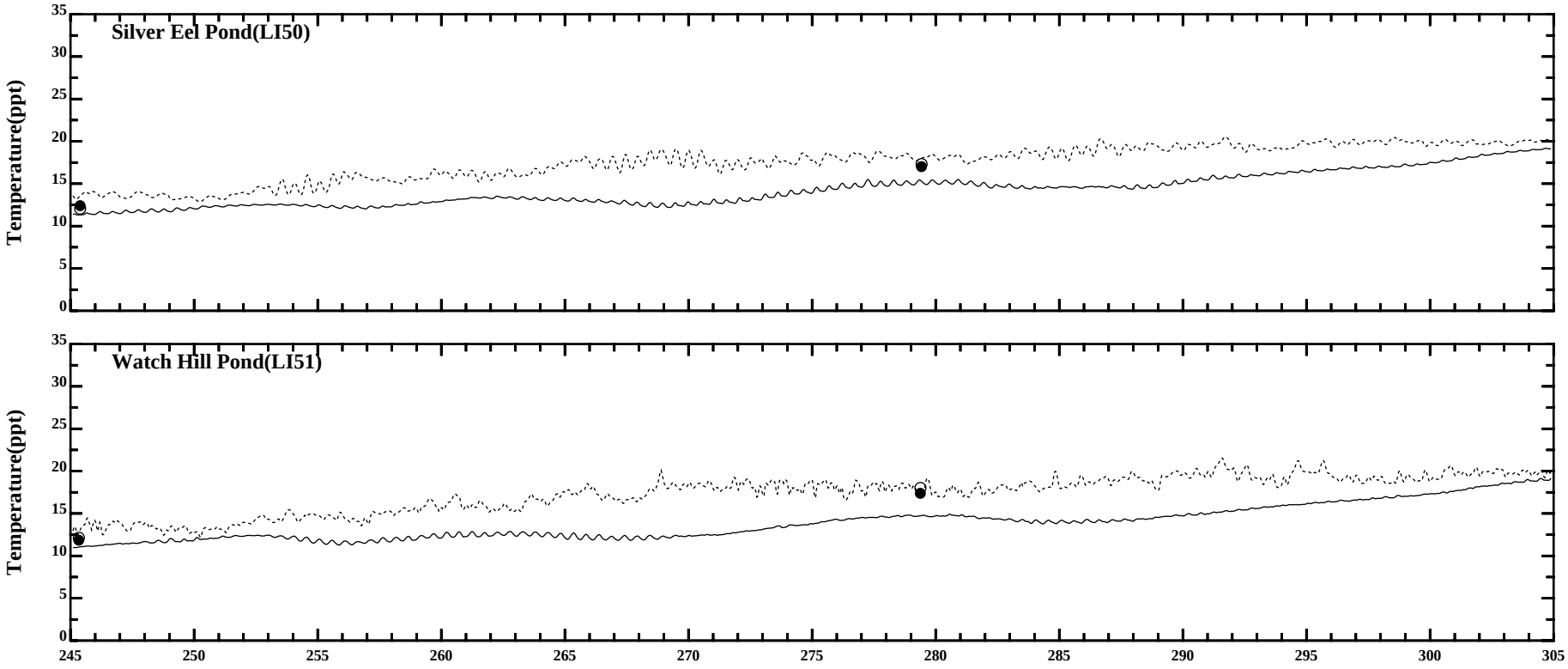

Comparison of Instantaneous Surface and Bottom Temperature

/erie1/hrfo0010/HYDRORUNS/CARP9900/PLOTS/TANDS/temp41

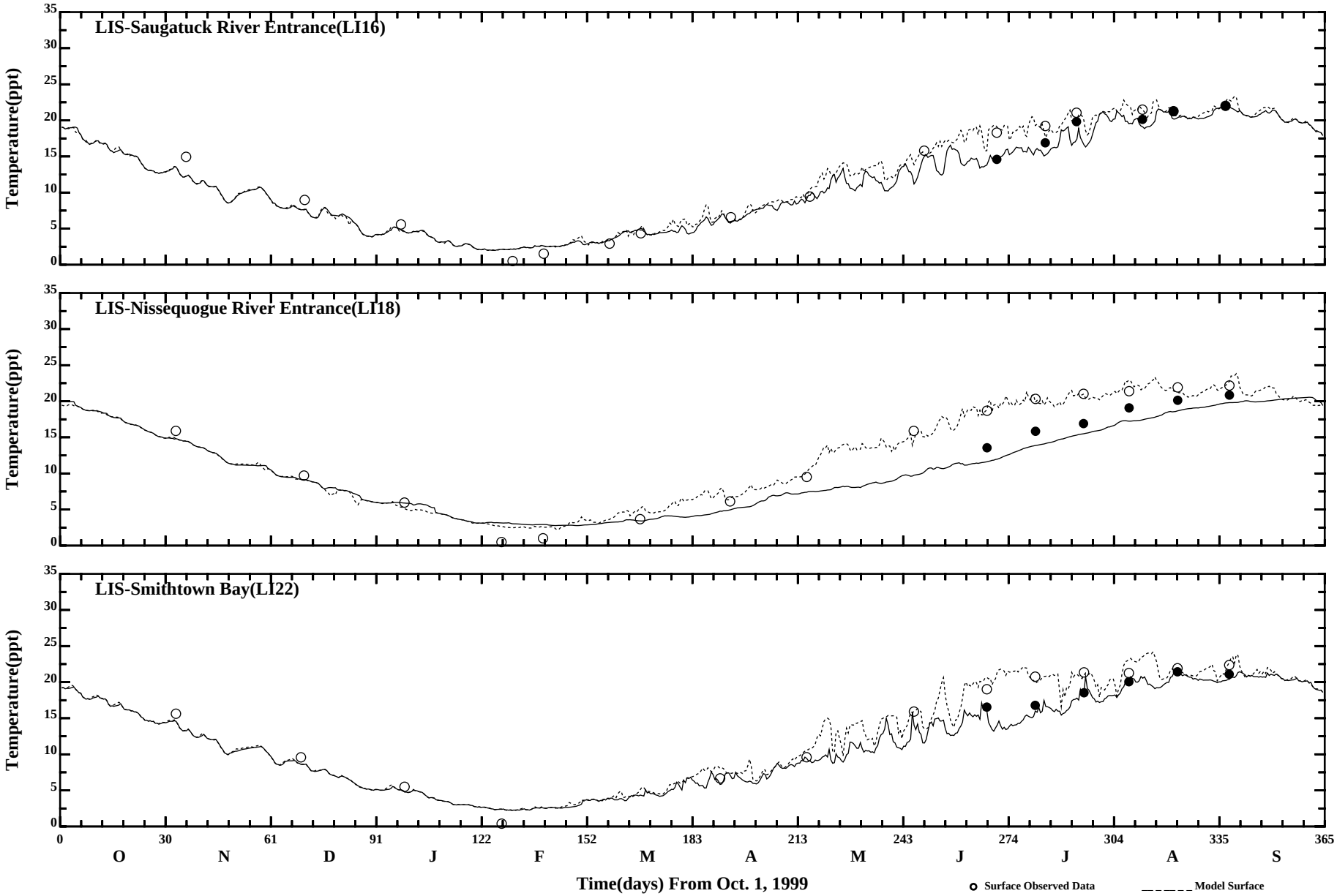

Comparison of 34 Hour Lowpass Surface and Bottom Temperature

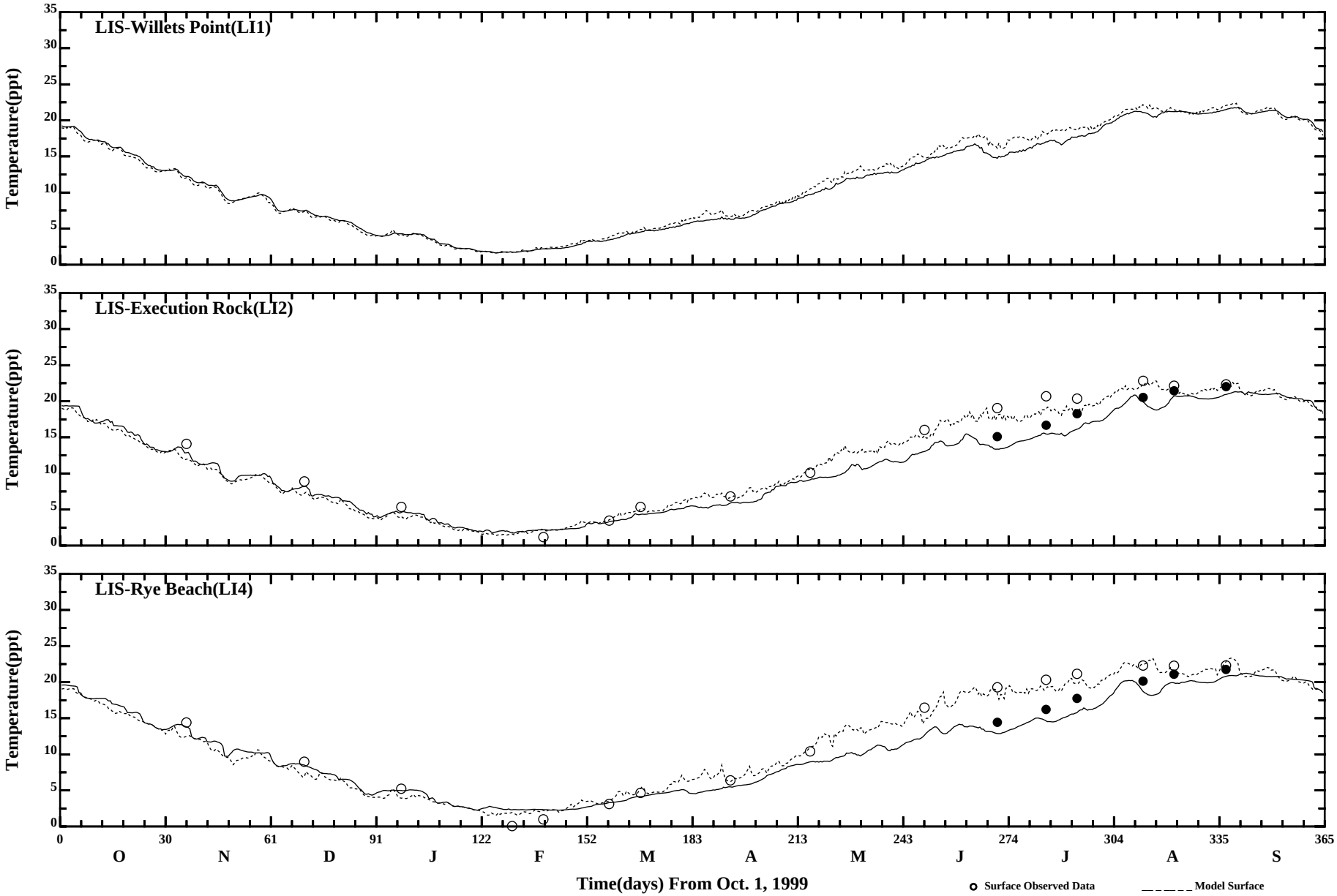

Comparison of 34 Hour Lowpass Surface and Bottom Temperature

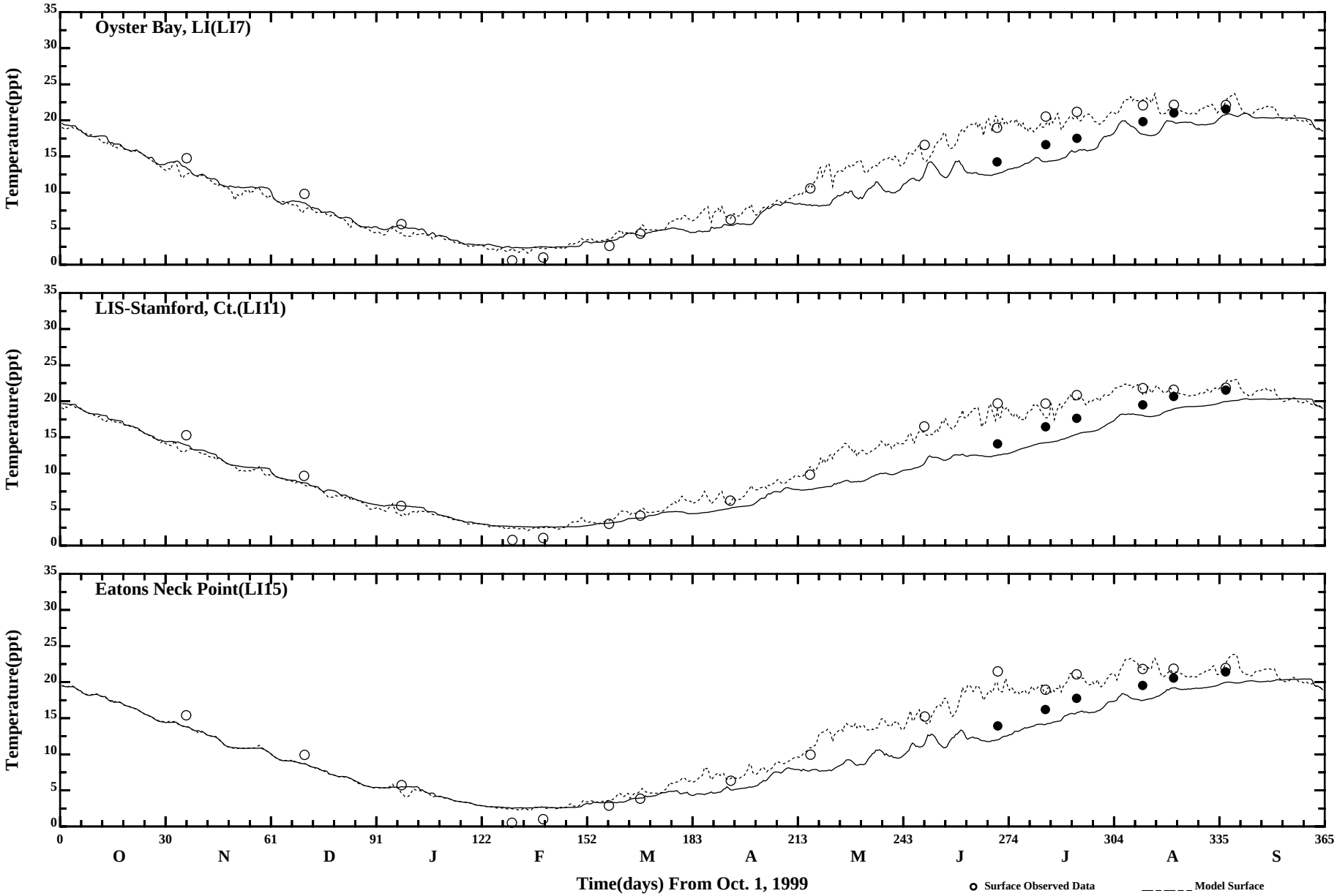

Comparison of 34 Hour Lowpass Surface and Bottom Temperature

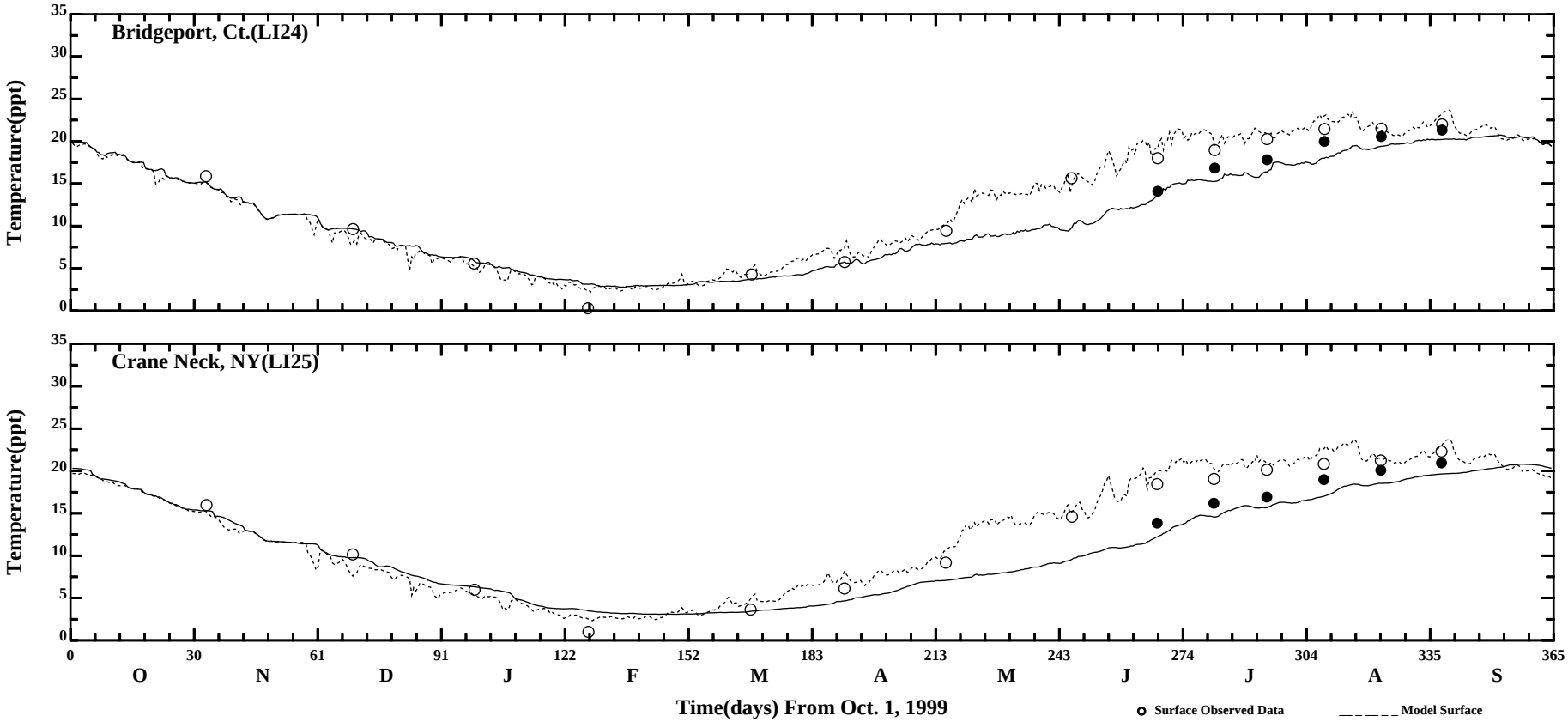

Comparison of 34 Hour Lowpass Surface and Bottom Temperature

/erie1/hrfo0010/HYDRORUNS/CARP9900/PLOTS/TANDS/ptemp41_34hlp

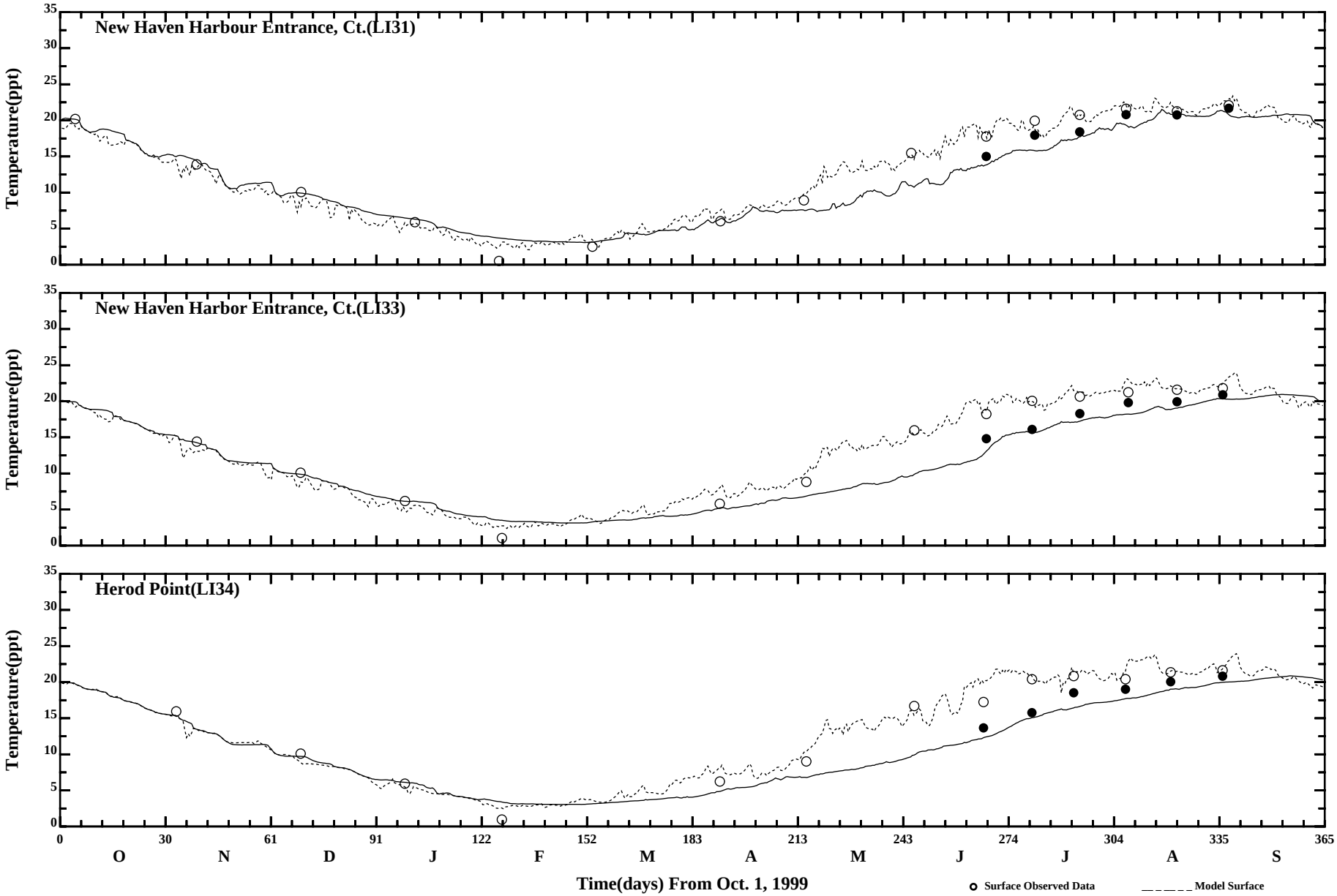

Comparison of 34 Hour Lowpass Surface and Bottom Temperature

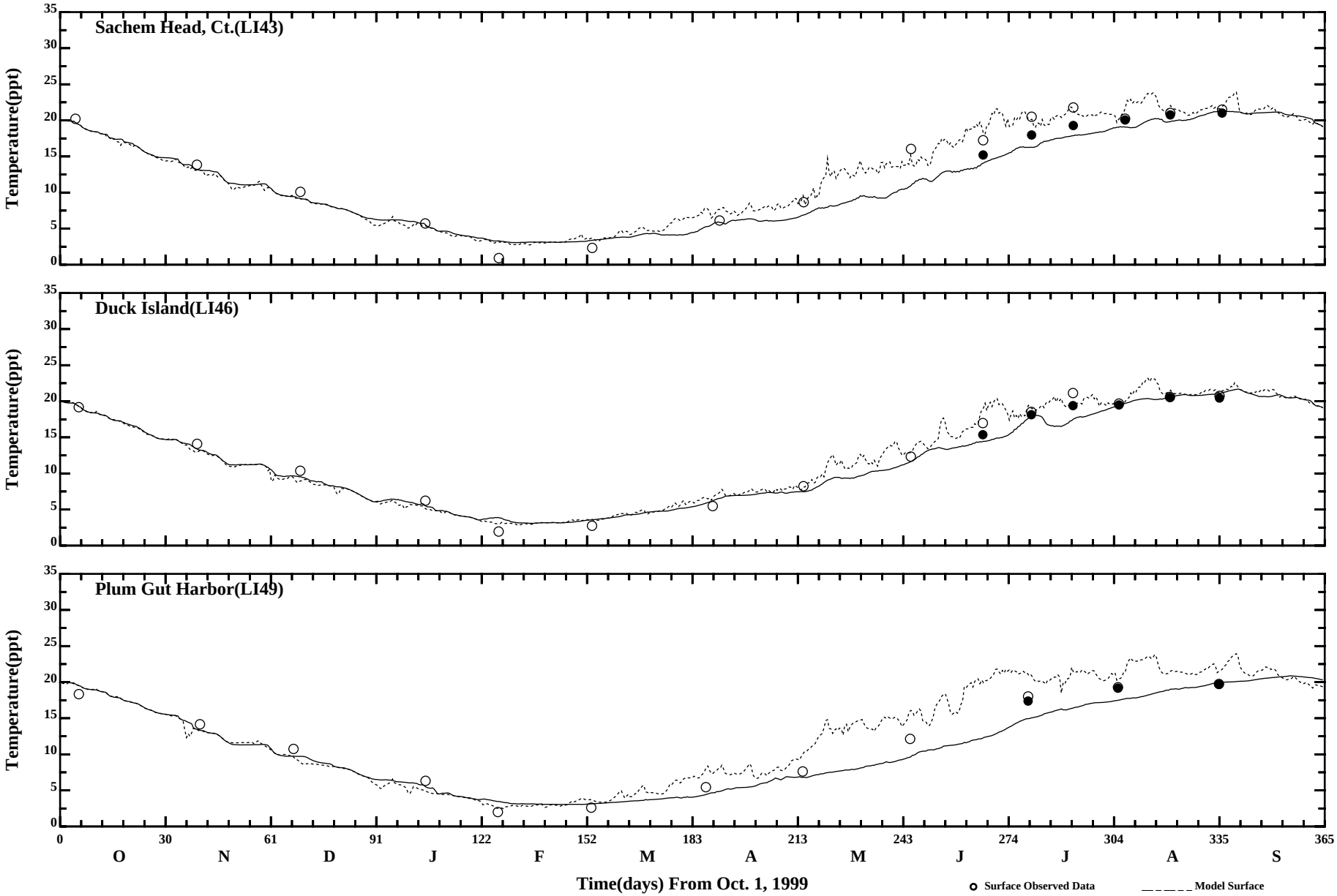

Comparison of 34 Hour Lowpass Surface and Bottom Temperature

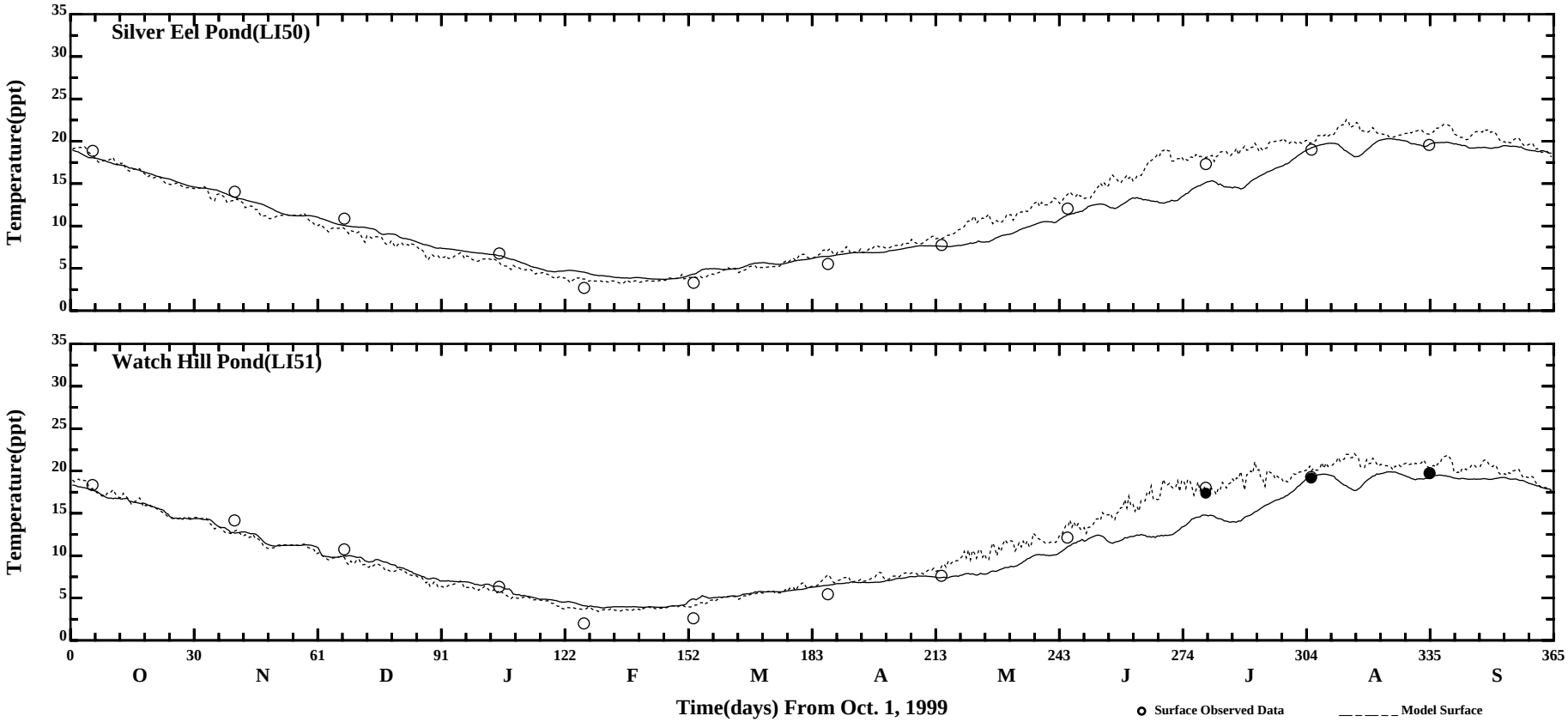

Comparison of 34 Hour Lowpass Surface and Bottom Temperature

/erie1/hrfo0010/HYDRORUNS/CARP9900/PLOTS/TANDS/ptemp41_34hlp

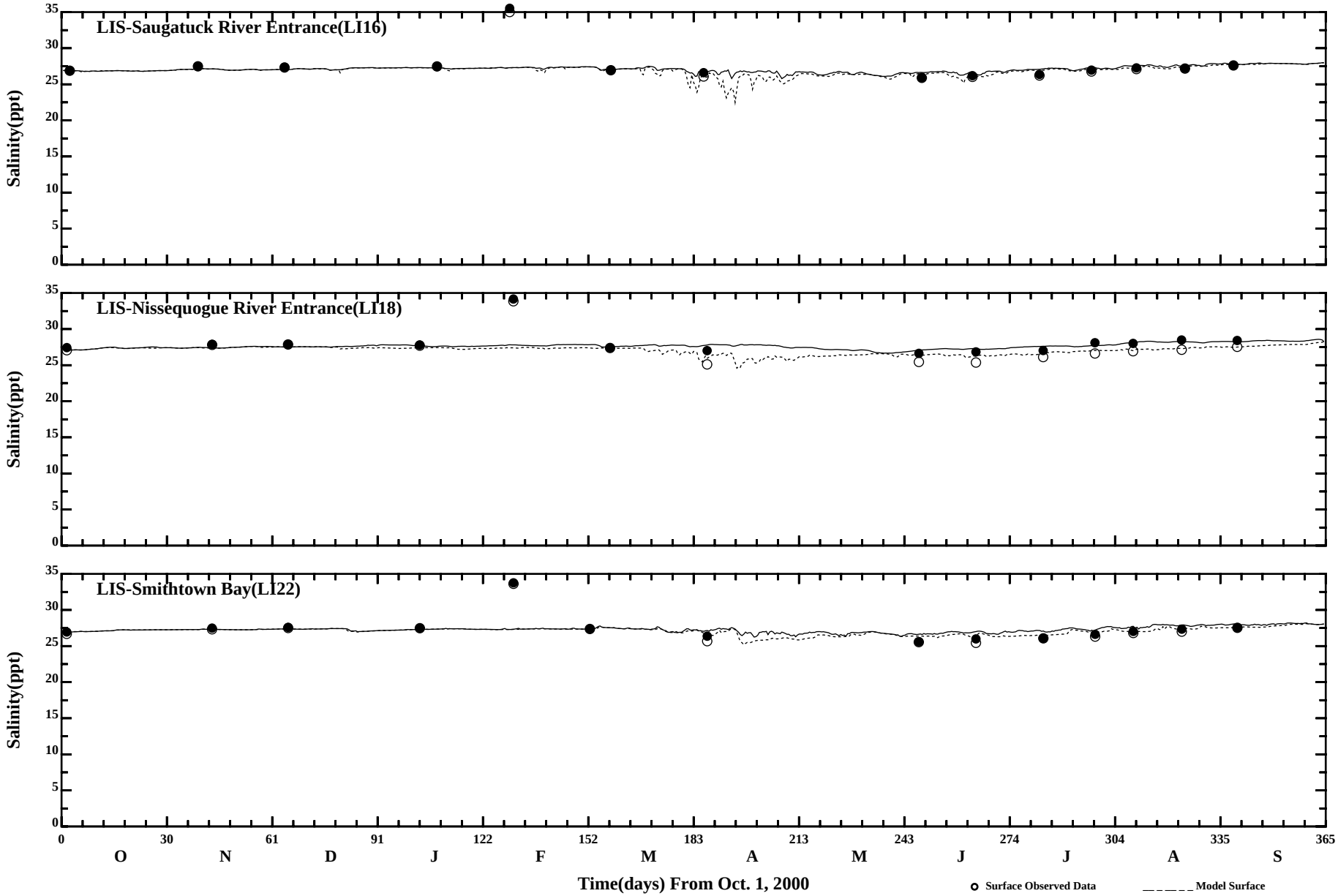

Comparison of 35 Hour Lowpass Surface and Bottom Salinity

DATE: 8/02/2004 TIME: 12:29:54

/erie1/hrfo0010/HYDRORUNS/CARP0001/PLOTS/TANDS/psalt41_35hlp

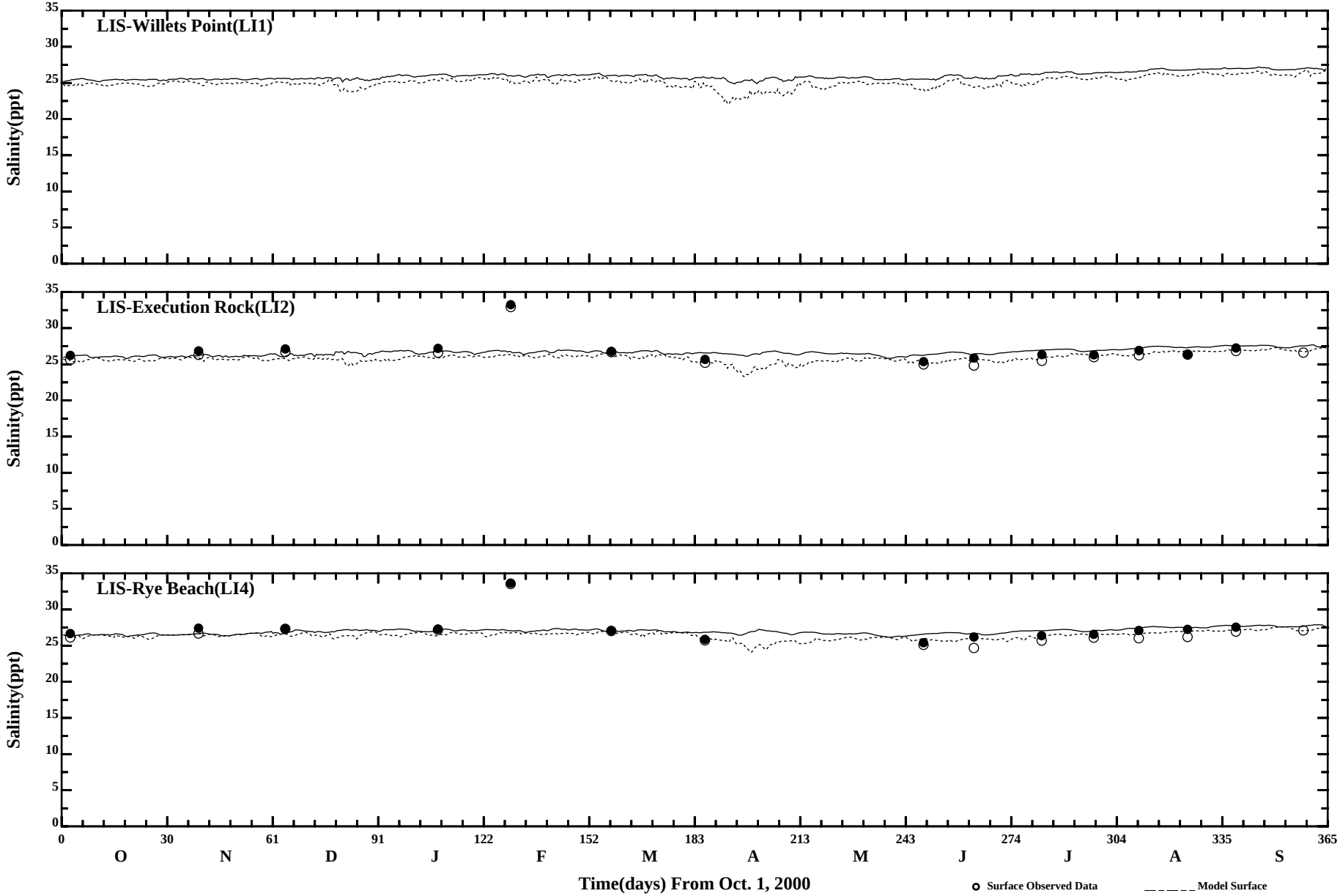

Comparison of 35 Hour Lowpass Surface and Bottom Salinity

DATE: 8/02/2004 TIME: 12:29:54

/erie1/hrfo0010/HYDRORUNS/CARP0001/PLOTS/TANDS/psalt41_35hlp

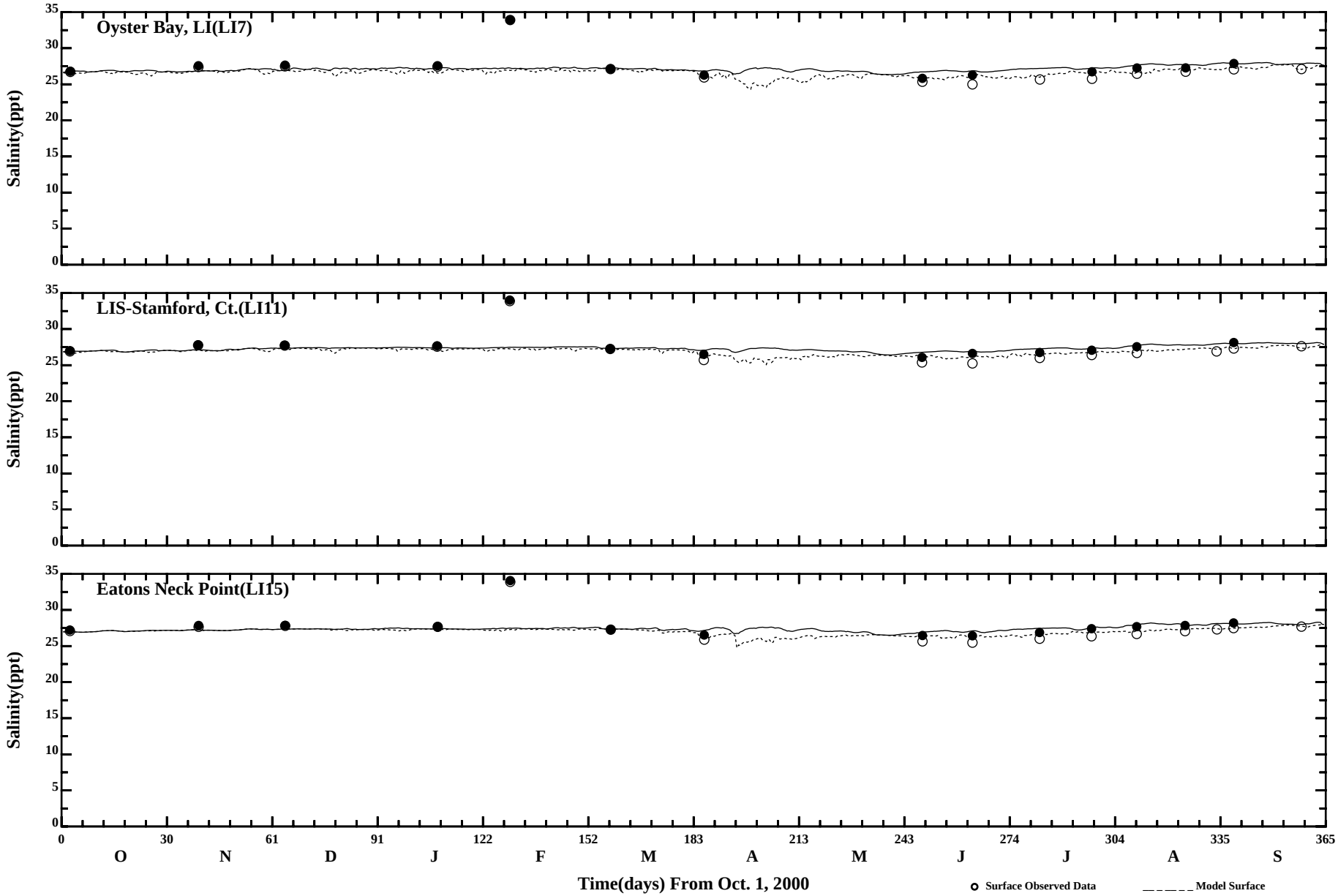

Comparison of 35 Hour Lowpass Surface and Bottom Salinity

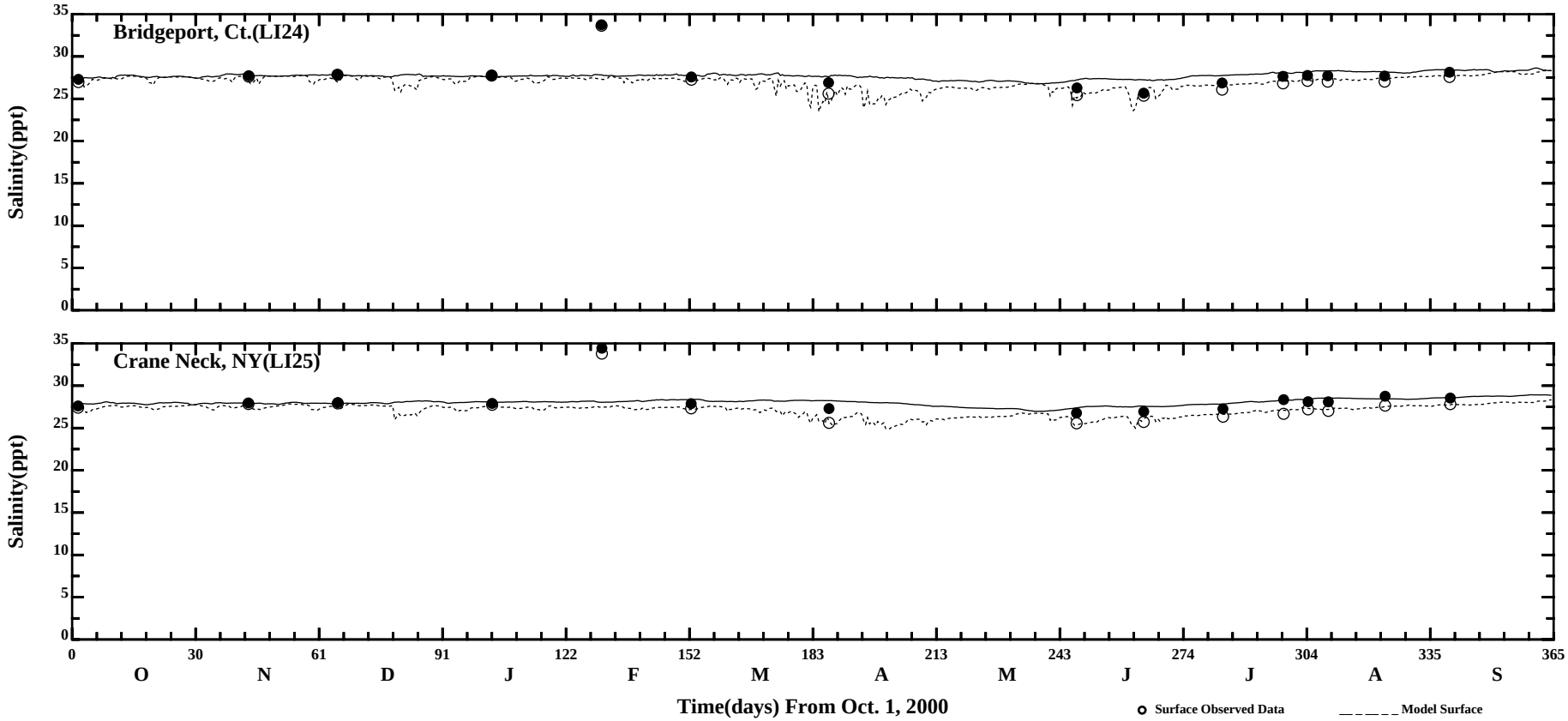

Comparison of 35 Hour Lowpass Surface and Bottom Salinity

/erie1/hrfo0010/HYDRORUNS/CARP0001/PLOTS/TANDS/psalt41_35hlp

DATE: 8/02/2004 TIME: 12:29:54

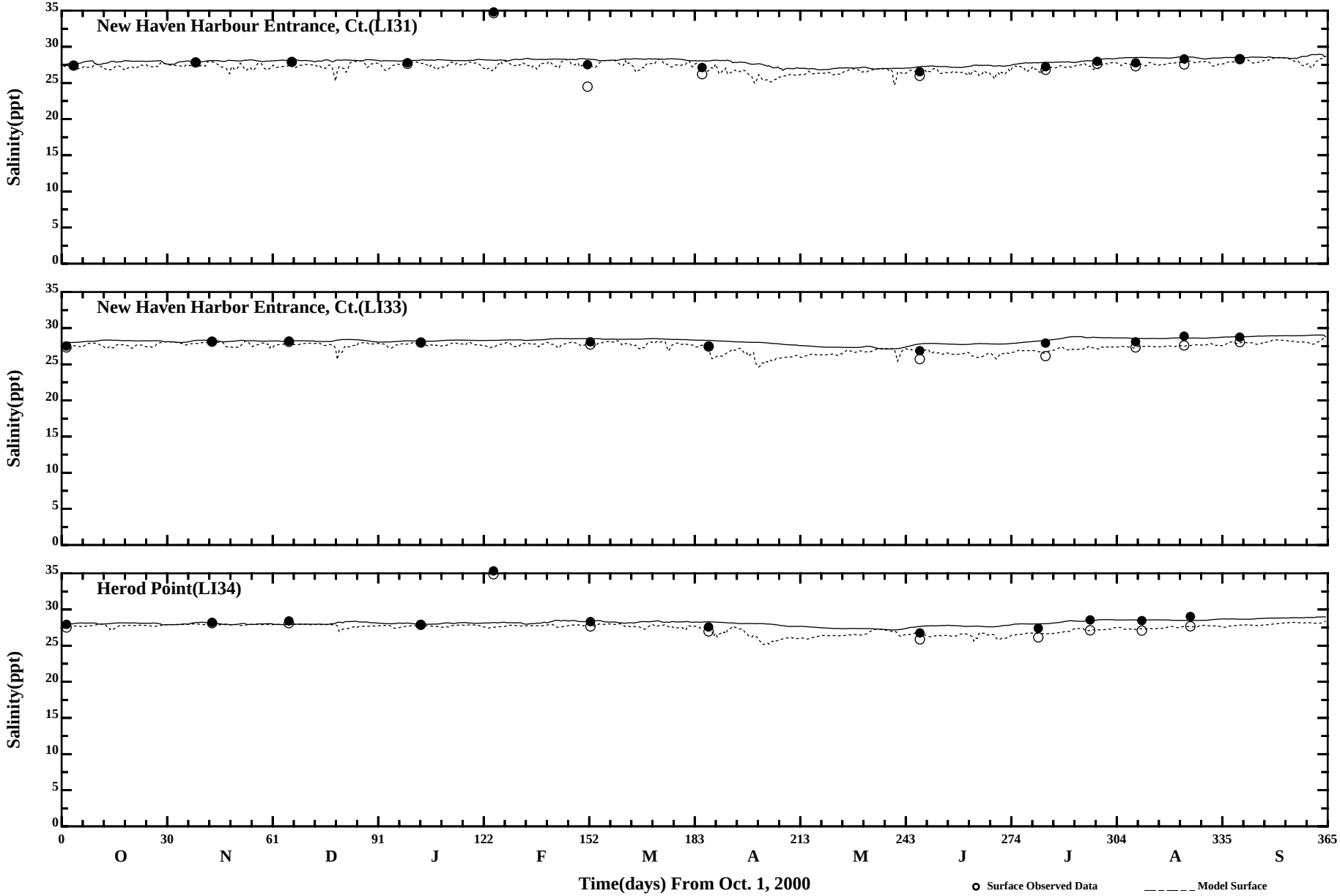

Comparison of 35 Hour Lowpass Surface and Bottom Salinity

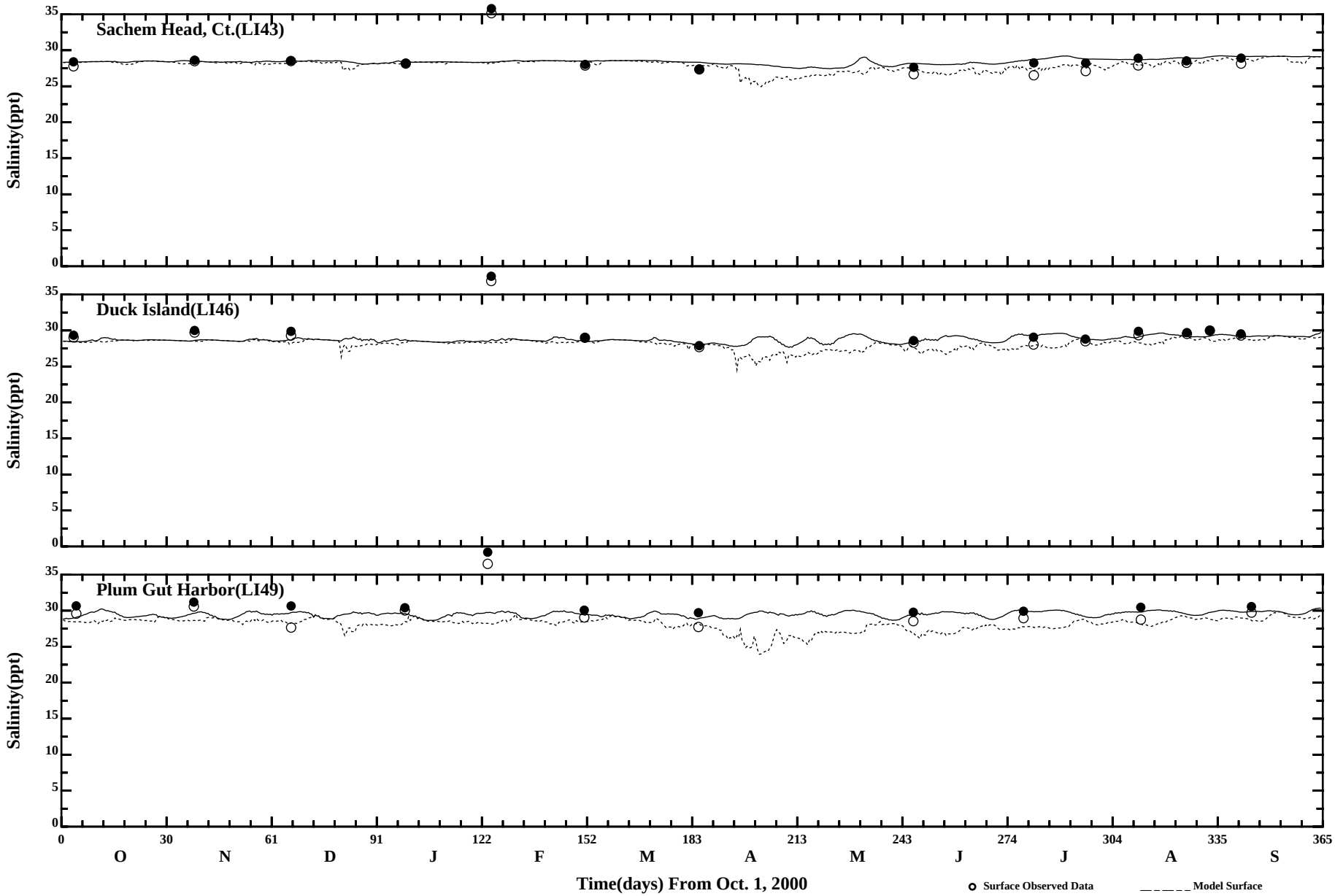

Comparison of 35 Hour Lowpass Surface and Bottom Salinity

DATE: 8/02/2004 TIME: 12:29:54

/erie1/hrfo0010/HYDRORUNS/CARP0001/PLOTS/TANDS/psalt41_35hlp

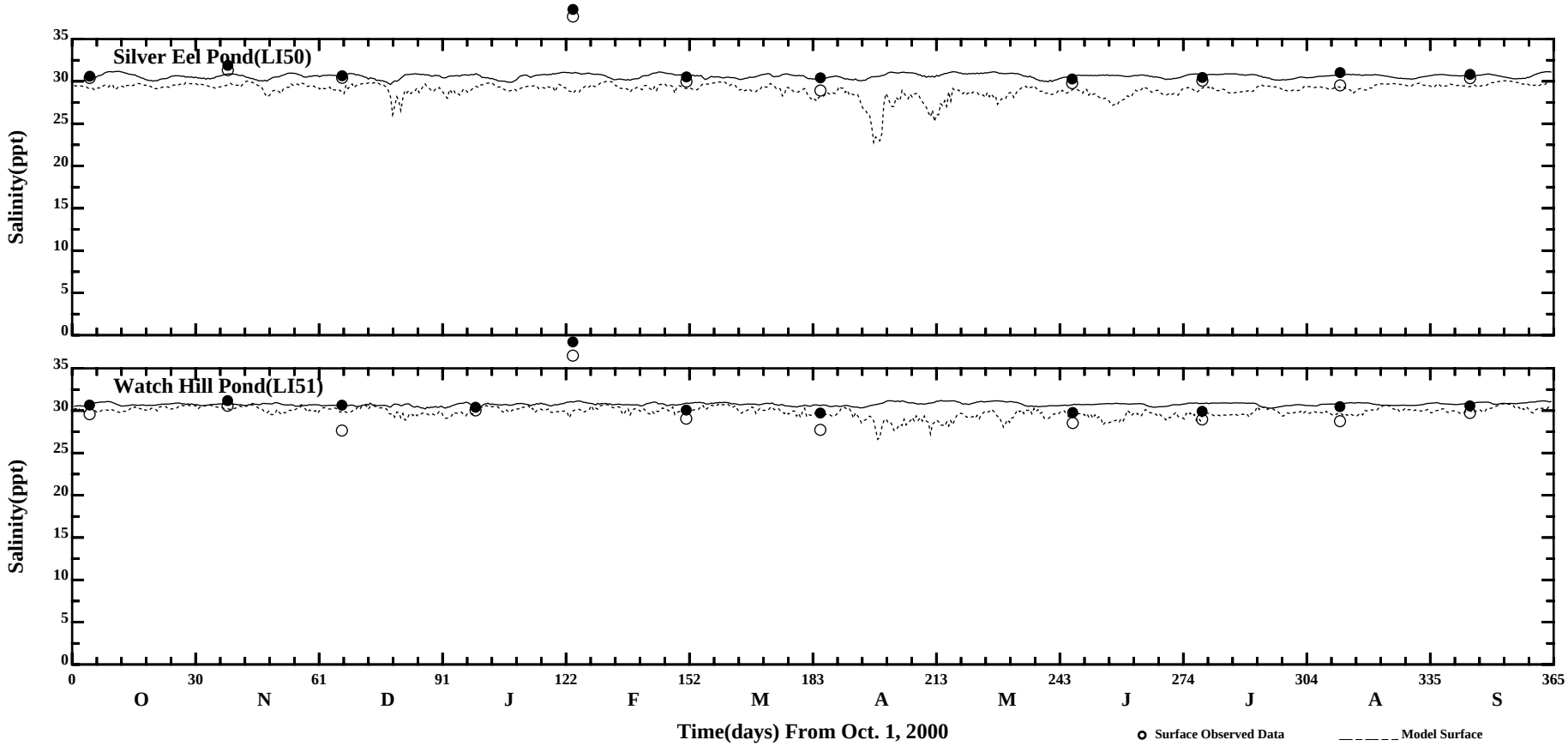

Comparison of 35 Hour Lowpass Surface and Bottom Salinity

/erie1/hrfo0010/HYDRORUNS/CARP0001/PLOTS/TANDS/psalt41_35hlp

DATE: 8/02/2004 TIME: 12:29:54

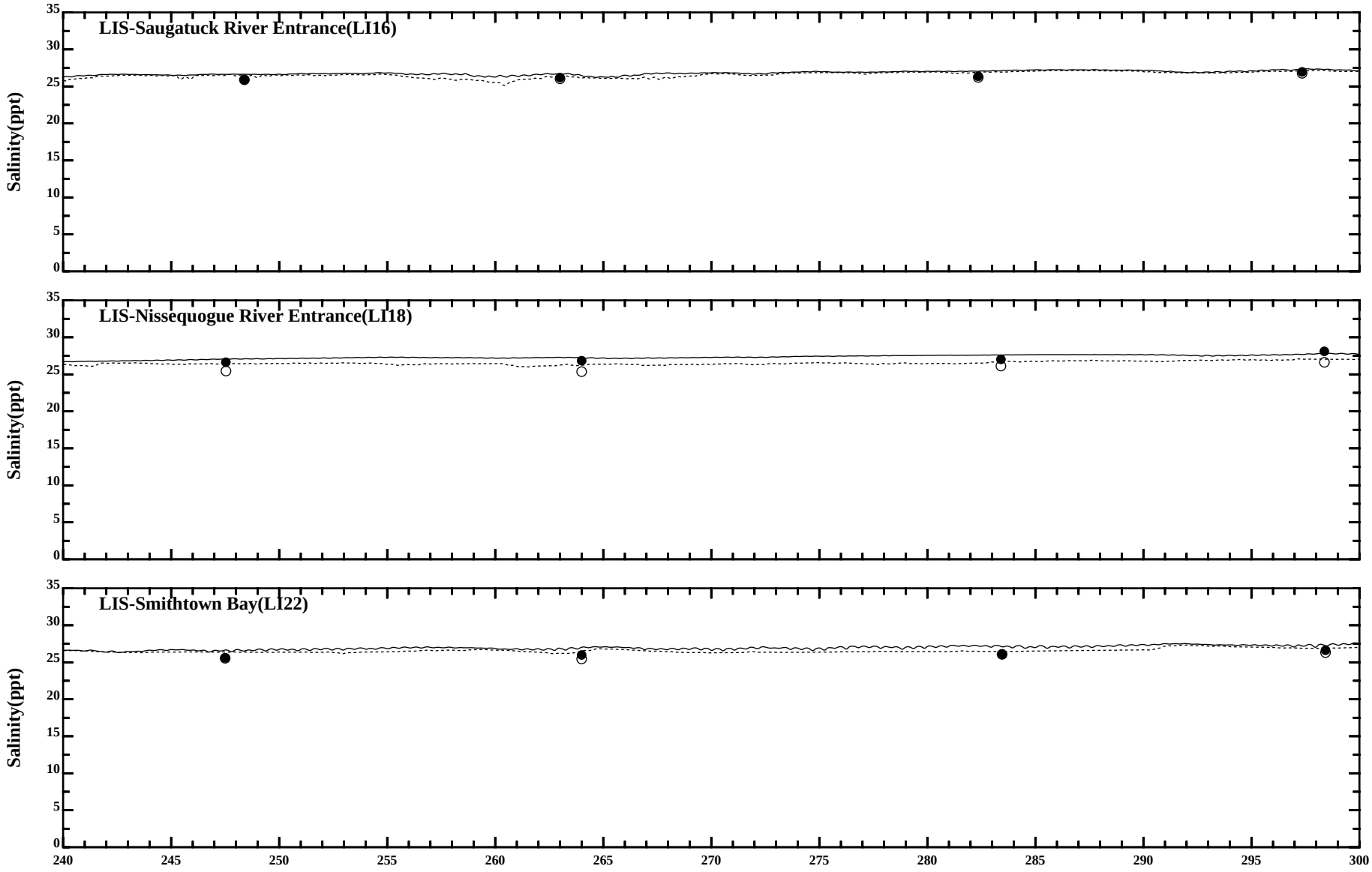

Comparison of Instantaneous Surface and Bottom Salinity

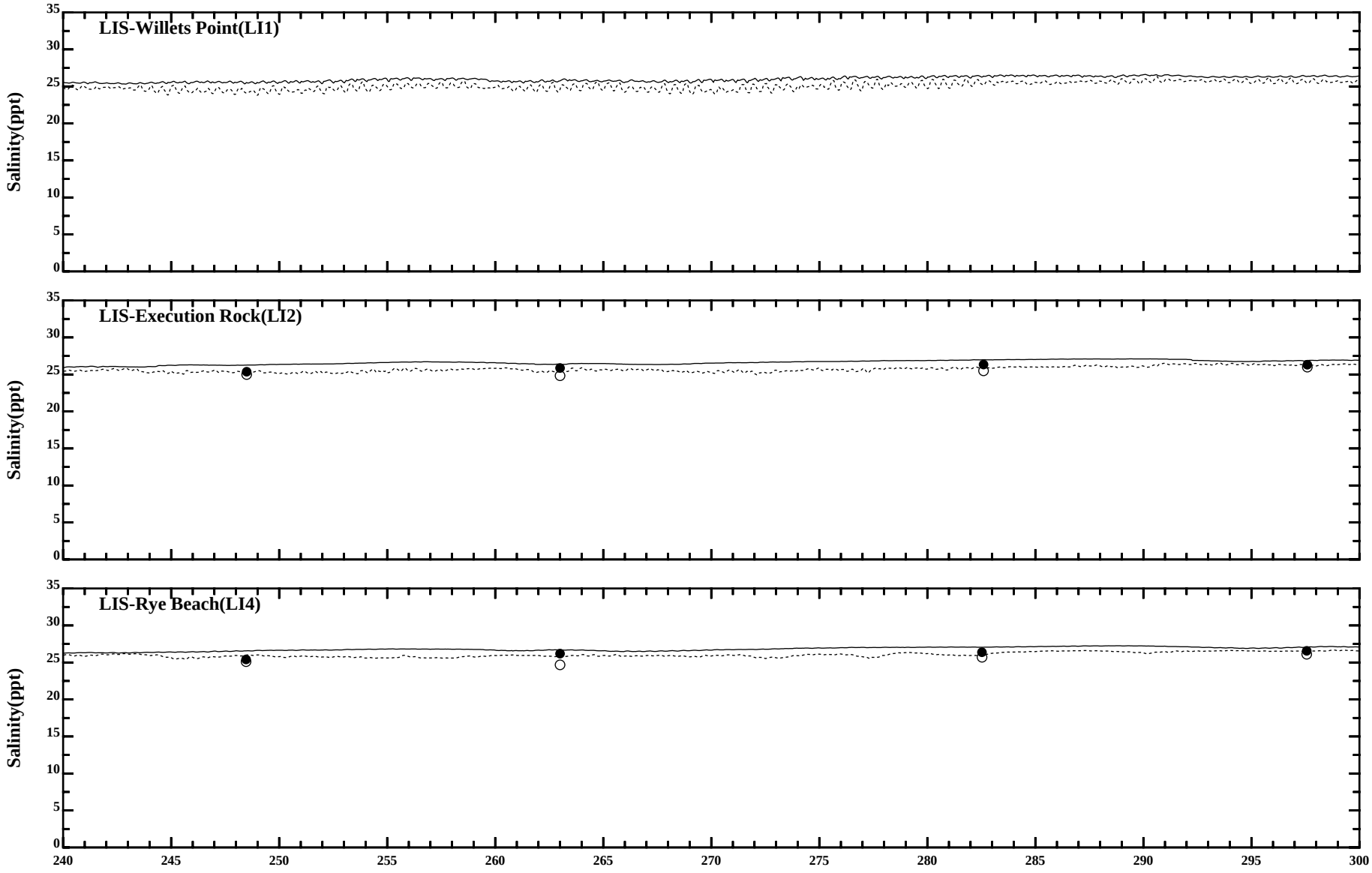

Comparison of Instantaneous Surface and Bottom Salinity

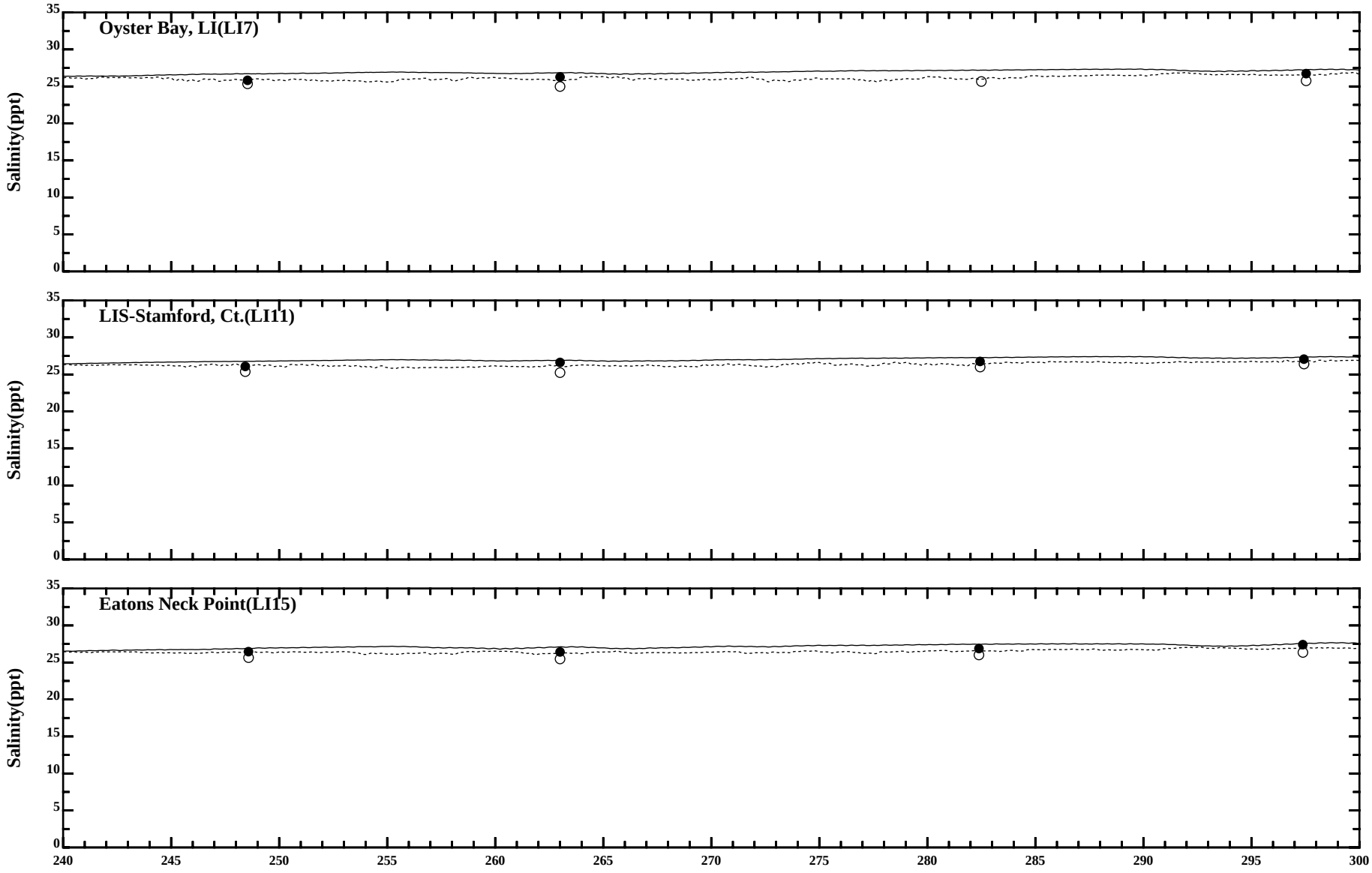

Comparison of Instantaneous Surface and Bottom Salinity

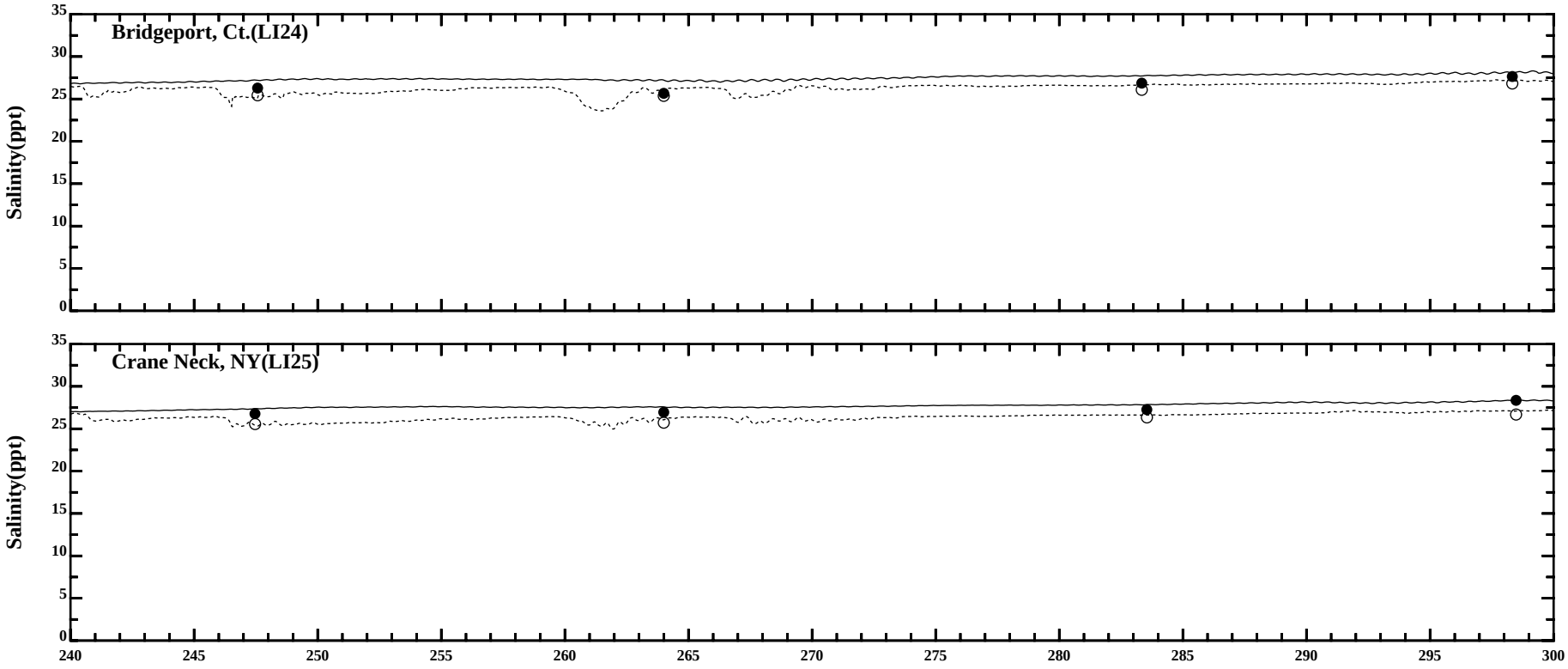

Comparison of Instantaneous Surface and Bottom Salinity

/erie1/hrfo0010/HYDRORUNS/CARP0001/PLOTS/TANDS/salt41

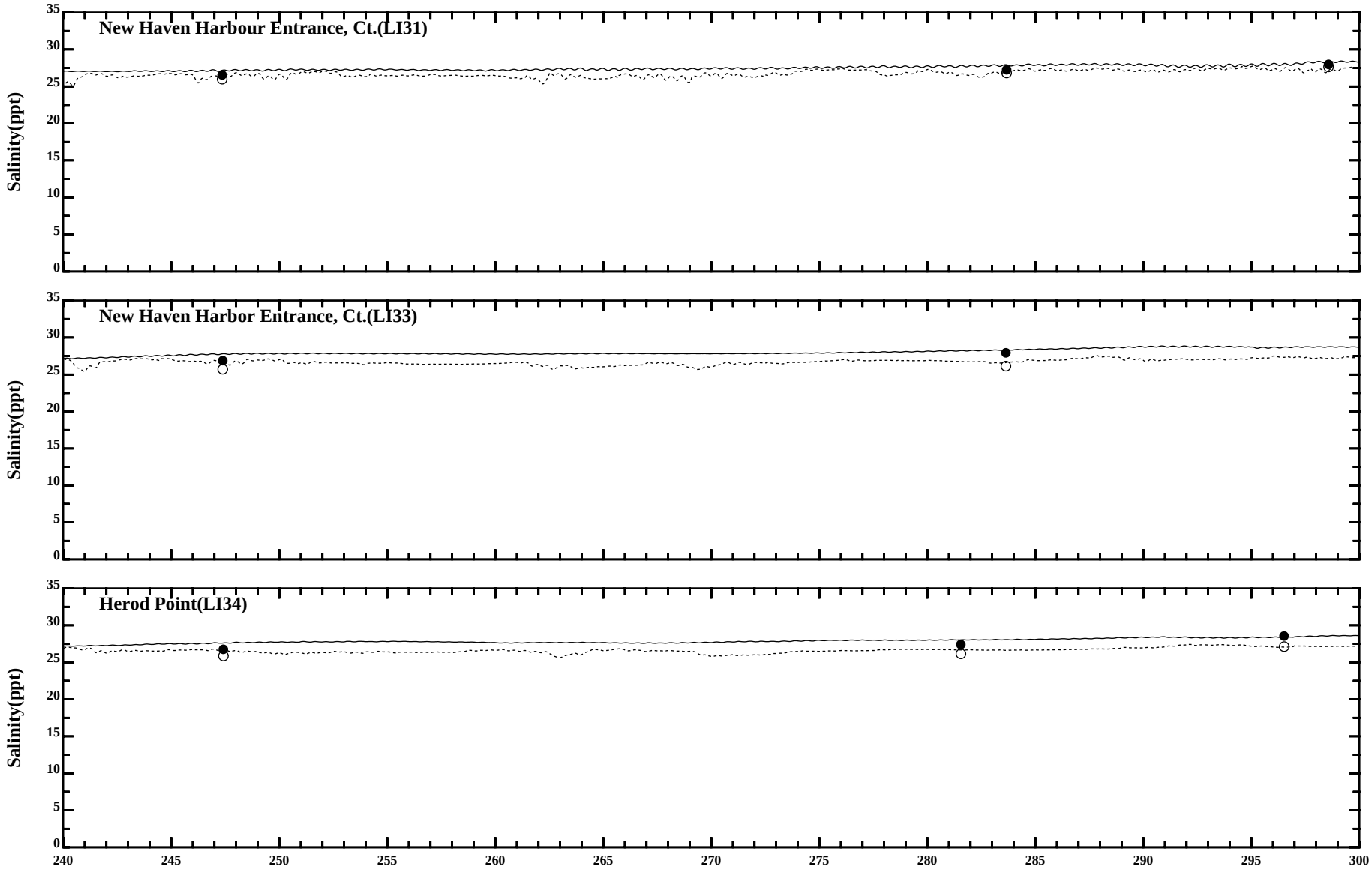

Comparison of Instantaneous Surface and Bottom Salinity

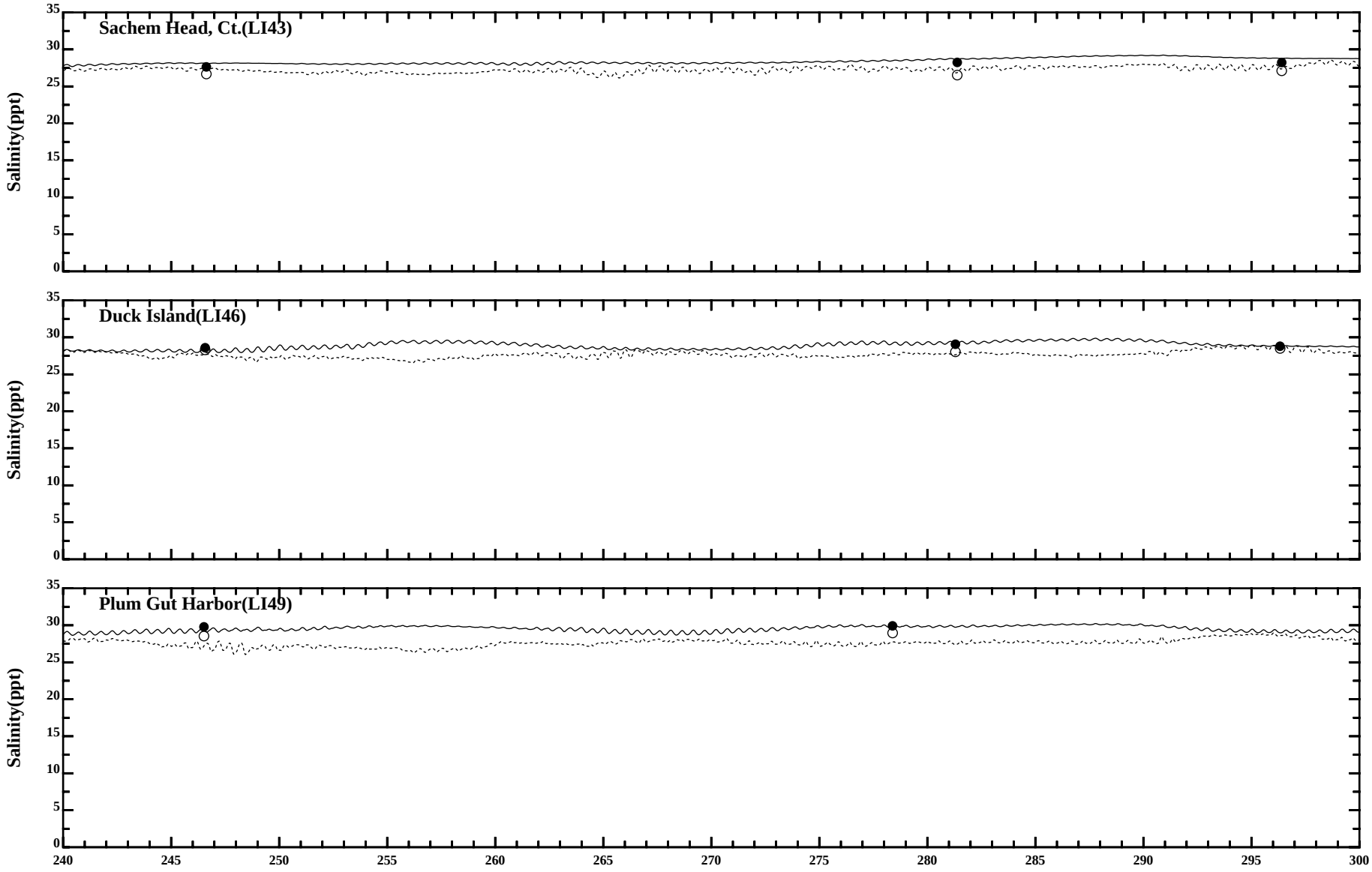

Comparison of Instantaneous Surface and Bottom Salinity

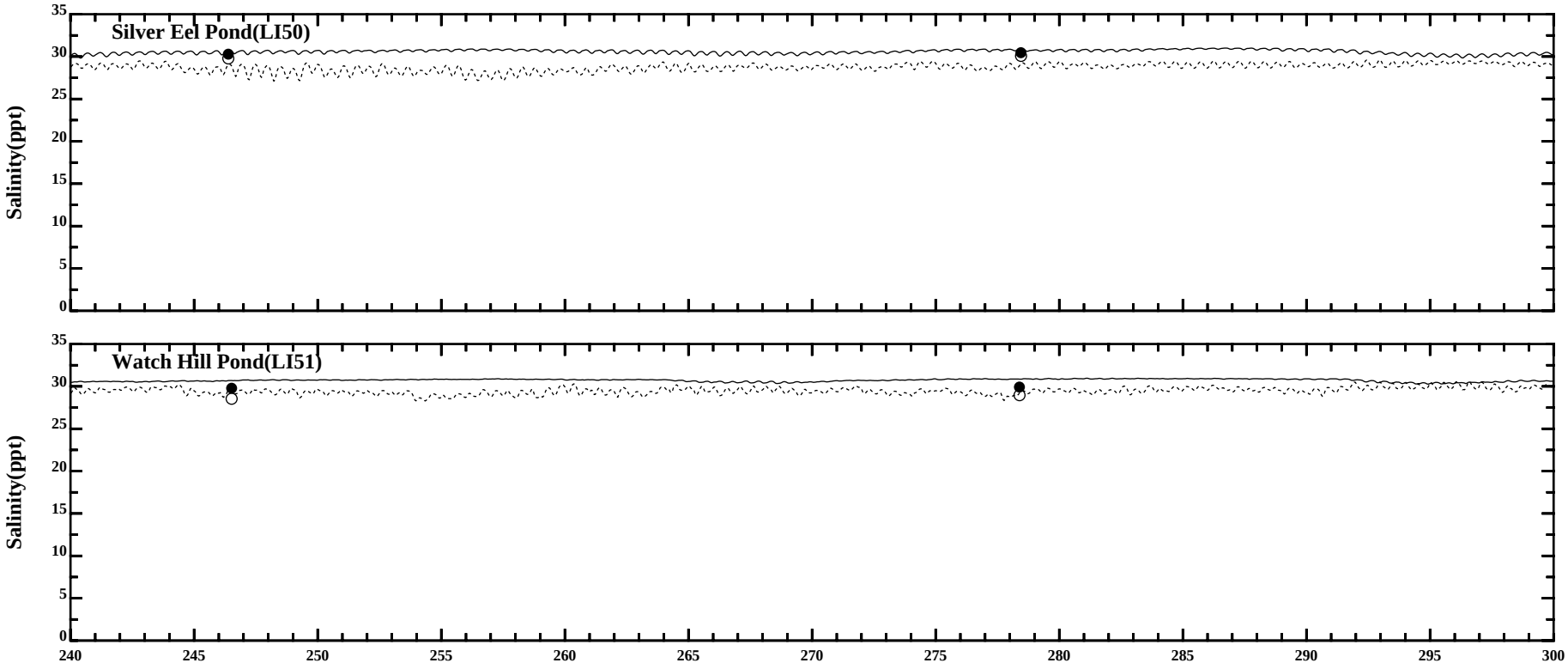

Comparison of Instantaneous Surface and Bottom Salinity

/erie1/hrfo0010/HYDRORUNS/CARP0001/PLOTS/TANDS/salt41

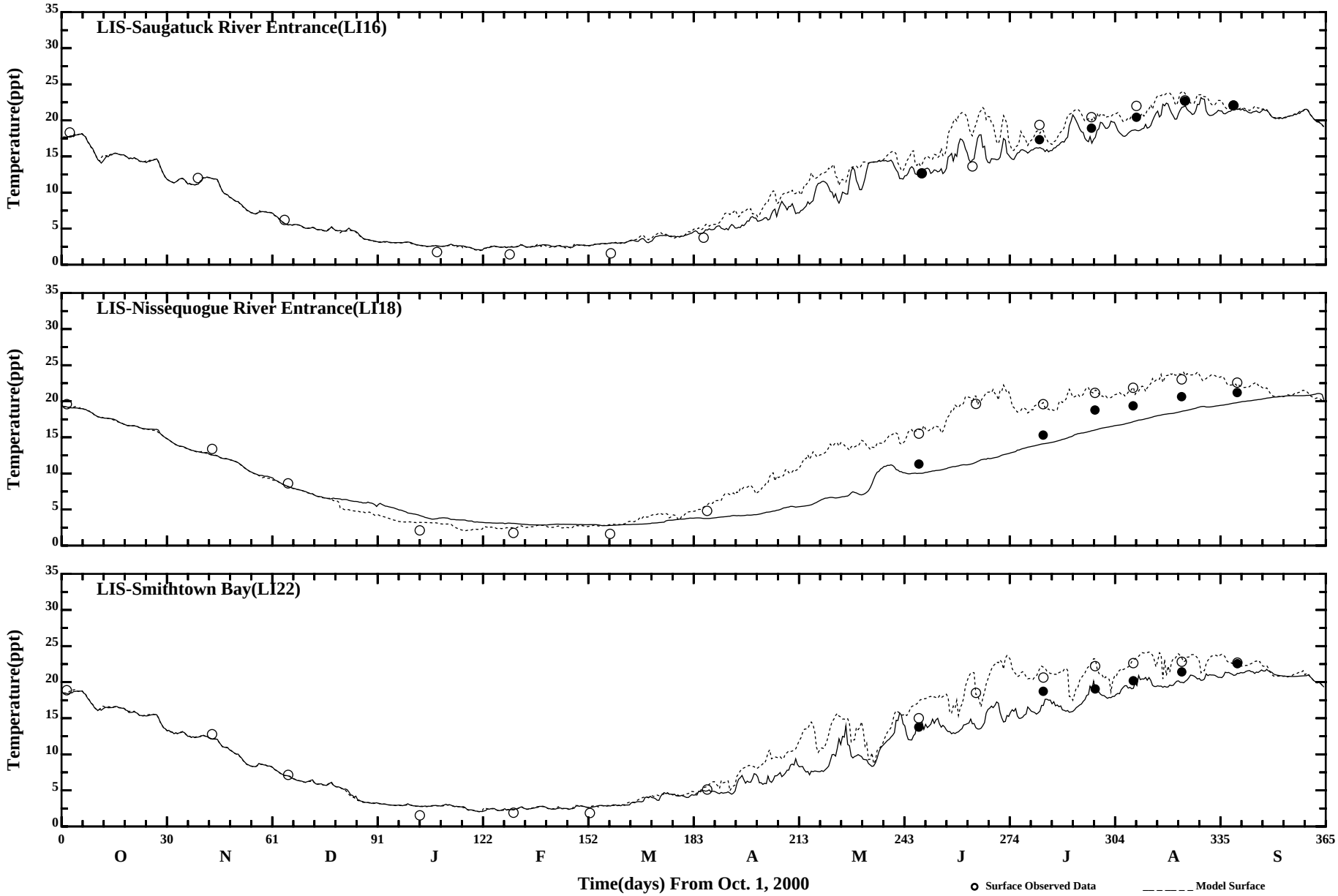

Comparison of 35 Hour Lowpass Surface and Bottom Temperature

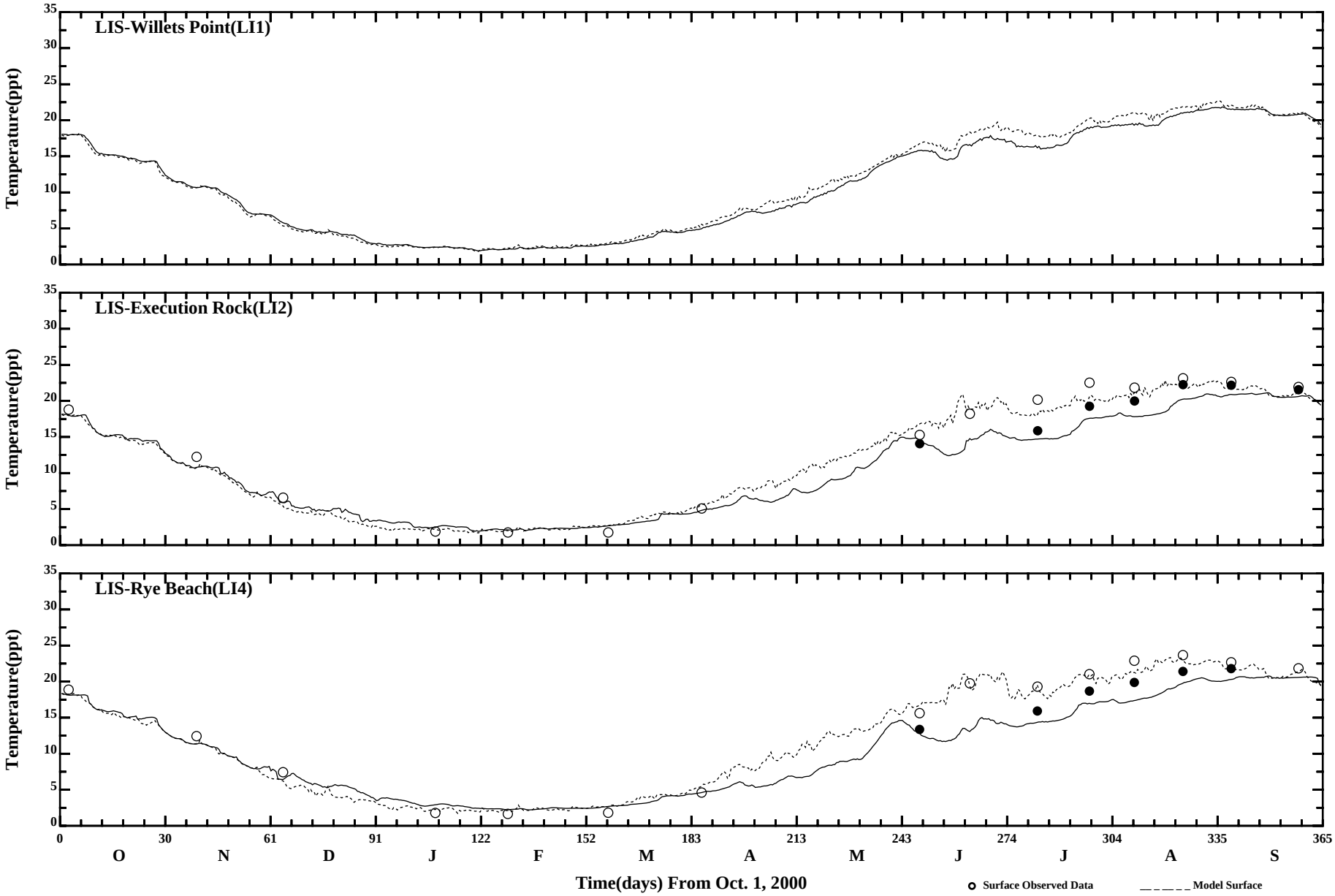

Comparison of 35 Hour Lowpass Surface and Bottom Temperature

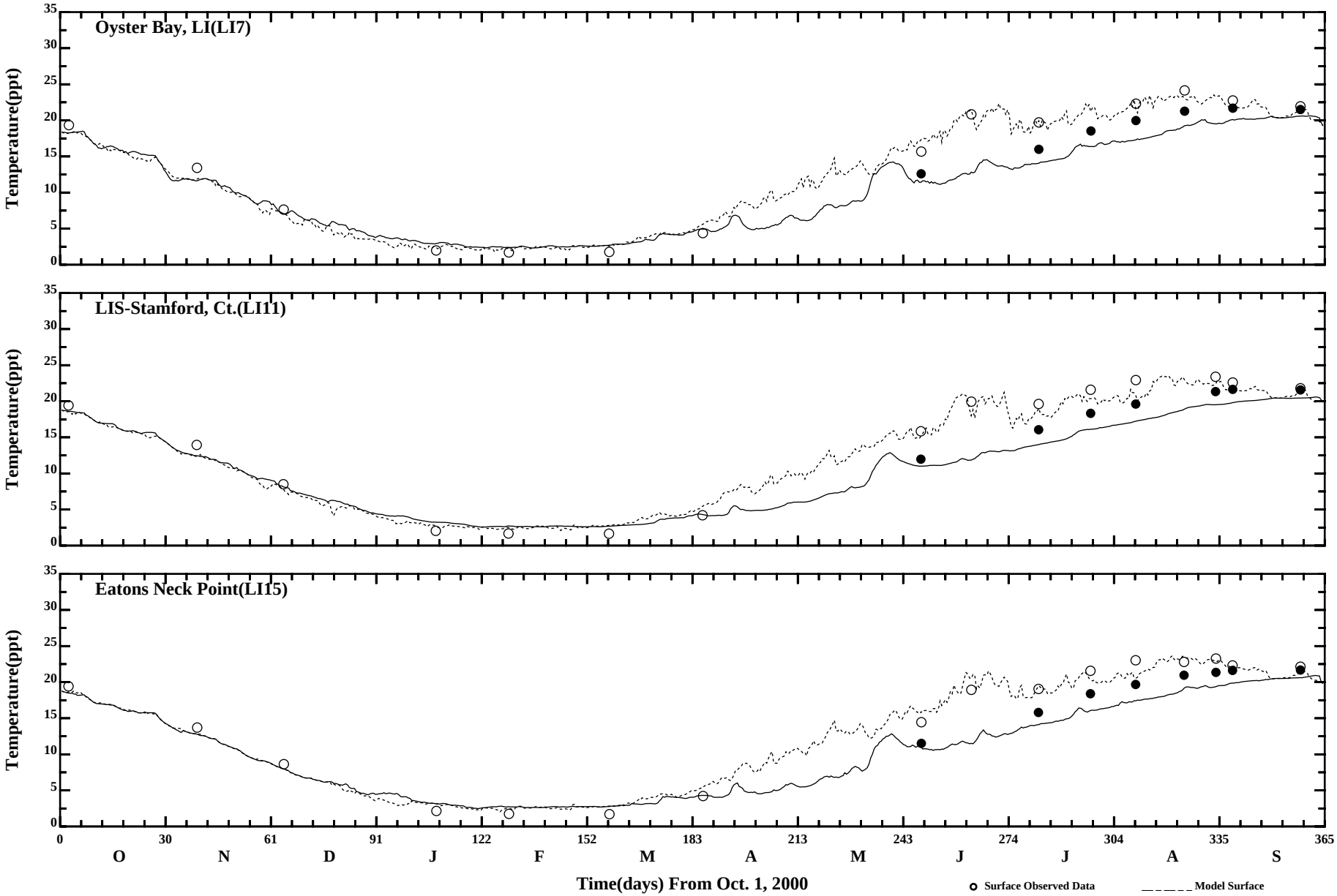

Comparison of 35 Hour Lowpass Surface and Bottom Temperature

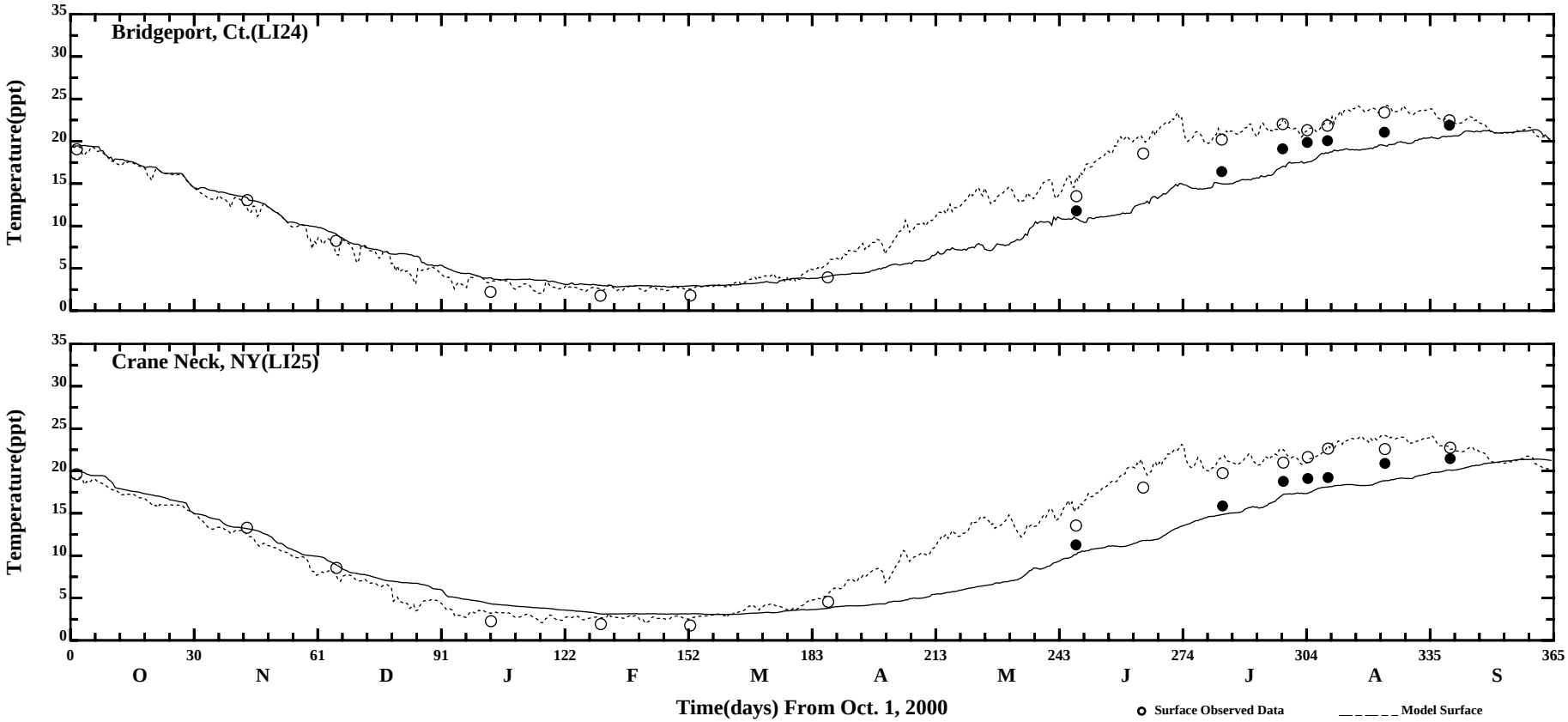

Comparison of 35 Hour Lowpass Surface and Bottom Temperature

/e1/hrfo0010/HYDRORUNS/CARP0001/PLOTS/TANDS/ptemp41_35hlp

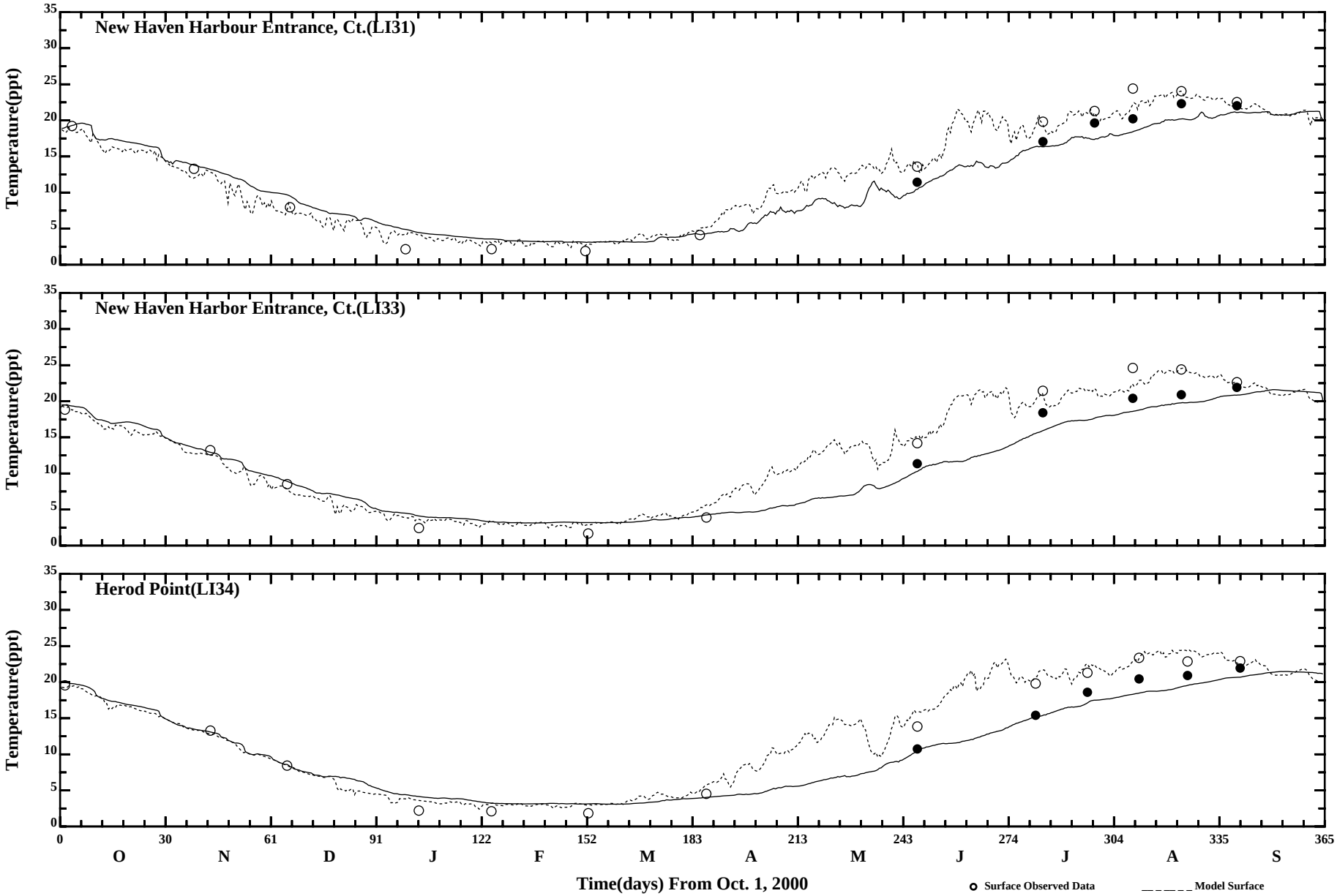

Comparison of 35 Hour Lowpass Surface and Bottom Temperature

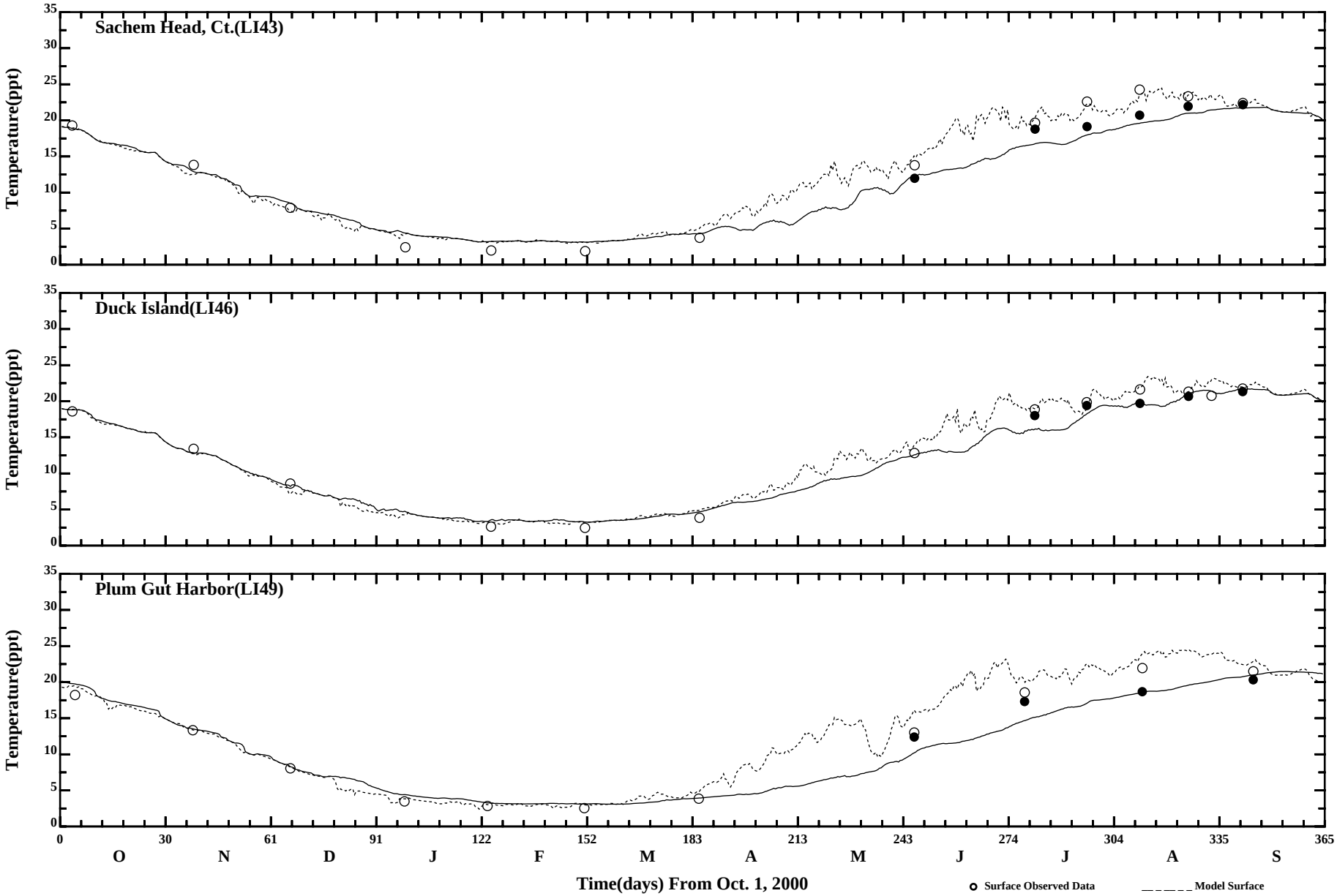

Comparison of 35 Hour Lowpass Surface and Bottom Temperature

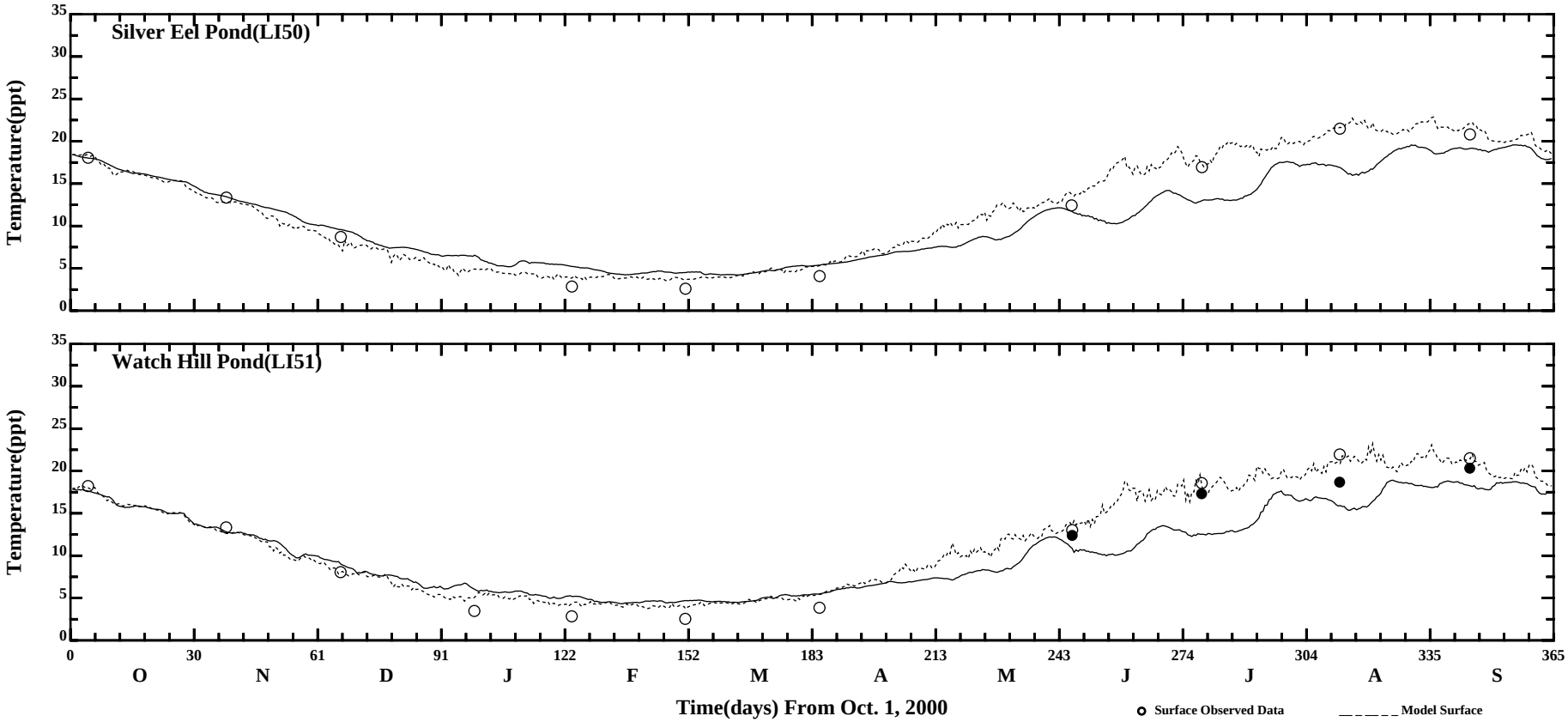

Comparison of 35 Hour Lowpass Surface and Bottom Temperature

/e1/hrfo0010/HYDRORUNS/CARP0001/PLOTS/TANDS/ptemp41_35hlp

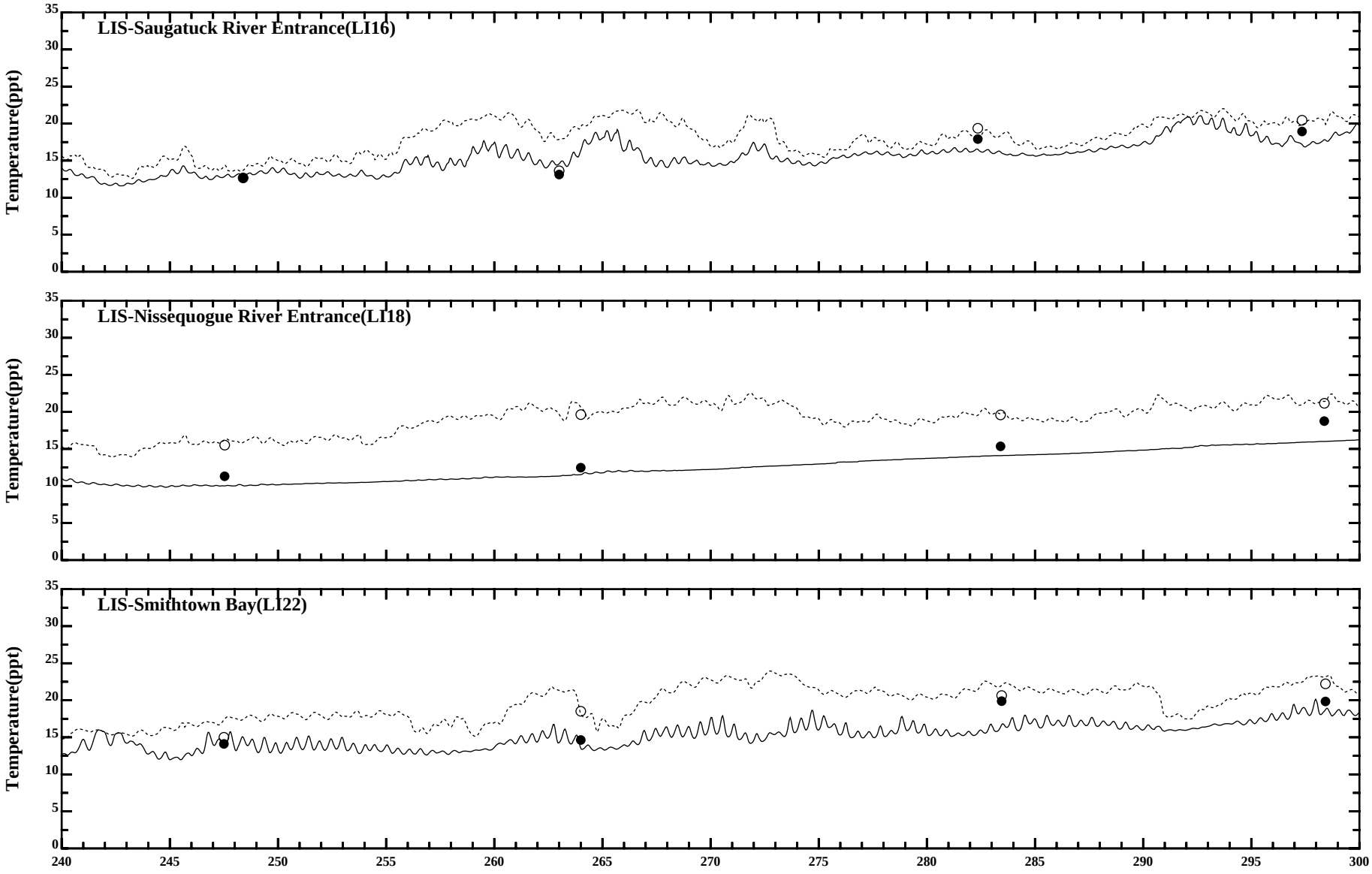

Comparison of Instantaneous Surface and Bottom Temperature

DATE: 8/02/2004 TIME: 12:28:51

/erie1/hrfo0010/HYDRORUNS/CARP0001/PLOTS/TANDS/temp41

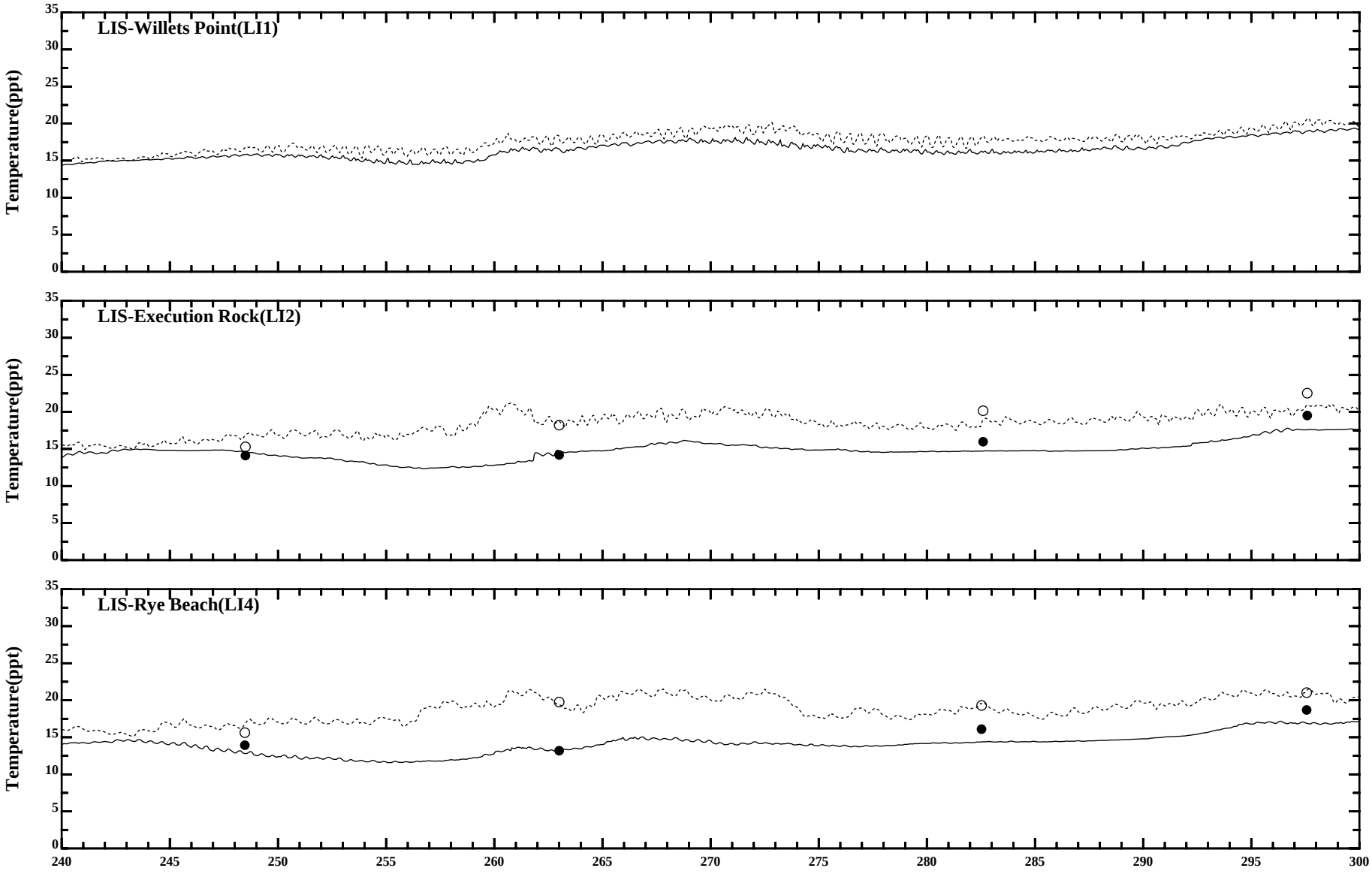

Comparison of Instantaneous Surface and Bottom Temperature

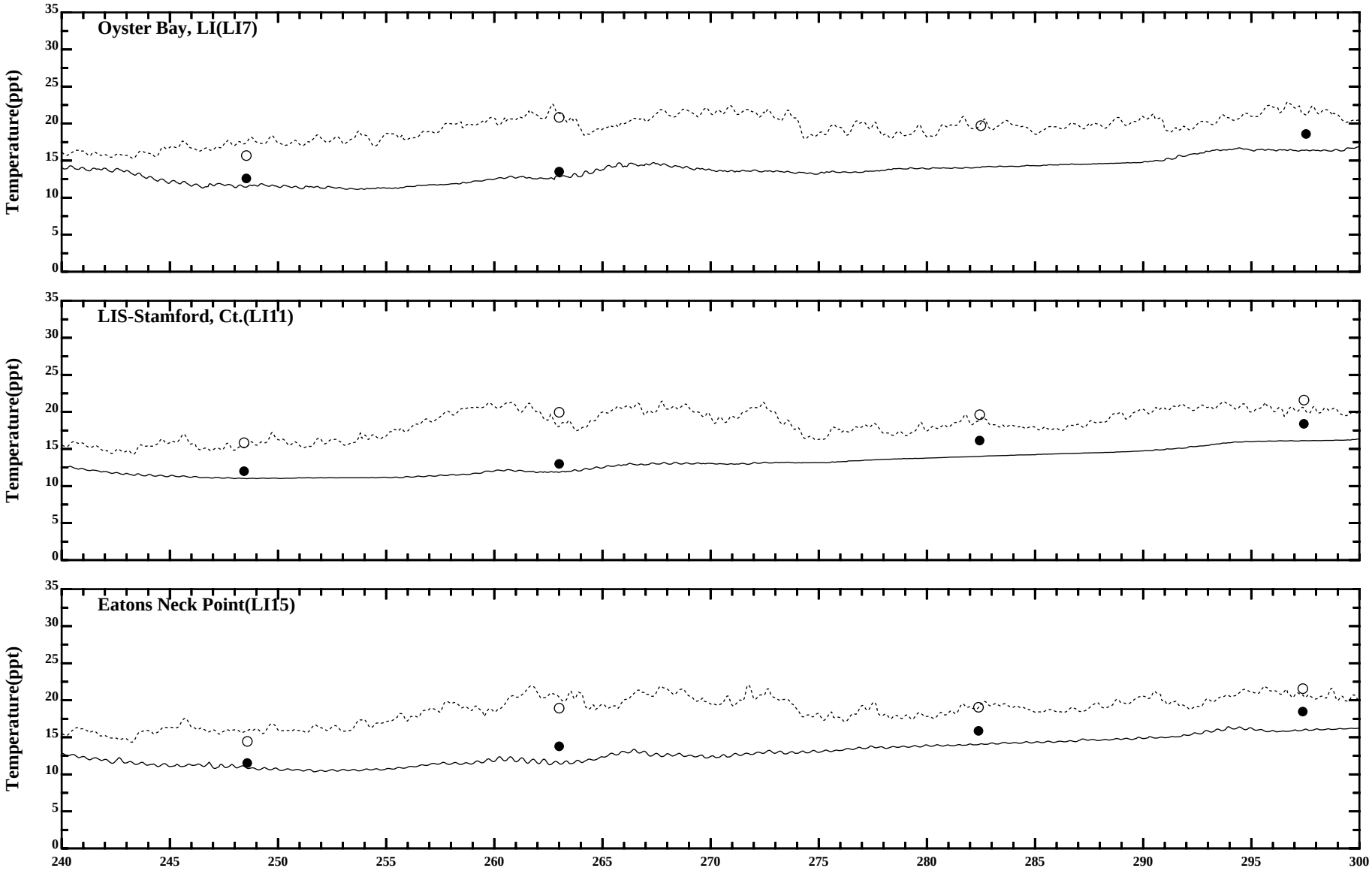

Comparison of Instantaneous Surface and Bottom Temperature

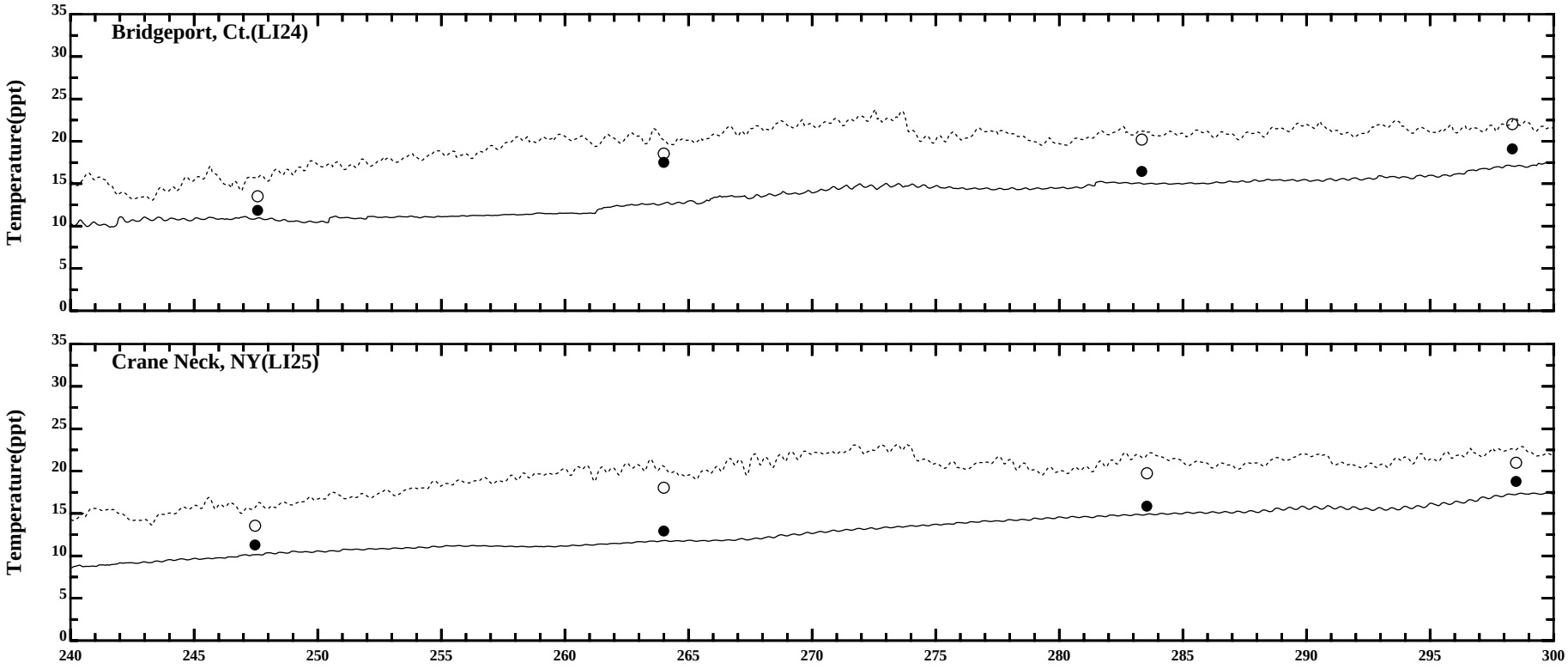

Comparison of Instantaneous Surface and Bottom Temperature

/erie1/hrfo0010/HYDRORUNS/CARP0001/PLOTS/TANDS/temp41

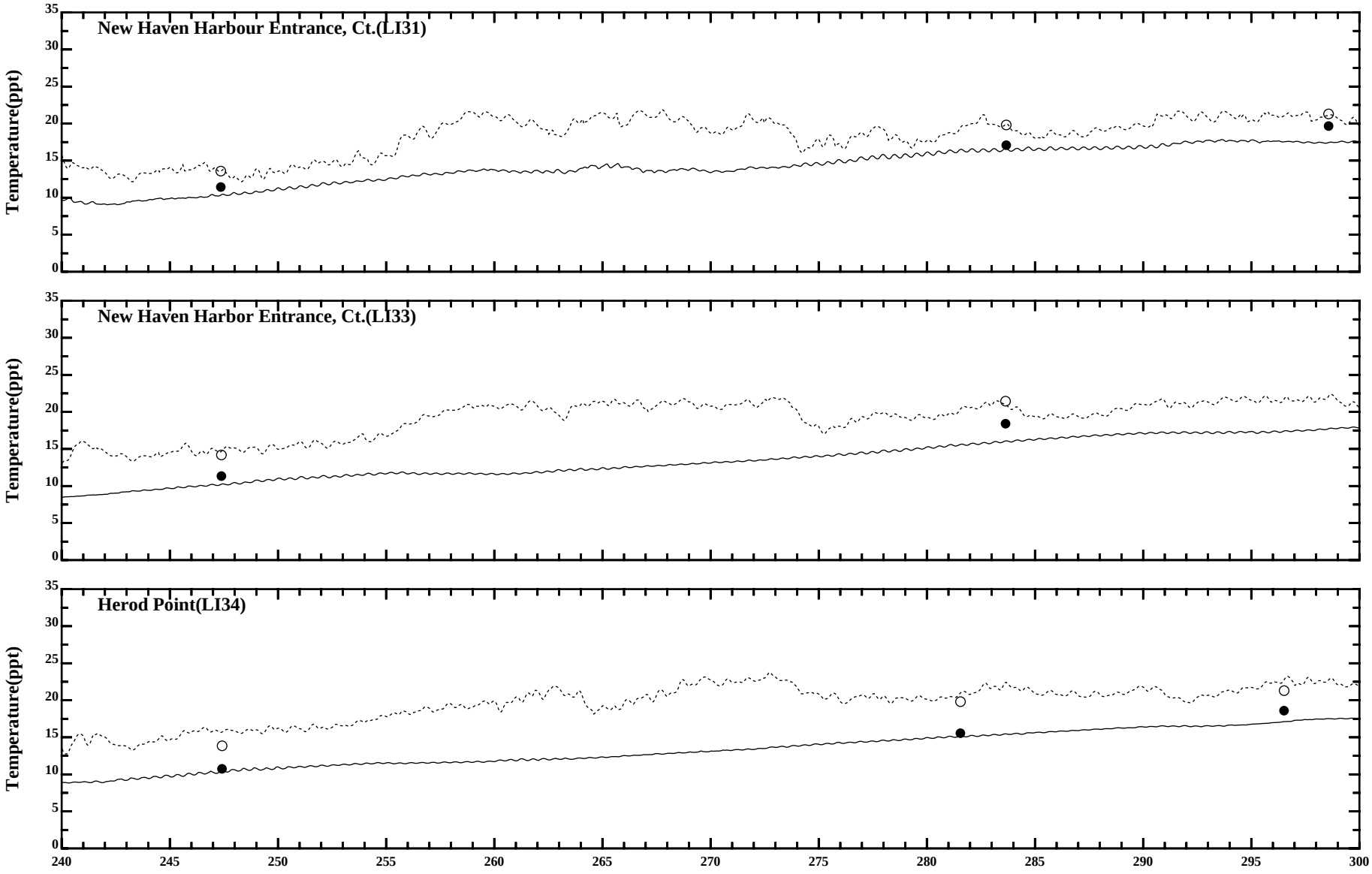

Comparison of Instantaneous Surface and Bottom Temperature

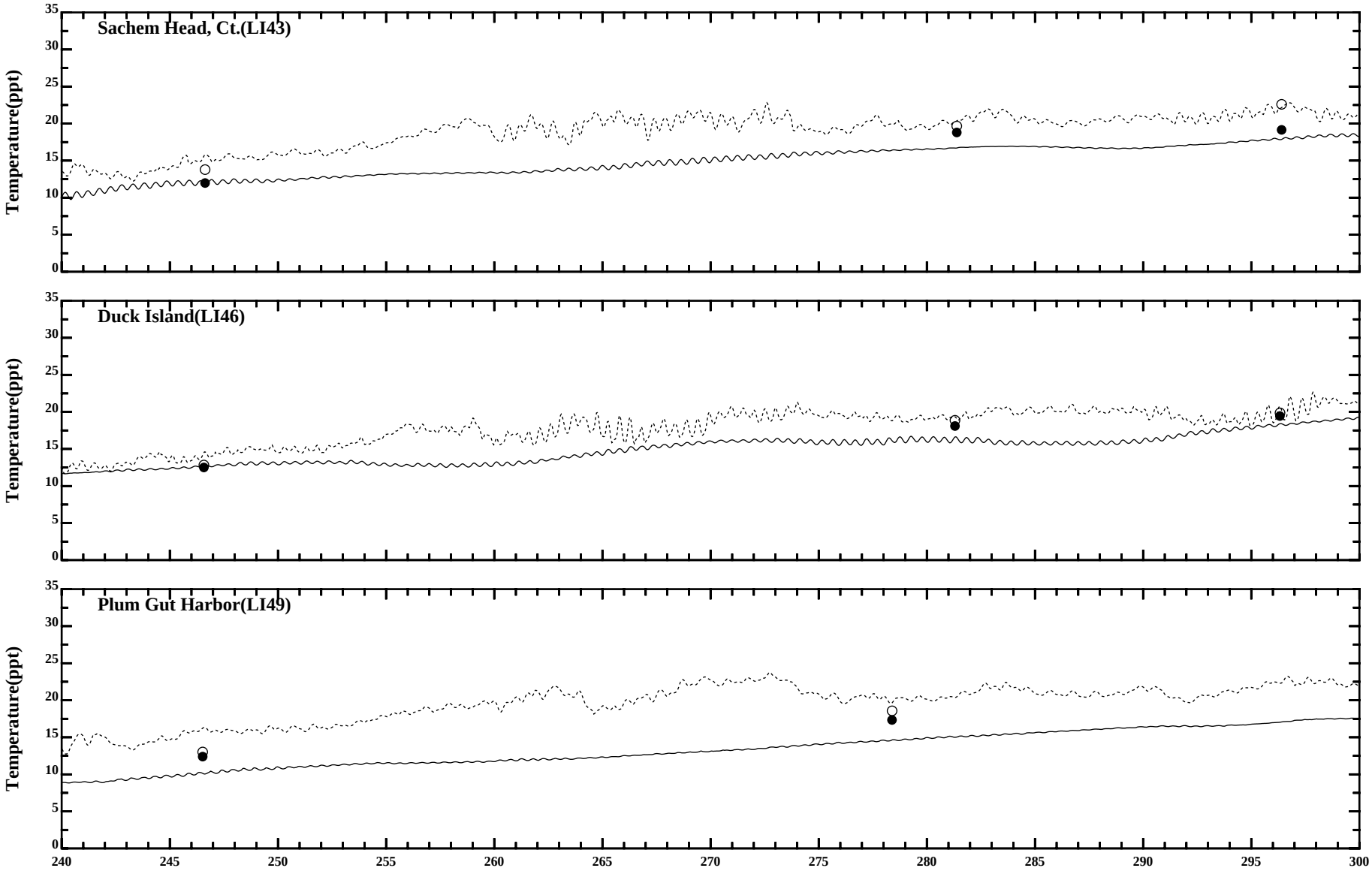

Comparison of Instantaneous Surface and Bottom Temperature

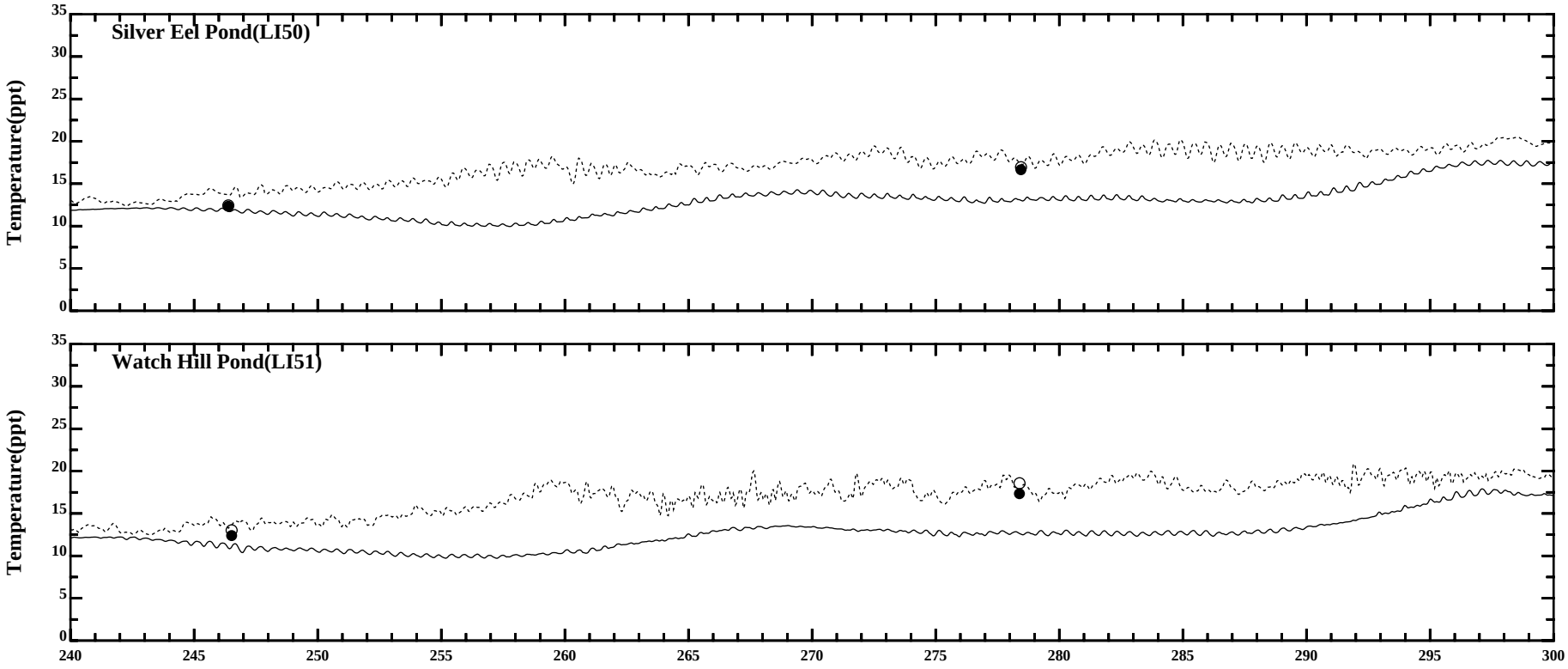

Comparison of Instantaneous Surface and Bottom Temperature

/erie1/hrfo0010/HYDRORUNS/CARP0001/PLOTS/TANDS/temp41

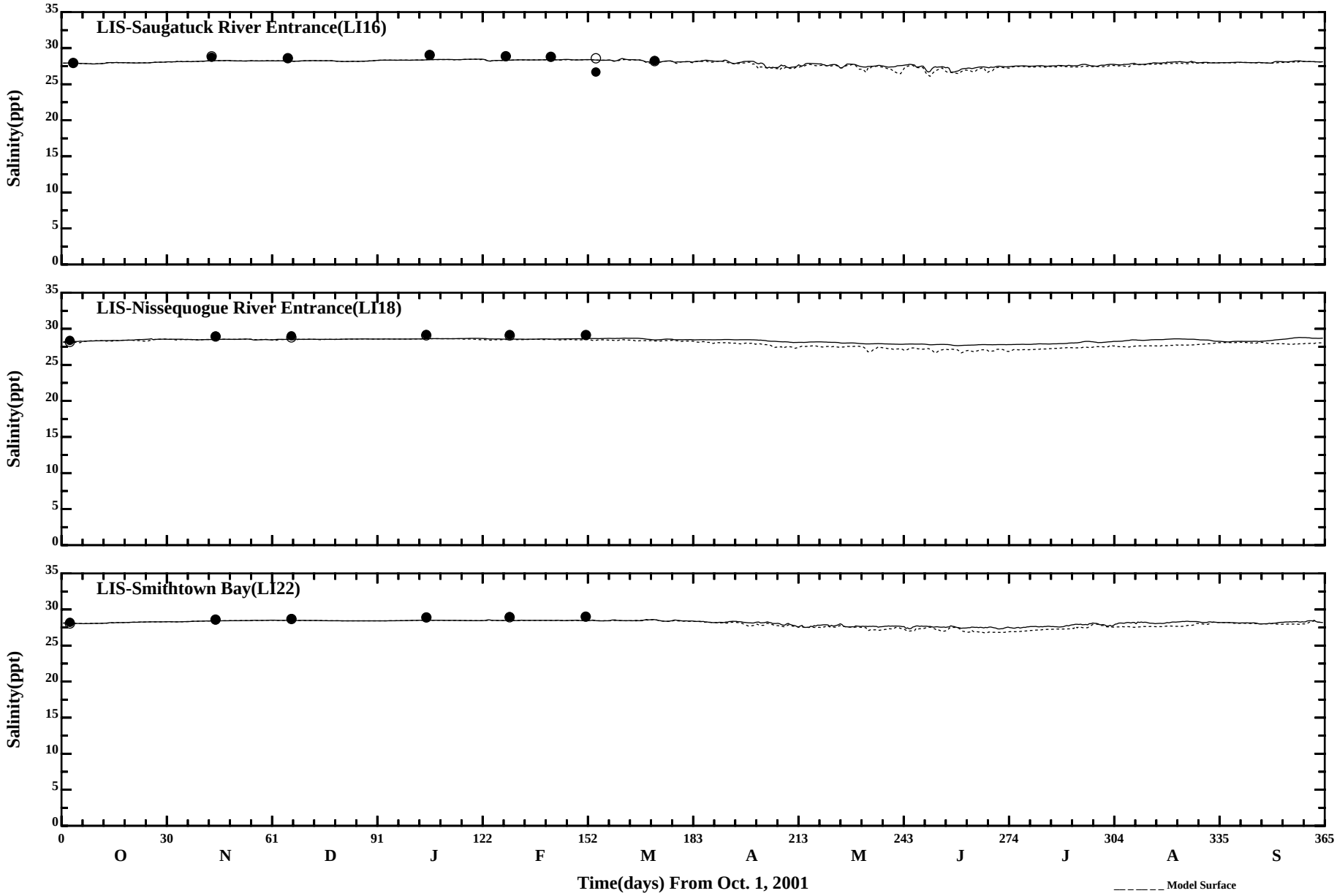

Comparison of 35 Hour Lowpass Surface and Bottom Salinity

/ont6/hrfo0010/RUNS/ECOMSED-SED/ECOMSED-0102/PLOTS/TANDS/salt_lis_35hlp

DATE: 11/21/2003 TIME: 10:41:32

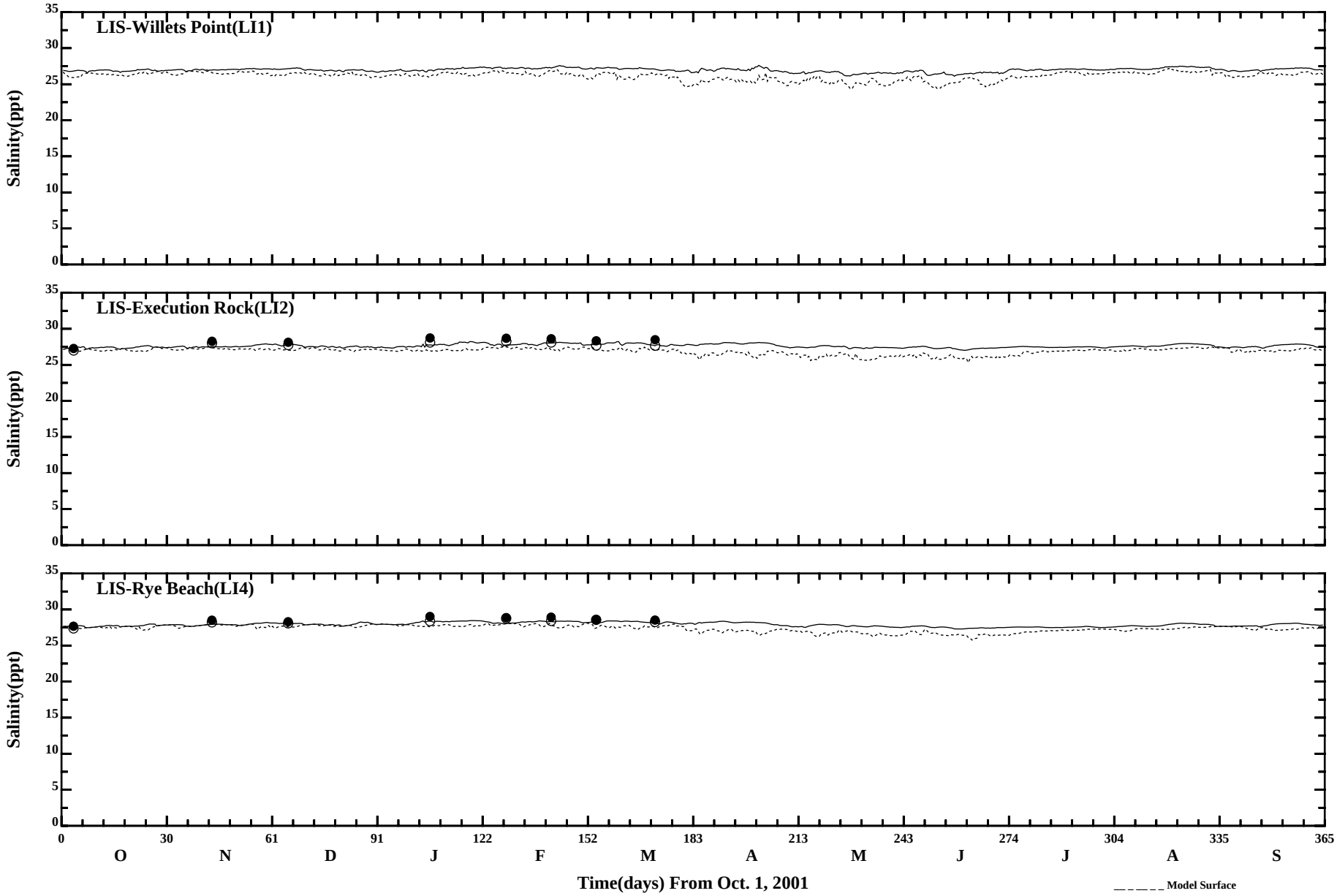

Comparison of 35 Hour Lowpass Surface and Bottom Salinity

/ont6/hrfo0010/RUNS/ECOMSED-SED/ECOMSED-0102/PLOTS/TANDS/salt_lis_35hlp

DATE: 11/21/2003 TIME: 10:41:32

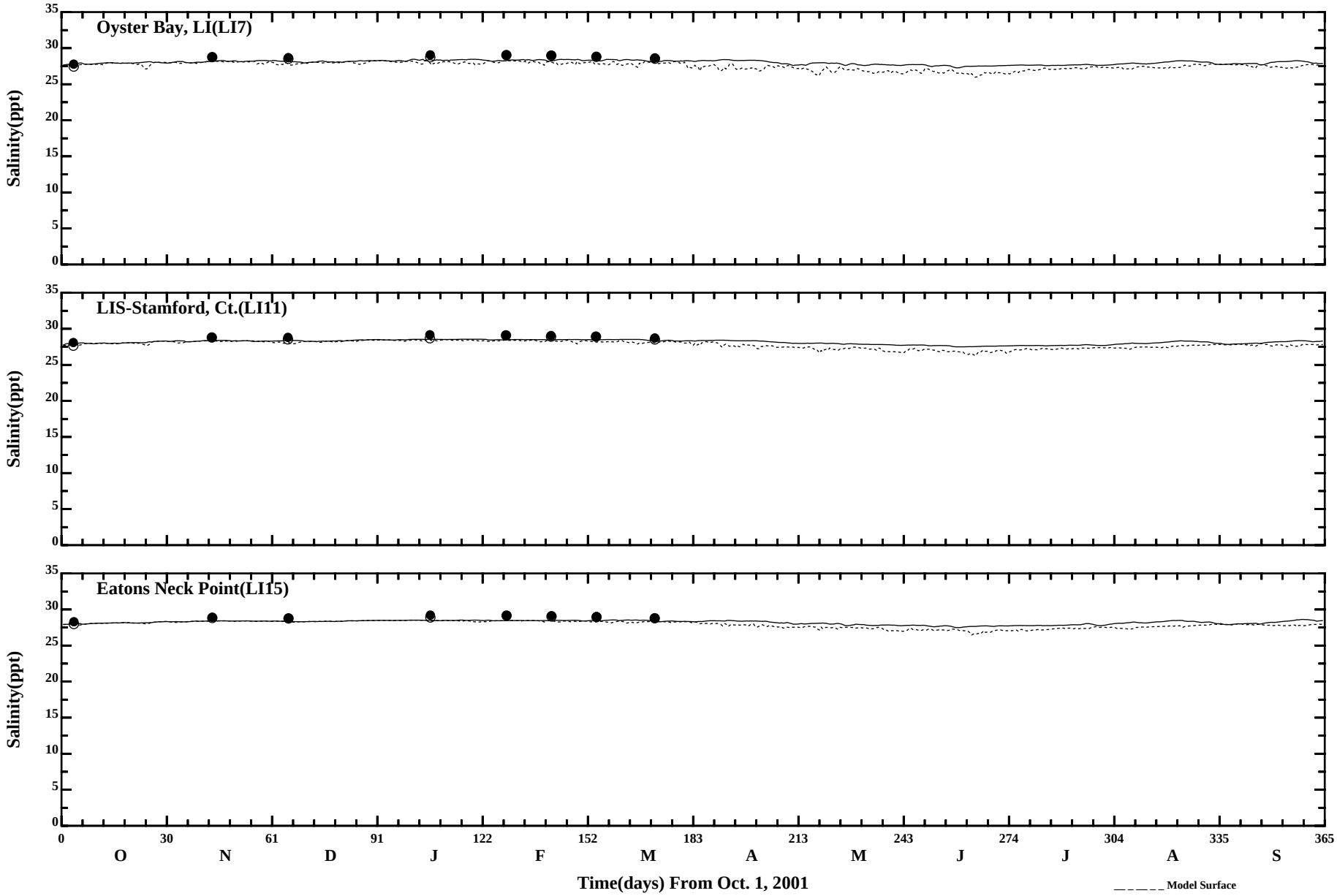

Comparison of 35 Hour Lowpass Surface and Bottom Salinity

/ont6/hrfo0010/RUNS/ECOMSED-SED/ECOMSED-0102/PLOTS/TANDS/salt_lis_35hlp

DATE: 11/21/2003 TIME: 10:41:32

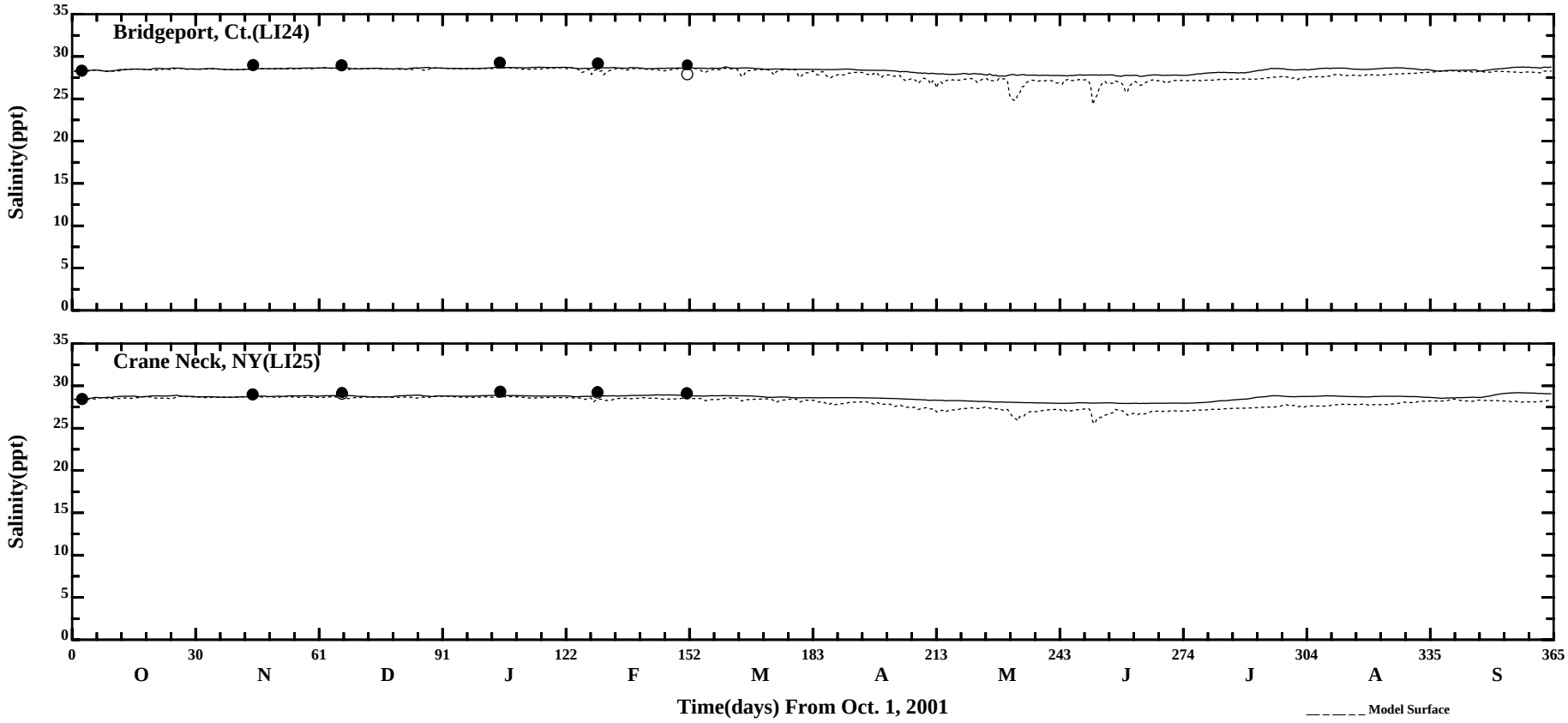

Comparison of 35 Hour Lowpass Surface and Bottom Salinity

/ont6/hrfo0010/RUNS/ECOMSED-SED/ECOMSED-0102/PLOTS/TANDS/salt_lis_35hlp

DATE: 11/21/2003 TIME: 10:41:32

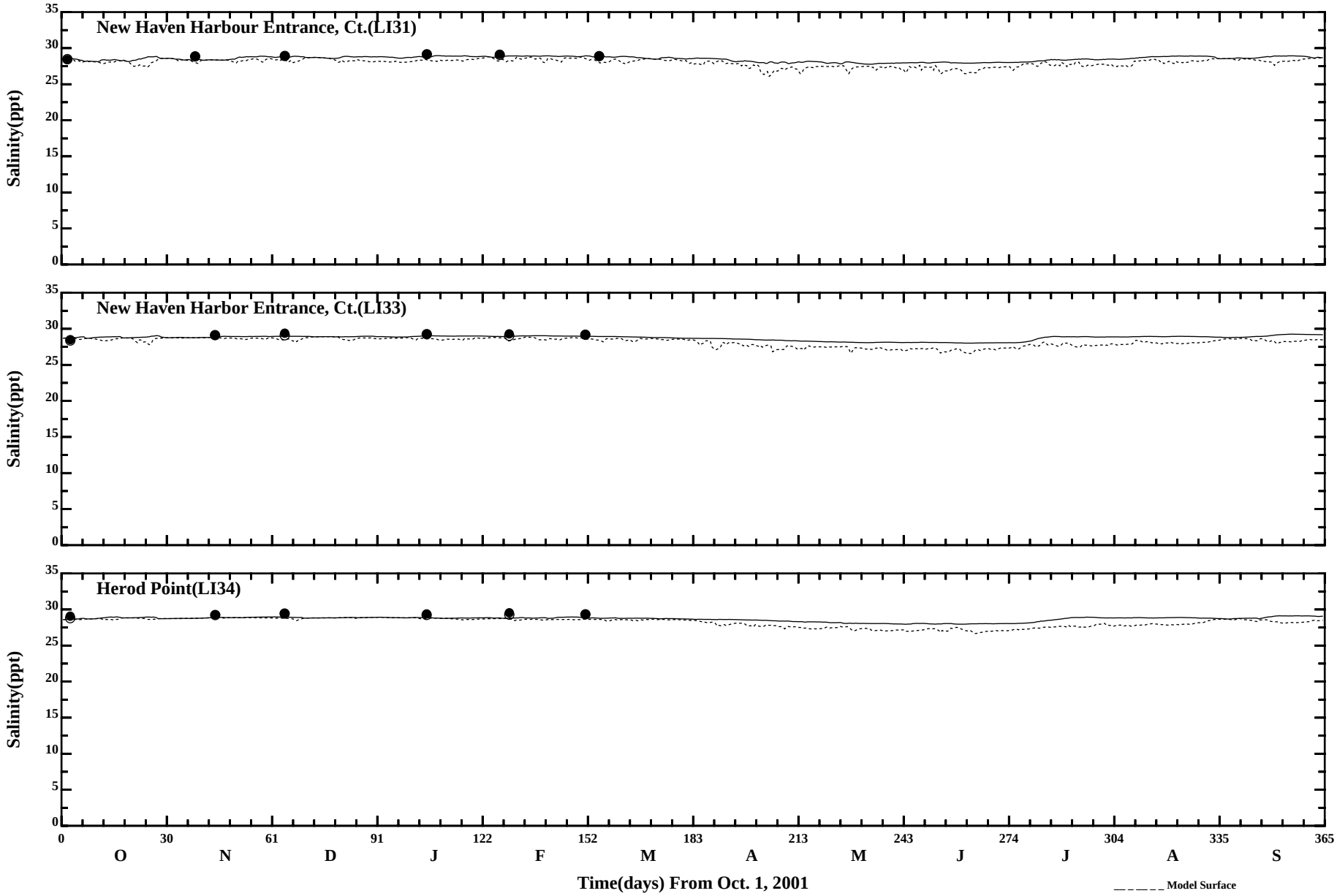

Comparison of 35 Hour Lowpass Surface and Bottom Salinity

/ont6/hrfo0010/RUNS/ECOMSED-SED/ECOMSED-0102/PLOTS/TANDS/salt_lis_35hlp

DATE: 11/21/2003 TIME: 10:41:32

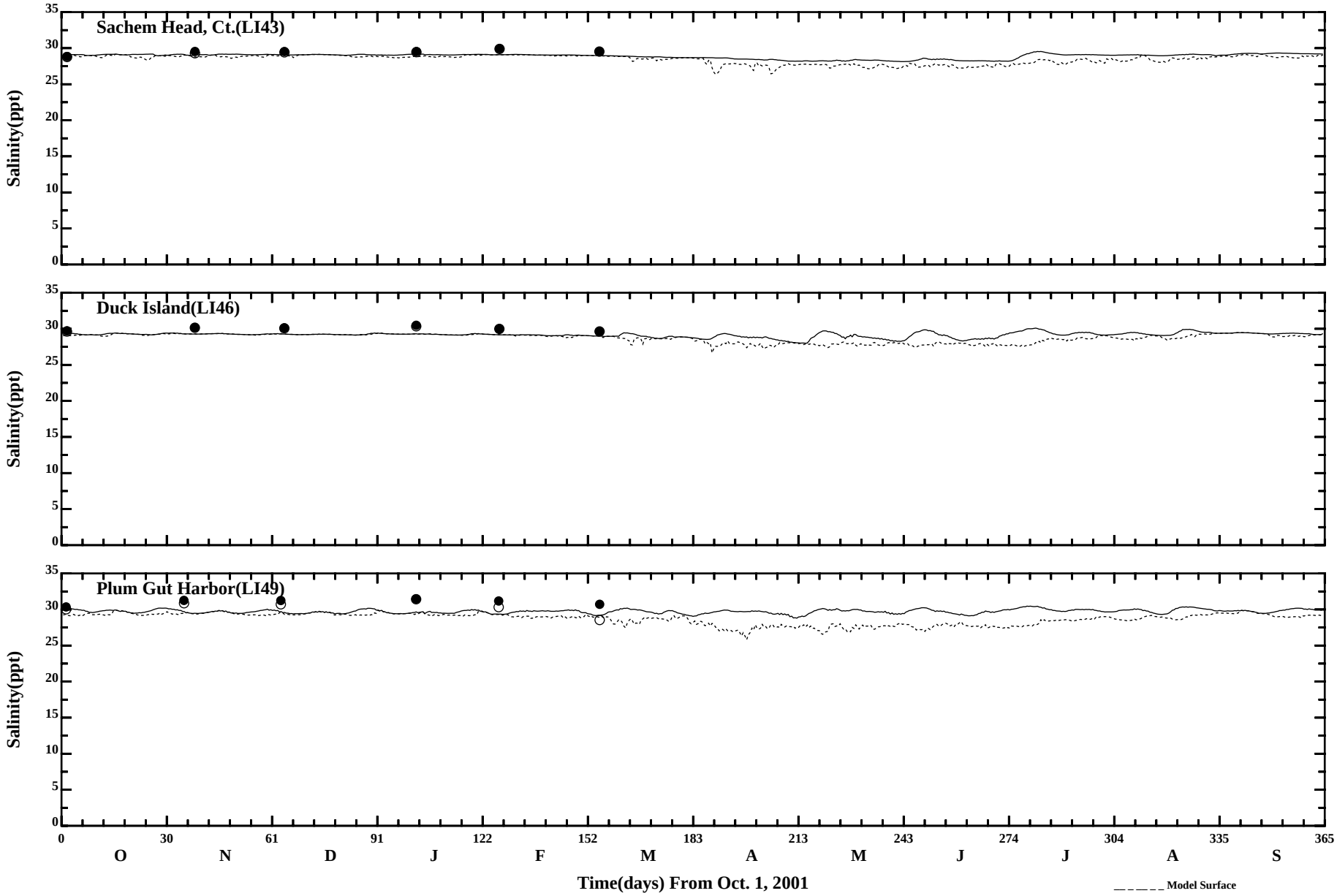

Comparison of 35 Hour Lowpass Surface and Bottom Salinity

/ont6/hrfo0010/RUNS/ECOMSED-SED/ECOMSED-0102/PLOTS/TANDS/salt_lis_35hlp

DATE: 11/21/2003 TIME: 10:41:32

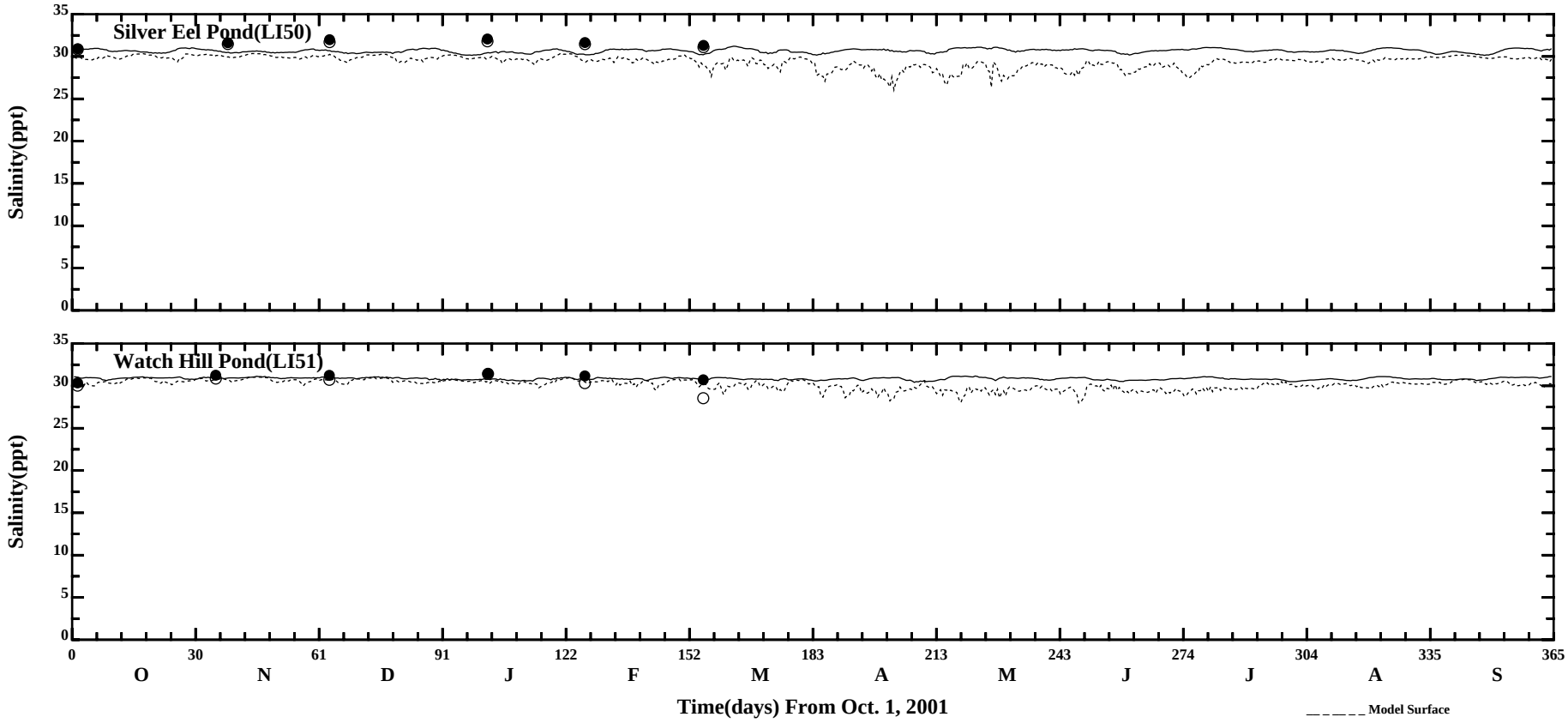

Comparison of 35 Hour Lowpass Surface and Bottom Salinity

/ont6/hrfo0010/RUNS/ECOMSED-SED/ECOMSED-0102/PLOTS/TANDS/salt_lis_35hlp

DATE: 11/21/2003 TIME: 10:41:32

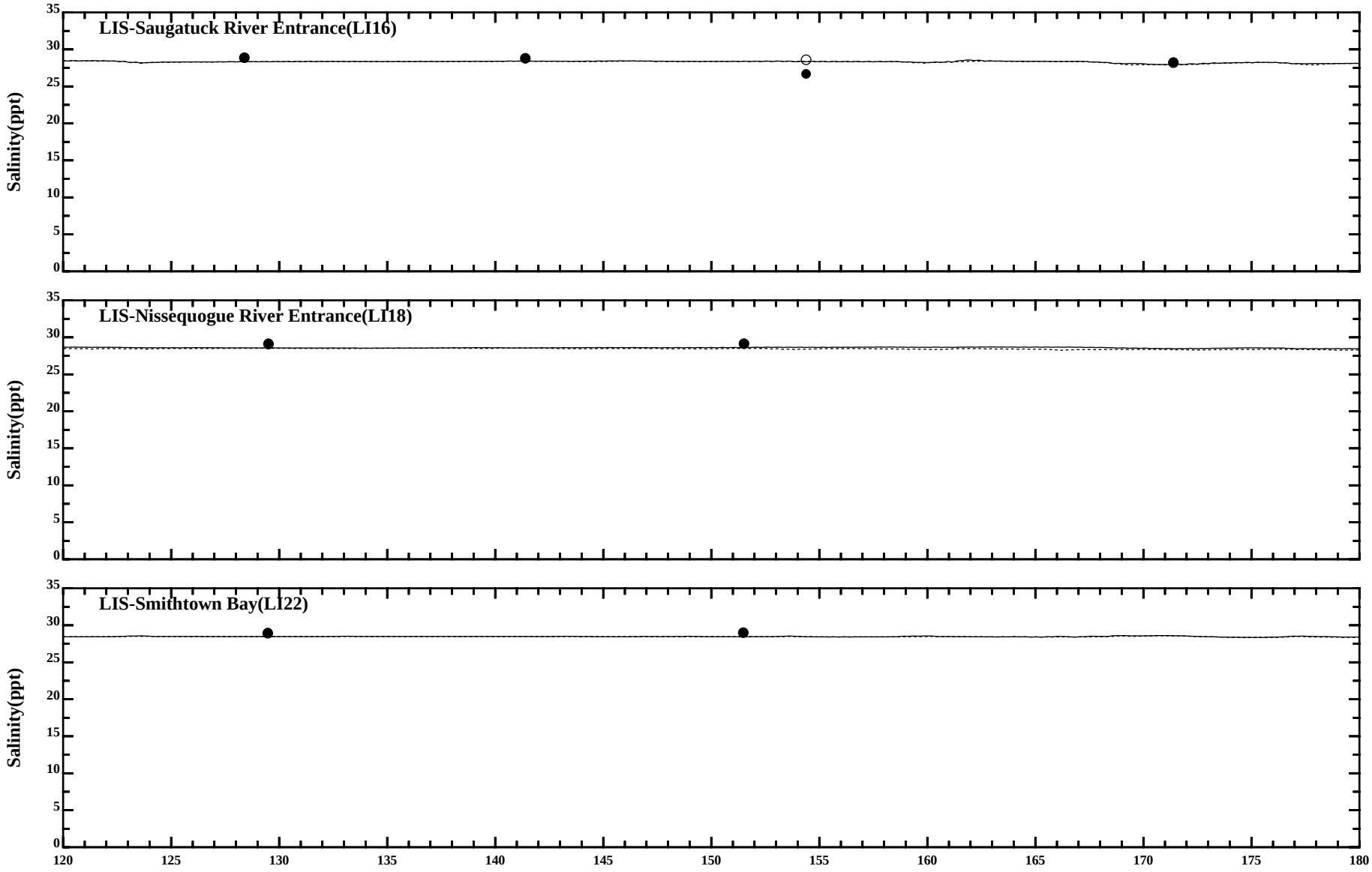

Comparison of Instantaneous Surface and Bottom Salinity

/ont6/hrfo0010/RUNS/ECOMSED-SED/ECOMSED-0102/PLOTS/TANDS/salt_lis_hourly

DATE: 11/21/2003 TIME: 10:41:43

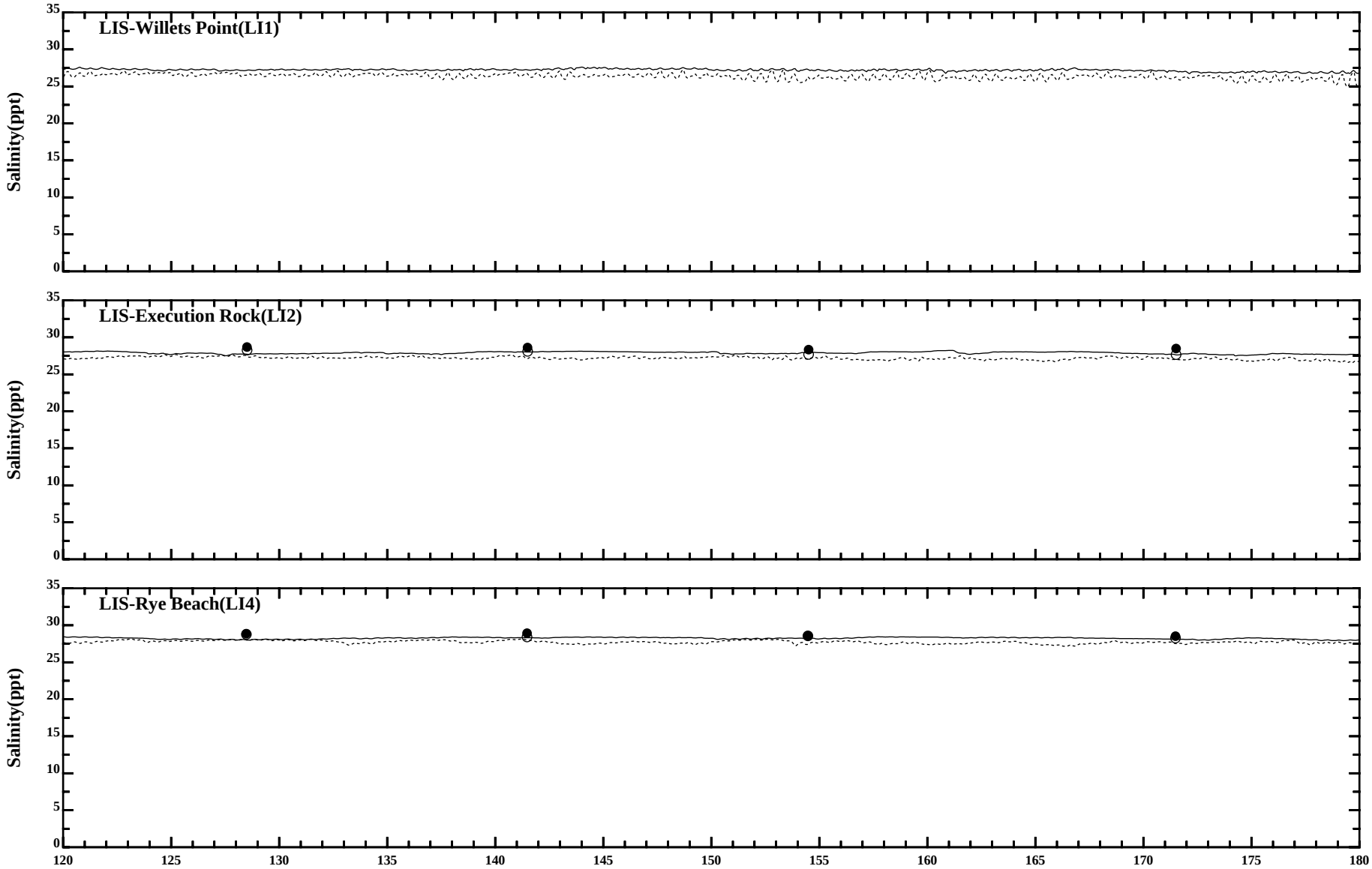

Comparison of Instantaneous Surface and Bottom Salinity

/ont6/hrfo0010/RUNS/ECOMSED-SED/ECOMSED-0102/PLOTS/TANDS/salt_lis_hourly

DATE: 11/21/2003 TIME: 10:41:43

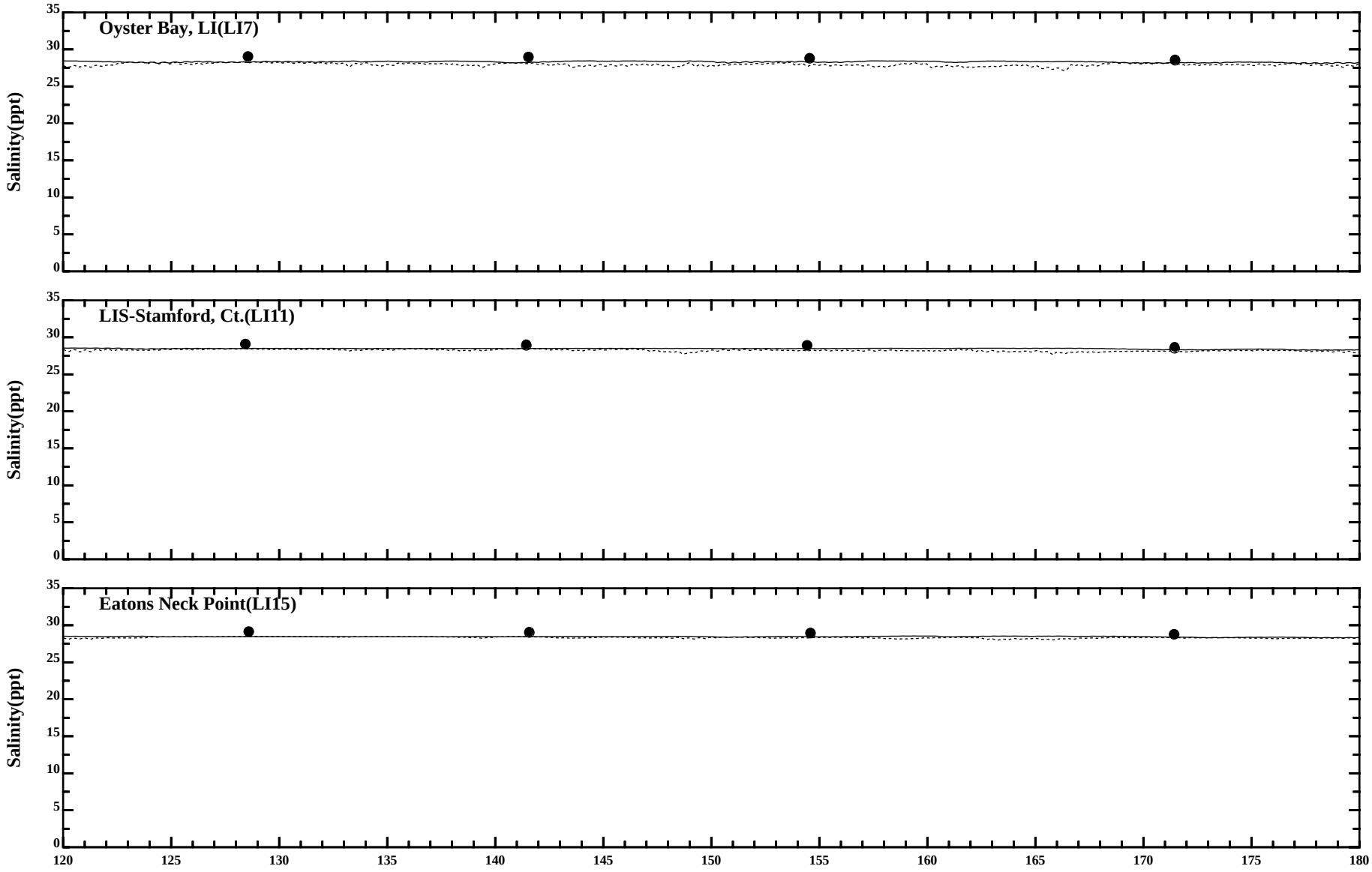

Comparison of Instantaneous Surface and Bottom Salinity

/ont6/hrfo0010/RUNS/ECOMSED-SED/ECOMSED-0102/PLOTS/TANDS/salt_lis_hourly

DATE: 11/21/2003 TIME: 10:41:43

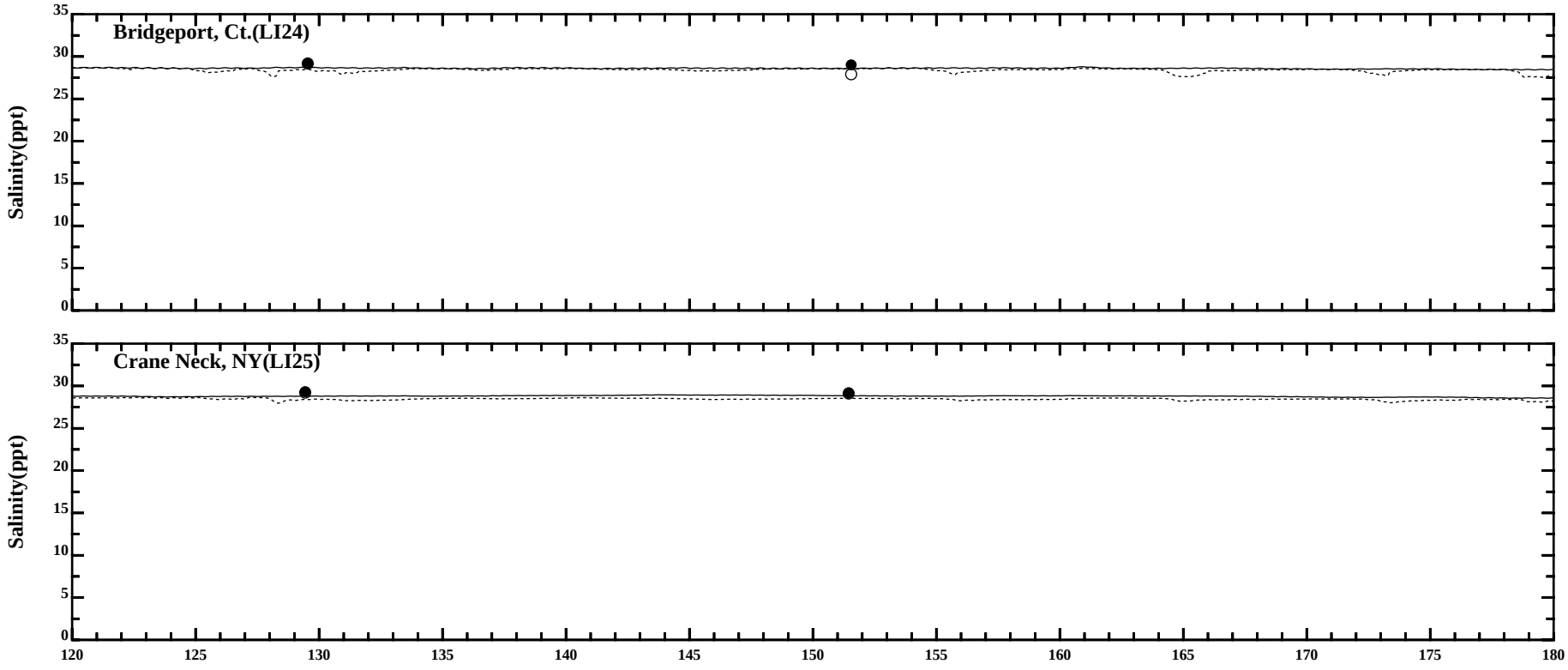

Comparison of Instantaneous Surface and Bottom Salinity

/ont6/hrfo0010/RUNS/ECOMSED-SED/ECOMSED-0102/PLOTS/TANDS/salt_lis_hourly

DATE: 11/21/2003 TIME: 10:41:43

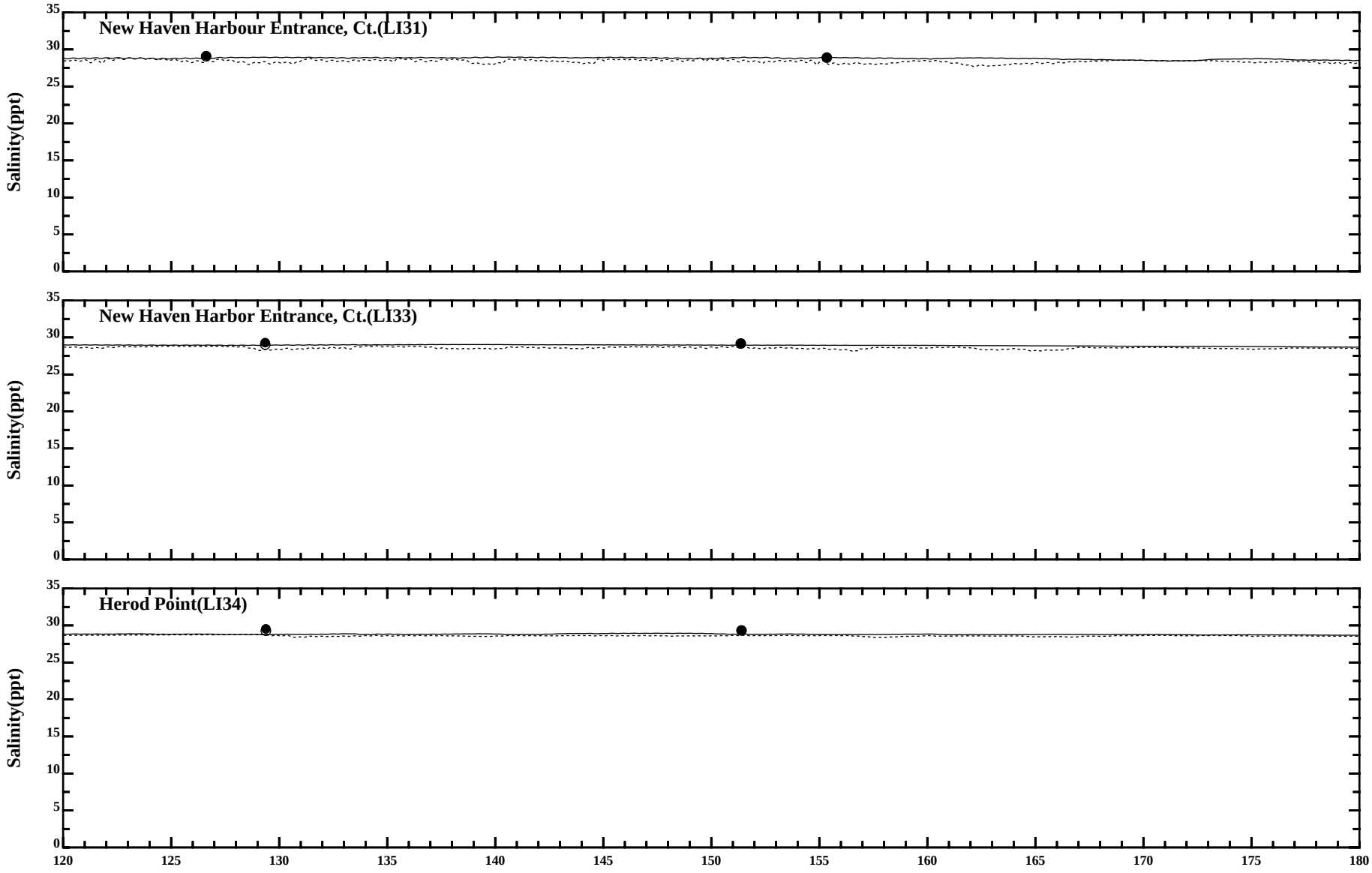

Comparison of Instantaneous Surface and Bottom Salinity

/ont6/hrfo0010/RUNS/ECOMSED-SED/ECOMSED-0102/PLOTS/TANDS/salt_lis_hourly

DATE: 11/21/2003 TIME: 10:41:43

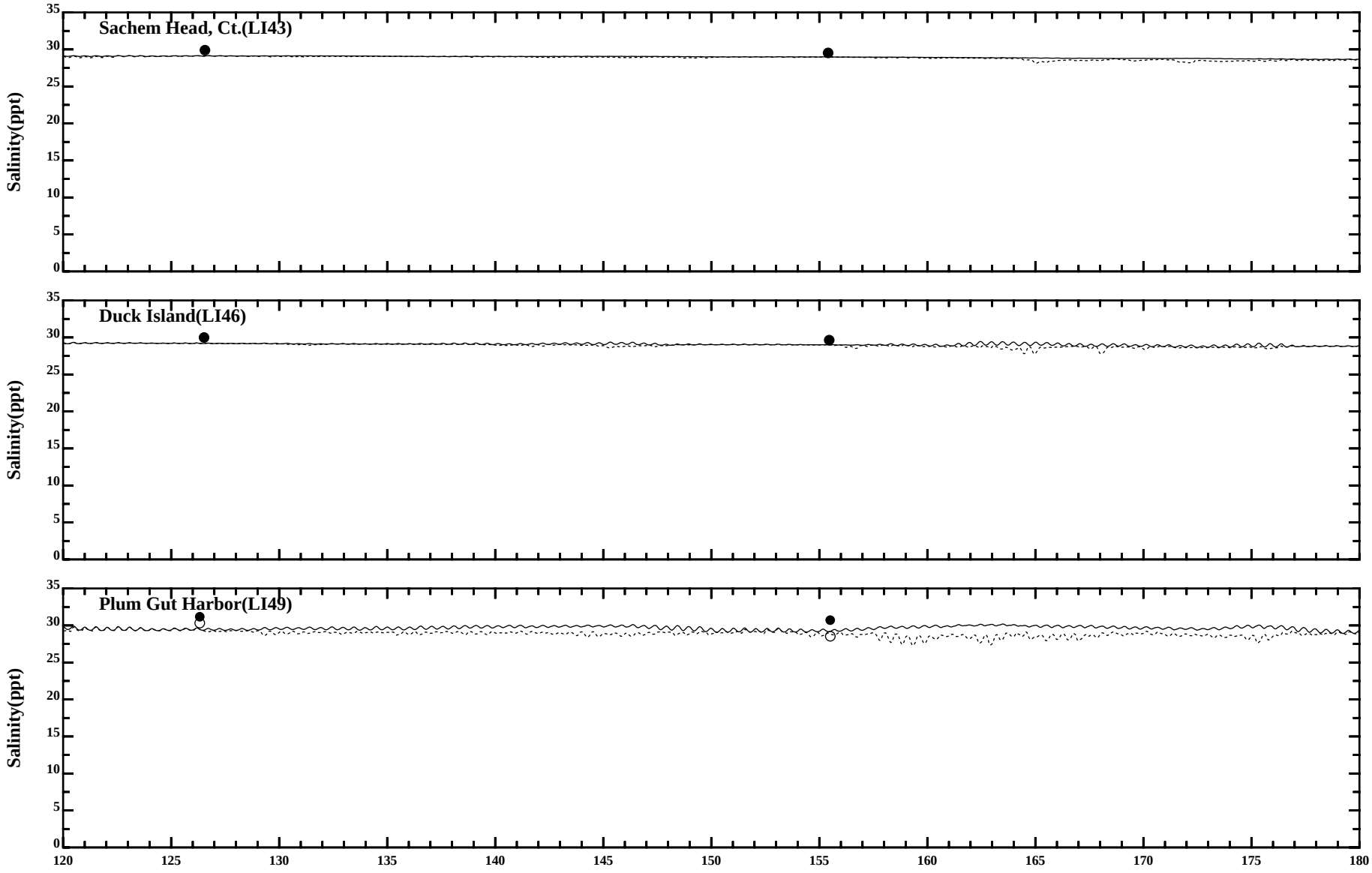

Comparison of Instantaneous Surface and Bottom Salinity

/ont6/hrfo0010/RUNS/ECOMSED-SED/ECOMSED-0102/PLOTS/TANDS/salt_lis_hourly

DATE: 11/21/2003 TIME: 10:41:43

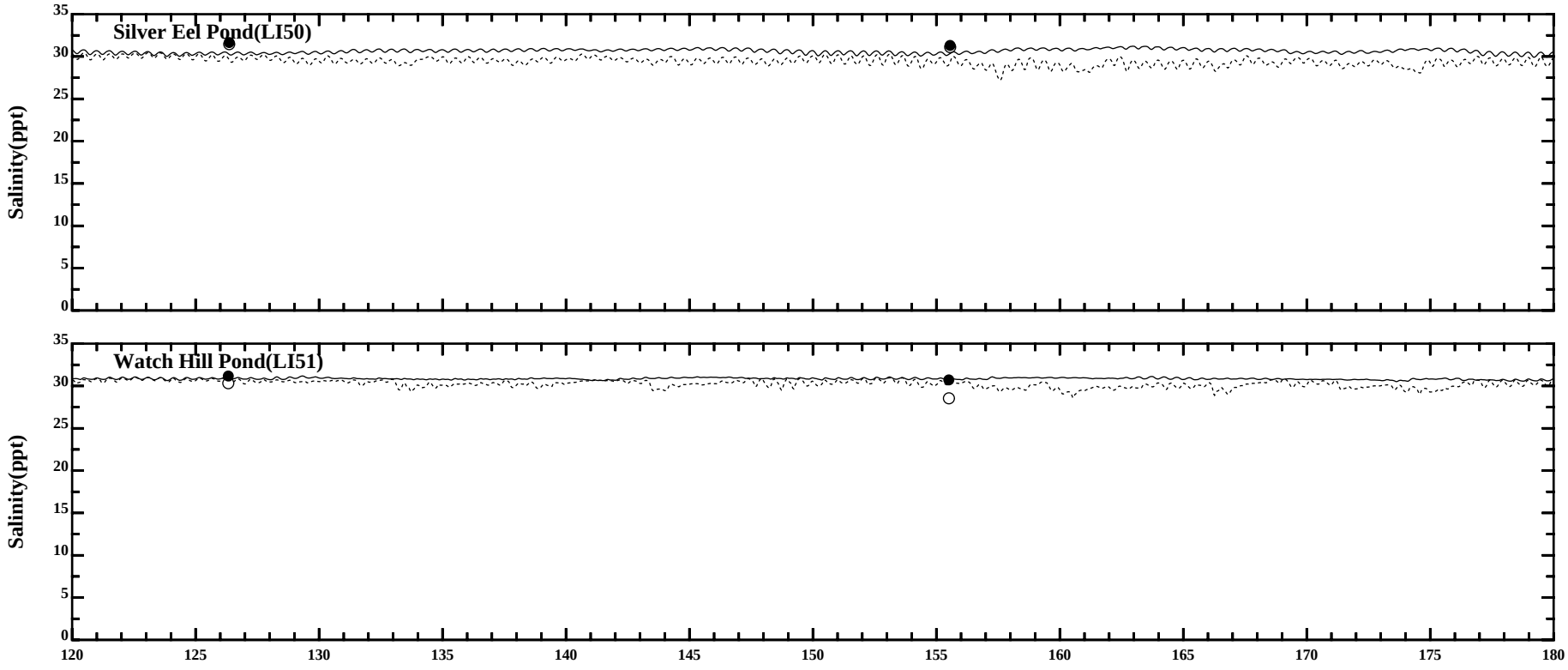

Comparison of Instantaneous Surface and Bottom Salinity

/ont6/hrfo0010/RUNS/ECOMSED-SED/ECOMSED-0102/PLOTS/TANDS/salt_lis_hourly

DATE: 11/21/2003 TIME: 10:41:43

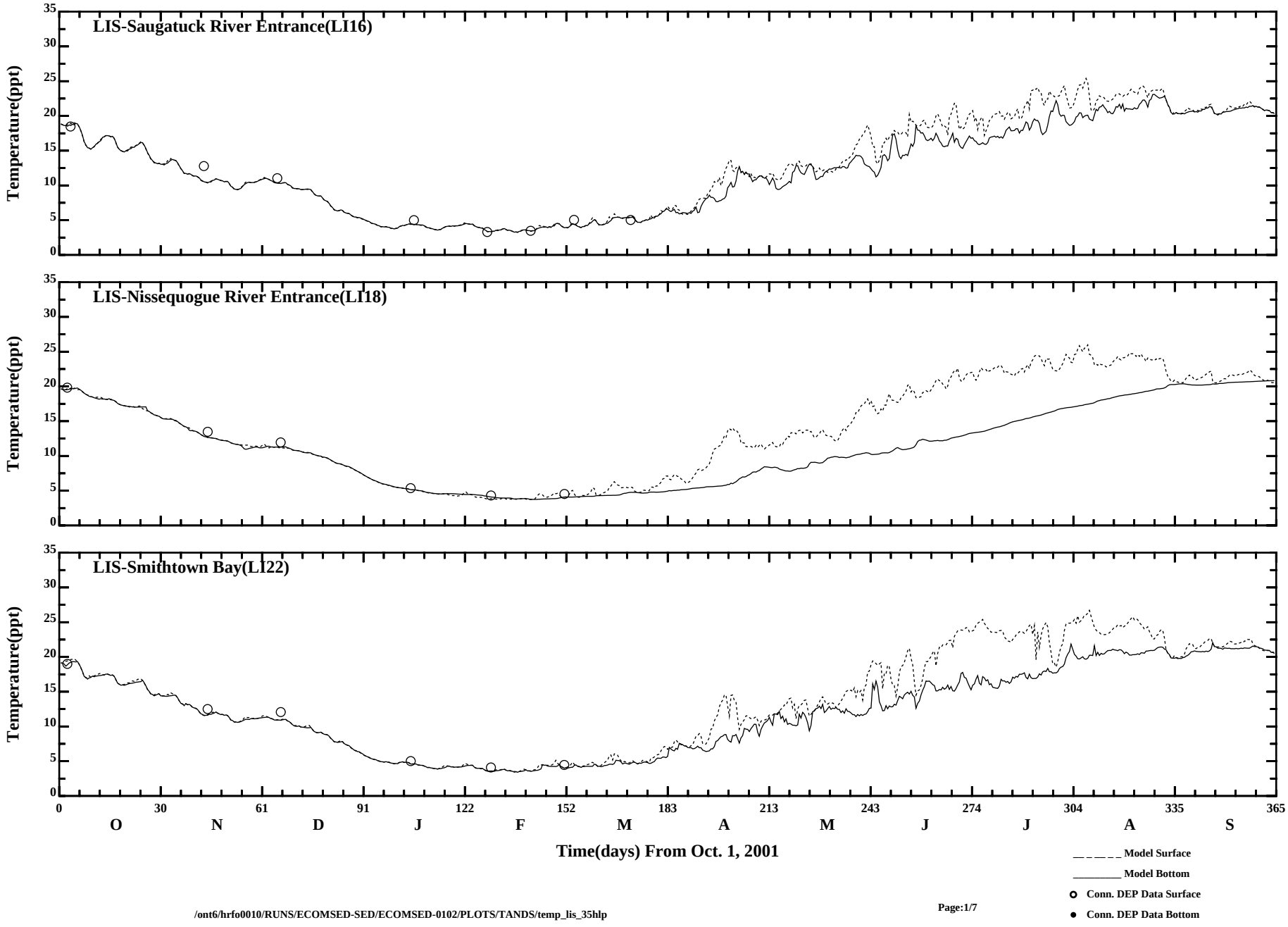

/ont6/hrfo0010/RUNS/ECOMSED-SED/ECOMSED-0102/PLOTS/TANDS/temp_lis_35hlp

DATE: 11/21/2003 TIME: 10:39:55

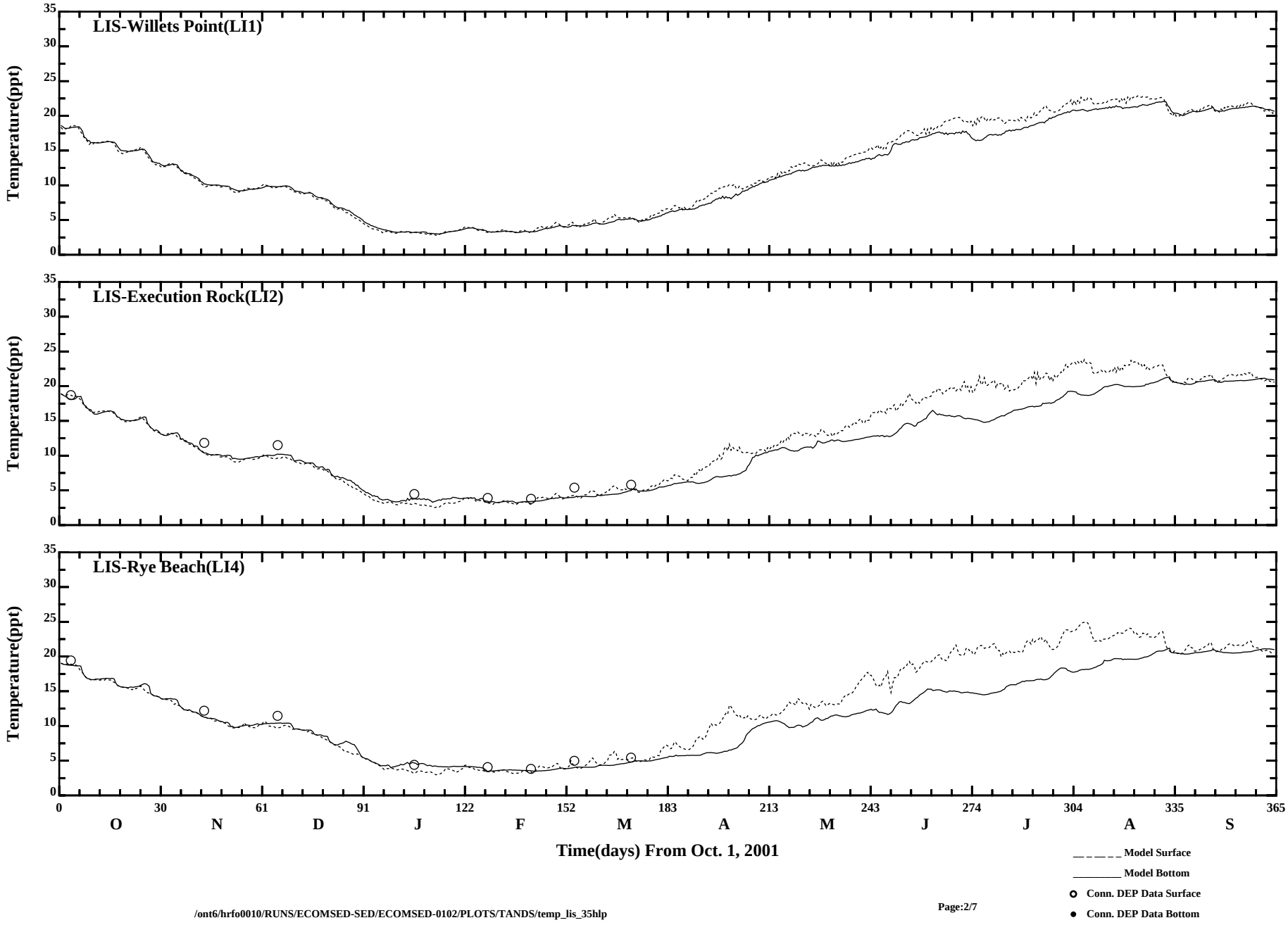

/ont6/hrfo0010/RUNS/ECOMSED-SED/ECOMSED-0102/PLOTS/TANDS/temp_lis_35hlp

DATE: 11/21/2003 TIME: 10:39:55

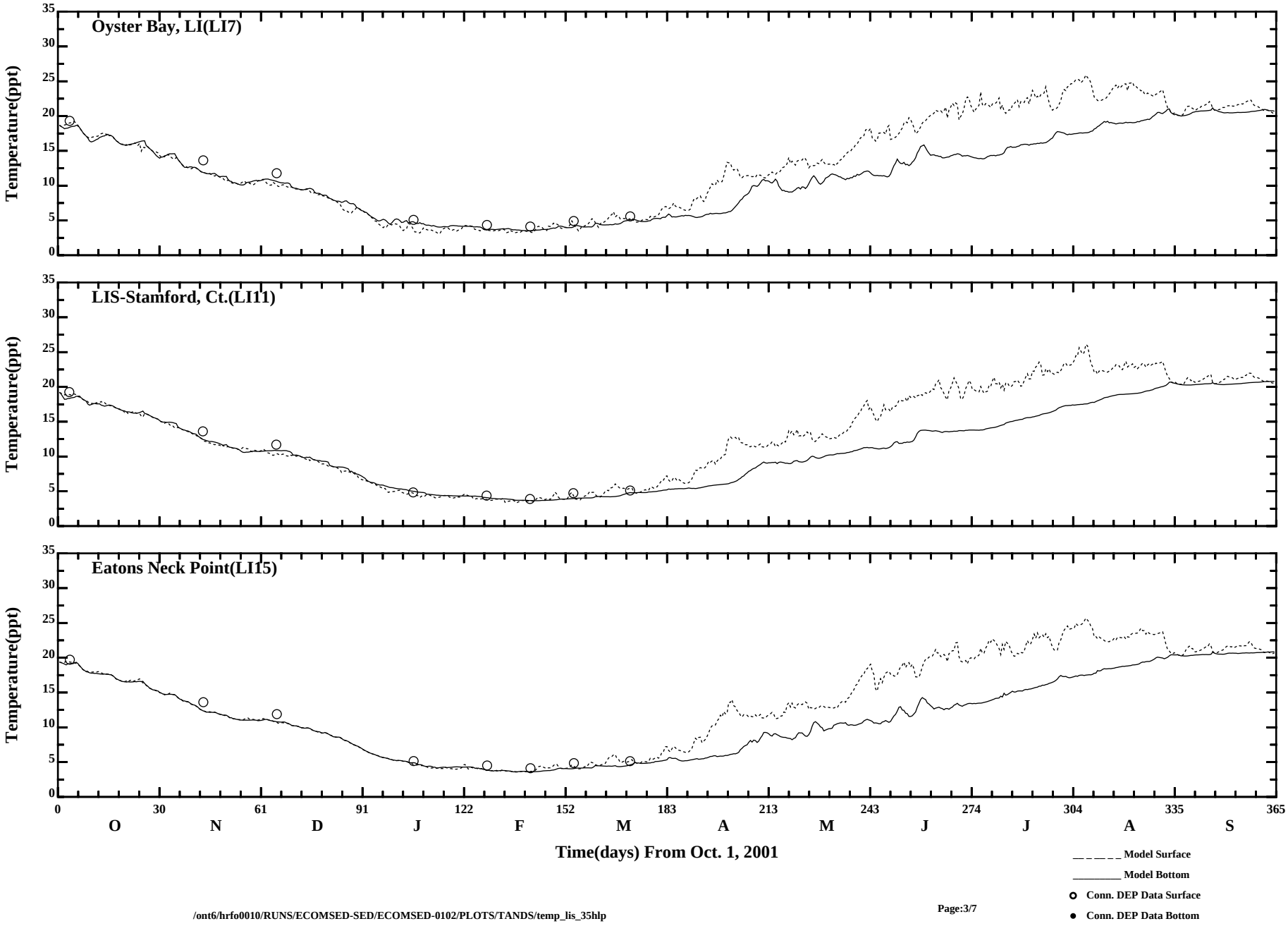
Oyster Bay, LI(LI7)
LIS-Stamford, Ct.(LI11)
Eatons Neck Point(LI15)
Temperature(ppt)
0
5
10
15
20
25
30
35
0
30
61
91
122
152
183
213
243
274
304
335
365
O
N
D
J
F
M
A
M
J
J
A
S
Time(days) From Oct. 1, 2001
Model Surface
Model Bottom
Conn. DEP Data Surface
Conn. DEP Data Bottom

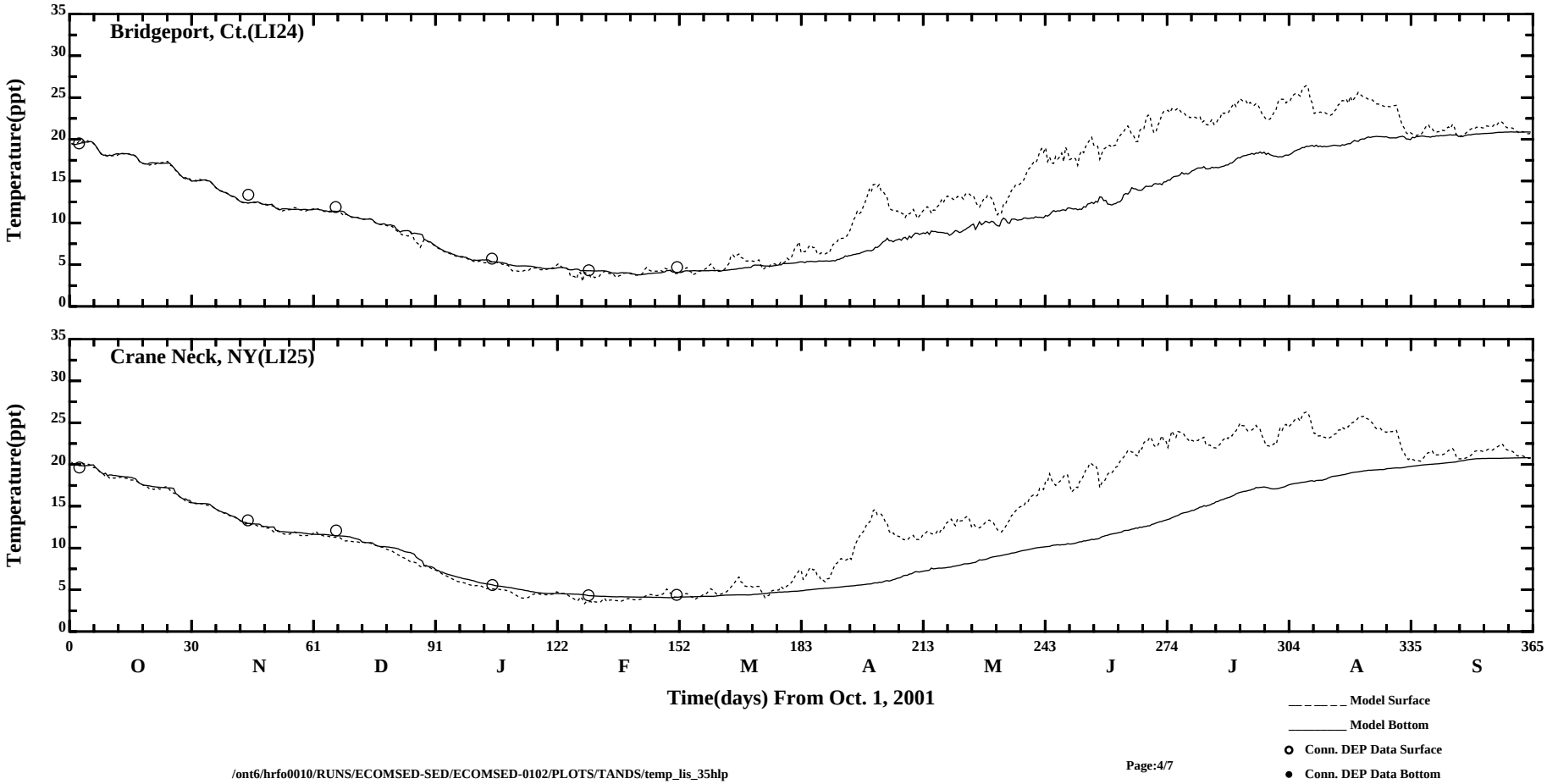

/ont6/hrfo0010/RUNS/ECOMSED-SED/ECOMSED-0102/PLOTS/TANDS/temp_lis_35hlp

DATE: 11/21/2003 TIME: 10:39:55

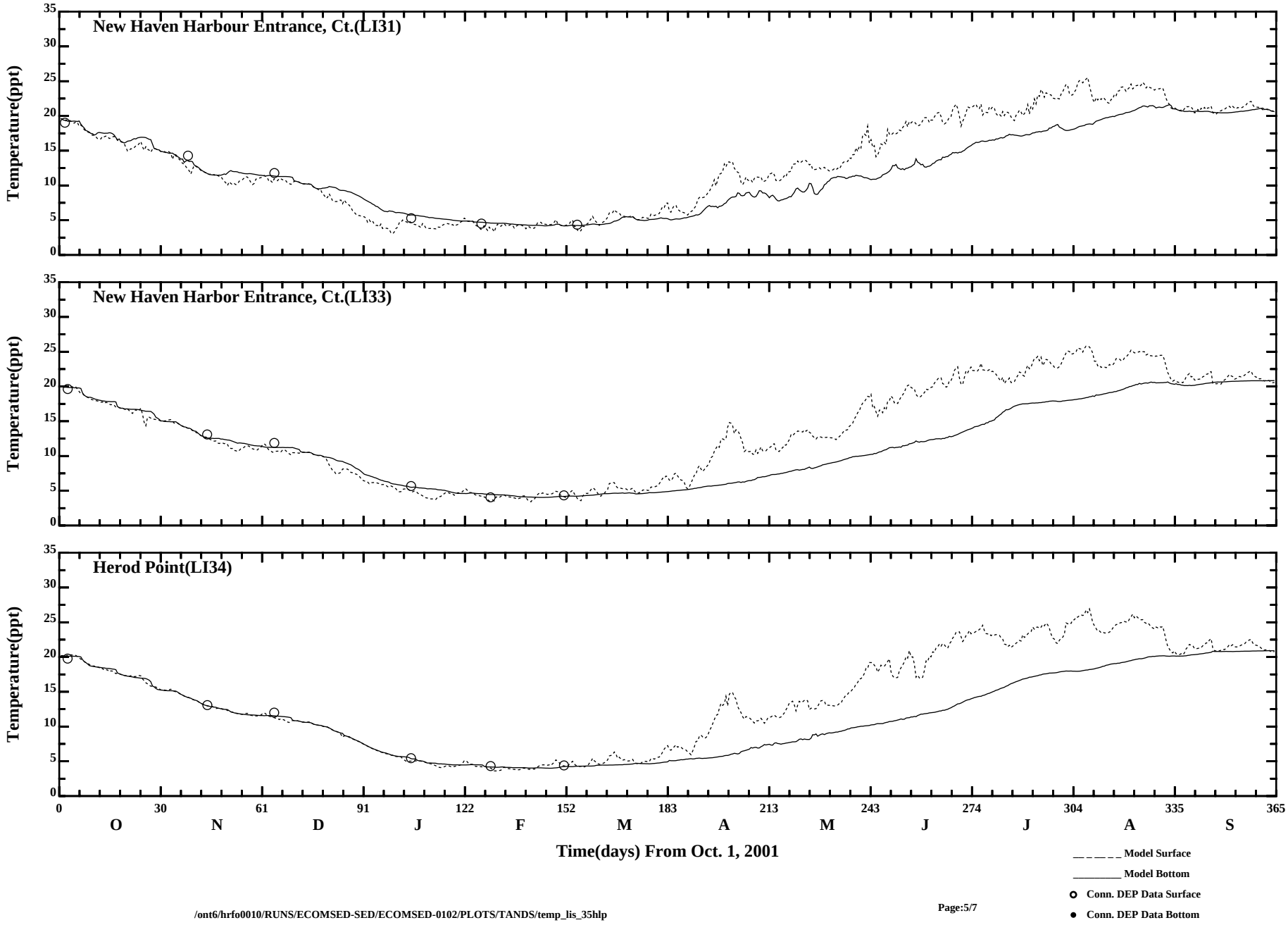
New Haven Harbour Entrance, Ct.(LI31)
New Haven Harbor Entrance, Ct.(LI33)
Herod Point(LI34)
Temperature(ppt)
0
5
10
15
20
25
30
35
0
30
61
91
122
152
183
213
243
274
304
335
365
O
N
D
J
F
M
A
M
J
J
A
S
Time(days) From Oct. 1, 2001
Model Surface
Model Bottom
Conn. DEP Data Surface
Conn. DEP Data Bottom

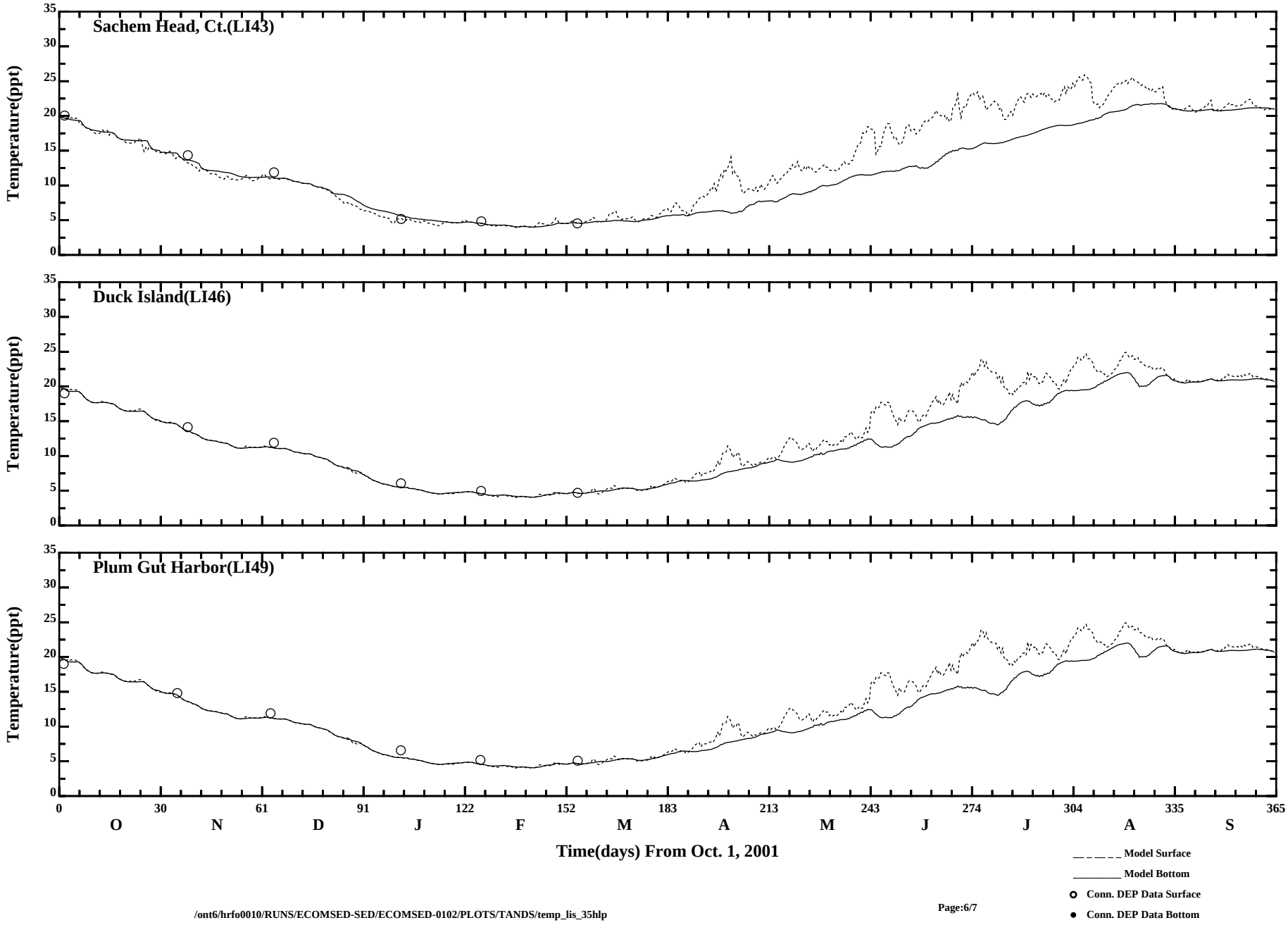

/ont6/hrfo0010/RUNS/ECOMSED-SED/ECOMSED-0102/PLOTS/TANDS/temp_lis_35hlp

DATE: 11/21/2003 TIME: 10:39:55

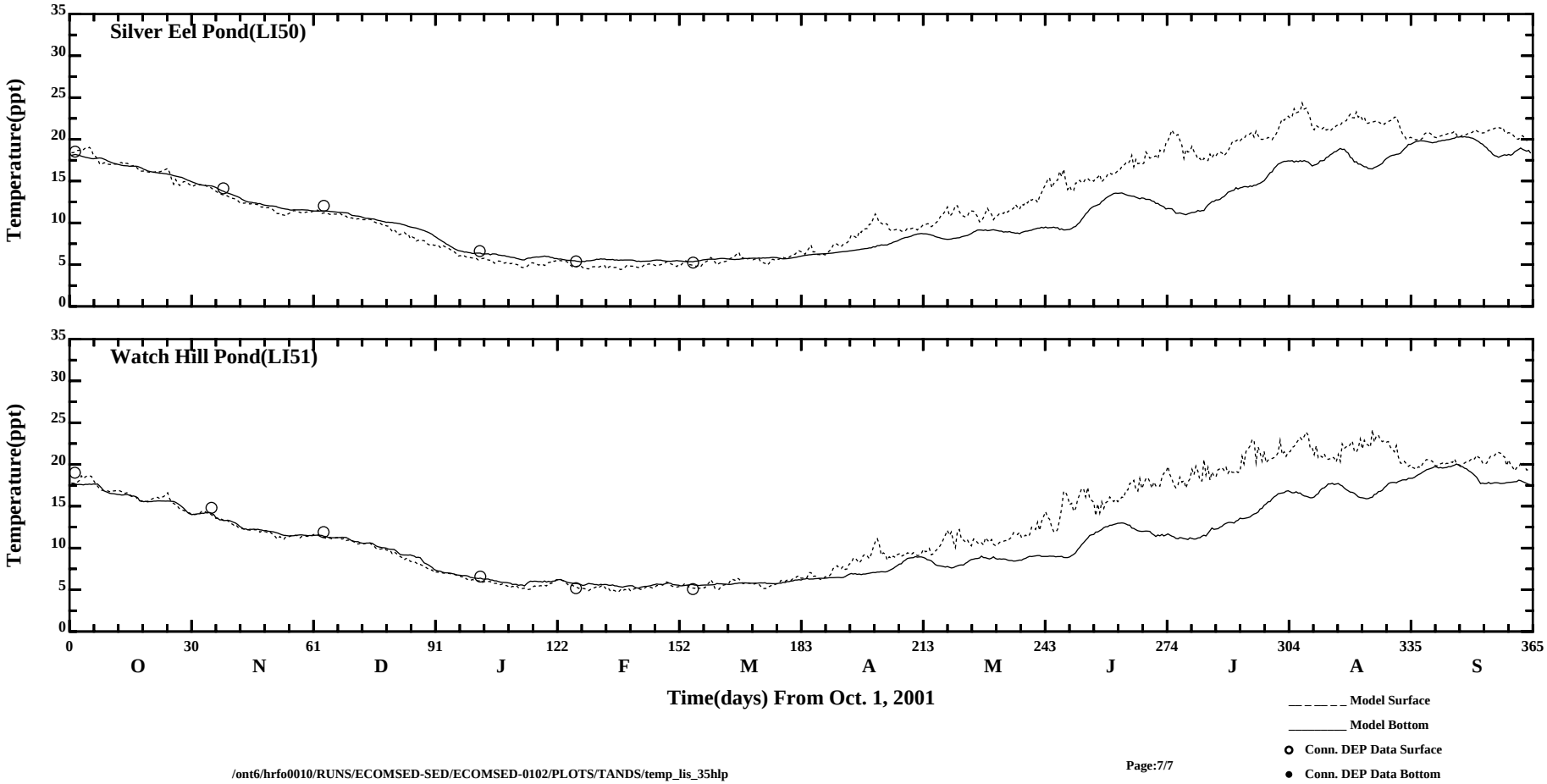

/ont6/hrfo0010/RUNS/ECOMSED-SED/ECOMSED-0102/PLOTS/TANDS/temp_lis_35hlp

DATE: 11/21/2003 TIME: 10:39:55

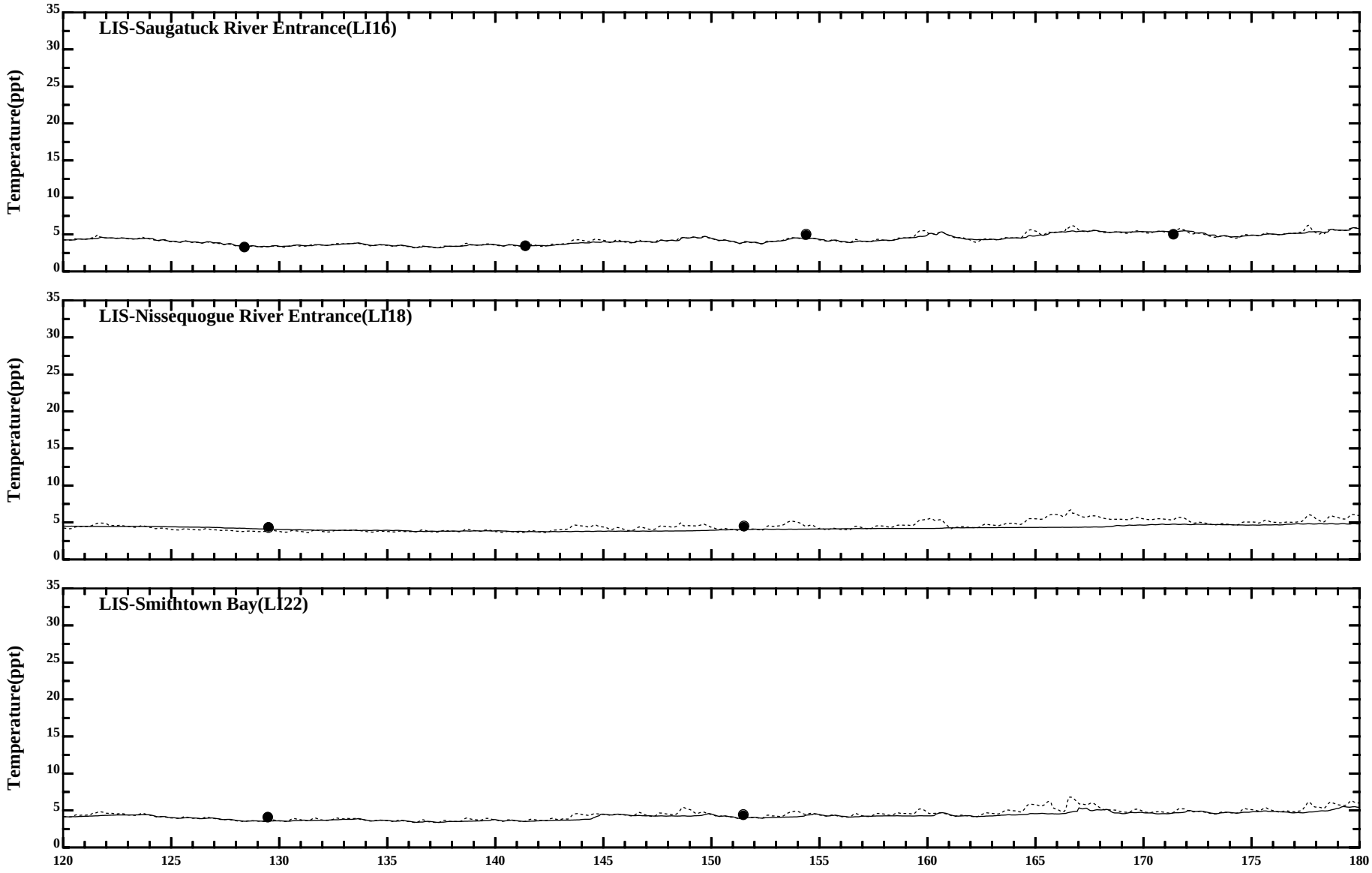
LIS-Saugatuck River Entrance(LI16)
LIS-Nissequogue River Entrance(LI18)
LIS-Smithtown Bay(LI22)
Temperature(ppt)
0
5
10
15
20
25
30
35
120
125
130
135
140
145
150
155
160
165
170
175
180
Time(days) From Oct. 1, 2001
Model Surface
Model Bottom
Conn. DEP Data Surface
Conn. DEP Data Bottom

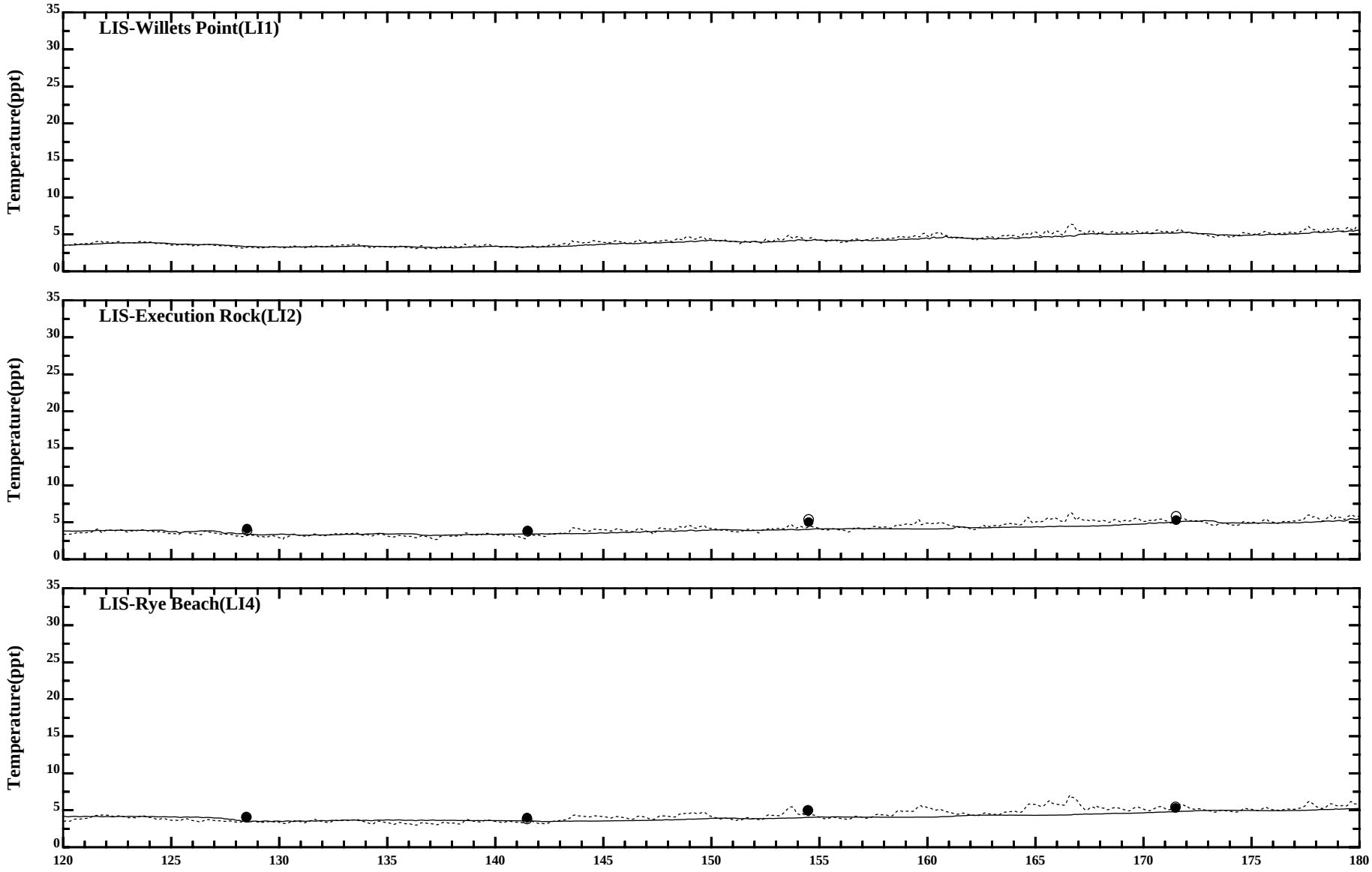
LIS-Willets Point(LI1)
LIS-Execution Rock(LI2)
LIS-Rye Beach(LI4)
Temperature(ppt)
0
5
10
15
20
25
30
35
120
125
130
135
140
145
150
155
160
165
170
175
180
Time(days) From Oct. 1, 2001
Model Surface
Model Bottom
Conn. DEP Data Surface
Conn. DEP Data Bottom

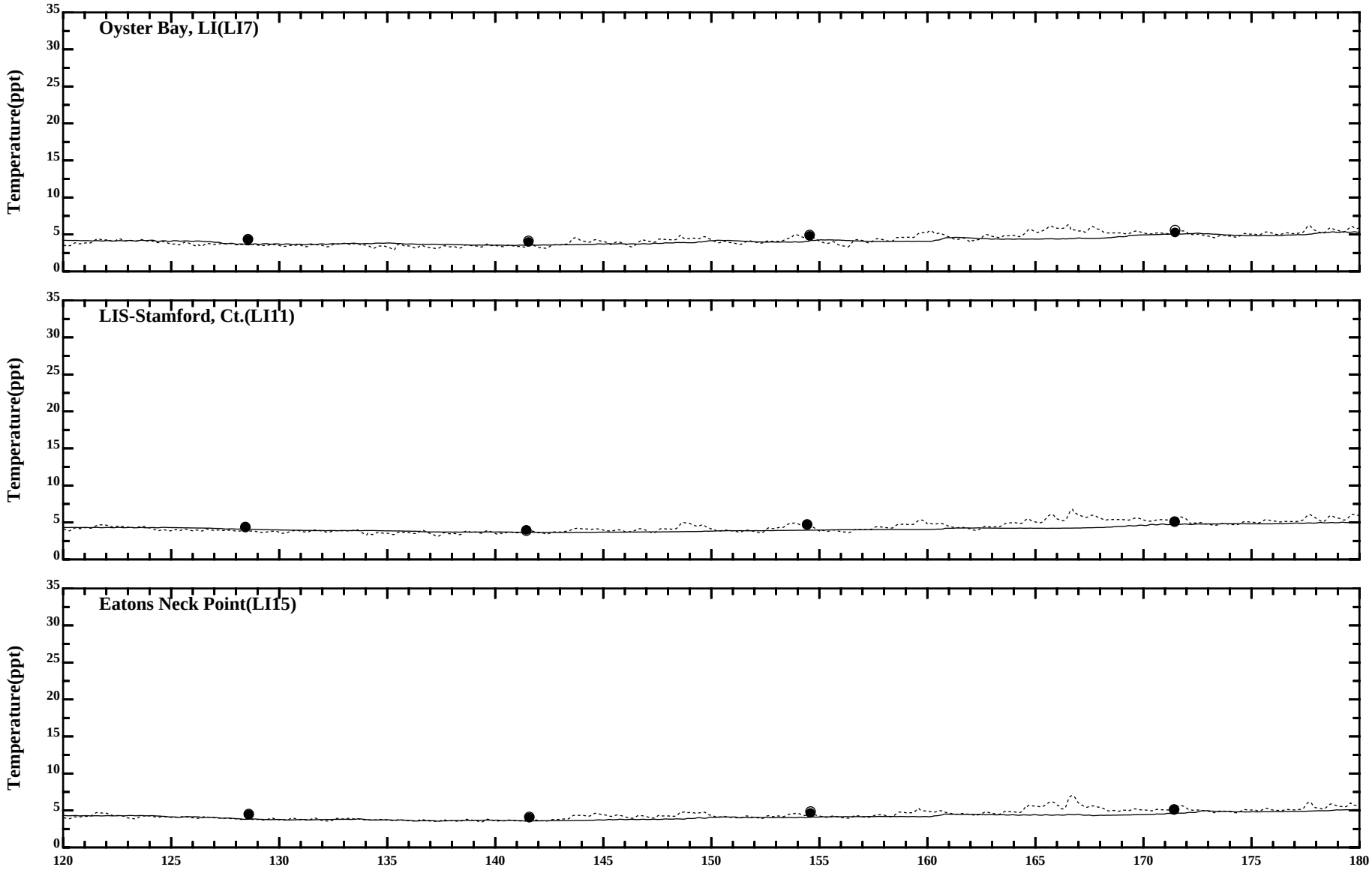
Oyster Bay, LI(LI7)
LIS-Stamford, Ct.(LI11)
Eatons Neck Point(LI15)
Temperature(ppt)
0
5
10
15
20
25
30
35
120
125
130
135
140
145
150
155
160
165
170
175
180
Time(days) From Oct. 1, 2001
Model Surface
Model Bottom
Conn. DEP Data Surface
Conn. DEP Data Bottom

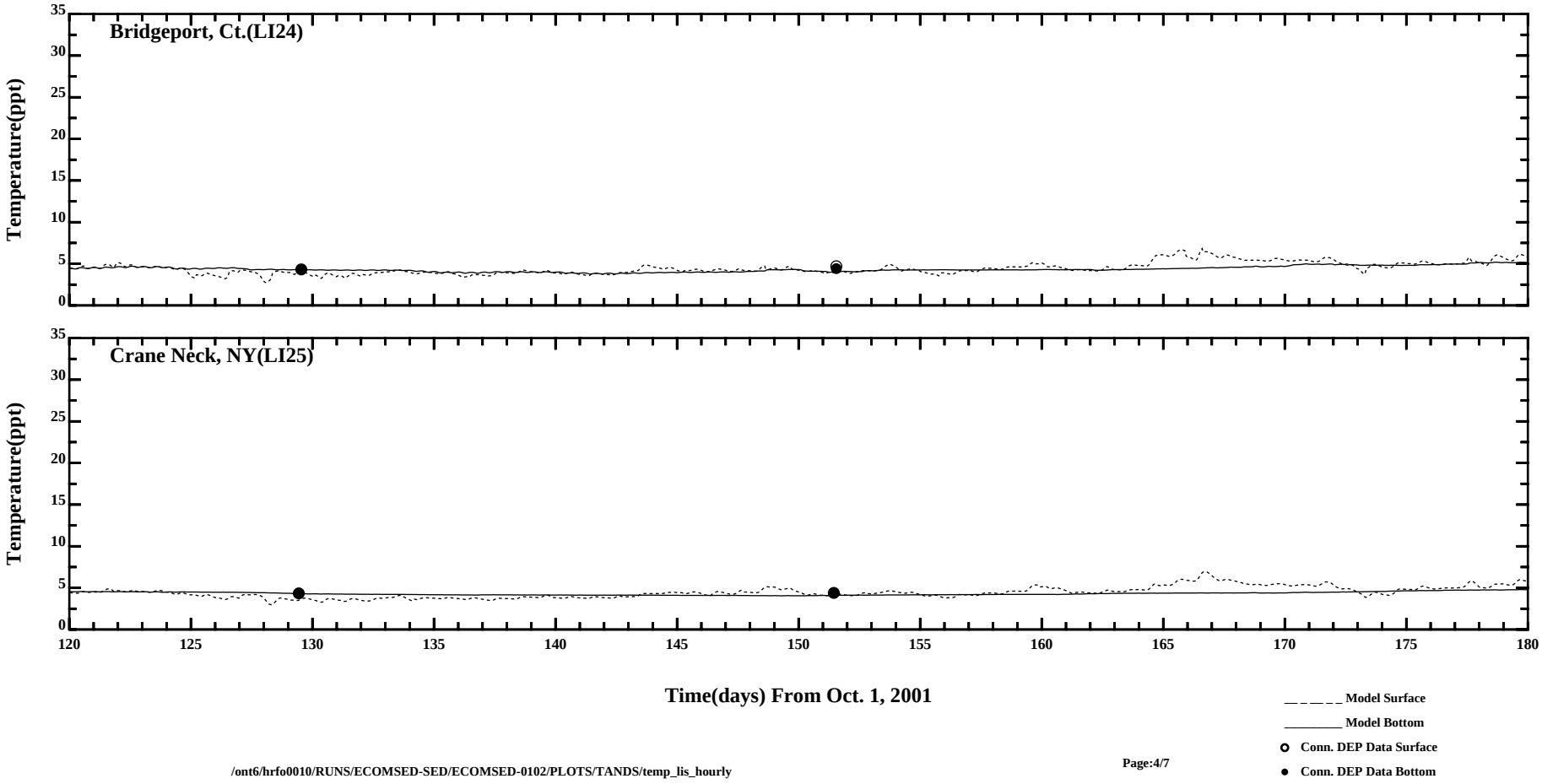

/ont6/hrfo0010/RUNS/ECOMSED-SED/ECOMSED-0102/PLOTS/TANDS/temp_lis_hourly

DATE: 11/21/2003 TIME: 10:40: 7

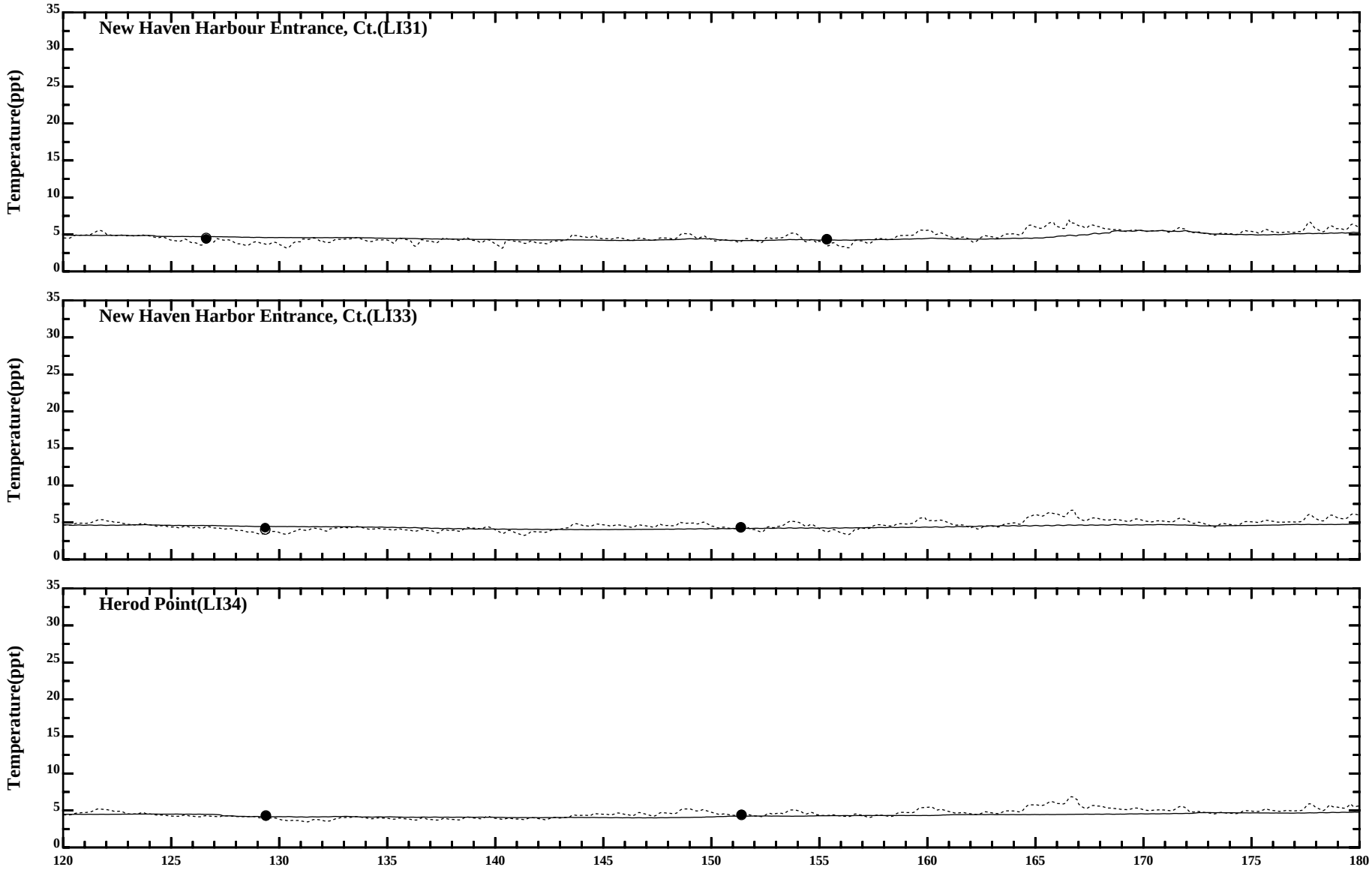
New Haven Harbour Entrance, Ct.(LI31)
New Haven Harbor Entrance, Ct.(LI33)
Herod Point(LI34)
Temperature(ppt)
0
5
10
15
20
25
30
35
120
125
130
135
140
145
150
155
160
165
170
175
180
Time(days) From Oct. 1, 2001
Model Surface
Model Bottom
Conn. DEP Data Surface
Conn. DEP Data Bottom

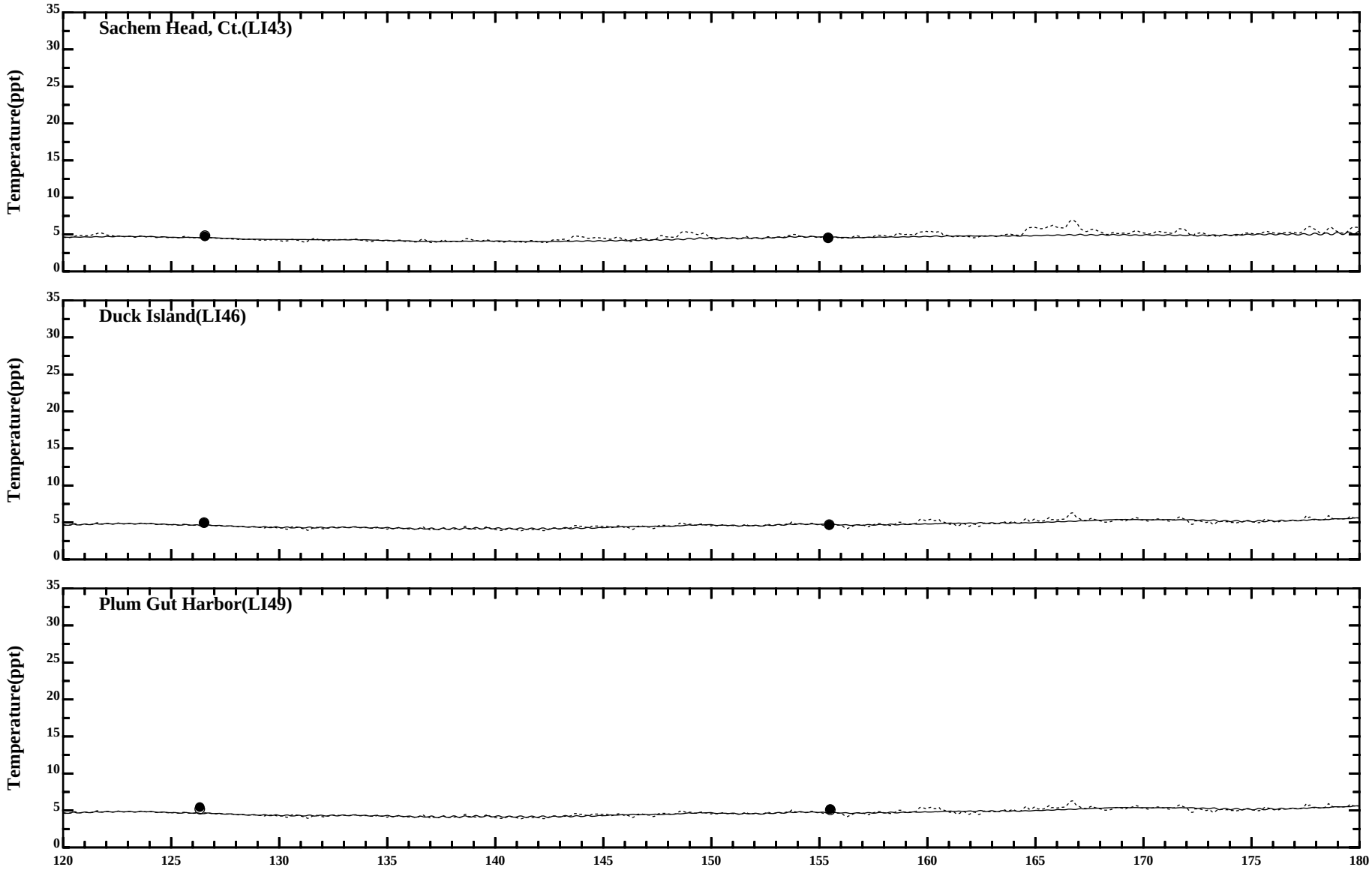
Sachem Head, Ct.(LI43)
Duck Island(LI46)
Plum Gut Harbor(LI49)
Temperature(ppt)
0
5
10
15
20
25
30
35
120
125
130
135
140
145
150
155
160
165
170
175
180
Time(days) From Oct. 1, 2001
Model Surface
Model Bottom
Conn. DEP Data Surface
Conn. DEP Data Bottom

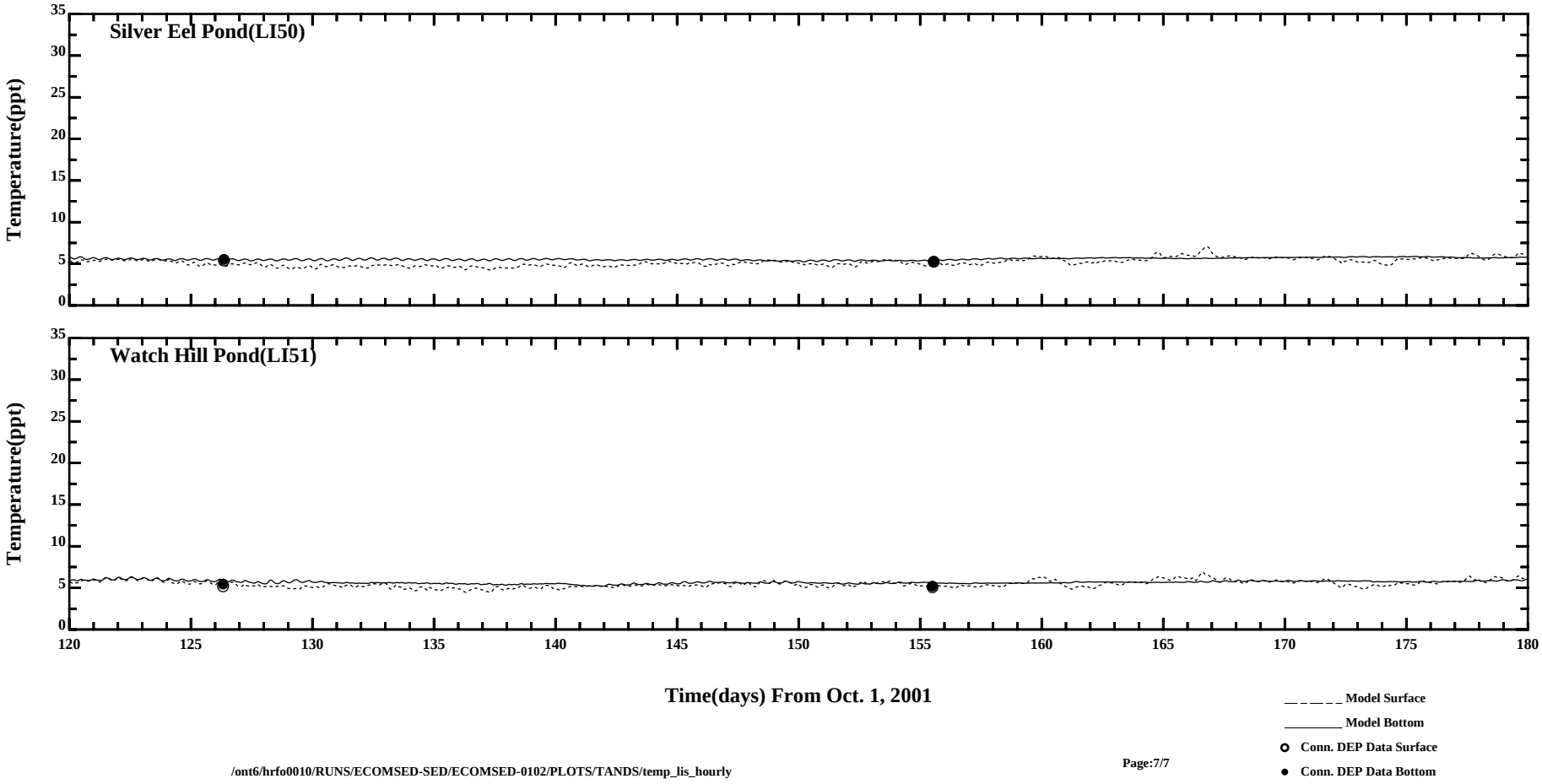

/ont6/hrfo0010/RUNS/ECOMSED-SED/ECOMSED-0102/PLOTS/TANDS/temp_lis_hourly

DATE: 11/21/2003 TIME: 10:40: 7

APPENDIX 9

MODEL EVALUATION GROUP (MEG)
FINAL HYDRODYNAMIC REVIEW COMMENTS
AND HYDROQUAL RESPONSE

Model Evaluation Group (MEG) Review of: "A Model for the Evaluation and Management of Contaminants of Concern in Water, Sediment, and Biota in the NY/NJ Harbor Estuary Hydrodynamic Sub-Model" by HydroQual, Inc.

This review examines HydroQual's Hydrodynamic Sub-Model Report (the "Report") for the Contaminant Assessment and Reduction Project (CARP). The objective of the Report is to provide a comprehensive description of the CARP hydrodynamic sub-model and its suitability for use in CARP fate and transport calculations. The Report provides a comprehensive description of the application of the CARP hydrodynamic model, but not of the model itself. However, the reader is provided with ample references (e.g., Blumberg et al. 1999) and cross-references (e.g., Blumberg and Mellor, 1987) that describe this well-known and frequently used model. The objective of the CARP hydrodynamic sub-model computations is to provide time series of water depths, current velocities, volume transport rates (in three dimensions), salinities, temperatures and dispersion coefficients. These hourly averaged variables are passed to other CARP sub-models to calculate advective and dispersive fluxes, temperature-and-salinity–dependent rate constants and kinetics coefficients, bottom shear stresses, etc.

Many others have reviewed previous applications of this hydrodynamic model to the NY-NJ Harbor Estuary. These include peer reviews in scientific and engineering journals (Blumberg et al. 1999; Blumberg and Pritchard, 1997), reviews by three previous Model Evaluation Groups (MEGs), and reviews by various government agencies and their consultants. Accordingly, this review focuses primarily on the performance of this model in its present application (CARP).

The model's computational grid is similar to previously reported versions. The specified horizontal grid spacing ranges from a minimum of about 100 m in inland rivers to 50 km in New York Bight. The grid still appears somewhat coarse in the important Newark Bay region, with 1-2 computational cell widths. The model grid includes ten vertical layers to resolve the estuarine vertical structure.

The model is forced primarily with observed physical data (with some empirical adjustments) at the model's boundaries. As in previous applications (Blumberg et al. 1999), the modelers assume that the water surface elevation at the offshore boundaries is a superposition of an astronomical tidal component, a sub-tidal component (assumed to be proportional to observed, low-pass-filtered sea level at Sandy Hook), and a prescribed steady geostrophic component (based on surface slope data collected in August 1978). The model includes a well-documented radiation boundary condition (Blumberg and Kantha, 1985). Also, salinity and temperature are prescribed at the offshore boundary based on mean monthly climatological data reported in the 1998 NOAA World Ocean Atlas (adjusted by 2 ppt or 2°C).

At the water surface, wind stress and heat flux are calculated based on the usual suite of observed meteorological variables (at J.F.K airport, Albany airport, Bridgeport airport and several offshore buoys). Fresh water inflows are input to the model at 25 locations based on flow data recorded at the limited number (34) of available U.S.G.S. gaging station in the tributary rivers. Also, river discharge temperatures are assumed to be the same as daily surface temperatures recorded at the Battery (a first-order approximation). The model benefits from HydroQuals' extensive database of reported wastewater treatment plant discharge data (and flow statistics) and previous model estimates for discharges from CSOs and stormwater runoff.

The Report does not provide the selected values for some of the model calibration coefficients. These include the selected bottom drag coefficients and horizontal diffusion parameter, C_s. However, previously selected values for these adjustable parameters are provided in Blumberg et al. (1999).

The validity of model assumptions and parameter selections may be assessed through the Report's numerous comparisons of model results with observed data. These include some continuous model-data comparisons for four variables (tidal elevation, temperature, bottom salinity and velocity) at the CARP Newark Bay/Kills monitoring stations, and continuous comparisons for one variable (tidal elevation) at various additional NOAA monitoring stations. Continuous comparisons for temperature, bottom salinity and velocity are not provided outside of the Newark Bay/Kills complex. Instead, model results are compared to discrete data collected by several agencies at varying intervals (e.g., weekly, bi-weekly, monthly, seasonal, etc.) throughout the model domain.

Visually, the model appears to reproduce well the observed tidal elevation variations at almost all stations. This includes the timing and magnitude of the observed peaks and troughs, the spring-neap variation, the sub-tidal variability, and the low sub-tidal variability. In particular, there is good agreement displayed (in Appendix 4) for the sub-tidal sea level components at several stations. This agreement suggests that the model adequately simulates the sub-tidal volume transport. Model agreement is less favorable at Montauk Point, though this station is beyond the main area of interest (and located within a small embayment). Unfortunately, the Report provides no quantitative skill assessment for simulated water surface elevations or currents. However, a favorable quantitative assessment was provided in the previous paper (Blumberg et al. 1999; Tables 1-2), and similar results are anticipated here.

Also, the present (CARP) model appears to reproduce well the observed tidal current variations at Newark Bay station 3 (Lower Newark Bay) and Perth Amboy. Also, a good visual comparison is presented in year 2002 for the two Kills stations. At Newark Bay station 1 (upper Newark Bay), the model appears to reproduce the observed velocity pattern at the surface; however, the model appears to underestimate observed bottom currents consistently (by a factor of 2 or more). This disagreement

should be investigated, since the model's bottom stress calculation would magnify this discrepancy and thereby underestimate the potential for tidal resuspension in this region.

Salinity comparisons are useful indicators of the ability of a model to simulate constituent transport (a main issue here). Water temperatures calibrations are also useful in as much as temperature influences various modeled biogeochemical processes. Model-data comparisons for salinity and temperature are presented at two levels of temporal resolution: continuous and discrete. Comparisons to continuous observed data are provided for the Newark Bay/Kill complex using available CARP data. Comparisons to discrete observations (collected weekly, bi-weekly, monthly, seasonal, etc.) are provided at various stations outside the Newark Bay/kills complex using data provided by various sources. Note that the previous published study (Blumberg et al. 1999) provided comparisons to discrete salinity and temperature observations.

Overall, the model appears to track the observed sub-tidal salinity trends and seasonal stratification cycles in the Hudson Estuary and Upper/Lower Bay. The exception is the summer of 2002 -- when the model appears to underestimate observed salinities at most stations. Also, the model tends to smooth out some of the observed tidal oscillations (translations) in bottom salinity, especially at Newark Bay station 1 (upper Newark Bay). This result may be related to the coarse computational grid applied in this area (Figure 3-1) and uncertainty in model bathymetry. The Report does not provide an assessment of the model's ability to track tidal (semi-diurnal) salinity variations outside of the Newark Bay/Kills complex (e.g., at NOAA's Sandy Hook station).

At many stations (e.g., Hudson Estuary, Upper and Lower Bay), the model appears to simulate fortnightly variations in the vertical salinity structure, with neap-to-spring tide transitions from stratified to less-stratified conditions. This is an important feature that modulates the estuarine gravitational circulation. Unfortunately, the selected CARP data does not resolve this variability for model-data comparisons.

The Report's discussion of correlation analyses for salinity (figure 3-22a) and temperature lack some important details regarding method assumptions and limitations. Clearly, there is a mismatch in the time scales of observed (discrete) and simulated ("continuous" or hourly) salinity and temperature data outside the Newark Bay/Kills complex. Typically, this results in comparisons to only a limited number of points within each graph (e.g., Figs. 3-12 through 3-19). This reduces the significance of any statistical assessment of model error, although there are many such graphs. The fact that the discrete data are aliased with regard to tidal fluctuations further confounds the analysis. The Report does not state whether discrete observations are being correlated with instantaneous model data, low-pass-filtered model data, or both. If correlations are made only to filtered model data, then this should be stated (along with its inherent limitation of tracking only sub-tidal and seasonal trends and excluding short-

term tidal variations). If this includes correlations with instantaneous model data, then small timing errors can result in relatively large model-data discrepancies (i.e., lower correlations) which would make the comparisons appear worse than they actually are. For these reasons, simple correlation analyses (alone) may not be the best technique to assess model skill. It is curious that other common metrics (e.g., RMS error, relative error, etc.) were not provided in the Report.

Also, the true regression lines are not shown (Figure 3-22a), only the zero-intercept, unit-slope line. The latter suggests that the model often underestimates the observed salinity data at several locations (Newark Bay/Kills, Raritan Bay, Inner Harbor). No correlation analysis is provided for Hudson River salinities (an obvious choice), though it probably would be favorable.

The model accurately tracks the observed subtidal and seasonal trends in water temperature at most stations. The model appears to follow the observed (continuous) trends in bottom temperature at the Newark Bay/Kills stations during 2001. Again, there is some evidence of tidal smoothing, but temperature trends are generally well reproduced in this region. The Report identifies some model discrepancies in the Hackensack Meadowlands region, but such inaccuracies are understandable given the complexities of this marsh system. Also, at estuarine monitoring stations outside the Newark Bay/Kills complex, the comparisons to discrete observations (collected weekly, bi-weekly, monthly, seasonal, etc.) demonstrate that the model reproduces low sub-tidal and seasonal trends.

Overall, the Report demonstrates that the CARP hydrodynamic model is a useful tool for simulating the hydrodynamics of the NY/NJ Harbor Estuary during the CARP years. The model is capable of passing accurate water surface elevations to other sub-models. Also, the model passes representative water temperatures for computation of temperature-dependent rate constants and kinetics. Bottom currents (and associated bottom shear) are generally well-reproduced in the Lower Newark Bay/Kills, where the model should be capable of simulating resuspension of particulate matter. However, the model tends to underestimated current speeds, and smooth tidal translations, in Upper Newark Bay – an issue that should be investigated further. Finally, the model appears to provide an adequate simulation of salt transport, except during the summer of 2002. Thus, the model should be capable of passing representative volume transports and diffusivities to other CARP sub-models.

In the future, the model's documentation may be enhanced by providing alternate quantitative measures of model skill (e.g., RMS error for all variables). Also, additional model-data comparisons may be performed at Hudson River and Sandy Hook monitoring sites where continuous temperature, salinity and/or velocity data are available. Such analyses would provide a more rigorous test of the model's fidelity, including the ability to simulate documented patterns of fortnightly variability in stratification/de-stratification (Warner et al. 2005).

Finally, the scientific merit of the Report would benefit from a discussion of the model results in light of the salient estuarine hydrodynamic features (e.g. tidal monthly variability, tidal straining, estuarine circulation patterns, meteorological forcing, etc.) and related transport processes. Unlike the previous paper (Blumberg et al. 1999), the present Report does not discuss model results in light of relevant physical transport processes. This omission limits the usefulness of the report in documenting the scientific tool developed in this study. However, this issue may be addressed in future publications.

References

Blumberg, A.F., L.A. Khan, and J.P. St. John. 1999. "Three dimensional hydrodynamic model of New York Harbor region." ASCE *Journal of Hydraulic Engineering*, 125: 799-816.

Blumberg, A.F., and D.W. Pritchard. 1997. "Estimates of the transport through the East River." *Journal of Geophysical Research*, 102: 5685-5703.

Blumberg, A.F., and G.L. Mellor. 1987. "A description of a three-dimensional coastal ocean circulation model." In: Coastal and estuarine sciences, Vol. 4, N. Heaps, ed. American Geophysical Union, Washington, D.C., 1-16.

Blumberg, A.F., and L.H. Kantha. 1985. "Open boundary condition for circulation models." ASCE *Journal of Hydraulic Engineering*, 111: 237-255.

Warner, J.C., W. R. Geyer, and J.A. Lerczak. 2005. "Numerical modeling of an estuary: a comprehensive skill assessment." *Journal of Geophysical Research*, 110, C05001.

HydroQual Inc. Response to: Model Evaluation Group (MEG) Review of: "A Model for the Evaluation and Management of Contaminants of Concern in Water, Sediment, and Biota in the NY/NJ Harbor Estuary Hydrodynamic Sub-Model" by HydroQual, Inc.

HydroQual's effort on the CARP hydrodynamic model included the application of a previously calibrated and validated hydrodynamic transport model for purposes of CARP (i.e., driving sediment transport, contaminant fate, and bioaccumulation models) as well as an additional skill assessment of the hydrodynamic model's performance using data collected by CARP and other agencies during the 1998-2002 period. HydroQual is appreciative of the MEG's involvement in the application of the hydrodynamic model and the review provided above. It is noted that the hydrodynamic model was not a focus of HydroQual's CARP effort nor that of the MEG. Greater emphasis was placed on the models developed specifically for CARP (i.e., the sediment transport model, the contaminant fate and transport models and the bioaccumulation models). Further, successful calibration of these others models demonstrates the validity of the underlying hydrodynamic model construct, calibration, validation, and skill assessments.

It was not intended that HydroQual would formally respond to or act upon the final MEG review comments. Accordingly, no scope or budget had been aloted for this purpose in HydroQual's contract agreement with the Hudson River Foundation. Rather the intention of the final MEG review was to provide guidance for future users of the CARP model. It is noted that HydroQual had been working cooperatively with the MEG throughout the CARP model development process and that many interim MEG recommendations and suggestions were incorporated into the CARP model along the way. In that sense, there has already been a significant effort by HydroQual to respond to MEG comments and feedback.

While the purposes of HydroQual's response is not to refute or rebut the MEG's final review, the HydroQual response is intended to provide HydroQual with the opportunity to clarify for potential future users of the model (e.g., EPA and State TMDL programs, Superfund, restoration, etc.) any misunderstandings that may be inherent in the MEG review. Overall, HydroQual has found the final MEG review of the hydrodynamic model to be technically accurate with few exceptions. These few exceptions and other points of clarification are noted below.

The MEG review notes the underestimation of salinity measurements at most data stations in 2002 but does not mention HydroQual's explanation for these discrepancies. Specifically, HydroQual had described the in-progress Harbor-deepening project which caused bathymetries to change during the data collection period. The MEG review also notes, and HydroQual agrees, that observed current velocities in upper Newark Bay during 2000-2002 are underestimated by the model. The velocity underestimation may be related, in part, to the deepening activities in-progress at that time. More

likely, the low calculations are related to the computational grid resolution in Newark Bay which tends to oversimplify (i.e., shipping channels in the Bay are not resolved) the detailed current distributions in deep and shallow portions of the Bay.

As the MEG indicated, HydroQual's report on the CARP hydrodynamic model did not include an exhaustive articulation of the calibration process, parameter selection, and salient estuarine hydrodynamic features as would typically be included in a publication in the peer-reviewed literature or a technical report describing the construct of a model. This is because the CARP hydrodynamics are an extension of the previous effort on SWEM. No calibration or adjustment of model parameters was attempted for purposes of CARP. All model forcing development procedures used for the CARP hydrodynamic model are the same as those used for SWEM.

HydroQual acknowledges the many excellent suggestions that the MEG has made regarding incorporating additional and perhaps more statistically rigorous skill assessments into future endeavors with the CARP hydrodynamic model. Hopefully, these may be incorporated in future modeling work or other upcoming efforts within the region. Once again, HydroQual gratefully acknowledges and thanks the MEG members for all of their assistance with the CARP modeling effort. In particular, HydroQual thanks Joe DiLorenzo who was the lead author of the MEG final review comments for the CARP hydrodynamic model.